ISSUED

DOE/WIPP-15-3556
Volume 1

Waste Isolation Pilot Plant

Geotechnical Analysis Report For July 2013 – June 2014

U.S. Department of Energy

October 2015

This page was intentionally left blank.

This document has been submitted as required to:

U.S. Department of Energy
Office of Scientific and Technical Information
PO Box 62
Oak Ridge, TN 37831
(865) 576-8401

Additional information about this document may be obtained by calling 1-800-336-9477

Unlimited, publicly available full-text scientific and technical reports produced since 1991 are available online at Information Bridge (www.osti.gov/bridge).

U.S Department of Energy and its contractors may obtain full-text reports produced prior to 1991 in paper form for a processing fee from:

U.S. Department of Energy
Office of Scientific and Technical Information
P.O. Box 62
Oak Ridge, TN 37831-0062
Telephone: (865) 576-8401
Facsimile: (865) 576-5728
E-mail: reports@osti.gov

Available for sale to the public from:

U.S. Department of Commerce
National Technical Information Service
5301 Shawnee Rd
Alexandra, VA 22312
Phone: (800) 553-6847 or (703) 605-6000
Fax: (703) 605-6900
Email: info@ntis.gov

This page was intentionally left blank.

FOREWORD AND ACKNOWLEDGMENTS

This report contains an assessment of the geotechnical status of the Waste Isolation Pilot Plant (WIPP). During the excavation of the principal underground access and experimental areas, the status was reported quarterly. Since 1987, when the initial construction phase was completed, reports have been published annually. This report presents and analyzes data collected from July 1, 2013, to June 30, 2014.

This Geotechnical Analysis Report (GAR) was written to meet the needs of several audiences. It satisfies requirements contained in the WIPP Hazardous Waste Facility Permit[1] (HWFP) and the Certification of Compliance[2] with Subparts B and C, Title 40 *Code of Federal Regulations* (CFR) Part 191, "Environmental Radiation Protection Standards for Management and Disposal of Spent Nuclear Fuel, High-Level and Transuranic Radioactive Wastes." It focuses on the geotechnical performance of the various components of the underground facility, including the shafts, shaft stations, access drifts, and waste disposal areas. The results of investigations of excavation effects and other geotechnical studies are also included.

The report compares the geotechnical performance of the repository to the design criteria. It describes the techniques that were used to acquire the data. The depth and breadth of the evaluation of the different components of the underground facility vary according to the types and quantities of data available and the complexity of the recorded geotechnical responses. Graphic documentation of data and tabular documentation of instrument history can be provided upon request.

This GAR was prepared by Nuclear Waste Partnership LLC (NWP) for the U.S. Department of Energy (DOE), Carlsbad Field Office (CBFO), in Carlsbad, New Mexico. Work was supported by the DOE under Contract No. DE-EM0001971.

[1] New Mexico Environment Department (NMED), 2012, Waste Isolation Pilot Plant Hazardous Waste Facility Permit, NM4890139088-TSDF, Santa Fe, NM

[2] U.S. Environmental Protection Agency, 1998, "Criteria for the Certification and Recertification of the Waste Isolation Pilot Plant's Compliance with the Disposal Regulations: Certification Decision," Federal Register, Vol. 63, No. 95, pp. 27354, May 18, 1998, Washington, DC

This page was intentionally left blank.

TABLE OF CONTENTS

LIST OF TABLES

LIST OF FIGURES

This page was intentionally left blank.

ACRONYMS AND ABBREVIATIONS

ASTM	American Society for Testing and Materials
bp	before present
bsc	below shaft collar
CAO	Carlsbad Area Office
CBFO	Carlsbad Field Office
CFR	Code of Federal Regulations
CH	contact-handled
cm	centimeter(s)
DOE	U.S. Department of Energy
EPA	U.S. Environmental Protection Agency
ft	foot (feet)
GAR	Geotechnical Analysis Report
GIS	Geomechanical Instrumentation System
HWFP	Hazardous Waste Facility Permit
in	inch(es)
km	kilometer(s)
kPa	kilopascal(s)
kVA	kilovolt ampere(s)
LANL	Los Alamos National Laboratory
lb	pound(s)
m	meter(s)
Ma	million years
MB	marker bed
NMED	New Mexico Environment Department
NWP	Nuclear Waste Partnership LLC
OMB	orange marker bed
psi	pound(s) per square inch
RH	remote-handled

SDI	Salt Disposal Investigation
SDDI	Salt Defense Disposal Investigation
SPDV	Site and Preliminary Design Validation
TRU	transuranic
WIPP	Waste Isolation Pilot Plant
VOC	Volatile Organic Compound
yr(s)	year(s)

1.0 INTRODUCTION

This Geotechnical Analysis Report (GAR) presents and interprets geotechnical data from the underground excavations at the Waste Isolation Pilot Plant (WIPP). The data, which are obtained as part of a regular monitoring program, are used to characterize conditions, to compare actual performance to the design criteria and to evaluate and forecast the performance of the underground excavations.

GARs have been available to the public since 1983. During the Site and Preliminary Design Validation (SPDV) Program, the architect/engineer for the project produced these reports quarterly to document the geomechanical performance during and immediately after early excavations of the underground facility. Since completion of the construction phase of the project in 1987, the management and operating contractor for the facility has prepared these reports annually. This report describes the performance and condition of selected areas from July 1, 2013, to June 30, 2014. It is divided into nine chapters.

Chapter 1 provides background information on WIPP, its mission, and the purpose and scope of the geomechanical monitoring program. Chapter 2 describes the local and regional geology of the WIPP site. Chapters 3 and 4 describe the geomechanical instrumentation in the shafts and shaft stations, present the data collected by that instrumentation, and provide interpretation of these data. Chapters 5 and 6 present the results of geomechanical monitoring in the two main portions of the WIPP underground (the access drifts and the waste disposal area). Chapter 7 introduces the Salt Disposal and Salt Defense Disposal Investigation Areas. Chapter 8 discusses the results of the Geoscience Program, which include fracture mapping and observation hole observations. Chapter 9 summarizes the results of geomechanical monitoring and compares the current excavation performance to the design requirements. Chapter 10 lists references.

1.1 Location and Description

WIPP is located in southeastern New Mexico, 26 miles (42 kilometers [km]) east of Carlsbad (Figure 1-1). The surface facilities were built on the flat to gently rolling terrain that is characteristic of the Los Medaños area. The underground facility is being excavated approximately 2,150 feet (ft) (655 meters [m]) beneath the surface in the Salado Formation. Figure 1-2 shows a plan view of the underground configuration of WIPP as of June 30, 2013.

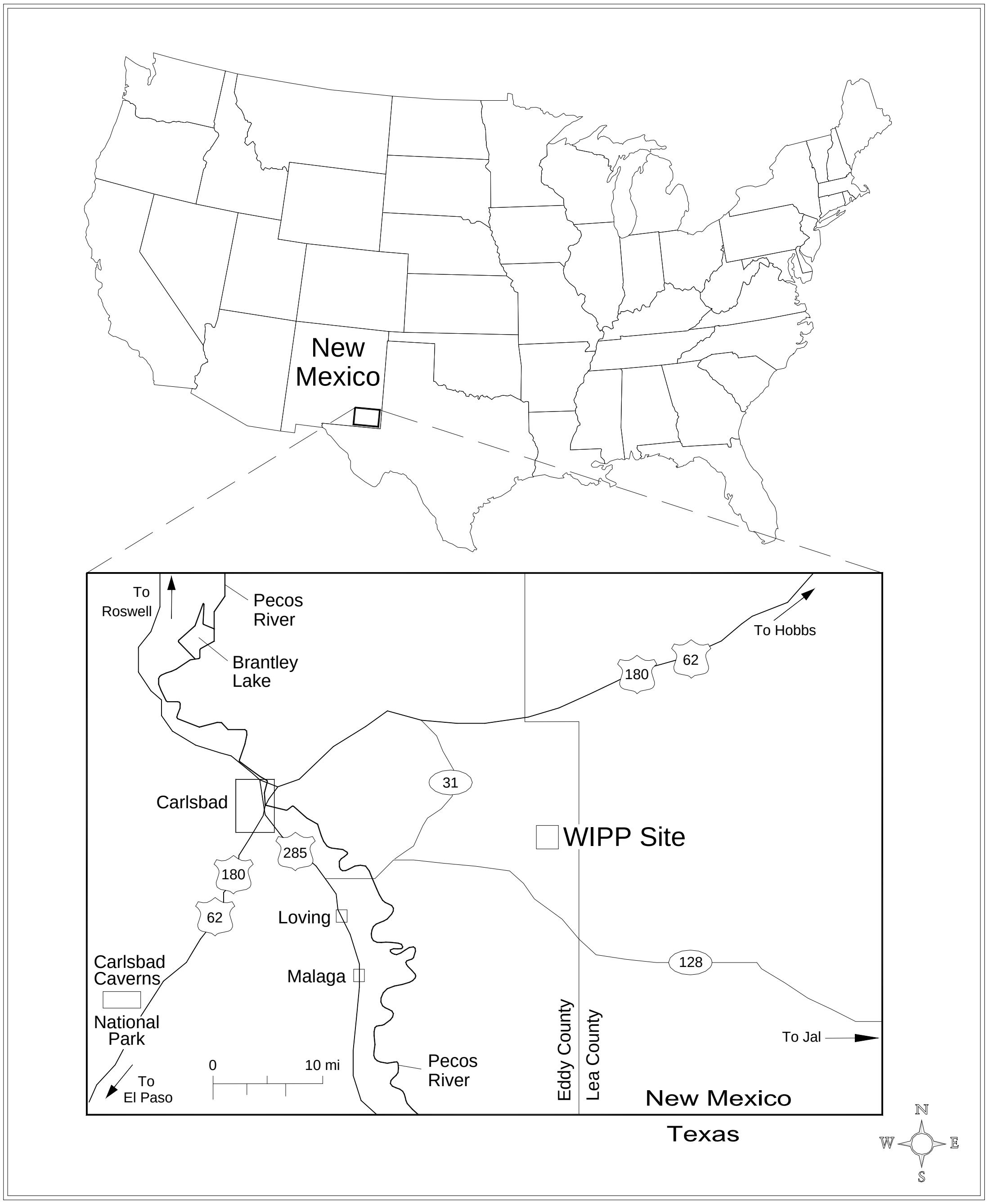

Figure 1 - 1 WIPP Location

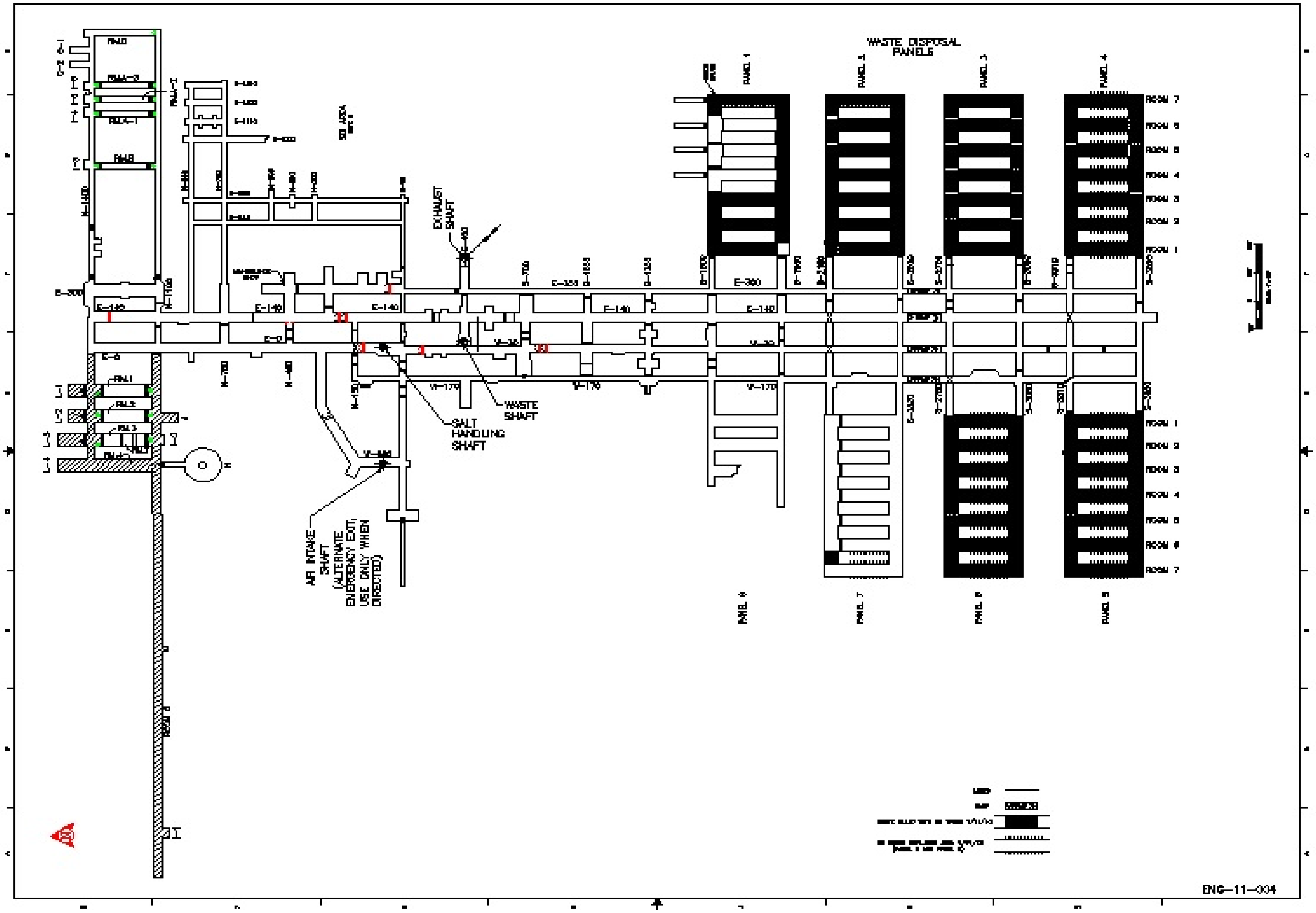

Figure 1 - 2 Underground Mining and Waste Disposal Configuration as of June 30, 2014

1.2 Mission

In 1979 Congress authorized WIPP (Public Law 96-164, National Security and Military Applications of Nuclear Energy Authorization Act of 1980) to provide ". . . a research and development facility to demonstrate the safe disposal of radioactive wastes resulting from the defense activities and programs of the United States exempted from regulation by the Nuclear Regulatory Commission." To fulfill this mission, the DOE constructed a full-scale facility to demonstrate both technical and operational principles of the permanent disposal of transuranic (TRU) and TRU mixed wastes. Technical aspects are those concerned with the design, construction, and performance of the subsurface excavations. Operational aspects refer to the receiving, handling, and emplacement of TRU wastes in the facility. The facility was first used for *in situ* studies and experiments without the use of radioactive waste. WIPP now receives handles, and permanently disposes of TRU waste and TRU mixed waste.

1.3 Development Status

To fulfill its mission, the DOE developed WIPP in a phased manner. The goal of the SPDV phase, begun in 1980, was to characterize the site and obtain *in situ* geotechnical data from underground excavations to determine whether site characteristics and *in situ* conditions were suitable for permanent disposal. During this phase, the Salt Shaft, a ventilation shaft, a drift to the southernmost extent of the proposed waste disposal area, a four-room experimental panel, and access drifts were excavated. Surface-based geological and hydrological investigations were also conducted. The data obtained from the SPDV investigations were reported in the "Summary of the Results of the Evaluation of the WIPP Site and Preliminary Design Validation Program" (DOE, 1983).

Based upon the favorable results of the SPDV investigations, additional activities were initiated in 1983. These included the construction of surface structures, conversion of the ventilation shaft for use as the Waste Shaft, excavation of the Exhaust Shaft, development of additional access drifts to the waste disposal area, excavation of the Air Intake Shaft, and excavation of additional experimental rooms to support research and development. Geotechnical data acquired during this phase were used to evaluate the performance of the excavations in the context of established design criteria (DOE, 1984). Results of these evaluations were reported in *Geotechnical Field Data Reports* (DOE, 1985; DOE, 1986a) and were summarized in the *Design Validation Final Report* (DOE, 1986b).

The *Design Validation Final Report* concluded that the facility, including waste disposal areas, could be developed and operated to fulfill the long-term mission of WIPP (DOE, 1986b). All available information validated the design of underground openings to safely accommodate the permanent disposal of waste under routine operating conditions.

Panel 1 mining began in 1986 and was completed in 1988. Panel 1 was intended to receive waste for an initial operations demonstration and pilot plant phase that was scheduled to start in October 1988; however, the demonstration and pilot plant phase was not put into effect because waste could not be emplaced until permits were acquired.

In October 1996, the DOE submitted to the U.S. Environmental Protection Agency (EPA) a compliance certification application in accordance with 40 CFR Parts 191 and 194, which addressed the long-term (10,000-year) performance criteria for the disposal system. On May 18, 1998, the EPA published the final certification that allowed for the receipt of TRU waste at WIPP. Immediately before this certification, the DOE Carlsbad Area Office (CAO) completed an Operational Readiness Review, which is required by the DOE before the start-up or a process change of any nuclear facility. As a result of the review, the CAO notified the Energy Secretary on April 1, 1998, that WIPP was operationally ready to receive waste. On March 26, 1999, the first shipment of TRU waste was received from Los Alamos National Laboratory (LANL). By the end of June 2013, many additional generator sites had shipped waste to WIPP. The cleanup of several small-quantity generator sites, as well as one large-quantity site (Rocky Flats Environmental Technology Site) is now complete.

Waste disposal in Panels 1, 2, 3, 4 and 5 is complete. Panels 1, 2, and 3 contain only CH waste. The first RH waste shipment arrived January 24, 2007. Panel 4 was the first to receive both CH and RH waste. As of June 30, 2014, waste handling activities included RH disposal in Room 1 of Panel 6 and CH disposal in Room 2 of Panel 6. Mining of Panel 7 was completed in January 2013.

1.4 Purpose and Scope of Geomechanical Monitoring Program

As specified in the WIPP HWFP (NMED, 2012), the purpose of the geomechanical monitoring program is to obtain *in situ* data to support the continuous assessment of the design for underground facilities.

Specifically, the program provides for:

- Early detection of conditions that could affect operational safety.
- Evaluation of disposal room closure that ensures adequate access.
- Guidance for design modifications and remedial actions.
- Data for interpreting the behavior of underground openings, in comparison with the established design criteria.

Data taken by or input into the geomechanical instrumentation system (GIS) are evaluated and reported in this GAR. This annual report fulfills the requirements set forth in Part 4.6.1.2, Attachment A3, Section A2-5b (2) of the WIPP HWFP (NMED, 2011), and 40 CFR §191.14, "Assurance Requirements," implemented through the certification criteria, 40 CFR Part 194.

The Geomechanical Monitoring Program generates the data for four of the compliance monitoring parameters:

- Creep closure and stresses
- Extent of deformation
- Initiation of brittle deformation
- Displacement of deformation features

The instrumentation system for geomechanical monitoring provides data for routine evaluations of safety, stability, and performance of underground openings. *In situ* data are also used to model long-term disposal system performance. Changes resulting from excavations are monitored by routine inspections of selected observation hole arrays and fracture mapping to detect and quantify occurrences of discontinuities such as fractures and bed separations. Analysis of data indicating areas of potential instability allows timely corrective action before they could become safety issues. Other geoscience activities include geologic mapping and sampling, and seismic monitoring.

The GIS provides data that are collected, processed, and stored for analysis. The following subsections briefly describe the major components of the GIS.

1.4.1 Instrumentation

Instrumentation installed for measuring the geomechanical response of the shafts, drifts, and other underground openings includes convergence points, convergence meters, extensometers, rock bolt load cells, pressure cells, strain gauges, piezometers, and joint meters. Table 1-1 lists a summary of the specifications for geomechanical instrumentation.

Table 1 - 1 Geomechanical Instrumentation System

Instrument Type	Measures	Range[1]	Resolution[1]
Sonic probe extensometer	Cumulative deformation	0–2 in	0.001 in
Convergence point (tape extensometer)	Cumulative deformation	2–50 ft	0.001 in
Wire convergence meter	Cumulative deformation	0–3.5 ft	0.001 in
Embedded strain gauge	Cumulative strain	0–3000 μin/in	1 μin/in
Spot-welded strain gauge	Cumulative strain	0–2500 μin/in	1 μin/in
Rock bolt load cell	Load	0–50 tons	40 lb
Earth pressure cell	Pressure	0–1000 psi	1 psi
Piezometer	Fluid pressure	0–500 psi	0.5 psi
Joint meter	Cumulative deformation	0–4 in	0.001 in
Vibrating wire extensometer	Cumulative deformation	0–4 in	0.001 in
Wire extensometer	Cumulative deformation	0–20 in	0.001 in
Linear potentiometric extensometer	Cumulative deformation	0–6 in	0.001 in

[1] Manual readout boxes for the instruments were manufactured to render measurements in U.S. customary units. Range and resolution measurement units have not been converted to metric units. Measurements from these instruments have been converted for presentation elsewhere in this report.

1.4.2 Data Acquisition

Geomechanical instruments are read either manually, using portable devices, or remotely by electronically polling the stations from the surface in accordance with approved operating procedures. Remotely read instruments are connected to one of the underground data loggers, and readings are collected by initiating the appropriate polling routine. Upon completion of a verification process, data are transferred to a computer database. Manual readout devices are taken to instrument locations underground. Data are recorded on data sheets and later entered into an electronic database.

The underground data acquisition system consists of instruments, polling devices, and a communications network. Instruments are connected to polling devices that are installed in electrical enclosures near the instrument locations. Polling devices are connected by a data link to a surface computer.

Whether acquired manually or remotely, geomechanical data are entered into the database files of the GIS data processing system. The data processing system consists of computer programs that are used to enter, reduce, and transfer the data to permanent storage files. Additional routines allow access to the permanent storage files for numerical analysis, tabular reporting, and graphical plotting. Copies of the instrumentation database and data plots are available upon request.[3]

[3] Instrumentation data and data plots are presented in "Geotechnical Analysis Report for July 2013-June 2014 Supporting Data" (DOE/WIPP-15-3556 Volume 2).
The document is available upon request from the National Technical Information Service. See page 3 for details and addresses.

1.4.3 Data Evaluation

Rounding and significant digits are used in the data tables of this document. The reference document is American Society for Testing and Materials (ASTM) document ASTM D 6026-06, "Standard Practice for Using Significant Digits in Geotechnical Data."

Closure measurements are acquired manually from convergence point anchors and remotely from convergence meters. Data are presented in plots of closure versus time. Closure rate data are calculated and presented as part of the data analysis. Extensometers provide displacement data from instrumented rods or wires anchored at various depths. Plots show displacement versus time for individual anchors.

Displacement rate data from the hole (collar) to the deepest anchor are presented in the data analysis.

The annual closure rate is calculated as follows:

$$rate(inches/year) = (cfi_2 - cfi_1)/(date_2 - date_1) \times 365.25\, days/year$$

$$where\ cfi = the\ change\ from\ the\ initial\ reading\ (inches)$$

$$cfi_1 = cfi\ reading\ closest\ to\ the\ beginning\ of\ the\ reporting\ period$$

$$cfi_2 = cfi\ reading\ closest\ to\ the\ end\ of\ the\ reporting\ period$$

Comparisons between closure rates of the previous and current reporting periods are presented as percent changes in rate and are calculated as follows:

$$percent\ change\ in\ rate = (Rate_{Current\,Period} - Rate_{Previous\,Period})/(Rate_{Previous\,Period}) \times 100\%$$

Rock bolt load cells are used to determine bolt support performance. Plots show load versus time for each instrumented bolt.

Earth pressure cells and strain gauges are used to determine the stresses and deformation in and around the shaft liners. Data are depicted in time-based plots.

Piezometers are used to measure the gauge pressure of groundwater and are installed in the shafts at varying elevations to monitor the hydraulic head acting on the shaft liners. Data are plotted as pressure versus time.

Joint meters, installed perpendicular to a crack, monitor the dilation of the crack with time. Data are presented as displacement versus time.

1.4.4 Data Errors

GIS data are processed through a comprehensive database management system. Whether acquired manually or remotely, GIS data are processed and permanently stored according to approved procedures. On occasion, erroneous readings can occur. There are several possible explanations for erroneous readings, including the following:

- The measuring device was misread.
- The reading was recorded incorrectly.
- The measuring device was not functioning within specifications.

When a reading is believed to be erroneous, the suspect reading is evaluated, and, if necessary, a second reading is collected. If the second reading falls in line with the instrument trend, the first reading is discarded and the second reading is entered in the database. If the second reading and subsequent readings remain out of the instrument trend, the ground conditions in the vicinity of the instrument are assessed to determine the reason for the discrepancy. In addition, the reading frequency may be increased.

2.0 GEOLOGY

This chapter provides a summary of the stratigraphy of the WIPP region and the site. Readers desiring further geologic information may consult the "Geological Characterization Report, WIPP Site, Southeastern New Mexico" (Powers et al., 1978). This report was developed as a source document on the geology of the WIPP site for individuals, groups, or agencies seeking basic information on geologic history, hydrology, geochemistry, or detailed information, such as physical and chemical properties of repository rocks. A more recent survey of WIPP stratigraphy is included in Holt and Powers (1990).

2.1 Regional Stratigraphy

The stratigraphy in the vicinity of the WIPP site includes rocks of Permian (295 to 250 million years [Ma] before present [bp]), Triassic (250 to 203 Ma), and Quaternary (1.75 Ma to present) ages. The descriptions of formations provided in this section are given in order of deposition (oldest to youngest), beginning with the Castile Formation (Figure 2-1).

2.1.1 Permian

The Permian system in southwestern North America is divided into four series. The last of these, the Ochoan Series, contains the host rock in which the WIPP repository is located.

The Ochoan Series is of mostly marine origin and consists of four formations: three evaporite formations (the Castile, the Salado, and the Rustler) and one redbeds formation (the Dewey Lake). The Ochoan evaporites overlie marine limestones and sandstones of the Guadalupian Series (Delaware Mountain Group). The younger redbeds represent a transition from the lower evaporite deposition to fluvial deposition on a broad, low-relief, fluvial plain. The Permian rocks are overlain by fluvial deposits of the Triassic and Quaternary periods.

2.1.1.1 Castile Formation

The Castile Formation, lowermost of the four Ochoan formations, is approximately 1,250 ft (380 m) thick in the WIPP vicinity. Lithologically, the Castile is the least complex of the evaporite formations and is composed chiefly of interbedded anhydrite and halite, with limestone present in minor amounts.

2.1.1.2 Salado Formation

The Salado Formation comprises nearly 2,000 ft (610 m) of evaporites, primarily halite. The formation is subdivided into three informal members: the unnamed lower member, the McNutt potash zone, and the unnamed upper member. Each member contains similar amounts of halite, anhydrite, and polyhalite and is differentiated on the basis of soluble potassium- and magnesium-bearing minerals. The WIPP disposal horizon is located within the unnamed lower member, 2,150 ft (655 m) below the surface.

2.1.1.3 Rustler Formation

The Rustler Formation is subdivided into five members, starting from its base: the Los Medaños Member, the Culebra Dolomite Member, the Tamarisk Member, the Magenta Dolomite Member, and the Forty-niner Member.

In the vicinity of the WIPP site, the Rustler is approximately 310 ft (95 m) thick and thickens to the east. The lower portion (Los Medaños Member) contains primarily fine sandstone to mudstone with lesser amounts of anhydrite, polyhalite, and halite. Bedded and burrowed siliciclastic sedimentary rocks with cross-bedding and fossil remains signify the transition from the strongly evaporitic environments of the Salado to the brackish lagoonal environments of the Rustler (Holt and Powers, 1990).

The upper portion of the Rustler contains interbeds of anhydrite, dolomite, and mudstone. The Culebra Dolomite member is generally brown, finely crystalline, and locally argillaceous. The Culebra contains rare to abundant vugs with variable gypsum and anhydrite filling and is the most transmissive hydrologic unit within the Rustler. The Tamarisk Member consists of lower and upper sulfate units separated by a unit that varies laterally from mudstone to mainly halite. The Magenta Dolomite Member is a gypsiferous dolomite with abundant primary sedimentary structures and well-developed algal features. The Forty-niner Member consists of lower and upper sulfate units separated by a mudstone that displays sedimentary features and bedding. East of the site area, halite correlates with the mudstone. The Culebra and Magenta Dolomite members are persistent and serve as important marker units.

2.1.1.4 Dewey Lake Redbeds

The Dewey Lake Redbeds is the uppermost of the Ochoan Series formations. Within the series, the Dewey Lake represents a transition from the lower marine evaporite deposition to fluvial deposition on a broad, low-relief, fluvial plain. The redbeds, approximately 475 ft (145 m) thick, consist of predominantly reddish-brown interbedded fine-grained sandstone, siltstone, and claystone. This formation is differentiated from others by its lithology and distinctive color (both of which are remarkably uniform), and by sedimentary structures, including horizontal- and cross-laminae and ripple marks. The redbeds also contain locally abundant greenish-gray reduction spots and gypsum filled fractures. The formation thickens from west to east due to eastward dips and erosion to the west.

2.1.2 Triassic

The only Triassic rocks present in the WIPP region belong to the Dockum Group.

2.1.2.1 Dockum Group

The Dockum Group consists of fine-grained floodplain sediments and coarse alluvial debris of Triassic age. From a pinch-out near the center of the WIPP site it thickens eastward, forming an erosional wedge. Local subdivisions of the Dockum Group are the Santa Rosa Sandstone and the Chinle Formation; however, only the Santa Rosa occurs in the vicinity of the site. It consists primarily of poorly sorted sandstone with conglomerate lenses and thin mudstone partings and contains impressions and remnants of fossils. These rocks have more variegated hues than the underlying uniformly colored Dewey Lake.

2.1.3 Quaternary

Quaternary Period deposits include the Gatuña Formation, Mescalero Caliche, and surficial sediments.

2.1.3.1 Gatuña Formation, Mescalero Caliche, and Surficial Sediments

The Gatuña Formation (ranging in age from approximately 1.3 million to 600,000 years bp) (Powers and Holt, 1993) is a stream-laid deposit overlying the Dockum Group in the WIPP vicinity. At the site center, the formation consists of approximately 13 ft (4 m) of poorly consolidated sand, gravel, and silty clay. The Gatuña Formation is light red and mottled with dark stains. The unit contains abundant calcium carbonate, but is poorly cemented. Sedimentary structures are abundant (Powers and Holt, 1993, 1995).

The Mescalero Caliche (approximately 500,000 years bp) is approximately 4 ft (1.2 m) thick in the WIPP vicinity. The Mescalero is a hard, resistant soil horizon that lies beneath a cover of wind-blown sand. The horizon is petrocalcic (i.e., very strongly cemented with calcium carbonate). Petrocalcic horizons form slowly beneath a stable landscape at the average depth of infiltration of soil moisture and indicate stability and integrity of the land surface. Many of the surface buildings at WIPP are founded on top of the Mescalero Caliche.

Surficial sediments include sandy soils developed from eolian material and active dune areas. The Berino Series (a soil type) covers about 50 percent of the site and consists of deep sandy soils that developed from wind-worked material of mixed origin. Based on sample analyses, the Berino soil from the WIPP site formed 330,000 ± 75,000 years bp.

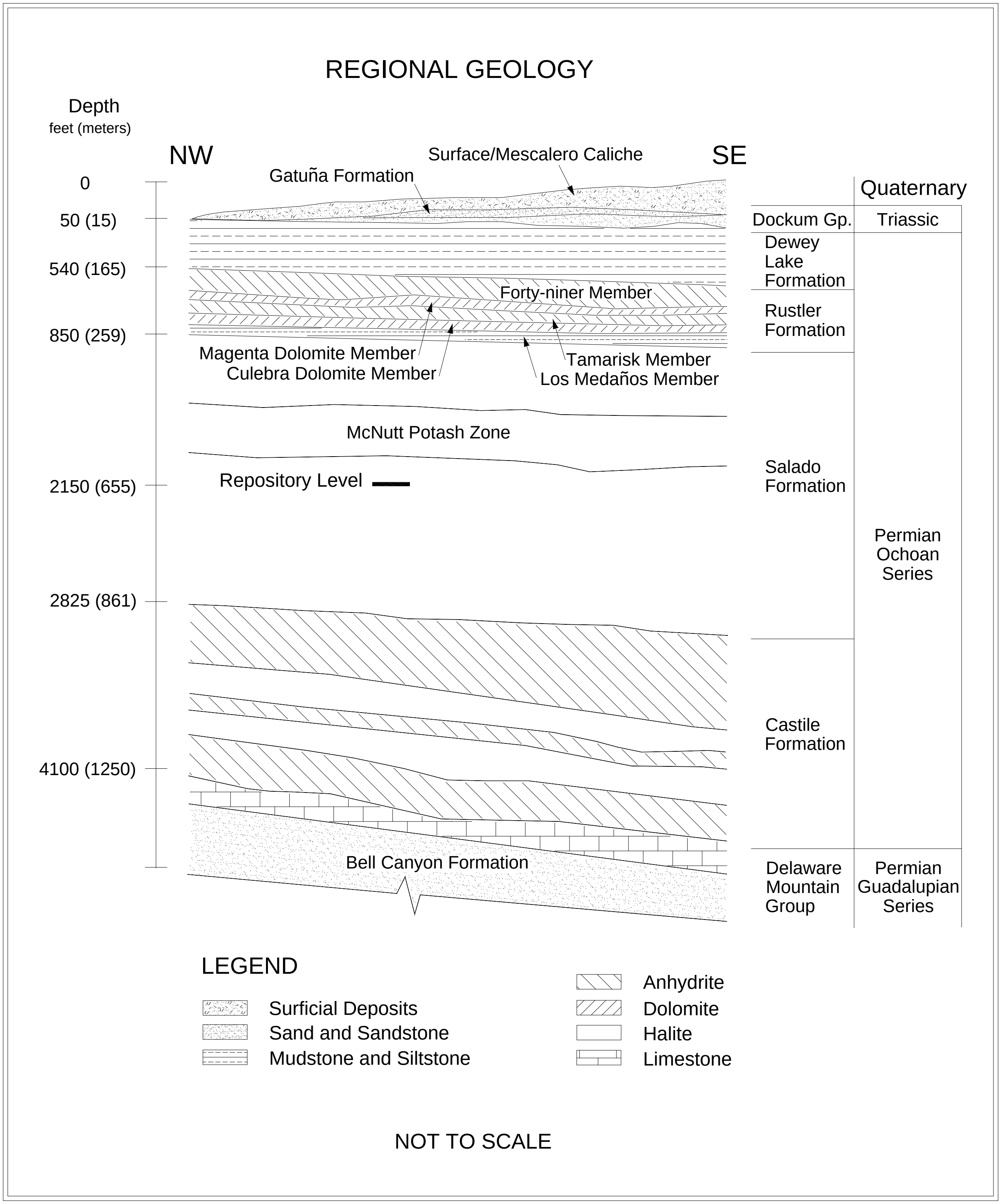

Figure 2 - 1 Regional Geology

2.2 Underground Facility Stratigraphy

The WIPP disposal horizon lies near the midpoint of the Salado Formation. The Salado was deposited in a shallow saline lagoon environment, which progressed through numerous inundation and desiccation cycles that are reflected in the formation. An "ideal" cycle progresses upward as follows: a basal layer consisting predominantly of claystone, followed by a layer of sulfate, which is in turn followed by a layer of halite. The entire sequence is capped by a bed of argillaceous (clay-rich) halite accumulated during a period of mainly subaerial exposure.

A regional system used for numbering the more significant sulfate beds within the Salado designates these beds as marker beds (MBs), counted from MB100 near the top of the formation to MB144 near the base. The repository is located between MB138 and MB139 within a sequence of laterally continuous depositional cycles as described above. Within this sequence, layers of clay and anhydrite that are locally designated (as shown) can have a significant impact on the geomechanical performance of the excavations. Clay layers provide surfaces along which slip and separation can occur, whereas anhydrites form brittle layers that do not deform plastically.

In the vicinity of WIPP, the stratigraphy is fairly continuous and uniform. Beds generally dip toward the south-southeast at a slope of approximately 3 percent.

2.2.1 Disposal Horizon Stratigraphy of Panels 1, 2, 7, and 8

This disposal horizon contains Panels 1, 2, 7, and 8, all the shaft areas, the shop areas, the SPDV areas (which are now closed), and all the access drifts north of S-2620. Farther south, the four main entries rise in a ramp that starts at S-2620 and ends at S-2740. Panel 7 is excavation was completed in January of 2013. Panel 8 has been partially excavated.

Most underground excavations are located within this disposal horizon (Figure 2-2). In it, the Orange Marker Bed (OMB) lies near the middle of the rib (i.e., the excavation wall). The OMB is a laterally consistent unit of moderate to light reddish-orange translucent halite about 6 inches (in) (15 centimeters [cm]) thick that is used as a point of reference during excavation.

MB139 lies approximately 11.5 ft (3.5 m) below the OMB. MB139 is a 20 to 32 in (50 to-80 cm) thick layer of polyhalitic anhydrite. The top of the anhydrite undulates up to 15 in (38 cm), while the bottom is sub-horizontal and is underlain by Clay E.

Above MB139 is a unit of halite that terminates at the base of the OMB. Within this unit, polyhalite is locally abundant and decreases upward, while argillaceous material increases upward.

Above the OMB, a thin band of argillaceous halite gives way to a thick sequence of clear halite that becomes increasingly argillaceous upward and is capped by Clay F. This constitutes a thin layer occasionally interrupted by partings and breaks and is readily visible in the upper ribs. Above Clay F, another sequence of halite begins that, as in lower sequences, becomes increasingly argillaceous upward. This sequence terminates at the Clay G/Anhydrite "b" interface, approximately 6.5 ft (2 m) above the roof of most disposal horizon excavations, forming a roof beam that typically acts as a structural unit.

The roof of some disposal horizon excavations (e.g., the E-140 drift between S-1000 and S-1950), has been excavated to the upper contact of Anhydrite "b." In this case, a roof beam is formed by the next depositional sequence beginning with Anhydrite "b" and progressing upward to the Clay H/Anhydrite "a" interface, approximately 6.5 ft (2 m) above the upper contact of Anhydrite "b."

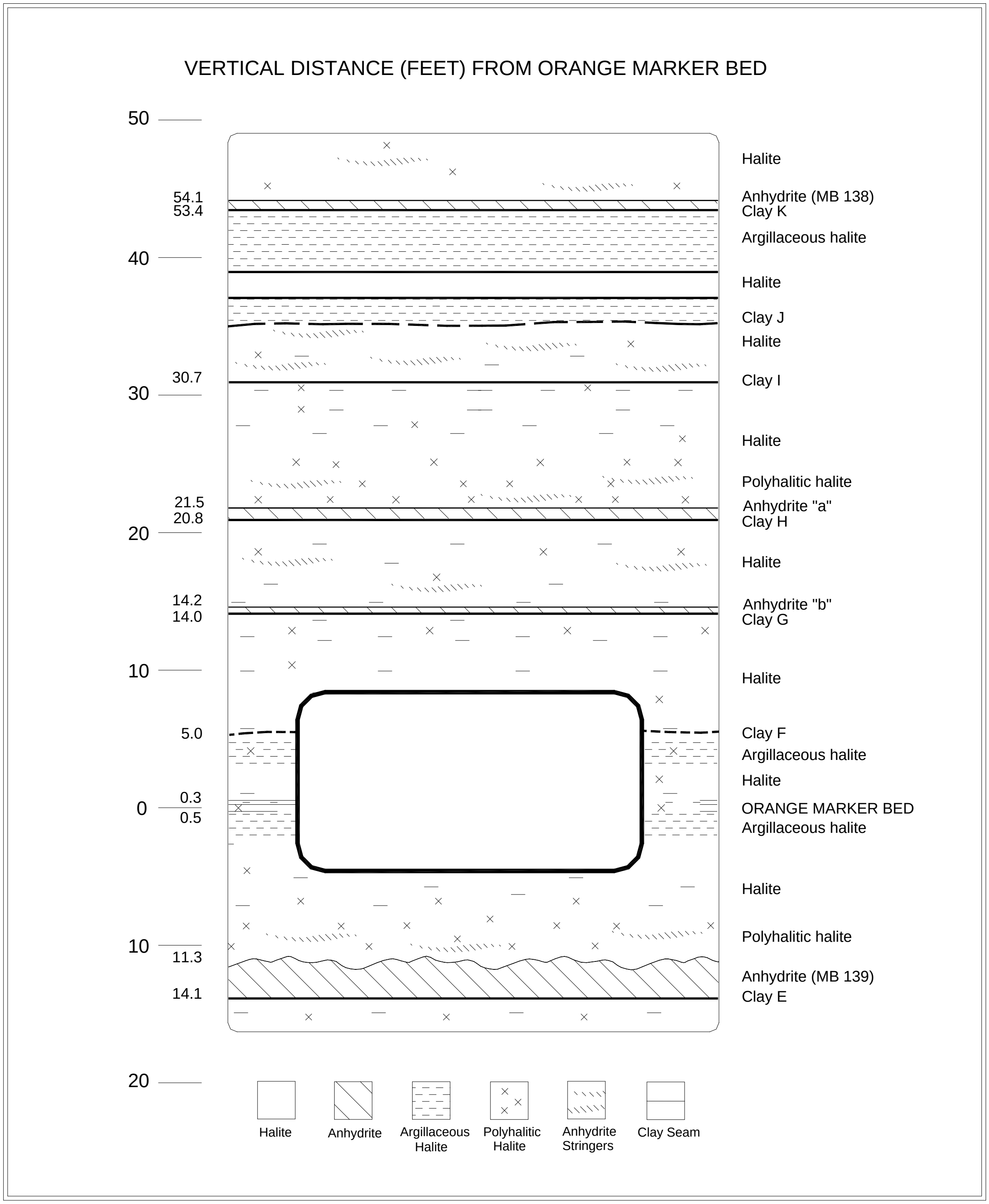

Figure 2 - 2 Repository Level Stratigraphy of Panels 1, 2, 7, and 8

2.2.2 Disposal Horizon Stratigraphy of Panels 3, 4, 5, and 6

Field observations and computer modeling indicated that moving the disposal horizon stratigraphically upward (so that the roof was located at Clay G) would improve long term ground conditions and provide a more stable roof configuration without significantly impacting repository performance. In 2000, the decision was made to implement this change by moving the mining horizon up approximately six feet. Subsequently, in 2000 and 2001, ramps were mined in the W-170, W-30, E-140, and E 300 drifts between S-2620 and S-2750 (Figure 1-2). As a result, the disposal horizon for Panels 3, 4, 5, and 6, and the associated connecting drifts lies above the horizon for the other panels (Figure 2-3).

In this horizon, the OMB lies at or below the floor. MB139 lies about 12 ft (3.7 m) below the floor. The roof lies at or slightly above Anhydrite "b." Clay G/ Anhydrite "b" is used as the mining reference during excavation of this disposal horizon. Locally continuous anhydrite stringers are found within this beam, generally concentrated in the lower portion toward Anhydrite "b". These effectively divide the roof beam itself into a series of thinner, independent beams.

2.2.3 Northeast Area Stratigraphy

All of the Northeast Area, a former experimental area, is now deactivated and closed to access. These excavations lie at a higher stratigraphic level than the disposal excavations. Floors are at Anhydrite "b." As in the lower units, the halite intervals between the clay seams/anhydrite beds contain relatively pure halite that becomes increasingly argillaceous upward. Above clay I, two more halite intervals complete the underground facility stratigraphy. Clay J, at the top of the first of these intervals, may consist of a distinct seam or merely an argillaceous zone. Clay K tops the second interval and is overlain by MB138.

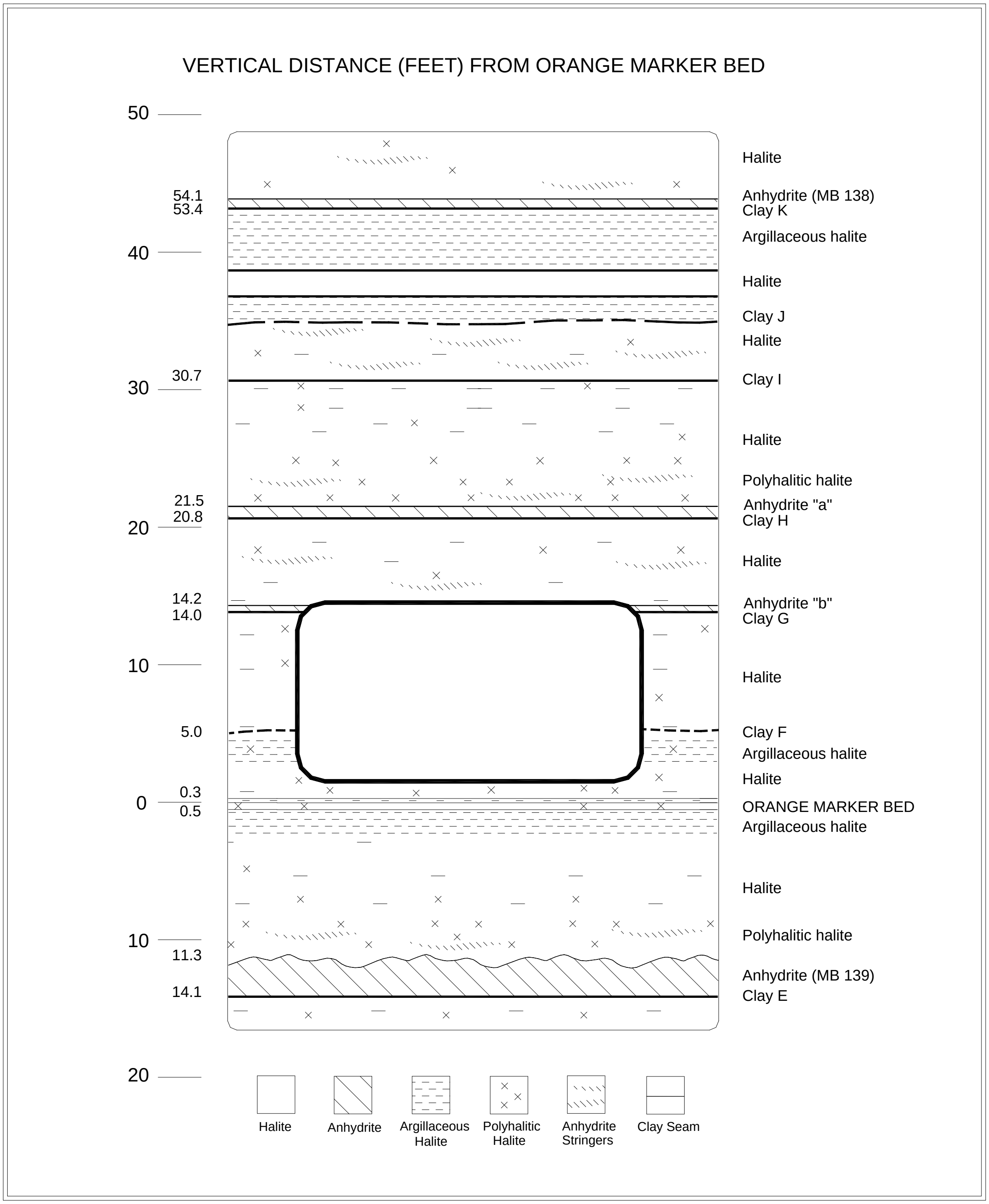

Figure 2 - 3 Repository Level Stratigraphy of Panels 3, 4, 5, and 6

3.0 PERFORMANCE OF SHAFTS AND KEYS

Four shafts connect the surface with the underground. They are the Salt Shaft, which is used primarily for removing excavated salt from the underground and for transporting personnel and material; the Waste Shaft, which is used primarily for transporting TRU waste to the underground and for transporting personnel and materials; the Exhaust Shaft, which is used to exhaust the ventilation air from the underground; and the Air Intake Shaft, which is the primary source of fresh air ventilation to the underground. This chapter describes the geomechanical performance of these shafts.

Although through the years much of the instrumentation installed in the shafts has failed, there are no plans to replace it. The project has a good understanding of the expected movements in the shafts. Monitoring results up to the point of instrument failure did not indicate unusual shaft movements or displacements. Continued periodic visual inspections confirm the expected shaft performance and provide necessary observations to evaluate shaft performance. Replacement of failed instrumentation will not provide significant additional information.

3.1 Salt Shaft

The first construction activity undertaken during the SPDV Program was the excavation of the Exploratory Shaft. This shaft was subsequently referred to as the Construction and Salt Shaft and is currently designated the Salt Shaft (see Figure 1-2). The shaft was drilled from July 4 to October 24, 1981, and geologically mapped in the spring of 1982 (DOE, 1983). Figure 3-1 presents the stratigraphy in the shaft.

The Salt Shaft is lined from the surface to 846 ft (258 m) with steel casing having an inside diameter of 10 ft (3-m). The thickness of the steel liner (including external stiffener rings) increases from 0.62 in (1.6 cm) at the top to 1.5 in (3.8 cm) at the key. Cement grout was placed between the liner and the rock face. The 10-ft (3-m) diameter extends through the concrete shaft key to 880 ft (268 m). The shaft key is a 37.5 ft (11.4-m) long, reinforced-concrete structure that begins 3.5 ft (1.07 m) above the bottom of the steel liner. From the key to the bottom at 2,298 ft (700 m), the shaft has a nominal diameter of 12 ft (4 m).

Wire mesh anchored by rock bolts is installed in sections of the lower shaft as a safety screen to contain rock fragments that may become detached. The shaft extends approximately 140 ft (43 m) below the repository horizon in order to accommodate the skip loading equipment and a sump.

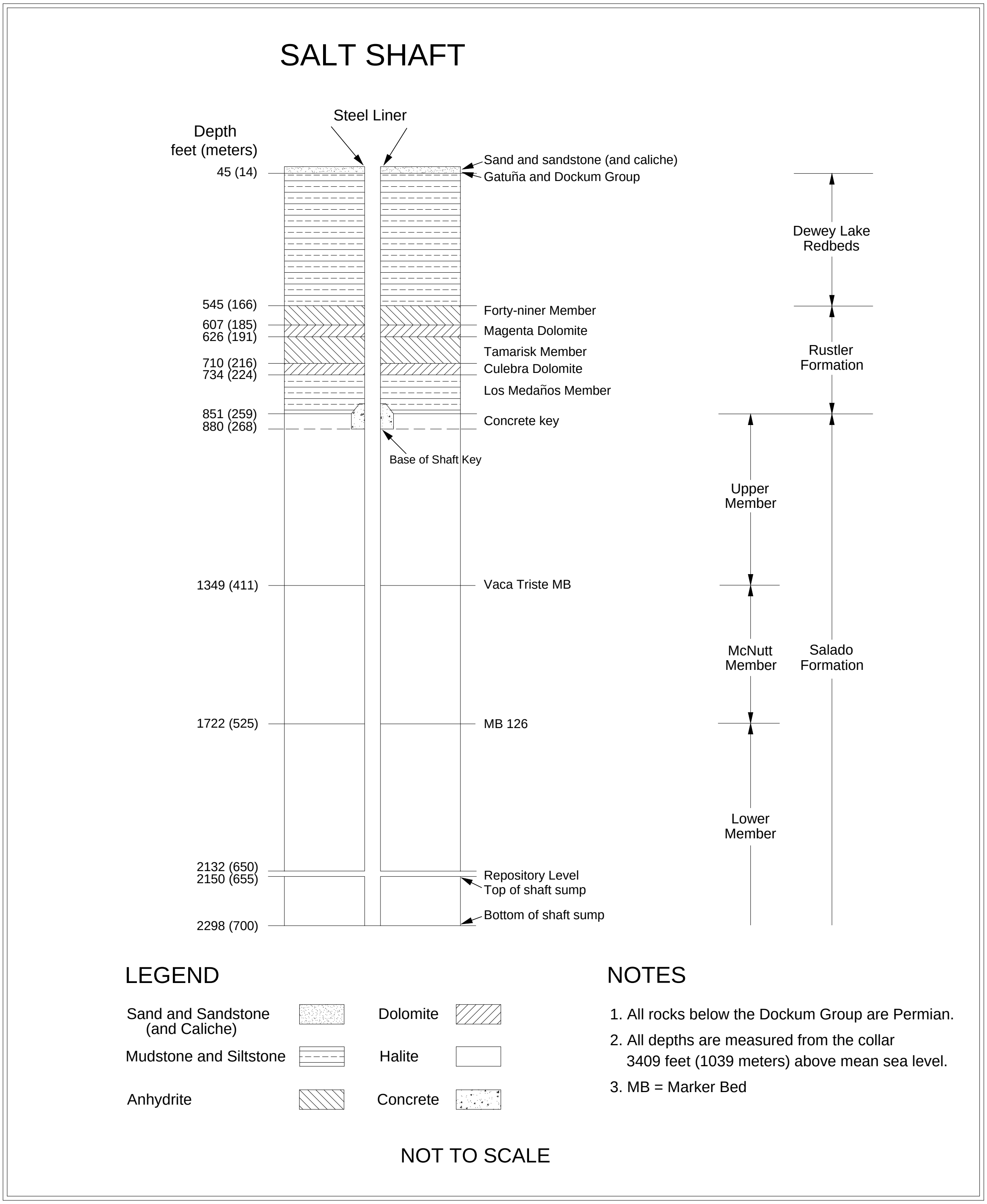

Figure 3 - 1 Salt Shaft Stratigraphy

3.1.1 Shaft Observations

Underground operations personnel conducted weekly visual inspections up until the fire and radiological release. These inspections are performed principally to assess the condition of the hoisting and mechanical systems, but they also include examining the shaft walls for water seepage, loose rock, or sloughing. Visual inspections during this reporting period found that the shaft remained in satisfactory condition. Only routine ground control activities were required.

3.1.2 Instrumentation

Geomechanical instruments (radial convergence points, extensometers, and piezometers) were installed at various levels in the shaft from April through July of 1982 (Figures 3-2 and 3-3). In the shaft key, instruments included strain gauges, pressure cells, and piezometers. Radial convergence points were installed prior to outfitting. Upon completion of shaft outfitting, no more readings were taken.

Ten of the 12 piezometers continue to provide data. The fluid pressures recorded at the end of this reporting period range from approximately 59 pounds per square inch (psi) (407 kilopascals [kPa]) at the 802-ft (244-m) level in the Los Medaños Member to 164 psi (1131 kPa) at the 691-ft (211-m) level in the Tamarisk Member. The recorded pressures for this reporting period are generally consistent with the readings from the previous reporting period. The fluid pressure on the shaft liner will continue to be monitored on a regular basis.

Four earth pressure cells were installed in the key section during concrete emplacement at the 860-ft (262-m) level. These instruments measure the normal stress between the concrete key and the Salado Formation as salt creep loads up the key structure. Three of the four earth pressure cells continue to provide data. These instruments have indicated essentially no contact pressure since their installation (readings resemble instrument drift at a zero pressure). The maximum contact pressure recorded by the instruments for this reporting period is 6 psi (41 kPa).

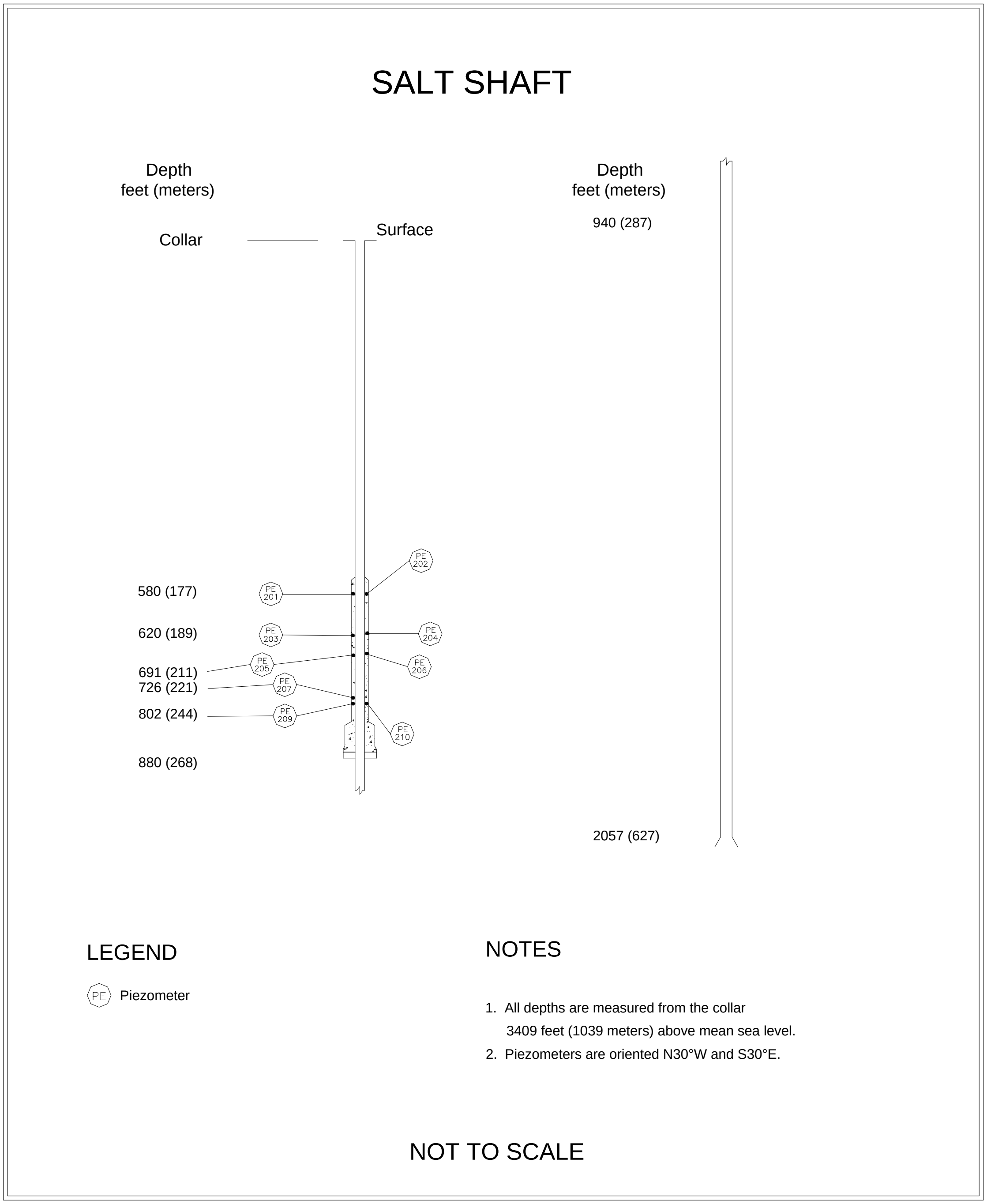

Figure 3 - 2 Salt Shaft Instrumentation (Without Shaft Key)

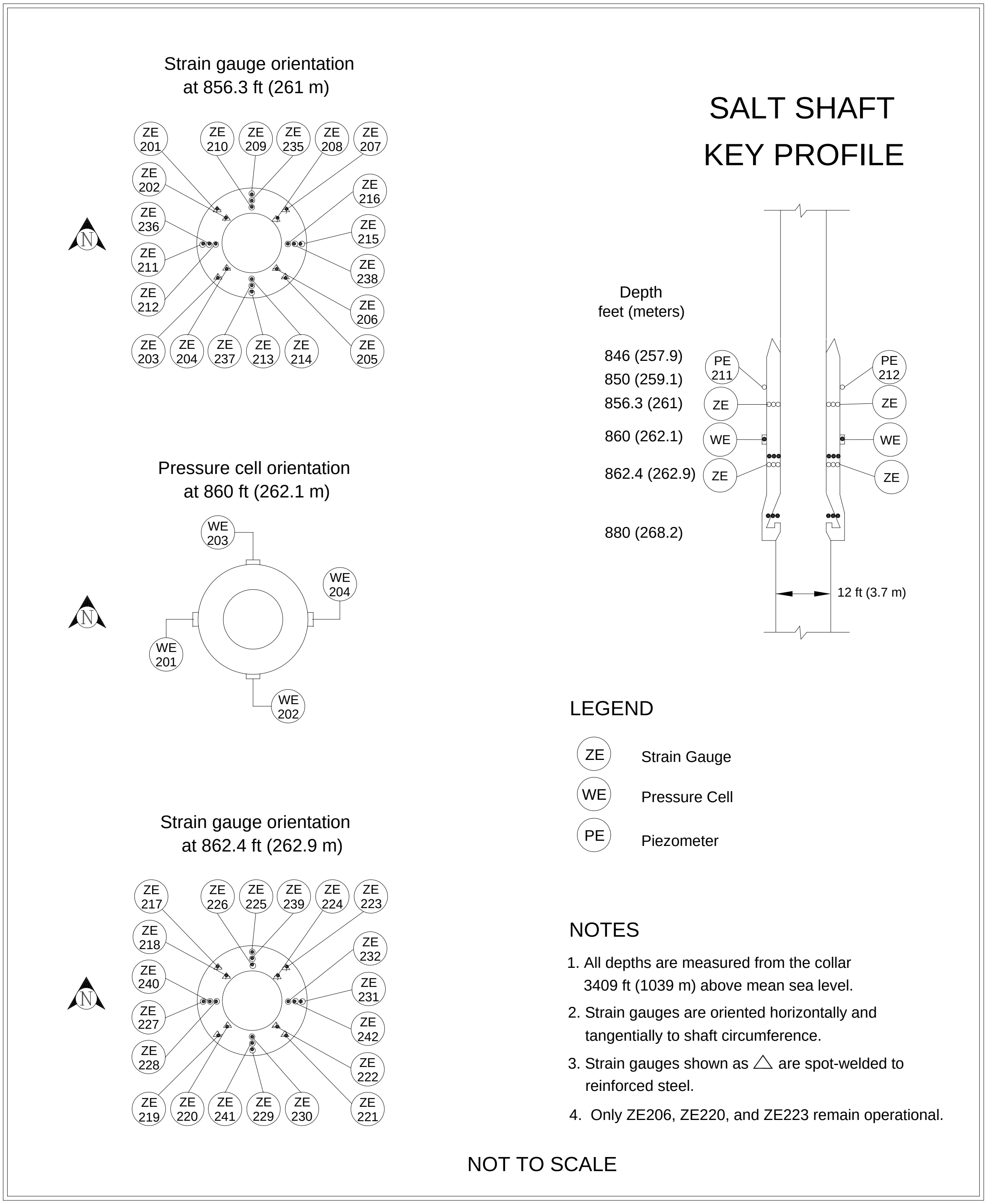

Figure 3 - 3 Salt Shaft Key Instrumentation

Sixteen spot-welded and twenty-four embedment strain gauges were installed on and in the shaft key concrete at both the 856.3-ft (261-m) level and at the 862.4-ft (263-m) level. Three spot-welded strain gauges are still functioning at these levels. Strain at the 856.3-ft (261-m) level recorded a maximum strain of 652 microstrain. Strains at the 862.4 ft (263 m) level were 690 and 957 microstrain.

Fourteen embedment strain gauges are still functioning. The strains at the 856.3-ft (261-m) level ranged from -928 to 1017 microstrain. The strains from the two embedment strain gauges at the 862.4 ft (263-m) level were 315 to 425 microstrain. The strains recorded by the spot-welded strain gauges and the embedment strain gauges during this reporting period are largely similar to the strains recorded by these instruments at the end of the previous reporting period.

3.2 Waste Shaft

As part of the SPDV Program, a 6-ft (2-m) diameter ventilation shaft, now referred to as the Waste Shaft, was excavated from December 1981 through February 1982 (see Figure 1-2). This shaft, in combination with the Salt Shaft, provided a two-shaft underground air circulation system. From October 11, 1983, to June 11, 1984, the shaft was enlarged to a diameter of 20 to 23 ft (6 to 7 m) and lined above the key. Stratigraphic mapping (Figure 3-4) was conducted during shaft enlargement from December 9, 1983, to June 5, 1984 (Holt and Powers, 1984).

The Waste Shaft is lined with non-reinforced concrete having a 19 ft (6 m) inside diameter from the surface to the top of the key at 837 ft (255 m). Liner thickness increases from 10 in (25 cm) at the surface to 20 in (51 cm) at the key. The key is 63 ft (19 m) long and 4.25 ft (1.3 m) thick and is constructed of reinforced concrete. The bottom of the key is 900 ft (274 m) below the surface. The diameter of the shaft is 20 ft (6 m) at the bottom of the key and increases to 23 ft (7 m) just above the shaft station. The shaft below the key is lined with wire mesh anchored by rock bolts. The diameter of 23 ft (7 m) extends to a depth of approximately 2,286 ft (697 m), with the shaft sump comprising the lower 119 ft (36 m) of that interval.

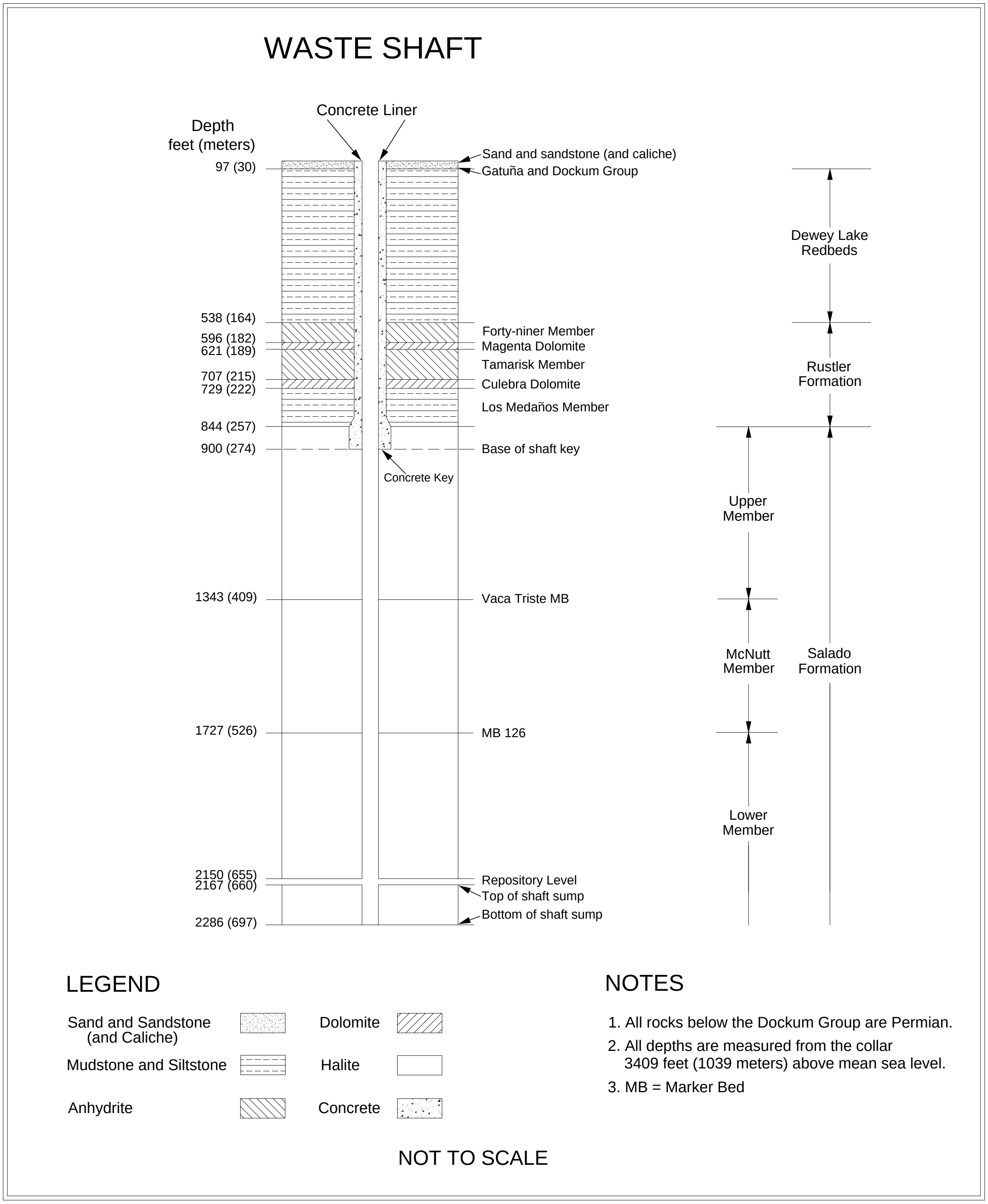

Figure 3 - 4 Waste Shaft Stratigraphy

3.2.1 Shaft Observations

Underground operations personnel conduct weekly visual inspections, principally to assess the condition of the hoisting and mechanical systems, but also include observation of the shaft walls for water seepage, loose rock, or sloughing. The visual inspections found that the shaft was in satisfactory condition. No ground control activities other than routine maintenance were required.

3.2.2 Instrumentation

Radial convergence points, extensometers, piezometers, and earth pressure cells were installed in the Waste Shaft between August 27 and September 10, 1984. Radial convergence points were installed prior to the outfitting. Upon completion of shaft outfitting, no more radial convergence readings were taken. Figure 3-5 and Figure 3-6 show the instrument locations.

Nine multi-position extensometers were installed in arrays 1,071 ft (326 m), 1,566 ft (477 m), and 2,059 ft (628 m) below the surface as shown in Figure 3-5. Each array consists of three extensometers. No extensometer data have been collected in recent years due to the malfunction of the data acquisition equipment. Since the type of extensometers installed in the shaft over 29 years ago is no longer manufactured, remote data acquisition equipment for these extensometers is also unavailable.

Twelve piezometers were installed in the lined section of the Waste Shaft on September 7 and 8, 1984, to monitor fluid pressure behind the shaft liner and the key section. As of this reporting period, data is no longer being received from any of the piezometers.

Four earth pressure cells were installed in the key section of the Waste Shaft during concrete emplacement between March 23 and April 3, 1984. Earth pressure cells measure the normal stress between the concrete key and the Salado Formation as salt creep loads the key structure. As of this reporting period, data is no longer being received from any of the earth pressure cells.

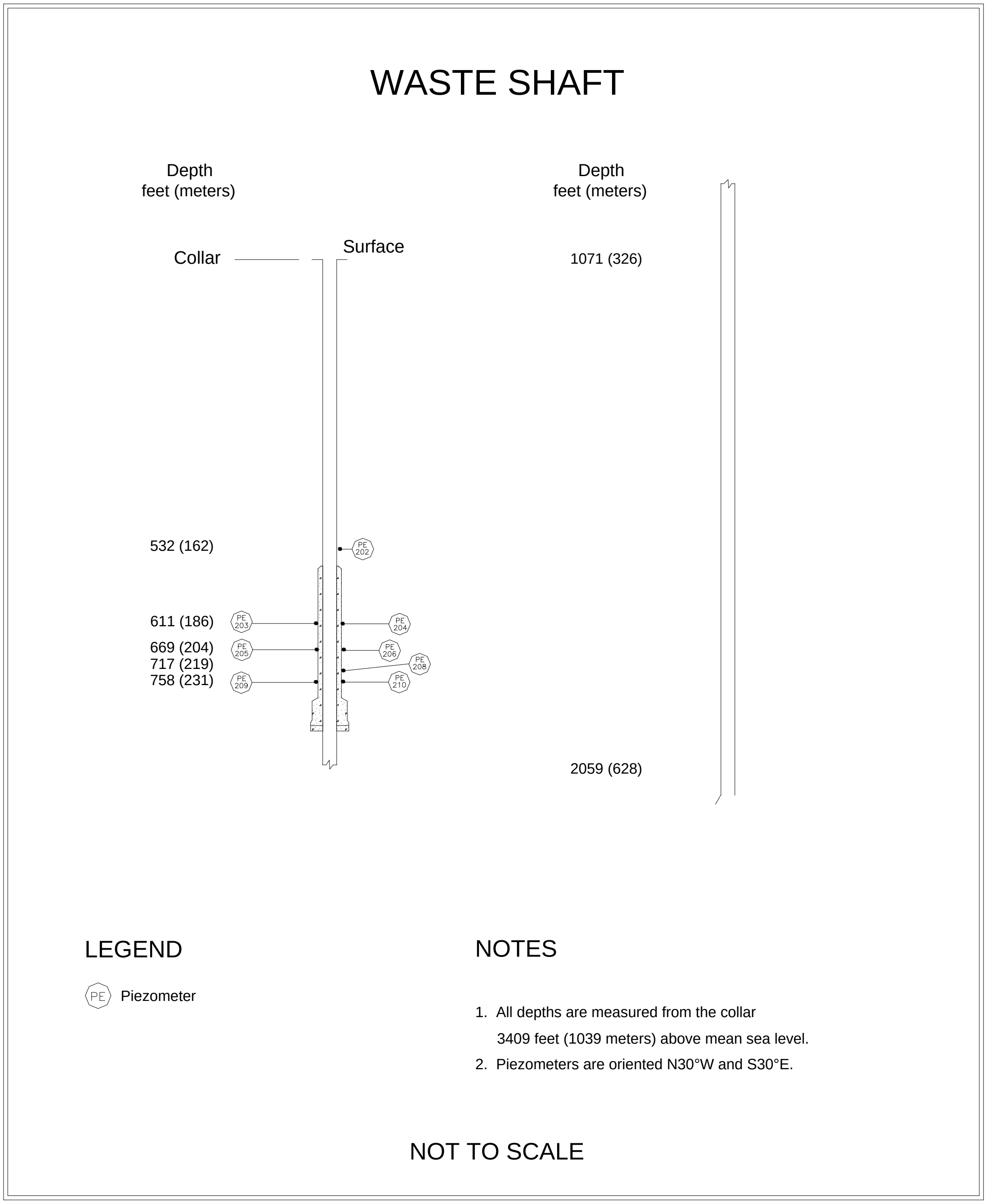

Figure 3 - 5 Waste Shaft Instrumentation (Without Shaft Key)

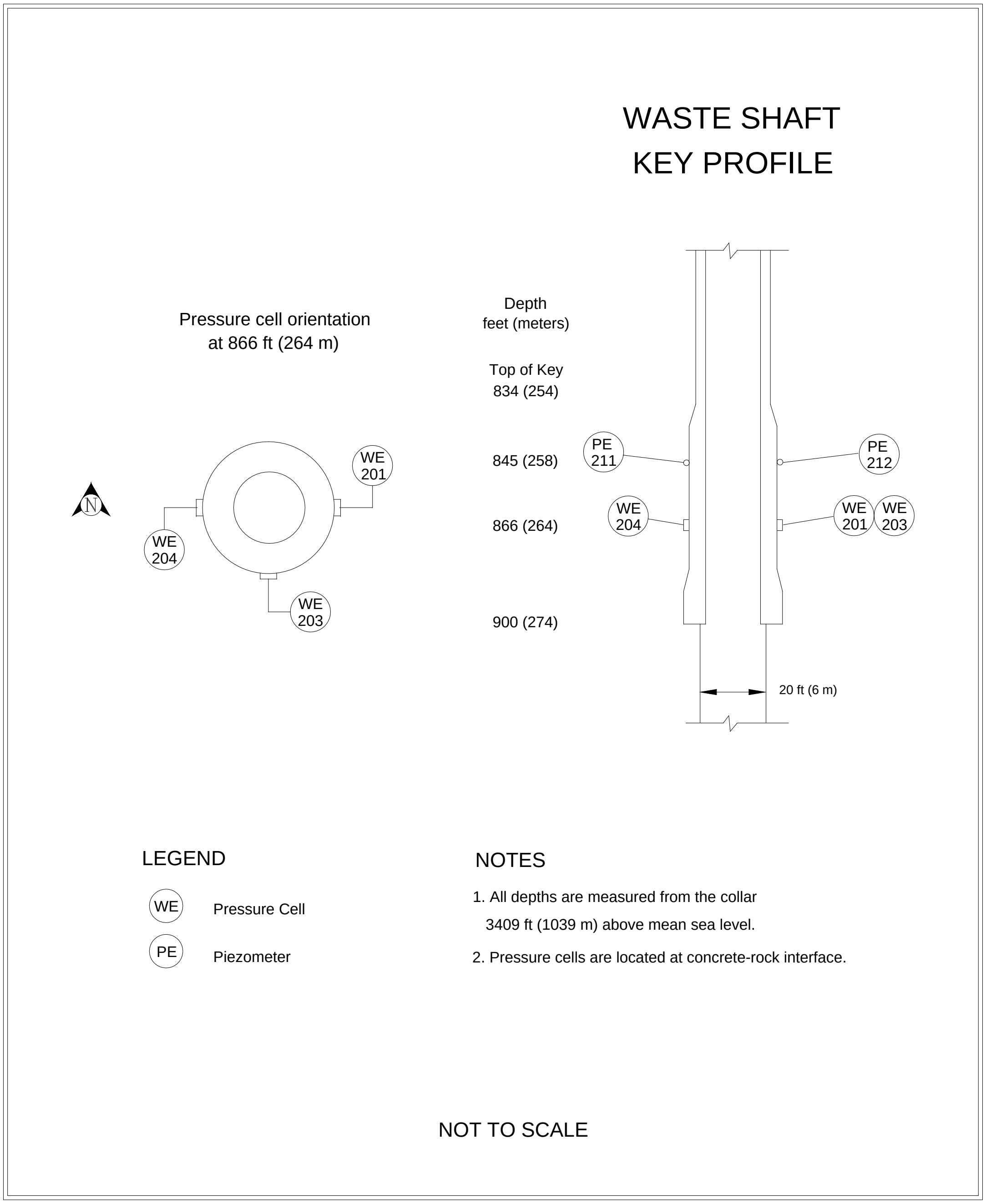

Figure 3 - 6 Waste Shaft Key Instrumentation

3.3 Exhaust Shaft

The Exhaust Shaft was drilled from September 22, 1983, to November 29, 1984, to establish a route from the underground to the surface for exhaust air (Figure 1-2). Stratigraphic mapping was conducted from July 16, 1984, to January 18, 1985 (DOE, 1986c). Figure 3-7 illustrates the shaft stratigraphy.

The Exhaust Shaft is lined with non-reinforced concrete from the surface to the top of the shaft key at 844 ft (257 m). The liner thickness increases from 10 to 16 in (25 to 41 cm) over that interval. The key is 63 ft (19 m) long and 3.5 ft (1 m) thick. The shaft diameter below the key is 15 ft (5 m), and the interval below the key is lined with wire mesh anchored by rock bolts. The shaft terminates at the facility horizon, approximately 2,150 ft (655 m) deep. This shaft has no sump.

3.3.1 Exhaust Shaft Observations

Quarterly video inspections were conducted according to approved WIPP procedures. Inspections were performed to evaluate the condition and to verify the integrity of the shaft. The shaft was examined for cracks, corrosion, salt buildup, seeps, and debris. In addition, inspections examined the condition of anchors, brackets, and down-hole equipment. Between July 2013 and June 2014, two quarterly shaft inspections were conducted on September 5, 2013 and November 14, 2014.

3.3.1.1 Video Camera

Video inspections use a custom-designed vertical-drop color camera in an aerodynamic housing, suspended by a dual-armored cable, with pan, tilt, and zoom capability. The cable contains five copper conductors and two multi-mode optical fibers. It is reeled out by a winch mounted in a control van. Inspections are recorded electronically.

3.3.1.2 Shaft Inspection Observations

Quarterly video inspection observations concentrate on four major areas: air monitoring components, shaft liner, shaft walls, and equipment support and cabling. The air monitoring components consist of one air-velocity and three air-monitoring devices as shown in Figure 3-8. The video inspection includes examination of each device, including the transport assembly, guide tubes, the sample intake, and the support brackets that extend from Station "A" above the shaft to the shaft collar. Air monitoring components extend from the collar 21 ft into the shaft. Video inspections indicate that the air-sampling components can accumulate salt buildup of up to several inches thick.

The Exhaust Shaft liner is examined for cracks, seepage, and general shaft stability. Currently, there are three principal zones of seepage in the shaft. The first is about 50 to 55 ft below the shaft collar (bsc). The second is about 60 to 65 ft bsc. The third is about 75 to 80 ft bsc, as shown in Figure 3-9. Monitoring of seepage horizons started before 1995. Water entering the shaft through these cracks is believed to originate from a perched aquifer at the base of the Santa Rosa Formation that is being recharged as the result of surface modifications at the site. The fluid level in the Santa Rosa near the shaft is about 46 to 47 ft below the surface. Based on examination of inspection videos, the flow rate into the shaft during this reporting period is estimated at about 1 to

1 ½ gallons per minute, most of which is carried out of the shaft by the exhaust air. Seepage cracks are confined primarily to the eastern side of the shaft wall.

When fluid was detected seeping into the shaft, a catch basin was designed and installed at the base of the Exhaust Shaft to intercept water and prevent it from draining into the Waste Shaft Sump. Fluid was removed from the catch basin from March 1996 through October 2005 as needed. The catch basin was damaged in 2004 by fallen debris, either salt or instrumentation cables or both. A new catch basin was fabricated and installed in December 2004. This basin was damaged in August 2005, most likely the result of fallen debris. An interception well system was installed between November 2005 and March 2006 to replace the catch basin. Interception wells were drilled down gradient in S-400 between E-140 and E 300 (Figure 3-10). The interception well system initially consisted of four 30-ft deep 9-7/8-in diameter fluid collection holes with a submersible pump and pressure transducer in each. Fluid is pumped from each hole to a series of storage containers in S-550. A data-acquisition system monitors the fluid level in each hole, turning the pump on and off between set limits as needed.

Between February 2 and 6, 2008, two additional fluid collection holes, OH631 and OH632, were drilled in S-400 to improve the total volume of fluid recovered by the interception well system. They replaced OH613 and OH614 which generated little fluid. As with the previous four holes, the additional holes were drilled at 9-7/8-inch diameter to a total depth of 30 feet. Pumps were pulled from OH613 and OH614 and installed in OH631 and OH632. Figure 3-10 shows the location of the interception wells system and the 500-gallons storage containers.

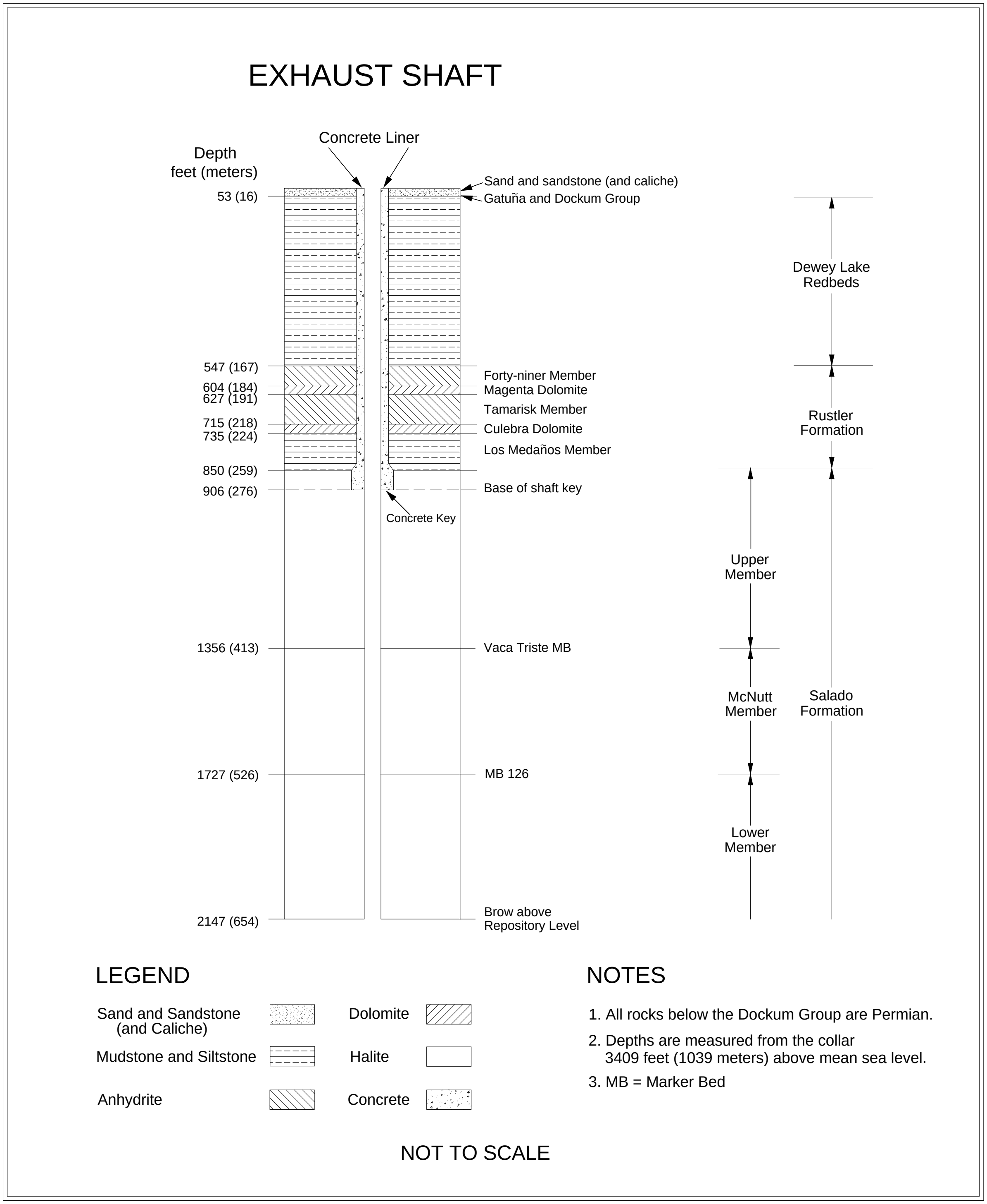

Figure 3 - 7 Exhaust Shaft Stratigraphy

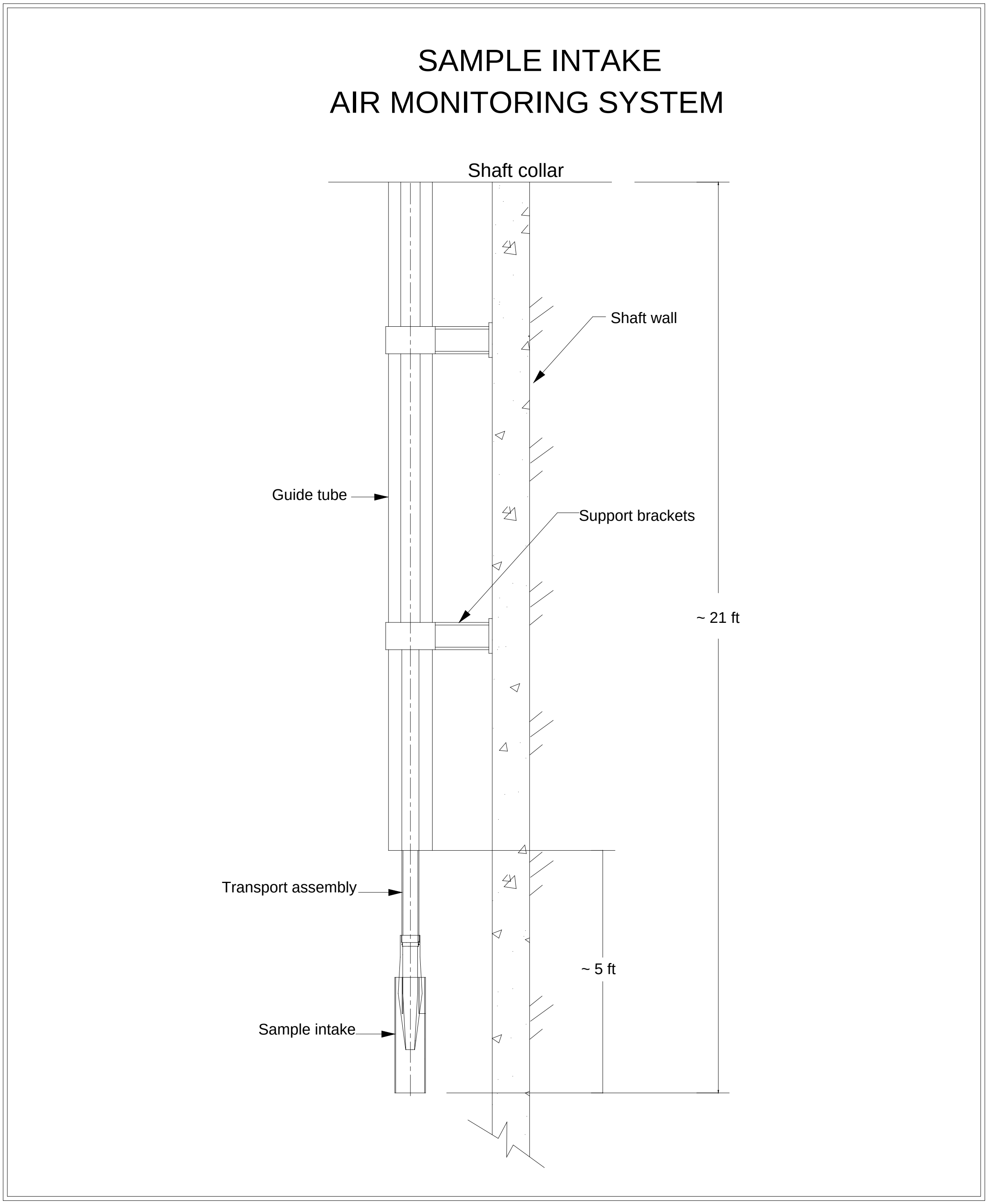

Figure 3 - 8 Sample Intake of Exhaust Shaft Air Monitoring System

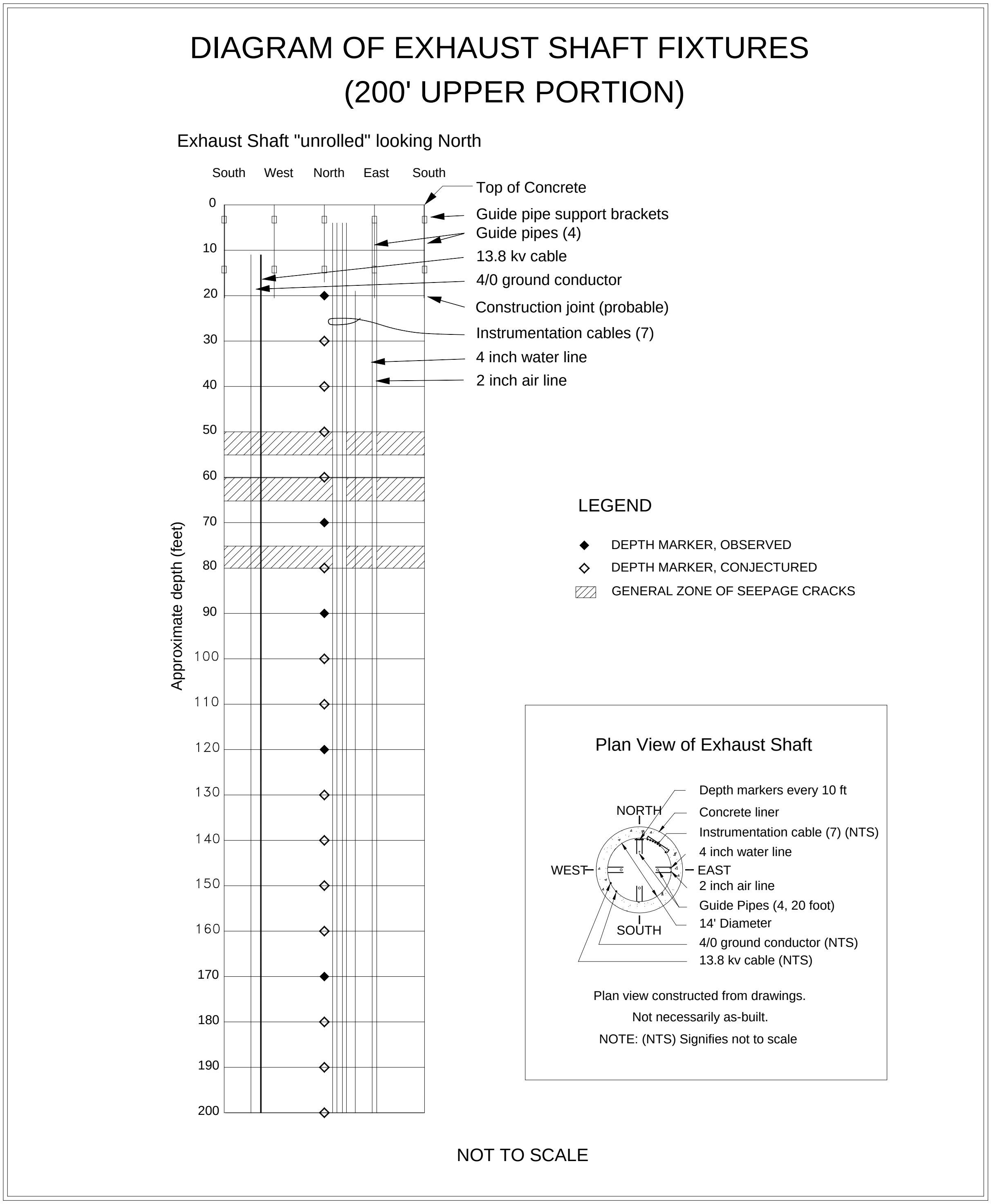

Figure 3 - 9 Diagram of Exhaust Shaft Fixtures and Seepage Zones (Upper 200 ft)

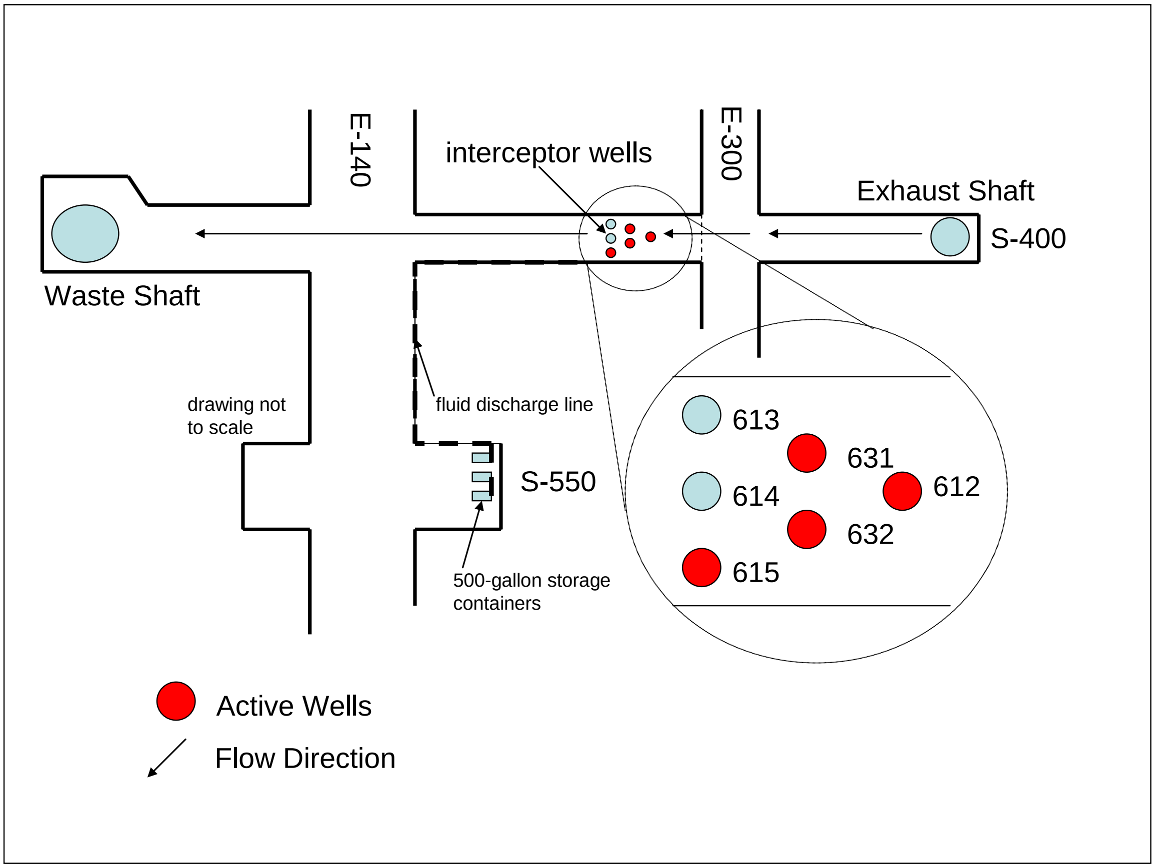

Figure 3 - 10 Location of Interception Wells and Storage Containers

Figure 3-11 presents the volume of fluid removed from the catch basin from July 1997 through June 2006, and by the interception well system from July 2006 through June 2014. The largest reported volumes are typically associated with periods of reduced ventilation and increased humidity. For a discussion of the factors affecting the quantity of fluid produced in the Exhaust Shaft, refer to DOE/WIPP-00-2000, *Brine Generation Study*.

The shaft walls were examined for salt buildup, cracks, moisture, and encrustations, with particular attention paid to power cables, instrument cables, air lines and water-lines, and the three water rings at the base of the Magenta and Culebra members of the Rustler Formation and the bottom of the shaft key. The condition of the shaft wall varies depending on airflow, humidity, temperature, and underground mining activities. During this reporting period, significant mining activity continued in Panel 7 and the Salt Disposal Investigation (SDI) area. The principal areas in the shaft with significant salt buildup were the three water rings at the Magenta, the Culebra, and the key, and along upper portions of the shaft generally associated with power cables, support brackets, instrument cables, and the air lines and water-lines.

Though the Magenta and Culebra water rings are encrusted with salt buildup, no water appears to originate from the liner or water rings. Most of the seepage was observed along the east face of the shaft wall near the instrumentation cables and the air lines and water-lines in the upper section of the shaft. Though the presence of water is an inconvenience requiring periodic disposal, at this time it does not appear to have created any hazard or affected the structural integrity of the shaft. However, brine increases the probability of corrosion and deterioration of utility hangers and brackets. There are no visible signs of dissolution of the salt below the key.

The video inspections also focused on the installed utilities and support brackets. These include a 13.8 kVA power cable that is no longer active and the grounding cable on the west wall of the shaft, the instrumentation cables on the northeast wall of the shaft, and the 4 in. air-line and the 2-in. water-line on the east wall of the shaft.

Sporadic salt buildup continues on all cables. The long-term implication of salt buildup is increased loading on cables and cable hangers, accompanied by intermittent falls of debris. The 4-in. compressed air-line and the 2-in. water-line extend from the surface to the bottom of the shaft. At present, neither line is being used. The integrity of the brackets holding the air-line and water-line was difficult to assess because of salt buildup; however, there was no indication that the brackets were broken. Instrumentation cable breaks were observed in the shaft; however, most of these breaks affected abandoned cables, with negligible impact on shaft monitoring and operations.

3.3.1.3 Instrumentation

The Exhaust Shaft was equipped with geomechanical instrumentation in two stages. Earth pressure cells were installed behind the liner key in November 1984. Piezometers and nine multi-position extensometers were installed during November and December 1985. Figure 3-12 and Figure 3-13 show the instrument locations. None of these instruments continues to provide data.

3.4 Air Intake Shaft

The Air Intake Shaft was drilled from December 4, 1987, to August 31, 1988, to establish a primary route for surface air to enter the repository (see Figure 1-2). The stratigraphy was mapped from September 14, 1988, to November 14, 1989 (Holt and Powers, 1990). Figure 3-14 summarizes the shaft stratigraphy.

The Air Intake Shaft is lined with non-reinforced concrete from the surface to the bottom of the shaft key at 903 ft (275 m). The key is 81 ft (25 m) long with an inside diameter of 16 ft (5 m). The shaft diameter below the key is 20 ft (6 m), and the shaft below the key is unlined to the facility horizon at 2,150 ft (655 m). The shaft walls are bolted and meshed from just below the key all the way down to the shaft station. This shaft has no sump.

3.4.1 Shaft Performance

Weekly visual inspections were performed on the Air Intake Shaft during this reporting period, and the shaft was found to be in satisfactory condition. No ground control activities other than routine maintenance were required during this reporting period.

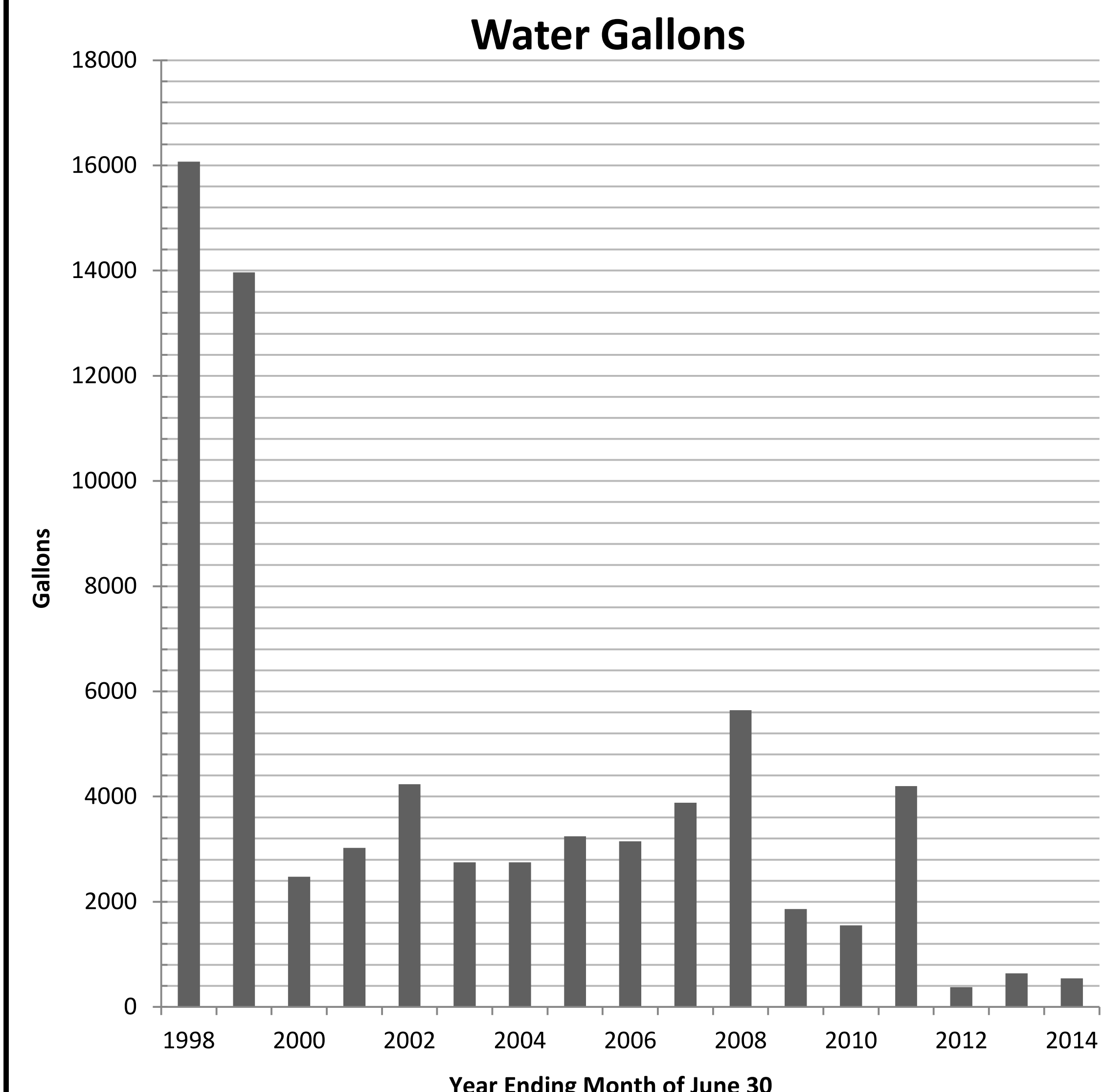

Figure 3 - 11 Water Removed from the Exhaust Shaft Catch Basin and the Interception Well System

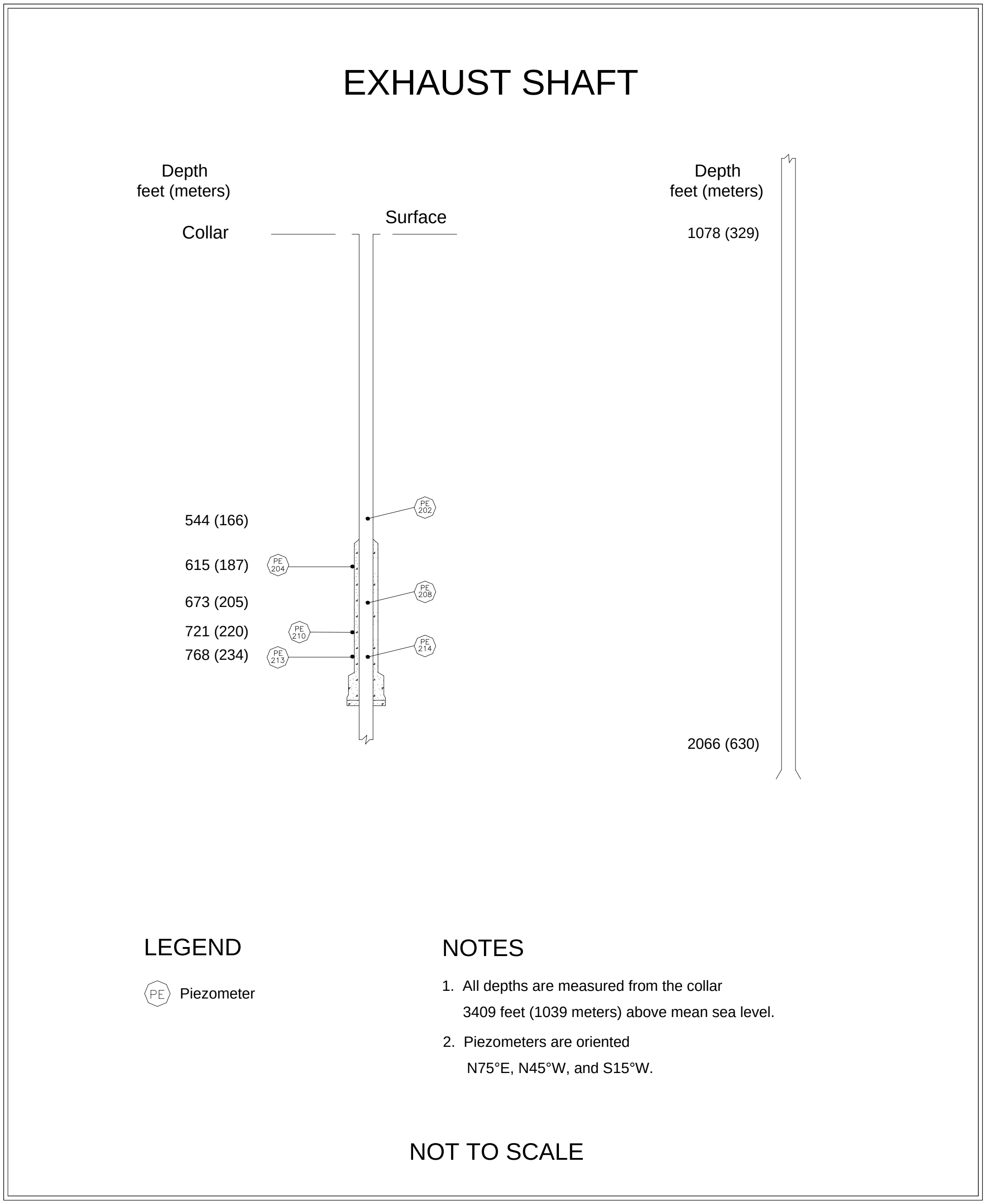

Figure 3 - 12 Exhaust Shaft Instrumentation (Without Shaft Key)

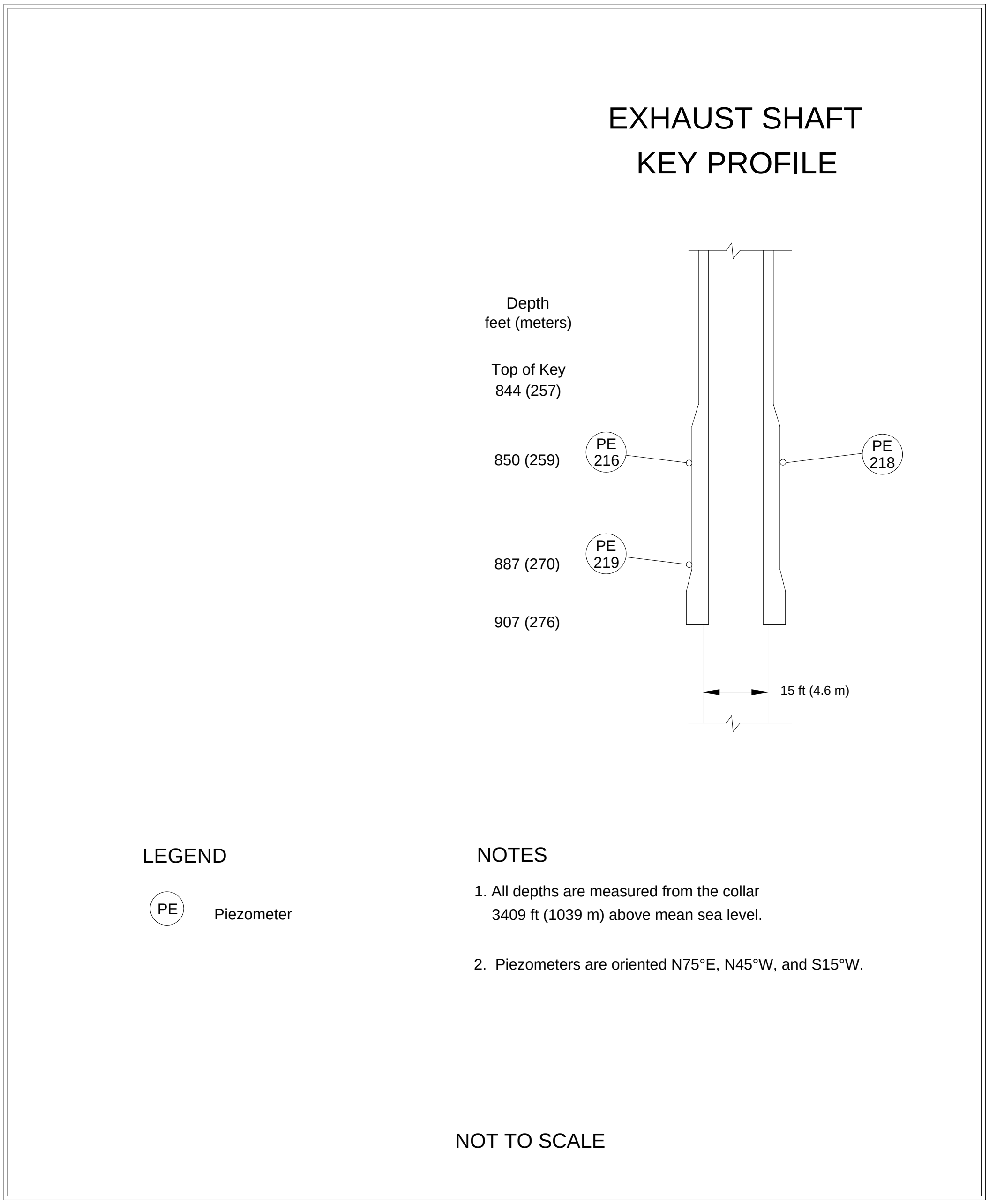

Figure 3 - 13 Exhaust Shaft Key Instrumentation

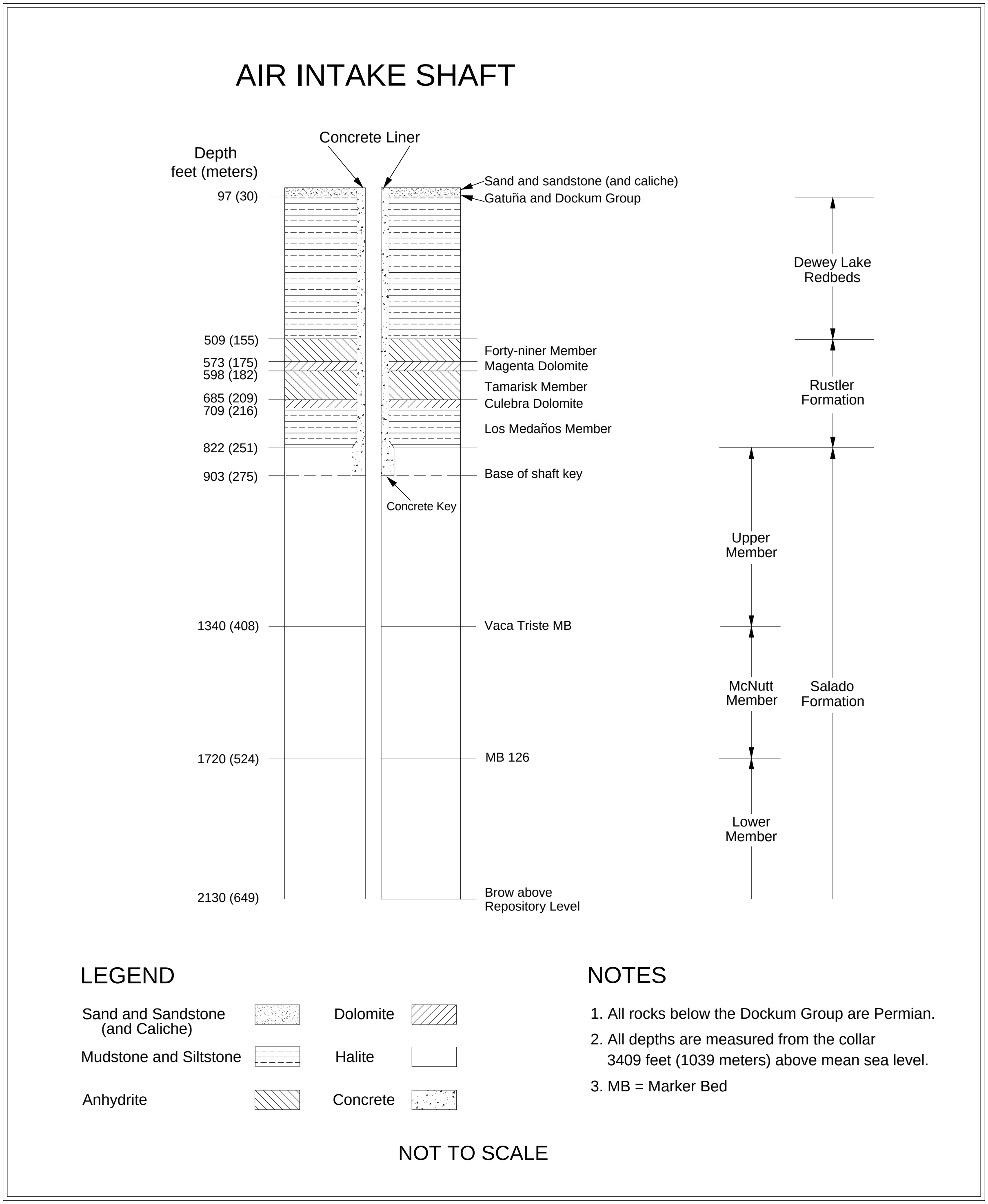

Figure 3 - 14 Air Intake Shaft Stratigraphy

4.0 PERFORMANCE OF SHAFT STATIONS

This chapter describes the instrumentation and geomechanical performance of the shaft stations at the base of the Salt Shaft, the Waste Shaft, and the Air Intake Shaft. The Exhaust Shaft does not have an enlarged shaft station; therefore, it is not included in this chapter.

4.1 Salt Shaft Station

The Salt Shaft Station was excavated by drilling and blasting between May 2 and June 3, 1982. In 1987 the station was enlarged by removing the roof beam up to Anhydrite "b" between S-90 and N-20 using a mechanical scaler. In 1995, the remaining roof beam at the north end of the station was also removed up to Anhydrite "b." The station area south of the shaft is 90 ft (27.5 m) long and 32 to 38 ft (10 to 12 m) wide. The height of the station south of the shaft is 18 ft (5.5 m). The station dimensions north of the shaft are approximately 30 ft (9 m) long, 32 to 35 ft (10 to 11 m) wide, and 18 ft (5.5 m) high. The shaft extends approximately 140 ft (43 m) below the facility horizon to accommodate the skip loading equipment and a sump. Figure 4-1 shows a cross section of the station.

4.1.1 Modifications to Excavation and Ground Control Activities

The Salt Shaft Station was not modified during this reporting period. Ground control activities were limited to routine maintenance.

4.1.2 Instrumentation

Geomechanical instrumentation was installed in the Salt Shaft Station between June 1982 and February 1983, with subsequent re-installation of extensometers and convergence points as necessary. Figure 4-2 shows the instrument locations after the roof beam was taken down.

Five vertical convergence points are currently monitored. Table 4-1 summarizes the vertical closure rates in the Salt Shaft Station from July 2013 through June 2014. Salt Shaft Station vertical closure rates indicate that the rates are lower than during the previous reporting period.

Table 4-2 summarizes the recent history of the roof extensometers in the Salt Shaft Station. Extensometers 51X-GE-01026-2 (S-30) and 51X-GE-01027-2 (S60) are located in the roof of the station.

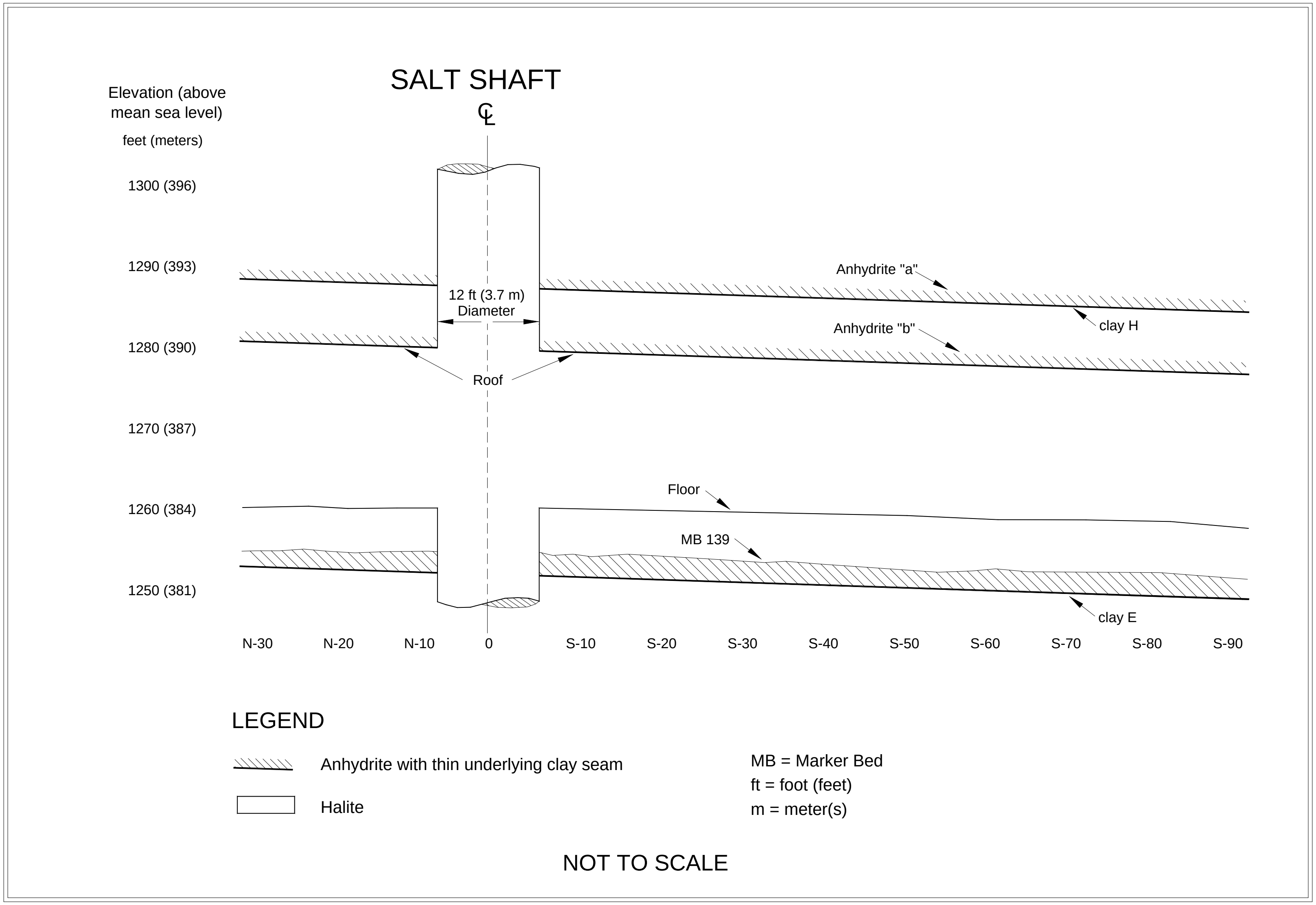

Figure 4 - 1 Salt Shaft Station Stratigraphy

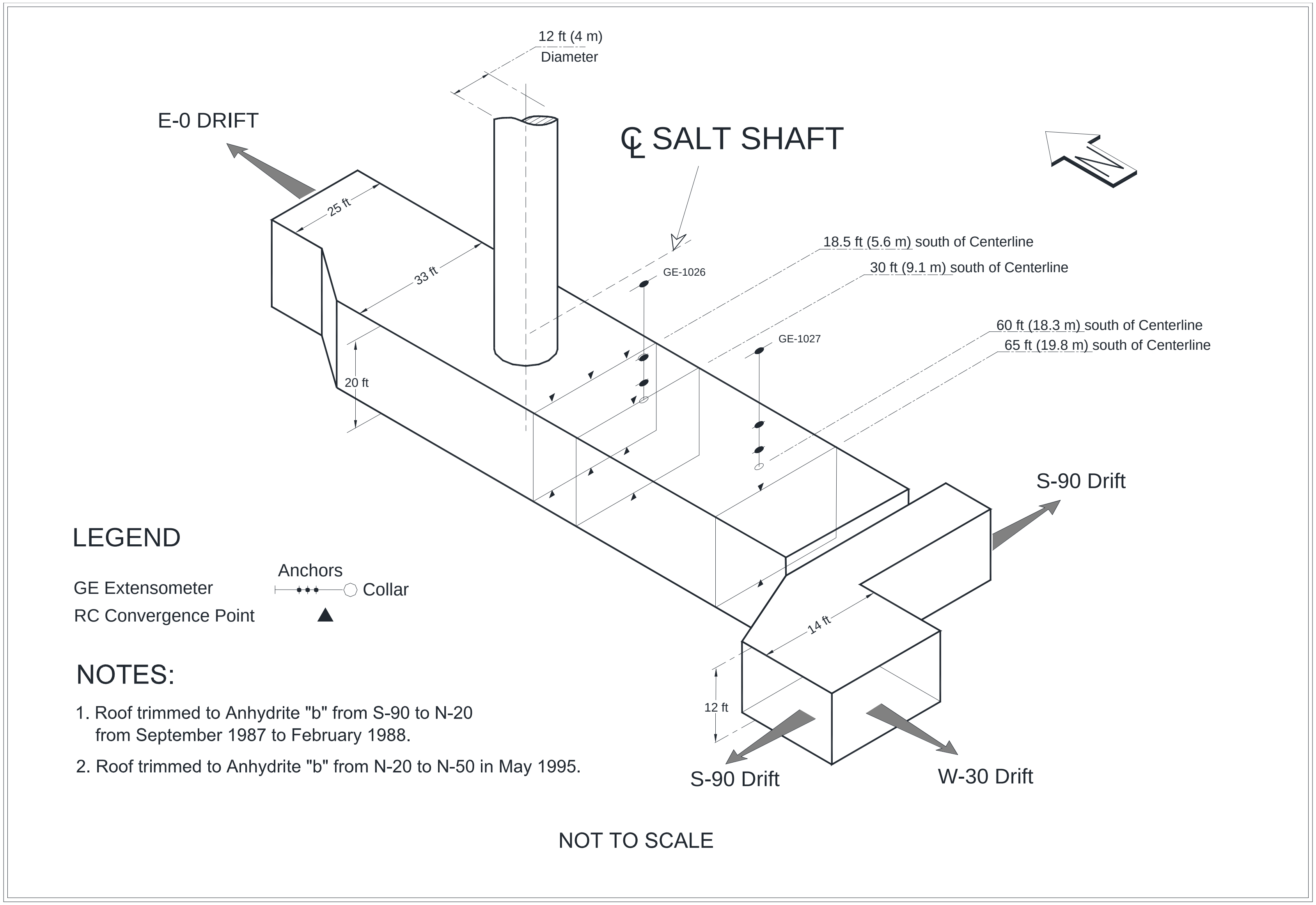

Figure 4 - 2 Salt Shart Station Instrumentation after Roof Beam Excavation

Table 4 - 1 Closure Rates in the Salt Shaft Station						
Location	Chord[1]	Last Reading	Total Cumulative Displacement in (cm)	Closure Rate 2013-2014 in/yr (cm/yr)	Closure Rate 2012-2013 in/yr (cm/yr)	Rate Percent Change
E0-S18	A-E	11/18/13	24.646 (62.601)	1.8 (4.6)	1.7 (4.3)	6%
E0-S18	B-D	01/21/14	27.266 (69.256)	1.9 (4.8)	1.9 (4.8)	0%
E0-S18	H-F	11/18/13	16.663 (42.324)	1.1 (2.8)	1.1 (2.8)	0%
E0-S30	A-C	01/21/14	25.727 (65.347)	1.6 (4.1)	1.7 (4.3)	-6%
E0-S65	A-C	01/21/14	17.892 (45.446)	1.1 (2.8)	1.2 (3.0)	-8%

[1] Chord is defined in Section 5.3

Table 4 - 2 Roof Beam Displacement in the Salt Shaft Station						
Instrument	Location	Last Reading	Displacement Relative to Deepest Anchor in (cm)	Displacement Rate 2014 to 2013 in/yr (cm/yr)	Displacement Rate 2012 to 2013 in/yr (cm/yr)	Rate Percent Change
51X-GE-01026-2	E0-S30	01/22/14	1.453 (3.691)	0.2 (0.5)	0.4 (1.0)	-50%
51X-GE-01027-2	E0-S60	01/22/14	0.987 (2.507)	0.2 (0.5)	0.3 (0.8)	-33%

4.2 Waste Shaft Station

The Waste Shaft Station was initially excavated with a continuous miner as a ventilation connection to a 6-ft (2-m) diameter exhaust shaft in November 1982. In 1984, the station was enlarged to a height of 15 to 20 ft (4.5 to 6 m) and a width of 20 to 30 ft (6 to 9 m). The station is approximately 150 ft (46 m) long. In 1988, the station walls were trimmed, and concrete was placed on the floor. Since 1988, the Waste Shaft Station has undergone five major floor renovations. A 53-ft (16-m)-long section of the reinforced concrete was removed in February 1991, in 1995 an additional 30-ft (9-m) section was removed, and in 2000 floor maintenance included trimming of the floor and reinstallation of the rails supported by segmented concrete panels on a crushed rock backfill. The roof of the Waste Shaft station was mined up to Clay G in December 2008 to assure adequate operational clearance. 12-ft resin-anchored roof bolts and chain link were installed for ground support. Figure 4-3 shows a cross-section of the Waste Shaft Station.

4.2.1 Modifications to Excavation and Ground Control Activities

No modifications to the Waste Shaft Station were made during this reporting period. Ground control activities were limited to routine maintenance.

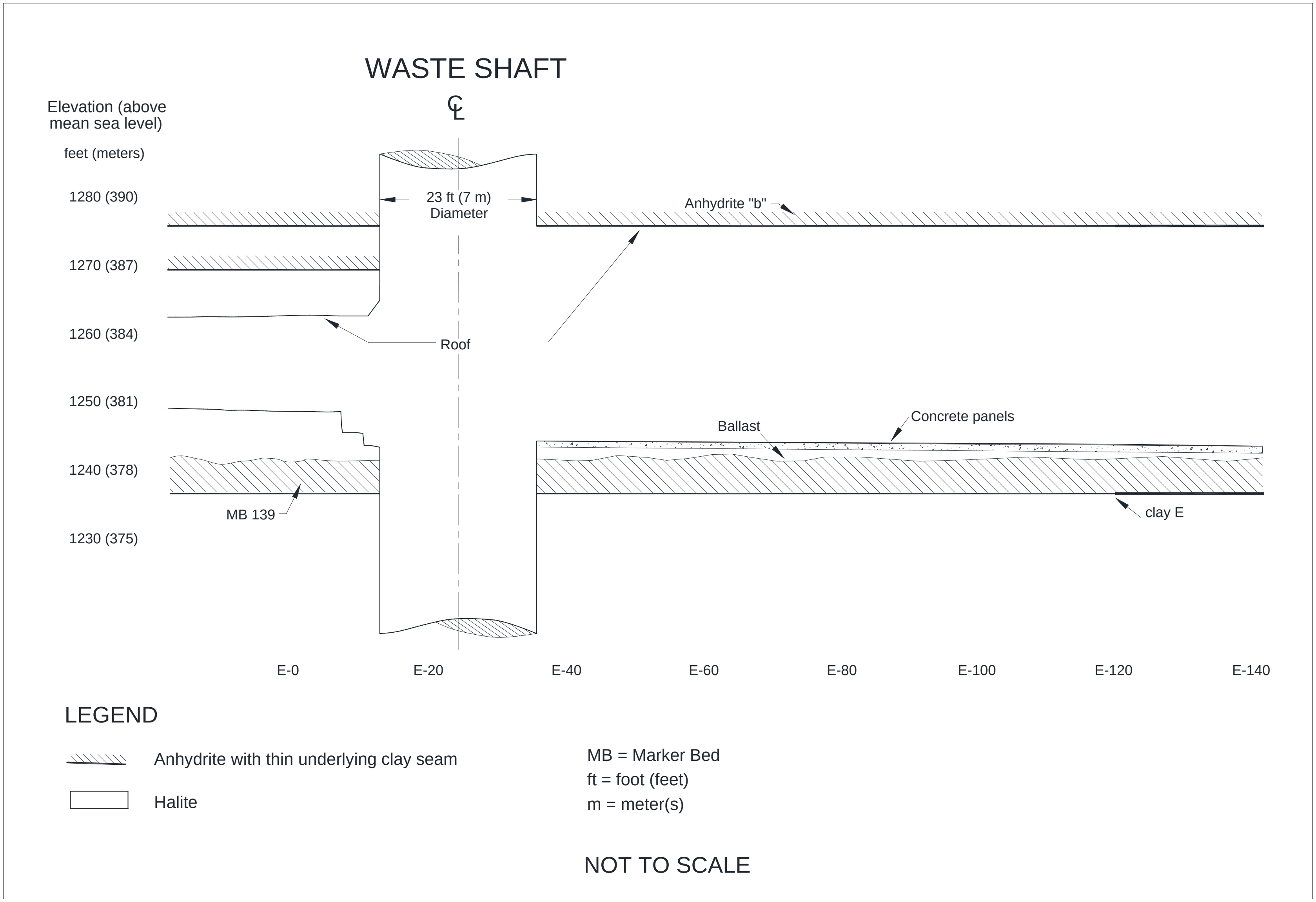

Figure 4 - 3 Waste Shaft Station Stratigraphy

4.2.2 Instrumentation

Instruments were initially installed in the Waste Shaft Station between November 12 and December 2, 1982. Figure 4-4 illustrates the locations after enlargement. Two extensometers in the Waste Shaft Station are currently being monitored. In addition, horizontal convergence is being monitored at E-32 and E-85.

Table 4-3 summarizes the recent history of the roof extensometers in the Waste Shaft Station. Extensometer 51X-GE-00404-2 is located at approximately S400-E35.

Table 4-4 summarizes the annual horizontal closure rates calculated from convergence point data for this reporting period. The data indicate that the horizontal closure rates at both E-32 and E-85 have not changed significantly from the previous reporting period.

Table 4 - 3 Summary of Roof Extensometers in Waste Shaft Station

Instrument	Location	Last Reading	Displacement Relative to Deepest Anchor in (cm)	Displacement Rate 2013 to 2014 in/yr (cm/yr)	Displacement Rate 2012 to 2013 in/yr (cm/yr)	Rate Change Percent
51X-GE-00268	S400-W30	01/22/14	7.051 (17.909)	0.1 (0.3)	0.1 (0.3)	0%
51X-GE-00404-2	S400-E35	06/24/14	1.222 (3.103)	0.3 (0.8)	0.3 (0.8)	0%

Table 4 - 4 Closure Rates in the Waste Shaft Station

Location	Chord[1]	Last Reading	Cumulative Displacement in (cm)	Closure Rate 2013 to 2014 in/yr (cm/yr)	Closure Rate 2012 to 2013 in/yr (cm/yr)	Rate Change Percent
S400-E32	B-D	02/05/14	6.435 (16.345)	1.1 (2.8)	1.4 (3.6)	-21%
S400-E85	B-D	02/05/14	6.590 (16.739)	1.2 (3.0)	1.4 (3.6)	-14%

[1] Chord is defined in Section 5.3

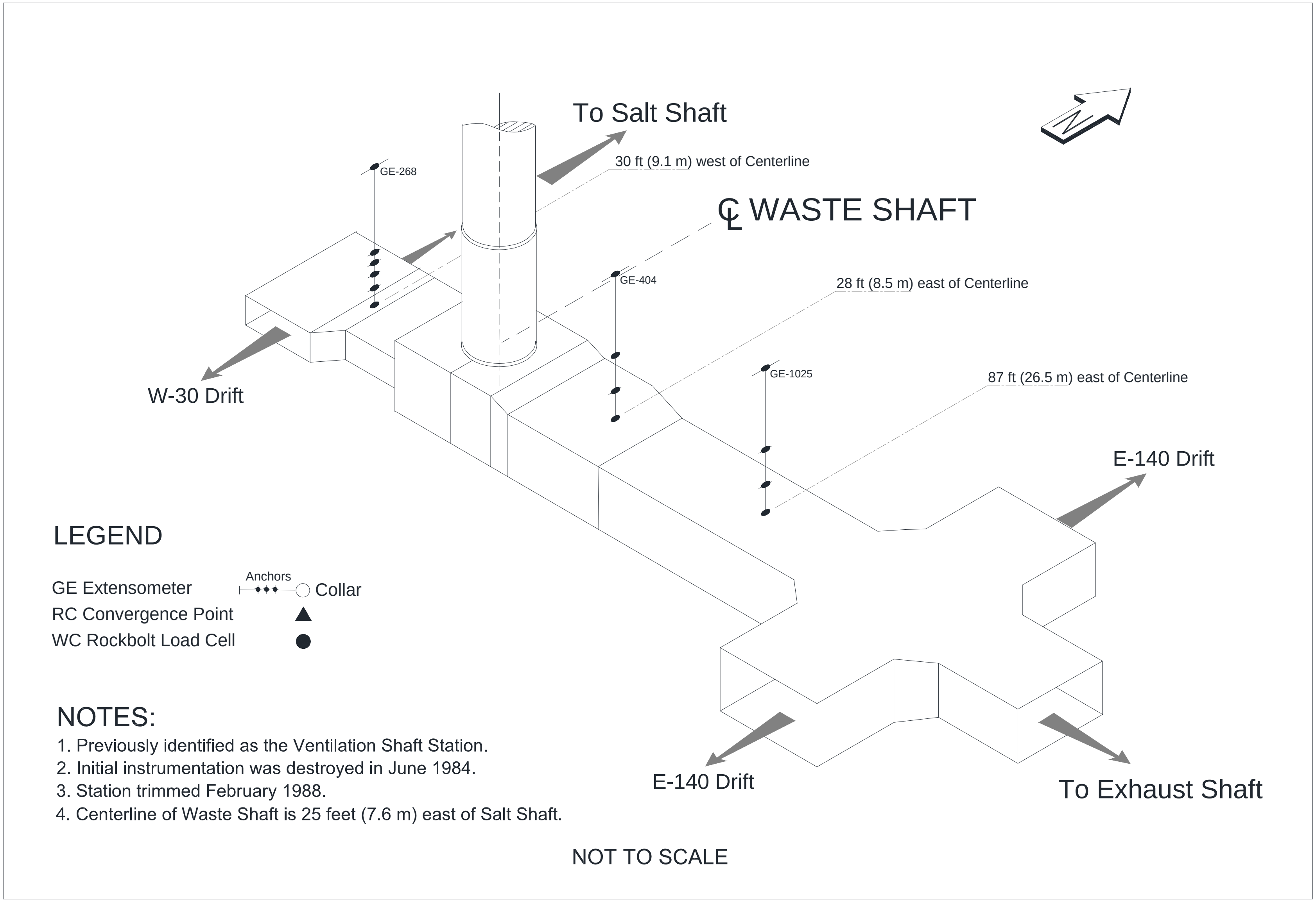

Figure 4 - 4 Waste Shaft Station Instrumentation after Roof Beam Excavation

4.3 Air Intake Shaft Station

The Air Intake Shaft Station was excavated in late 1987 and early 1988, using a continuous miner. The Air Intake Shaft is furnished with a work platform and a small cage that can be raised and lowered to perform routine ground maintenance. The principal purpose of that equipment is to provide emergency access.

4.3.1 Modifications to Excavation and Ground Control Activities

The AIS station was not modified during this reporting period. Ground control activities were limited to routine maintenance.

4.3.2 Instrumentation

Radial convergence point and extensometer instrumentation data near the Air Intake Shaft Station are presented in Chapter 5.0 as part of the discussion on the performance of the access drifts. Twenty rock bolt load cells are installed in the Air Intake Shaft Station area and are monitored regularly.

5.0 PERFORMANCE OF ACCESS DRIFTS

This chapter describes the geomechanical performance of the underground access drifts. The Waste Disposal Area is discussed in Chapter 6.0 and the Salt Disposal Investigation areas are discussed in Chapter 7.0. Four major north-south drifts in the WIPP underground are intersected by shorter east-west cross-drifts. Drift dimensions range from 13 ft (4 m) to 21 ft (6.4 m) high and from 14 ft (4.3 m) to 33 ft (9.2 m) wide.

5.1 Modifications to Excavation and Ground Control Activities

Trimming, scaling, and floor milling activities were performed as necessary in many areas. Table 5-1 summarizes these activities. It also summarizes ground control activities (e.g., rock bolting and installing wire mesh) in various locations in the access drifts.

5.2 Instrumentation

This section discusses instrumentation details and locations for each instrumentation type.

5.2.1 Extensometers

Thirty-two extensometers continue to be monitored at various locations in the access drifts. Where displacement data were available, annual displacement rates were calculated (see Section 1.4.3) for each active installation and compared to the annual displacement rates from the previous reporting period.

Table 5 - 1 Summary of Modifications and Ground Control Activities in the Access Drifts July 1, 2013 to June 30, 2014

Location	Work Activity
W30 drift from S1125 to S1175	Replaced broken Dywidag roof bolts
W30 drift from S2520 to S3310	Replaced broken Dywidag roof bolts
W170 drift from S2520 to S3310	Replaced broken Dywidag roof bolts
S1000 drift from E140 to W170	Replaced broken Dywidag roof bolts
S2180 from W30 to W170	Replaced broken Dywidag roof bolts
S2750 drift from E140 to E300	Replaced broken Dywidag roof bolts
S3080 drift from W30 to W170	Replaced broken Dywidag roof bolts
N215/N300 drift (Air Intake Shaft Access Drift)	Replaced broken Dywidag roof bolts
N620 alcove	Replaced broken Dywidag roof bolts
Panel 6, Room 1	Replaced broken Dywidag roof bolts
Mine wide	Replaced broken Dywidag roof bolts
E140 drift from S700 to S2180 (Ribs)	Installed 4-ft Mechanical roof bolt and chain link mesh
E140-S400 intersection (Rib/back intersection)	Installed 4-ft Mechanical roof bolt and chain link mesh
W170 drift from S2520 to S2750 (Ribs)	Installed 4-ft Mechanical roof bolt and chain link mesh
S90 drift from E140 to E300 (Back)	Installed 4-ft Mechanical roof bolt and chain link mesh
S1950 drift from W170 to Panel 8, Room 1	Installed 4-ft Mechanical roof bolts (spot bolting)
Panel 8	Installed 4-ft Mechanical roof bolts (spot bolting)
E0 drift from N150 to N460	Installed 14-ft Dywidag roof bolts

Extensometer data are obtained by measuring the displacement from the reference head anchor (collar) to each fixed anchor of the extensometer. These measurements are scheduled to be made at least monthly throughout the WIPP underground.

Many of the E-140 extensometers indicate movement in the roof beam that may be attributed to shallow fracturing and the effects of anhydrite stringer separations in the roof. Lateral deformation in the roof beam may influence the extensometer readings, causing an increase in the measured displacement. Although the extensometer data indicate continued deformation and breakup of the lower beam, the roof bolt anchorage zone remains competent.

5.2.2 Convergence Points

Convergence point data are obtained by measuring the change in distance between fixed points anchored into the rock across an opening, either from rib to rib or from roof to floor. The measurement end-points constitute a "chord." Figure 5-1 shows typical convergence point array configurations along with typical chord designations.

Convergence points installed during this reporting period involved the replacement of arrays in previously mined areas and the installation of new monitoring arrays in newly mined areas. Replacement convergence points were installed in twenty-three locations throughout the WIPP underground access drifts. Most of these installations were located in E-140 and W-30, where floor trimming activities removed the existing points. Table 5-2 lists the replacement convergence points that were installed during this reporting period.

Where possible, annual closure rates were calculated from convergence point array data gathered in the access drifts. Approximately 360 convergence points are located in the access drifts. A complete tabulation of these convergence point data and calculated closure rates is presented in the supporting data document for this report.

Locations with increases in annual vertical closure rates of greater than twenty percent are shown in Table 5-3.

Table 5 - 2 New and Replacement Convergence Points Installed In the Access Drifts July 1, 2013 through June 30, 2014

LOCATION	New/Replaced	Fieldtag[1]	CHORD[2]	Date Installed
E690-N570	N	E690-N570	A-C	07/09/13
E690-N640	R	E690-N640-2	A-C	07/09/13
E690-N710	N	E690-N710	A-C	07/09/13
N250-E220	R	N250-E220-3	A-E	07/11/13
N250-E220	R	N250-E220-3	B-D	07/11/13
N250-E220	R	N250-E220-3	H-F	07/11/13
E300-N250	R	E300-N250-4	A-C	07/11/13
E300-N170	R	E300-N170-3	A-E	07/11/13
E300-N170	R	E300-N170-3	H-F	07/11/13
E300-N45	R	E300-N45-2	A-E	07/11/13
E300-N45	R	E300-N45-2	H-F	07/11/13
E300-S45	R	E300-S45-3	H-F	07/11/13
E300-S45	R	E300-S45-3	A-E	07/11/13
E300-S45	R	E300-S45-3	B-D	07/11/13
W170-S2998	R	W170-S2998-2	A-C	07/25/13
W170-S2833	R	W170-S2833-2	A-C	07/25/13
S90-E220	N	S90-E220	A-C	08/07/13
W30-S1775	R	W30-S1775-4	A-C	09/19/13

Table 5 - 2 New and Replacement Convergence Points Installed In the Access Drifts July 1, 2013 through June 30, 2014

LOCATION	New/Replaced	Fieldtag[1]	CHORD[2]	Date Installed
W30-S1950	R	W30-S1950-3	A-C	09/19/13
W30-S2067	R	W30-S2067-4	A-C	09/19/13
W30-S850	R	W30-S850-6	A-E	09/19/13
W30-S850	R	W30-S850-5	B-D	09/19/13
W30-S850	R	W30-S850-4	H-F	09/19/13
E300-S90	R	E300-S90-3	A-C	09/19/13
N940-E768	R	N940-E768-2	A-C	09/19/13
N940-E845	R	N940-E845-2	A-C	09/19/13
N940-E922	R	N940-E922-2	A-C	09/19/13
N940-E1000	N	N940-E1000	A-C	09/19/13
N1100-E300	R	N1100-E300-2	A-C	09/25/13
N940-E1050	R	N940-E1050-2	A-C	09/25/13
N940-E1100	N	N940-E1100	A-C	09/25/13
N940-E1150	N	N940-E1150	A-C	09/25/13
N940-E1200	N	N940-E1200	A-C	09/25/13
N940-E1250	N	N940-E1250	A-C	09/25/13
N940-E1300	N	N940-E1300	A-C	09/25/13
E1300-N860	N	E1300-N860	A-C	09/25/13
N780-E1300	N	N780-E1300	A-C	09/25/13
W30-S2520	R	W30-S2520-4	A-C	11/18/13
W30-S120	R	W30-S120-3	A-C	12/04/13
W30-S500	R	W30-S500-3	A-C	12/04/13
W30-S500	R	W30-S500-2	B-D	12/04/13
S2520-E55	R	S2520-E55-2	A-C	12/04/13
S90-W400	R	S90-W400-3	B-D	12/04/13
W170-S700	R	W170-S700-3	A-C	12/11/13
W170-S850	R	W170-S850-8	B-D	12/11/13
W170-S850	R	W170-S850-8	A-E	12/11/13
W170-S850	R	W170-S850-8	H-F	12/11/13
W170-S1150	R	W170-S1150-5	B-D	12/11/13
W170-S1150	R	W170-S1150-5	A-E	12/11/13
W170-S1150	R	W170-S1150-3	H-F	12/11/13
W170-S5	R	W170-S5-2	A-C	12/11/13
S1600-W285	N	S1600-W285	A-C	01/07/14
S1600-W390	N	S1600-W390	A-C	01/07/14
S1600-W455	N	S1600-W455	A-C	01/07/14
S1600-W520	N	S1600-W520	A-C	01/07/14

Table 5 - 2 New and Replacement Convergence Points Installed In the Access Drifts July 1, 2013 through June 30, 2014

LOCATION	New/Replaced	Fieldtag[1]	CHORD[2]	Date Installed
W390-S1682	N	W390-S1682	A-C	01/07/14
W390-S1765	N	W390-S1765	A-C	01/07/14
W390-S1846	N	W390-S1846	A-C	01/07/14
S1950-W790	N	S1950-W790	A-C	01/08/14
S1950-W725	N	S1950-W725	A-C	01/08/14
S1950-W660	N	S1950-W660	A-C	01/08/14
S1950-W585	N	S1950-W585	A-C	01/08/14
S1950-W520	N	S1950-W520	A-C	01/08/14
S1950-W455	N	S1950-W455	A-C	01/08/14
S1950-W390	N	S1950-W390	A-C	01/08/14
S1950-W285	N	S1950-W285	A-C	01/08/14
N140-E90	R	N140-E90-3	A-C	01/16/14
N140-E90	R	N140-E90-2	B-D	01/16/14
S1600-E311	R	S1600-E311-3	A-C	01/23/14
S1600-E332	R	S1600-E332-4	A-C	01/23/14
S1600-E357	R	S1600-E357-3	A-C	01/23/14
S1600-E382	R	S1600-E382-3	A-C	01/23/14
S1950-W455	N	S1950-W455	A-C	01/08/14
S1950-W390	N	S1950-W390	A-C	01/08/14
S1950-W285	N	S1950-W285	A-C	01/08/14
N140-E90	R	N140-E90-3	A-C	01/16/14
S1600-E407	R	S1600-E407-3	A-G	01/23/14
S1600-E407	R	S1600-E407-3	B-F	01/23/14
S1600-E407	R	S1600-E407-3	L-H	01/23/14
S1600-E432	R	S1600-E432-3	A-C	01/23/14
S1950-E357	R	S1950-E357-8	A-C	01/23/14
S1950-E357	R	S1950-E357-5	B-D	01/23/14
S1950-E432	R	S1950-E432-4	A-C	01/23/14
W170-S2833	R	W170-S2833-3	A-C	01/23/14
W520-S1682	N	W520-S1682	A-C	02/04/14
W520-S1765	N	W520-S1765	A-C	02/04/14
W520-S1846	N	W520-S1846	A-C	02/04/14
S1950-E332	R	S1950-E332-5	B-D	01/23/14

N = New installation.
R = Replacement installation (i.e., instrument replaces older instrument that has failed or has been mined out).
[1] This column is a combination of the convergence point location followed by a "-X," where X represents the reinstallation number, when applicable.
[2] A unique letter is assigned to each convergence array element around a particular opening. Chord refers to a particular array pair. The various array lettering schemes are shown in Figure 5-1.

5.3 Analysis of Convergence Point and Extensometer Data

Vertical loading on mine pillars results in lateral stresses on the roof and floor beams. The composition of those beams, in part, determines how these structures will react to the horizontal stresses. In particular, horizontally continuous anhydrite stringers (see Section 2.2.2) divide the beam itself into a series of smaller independent beams.

Lateral strain on the beam imposed by vertical loading on the pillars is accommodated by vertical displacement over the mined opening. This requires that the horizontally oriented beam separate along the most favorable, or weakest, planes.

Where anhydrite stringers interpose the beam, they constitute a plane of weakness, and delamination occurs. The material is confined in the plane above, so that the roof accommodates the lateral strain by bending convex into the mined opening.

Two distinct results come of this action. First, voids form within the beam as the portions closer to the opening move away from those deeper within the beam. Second, the convex portion of the bended plane is subjected to tensile loading perpendicular to the axis of the drift and superficial tears known as "tensile fractures" develop generally parallel to the axis of the drift.

Where anhydrite stringers are small and discontinuous or not present at all within the beam, horizontal loading is accommodated along shear planes. These develop at angles of approximately 35 degrees with respect to the horizontal. In some cases, a plane develops preferentially on one side of the drift, and the bulk of material is pushed into the mined opening on that side. This may be thought of as a cantilevered beam.

Whatever the mechanism, vertical displacement into the mined opening is measured by convergence monitoring. Convergence points consider the displacement between two opposing surfaces: either the roof and floor or the two ribs. Extensometers consider the displacement between one surface (usually the back) and one or more points within the beam. Where a convergence point and an extensometer are adjacent to one another, it is possible to determine the individual displacements of both floor and roof beams.

This data is used to analyze the stability and mechanics of the beam, and in determining what actions may be taken to ensure the safety of personnel and equipment consistent with the safe operation of the facility.

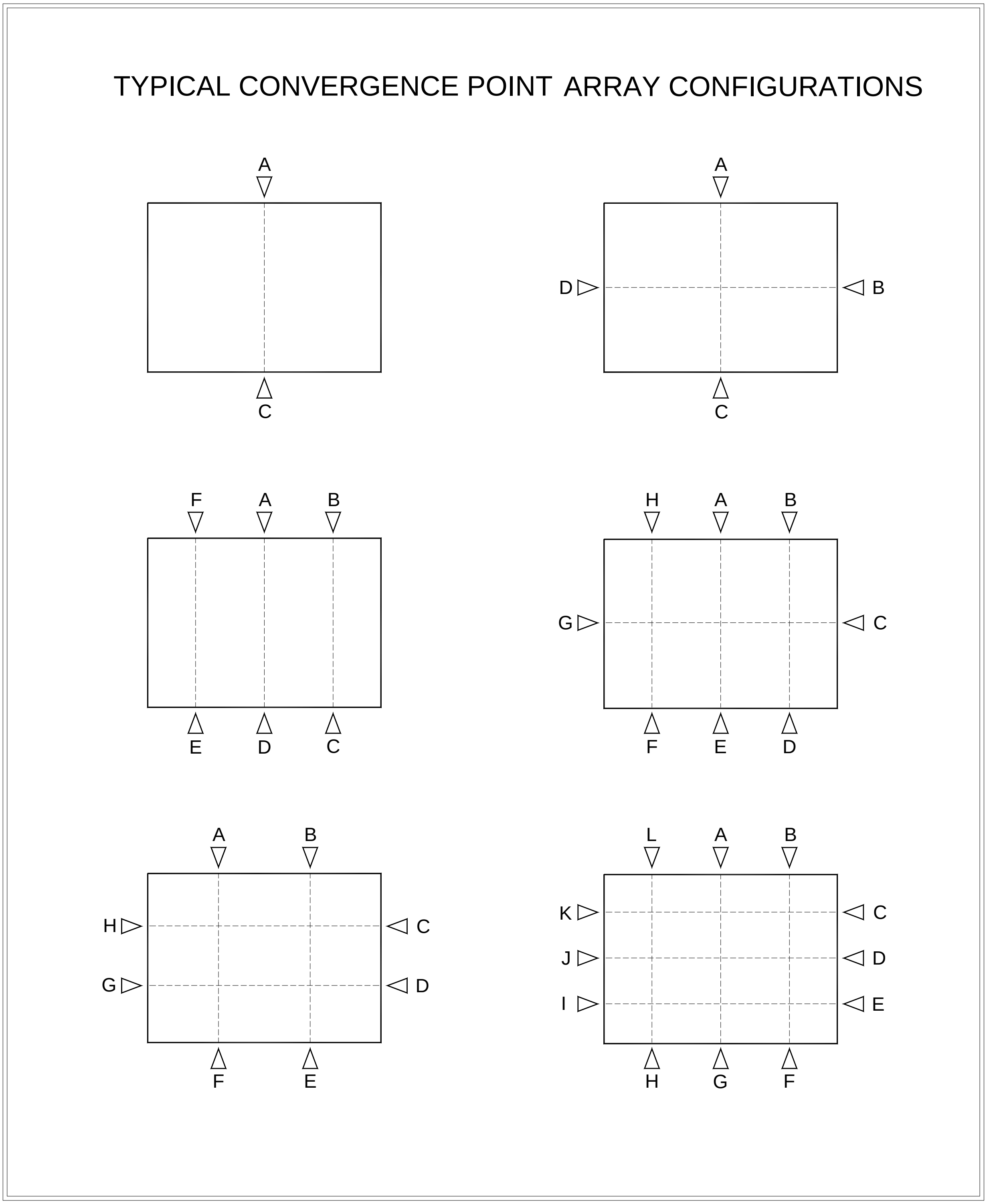

Figure 5 - 1 Typical Convergence Point Array Configurations Showing Anchor Designations

Table 5 - 3 Vertical Closure Rate Changes in Excess of Twenty Percent in the Access Drifts

Location	Chord	Last Reading Date	Closure Rate 2013 to 2014 in/yr (cm/yr)	Closure Rate 2012 to 2013 in/yr (cm/yr)	Rate Percent Change
W170-S850-7	B-D	12/17/2013	2.1 (5.3)	0.7 (1.8)	200%
W170-S1600-4	A-C	5/29/2014	4.1 (10.4)	1.8 (4.6)	128%
S3310-E220	A-C	1/27/2014	3.9 (9.9)	2.1 (5.3)	86%
W170-S1950-3	A-C	5/29/2014	2.6 (6.6)	1.4 (3.6)	86%
E300-N250-4	A-C	1/13/2014	3.2 (8.1)	1.9 (4.8)	68%
W170-S1150-3	H-F	12/17/2013	1.1 (2.8)	0.7 (1.8)	57%
W170-S1779-2	B-D	12/17/2013	2.2 (5.6)	1.4 (3.6)	57%
W170-S1779-3	A-C	5/29/2014	2.5 (6.4)	1.6 (4.1)	56%
E300-S2833-2	A-C	1/13/2014	3.0 (7.6)	2.1 (5.3)	43%
E300-S2425-2	A-C	1/13/2014	4.3 (10.9)	3.1 (7.9)	39%
E140-S2122-7	A-C	2/5/2014	4.1 (10.4)	3.0 (7.6)	37%
E140-S1775-4	L-H	2/3/2014	1.5 (3.8)	1.1 (2.8)	36%
S1950-E284-3	A-C	12/11/2013	1.6 (4.1)	1.2 (3.0)	33%
W30-S1775-4	A-C	5/29/2014	4.1 (10.4)	3.1 (7.9)	32%
W170-S3195	A-C	1/20/2014	3.9 (9.9)	3.0 (7.6)	30%
E140-S1687-4	B-D	2/3/2014	2.3 (5.8)	1.8 (4.6)	28%
W30-S2833-4	A-C	2/5/2014	4.2 (10.7)	3.3 (8.4)	27%
S3310-E55	A-C	1/27/2014	4.0 (10.2)	3.2 (8.1)	25%
W170-S1445-4	A-C	5/29/2014	2.0 (5.1)	1.6 (4.1)	25%
W30-S1600-3	A-C	5/29/2014	2.5 (6.4)	2.0 (5.1)	25%
E300-S2350-2	A-C	1/13/2014	4.7 (11.9)	3.8 (9.7)	24%
E300-S2998-4	A-C	1/13/2014	4.3 (10.9)	3.5 (8.9)	23%
E140-S1450-4	B-F	2/3/2014	1.6 (4.1)	1.3 (3.3)	23%

5.4 Excavation Performance

Approximately 500 readings are collected and assessed regularly from convergence point arrays throughout the WIPP underground. Convergence rates continue to vary seasonally, typically increasing during the warmer summer months and decreasing during the cooler and drier winter months.

The performance of the access drift excavations during this reporting period was within acceptable criteria. "Acceptable criteria" means that a drift remains accessible, and the ground can be controlled by routine maintenance. Standard remedial ground control in some areas was required to maintain the performance of the excavations. The drifts remain stable and controlled. Most of the annualized rates remain steady, indicating stability. In some locations, where the rates are high, nearby mining activity or gradual deterioration of the roof beam along anhydrite stringers is most likely the cause. Where necessary, additional ground control measures have been or will be installed.

6.0 PERFORMANCE OF WASTE DISPOSAL AREA

The Waste Disposal Area as of June 30, 2014, consisted of Panels 1, 2, 3, 4, 5, 6, and 7. Panels 1, 2, 3 4, and 5 were closed during previous reporting periods. Waste disposal in Panel 7 and mining in Panel 8 were interrupted by the radiological release.

6.1 History

Excavation of Panel 1 began in May 1986 with the mining of the access entries. Initially, the disposal rooms and drifts were developed as pilot drifts that were later excavated to nominal operational dimensions of 13 ft (4 m) high, 33 ft (10 m) wide, and 300 ft (91 m) long. Room 1 was completed to these dimensions in August 1986, and pilot drifts for Rooms 2 and 3 were excavated in January and February 1987. Rooms 2 and 3 were completed in February and March 1988, and Rooms 4 through 7 were completed in May 1988. Four short access drifts designed to lead to smaller test alcoves were excavated north off the S-1600 drift and Rooms 4-7 in June 1989. Only the access drifts to the alcoves were completed; the alcoves themselves were not excavated. Panel 1 waste emplacement (in Rooms 1, 2, 3, 7, adjacent areas of S 1600, and all of S-1950) was completed during a prior reporting period, and the panel is closed to all access. The Panel 1 access entries, S-1600 and S-1950, which extend from the E-300 drift to the isolation walls, remain open, and the instrumentation in this area continues to be maintained and monitored.

Excavation of the Panel 2 waste disposal area began in September 1999 with the mining of access entries. Initially, the disposal rooms and drifts were developed as pilot drifts that were trimmed to finished dimensions. Room 1 was completed in January 2000, and pilot drifts for Rooms 2 and 3 were excavated in February 2000. Pilot drifts were completed for Rooms 4 through 6 in April 2000. The pilot drift for Room 7 was excavated in May 2000. All the rooms were excavated to final dimensions by August 2000. Waste emplacement in Panel 2 was completed during a prior reporting period, and the panel is closed to all access. The Panel 2 access entries, S-2150 and S-2520, which extend from the E-300 drift to the isolation walls, remain open, and the instrumentation in this area continues to be maintained and monitored.

Excavation of Panel 3 waste disposal rooms began in May 2002 with the mining of access entries to Panel 3. As with Panel 2, initially, the disposal rooms and drifts were developed as pilot drifts that were trimmed to finished dimensions. All the rooms were excavated to final dimensions by the end of March 2004. Waste emplacement in Panel 3 was completed in February 2007. Substantial barriers and bulkheads were installed in the exhaust and intake drifts of Panel 3 to prevent access into the panel and to isolate it from the ventilation circuit.

Panel 4 access drift mining began in January 2005. The disposal rooms were initially developed as pilot drifts and were later trimmed to final dimensions. Mining was completed by June 2006. Waste emplacement in Panel 4 was completed in March 2009. Substantial barriers and bulkheads were installed in the exhaust and intake drifts of Panel 4 to prevent access into the panel and to isolate it from the ventilation circuit.

Panel 5 excavation activities began in June 2006. The panel was initially mined to less than-final dimensions and later trimmed to specification. Mining was complete by February 2008. Waste emplacement was conducted from March 2009 through July 2011. Isolation walls were completed in November 2011. Instrumentation and regular observations will continue in the accessible area up to the isolation walls.

Panel 6 mining began in June 2008. The panel was initially mined to less- than-final dimensions and later trimmed to specification. Mining was complete by April 2010. Waste emplacement began in March of 2011. As of the end of this reporting period, CH Waste was being emplaced in Panel 6, Room 2 and RH Waste in Panel 6, Room 1.

Panel 7 mining activities began in April 2010 and were complete in January 2013.

Panel 8 mining activities began in September 2013 and have not resumed since the radiological release.

6.2 Modifications to Excavations and Ground Control Activities

Routine maintenance and ground control activities in the form of trimming, scaling, rock bolt replacement, and installing wire mesh were performed on ribs, floor, and roof throughout accessible areas of the disposal panels.

The original floor of Panel 7 lay within two feet of a stiff polyhalite bed which rested atop a hard anhydrite bed. These beds, being stiffer than the adjacent salt, resisted the lateral loading imposed by creep deformation of the pillars and bow upward into the mined openings. To provide a stable floor for the lifetime of the panel, a wide channel was mined through the two beds, and is backfilled with run-of-mine salt. The backfilled salt will offer less resistance to the lateral loading and result in a more even uplift, rather than the severe bowing and fracturing that was experienced with the removed materials.

Table 6-1 summarizes modifications and ground control activities performed in the disposal panels during this reporting period.

6.3 Instrumentation

There were no changes to the Panel 6 instrumentation layout. Convergence monitoring continued in all accessible areas up to the time that the waste stack front passed the instrument location. Remote monitoring of extensometers continues.

Panel 7 instrumentation consists of the following:

- Forty-nine vertical convergence points, distributed as fourteen each in the intake and exhaust drifts and three in each of the rooms; and
- Eleven wire extensometers, distributed as two in each of the intake and exhaust drifts and one in each of the rooms.

A schematic of the geomechanical instrumentation layout found in Panels 6 and 7 is shown in Figure 6-1.

Table 6- 1 Summary of Modifications and Ground Control Activities in the Waste Disposal Area July 1, 2013 to June 30, 2014

Location	Work Activity
S2750 from W170 to Panel 6 Room 1	Replaced broken Dywidag roof bolts
S3080 from W170 to Panel 6 Room 1	Replaced broken Dywidag roof bolts
Panel 7	Replaced broken Dywidag roof bolts
Panel 7, Room 1 (Rib/back intersection)	Installed 4-ft Mechanical roof bolt and chainlink mesh
Panel 7, S2180 at Room 2 (Rib/back intersection)	Installed 4-ft Mechanical roof bolt and chainlink mesh
Panel 7, S2520 drift from Room 1 to Room 2	Installed 14-ft Dywidag roof bolts

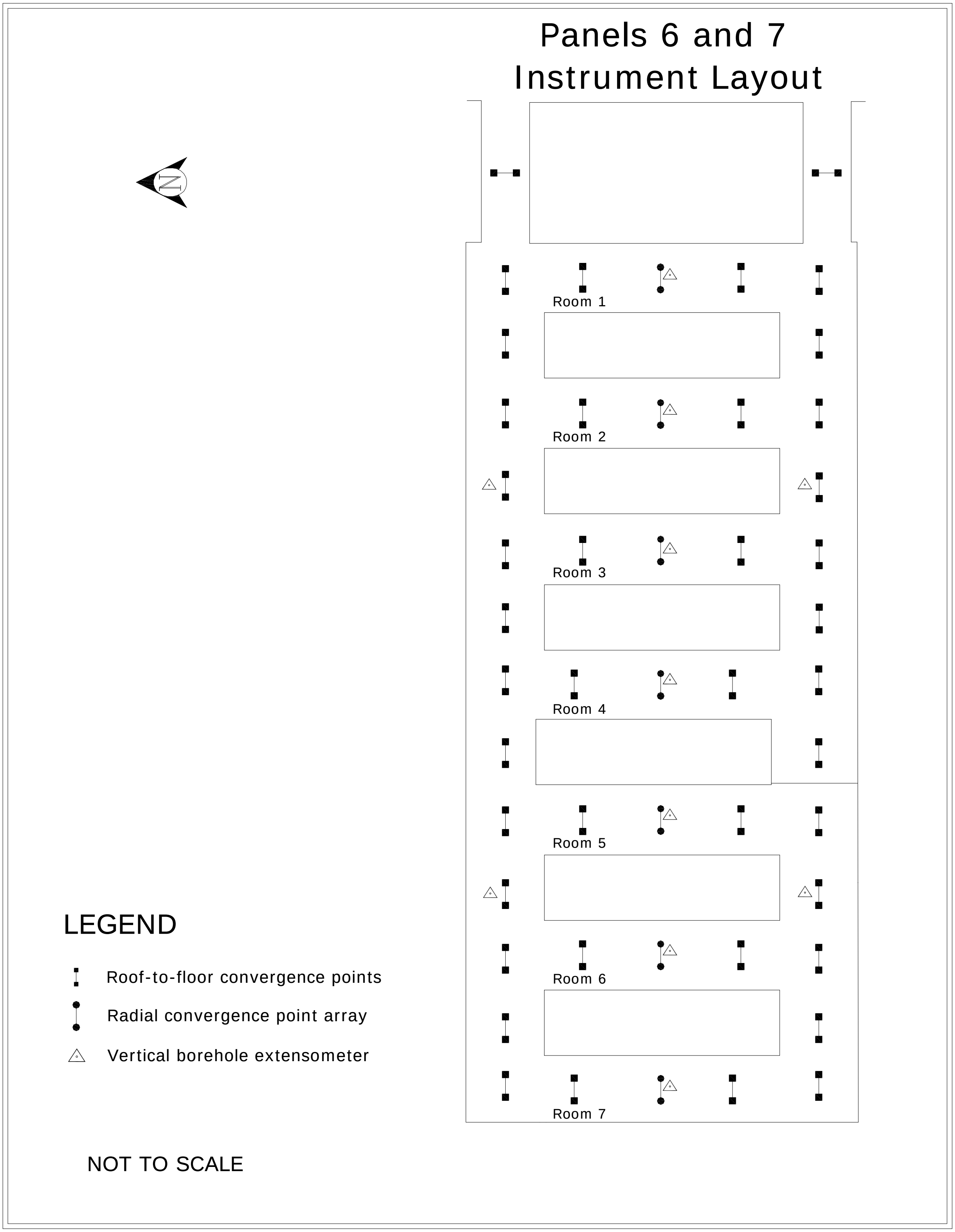

Figure 6 - 1 Location of Geomechanical Instruments in Panels 6 and 7

6.4 Excavation Performance

Waste handling activities in Panels 1-5 have been completed, and geomechanical monitoring inside these panels has been discontinued.

In accessible underground areas, horizontal and vertical convergence rates, calculated at the center of each of the rooms, were compared between this and the previous reporting period. Generally, convergence rates have declined from initial post-mining levels. Localized increases occur with seasonal creep trends, the presence of continuous anhydrite stringers, and coincident with adjacent mining activities. These increases are addressed, where necessary, with additional ground support selected for conditions prevailing at the specific location of installation.

6.5 Analysis of Extensometer and Convergence Point Data

Geomechanical instrumentation is installed in each disposal room and at select locations in the panel access drifts. As anticipated, these installations showed a general decrease in room closure rate and roof beam deformation with time. At some locations, deformation rates increased as roof sag and roof beam deterioration developed. Supplemental ground control support was installed in these areas and has subsequently reduced the observed rates.

Although Panels 1 through 5 are closed and Panel 6 is in the process of being closed, convergence monitoring continues in the panel entries between E-300 and the explosion isolation walls (Panels 1 and 2) and substantial and isolation barriers (Panels 3 and 4). The exception is the Panel 4 intake drift (S3650) which is closed to access due to elevated volatile organic compound (VOC) levels. Monitoring data indicate generally steady long term trends. Incidences of short term acceleration are largely attributed to creep deformation of the pillars, which results in increasing lateral loading of the roof beam and the growth of separations along anhydrite stringers.

All but four of the extensometers in Panel 6 were returning increasing rates of closure throughout this reporting period. The much younger Panel 7 had one location with very modest, increasing rates of beam expansion. The remaining extensometers indicated low and steady trends.

7.0 PERFORMANCE OF THE SALT DISPOSAL INVESTIGATIONS AND SALT DEFENSE DISPOSAL INVESTIGATIONS AREAS

This chapter describes the geomechanical performance of the SDI and SDDI areas (hereafter referred to as SDI). Development of the area began during the previous reporting period, in January 2012. When completed, most of the area will have nominal dimensions of 13 feet high and 16 feet wide.

7.1 Ground Control Program

Due to the relatively narrow drifts (nominally 16 feet across) and favorable mining horizon, ground control plans in the SDI area are confined to routine maintenance such as spot-bolting where localized drummy surface features develop. More substantial engineered ground control systems may be applied in the event that ongoing geomechanical monitoring and analysis of the area identify a need.

7.2 Instrumentation

Convergence point data are obtained by measuring the change in distance between fixed points anchored into the rock across an opening, either from rib to rib or from roof to floor. The measurement end-points constitute a "chord." Figure 5-1 shows typical convergence point array configurations along with typical chord designations.

7.3 Analysis of Convergence Point Data

As of this reporting period, fifty-seven convergence points have produced preliminary data on the behavior of the SDI openings. As a rule, the area behaves as expected, with relatively high initial rates rapidly decreasing as the stresses redistribute to load the surrounding salt pillars.

7.4 Excavation Performance

One object of the SDI project is to observe the behavior of the salt in response to high heat sources emplaced within the mined openings. It is expected that the performance of these areas, in particular those nearest the experimental heat sources, will exhibit rapid creep movement. The necessity for ground control has not yet been determined. As the development of the area progresses and as the experiments begin to come on line, geotechnical observations will be closely analyzed for any need of external control.

8.0 GEOSCIENCE PROGRAM

The Geoscience Program confirms the suitability of the site through the collection of various geologic data and excavation characteristics from the underground. These include the inspection of open observation holes for fractures (separations) and offsets (lateral displacements) in roof beams and the mapping of fracture development on roof surfaces. Data collected through these activities support the design and evaluation of ground support systems.

During this reporting period, the following activities were performed:

- Observation hole inspections
- Fracture mapping
- Stratigraphic Mapping
- Drilling and Geologic Core Descriptions

Fracture development in the roof is primarily caused by the concentration of compressive stresses in the roof beam and is influenced by the size and shape of the excavation and the stratigraphy in the immediate vicinity of the opening. In a thick roof beam, pillar deformations induce lateral compressive stresses into the immediate roof and floor. With time, the buildup of stress causes differential movement along stratigraphic boundaries. This differential movement is identified as offsets in observation holes and by the bends in failed rock bolts. Large strains associated with lateral movements can induce fracturing in the roof, which is frequently seen near the ribs; however, this process may take a long time (years) to develop.

At the upper repository horizon, clay or anhydrite stringers exert significant influence over the effective thickness of the roof beam. The presence of these stringers causes the roof beam to behave as a series of thin independent beams. Little or no tensile support is provided across the stringer interface. As horizontal end-loading continues, each beam can deflect downward causing a tensile fracture to develop along the bottom of the beam. These tensile fractures can develop in relatively new excavations soon after separation occurs along the stringer interface.

8.1 Observation Hole Inspections

Geotechnical observation holes are drilled at various locations throughout the underground facility. A location may contain one or more holes arranged in an array. These holes are drilled to depths that allow the monitoring of fracture development and offsetting and are inspected for the development of those features. Roof observation holes usually extend up past clays G and H (Figure 8-1 and Figure 8-2).

The clay seams nearest the excavation surfaces define the immediate roof beam. The roof beam is bounded by Clay G in most of the access drifts and Panels 1 and 2. Some areas, such as the Salt Shaft Station, portions of the E-0 and E-140 drifts, the south mains south of S-2620, and Panels 3, 4, 5, and 6 are excavated to Clay G and so have roof beams bounded by Clay H.

The offset in an observation hole is determined by visually estimating the degree of occlusion. The direction of offset along clay seams is observed as the movement of the strata nearer to the observer relative to the strata farther away. Typically, the nearer strata move toward the center of the excavation (Figure 8-3 and Figure 8-4). Based on previous observations in the underground, the magnitude of offset is usually greater in holes located near ribs than in those located along excavation centerlines. Offsetting along the clay layers is observable until total offset is reached or visibility is obstructed by intervening offsets at other clay seams or fractures.

Observation holes are inspected for fractures, using an aluminum rod with a flattened steel wire probe attached to one end perpendicular to the rod (referred to as a "scratch rod"). Fractures and clay seams are located by moving the probe along the inside of the hole until it is snagged in one of these features. Depth to each feature is recorded, as is the magnitude of separations encountered. A fiber scope camera is available for use in addition to the scratch rod to visually document features of interest in a hole.

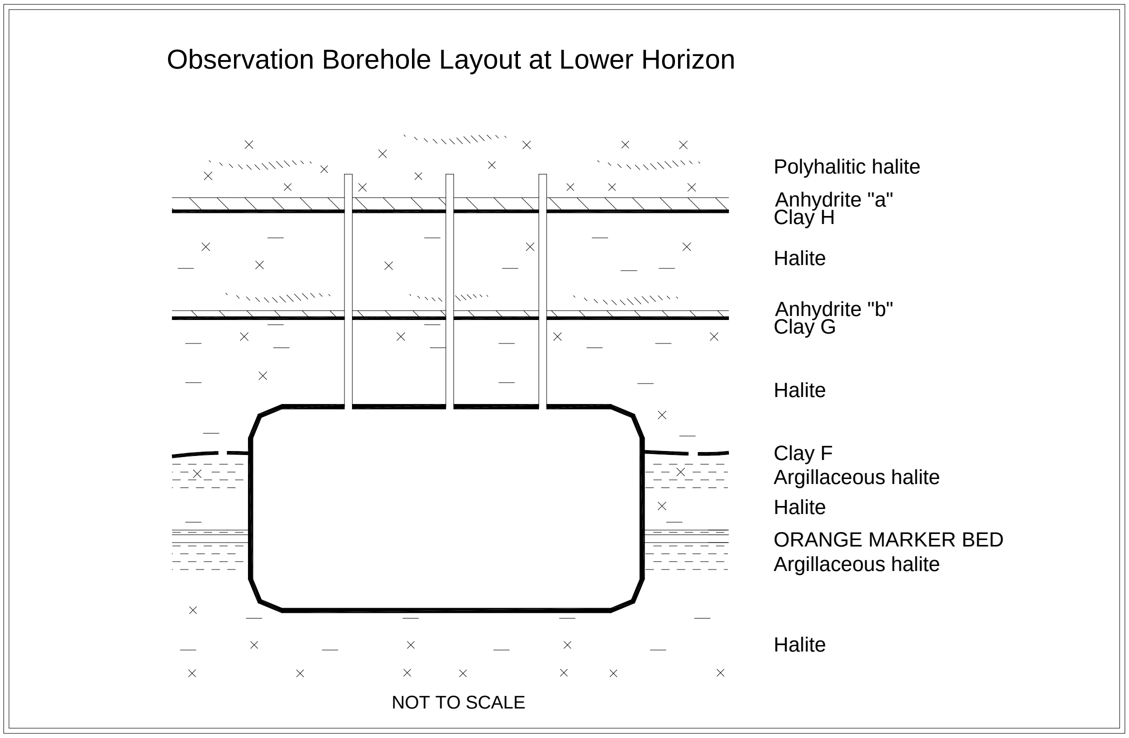

Figure 8 - 1 Example of Observation Hole Layout at Lower Horizon

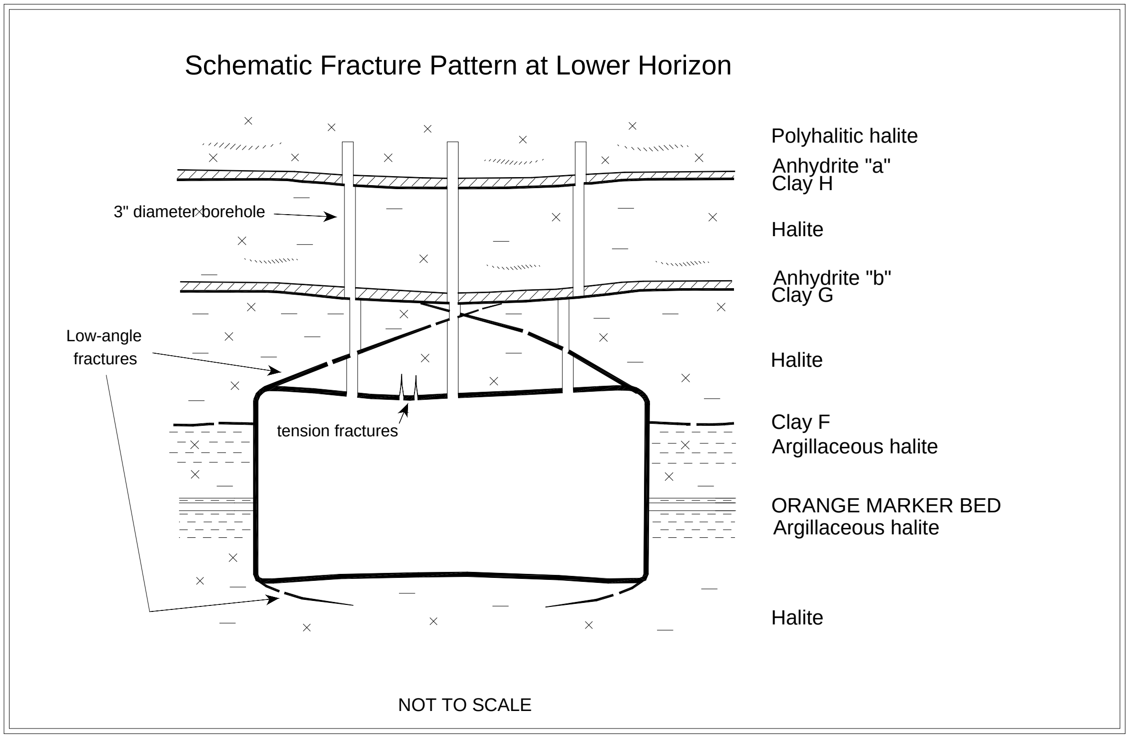

Figure 8 - 2 Typical Fracture Pattern at Lower Horizon

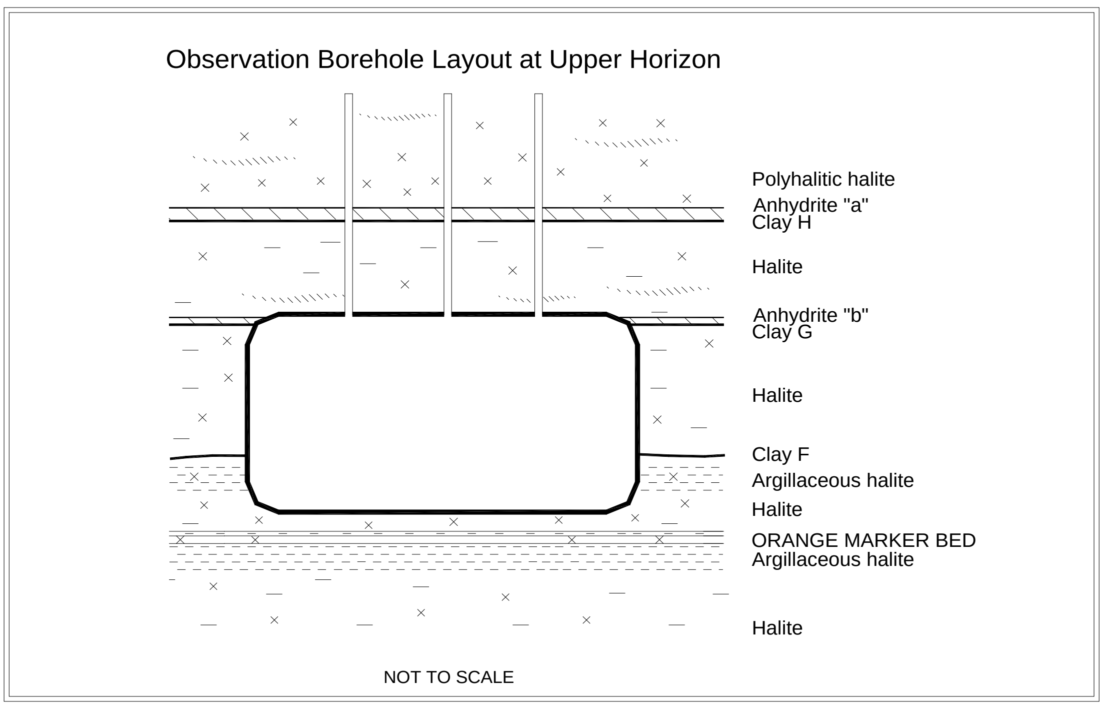

Figure 8 - 3 Example Observation Hole Layout at Upper Horizon

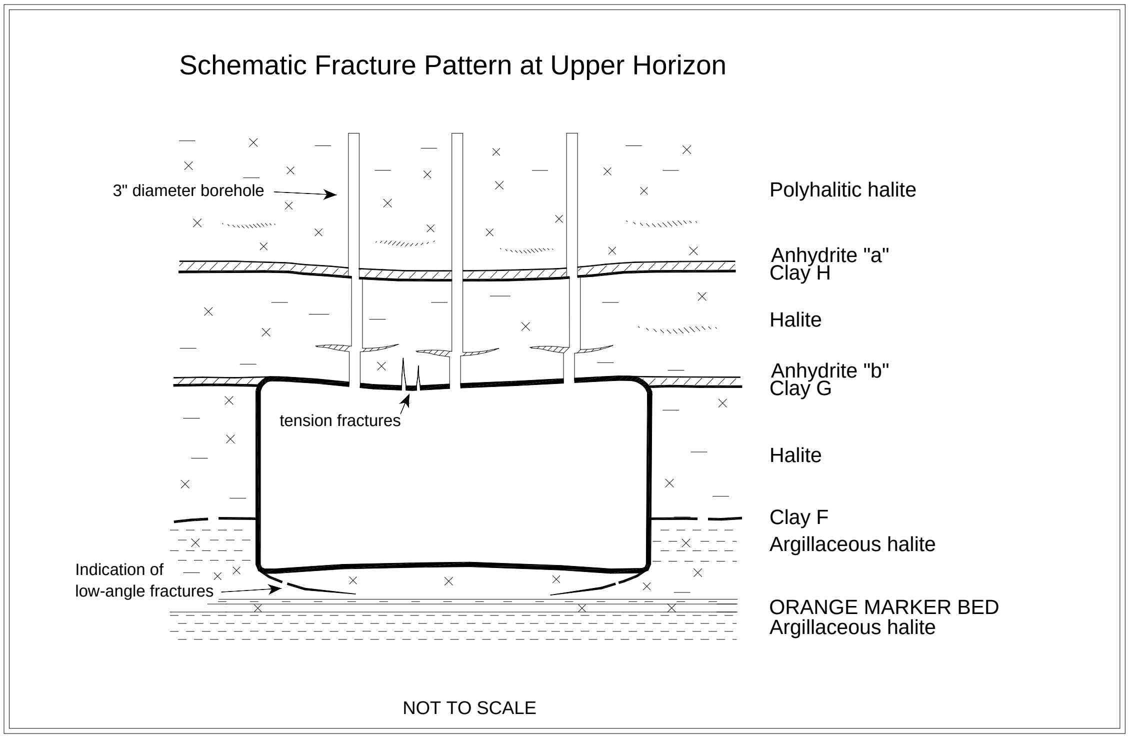

Figure 8 - 4 Typical Fracture Patterns at Upper Horizon

The separation and offset data observed in accessible observation holes in the back are presented in the supporting data document for this report. Thirty-nine accessible holes were monitored in Panel 7, and twenty in the E140 transport route between S400 and S2520. In Panel 7, thirty-nine of thirty-nine holes had separations/hangups associated with Clay G and Anhydrite "b" with an average beam height of 7.8 feet. In E140, the greatest separations were associated with Clay H and Anhydrite "a" with an average beam height of 5.6 feet. In addition, eleven holes in E140 had separations associated with anhydrite stringers in the lower portion (first three feet) of the roof beam. Twenty-two of thirty-nine holes in Panel 7, and eight of twenty holes in E140 showed some horizontal offset.

8.2 Fracture Mapping

Routine mapping documents the progression of fractures in the roof exposed on the excavation surfaces of the drifts and rooms in the underground repository. The fracture surveys are generally performed on an annual basis, and the fracture maps are updated. The fracture maps facilitate the analysis of strain in the immediate roof-beam, because they document the development and propagation of fractures through time. The supporting data in Volume II contains fracture maps for Panels 6 and 7. During this reporting period, Panel 6 fractures were mapped in Rooms 1 and in S2520 between W377 and W527, and in S3080 between W370 and W519. All areas in Panel 7 were mapped.

8.3 Stratigraphic Mapping

Stratigraphic mapping is the identification and partitioning of the sequence of rock strata based on their form, distribution, and lithologic composition. It is used to verify that there are no nonconformities in the geology within the waste disposal horizon at WIPP. During this reporting period, stratigraphic mapping was performed in the SDI areas located in the northeast portion of the WIPP underground between S90 and N940 and E300 and E1310.

8.4 Drilling and Geologic Core Descriptions

As new panels and experimental areas are excavated, holes are typically drilled and cored vertically into the back and into the floor to a nominal depth of 50 feet to verify and to describe the stratigraphic units present. During this recording period two boreholes were drilled at the intersection of N780 and S1310. A vertical up hole (SDI-BH00005) and a vertical down hole (SDI-BH00004) were drilled to a depth of 50.8 feet and 50.6 feet, respectfully. During the drilling core were collected, photographed and geologic descriptions of core were documented. The core logs are presented in Volume II.

9.0 SUMMARY

At the inception of WIPP, criteria were developed that address the design requirements (DOE, 1984). They pertained to all aspects of the mined facility and its operation as a pilot plant for the demonstration of technical and operational methods for permanent disposal of contact-handled and remote-handled TRU waste. In 1994, as the WIPP focus moved toward the permanent disposal of TRU waste, these design requirements were reassessed and replaced by a new set of requirements called system design descriptions. Table 9-1 shows the comparison of these design requirements with conditions actually observed in the underground from July 2013 through June 2014.

Underground activities were severely restricted during the months between the February 14, 2014 radiological release and the end of the reporting period. However, normal drift and room maintenance were performed during the pre-release portion of the reporting period with rib, roof, and floor scaling and trimming in various locations, and rock bolts and wire mesh installed as needed.

Panel 6 extensometers were monitored remotely and manual convergence data were collected in the accessible areas of the panel. Data from the remote and manually read instrumentation in Panel 7 were being acquired for some time prior to waste emplacement in Panel 7. All accessible areas of the underground are connected to data-loggers or are monitored manually.

The *in situ* performance of the excavations generally continues to satisfy the appropriate design criteria, although specific areas are being identified where deterioration resulting from ageing must be addressed through routine maintenance and installation of engineered systems. This deterioration has been identified through the analysis of data acquired from geomechanical instrumentation and the Geoscience Program. If the planned life of some of the openings needs to be extended, changing the geometry of the access drifts (removing unstable roof beam or rib spalls, or milling the floor for added clearance), or additional ground control (roof removal, installing bolts, mesh, or straps) may be necessary. The ground conditions in the waste disposal area and associated waste transport routes continue to slowly deteriorate; however, routine ground control installations and maintenance continue to allow safe access in the underground facility.

In addition to underground instrumentation, qualitative assessments of fracture development are documented through mapping the underground repository and inspecting the observation holes. The information acquired from these programs provides early detection of ground deterioration, contributes to the understanding of the dynamic geomechanical processes in the WIPP underground, and aids in the design of effective ground control and support systems.

Table 9 - 1 Comparison of Excavation Performance to System Design Requirements

Requirement	Comments
"The lining shall be designed for a hydrostatic pressure. . . ."	Water pressure observed on piezometers located behind the shaft liners remains below design levels.
"The key shall be designed to resist the lateral pressure generated by salt creep."	Geomechanical data from the Waste Shaft indicate that the shaft key is minimally loaded and is structurally stable. Visual inspections of all shaft keys do not indicate any deterioration due to creep loading.
"The key shall be designed to retain the rock formation and will be provided with chemical seal rings and a water collection ring with drains to prevent water from flowing down the unlined shaft from the lining above."	Shaft inspection observations and instrumentation show no indication of instability due to salt dissolution. No water has been observed flowing along the rock-liner interface.
"The underground waste disposal facilities shall be designed to provide space and adequate access for the underground equipment and temporary storage space to support underground operations."	Geomechanical instrument data and visual observations indicate that the current design provides adequate access and storage and disposal space. Ground control maintenance is performed as necessary to maintain access.
"Entries and subentries to the underground disposal area and the experimental areas shall be provided and sized for personnel safety, adequate air flow, and space for equipment."	Deformation of excavation remains within the required limits. Normal periodic maintenance consisting of rock bolting, wire meshing, trimming, and scaling continue throughout the repository. Areas such as the waste transport route undergo periodic floor trims in order to maintain adequate operating height.
"Geomechanical instrumentation shall be provided to measure the cumulative deformation of the rock mass surrounding mined drifts. . . ."	Geomechanical instrumentation is operated and maintained to meet this requirement. This annual report provides a summary and analysis of the geomechanical data.

10.0 REFERENCES

ASTM, 2006, D6026-06, *Standard Practice for Using Significant Digits in Geotechnical Data*.

Public Law 96-164, *Department of Energy National Security and Military Applications of Nuclear Energy Authorization Act of 1980*.

Title 40 CFR Part 191, "Environmental Radiation Protection Standards for Management and Disposal of Spent Nuclear Fuel, High-Level and Transuranic Radioactive Wastes."

Title 40 CFR Part 194, "Criteria for the Certification and Re-certification of the Waste Isolation Pilot Plant's Compliance with the 40 CFR Part 191 Disposal Regulations."

U.S. Environmental Protection Agency, 1998, "Criteria for the Certification and Recertification of the Waste Isolation Pilot Plant's Compliance with the Disposal Regulations: Certification Decision," Federal Register, Vol. 63, No. 95, pp. 27354, May 18, 1998, Washington, DC

Holt, R. M., and D. W. Powers, 1990, *Geologic Mapping of the Air Intake Shaft at the Waste Isolation Pilot Plant*, DOE/WIPP 90-051, Waste Isolation Pilot Plant, Carlsbad, New Mexico.

Holt, R. M., and D. W. Powers, 1984, *Geotechnical Activities in the Waste Handling Shaft, Waste Isolation Pilot Plant (WIPP) Project, Southeastern New Mexico*, WTSD TME 038, Waste Isolation Pilot Plant, Carlsbad, New Mexico.

New Mexico Environment Department (NMED), 2010, Waste Isolation Pilot Plant Hazardous Waste Facility Permit, NM4890139088-TSDF, Santa Fe, New Mexico.

Powers, D. W., and R. M. Holt, 1993, *The Upper Cenozoic Gatuña Formation of Southeastern New Mexico, New Mexico Geological Society Guidebook*, 44th Field Conference, Carlsbad Region, New Mexico and West Texas, D. W. Love et al., Eds., pp 271-282.

Powers, D. W., and R. M. Holt, 1995, *Gatuña Formation (Miocene to Pleistocene) Geology and Paleohydrology*, prepared for Westinghouse Waste Isolation Division by International Technology Corporation, Albuquerque, New Mexico.

Powers, D. W., S. J. Lambert, S. E. Shaffer, L. R. Hill, and W. D. Weart, Eds.,1978, *Geological Characterization Report, Waste Isolation Pilot Plant (WIPP) Site, Southeastern New Mexico, Vols. I and II*, SAND 78 1596; Sandia National Laboratories, Albuquerque, New Mexico.

U.S. Department of Energy (DOE), 2000, *Brine Generation Study, DOE/WIPP 00-2000, Waste Isolation Pilot Plant*, Carlsbad, New Mexico.

U.S. Department of Energy (DOE), 1986a, *Interim Geotechnical Field Data Report, DOE/WIPP 86-012*, Waste Isolation Pilot Plant, Carlsbad, New Mexico.

U.S. Department of Energy (DOE), 1986b, *Waste Isolation Pilot Plant Design Validation Final Report*, DOE/WIPP 86-010; Prepared by Bechtel National, Inc., for the U.S. Department of Energy, San Francisco, California.

U.S. Department of Energy (DOE), 1986c, *Geotechnical Activities in the Exhaust Shaft*, DOE/WIPP 86-008, Waste Isolation Pilot Plant, Carlsbad, New Mexico.

U.S. Department of Energy (DOE), 1985, *Quarterly Geotechnical Field Data Report*, DOE/WIPP-221, Waste Isolation Pilot Plant, Carlsbad, New Mexico.

U.S. Department of Energy (DOE), 1984, *Design Criteria, Waste Isolation Pilot Plant (WIPP) Revised Mission Concept-IIA*, DOE/WIPP-071; Waste Isolation Pilot Plant, Carlsbad, New Mexico.

U.S. Department of Energy (DOE), 1983, *Summary of the Results of the Evaluation of the WIPP Site and Preliminary Design Validation Program*, DOE/WIPP-161; Waste Isolation Pilot Plant, Carlsbad, New Mexico.

DRAFT

DOE/WIPP-15-3556
Volume 2

Waste Isolation Pilot Plant

Geotechnical Analysis Report For July 2013 – June 2014

Supporting Data

U.S. Department of Energy

October 2015

This page was intentionally left blank.

This document has been submitted as required to:

U.S. Department of Energy
Office of Scientific and Technical Information
PO Box 62
Oak Ridge, TN 37831
(865) 576-8401

Additional information about this document may be obtained by calling 1-800-336-9477

Unlimited, publicly available full-text scientific and technical reports produced since 1991 are available online at Information Bridge (www.osti.gov/bridge).

U.S Department of Energy and its contractors may obtain full-text reports produced prior to 1991 in paper form for a processing fee from:

U.S. Department of Energy
Office of Scientific and Technical Information
P.O. Box 62
Oak Ridge, TN 37831-0062
Telephone: (865) 576-8401
Facsimile: (865) 576-5728
E-mail: reports@osti.gov

Available for sale to the public from:

U.S. Department of Commerce
National Technical Information Service
5301 Shawnee Rd
Alexandra, VA 22312
Phone: (800) 553-6847 or (703) 605-6000
Fax: (703) 605-6900
Email: info@ntis.gov

This page was intentionally left blank.

FOREWORD AND ACKNOWLEDGMENTS

This report contains an assessment of the geotechnical status of the Waste Isolation Pilot Plant (WIPP). During the excavation of the principal underground access and experimental areas, the status was reported quarterly. Since 1987, when the initial construction phase was completed, reports have been published annually. This report presents and analyzes data collected from July 1, 2013, to June 30, 2014.

This Geotechnical Analysis Report (GAR) was written to meet the needs of several audiences. It satisfies requirements contained in the WIPP Hazardous Waste Facility Permit[1] (HWFP) and the Certification of Compliance[2] with Subparts B and C, Title 40 *Code of Federal Regulations* (CFR) Part 191, "Environmental Radiation Protection Standards for Management and Disposal of Spent Nuclear Fuel, High-Level and Transuranic Radioactive Wastes." It focuses on the geotechnical performance of the various components of the underground facility, including the shafts, shaft stations, access drifts, and waste disposal areas. The results of investigations of excavation effects and other geotechnical studies are also included.

The report compares the geotechnical performance of the repository to the design criteria. It describes the techniques that were used to acquire the data. The depth and breadth of the evaluation of the different components of the underground facility vary according to the types and quantities of data available and the complexity of the recorded geotechnical responses. Graphic documentation of data and tabular documentation of instrument history can be provided upon request.

This GAR was prepared by Nuclear Waste Partnership LLC (NWP) for the U.S. Department of Energy (DOE), Carlsbad Field Office (CBFO), in Carlsbad, New Mexico. Work was supported by the DOE under Contract No. DE-EM0001971.

[1] New Mexico Environment Department (NMED), 2012, Waste Isolation Pilot Plant Hazardous Waste Facility Permit, NM4890139088-TSDF, Santa Fe, NM

[2] U.S. Environmental Protection Agency, 1998, "Criteria for the Certification and Recertification of the Waste Isolation Pilot Plant's Compliance with the Disposal Regulations: Certification Decision," Federal Register, Vol. 63, No. 95, pp. 27354, May 18, 1998, Washington, DC

Table of Contents

List of Tables

SHAFTS AND KEYS

Salt Handling Shaft

SHAFT STATIONS

Salt Handling Shaft Station

Waste Disposal Area Panel 1

Waste Disposal Area Panel 2

Waste Disposal Area Panel 3

Waste Disposal Area Panel 4

Waste Disposal Area Panel 5

Waste Disposal Area Panel 6

Salt Disposal Investigations (Continued)

Geosciences Program

Geosciences Program (continued)

1.0 Introduction

This report is a compilation of geotechnical data presented as plots for each active instrument installed in the underground at the Waste Isolation Pilot Plant (WIPP) through June 30, 2014. A summary of the geotechnical analyses that were performed using the enclosed data is provided in Volume 1 of the Geotechnical Analysis Report (GAR).

1.1 Instrumentation

Geomechanical instrument data included in this report reflect the measurements of the geomechanical response of the underground and shafts. The instruments consist of convergence points, borehole extensometers, rockbolt load cells, pressure cells, strain gages, piezometers, and joint meters.

Closure measurements are taken at convergence points. Rock displacement is calculated by measuring the distance between two opposing points. Displacement is monitored over time and is plotted as closure versus time. Annual rates of closure are calculated for the convergence data and are compared with annual closure rates from previous reporting periods.

Borehole extensometers are used to determine the absolute movements of the ground around the openings. With these instruments, rods or wires are placed into a hole and anchored at various depths. The displacement at the extensometer head (located near the excavation face) is measured relative to each of the fixed anchors. These data are used in the extensometer *displacement* plots presented here. As part of the post-processing of acquired extensometer data a *relative displacement* value is calculated. The deepest anchor is assumed to be fixed in undisturbed ground and a displacement for the remaining anchors relative to the deepest anchor is calculated. Annual rates of collar displacement are calculated for each extensometer and are compared with the annual displacement rate reported during the previous reporting period.

Rockbolt load cells are used to determine the ground loading and the effectiveness of rockbolts. Plots consist of load versus time for each instrumented bolt.

Earth pressure cells and strain gages are used in and around the shaft liners to determine their loads. These are also depicted in time-based plots. Monitoring of these instruments indicates whether there is any stress buildup in the shaft lining systems.

Piezometers are used to measure the gauge pressure of groundwater. They have been installed in the shafts at varying elevations to monitor the hydraulic head acting on the shaft liners. Plots from piezometers are presented as pressure versus time.

Joint meters are installed perpendicular to a crack and monitor any changes in separation of the crack which may occur over time.

1.2 Data Plot Explanation

Data are presented in graphical form for ease in interpretation. Time-based plots are used in this report. Each plot generally consists of a legend in the upper right-hand corner that gives the array name and specific location of the instrument or point evaluated. The legend ties the graphical cross-sectional representation of the drift or shaft typically presented in the lower right-hand corner to the symbols on the curve in the graph. For extensometers, each anchor is designated with an alpha character "A" closest to the collar and "B," "C," "D," or "E" for the furthest point from the collar (the deepest anchor). For convergence points, the horizontal and vertical sections of the drift are referred to as chords. Breaks in the graph for convergence data and a numeric designator added to the legend typically indicate that the convergence point was lost due to normal mine maintenance activities and later reinstalled.

1.3 Report Organization

Chapter 1.0 provides an introduction to this Supporting Data volume of the GAR. Chapter 2.0 provides instrument data analysis for the Salt Handling Shaft, Waste Shaft, and Exhaust Shaft followed by data plots for the extensometers, piezometers, earth pressure cells, spot welded strain gages, and embedment strain gages installed in the shafts. Chapter 3.0 provides instrument data analysis for the Salt Handling Shaft Station and Waste Shaft Station, an instrument data summary only for the area immediately surrounding the Air Intake Shaft, and data plots for extensometers, convergence points, and rockbolt load cells for all three locations. Chapter 4.0 provides instrument data analysis for the access drifts followed by data plots for the extensometers, convergence points, joint meters and rock bolt load cells. Chapter 5.0 provides instrument data analysis for the Waste Disposal Area followed by data plots for the extensometers, rock bolt load cells and convergence points. Chapter 6.0 provides convergence point instrument data analysis for the Salt Disposal Investigations (SDI) area. Chapter 7.0 provides geologic data collected through the mapping of fractures, stratigraphic mapping and the observed displacements in vertical boreholes.

2.0 Instrumentation Summary for Shafts

Originally, the Salt, Waste and Exhaust Shafts were instrumented with geomechanical instrumentation. The instrument readings from the Waste and Exhaust Shafts are no longer available due to failed instruments, broken cabling and/or inoperative, obsolete data acquisition equipment. Table 2-1 presents data and analysis of the Salt Shaft. Plots of the instrument data are presented as Figures 2-1 through 2-12.

Table 2-1
Salt Handling Shaft Data Analysis

Piezometers

Field Tag	Level feet	Figure Number	Date of 2013-2014 Max. Reading	2013-2014 Maximum Pressure Readings (psi)	Date of 2012-2013 Max. Reading	2012-2013 Maximum Pressure Readings (psi)	Change in Maximum Pressure From Previous Year (psi)	Comments
37X-PE-00201	580	2-1	05/20/14	87	03/08/13	88	-1	
37X-PE-00202	580	2-1	05/20/14	99	05/09/13	96	4	
37X-PE-00203	620	2-2	05/20/14	192	03/08/13	192	1	
37X-PE-00204	620	2-2	05/20/14	167	07/30/12	155	12	
37X-PE-00205	691	2-3	08/01/13	164	06/06/13	199	-35	
37X-PE-00206	691	2-3	08/01/13	161	06/06/13	196	-35	
37X-PE-00209	802	2-4	09/06/13	59	08/08/12	62	-3	
37X-PE-00210	802	2-4	09/06/13	60	09/27/12	62	-2	
37X-PE-00211	850	2-5	07/03/13	105	08/08/12	96	9	
37X-PE-00212	850	2-5	07/03/13	98	06/06/13	131	-33	

Earth Pressure Cells

Field Tag	Level feet	Figure Number	Date of 2013-2014 Max. Reading	2013-2014 Maximum Pressure Readings (psi)	Date of 2012-2013 Max. Reading	2012-2013 Maximum Pressure Readings (psi)	Change in Maximum Pressure From Previous Year (psi)	Comments
37X-WE-00201	862.4	2-6	09/06/13	-9	08/08/12	-6	-3	
37X-WE-00202	862.4	2-6	08/01/13	-26	08/08/12	-26	-1	
37X-WE-00203	862.4	2-6	05/13/14	6	05/09/13	6	0	

Spot-Welded Strain Gages

Field Tag	Level feet	Figure Number	Date of 2013-2014 Max. Reading	2013-2014 Maximum Pressure Readings (psi)	Date of 2012-2013 Max. Reading	2012-2013 Maximum Pressure Readings (psi)	Change in Maximum Pressure From Previous Year (psi)	Comments
37X-ZE-00206	856.3	2-7	09/06/13	652	08/08/12	686	-34	
37X-ZE-00220	862.4	2-8	09/06/13	957	09/19/12	956	1	
37X-ZE-00223	862.4	2-8	03/04/14	690	11/12/12	714	-24	

Table 2-1
Salt Handling Shaft Data Analysis (Continued)

Embedment Strain Gages								
Field Tag	Level feet	Figure Number	Date of 2013-2014 Max. Reading	2013-2014 Maximum Strain Readings (με)	Date of 2012-2013 Max. Reading	2012-2013 Maximum Strain Readings (με)	Change in Maximum Strain From Previous Year (με)	Comments
37X-ZE-00209	856.3	2-9	01/10/14	-538	03/08/13	-536	-2	
37X-ZE-00210	856.3	2-9	09/06/13	1017	08/08/12	1030	-13	
37X-ZE-00211	856.3	2-9	07/03/13	363	08/08/12	364	-1	
37X-ZE-00212	856.3	2-9	02/07/14	-928	01/02/13	-858	-70	
37X-ZE-00213	856.3	2-9	07/03/13	404	08/08/12	402	2	
37X-ZE-00214	856.3	2-9	09/06/13	140	08/08/12	166	-26	
37X-ZE-00215	856.3	2-9	07/03/13	155	08/08/12	155	0	
37X-ZE-00216	856.3	2-9	08/01/13	680	08/08/12	694	-14	
37X-ZE-00235	856.3	2-10	09/06/13	315	08/08/12	314	1	
37X-ZE-00236	856.3	2-10	01/10/14	-406	02/04/13	-403	-3	
37X-ZE-00237	856.3	2-10	02/07/14	-181	08/08/12	155	-336	
37X-ZE-00238	856.3	2-10	08/01/13	128	08/08/12	150	-22	
37X-ZE-00225	862.4	2-11	08/01/13	564	08/08/12	575	-11	
37X-ZE-00239	862.4	2-12	09/06/13	425	08/08/12	429	-4	

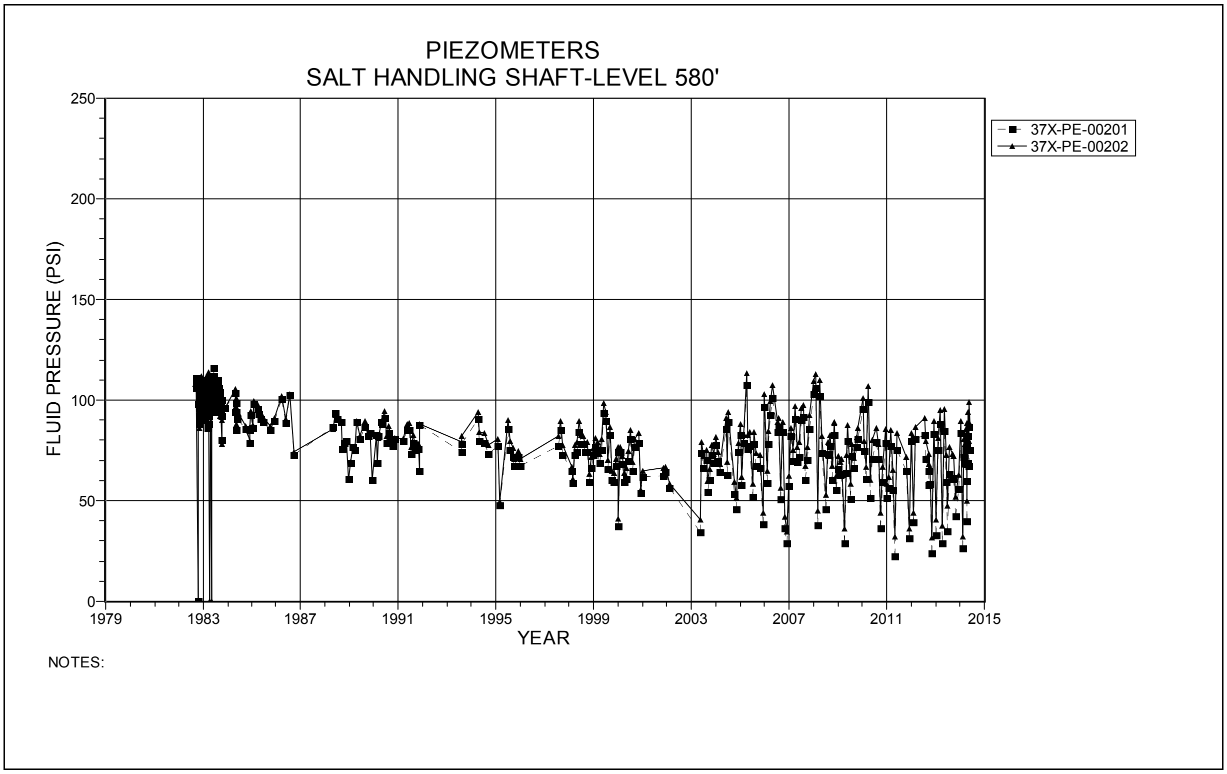

Figure 2-1 Piezometers Salt Handling Shaft
–Level 580 at the Forty-niner Member

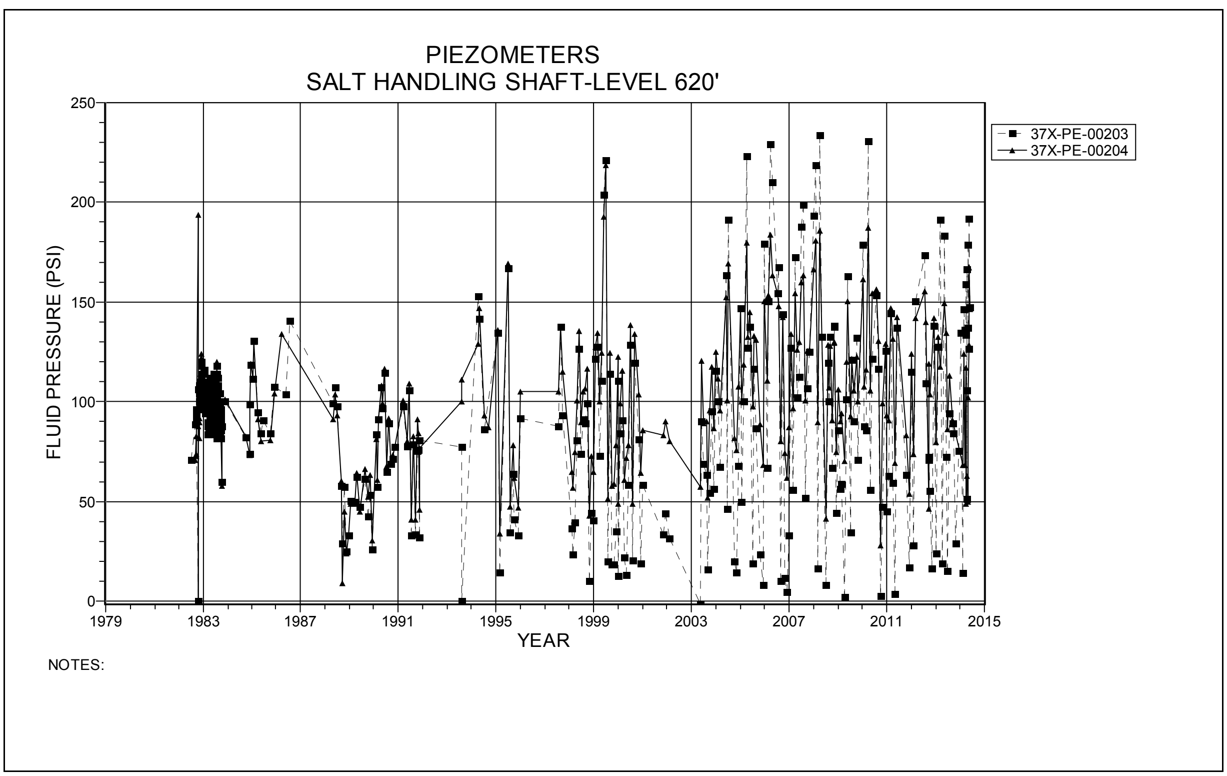

Figure 2-2 Piezometers Salt Handling Shaft
– Level 620 at the Magenta Dolomite Member

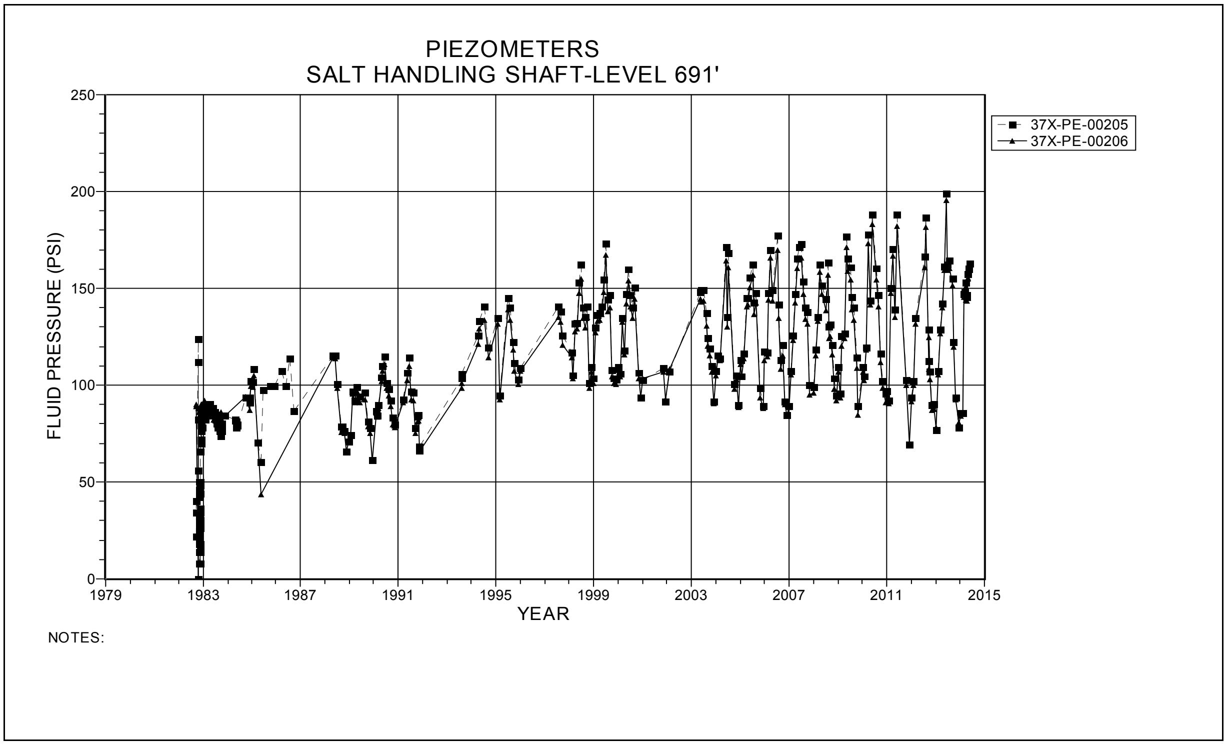

Figure 2-3 Piezometers Salt Handling Shaft
– Level 691 at the Tamarisk Member

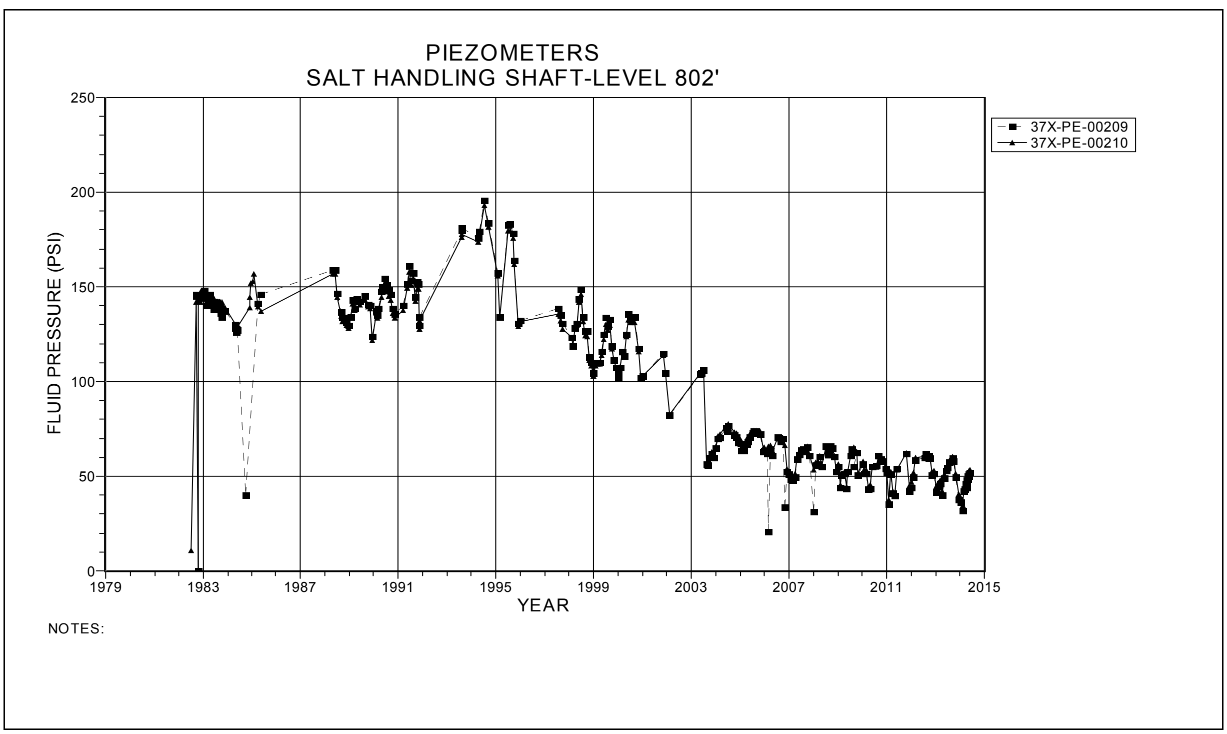

Figure 2-4 Piezometers Salt Handling Shaft
– Level 802 at the Los Medaños Member

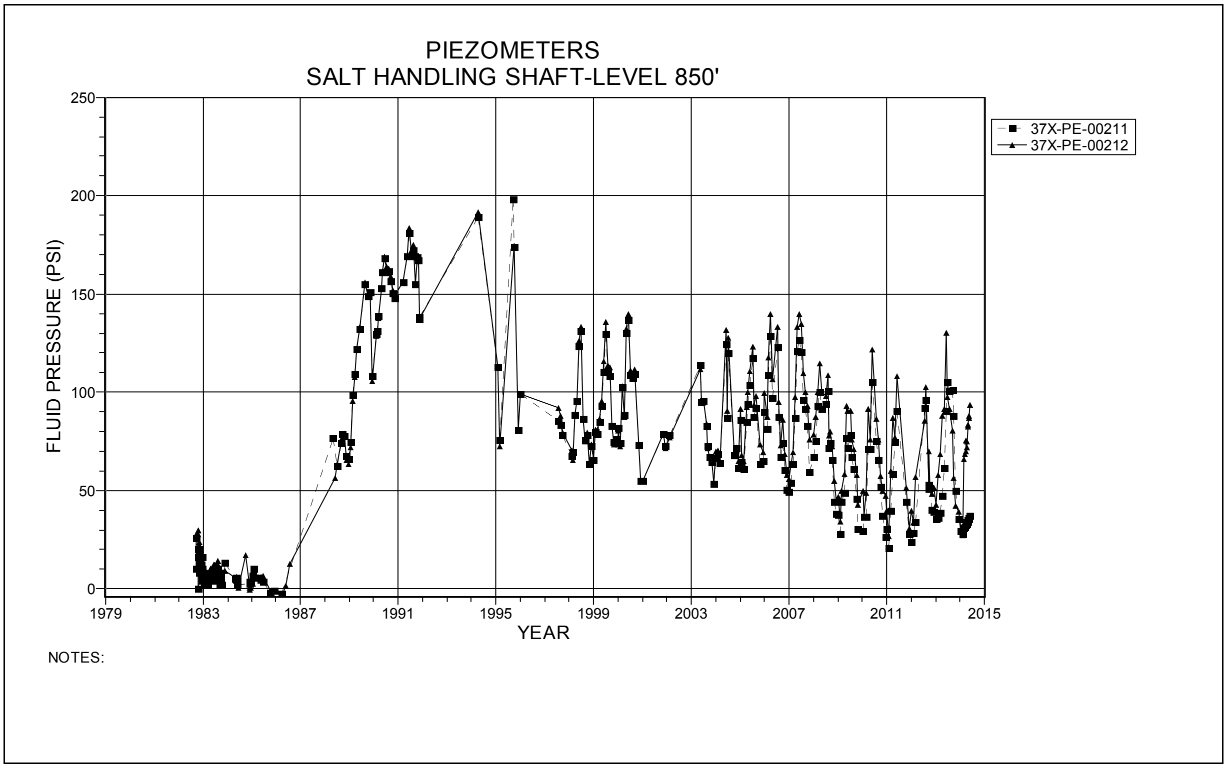

Figure 2-5 Piezometers Salt Handling Shaft
– Level 850 at the Rustler-Salado Contact

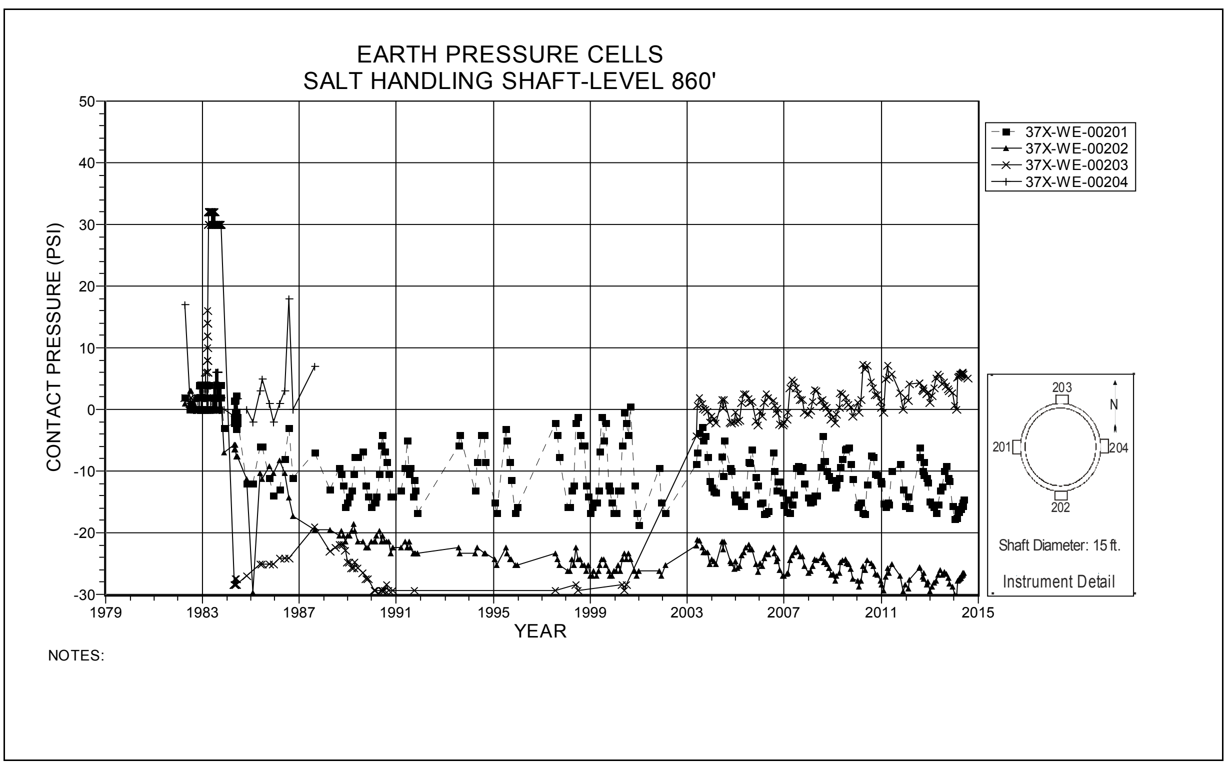

Figure 2-6 Earth Pressure Cells Behind Shaft Key
Salt Handling Shaft Key – Level 860

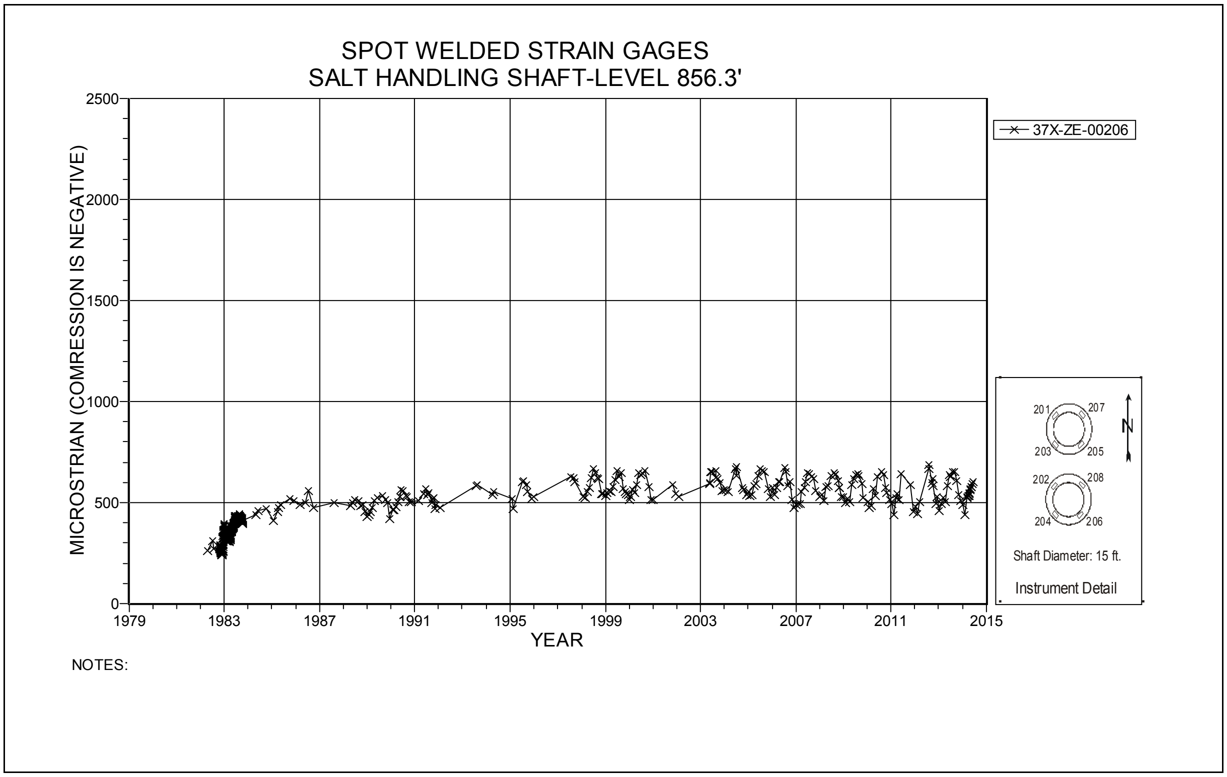

Figure 2-7 Spot-Welded Strain Gage
Salt Handling Shaft Key – Level 856.3

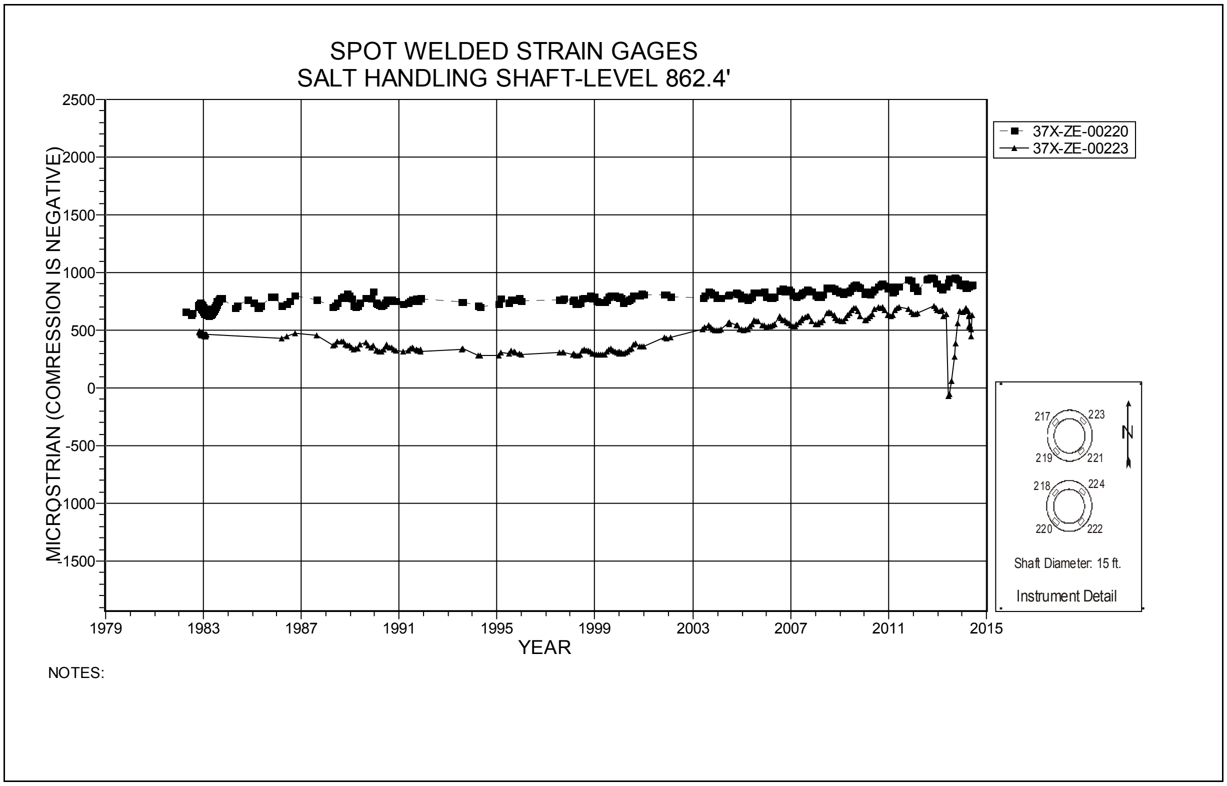

Figure 2-8 Spot-Welded Strain Gages
Salt Handling Shaft Key – Level 862.4

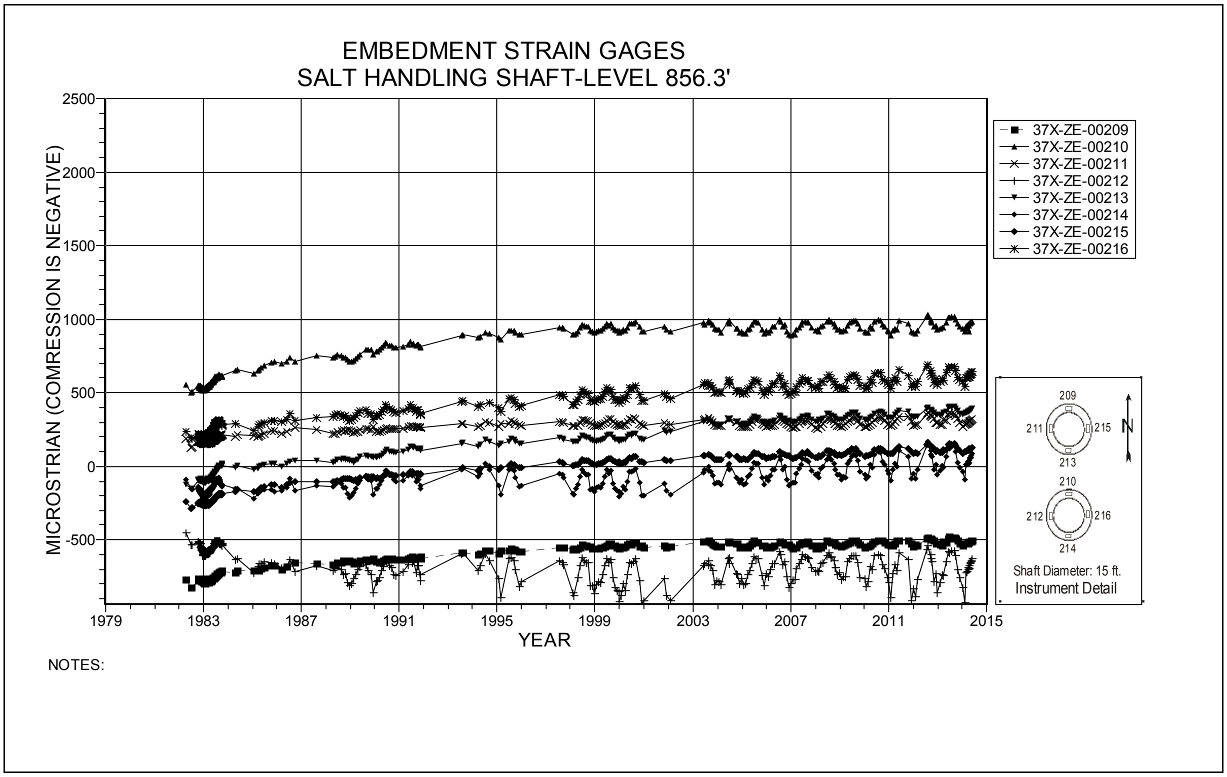

Figure 2-9 Embedment Strain Gages
Salt Handling Shaft Key – Level 856.3

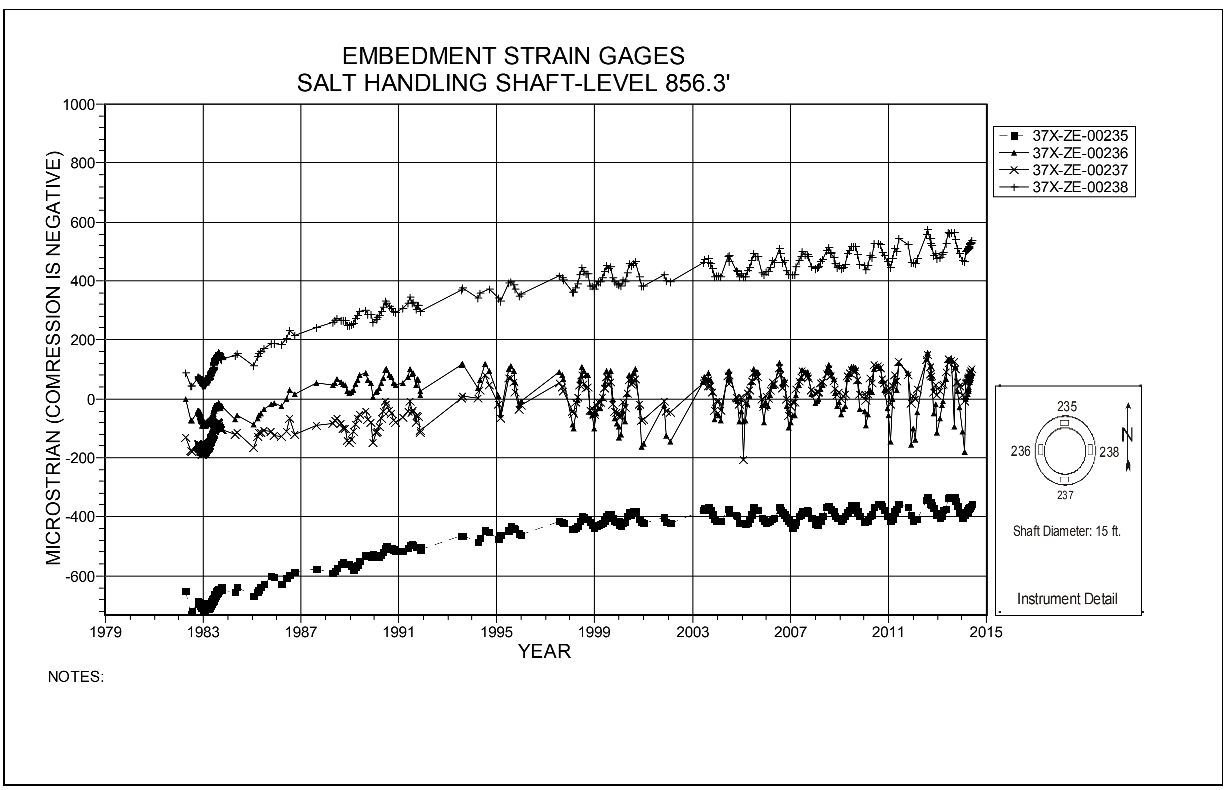

Figure 2-10 Embedment Strain Gages
Salt Handling Shaft Key Level 856.3

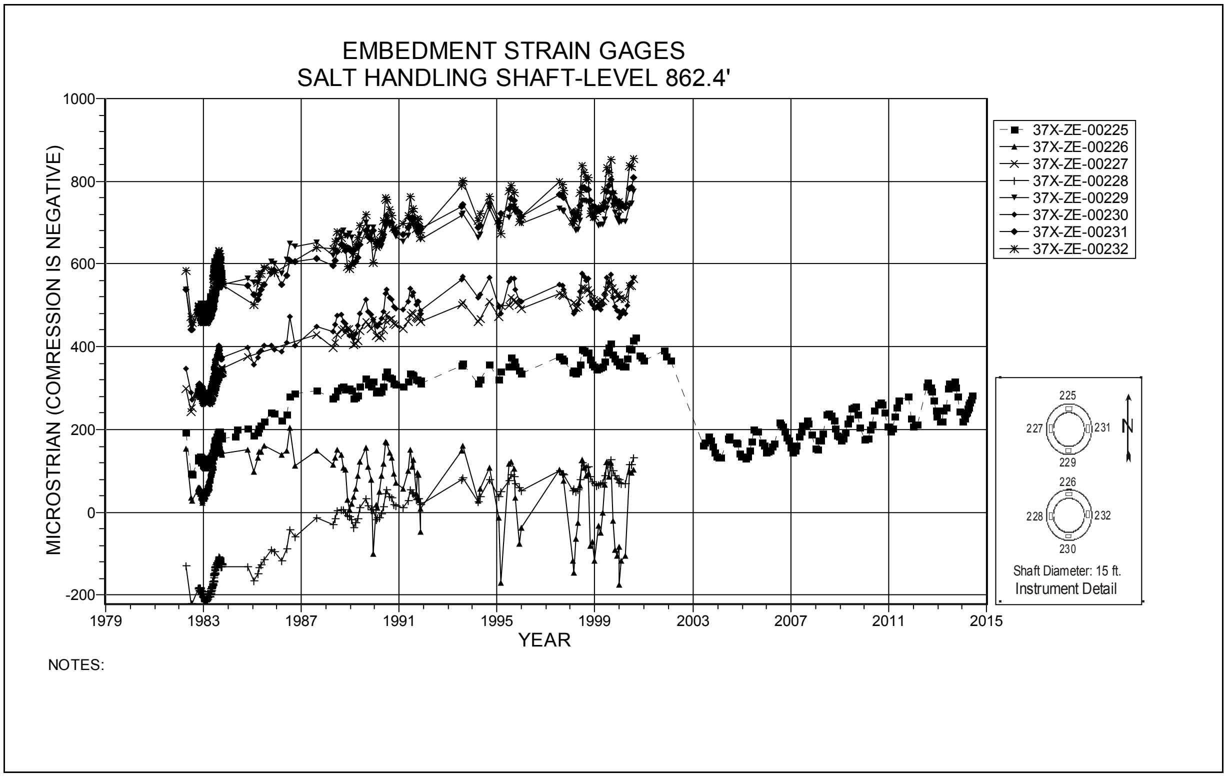

Figure 2-11 Embedment Strain Gage
Salt Handling Shaft Key Level 862.4

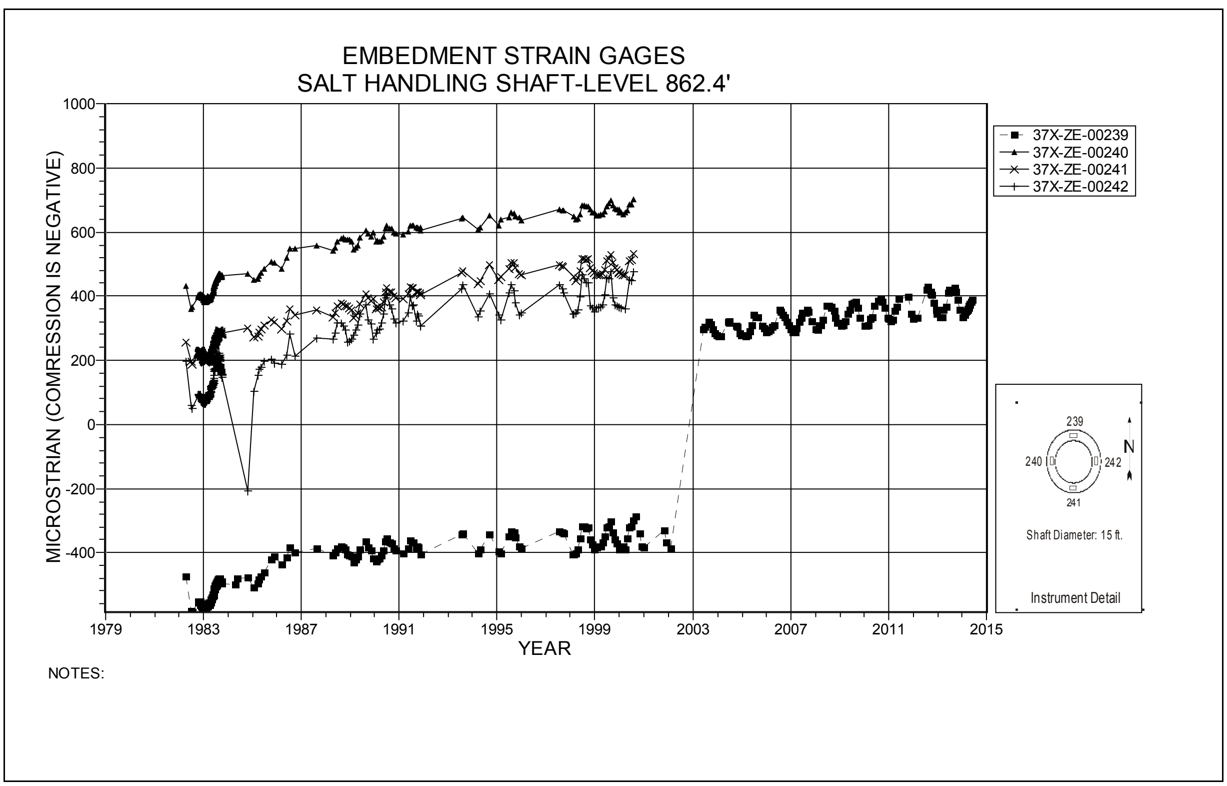

Figure 2-12 Embedment Strain Gage
Salt Handling Shaft Key – Level 862.4

This page was intentionally left blank.

3.0 Instrumentation Summary for Shaft Stations

Instrumentation data analysis for the Salt Handling Shaft Station, Waste Shaft Station, and the area around the Air Intake Shaft follow. Table 3-1 presents data analyses for each of the Salt Handling Shaft Station instruments. Figures 3-1 through 3-6 present plots of the instrumentation data for the Salt Handling Shaft Station.

Table 3-2 presents data and analysis for the Waste Shaft Station. Plots from the instrumentation in the Waste Shaft Station are presented as Figures 3-7 through 3-10.

Table 3-3 and Figures 3-11 through 3-16 present the data from rock bolt load cells and borehole extensometers located in the immediate area around the Air Intake Shaft.

Table 3-1
Salt Handling Shaft Station Data Analysis

Convergence Points

Field Tag	Location	Figure Number	Last Reading 2013-2014 Date	Last Reading 2013-2014 Inches	Cumulative Displacement (inches)	Closure Rate 2013 to 2014 (in/year)	Closure Rate 2012 to 2013 (in/year)	Rate Change Percent	Comments
E0-S18-8 A-E	E0 Drift-S18	3-1	11/18/13	3.494	24.646	1.8	1.7	6%	
E0-S18-6 B-D	E0 Drift-S18	3-2	01/21/14	4.167	27.266	1.9	1.9	0%	
E0-S18-5 H-F	E0 Drift-S18	3-2	11/18/13	2.202	16.663	1.1	1.1	0%	
E0-S30-6 A-C	E0 Drift-S30	3-3	01/21/14	3.696	25.727	1.6	1.7	-6%	
E0-S65-5 A-C	E0 Drift-S65	3-4	01/21/14	2.532	17.892	1.1	1.2	-8%	

Extensometers

Field Tag	Location	Figure Number	Date of Last Reading	Collar Displacement Relative to Deepest Anchor (inches)	Displacement Rate 2013 to 2014 (in/year)	Displacement Rate 2012 to 2013 (in/year)	Rate Change Percent	Comments
51X-GE-01026-2	E0-S30 Roof	3-5	01/22/14	1.453	0.2	0.4	-50%	
51X-GE-01027-2	E0-S60 Roof	3-6	01/22/14	0.987	0.2	0.3	-33%	

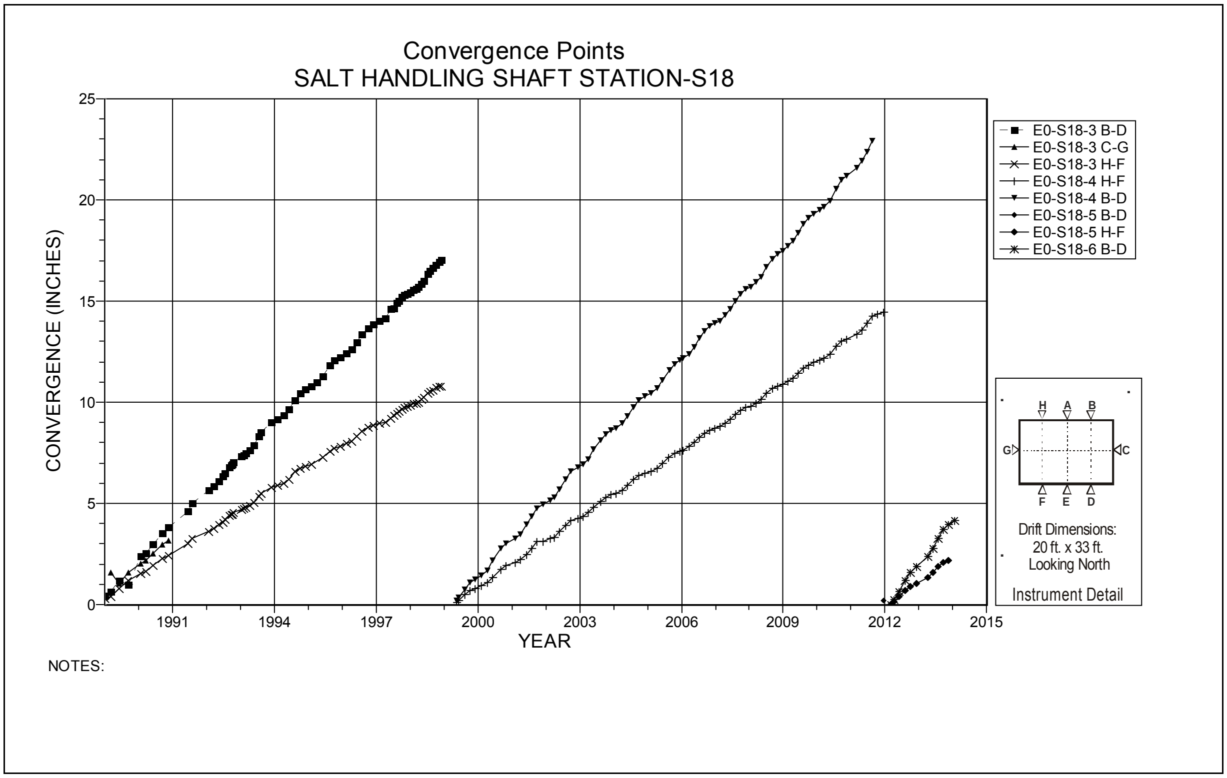

Figure 3-1 Convergence Point Array
Salt Handling Shaft Station at S18 – Centerline – Roof to Floor

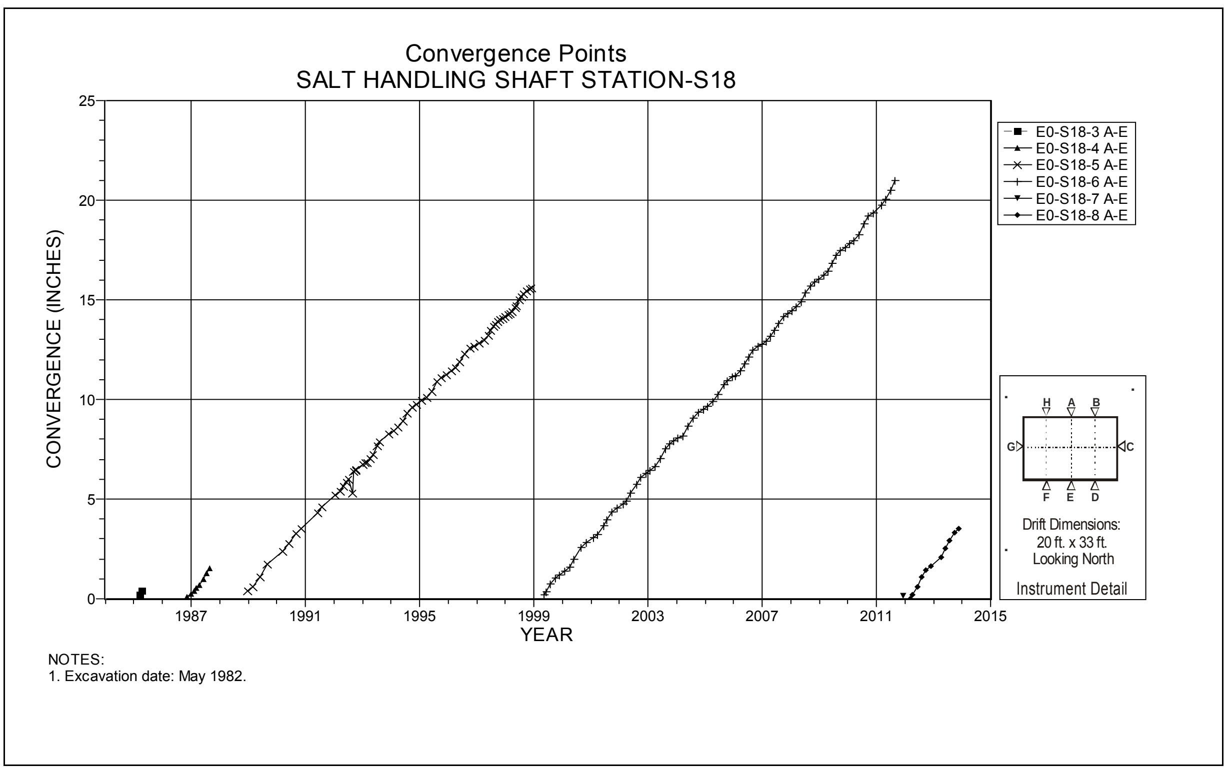

Figure 3-2 Convergence Point Array
Salt Handling Shaft Station at S18 – Quarter Points – Roof to Floor

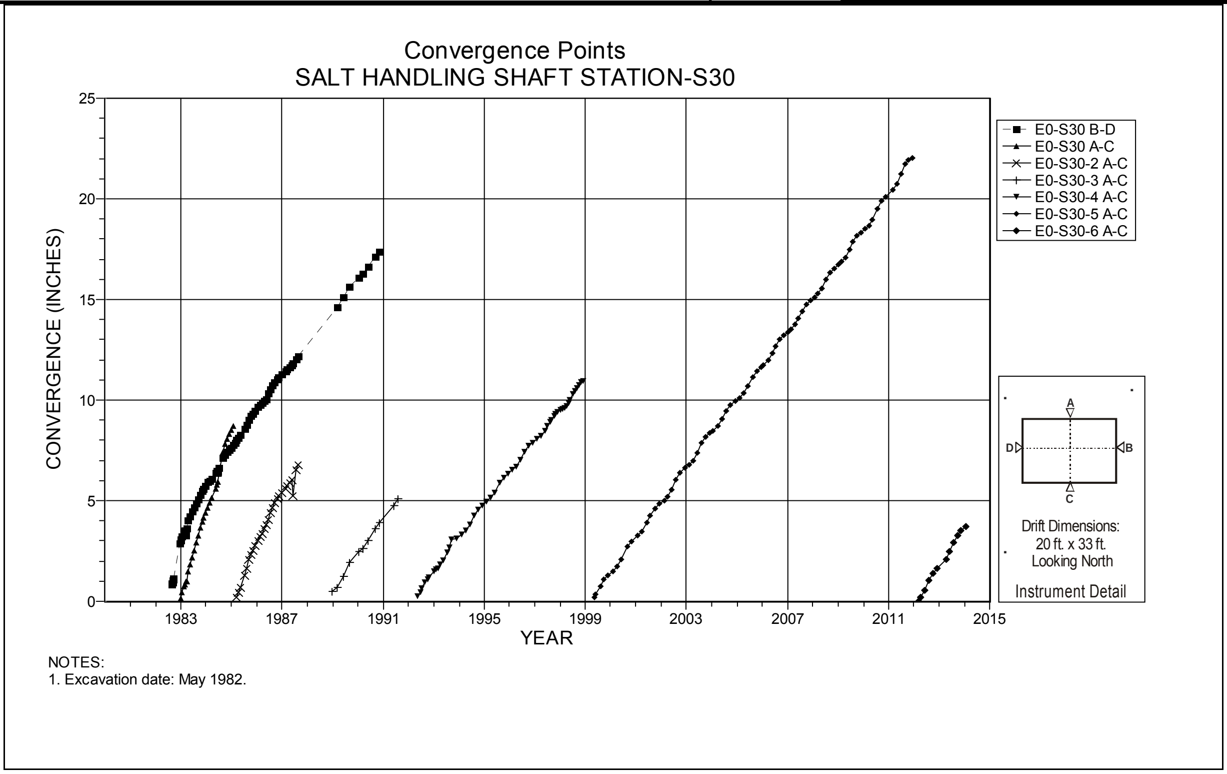

Figure 3-3 Convergence Point Array
Salt Handling Shaft Station at S30 – Roof to Floor

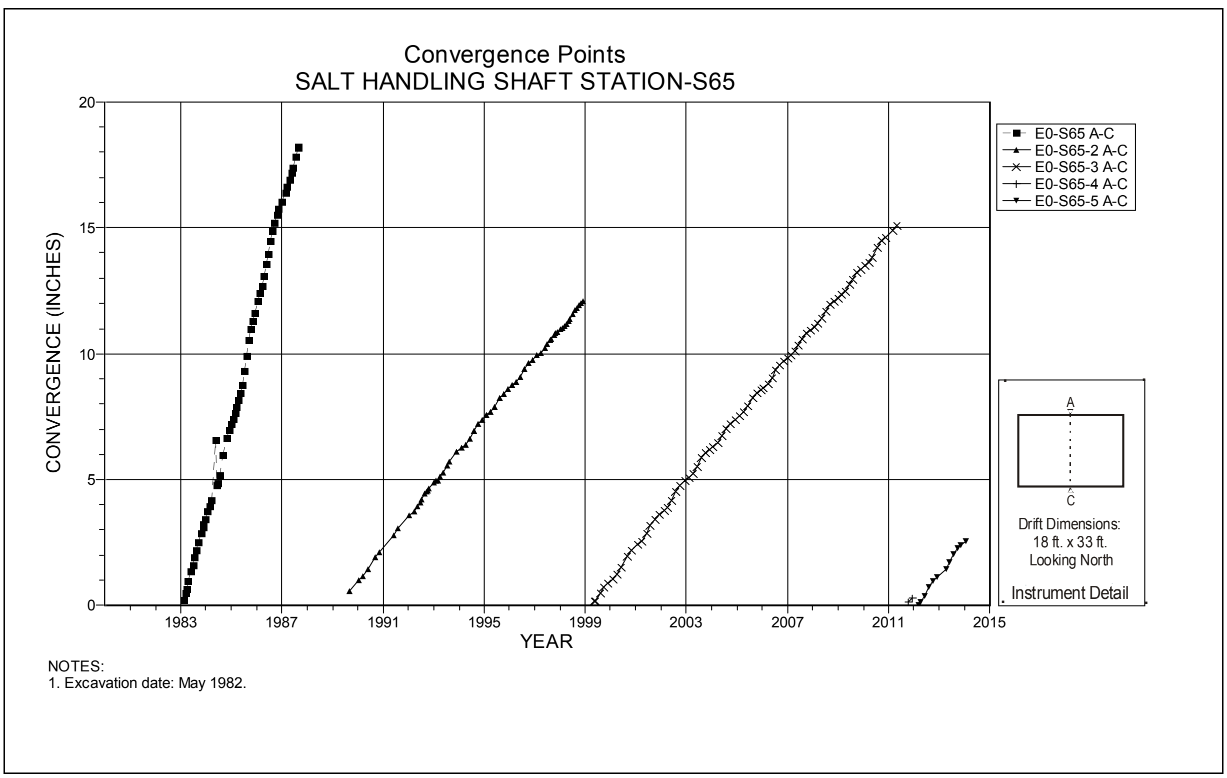

Figure 3-4 Convergence Point Array
Salt Handling Shaft Station at S65 – Roof to Floor

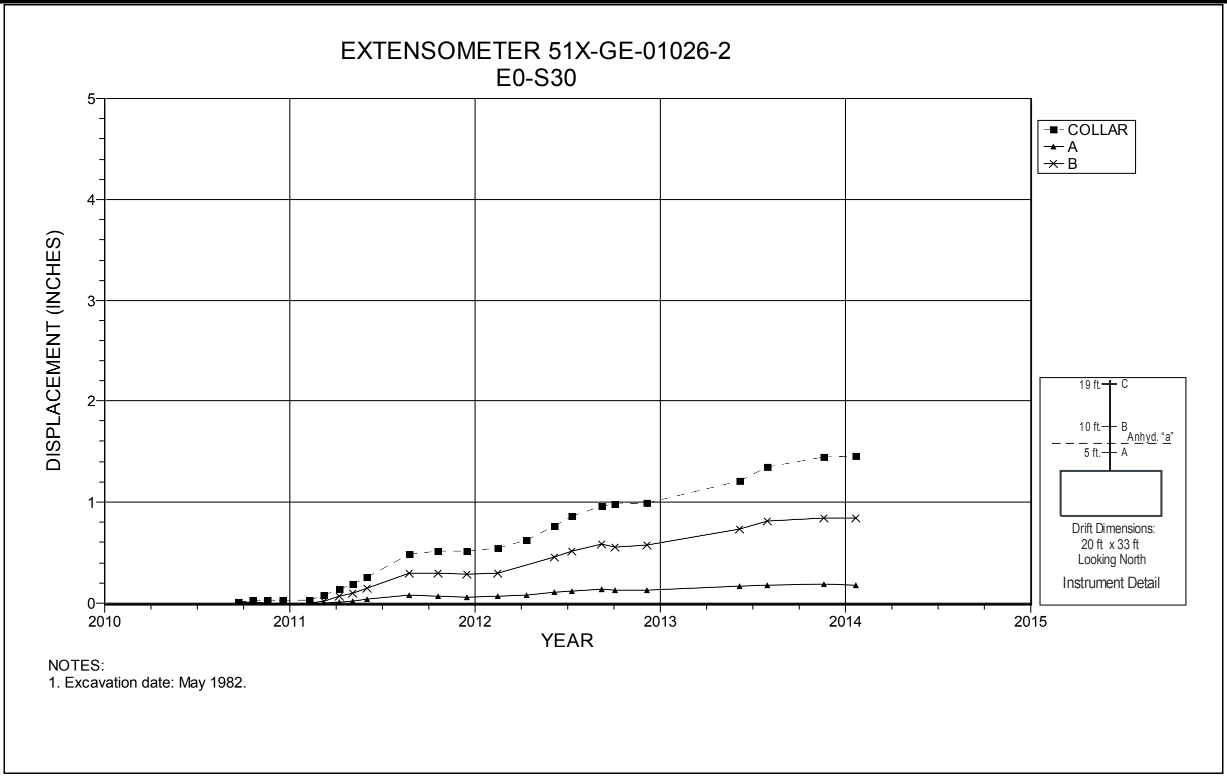

Figure 3-5 Extensometer 51X-GE-01026-2
Salt Handling Shaft Station at S30 – Roof

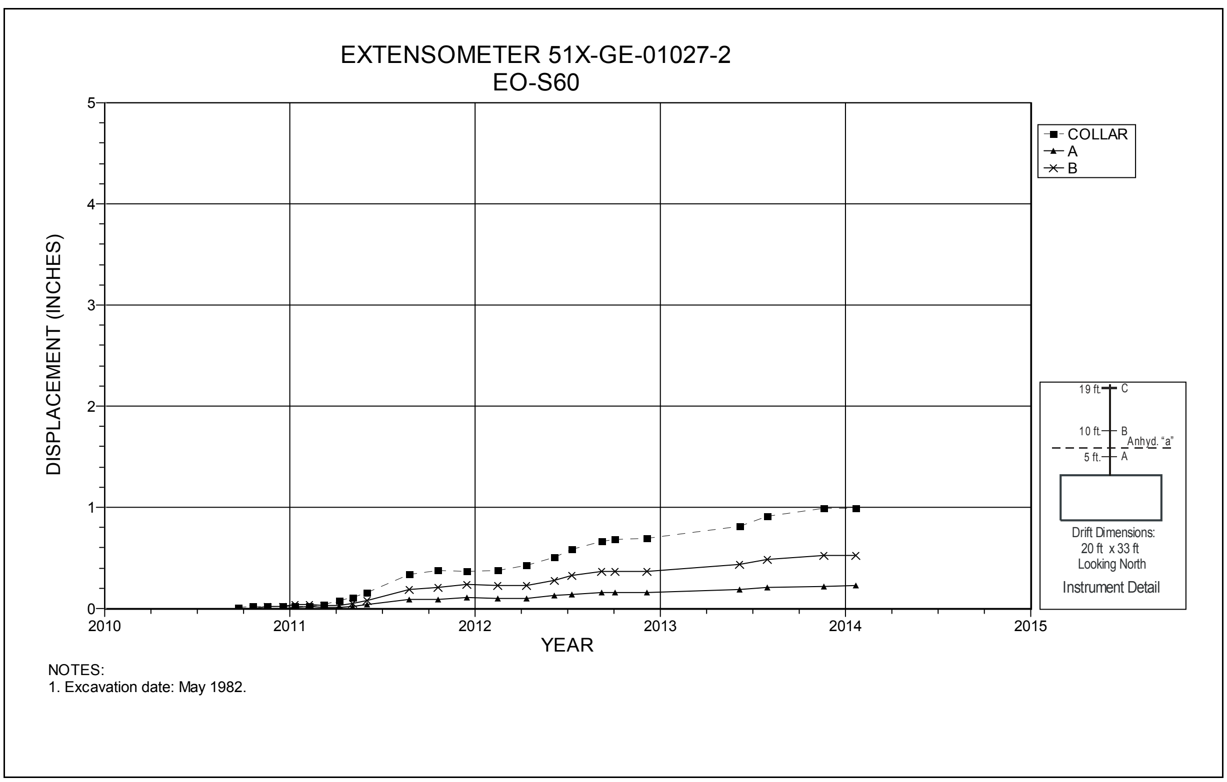

Figure 3-6 Extensometer 51X-GE-01027-2
Salt Handling Shaft Station at S60 – Roof

Table 3-2
Waste Shaft Station Data Analysis

Extensometers

Fieldtag	Location	Figure Number	Date of Last Reading	Collar Displacement Relative to Deepest Anchor (inches)	Displacement Rate 2013 to 2014 (in/year)	Displacement Rate 2012 to 2013 (in/year)	Rate Change Percent	Comments
51X-GE-00268	Waste Shaft Station - W30	3-7	01/22/14	7.051	0.1	0.1	0%	
51X-GE-00404-2	Waste Shaft Station - E35	3-8	06/24/14	1.222	0.3	0.3	0%	

Convergence Points

Field Tag	Location	Figure Number	Last Reading 2013-2014		Cumulative Displacement (inches)	Closure Rate 2013 to 2014 (in/year)	Closure Rate 2012 to 2013 (in/year)	Rate Change Percent	Comments
			Date	Inches					
S400-E32 B-D	Waste Shaft Station - E32	3-9	02/05/14	6.435	6.435	1.1	1.4	-21%	
S400-E85 B-D	Waste Shaft Station - E85	3-10	02/05/14	6.590	6.590	1.2	1.4	-14%	

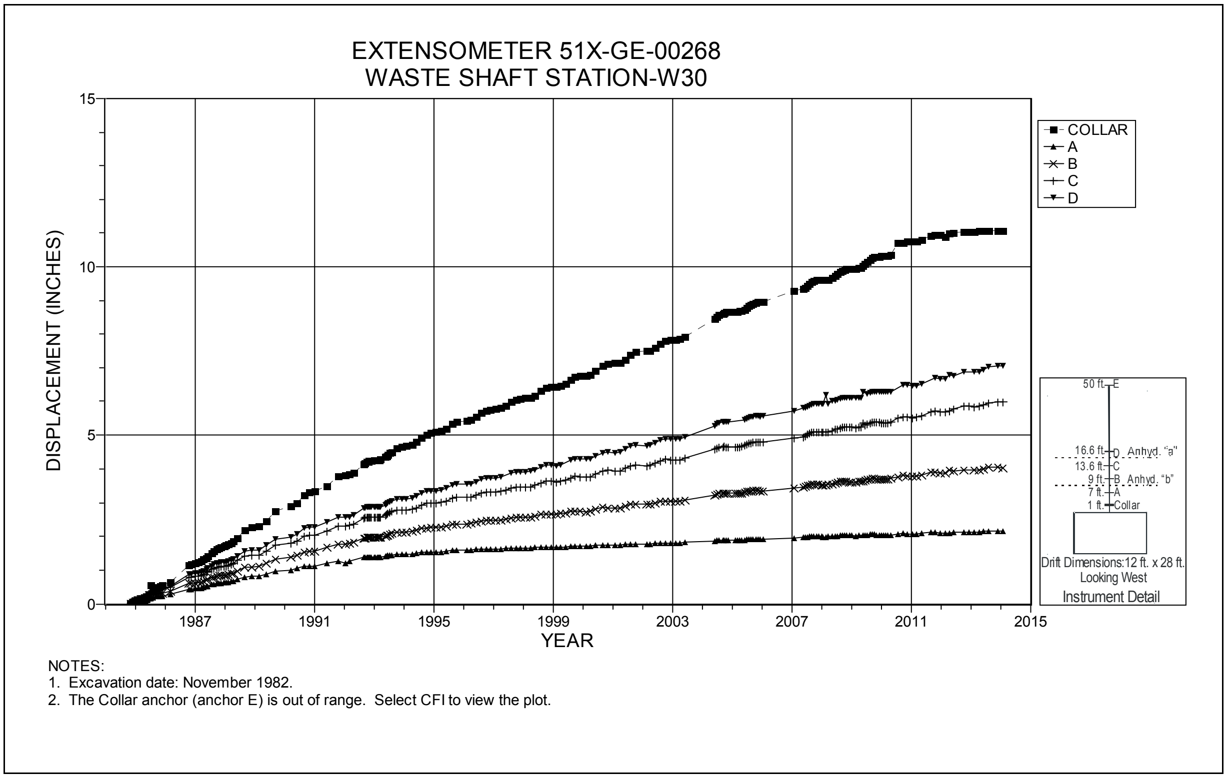

Figure 3-7 Extensometer 51X-GE-00268
Waste Shaft Station at S400 W30 – Roof

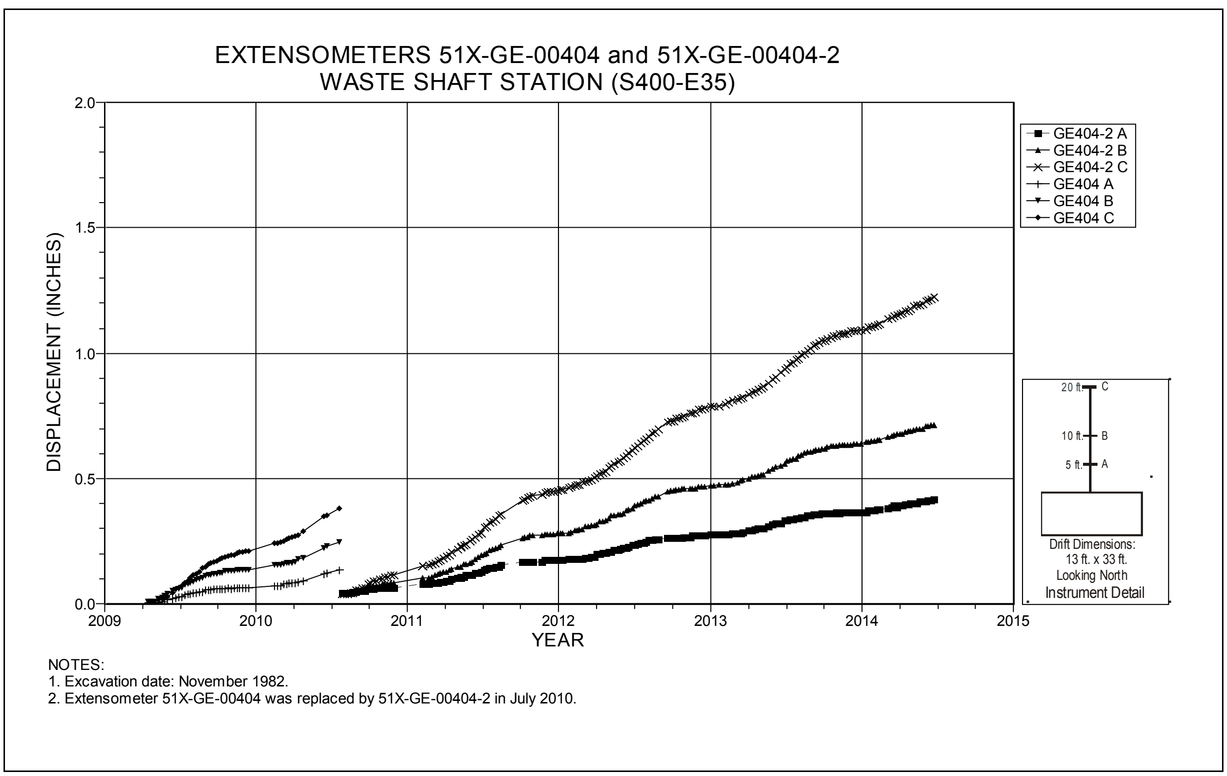

Figure 3-8 Extensometers 51X-GE-00404 and 51X-GE-00404-2
Waste Shaft Station at S400 E35 – Roof

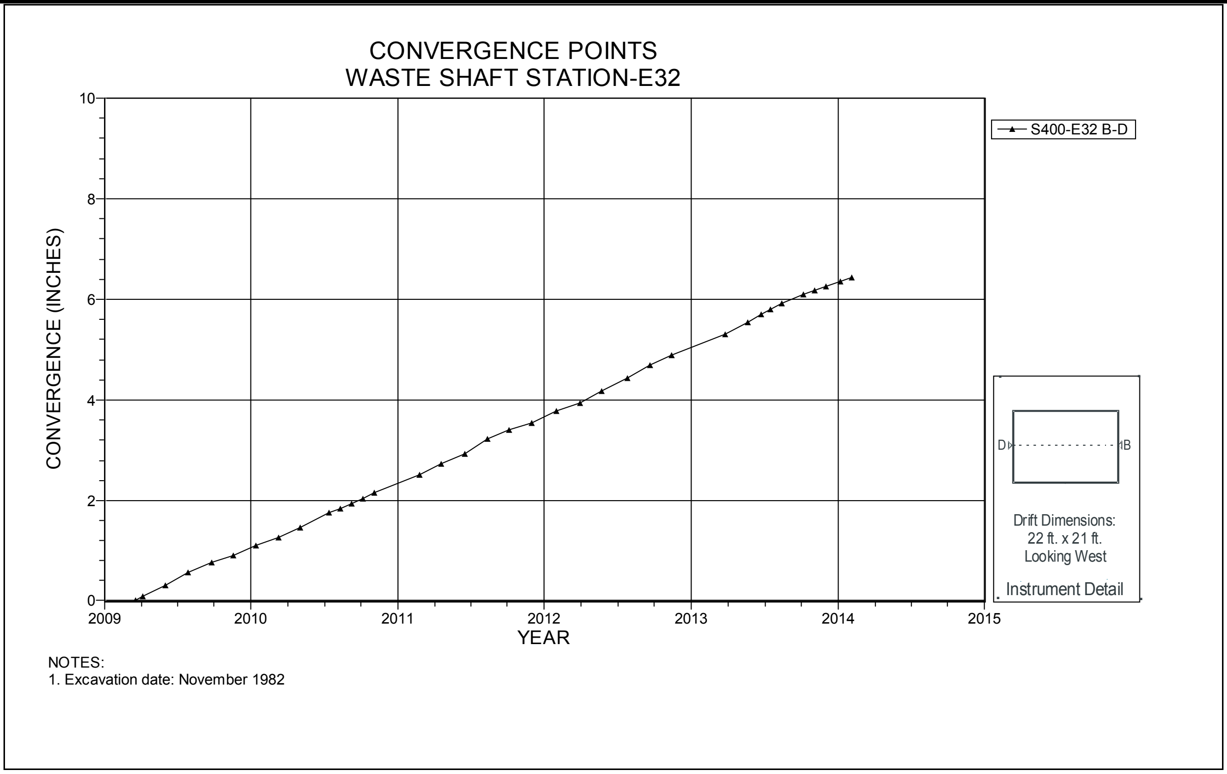

Figure 3-9 Convergence Point Array
Waste Shaft Station at S400 E32 – Rib to Rib

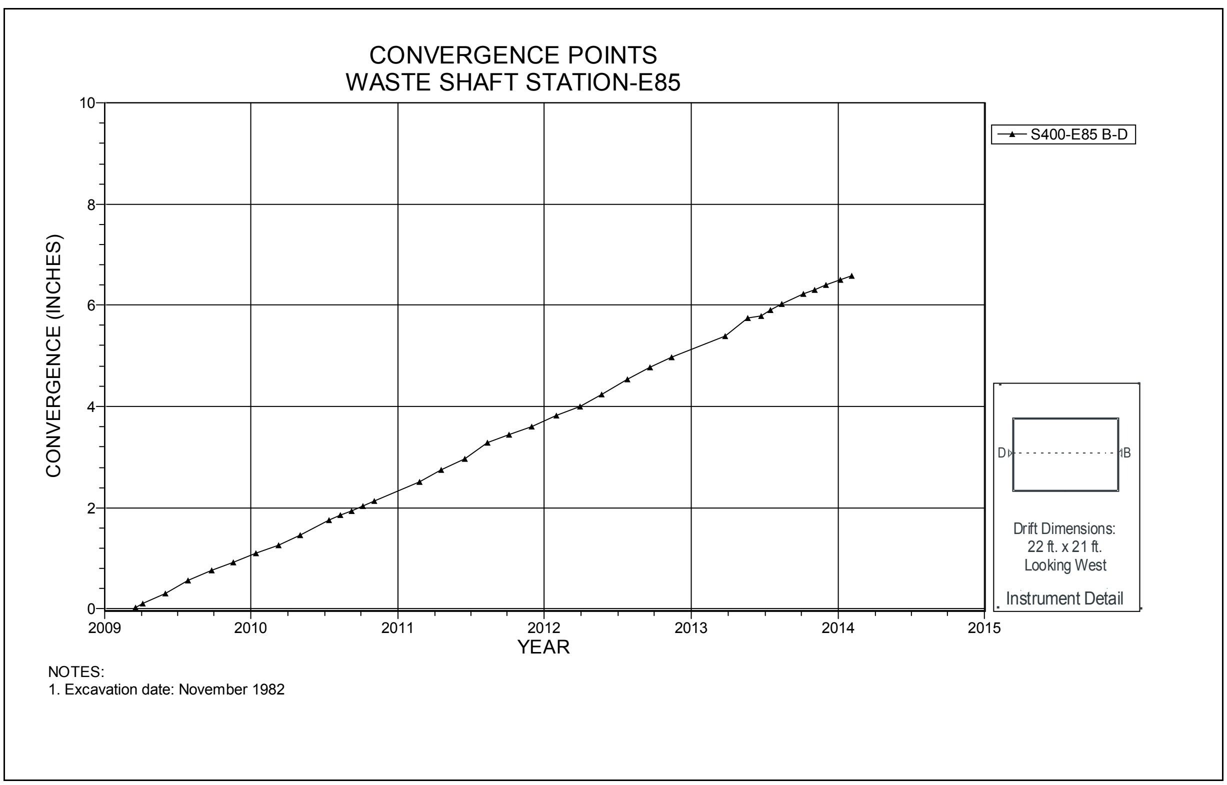

Figure 3-10 Convergence Point Array
Waste Shaft Station at S400 E85 – Rib to Rib

Table 3-3
Air Intake Shaft Station Data Analysis

Extensometers

Field Tag	Location	Figure Number	Date of Last Reading	Collar Displacement Relative to Deepest Anchor (Inches)	Displacement Rate 2013 to 2014 in/year	Displacement Rate 2012 to 2013 in/year	Rate Change Percent	Comments
41X-GE-00122	W620-S65	3-11	06/24/14	3.705	0.2	0.2	0%	Anchor "D" has reached its maximum range. Anchor "C" readings were used in the calculations.
41X-GE-00123	W620-N93	3-12	06/24/14	4.990	0.3	0.3	0%	The Collar and "C" anchors have reached their maximum range. Anchor "B" readings were used.

Rockbolt Load Cells

Field Tag	Location	Figure Number	Date of Initial Reading	Date of Last Reading	Load (kips)	Comments
51X-WG-00236	AIS Station Brow - South	3-13	01/19/93	03/04/14	66.4	
51X-WG-00237	AIS Station Brow - South	3-13	01/19/93	06/24/14	1.5	The rock bolt has failed.
51X-WG-00238	AIS Station Brow - South	3-13	01/19/93	06/24/14	1.6	
51X-WG-00239	AIS Station Brow - South	3-13	01/19/93	06/24/14	40.0	
51X-WG-00240	AIS Station Brow - South	3-13	01/19/93	06/24/14	1.7	
51X-WG-00241	AIS Station Brow - South	3-14	01/19/93	06/24/14	68.7	
51X-WG-00242	AIS Station Brow - South	3-14	01/19/93	06/24/14	36.9	
51X-WG-00243	AIS Station Brow - South	3-14	01/19/93	06/24/14	23.4	
51X-WG-00244	AIS Station Brow - South	3-14	12/24/94	06/24/14	27.5	
51X-WG-00245	AIS Station Brow - South	3-14	01/19/93	06/24/14	0.7	The rock bolt has failed.
51X-WG-00246	AIS Station Brow - North	3-15	01/19/93	06/24/14	24.7	
51X-WG-00247	AIS Station Brow - North	3-15	01/19/93	06/24/14	1.6	The rock bolt has failed.
51X-WG-00248	AIS Station Brow - North	3-15	01/19/93	06/24/14	13.6	
51X-WG-00249	AIS Station Brow - North	3-15	01/19/93	06/24/14	0.4	The rock bolt has failed.
51X-WG-00250	AIS Station Brow - North	3-15	12/24/94	06/24/14	14.0	
51X-WG-00251	AIS Station Brow - North	3-16	01/19/93	06/24/14	28.4	
51X-WG-00252	AIS Station Brow - North	3-16	01/19/93	05/27/14	3039.1	The load cell or the instrument cable to the cell has been damaged.
51X-WG-00253	AIS Station Brow - North	3-16	01/19/93	06/24/14	66.3	
51X-WG-00254	AIS Station Brow - North	3-16	01/19/93	06/24/14	9.2	
51X-WG-00255	AIS Station Brow - North	3-16	01/19/93	06/24/14	19.7	

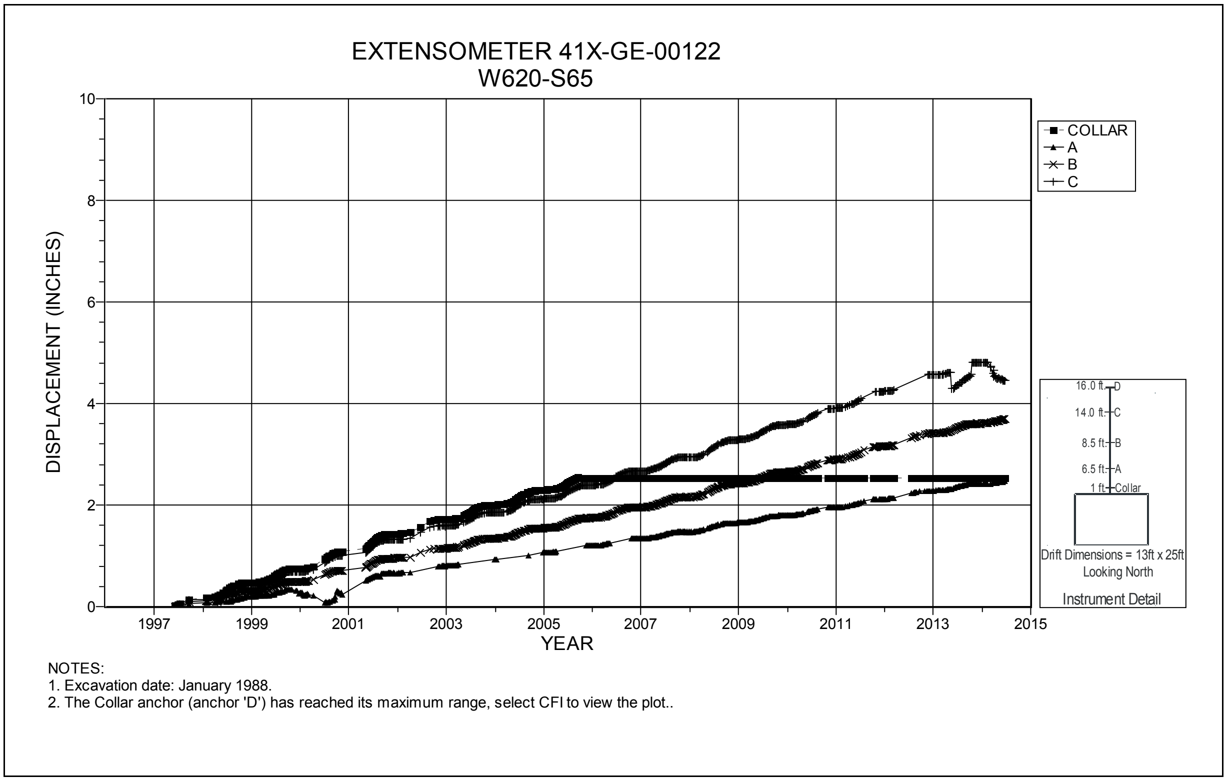

Figure 3-11 Extensometer 41X-GE-00122
Air Intake Shaft Station at S65 – Roof

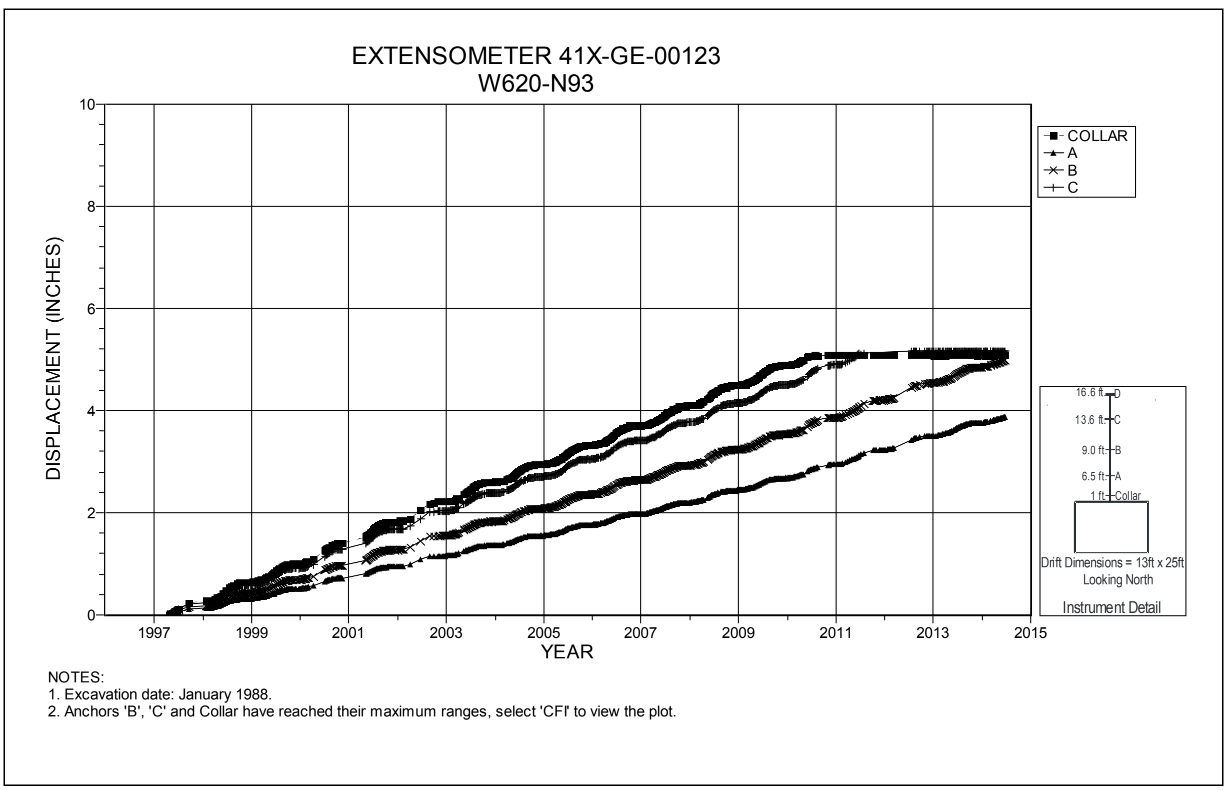

Figure 3-12 Extensometer 41X-GE-00123
Air Intake Shaft Station at N93 – Roof

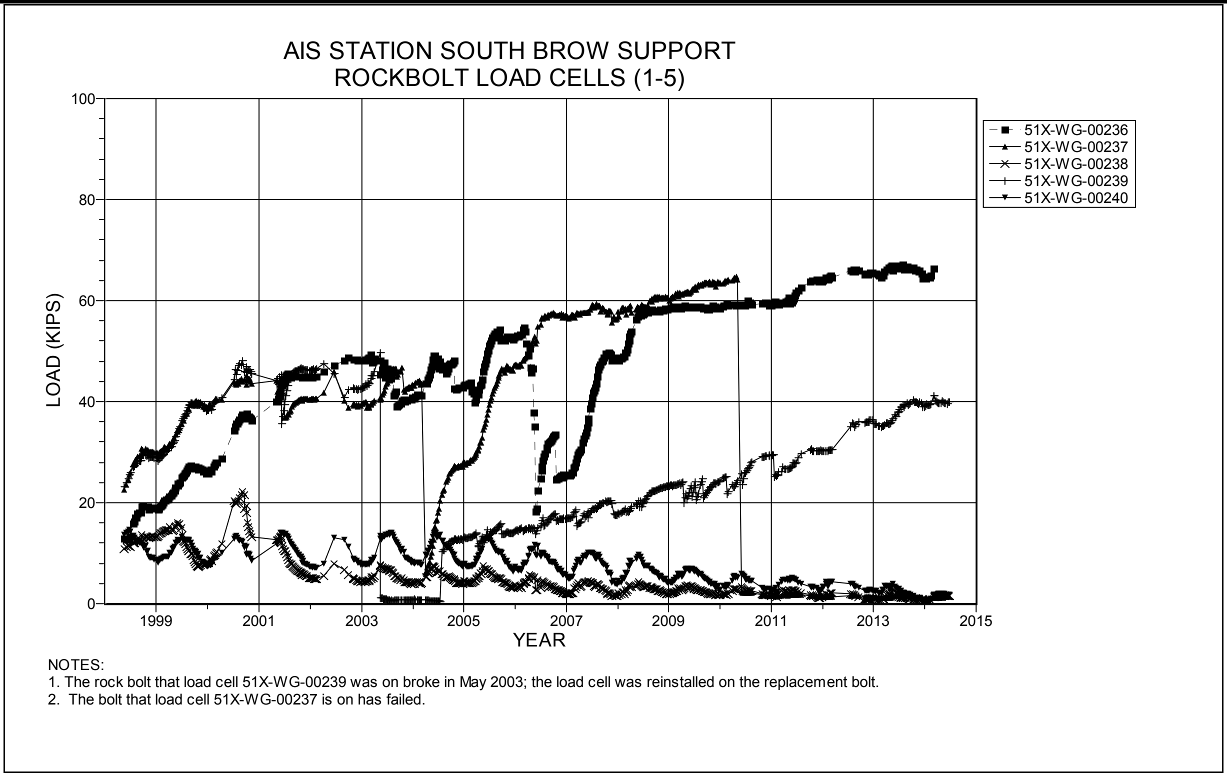

Figure 3-13 Rock Bolt Load Cells
Air Intake Shaft Station Brow – South Side Roof Bolts Set 1

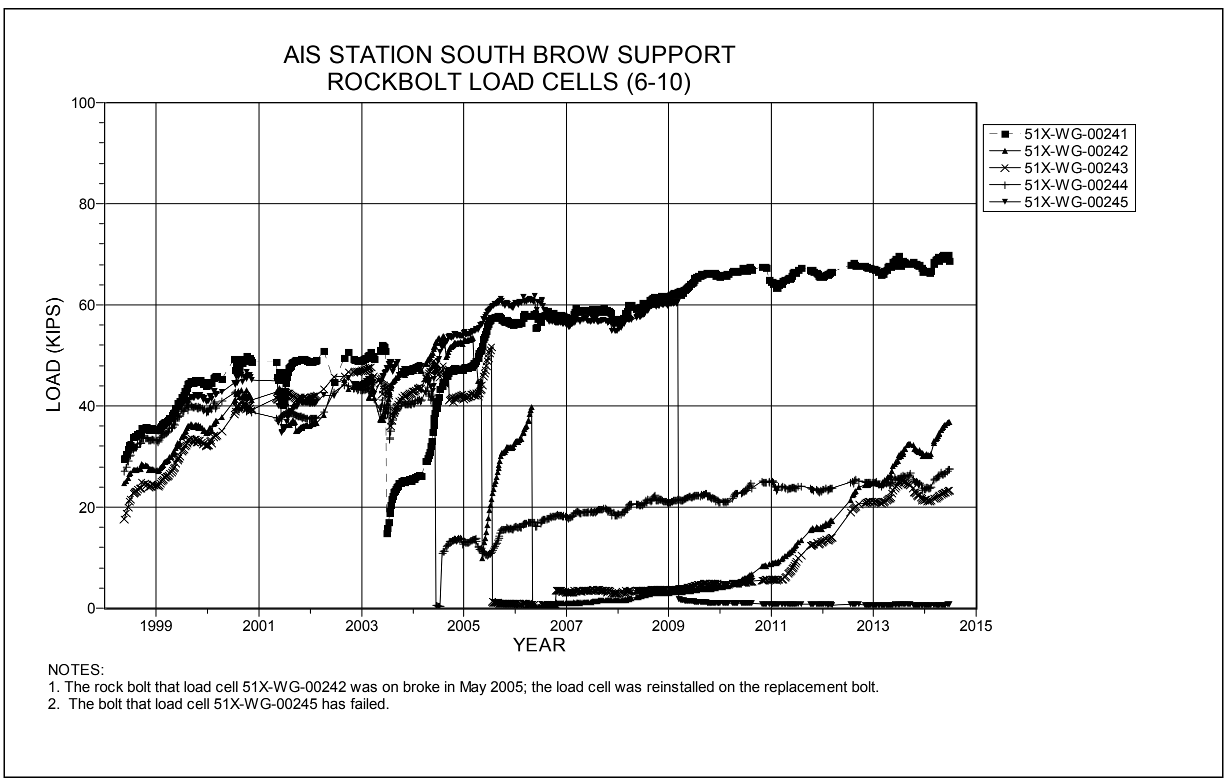

Figure 3-14 Rock Bolt Load Cells
Air Intake Shaft Station Brow – South Side Roof Bolts Set 2

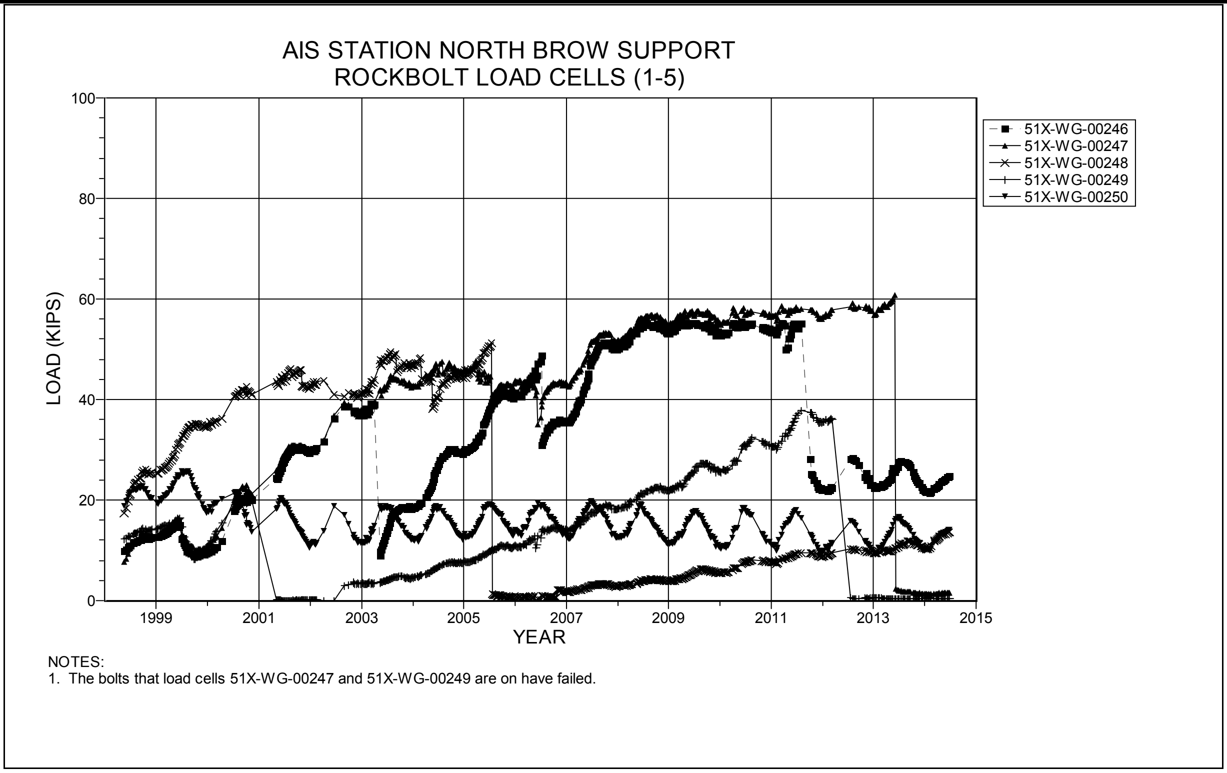

Figure 3-15 Rock Bolt Load Cells
Air Intake Shaft Station Brow – North Side Roof Bolts Set 1

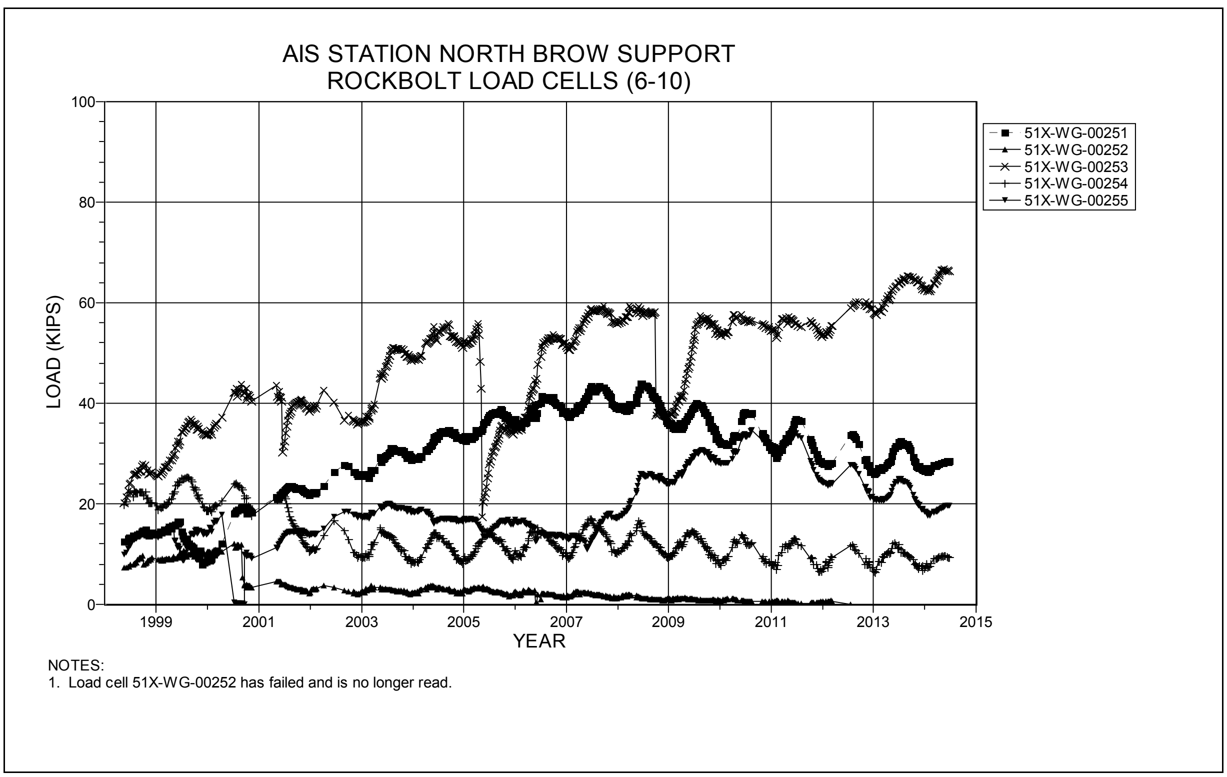

Figure 3-16 Rock Bolt Load Cells
Air Intake Shaft Station Brow – North Side Roof Bolts Set 2

4.0 Instrumentation Summary for the Access Drifts

This chapter presents the instrumentation data and data analyses for the access drifts throughout the WIPP underground. Table 4-1 provides the results of analyses performed on the instrument data including displacement, convergence rates, and rock bolt loading.

Figures 4-1 through 4-32 present data from borehole extensometers installed in the access drifts while Figures 4-33 through 4-261 present the convergence point data. Figure 4-262 through 4-267 presents data from joint meters installed at the S1950/E300 overcast and the access drifts. Figure 4-268 through 4-277 presents the data from rock bolt load cells installed in the E140 drift, the adjacent brows in E140-S1300 and at the E140-S1600 east brow.

Table 4-1
Access Drifts Data Analysis)

Extensometers

Field Tag	Location	Figure Number	Date of Last Reading	Collar Displacement Relative to Deepest Anchor (inches)	Displacement Rate 2013 to 2014 (in/year)	Displacement Rate 2012 to 2013 (in/year)	Rate Change Percent	Comments
51X-GE-00355	E0-N300	4-1	06/24/14	6.420	0.4	0.7	-43%	
51X-GE-00353	E0-N626	4-2	06/24/14	8.358	0.6	0.8	-25%	
51X-GE-00352	E0-N940	4-3	06/24/14	7.963	0.6	0.7	-14%	
51X-GE-00361	E0-N1266	4-4	06/24/14	12.018	0.6	0.7	-14%	
51X-GE-00105-3	E140-N150	4-5	01/28/14	4.501	0.2	0.3	-33%	
51X-GE-00364	E140-N1266	4-6	06/24/14	6.605	0.6	0.4	50%	
51X-GE-00372	E140-S146	4-7	06/24/14	4.937	0.7	0.5	40%	Data taken from anchor ‘B’.
51X-GE-00472	E140-S1000	4-8	02/03/14	6.353	0.2	0.4	-50%	
51X-GE-00464	E140-S1025	4-9	02/03/14	5.268	0.0	0.2	-100%	
51X-GE-00428-2	E140-S1150	4-10	01/14/14	3.595	1.8	2.2	-18%	Data taken from anchor ‘B’.
51X-GE-00429	E140-S1450	4-11	01/27/14	3.387	1.3	1.5	-13%	
51X-GE-00430	E140-S1669	4-12	01/27/14	3.617	1.4	1.6	-13%	
51X-GE-00431	E140-S1775	4-13	01/27/14	3.583	1.8	1.7	6%	
51X-GE-00432	E140-S1850	4-14	01/27/14	4.226	1.8	1.9	-5%	
51X-GE-00433-2	E140-S2065	4-15	01/27/14	4.115	2.4	2.1	14%	
51X-GE-00434	E140-S2265	4-16	01/27/14	2.264	0.7	0.8	-13%	
51X-GE-00435	E140-S2350	4-17	01/14/14	4.623	2.1	2.2	-5%	
51X-GE-00437	E140-S2635	4-18	01/14/14	4.417	2.1	3.1	-32%	
51X-GE-00492	E140-S2750	4-19	02/05/14	4.078	0.2	0.3	-33%	
51X-GE-00439	E140-S2916	4-20	01/14/14	0.875	0.4	0.5	-20%	See data plot Note 3.
51X-GE-00396	E140-S3493	4-21	06/24/14	12.656	3.4	2.4	42%	
51X-GE-00374	E300-N1186	4-22	06/24/14	6.776	0.9	0.6	50%	
51X-GE-00388	E300-N1266	4-23	06/24/14	4.985	0.9	0.6	50%	
51X-GE-00373	E300-N1341	4-24	06/24/14	5.386	0.4	0.3	33%	
51X-GE-00474	S1000-E120	4-25	12/10/13	1.499	0.1	0.0	100%	
51X-GE-00473	S1000-E160	4-26	12/10/13	1.292	0.0	0.1	-100%	
51X-GE-00462	S1300-E120	4-27	12/10/13	0.866	0.0	0.0	0%	

Table 4-1
Access Drifts Data Analysis

Extensometers (continued)

Field Tag	Location	Figure Number	Date of Last Reading	Collar Displacement Relative to Deepest Anchor (inches)	Displacement Rate 2013 to 2014 (in/year)	Displacement Rate 2012 to 2013 (in/year)	Rate Change Percent	Comments
51X-GE-00442	S1600-E120	4-28	10/16/13	1.252	0.1	0.1	0%	
51X-GE-00500/502	S2750-W93	4-29	01/28/14	0.449	0.6	0.3	100%	
51X-GE-00501-3	S2750-W285	4-30	1/28/2014	0.613	5.5	4.7	17%	
51X-GE-00490	W30-S2750	4-31	01/20/14	5.190	0.8	0.8	0%	
51X-GE-00415	W170-S2998	4-32	06/24/14	13.437	2.2	3.0	-27%	

Convergence Points

Field Tag	Location	Figure Number	Last Reading 2013-2014		Cumulative Displacement (inches)	Closure Rate 2013 to 2014 (in/year)	Closure Rate 2012 to 2013 (in/year)	Rate Change Percent	Comments
			Date	Inches					
CORE-W10 A-C	Core Storage W10	4-33	12/17/13	24.371	24.371	0.8	0.9	-11%	
CORE-W20 A-C	Core Storage W20	4-33	12/17/13	23.204	23.204	1.0	0.9	11%	
CORE-W30 A-C	Core Storage W30	4-33	12/17/13	24.477	24.477	1.1	1.0	10%	
CORE-W51 A-C	Core Storage W51	4-33	12/17/13	28.395	28.395	1.2	1.2	0%	
CORE-W62 A-C	Core Storage W62	4-33	12/17/13	29.670	29.670	1.2	1.2	0%	
CORE-W73 A-C	Core Storage W73	4-33	12/17/13	29.946	29.946	1.2	1.2	0%	
CORE-W101 A-C	Core Storage W101	4-33	12/17/13	28.864	28.864	1.1	1.1	0%	
CORE-W117 A-C	Core Storage W117	4-33	12/17/13	25.914	25.914	1.0	1.0	0%	
CORE-W133 A-C	Core Storage W133	4-33	10/30/12	20.677	20.677	0.9	0.9	0%	Instrument is inaccessible.
E0-N75 A-C	E0-N80	4-34	01/21/14	23.174	23.174	1.9	2.0	-5%	
E0-N75 B-D	E0-N80	4-34	01/21/14	15.866	15.866	1.1	1.2	-8%	
E0-N225-2 A-C	E0-N225	4-35	01/21/14	22.714	22.761	1.6	1.9	-16%	
E0-N225-2 B-D	E0-N225	4-35	01/21/14	5.329	17.634	1.2	1.4	-14%	
E0-N300-6 A-C	E0-N290	4-36	11/19/13	6.045	57.090	1.7	1.8	-6%	
E0-N460-3 A-C	E0-N460	4-37	01/21/14	27.343	47.432	1.8	2.3	-22%	

Table 4-1
Access Drifts Data Analysis (Continued

Convergence Points									
			Last Reading 2013-2014						
Field Tag	Location	Figure Number	Date	Inches	Cumulative Displacement (inches)	Closure Rate 2013 to 2014 (in/year)	Closure Rate 2012 to 2013 (in/year)	Rate Change Percent	Comments
E0-N562 A-C	E0-N562	4-38	09/23/13	20.619	20.619	2.4	2.1	14%	Cannot read, muck pile on floor point.
E0-N562 B-D	E0-N562	4-38	09/23/13	17.211	17.211	1.9	1.7	12%	Cannot access rib point.
E0-N626-4 A-C	E0-N626	4-39	07/30/13	25.324	66.283	N/A	2.3	N/A	Cannot read, muck pile on floor point.
E0-N686 A-C	E0-N686	4-40	06/05/12	27.073	27.073	N/A	N/A	N/A	Cannot read, muck pile on floor point.
E0-N686 B-D	E0-N686	4-40	06/05/12	15.254	15.254	N/A	N/A	N/A	Cannot access rib point.
E0-N780-2 A-C	E0-N780	4-41	01/21/14	22.770	43.192	1.9	2.1	-10%	
E0-N940-5 A-C	E0-N940	4-42	01/21/14	23.347	71.399	2.0	2.2	-9%	
E0-N1110-5 A-C	E0-N1110	4-43	01/21/14	15.656	50.080	1.2	1.3	-8%	..
E0-N1266-4 A-C	E0-N1266	4-44	01/21/14	24.915	61.822	1.7	2.2	-23%	
E140-N5-7 A-C	E140-N5	4-45	01/28/14	2.380	49.273	2.8	3.0	-7%	
E140-N5-3 B-D	E140-N5	4-45	01/28/14	19.746	34.987	1.4	1.5	-7%	
E140-N150-6 A-C	E140-N150	4-46	01/28/14	1.637	32.383	1.7	2.2	-23%	
E140-N220-4 A-C	E140-N220	4-47	01/28/14	2.458	44.615	2.9	3.6	-19%	
E140-N355-2 A-C	E140-N355	4-48	01/28/14	16.110	24.654	2.3	2.5	-8%	
E140-N355 B-D	E140-N355	4-48	01/28/14	20.069	20.069	1.7	1.8	-6%	
E140-N460-3 A-C	E140-N460	4-49	01/28/14	25.209	46.040	1.9	2.1	-10%	
E140-N562-2 A-C	E140-N562	4-50	01/28/14	25.268	37.085	2.6	2.7	-4%	
E140-N562-2 B-D	E140-N562	4-50	01/28/14	17.563	25.840	1.6	1.8	-11%	
E140-N626-3 A-C	E140-N626	4-51	01/28/14	34.275	66.845	3.0	3.5	-14%	
E140-N626-4 B-D	E140-N626	4-51	01/28/14	16.748	38.055	1.5	1.6	-6%	
E140-N686-2 A-C	E140-N686	4-52	01/28/14	27.179	27.179	2.3	2.6	-12%	
E140-N686-2 B-D	E140-N686	4-52	01/28/14	16.908	27.926	1.6	1.7	-6%	
E140-N780-2 A-C	E140-N780	4-53	01/28/14	32.021	63.778	2.1	2.8	-25%	
E140-N940-2 A-C	E140-N940	4-54	01/28/14	31.393	31.393	2.8	3.4	-18%	
E140-N1100-2 A-C	E140-N1100	4-55	01/28/14	15.062	34.785	1.5	1.5	0%	
E140-N1266-3 A-C	E140-N1266	4-56	01/29/14	23.775	61.530	1.9	2.3	-17%	The initial installation was at N952.

Table 4-1
Access Drifts Data Analysis (Continued)

Convergence Points

Field Tag	Location	Figure Number	Last Reading 2013-2014		Cumulative Displacement (inches)	Closure Rate 2013 to 2014 (in/year)	Closure Rate 2012 to 2013 (in/year)	Rate Change Percent	Comments
			Date	Inches					
E140-N1266-4 B-D	E140-N1266	4-56	01/29/14	12.068	34.073	1.1	1.3	-15%	
E140-N1420-2 A-C	E140-N1420	4-57	01/29/14	16.455	32.925	1.4	1.4	0%	
E140-S90-4 A-C	E140-S90	4-58	02/03/14	12.967	30.680	2.2	2.1	5%	
E140-S262-5 A-C	E140-S262	4-59	02/03/14	2.725	39.746	2.3	2.2	5%	
E140-S460-6 A-C	E140-S460	4-60	02/03/14	6.359	57.095	2.1	2.1	0%	
E140-S460-2 B-D	E140-S460	4-60	02/03/14	29.129	35.073	1.2	1.3	-8%	
E140-S550-6 A-C	E140-S550	4-61	02/03/14	5.898	47.865	1.9	1.9	0%	
E140-S550-4 B-D	E140-S550	4-61	02/03/14	32.091	40.733	1.4	1.6	-13%	
E140-S700-8 A-D	E140-S700	4-62	02/03/14	6.951	36.991	2.1	2.2	-5%	
E140-S700-6 B-C	E140-S700	4-63	02/03/14	9.707	39.739	2.3	2.2	5%	
E140-S700-6 E-F	E140-S700	4-64	02/03/14	5.510	25.507	1.3	1.4	-7%	
E140-S850-10 A-C	E140-S850	4-65	05/29/14	3.009	60.745	2.5	2.6	-4%	
E140-S850-4 B-D	E140-S850	4-66	02/03/14	21.890	37.837	1.2	1.4	-14%	
E140-S1000-4 A-C	E140-S1000	4-67	05/29/14	2.093	42.440	1.5	2.3	-35%	
E140-S1025-5 A-C	E140-S1025	4-68	05/29/14	2.347	29.754	1.8	2.3	-22%	
E140-S1075-5 A-E	E140-S1075	4-69	05/30/14	3.328	32.130	2.5	3.2	-22%	
E140-S1075-5 B-D	E140-S1075	4-70	02/03/14	1.137	23.228	1.2	1.4	-14%	
E140-S1075-5 H-F	E140-S1075	4-70	02/03/14	1.599	22.919	1.5	2.1	-29%	
E140-S1075-2 C-G	E140-S1075	4-71	02/03/14	20.458	21.280	1.2	1.4	-14%	
E140-S1150-5 A-G	E140-S1150	4-72	05/30/14	4.866	75.040	3.7	5.1	-27%	
E140-S1150-7 B-F	E140-S1150	4-73	02/03/14	2.734	35.191	2.7	3.2	-16%	
E140-S1150 C-K	E140-S1150	4-74	02/03/14	20.665	20.665	1.2	1.3	-8%	
E140-S1150-2 D-J	E140-S1150	4-74	02/03/14	22.289	40.210	1.4	1.6	-13%	
E140-S1150-2 E-I	E140-S1150	4-74	02/03/14	20.095	20.956	1.2	1.4	-14%	
E140-S1150-6 L-H	E140-S1150	4-75	02/03/14	1.729	27.527	1.8	2.3	-22%	
E140-S1225-5 A-E	E140-S1225	4-76	05/30/14	4.751	41.246	3.7	4.6	-20%	

Table 4-1
Access Drifts Data Analysis (Continued)

Convergence Points									
			Last Reading 2013-2014						
Field Tag	Location	Figure Number	Date	Inches	Cumulative Displacement (inches)	Closure Rate 2013 to 2014 (in/year)	Closure Rate 2012 to 2013 (in/year)	Rate Change Percent	Comments
E140-S1225-5 B-D	E140-S1225	4-77	02/03/14	1.916	37.840	2.1	2.1	0%	
E140-S1300-5 A-C	E140-S1300	4-78	05/30/14	1.947	39.890	1.5	1.9	-21%	
E140-S1378-4 A-E	E140-S1375/1378	4-79	02/03/14	3.464	46.005	3.4	4.5	-24%	
E140-S1378-4 B-D	E140-S1375/1378	4-80	02/03/14	1.833	31.371	1.8	2.3	-22%	
E140-S1378 C-G	E140-S1375/1378	4-81	02/03/14	25.095	29.265	1.6	1.8	-11%	
E140-S1378-4 H-F	E140-S1375/1378	4-80	02/03/14	3.929	49.791	3.9	5.0	-22%	
E140-S1450-6 A-G	E140-S1450/1456	4-82	05/30/14	4.733	85.540	3.7	4.3	-14%	
E140-S1450-4 B-F	E140-S1450/1456	4-83	02/03/14	1.412	48.900	1.6	1.3	23%	
E140-S1450-3 I-E	E140-S1450/1456	4-84	02/03/14	5.100	23.192	1.3	1.5	-13%	
E140-S1450-4 L-H	E140-S1450/1456	4-85	02/03/14	2.726	44.546	2.7	3.5	-23%	
E140-S1456-2 D-J	E140-S1450/1456	4-86	02/03/14	26.933	48.228	1.8	2.0	-10%	
E140-S1456 K-C	E140-S1450/1456	4-84	02/03/14	23.552	23.552	1.4	1.5	-7%	
E140-S1534-4 A-E	E140-S1534	4-87	05/30/14	3.565	57.048	2.8	3.3	-15%	
E140-S1534-5 B-D	E140-S1534	4-88	02/03/14	2.138	36.685	2.1	2.7	-22%	
E140-S1534-2 C-G	E140-S1534	4-87	02/03/14	23.821	25.292	1.6	1.7	-6%	
E140-S1534-4 H-F	E140-S1534	4-89	02/03/14	2.564	40.502	2.8	2.9	-3%	
E140-S1600-7 A-C	E140-S1600	4-90	05/30/14	2.798	44.744	2.1	2.7	-22%	
E140-S1687-4 A-E	E140-S1687	4-91	05/30/14	4.271	53.410	3.3	3.8	-13%	
E140-S1687-4 B-D	E140-S1687	4-92	02/03/14	1.978	38.720	2.3	1.8	28%	
E140-S1687 C-G	E140-S1687	4-92	02/03/14	26.621	26.621	1.9	2.0	-5%	
E140-S1687-4 H-F	E140-S1687	4-92	02/03/14	2.476	39.244	2.6	2.8	-7%	
E140-S1775-4 A-G	E140-S1775	4-93	05/30/14	5.066	73.252	4.0	4.3	-7%	
E140-S1775-5 B-F	E140-S1775	4-94	02/03/14	3.620	61.033	3.8	4.2	-10%	
E140-S1775-4 L-H	E140-S1775	4-94	02/03/14	1.271	33.856	1.5	1.1	36%	
E140-S1775 C-K	E140-S1775	4-95	02/03/14	25.146	25.146	1.7	1.7	0%	
E140-S1775-2 D-J	E140-S1775	4-95	02/03/14	27.893	29.144	2.4	2.5	-4%	

Table 4-1
Access Drifts Data Analysis (Continued)

Convergence Points									
			Last Reading 2013-2014						
Field Tag	Location	Figure Number	Date	Inches	Cumulative Displacement (inches)	Closure Rate 2013 to 2014 (in/year)	Closure Rate 2012 to 2013 (in/year)	Rate Change Percent	Comments
E140-S1775-3 I-E	E140-S1775	4-95	02/03/14	12.464	26.685	1.8	1.9	-5%	
E140-S1862-4 A-E	E140-S1862	4-96	05/30/14	4.816	57.814	3.7	4.3	-14%	
E140-S1862-4 B-D	E140-S1862	4-97	02/05/14	3.681	52.342	3.9	4.1	-5%	
E140-S1862-3 C-G	E140-S1862	4-96	02/05/14	20.957	27.262	2.2	2.3	-4%	
E140-S1862-4 H-F	E140-S1862	4-97	02/05/14	1.979	28.332	2.0	2.3	-13%	
E140-S1950-7 A-C	E140-S1950	4-98	05/30/14	4.640	61.030	3.4	4.4	-23%	
E140-S2007-8 A-C	E140-S2007	4-99	02/05/14	4.513	49.040	4.5	5.4	-17%	
E140-S2065-7 A-C	E140-S2065	4-100	02/05/14	4.493	57.259	4.5	5.4	-17%	
E140-S2065-2 B-D	E140-S2065	4-100	02/05/14	20.917	27.565	2.1	2.2	-5%	
E140-S2122-7 A-C	E140-S2122	4-101	02/05/14	3.092	53.332	4.1	3.0	37%	
E140-S2275-7 A-C	E140-S2275	4-102	02/05/14	4.964	83.901	5.3	5.4	-2%	
E140-S2275 B-D	E140-S2275	4-102	02/05/14	29.661	29.661	2.3	2.4	-4%	
E140-S2350-7 A-C	E140-S2350	4-103	02/05/14	4.888	87.601	5.0	5.7	-12%	
E140-S2350-2 B-D	E140-S2350	4-103	02/05/14	31.410	38.301	2.5	2.6	-4%	
E140-S2425-6 A-C	E140-S2425	4-104	02/05/14	4.267	59.773	4.4	4.9	-10%	
E140-S2425 B-D	E140-S2425	4-104	02/05/14	31.007	31.007	2.5	2.6	-4%	
E140-S2520-4 A-C	E140-S2520	4-105	02/05/14	3.394	44.170	3.2	4.2	-24%	
E140-S2634-2 A-C	E140-S2634	4-106	02/05/14	4.949	61.924	5.0	5.9	-15%	
E140-S2634 B-D	E140-S2634	4-106	02/05/14	25.100	25.100	2.5	2.6	-4%	
E140-S2750-4 A-C	E140-S2750	4-107	02/05/14	2.897	29.232	2.7	3.6	-25%	
E140-S2833-3 A-C	E140-S2833	4-108	02/05/14	23.822	44.621	4.5	4.7	-4%	
E140-S2833 B-D	E140-S2833	4-108	02/05/14	22.010	22.010	2.2	2.3	-4%	
E140-S2915-3 A-C	E140-S2915	4-109	02/05/14	16.633	42.849	2.6	2.7	-4%	
E140-S2915 B-D	E140-S2915	4-109	02/05/14	23.845	23.845	2.4	2.4	0%	
E140-S2998-3 A-C	E140-S2998	4-110	02/05/14	18.211	45.366	3.2	3.5	-9%	
E140-S2998 B-D	E140-S2998	4-110	02/05/14	21.746	21.746	2.1	2.1	0%	

Table 4-1
Access Drifts Data Analysis (Continued)

Convergence Points									
Field Tag	Location	Figure Number	Last Reading 2013-2014 Date	Last Reading 2013-2014 Inches	Cumulative Displacement (inches)	Closure Rate 2013 to 2014 (in/year)	Closure Rate 2012 to 2013 (in/year)	Rate Change Percent	Comments
E140-S3080-2 A-C	E140-S3080	4-111	02/05/14	17.382	33.521	3.7	3.7	0%	
E140-S3195-2 A-C	E140-S3195	4-112	02/05/14	20.065	46.320	4.0	4.3	-7%	
E140-S3195 B-D	E140-S3195	4-112	02/05/14	21.571	21.571	2.0	2.1	-5%	
E140-S3295-2 A-C	E140-S3295	4-113	02/05/14	12.361	20.066	2.4	2.4	0%	
E140-S3325 A-C	E140-S3325	4-114	02/05/14	19.596	19.596	2.4	2.3	4%	
E140-S3395-2 A-C	E140-S3395	4-115	02/05/14	18.097	33.255	3.5	3.3	6%	
E140-S3395 B-D	E140-S3395	4-115	02/05/14	15.590	15.590	1.8	1.7	6%	
E140-S3480-2 A-C	E140-S3480	4-116	02/05/14	20.949	35.249	4.8	4.3	12%	
E140-S3480 B-D	E140-S3480	4-116	02/05/14	16.001	16.001	1.8	1.8	0%	
E140-S3565-2 A-C	E140-S3565	4-117	02/05/14	15.888	27.216	3.9	3.3	18%	
E140-S3565 B-D	E140-S3565	4-117	02/05/14	15.182	15.182	1.8	1.6	13%	
E140-S3650-2 A-C	E140-S3650	4-118	01/27/14	10.250	16.870	2.0	1.9	5%	
E300-N45-2 A-E	E300-N45	4-119	01/13/14	1.102	33.983	2.2	1.9	16%	
E300-N45 C-G	E300-N45	4-119	01/13/14	26.536	26.536	1.8	1.7	6%	
E300-N45-2 H-F	E300-N45	4-119	11/12/13	0.674	30.213	2.0	1.8	11%	
E300-N170-3 A-E	E300-N170	4-120	01/13/14	1.158	34.632	2.3	2.3	0%	
E300-N170-2 C-G	E300-N170	4-120	01/13/14	13.183	28.027	1.8	1.8	0%	
E300-N170-3 H-F	E300-N170	4-120	01/13/14	0.932	31.227	1.8	2.3	-22%	
E300-N250-4 A-C	E300-N250	4-121	01/13/14	1.650	41.255	3.2	1.9	68%	
E300-N1262-4 A-C	E300-N1262	4-122	01/29/14	3.616	25.679	2.5	2.5	0%	
E300-N1341-3 A-C	E300-N1341	4-123	01/29/14	3.352	23.950	2.4	2.4	0%	
E300-S45-3 A-E	E300-S45	4-124	01/13/14	0.927	28.131	1.8	2.3	-22%	
E300-S45-3 B-D	E300-S45	4-124	01/13/14	1.076	26.267	2.1	2.8	-25%	
E300-S45 C-G	E300-S45	4-124	01/13/14	22.043	22.043	1.5	1.7	-12%	
E300-S45-3 H-F	E300-S45	4-124	01/13/14	0.764	24.013	1.5	1.7	-12%	
E300-S90-3 A-C	E300-S90	4-125	01/13/14	0.467	20.744	1.5	1.4	7%	

Table 4-1
Access Drifts Data Analysis (Continued)

Convergence Points

Field Tag	Location	Figure Number	Last Reading 2013-2014 Date	Last Reading 2013-2014 Inches	Cumulative Displacement (inches)	Closure Rate 2013 to 2014 (in/year)	Closure Rate 2012 to 2013 (in/year)	Rate Change Percent	Comments
E300-S250-2 A-C	E300-S250	4-126	01/13/14	10.483	14.868	0.8	0.8	0%	
E300-S250-2 B-D	E300-S250	4-126	01/13/14	11.231	15.277	0.8	0.8	0%	
E300-S700-2 A-C	E300-S700	4-127	01/13/14	4.273	24.003	1.4	1.3	8%	
E300-S850-2 A-E	E300-S850	4-128	01/13/14	2.235	17.317	0.7	0.7	0%	
E300-S850-2 B-D	E300-S850	4-128	01/13/14	1.899	13.200	0.6	0.6	0%	
E300-S850-2 C-G	E300-S850	4-128	01/13/14	10.433	19.711	0.8	0.8	0%	
E300-S850-2 H-F	E300-S850	4-128	01/13/14	1.698	12.161	0.6	0.6	0%	
E300-S1000-2 A-C	E300-S1000	4-129	01/13/14	3.077	22.622	1.0	1.0	0%	
E300-S1150-4 A-E	E300-S1150	4-130	01/13/14	7.035	24.114	1.9	2.0	-5%	
E300-S1150-4 B-D	E300-S1150	4-131	01/13/14	2.307	14.412	0.7	0.7	0%	
E300-S1150-2 C-G	E300-S1150	4-132	01/13/14	12.852	23.308	1.0	1.0	0%	
E300-S1150-4 H-F	E300-S1150	4-131	01/13/14	2.552	14.308	0.8	0.8	0%	
E300-S1300-2 A-C	E300-S1300	4-133	01/13/14	5.571	19.105	1.8	1.7	6%	
E300-S1450-2 A-C	E300-S1450	4-134	01/13/14	5.512	14.494	1.8	1.8	0%	
E300-S1450 B-D	E300-S1450	4-134	01/13/14	14.911	14.911	1.3	1.3	0%	
E300-S1687-2 A-C	E300-S1687	4-135	01/13/14	4.047	13.904	1.5	1.4	7%	
E300-S1687 B-D	E300-S1687	4-135	01/13/14	14.811	14.811	1.3	1.3	0%	
E300-S1775-2 A-C	E300-S1775	4-136	01/13/14	4.826	13.621	1.7	1.6	6%	
E300-S1775 B-D	E300-S1775	4-136	01/13/14	15.098	15.098	1.3	1.3	0%	
E300-S1862-2 A-C	E300-S1862	4-137	01/13/14	5.986	15.439	2.0	2.0	0%	
E300-S1862 B-D	E300-S1862	4-137	01/13/14	16.541	16.541	1.5	1.4	7%	
E300-S2065-2 A-C	E300-S2065	4-138	01/13/14	6.088	17.199	2.3	2.1	10%	
E300-S2065 B-D	E300-S2065	4-138	01/13/14	21.395	21.395	1.9	1.9	0%	
E300-S2275-2 A-C	E300-S2275	4-139	01/13/14	8.957	22.383	3.0	2.9	3%	
E300-S2275 B-D	E300-S2275	4-139	01/13/14	24.987	24.987	2.4	2.2	9%	
E300-S2350-2 A-C	E300-S2350	4-140	01/13/14	12.558	28.122	4.7	3.8	24%	

Table 4-1
Access Drifts Data Analysis (Continued)

Convergence Points									
Field Tag	Location	Figure Number	Last Reading 2013-2014 Date	Inches	Cumulative Displacement (inches)	Closure Rate 2013 to 2014 (in/year)	Closure Rate 2012 to 2013 (in/year)	Rate Change Percent	Comments
E300-S2350 B-D	E300-S2350	4-140	01/13/14	25.503	25.503	2.3	2.2	5%	
E300-S2425-2 A-C	E300-S2425	4-141	01/13/14	10.512	26.734	4.3	3.1	39%	
E300-S2425 B-D	E300-S2425	4-141	01/13/14	25.436	25.436	2.3	2.1	10%	
E300-S2634-2 A-C	E300-S2634	4-142	01/13/14	6.491	19.876	2.2	2.1	5%	
E300-S2634 B-D	E300-S2634	4-142	01/13/14	20.372	20.372	2.2	2.1	5%	
E300-S2833-2 A-C	E300-S2833	4-143	01/13/14	6.395	22.687	3.0	2.1	43%	
E300-S2833 B-D	E300-S2833	4-143	01/13/14	21.178	21.178	2.4	2.2	9%	
E300-S2916-4 A-C	E300-S2916	4-144	01/13/14	7.808	32.878	2.8	3.0	-7%	
E300-S2916 B-D	E300-S2916	4-144	01/13/14	23.771	23.771	2.7	2.6	4%	
E300-S2998-4 A-C	E300-S2998	4-144	01/13/14	10.409	45.159	4.3	3.5	23%	
E300-S2998 B-D	E300-S2998	4-145	01/13/14	23.757	23.757	2.7	2.7	0%	
E300-S3195 A-C	E300-S3195	4-146	01/13/14	28.314	28.314	3.8	3.4	12%	
E300-S3195 B-D	E300-S3195	4-146	01/13/14	21.022	21.022	2.2	2.0	10%	
E300-S3480 A-C	E300-S3480	4-147	01/13/14	16.073	16.073	2.5	2.3	9%	
E300-S3480 B-D	E300-S3480	4-147	01/13/14	12.336	12.336	1.9	1.8	6%	
N140-E90-3 A-C	N140-E90	4-148	11/26/13	4.498	18.635	0.6	0.8	-25%	
N140-E90-2 B-D	N140-E90	4-148	11/26/13	20.138	20.138	0.9	1.0	-10%	
N215-W500-2 A-C	N215-W500	4-149	01/29/14	14.373	32.702	1.0	1.2	-17%	
N215-W500-2 B-D	N215-W500	4-149	01/29/14	14.427	21.245	0.6	0.9	-33%	
N215-W620-2 A-C	N215-W620	4-150	01/29/14	11.049	27.267	0.8	1.0	-20%	
N250-E220-3 A-E	N250-E220	4-151	01/13/14	1.359	41.317	2.7	2.7	0%	
N250-E220-3 B-D	N250-E220	4-151	01/13/14	0.817	36.957	1.6	1.8	-11%	
N250-E220 C-G	N250-E220	4-151	01/13/14	28.501	28.501	1.5	1.5	0%	
N250-E220-3 H-F	N250-E220	4-151	01/13/14	0.850	29.138	1.7	1.7	0%	
N300-W170-2 A-C	N300-W170	4-152	01/29/14	17.285	39.545	1.4	1.6	-13%	
N300-W170-2 B-D	N300-W170	4-152	01/29/14	19.035	27.230	0.8	1.3	-38%	

Table 4-1
Access Drifts Data Analysis (Continued)

Convergence Points

Field Tag	Location	Figure Number	Last Reading 2013-2014 Date	Last Reading 2013-2014 Inches	Cumulative Displacement (inches)	Closure Rate 2013 to 2014 (in/year)	Closure Rate 2012 to 2013 (in/year)	Rate Change Percent	Comments
N460-E70-3 A-C	N460-E70	4-153	01/21/14	18.081	34.527	1.5	1.7	-12%	
N460-E70-2 B-D	N460-E70	4-153	01/21/14	18.761	30.459	1.5	1.6	-6%	
N780-E70 A-C	N780-E70	4-154	01/21/14	15.325	15.325	1.2		N/A	12'-13', one reading
N780-E70 B-D	N780-E70	4-154	01/21/14	15.060	15.060	1.1	N/A	N/A	Inaccessible.
S90-W120 A-C	S90-W120	4-155	12/16/13	9.143	9.143	0.7	0.6	17%	
S90-W120 B-D	S90-W120	4-155	12/16/13	9.767	9.767	0.7	0.7	0%	
S90-W400-2 A-C	S90-W400	4-156	10/22/13	5.503	18.852	0.5	0.6	-17%	
S90-W400-2 B-D	S90-W400	4-156	10/22/13	10.443	18.337	0.5	0.6	-17%	
S90-W590-2 A-C	S90-W590	4-157	12/16/13	5.395	14.724	0.5	0.6	-17%	
S90-W590-2 B-D	S90-W590	4-157	12/16/13	10.031	13.838	0.4	0.6	-33%	
S90-W620 A-C	S90-W620	4-158	12/16/13	27.923	27.923	0.9	1.0	-10%	
S90-W770 A-C	S90-W770	4-159	12/16/13	19.515	19.515	0.7	0.9	-22%	
S90-W770-3 B-D	S90-W770	4-159	12/16/13	4.610	17.931	0.7	0.8	-13%	
S90-W905 A-C	S90-W905	4-160	12/16/13	16.808	16.808	1.0	1.0	0%	
S105-W920 A-C	S105-W920	4-161	12/16/13	5.604	5.604	0.8	1.0	-20%	
S700-E55-2 A-C	S700-E55	4-162	12/10/13	7.102	11.236	1.9	1.8	6%	
S700-E55-2 B-D	S700-E55	4-162	12/10/13	4.454	8.596	1.1	1.1	0%	
S700-E180 A-C	S700-E180	4-163	12/10/13	14.810	14.810	2.0	1.9	5%	
S700-E180 B-D	S700-E180	4-163	12/10/13	8.505	8.505	1.0	1.1	-9%	
S700-E205-3 A-C	S700-E205	4-164	12/10/13	14.624	32.053	2.0	1.9	5%	
S700-W98-3 A-C	S700-W98	4-165	05/29/14	5.081	29.422	1.9	2.1	-10%	
S1000-E58-4 A-C	S1000-E58	4-166	12/10/13	11.582	27.048	1.2	1.3	-8%	
S1000-E58-2 B-D	S1000-E58	4-166	12/10/13	20.592	22.136	1.0	1.2	-17%	
S1000-E120-3 A-C	S1000-E120	4-167	12/10/13	10.274	18.714	1.1	1.1	0%	
S1000-E160 -3 A-C	S1000-E160	4-168	12/10/13	5.565	13.775	0.8	0.9	-11%	
S1000-W98-2 A-C	S1000-W98	4-169	12/09/13	18.791	37.539	2.2	2.1	5%	

Table 4-1
Access Drifts Data Analysis (Continued)

Convergence Points

Field Tag	Location	Figure Number	Last Reading 2013-2014 Date	Last Reading 2013-2014 Inches	Cumulative Displacement (inches)	Closure Rate 2013 to 2014 (in/year)	Closure Rate 2012 to 2013 (in/year)	Rate Change Percent	Comments
S1300-E24 A-C	S1300-E24	4-170	12/09/13	24.961	24.961	1.3	1.3	0%	
S1300-E120 A-C	S1300-E120	4-171	12/10/13	16.689	16.689	0.9	1.0	-10%	
S1300-E160 A-C	S1300-E160	4-172	12/10/13	26.945	26.945	1.6	1.8	-11%	
S1300-W100-3 A-C	S1300-W100	4-173	12/10/13	17.227	41.230	1.6	1.9	-16%	
S1600-E110-2 A-C	S1600-E110	4-174	12/10/13	0.743	17.465	0.9	1.5	-40%	
S1600-E170-2 A-C	S1600-E170	4-175	12/10/13	0.836	19.147	1.1	1.7	-35%	
S1950-E113-4 A-C	S1950-E113	4-176	12/09/13	11.638	15.514	1.3	1.2	8%	
S1950-E281-3 A-C	S1950-E281	4-177	12/11/13	17.470	24.012	1.5	1.2	25%	
S1950-E284-3 A-C	S1950-E284	4-178	12/11/13	17.859	24.471	1.6	1.2	33%	
S2180-E55-3 A-C	S2180-E55	4-179	01/28/14	10.346	21.193	2.2	2.2	0%	
S2180-E55 B-D	S2180-E55	4-179	01/28/14	18.851	18.851	1.9	1.9	0%	
S2180-E220 A-C	S2180-E220	4-180	01/29/14	18.637	18.637	1.7	1.7	0%	
S2180-E220 B-D	S2180-E220	4-180	01/29/14	20.794	20.794	2.0	2.0	0%	
S2180-W100-3 A-C	S2180-W100	4-181	01/27/14	11.134	29.317	3.5	3.4	3%	
S2180-W100-2 B-D	S2180-W100	4-181	01/27/14	18.161	18.302	2.1	2.1	0%	
S2520-E220 A-C	S2520-E220	4-182	01/29/14	23.351	23.351	1.7	1.7	0%	
S2520-E220 B-D	S2520-E220	4-182	01/29/14	24.318	24.318	1.9	1.9	0%	
S2520-W100-2 A-C	S2520-W100	4-183	01/28/14	6.687	26.367	3.1	3.0	3%	
S2520-W100-2 B-D	S2520-W100	4-183	01/28/14	8.479	24.102	2.2	2.4	-8%	
S2750-E55-2 A-C	S2750-E55	4-184	01/27/14	15.127	31.808	3.5	5.1	-31%	
S2750-E55 B-D	S2750-E55	4-184	01/27/14	21.466	21.466	2.3	2.4	-4%	
S2750-E220-2 A-C	S2750-E220	4-185	01/27/14	7.149	28.546	3.2	3.6	-11%	
S2750-E220 B-D	S2750-E220	4-185	01/27/14	19.308	19.308	2.0	2.0	0%	
S2750-E410 A-C	S2750-E410	4-186	01/27/14	33.070	33.070	4.2	4.6	-9%	
S2750-E410 B-D	S2750-E410	4-186	01/27/14	22.068	22.068	2.7	2.6	4%	
S2750-W93-3 A-C	S2750-W93	4-187	01/28/14	2.447	34.855	2.5	2.4	4%	

Table 4-1
Access Drifts Data Analysis (Continued)

Convergence Points

Field Tag	Location	Figure Number	Last Reading 2013-2014 Date	Last Reading 2013-2014 Inches	Cumulative Displacement (inches)	Closure Rate 2013 to 2014 (in/year)	Closure Rate 2012 to 2013 (in/year)	Rate Change Percent	Comments
S2750-W93 B-D	S2750-W93	4-188	01/28/14	18.057	18.057	2.1	2.2	-5%	
S3080-E220-2 A-C	S3080-E220	4-188	11/25/13	22.914	25.619	3.5	3.3	6%	
S3080-E220 B-D	S3080-E220	4-188	01/27/14	18.550	18.550	1.9	1.8	6%	
S3080-W100 A-C	S3080-W100	4-189	01/29/14	34.278	34.278	5.1	5.4	-6%	
S3080-W100 B-D	S3080-W100	4-189	01/29/14	20.363	20.363	2.6	2.6	0%	
S3310-E55 A-C	S3310-E55	4-190	01/27/14	26.651	26.651	4.0	3.2	25%	
S3310-E55 B-D	S3310-E55	4-190	01/27/14	18.838	18.838	2.3	2.1	10%	
S3310-E220 A-C	S3310-E220	4-191	01/27/14	33.506	33.506	3.9	2.1	86%	
S3310-E220 B-D	S3310-E220	4-191	01/27/14	21.089	21.089	2.3	2.1	10%	
S3310-W100-3 A-C	S3310-W100	4-192	01/27/14	25.367	31.645	4.3	4.1	5%	
S3310-W100 B-D	S3310-W100	4-192	01/27/14	18.939	18.939	1.9	1.8	6%	
S3650-E55-2 A-C	S3650-E55	4-193	01/27/14	11.269	14.602	2.4	2.8	-14%	
S3650-E220-2 A-C	S3650-E220	4-194	01/27/14	12.349	15.706	3.6	3.1	16%	
S3650-W100-2 A-C	S3650-W100	4-195	01/27/14	13.794	19.811	1.9	2.8	-32%	
S3650-W100 B-D	S3650-W100	4-195	01/27/14	13.337	13.337	1.6	1.7	-6%	
W30-S120-3 A-C	W30-S120	4-196	01/21/14	0.088	27.734	0.7	1.0	-30%	
W30-S250-5 A-C	W30-S250	4-197	01/21/14	9.233	35.466	1.2	1.1	9%	
W30-S250-5 B-D	W30-S250	4-197	01/21/14	19.482	30.436	1.0	1.0	0%	
W30-S400-2 A-C	W30-S400	4-198	01/21/14	7.069	24.897	0.7	0.8	-13%	
W30-S500-3 A-C	W30-S500	4-199	01/21/14	0.087	30.494	0.7	1.1	-36%	
W30-S500-2 B-D	W30-S500	4-199	01/21/14	0.101	28.921	0.8	1.0	-20%	
W30-S700-5 A-C	W30-S700	4-200	05/29/14	8.579	42.856	1.6	1.9	-16%	
W30-S850-6 A-E	W30-S850	4-201	01/21/14	0.489	30.506	1.4	2.9	-52%	
W30-S850-5 B-D	W30-S850	4-202	01/21/14	0.349	20.758	1.0	1.4	-28%	
W30-S850-4 H-F	W30-S850	4-202	01/21/14	0.530	22.727	1.6	2.0	-20%	
W30-S850-4 C-G	W30-S850	4-203	01/21/14	2.372	27.849	1.0	1.1	-9%	

Table 4-1
Access Drifts Data Analysis (Continued)

Convergence Points

Field Tag	Location	Figure Number	Last Reading 2013-2014 Date	Last Reading 2013-2014 Inches	Cumulative Displacement (inches)	Closure Rate 2013 to 2014 (in/year)	Closure Rate 2012 to 2013 (in/year)	Rate Change Percent	Comments
W30-S1000-5 A-C	W30-S1000	4-204	05/29/14	7.198	45.377	1.7	1.7	0%	
W30-S1150-2 A-C	W30-S1150	4-205	01/21/14	13.436	14.937	4.2	3.6	17%	
W30-S1300-2 A-C	W30-S1300	4-206	05/29/14	7.977	29.215	1.8	1.6	13%	
W30-S1453-2 A-C	W30-S1453	4-207	05/29/14	10.852	24.919	3.0	2.5	20%	
W30-S1453-3 B-D	W30-S1453	4-207	01/21/14	5.313	19.275	1.3	1.3	0%	
W30-S1600-3 A-C	W30-S1600	4-208	05/29/14	9.798	28.928	2.5	2.0	25%	
W30-S1775-4 A-C	W30-S1775	4-209	05/29/14	2.857	24.198	4.1	3.1	32%	
W30-S1775-3 B-D	W30-S1775	4-209	01/20/14	6.476	19.152	1.7	1.5	13%	
W30-S1950-3 A-C	W30-S1950	4-210	05/29/14	1.944	31.618	2.8	2.5	12%	
W30-S2067-4 A-C	W30-S2067	4-211	01/20/14	1.247	28.187	3.7	3.6	2%	
W30-S2067-4 B-D	W30-S2067	4-211	01/20/14	3.292	21.886	1.6	1.7	-6%	
W30-S2275-4 A-C	W30-S2275	4-212	01/20/14	9.979	30.659	4.8	4.4	9%	
W30-S2275-2 B-D	W30-S2275	4-212	01/20/14	7.818	18.998	2.0	1.9	5%	
W30-S2350-4 A-C	W30-S2350	4-213	01/20/14	13.430	32.739	5.8	6.2	-6%	
W30-S2350-2 B-D	W30-S2350	4-213	01/20/14	8.911	21.406	2.3	2.3	0%	
W30-S2425-4 A-C	W30-S2425	4-214	01/20/14	8.941	27.229	3.8	4.1	-7%	
W30-S2425-2 B-D	W30-S2425	4-214	01/20/14	8.835	22.319	2.3	2.3	0%	
W30-S2520-4 A-C	W30-S2520	4-215	01/20/14	0.355	29.344	2.1	3.0	-30%	
W30-S2685-3 A-C	W30-S2685	4-216	01/20/14	8.752	27.642	2.5	2.4	4%	
W30-S2685-3 B-D	W30-S2685	4-216	01/20/14	7.766	22.036	2.1	2.1	0%	
W30-S2750-3 A-C	W30-S2750	4-217	01/20/14	2.813	21.527	2.8	2.5	12%	
W30-S2833-4 A-C	W30-S2833	4-218	02/05/14	3.974	27.073	4.2	3.3	27%	
W30-S2833-2 B-D	W30-S2833	4-218	02/05/14	9.535	21.541	2.8	2.8	0%	
W30-S2916-2 A-C	W30-S2916	4-219	02/05/14	3.943	44.992	3.8	3.8	0%	
W30-S2916-2 B-D	W30-S2916	4-219	02/05/14	8.230	18.614	2.4	2.4	0%	
W30-S2998-2 A-C	W30-S2998	4-220	02/05/14	3.740	28.184	3.7	3.4	9%	

Table 4-1
Access Drifts Data Analysis (Continued)

Convergence Points

Field Tag	Location	Figure Number	Last Reading 2013-2014 Date	Last Reading 2013-2014 Inches	Cumulative Displacement (inches)	Closure Rate 2013 to 2014 (in/year)	Closure Rate 2012 to 2013 (in/year)	Rate Change Percent	Comments
W30-S2998-2 B-D	W30-S2998	4-220	02/05/14	7.204	17.921	2.2	2.1	5%	
W30-S3080 A-C	W30-S3080	4-221	01/20/14	27.573	27.573	2.1	2.1	0%	
W30-S3195 A-C	W30-S3195	4-222	01/20/14	24.325	24.325	2.8	2.8	0%	
W30-S3195 B-D	W30-S3195	4-222	01/20/14	17.132	17.132	1.7	1.7	0%	
W30-S3310 A-C	W30-S3310	4-223	01/20/14	20.050	20.050	1.9	1.7	12%	
W30-S3650-2 A-C	W30-S3650	4-224	01/27/14	10.137	15.789	1.8	2.2	-18%	
W170-N150-3 A-C	W170-N150	4-225	12/16/13	3.667	12.019	0.6	0.6	0%	
W170-S5-2 A-C	W170-S5	4-226	12/16/13	0.010	16.206	0.7	0.6	17%	
W170-S5-2 B-D	W170-S5	4-226	12/16/13	10.932	18.698	0.6	0.7	-14%	
W170-S90-3 A-C	W170-S90	4-227	12/17/13	10.732	17.934	0.9	0.8	13%	
W170-S232-2 A-C	W170-S232	4-228	12/17/13	7.892	13.481	0.6	0.6	0%	
W170-S232-2 B-D	W170-S232	4-228	12/17/13	11.210	13.852	0.6	0.6	0%	
W170-S400 A-C	W170-S400	4-229	12/17/13	16.462	16.462	0.8	0.7	14%	
W170-S560-4 A-C	W170-S560	4-230	12/17/13	4.135	14.954	0.8	0.7	14%	
W170-S560-3 B-D	W170-S560	4-230	12/17/13	3.234	16.062	0.8	0.7	14%	
W170-S700-3 A-C	W170-S700	4-231	05/29/14	0.451	25.729	1.0	1.1	-9%	
W170-S850-8 A-E	W170-S850	4-232	12/17/13	0.007	20.961	0.4	0.8	-50%	
W170-S850-7 B-D	W170-S850	4-233	12/17/13	0.035	16.226	2.1	0.7	200%	
W170-S850-3 C-G	W170-S850	4-234	12/17/13	13.672	24.485	1.0	0.9	11%	
W170-S850-8 H-F	W170-S850	4-235	12/17/13	0.011	14.470	0.7	0.6	17%	
W170-S1000-3 A-C	W170-S1000	4-236	05/29/14	6.512	29.425	1.1	1.1	0%	
W170-S1150-5 A-E	W170-S1150	4-237	05/29/14	0.401	25.442	0.9	0.9	0%	
W170-S1150-5 B-D	W170-S1150	4-239	12/17/13	0.017	18.016	1.0	0.9	11%	
W170-S1150-2 C-G	W170-S1150	4-238	12/17/13	15.530	27.107	1.2	1.1	9%	
W170-S1150-3 H-F	W170-S1150	4-239	12/17/13	0.018	17.175	1.1	0.7	57%	
W170-S1300-4 A-C	W170-S1300	4-240	05/29/14	11.755	32.713	2.0	1.7	18%	

Table 4-1
Access Drifts Data Analysis (Continued)

Convergence Points									
			Last Reading 2013-2014						
Field Tag	Location	Figure Number	Date	Inches	Cumulative Displacement (inches)	Closure Rate 2013 to 2014 (in/year)	Closure Rate 2012 to 2013 (in/year)	Rate Change Percent	Comments
W170-S1445-4 A-C	W170-S1445	4-241	05/29/14	9.917	21.209	2.0	1.6	25%	
W170-S1445-2 B-D	W170-S1445	4-241	12/17/13	14.942	17.600	1.3	1.1	18%	
W170-S1600-4 A-C	W170-S1600	4-242	05/29/14	10.831	25.596	4.1	1.8	128%	
W170-S1779-3 A-C	W170-S1779	4-243	05/29/14	10.173	25.144	2.5	1.6	56%	
W170-S1779-2 B-D	W170-S1779	4-243	12/17/13	18.418	21.553	2.2	1.4	57%	
W170-S1950-3 A-C	W170-S1950	4-244	05/29/14	8.877	22.058	2.6	1.4	86%	
W170-S2060-3 A-C	W170-S2060	4-245	12/16/13	3.003	21.247	1.8	1.5	20%	
W170-S2060-2 B-D	W170-S2060	4-245	12/16/13	20.198	23.522	2.0	1.8	11%	
W170-S2180-3 A-C	W170-S2180	4-246	01/20/14	4.064	27.628	2.2	2.0	10%	
W170-S2275 A-C	W170-S2275	4-247	01/20/14	18.262	18.262	1.8	1.7	6%	
W170-S2275 B-D	W170-S2275	4-247	01/20/14	21.560	21.560	2.5	2.4	4%	
W170-S2350 A-C	W170-S2350	4-248	01/20/14	24.021	24.021	2.2	2.2	0%	
W170-S2350 B-D	W170-S2350	4-248	01/20/14	21.017	21.017	2.0	2.1	-5%	
W170-S2425 A-C	W170-S2425	4-249	01/20/14	20.934	20.934	1.8	1.8	0%	
W170-S2425 B-D	W170-S2425	4-249	01/20/14	23.524	23.524	2.2	2.4	-8%	
W170-S2520-2 A-C	W170-S2520	4-250	01/20/14	7.752	28.347	3.4	3.4	0%	
W170-S2685-2 A-C	W170-S2685	4-251	12/16/13	25.144	26.990	2.0	1.8	11%	
W170-S2685-2 B-D	W170-S2685	4-251	12/16/13	21.692	23.555	2.3	2.2	5%	
W170-S2833-2 A-C	W170-S2833	4-252	01/20/14	2.766	37.913	5.6	5.8	3%	
W170-S2833 B-D	W170-S2833	4-252	01/20/14	22.484	22.484	2.9	2.9	0%	
W170-S2916 A-C	W170-S2916	4-253	01/20/14	32.306	32.306	2.7	2.9	-7%	
W170-S2916 B-D	W170-S2916	4-253	01/20/14	20.432	20.432	2.3	2.3	0%	
W170-S2998-2 A-C	W170-S2998	4-254	01/20/14	1.573	43.588	3.2	4.9	N/A	
W170-S2998-2 B-D	W170-S2998	4-254	01/20/14	10.937	23.630	3.2	3.3	-3%	
W170-S3080 A-C	W170-S3080	4-255	01/20/14	28.961	28.961	3.1	3.2	-3%	
W170-S3195 A-C	W170-S3195	4-256	01/20/14	27.973	27.973	3.9	3.0	30%	

Table 4-1
Access Drifts Data Analysis (Continued)

Convergence Points

Field Tag	Location	Figure Number	Last Reading 2013-2014 Date	Last Reading 2013-2014 Inches	Cumulative Displacement (inches)	Closure Rate 2013 to 2014 (in/year)	Closure Rate 2012 to 2013 (in/year)	Rate Change Percent	Comments
W170-S3195 B-D	W170-S3195	4-256	01/20/14	18.809	18.809	2.1	1.9	11%	
W170-S3310 A-C	W170-S3310	4-257	01/20/14	23.170	23.170	2.0	2.0	0%	
W170-S3395 A-C	W170-S3395	4-258	01/20/14	28.221	28.221	5.3	4.8	10%	
W170-S3395 B-D	W170-S3395	4-258	01/20/14	15.555	15.555	2.1	2.1	0%	
W170-S3480 A-C	W170-S3480	4-259	01/20/14	31.540	31.540	6.6	5.6	18%	
W170-S3480 B-D	W170-S3480	4-259	01/20/14	19.504	19.504	2.4	2.4	0%	
W170-S3565 A-C	W170-S3565	4-260	01/20/14	16.977	16.977	2.1	2.2	-5%	
W170-S3565 B-D	W170-S3565	4-260	01/20/14	13.586	13.586	1.5	1.6	-6%	
W170-S3650-2 A-C	W170-S3650	4-261	01/27/14	9.657	17.302	1.9	1.9	0%	

Joint Meters

Field Tag	Location	Figure Number	Date	Cumulative Displacement (inches)	Closure Rate 2013 to 2014 (in/year)	Closure Rate 2012 to 2013 (in/year)	Rate Change Percent	Comments
51X-CG-02706	S1950-E300	4-262	1/9/2014	2.246	0.2	0.2	0%	
51X-CG-02707	S1950-E300	4-262	1/9/2014	2.163	0.1	0.1	0%	
51X-CG-02876-2	E140-S1505	4-263	1/9/2014	-0.145	-0.2	-0.1	100%	
51X-CG-02883-3	E140-S1529	4-264	1/9/2014	-0.019	0.0	0.2	-100%	
51X-CG-02885-2	E140-S1545	4-265	1/9/2014	0.754	0.0	0.0	0%	
51X-CG-02875-2	E140-S1795	4-266	1/9/2014	0.511	0.0	0.1	-100%	
51X-CG-02713	E140-S2964	4-267	1/9/2014	-0.559	-0.3	-0.3	0%	

Table 4-1
Access Drifts Data Analysis (Continued)

Rockbolt Load Cells						
Field Tag	Location	Figure Number	Date of Initial Reading	Date of Last Reading	Load (klps)	Comments
51X-WG-00325	E140-N1266	4-268	09/23/10	01/29/14	43.5	
51X-WG-00326	E140-N1266	4-268	09/23/10	01/29/14	42.8	
51X-WG-00327	E140-N1266	4-268	09/23/10	01/29/14	40.2	
51X-WG-00328	E140-N1266	4-268	09/23/10	01/29/14	41.2	
51X-WG-00329	E140-N1266	4-268	09/23/10	01/29/14	44.8	
51X-WG-00330	E140-N1266	4-269	09/23/10	01/29/14	35.8	
51X-WG-00331	E140-N1266	4-269	09/23/10	01/29/14	39.4	
51X-WG-00332	E140-N1266	4-269	09/23/10	01/29/14	40.2	
51X-WG-00333	E140-N1266	4-269	09/23/10	01/29/14	37.0	
51X-WG-00216	E140-S910	4-270	06/26/97	06/24/14	44.1	
51X-WG-00219	E140-S975	4-271	06/26/97	06/24/14	29.0	
51X-WG-00220	E140-S1023	4-271	10/23/96	06/17/14	25.5	
51X-WG-00293	E140-S1550	4-272	03/17/04	02/04/14	56.4	
51X-WG-00295-2	E140-S2916	4-274	03/18/10	02/04/14	40.6	
51X-WG-00296-2	E140-S2916	4-274	03/18/10	02/04/14	36.3	
51X-WG-00223	S1600-E150	4-277	02/18/96	06/17/14	7.2	

[1] N/A – Insufficient data available to perform the calculation. This is usually due to the inability to read the instruments because of activities such as: the temporary removal of an instrument due to floor, rib or back trimming; locations blocked by equipment or waste disposal; installation timing, etc.
[2] During a period of inaccessibility, an additional 20.753 inches of displacement was recorded (not represented in the cumulative) by a remotely read convergence meter from June 1996 until May 2002. Remote readings were not taken at E300-N1341.

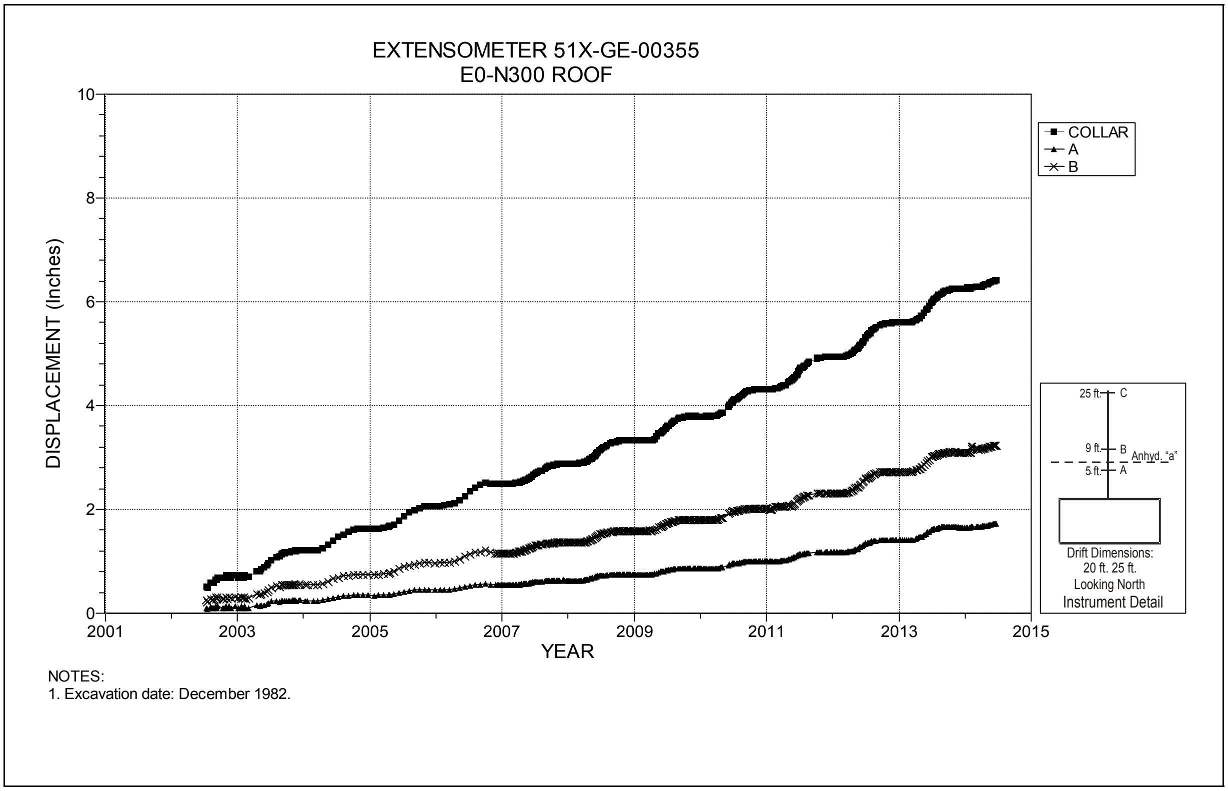

Figure 4-1 Extensometer 51X-GE-00355
E0 N300 – Roof

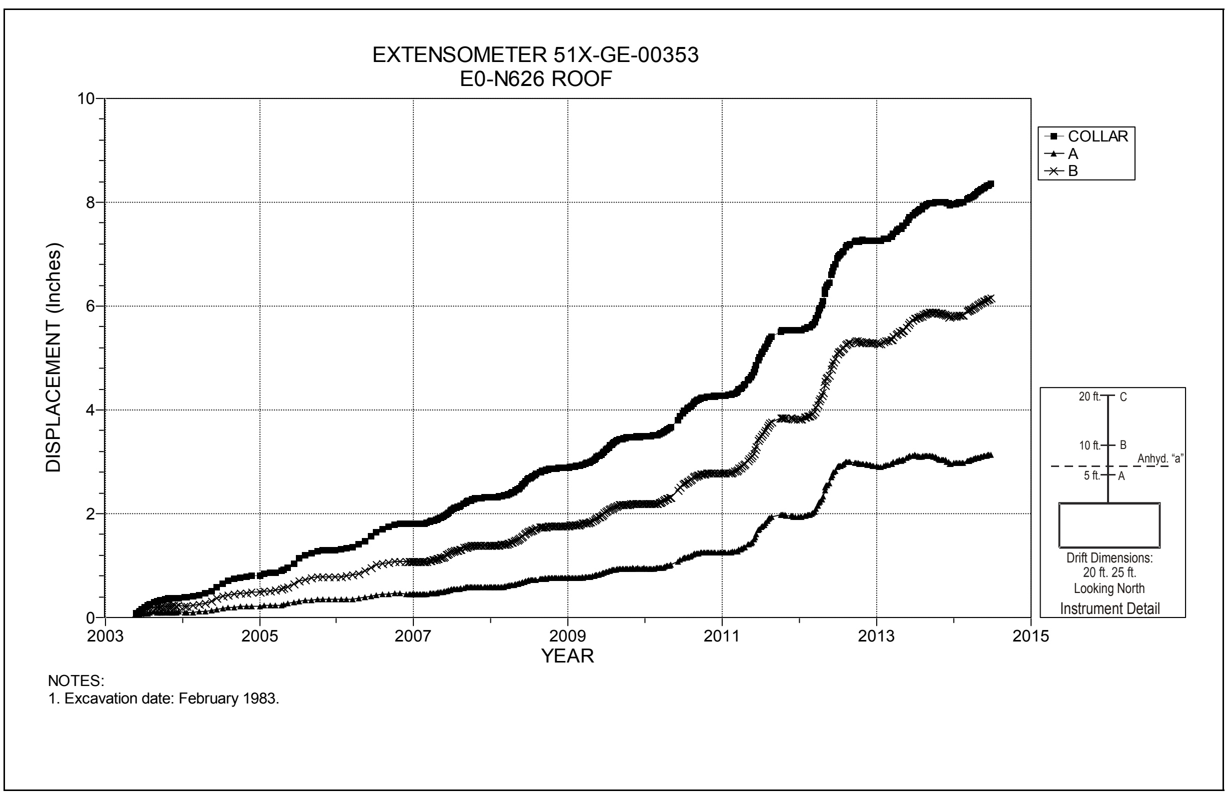

Figure 4-2 Extensometer 51X-GE-00353
E0-N626 – Roof

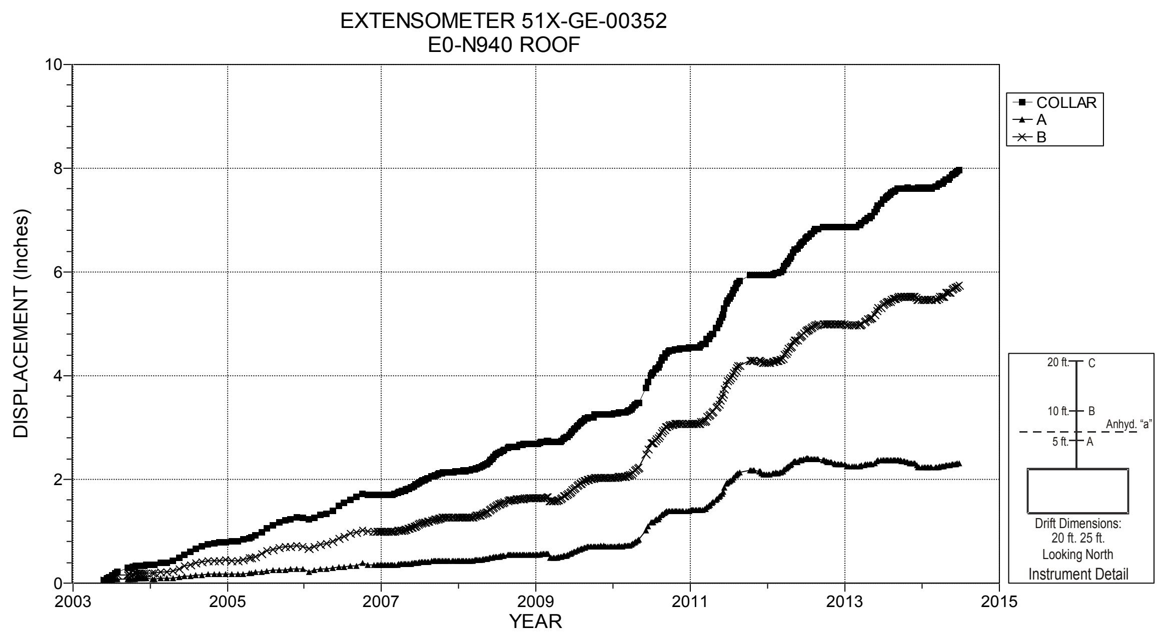

NOTES:
1. Excavation date: February 1983.

Figure 4-3 Extensometer 51X-GE-00352
E0 N940 – Roof

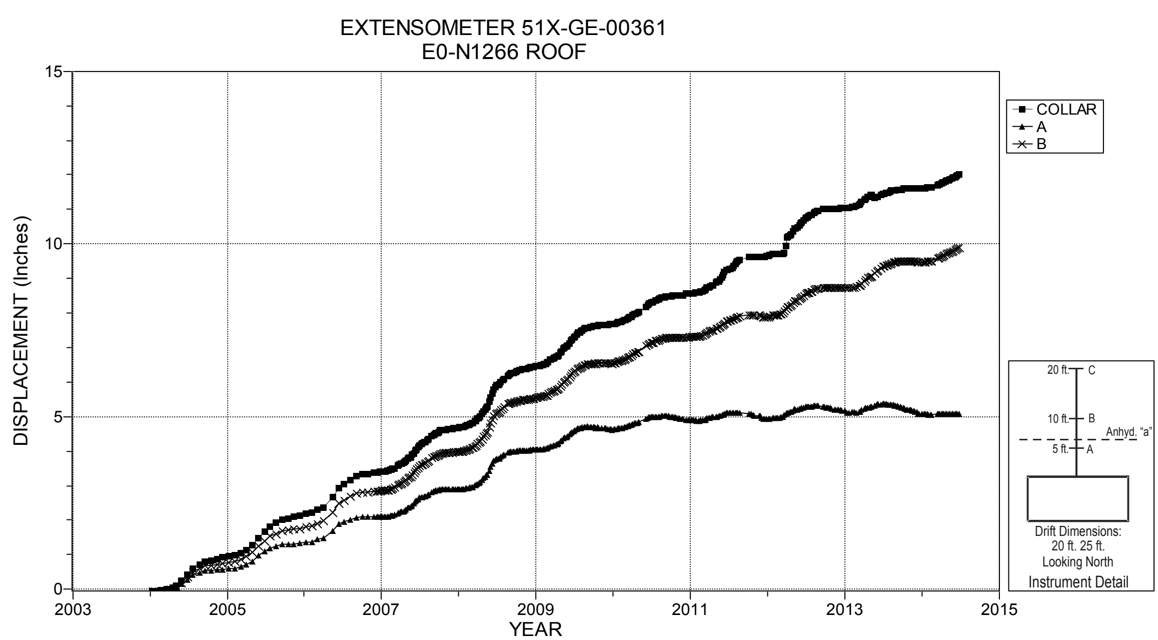

NOTES:
1. Excavation date: February 1983.

Figure 4-4 Extensometer 51X-GE-00361
E0-N1266 – Roof

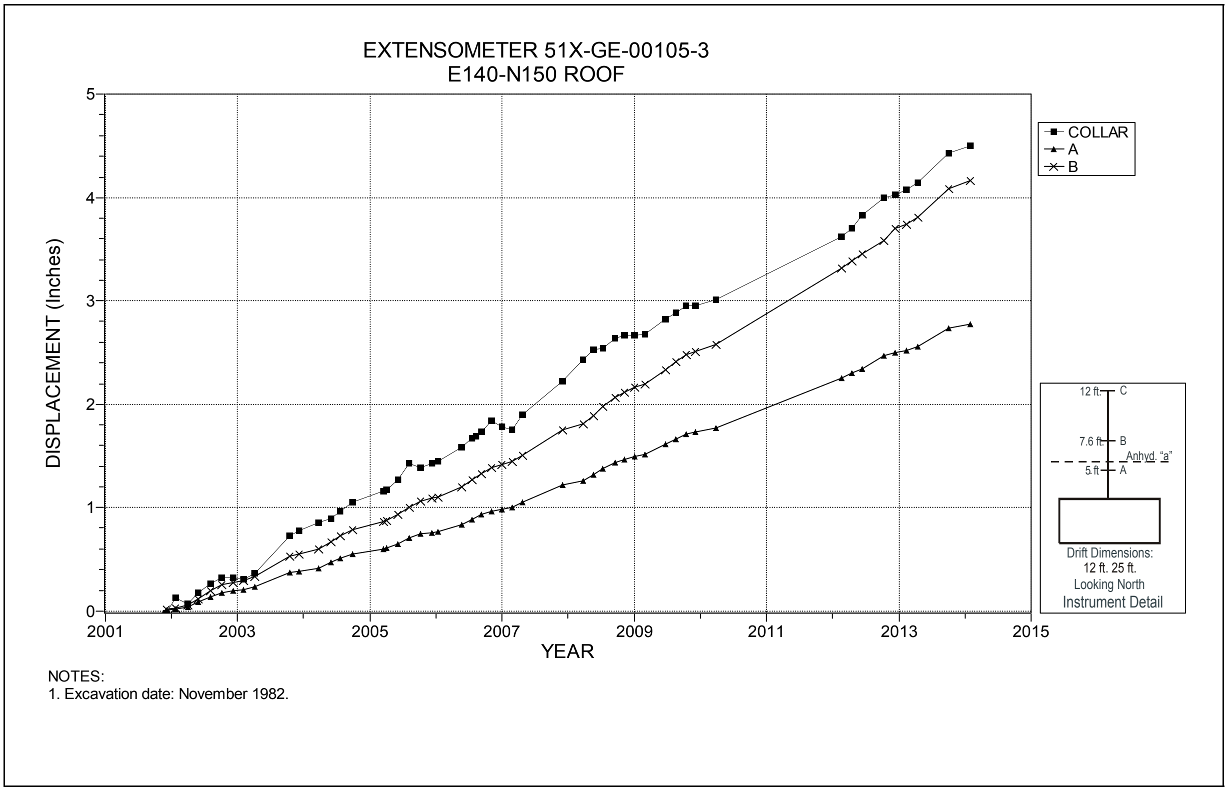

Figure 4-5 Extensometer 51X-GE-00105-3
E140 N150 – Roof

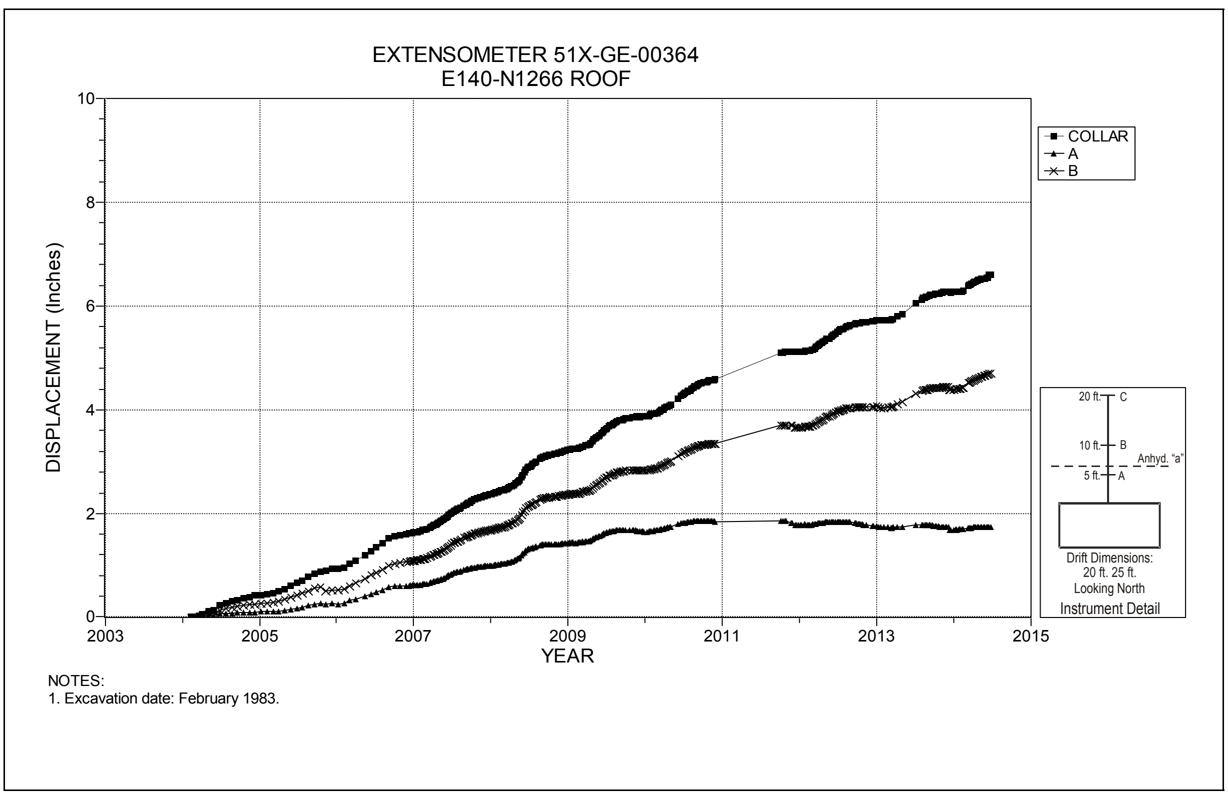

Figure 4-6 Extensometer 51X-GE-00364
E140 N1266 – Roof

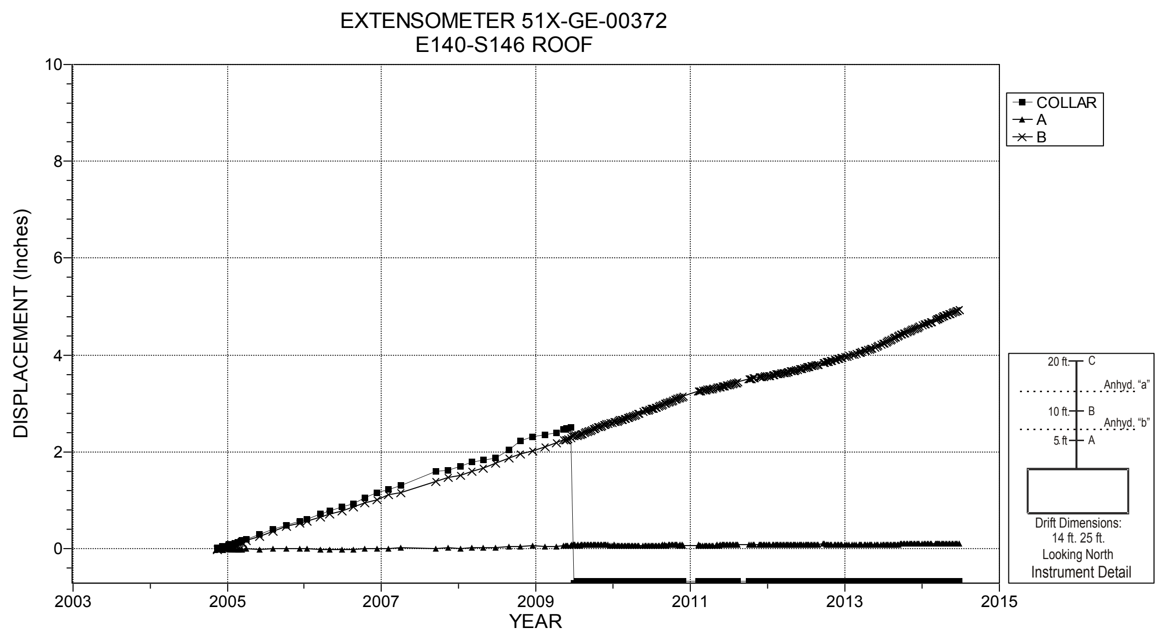

NOTES:
1. Excavation date: November 1982.
2. The mechanical connection to the Collar anchor has been lost.

Figure 4-7 Extensometer 51X-GE-00372
E140 S146 – Roof

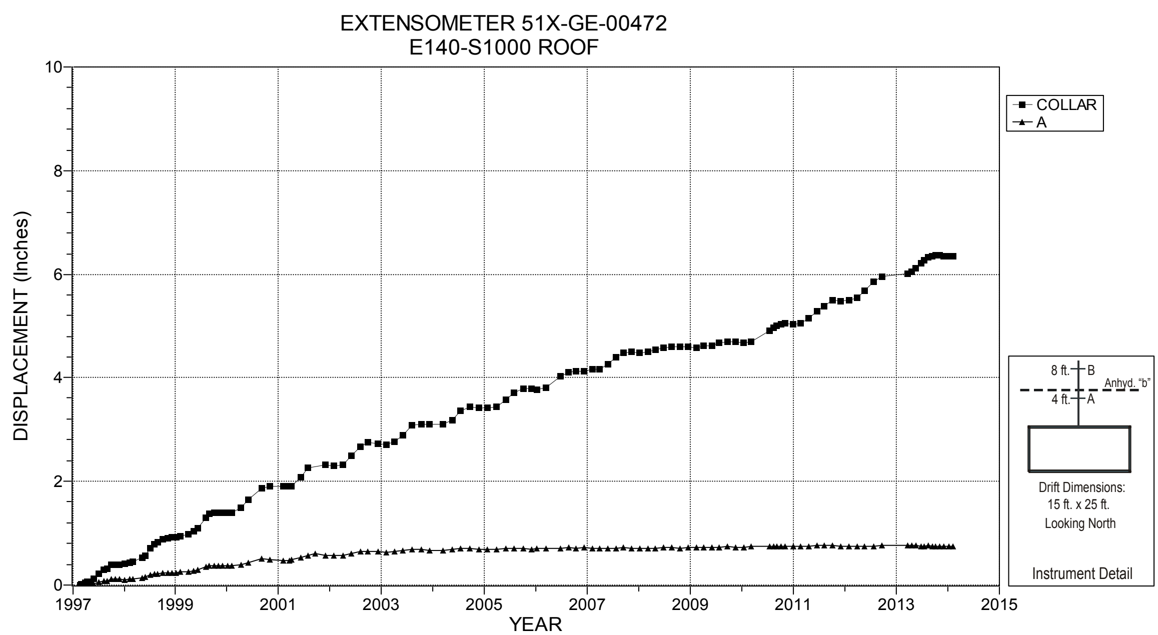

NOTES:
1. Excavation date: December 1982.

Figure 4-8 Extensometer 51X-GE-00472
E140 S1000 – Roof

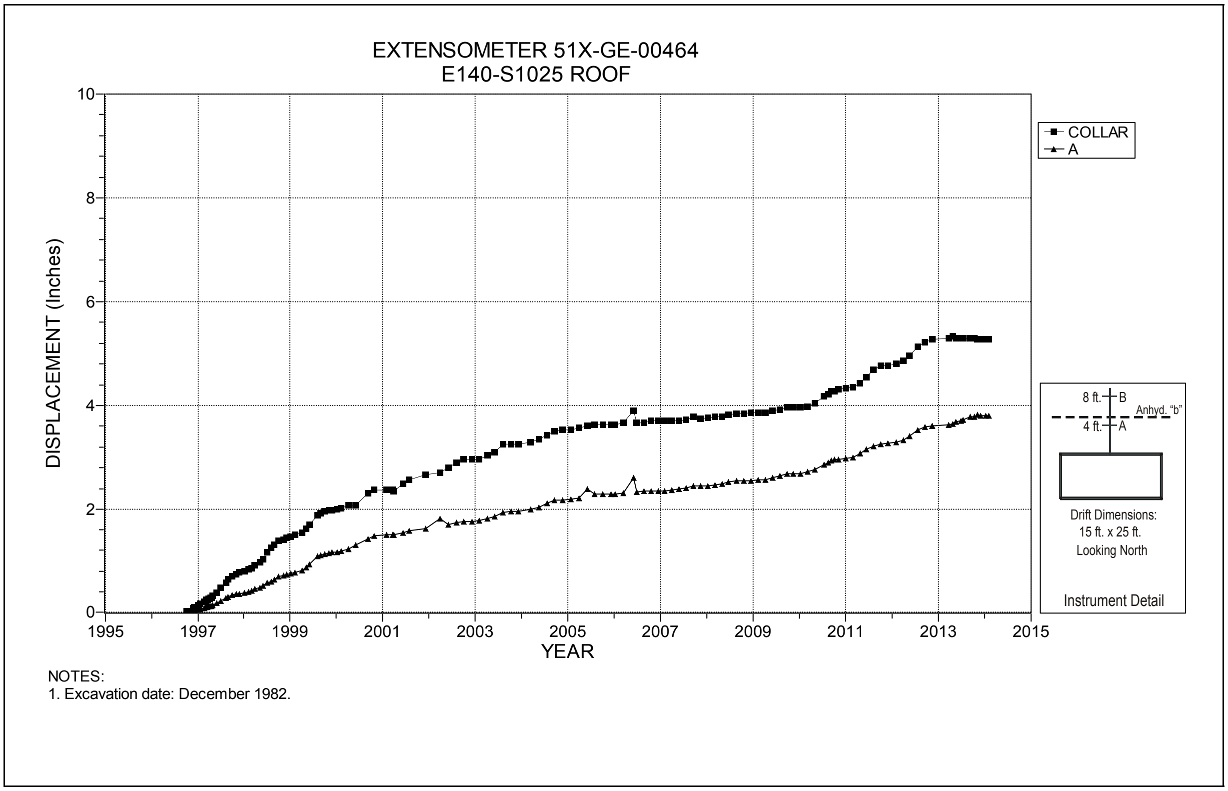

Figure 4-9 Extensometer 51X-GE-00464
E140 S1025 – Roof
Error! Bookmark not defined.

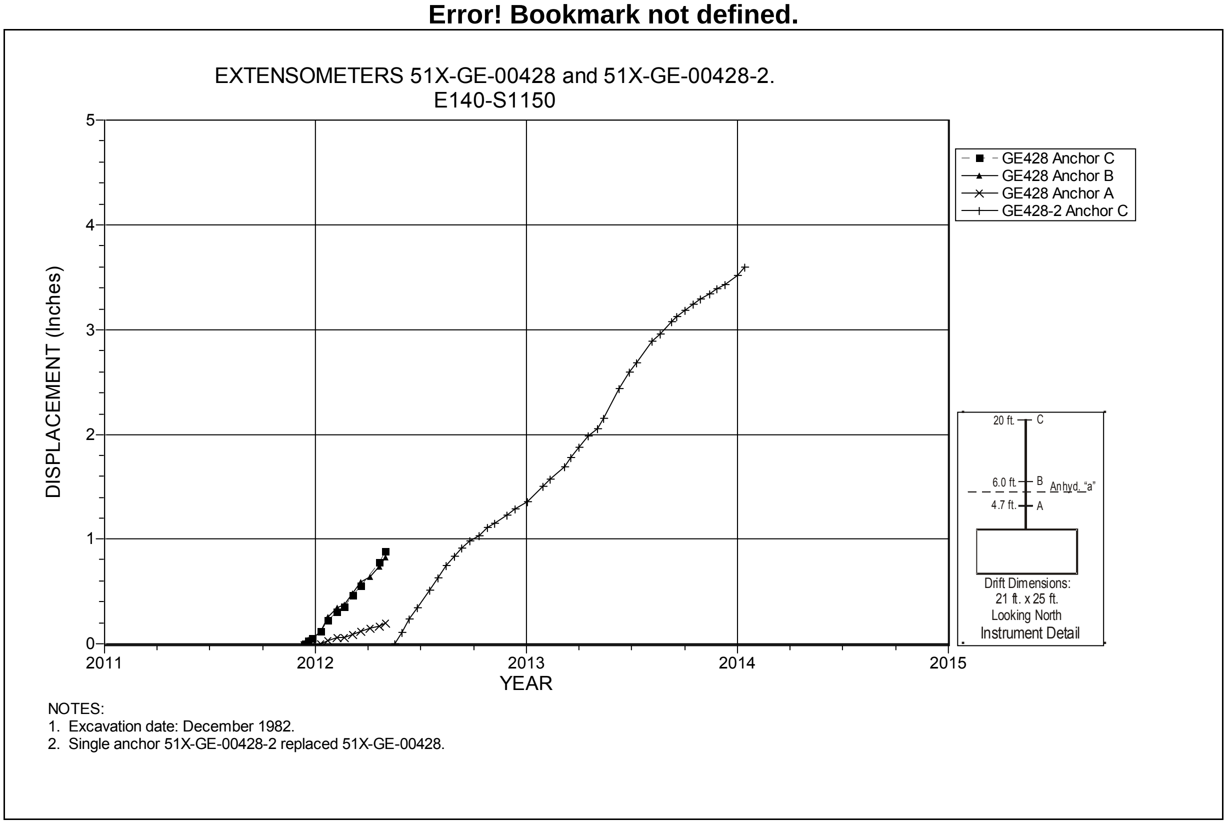

Figure 4-10 Extensometers 51X-GE-00428 and 51X-GE-00428-2
E140 S1150 – Roof

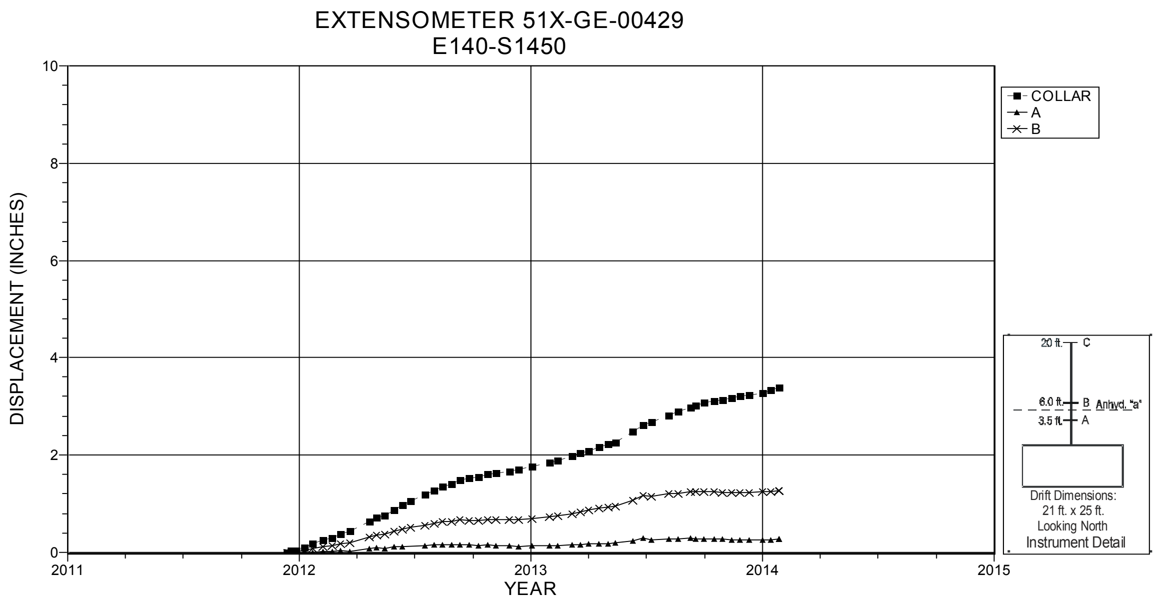

NOTES:
1. Excavation date: December 1982.

Figure 4-11 Extensometer 51X-GE-00429
E140 S1450 – Roof

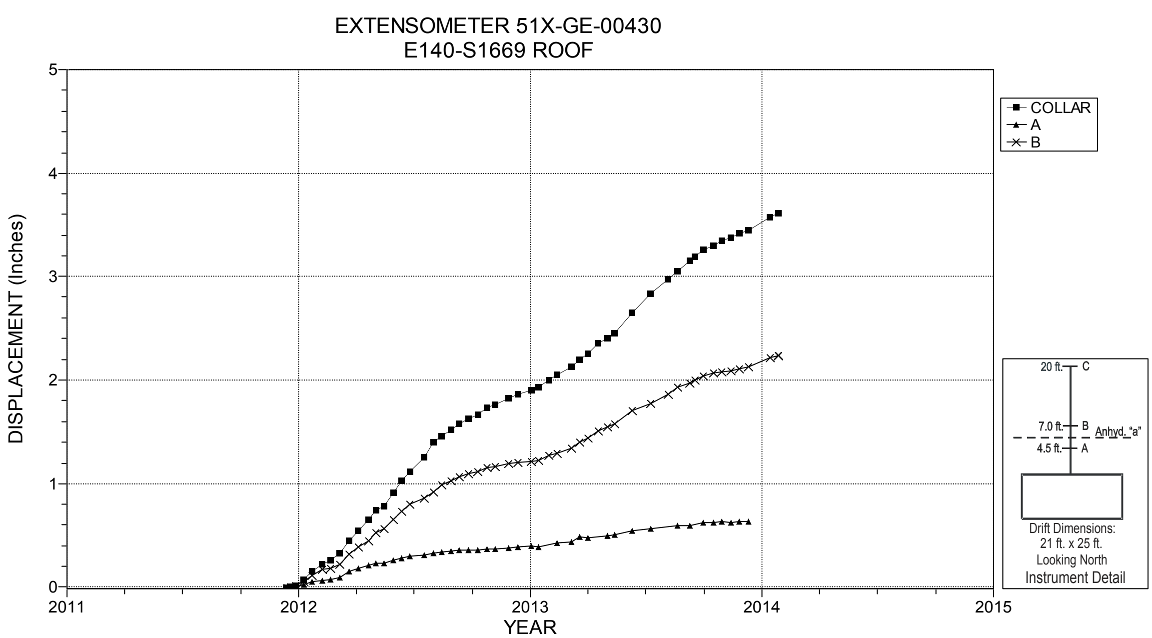

NOTES:
1. Excavation date: December 1982.

Figure 4-12 Extensometer 51X-GE-00430
E140 S1669 – Roof

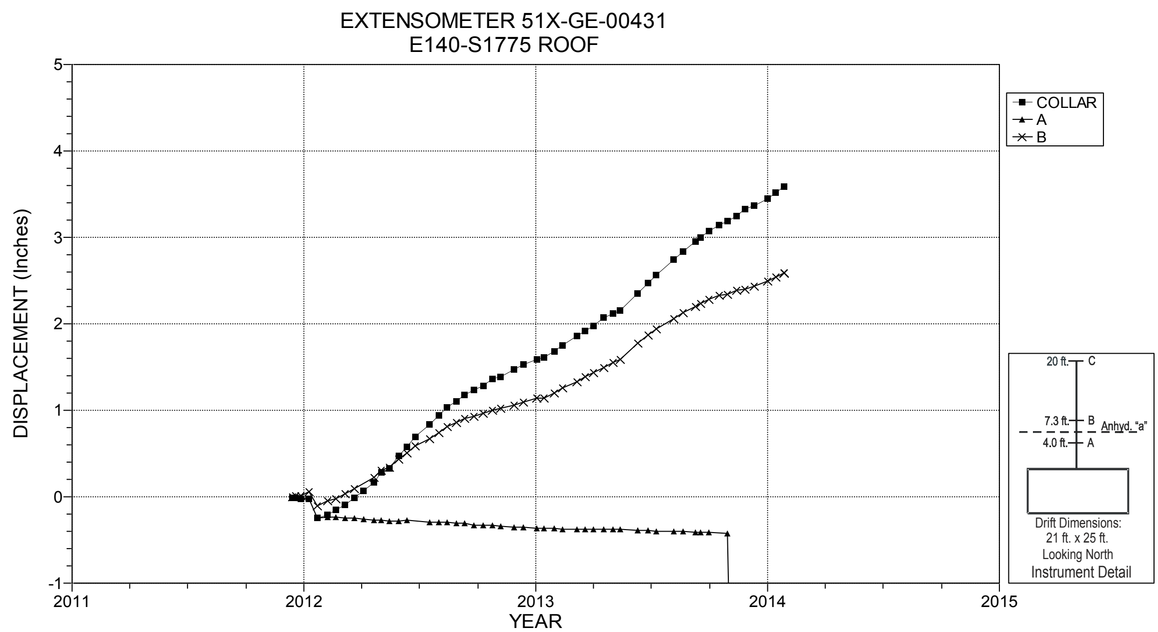

NOTES:
1. Excavation date: December 1982.
2. The negative offset that occurred not long after installation is due to the instrument being struck by a roof bolter.
3. Anchor "A" has failed.

Figure 4-13 Extensometer 51X-GE-00431
E140 S1775 – Roof

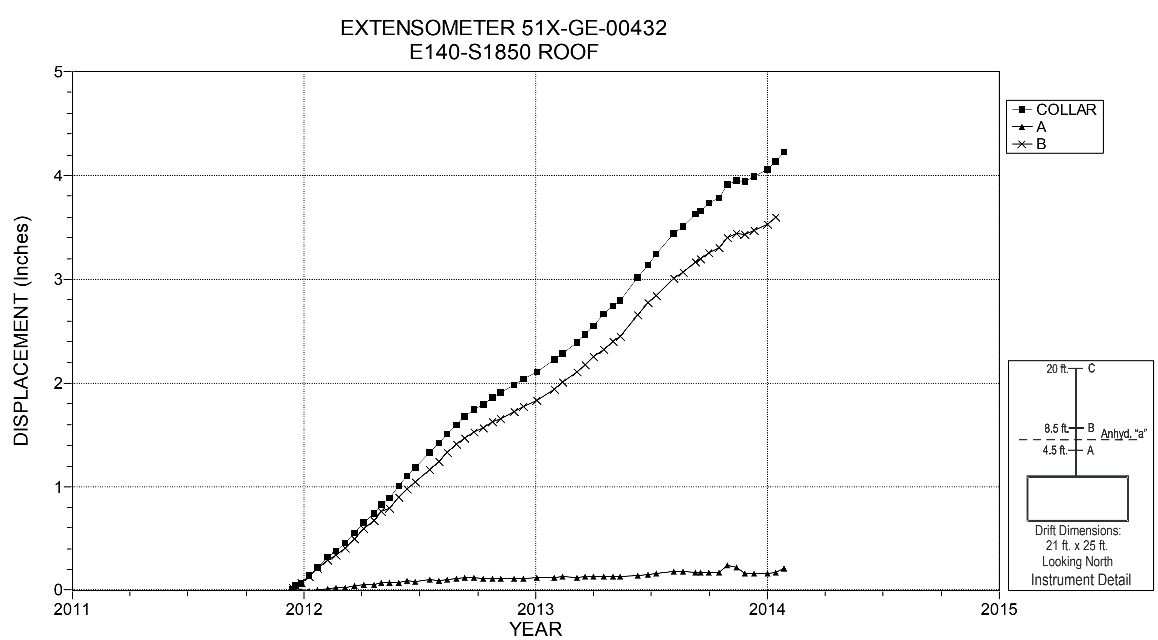

NOTES:
1. Excavation date: December 1982.

Figure 4-14 Extensometer 51X-GE-00432
E140 S1850 – Roof

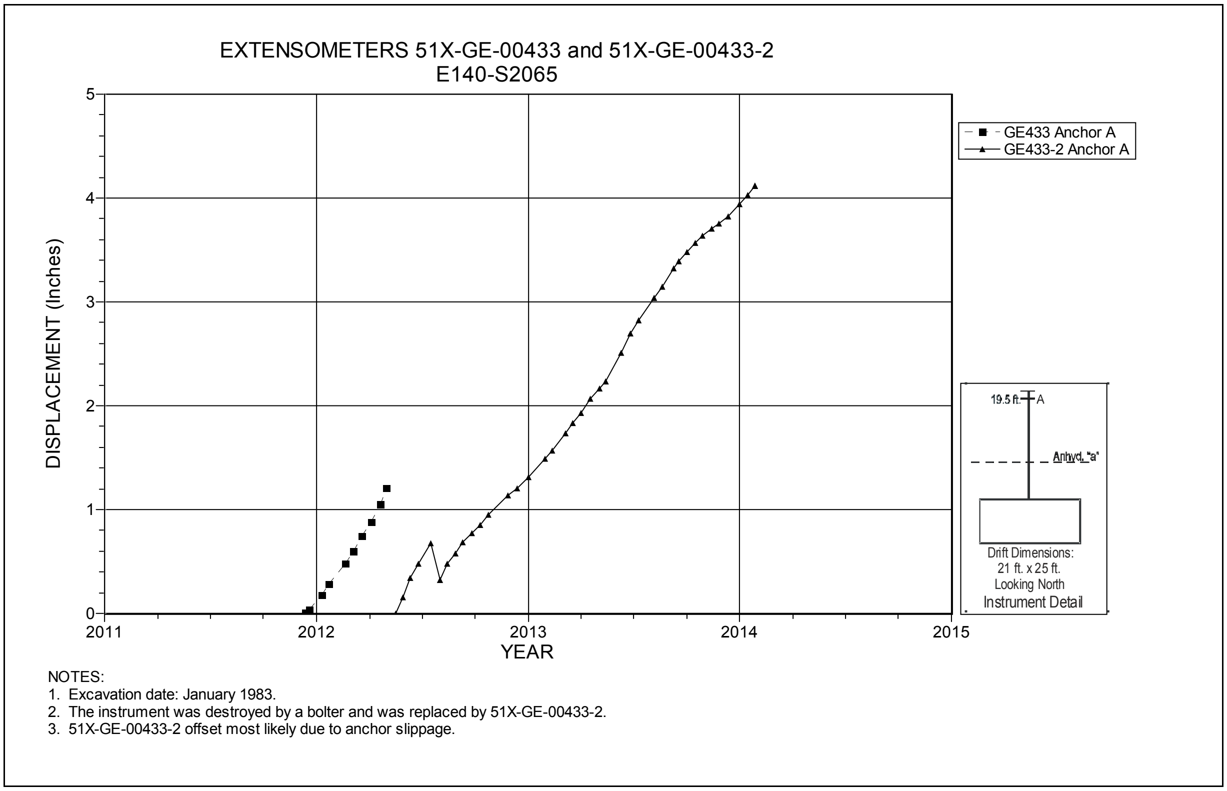

Figure 4-15 Extensometers 51X-GE-00433 and 51X-GE-00433-2
E140 S2065 – Roof

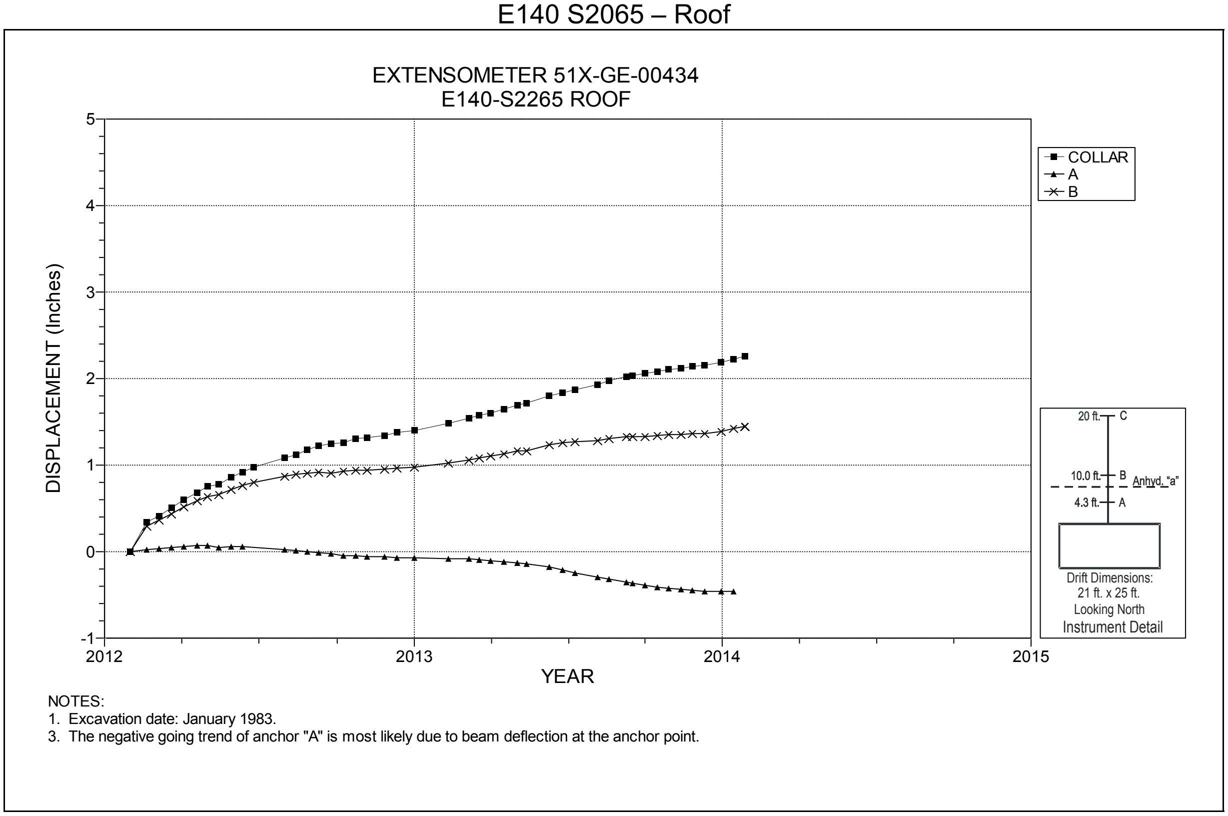

Figure 4-16 Extensometer 51X-GE-00434
E140 S2265 – Roof

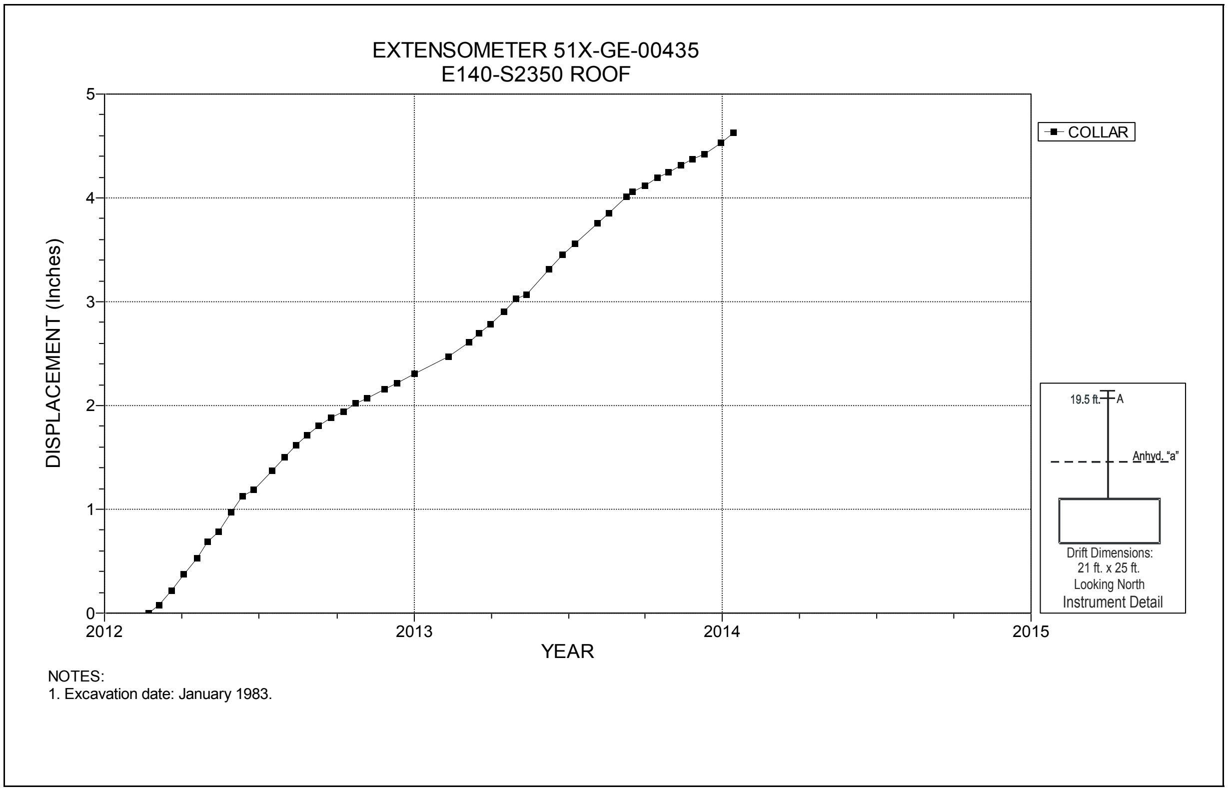

Figure 4-17 Extensometer 41X-GE-00435
E140 S2350 – Roof

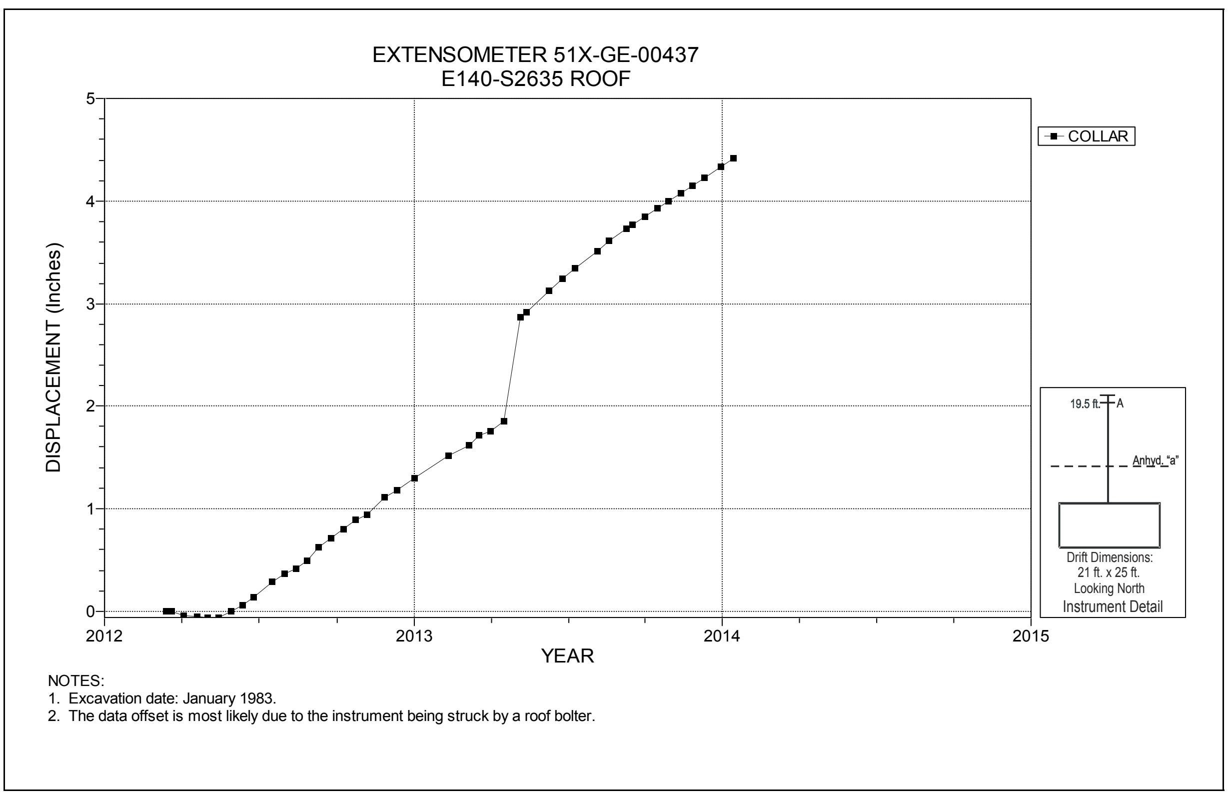

Figure 4-18 Extensometer 41X-GE-00437
E140 S2635 – Roof

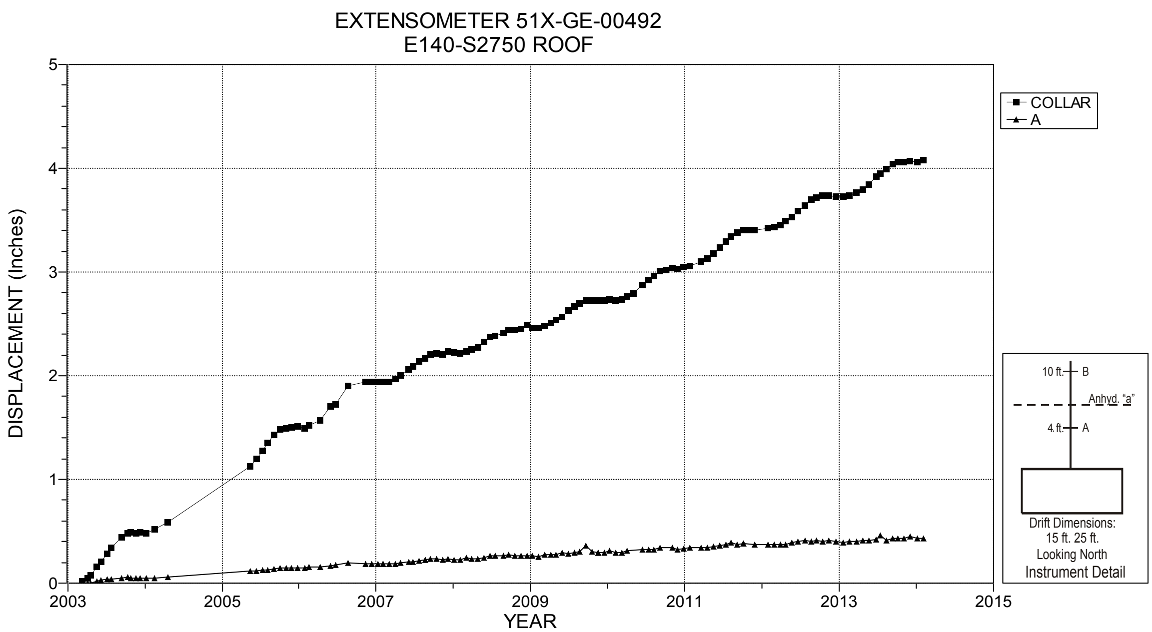

NOTES:
1. Excavation date: January 1983.

Figure 4-19 Extensometer 51X-GE-00492
E140 S2750 – Roof

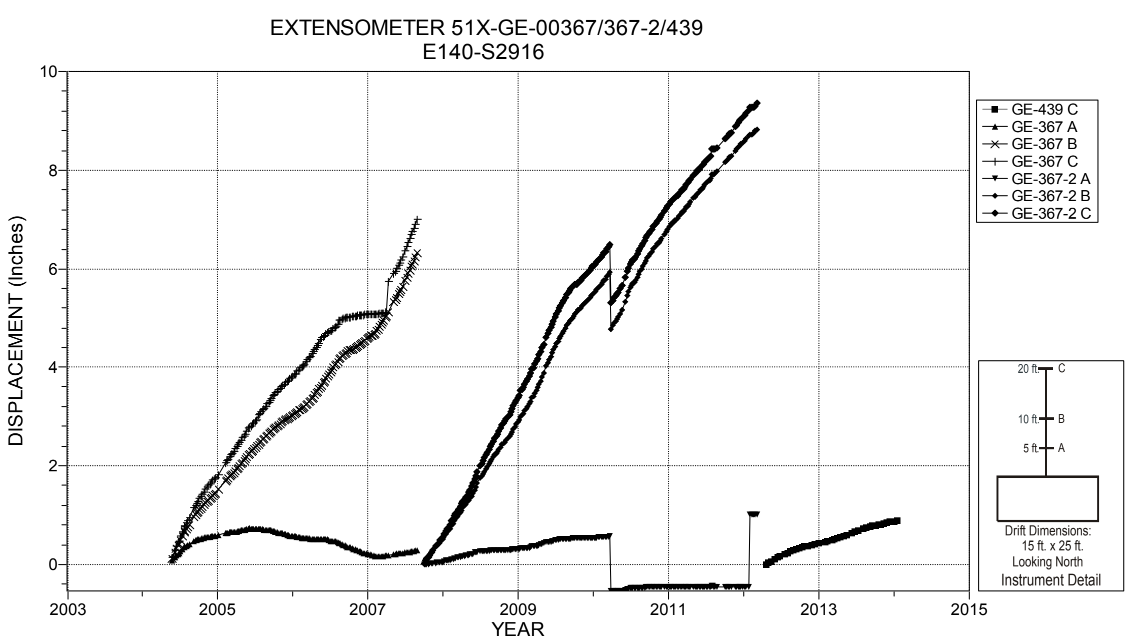

NOTES:
1. Excavation date: January 1983.
2. Instrument was reset April 2007 due to wire from collar anchor hanging-up inside the instrument.
3. GE367 was replaced by GE367-2 in 09/2007;
4. The data offset in 1Q 2010 was due to a bolter strike; GE439 replaced GE367-2.

Figure 4-20 Extensometers 51X-GE-00367, 51X-GE-00367-2 and 51X-GE-00439
E140 S2916 – Roof

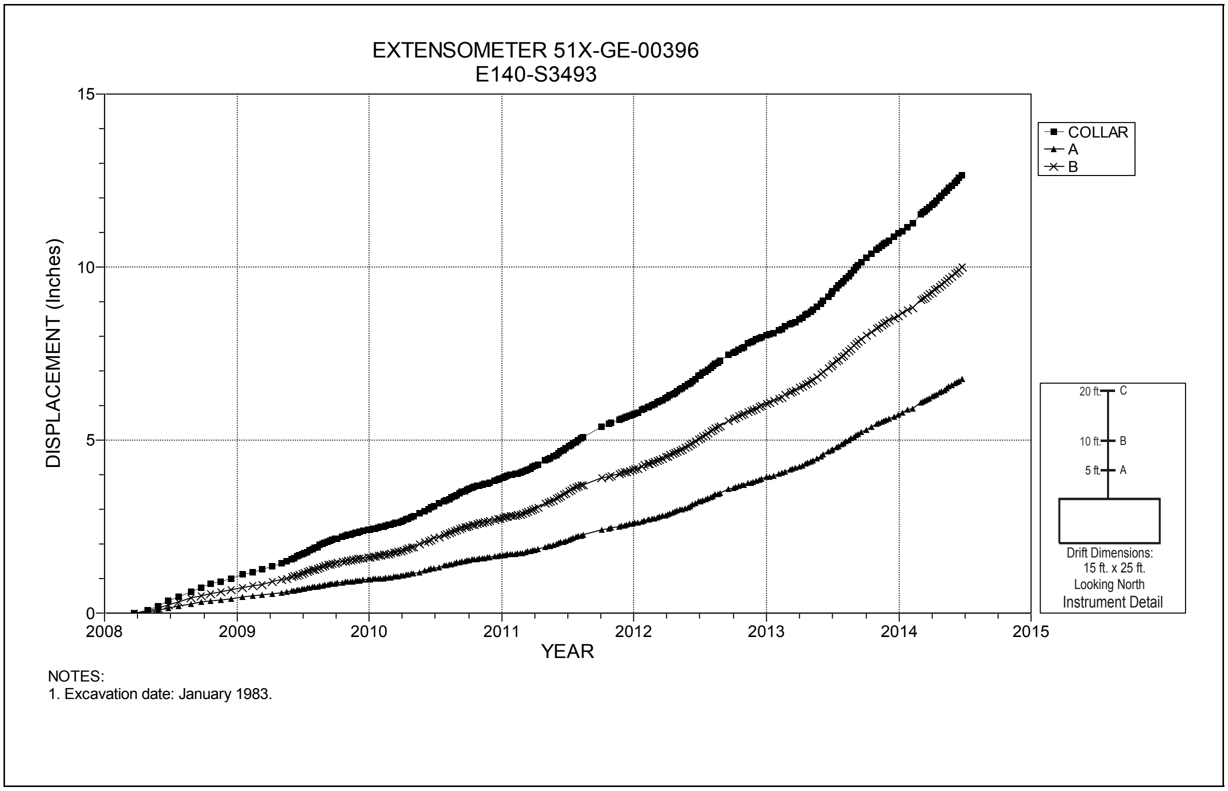

Figure 4-21 Extensometer 51X-GE-00396
E140 S3493 – Roof

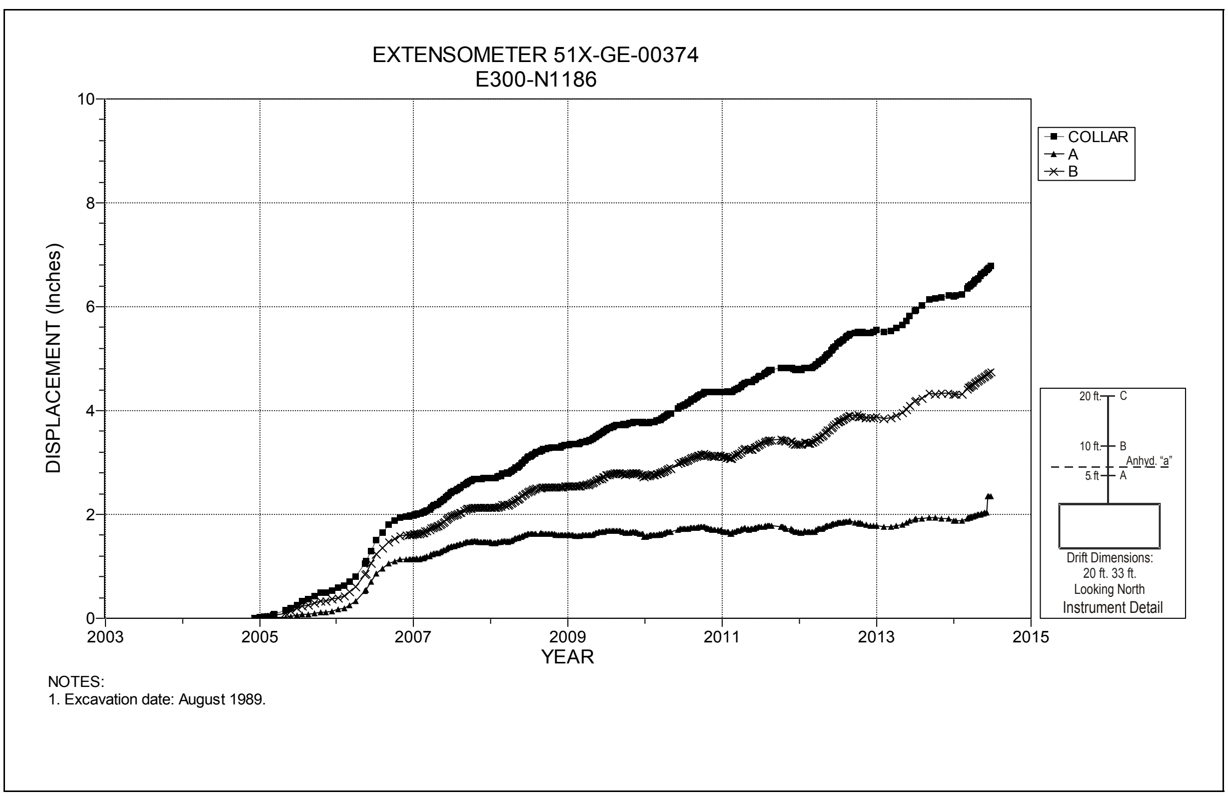

Figure 4-22 Extensometer 51X-GE-00374
E300 N1186 – Roof

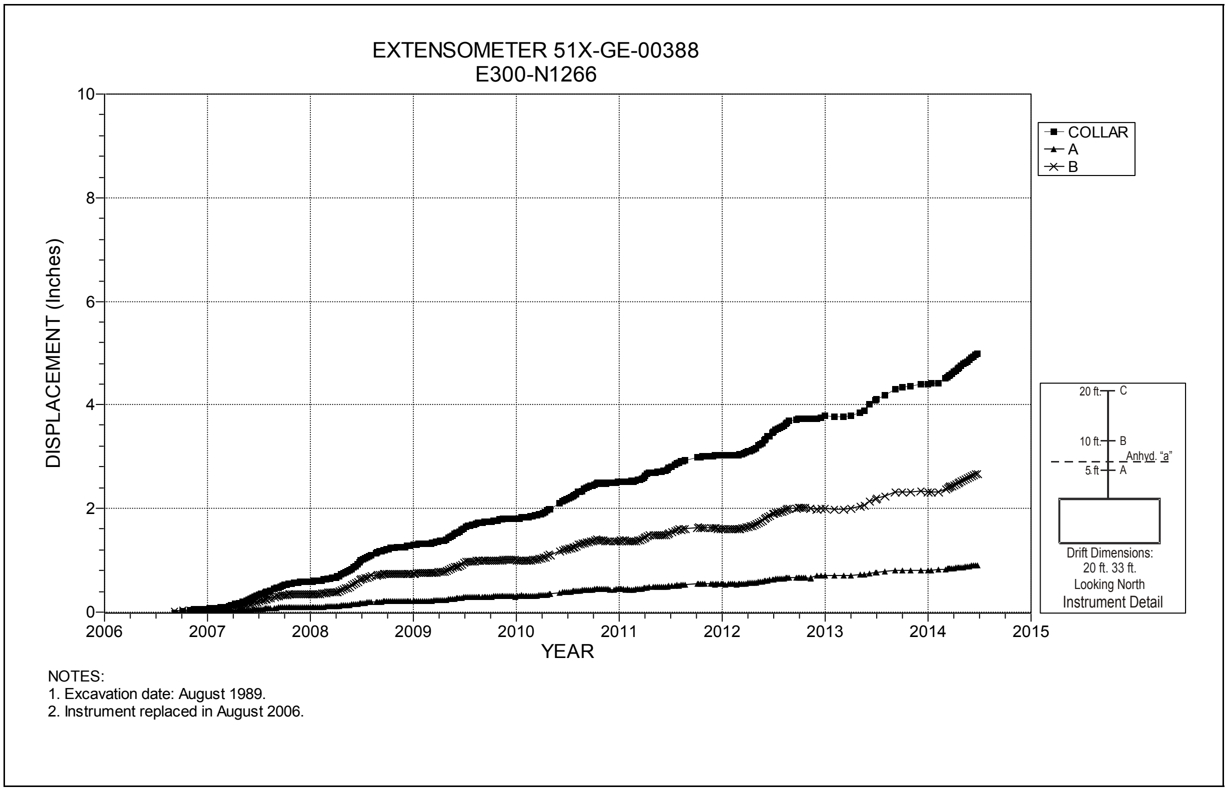

Figure 4-23 Extensometer 51X-GE-00388
E300 N1266 – Roof

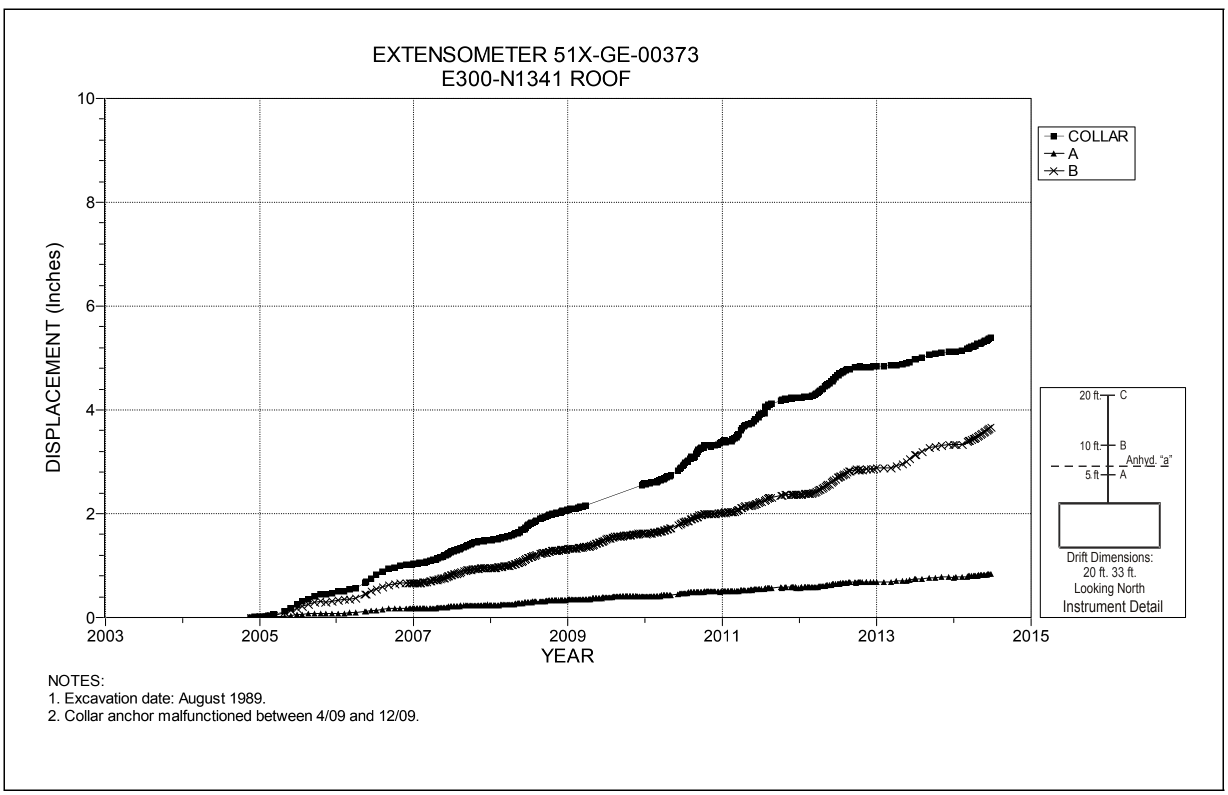

Figure 4-24 Extensometer 51X-GE-00373
E300 N1341 – Roof

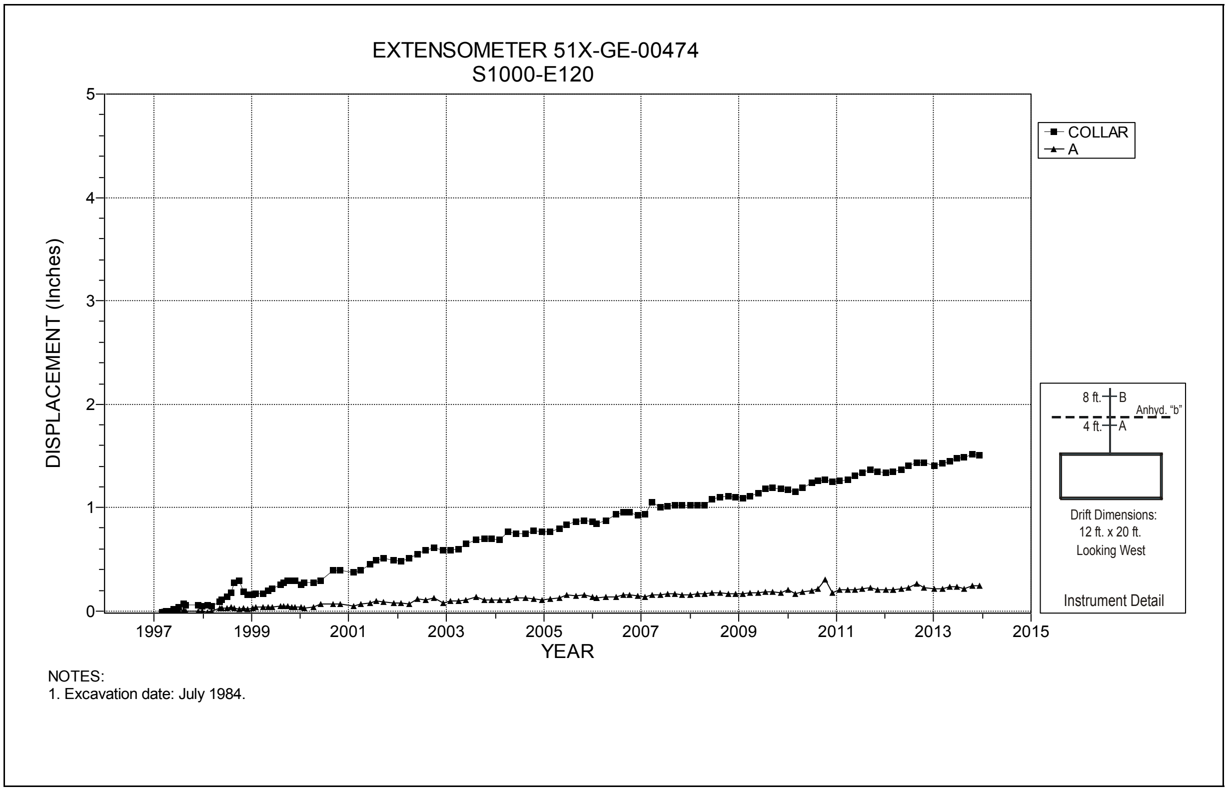

Figure 4-25 Extensometer 51X-GE-00474
S1000 E120 – Roof

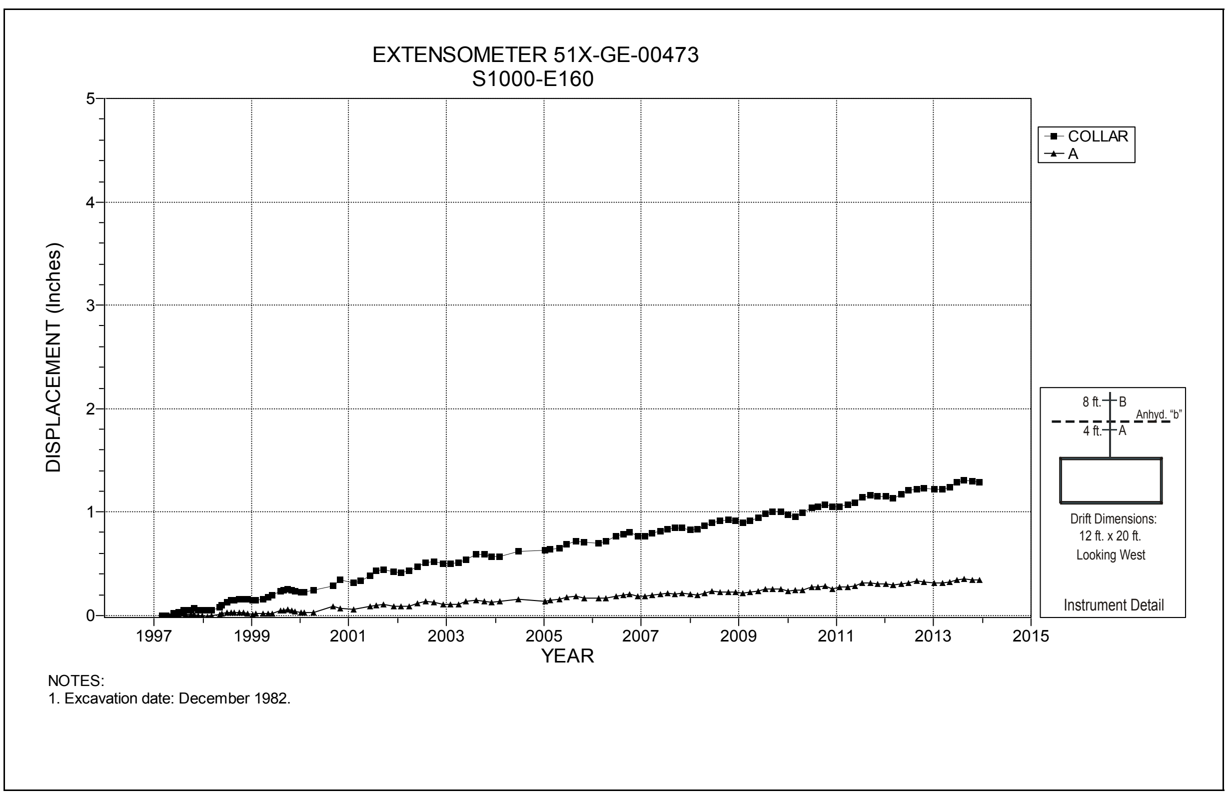

Figure 4-26 Extensometer 51X-GE-00473
S1000 E160 – Roof

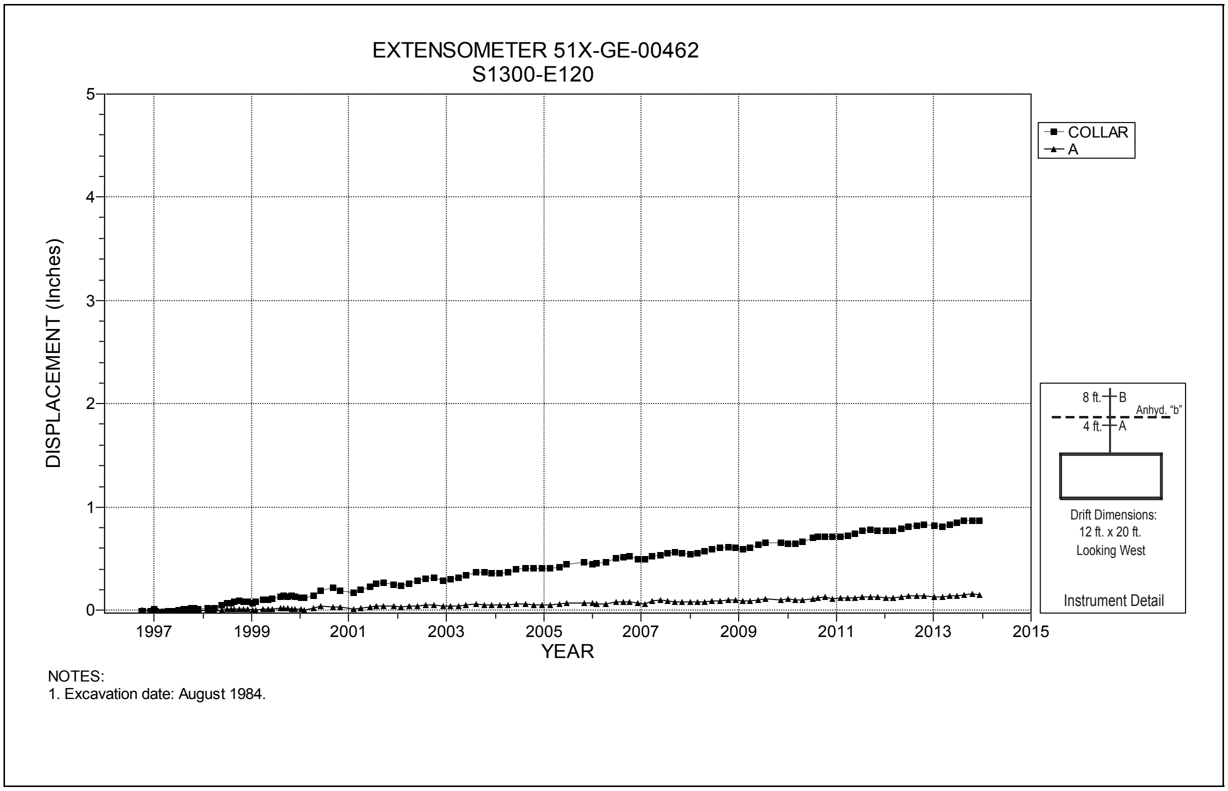

Figure 4-27 Extensometer 51X-GE-00462
S1300 E120 – Roof

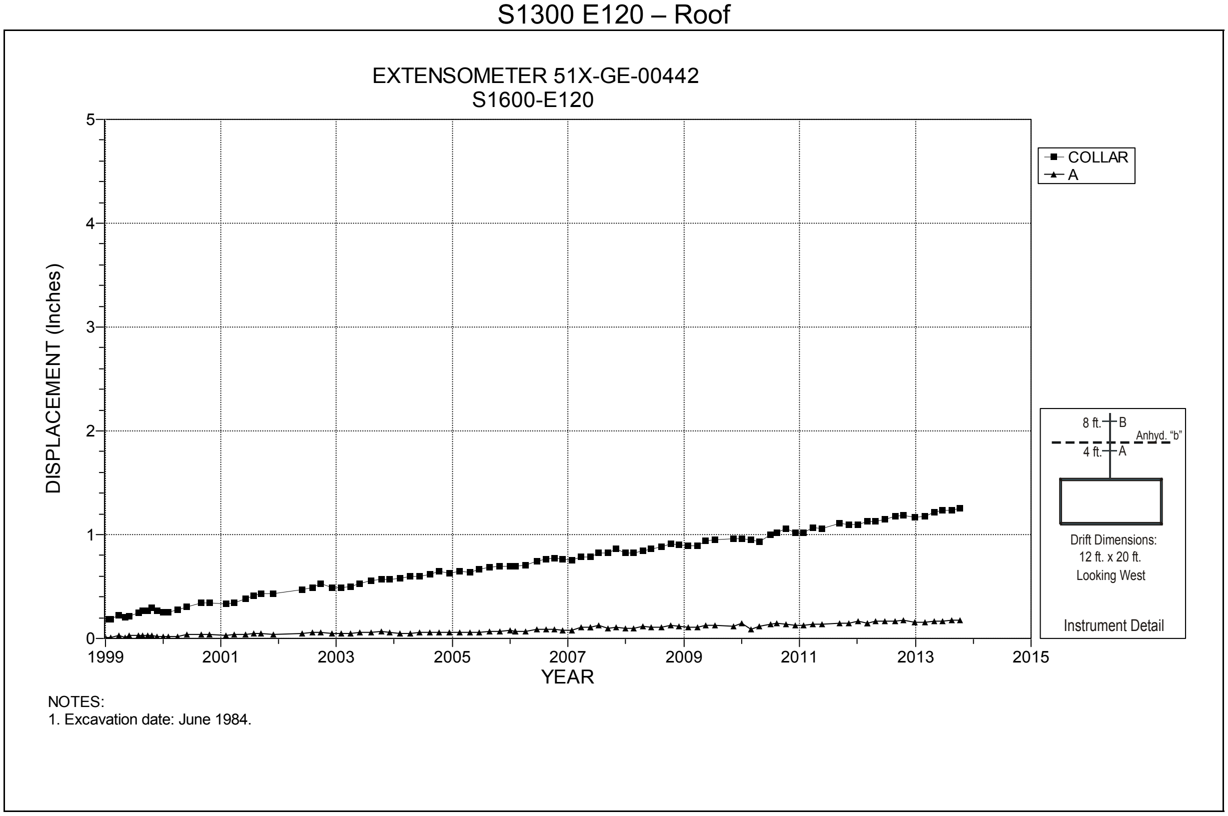

Figure 4-28 Extensometer 51X-GE-00442
S1600 E120 – Roof

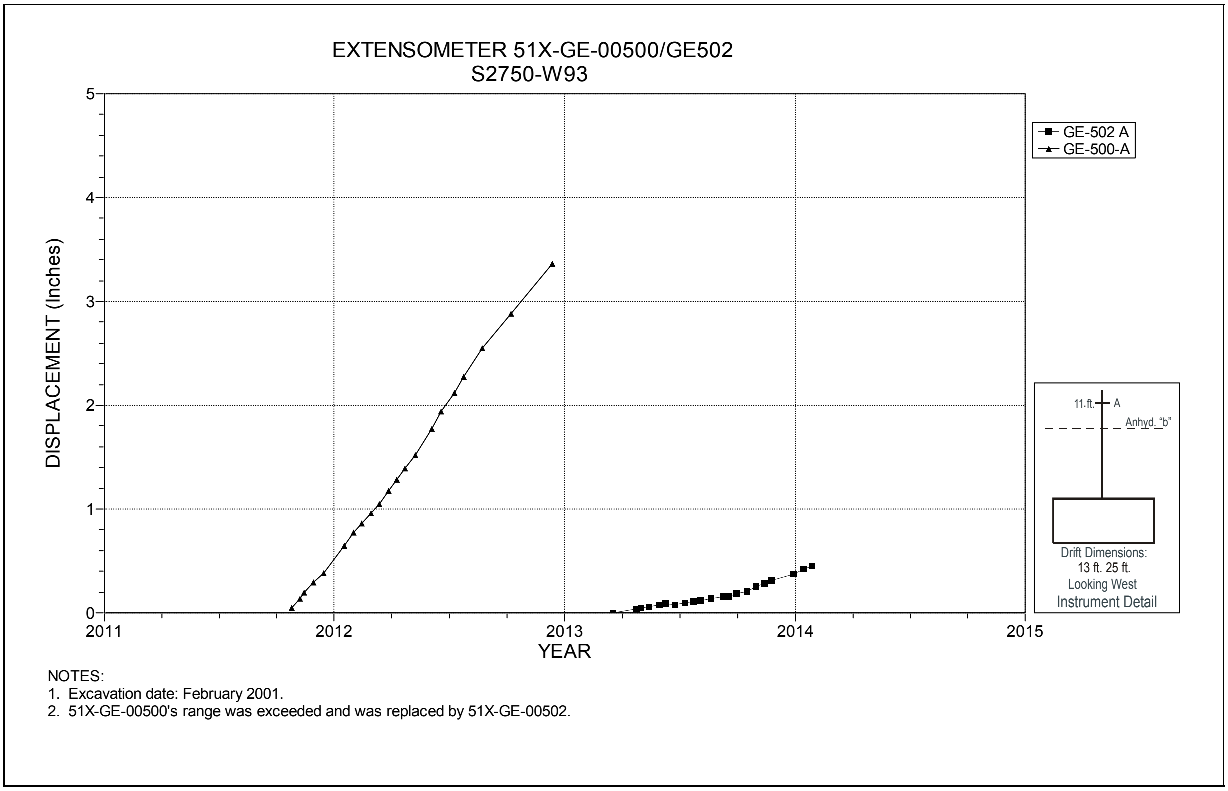

Figure 4-29 Extensometers 51X-GE-00500 and 51X-GE-00502
S2750 W93 – Roof

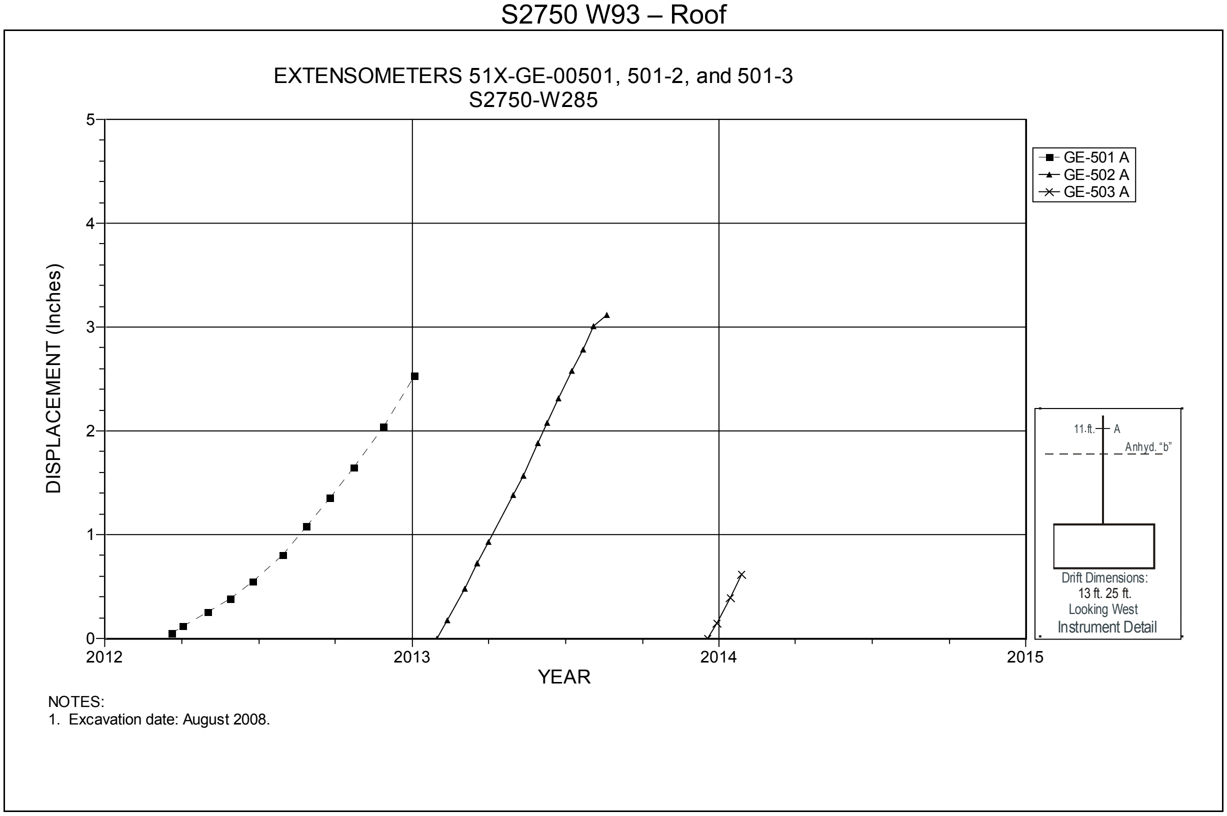

Figure 4-30 Extensometers 51X-GE-00501, 51X-GE-00501-2, and 51X-GE-00501-3
S2750 W285 – Roof

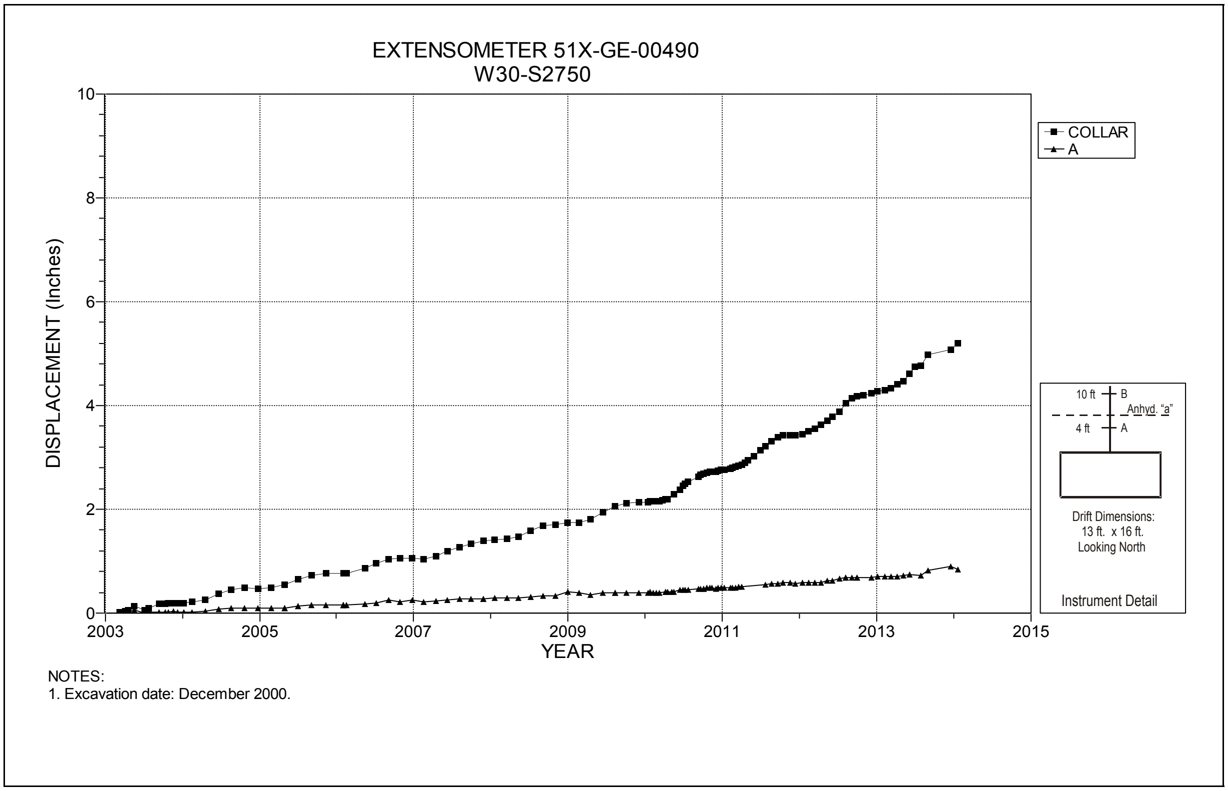

Figure 4-31 Extensometer 51X-GE-00490
W30 S2750 – Roof

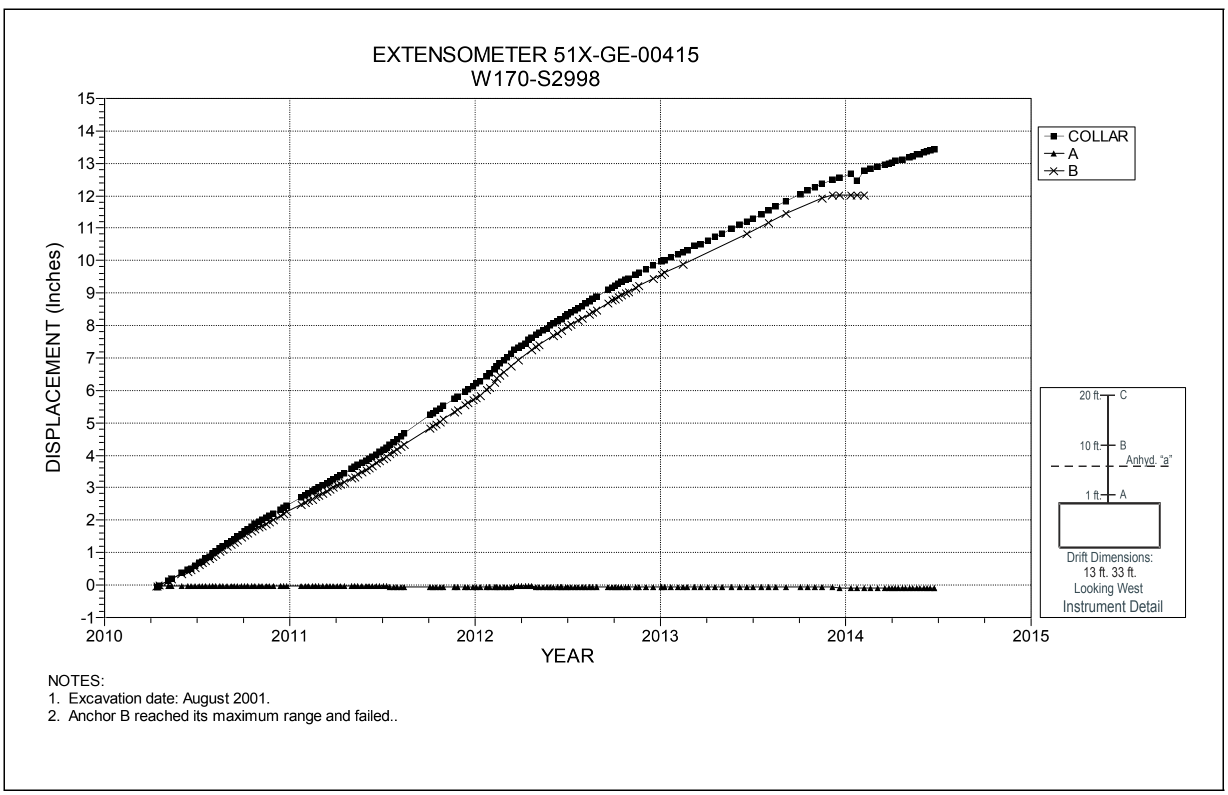

Figure 4-32 Extensometer 51X-GE-00415
W170 S2998 – Roof

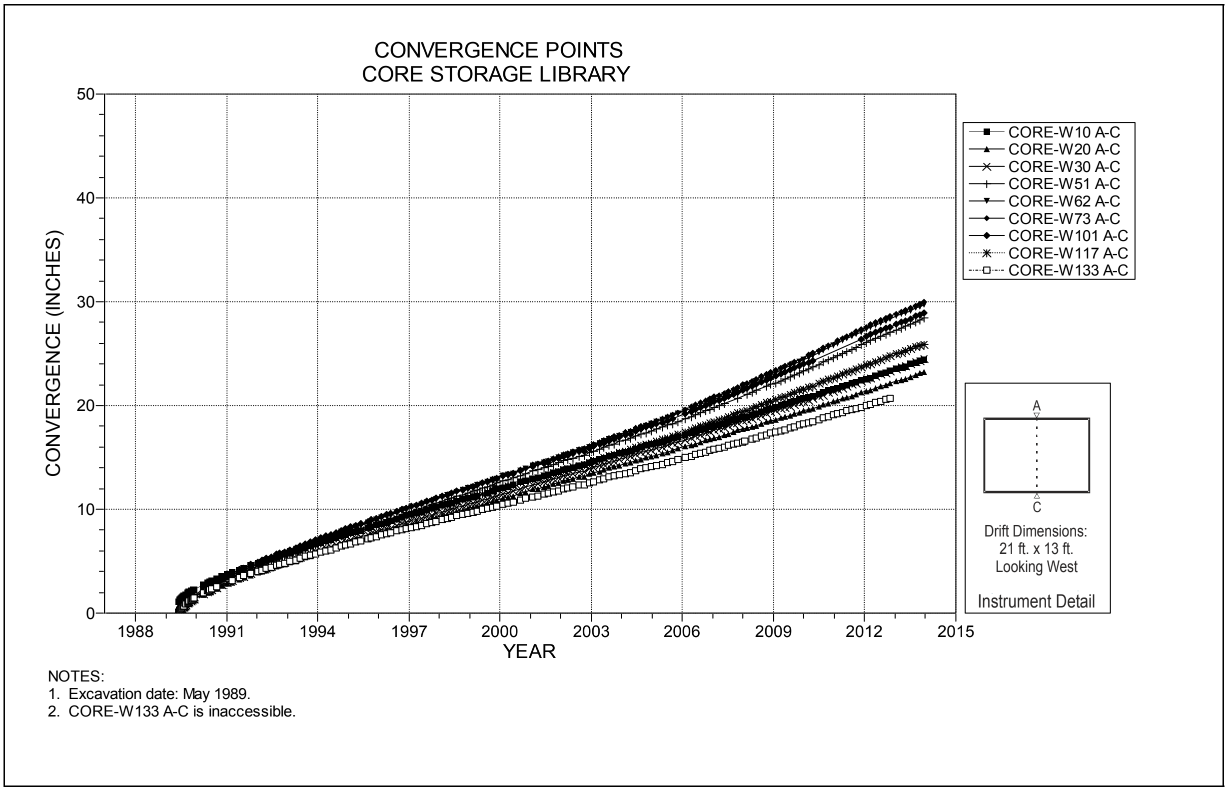

Figure 4-33 Convergence Point Array
Core Storage Library – Roof to Floor

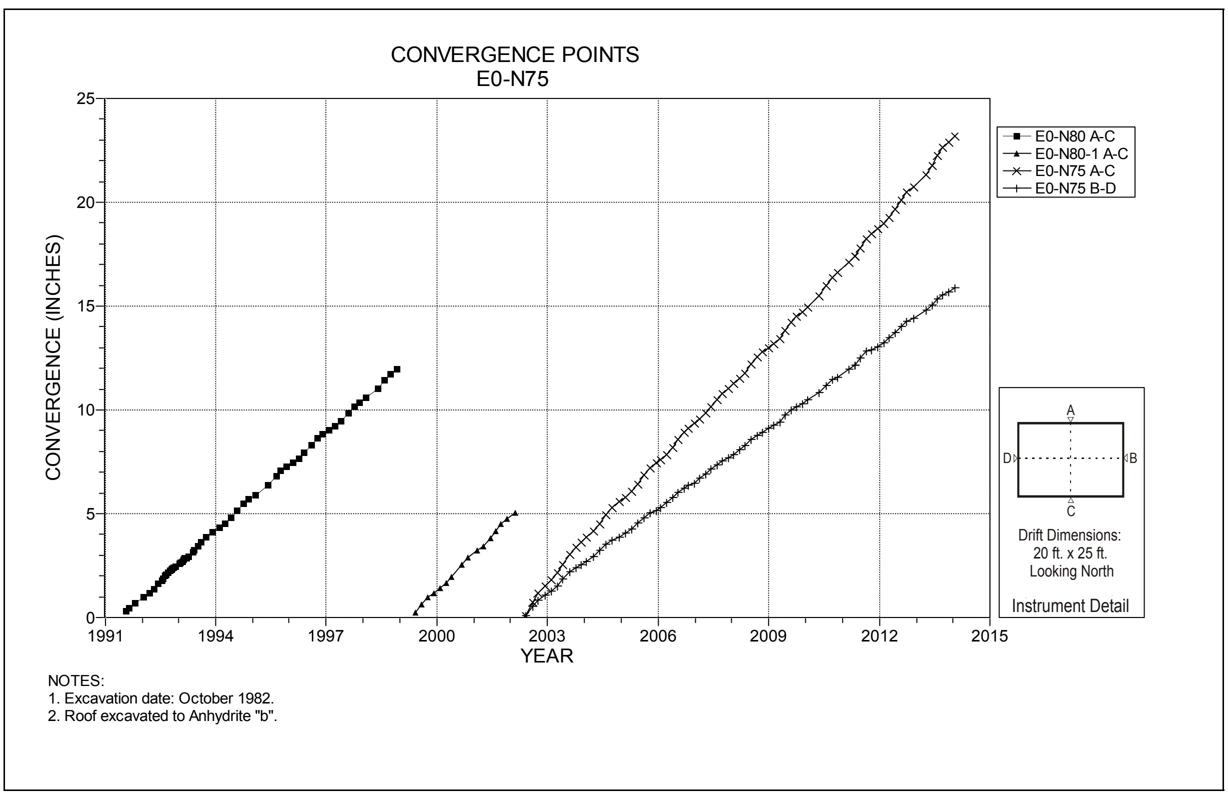

Figure 4-34 Convergence Point Array
E0 N75 – All Chords

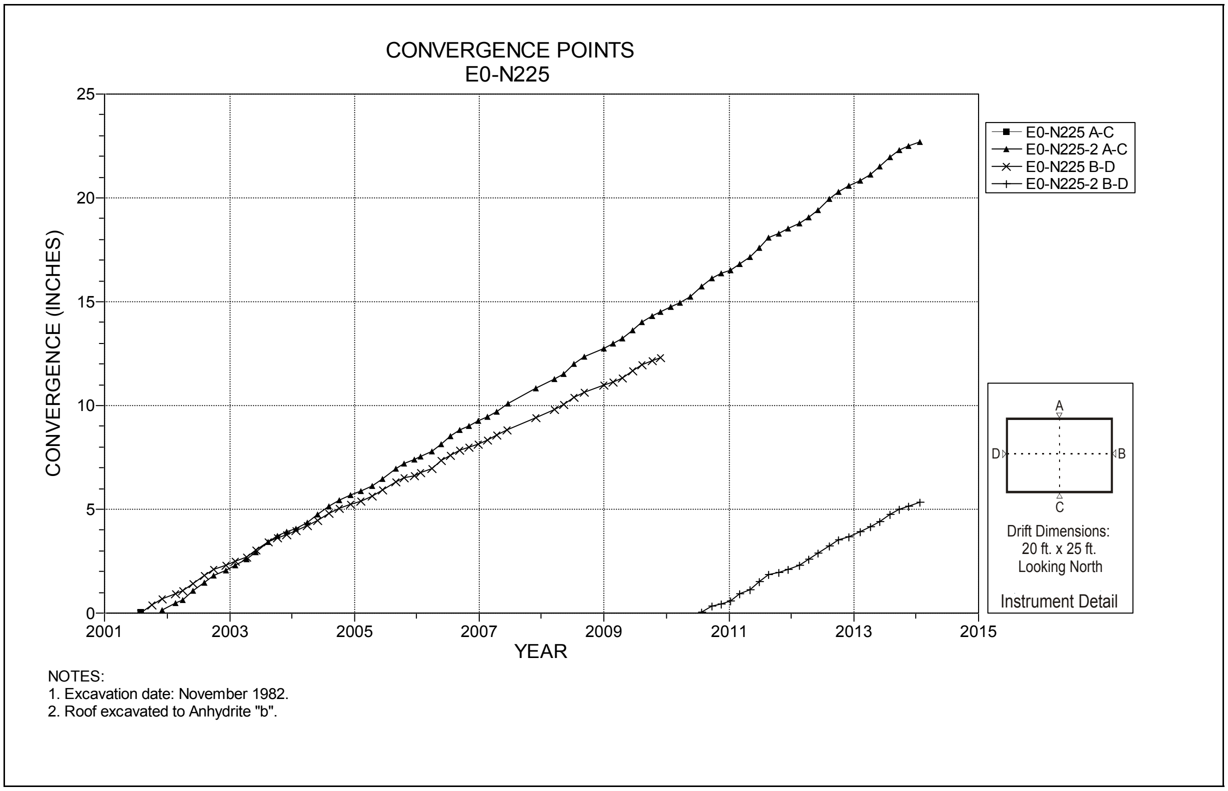

Figure 4-35 Convergence Point Array
E0 N225 – All Chords

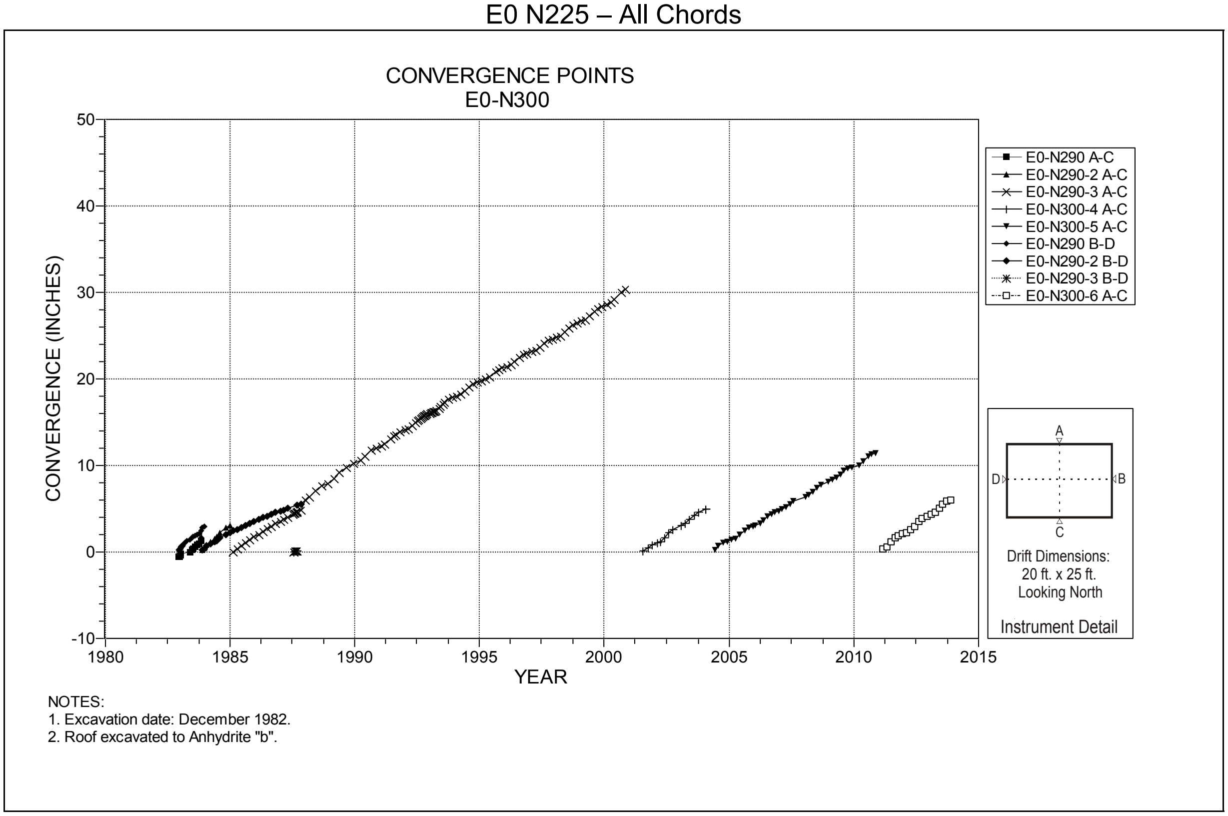

Figure 4-36 Convergence Point Array
E0 N300 – All Chords

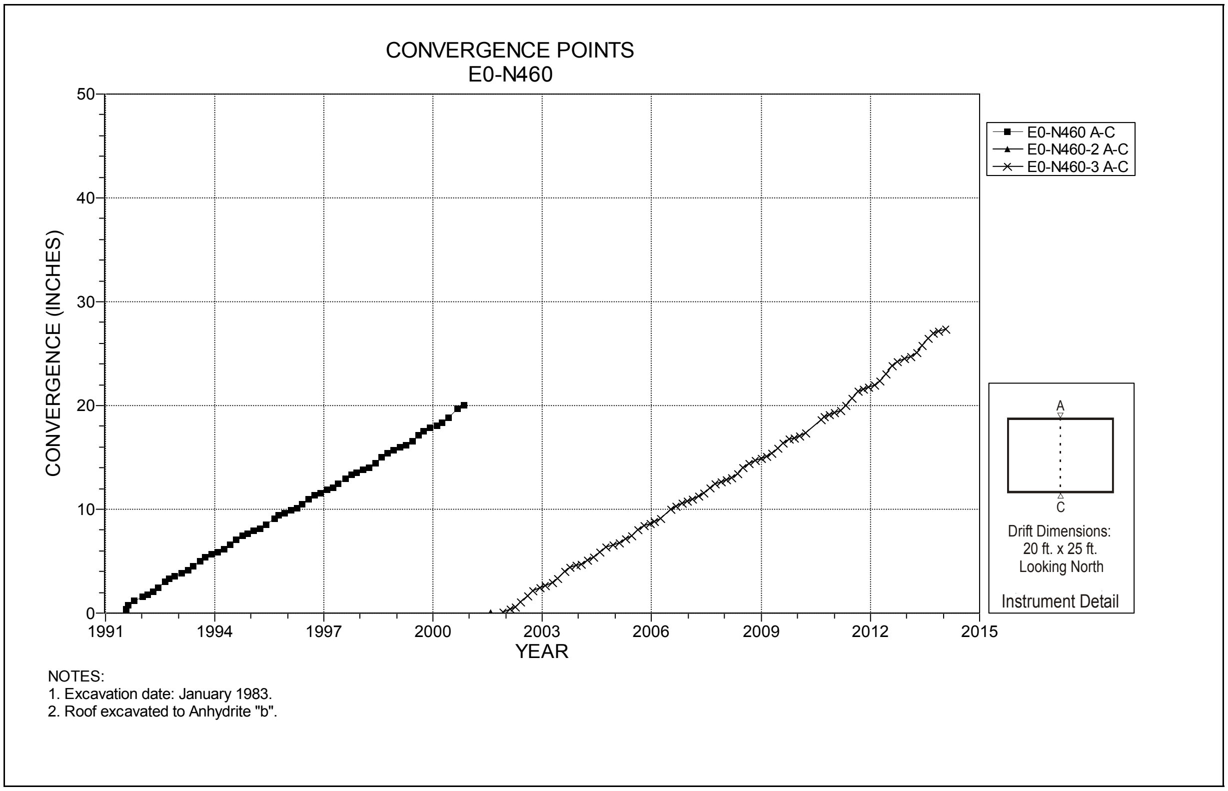

Figure 4-37 Convergence Point Array
E0 N460 – Roof to Floor

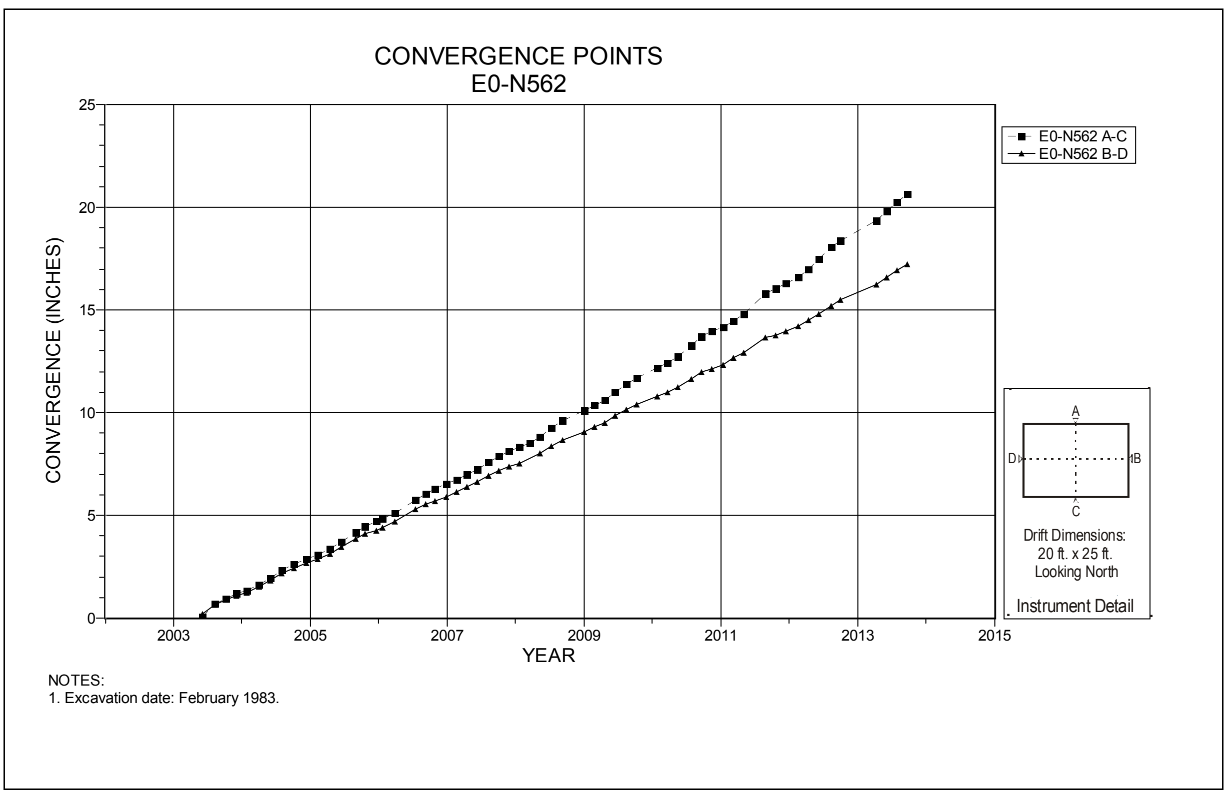

Figure 4-38 Convergence Point Array
E0 N562 – All Chords

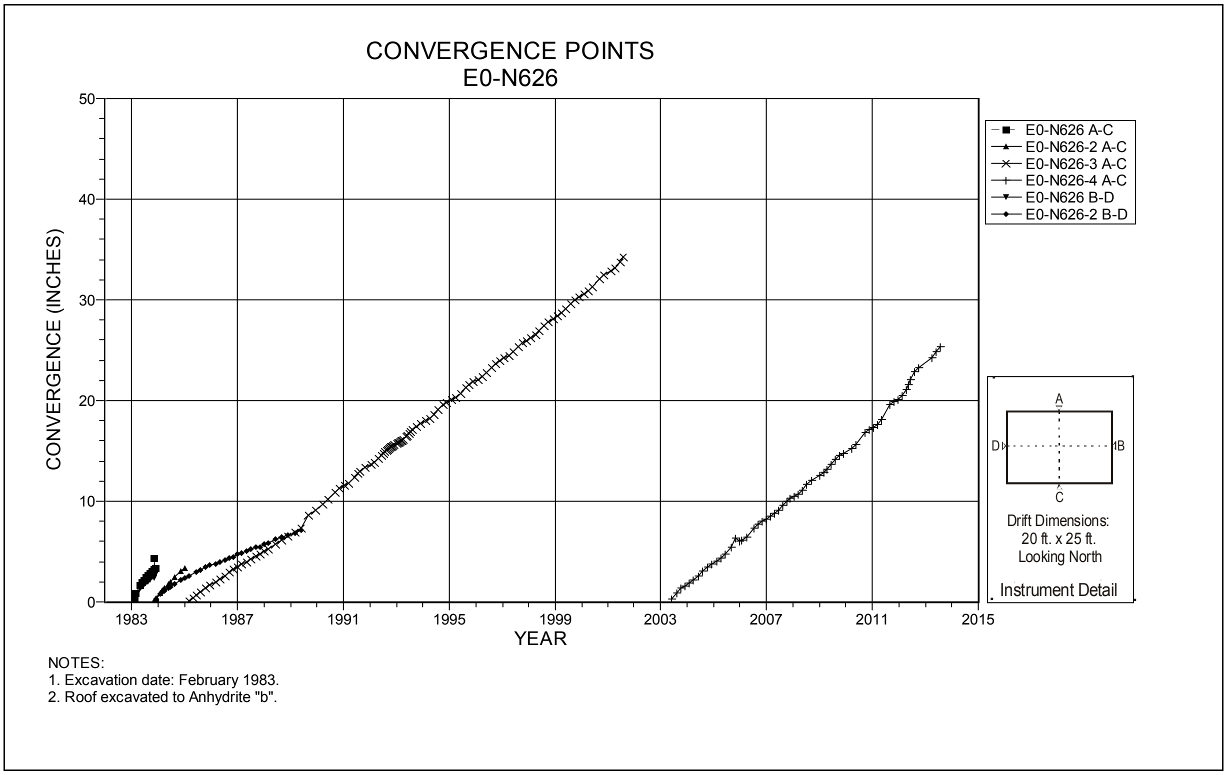

Figure 4-39 Convergence Point Array
E0 N626 – All Chords

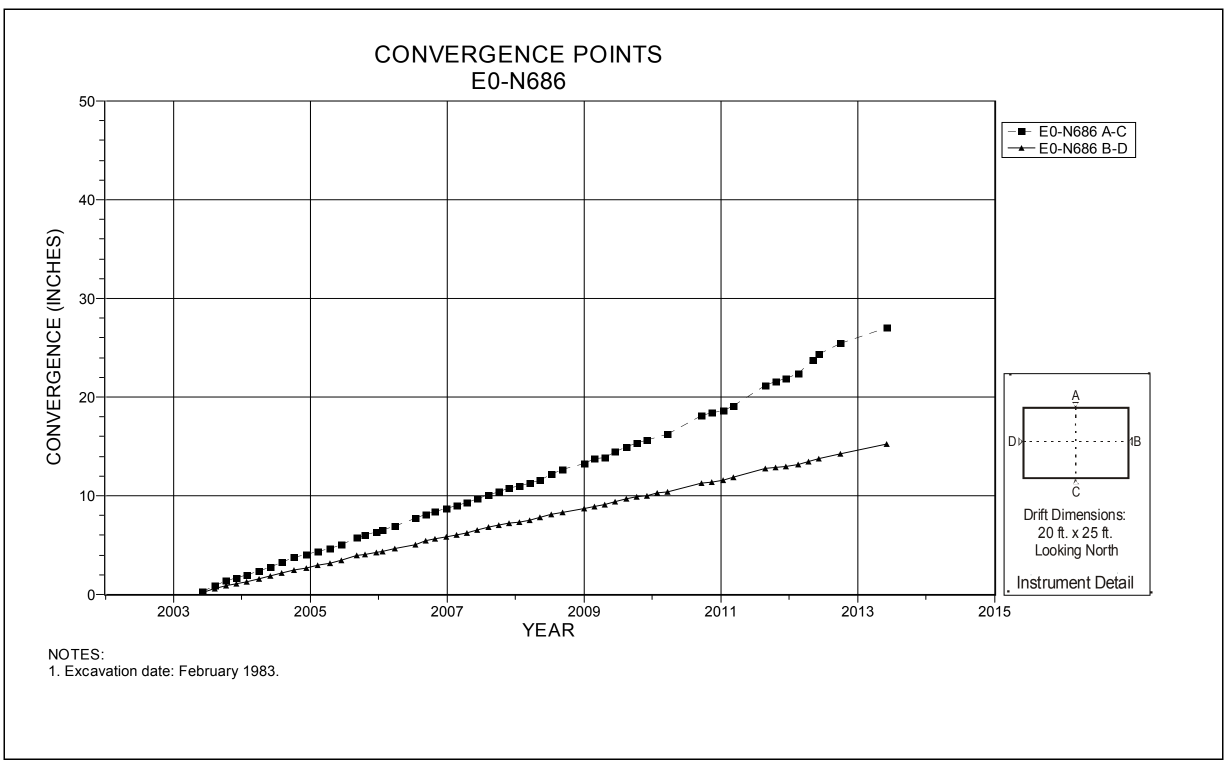

Figure 4-40 Convergence Point Array
E0 N686 – All Chords

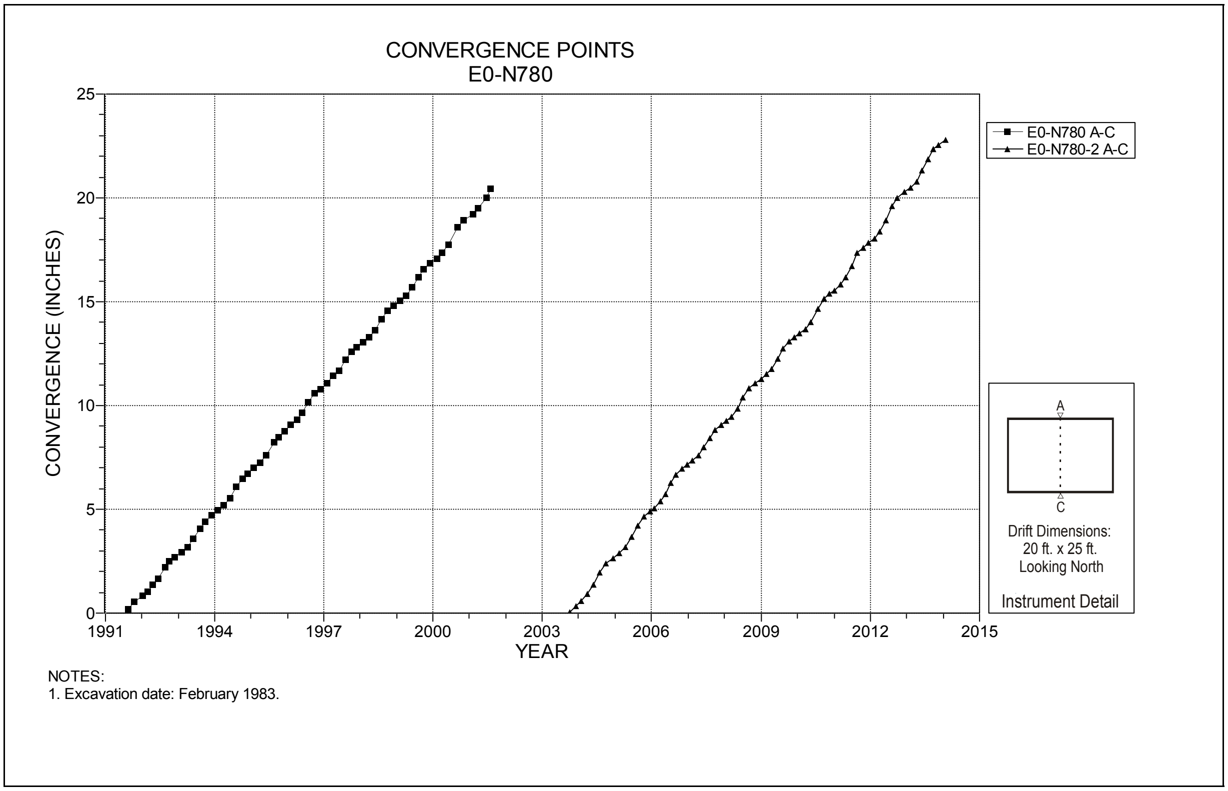

Figure 4-41 Convergence Point Array
E0 N780 – Roof to Floor

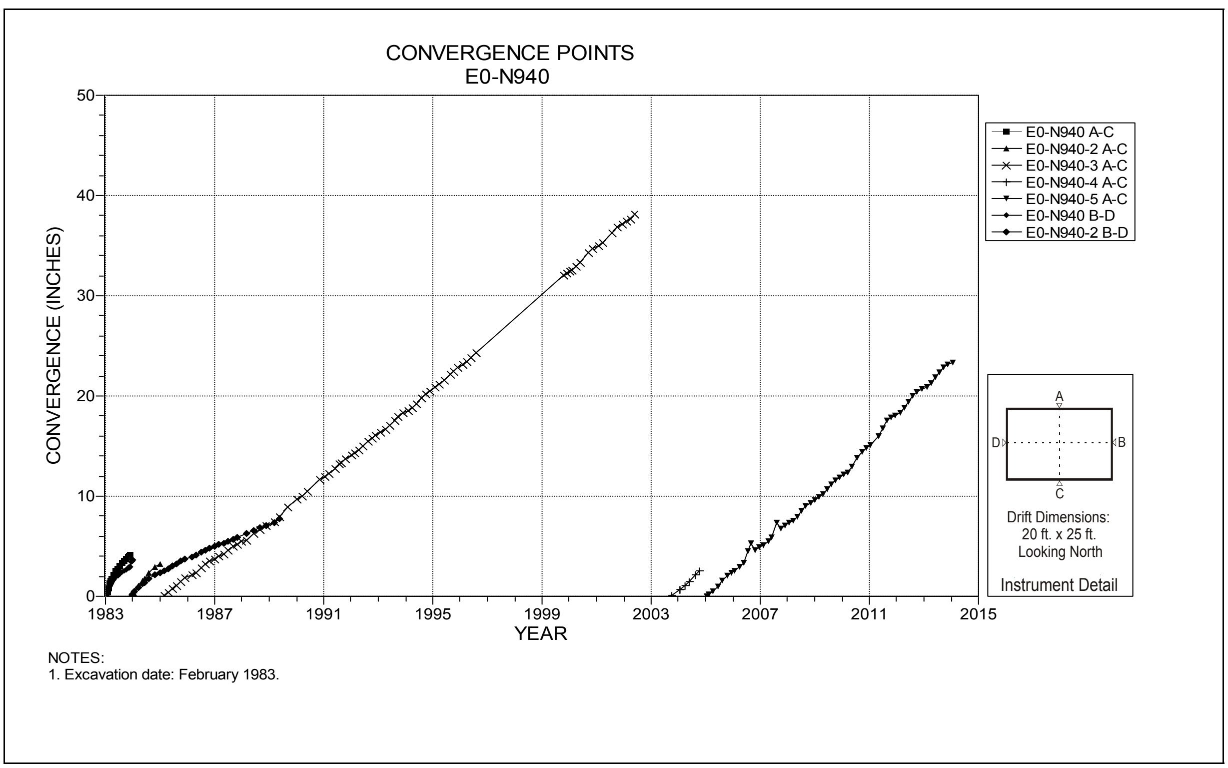

Figure 4-42 Convergence Point Array
E0 N940 – All Chords

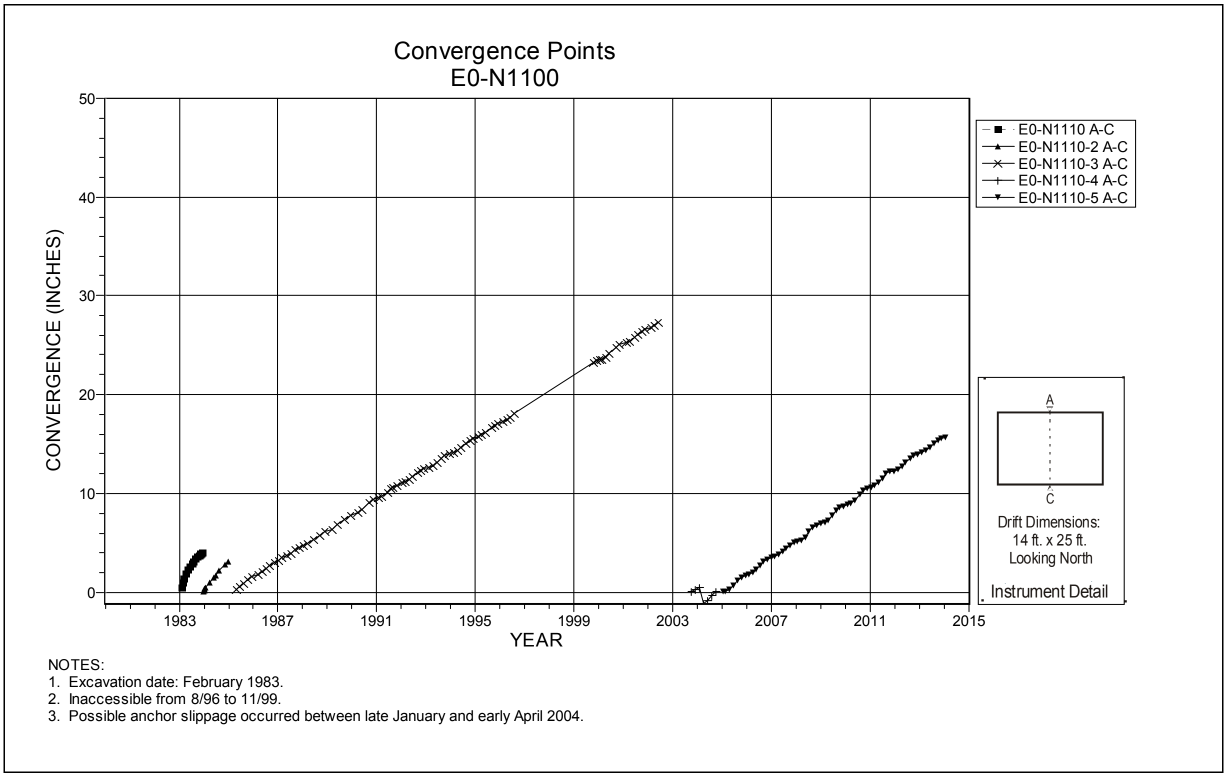

Figure 4-43 Convergence Point Array
E0 N1100 – Roof to Floor

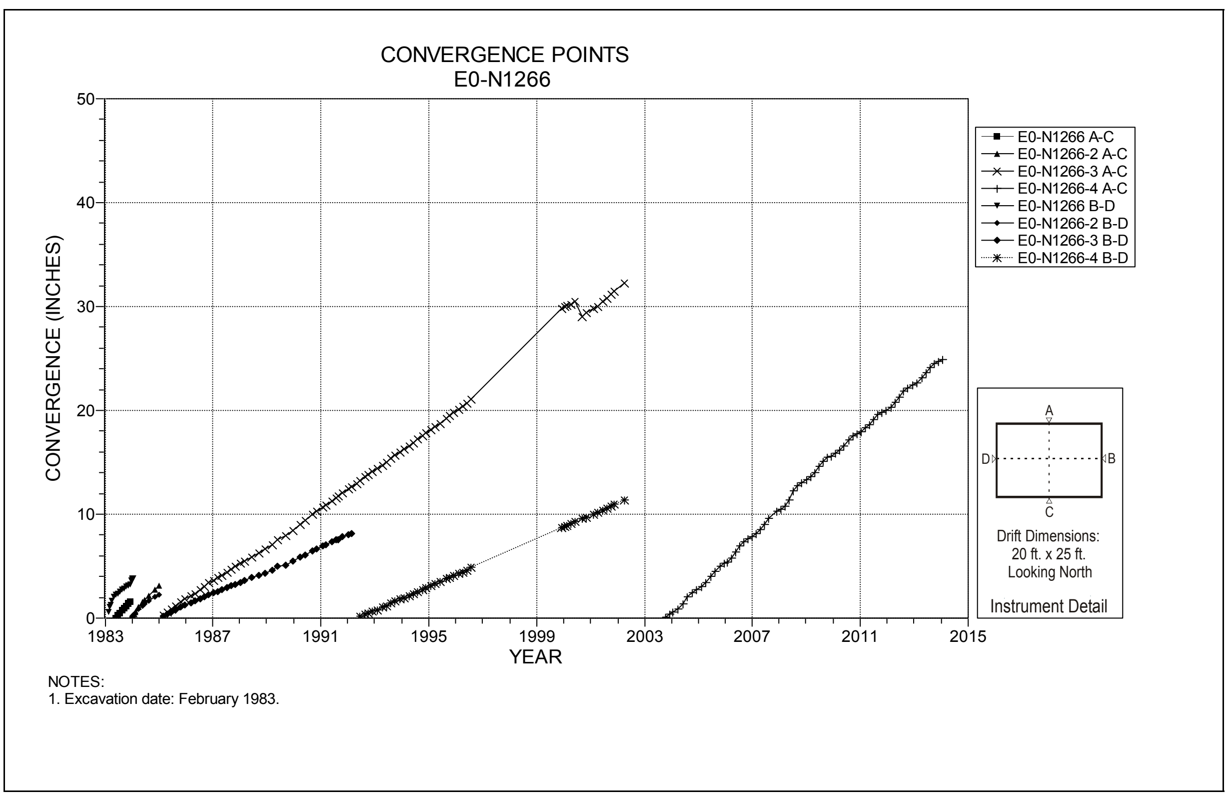

Figure 4-44 Convergence Point Array
E0 N1266 – All Chords

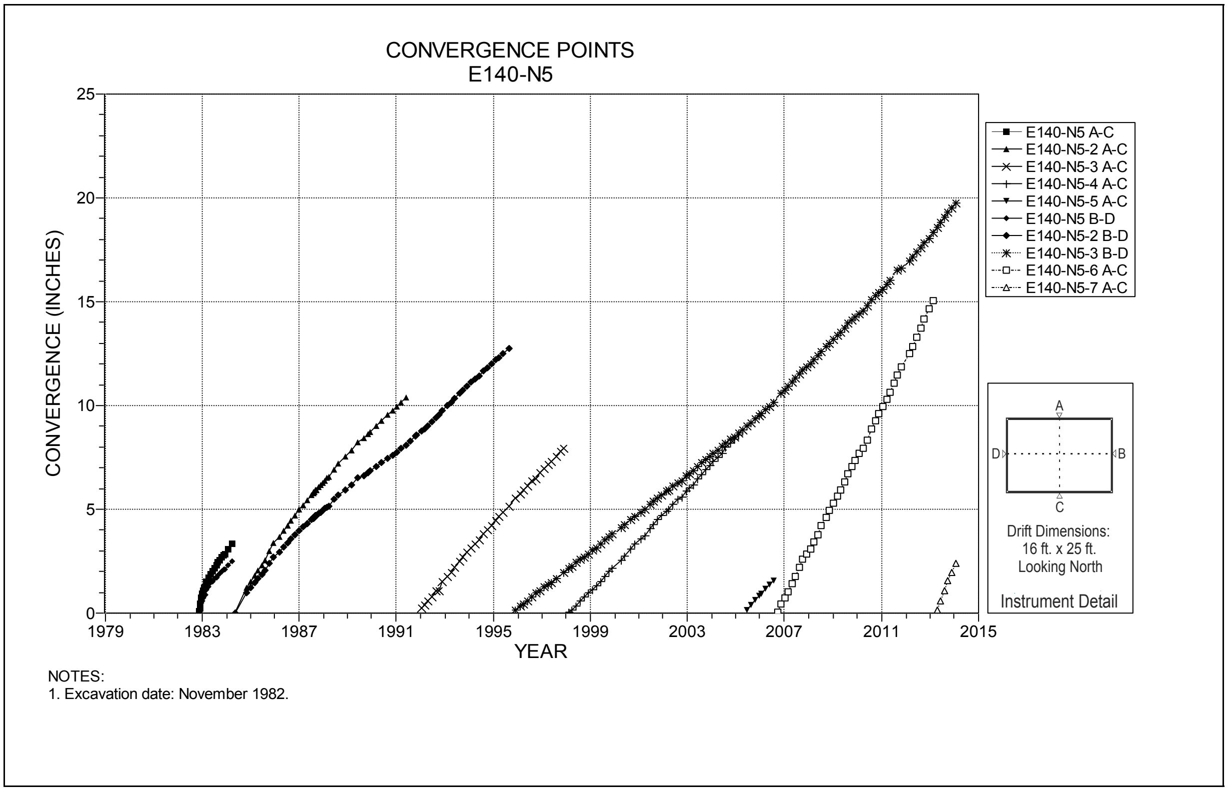

Figure 4-45 Convergence Point Array
E140 N5 – All Chords

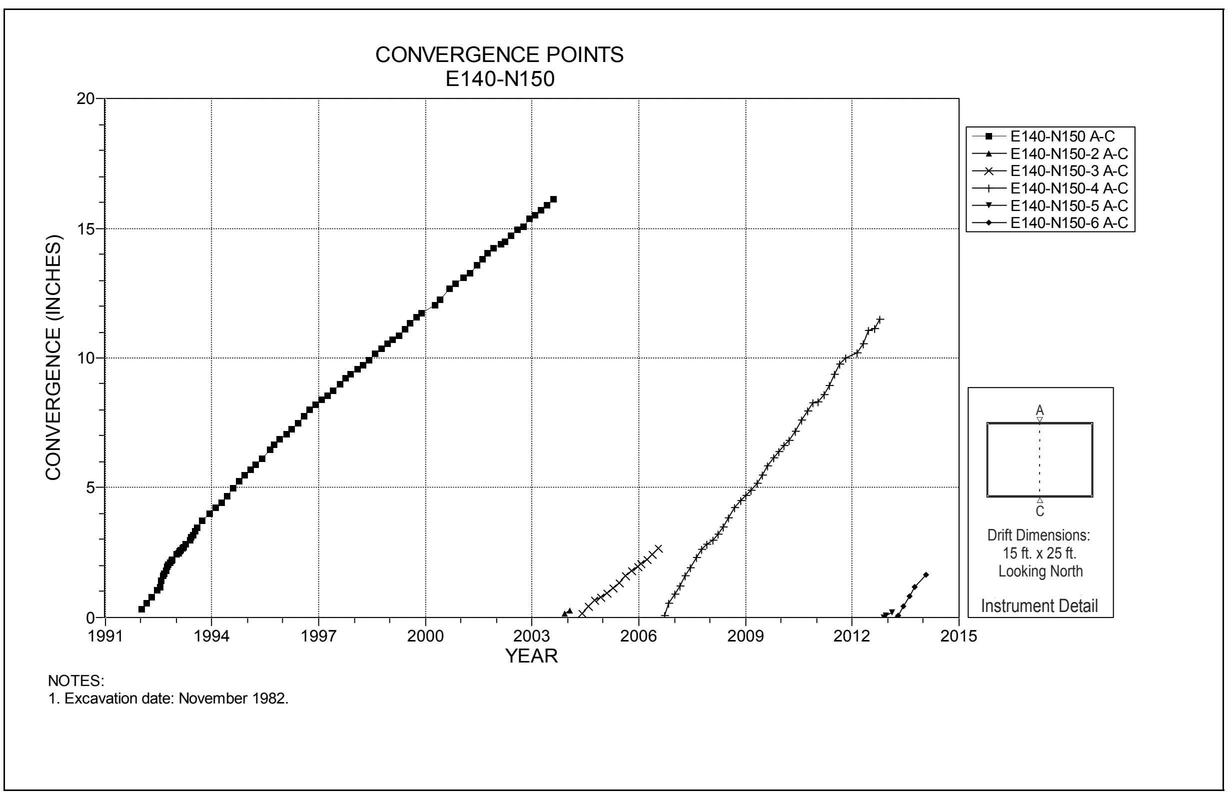

Figure 4-46 Convergence Point Array
E140 N150 – Roof to Floor

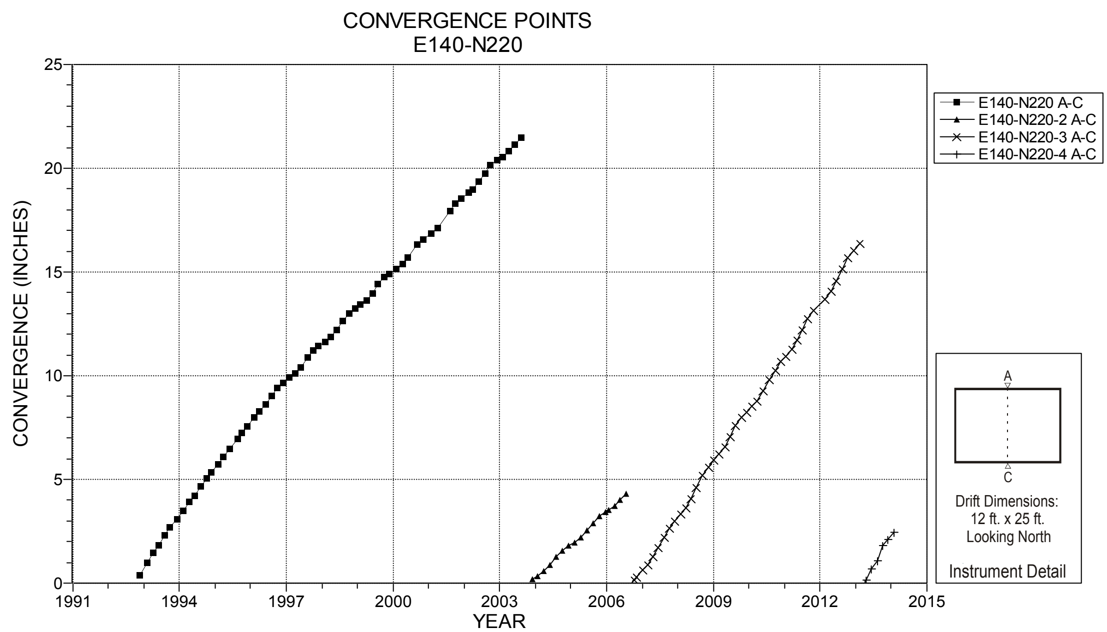

NOTES:
1. Excavation date: November 1982.
2. Reinstalled "C" point 9-27-2006.

Figure 4-47 Convergence Point Array
E140 N220 – Roof to Floor

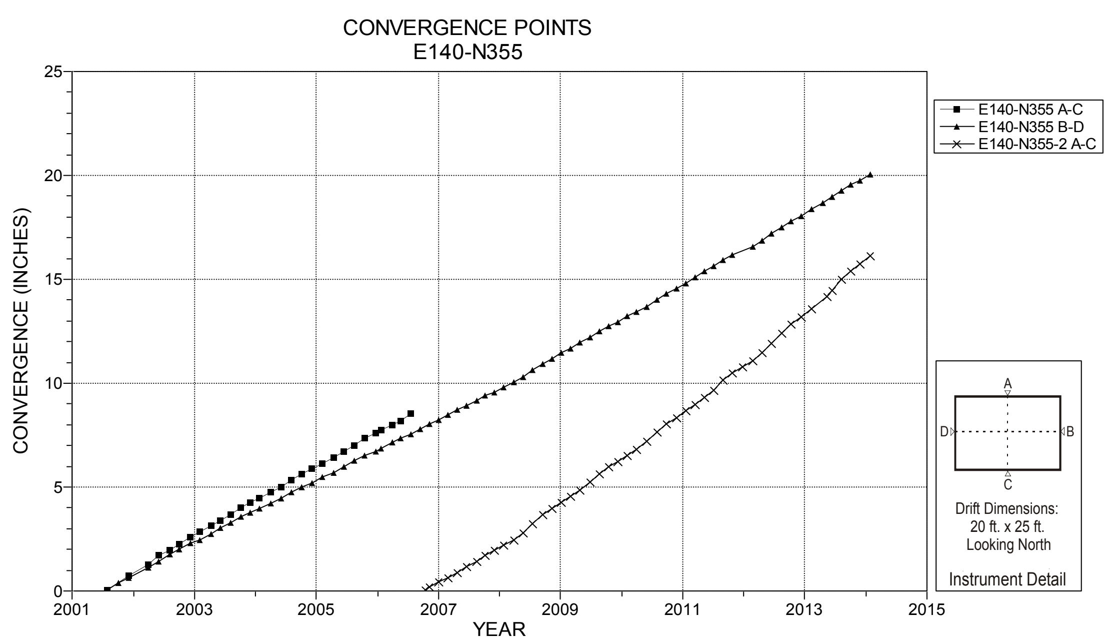

NOTES:
1. Excavation date: February 1983.
2. Roof excavated to Anhydrite 'b' in mid 2001.

Figure 4-48 Convergence Point Array
E140 N355 – All Chords

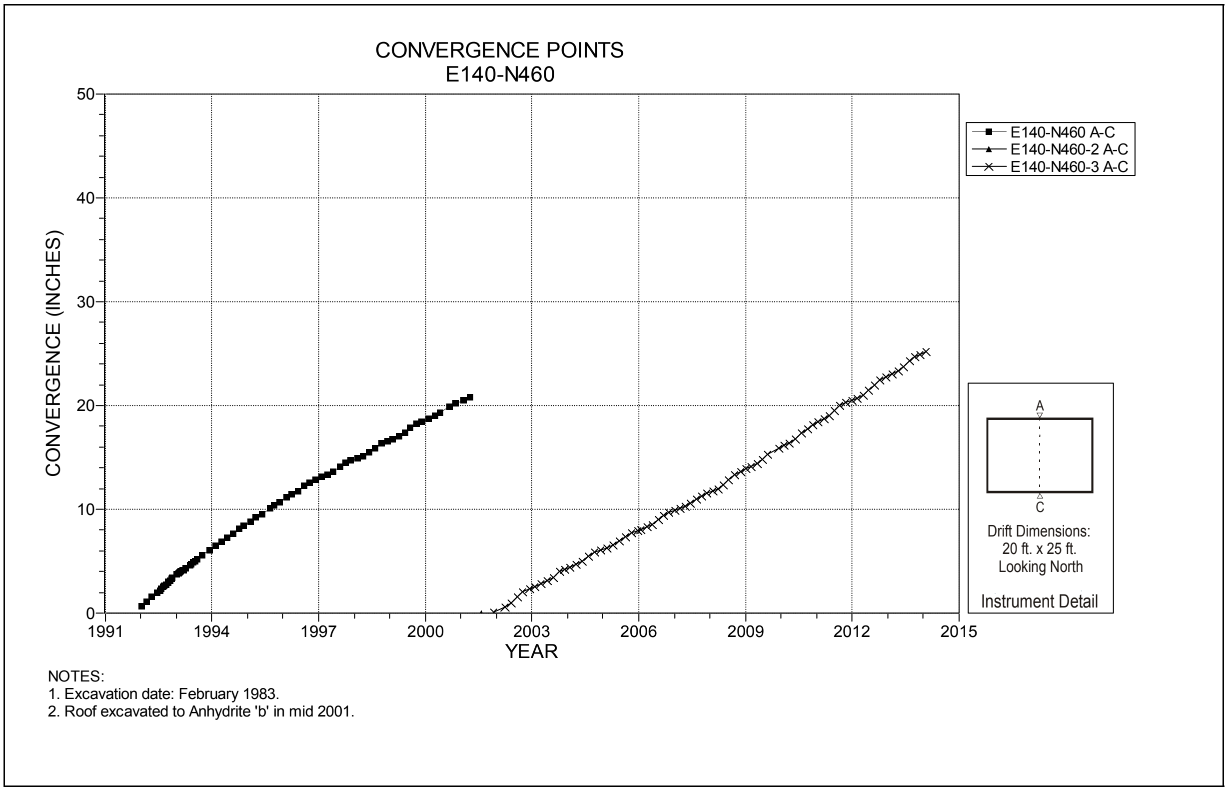

Figure 4-49 Convergence Point Array
E140 N460 – Roof to Floor

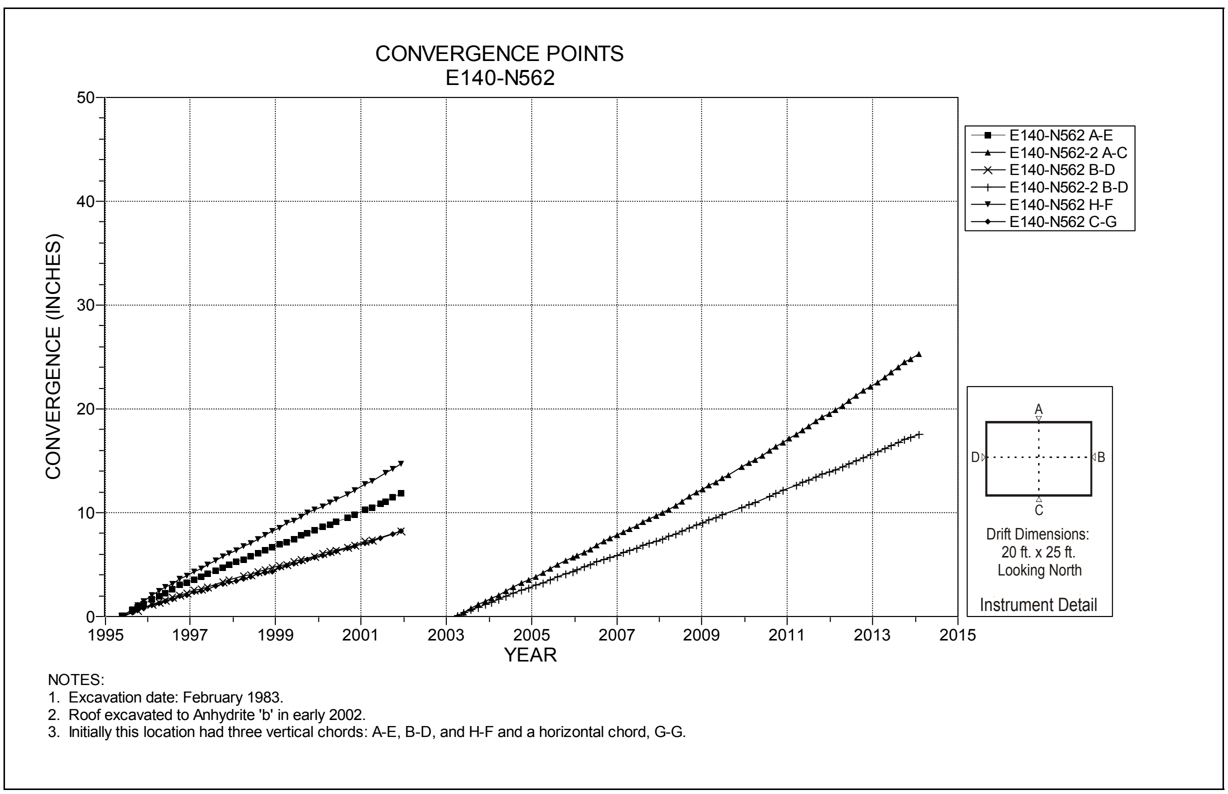

Figure 4-50 Convergence Point Array
E140 N562 – All Chords

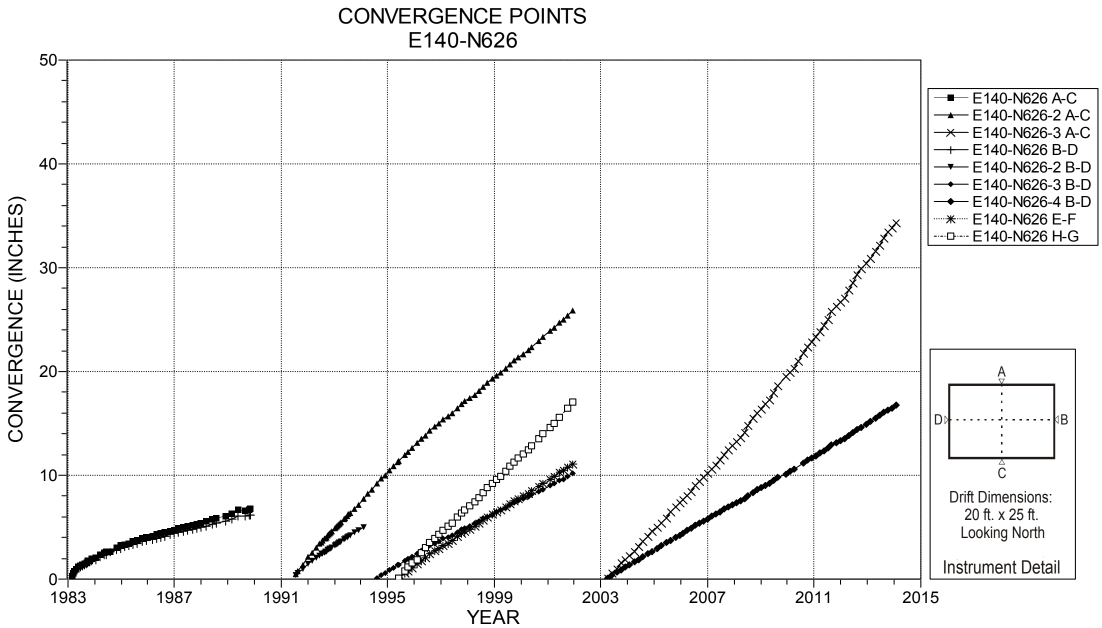

NOTES:
1. Excavation date: February 1983.
2. Roof excavated to Anhydrite 'b' in early 2002.
3. The A-E chord was physically located in the same position as the present A-C chord.

Figure 4-51 Convergence Point Array
E140 N626 – All Chords

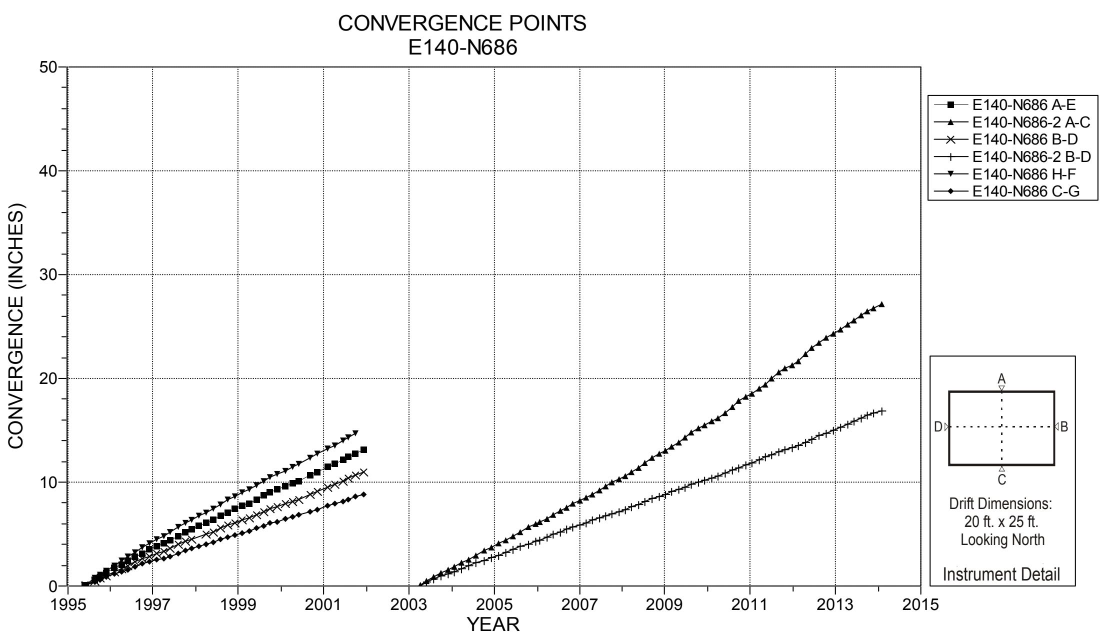

NOTES:
1. Excavation date: February 1983.
2. Roof excavated to Anhydrite 'b' in early 2002.
3. The A-E chord was physically located in the same position as the present A-C chord.

Figure 4-52 Convergence Point Array
E140 N686 – All Chords

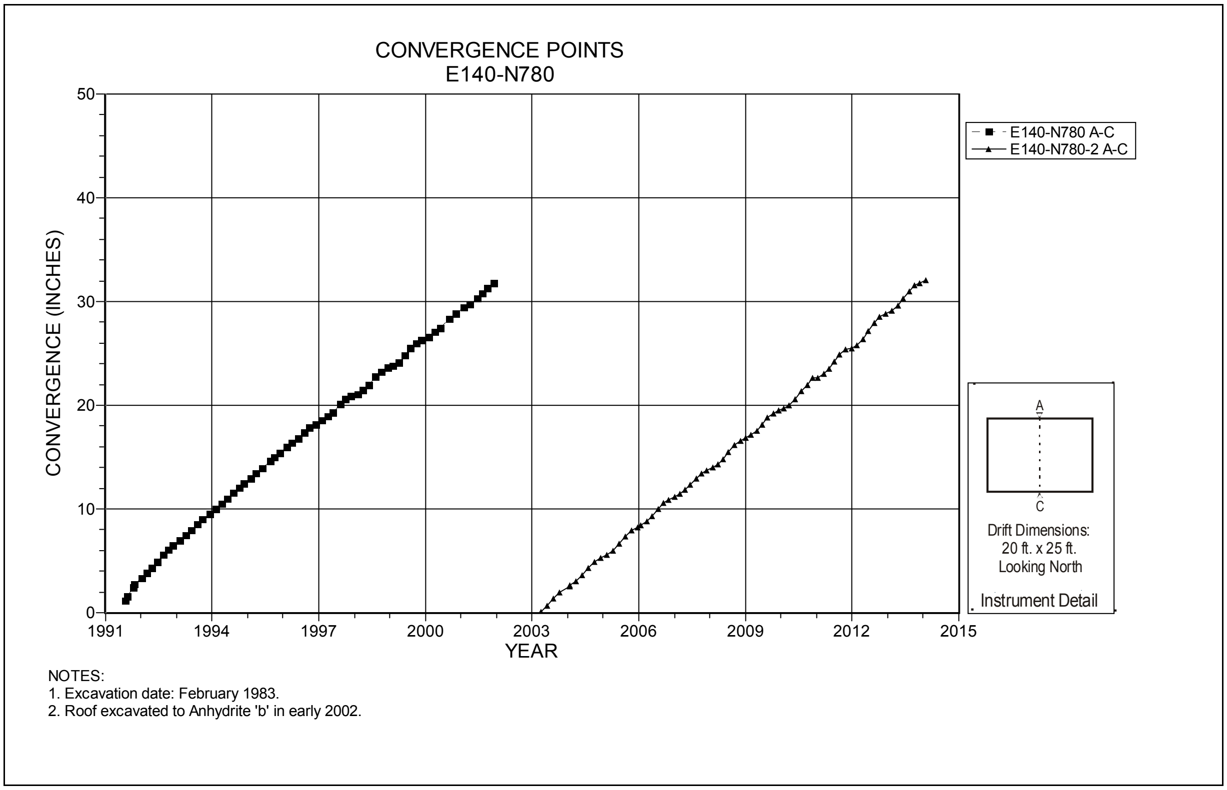

Figure 4-53 Convergence Point Array
E140 N780 – Roof to Floor

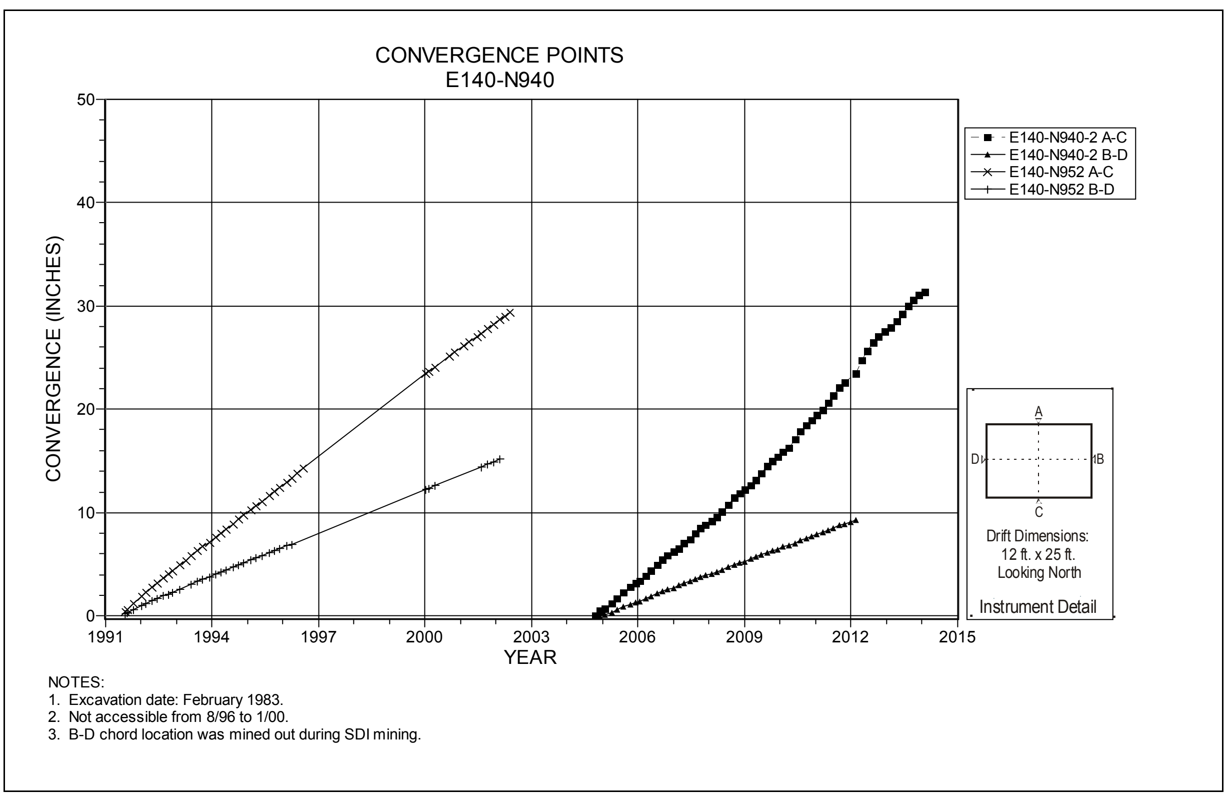

Figure 4-54 Convergence Point Array
E140 N940 – All Chords

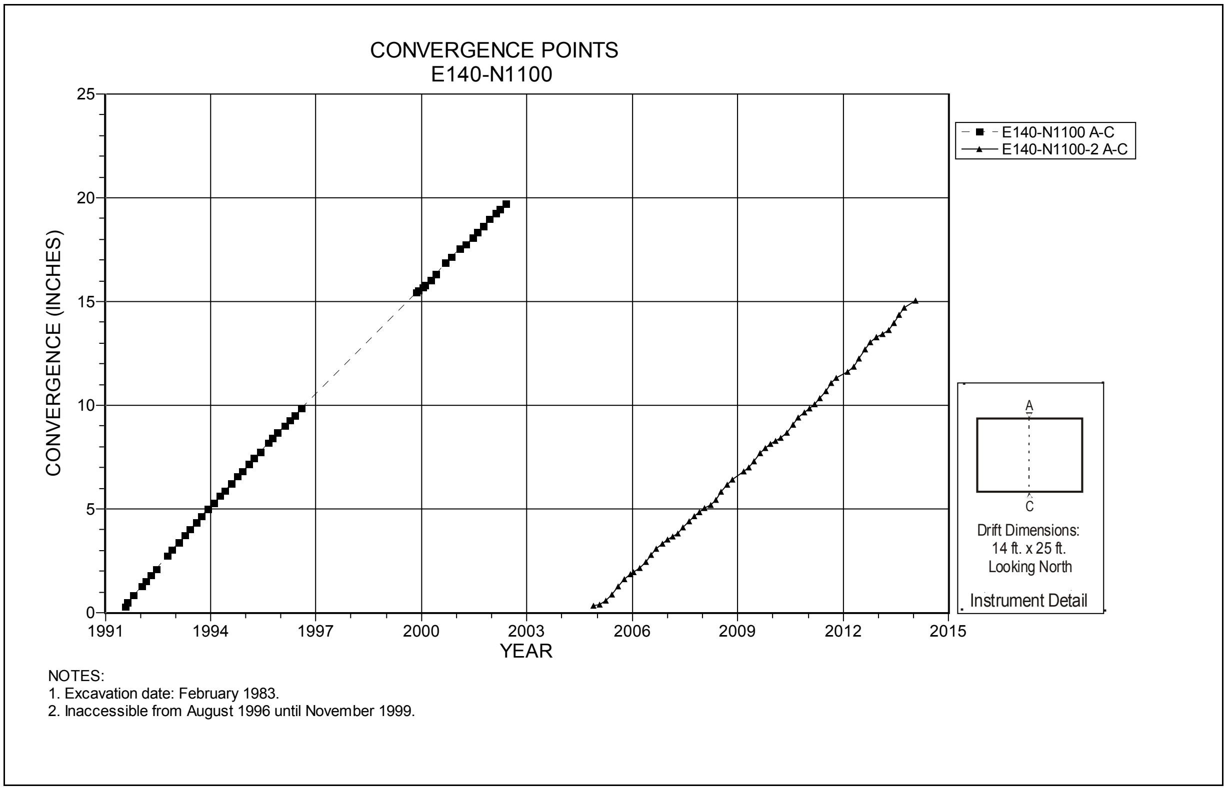

Figure 4-55 Convergence Point Array
E140 N1100 – Roof to Floor

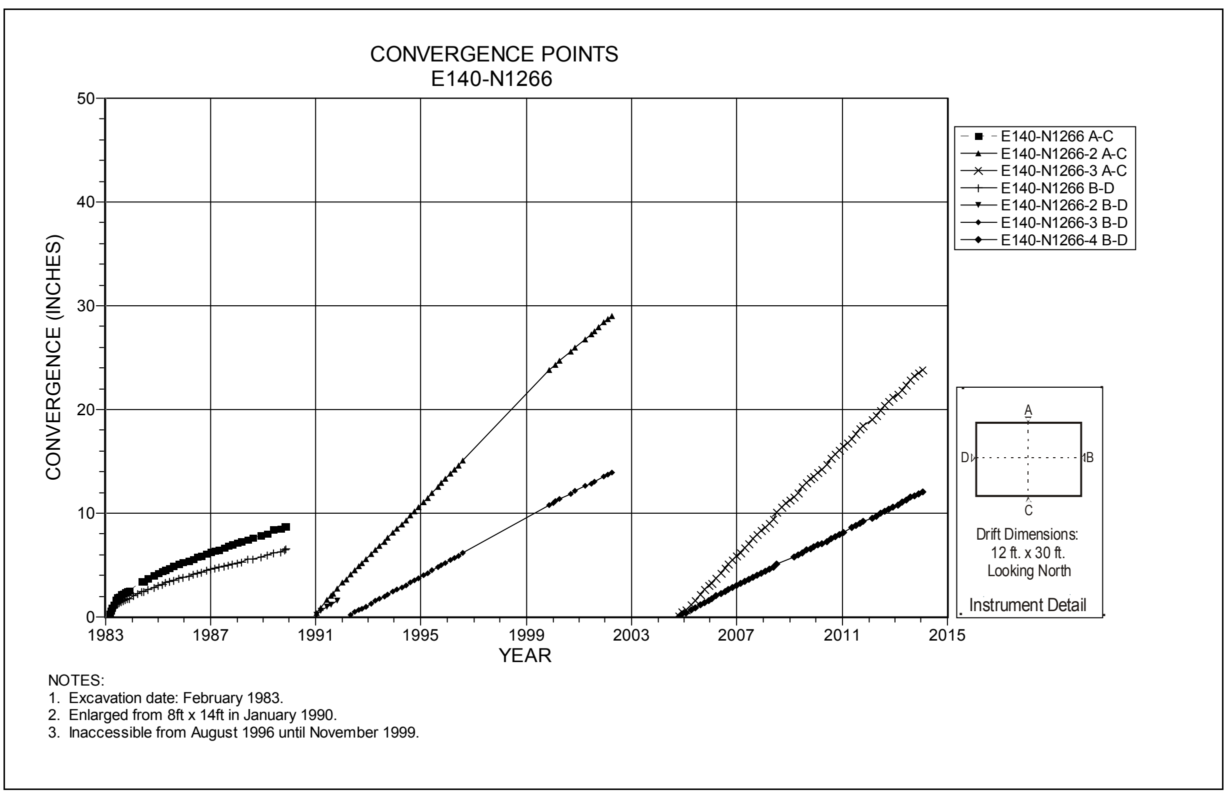

Figure 4-56 Convergence Point Array
E140 N1266 – All Chords

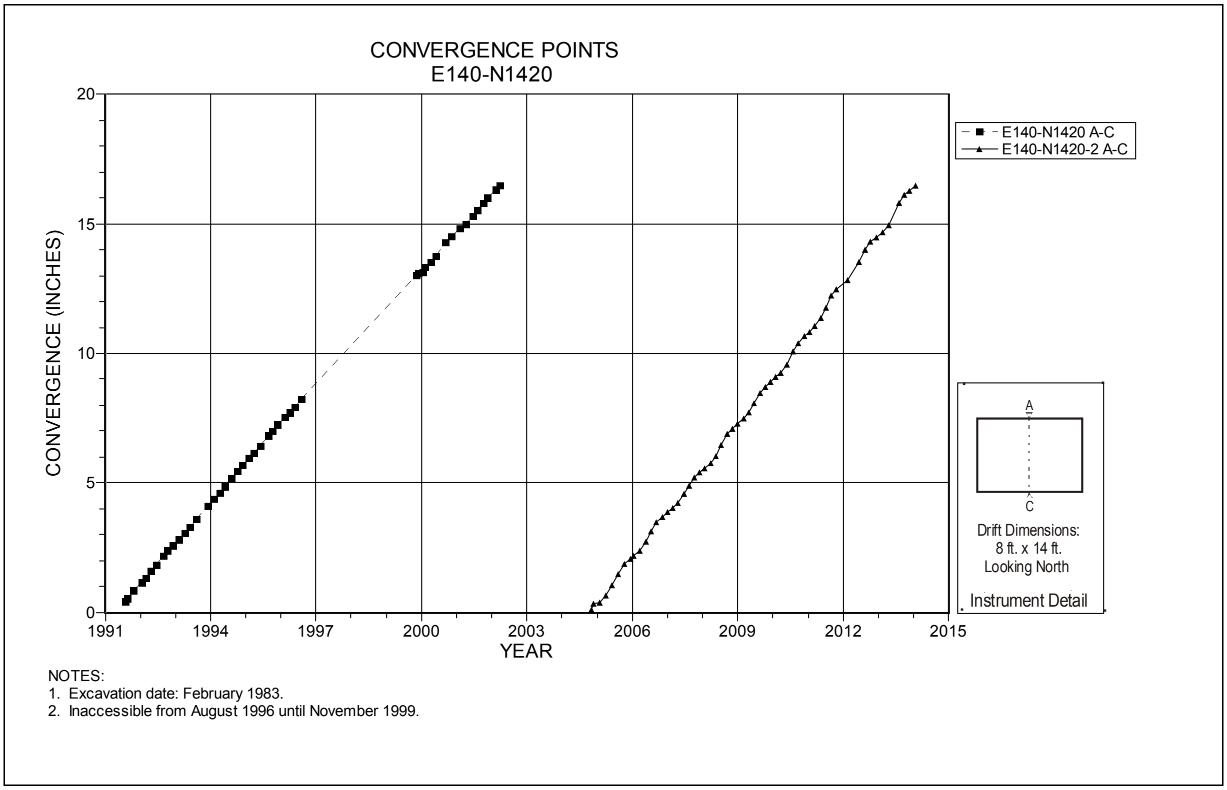

Figure 4-57 Convergence Point Array
E140 N1420 – Roof to Floor

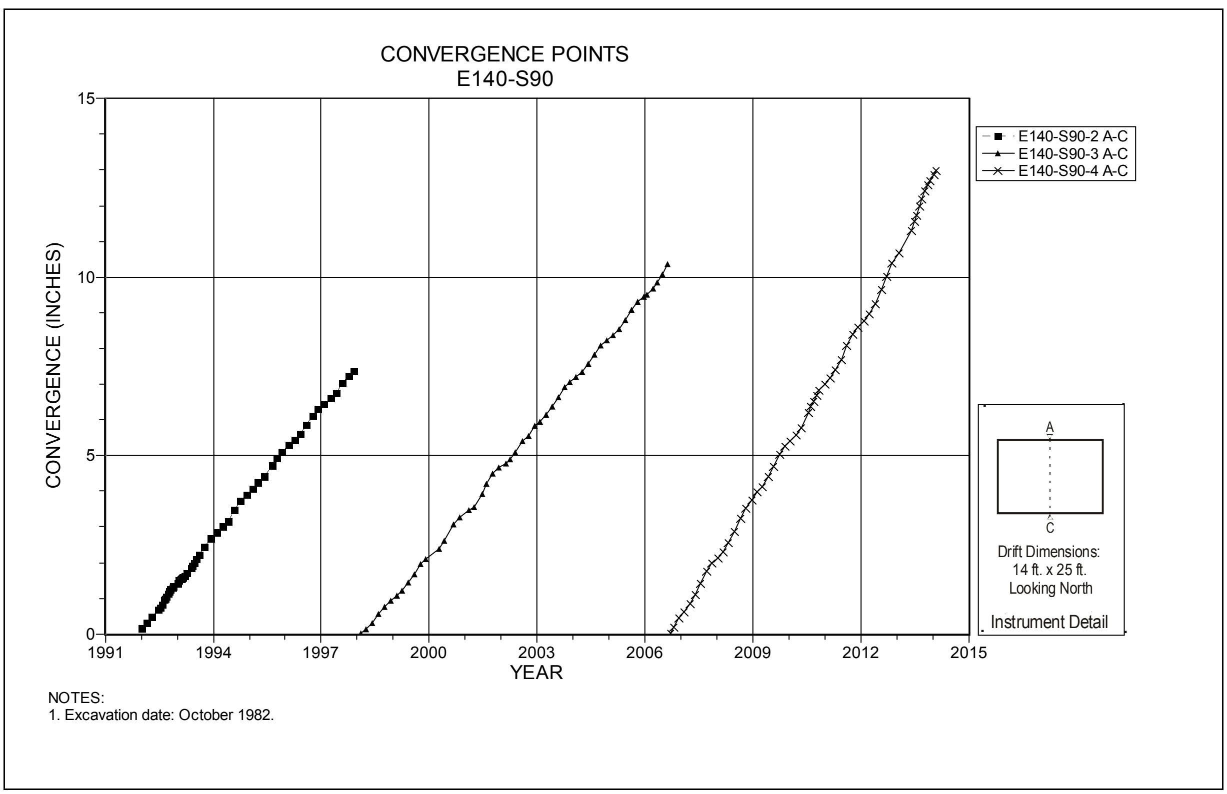

Figure 4-58 Convergence Point Array
E140 S90 – Roof to Floor

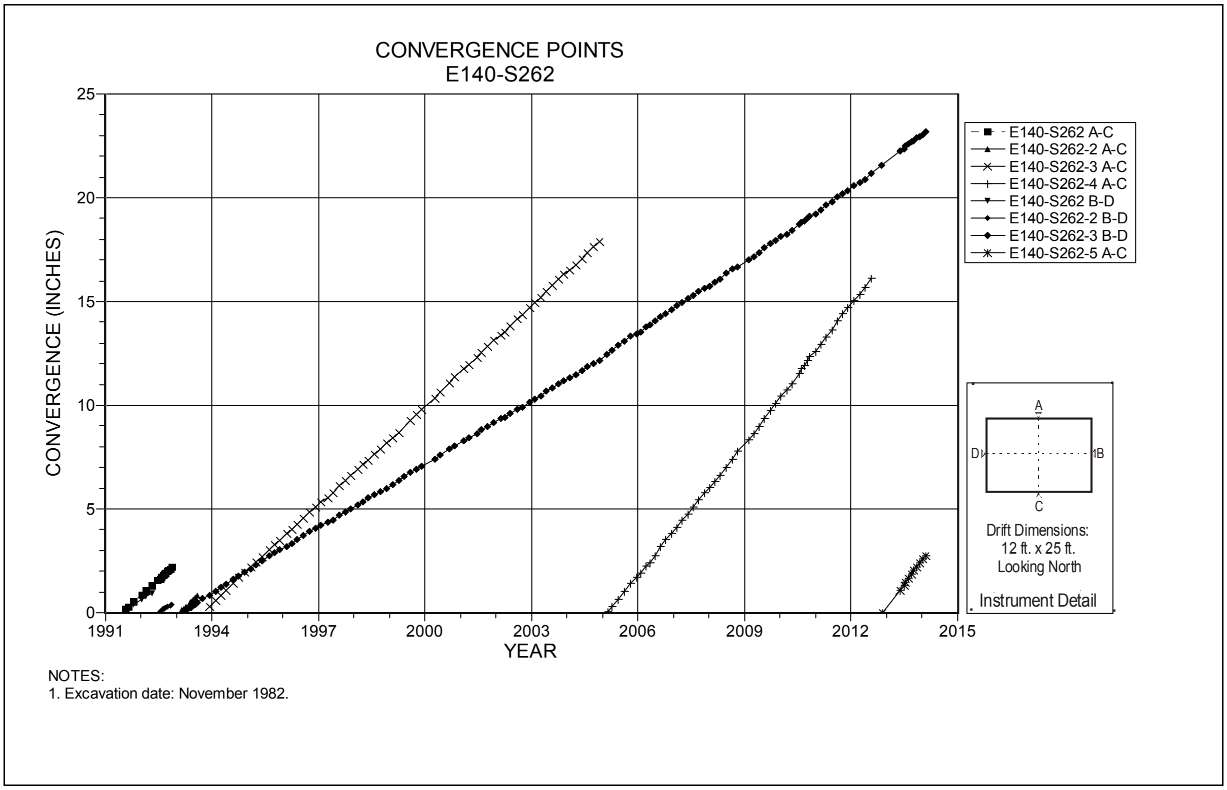

Figure 4-59 Convergence Point Array
E140 S262 – All Chords

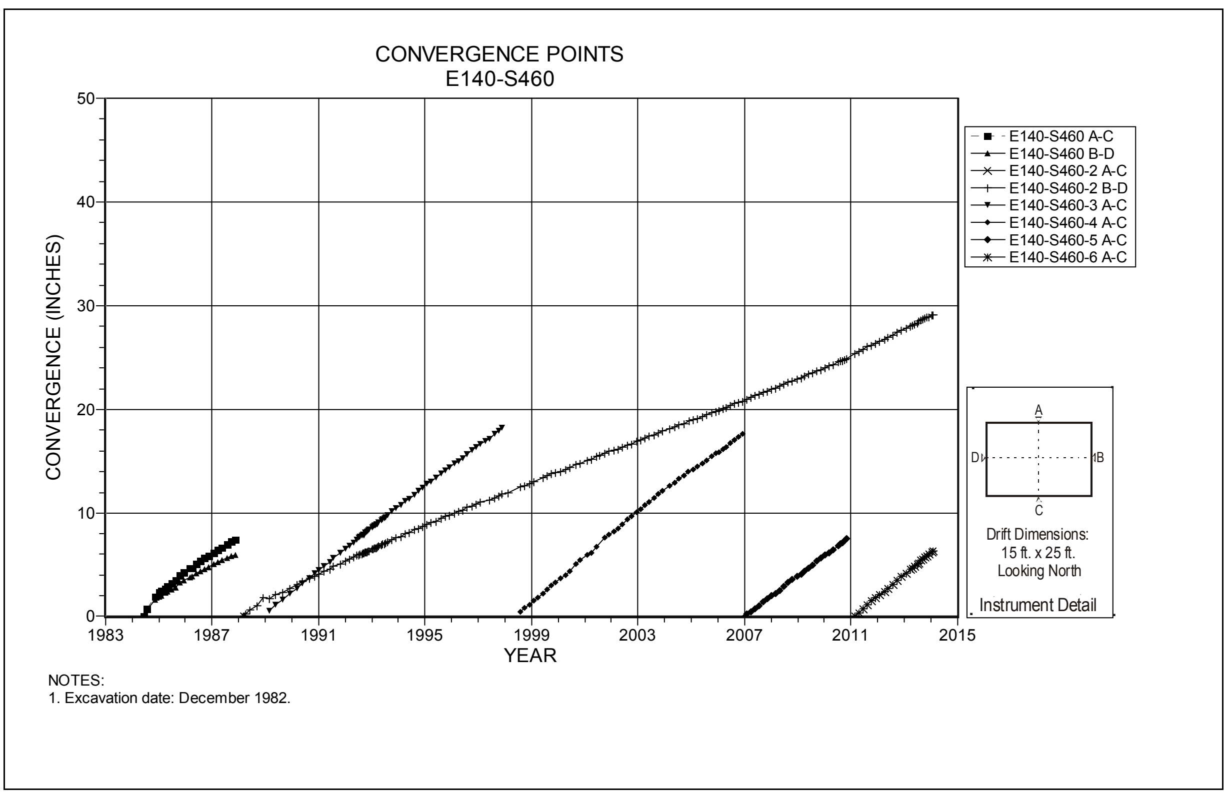

Figure 4-60 Convergence Point Array
E140 S460 – All Chords

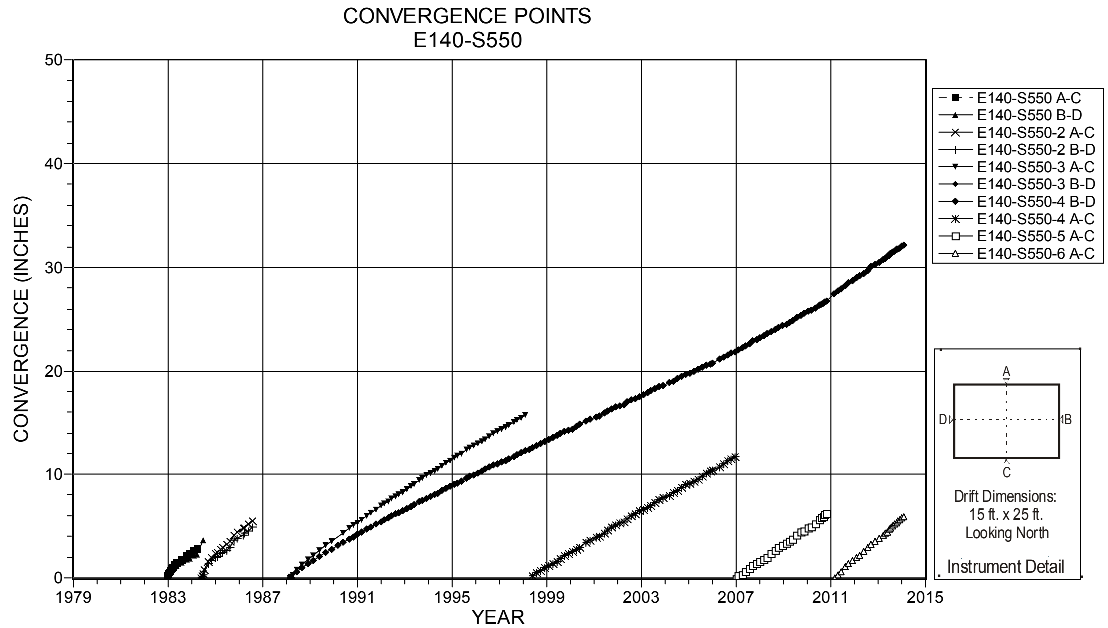

NOTES:
1. Excavation date: December 1982.

Figure 4-61 Convergence Point Array
E140 S550 – All Chords

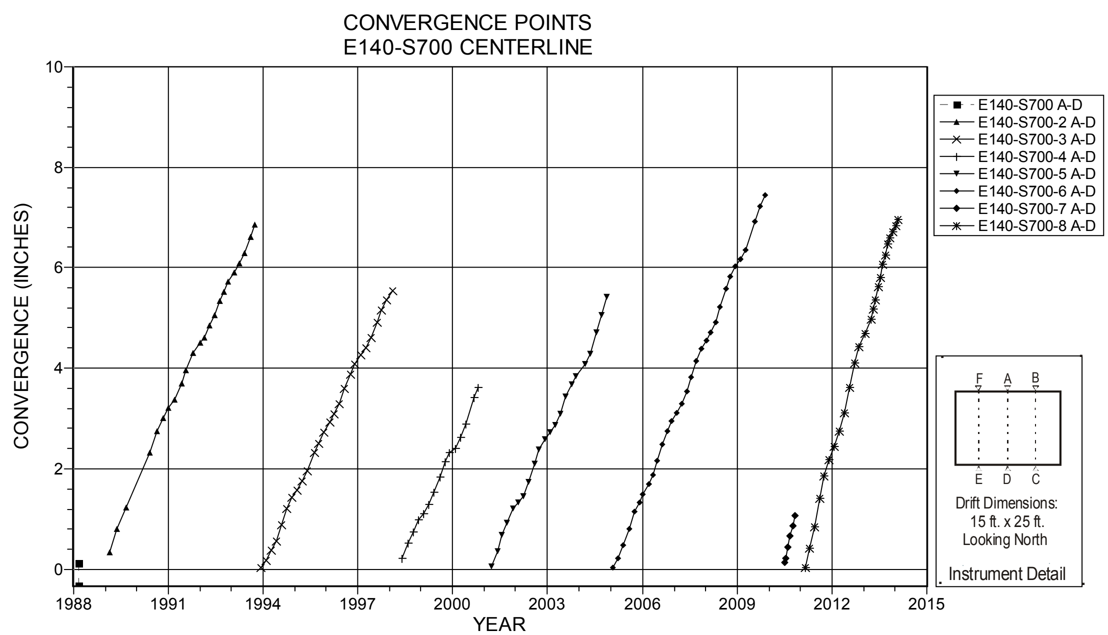

NOTES:
1. Excavation date: December 1982.

Figure 4-62 Convergence Point Array
E140 S700 – Roof to Floor – Centerline

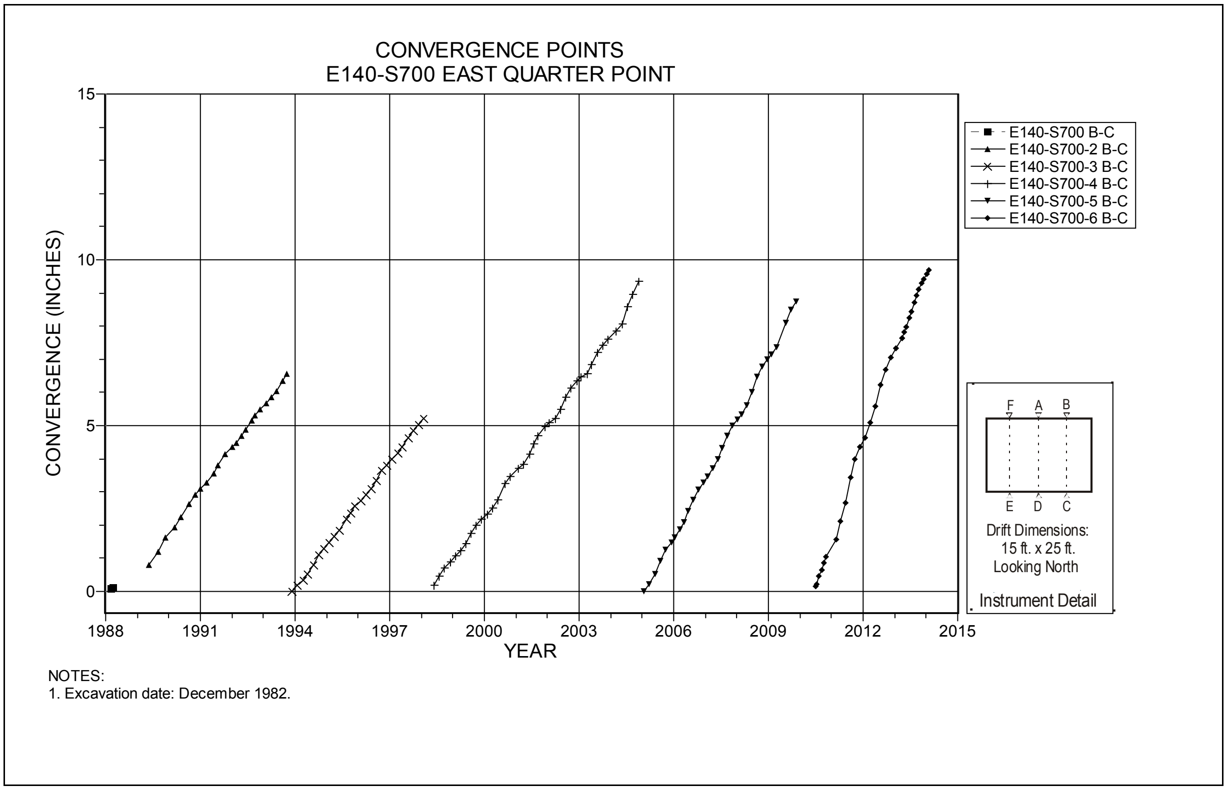

Figure 4-63 Convergence Point Array
E140 S700 – Roof to Floor – East Quarter Point

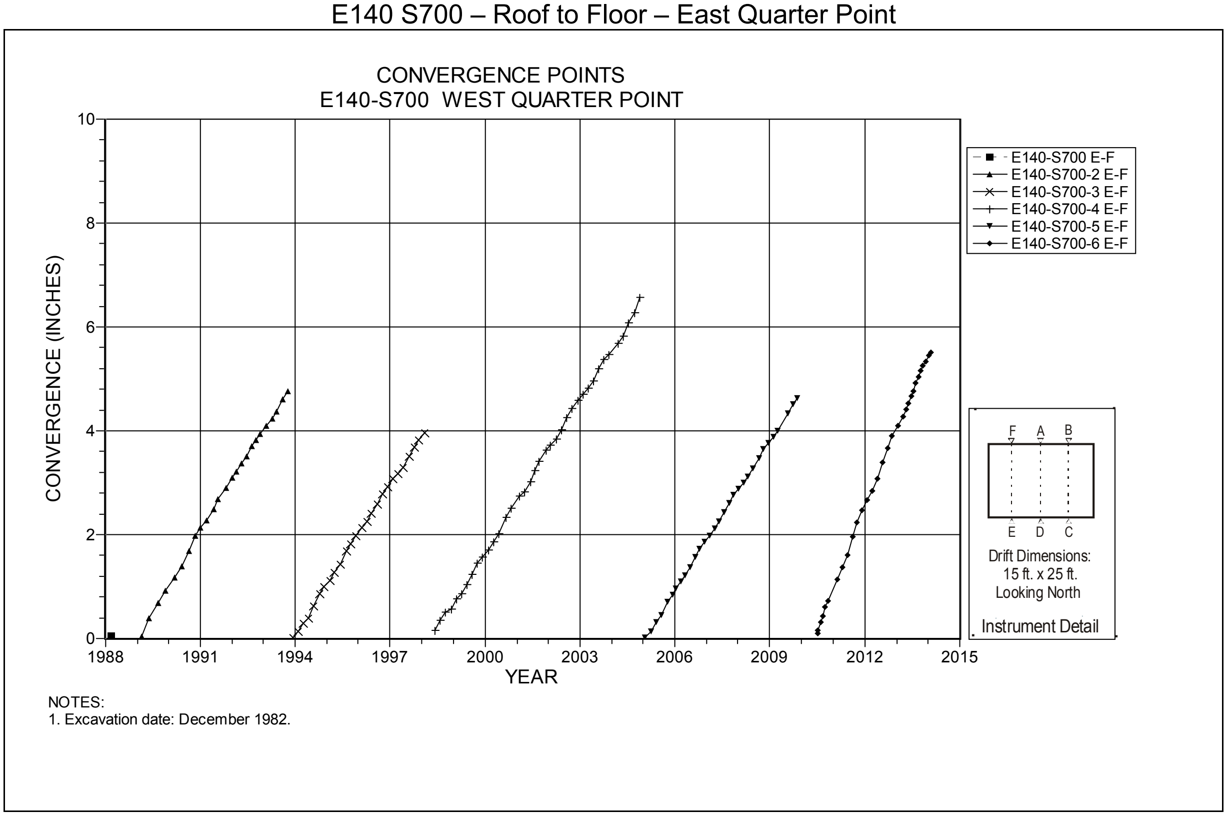

Figure 4-64 Convergence Point Array
E140 S700 – Roof to Floor – West Quarter Point

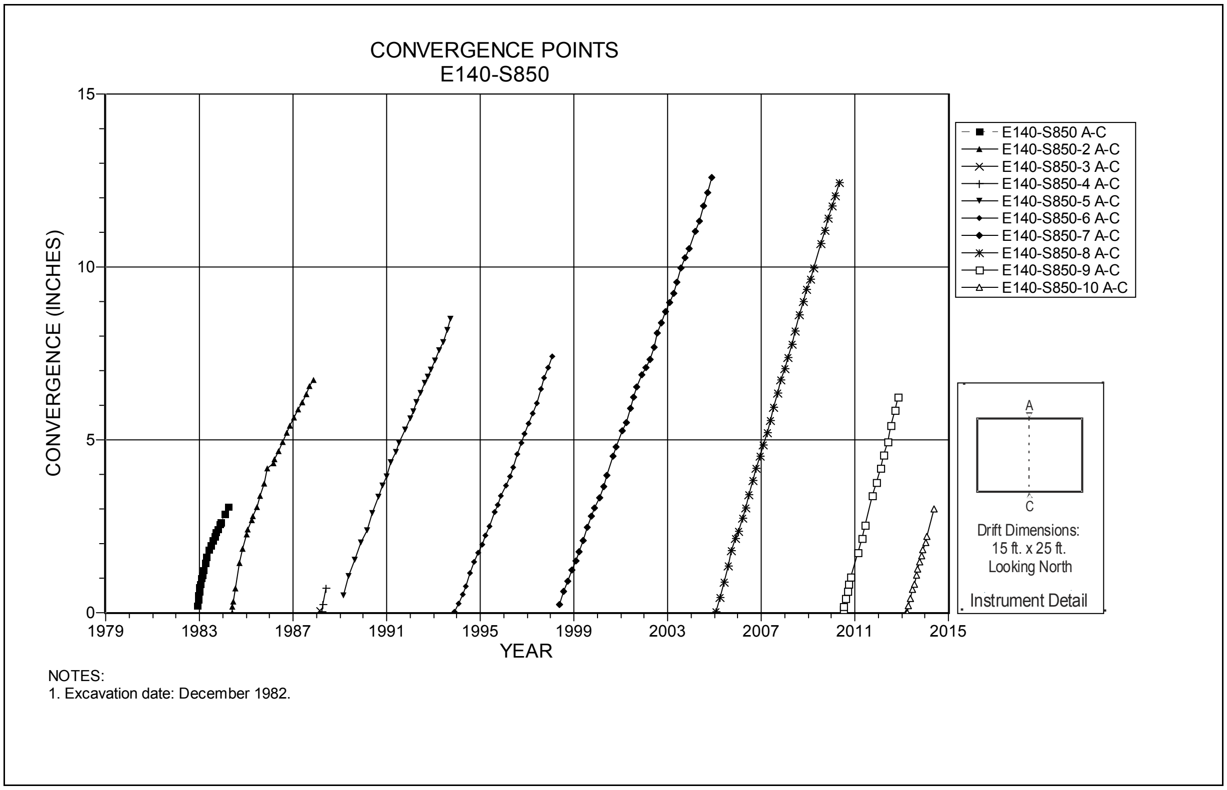

Figure 4-65 Convergence Point Array
E140 S850 – Roof to Floor

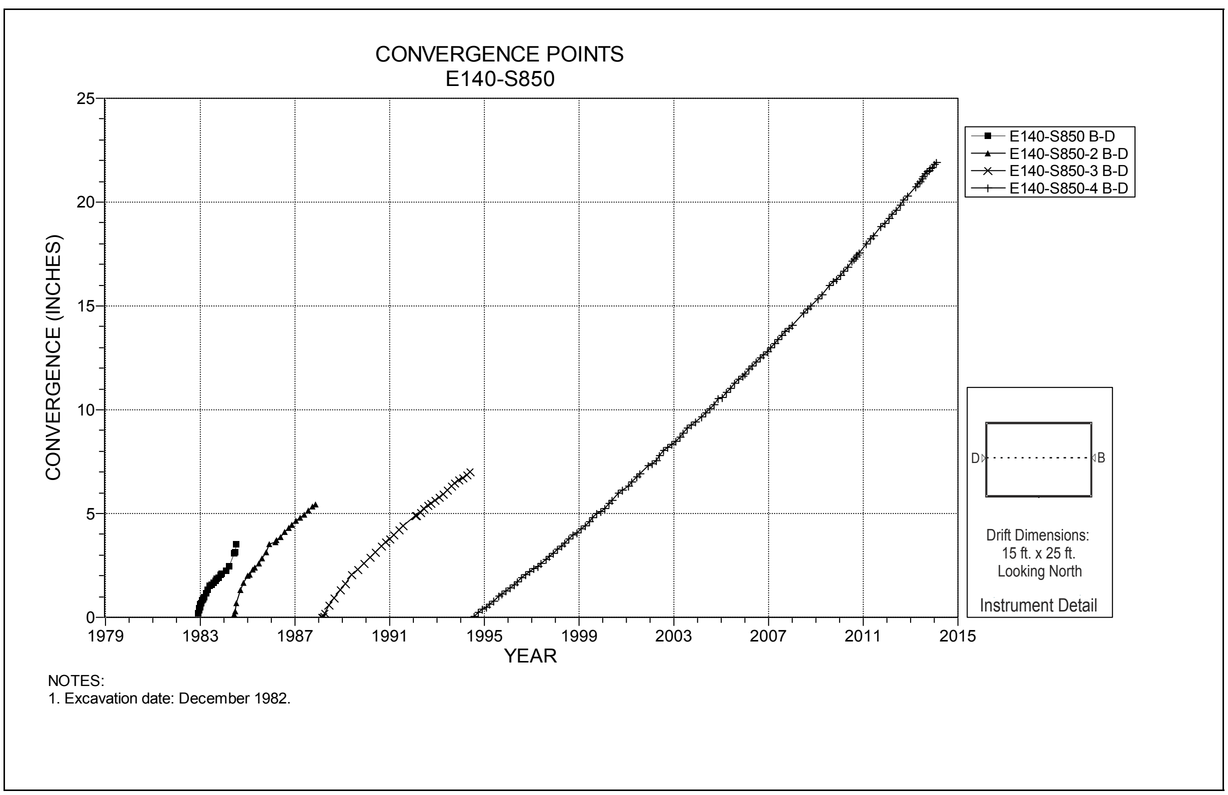

Figure 4-66 Convergence Point Array
E140 S850 – Rib to Rib

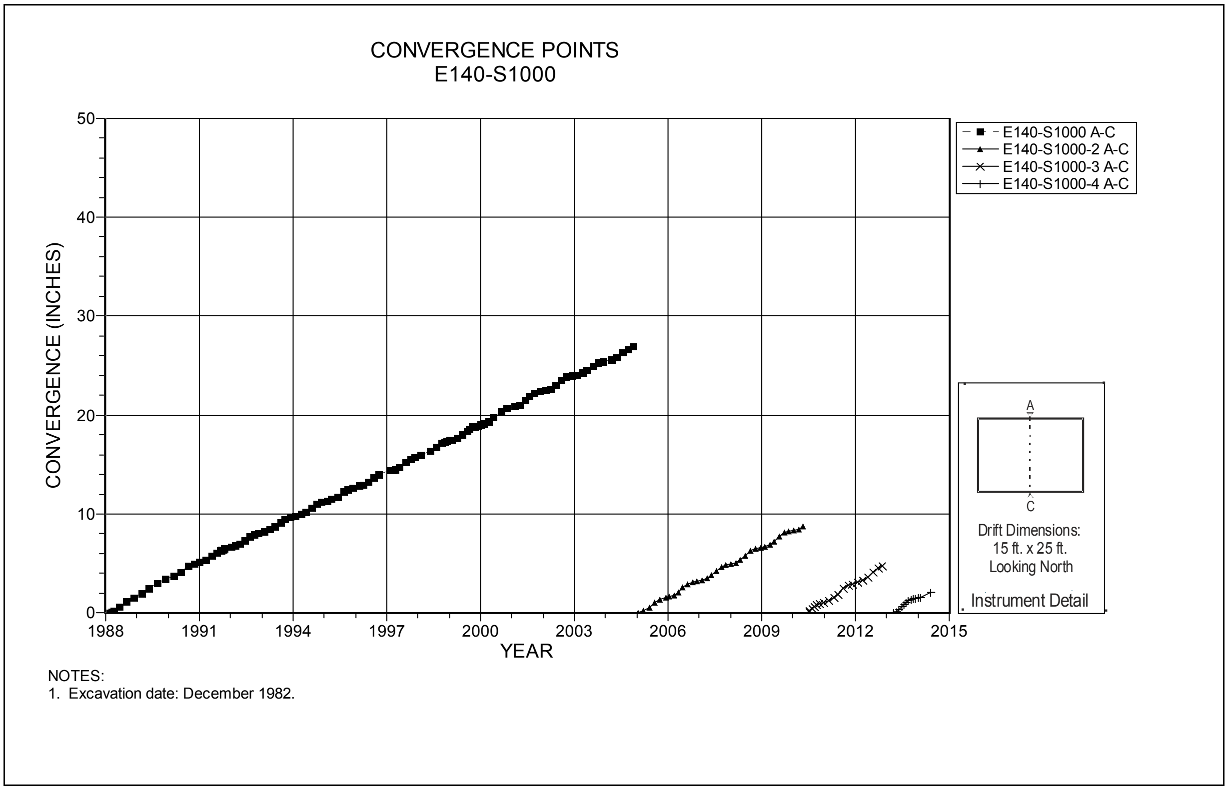

Figure 4-67 Convergence Point Array
E140 S1000 – Roof to Floor

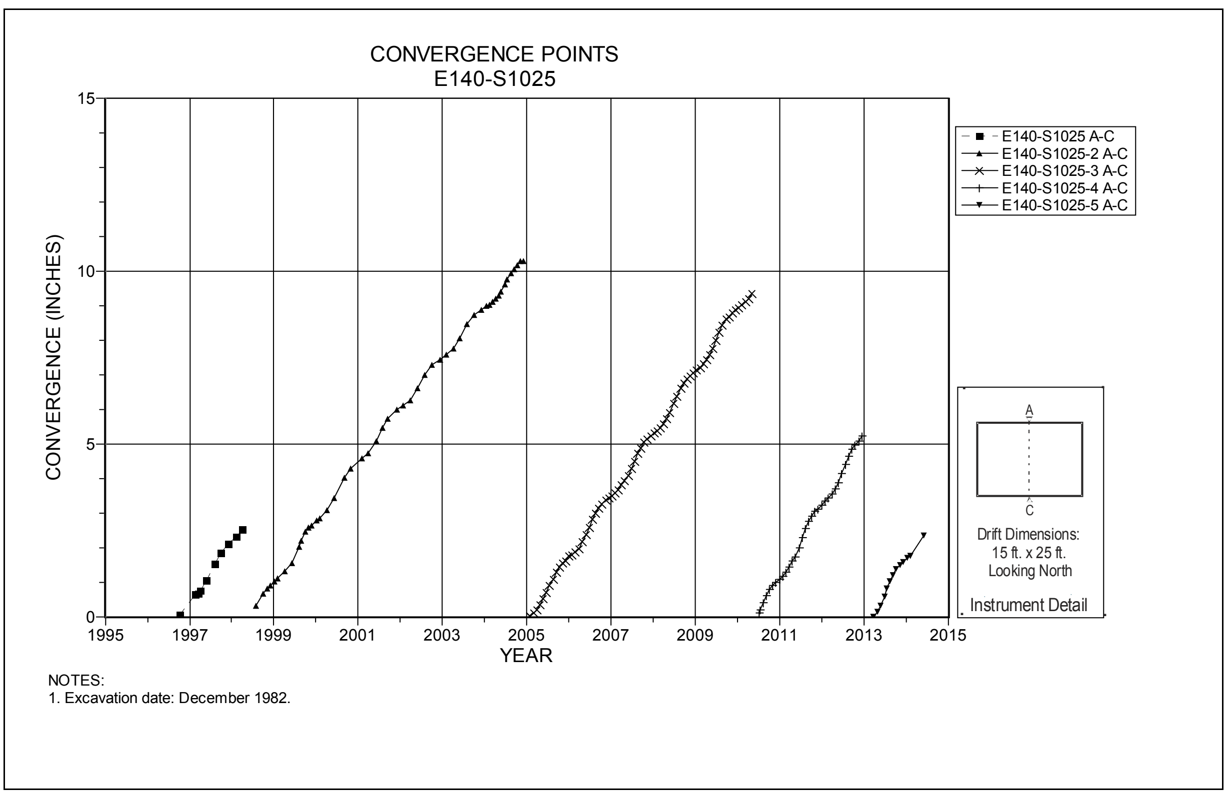

Figure 4-68 Convergence Point Array
E140 S1025 – Roof to Floor

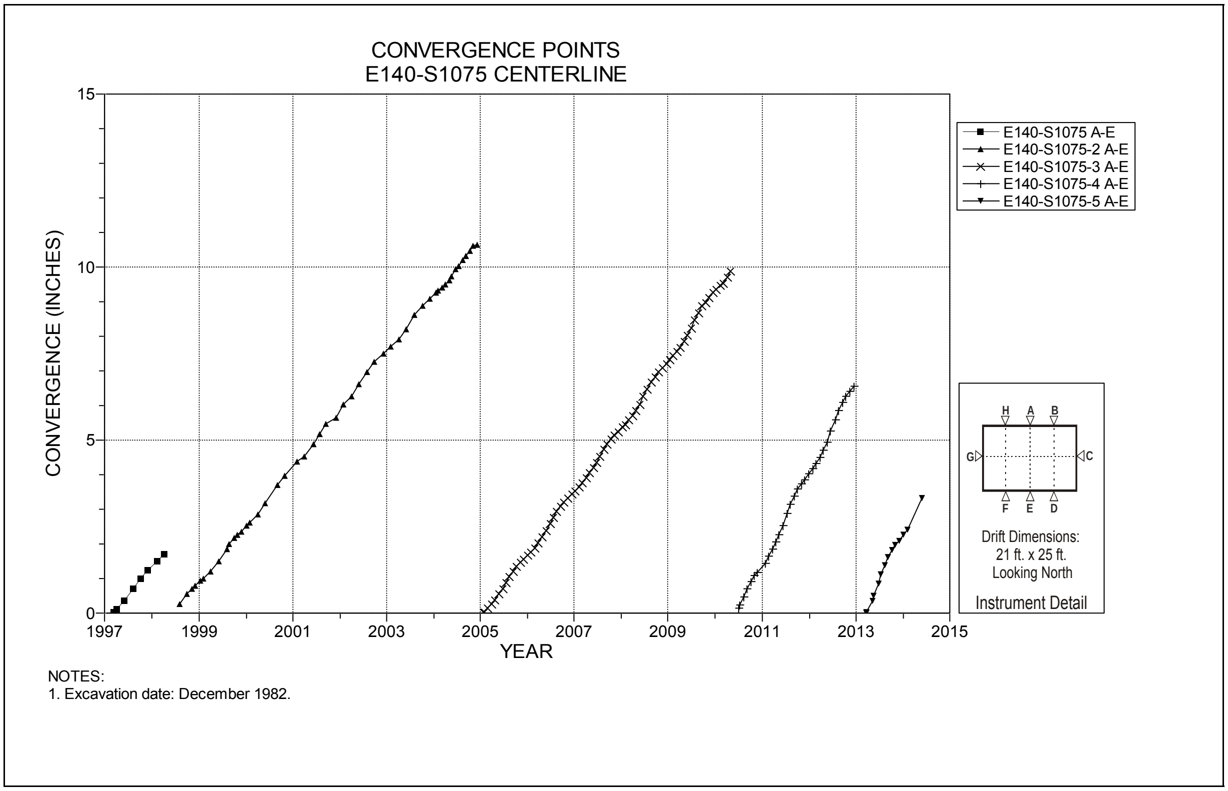

Figure 4-69 Convergence Point Array
E140 S1075 – Roof to Floor – Centerline

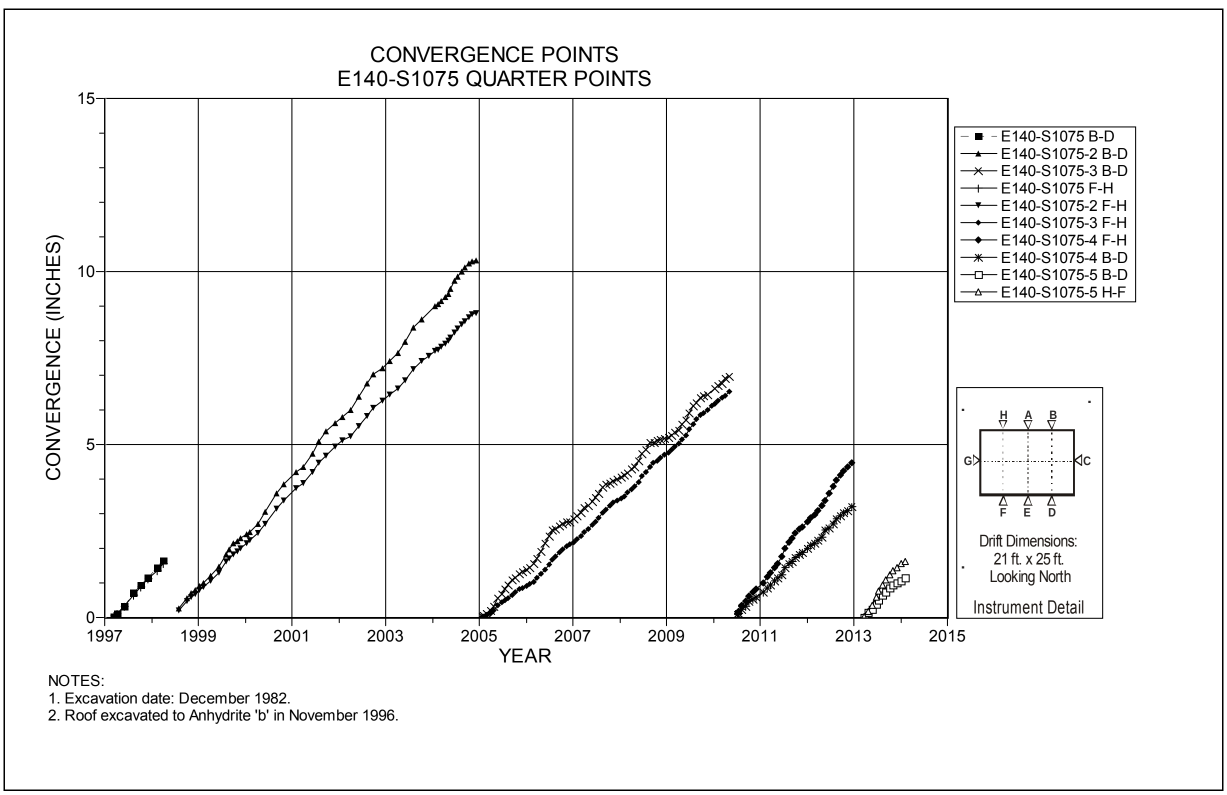

Figure 4-70 Convergence Point Array
E140 S1075 – Roof to Floor – Quarter Points

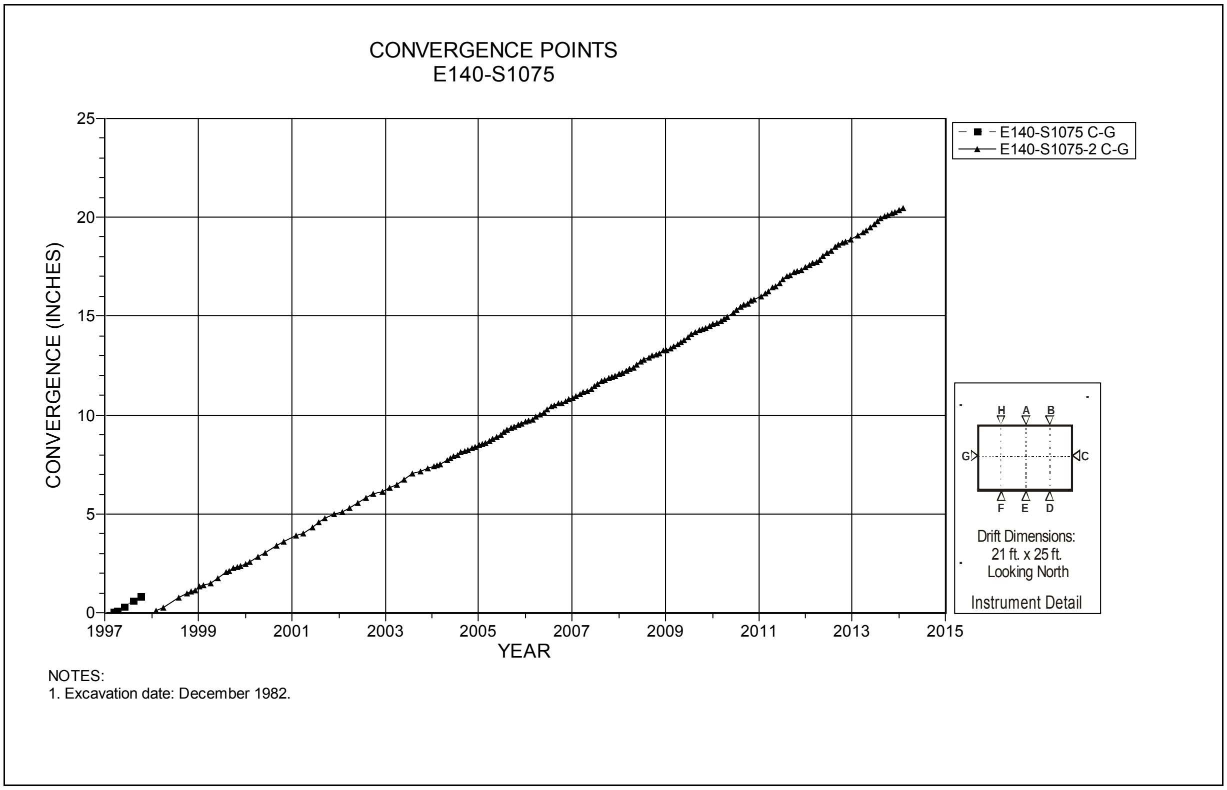

Figure 4-71 Convergence Point Array
E140 S1075 – Rib to Rib

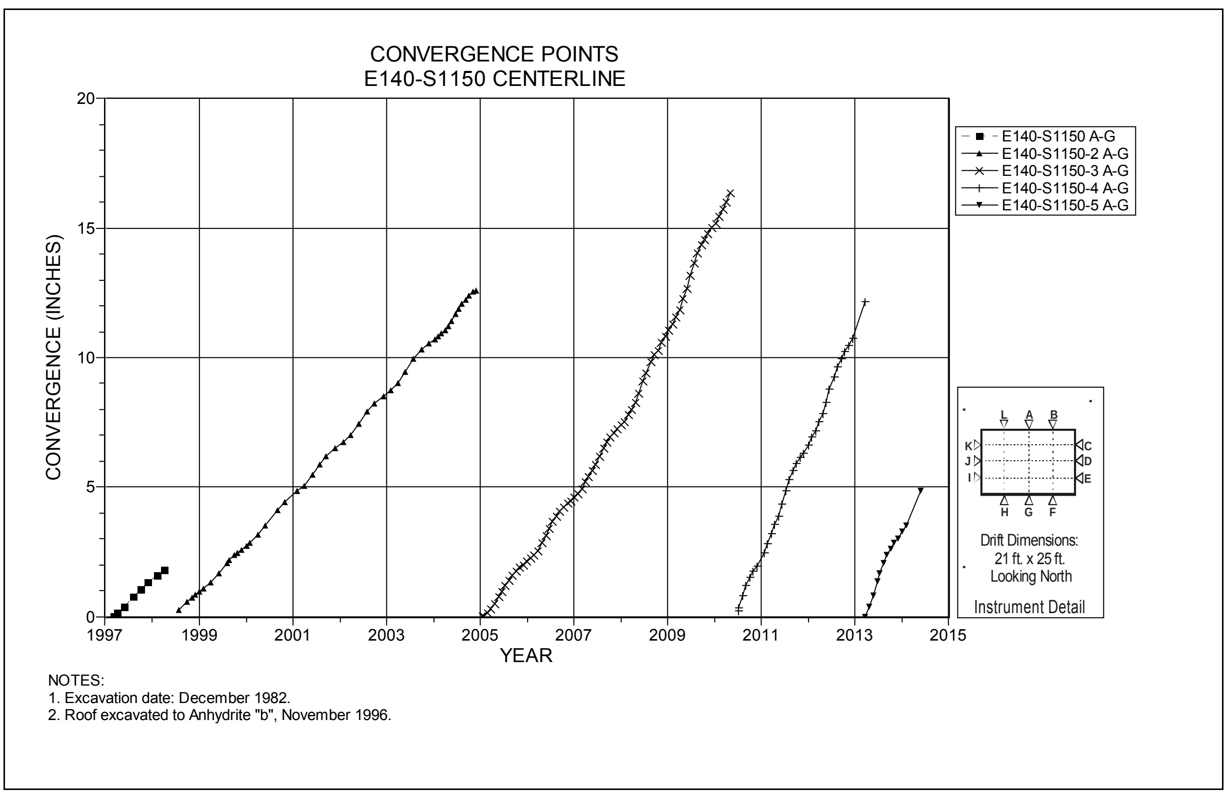

Figure 4-72 Convergence Point Array
E140 S1150 – Roof to Floor – Centerline

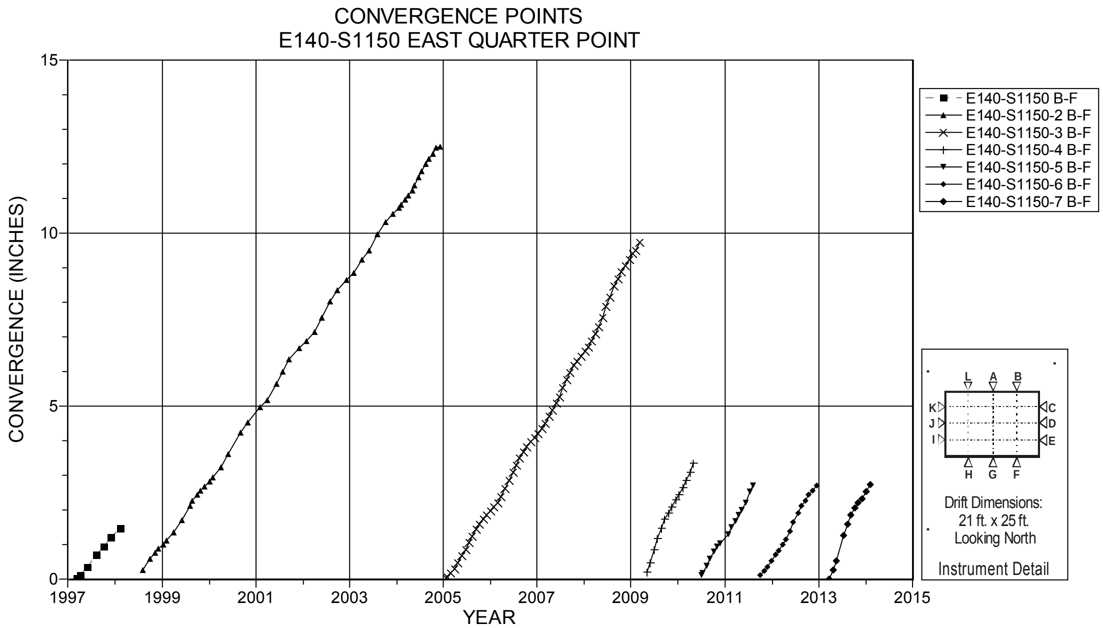

NOTES:
1. Excavation date: December 1982.
2. Roof excavated to Anhydrite "b", November 1996.

Figure 4-73 Convergence Point Array
E140 S1150 – Roof to Floor – East Quarter Point

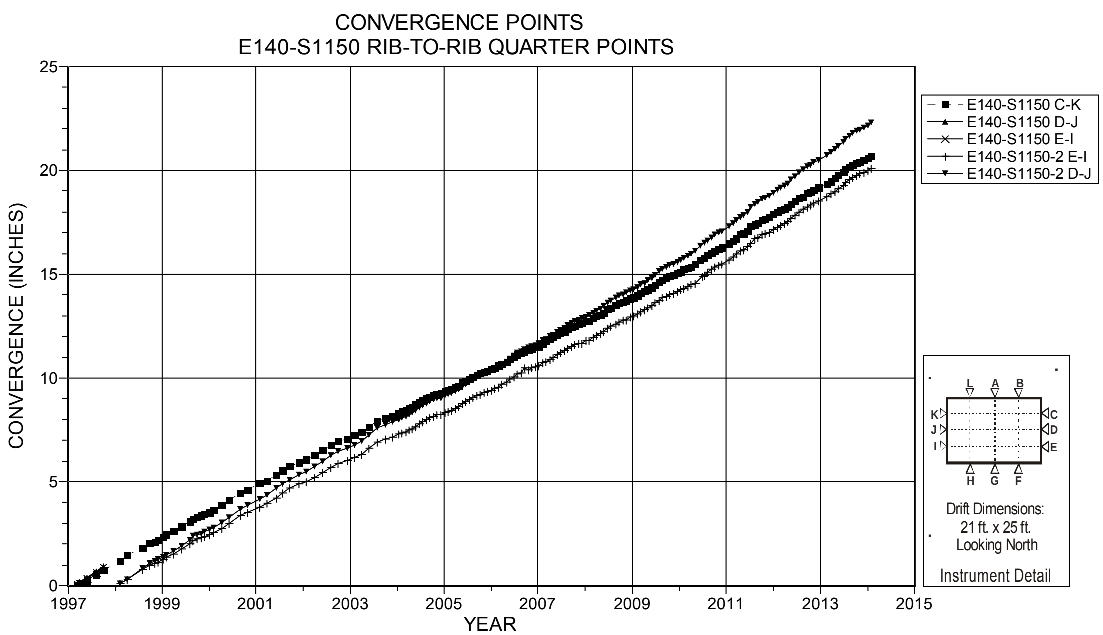

NOTES:
1. Excavation date: December 1982.
2. Roof excavated to Anhydrite 'b' in November 1996.

Figure 4-74 Convergence Point Array
E140 S1150 – Rib to Rib Quarter Points

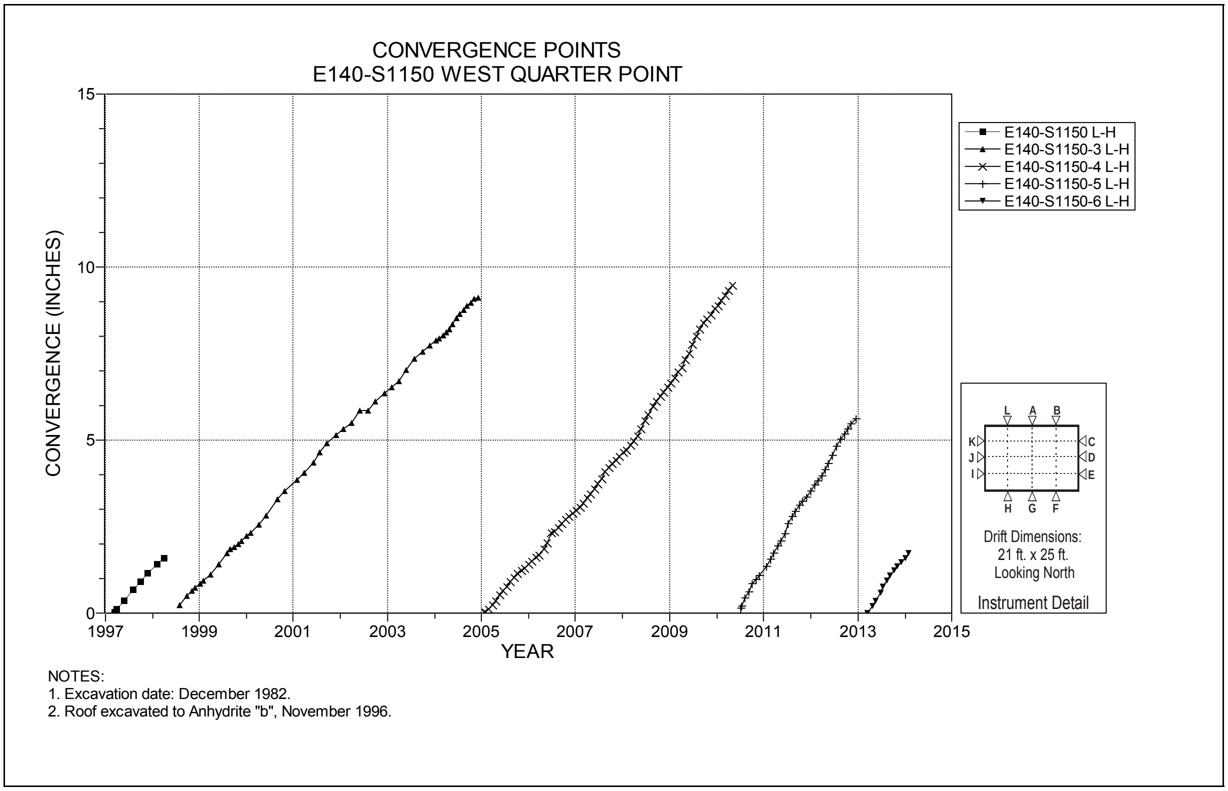

Figure 4-75 Convergence Point Array
E140 S1150 – Roof to Floor – West Quarter Point

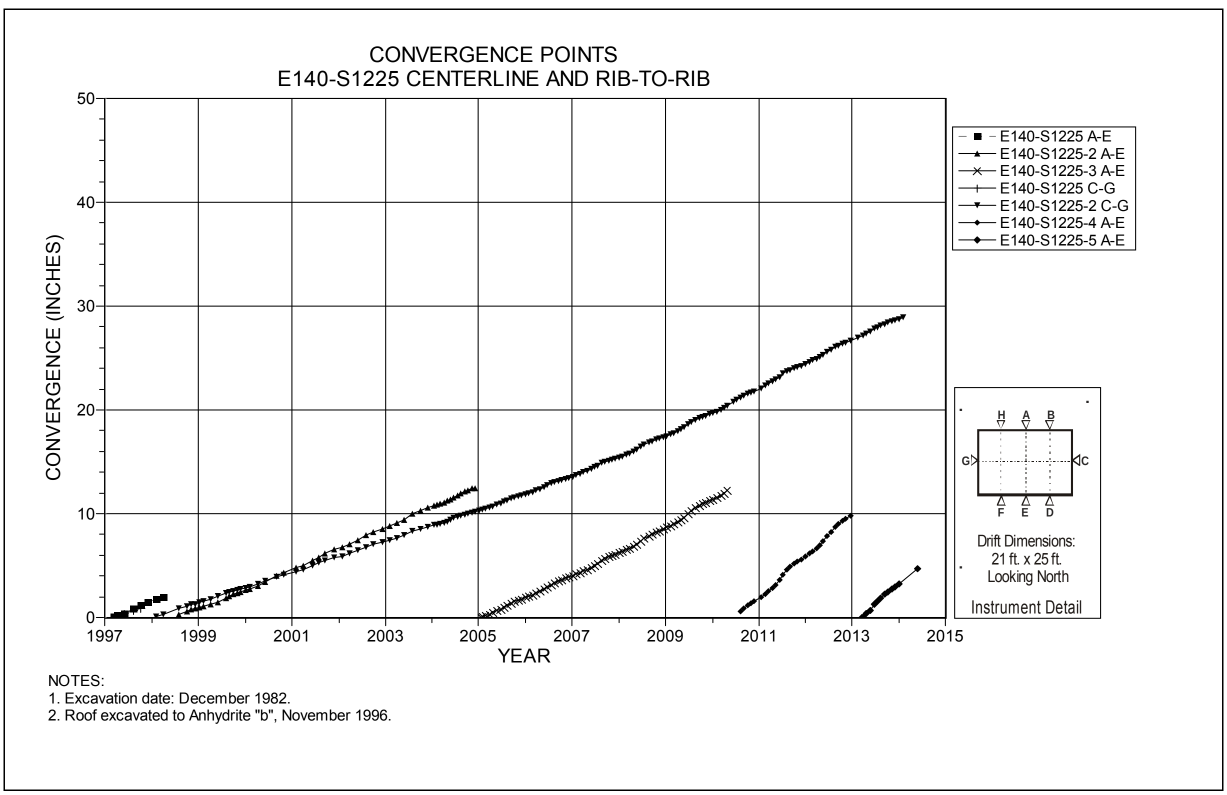

Figure 4-76 Convergence Point Array
E140 S1225 – Roof to Floor – Centerline and Rib to Rib

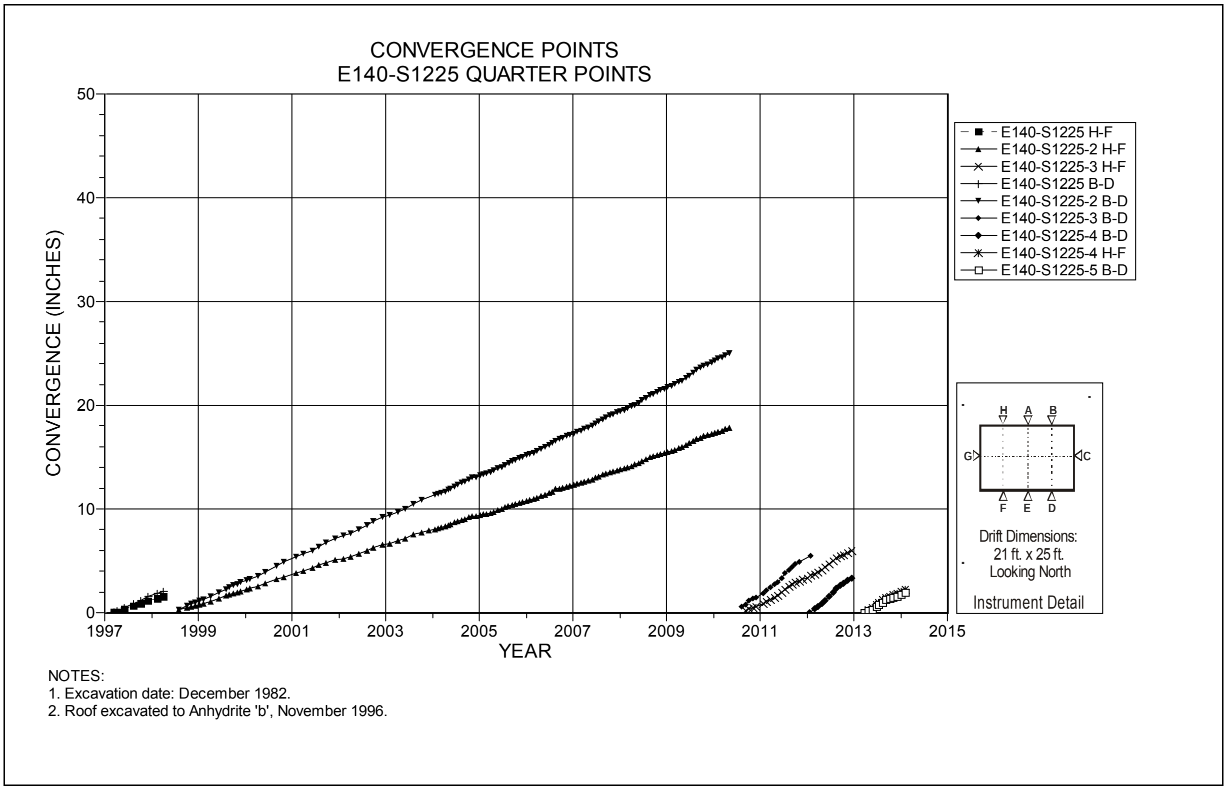

Figure 4-77 Convergence Point Array
E140 S1225 – Roof to Floor – Quarter Points

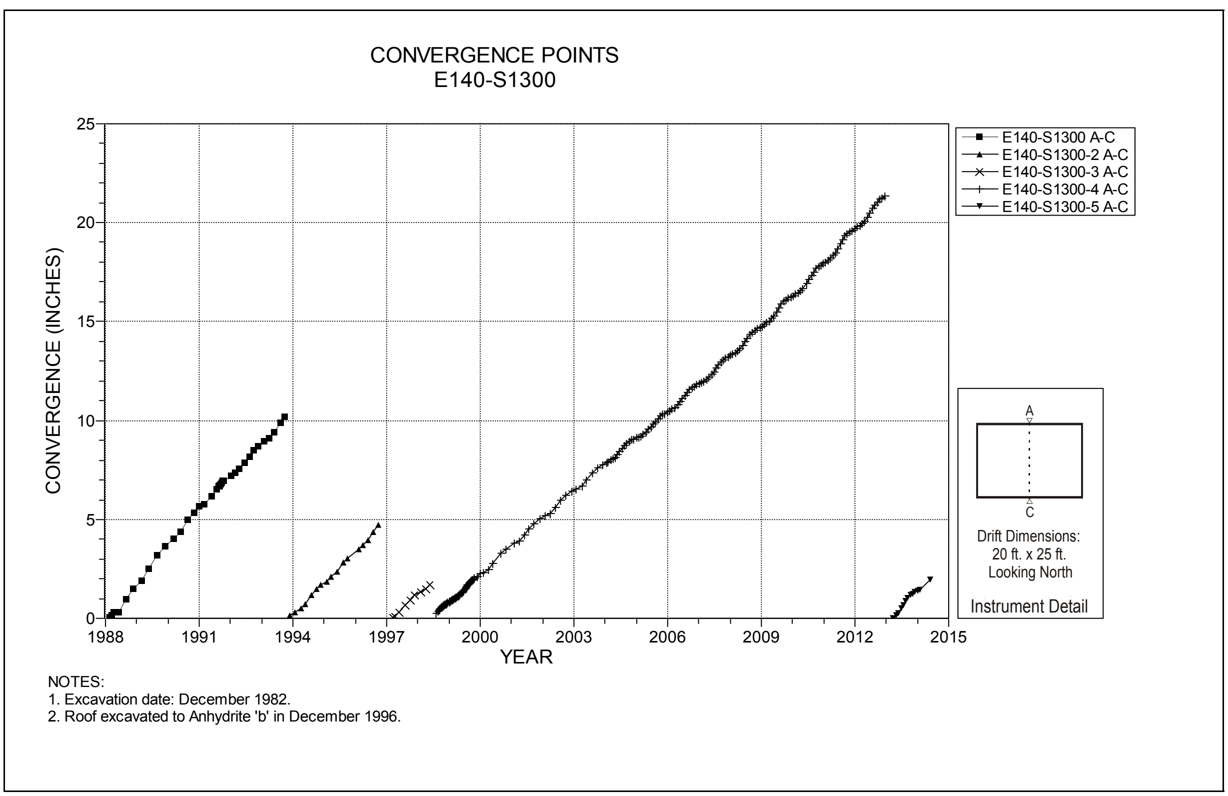

Figure 4-78 Convergence Point Array
E140 S1300 – Roof to Floor

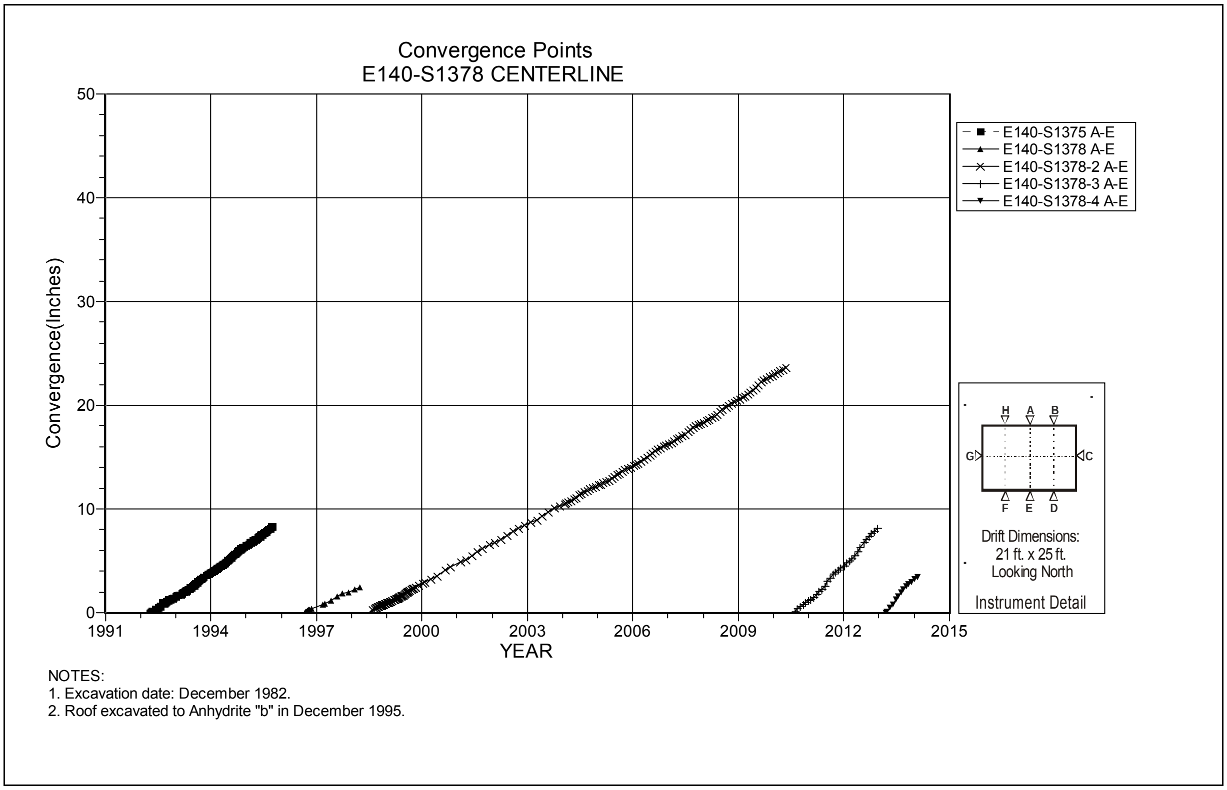

Figure 4-79 Convergence Point Array
E140 S1375/S1378 – Roof to Floor – Centerline

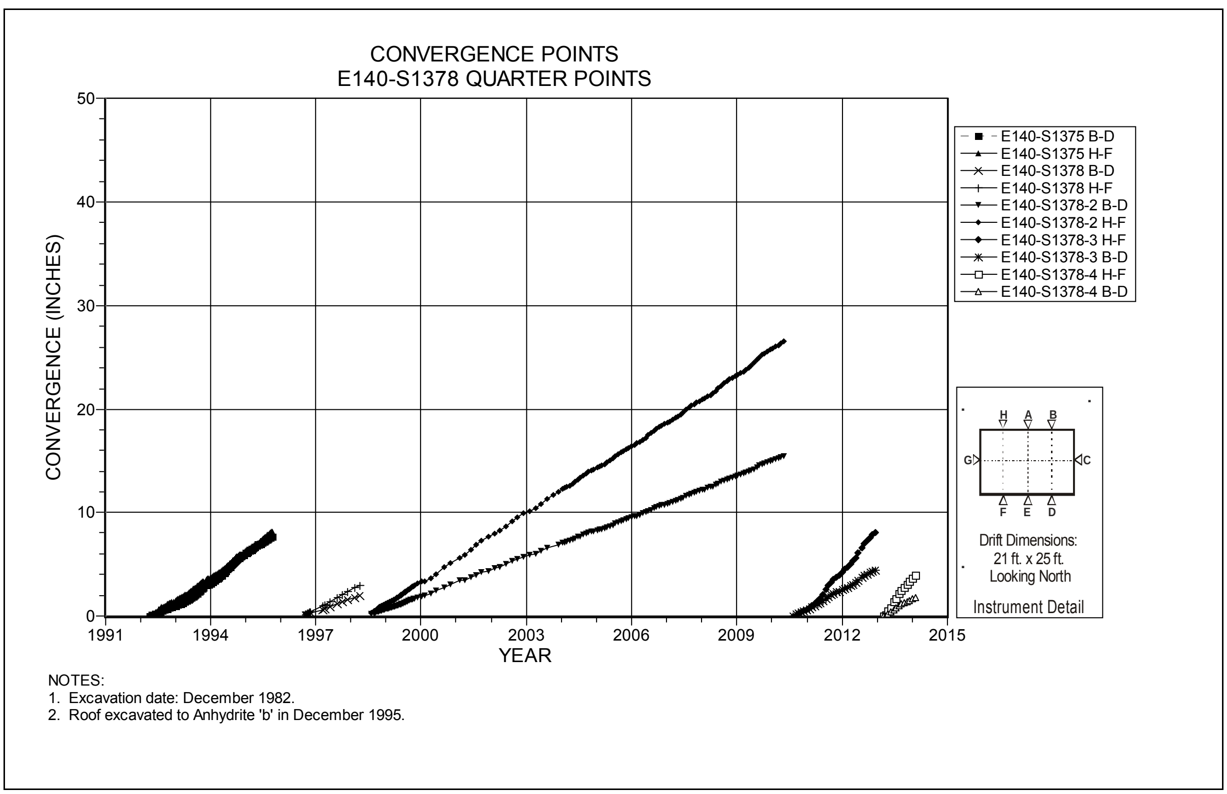

Figure 4-80 Convergence Point Array
E140 S1375/S1378 – Roof to Floor – Quarter Points

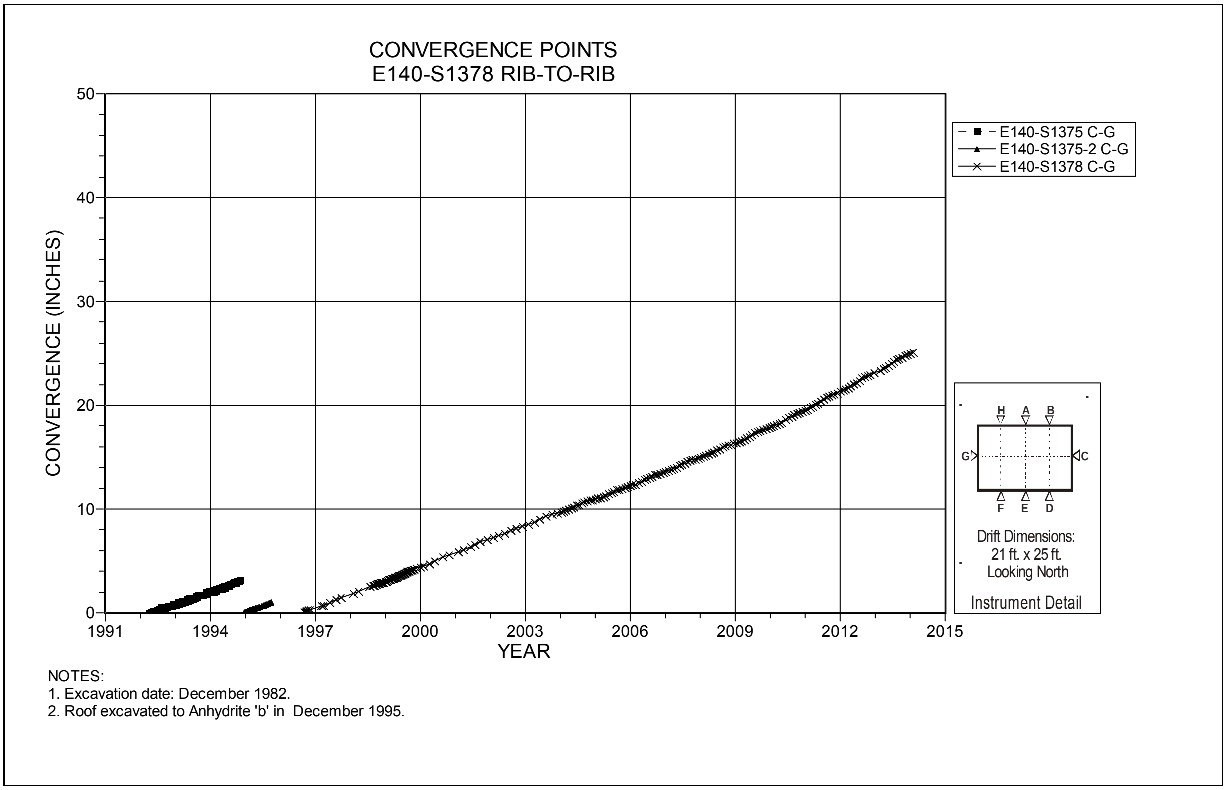

Figure 4-81 Convergence Point Array
E140 S1375/S1378 – Rib to Rib

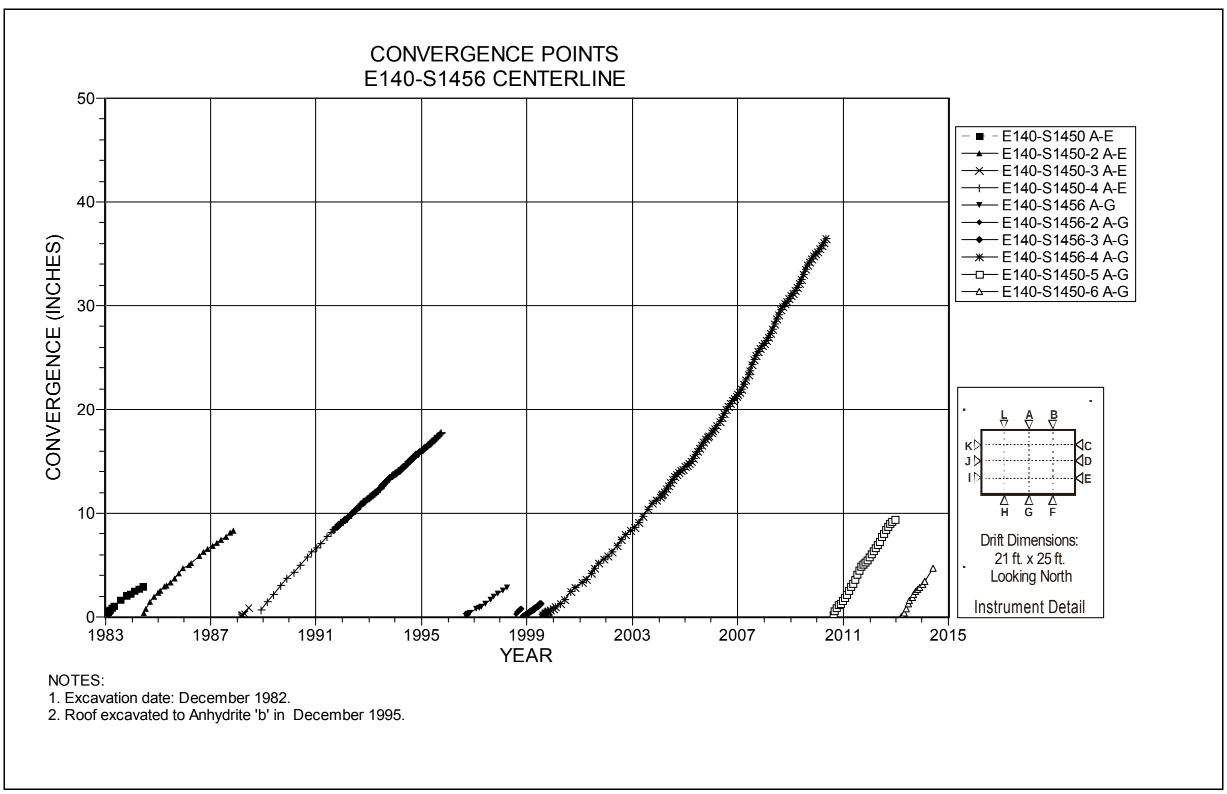

Figure 4-82 Convergence Point Array
E140 S1450/S1456 – Roof to Floor – Centerline

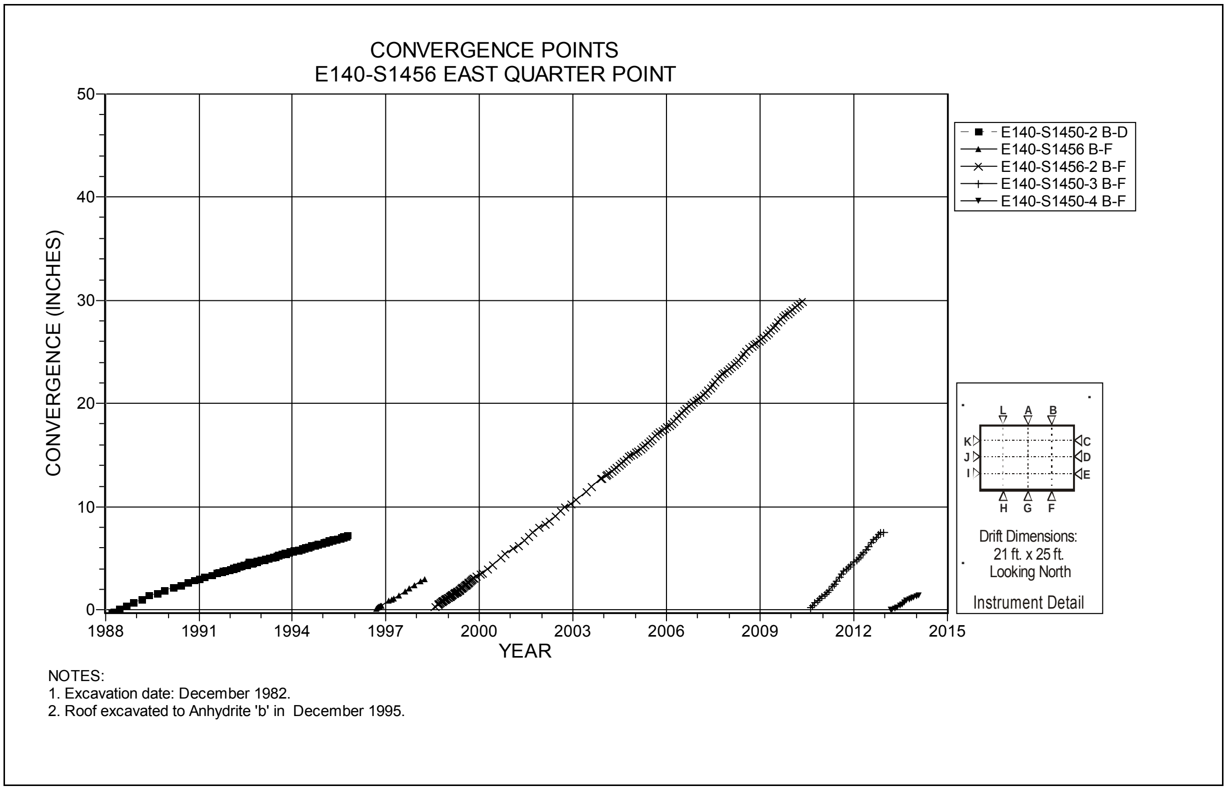

Figure 4-83 Convergence Point Array
E140 S1450/S1456 – Roof to Floor – East Quarter Point

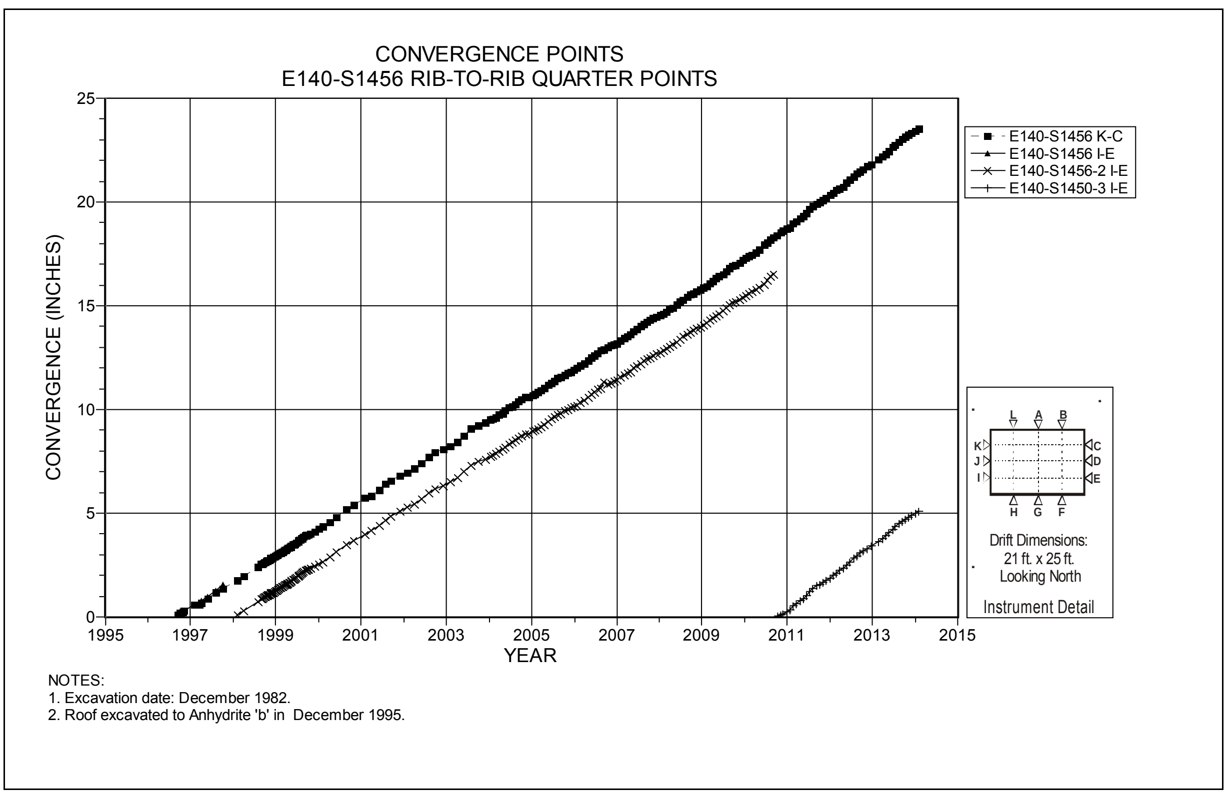

Figure 4-84 Convergence Point Array
E140 S1450/S1456 – Rib to Rib Quarter Points

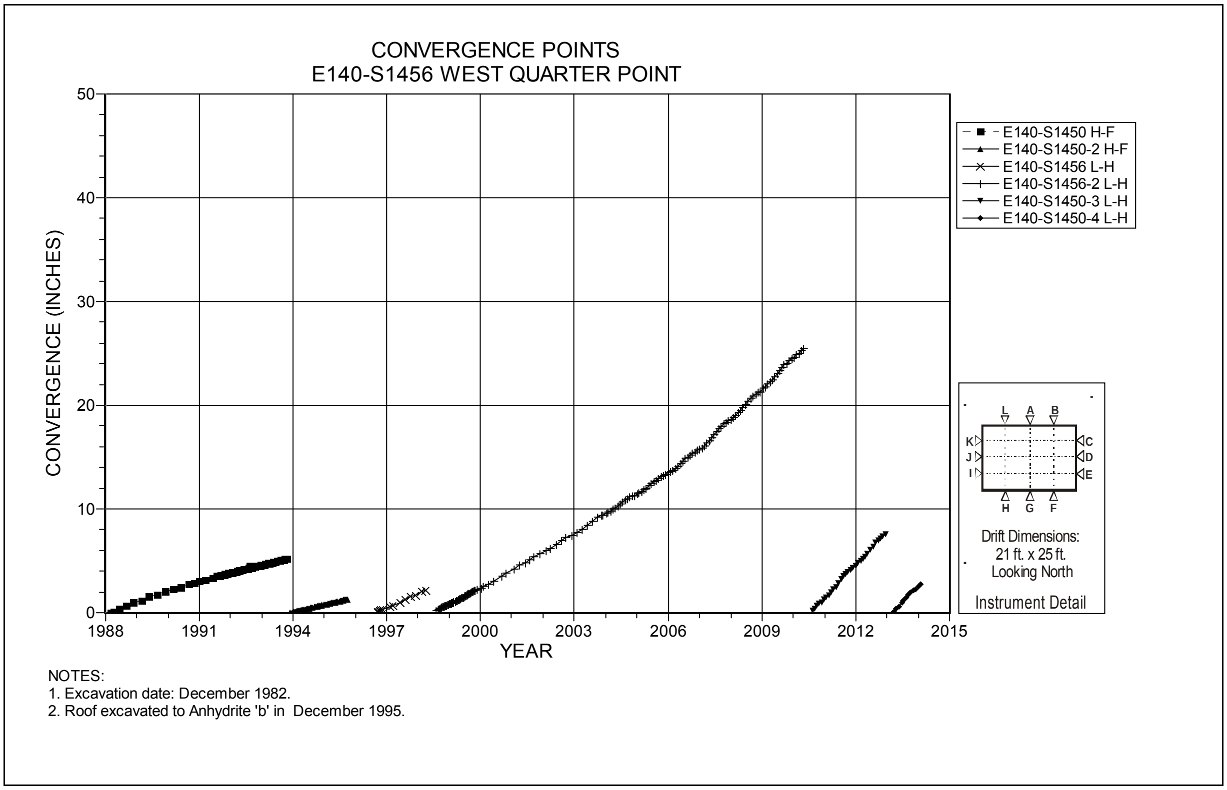

Figure 4-85 Convergence Point Array
E140 S1450/S1456 – Roof to Floor – West Quarter Point

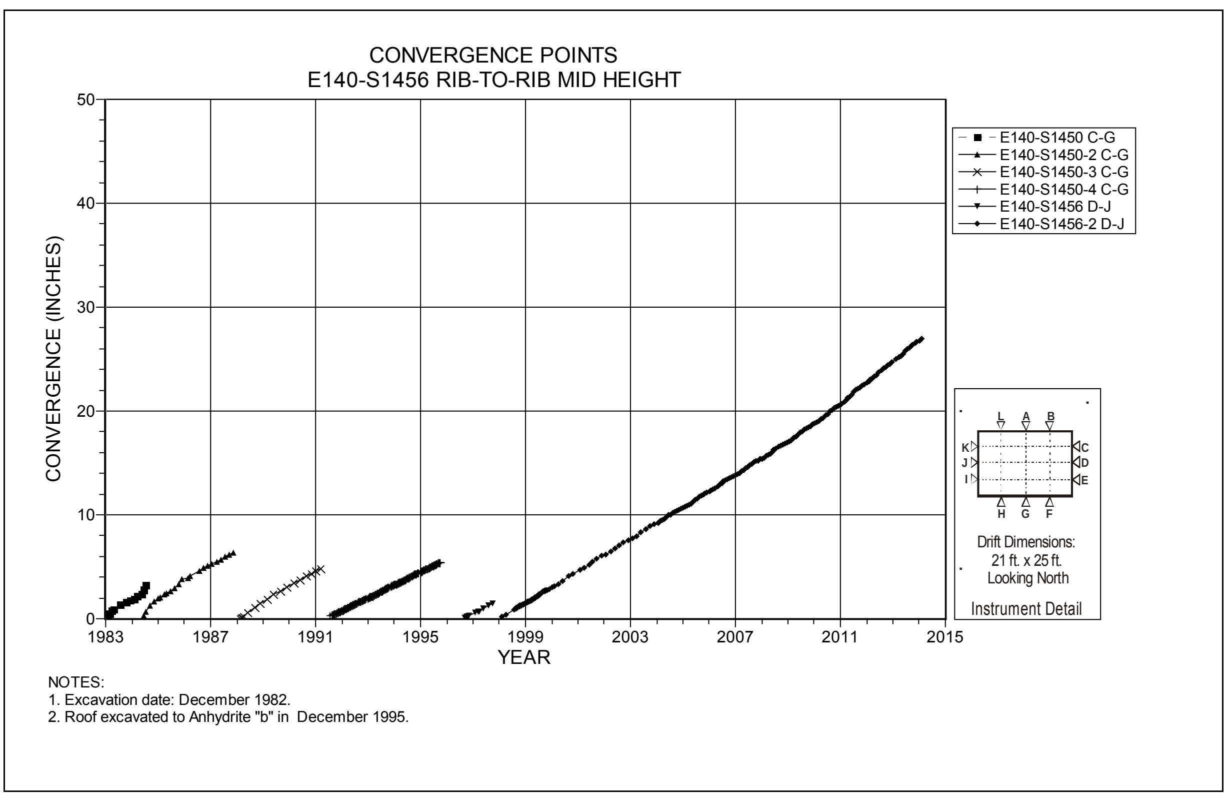

Figure 4-86 Convergence Point Array
E140 S1450/S1456 – Rib to Rib – Mid-Height

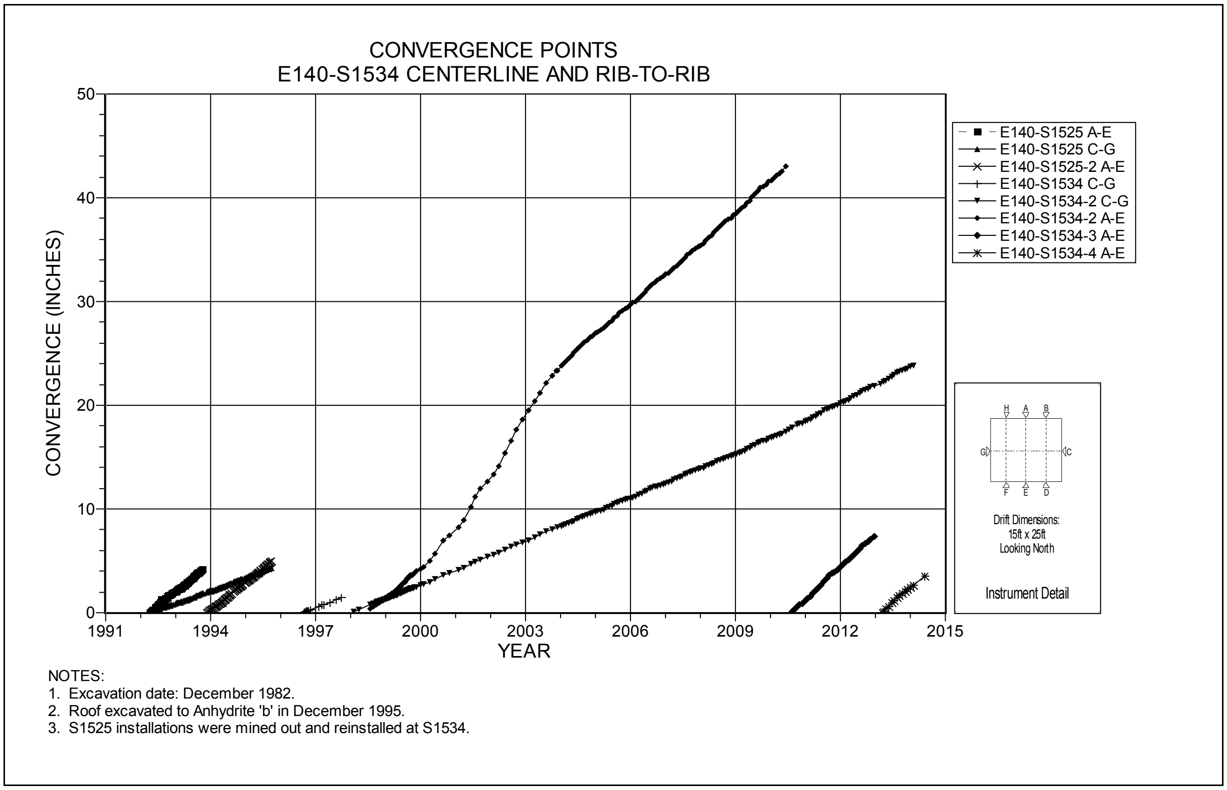

Figure 4-87 Convergence Point Array
E140 S1525/S1534 – Roof to Floor – Centerline and Rib to Rib

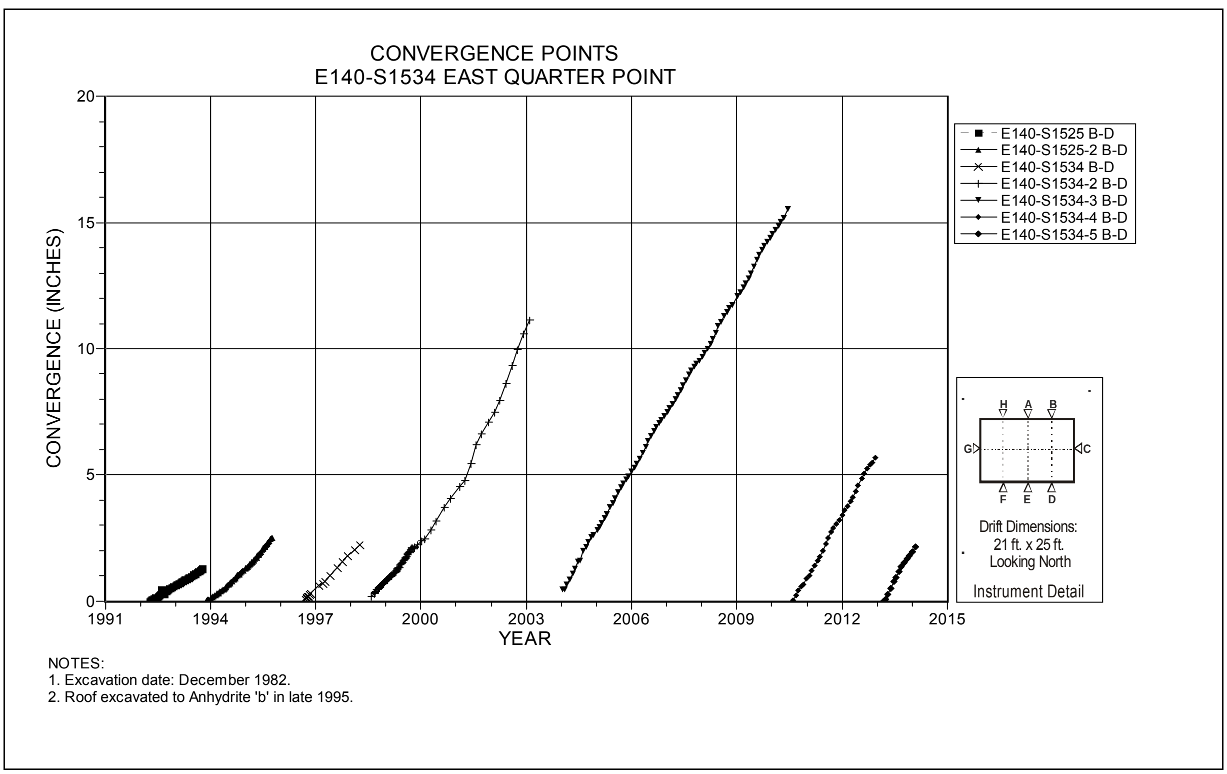

Figure 4-88 Convergence Point Array
E140 S1525/S1534 – Roof to Floor – East Quarter Point

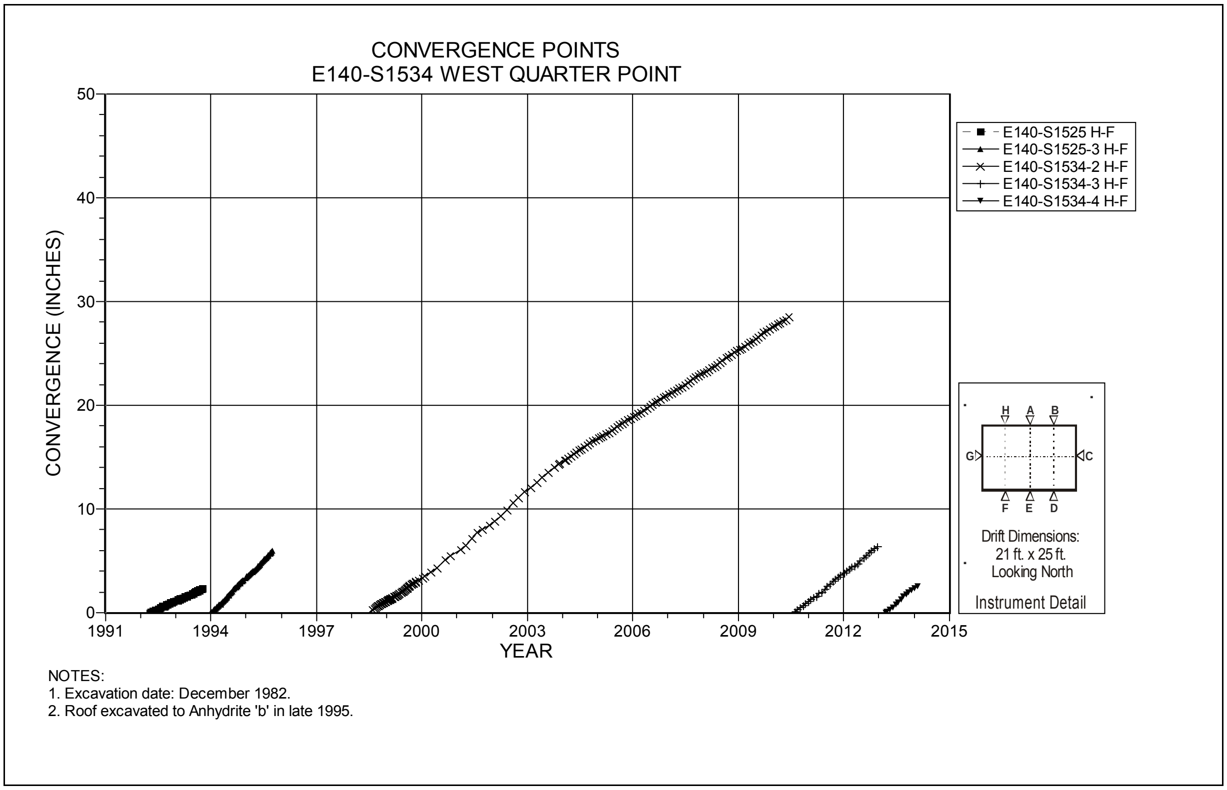

Figure 4-89 Convergence Point Array
E140 S1525/S1534 – Roof to Floor – West Quarter Point

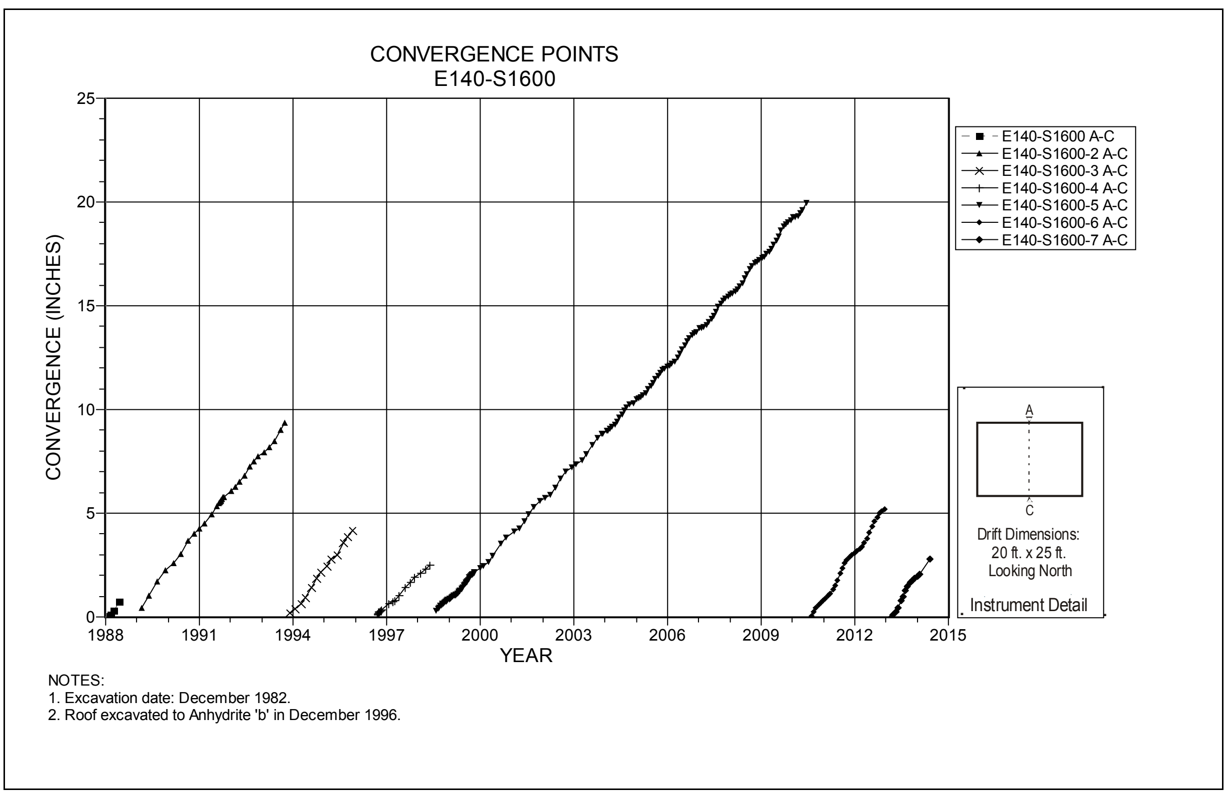

Figure 4-90 Convergence Point Array
E140 S1600 – Roof to Floor

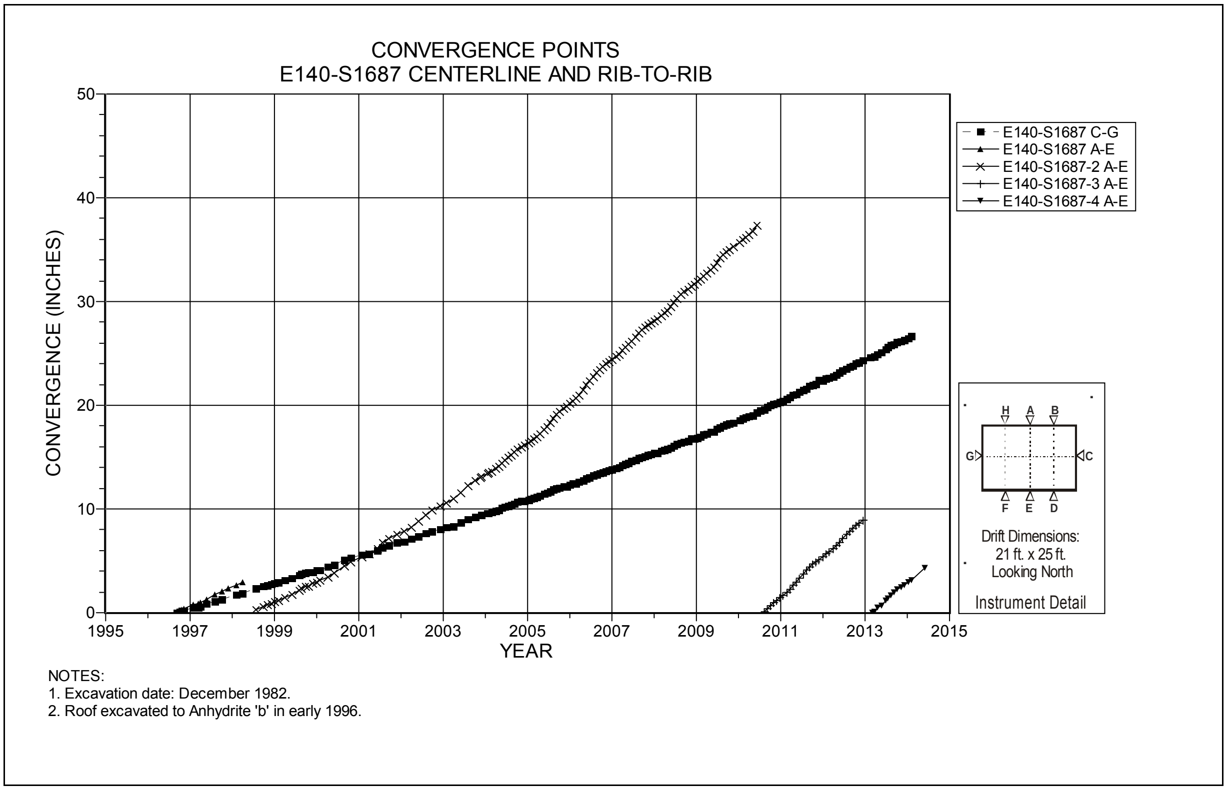

Figure 4-91 Convergence Point Array
E140 S1687 – Roof to Floor – Centerline and Rib to Rib

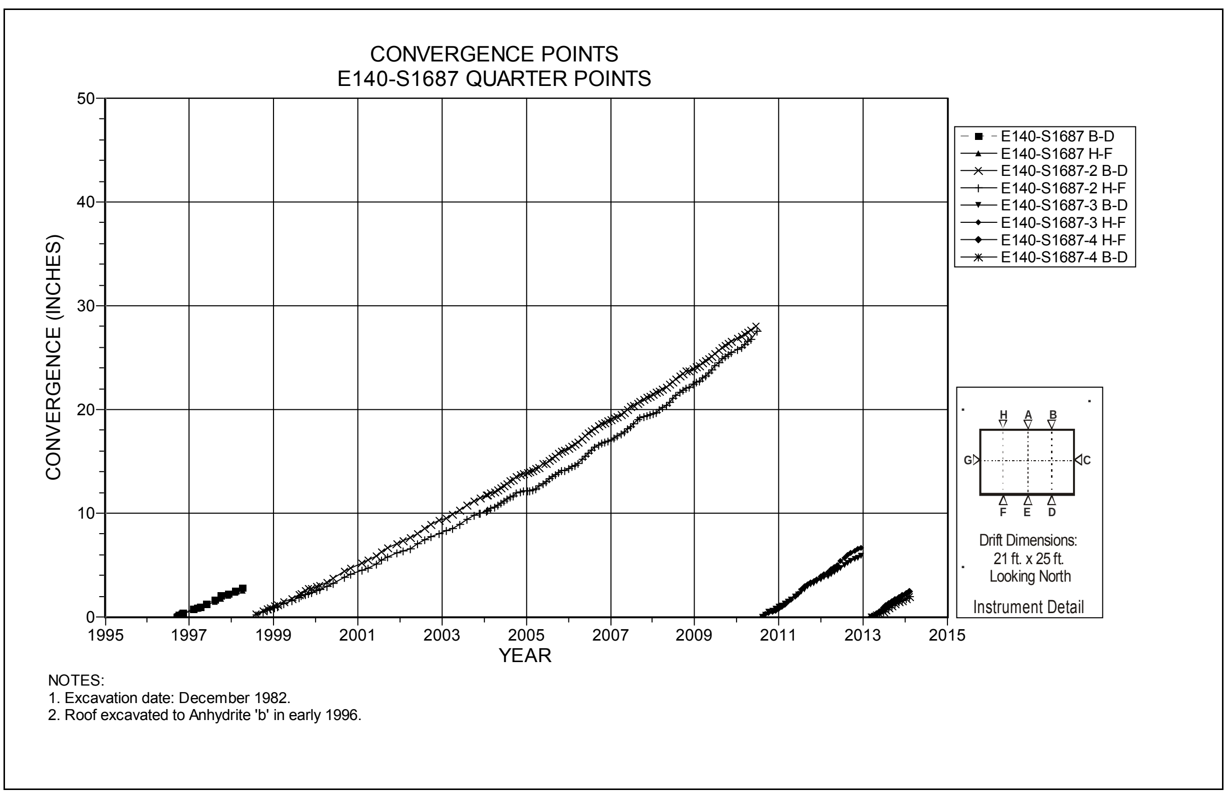

Figure 4-92 Convergence Point Array
E140 S1687 – Roof to Floor – Quarter Points

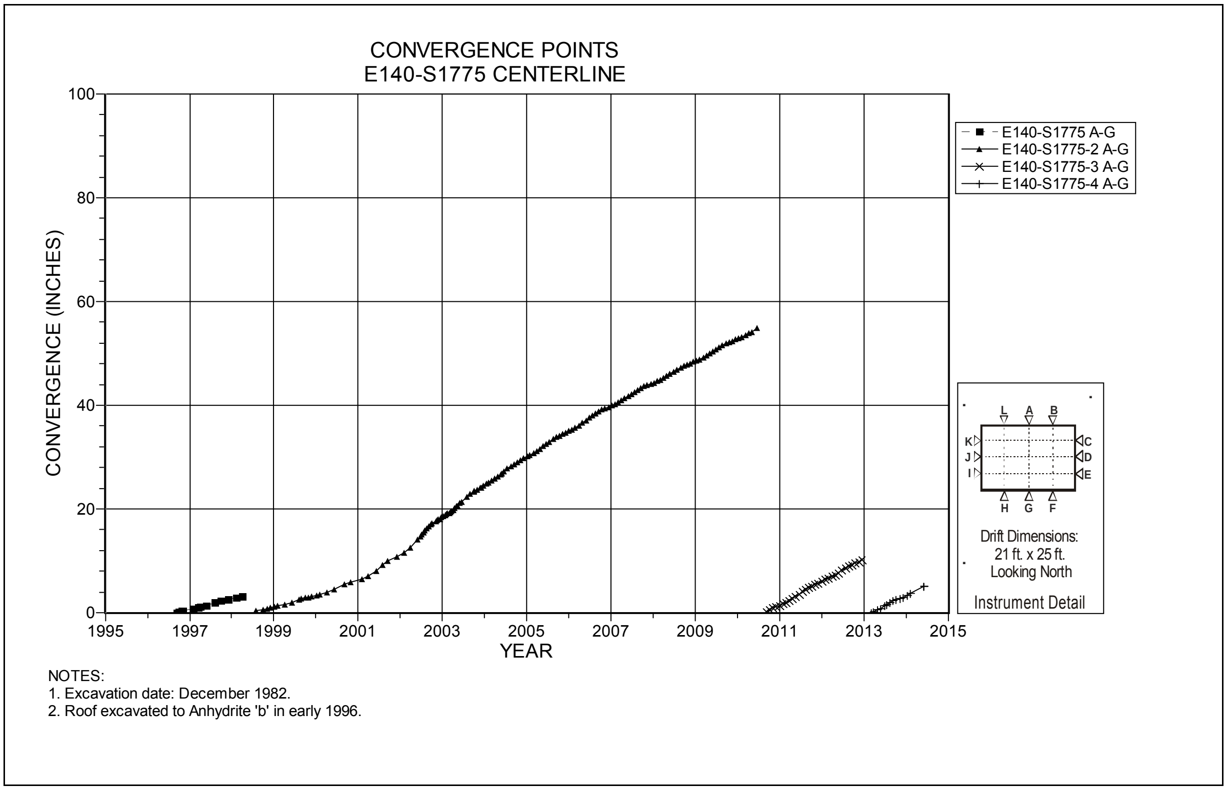

Figure 4-93 Convergence Point Array
E140 S1775 – Roof to Floor – Centerline

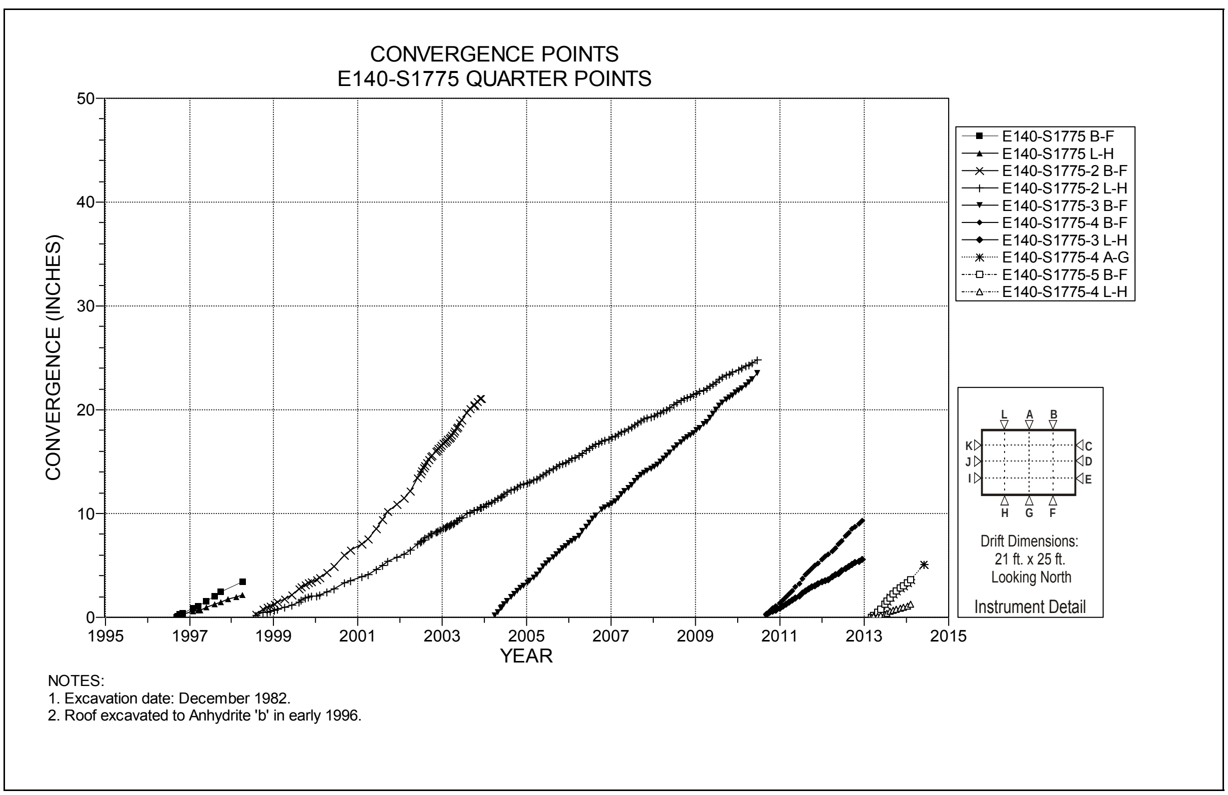

Figure 4-94 Convergence Point Array
E140 S1775 – Roof to Floor – Quarter Points

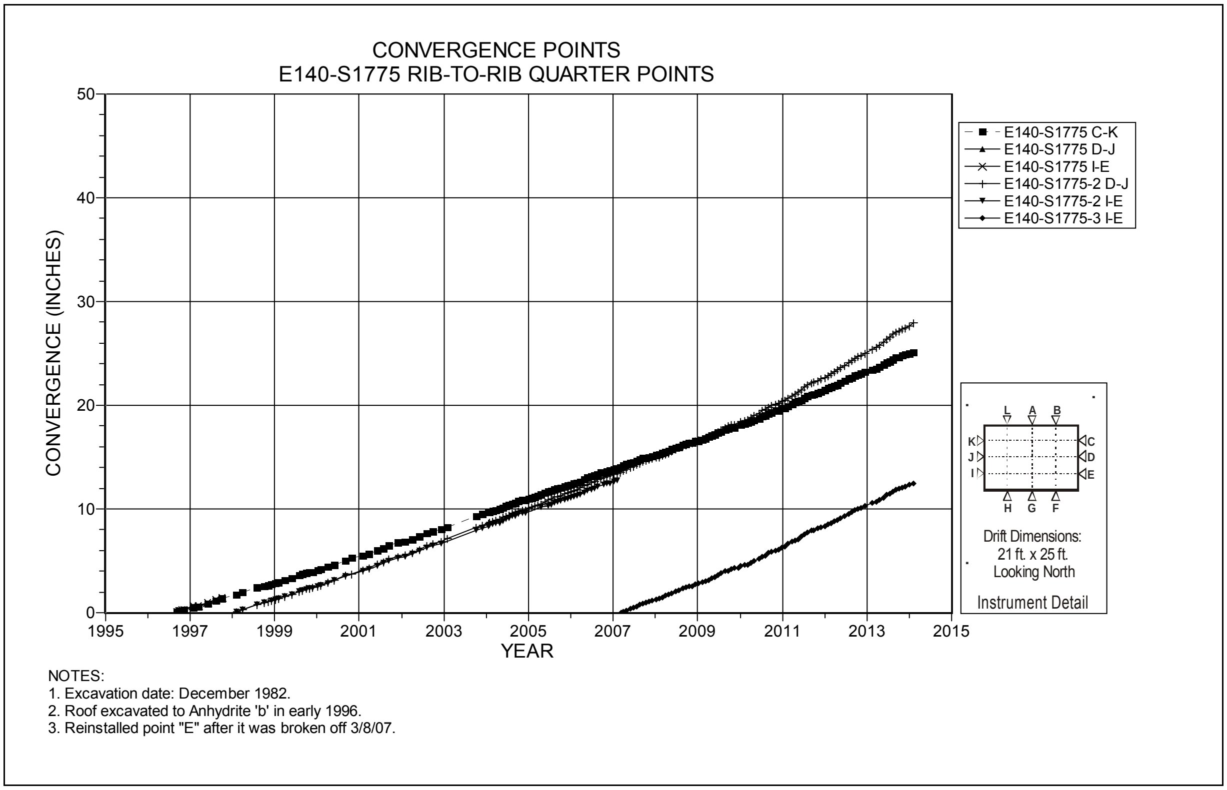

Figure 4-95 Convergence Point Array
E140 S1775 – Rib to Rib – Quarter Points

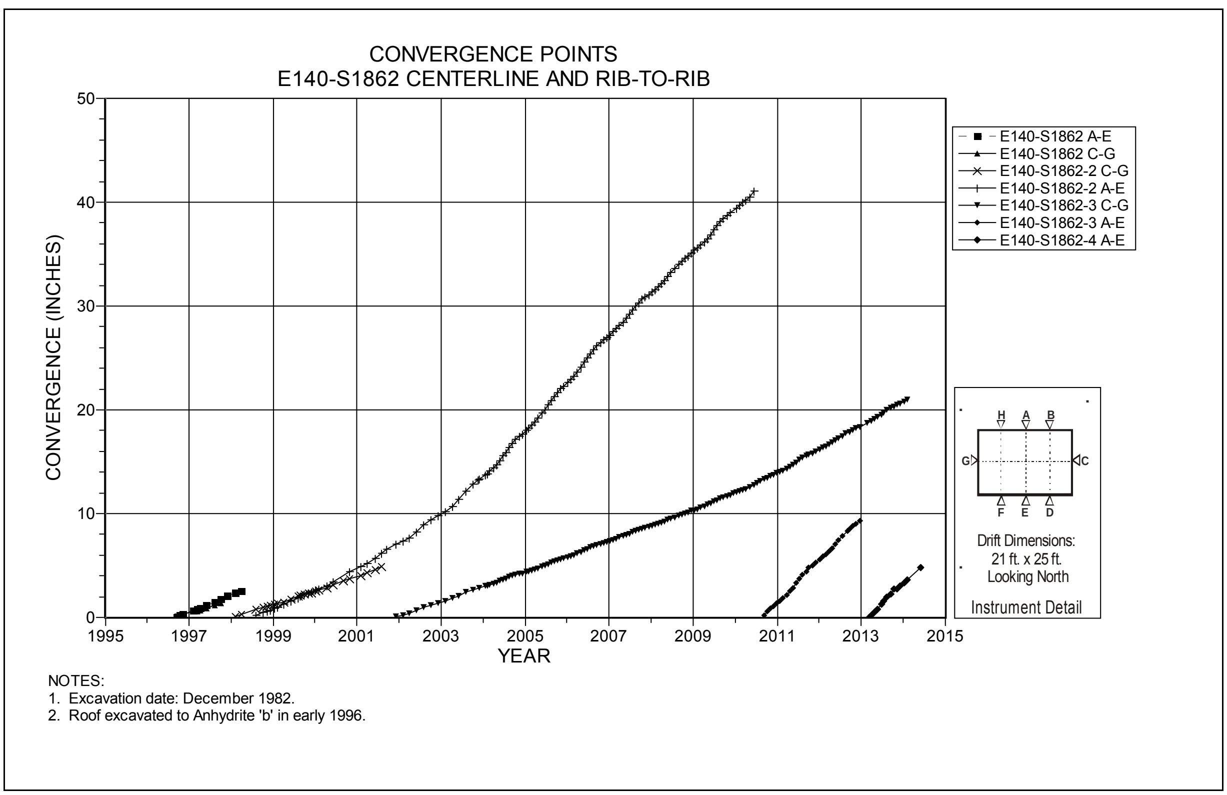

Figure 4-96 Convergence Point Array
E140 S1862 – Roof to Floor – Centerline and Rib to Rib

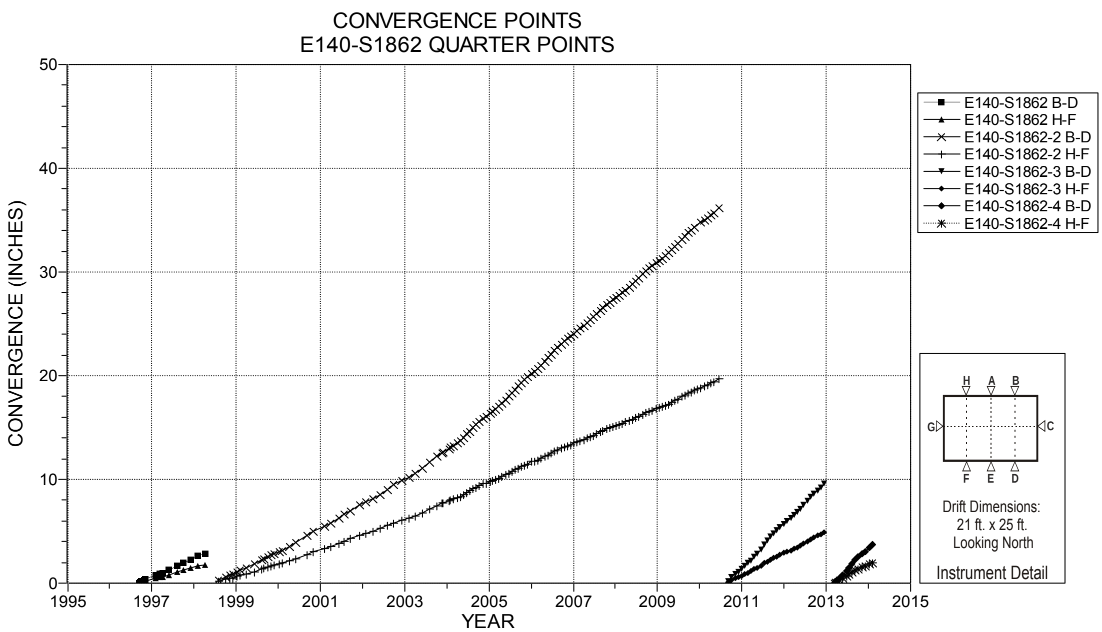

NOTES:
1. Excavation date: December 1982.
2. Roof excavated to Anhydrite 'b' in early 1996.

Figure 4-97 Convergence Point Array
E140 S1862 – Roof to Floor – Quarter Points

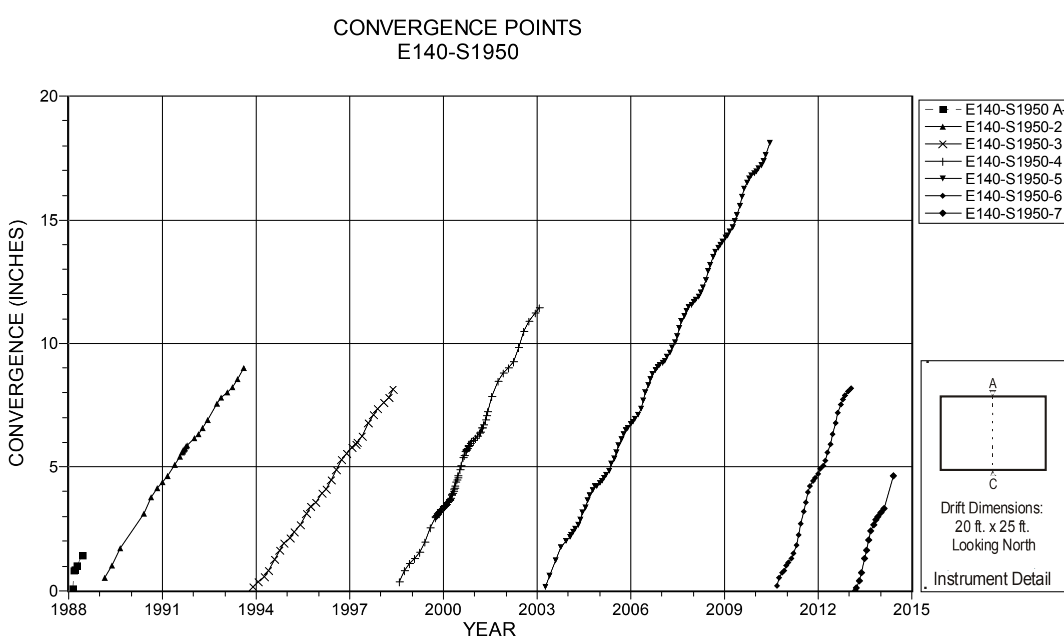

NOTES:
1. Excavation date: December 1982.
2. Roof excavated to Anhydrite 'b', March 2003.

Figure 4-98 Convergence Point Array
E140 S1950 – Roof to Floor

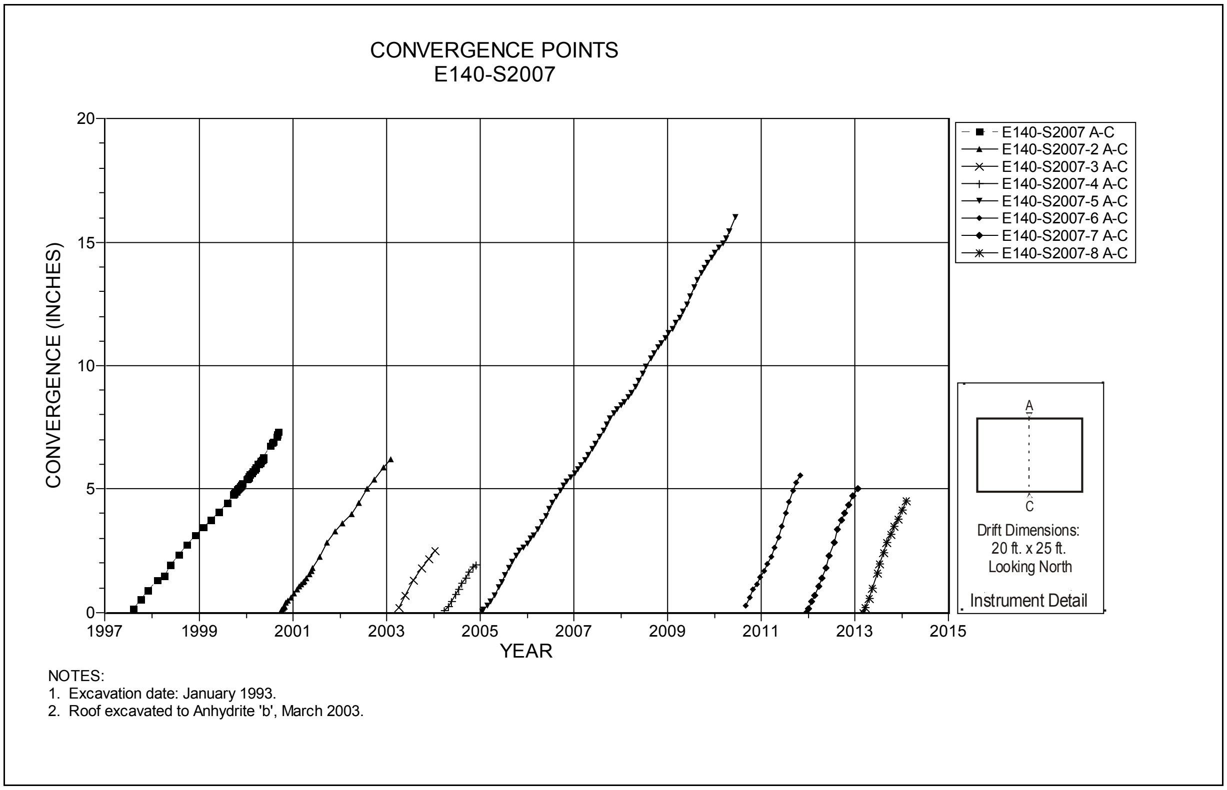

Figure 4-99 Convergence Point Array
E140 S2007 – Roof to Floor

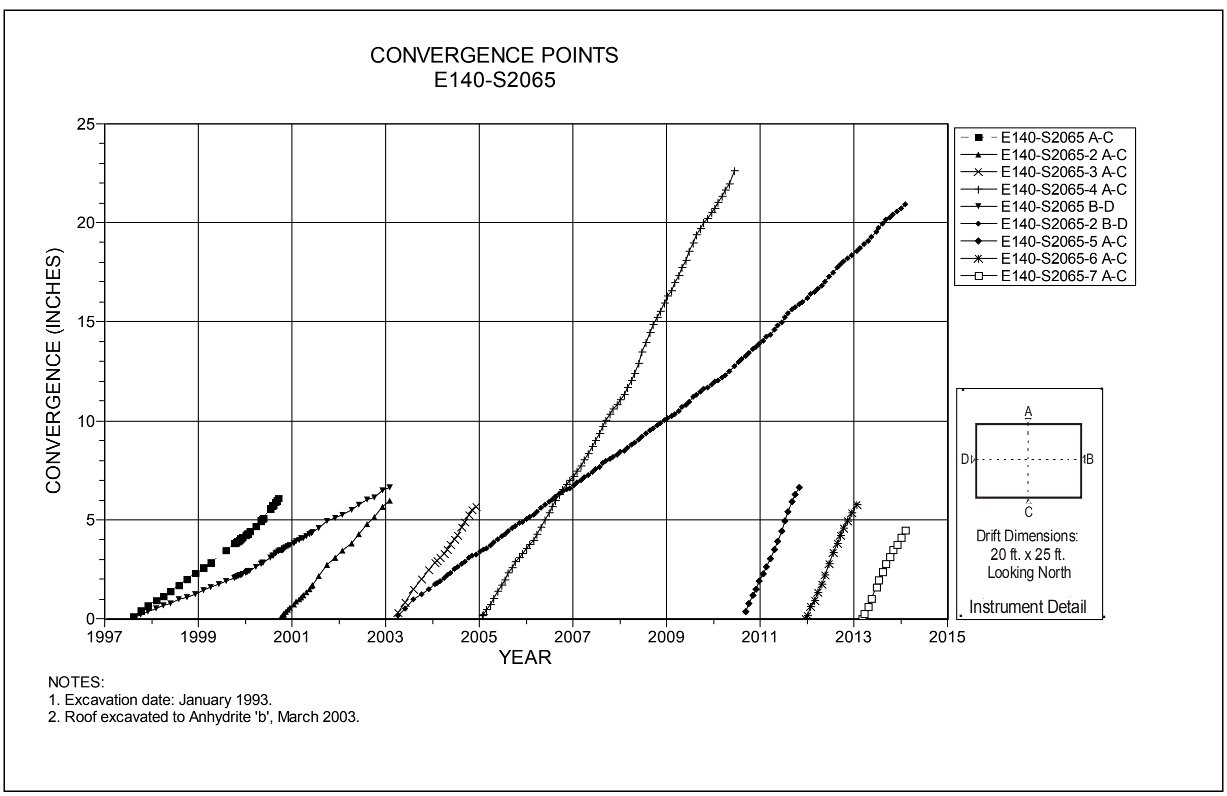

Figure 4-100 Convergence Point Array
E140 S2065 – All Chords

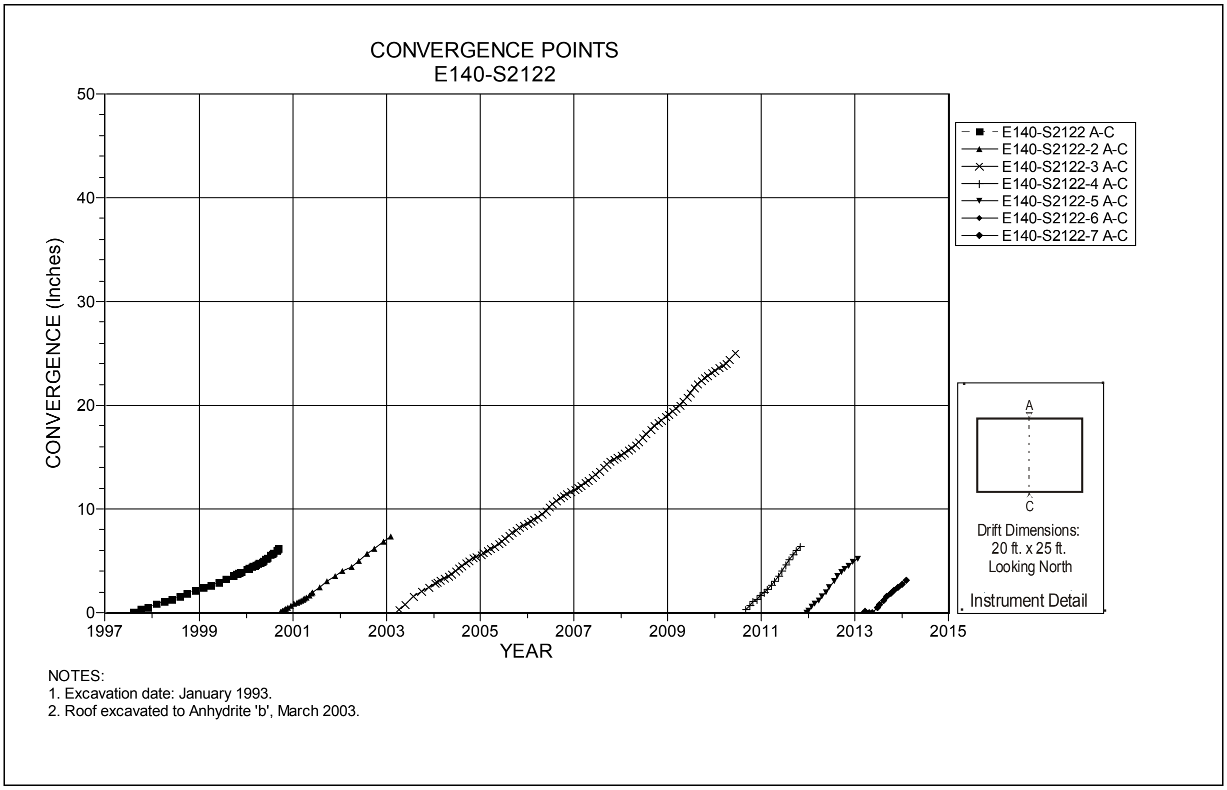

Figure 4-101 Convergence Point Array
E140 S2122 – Roof to Floor

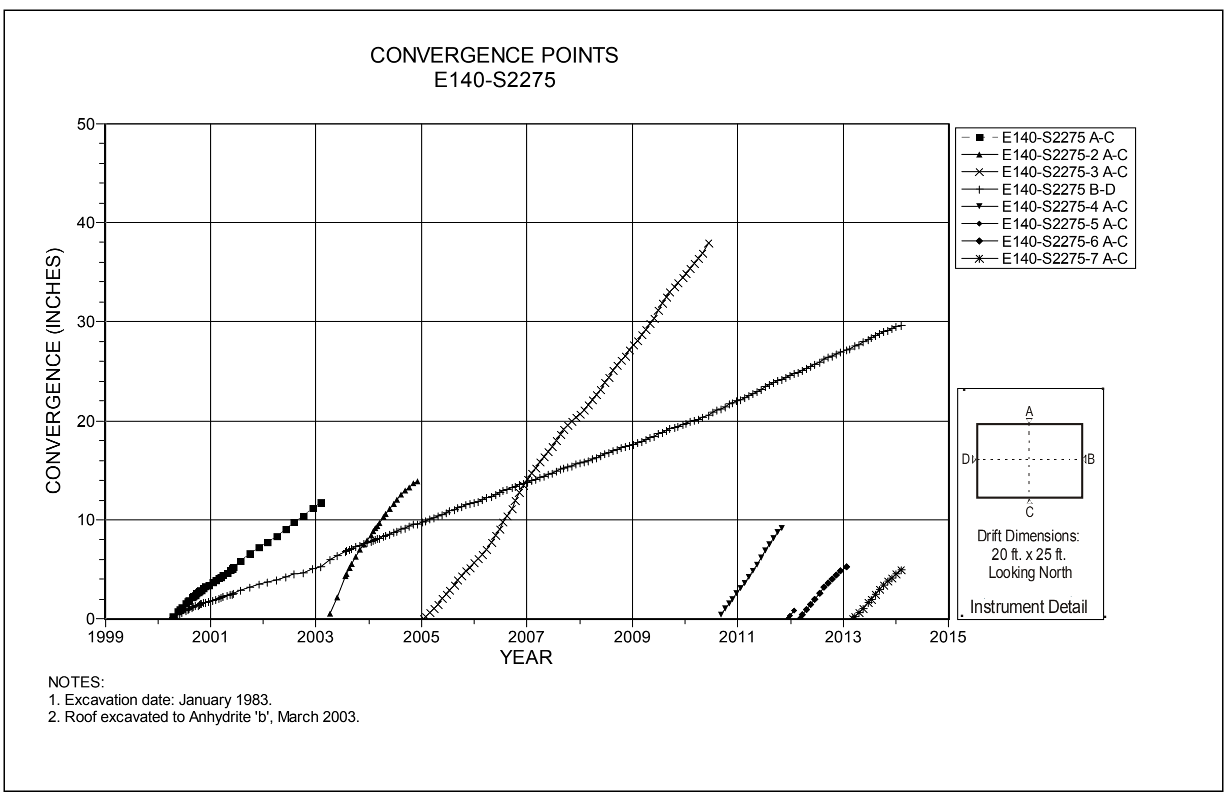

Figure 4-102 Convergence Point Array
E140 S2275 – All Chords

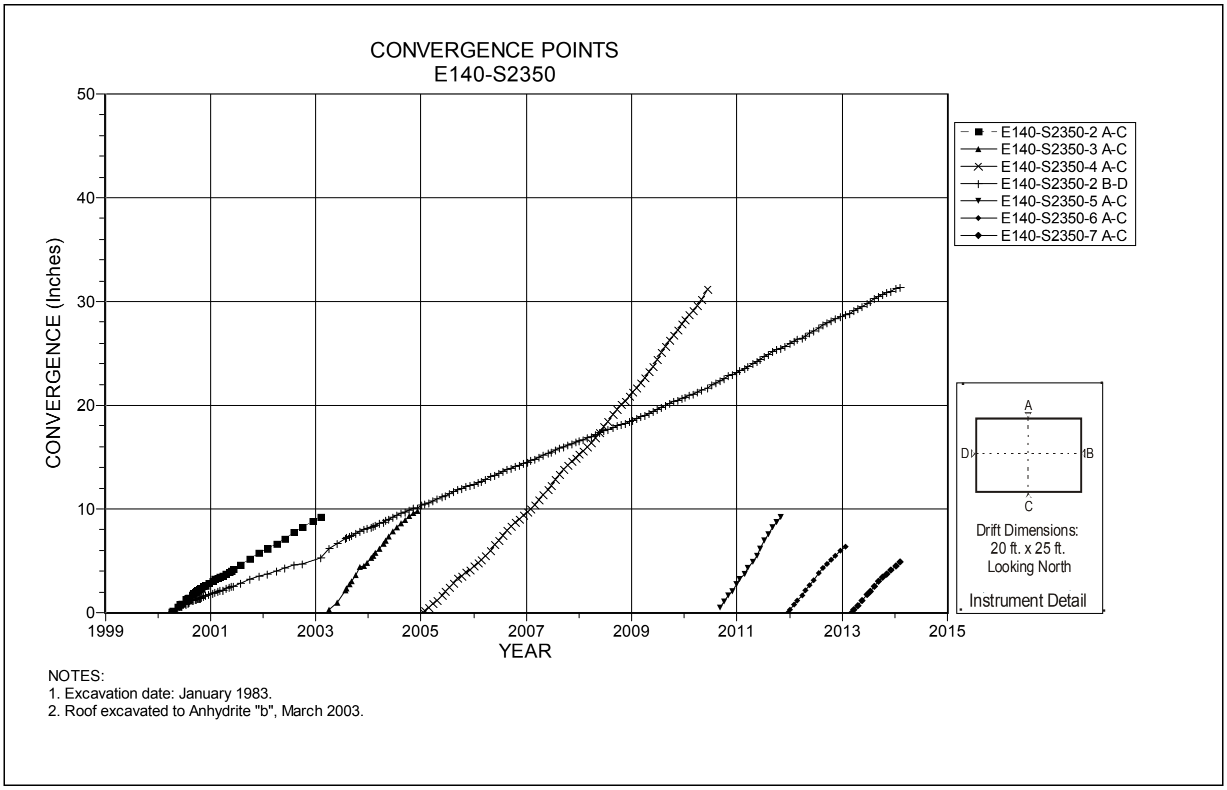

Figure 4-103 Convergence Point Array
E140 S2350 – All Chords

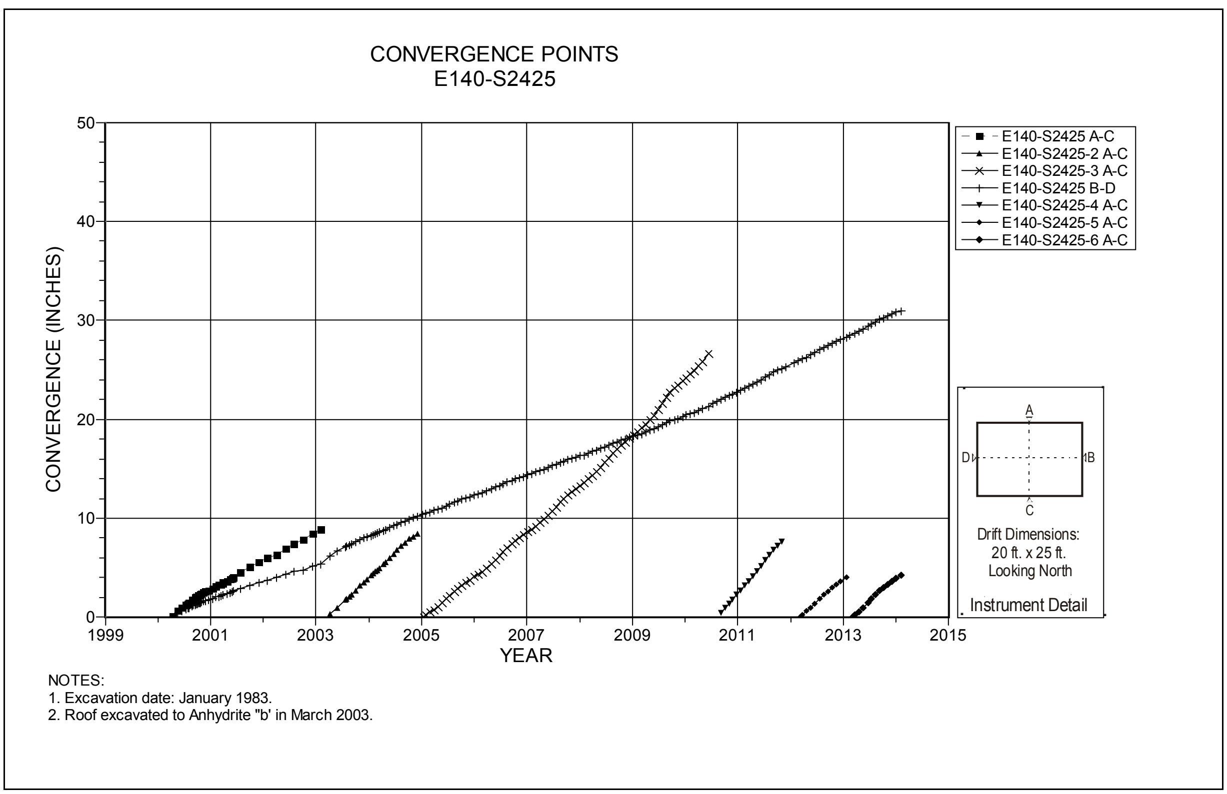

Figure 4-104 Convergence Point Array
E140 S2425 – All Chords

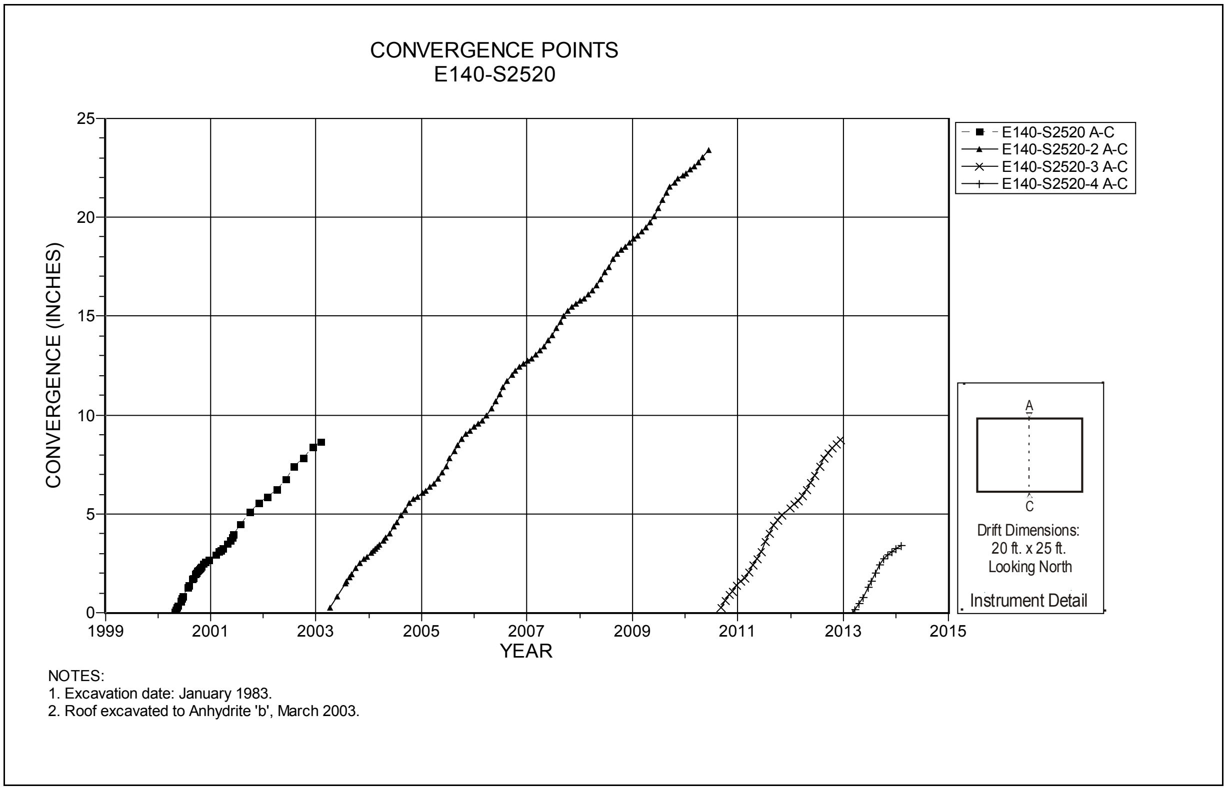

Figure 4-105 Convergence Point Array
E140 S2520 – Roof to Floor

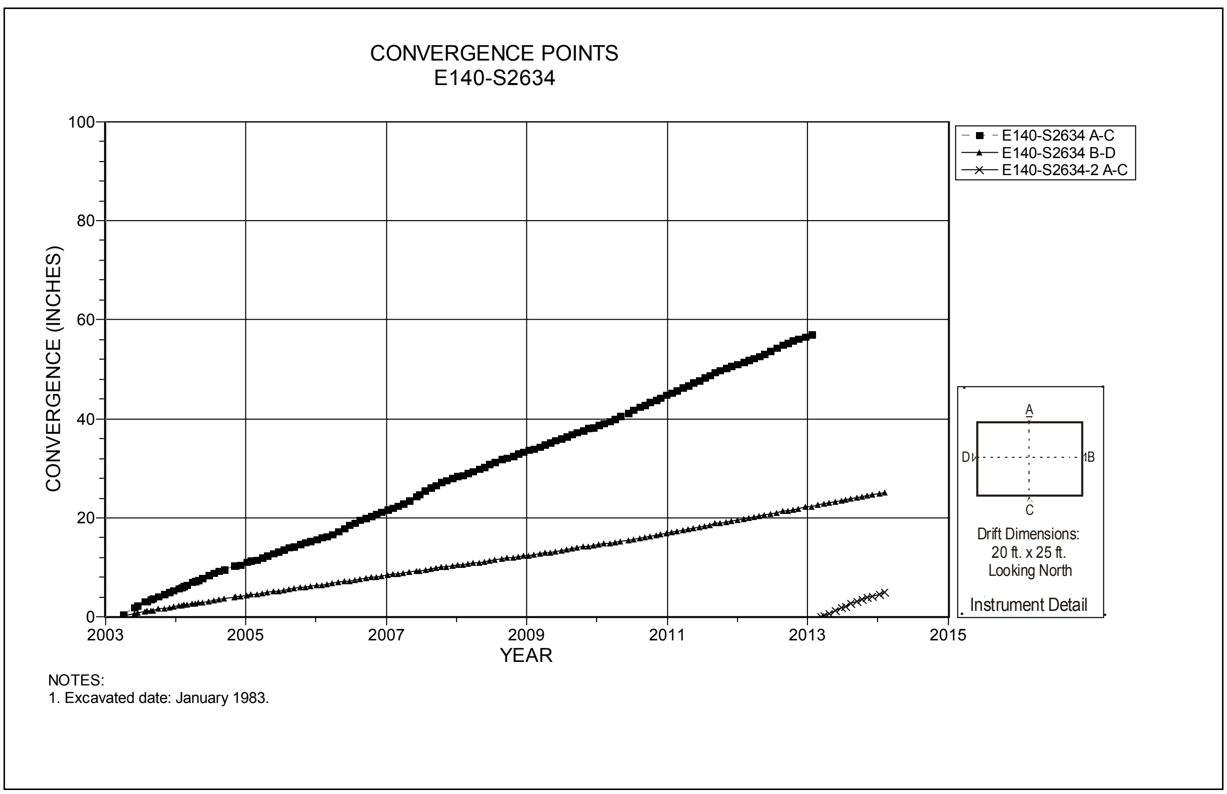

Figure 4-106 Convergence Point Array
E140 S2634 – All Chords

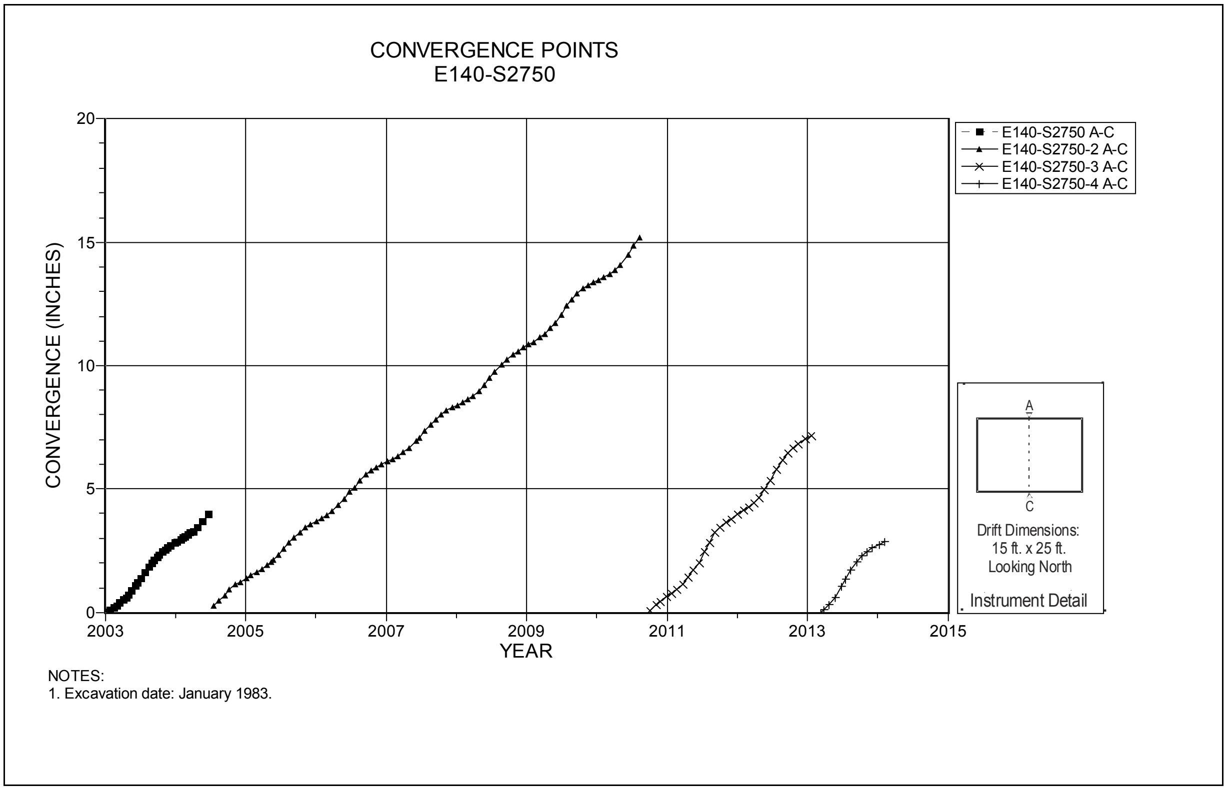

Figure 4-107 Convergence Point Array
E140 S2750 – Roof to Floor

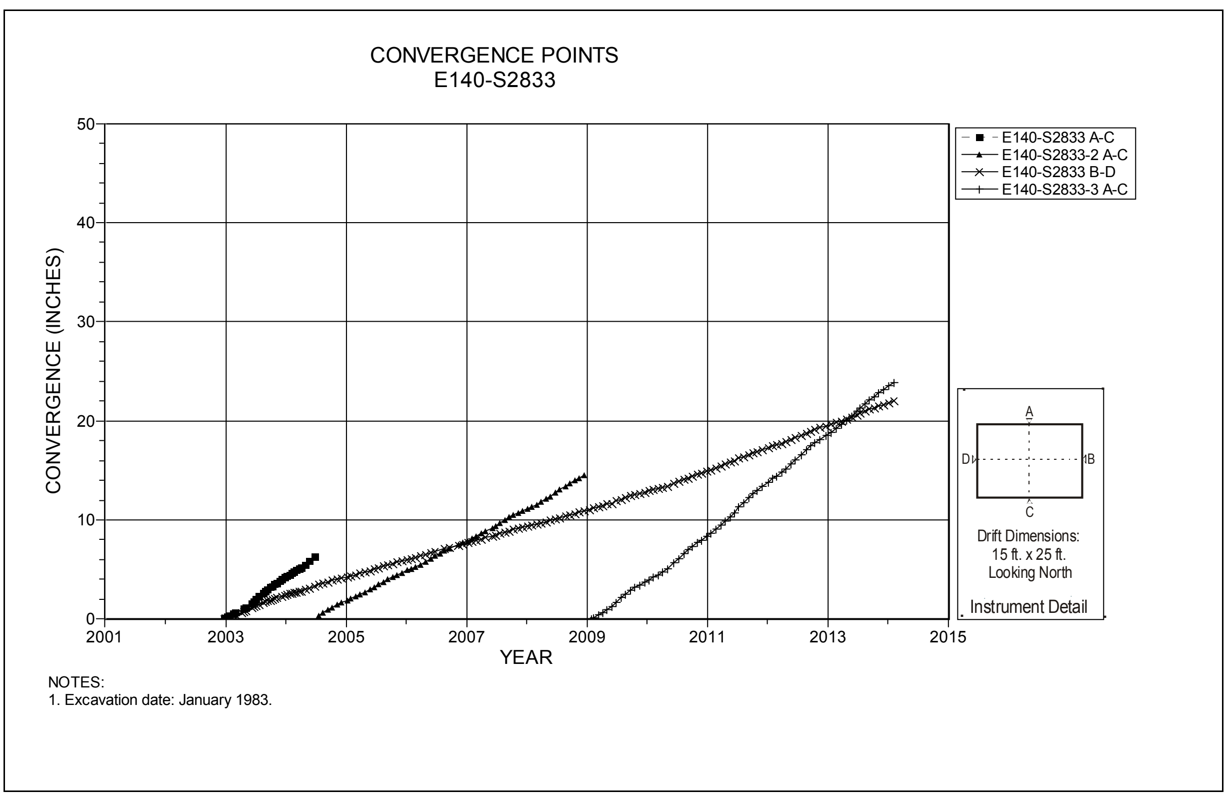

Figure 4-108 Convergence Point Array
E140 S2833 – All Chords

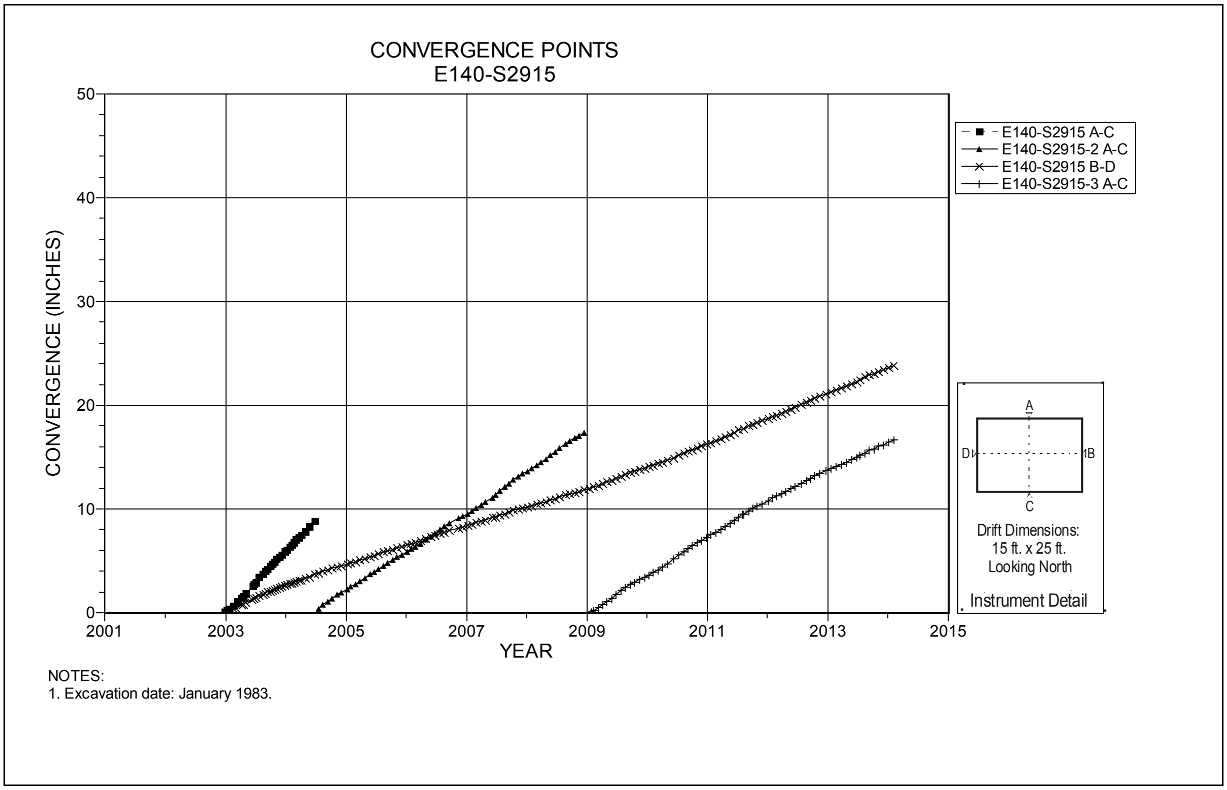

Figure 4-109 Convergence Point Array
E140 S2915 – All Chords

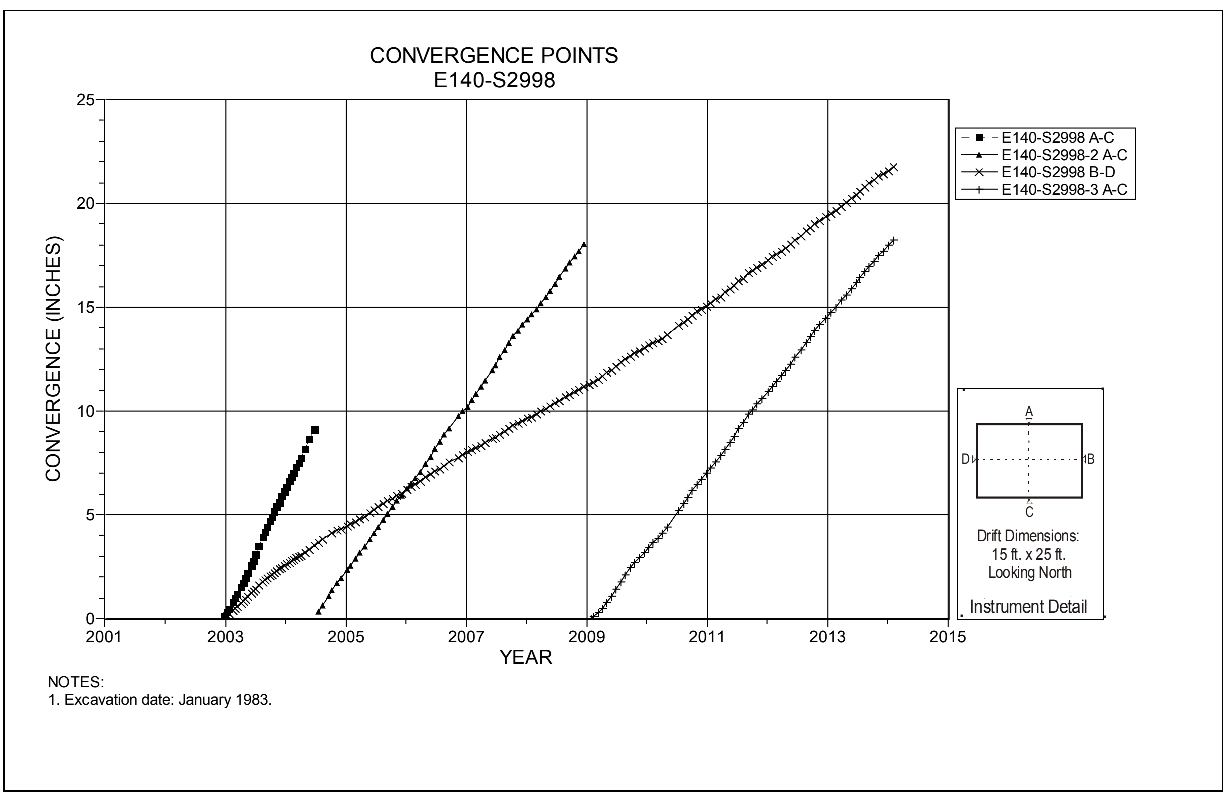

Figure 4-110 Convergence Point Array
E140 S2998 – All Chords

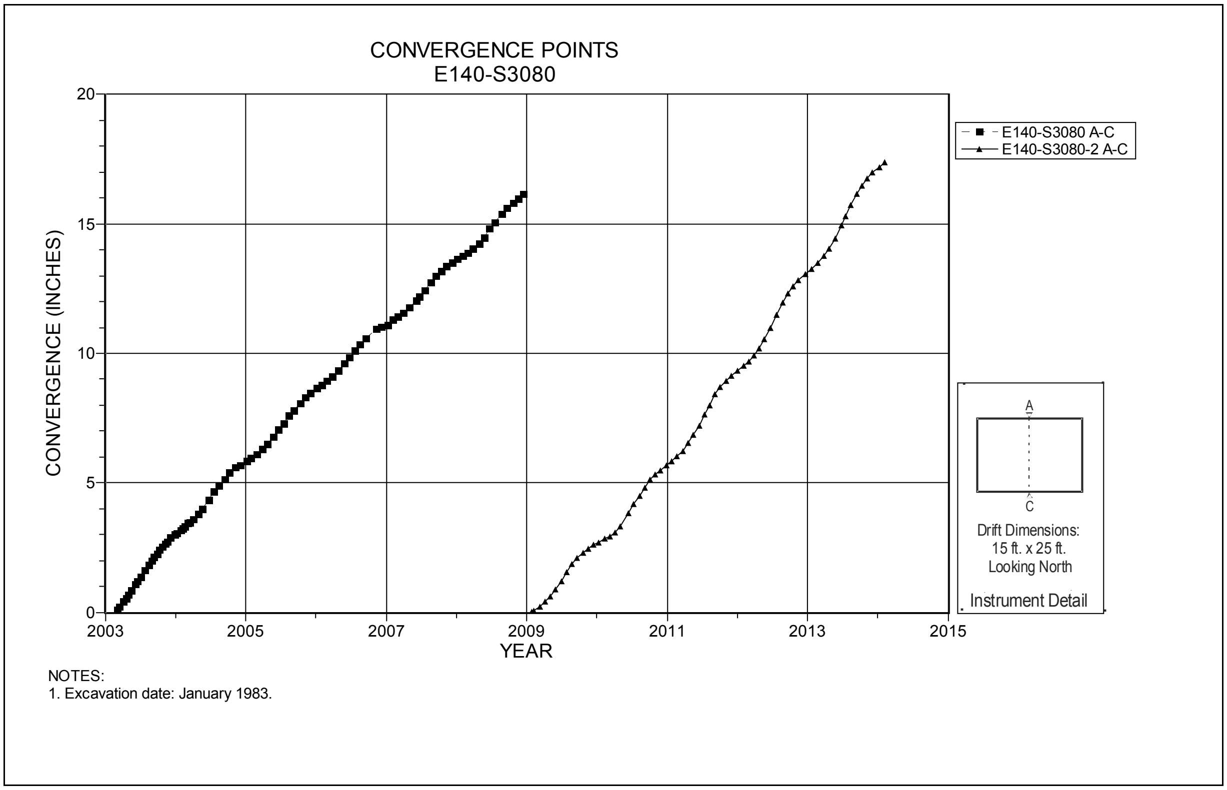

Figure 4-111 Convergence Point Array
E140 S3080 – Roof to Floor

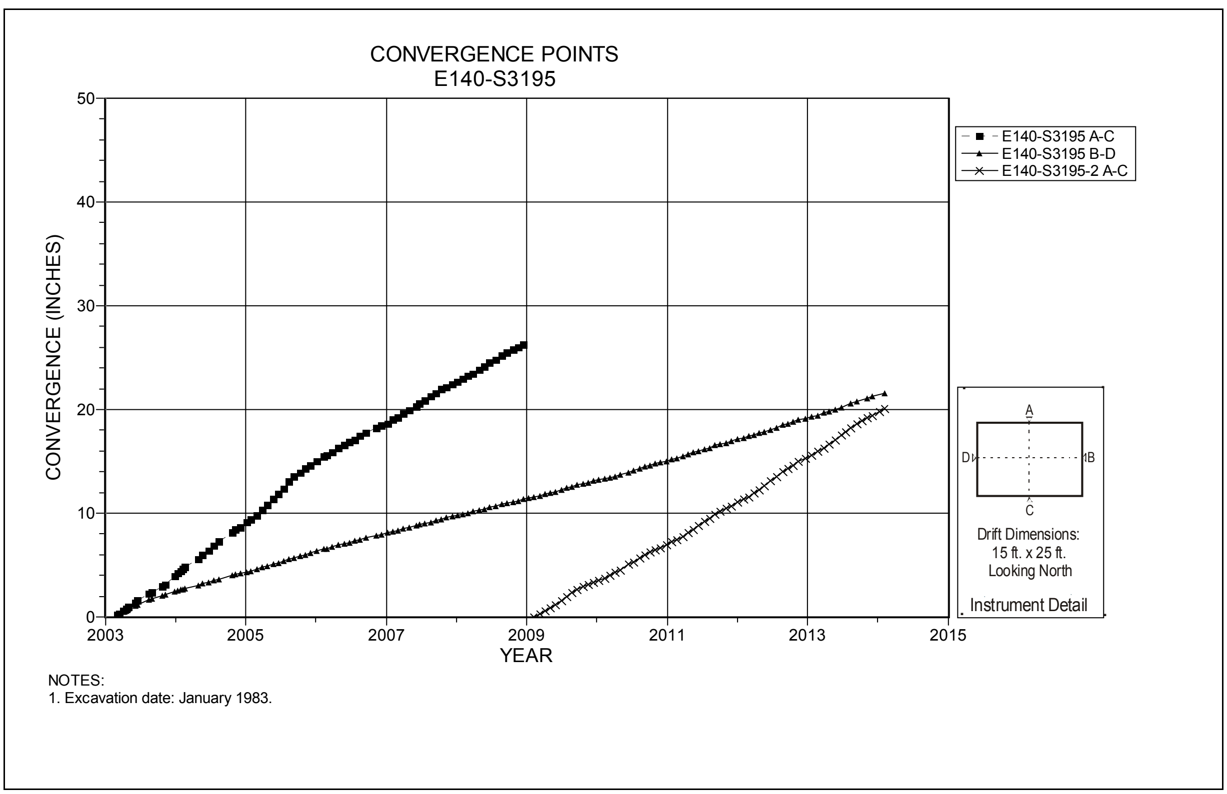

Figure 4-112 Convergence Point Array
E140 S3195 – All Chords

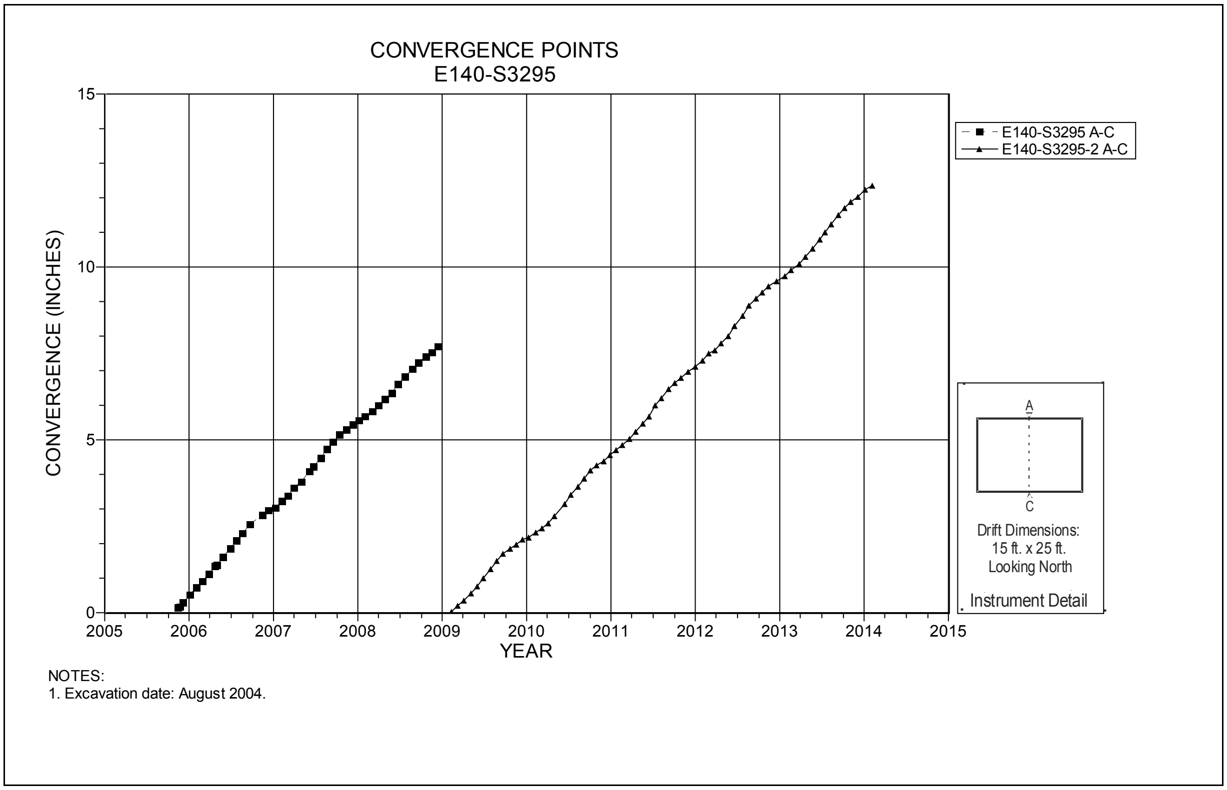

Figure 4-113 Convergence Point Array
E140 S3295 – Roof to Floor

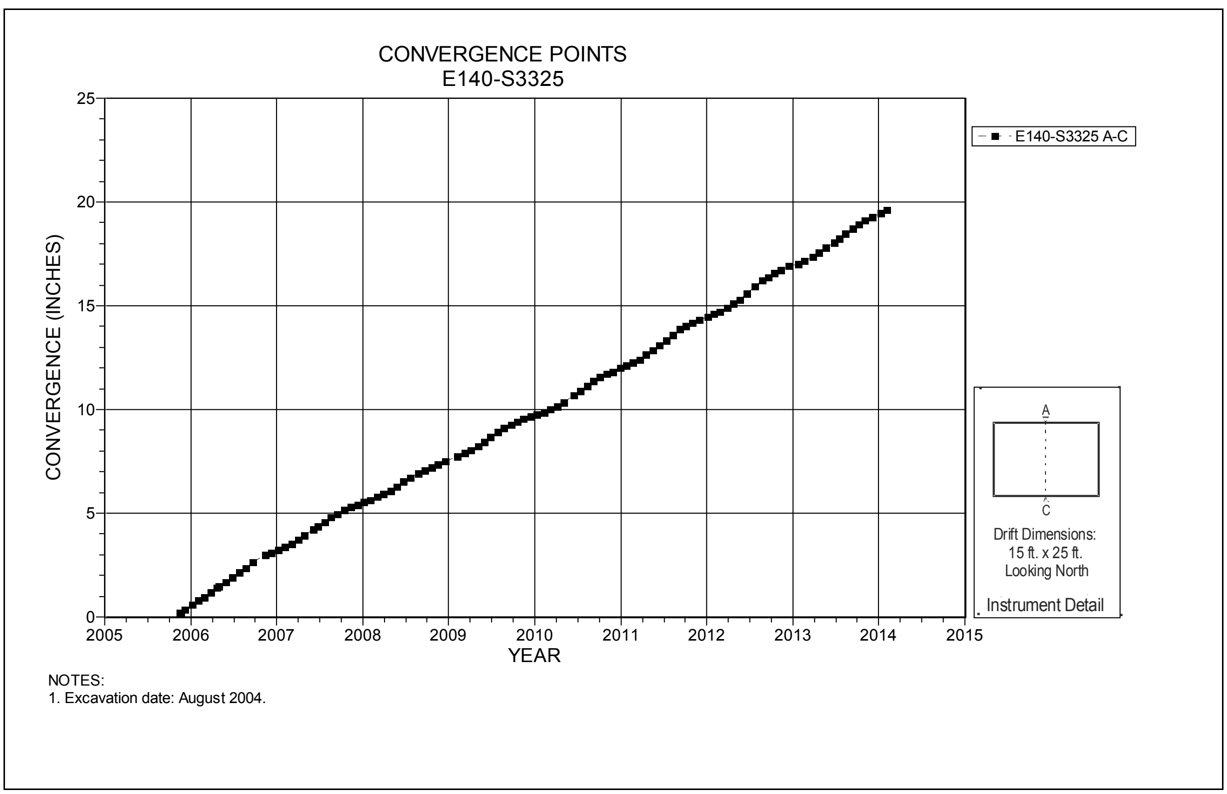

Figure 4-114 Convergence Point Array
E140 S3325 – Roof to Floor

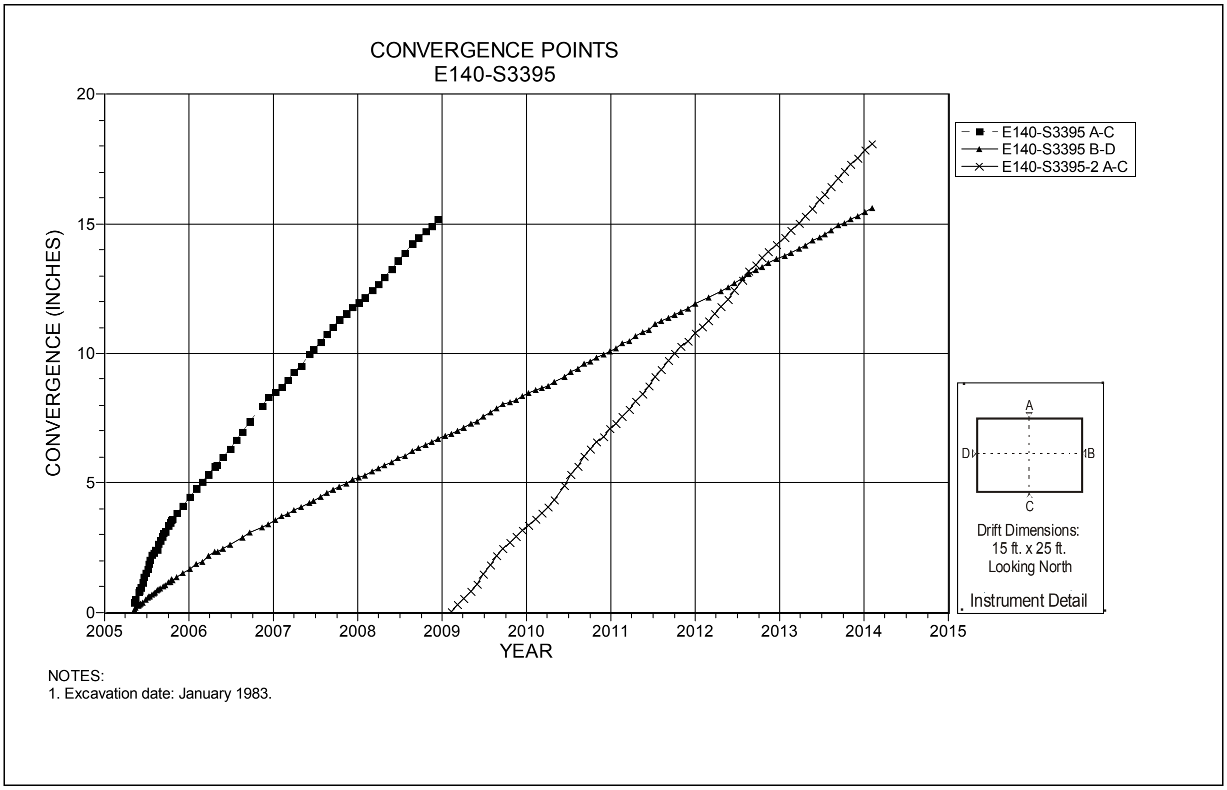

Figure 4-115 Convergence Point Array
E140 S3395 – All Chords

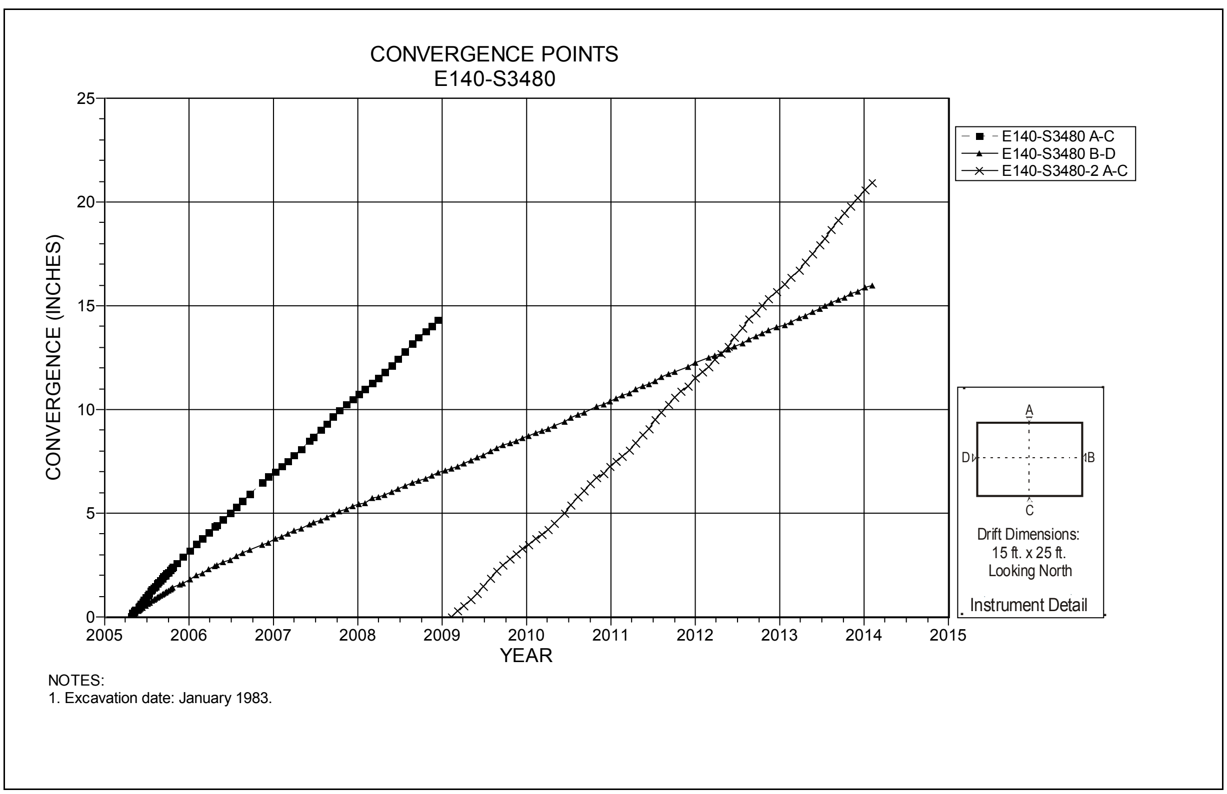

Figure 4-116 Convergence Point Array
E140 S3480 – All Chords

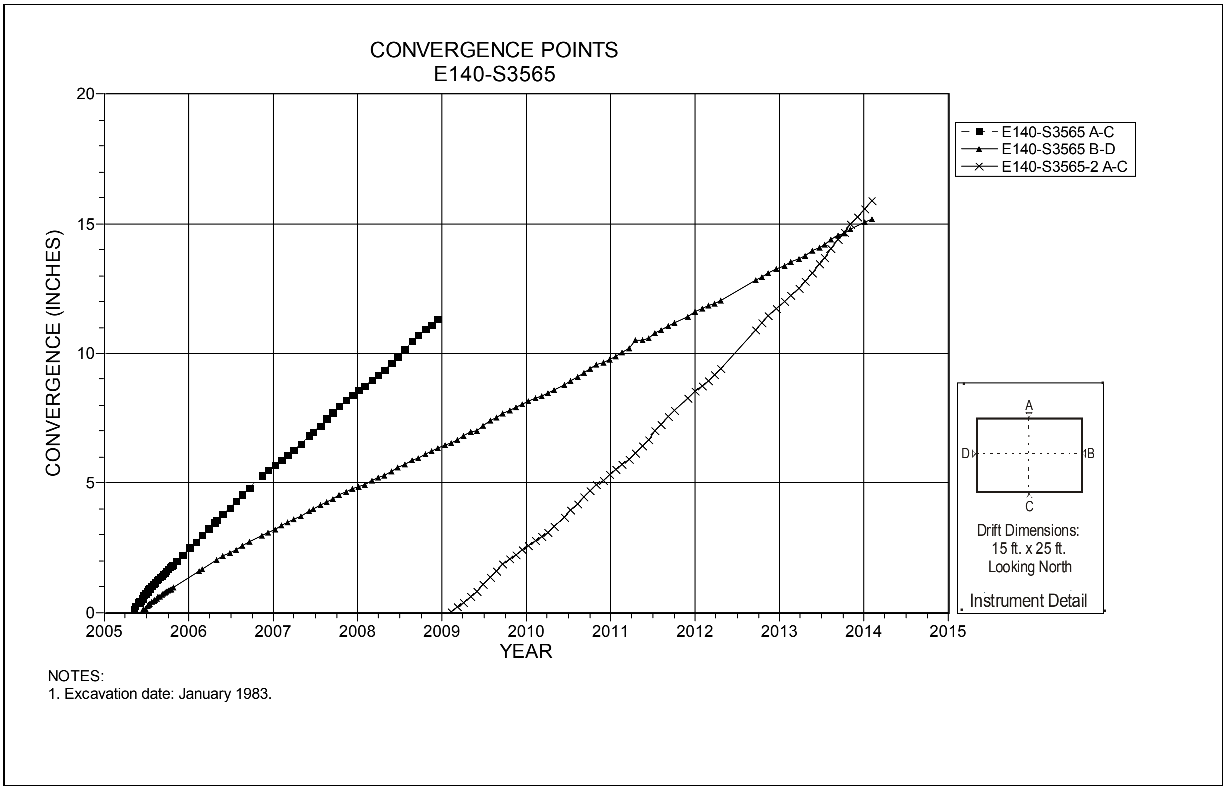

Figure 4-117 Convergence Point Array
E140 S3565 – All Chords

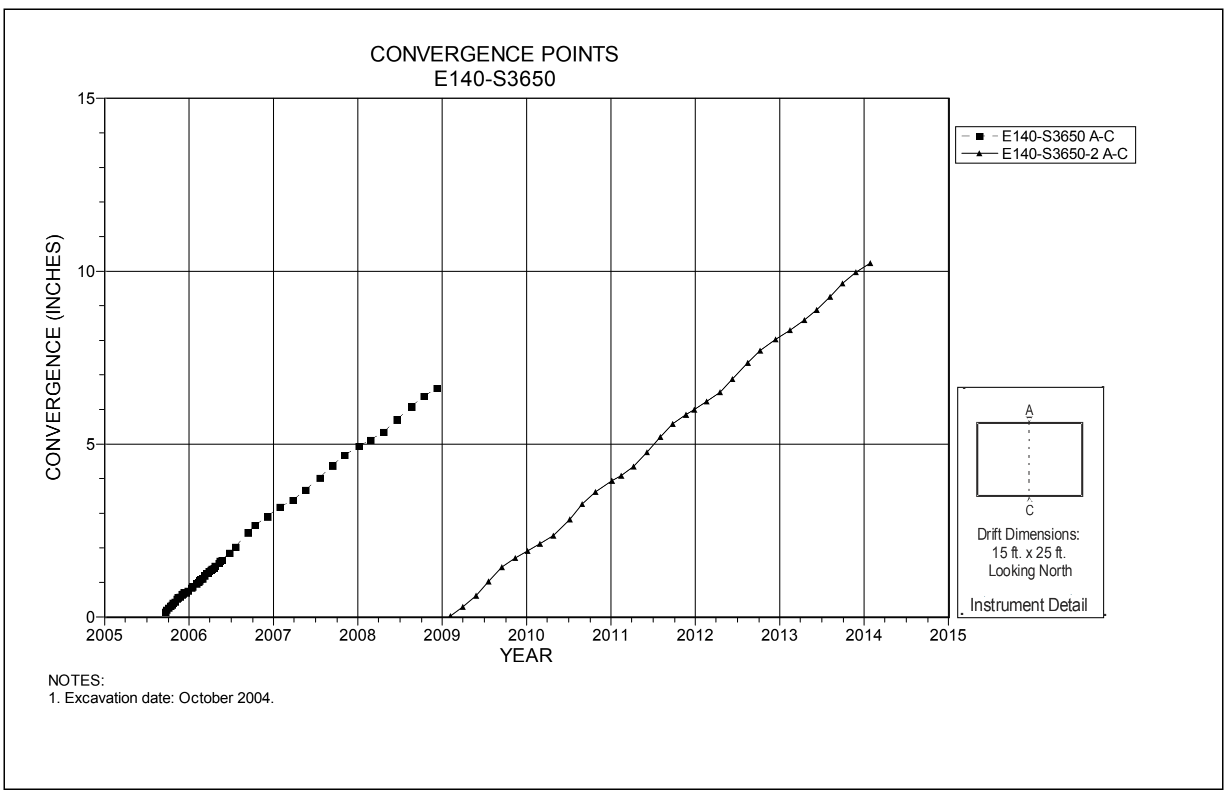

Figure 4-118 Convergence Point Array
E140 S3650 – Roof to Floor

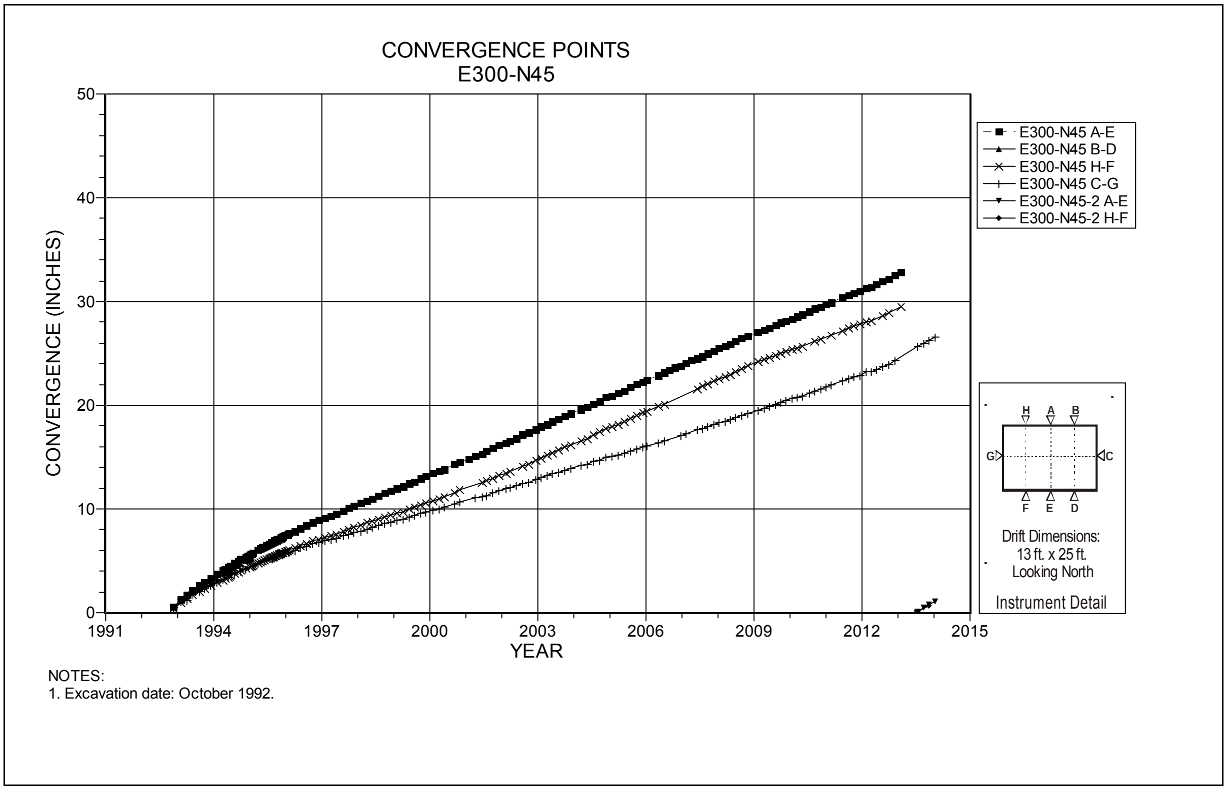

Figure 4-119 Convergence Point Array
E300 N45 – All Chords

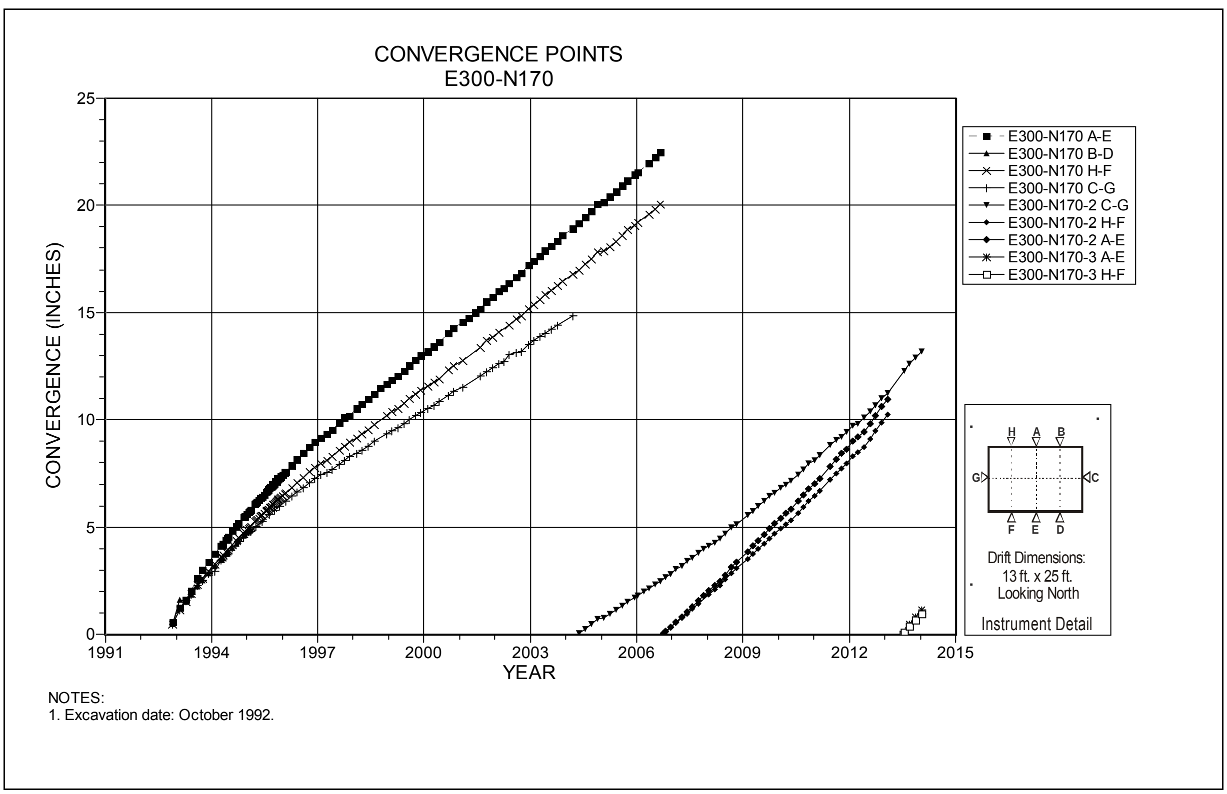

Figure 4-120 Convergence Point Array
E300 N170 – All Chords

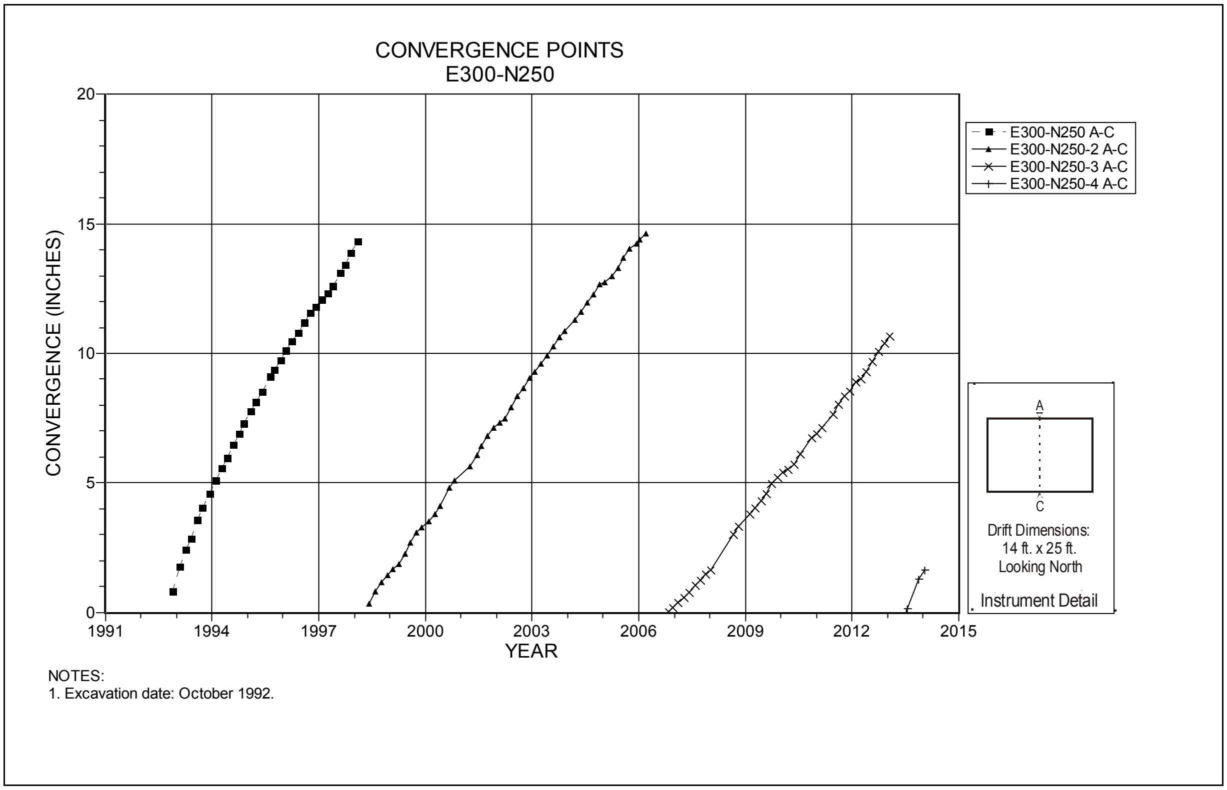

Figure 4-121 Convergence Point Array
E300 N250 – Roof to Floor

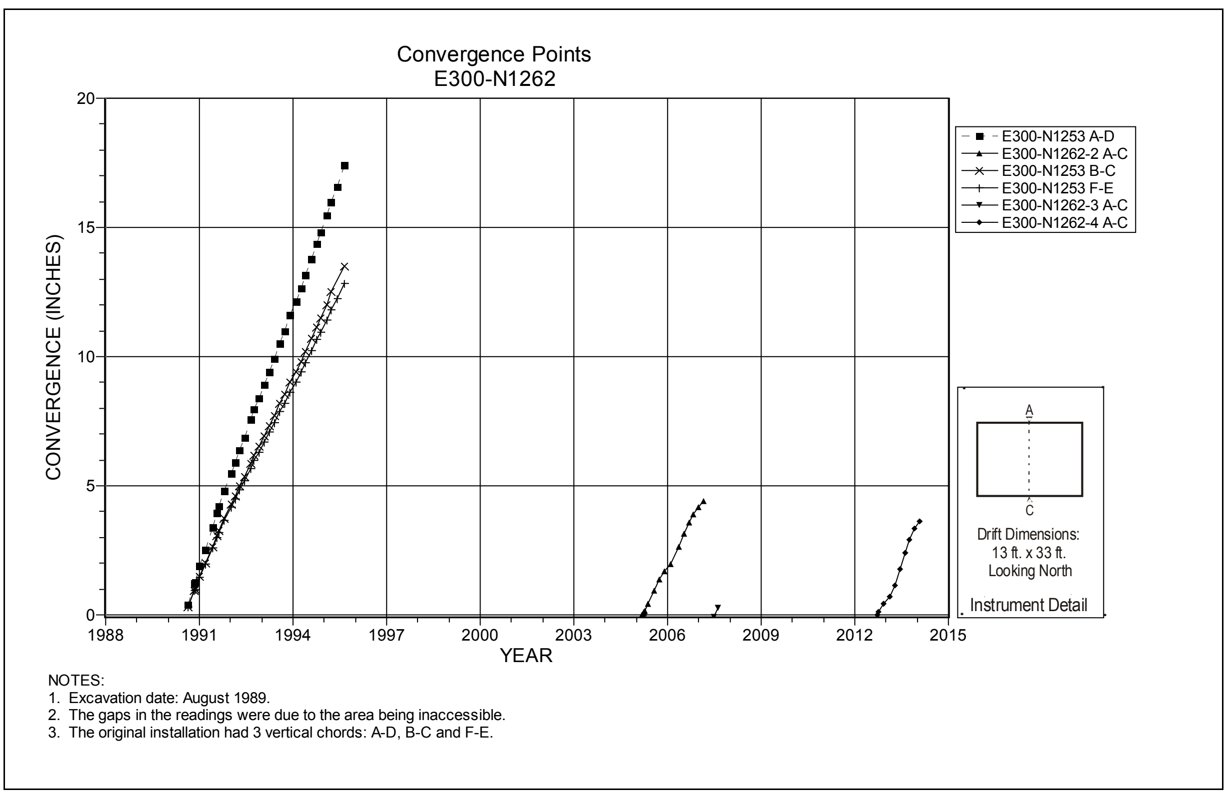

Figure 4-122 Convergence Point Array
E300 N1253/N1262 – Roof to Floor

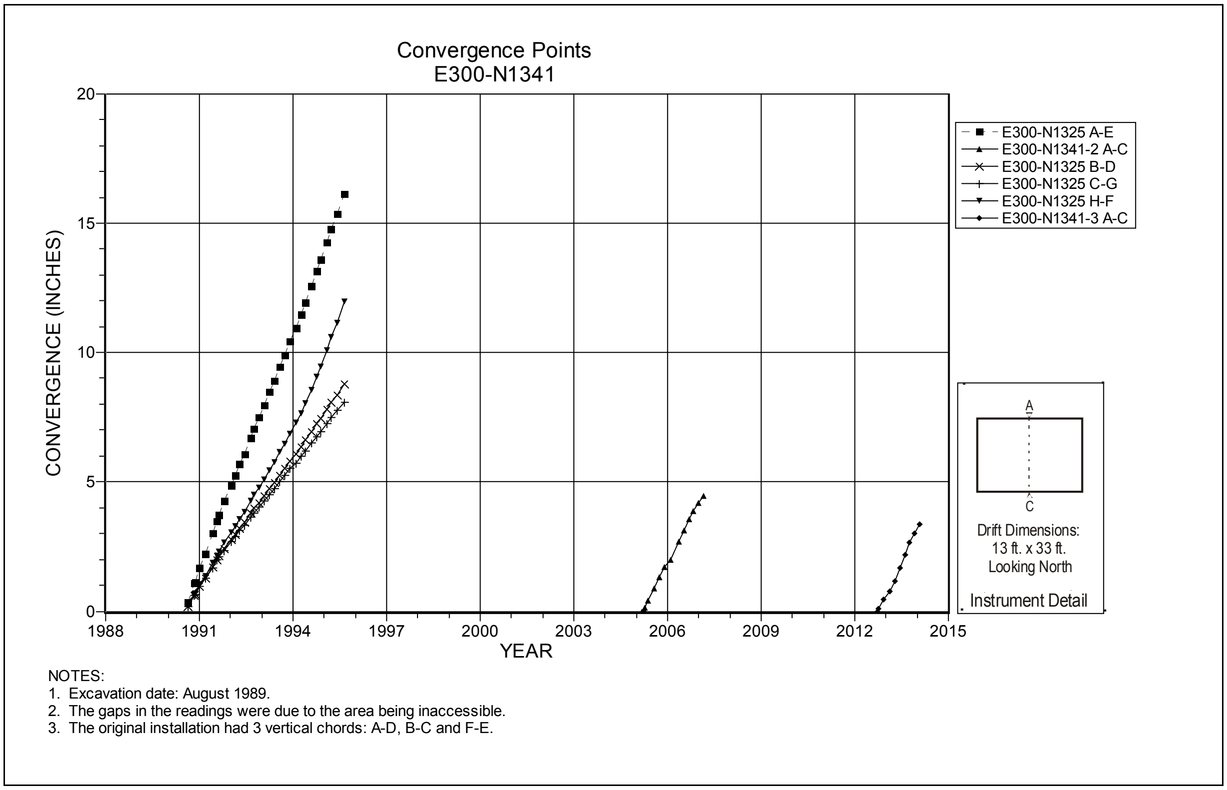

Figure 4-123 Convergence Point Array
E300 N1325/N1341 – All Chords

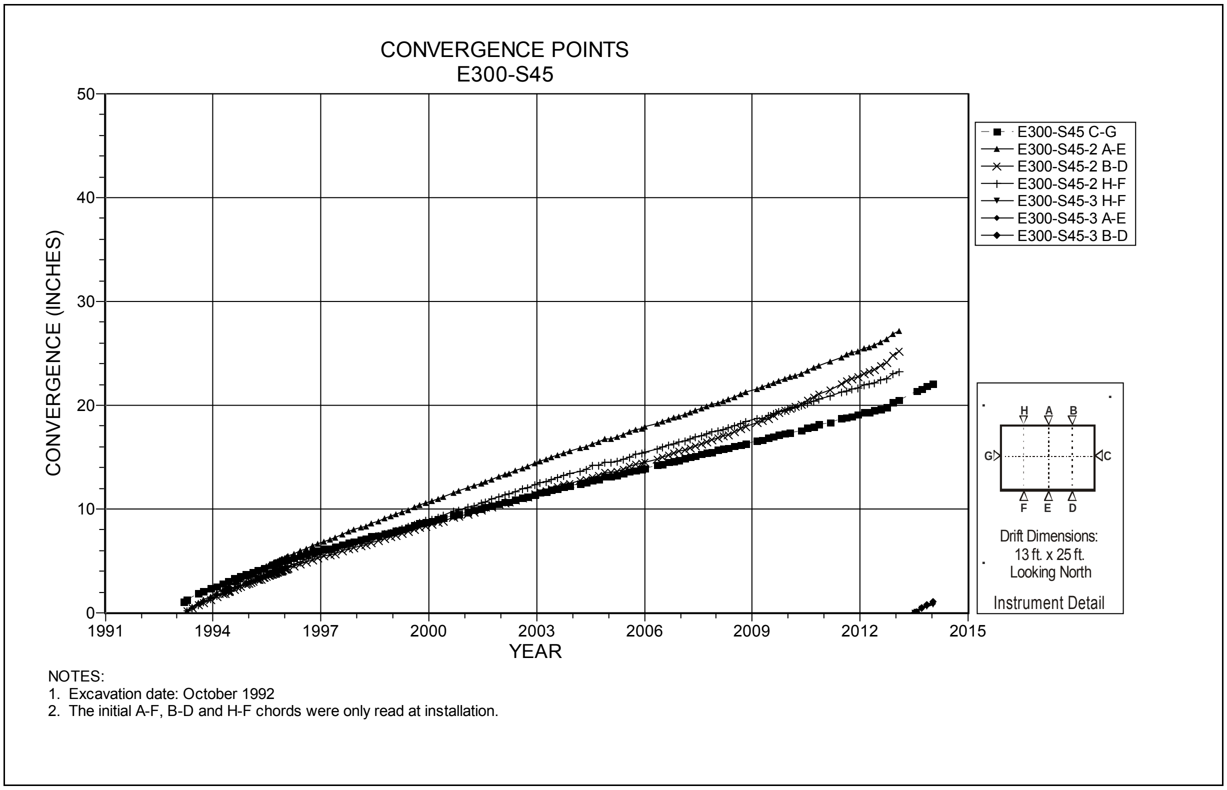

Figure 4-124 Convergence Point Array
E300 S45 – All Chords

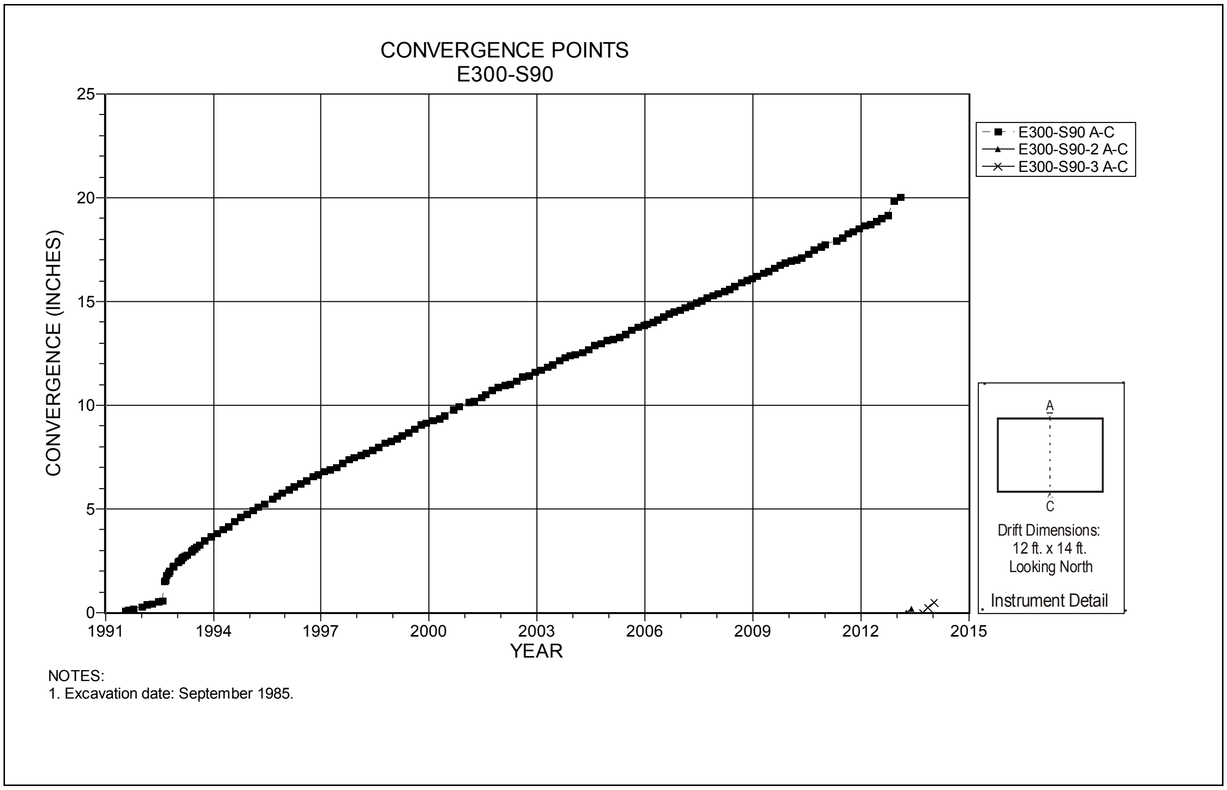

Figure 4-125 Convergence Point Array
E300 S90 – Roof to Floor

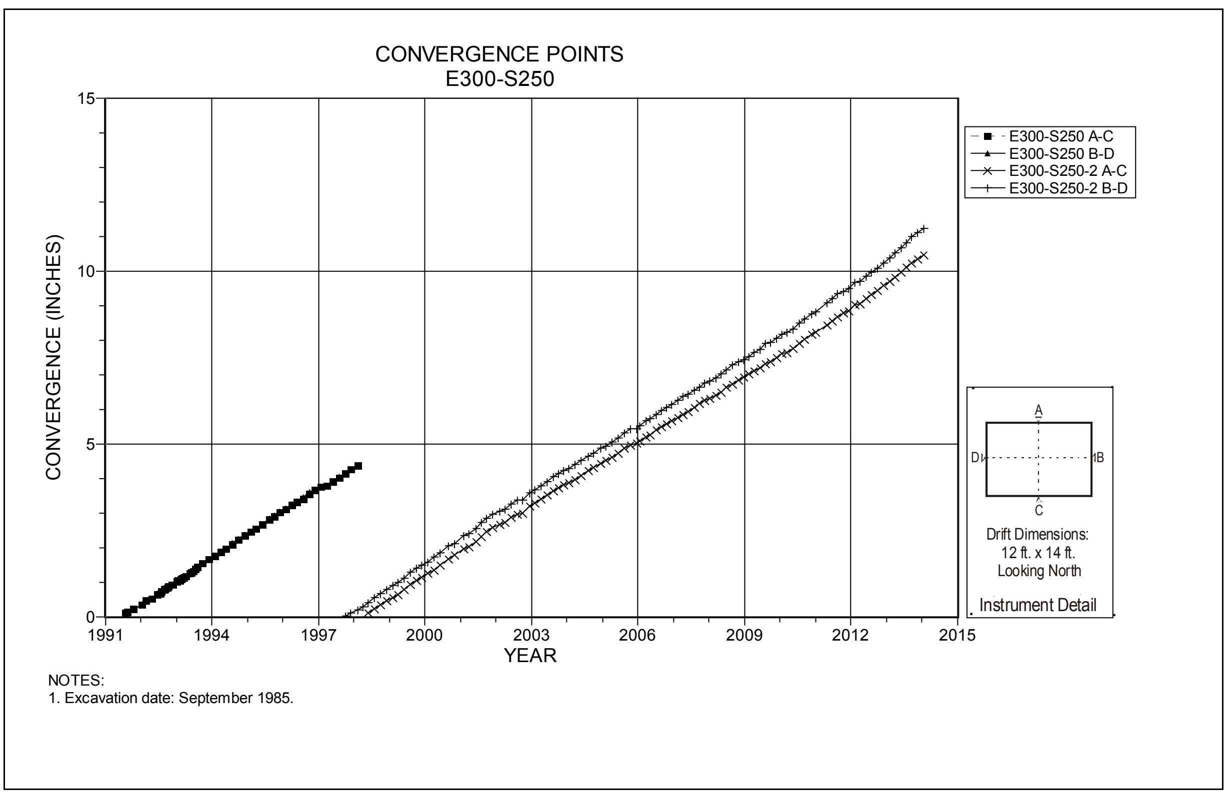

Figure 4-126 Convergence Point Array
E300 S250 – All Chords

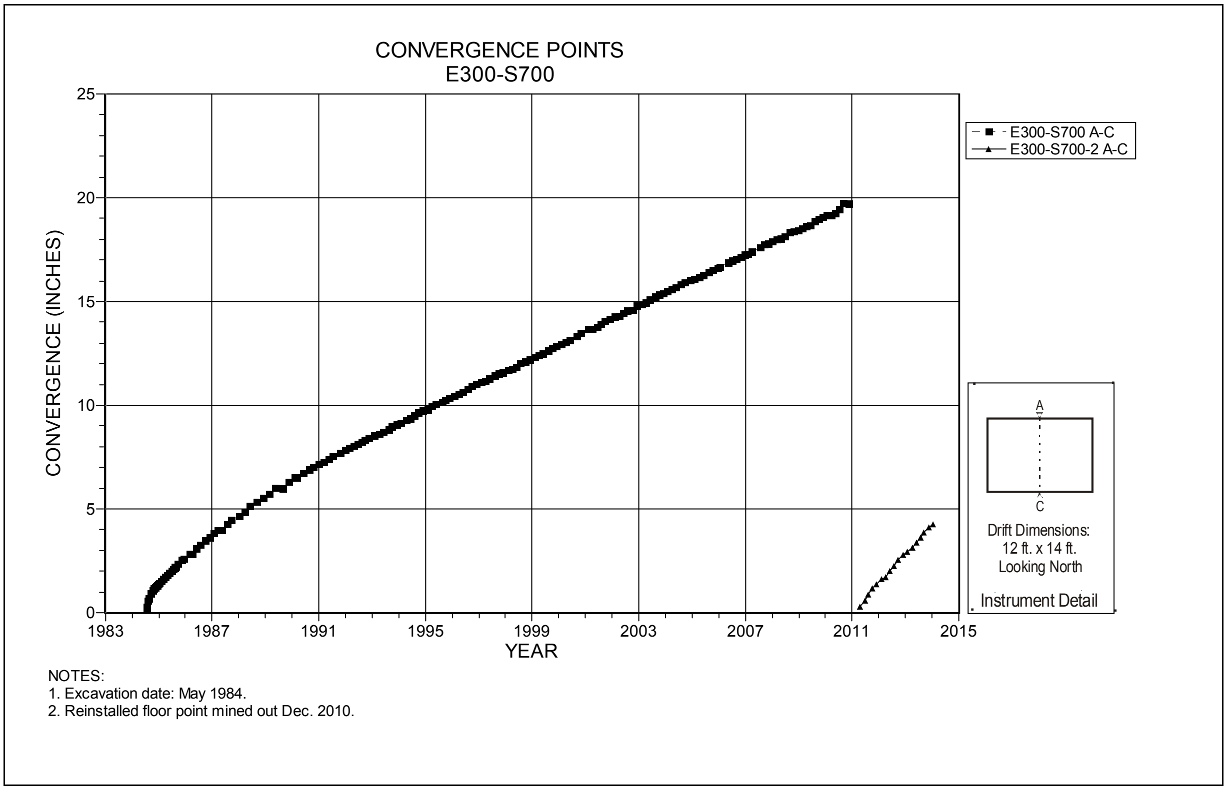

Figure 4-127 Convergence Point Array
E300 S700 – Roof to Floor

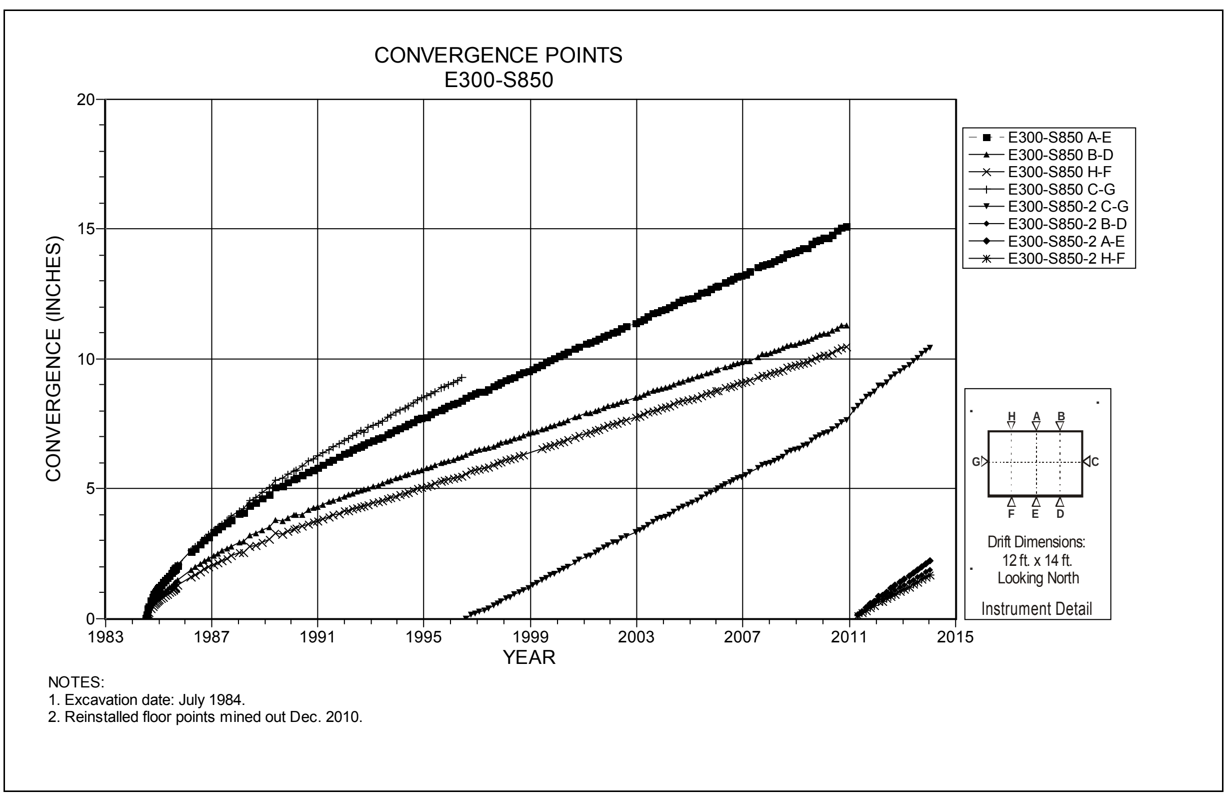

Figure 4-128 Convergence Point Array
E300 S850 – All Chords

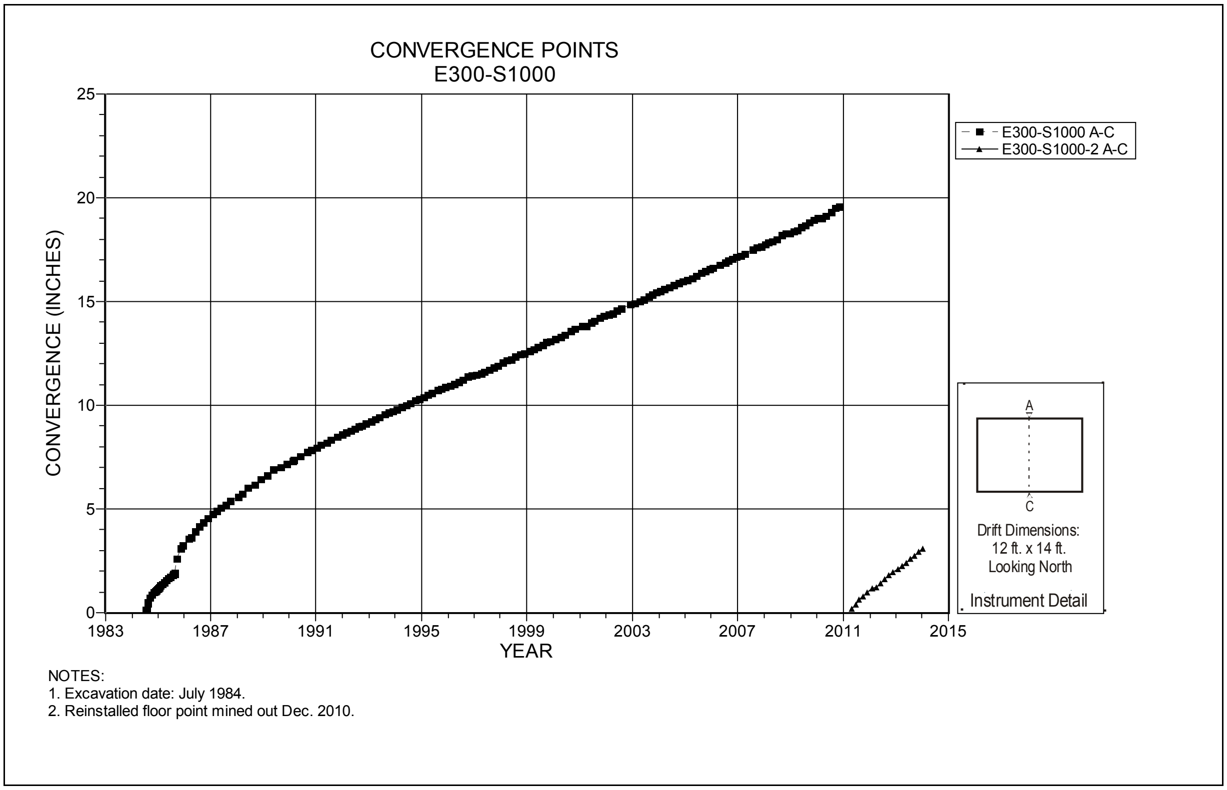

Figure 4-129 Convergence Point Array
E300 S1000 – Roof to Floor

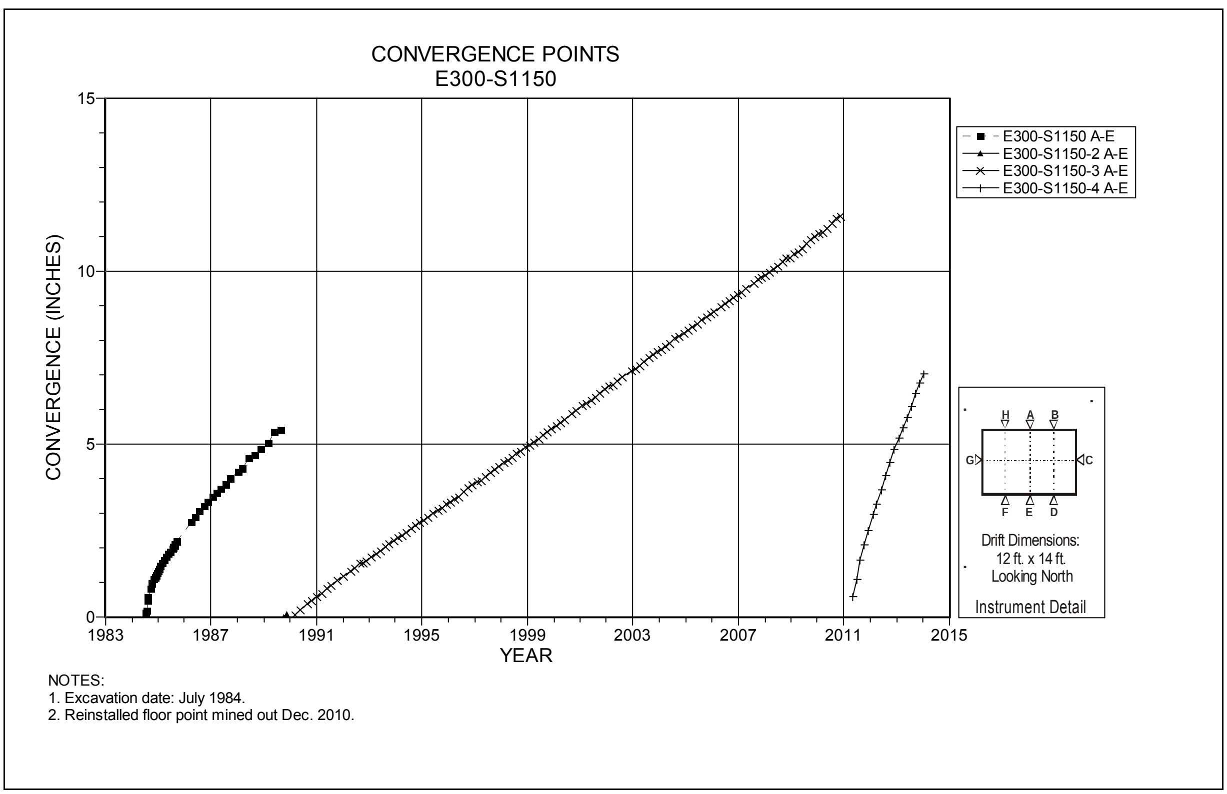

Figure 4-130 Convergence Point Array
E300 S1150 – Roof to Floor

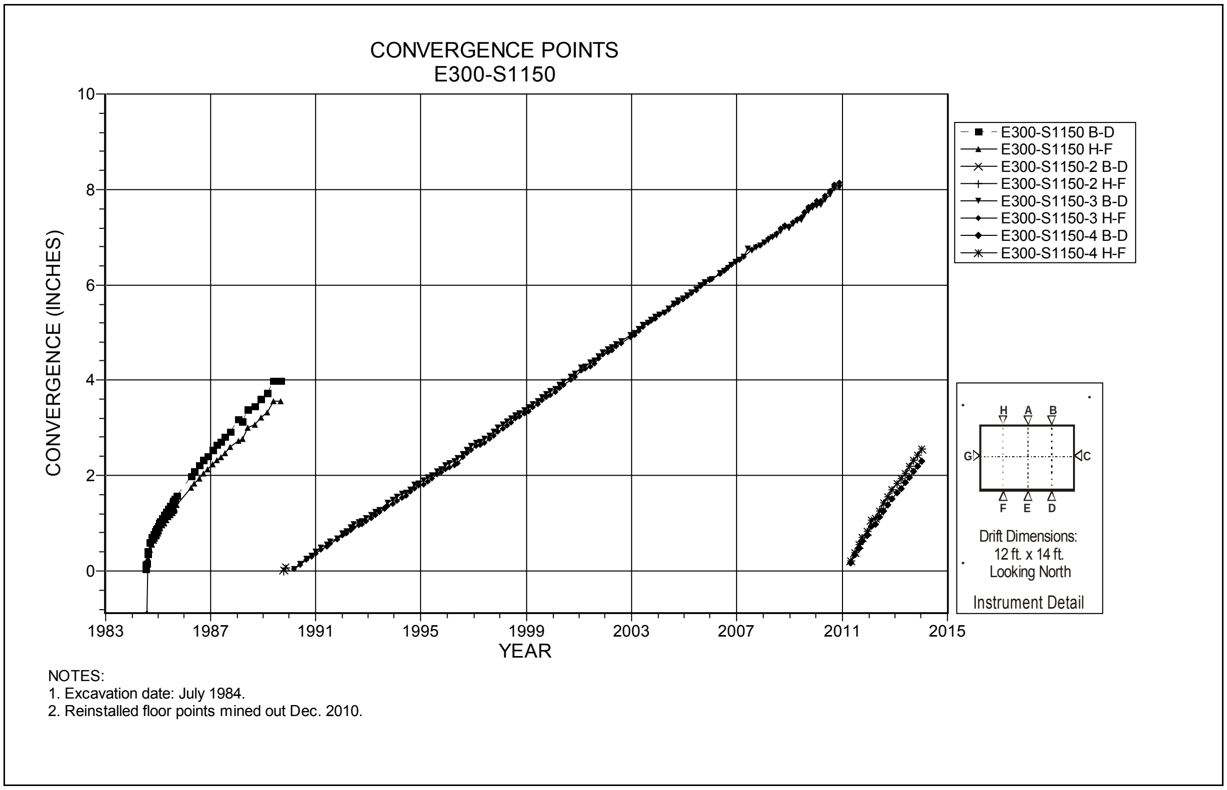

Figure 4-131 Convergence Point Array
E300 S1150 – Roof to Floor – Quarter Points

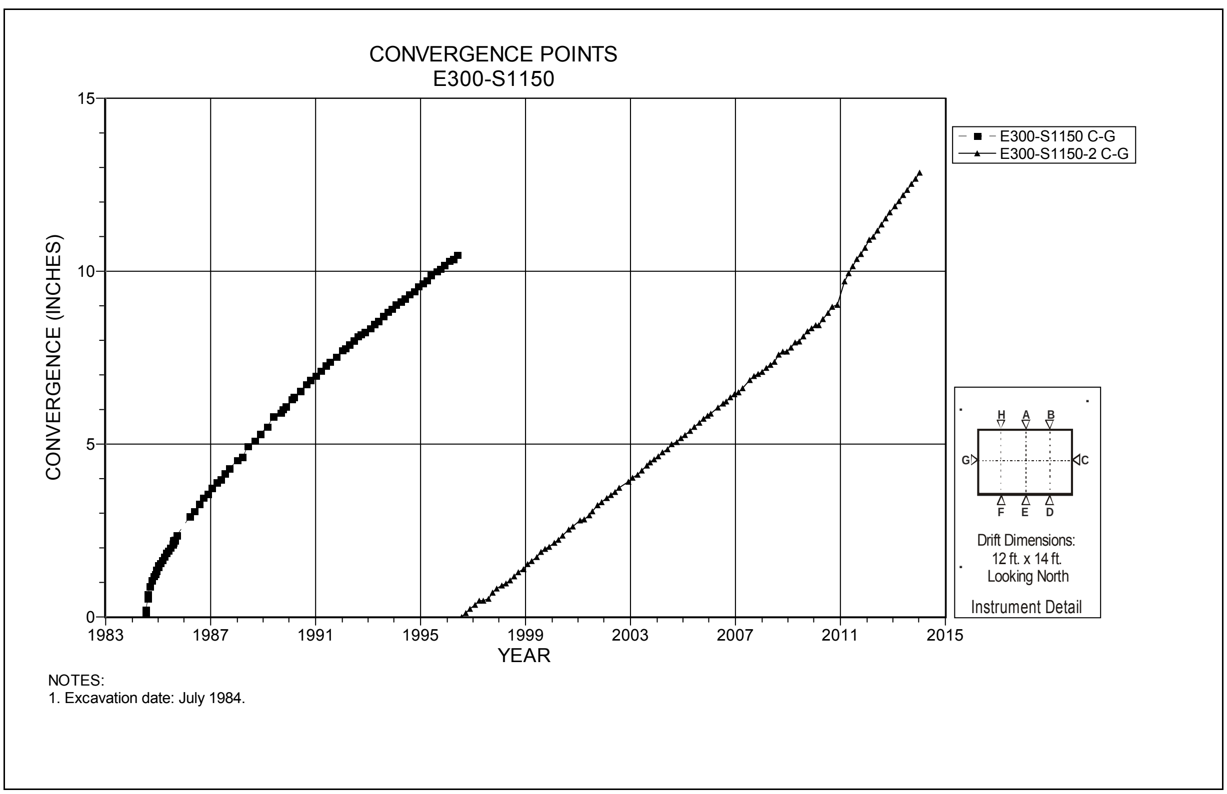

Figure 4-132 Convergence Point Array
E300 S1150 – Rib to Rib

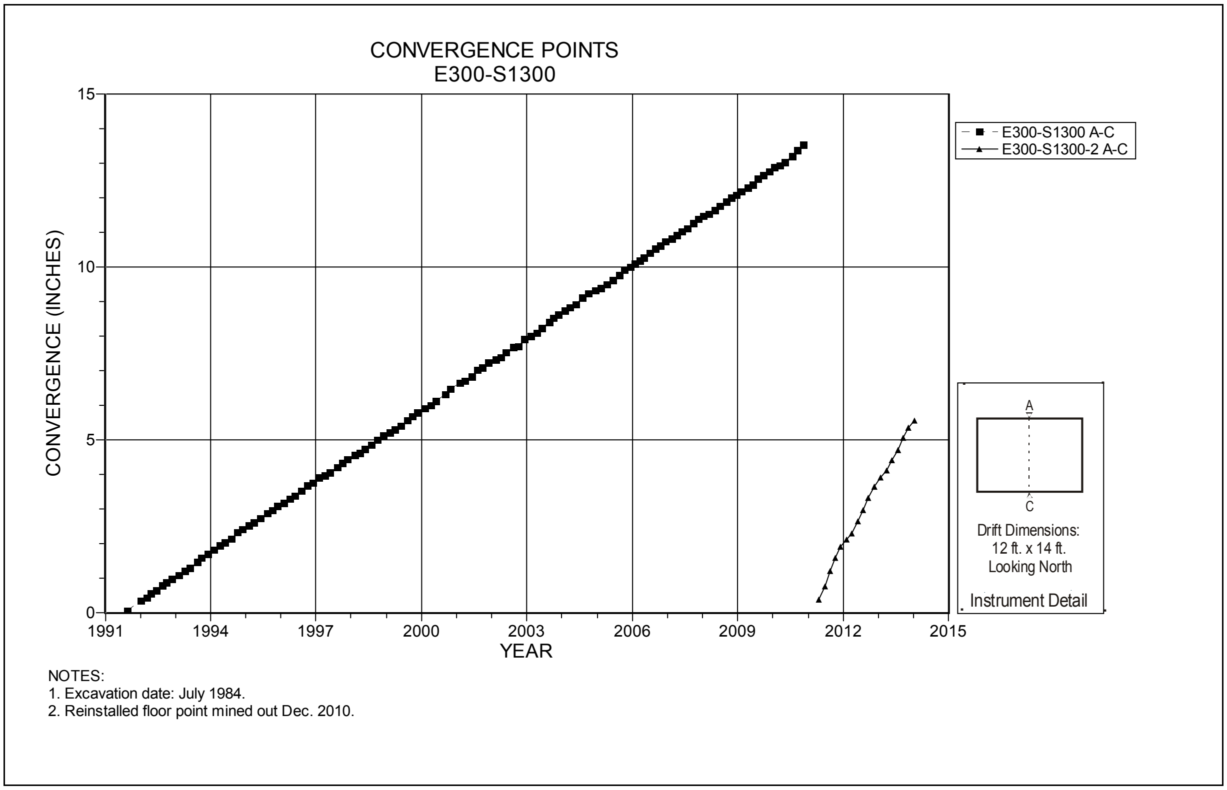

Figure 4-133 Convergence Point Array
E300 S1300 – Roof to Floor

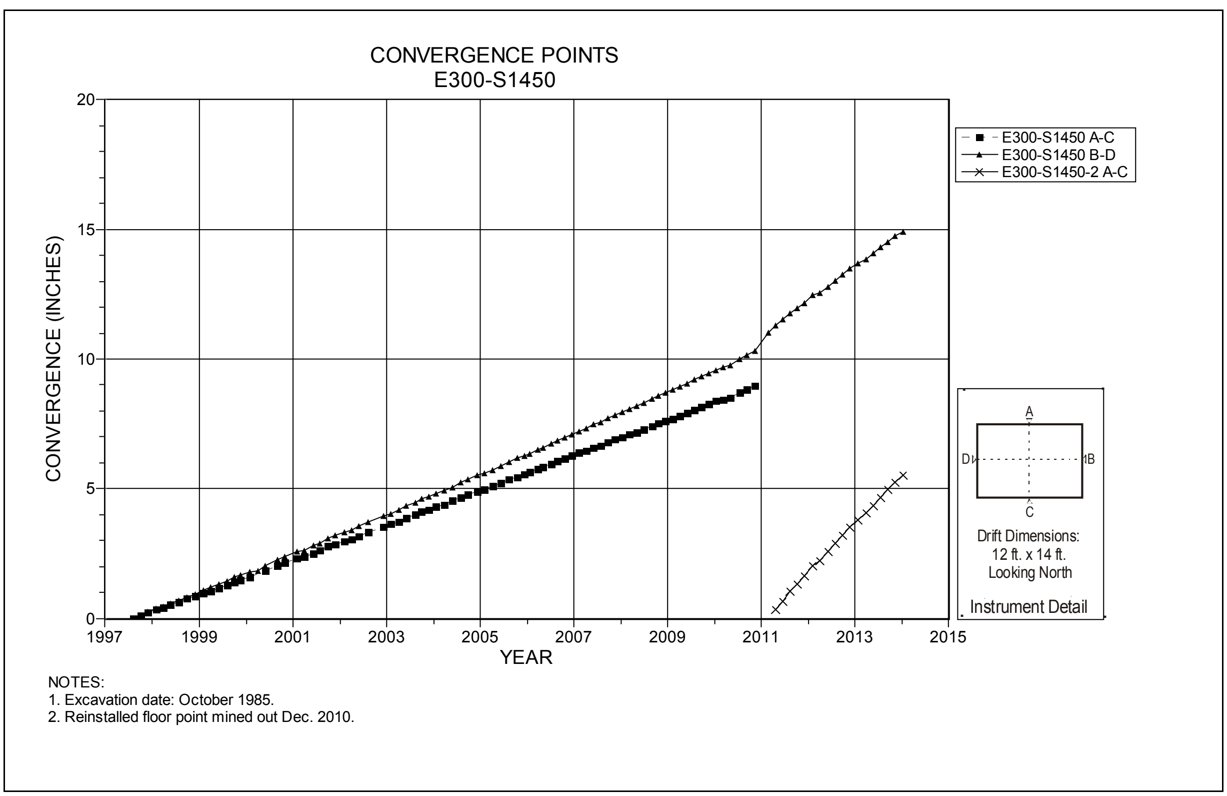

Figure 4-134 Convergence Point Array
E300 S1450 – All Chords

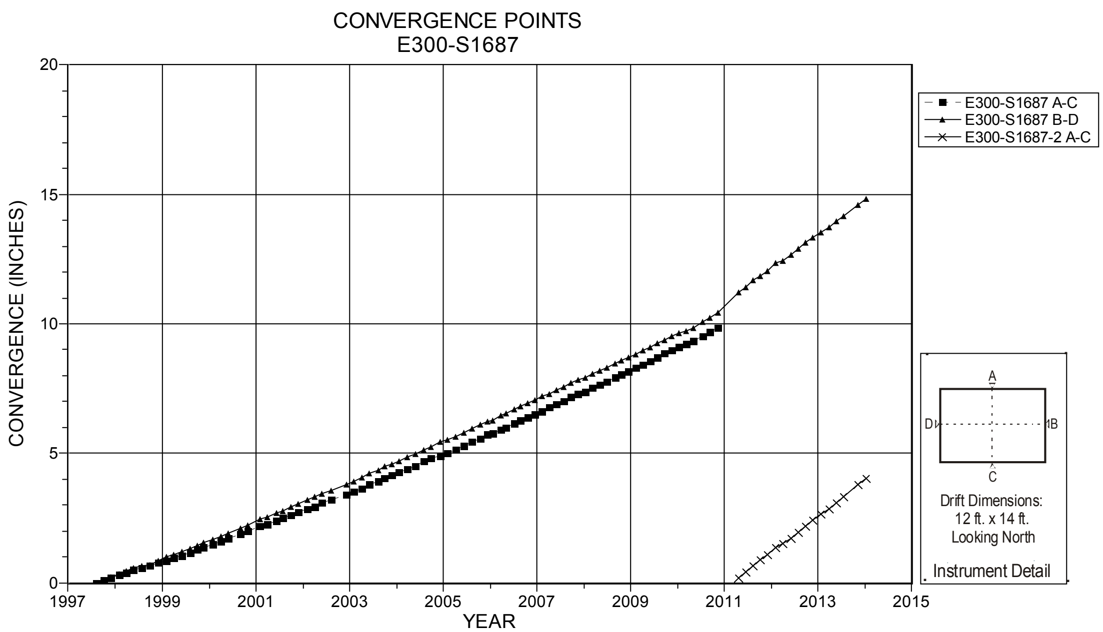

NOTES:
1. Excavation date: October 1985.

Figure 4-135 Convergence Point Array
E300 S1687 – All Chords

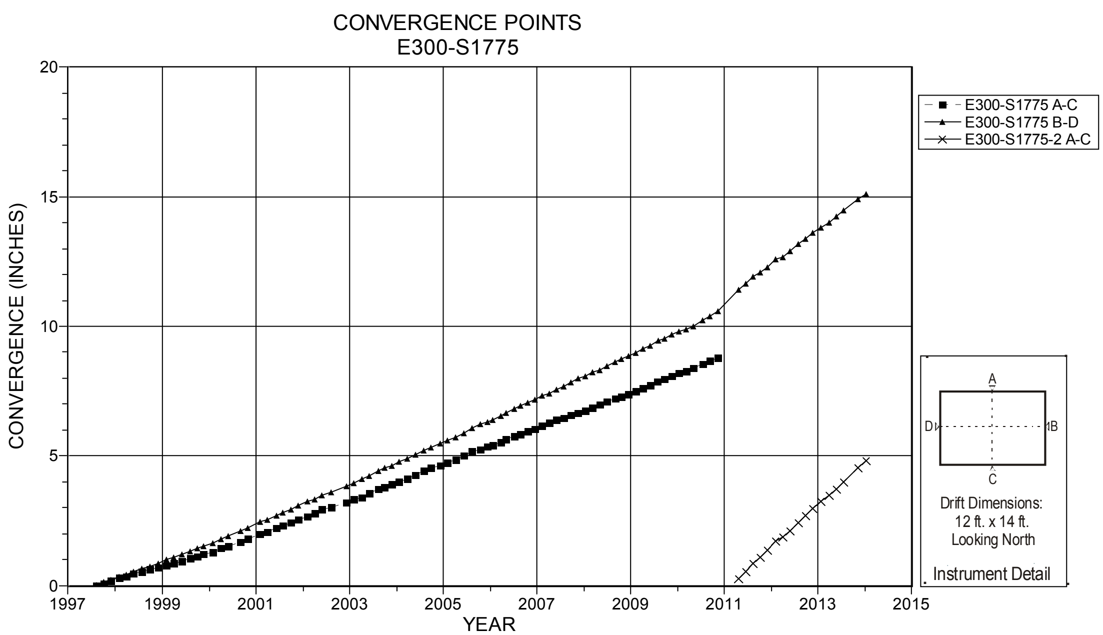

NOTES:
1. Excavation date: October 1985.

Figure 4-136 Convergence Point Array
E300 S1775 – All Chords

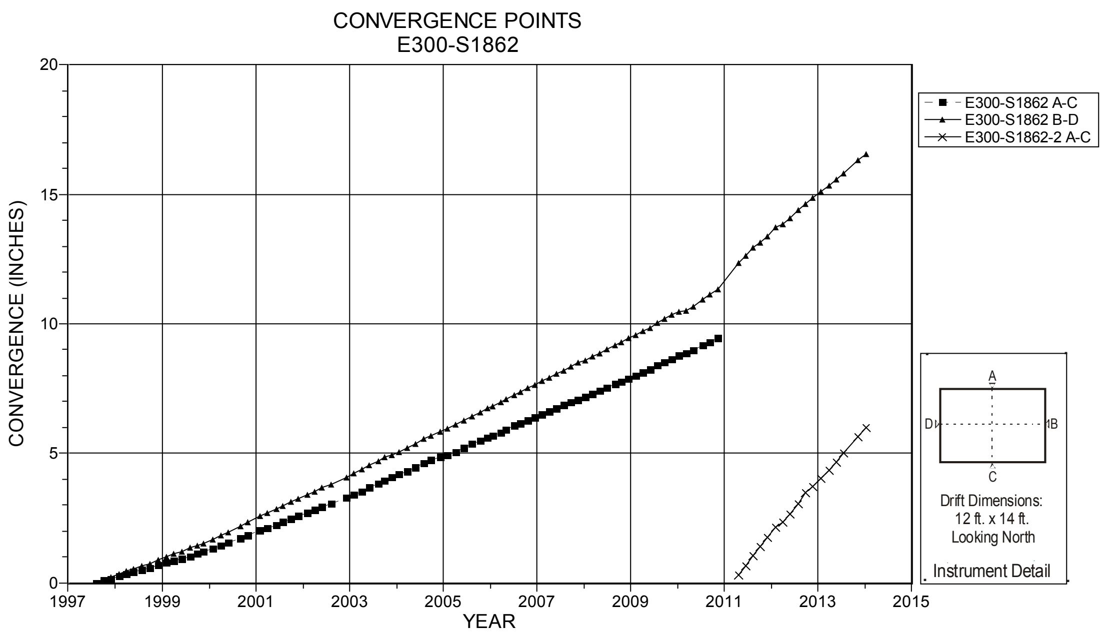

NOTES:
1. Excavation date: October 1985.

Figure 4-137 Convergence Point Array
E300 S1862 – All Chords

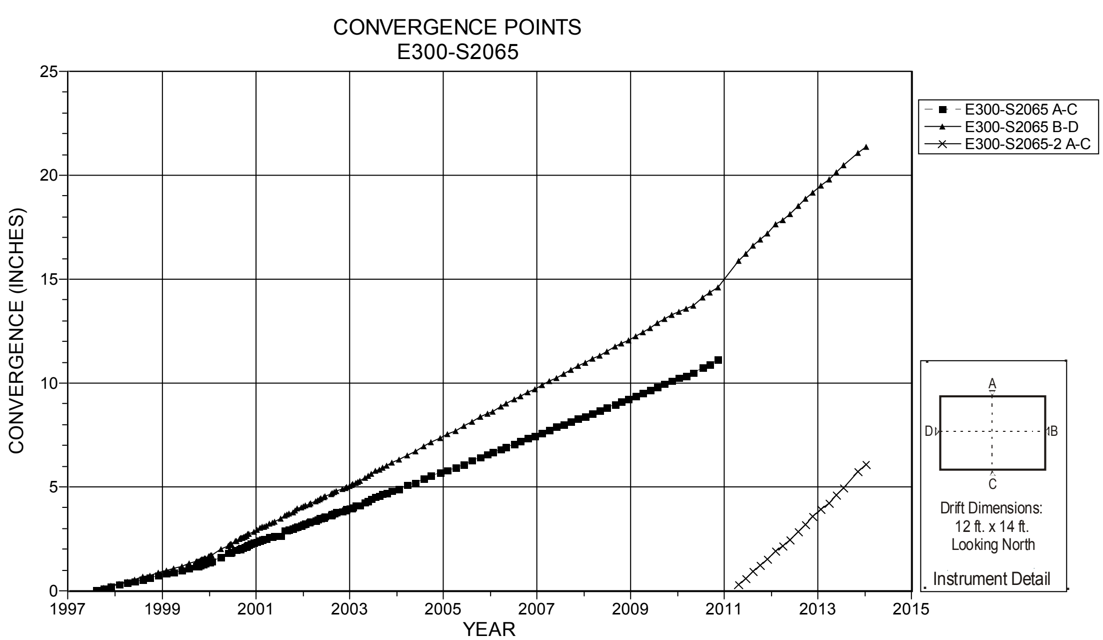

NOTES:
1. Excavation date: April 1986.

Figure 4-138 Convergence Point Array
E300 S2065 – All Chords

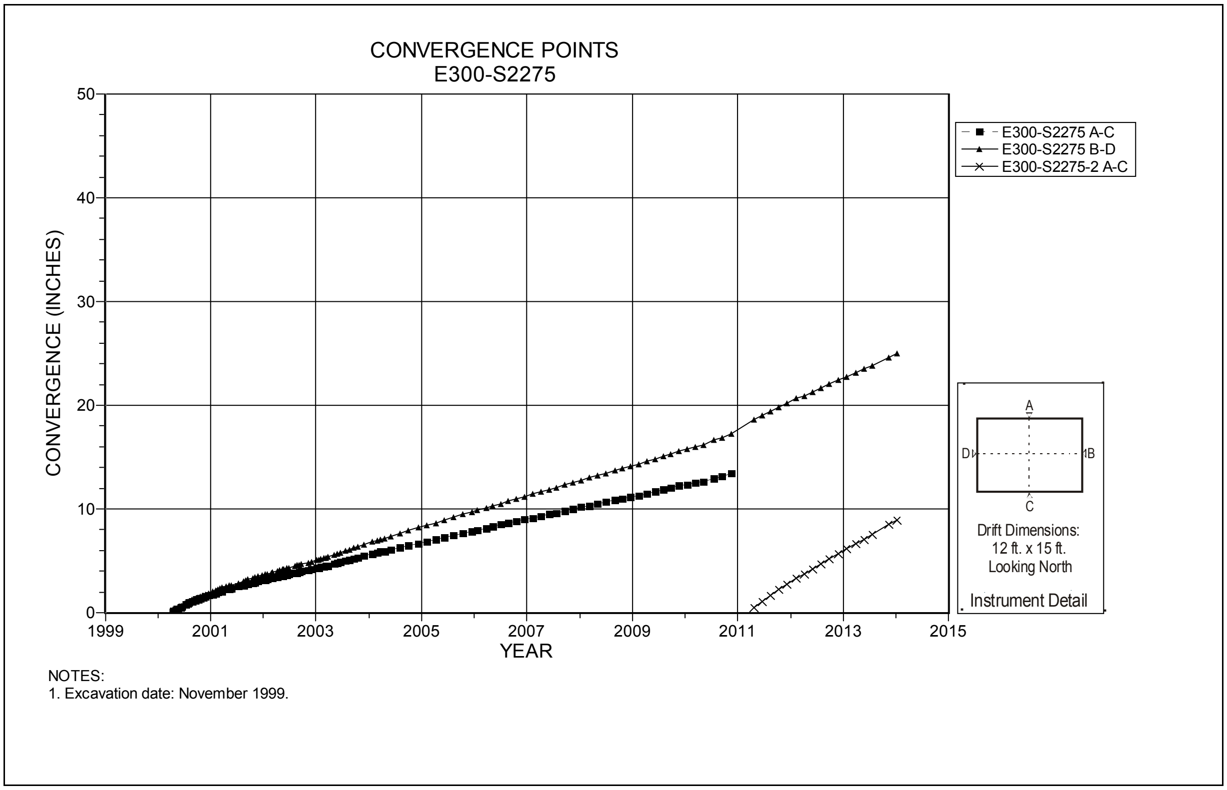

Figure 4-139 Convergence Point Array
E300 S2275 – All Chords

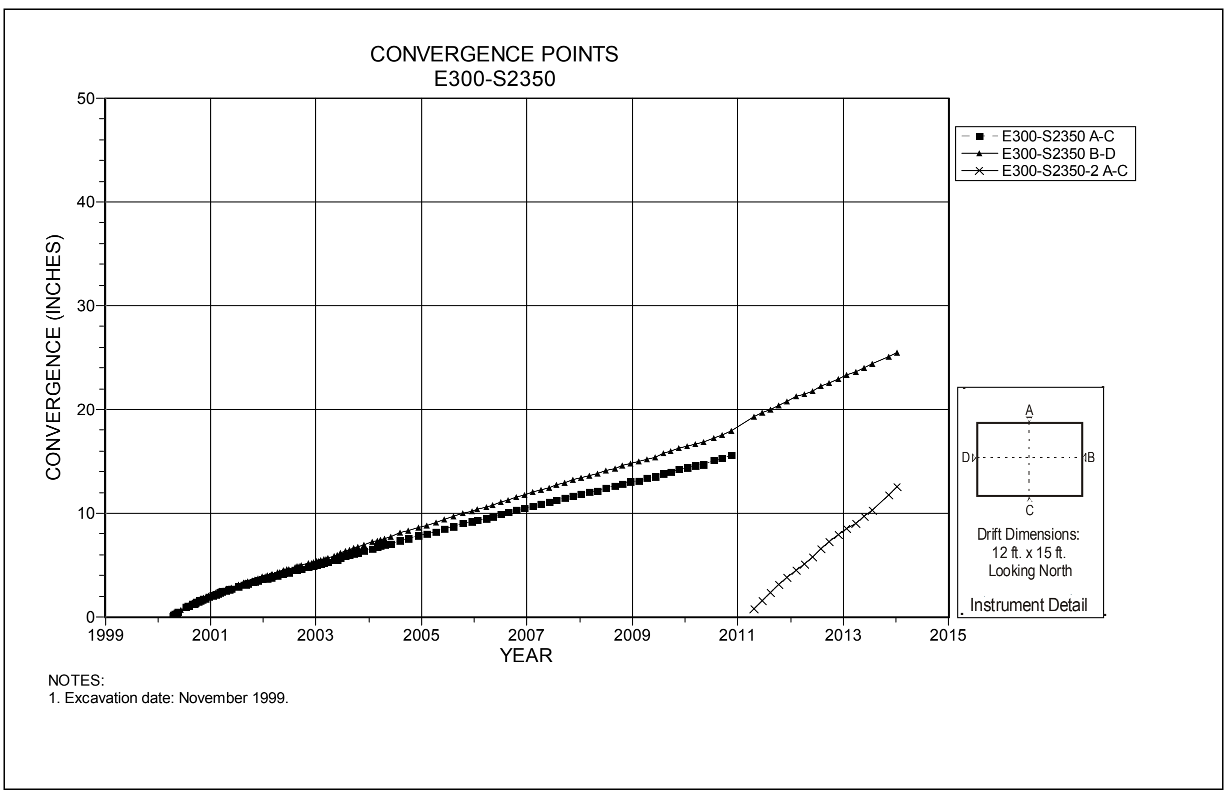

Figure 4-140 Convergence Point Array
E300 S2350 – All Chords

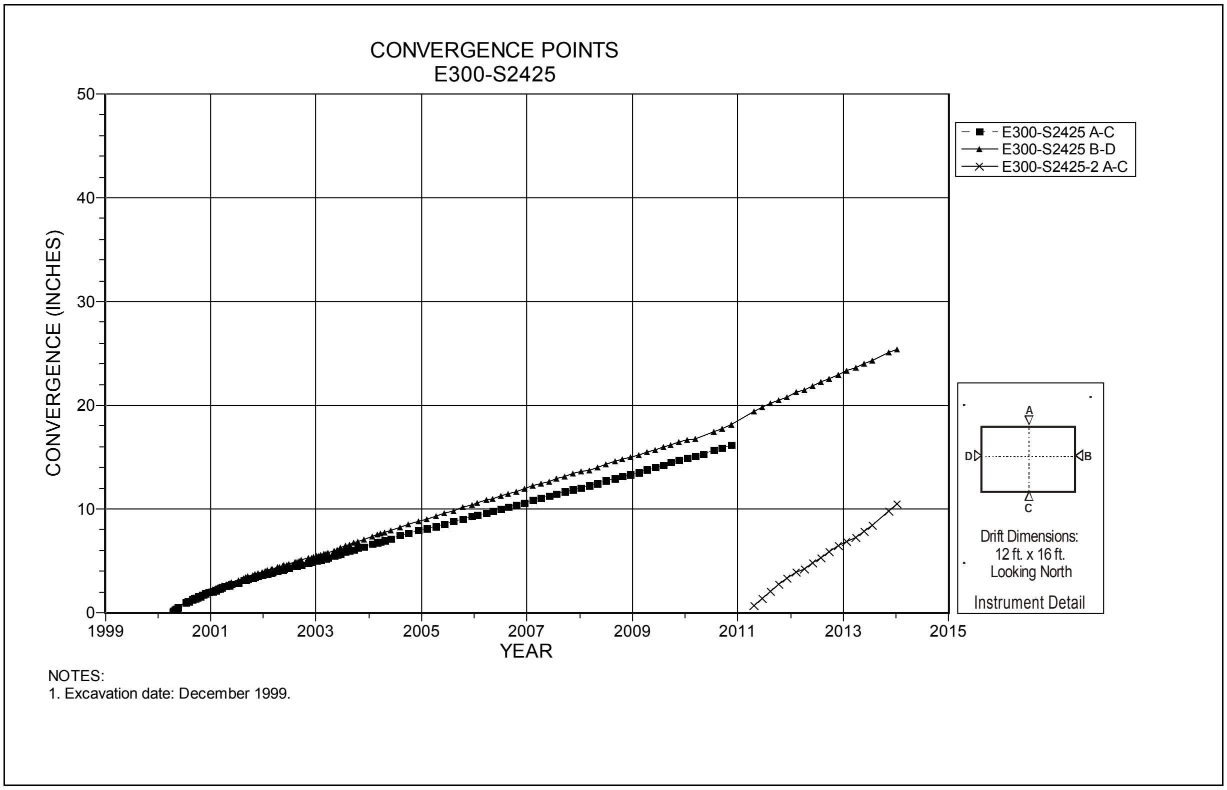

Figure 4-141 Convergence Point Array
E300 S2425 – All Chords

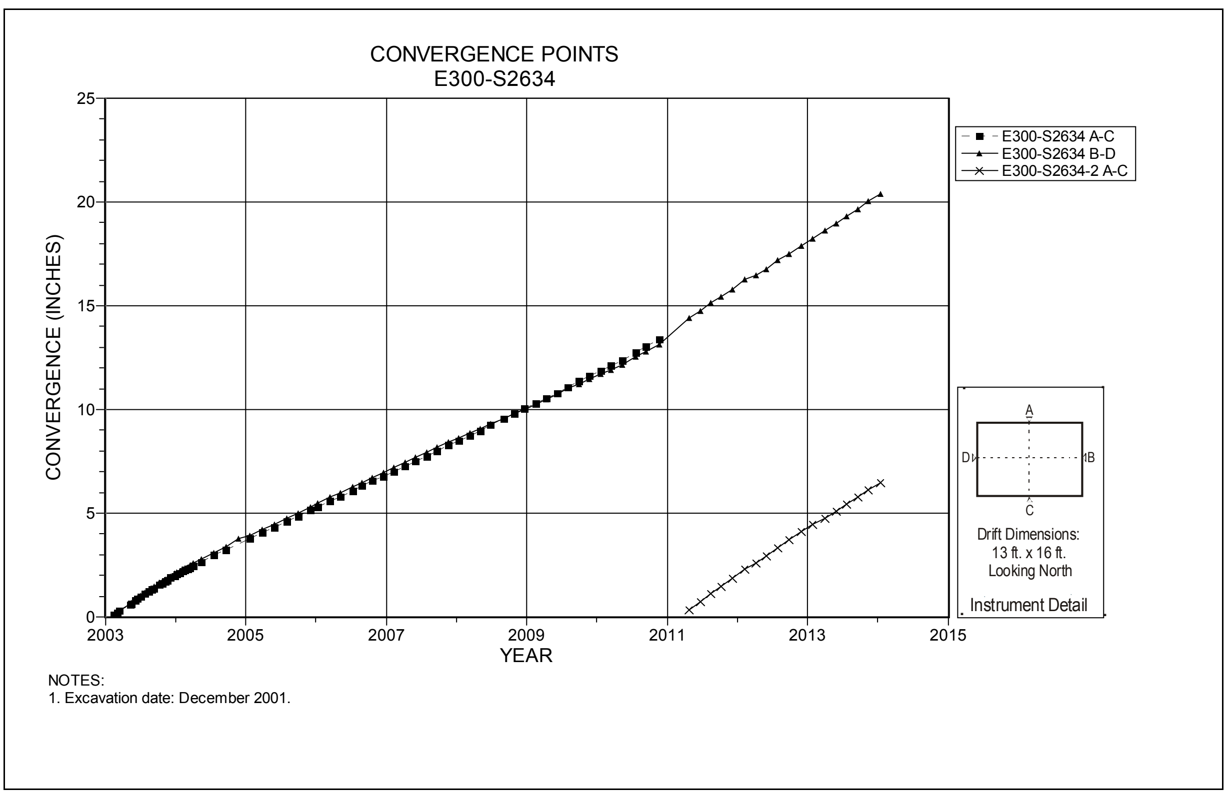

Figure 4-142 Convergence Point Array
E300 S2634 – All Chords

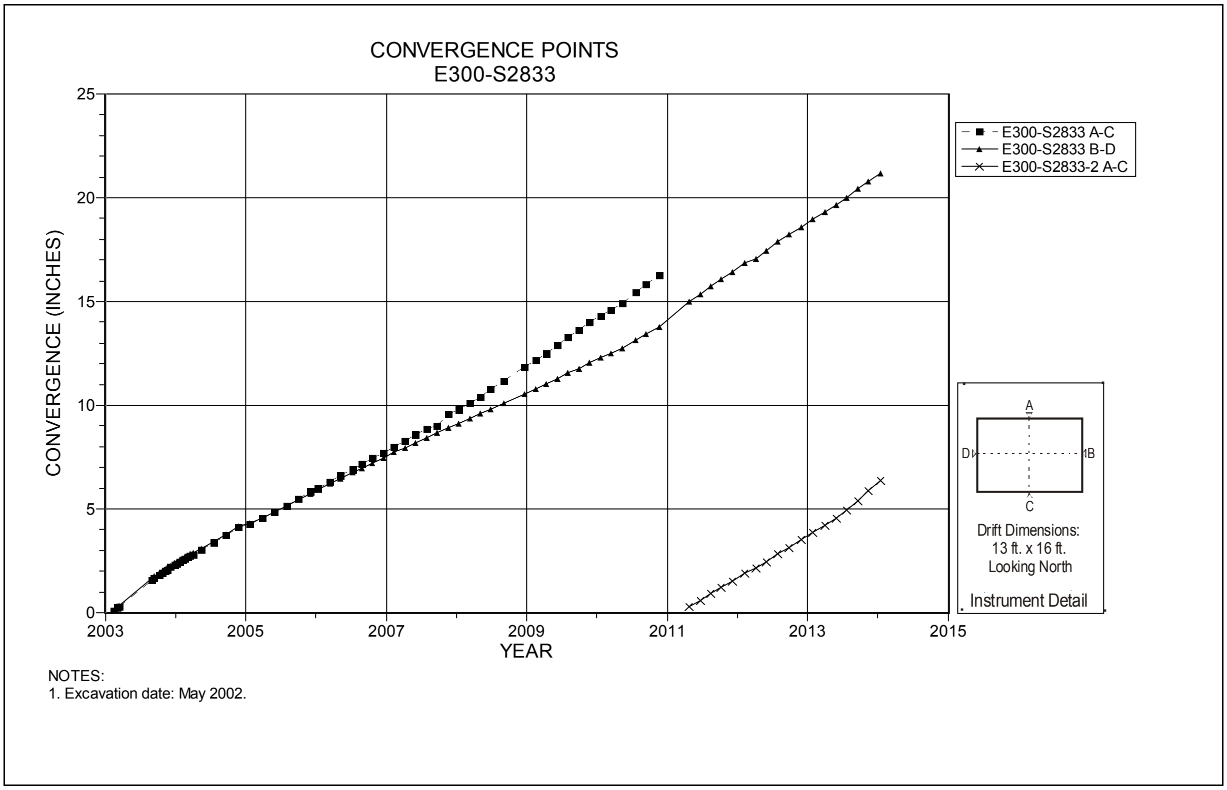

Figure 4-143 Convergence Point Array
E300 S2833 – All Chords

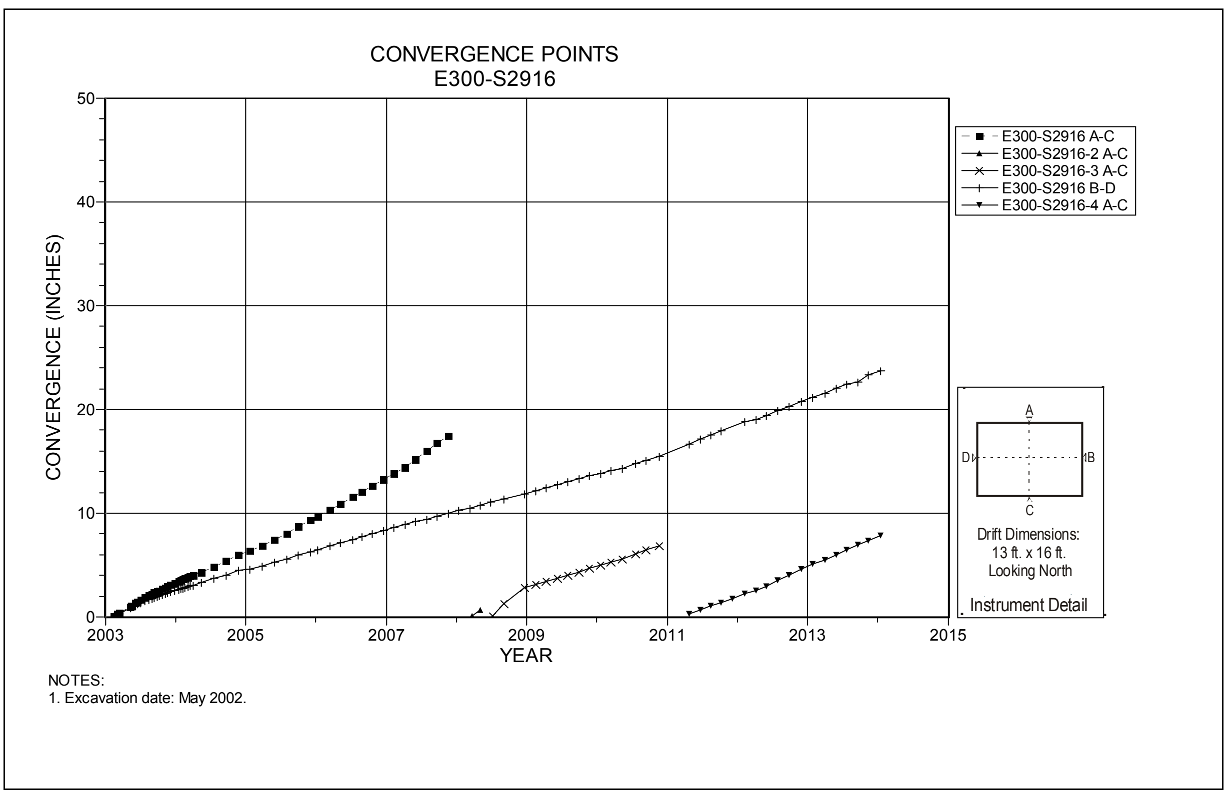

Figure 4-144 Convergence Point Array
E300 S2916 – All Chords

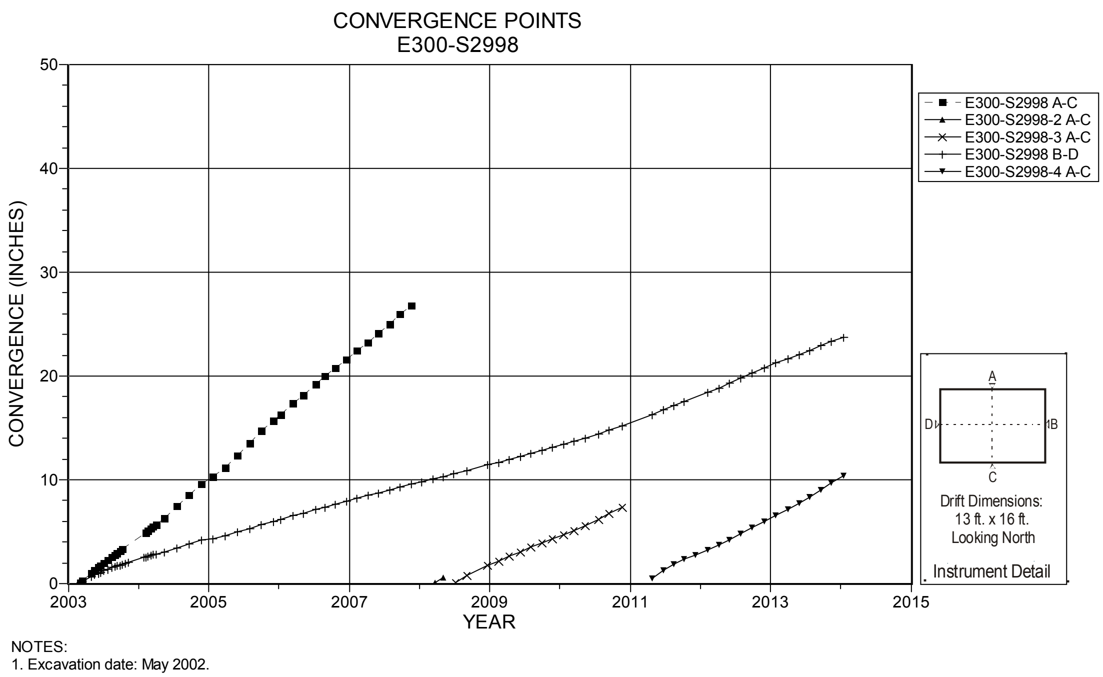

Figure 4-145 Convergence Point Array
E300 S2998 – All Chords

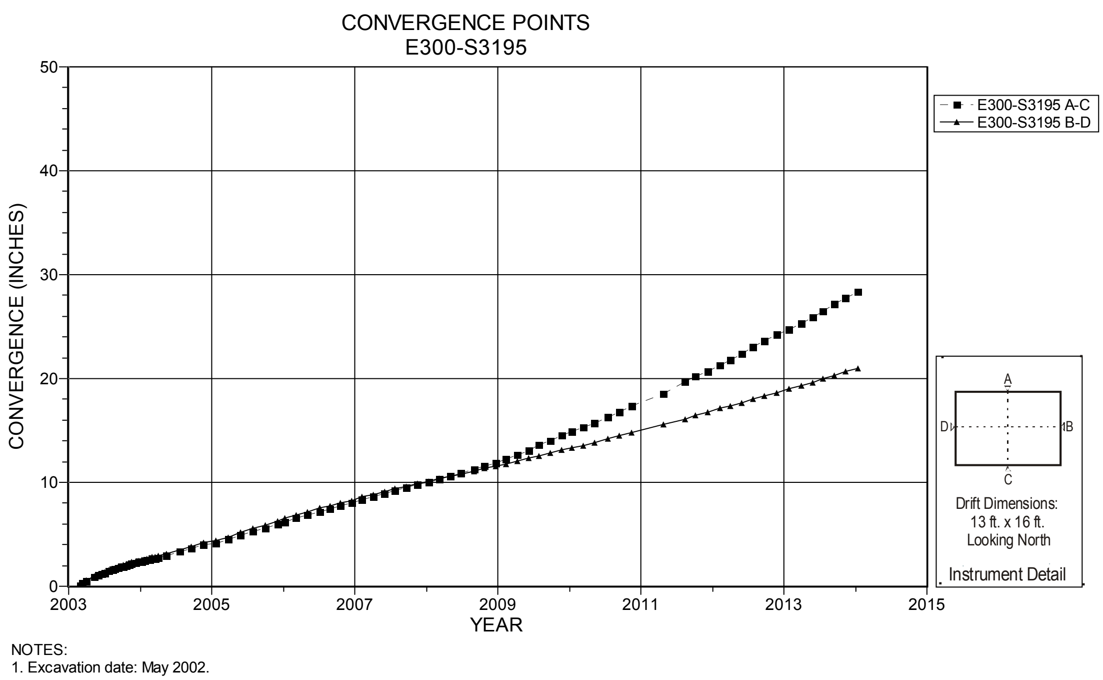

Figure 4-146 Convergence Point Array
E300 S3195 – All Chords

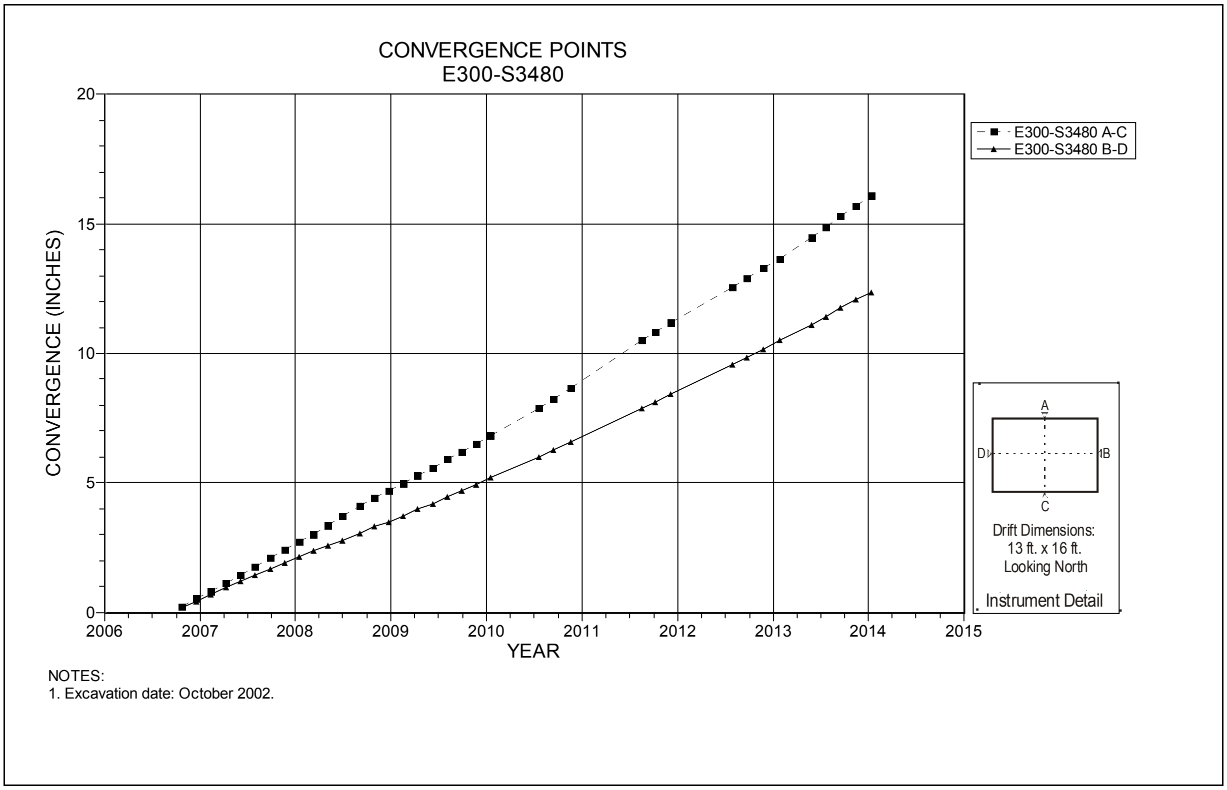

Figure 4-147 Convergence Point Array
E300 S3480 – All Chords

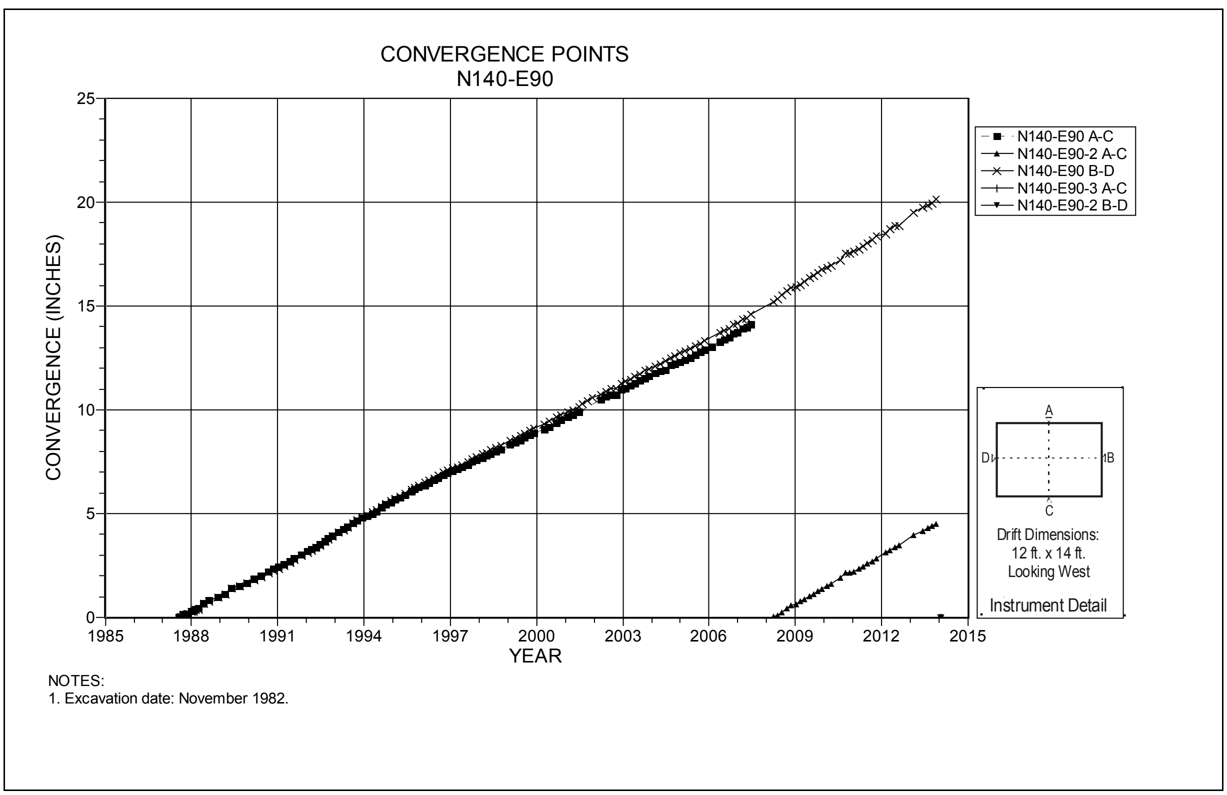

Figure 4-148 Convergence Point Array
N140 E90 – All Chords

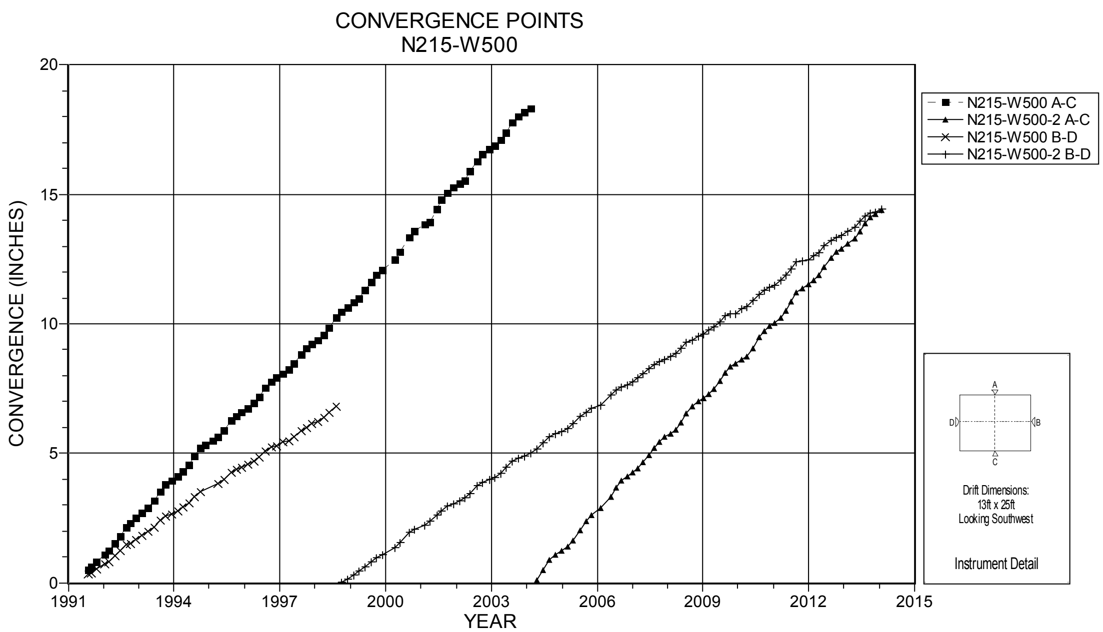

NOTES:
1. Excavation date: December 1987.

Figure 4-149 Convergence Point Array
N215 W500 – All Chords

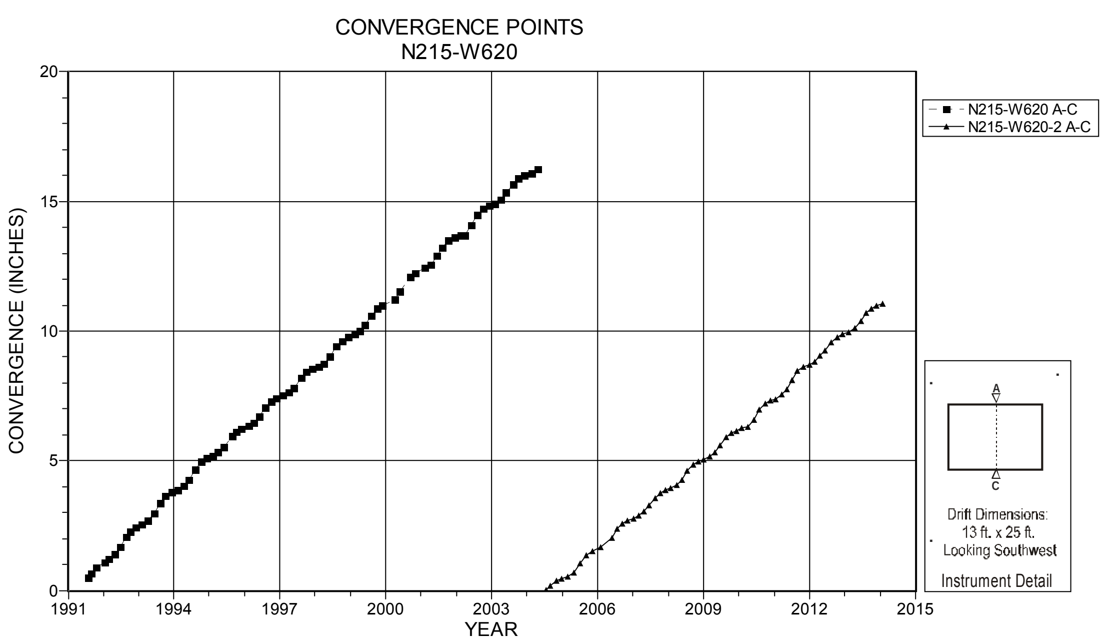

NOTES:
1. Excavation date: January 1988.

Figure 4-150 Convergence Point Array
N215 W620 – Roof to Floor

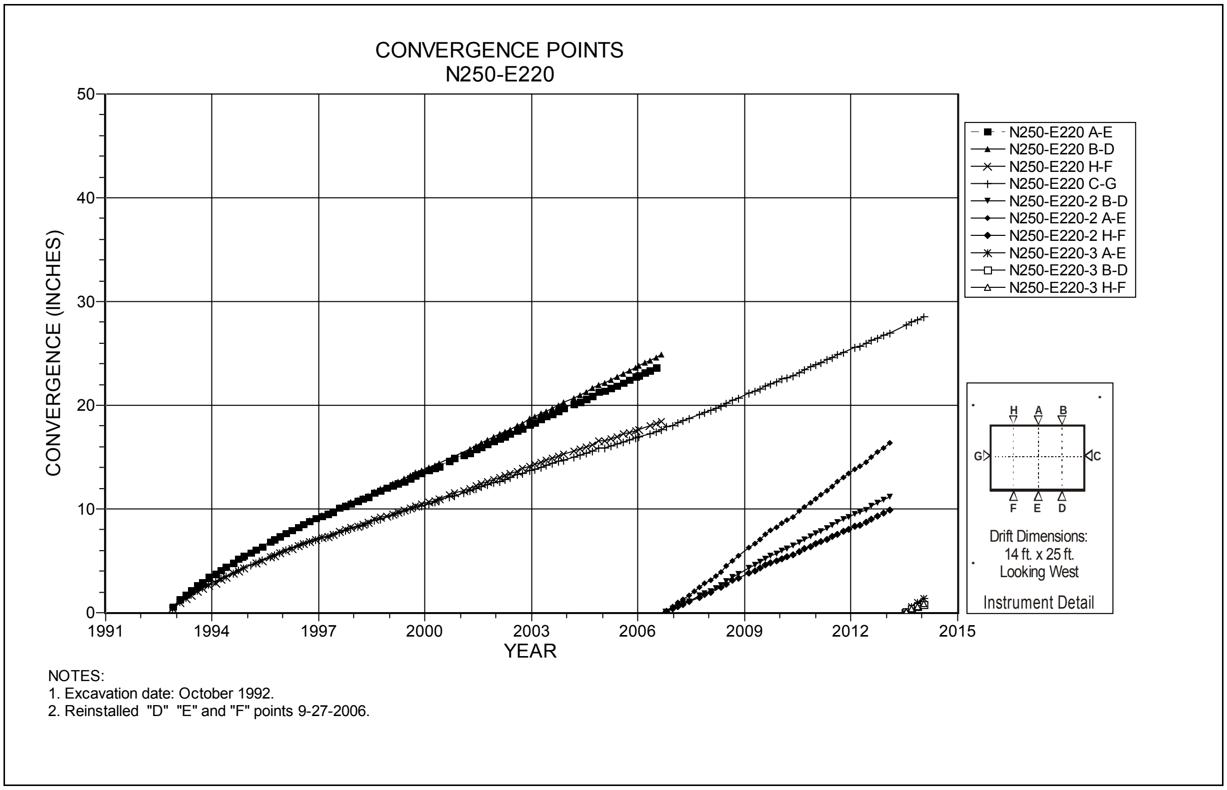

Figure 4-151 Convergence Point Array
N250 E220 – All Chords

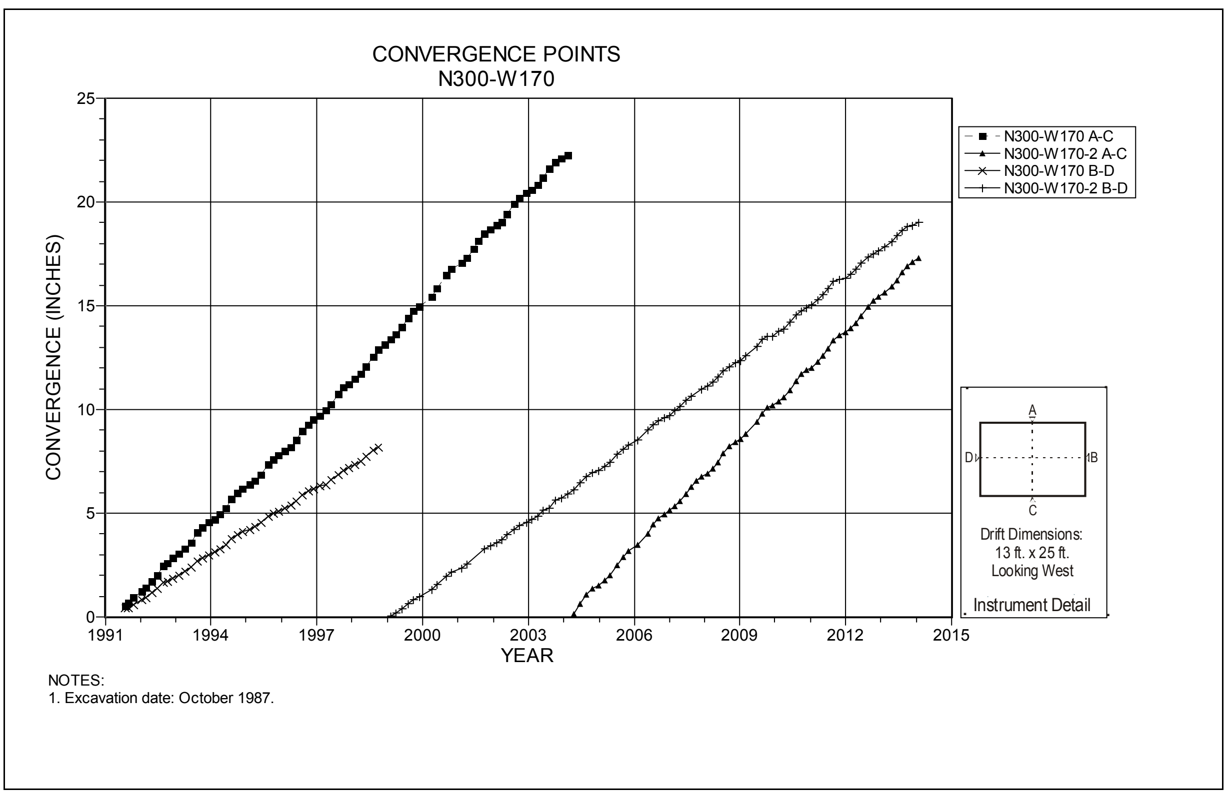

Figure 4-152 Convergence Point Array
N300 W170 – All Chords

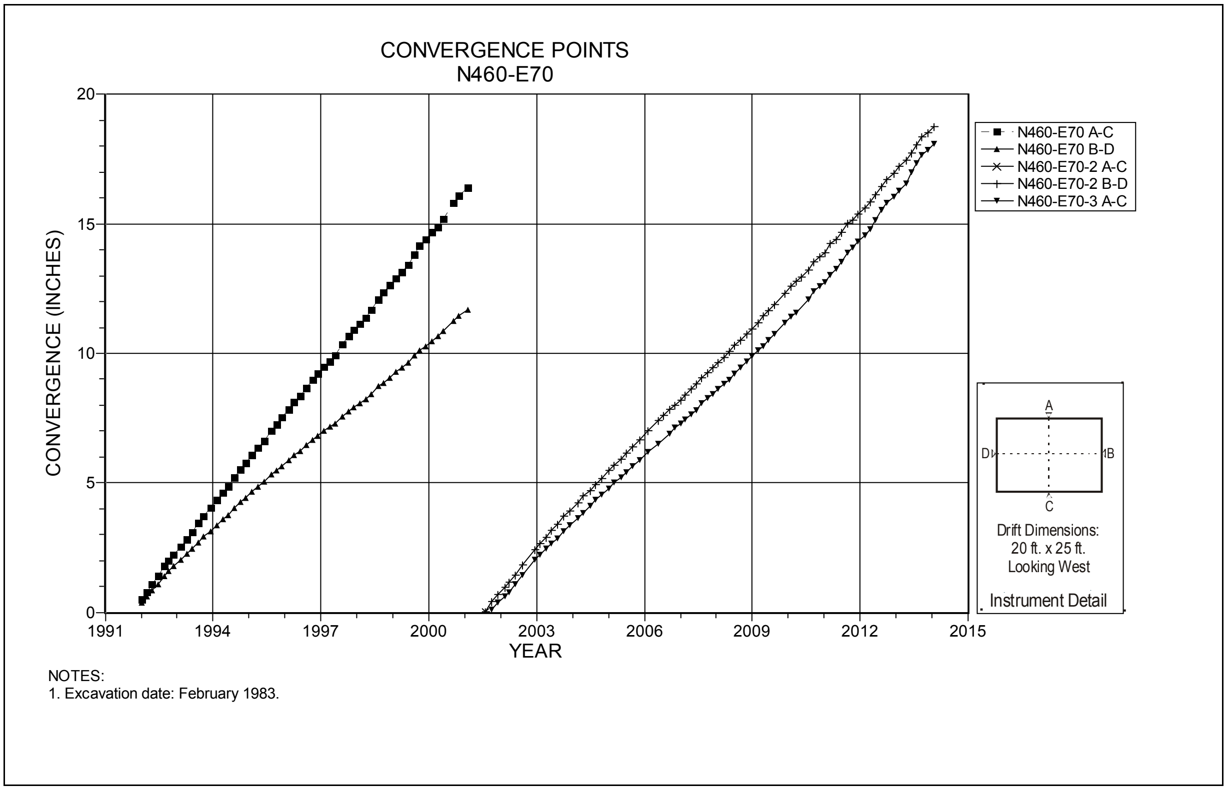

Figure 4-153 Convergence Point Array
N460 E70 – All Chords

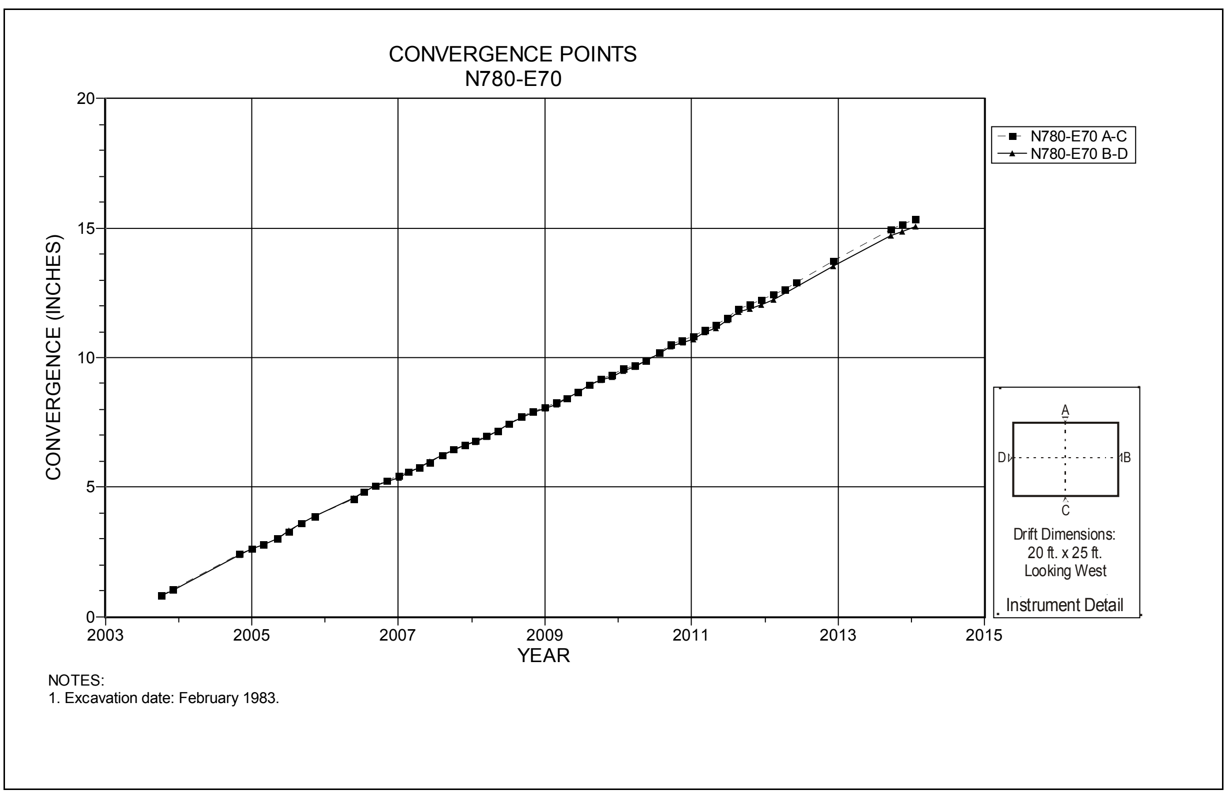

Figure 4-154 Convergence Point Array
N780 E70 – All Chords

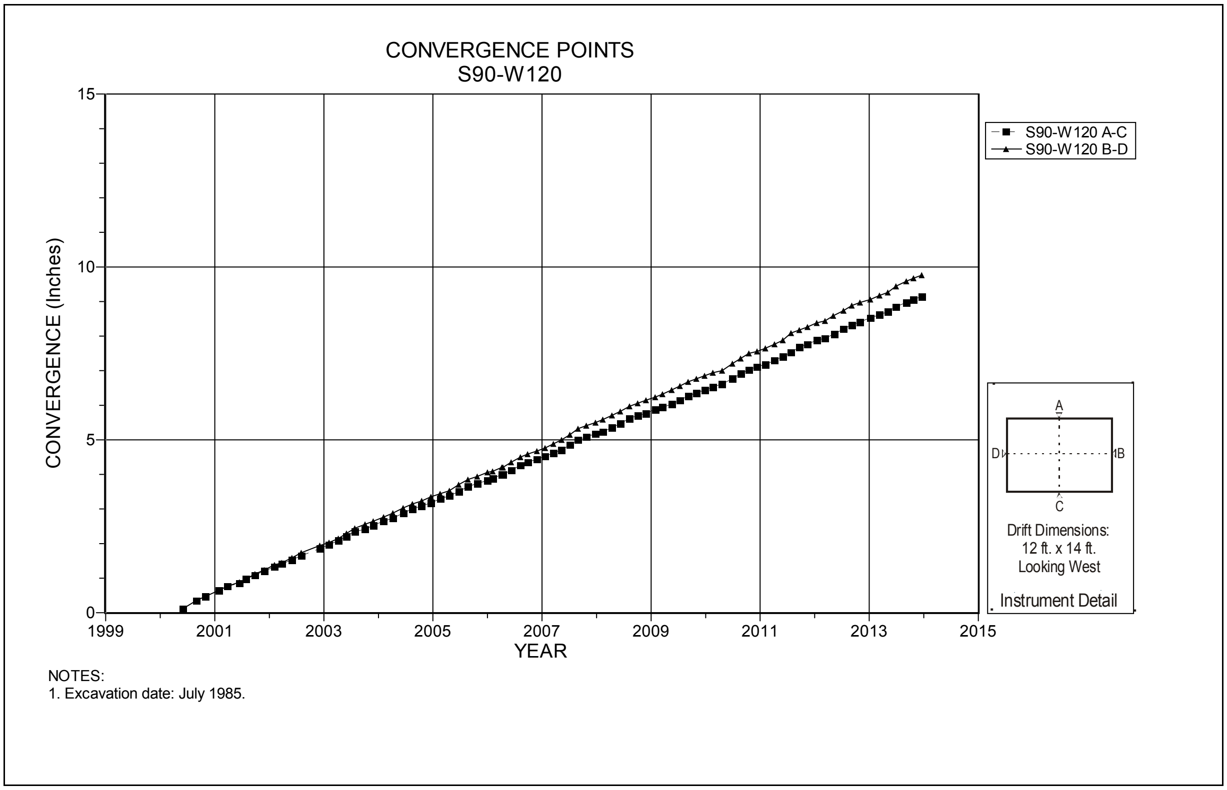

Figure 4-155 Convergence Point Array
S90 W120 – All Chords

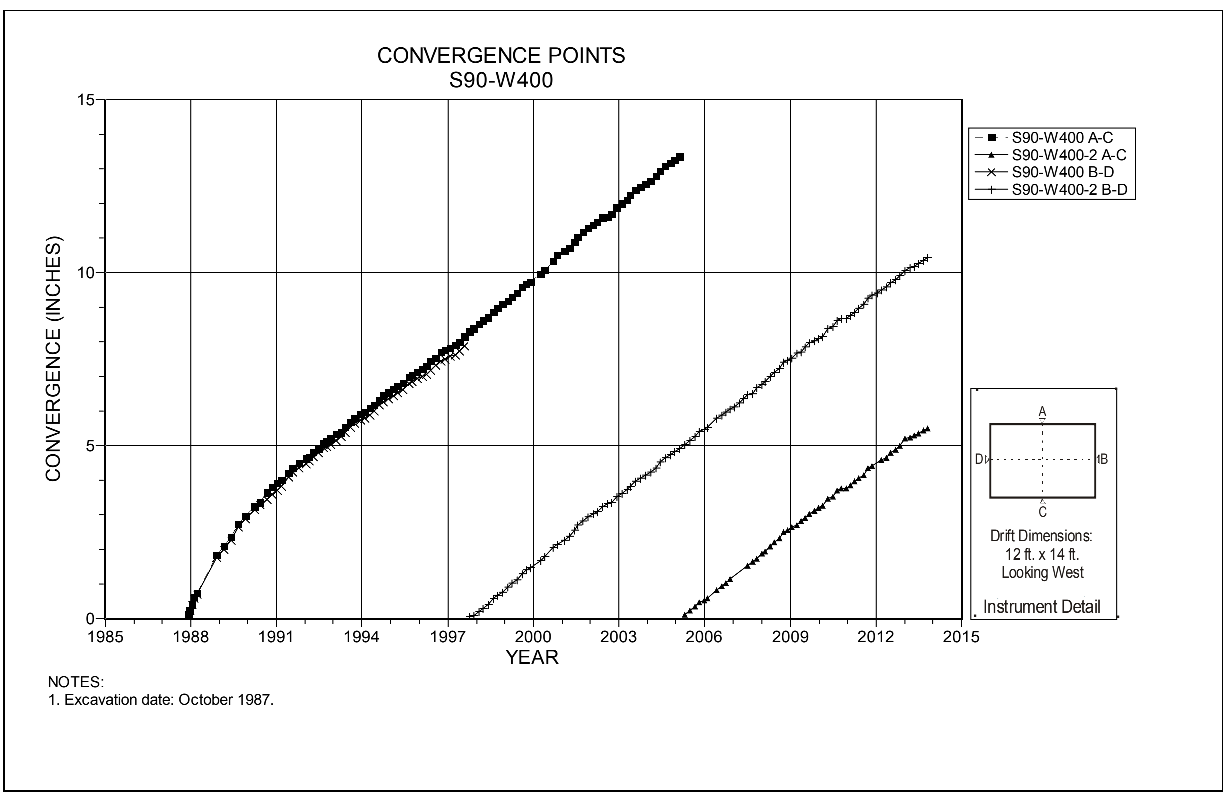

Figure 4-156 Convergence Point Array
S90 W400 – All Chords

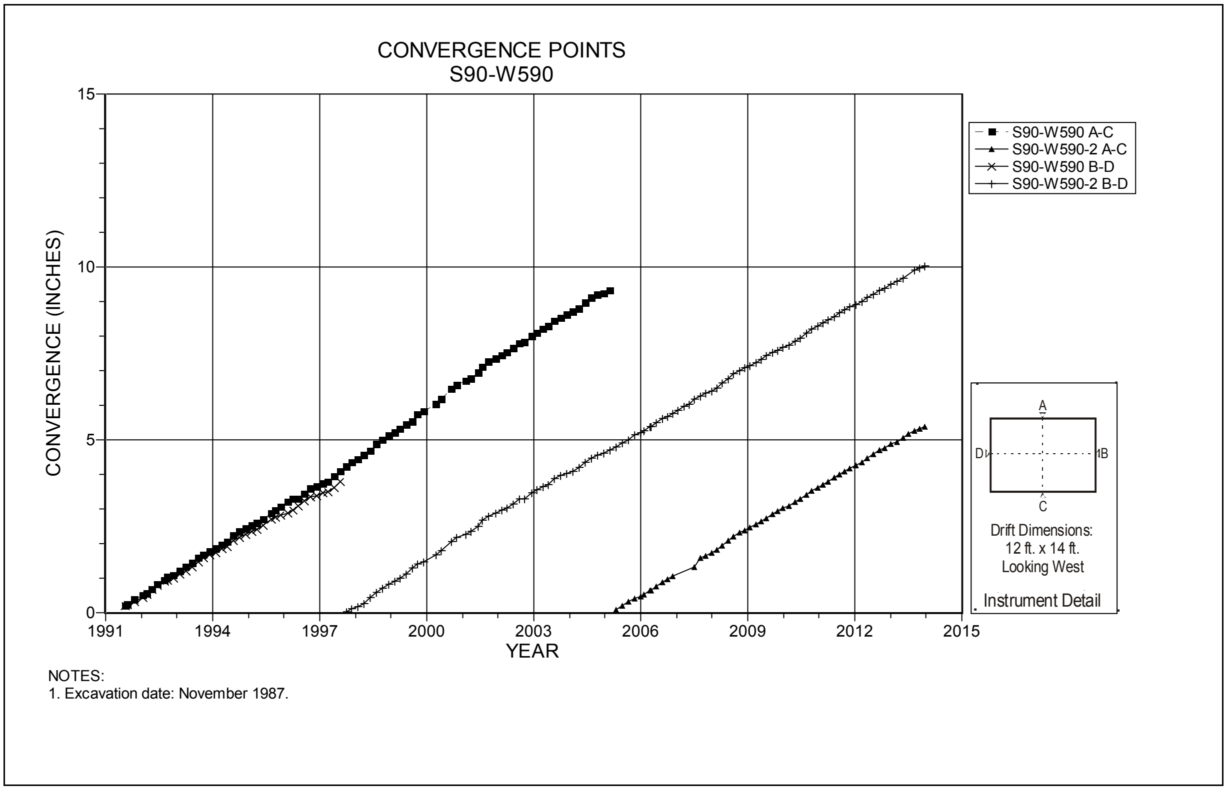

Figure 4-157 Convergence Point Array
S90 W590 – All Chords

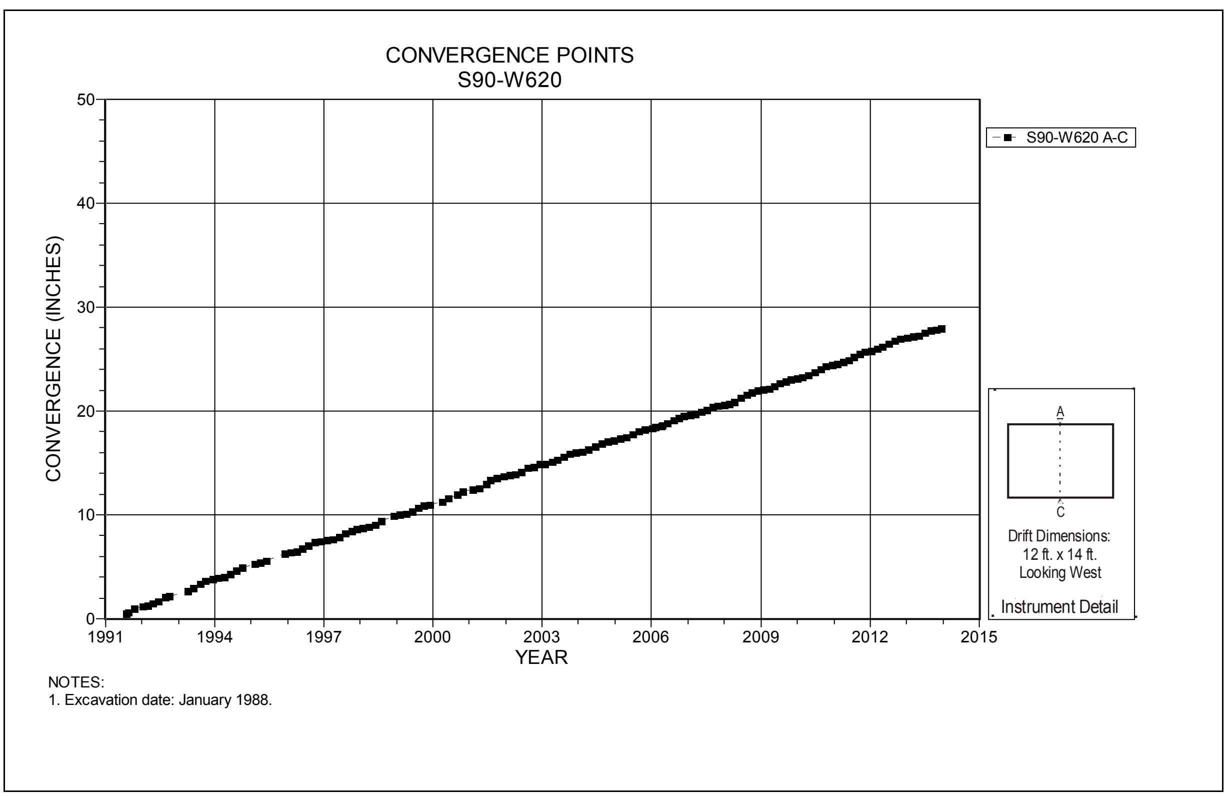

Figure 4-158 Convergence Point Array
S90 W620 – Roof to Floor

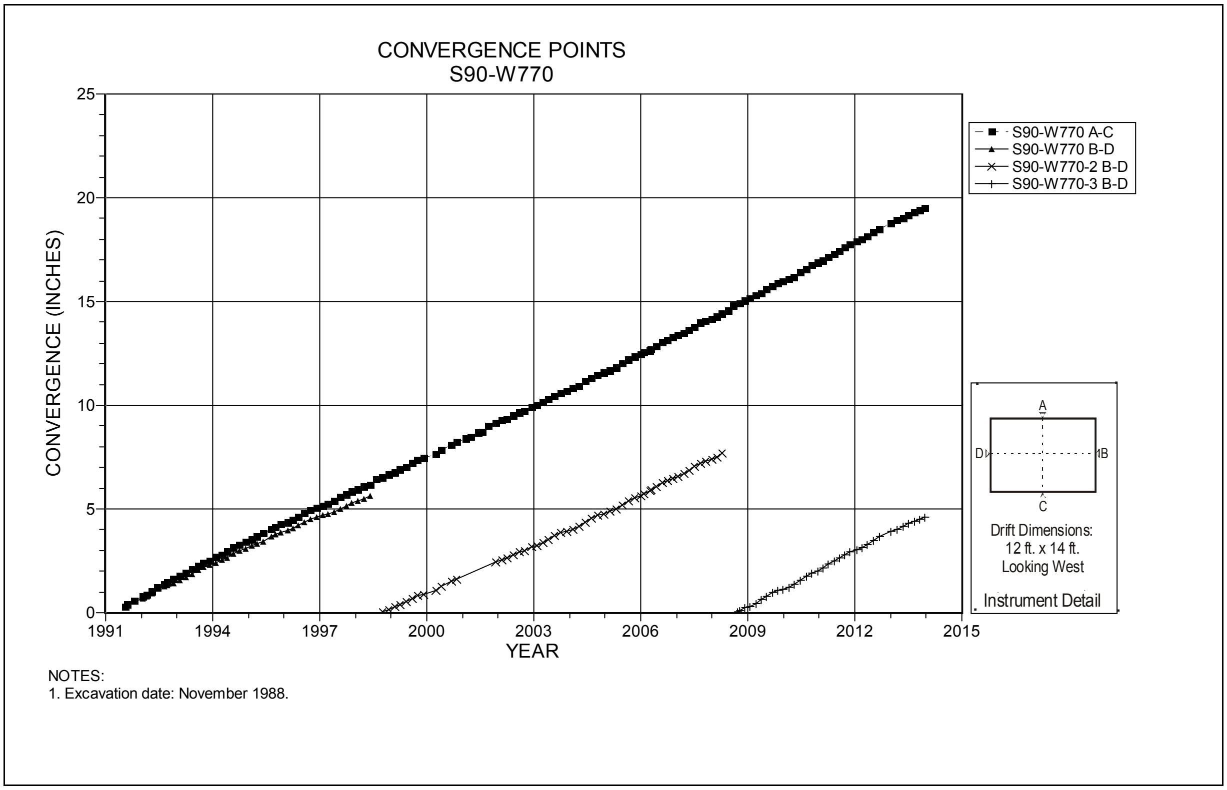

Figure 4-159 Convergence Point Array
S90 W770 – All Chords

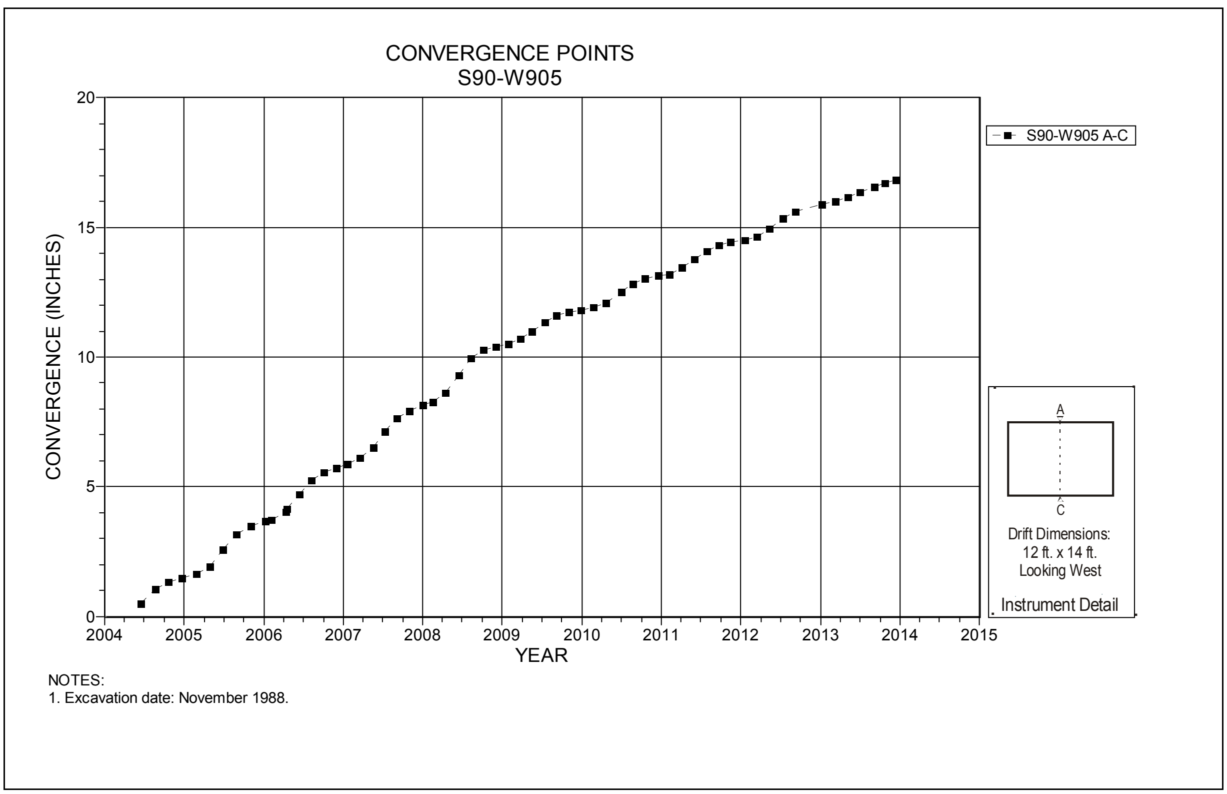

Figure 4-160 Convergence Point Array
S90 W905 – Roof to Floor

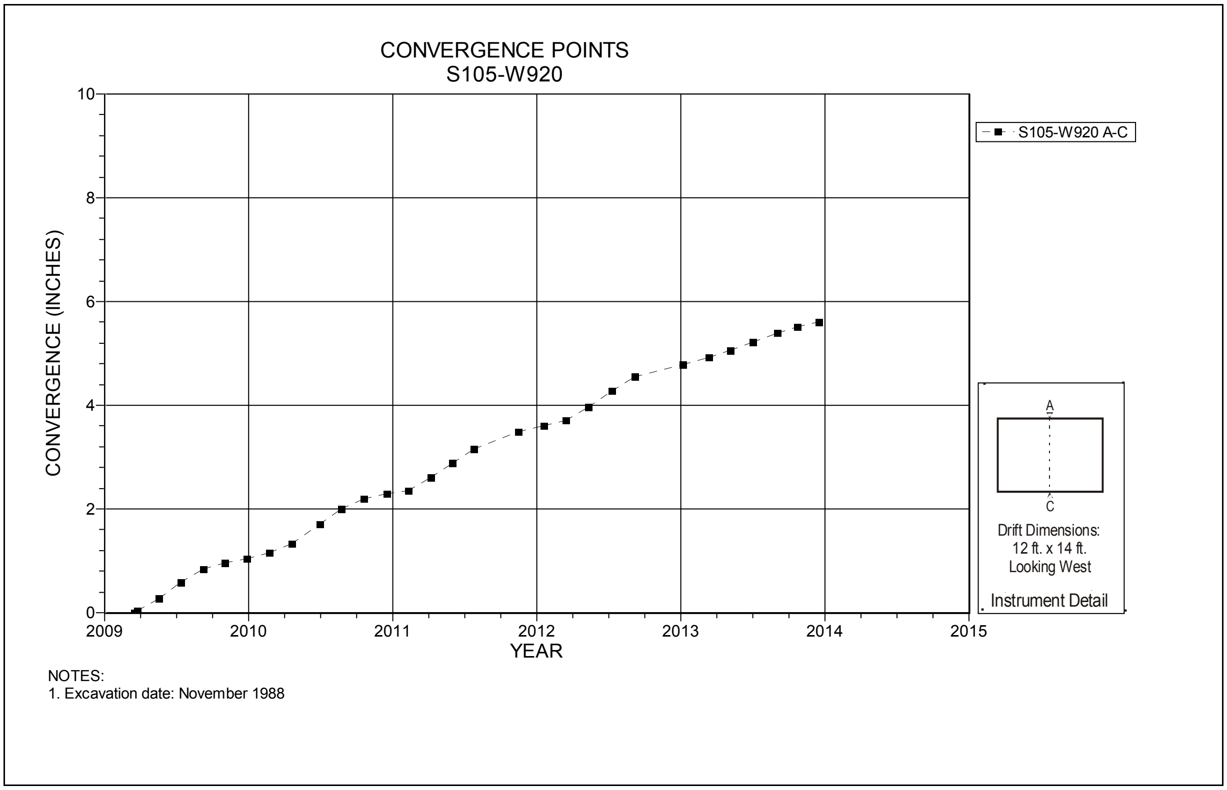

Figure 4-161 Convergence Point Array
S105 W920 – Roof to Floor

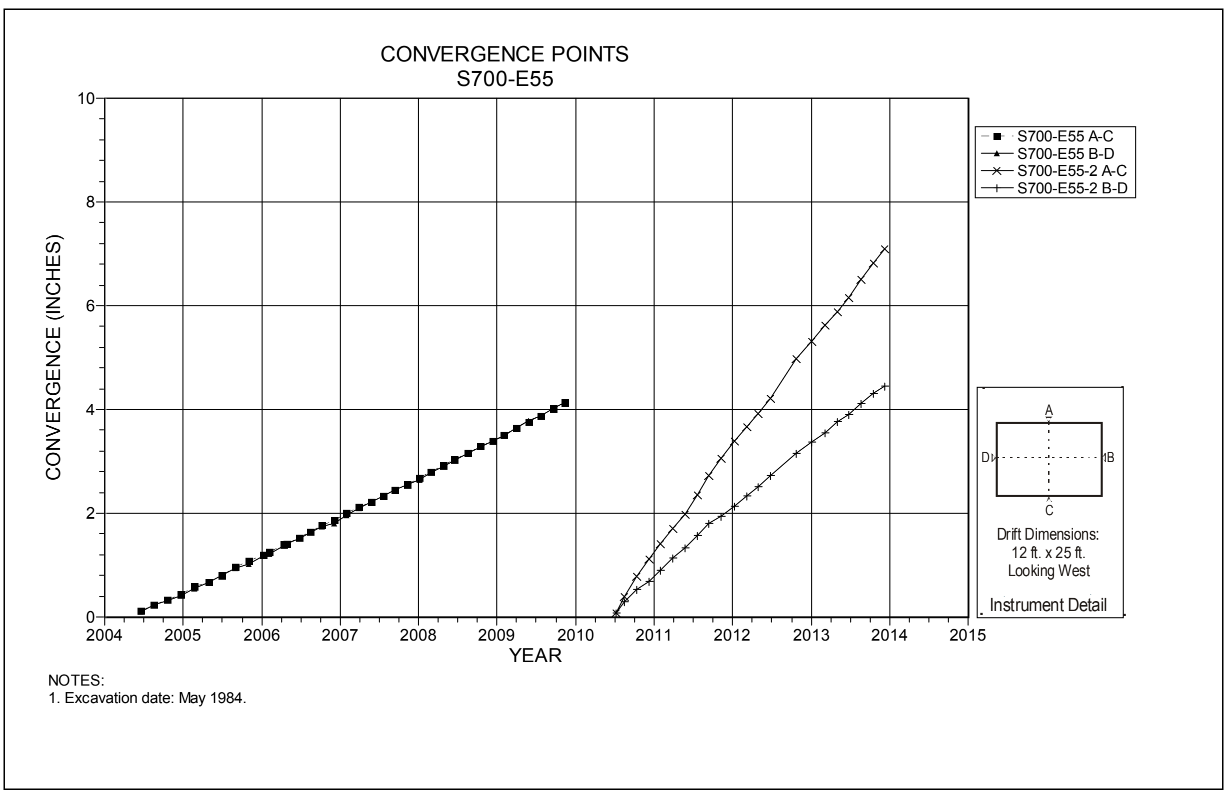

Figure 4-162 Convergence Point Array
S700 E55 – All Chords

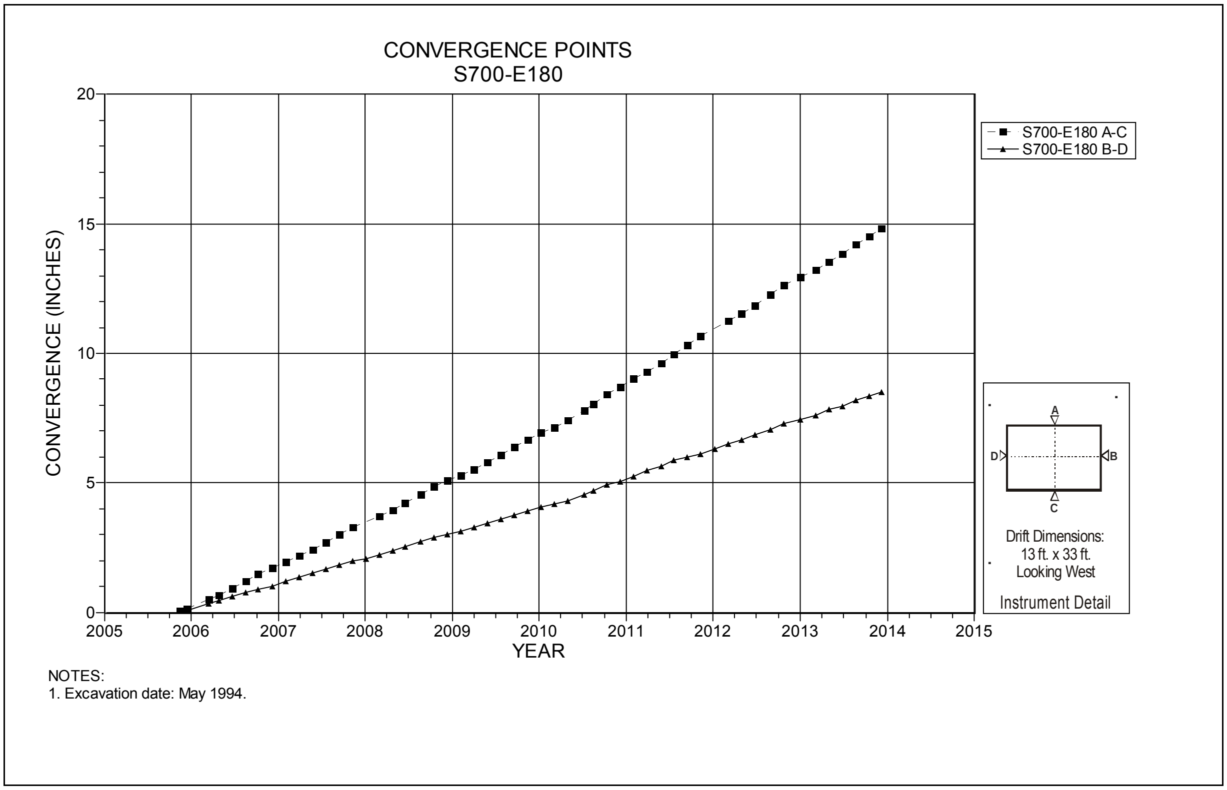

Figure 4-163 Convergence Point Array
S700 E180 – All Chords

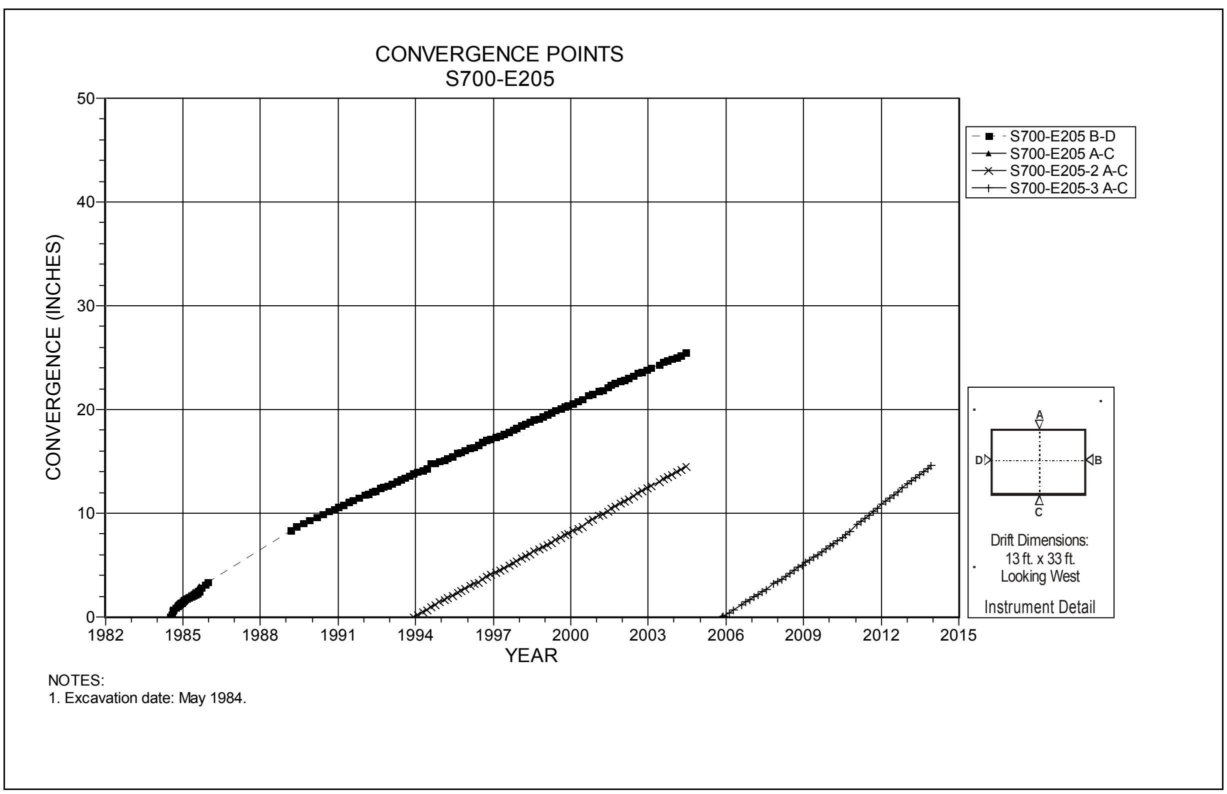

Figure 4-164 Convergence Point Array
S700 E205 – All Chords

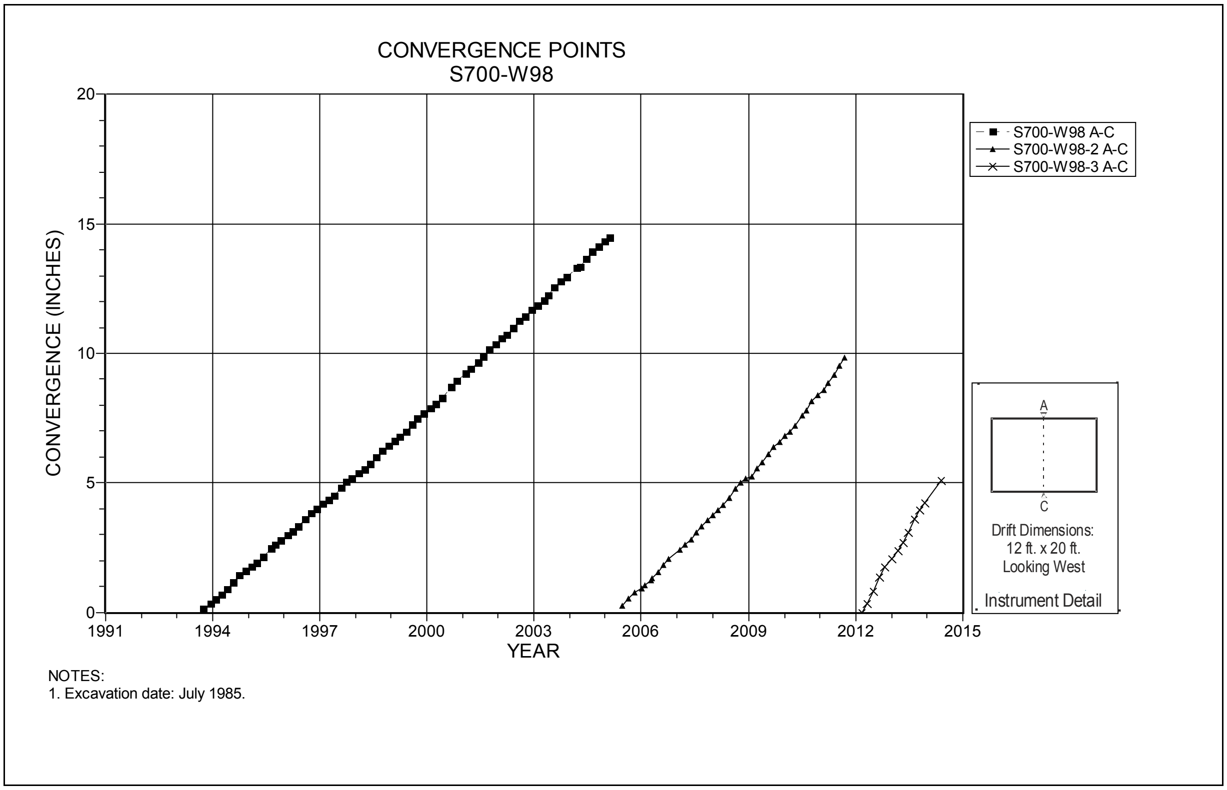

Figure 4-165 Convergence Point Array
S700 W98 – Roof to Floor

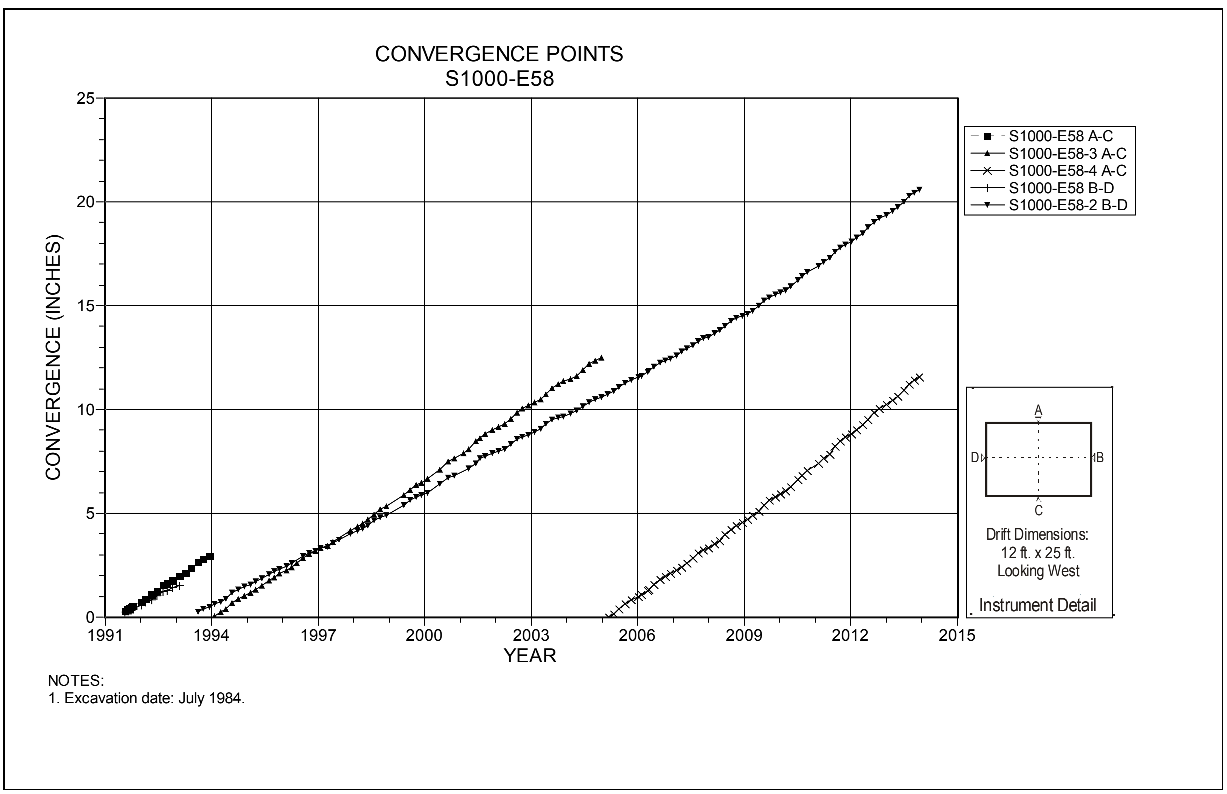

Figure 4-166 Convergence Point Array
S1000 E58 – All Chords

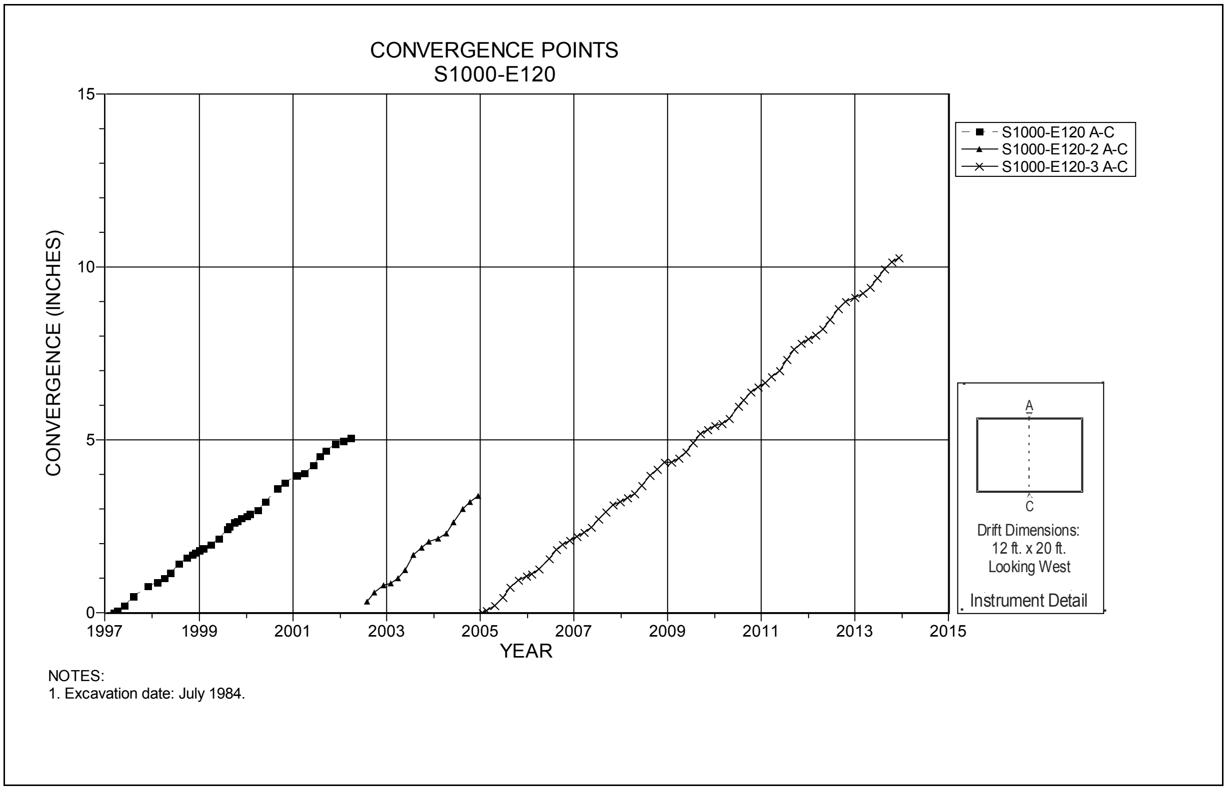

Figure 4-167 Convergence Point Array
S1000 E120 – Roof to Floor

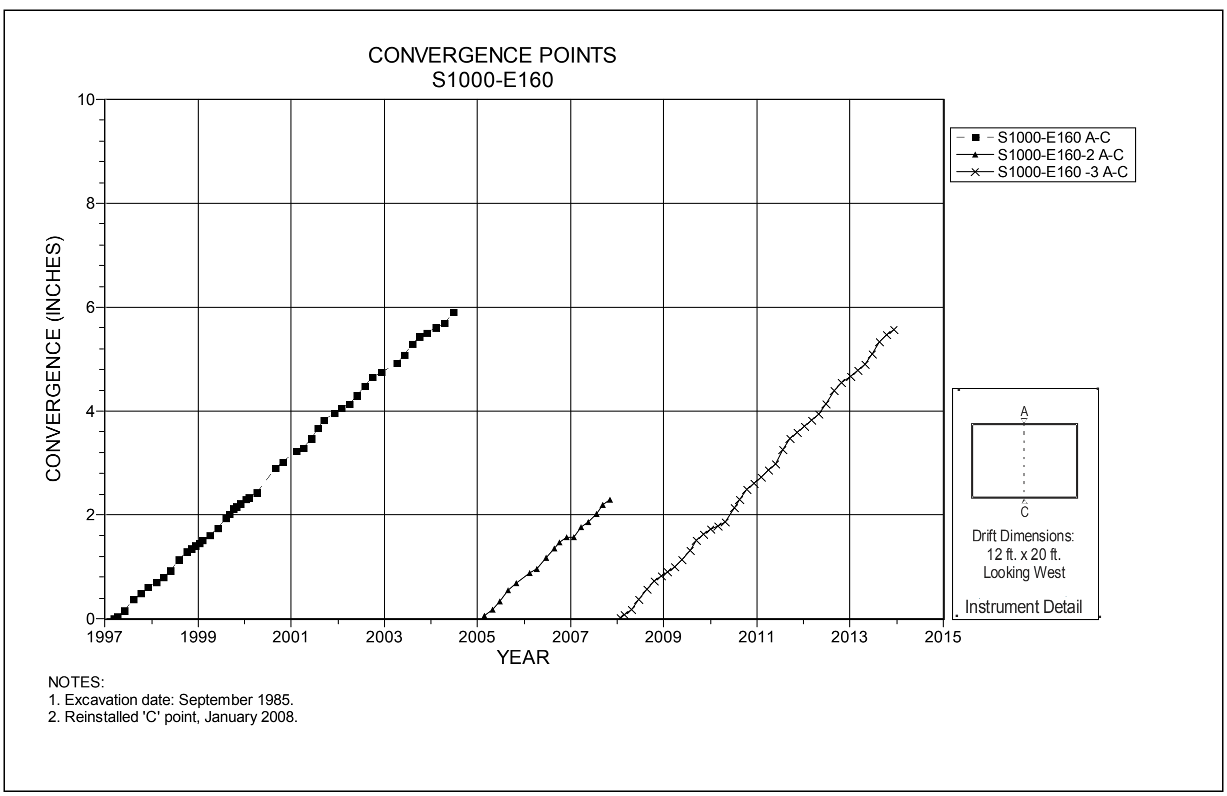

Figure 4-168 Convergence Point Array
S1000 E160 – Roof to Floor

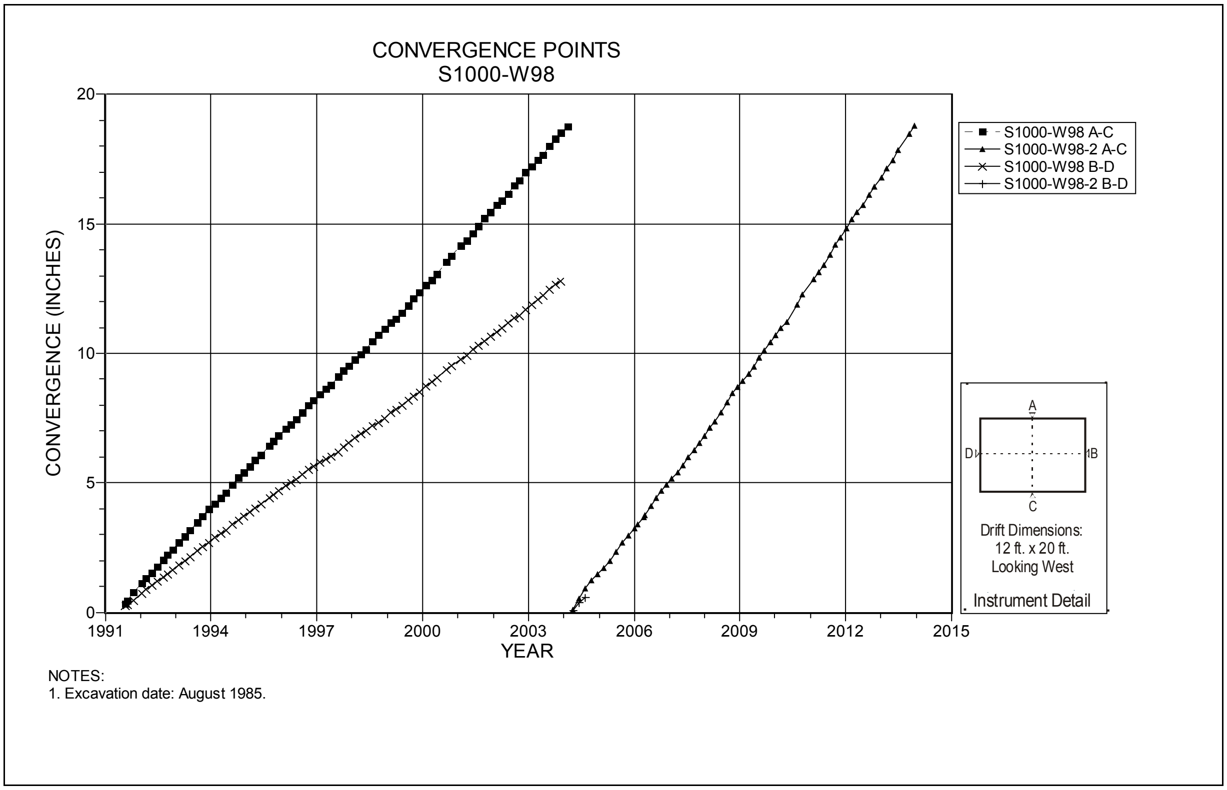

Figure 4-169 Convergence Point Array
S1000 W98 – All Chords

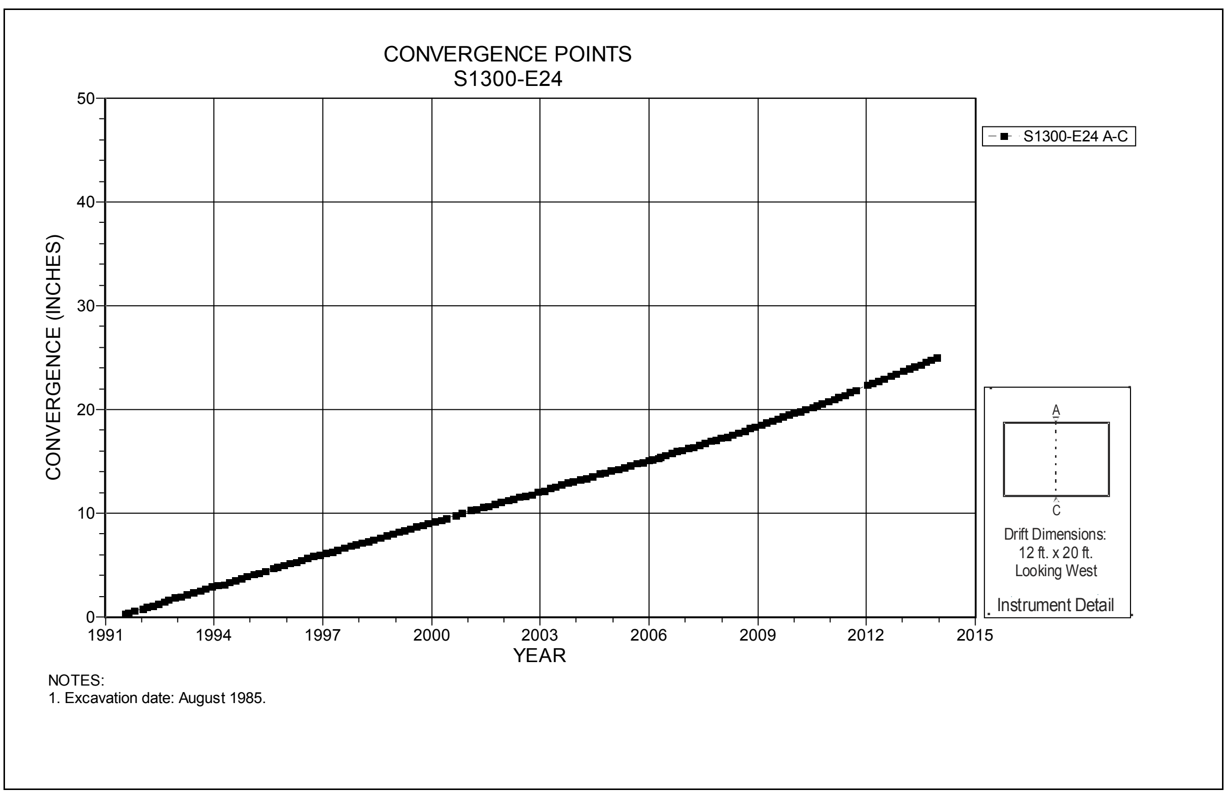

Figure 4-170 Convergence Point Array
S1300 E24 – Roof to Floor

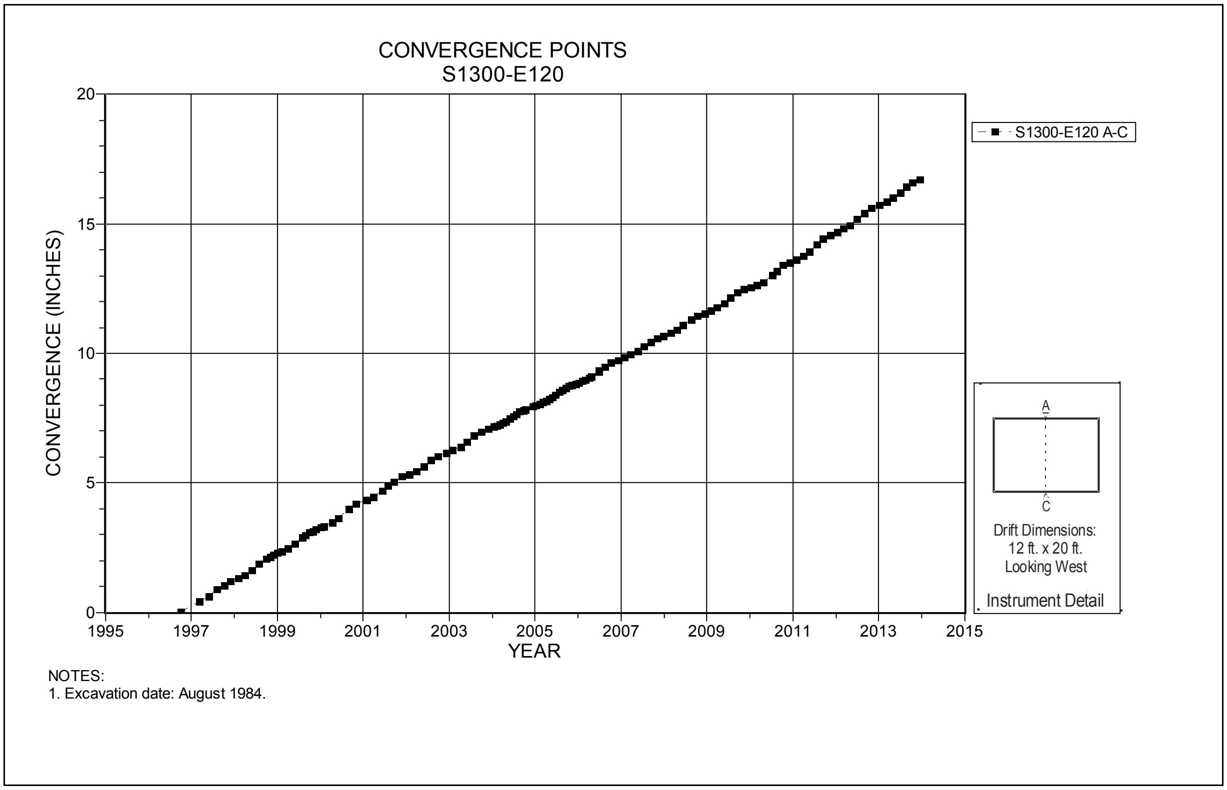

Figure 4-171 Convergence Point Array
S1300 E120 – Roof to Floor

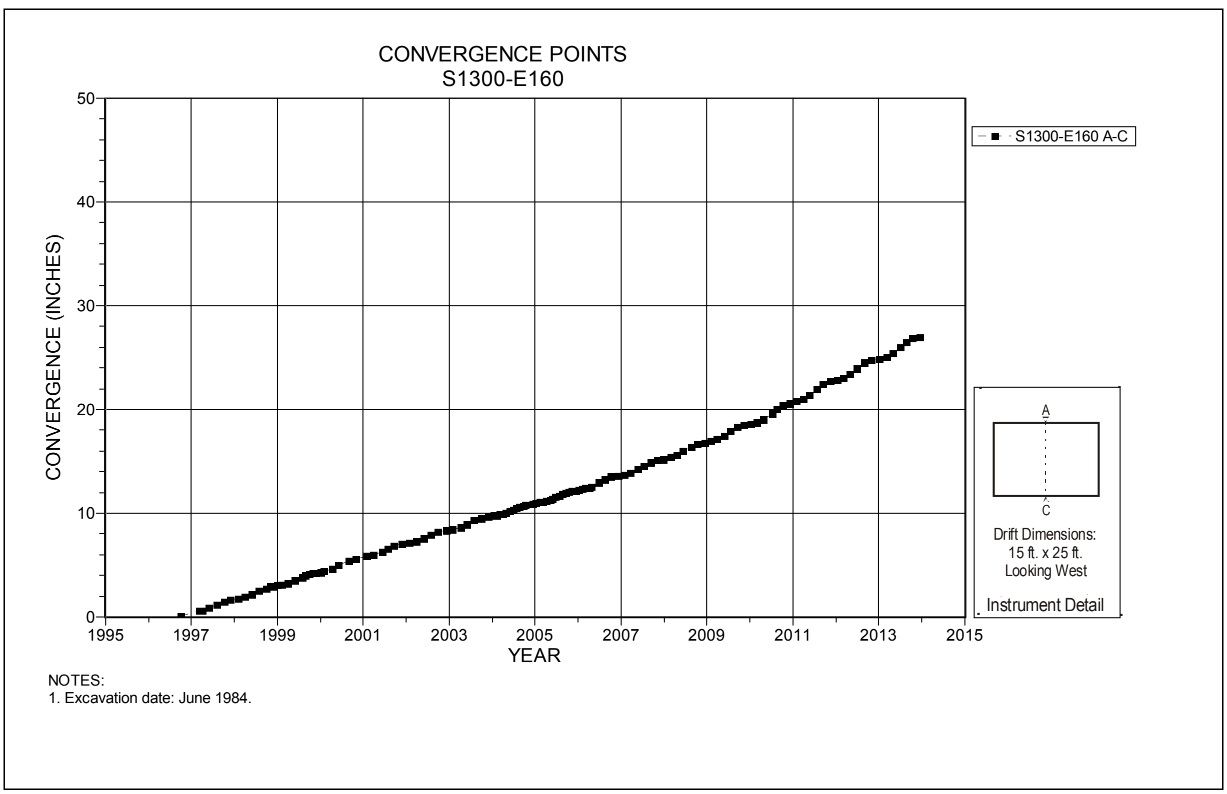

Figure 4-172 Convergence Point Array
S1300 E160 – Roof to Floor

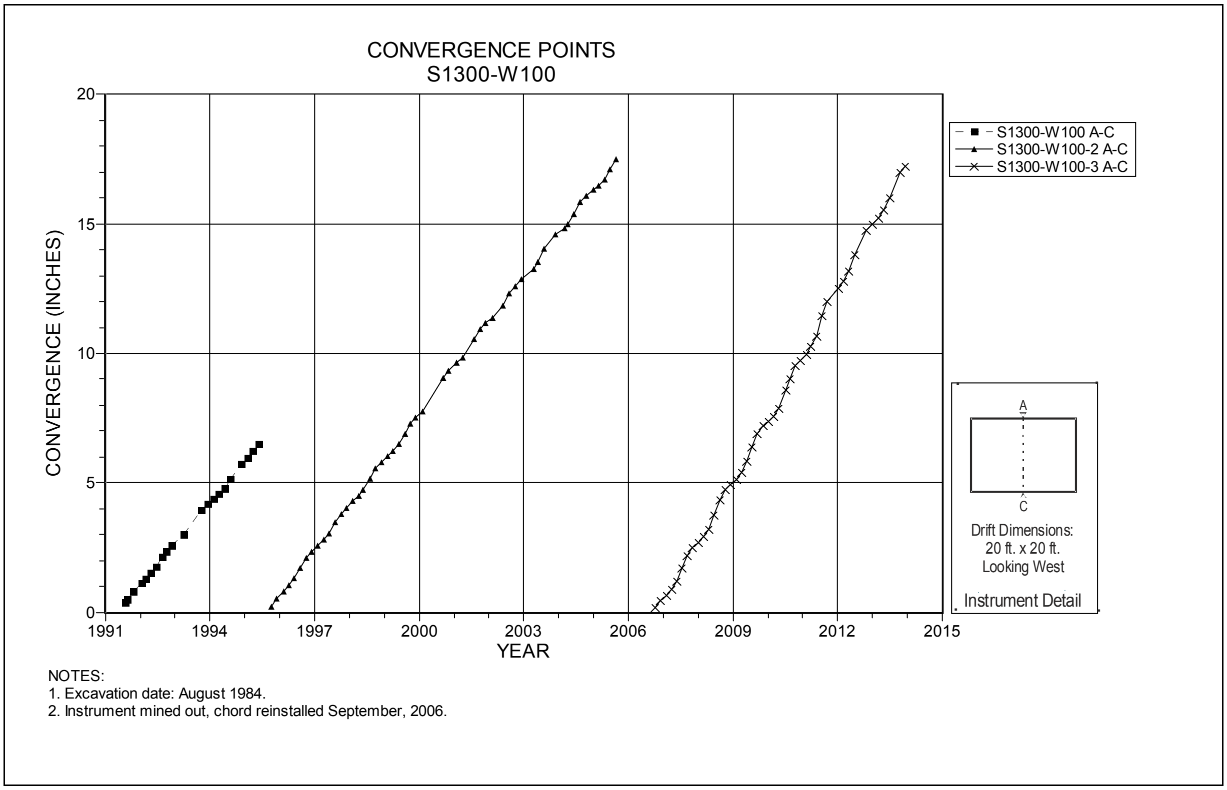

Figure 4-173 Convergence Point Array
S1300 W100 – Roof to Floor

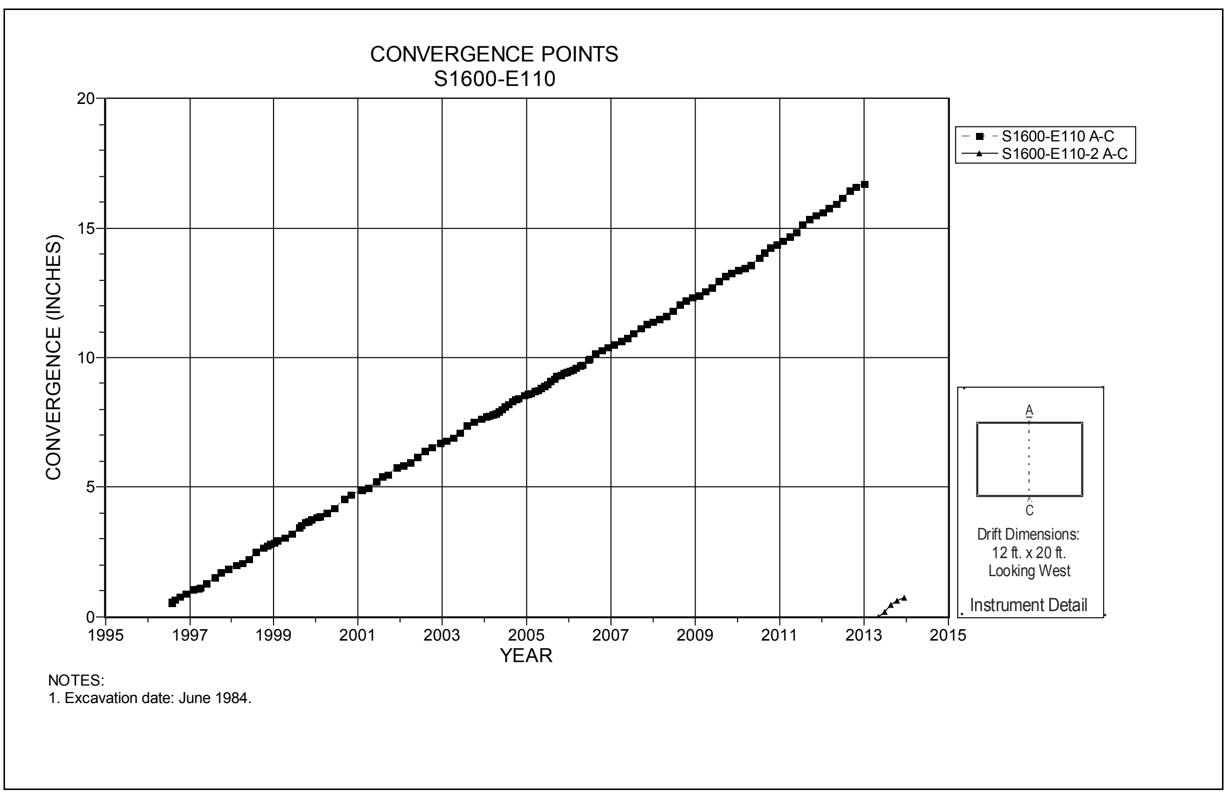

Figure 4-174 Convergence Point Array
S1600 E110 – Roof to Floor

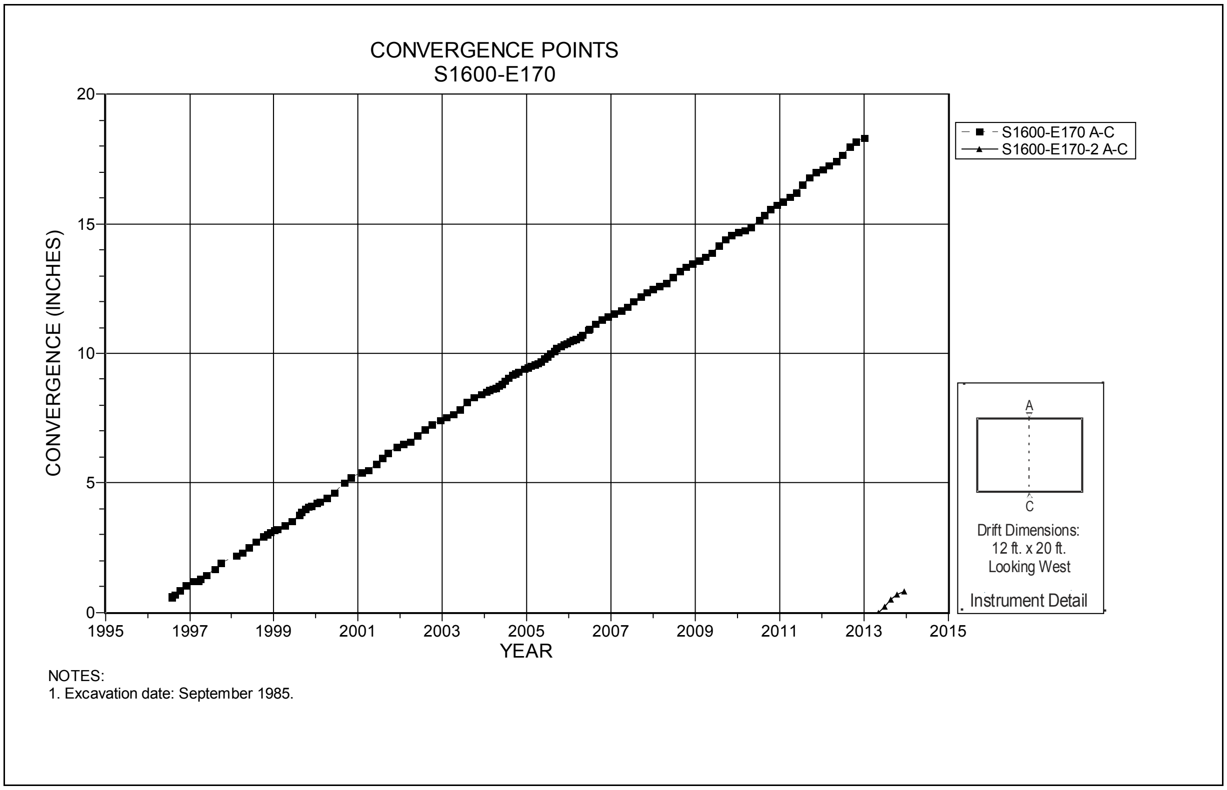

Figure 4-175 Convergence Point Array
S1600 E170 – Roof to Floor

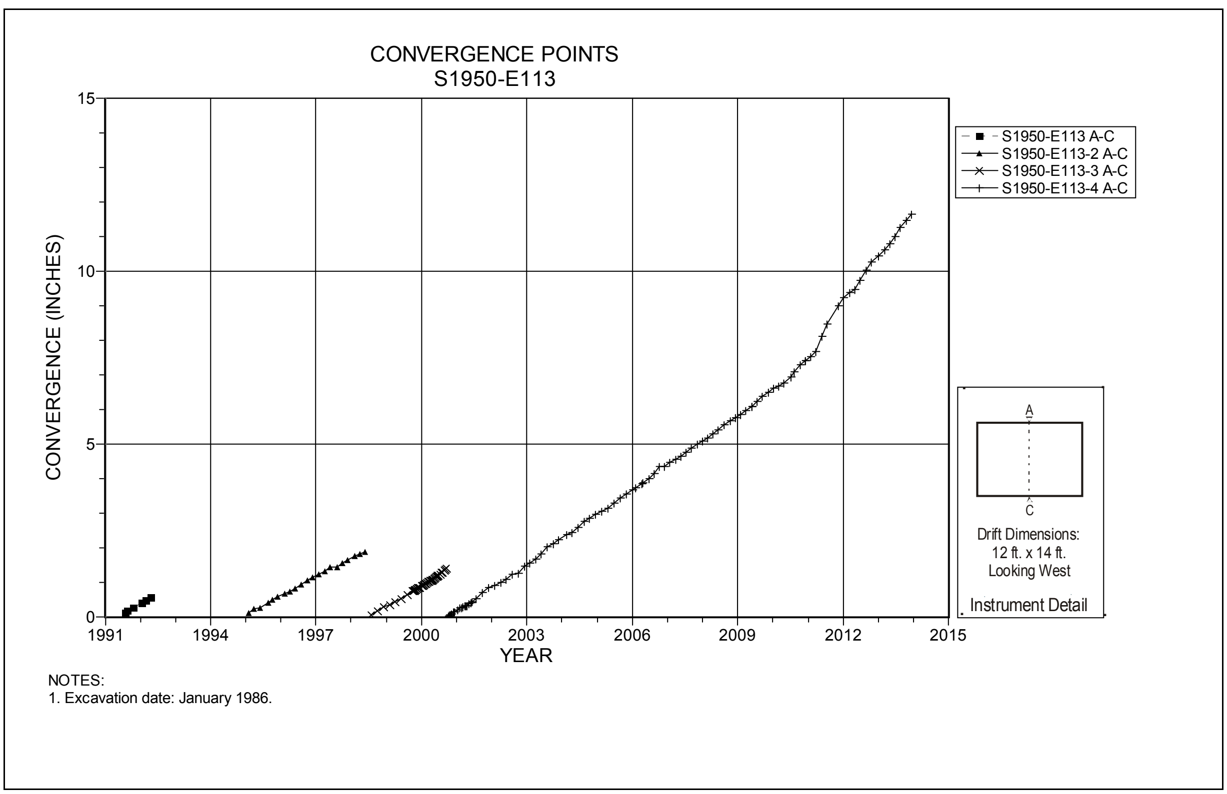

Figure 4-176 Convergence Point Array
S1950 E113 – Roof to Floor

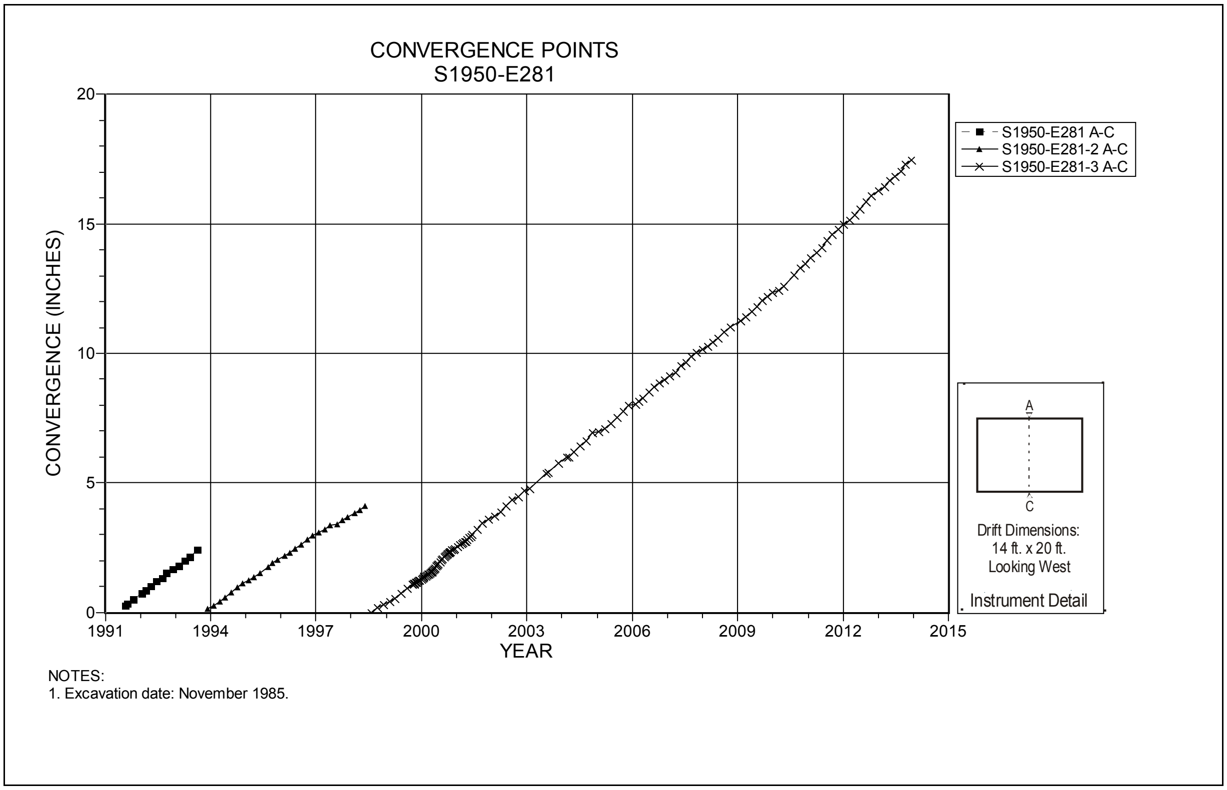

Figure 4-177 Convergence Point Array
S1950 E281 – Roof to Floor

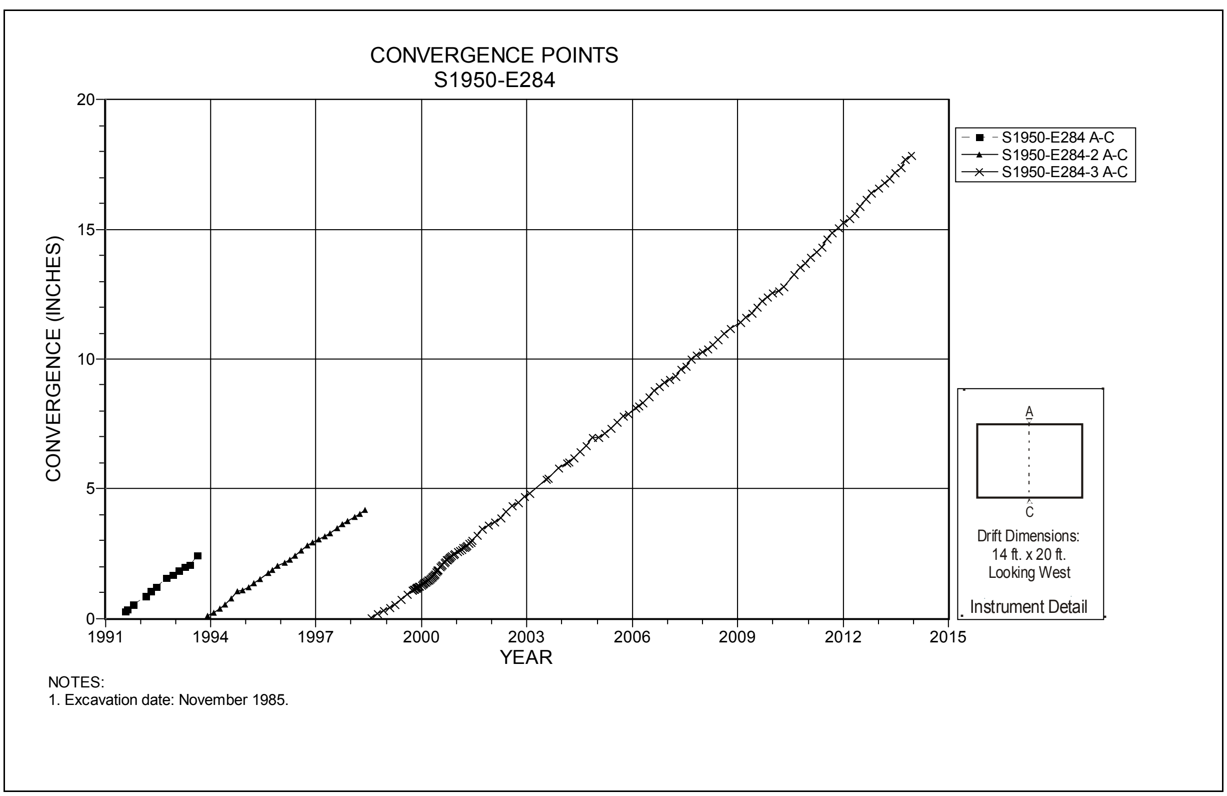

Figure 4-178 Convergence Point Array
S1950 E284 – Roof to Floor

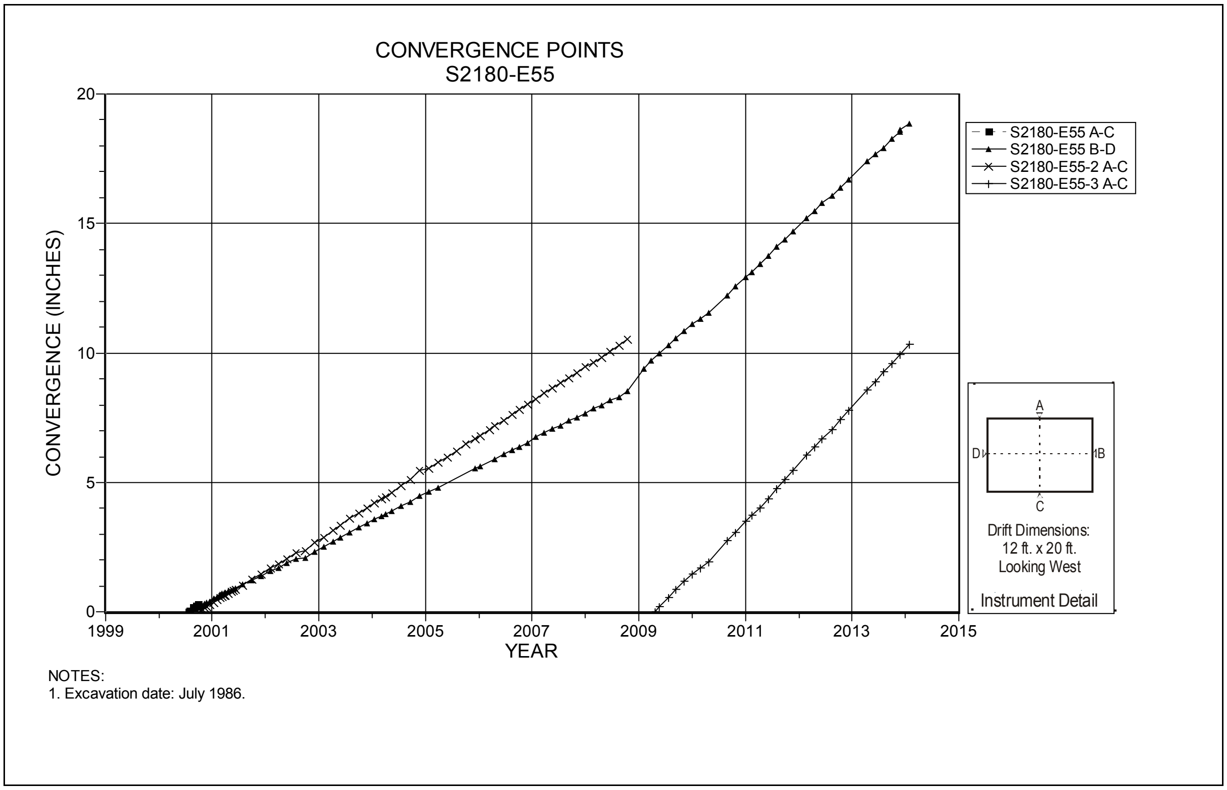

Figure 4-179 Convergence Point Array
S2180 E55 – All Chords

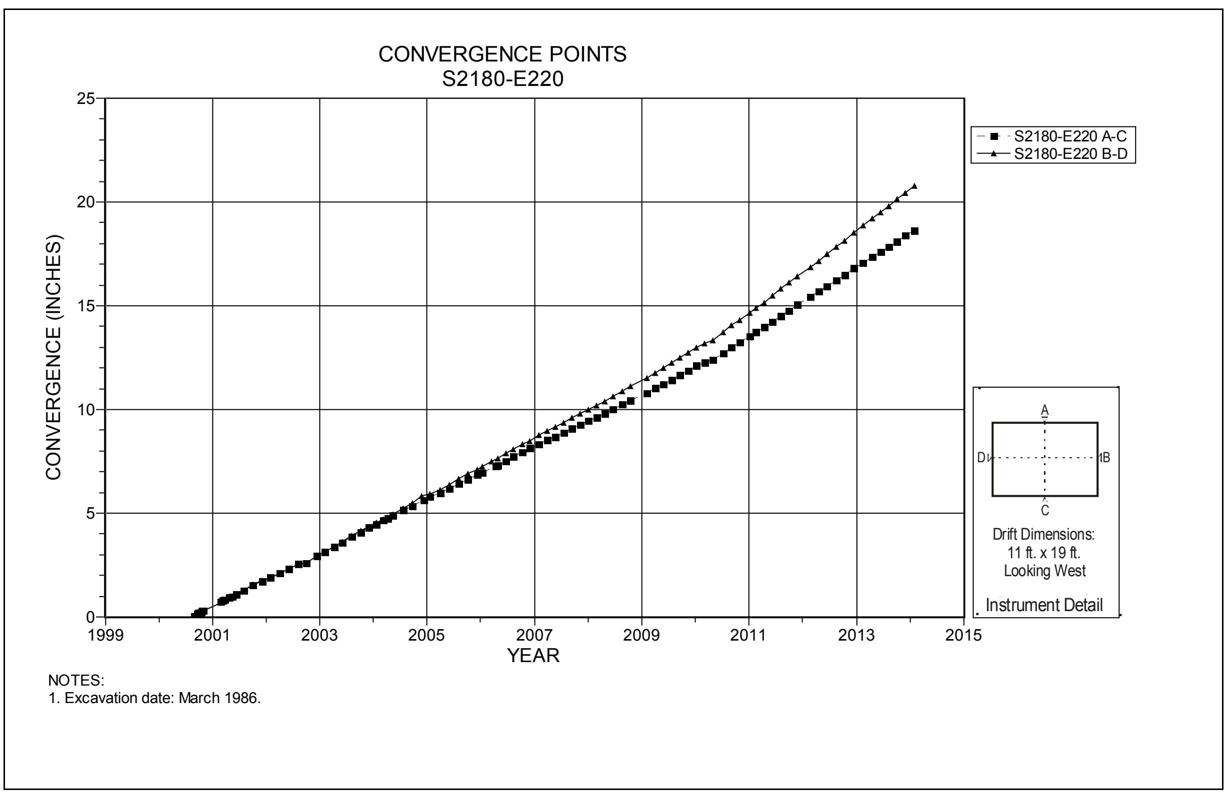

Figure 4-180 Convergence Point Array
S2180 E220 – All Chords

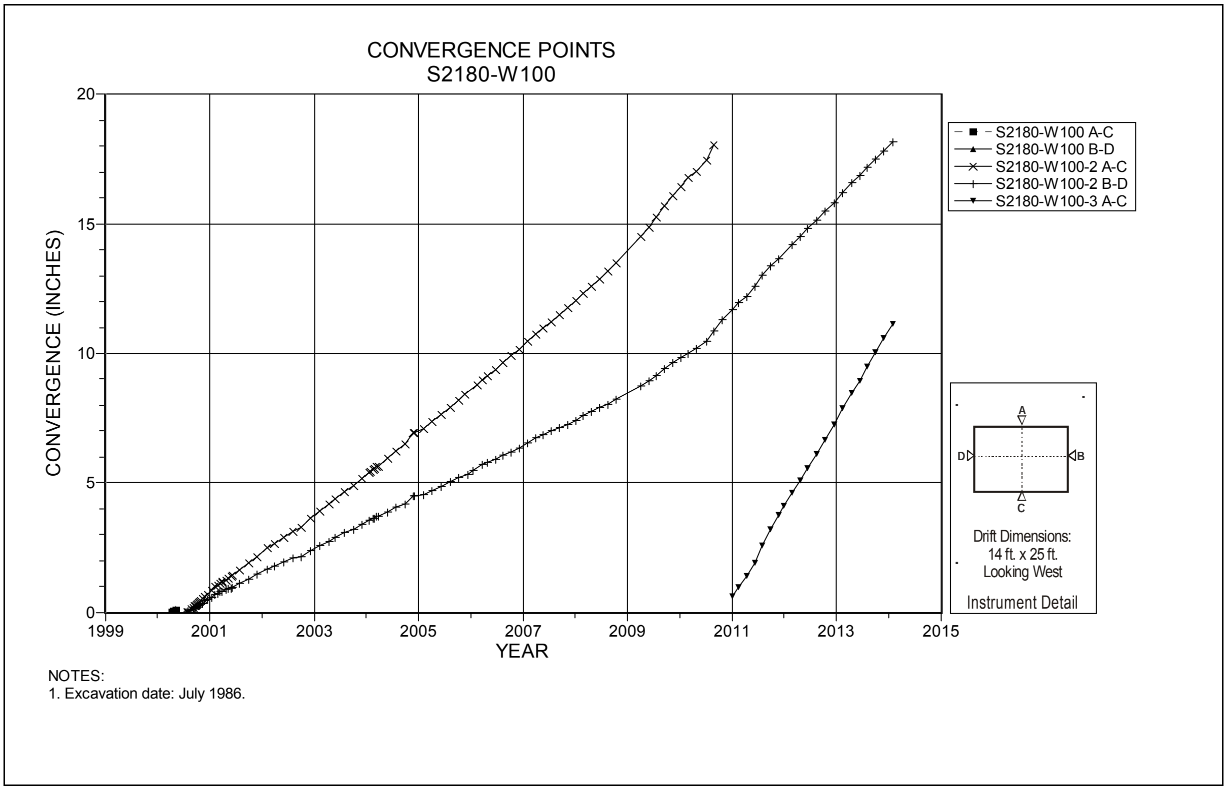

Figure 4-181 Convergence Point Array
S2180 W100 – All Chords

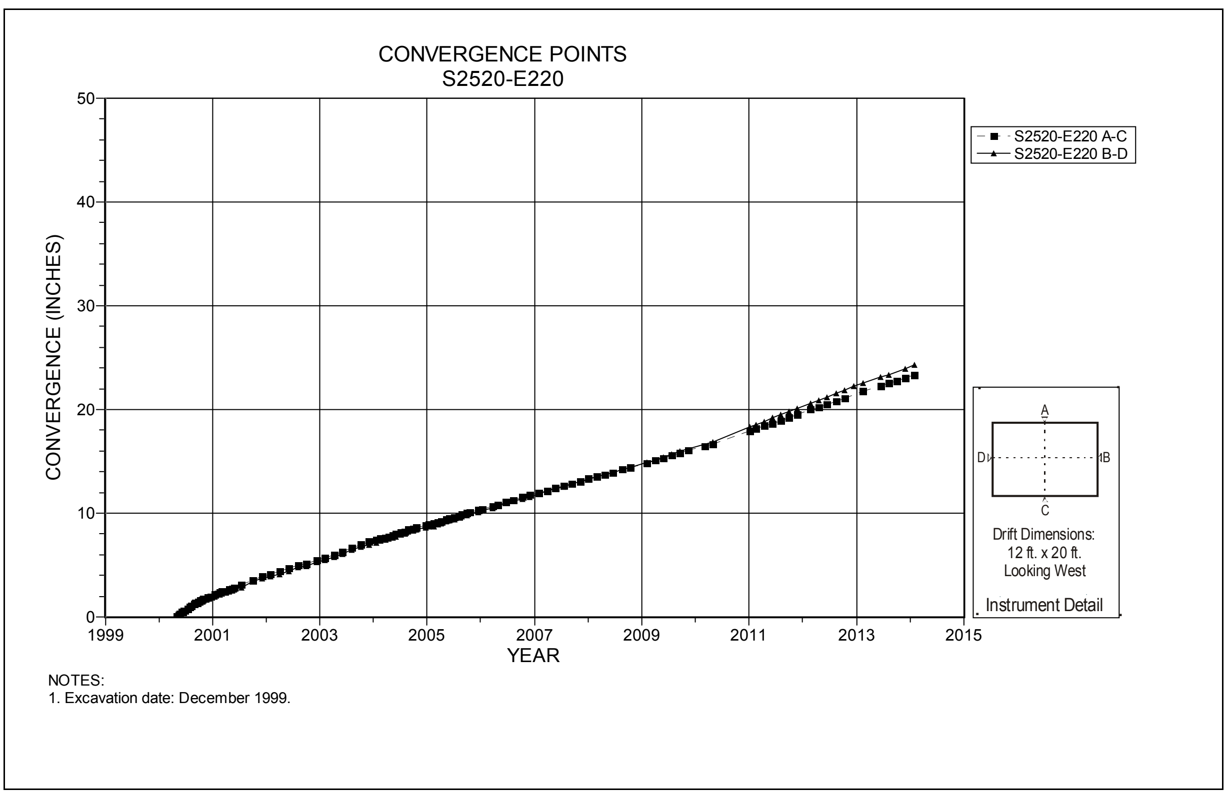

Figure 4-182 Convergence Point Array
S2520 E220 – All Chords

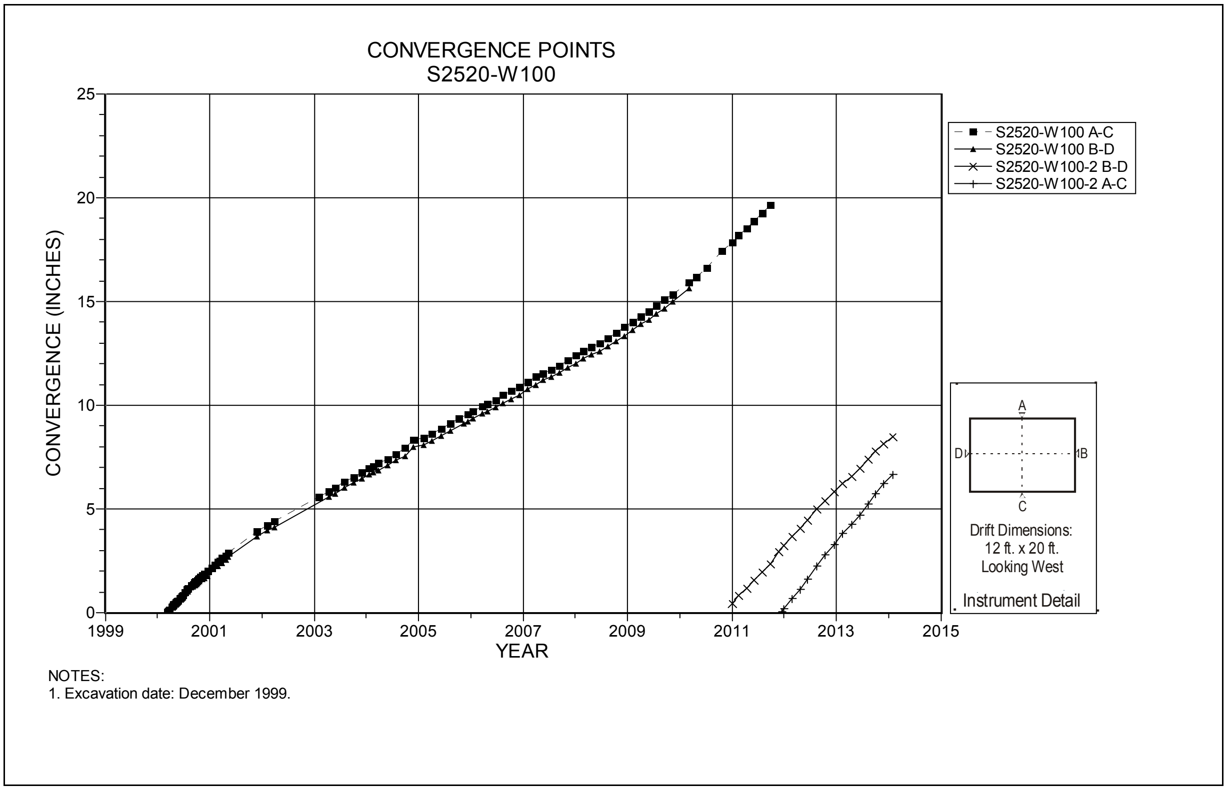

Figure 4-183 Convergence Point Array
S2520 W100 – All Chords

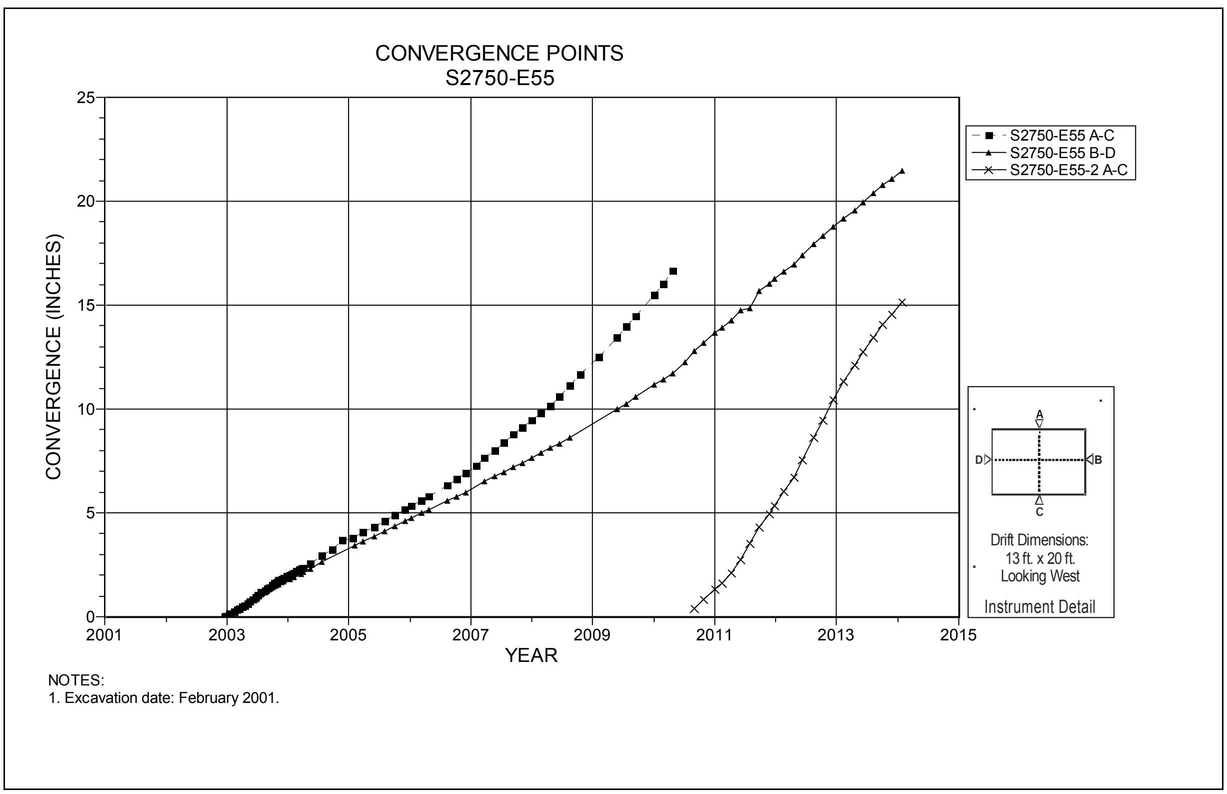

Figure 4-184 Convergence Point Array
S2750 E55 – All Chords

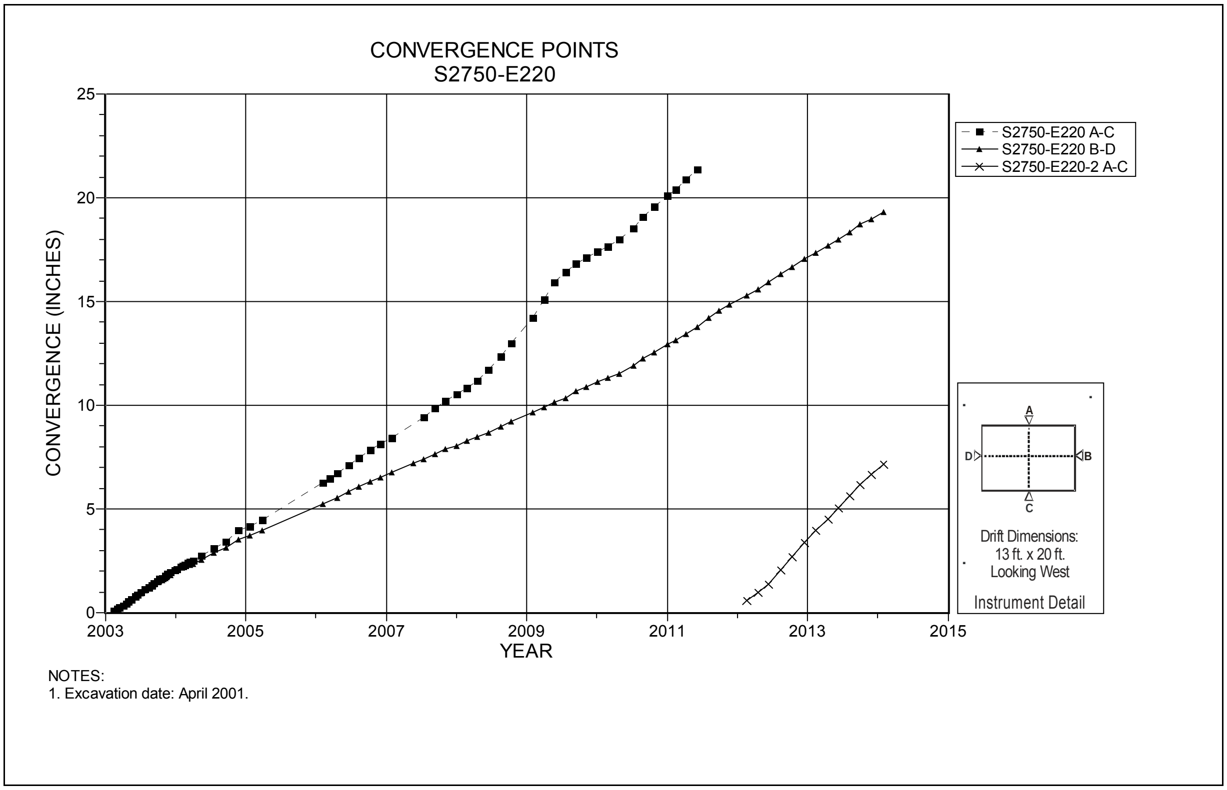

Figure 4-185 Convergence Point Array
S2750 E220 – All Chords

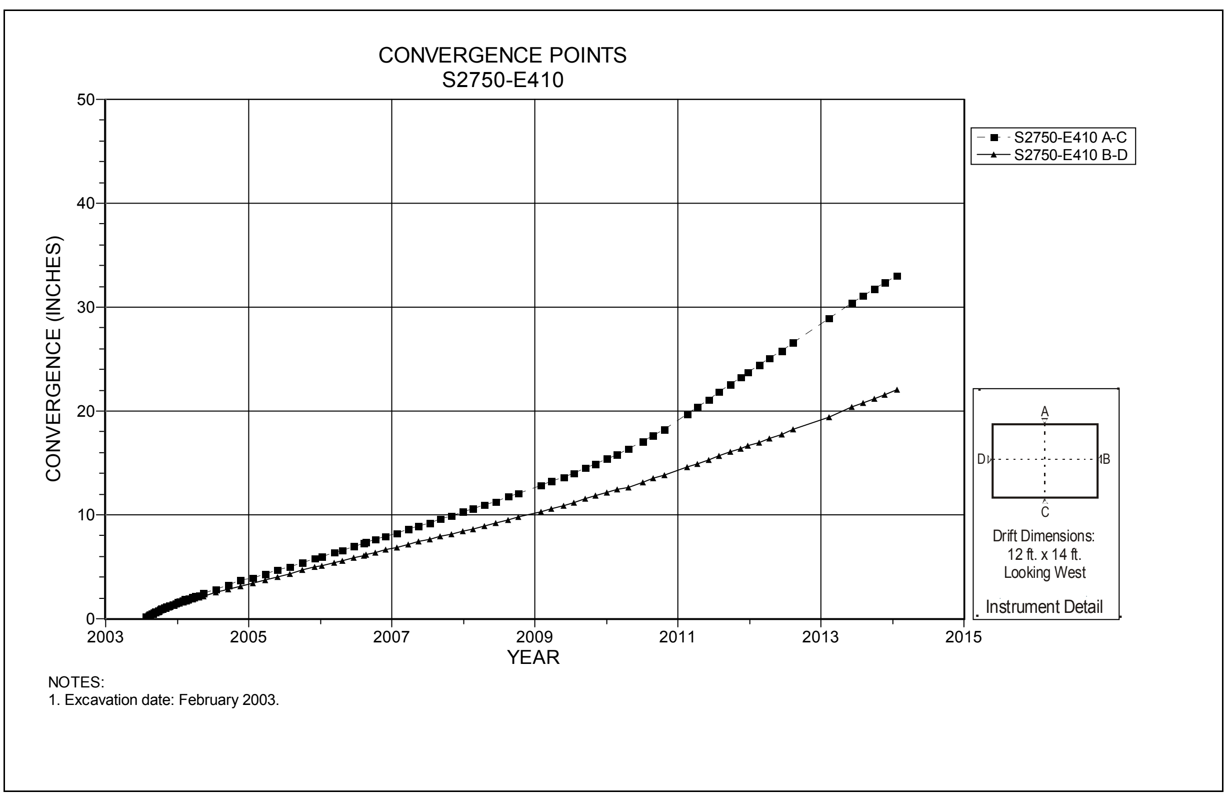

Figure 4-186 Convergence Point Array
S2750 E410 – All Chords

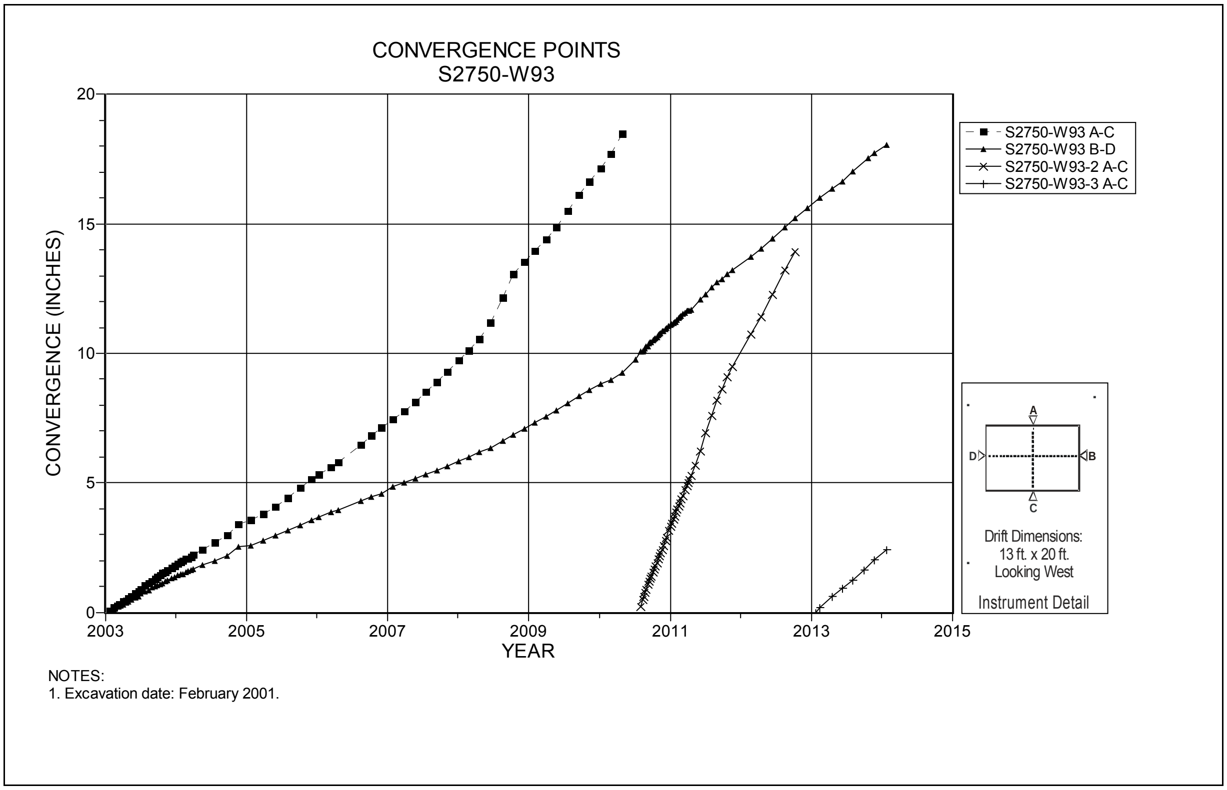

Figure 4-187 Convergence Point Array
S2750 W93 – All Chords

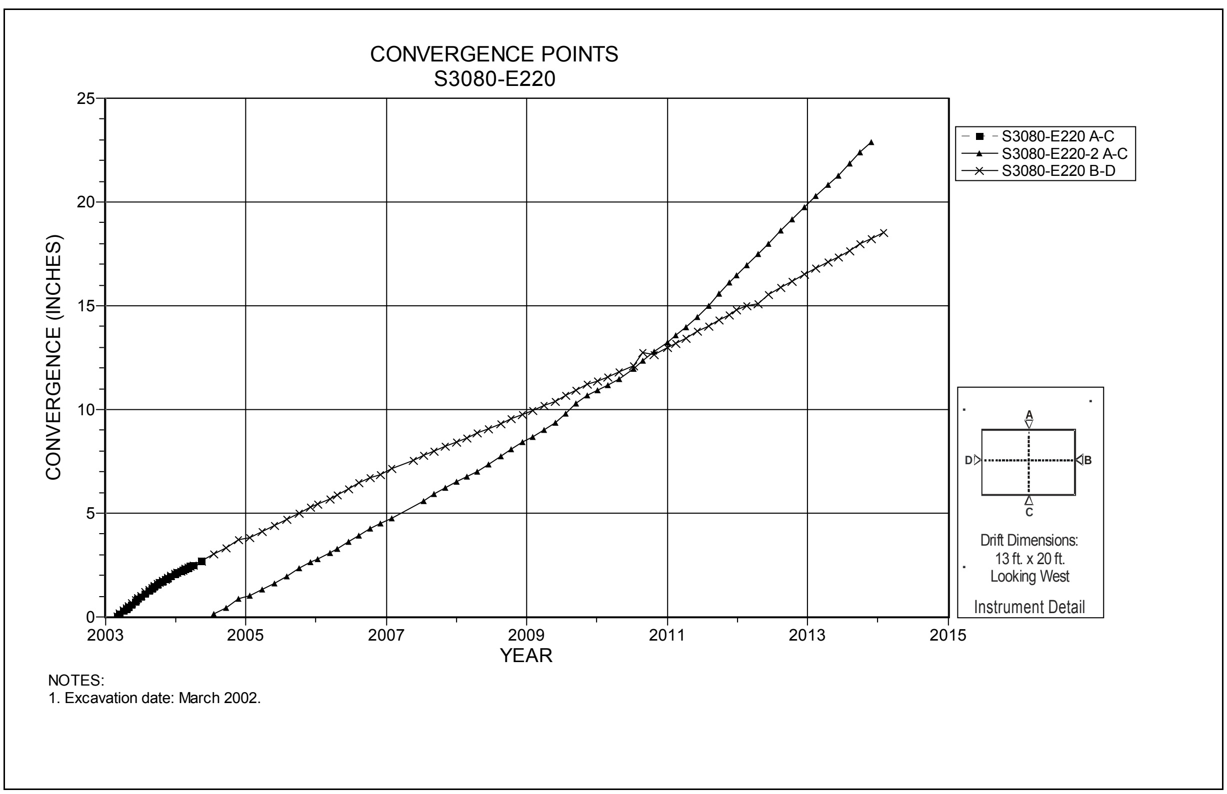

Figure 4-188 Convergence Point Array
S3080 E220 – All Chords

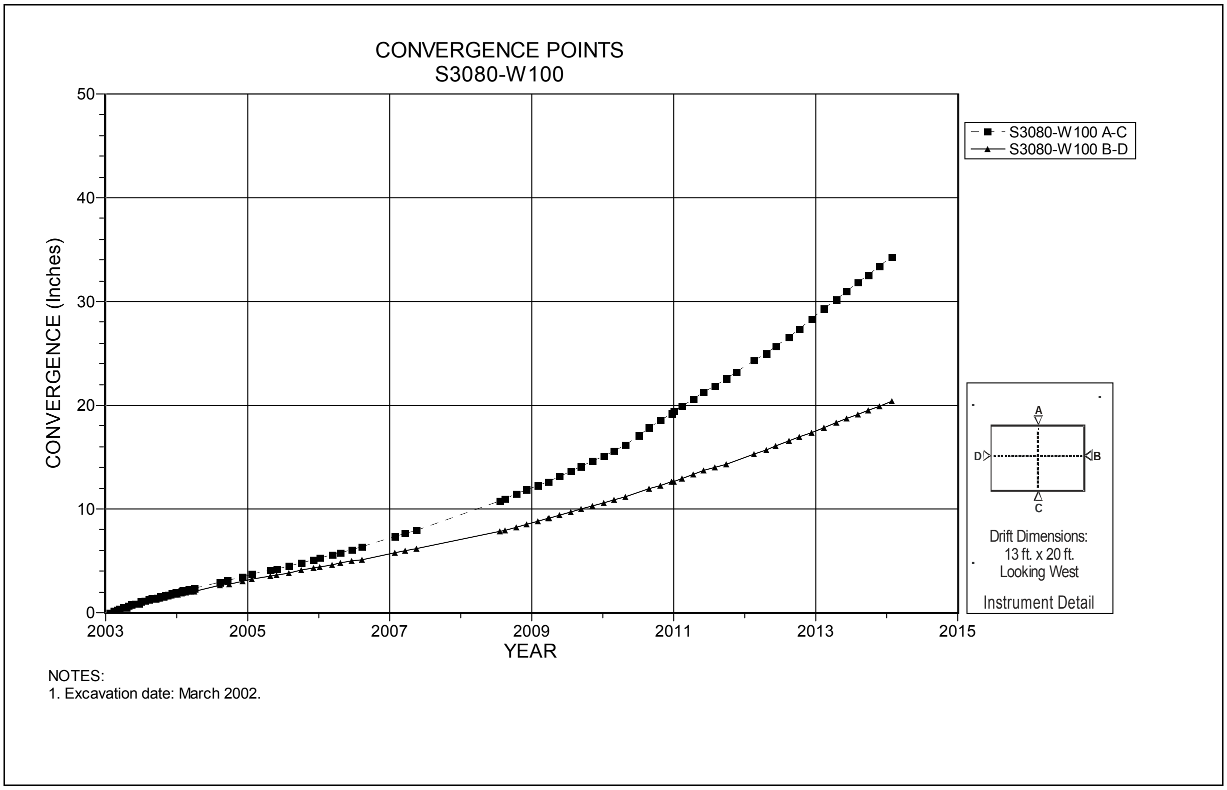

Figure 4-189 Convergence Point Array
S3080 W100 – All Chords

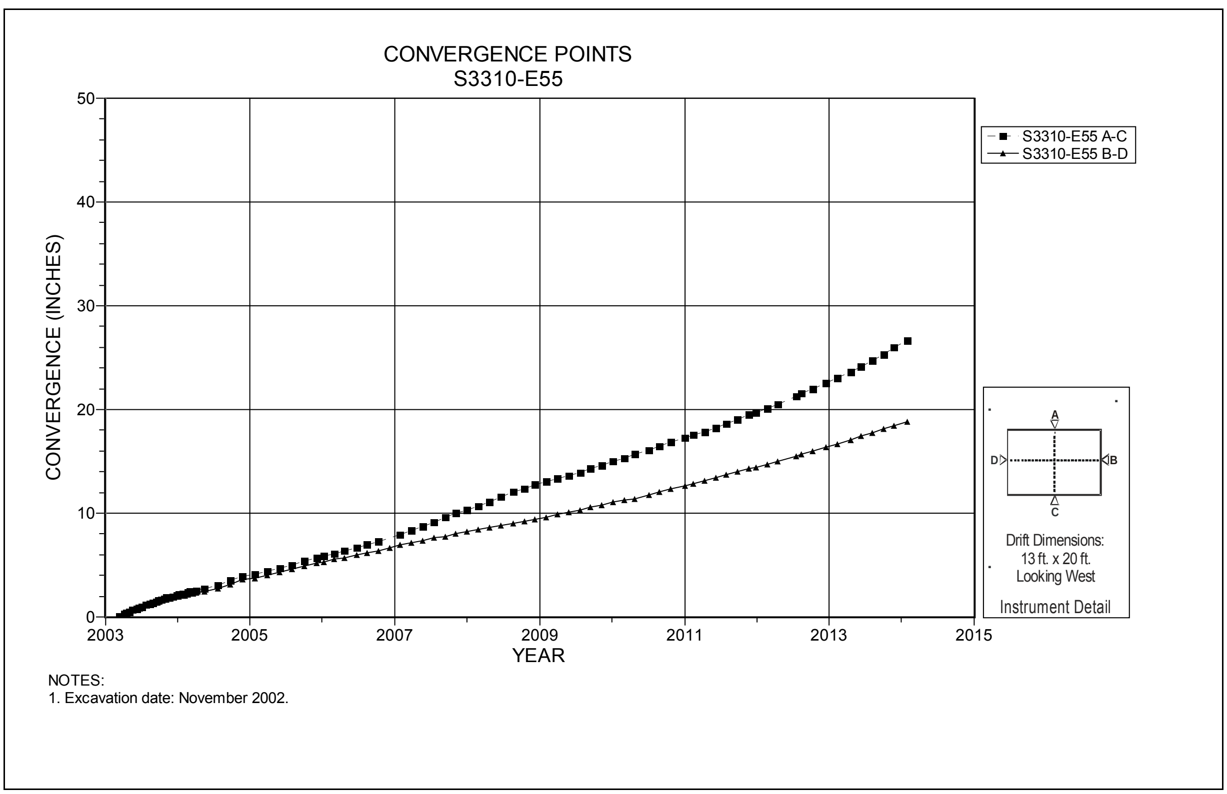

Figure 4-190 Convergence Point Array
S3310 E55 – All Chords

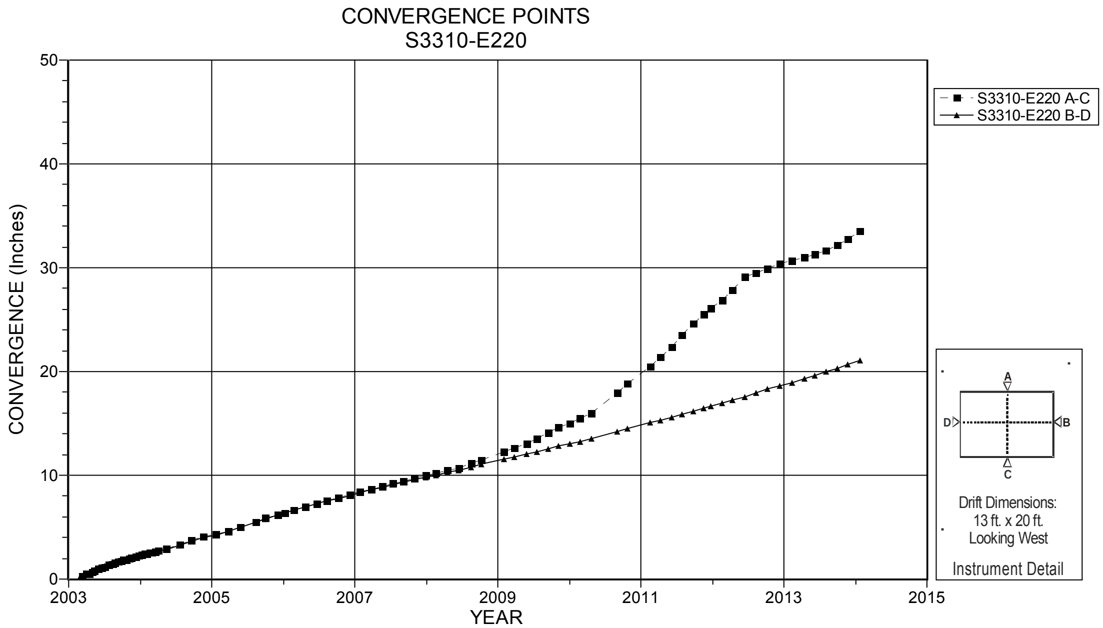

NOTES:
1. Excavation date: November 2002.

Figure 4-191 Convergence Point Array
S3310 E220 – All Chords

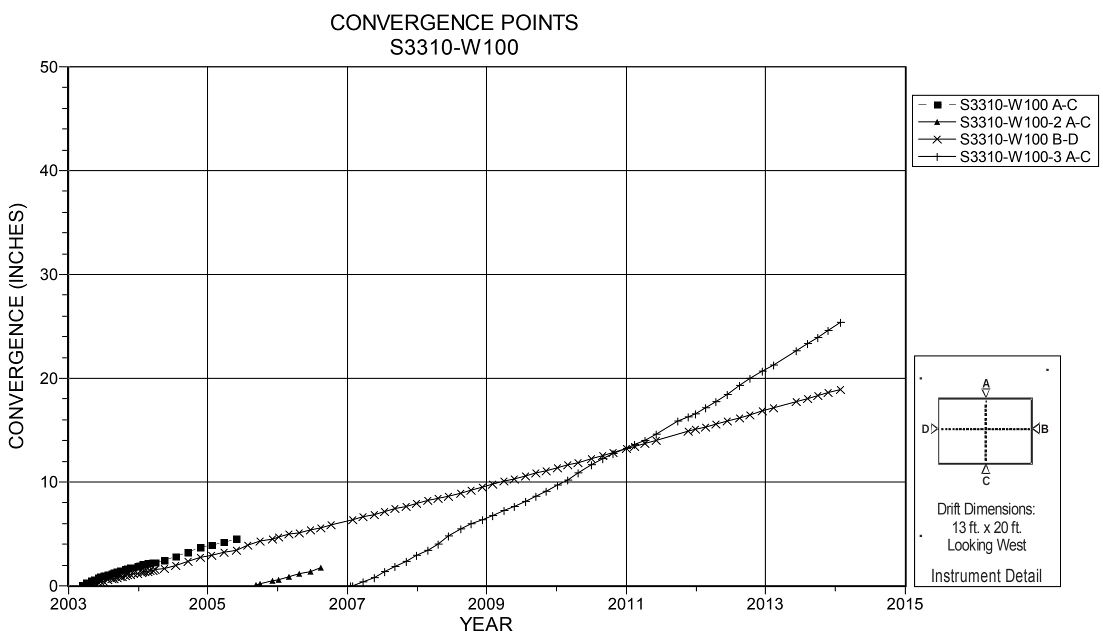

NOTES:
1. Excavation date: November 2002.

Figure 4-192 Convergence Point Array
S3310 W100 – All Chords

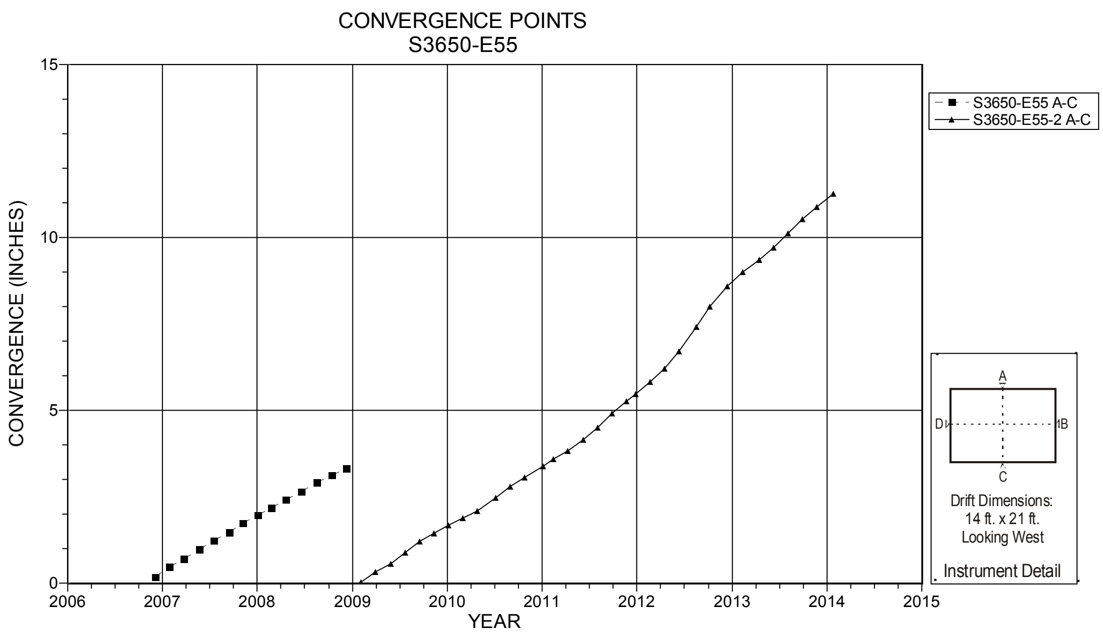

NOTES:
1. Excavation date: September 2004.

Figure 4-193 Convergence Point Array
S3650 E55 – Roof to Floor

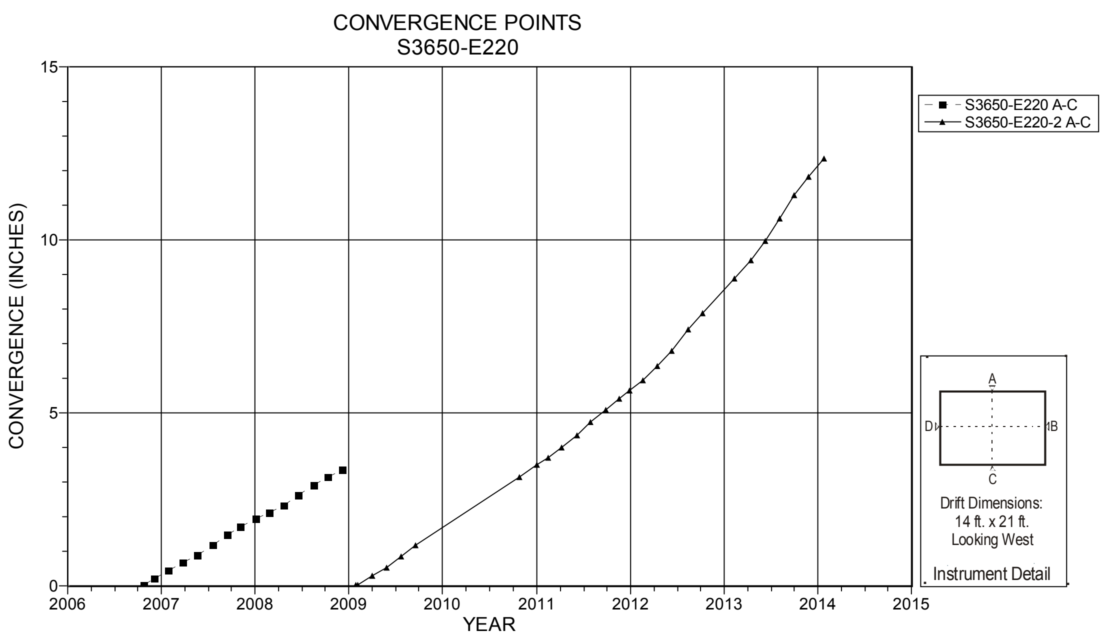

NOTES:
1. Excavation date: December 2004.

Figure 4-194 Convergence Point Array
S3650 E220 – Roof to Floor

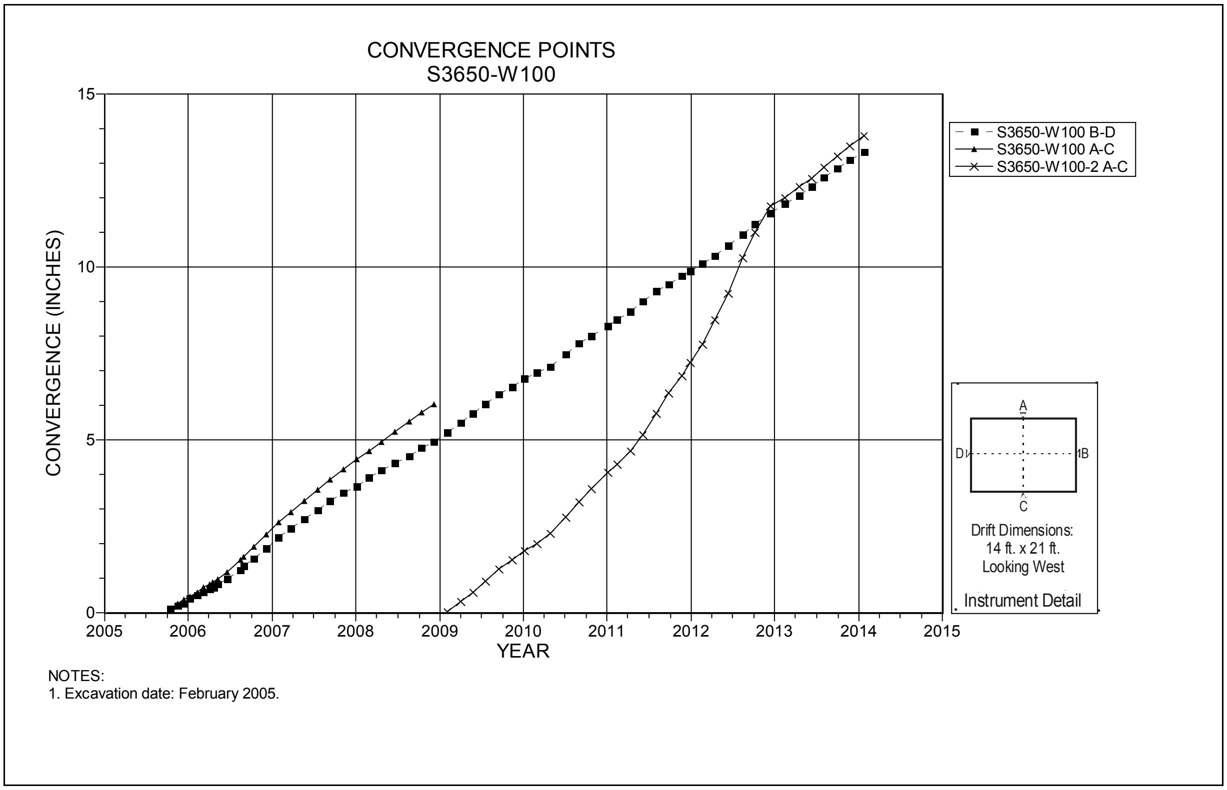

Figure 4-195 Convergence Point Array
S3650 W100 – All Chords

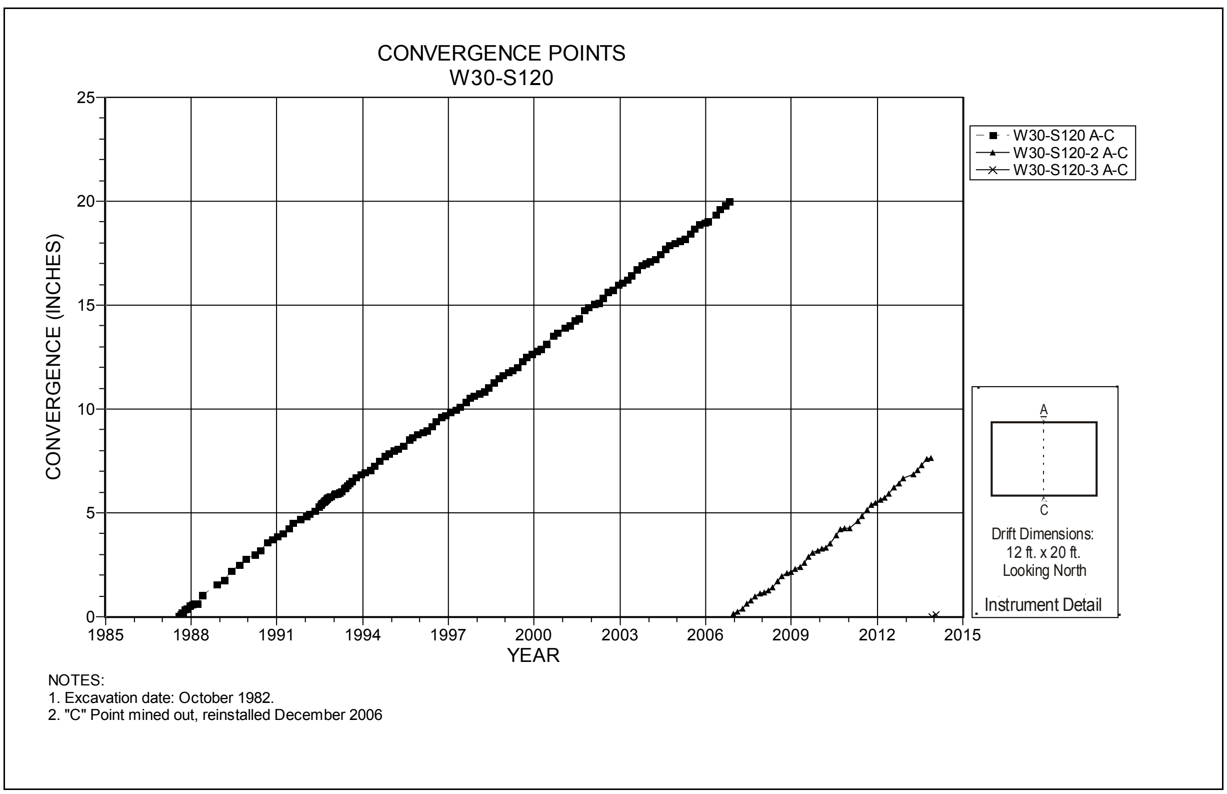

Figure 4-196 Convergence Point Array
W30 S120 – Roof to Floor

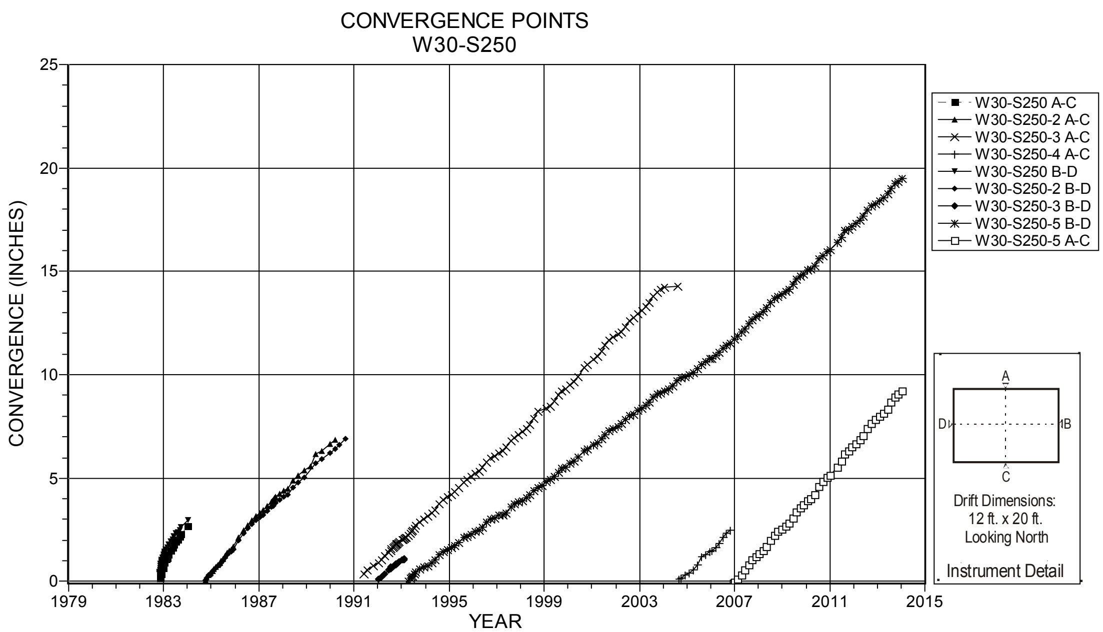

NOTES:
1. Excavation date: October 1982.

Figure 4-197 Convergence Point Array
W30 S250 – All Chords

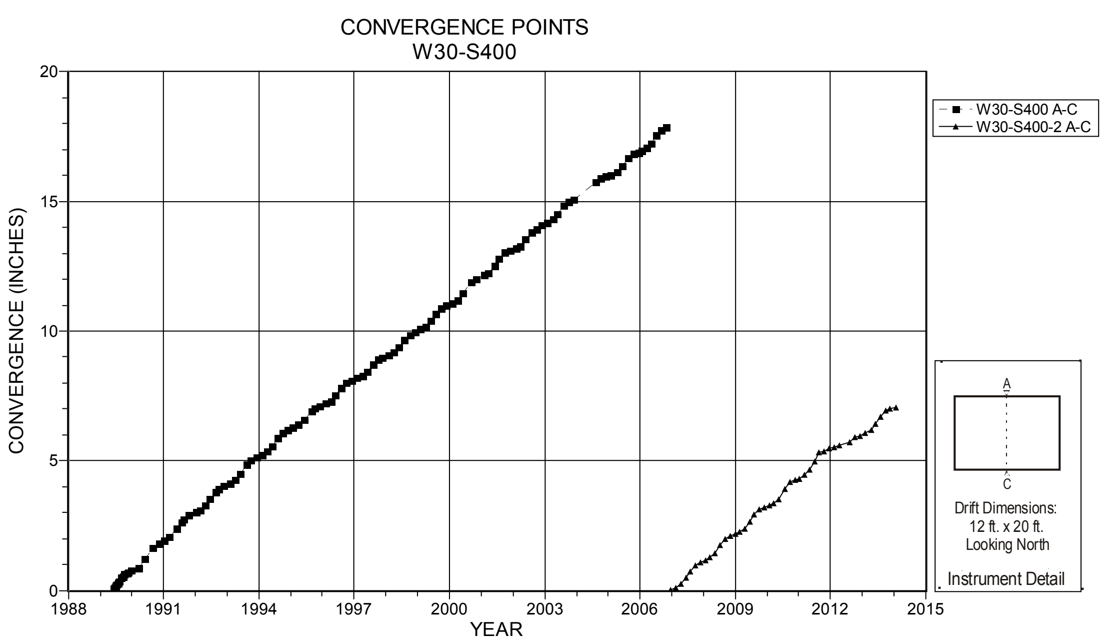

NOTES:
1. Excavation date: October 1982.
2. "C" Point mined out, reinstalled December 2006.

Figure 4-198 Convergence Point Array
W30 S400 – Roof to Floor

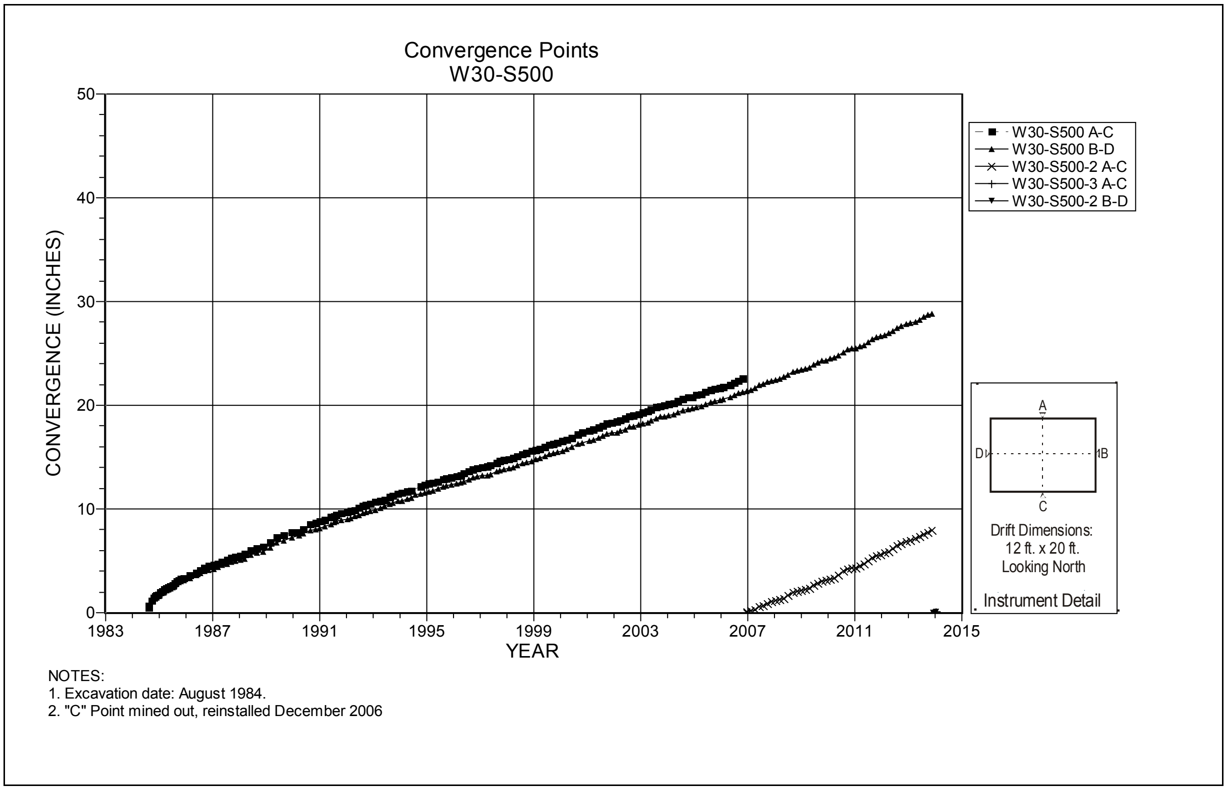

Figure 4-199 Convergence Point Array
W30 S500 – All Chords

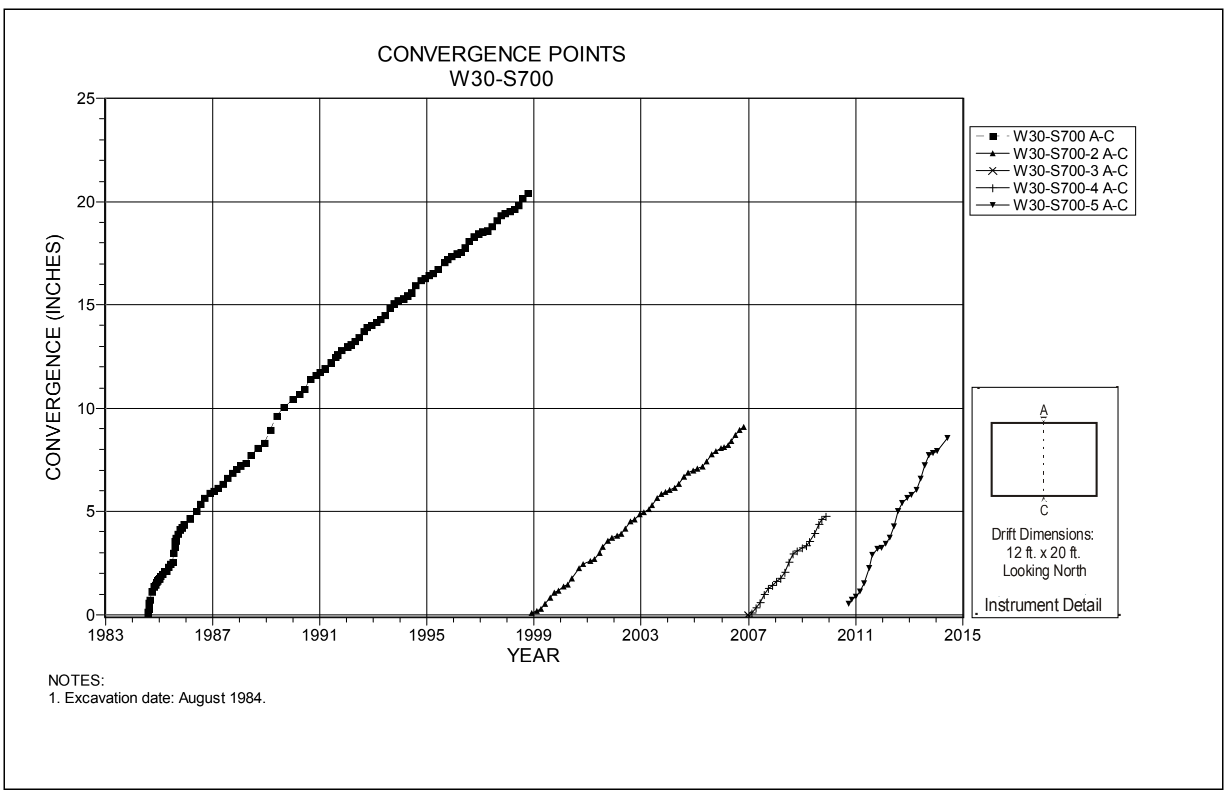

Figure 4-200 Convergence Point Array
W30 S700 – Roof to Floor

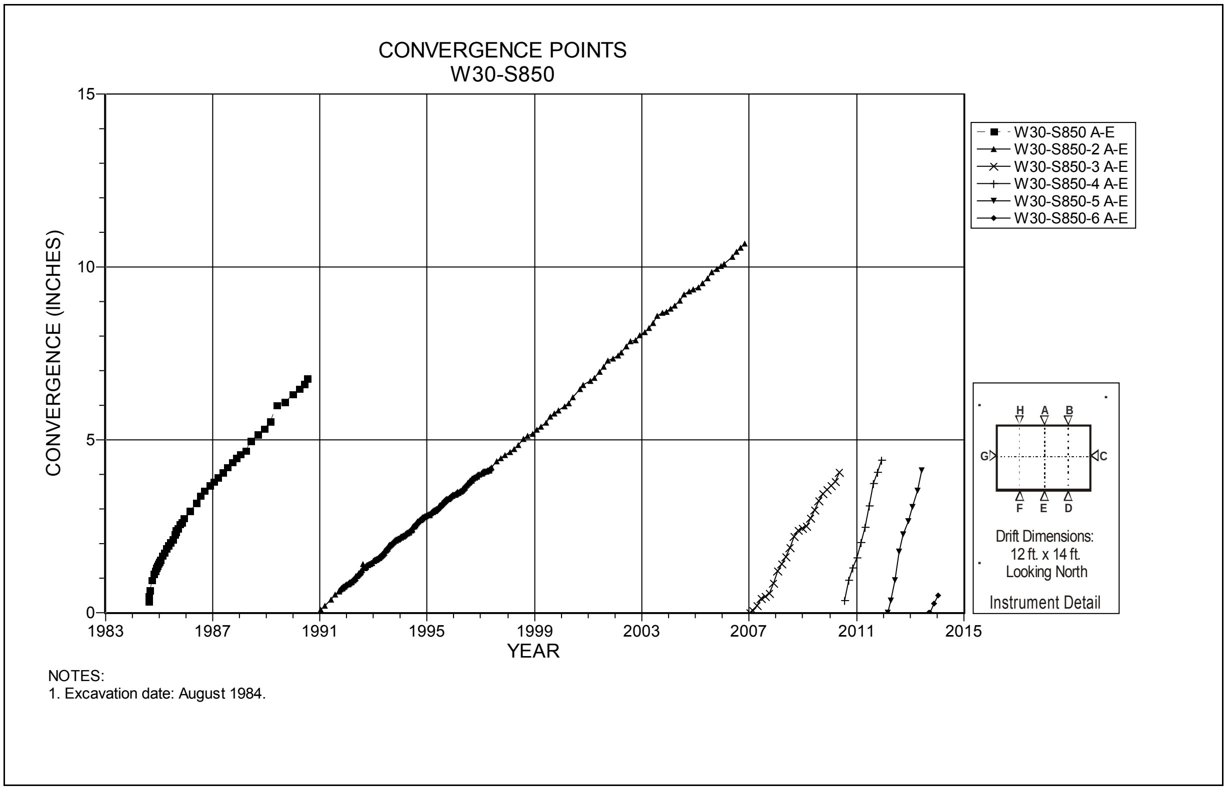

Figure 4-201 Convergence Point Array
W30 S850 – Roof to Floor – Centerline

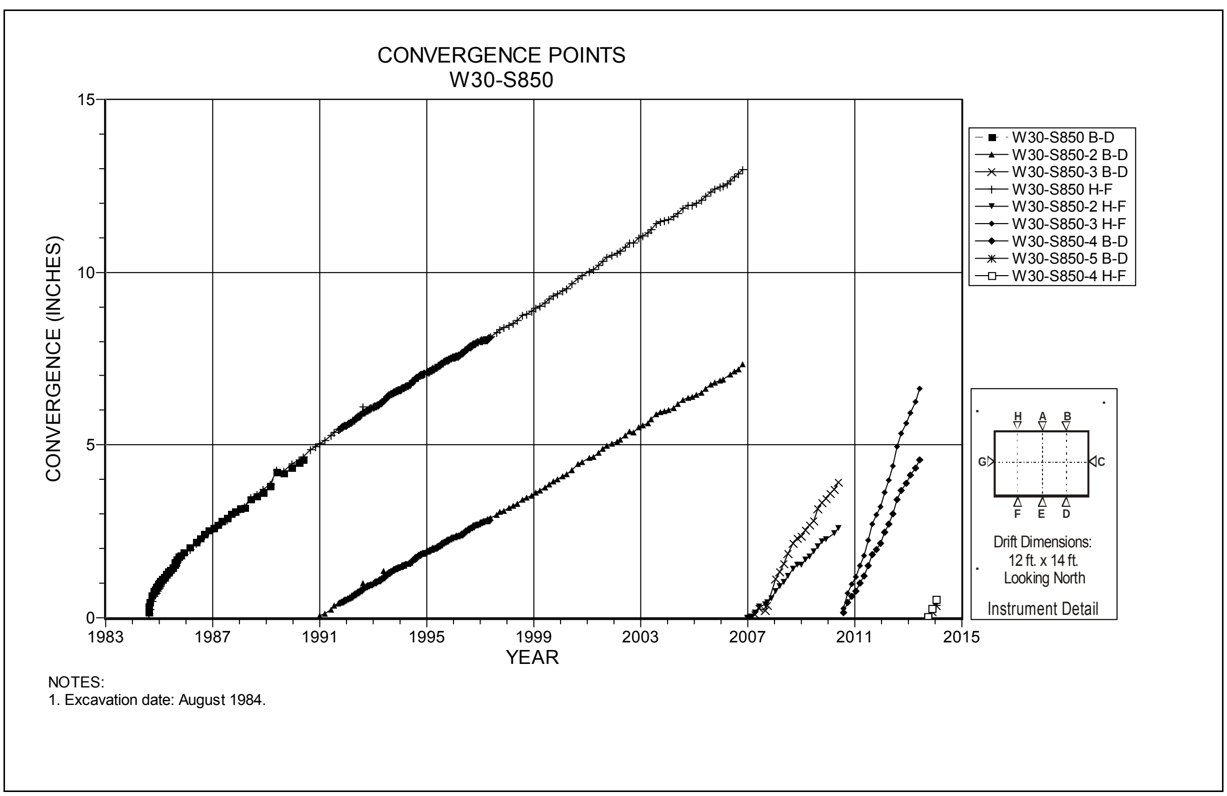

Figure 4-202 Convergence Point Array
W30 S850 – Roof to Floor – Quarter Points

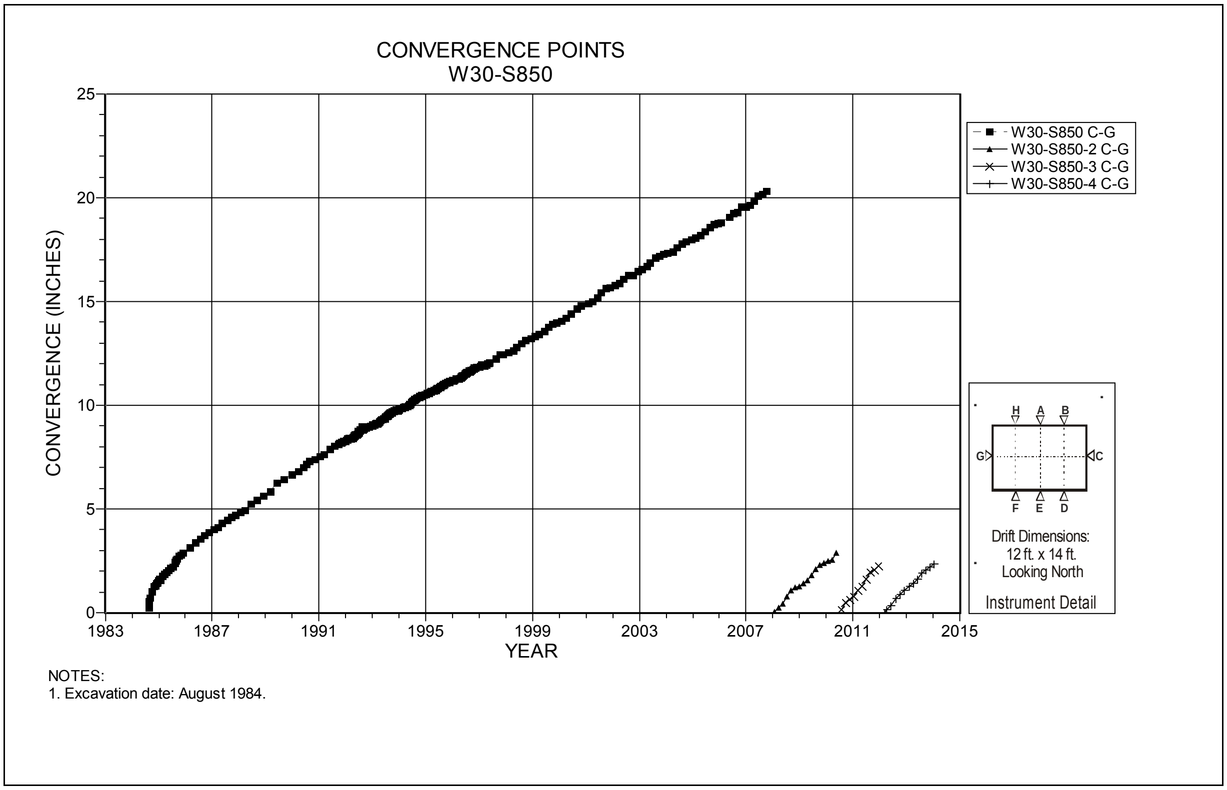

Figure 4-203 Convergence Point Array
W30 S850 – Rib to Rib

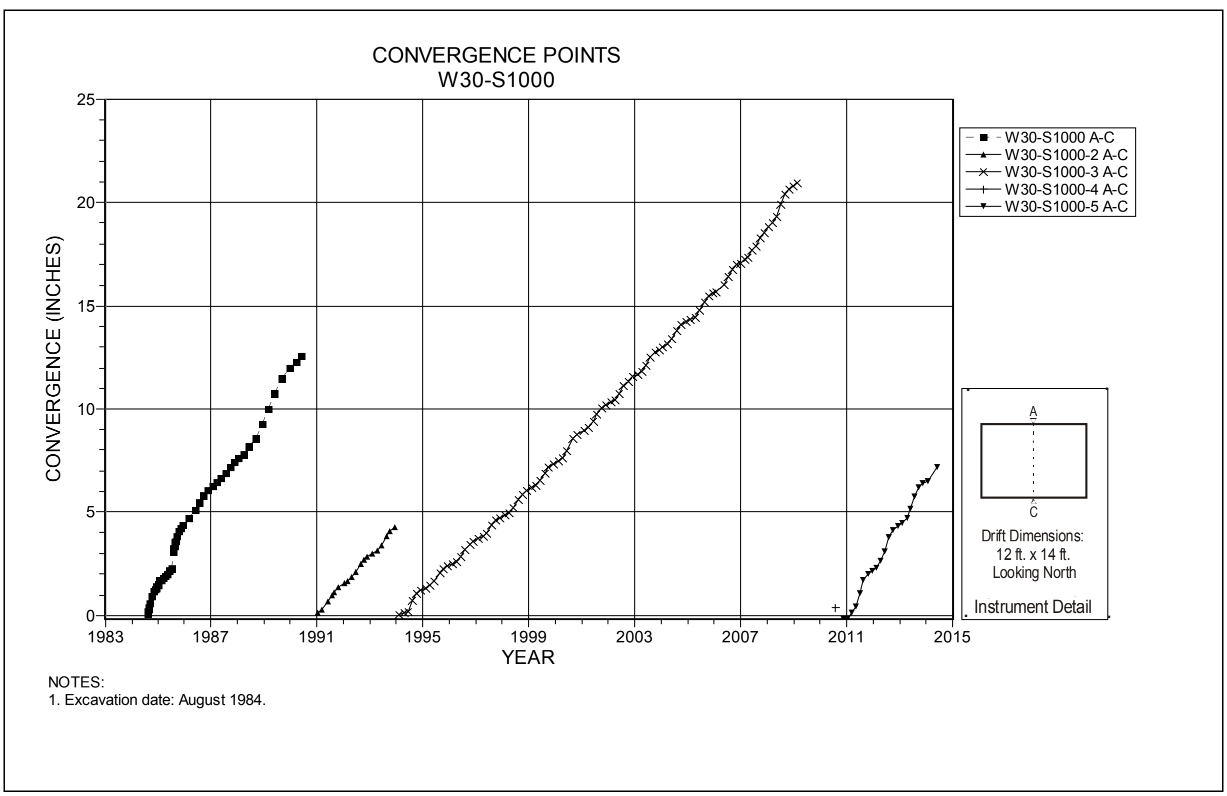

Figure 4-204 Convergence Point Array
W30 S1000 – Roof to Floor

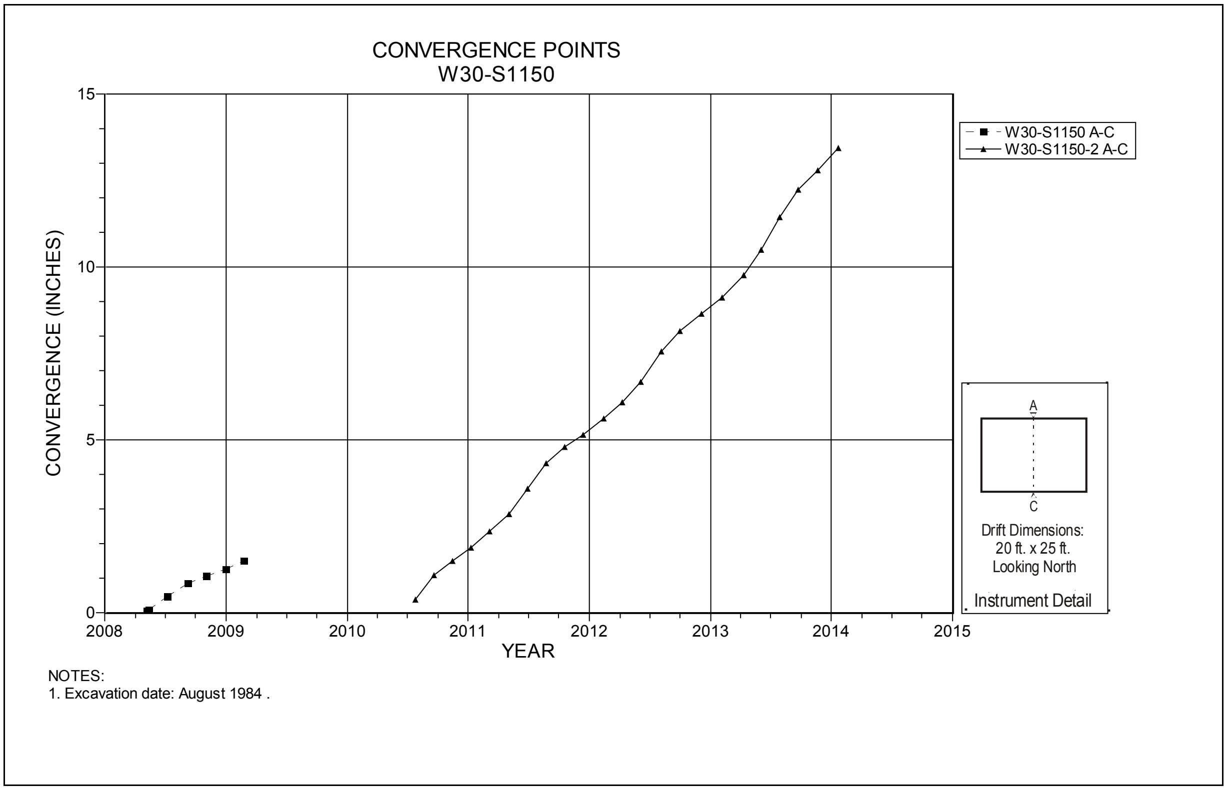

Figure 4-205 Convergence Point Array
W30 S1150 – Roof to Floor

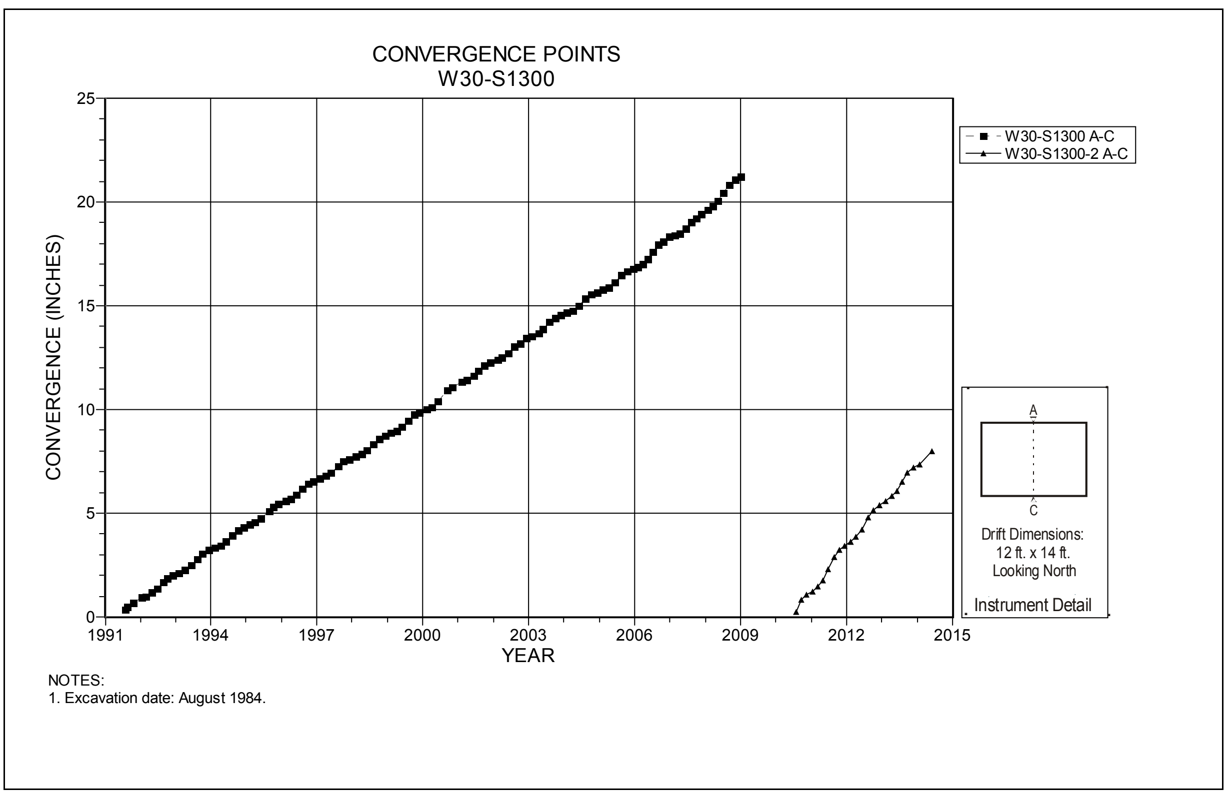

Figure 4-206 Convergence Point Array
W30 S1300 – Roof to Floor

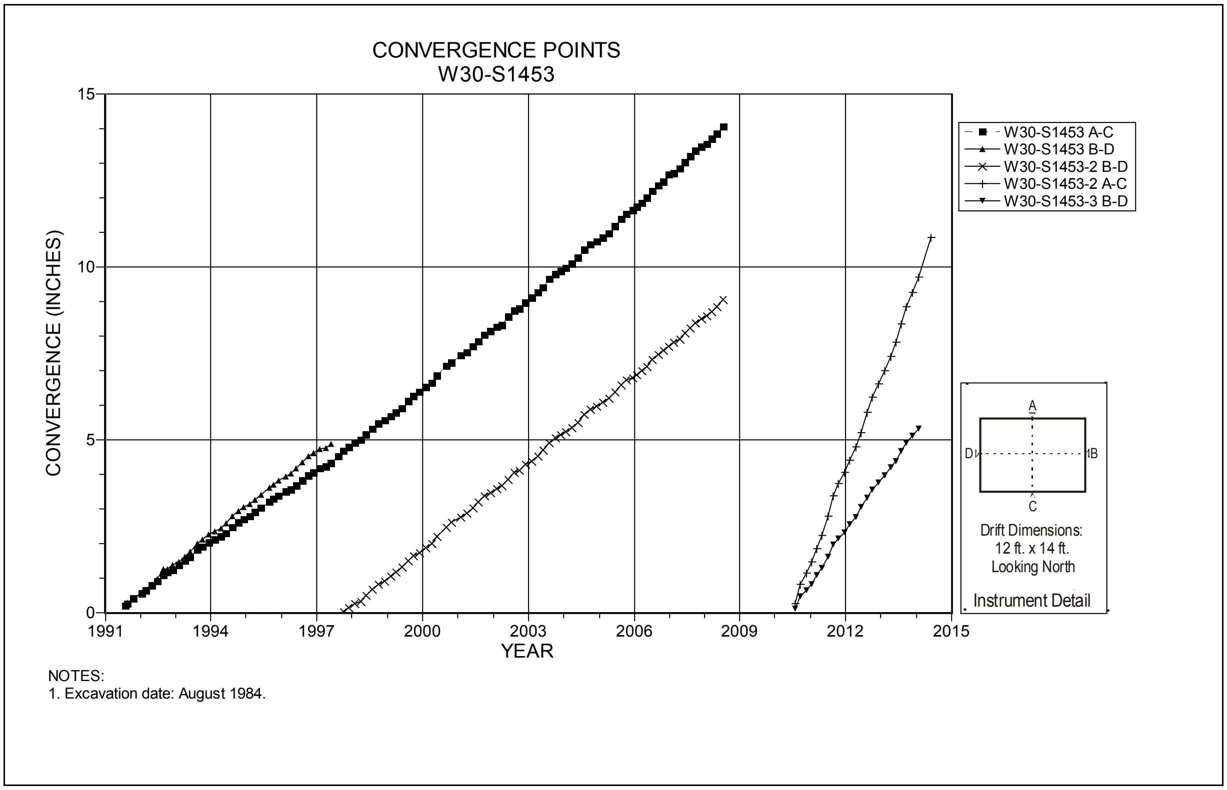

Figure 4-207 Convergence Point Array
W30 S1453 – All Chords

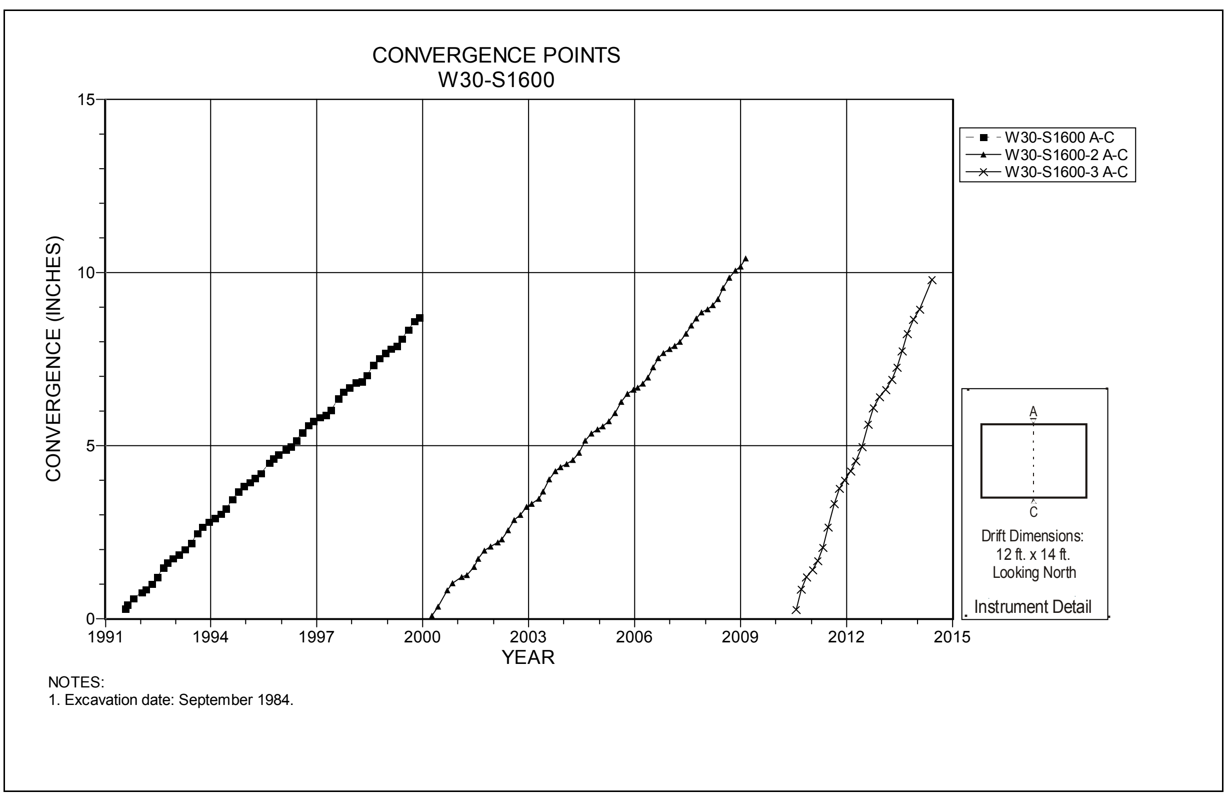

Figure 4-208 Convergence Point Array
W30 S1600 – Roof to Floor

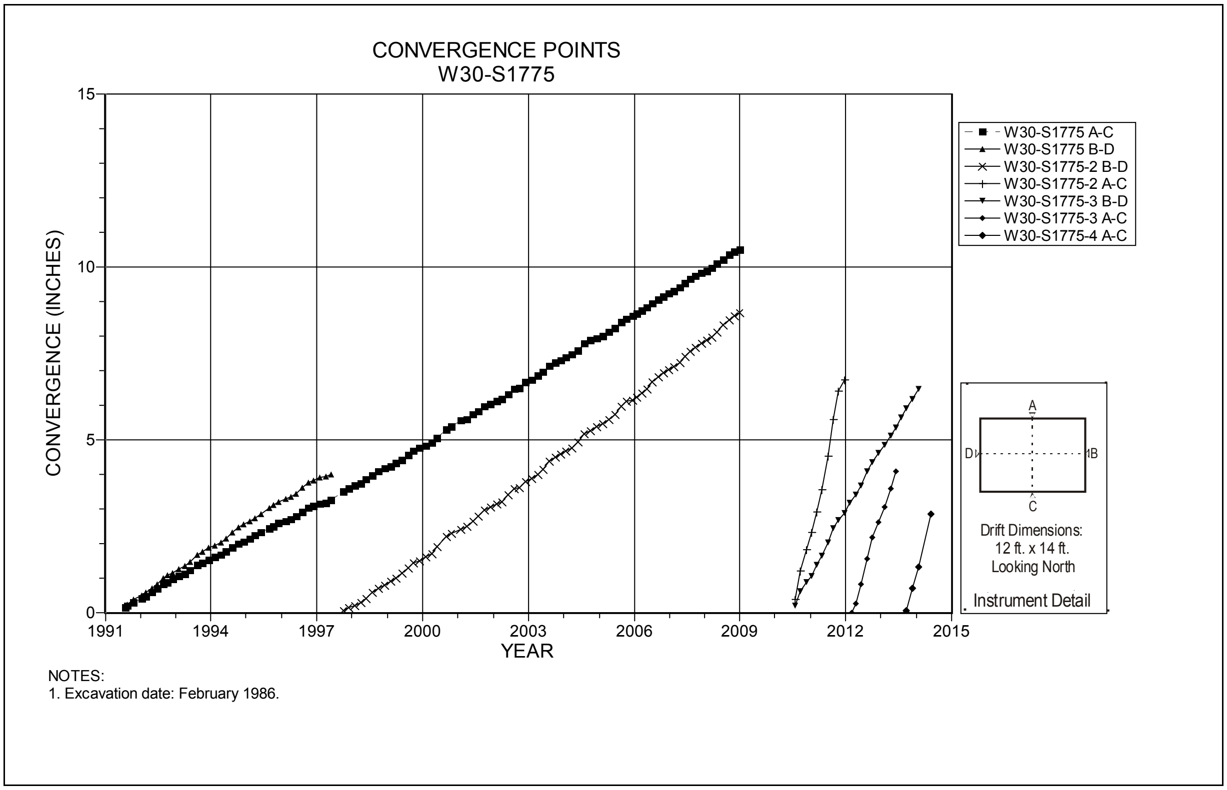

Figure 4-209 Convergence Point Array
W30 S1775 – All Chords

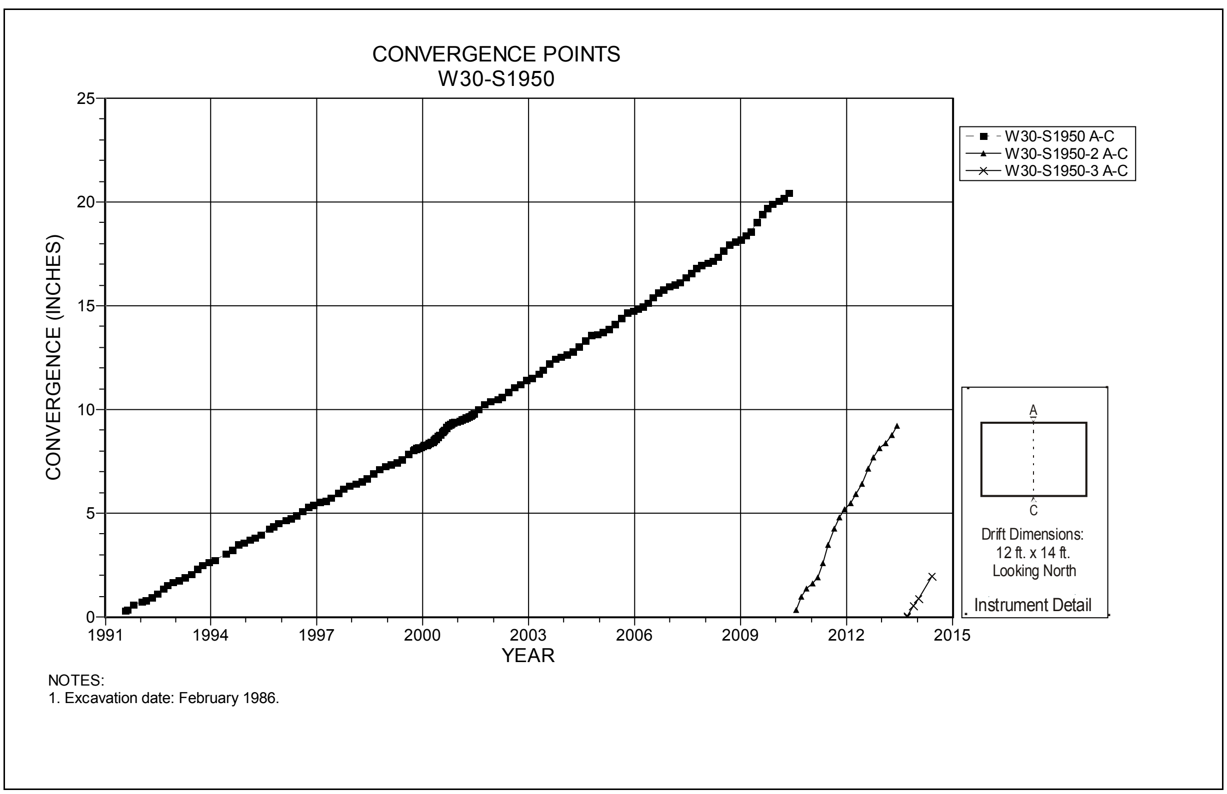

Figure 4-210 Convergence Point Array
W30 S1950 – Roof to Floor

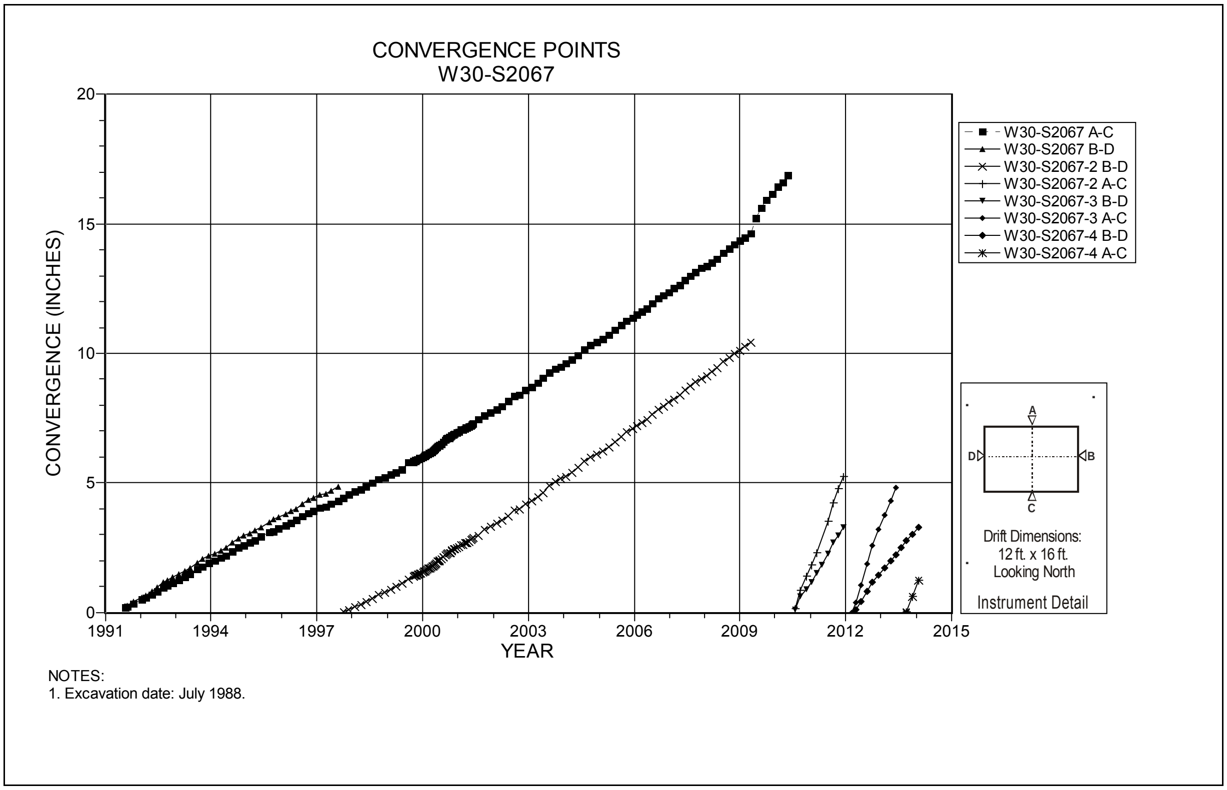

Figure 4-211 Convergence Point Array
W30 S2067 – All Chords

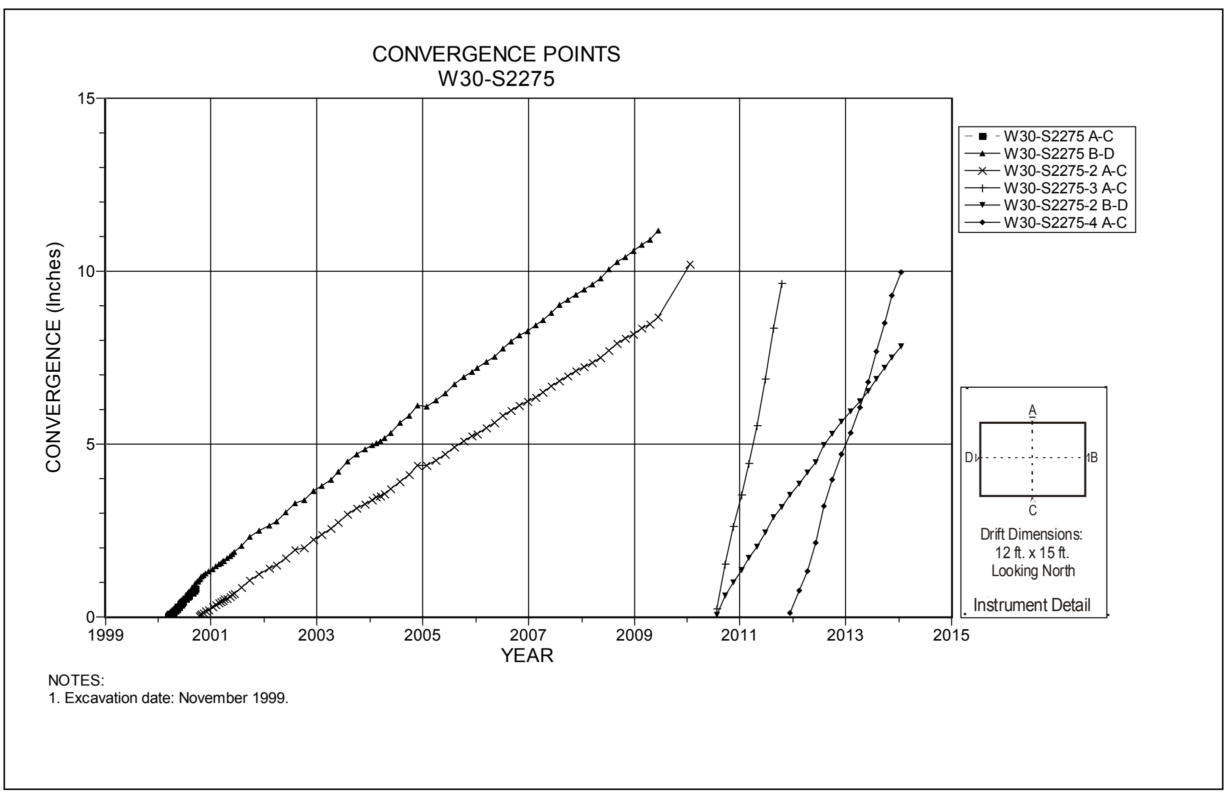

Figure 4-212 Convergence Point Array
W30 S2275 – All Chords

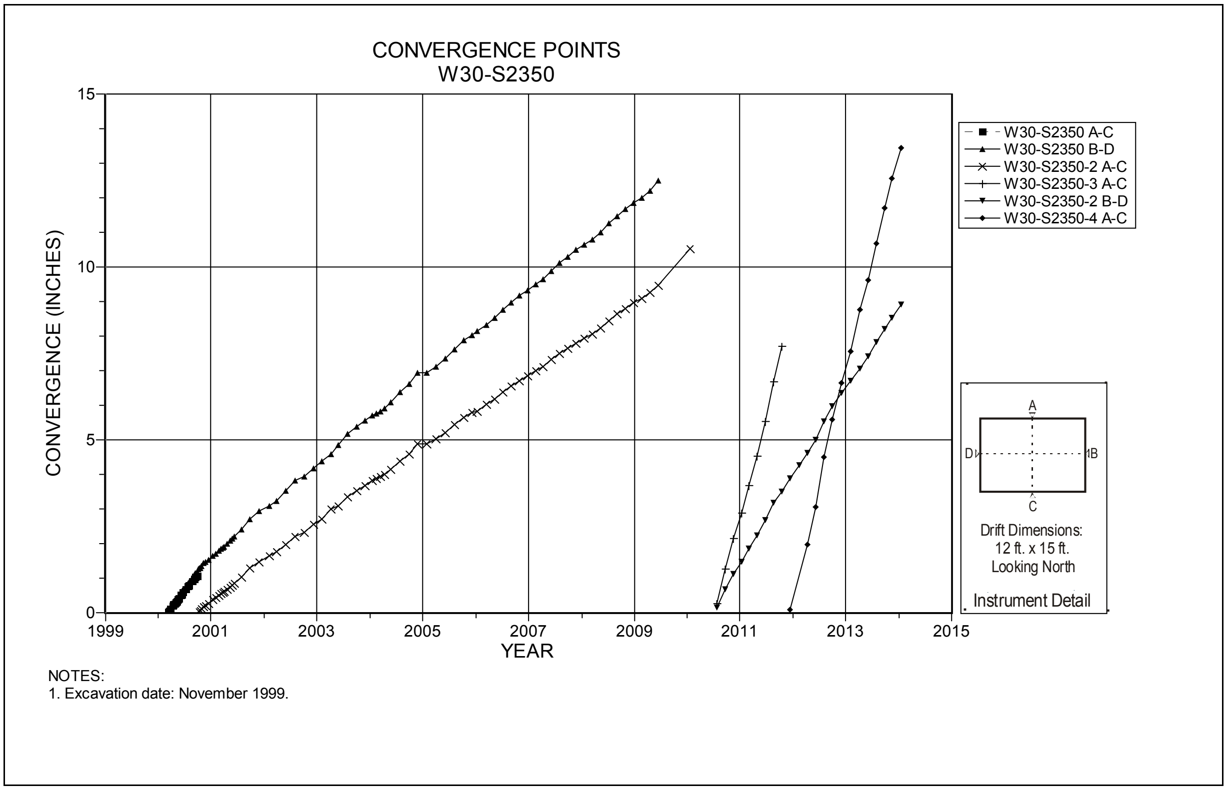

Figure 4-213 Convergence Point Array
W30 S2350 – All Chords

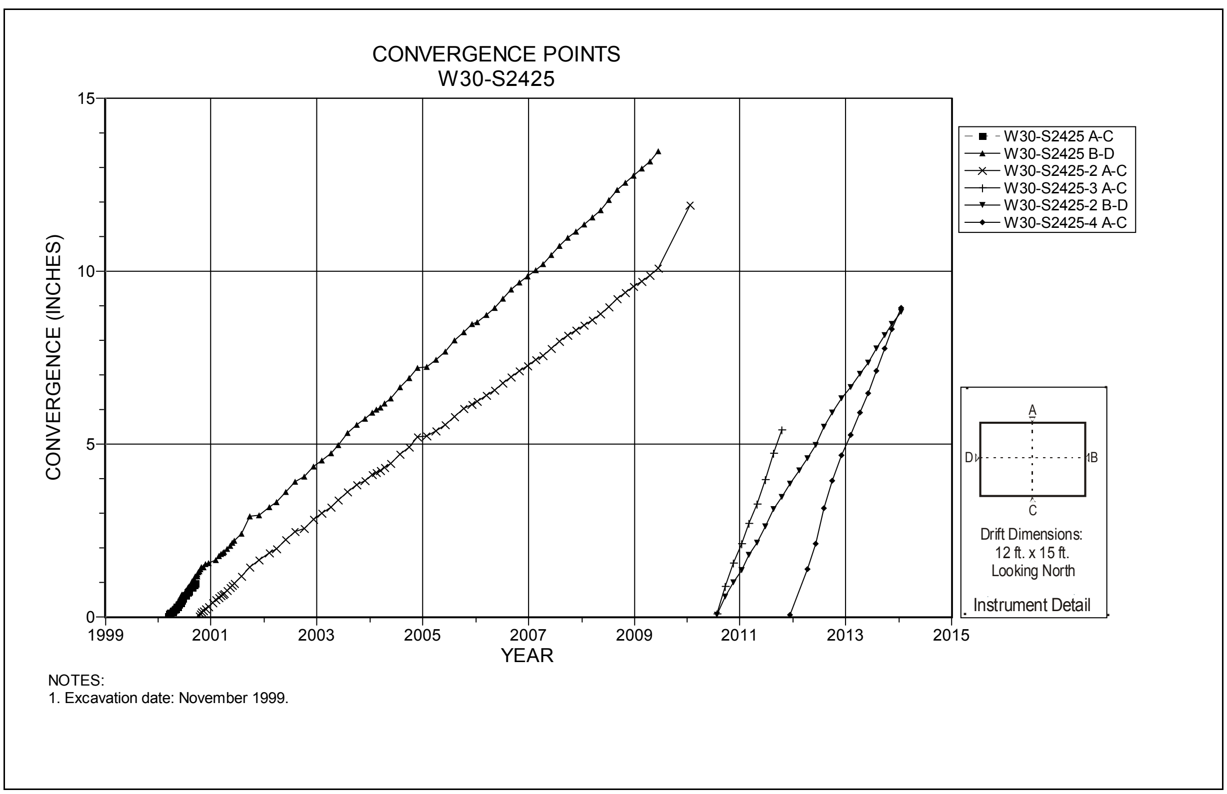

Figure 4-214 Convergence Point Array
W30 S2425 – All Chords

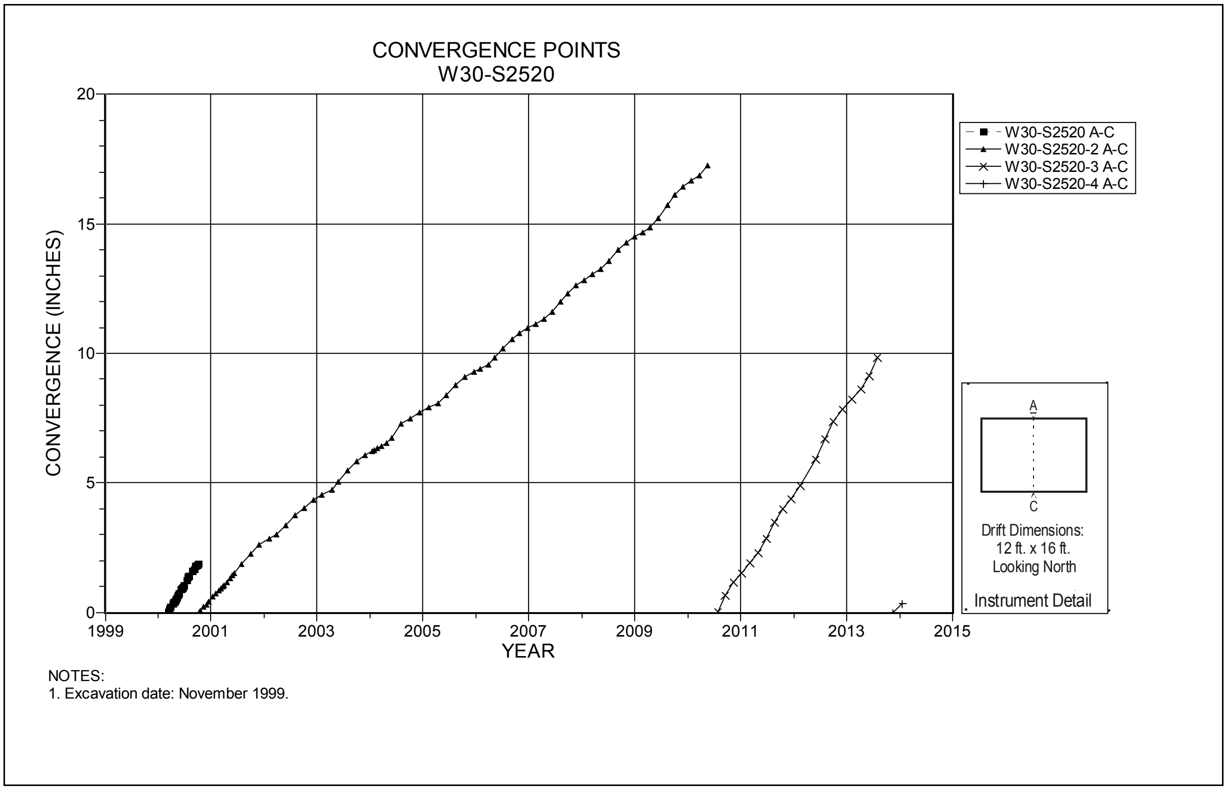

Figure 4-215 Convergence Point Array
W30 S2520 – Roof to Floor

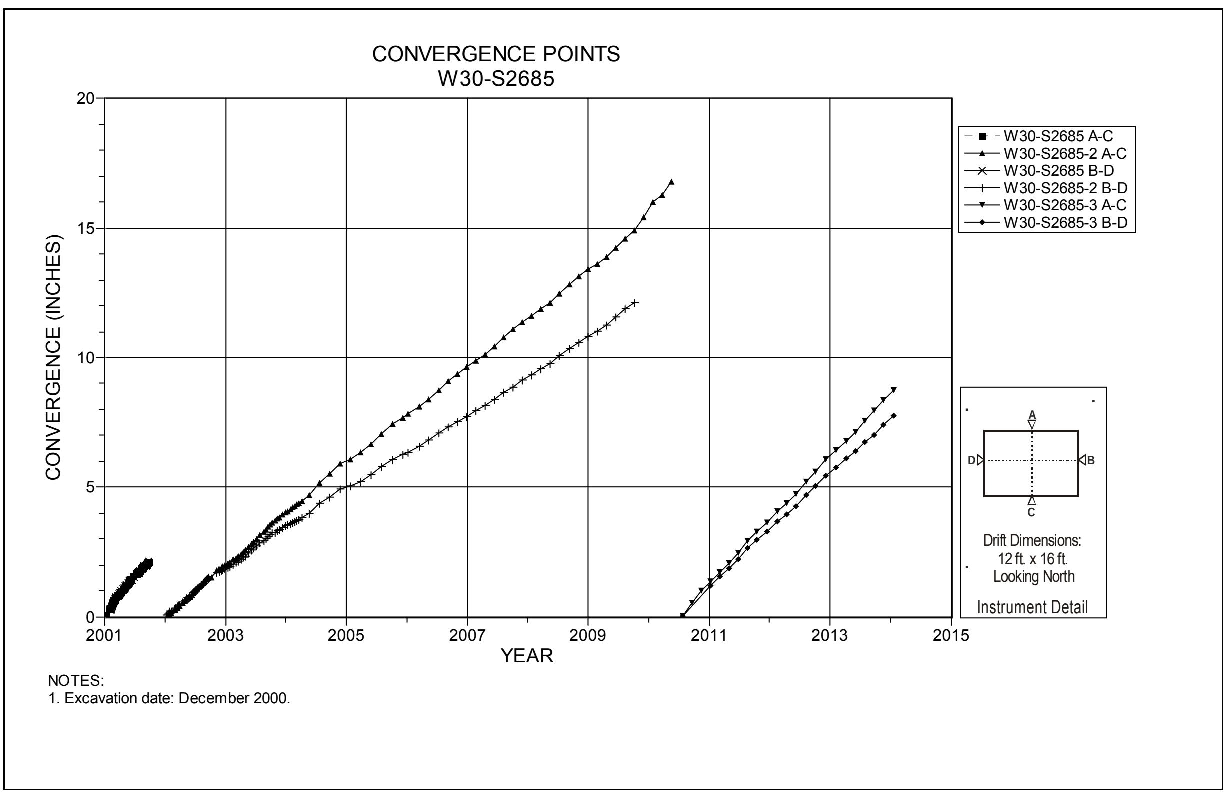

Figure 4-216 Convergence Point Array
W30 S2685 – All Chords

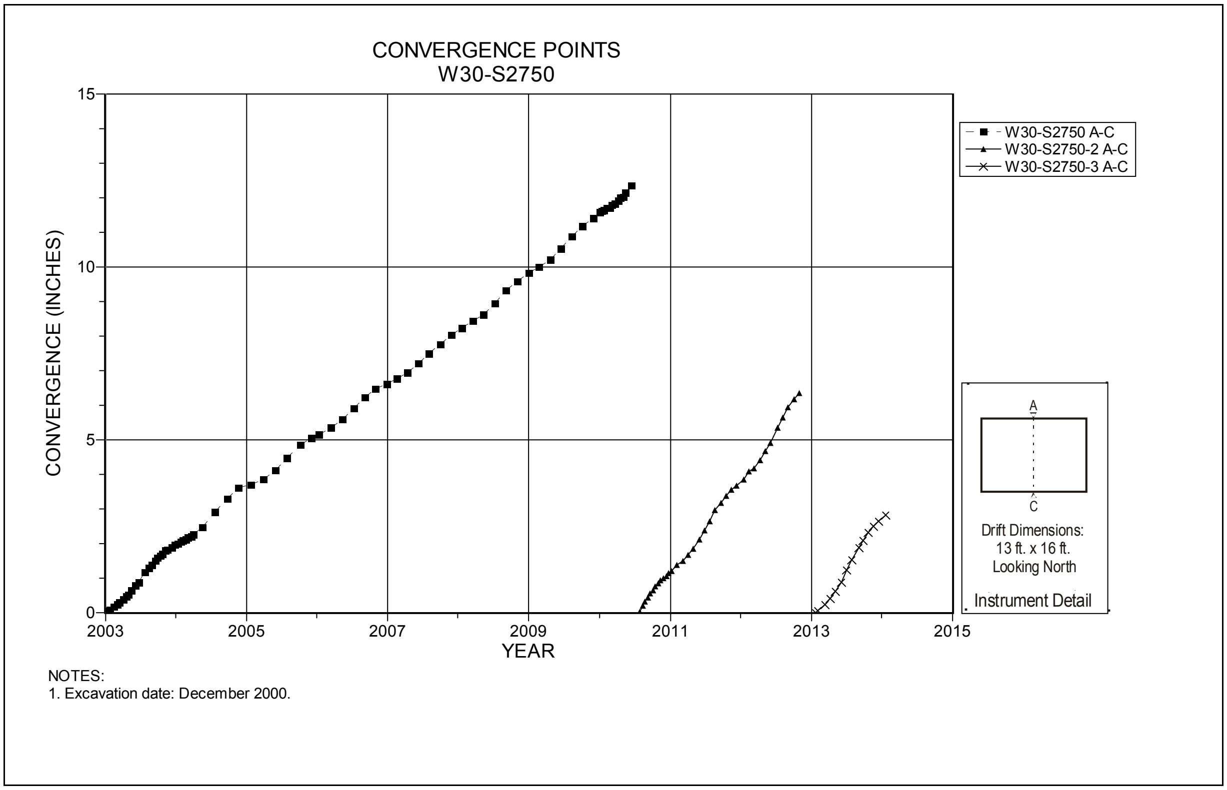

Figure 4-217 Convergence Point Array
W30 S2750 – Roof to Floor

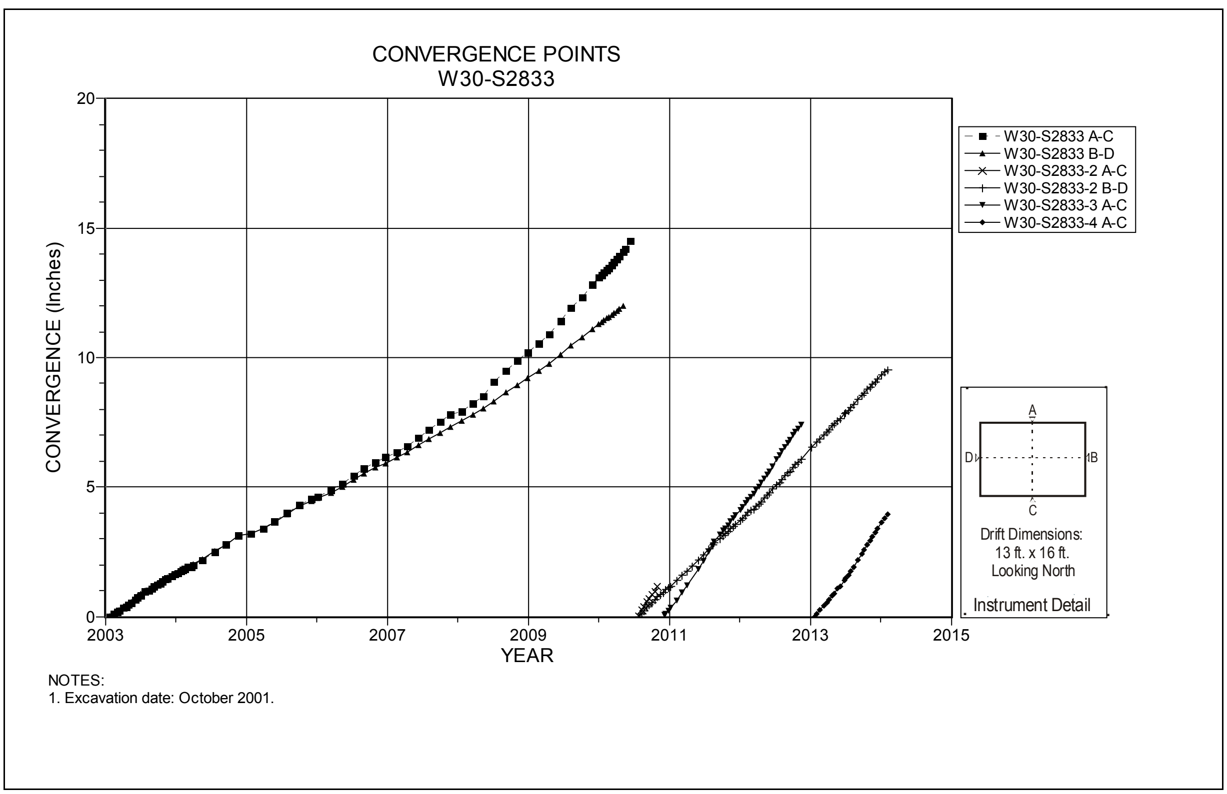

Figure 4-218 Convergence Point Array
W30 S2833 – All Chords

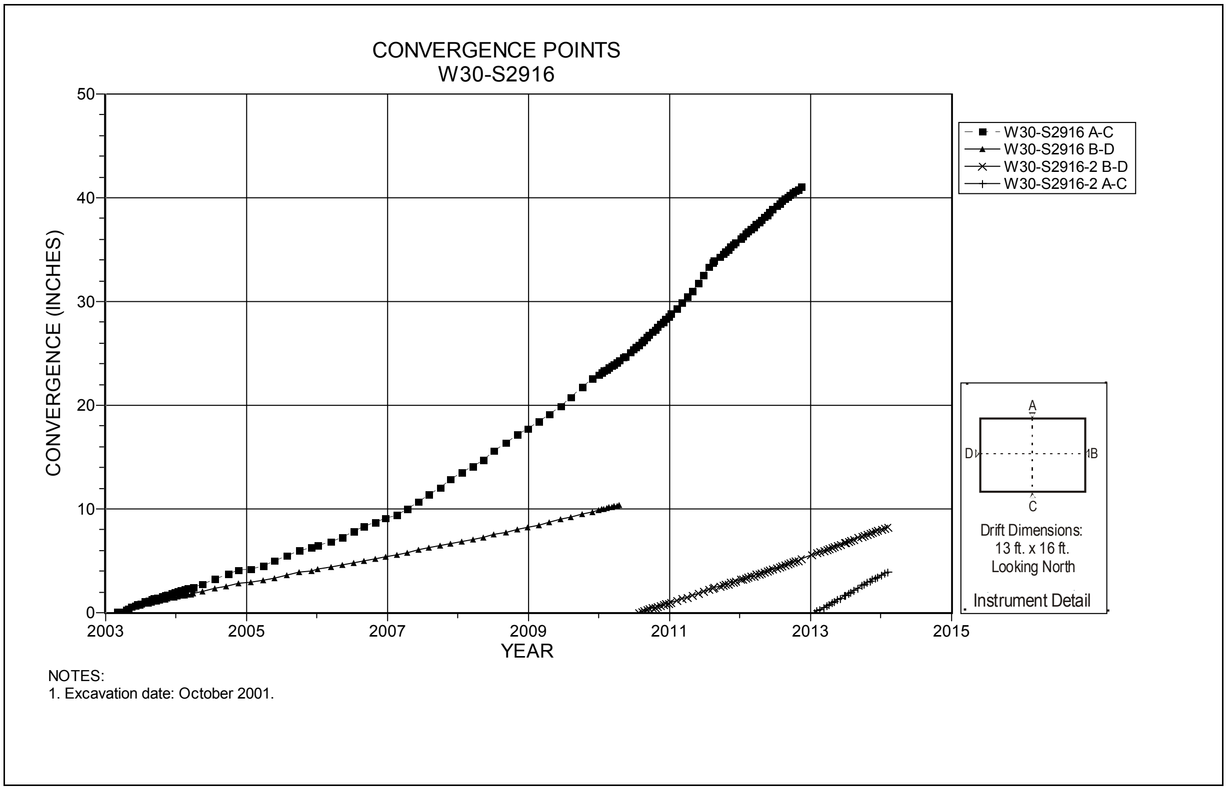

Figure 4-219 Convergence Point Array
W30 S2916 – All Chords

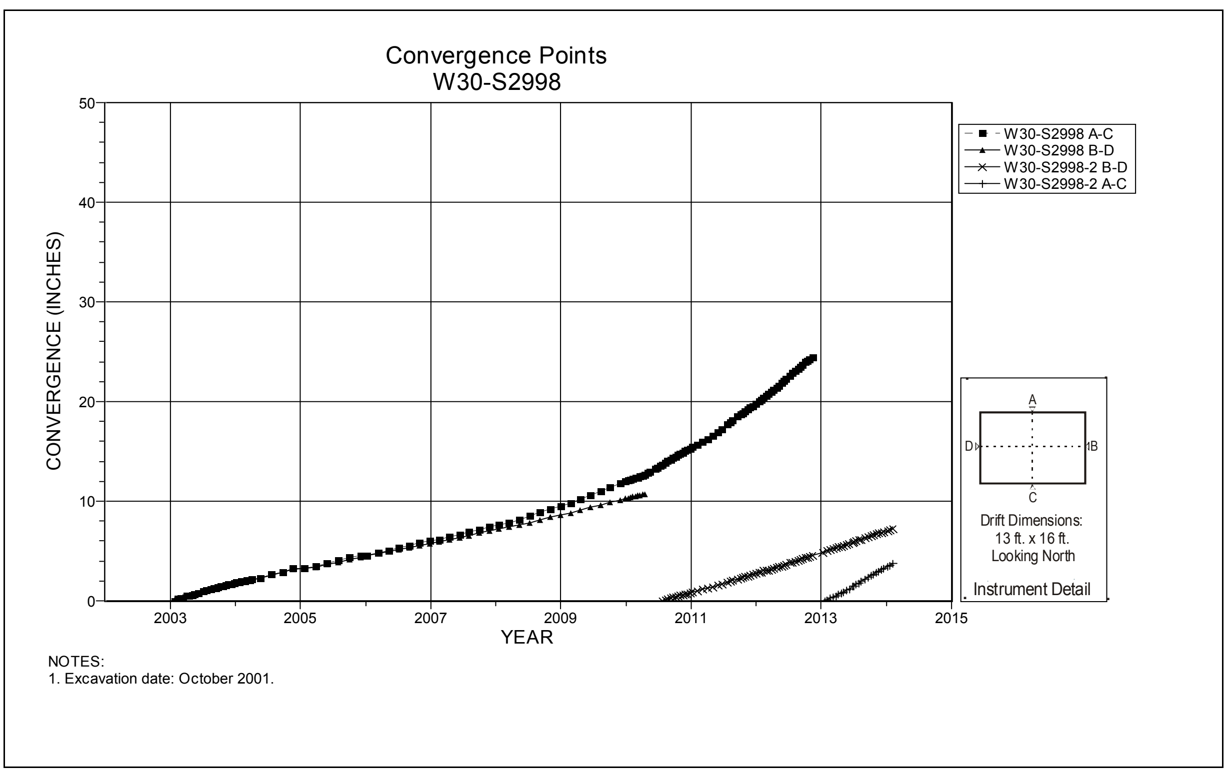

Figure 4-220 Convergence Point Array
W30 S2998 – All Chords

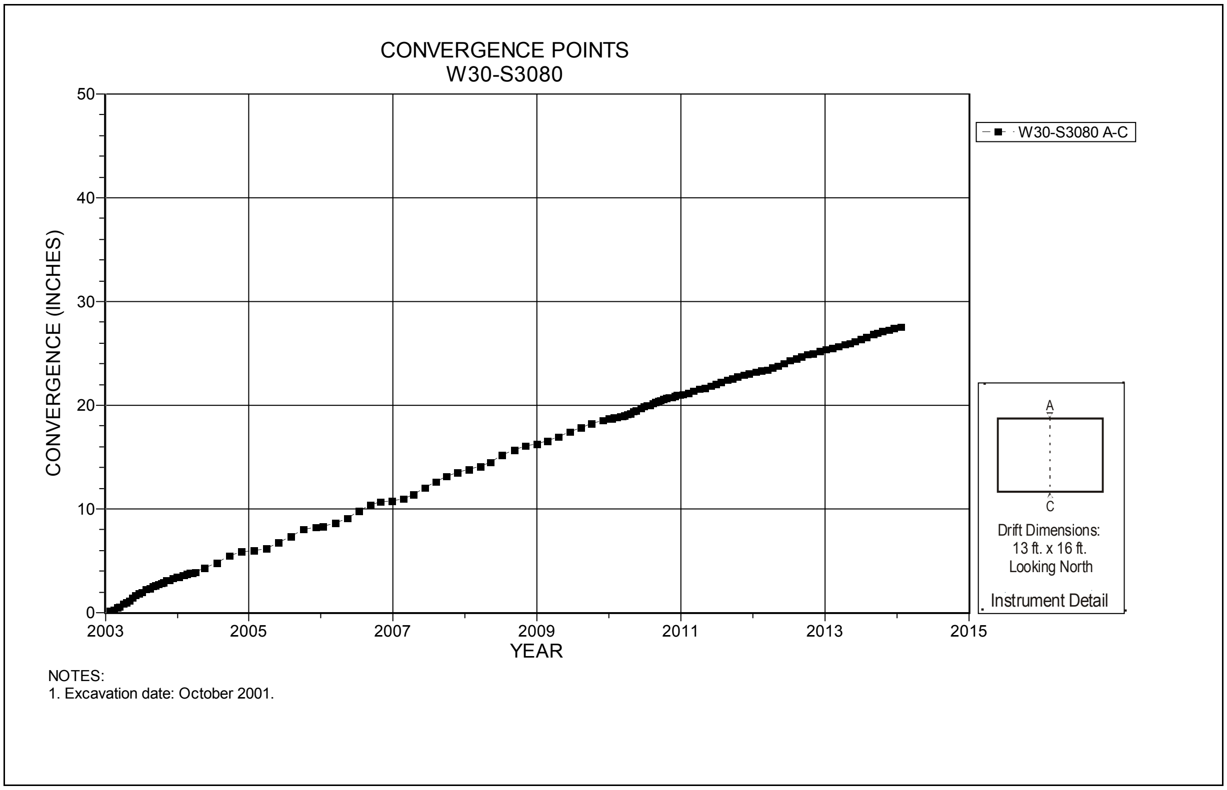

Figure 4-221 Convergence Point Array
W30 S3080 – Roof to Floor

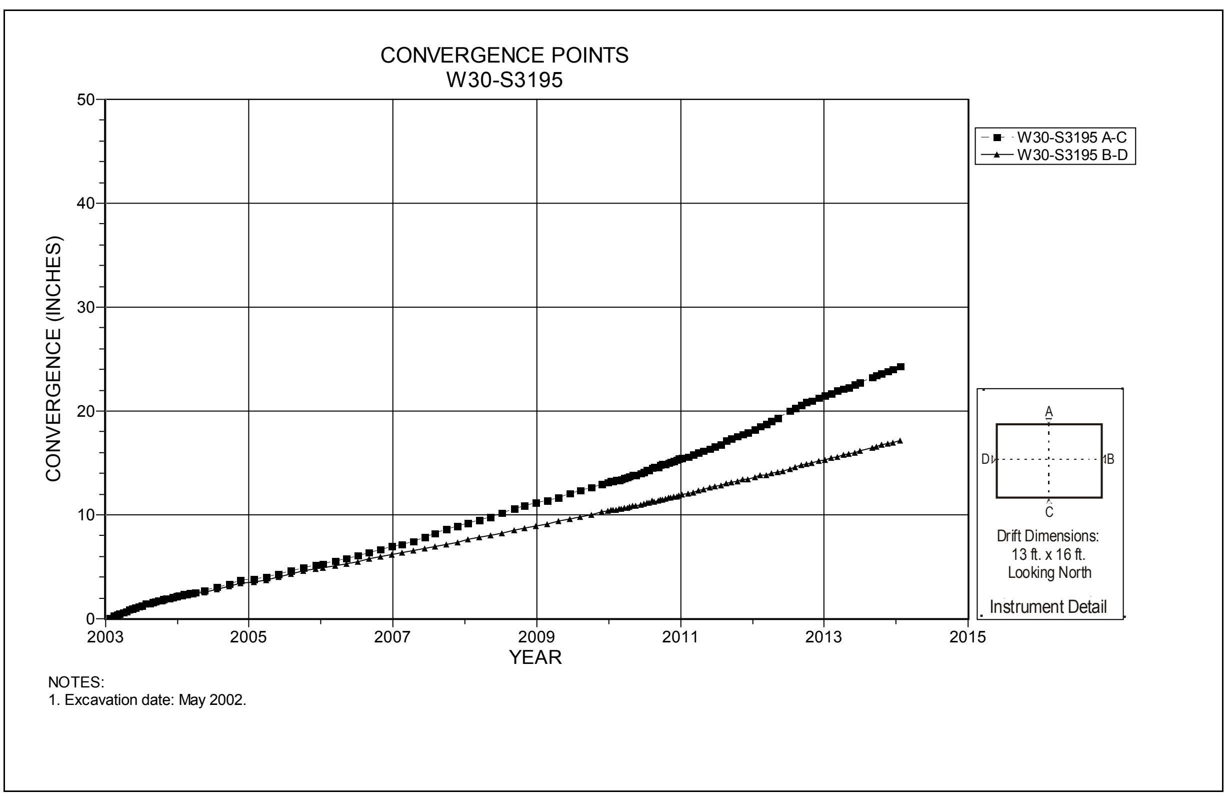

Figure 4-222 Convergence Point Array
W30 S3195 – All Chords

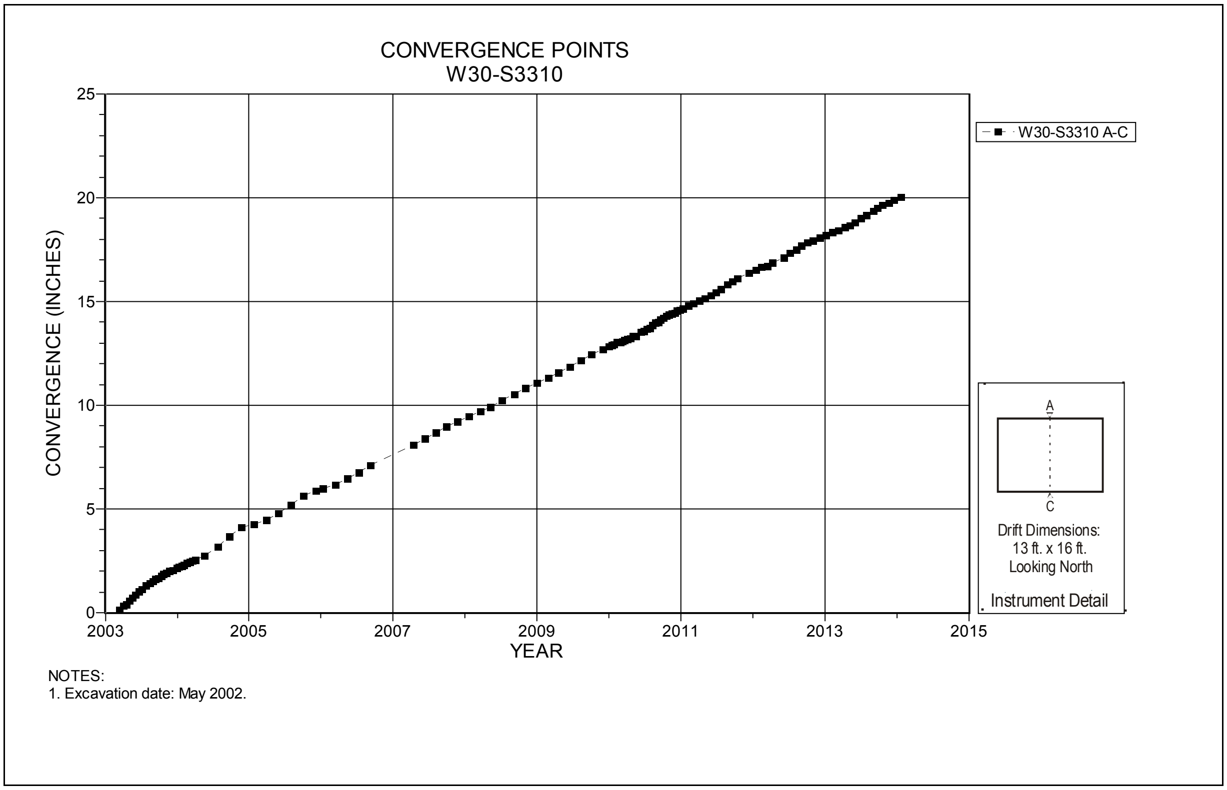

Figure 4-223 Convergence Point Array
W30 S3310 – Roof to Floor

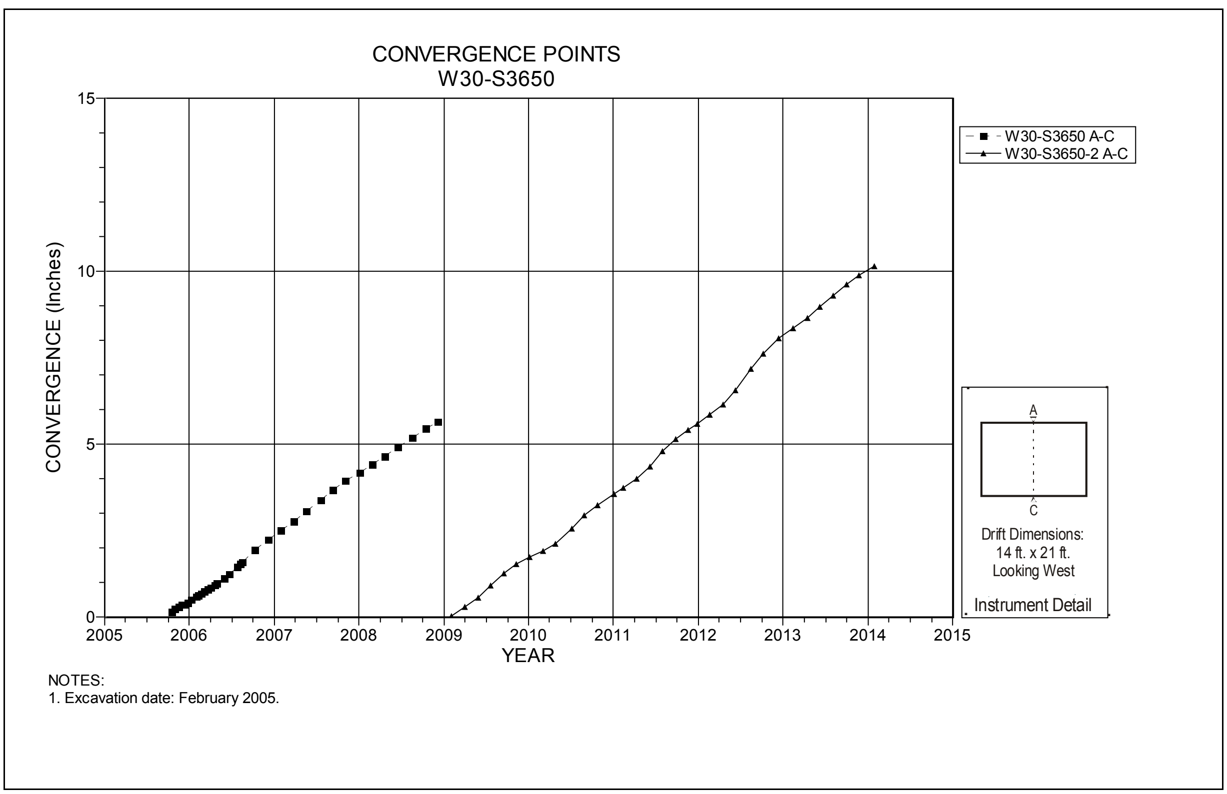

Figure 4-224 Convergence Point Array
W30 S3650 – Roof to Floor

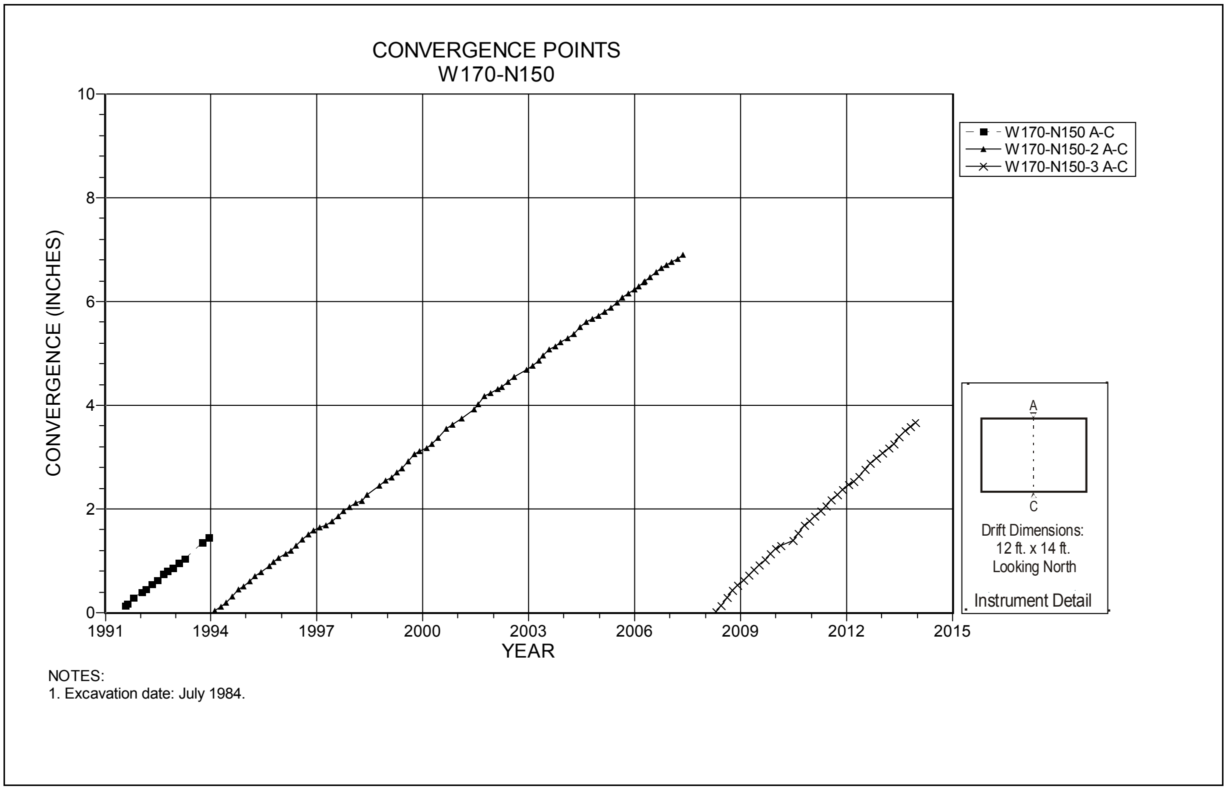

Figure 4-225 Convergence Point Array
W170 N150 – Roof to Floor

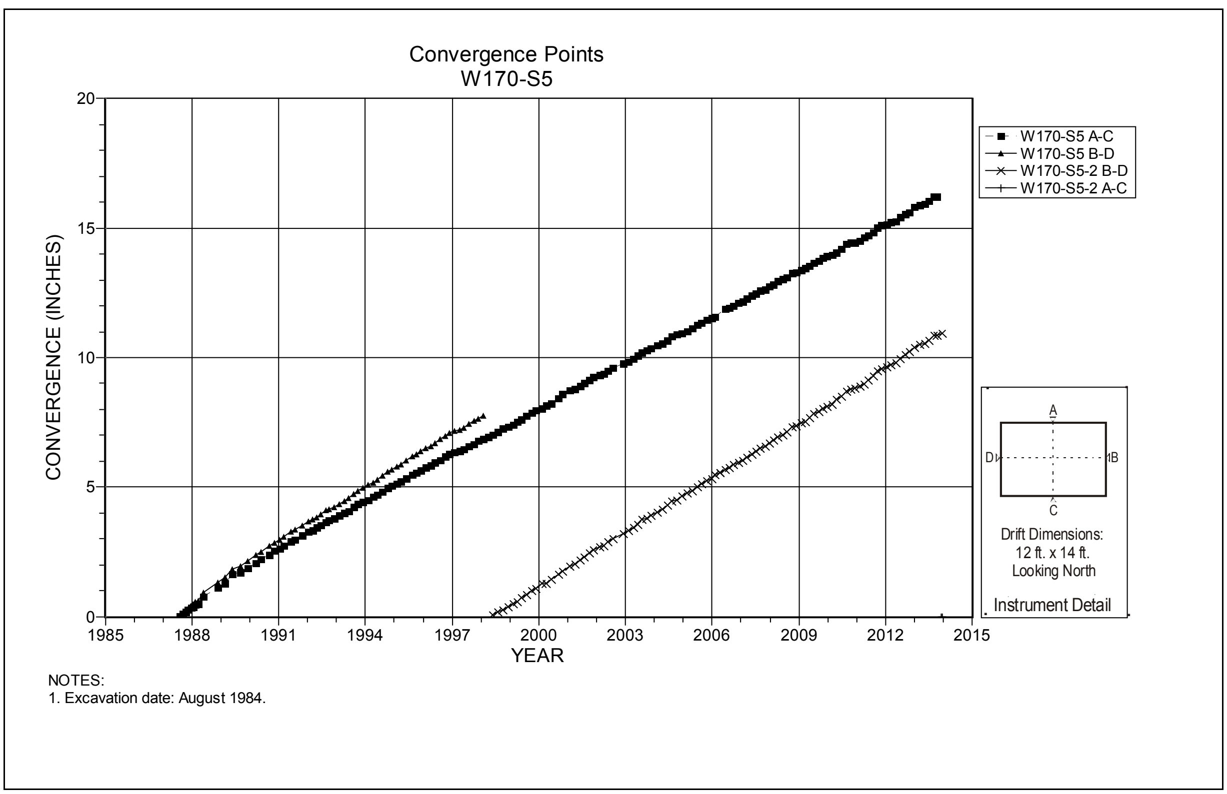

Figure 4-226 Convergence Point Array
W170 S5 – All Chords

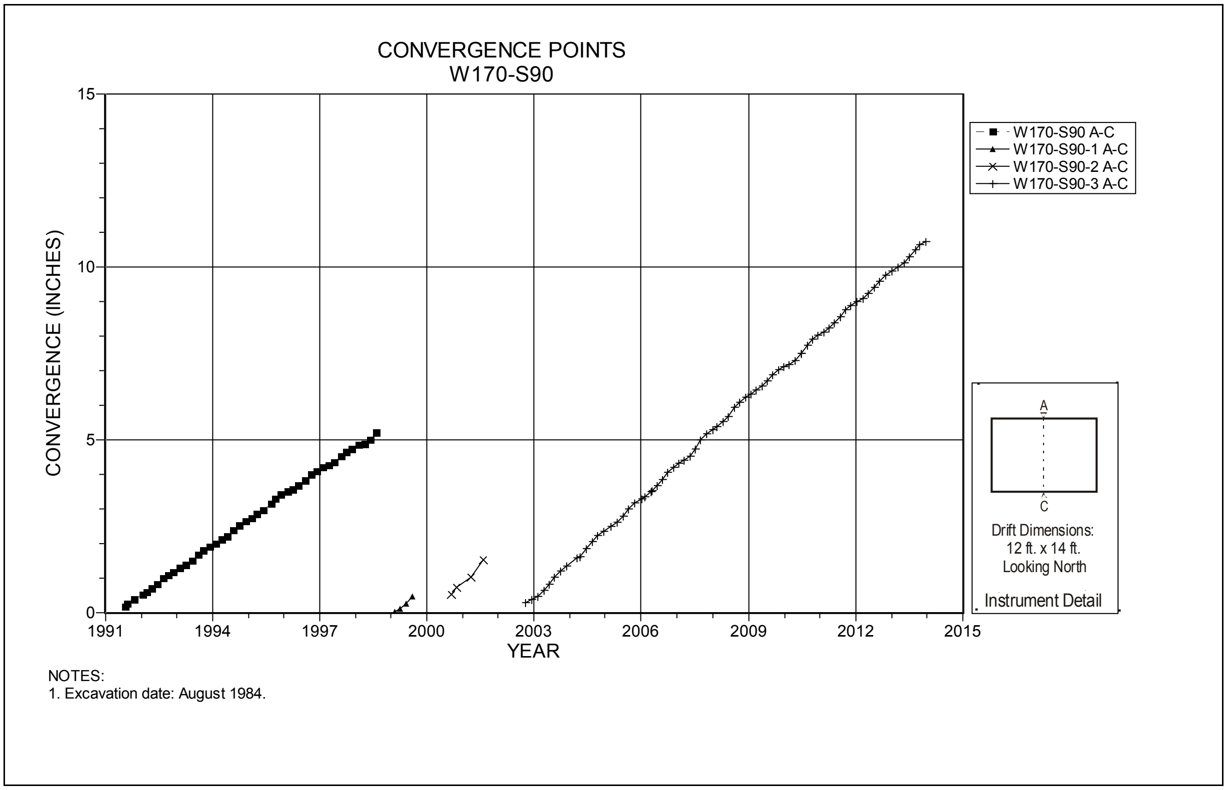

Figure 4-227 Convergence Point Array
W170 S90 – Roof to Floor

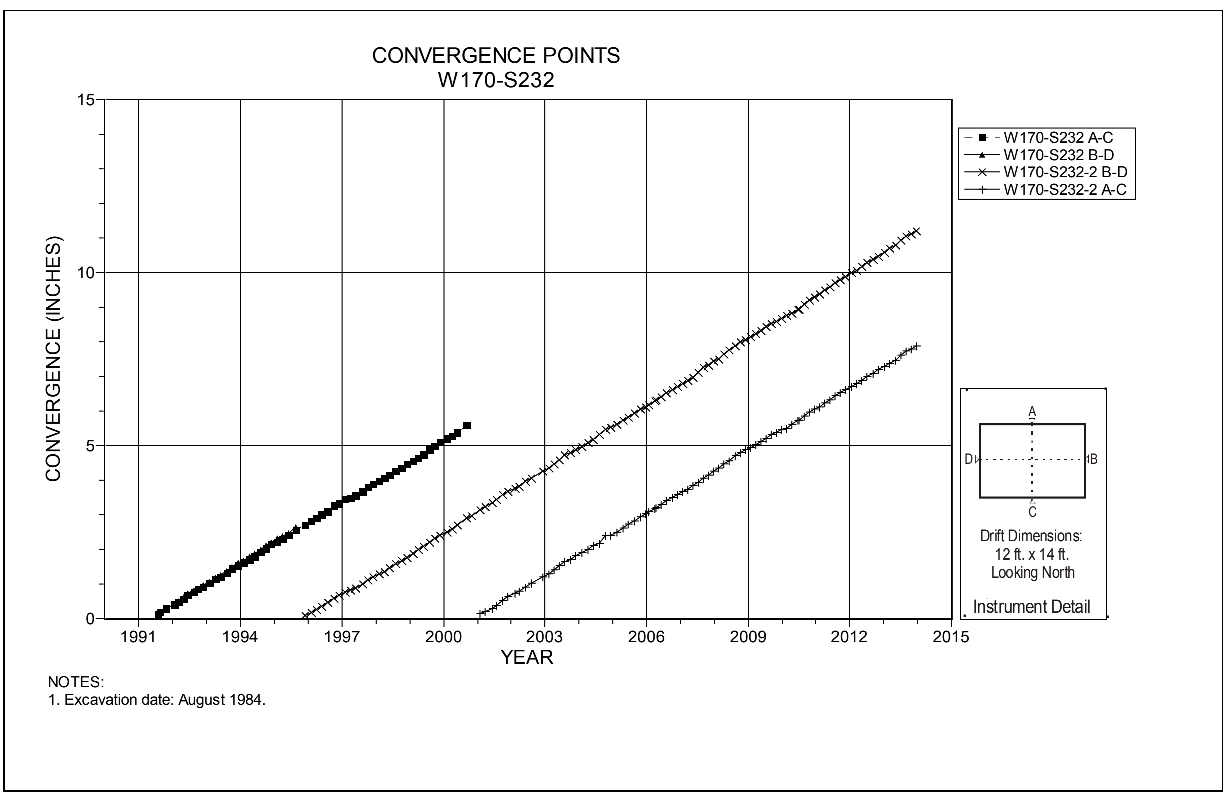

Figure 4-228 Convergence Point Array
W170 S232 – All Chords

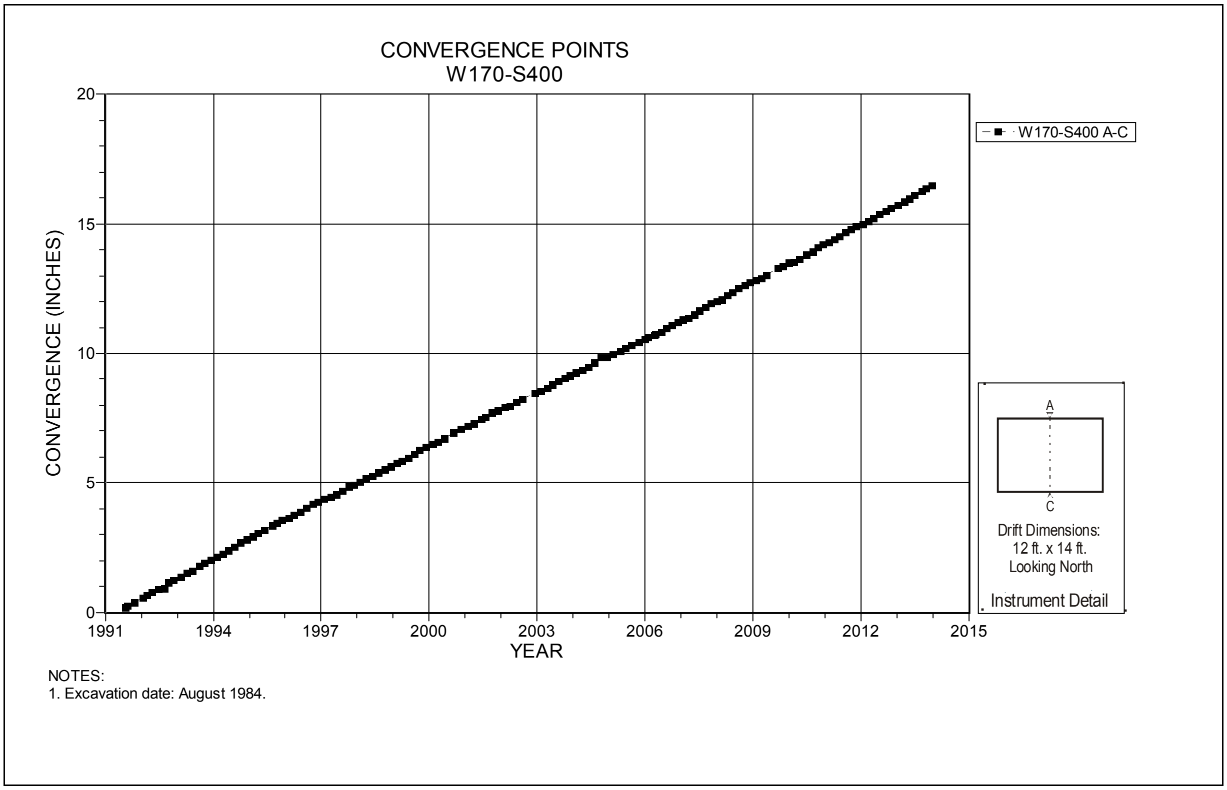

Figure 4-229 Convergence Point Array
W170 S400 – Roof to Floor

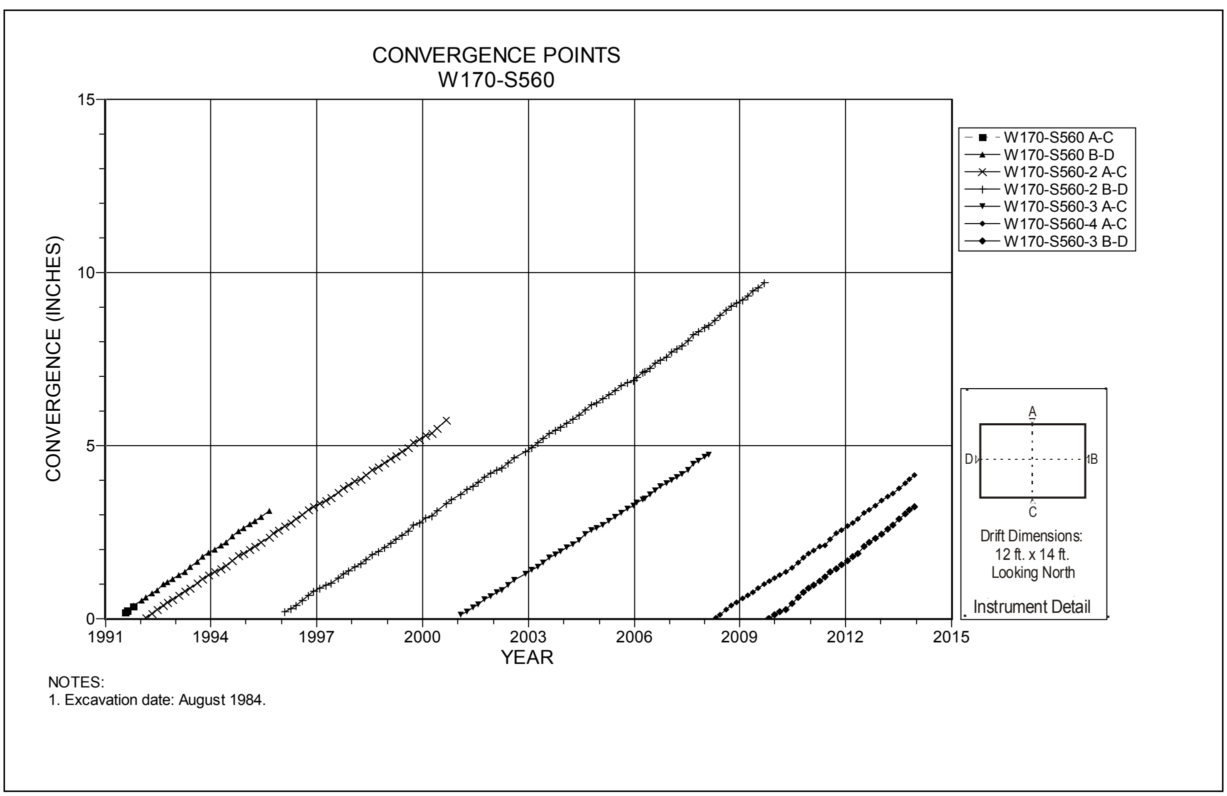

Figure 4-230 Convergence Point Array
W170 S560 – All Chords

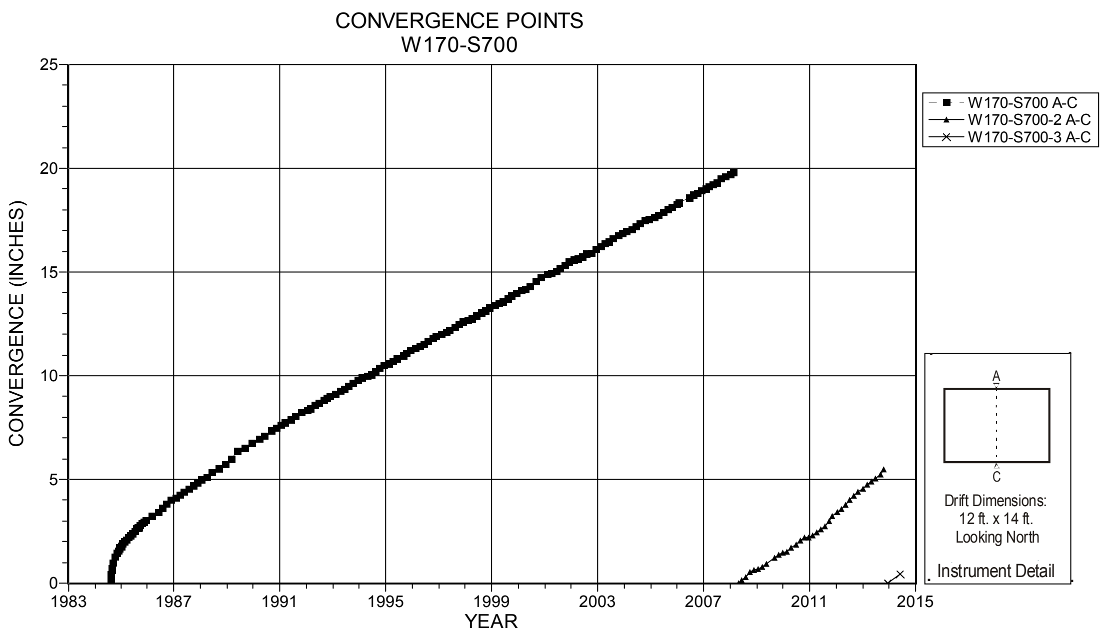

NOTES:
1. Excavation date: August 1984.

Figure 4-231 Convergence Point Array
W170 S700 – Roof to Floor

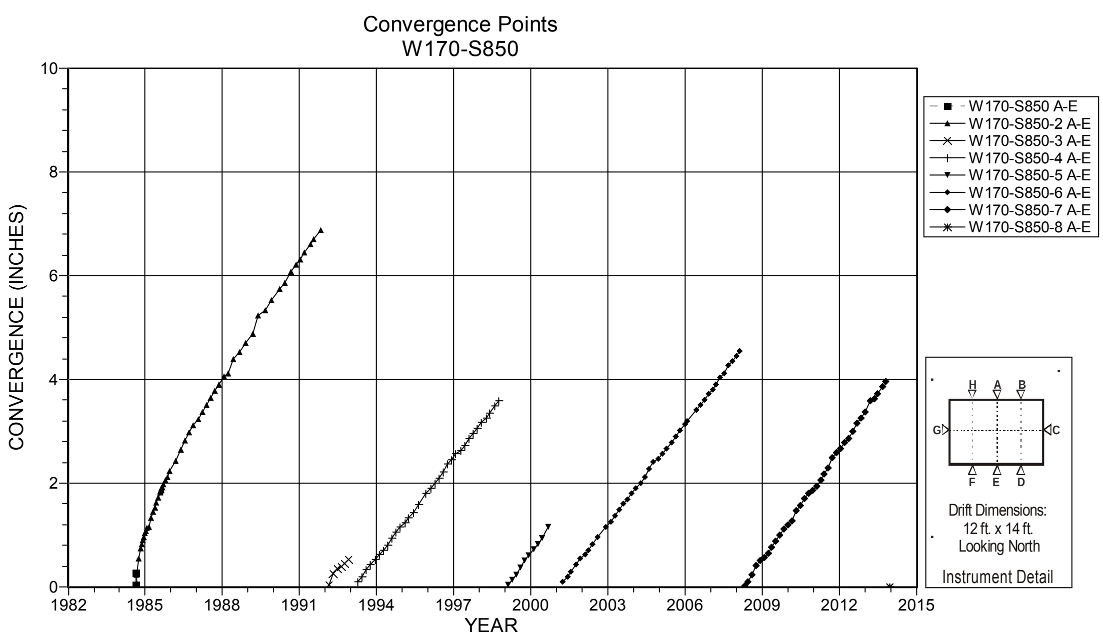

NOTES:
1. Excavation date: August 1984.
2. Chords for this location are on separate plots.

Figure 4-232 Convergence Point Array
W170 S850 – Roof to Floor – Centerline

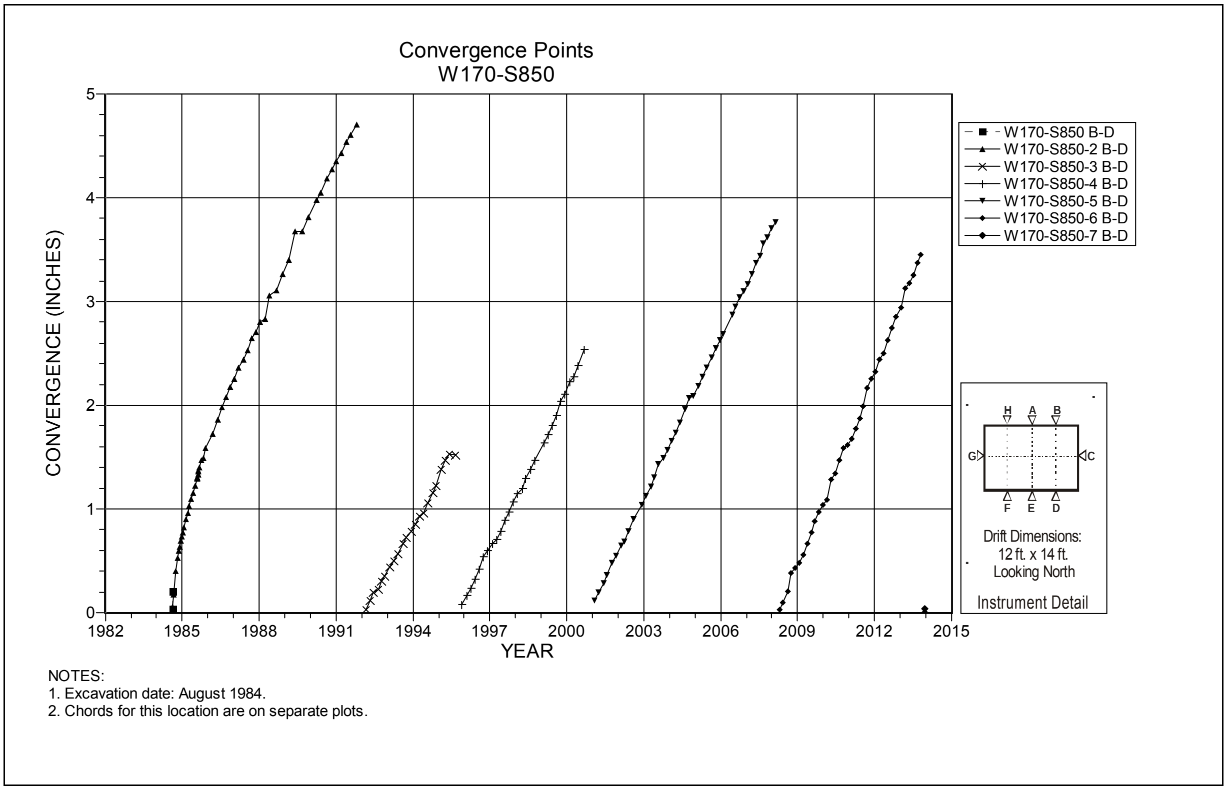

Figure 4-233 Convergence Point Array
W170 S850 – Roof to Floor – East Quarter Point

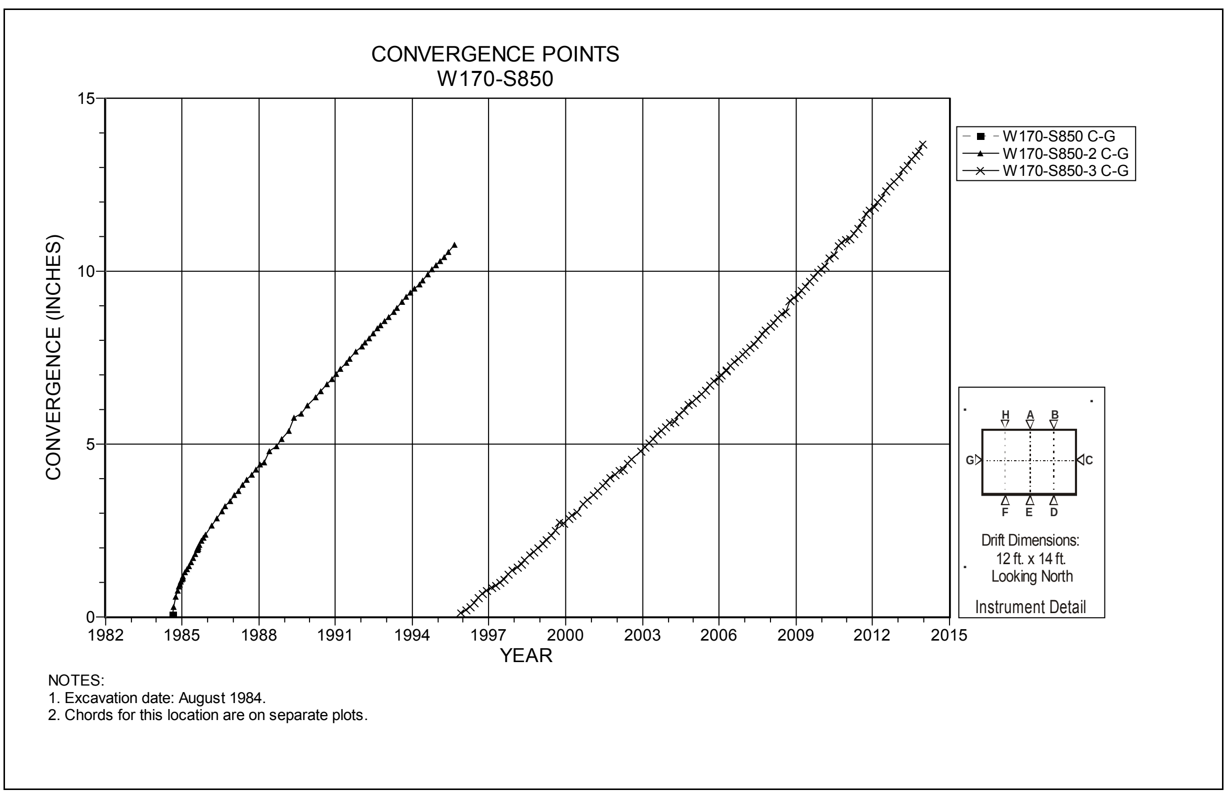

Figure 4-234 Convergence Point Array
W170 S850 – Rib to Rib

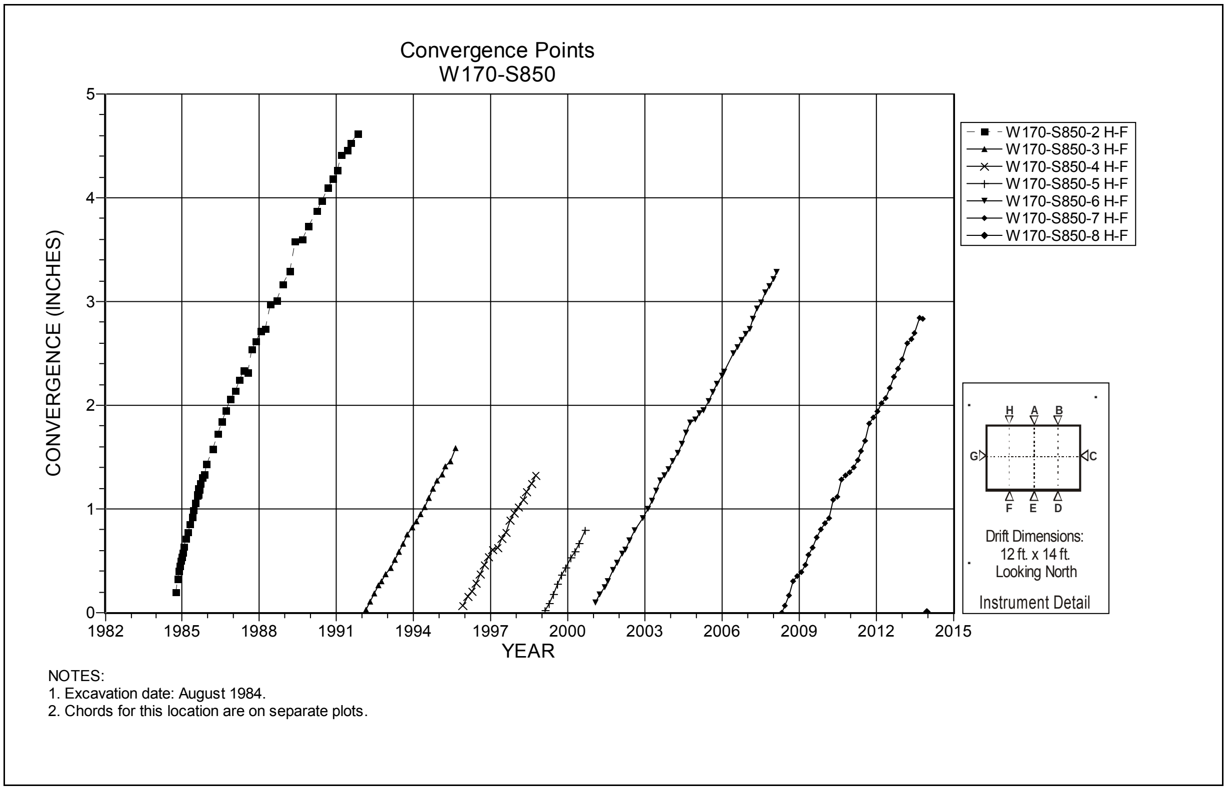

Figure 4-235 Convergence Point Array
W170 S850 – Roof to Floor – West Quarter Point

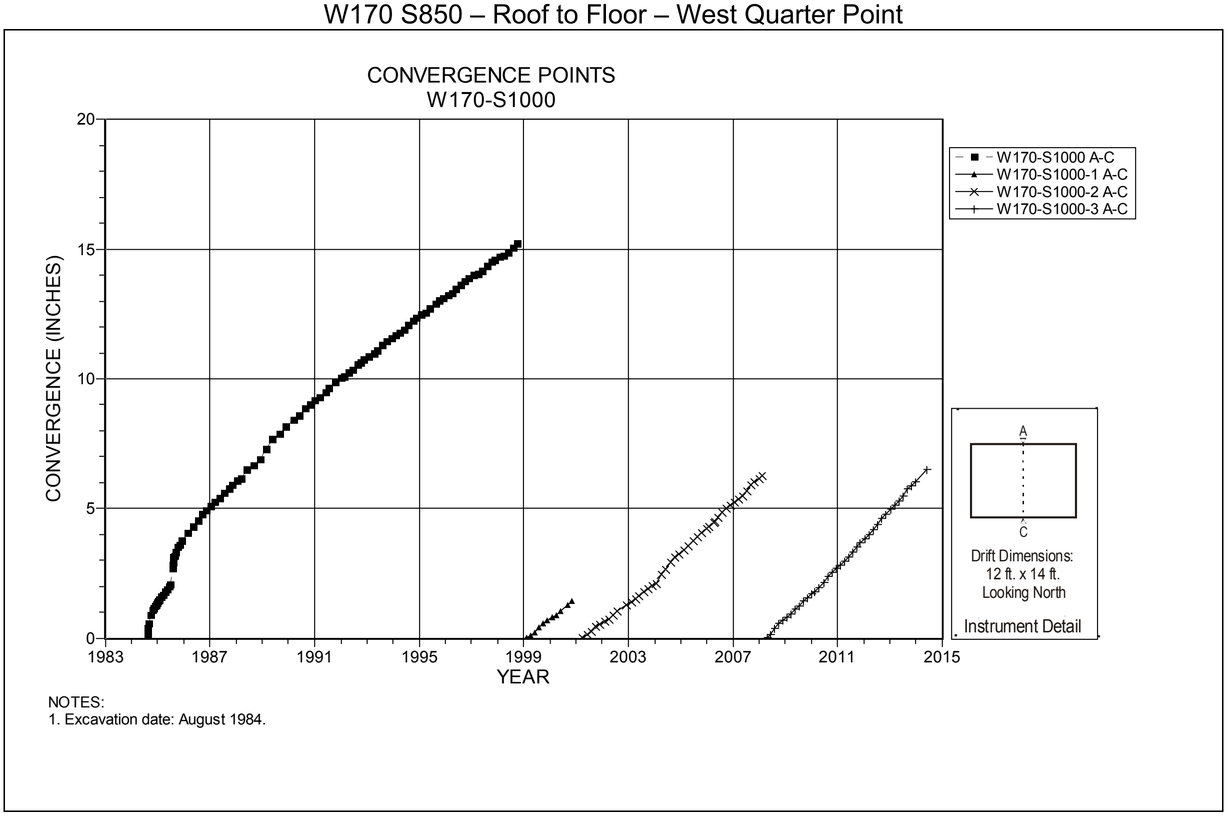

Figure 4-236 Convergence Point Array
W170 S1000 – Roof to Floor

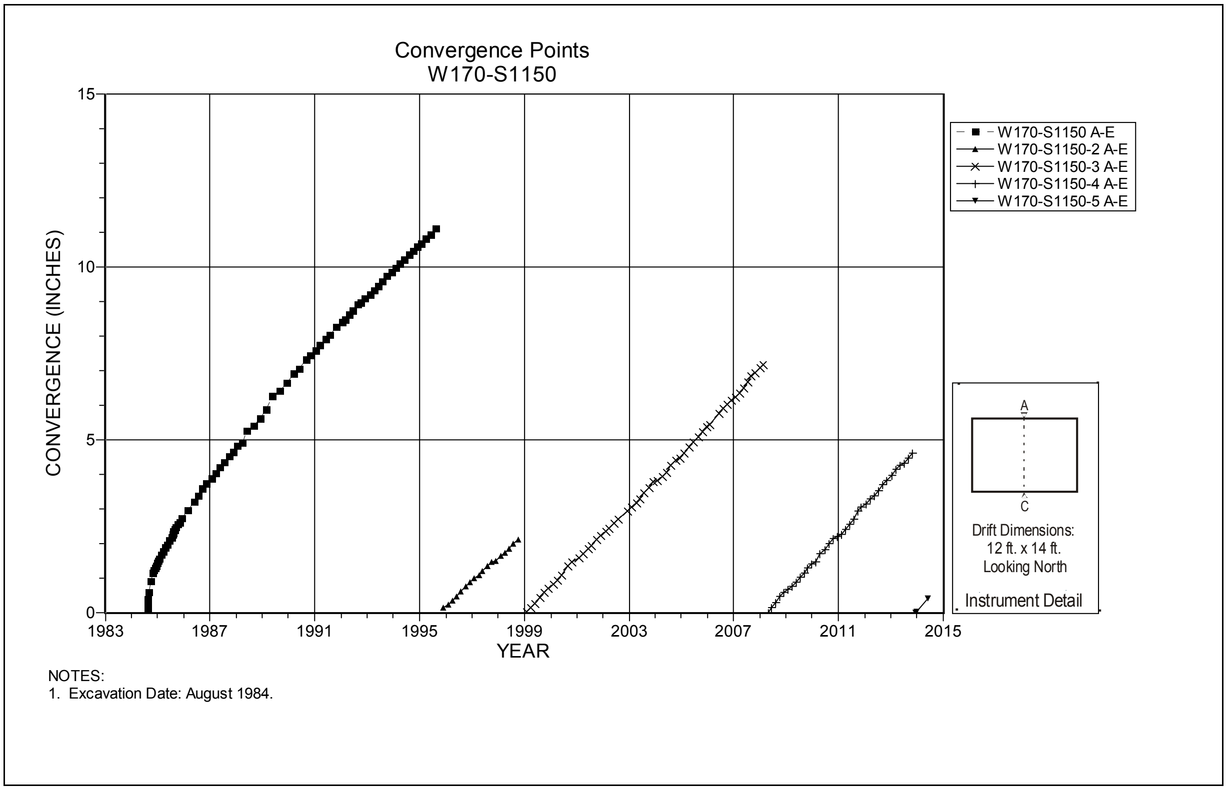

Figure 4-237 Convergence Point Array
W170 S1150 – Roof to Floor

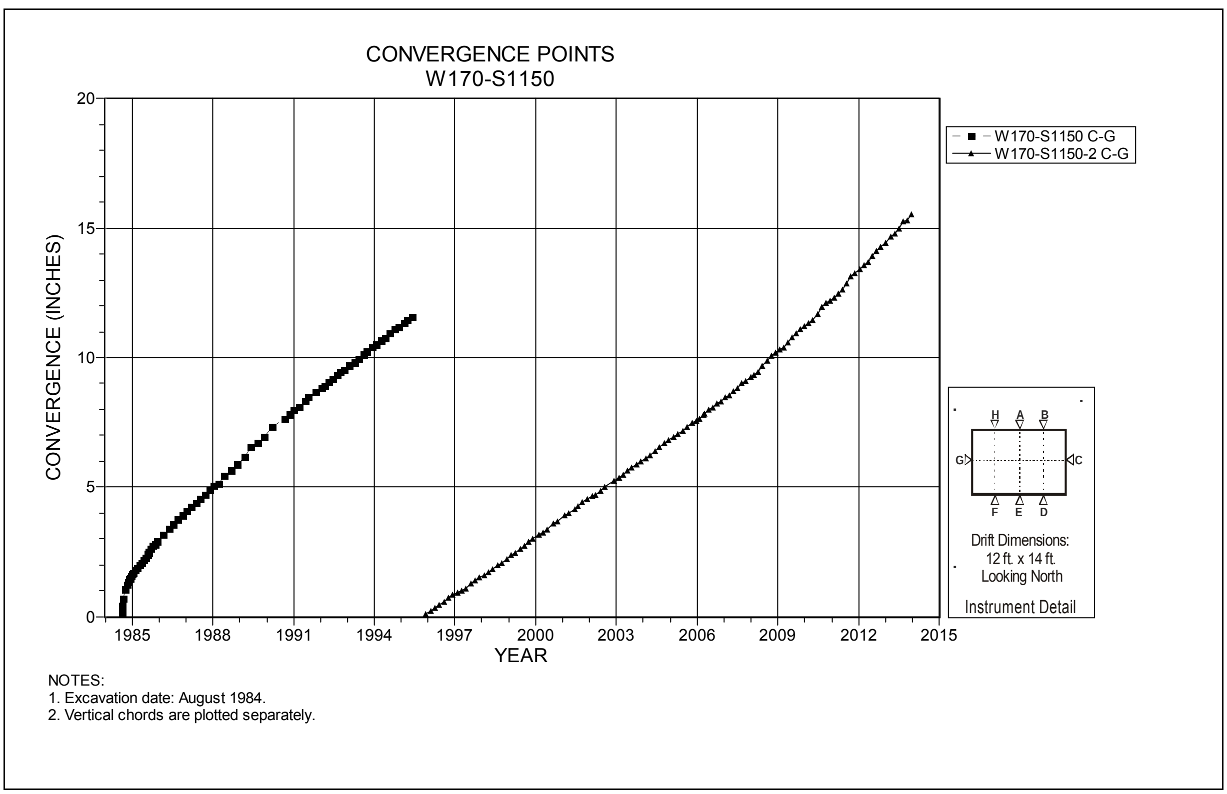

Figure 4-238 Convergence Point Array
W170 S1150 – Rib to Rib

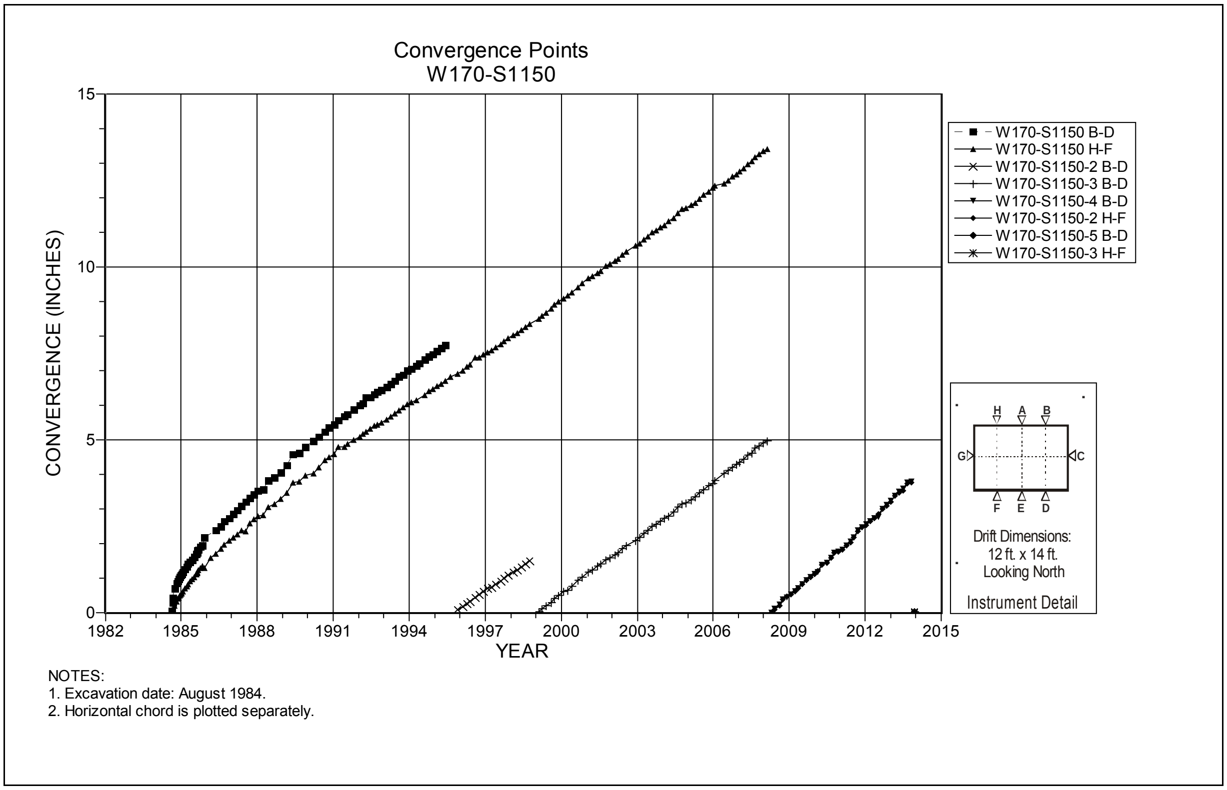

Figure 4-239 Convergence Point Array
W170 S1150 – Roof to Floor – Quarter Points

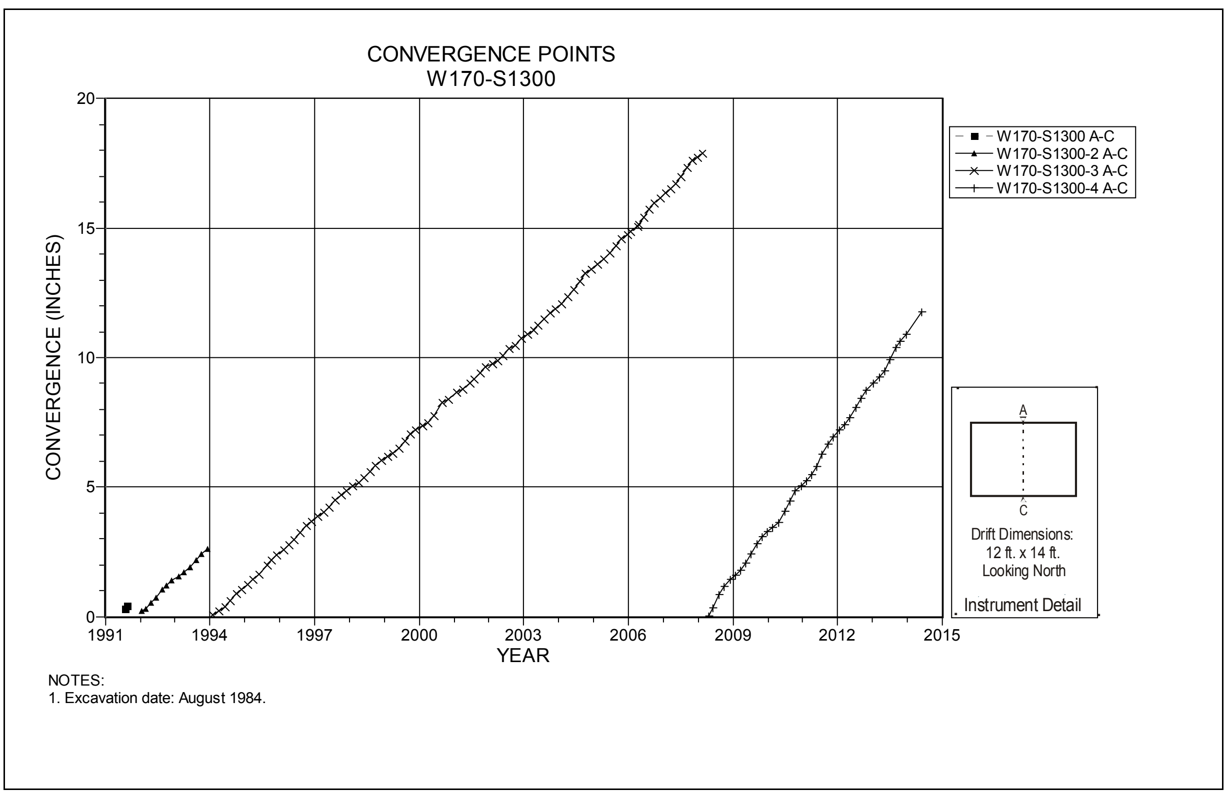

Figure 4-240 Convergence Point Array
W170 S1300 – Roof to Floor

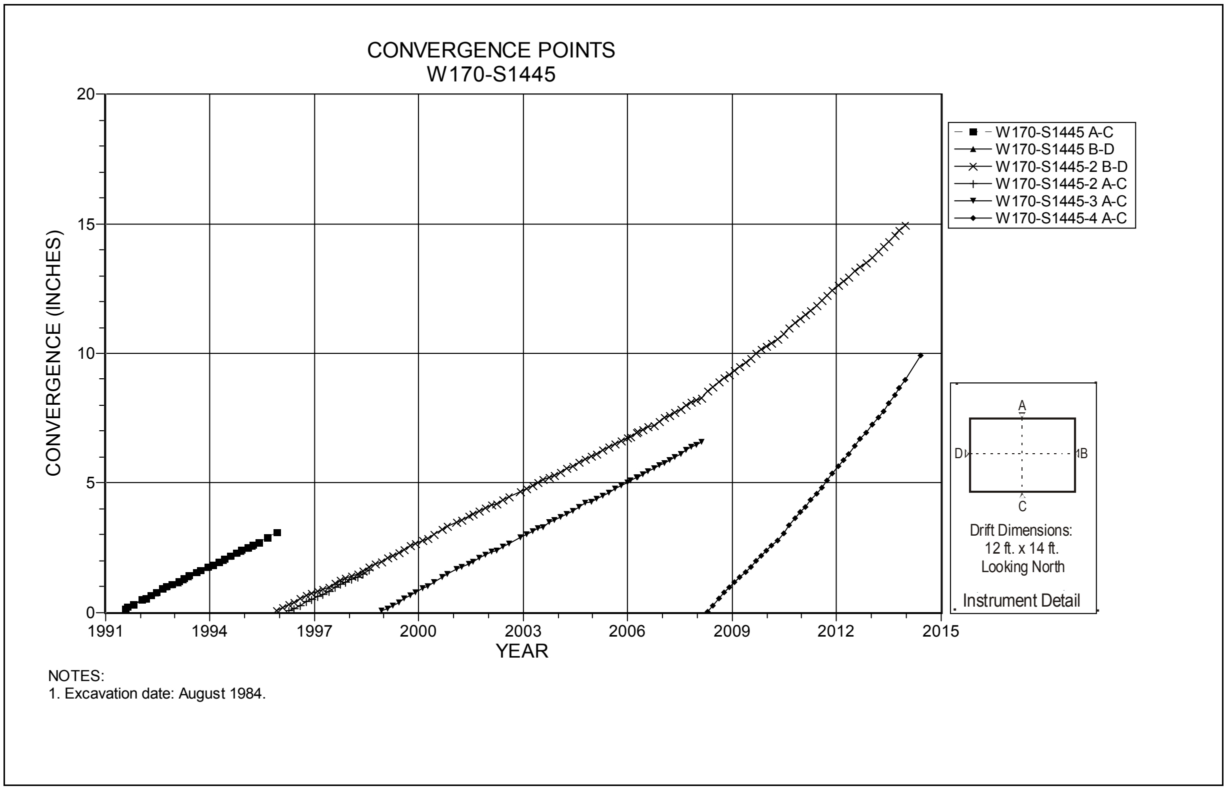

Figure 4-241 Convergence Point Array
W170 S1445 – All Chords

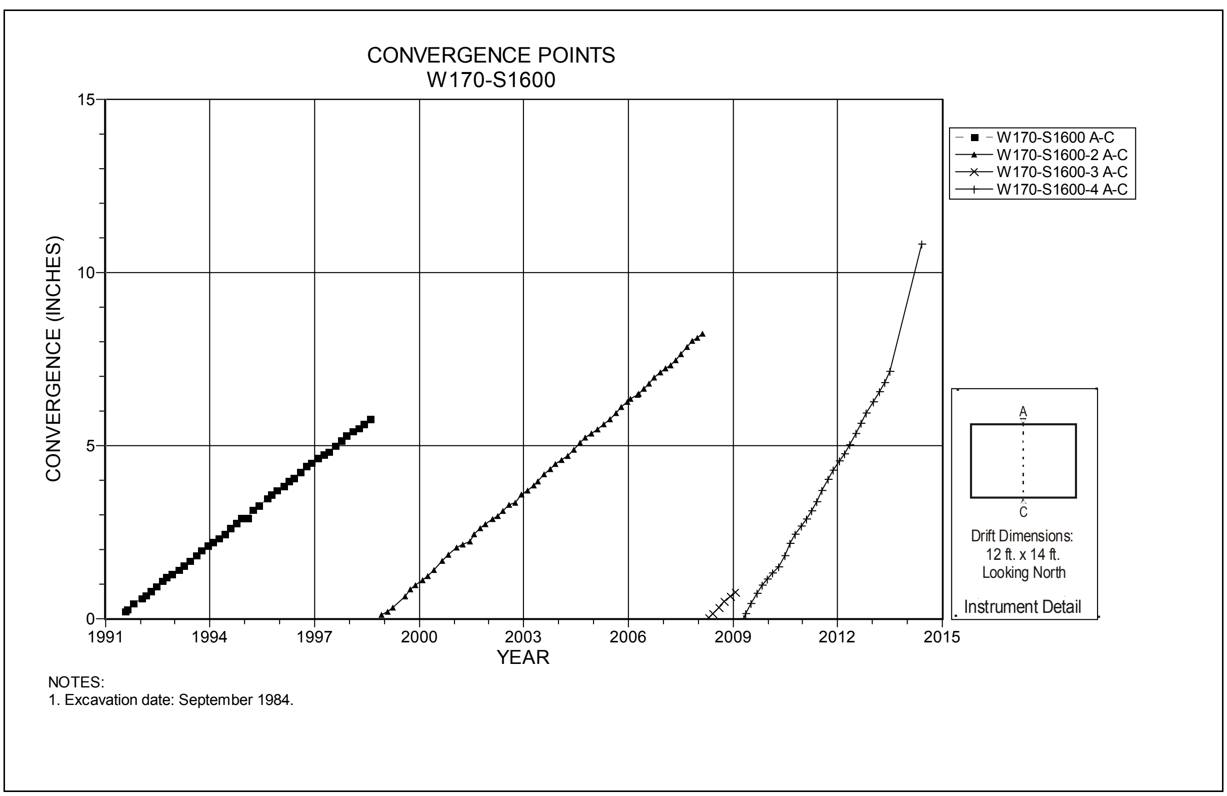

Figure 4-242 Convergence Point Array
W170 S1600 – Roof to Floor

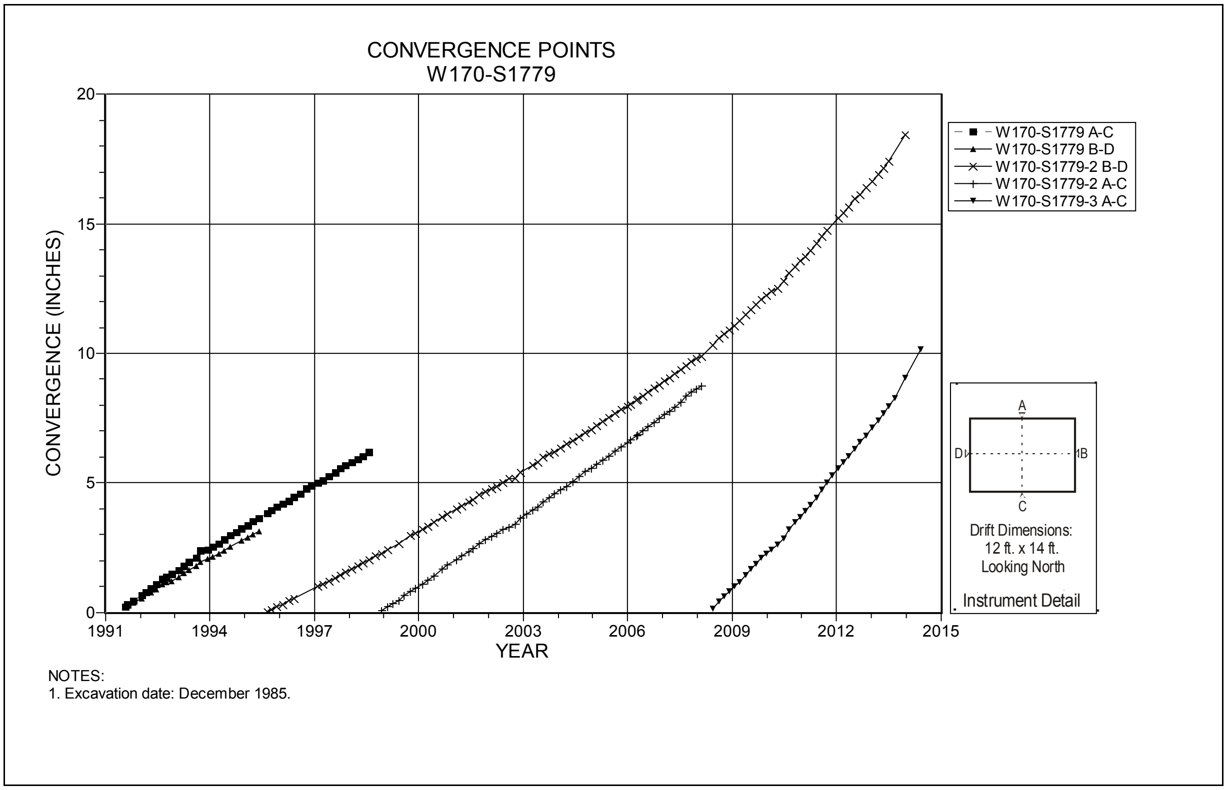

Figure 4-243 Convergence Point Array
W170 S1779 – All Chords

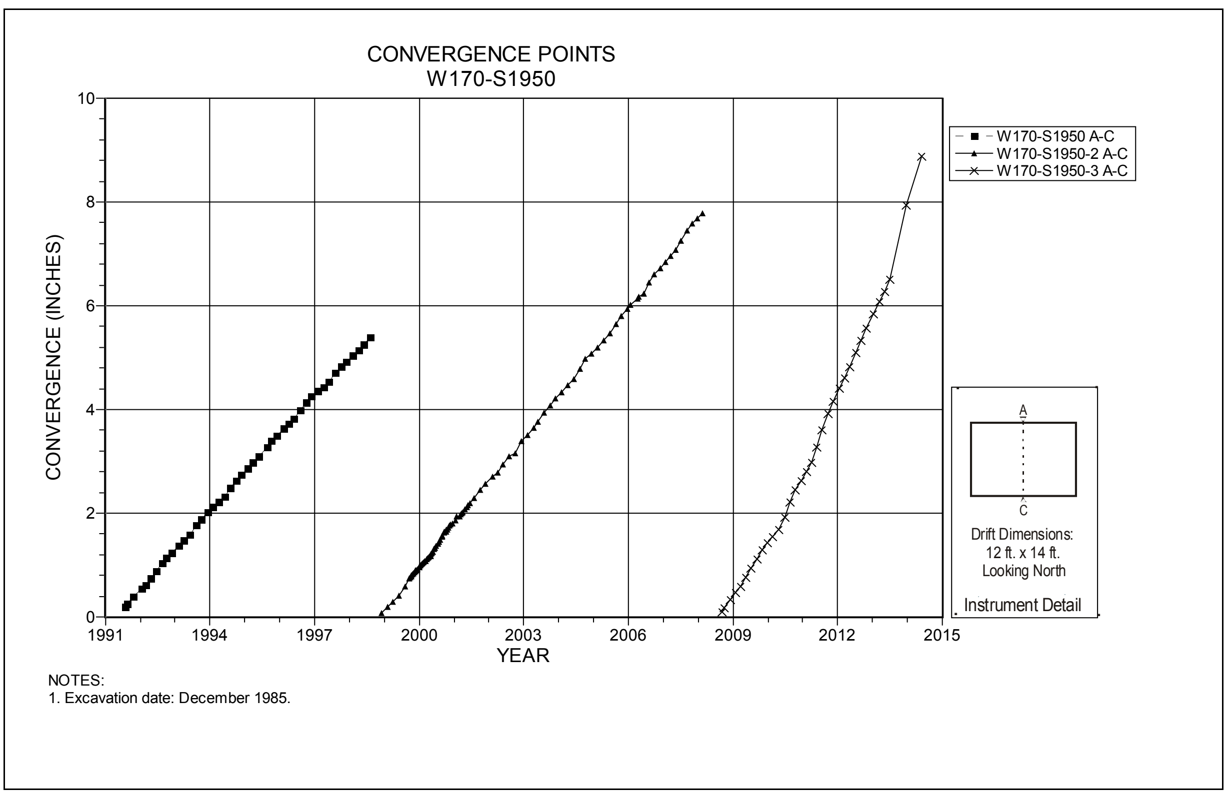

Figure 4-244 Convergence Point Array
W170 S1950 – Roof to Floor

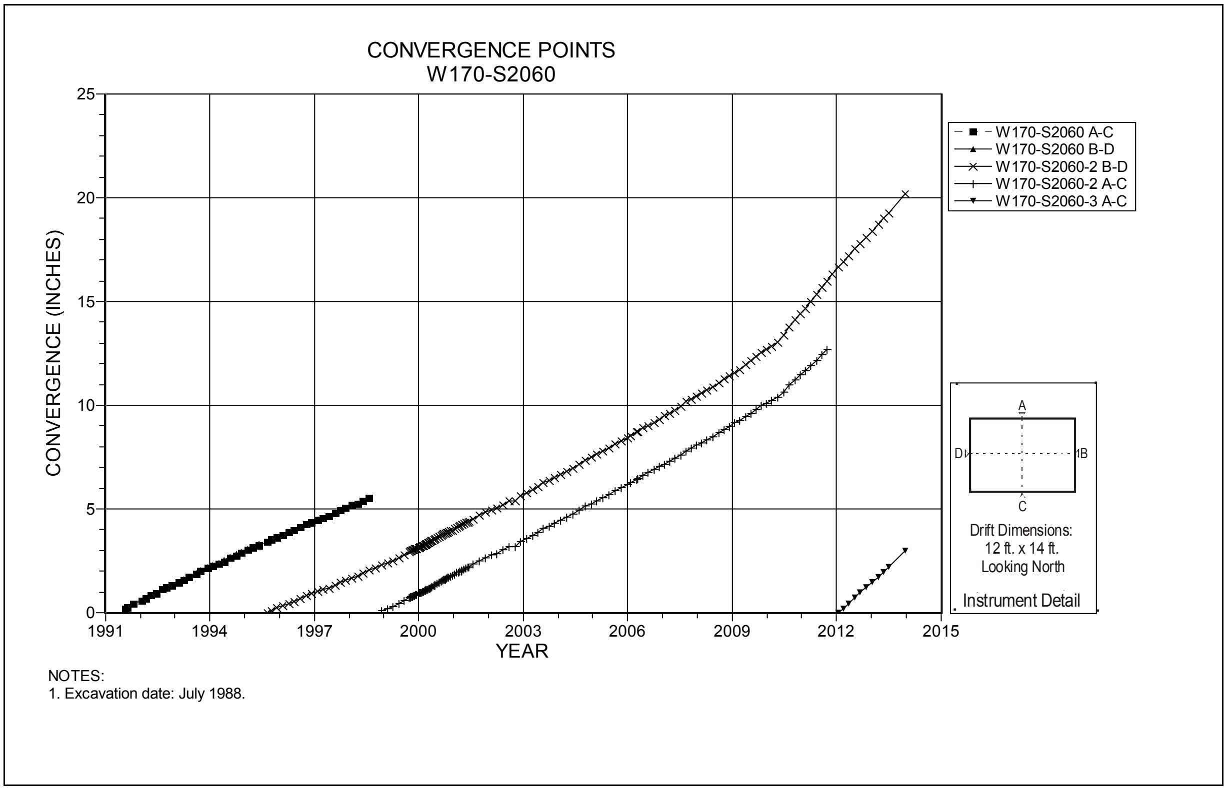

Figure 4-245 Convergence Point Array
W170 S2060 – All Chords

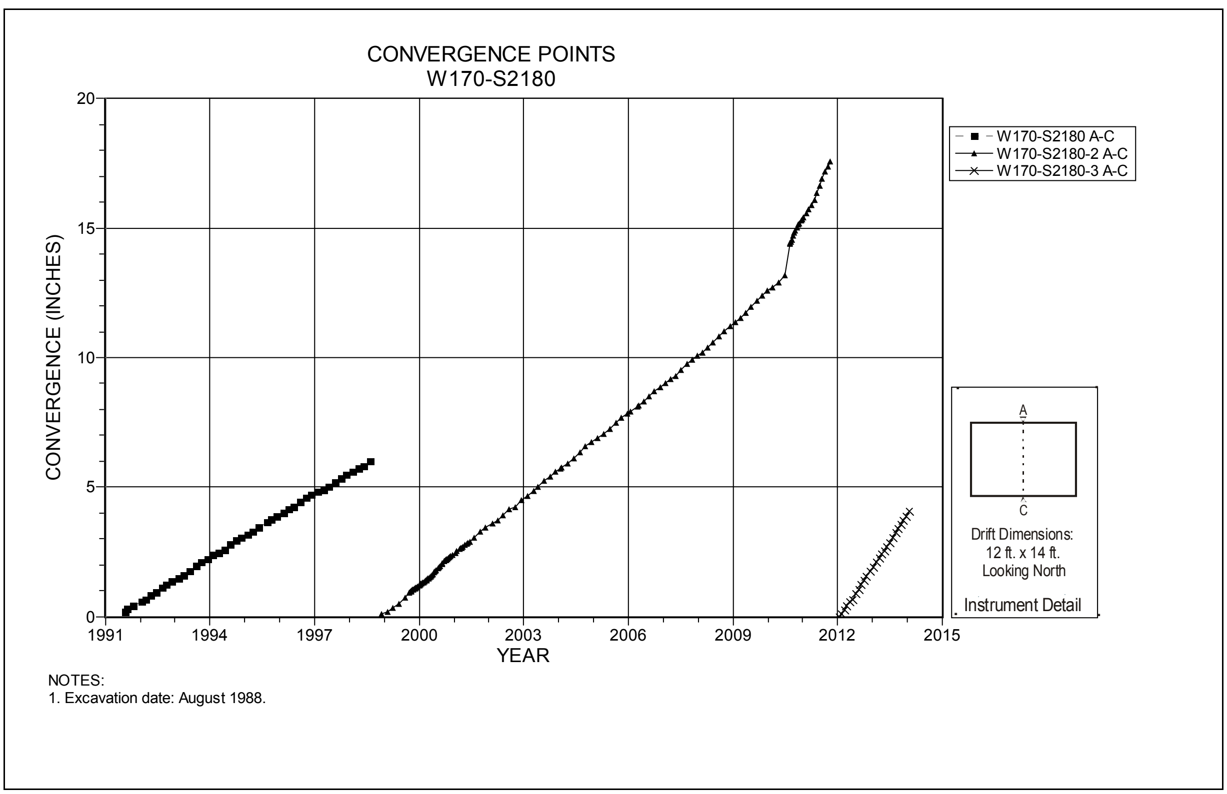

Figure 4-246 Convergence Point Array
W170 S2180 – Roof to Floor

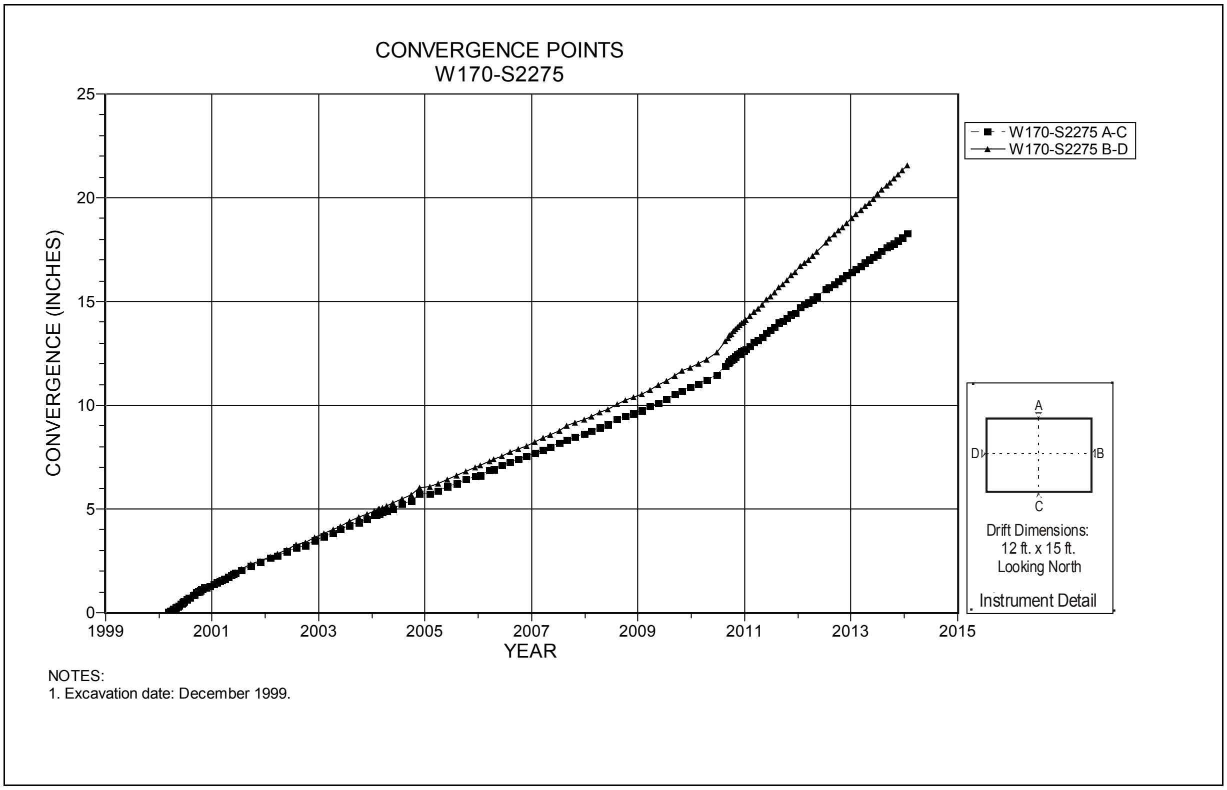

Figure 4-247 Convergence Point Array
W170 S2275 – All Chords

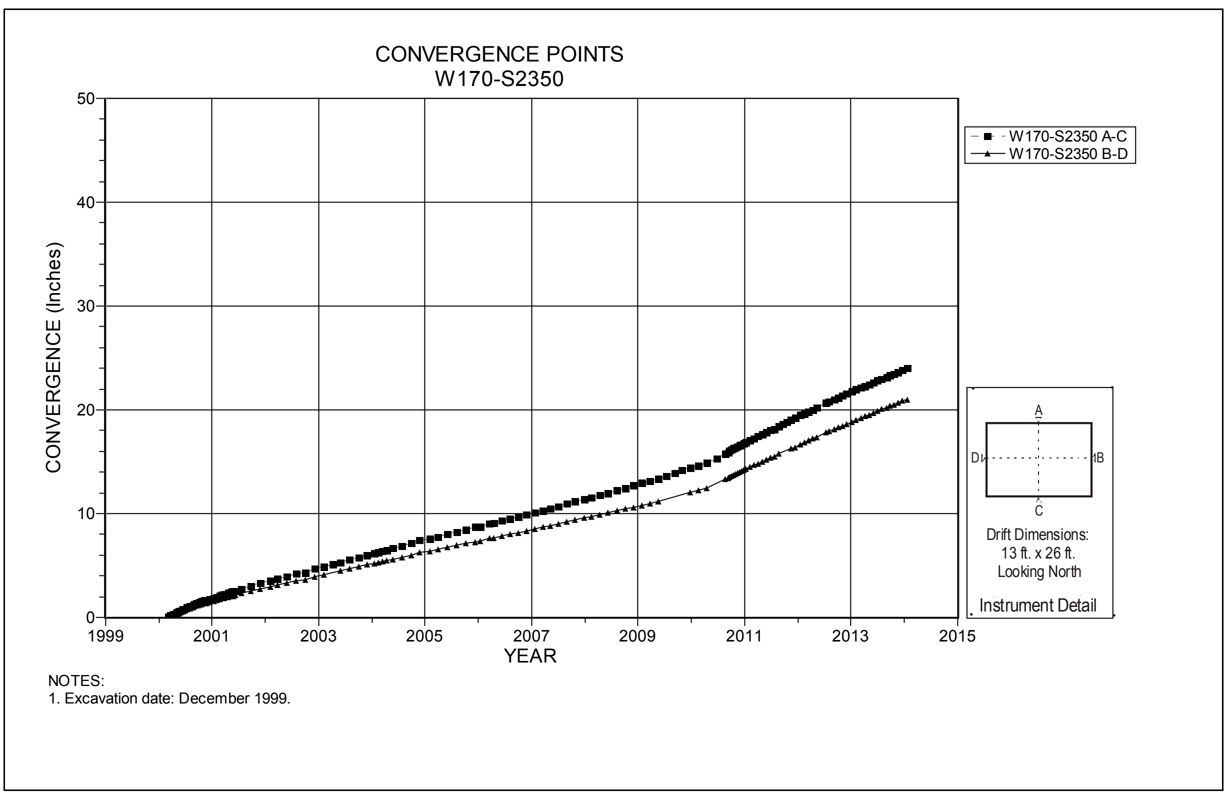

Figure 4-248 Convergence Point Array
W170 S2350 – All Chords

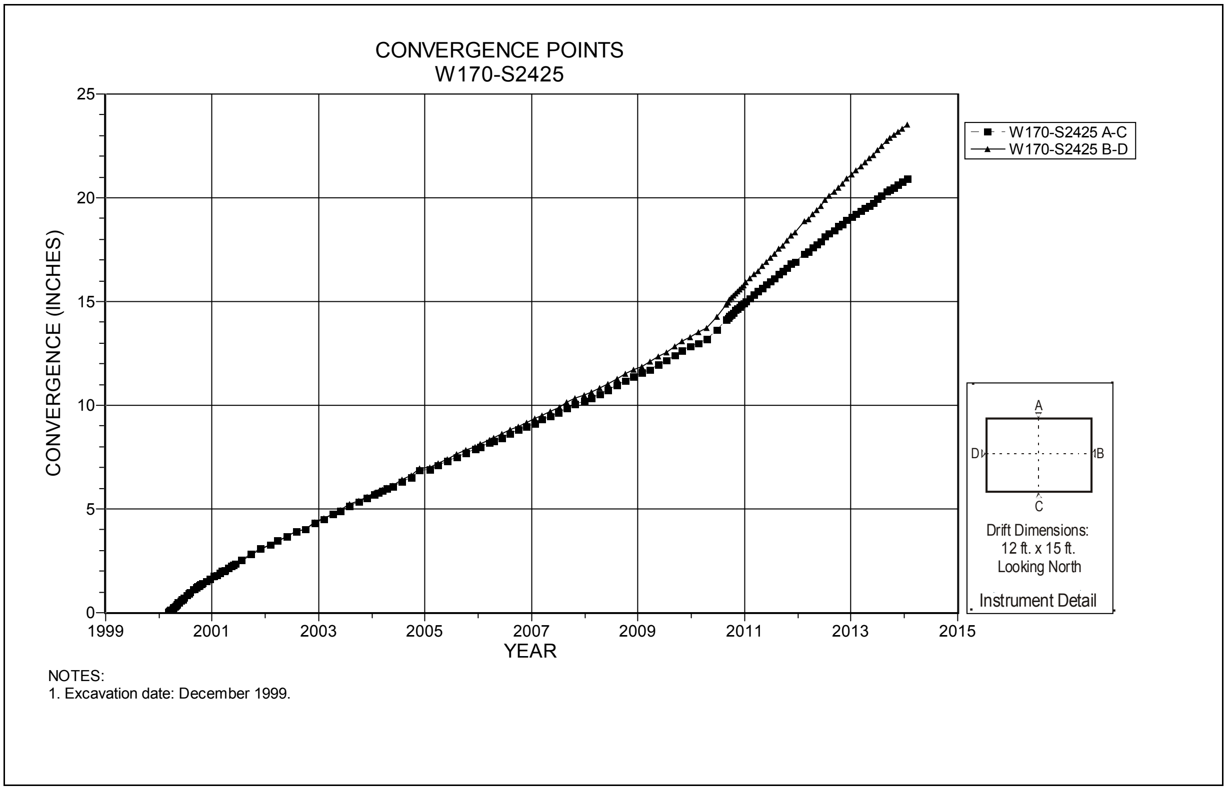

Figure 4-249 Convergence Point Array
W170 S2425 – All Chords

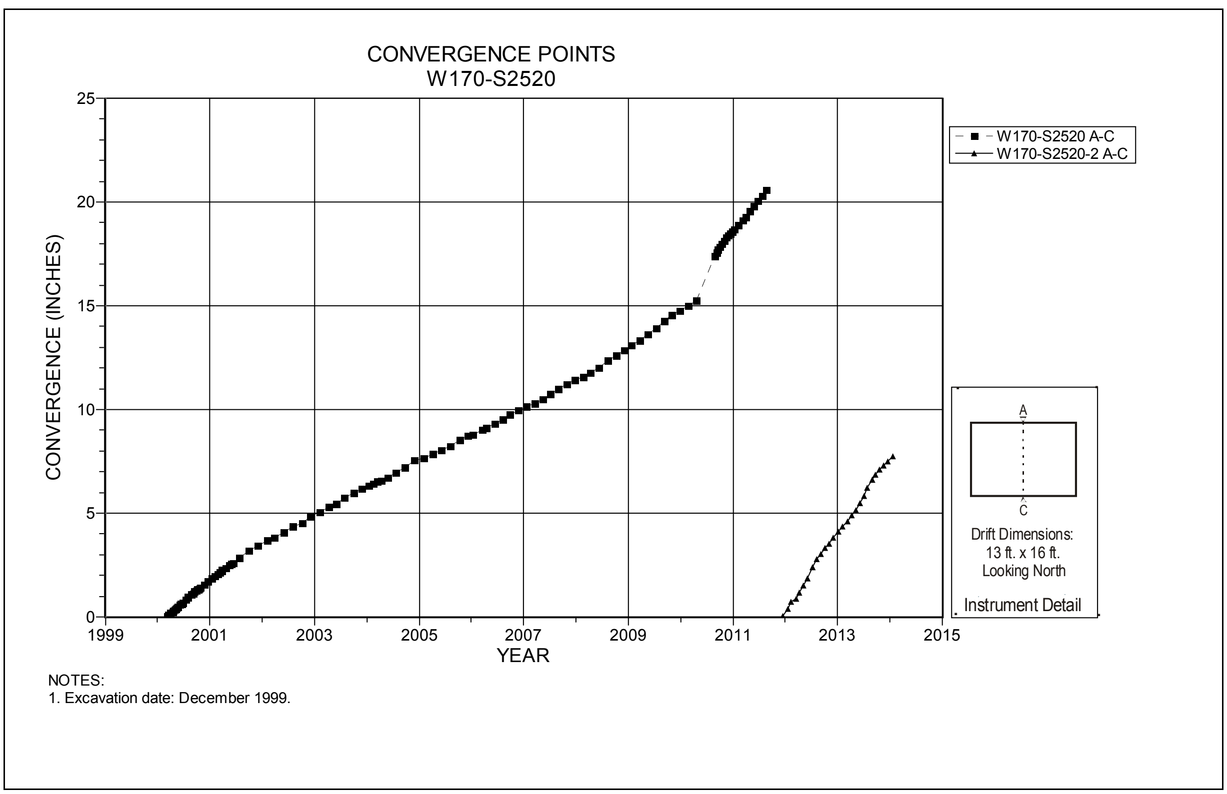

Figure 4-250 Convergence Point Array
W170 S2520 – Roof to Floor

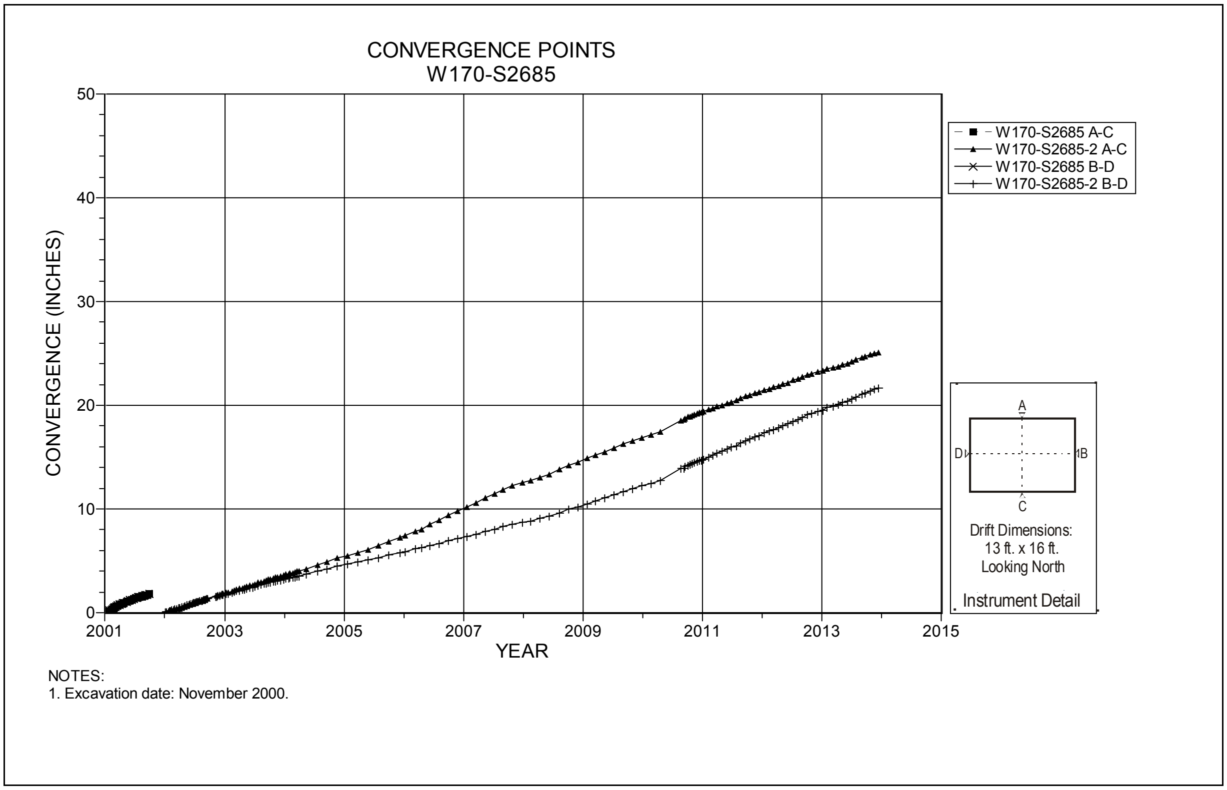

Figure 4-251 Convergence Point Array
W170 S2685 – All Chords

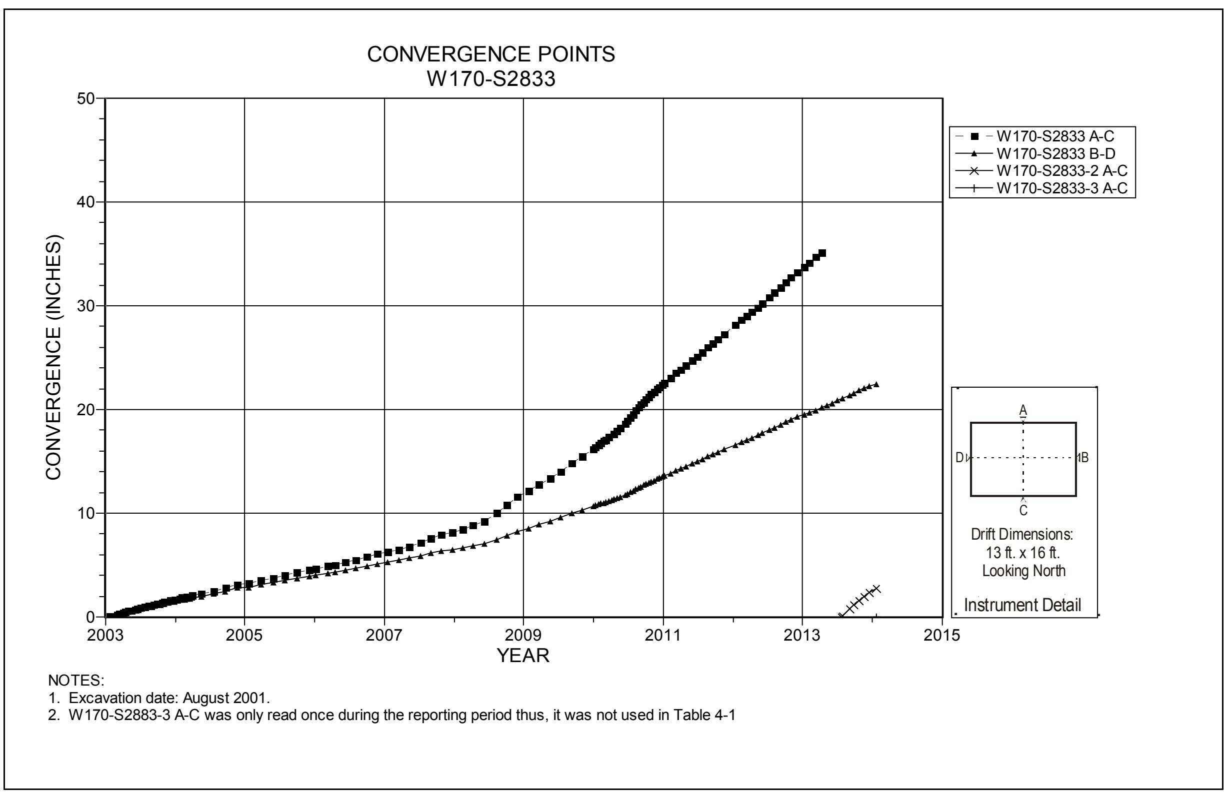

Figure 4-252 Convergence Point Array
W170 S2833 – All Chords

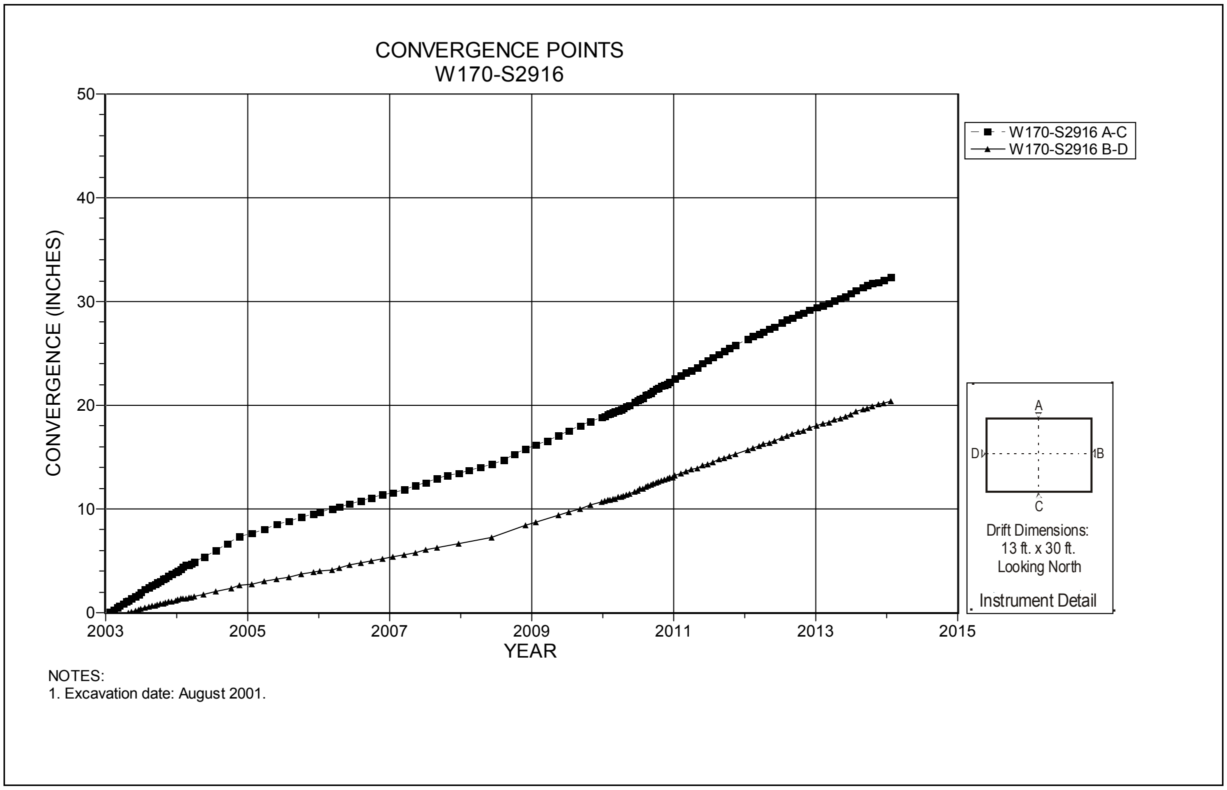

Figure 4-253 Convergence Point Array
W170 S2916 – All Chords

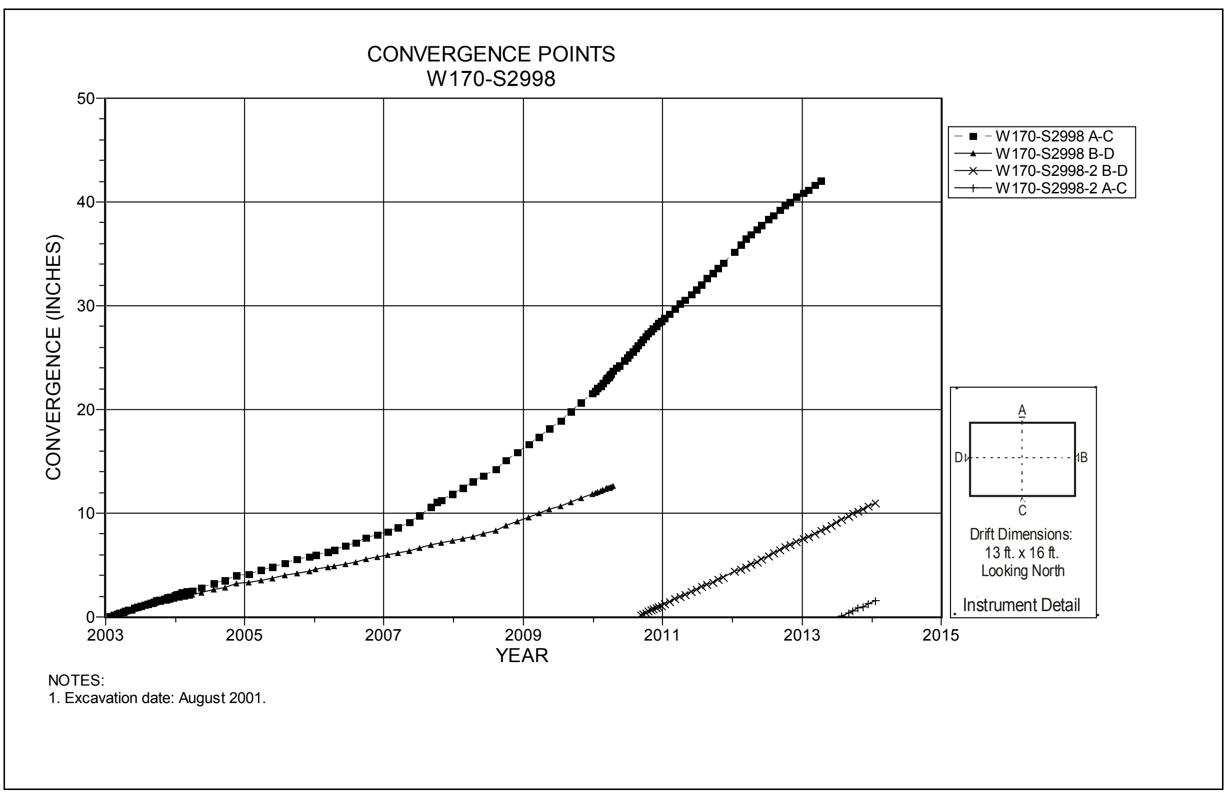

Figure 4-254 Convergence Point Array
W170 S2998 – All Chords

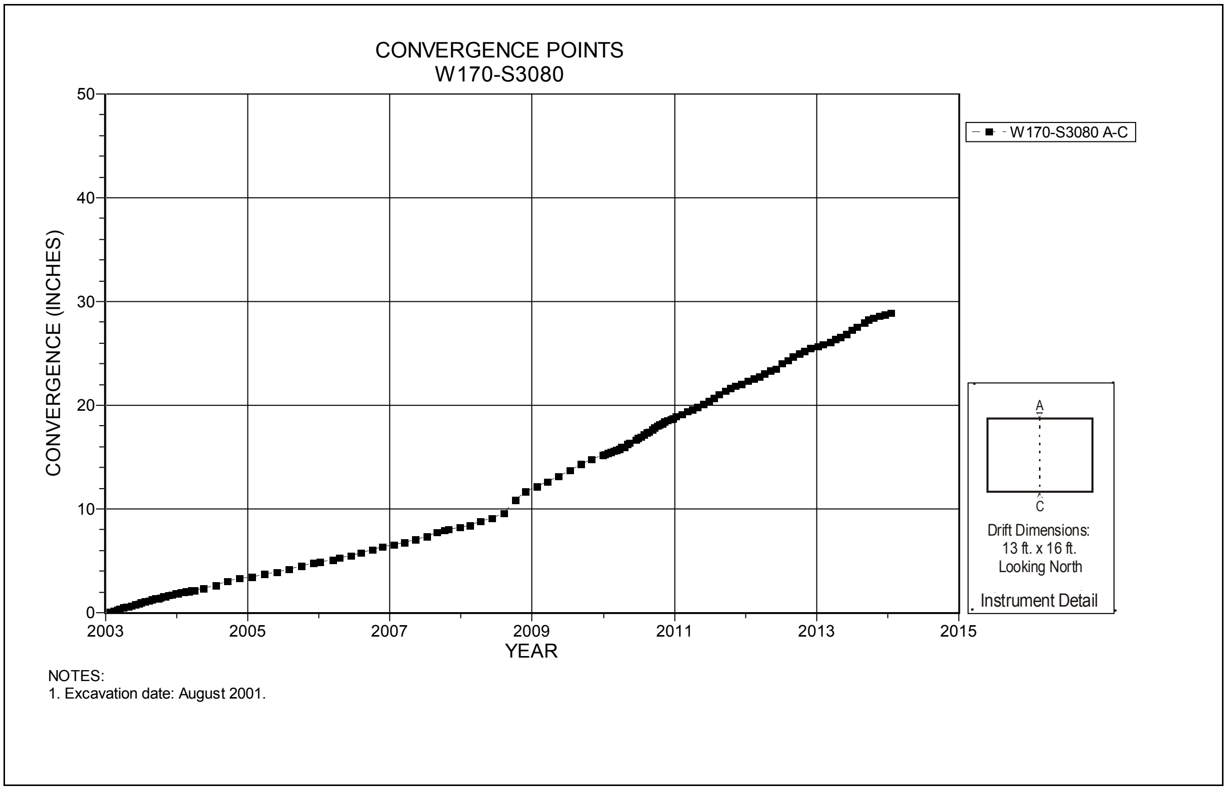

Figure 4-255 Convergence Point Array
W170 S3080 – Roof to Floor

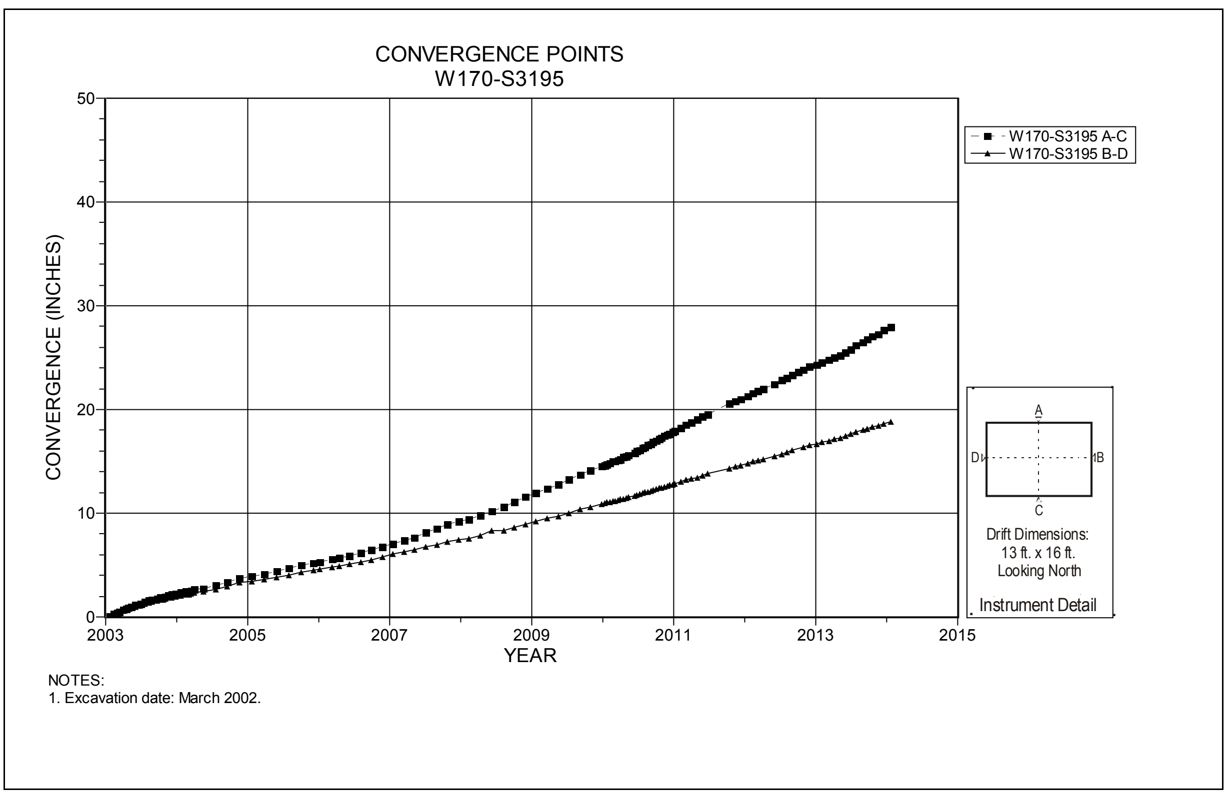

Figure 4-256 Convergence Point Array
W170 S3195 – All Chords

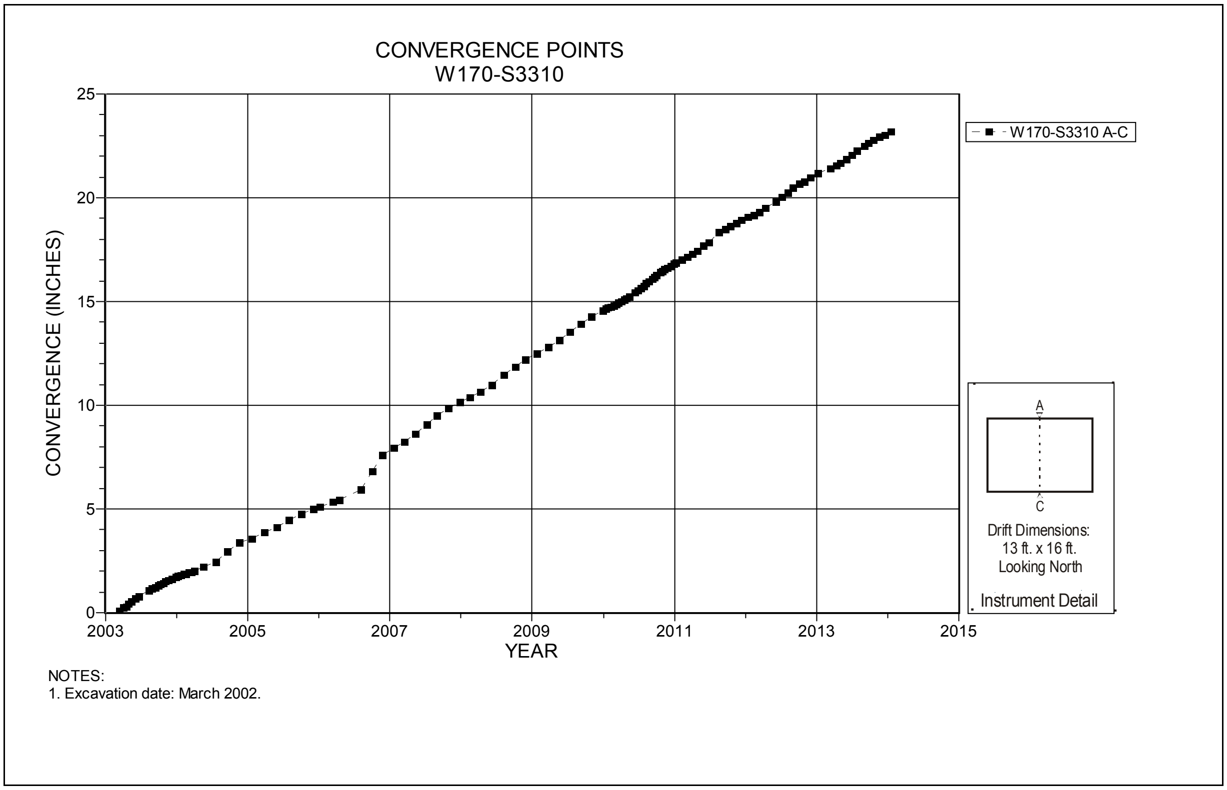

Figure 4-257 Convergence Point Array
W170 S3310 – Roof to Floor

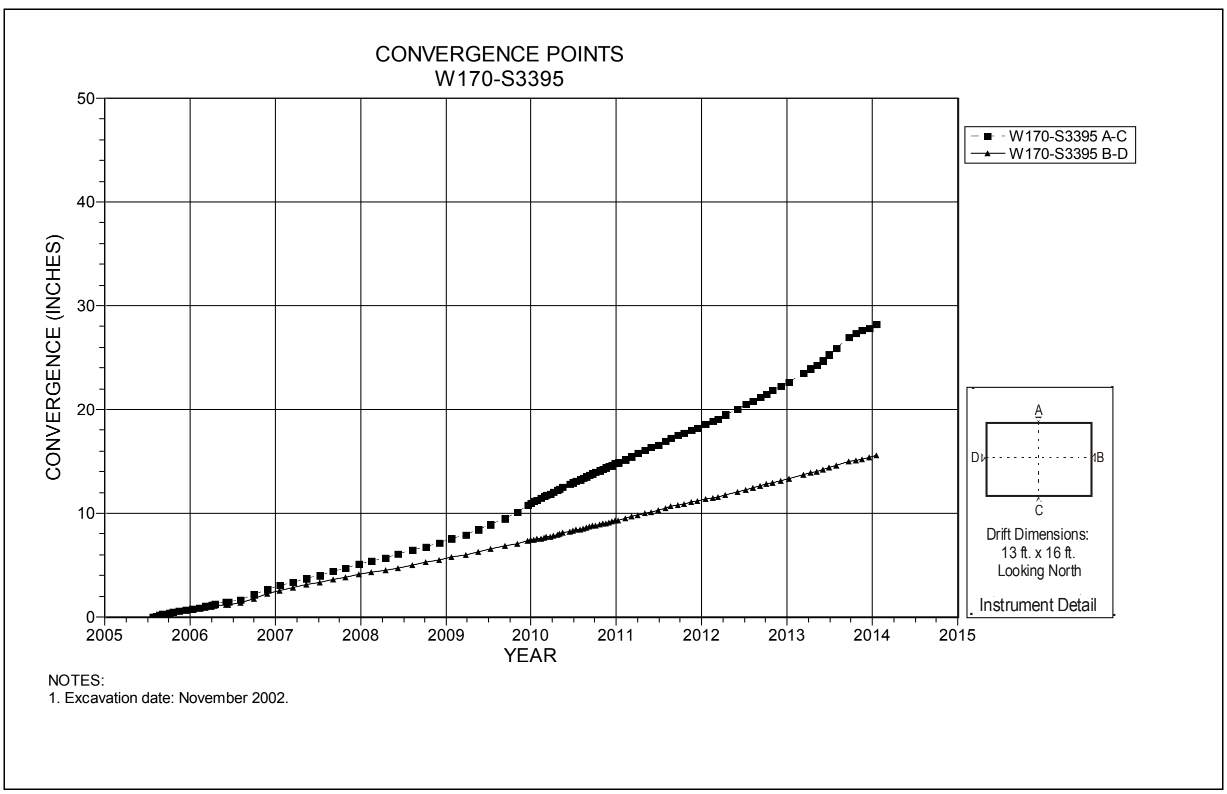

Figure 4-258 Convergence Point Array
W170 S3395 – All Chords

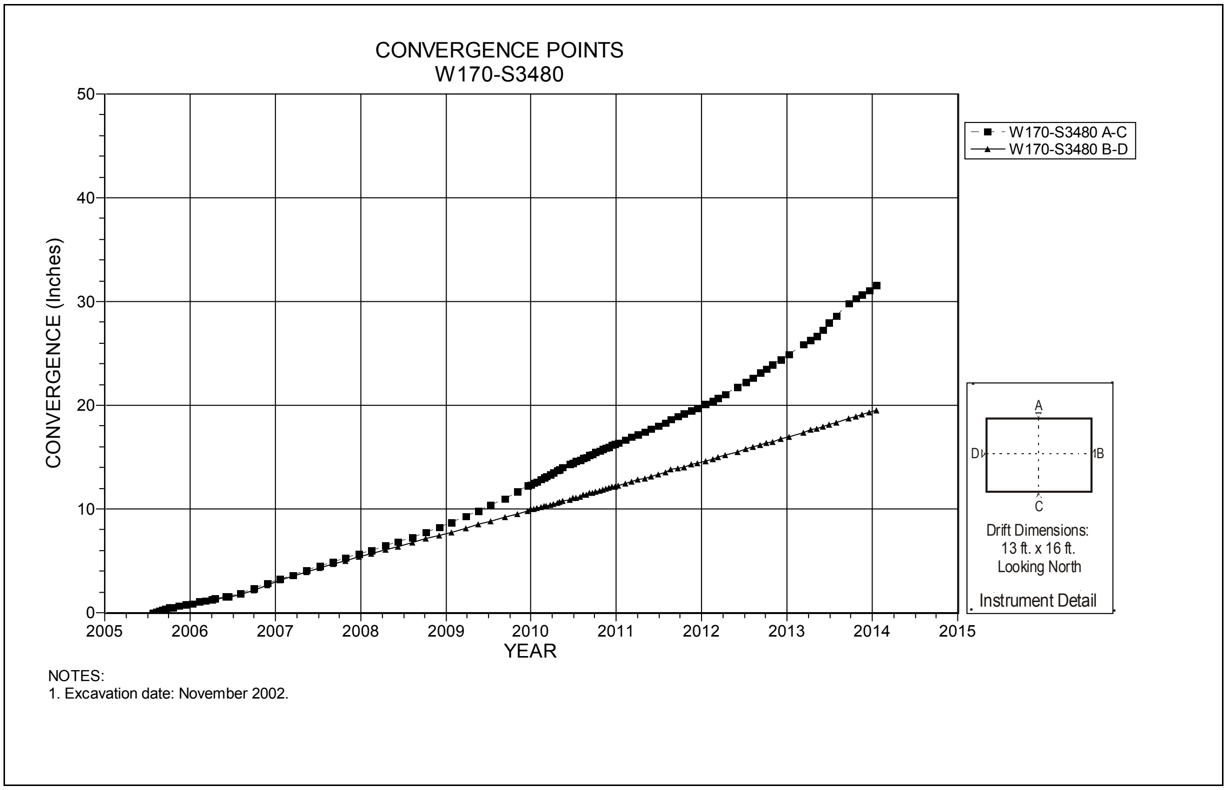

Figure 4-259 Convergence Point Array
W170 S3480 – All Chords

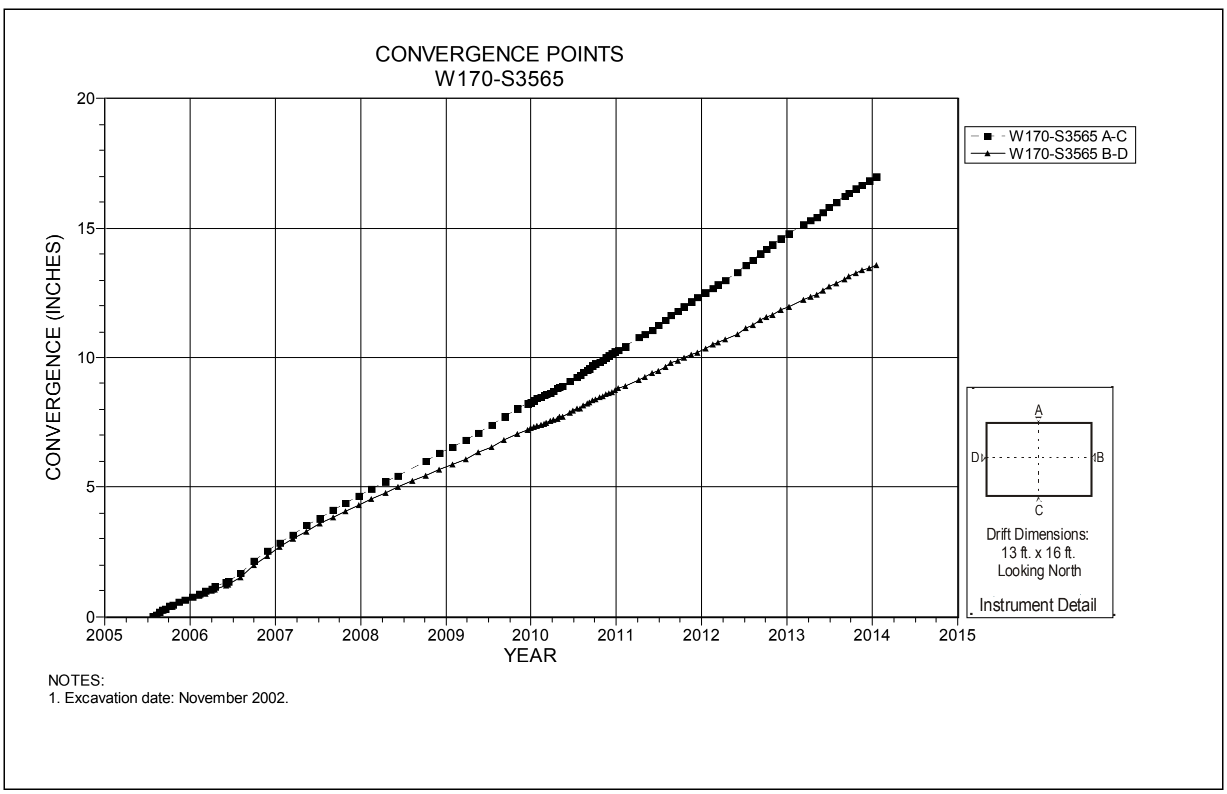

Figure 4-260 Convergence Point Array
W170 S3565 – All Chords

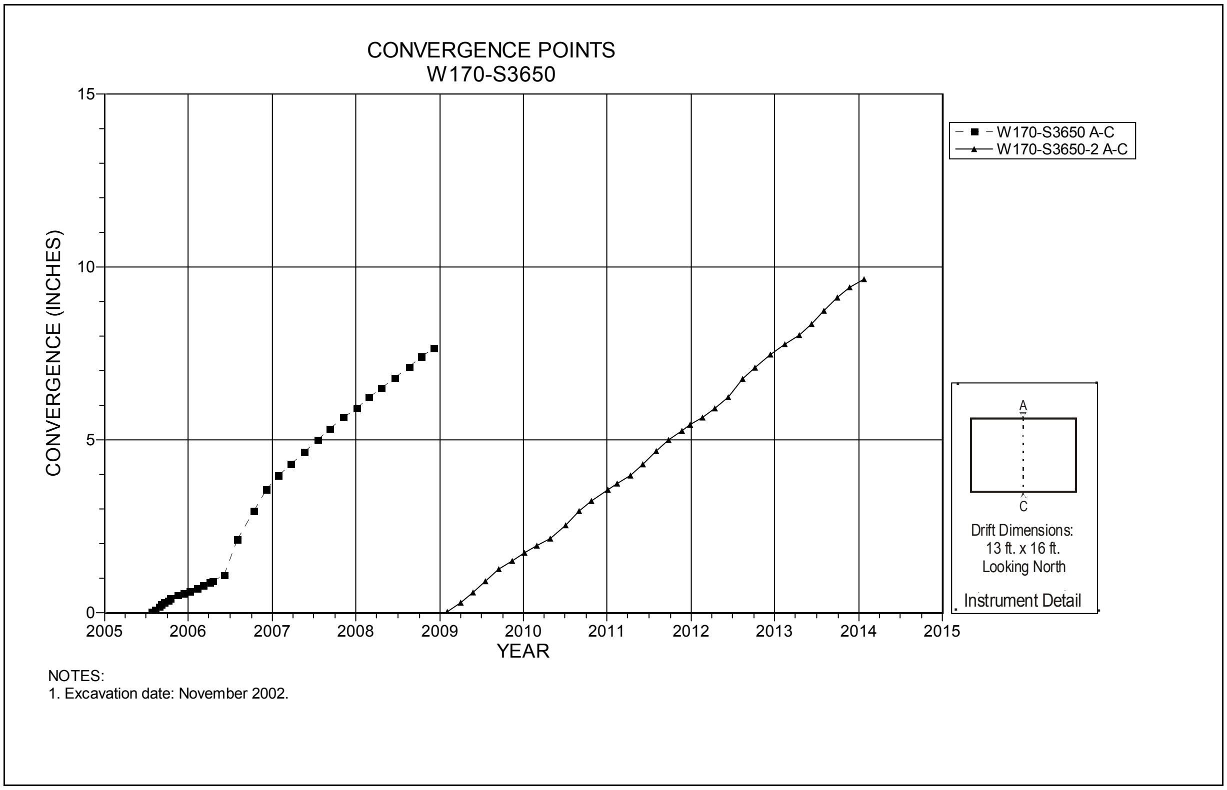

Figure 4-261 Convergence Point Array
W170 S3650 – Roof to Floor

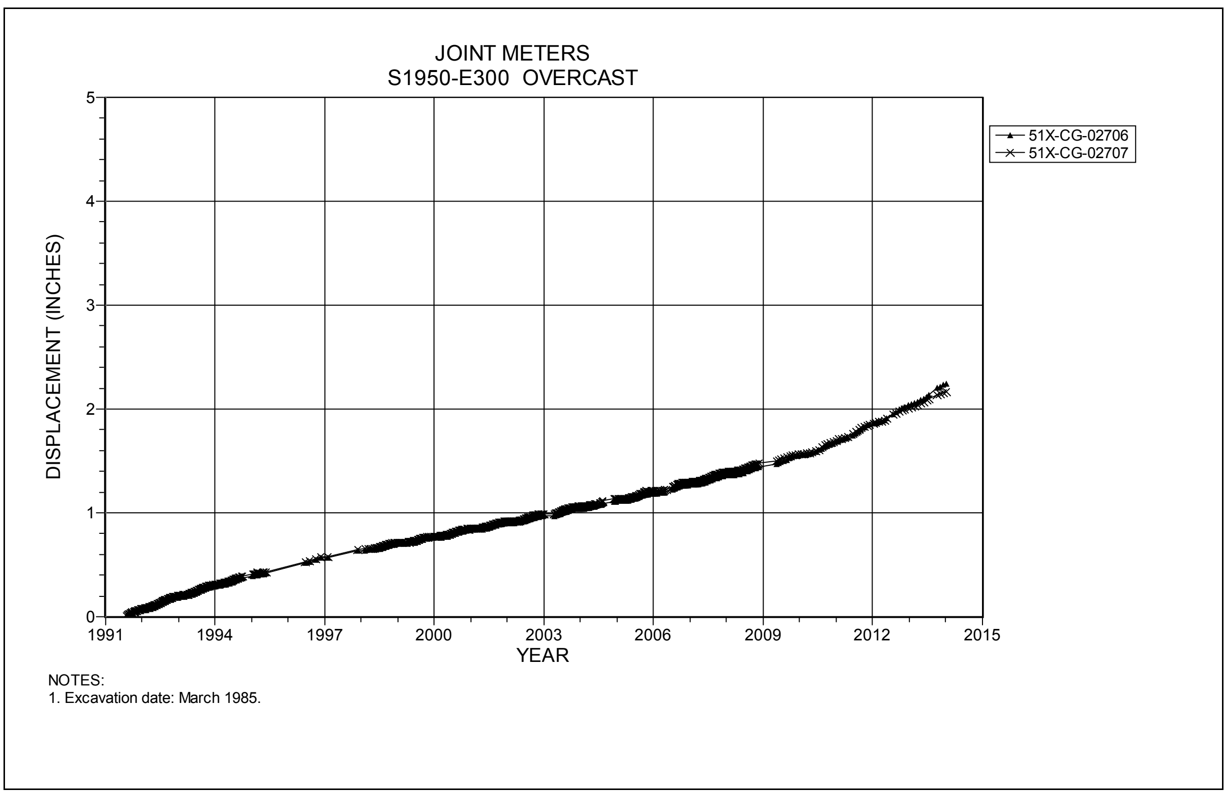

Figure 4-262 Joint Meters
S1950 E300 Overcast

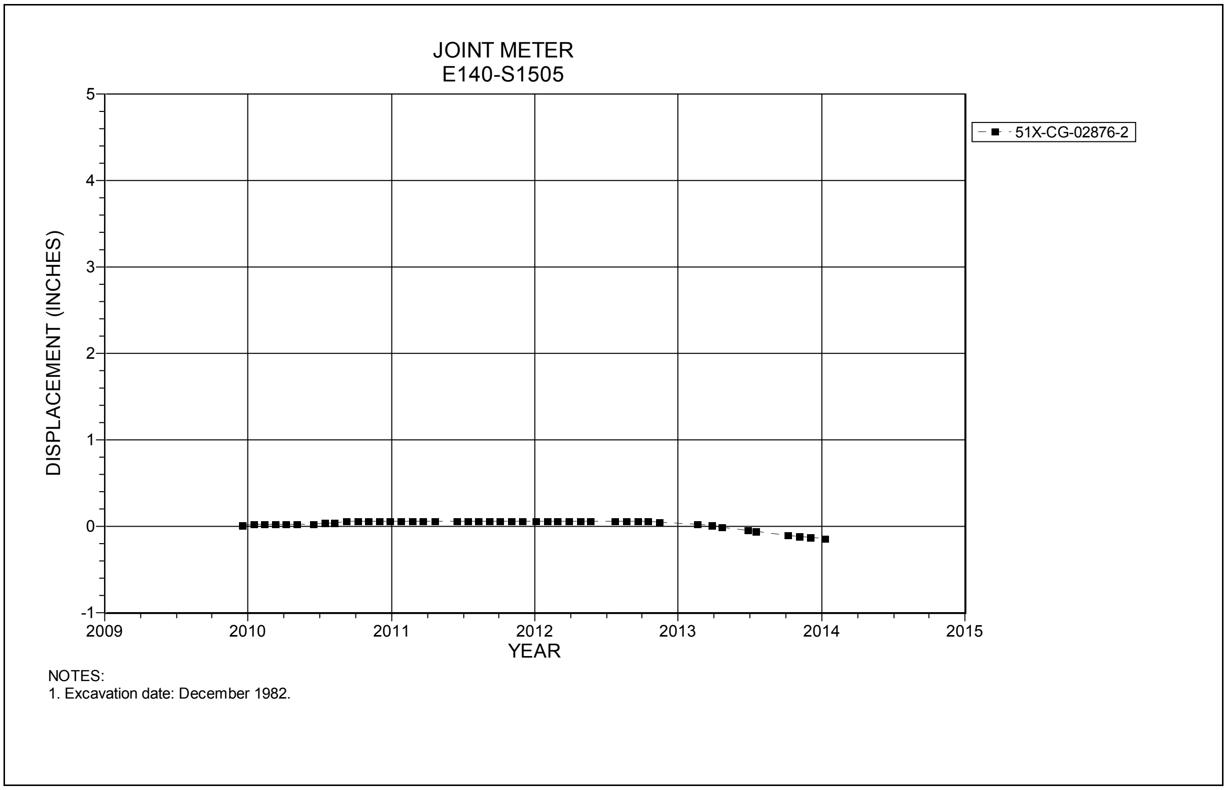

Figure 4-263 Joint Meter
E140 S1505

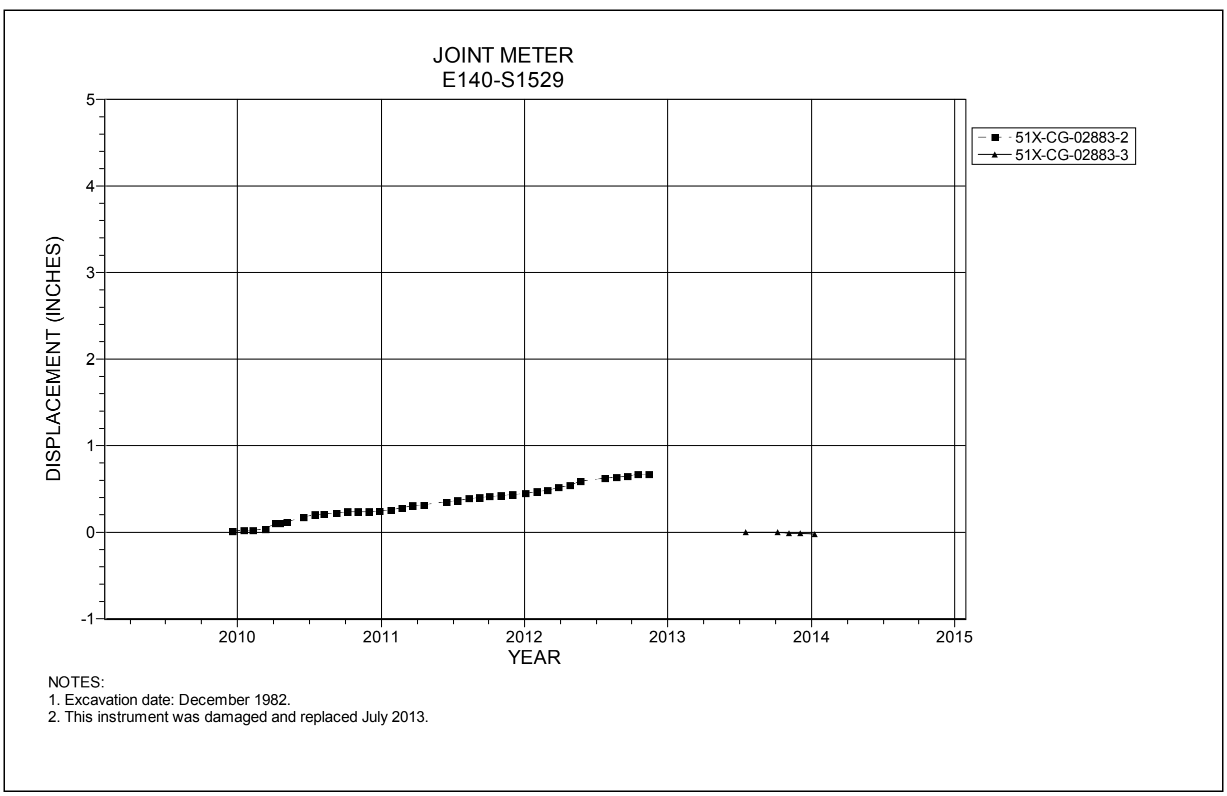

Figure 4-264 Joint Meter
E140 S1529

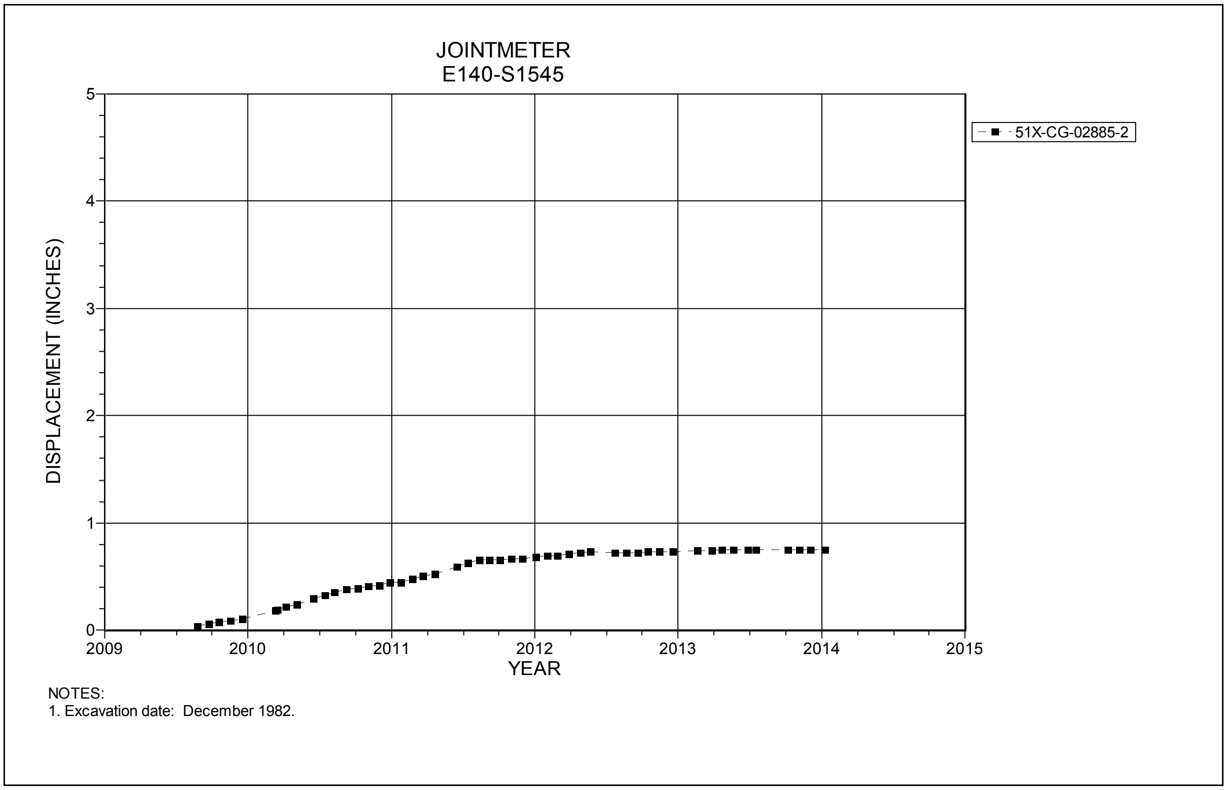

Figure 4-265 Joint Meter
E140 S1545

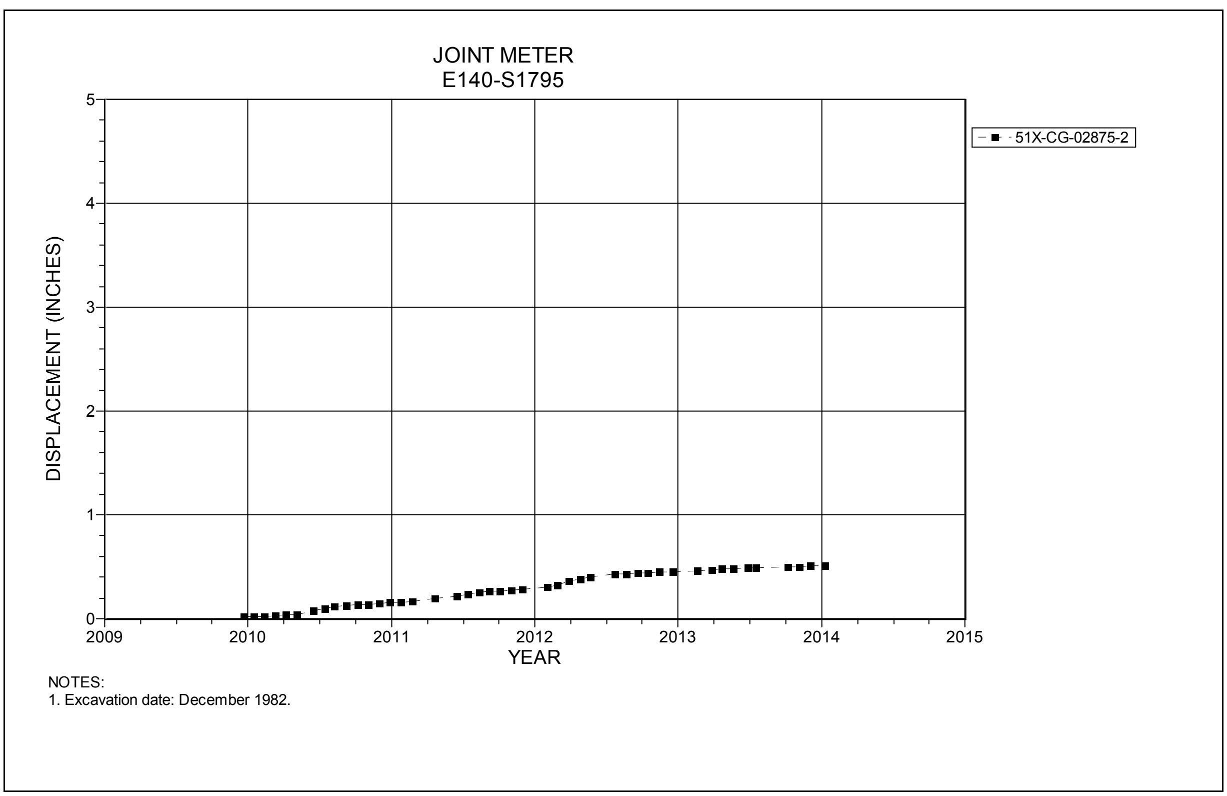

Figure 4-266 Joint Meter
E140 S1795

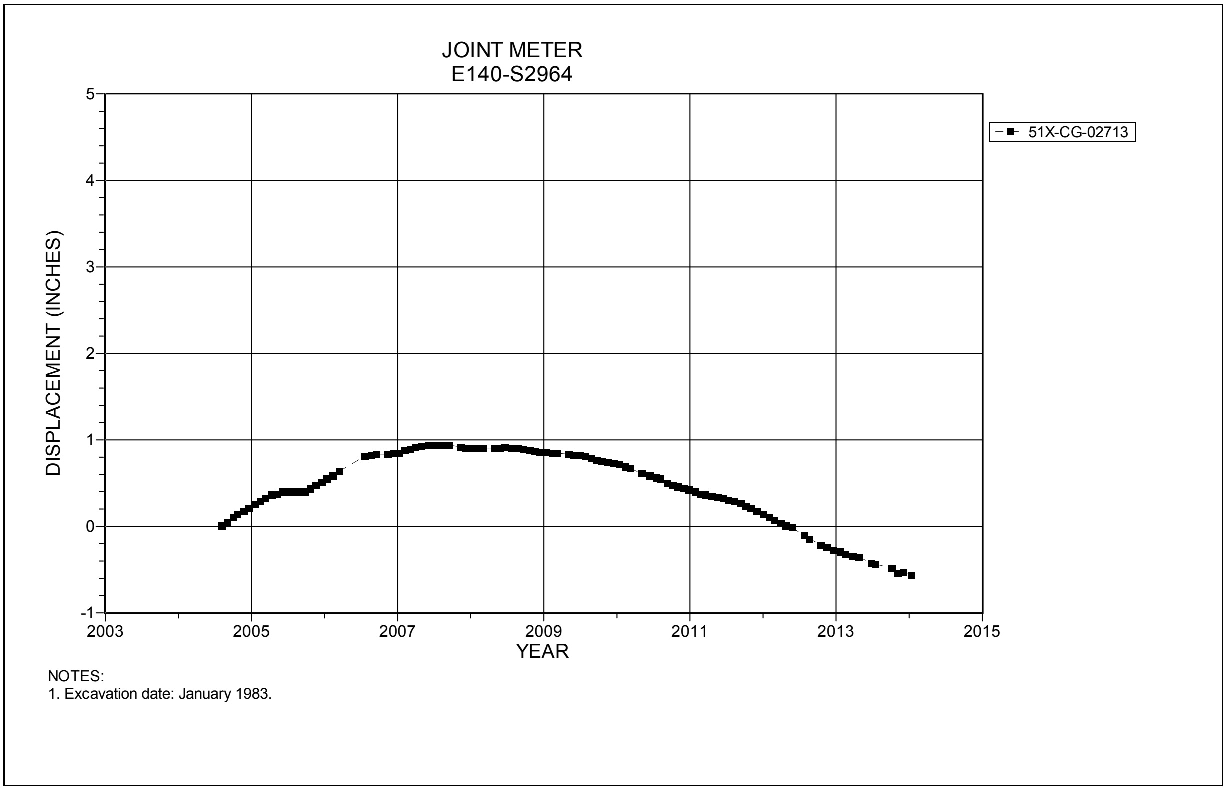

Figure 4-267 Joint Meter
E140 S2964

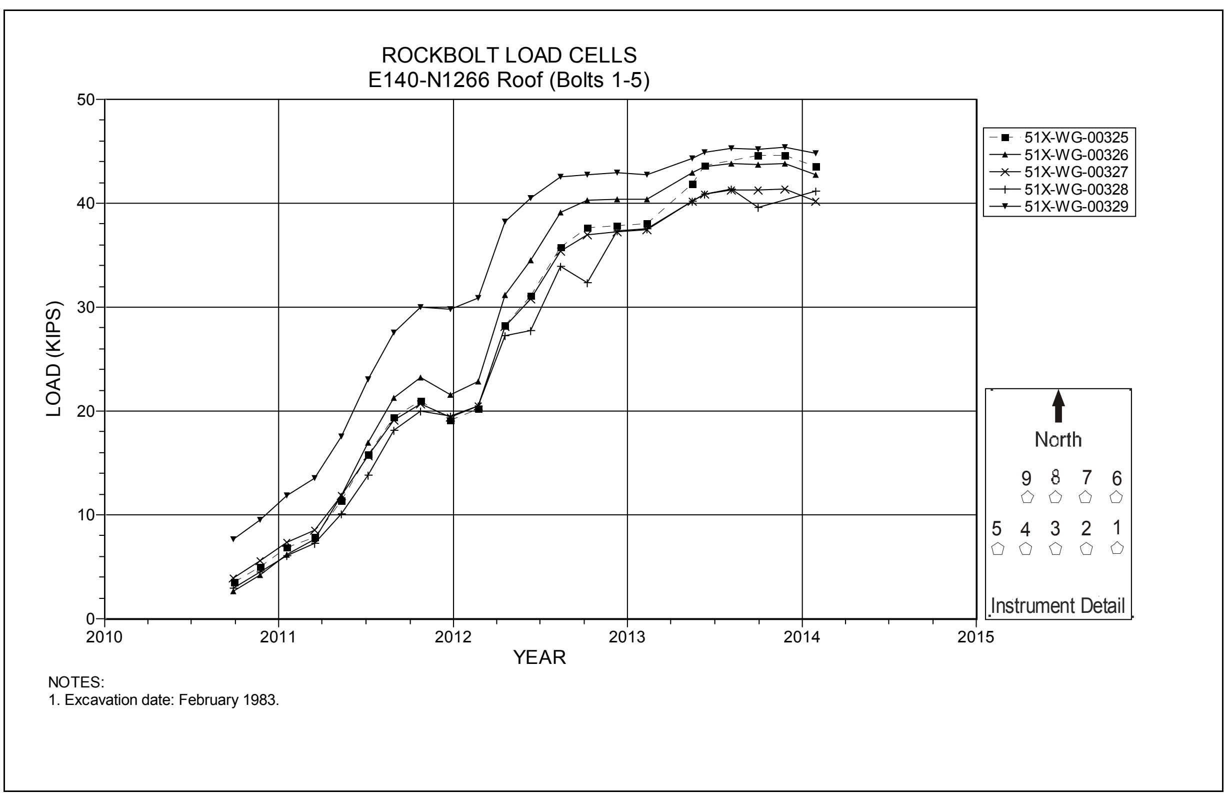

Figure 4-268 Rock Bolt Load Cells, Bolts 1-5
E140 N1266

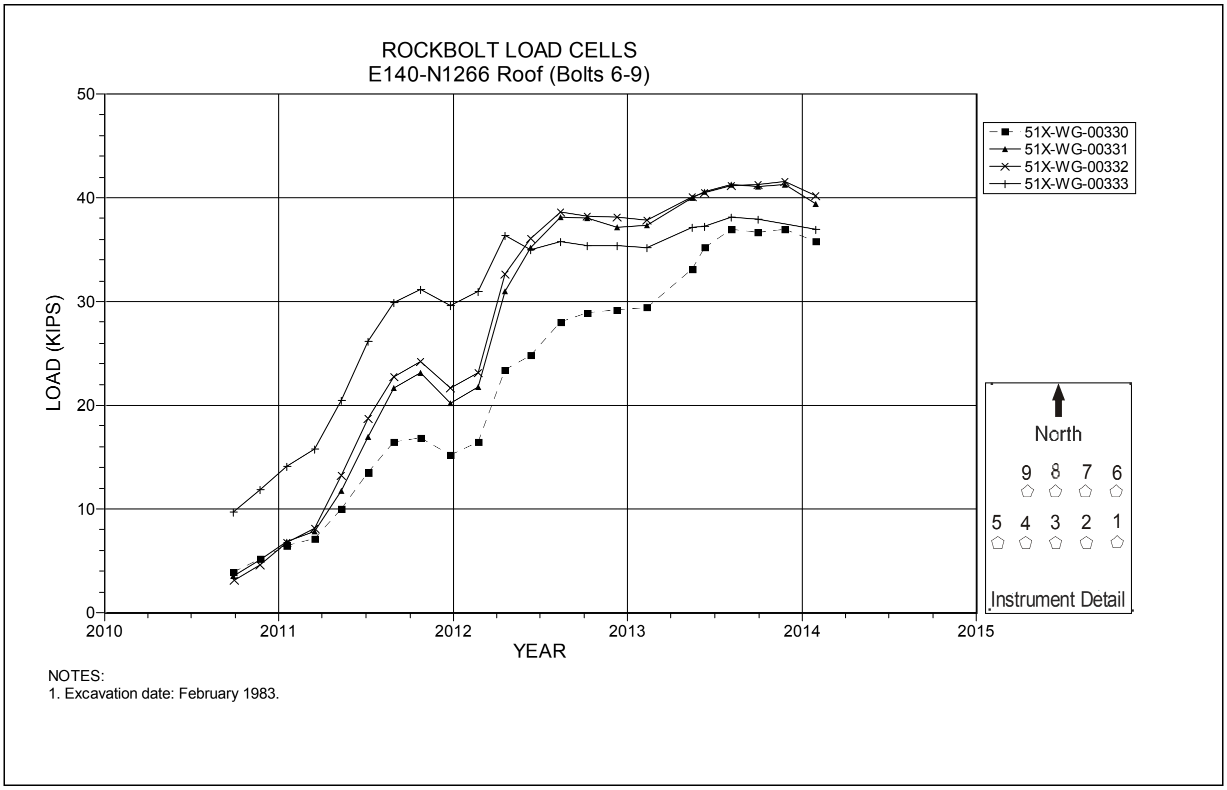

Figure 4-269 Rock Bolt Load Cells, Bolts 6-9
E140 N1266

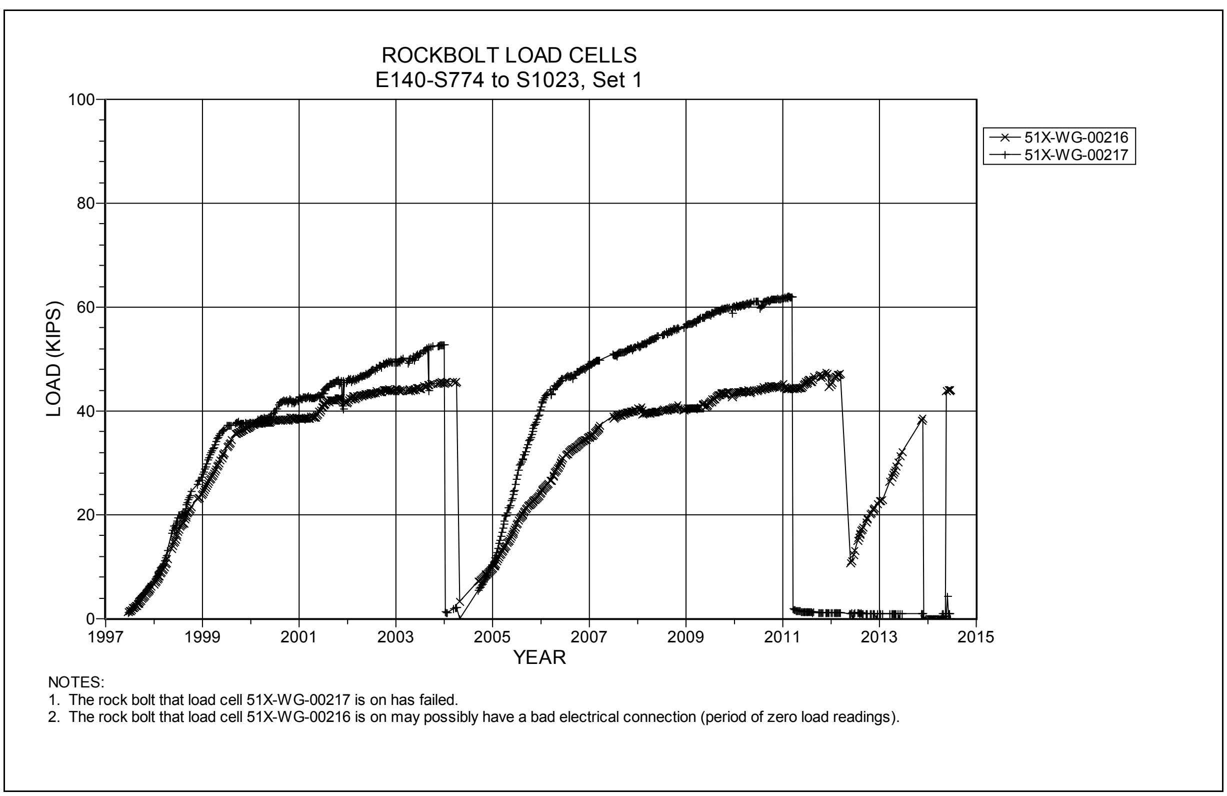

Figure 4-270 Rock Bolt Load Cells
E140 S774 – S1023

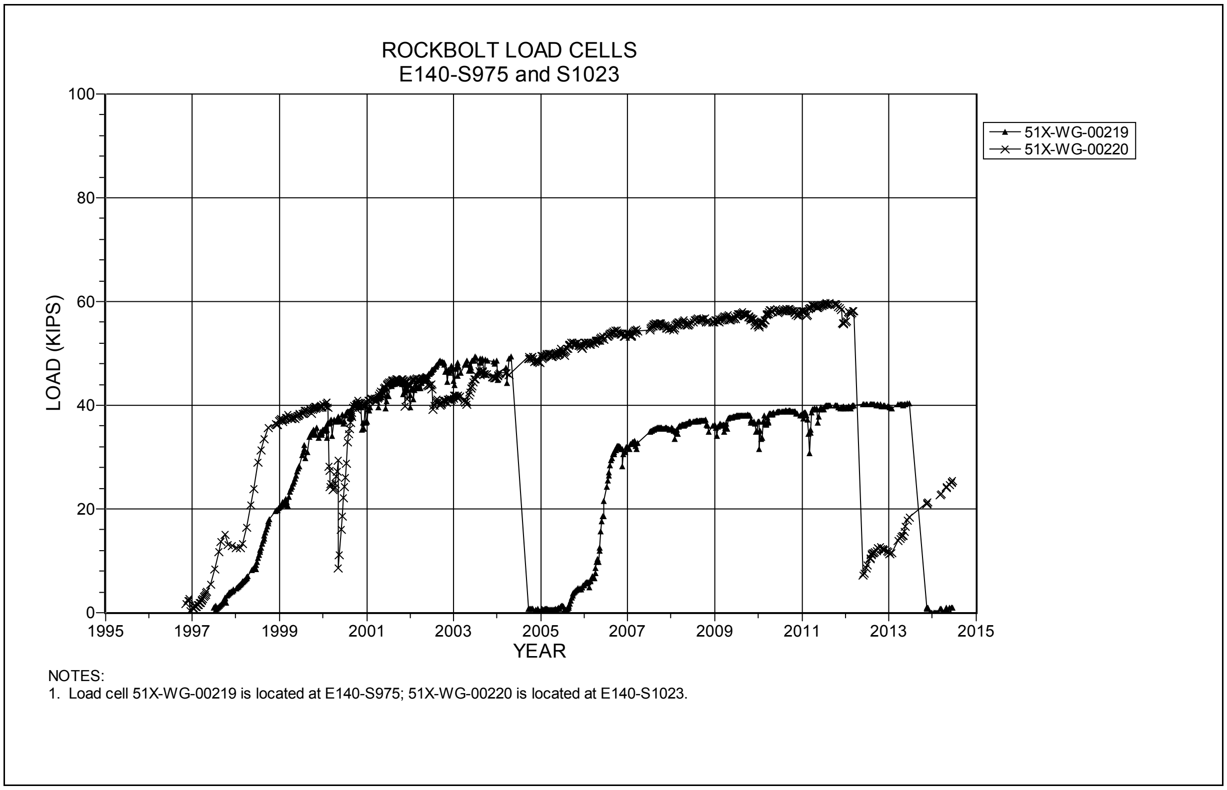

Figure 4-271 Rock Bolt Load Cells
E140 S975 and S1023

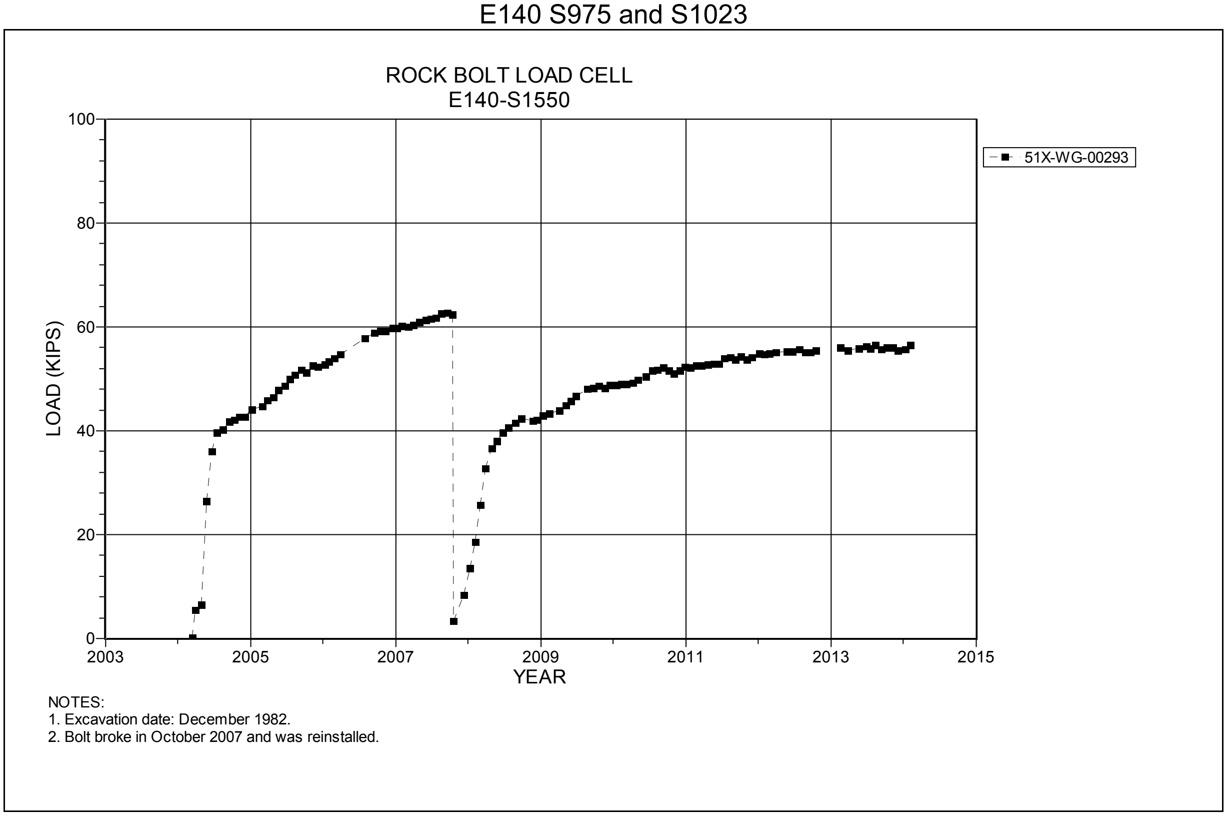

Figure 4-272 Rock Bolt Load Cell
E140 S1550

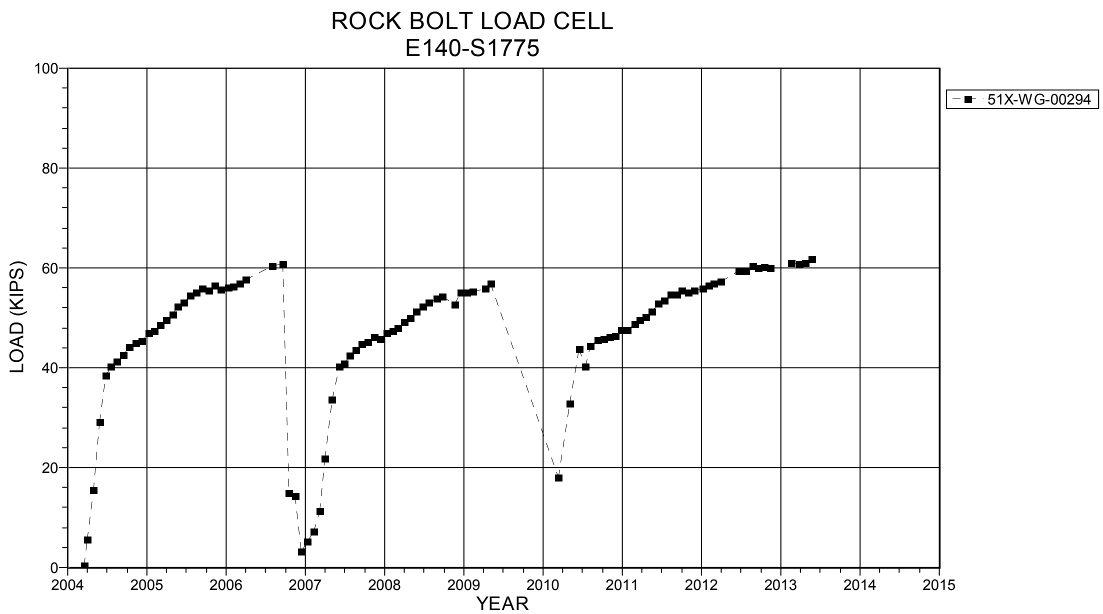

NOTES:
1. Excavation date: December 1982.
2. Reinstalled RBLC due to broken bolt, replaced Oct. 2006
3. Reinstalled RBLC due to broken bolt, replaced March 2010.

Figure 4-273 Rock Bolt Load Cell
E140 S1775

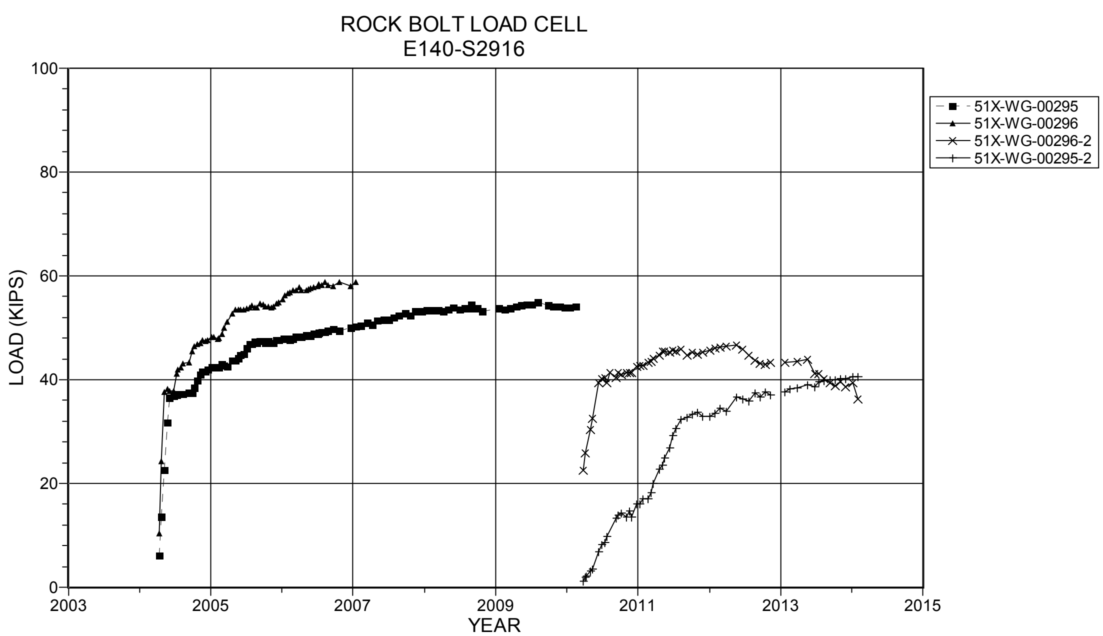

NOTES:
1. Excavation date: January 1983.
2. 51X-WG-00295-2 installed on replacement bolt in March 2010.
3. 51X-WG-00296-2 installed on replacement bolt in March 2010.

Figure 4-274 Rock Bolt Load Cells
E140 S2916

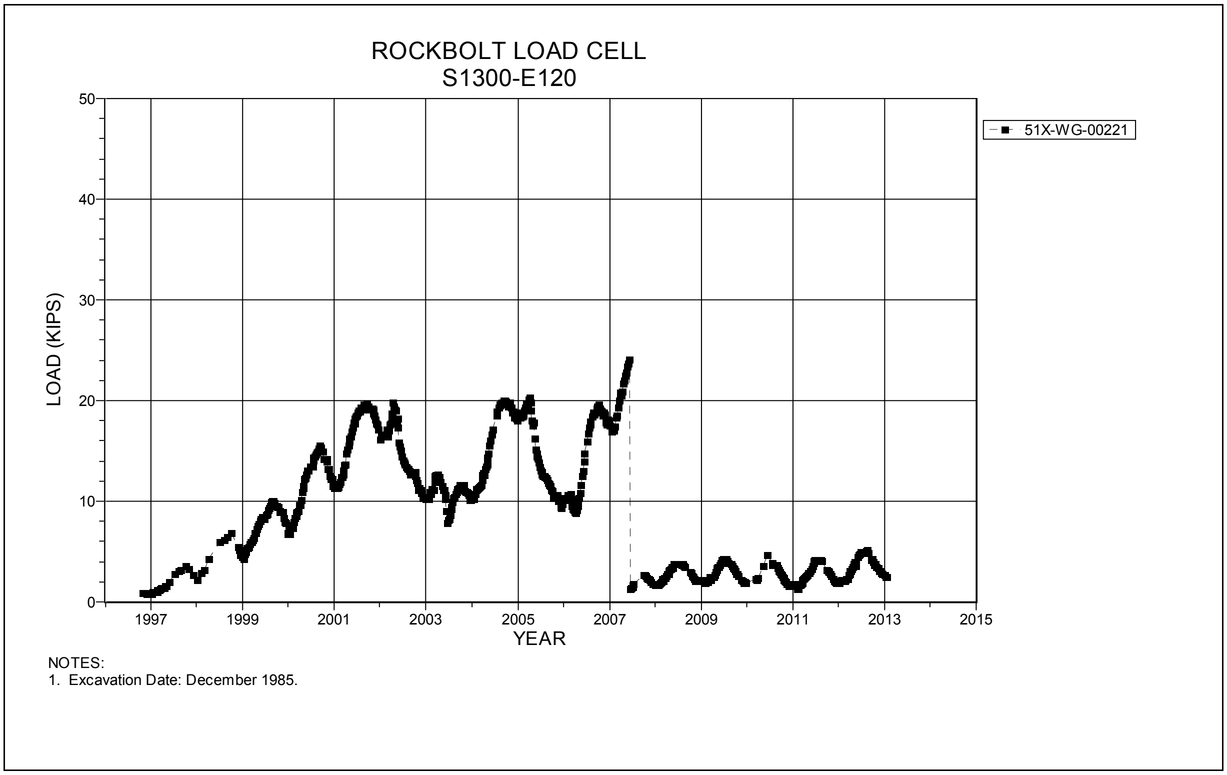

Figure 4-275 Rock Bolt Load Cell
S1300 E120

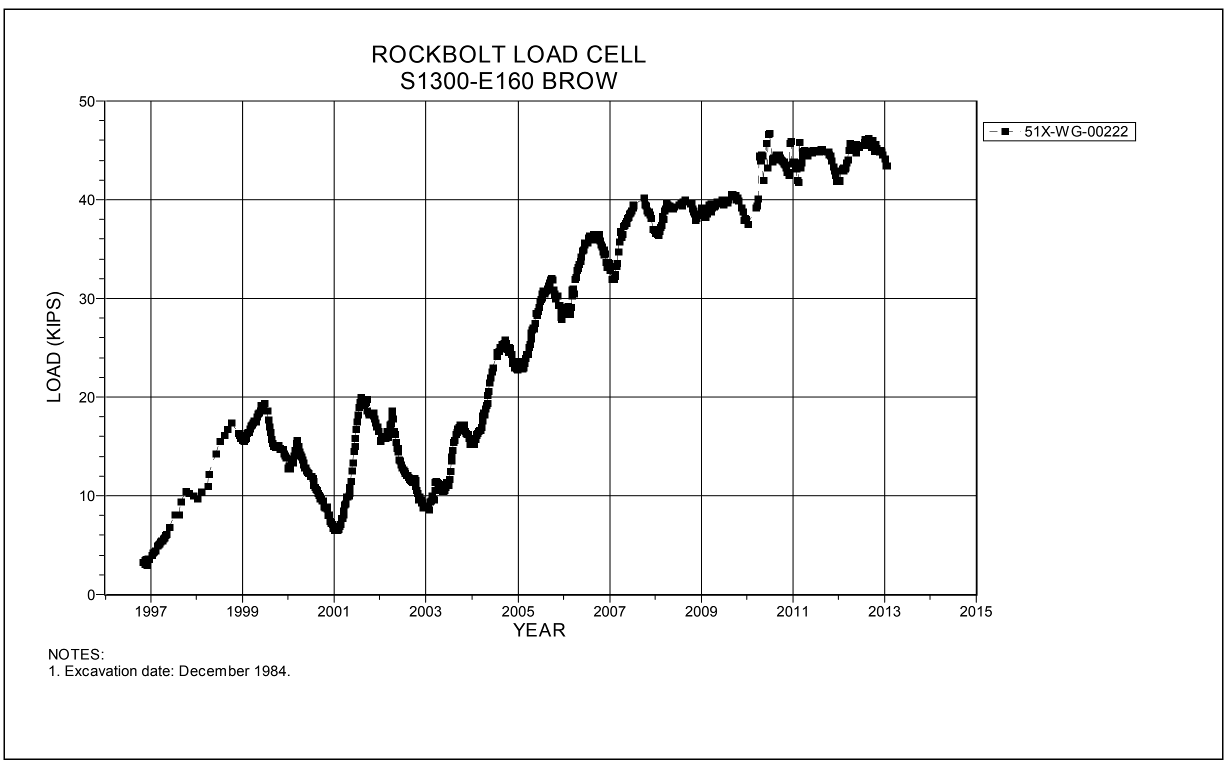

Figure 4-276 Rock Bolt Load Cell
S1300 E160

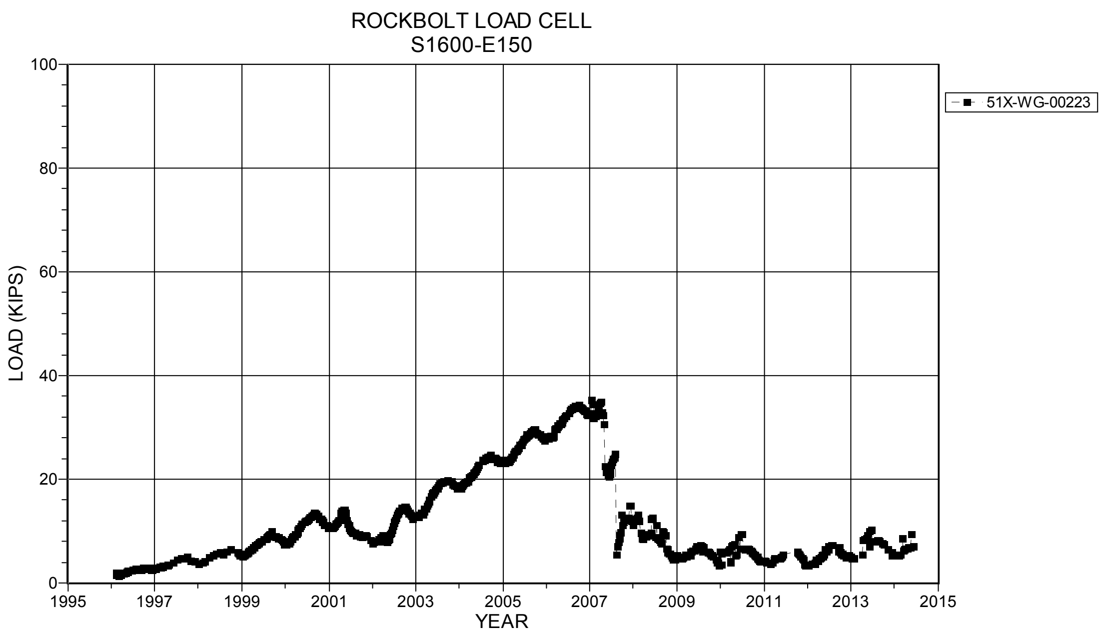

NOTES:
1. Excavation Date: September 1985.

Figure 4-277 Rock Bolt Load Cell
S1600 E150

5.0 Instrumentation Summary for the Waste Disposal Area

This chapter presents a summary of the data collected from instruments located in the Waste Disposal Area at the WIPP. Table 5-1 presents data and analysis of the access drifts associated with Panel 1. Plots of the instrument data are presented as Figures 5-1 through 5-15.

Table 5-2 presents data and analysis of the access drifts associated with Panel 2. Plots of the instrument data are presented as Figures 5-16 and 5-17.

Table 5-3 presents data and analysis of Panel 3. Plots of the instrument data are presented as Figures 5-18 through 5-19.

Table 5-4 presents data and analysis of Panel 4. The instrument data plot is presented as Figure 5-20.

Table 5-5 presents data and analysis of Panel 5. Plots of the instrument data are presented as Figures 5-21 and 5-22.

Table 5-6 presents data and analysis of Panel 6. Plots of the instrument data are presented as Figures 5-23 through 5-46.

Table 5-7 presents data and analysis of Panel 7. Plots of the instrument data are presented as Figures 5-47 through 5-106.

Table 5-1
Panel 1 Access Drifts Data Analysis

Convergence Points

Field Tag	Location	Figure Number	Last Reading 2013 to 2014		Cumulative Displacement (inches)	Closure Rate 2013 to 2014 (in/year)	Closure Rate 2012 to 2013 (in/year)	Rate Change Percent	Comments
			Date	Inches					
S1600-E311-2[1] A-C	S1600-E311	5-1	12/09/13	18.000	23.447	0.3	0.9	-67%	
S1600-E332-3[1] A-C	S1600-E332	5-2	12/09/13	17.663	22.090	0.8	1.0	-20%	
S1600-E357-2[1] A-C	S1600-E357	5-3	12/09/13	20.573	25.971	0.9	1.2	-25%	
S1600-E382-2[1] A-C	S1600-E382	5-4	12/09/13	20.299	25.679	0.9	1.1	-18%	
S1600-E407-2 A-G	S1600-E407	5-5	12/09/13	23.009	28.451	1.4	1.5	-7%	
S1600-E407-2 B-F	S1600-E407	5-5	12/09/13	21.237	26.243	1.3	1.3	0%	
S1600-E407-2[1] H-L	S1600-E407	5-5	12/09/13	22.313	27.378	1.2	1.4	-14%	
S1600-E432-2 A-C	S1600-E432	5-6	12/09/13	27.049	33.808	1.9	1.7	12%	
S1600-E453 B-D	S1600-E453	5-7	08/22/13	5.661	5.661	N/A	0.7	N/A	Inaccessible due to floor debris.
S1950-E311-7 A-C	S1950-E311	5-8	12/09/13	4.979	34.370	1.8	1.4	29%	
S1950-E311-3 B-D	S1950-E311	5-8	12/09/13	19.866	32.867	2.2	1.3	69%	
S1950-E332-4[1] A-C	S1950-E332	5-9	12/09/13	23.340	41.942	2.1	1.7	24%	
S1950-E332-4 B-D	S1950-E332	5-9	12/09/13	18.686	36.632	1.8	1.8	0%	
S1950-E357-7[1] A-C	S1950-E357	5-10	12/09/13	29.756	49.920	1.9	2.5	-24%	
S1950-E357-4[1] B-D	S1950-E357	5-11	12/09/13	19.783	38.242	1.5	1.9	-21%	
S1950-E382-5 A-C	S1950-E382	5-12	12/09/13	35.068	53.703	3.0	2.9	3%	
S1950-E382-3 B-D	S1950-E382	5-12	12/09/13	26.922	41.304	0.5	2.0	-75%	
S1950-E407-4 A-G	S1950-E407	5-13	12/09/13	34.403	56.227	2.6	2.7	-4%	
S1950-E407-3 H-L	S1950-E407	5-13	12/09/13	33.512	54.244	2.8	2.5	12%	
S1950-E407-3 D-J	S1950-E407	5-14	12/09/13	28.038	42.215	2.8	2.0	40%	
S1950-E432-3[1]A-C	S1950-E432	5-15	12/09/13	33.749	55.544	2.2	2.6	-15%	
S1950-E432-3 B-D	S1950-E432	5-15	12/09/13	26.220	40.621	1.7	1.9	-11%	

[1] The most recent installation was only read once before the radioactive release and is only presented in the data plots.

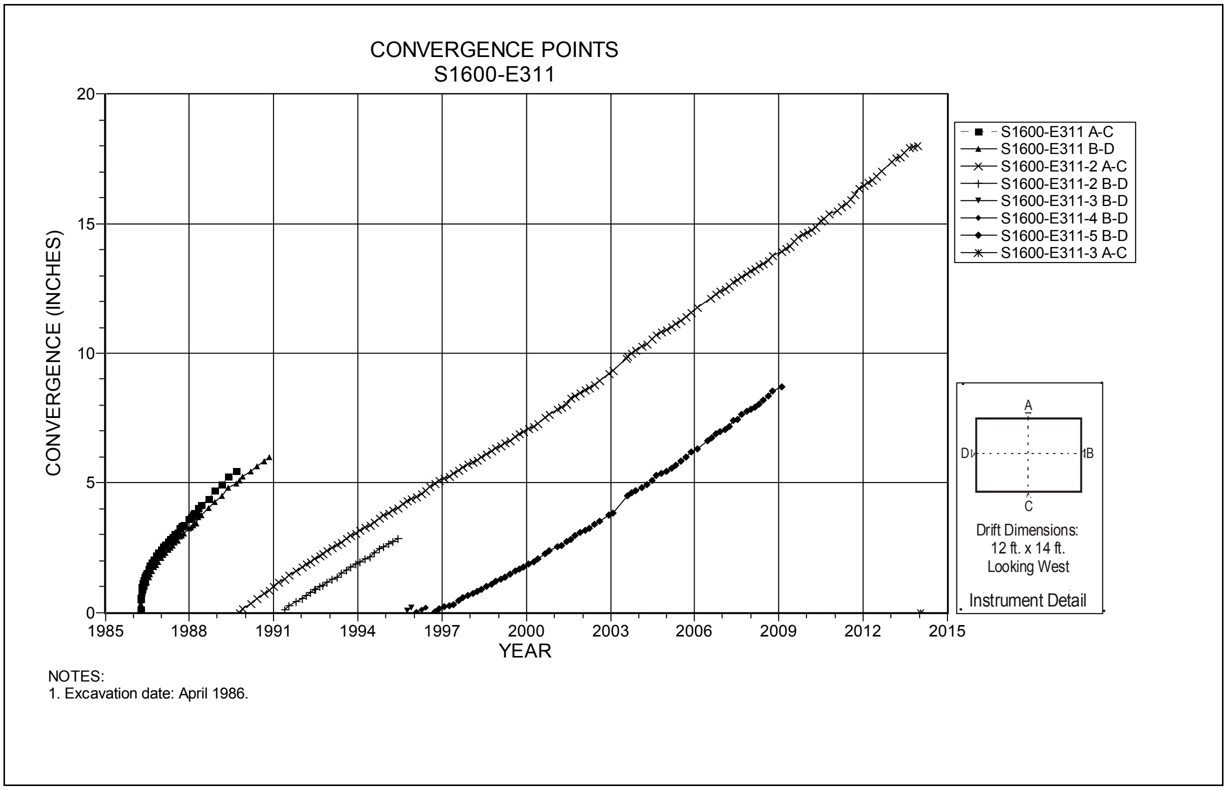

Figure 5-1 Convergence Point Array
S1600 E311 – All Chords

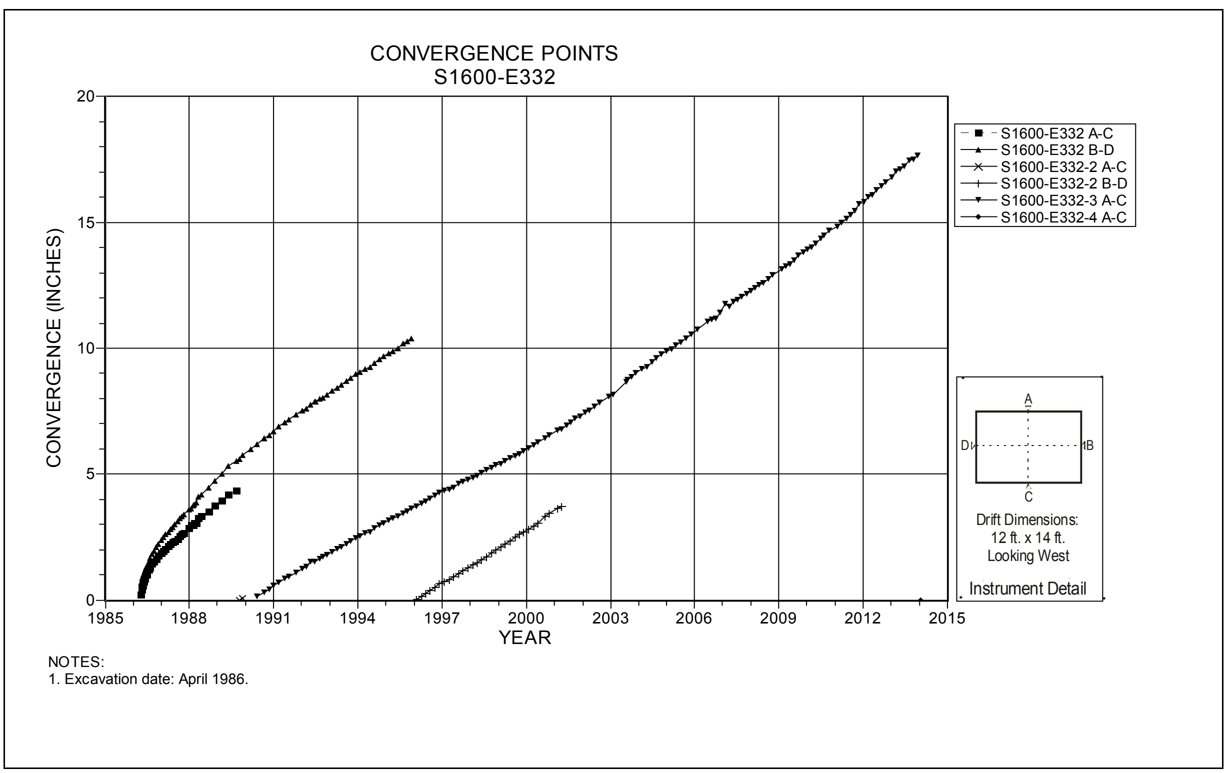

Figure 5-2 Convergence Point Array
S1600 E332 – All Chords

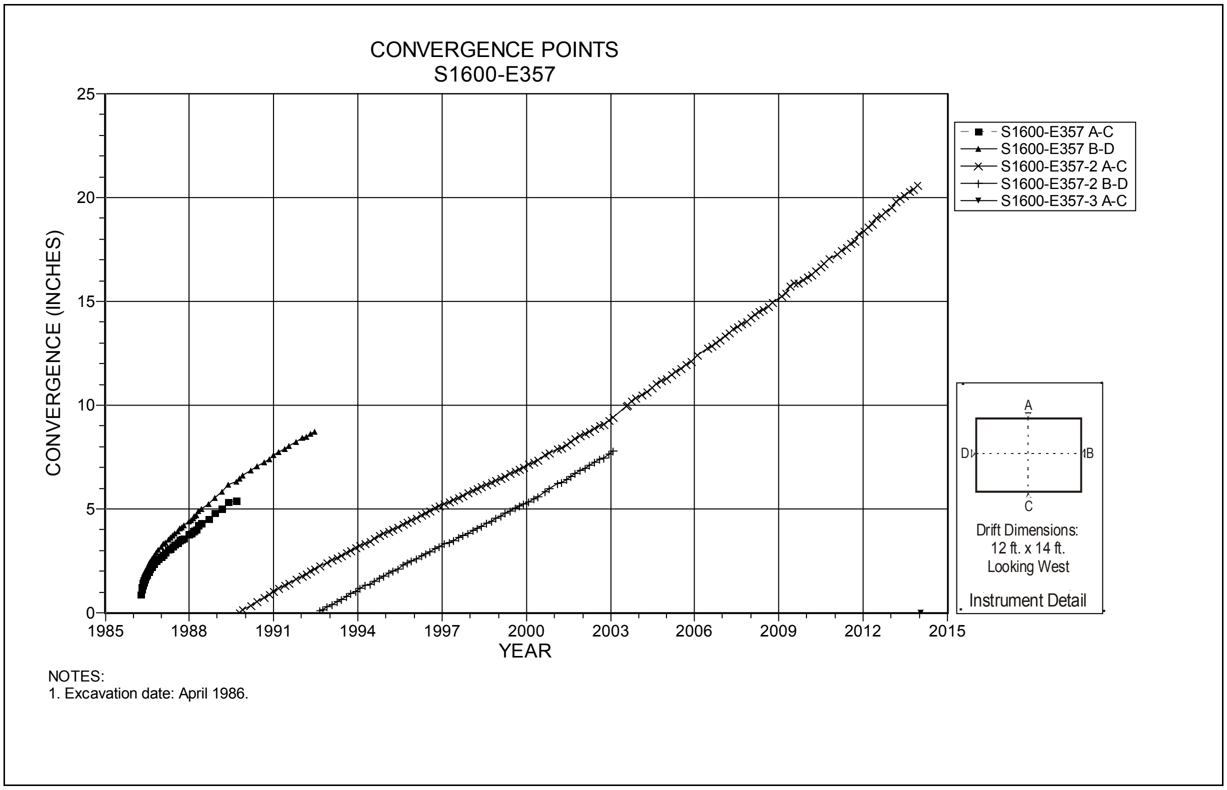

Figure 5-3 Convergence Point Array
S1600 E357 – All Chords

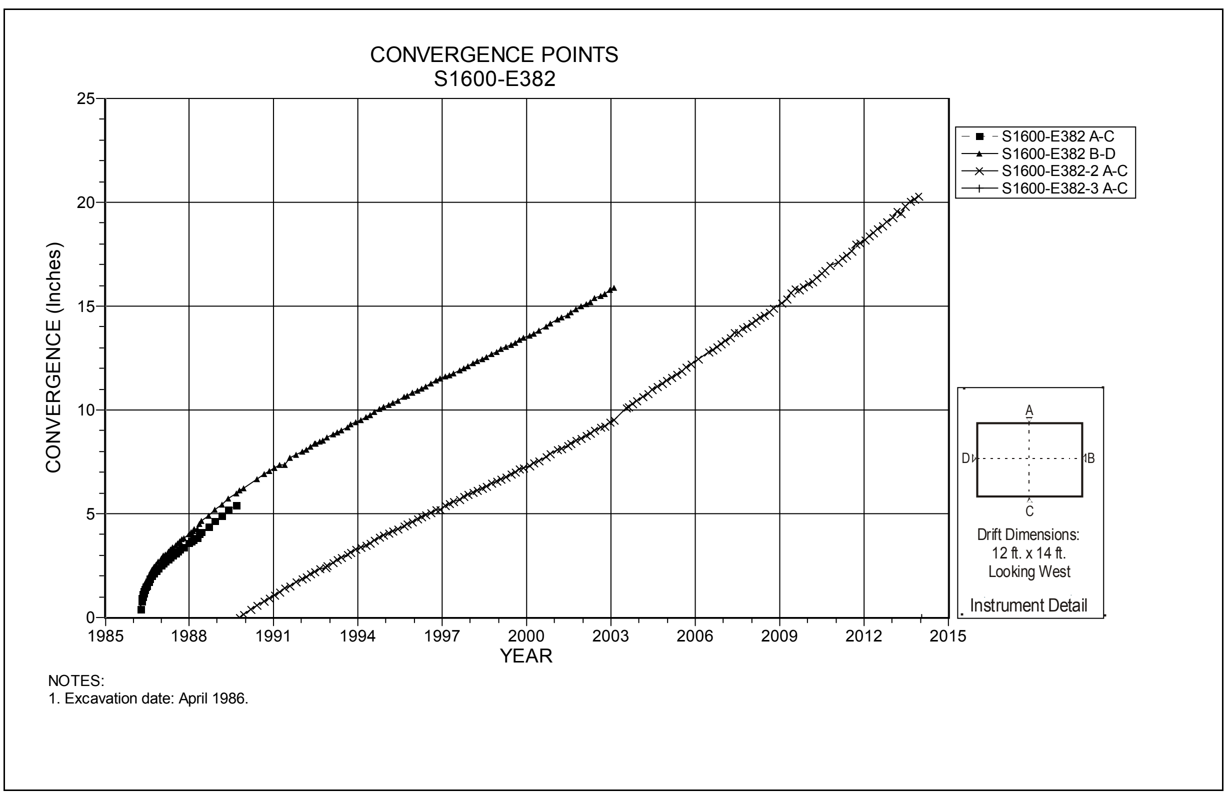

Figure 5-4 Convergence Point Array
S1600 E382 – All Chords

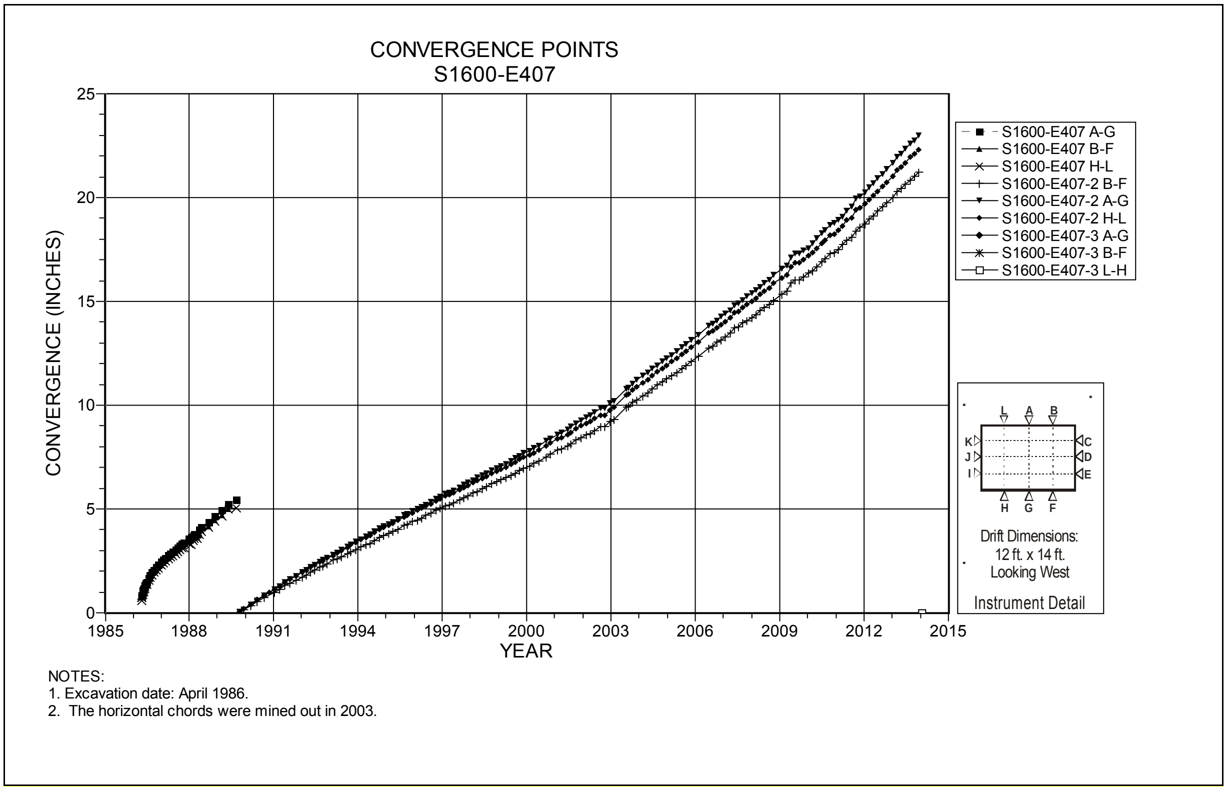

Figure 5-5 Convergence Point Array
S1600 E407 – Roof to Floor

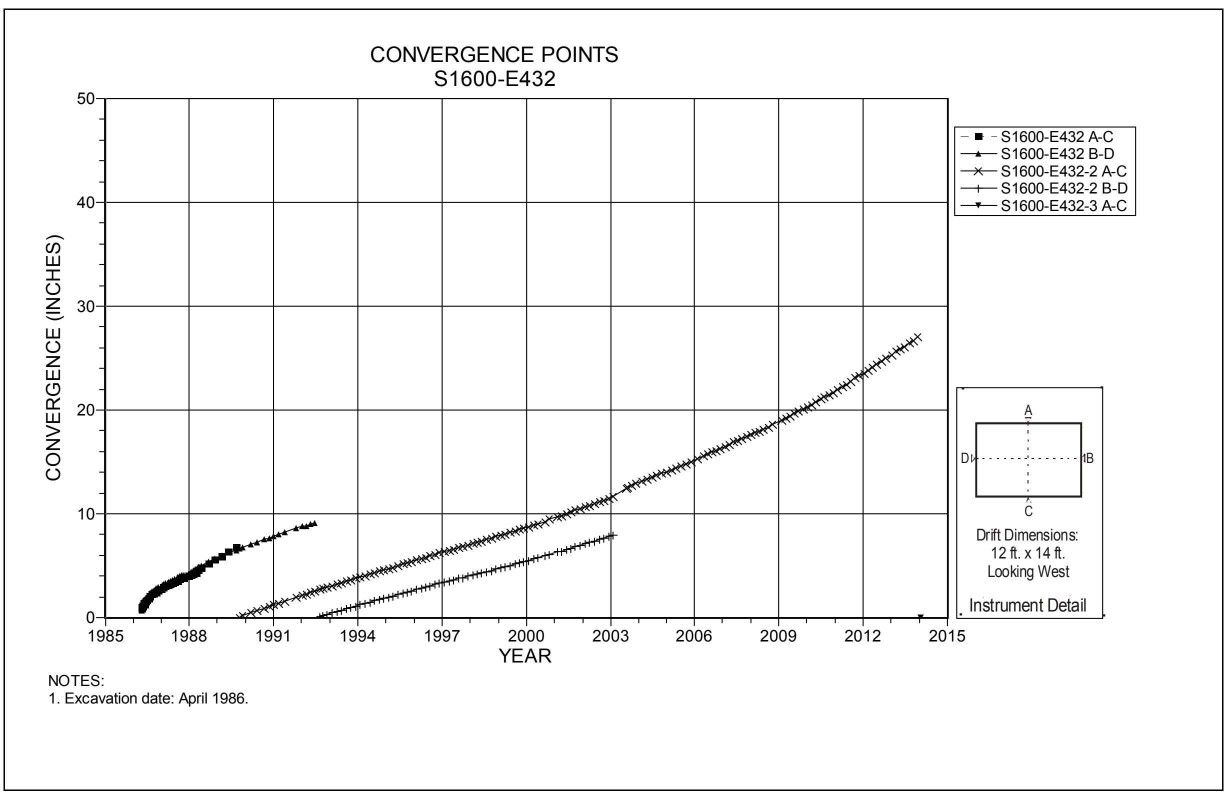

Figure 5-6 Convergence Point Array
S1600 E432 – All Chords

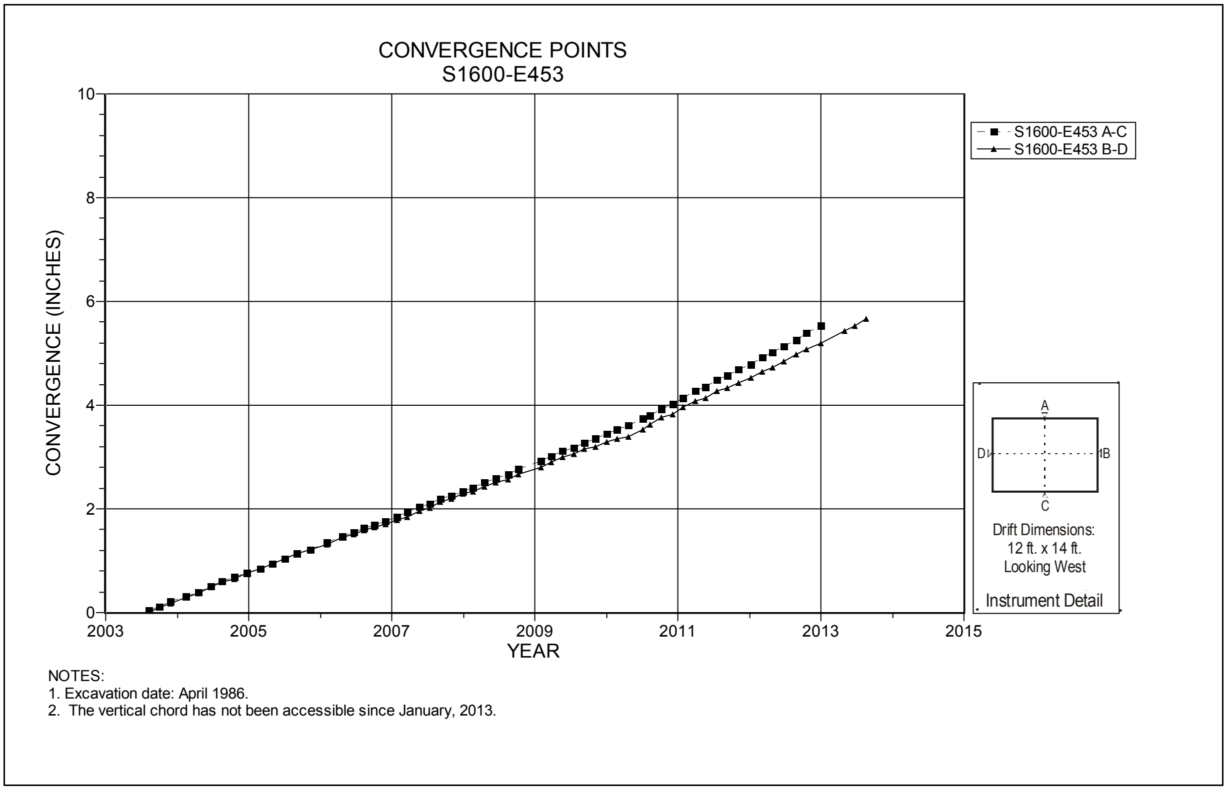

Figure 5-7 Convergence Point Array
S1600 E453 – All Chords

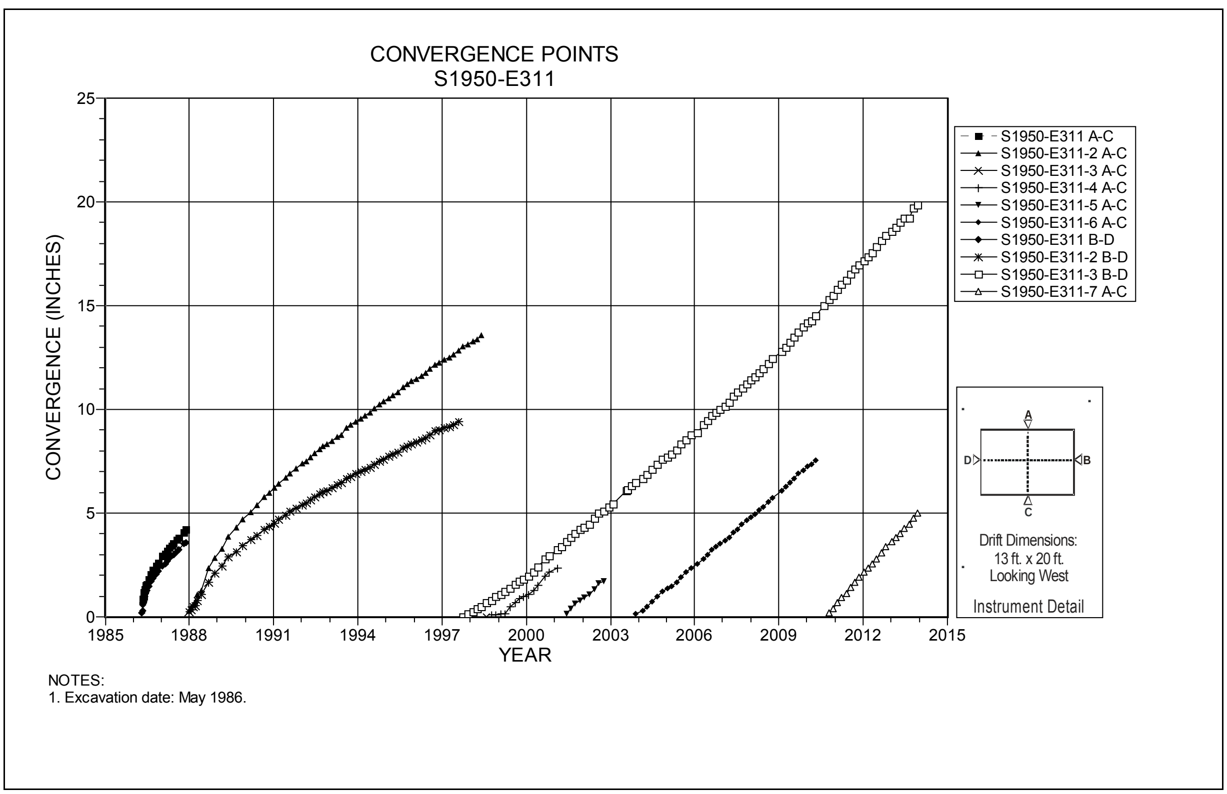

Figure 5-8 Convergence Point Array
S1950 E311 – All Chords

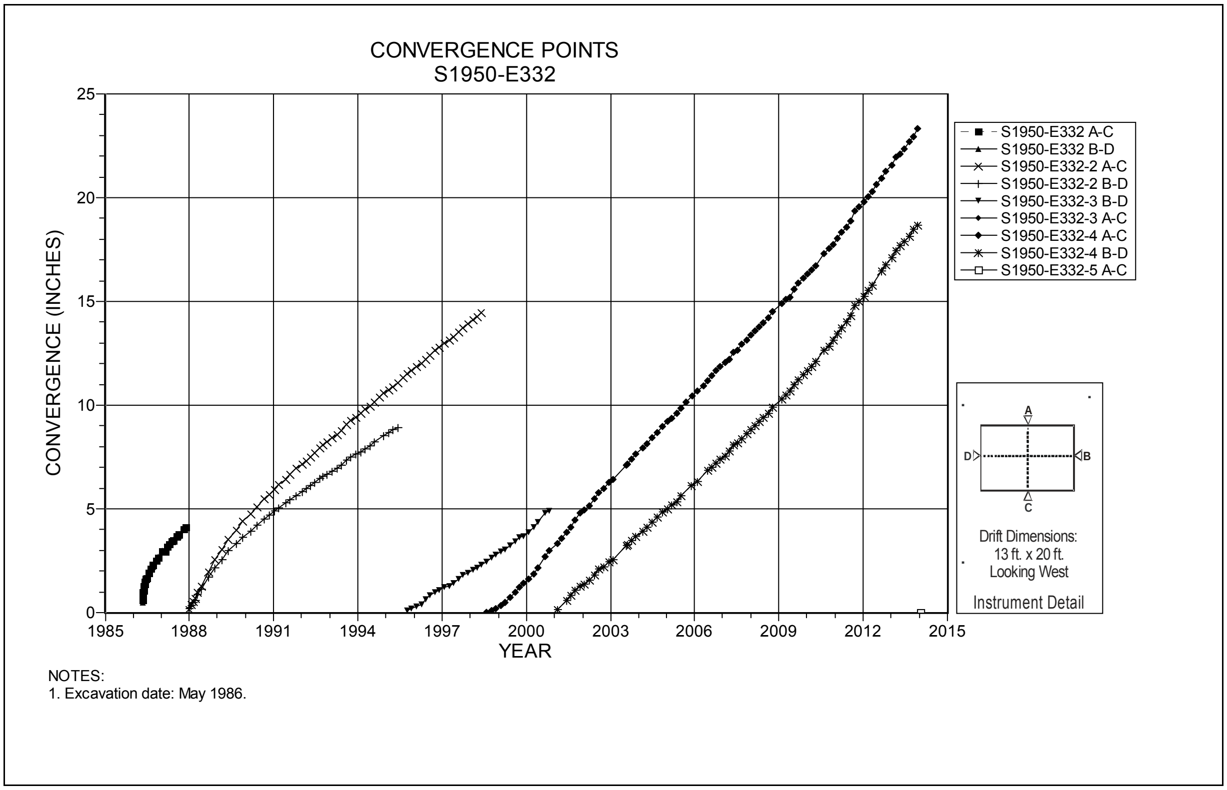

Figure 5-9 Convergence Point Array
S1950 E332 – All Chords

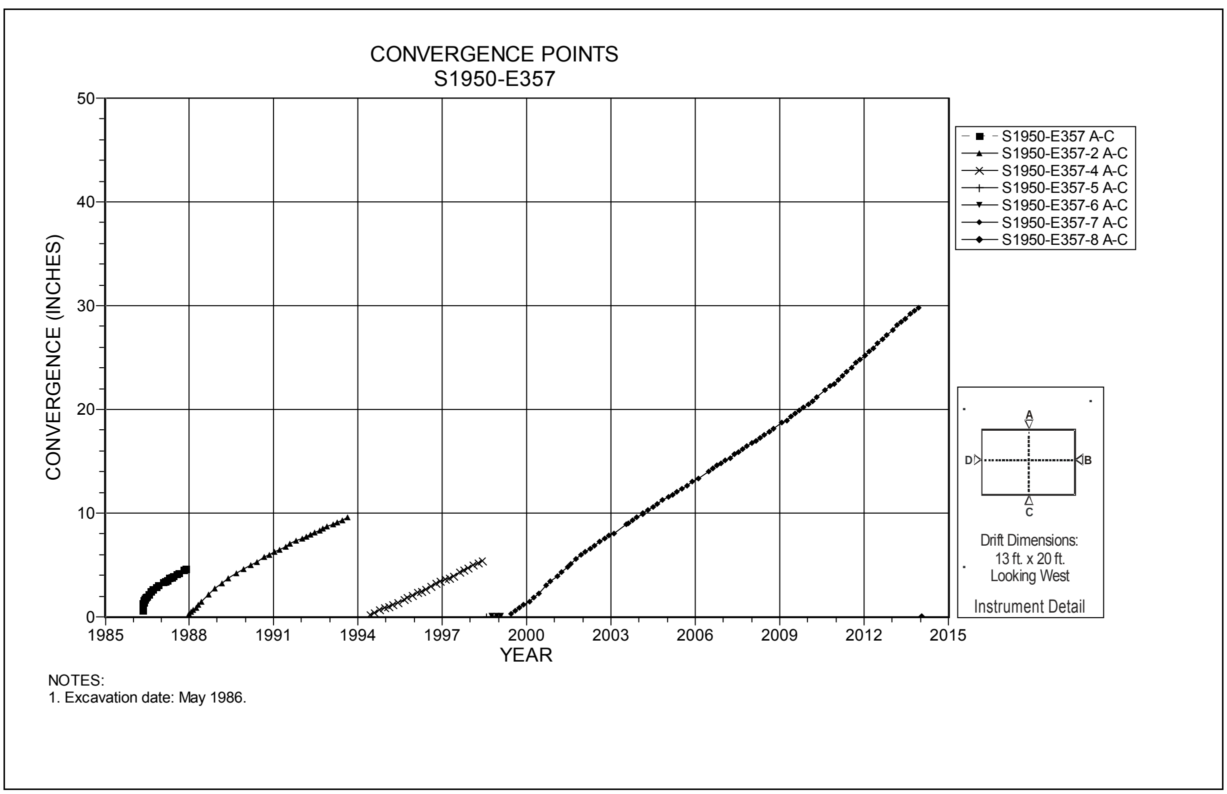

Figure 5-10 Convergence Point Array
S1950 E357 – Roof to Floor

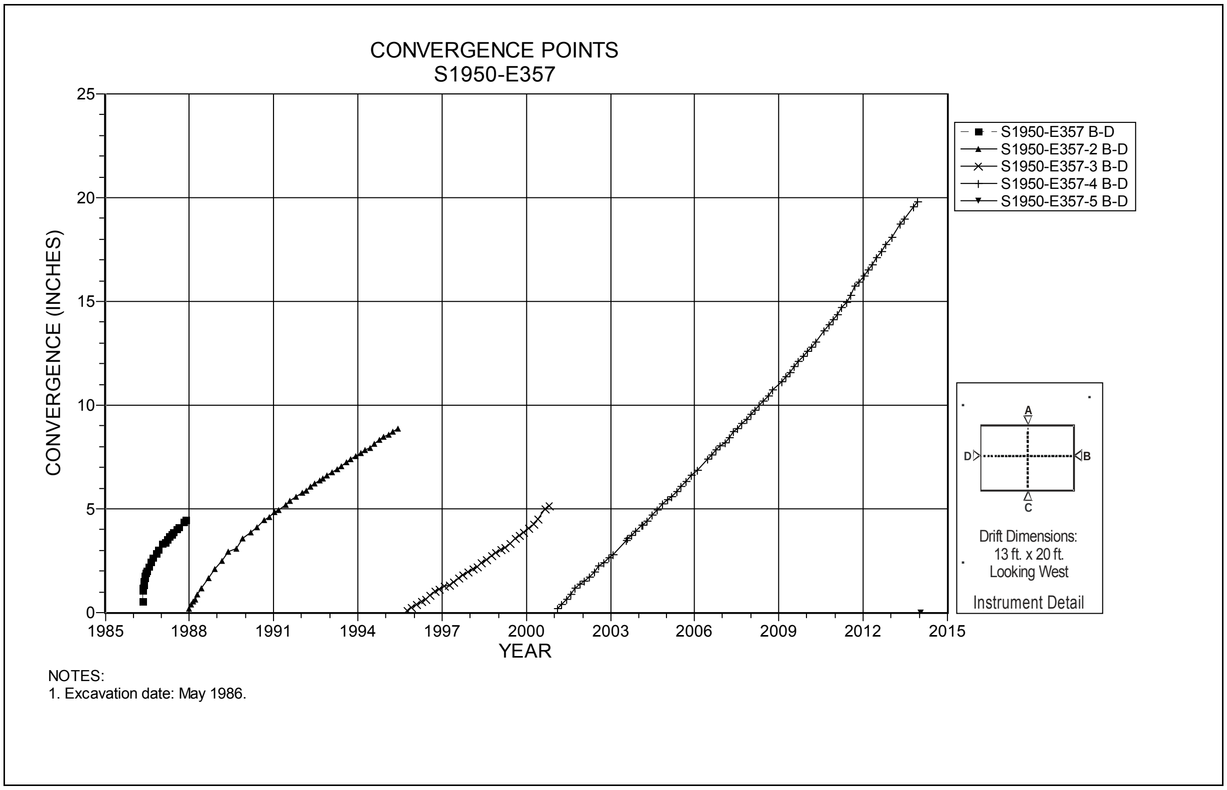

Figure 5-11 Convergence Point Array
S1950 E357 – Rib to Rib

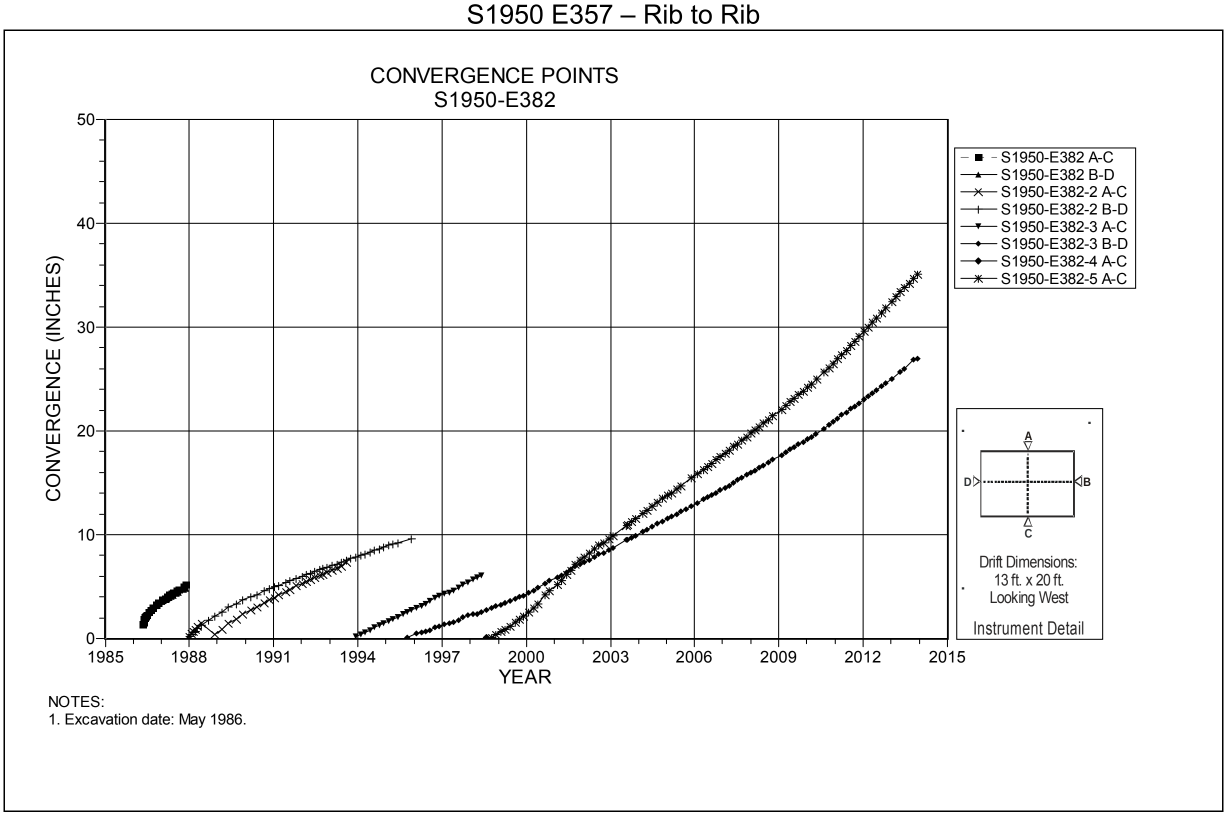

Figure 5-12 Convergence Point Array
S1950 E382 – All Chords

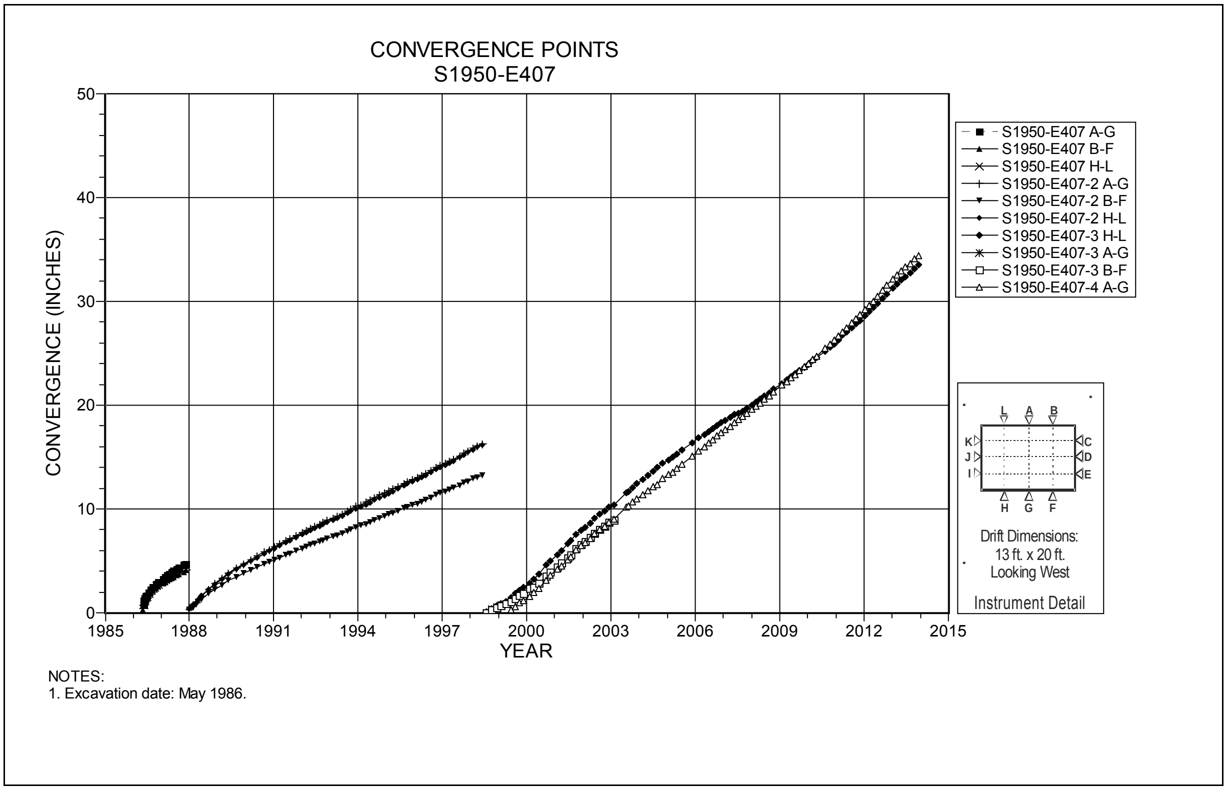

Figure 5-13 Convergence Point Array
S1950 E407 – Roof to Floor

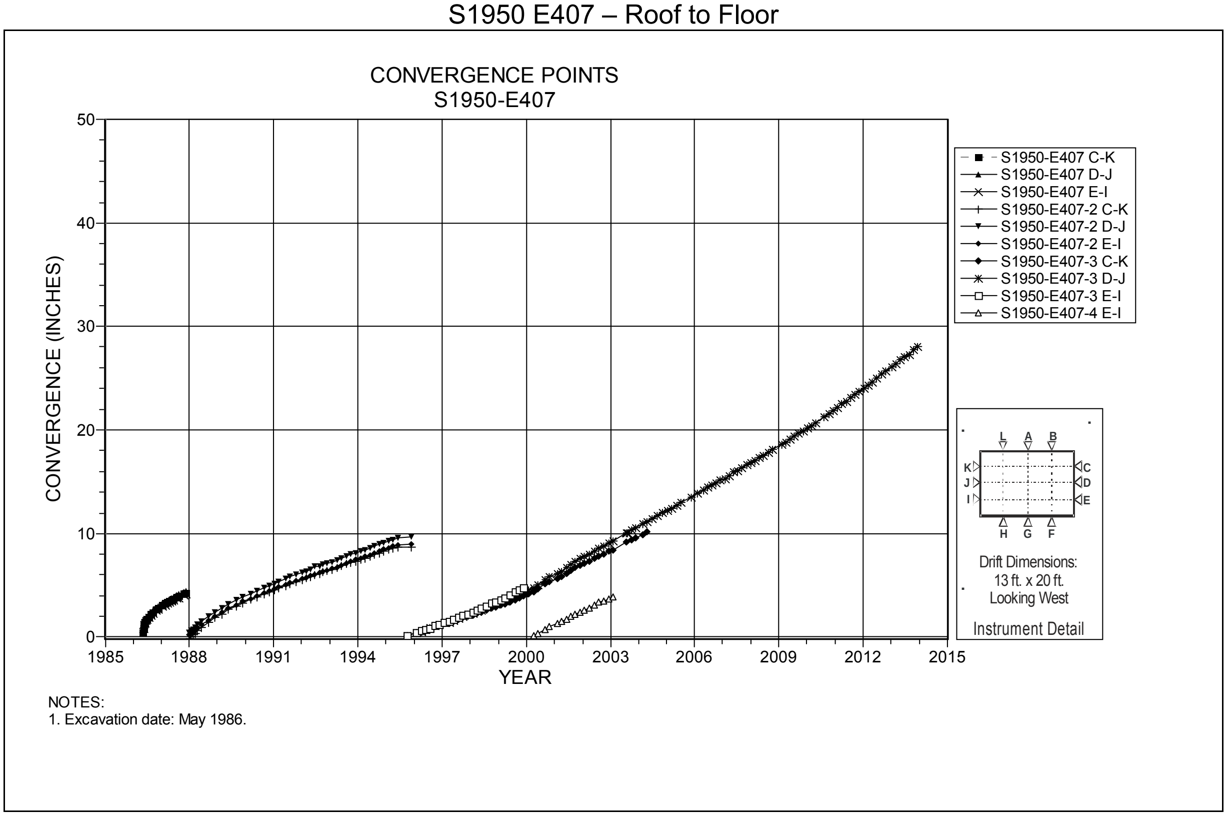

Figure 5-14 Convergence Point Array
S1950 E407 – Rib to Rib

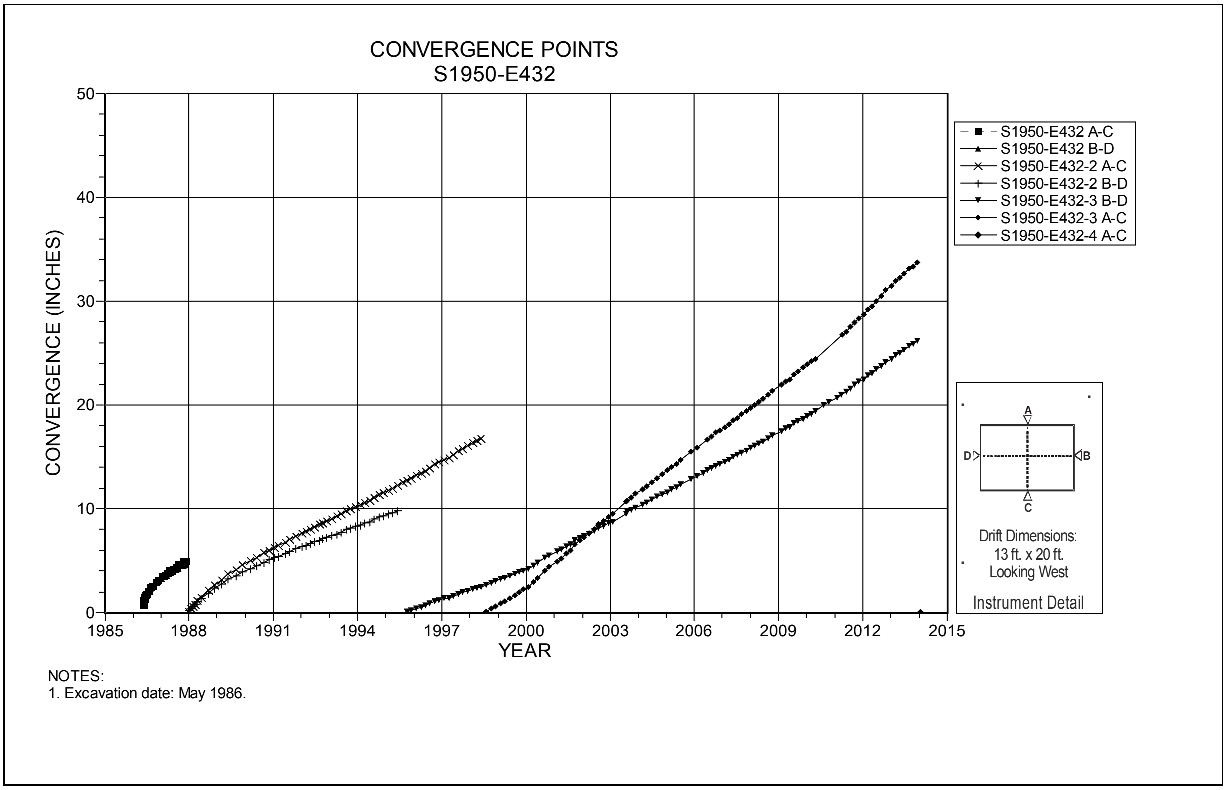

Figure 5-15 Convergence Point Array
S1950 E432 – All Chords

Table 5-2
Panel 2 Access Drift Data Analysis

Convergence Points

Field Tag	Location	Figure Number	Last Reading 2012 to 2013		Cumulative Displacement (inches)	Closure Rate 2012 to 2013 (in/year)	Closure Rate 2011 to 2012 (in/year)	Rate Change Percent	Comments
			Date	Inches					
S2180-E410-2 A-C	S2180-E410	5-16	01/29/14	13.286	18.083	1.6	1.6	0.00%	
S2180-E410 B-D	S2180-E410	5-16	01/29/14	24.001	24.001	2.4	2.5	-4.00%	
S2520-E410-3 A-C	S2520-E410	5-17	01/27/14	30.348	38.484	3.7	3.6	2.78%	

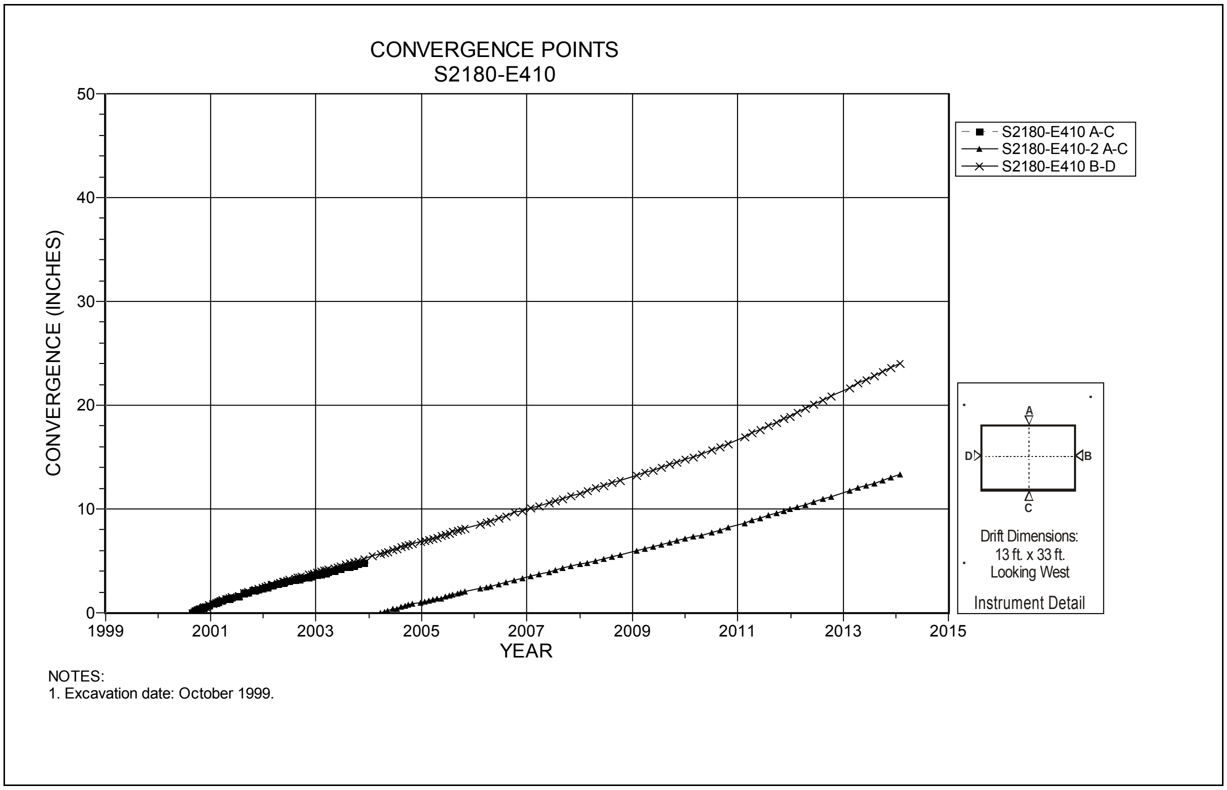

Figure 5-16 Convergence Point Array
S2180 E410 – All Chords

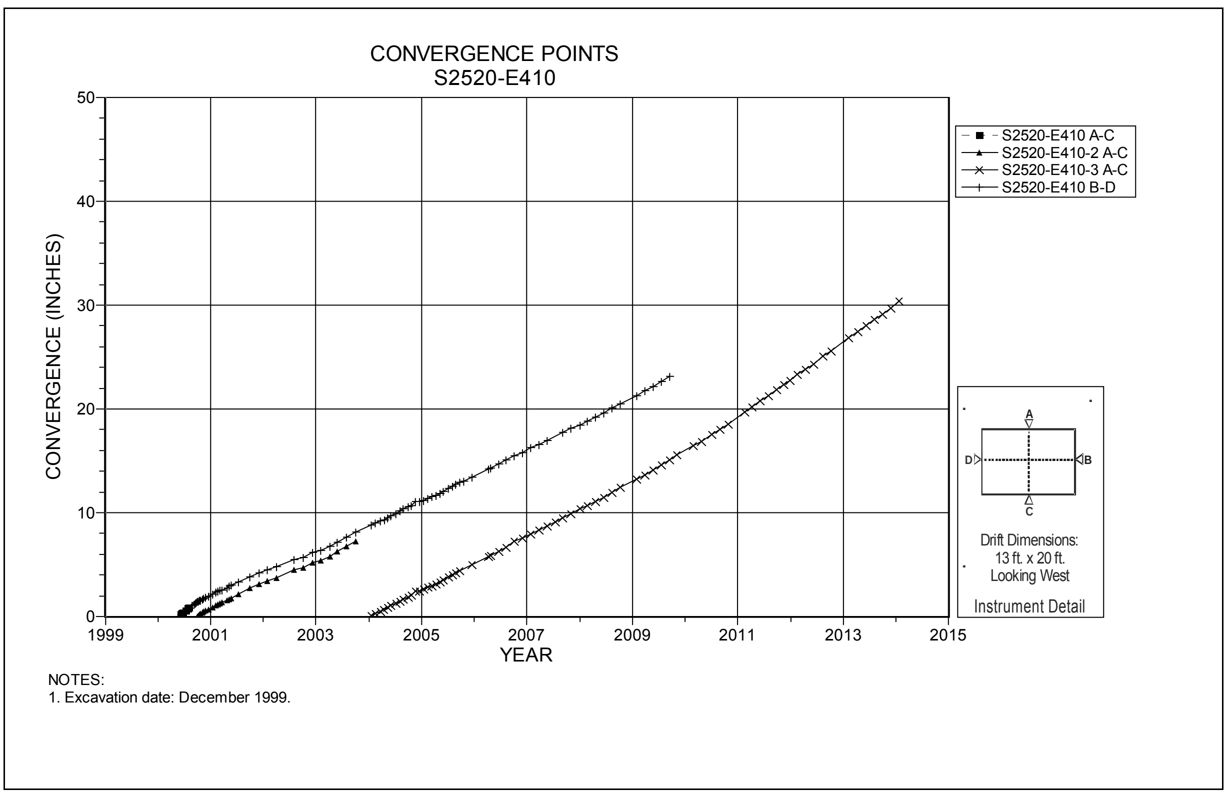

Figure 5-17 Convergence Point Array
S2520 E410 – All Chords

Table 5-3
Panel 3 Access Drift Data Analysis

Convergence Points

Field Tag	Location	Figure Number	Last Reading 2012 to 2013		Cumulative Displacement (inches)	Closure Rate 2012 to 2013 (in/year)	Closure Rate 2011 to 2012 (in/year)	Rate Change Percent	Comments
			Date	Inches					
S2750-E410 A-C	S2750-E410	5-18	01/27/14	33.070	33.070	4.2	4.6	-9%	
S2750-E410 B-D	S2750-E410	5-18	01/27/14	22.068	22.068	2.7	2.6	5%	
S3080-E410-2 A-C	S3080-E410	5-19	01/27/14	35.389	37.902	5.4	5.4	0%	
S3080-E410 B-D	S3080-E410	5-19	01/27/14	25.078	25.078	2.5	2.6	-4%	

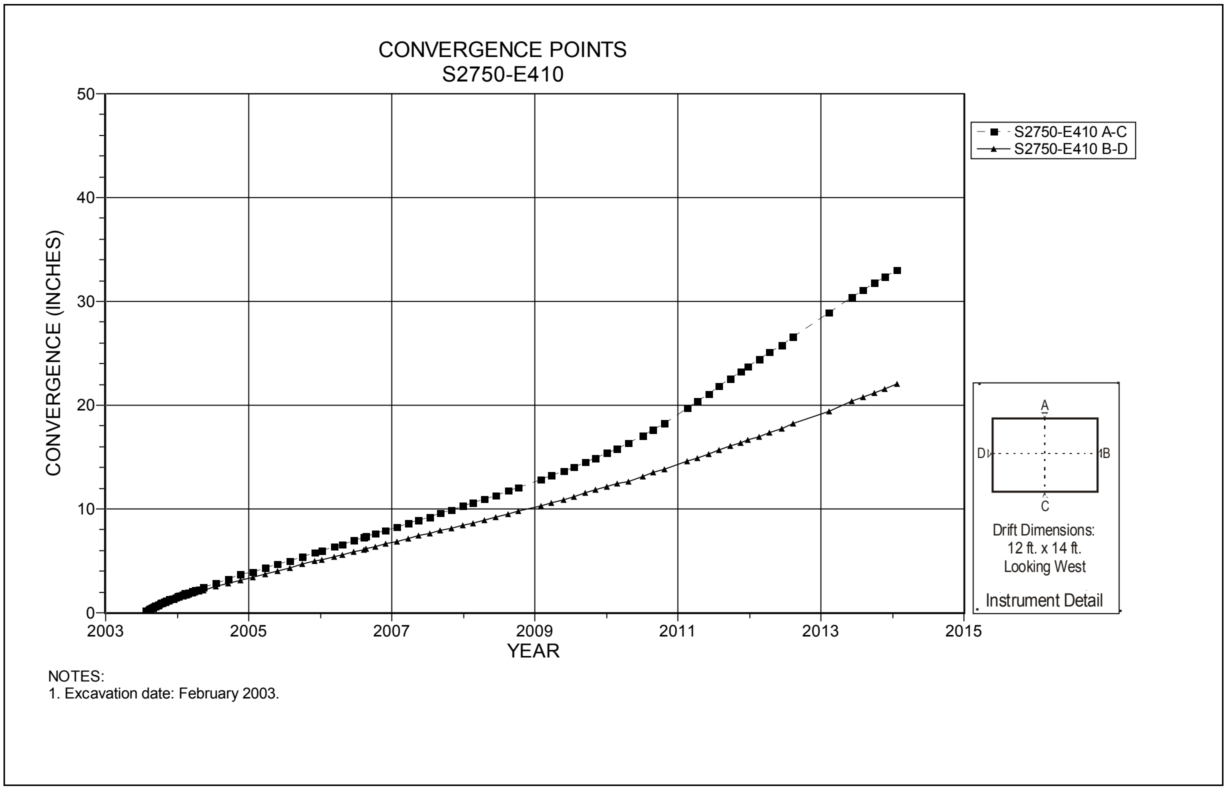

Figure 5-18 Convergence Point Array
S2750 E410 – All Chords

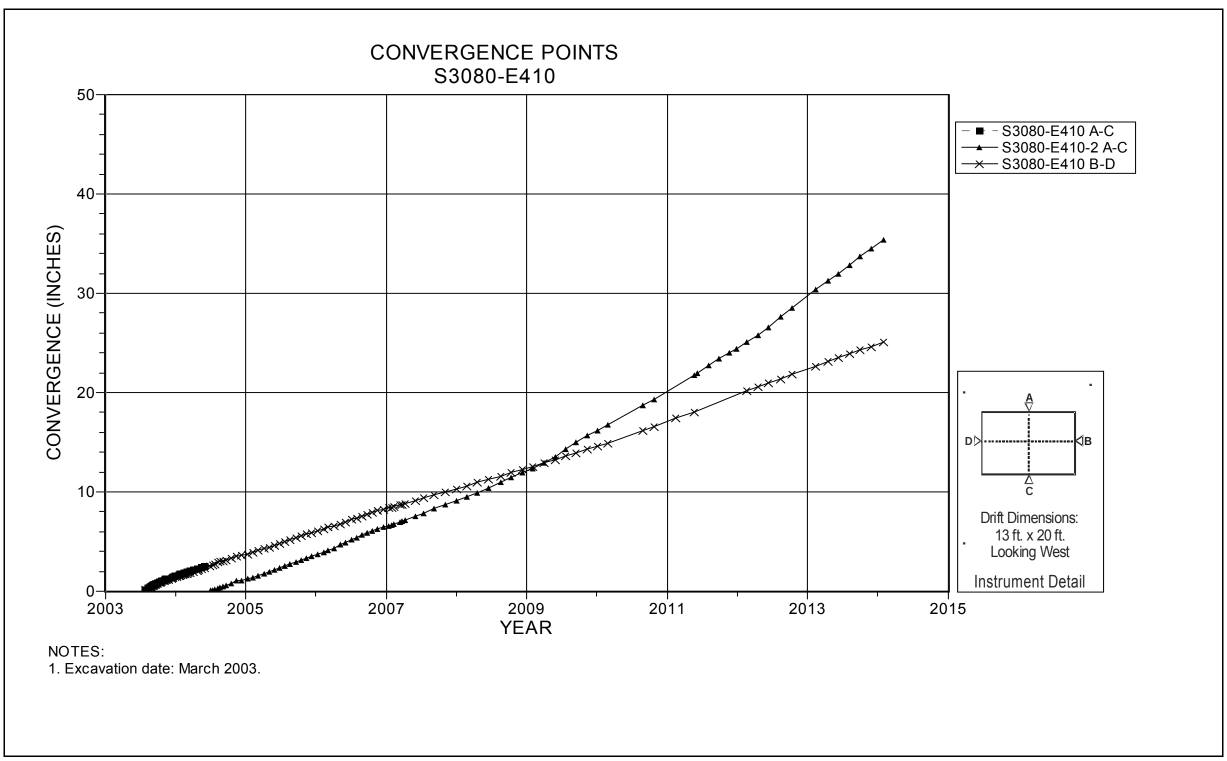

Figure 5-19 Convergence Point Array
S3080 E410 – All Chords

Table 5-4
Panel 4 Access Drift Data Analysis

Convergence Points

Field Tag	Location	Figure Number	Last Reading 2013 to 2014 Date	Last Reading 2013 to 2014 Inches	Cumulative Displacement (inches)	Closure Rate 2013 to 2014 (in/year)	Closure Rate[2] 2012 to 2013 (in/year)	Rate Change Percent[2]	Comments
S3310-E410 A-C	S3310-E410	5-20	01/27/14	17.652	17.652	2.0	N/A	N/A	One reading during ‘12 – ‘13 reporting period.

[2] N/A – Insufficient data available to perform the calculation. This is usually due to the inability to read the instruments because of activities such as: the temporary removal of an instrument due to floor, rib or back trimming; locations blocked by equipment or waste disposal, installation timing, etc.

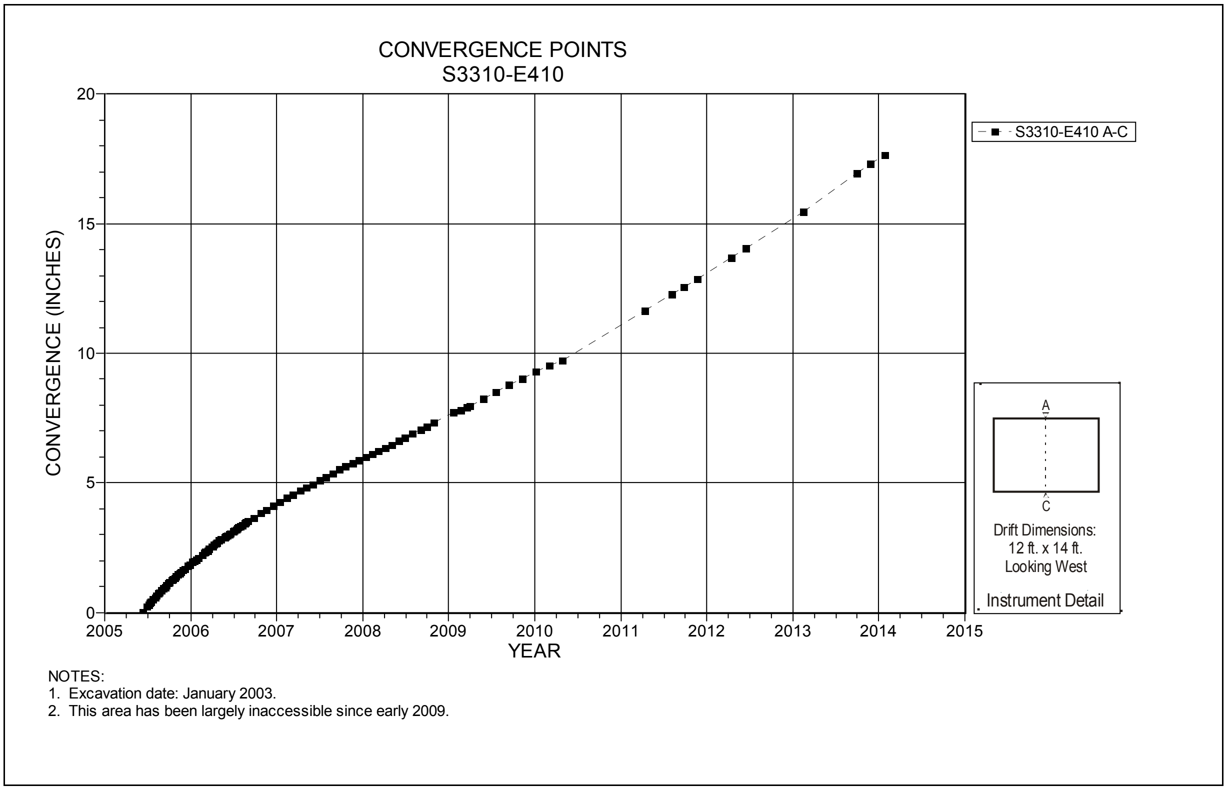

Figure 5-20 Convergence Point Array
S3310 E410 – Roof to Floor

Table 5-5
Panel 5 Access Data Analysis

Convergence Points

Field Tag	Location	Figure Number	Last Reading 2013 to 2014		Cumulative Displacement (inches)	Closure Rate 2013 to 2014 (in/year)	Closure Rate 2012 to 2013 (in/year)	Rate Change Percent	Comments
			Date	Inches					
S3310-W285 A-C	S3310-W285	5-21	01/27/14	16.014	16.014	2.1	4.4	-52%	
S3650-W285-2 A-C	S3650-W285	5-22	01/27/14	17.489	19.930	4.1	5.8	-29%	

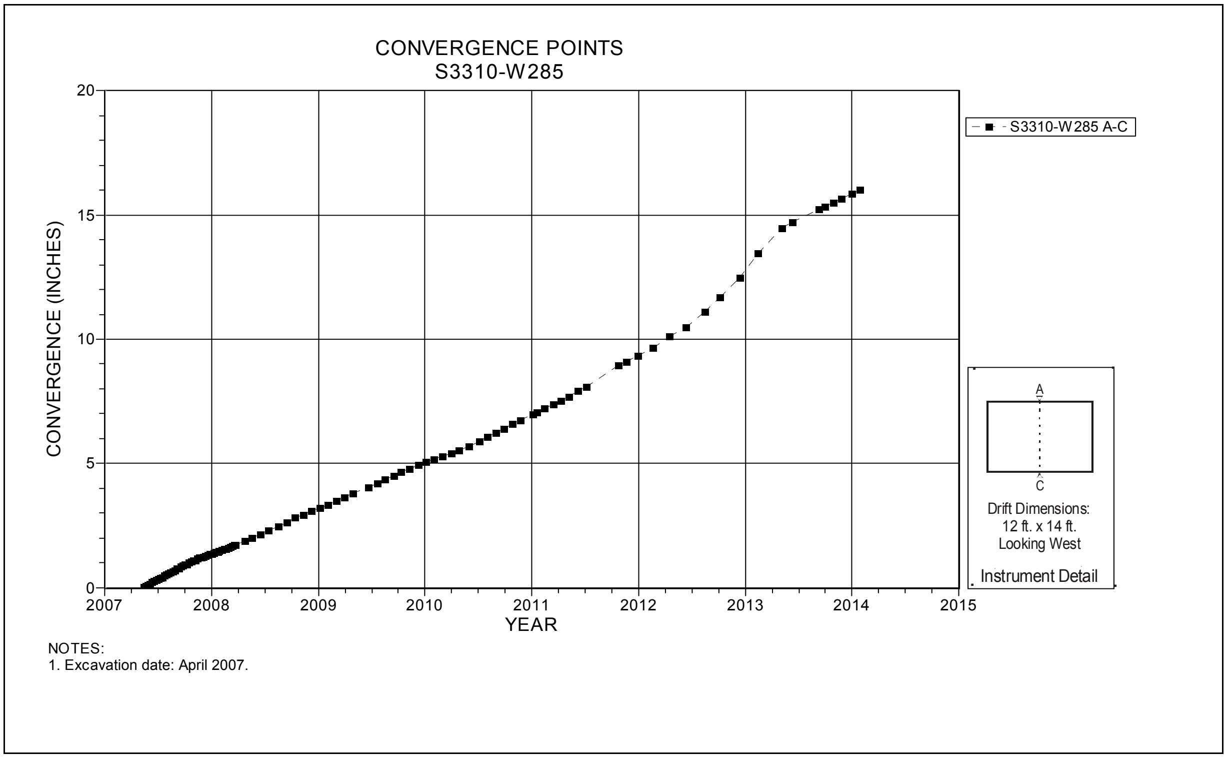

Figure 5-21 Convergence Point Array
S3310 W285 – Roof to Floor

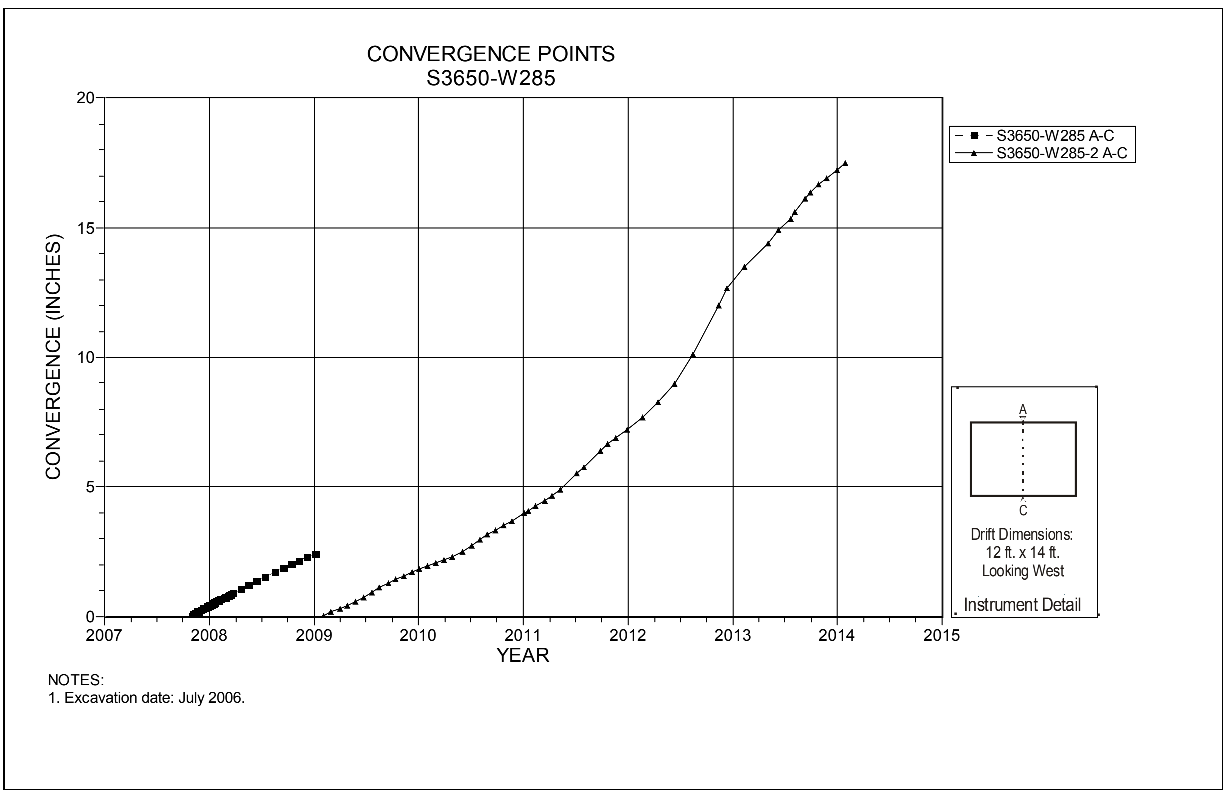

Figure 5-22 Convergence Point Array
S3650 W285 – Roof to Floor

Table 5-6
Panel 6 Data Analysis

Extensometers

Field Tag	Location	Figure Number	Date of Last Reading	Collar Displacement Relative to Deepest Anchor (inches)	Displacement Rate 2013 to 2014 (in/year)	Displacement Rate 2012 to 2013 (in/year)	Rate Change Percent	Comments
51X-GE-00501-3	S2750-W285	5-23	01/28/14	0.613	5.5	5.9	-20%	'12-'13 rate taken from 51X-GE-00501-2
51X-GE-00413-2	S2750-W585	5.24	06/24/14	9.764	2.9	2.5	16%	
51X-GE-00414	S2750-W985	5-25	06/24/14	8.478	3.4	1.8	89%	
51X-GE-00403-2	W390-S2916	5-26	02/13/14	1.572	0.3	1.4	-79%	
51X-GE-00405-2	W520-S2916	5-27	06/24/14	8.915	5.3	3.8	39%	
51X-GE-00406	W660-S2916	5-28	06/24/14	1.549	0.04	0.09	-56%	Anchor "A" was used in the calc.
51X-GE-00407	W790-S2916	5-29	06/24/14	13.311	5.7	2.1	171%	
51X-GE-00408-2	W920-S2916	5-30	06/24/14	7.417	3.3	1.7	94%	Anchor "B" was used (anchor "C" has failed).
51X-GE-00409	W1050-S2916	5-31	06/24/14	9.701	2.9	2.1	38%	
51X-GE-00410	W1190-S2916	5-32	06/24/14	7.904	2.6	1.5	73%	
51X-GE-00411	S3080-W585	5-33	06/24/14					
51X-GE-00412	S3080-W985	5-34	06/24/14	9.217	3.5	1.9	84%	

Convergence Points

Field Tag	Location	Figure Number	Last Reading 2013 to 2014		Cumulative Displacement (inches)	Closure Rate[1] 2013 to 2014 (in/year)	Closure Rate 2012 to 2013 (in/year)	Rate Change Percent[1]	Comments
			Date	Inches					
S2750-W285-2 A-C	S2750-W285	5-35	01/28/14	26.020	30.701	8.1	7.0	16%	
S2750-W390-2 A-C	S2750-W390	5-36	12/09/13	19.103	26.229	5.4	4.9	10%	
S2750-W460-2 A-C	S2750-W460	5-37	09/18/13	23.067	29.093	6.5	5.7	14%	
S2750-W520-2 A-C	S2750-W520	5-38	08/26/13	17.201	23.917	4.5	4.2	7%	
W390-S2833-3 A-C	W390-S2833	5-39	12/09/13	7.050	35.680	6.5	6.9	-6%	
W390-S2916-3 A-C	W390-S2916	5-40	11/13/13	3.541	30.739	3.1	4.3	-28%	
W390-S2916 B-D	W390-S2916	5-40	11/13/13	8.997	8.997	3.7	3.7	0%	
W390-S2998-2 A-C	W390-S2998	5-41	10/16/13	16.822	25.875	4.6	4.3	7%	
W520-S2833-2 A-C	W520-S2833	5-42	07/22/13	15.175	21.183	N/A	3.9	N/A	Waste emplacement, one reading this period.

Table 5-6
Panel 6 Data Analysis (Continued)

Convergence Points (Continued)

Field Tag	Location	Figure Number	Last Reading 2013 to 2014 Date	Last Reading 2013 to 2014 Inches	Cumulative Displacement (inches)	Closure Rate[1] 2013 to 2014 (in/year)	Closure Rate 2012 to 2013 (in/year)	Rate Change Percent[1]	Comments
W520-S2916-2 A-C	W520-S2916	5-43	07/22/13	20.815	26.918	N/A	5.5	N/A	Waste emplacement, one reading this period.
W520-S2916 B-D	W520-S2916	5-43	07/22/13	9.067	9.067	N/A	3.3	N/A	Waste emplacement, one reading this period.
W520-S2998-2 A-C	W520-S2998	5-44	07/22/13	14.886	20.596	N/A	4.0	N/A	Waste emplacement, one reading this period.
S3080-W285-2 A-C	S3080-W285	5-45	01/29/14	11.028	14.995	3.3	3.2	3%	
S3080-W390-2 A-C	S3080-W390	5-46	09/18/13	12.724	20.922	3.8	3.0	27%	

[1] N/A – Insufficient data available to perform the calculation. This is usually due to the inability to read the instruments because of activities such as: the temporary removal of an instrument due to floor, rib or back trimming; locations blocked by equipment or waste disposal, installation timing, etc.

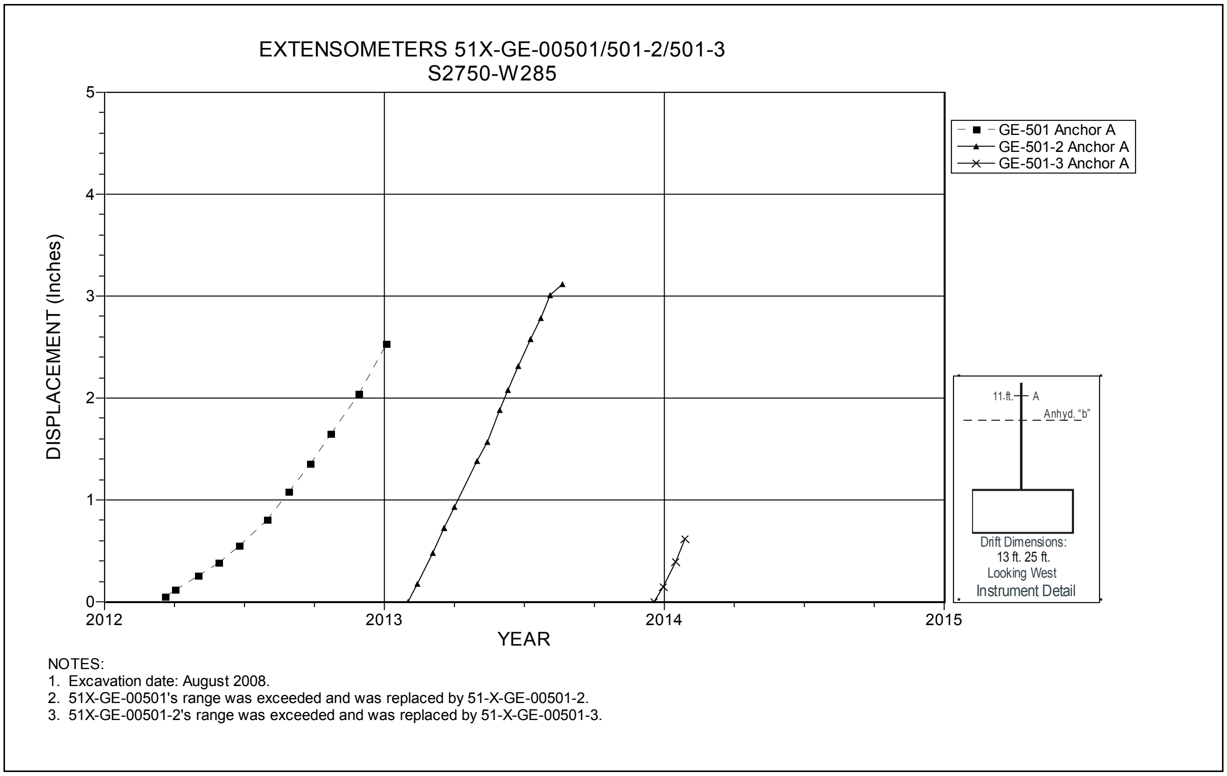

Figure 5-23 Extensometers 51X-GE-00501, 51X-GE-00501-2 and 51X-GE-00501-3
S2750 W285 – Roof

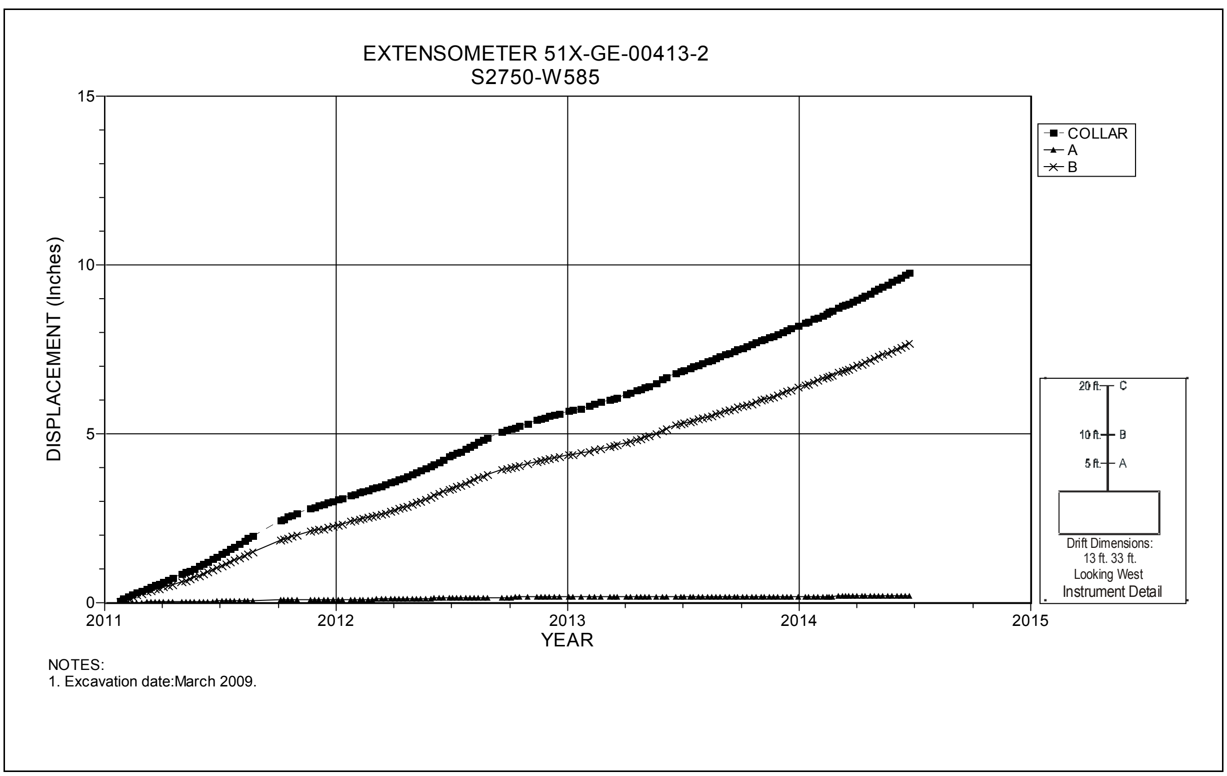

Figure 5-24 Extensometer 51X-GE-00413-2
S2750 W585 – Roof

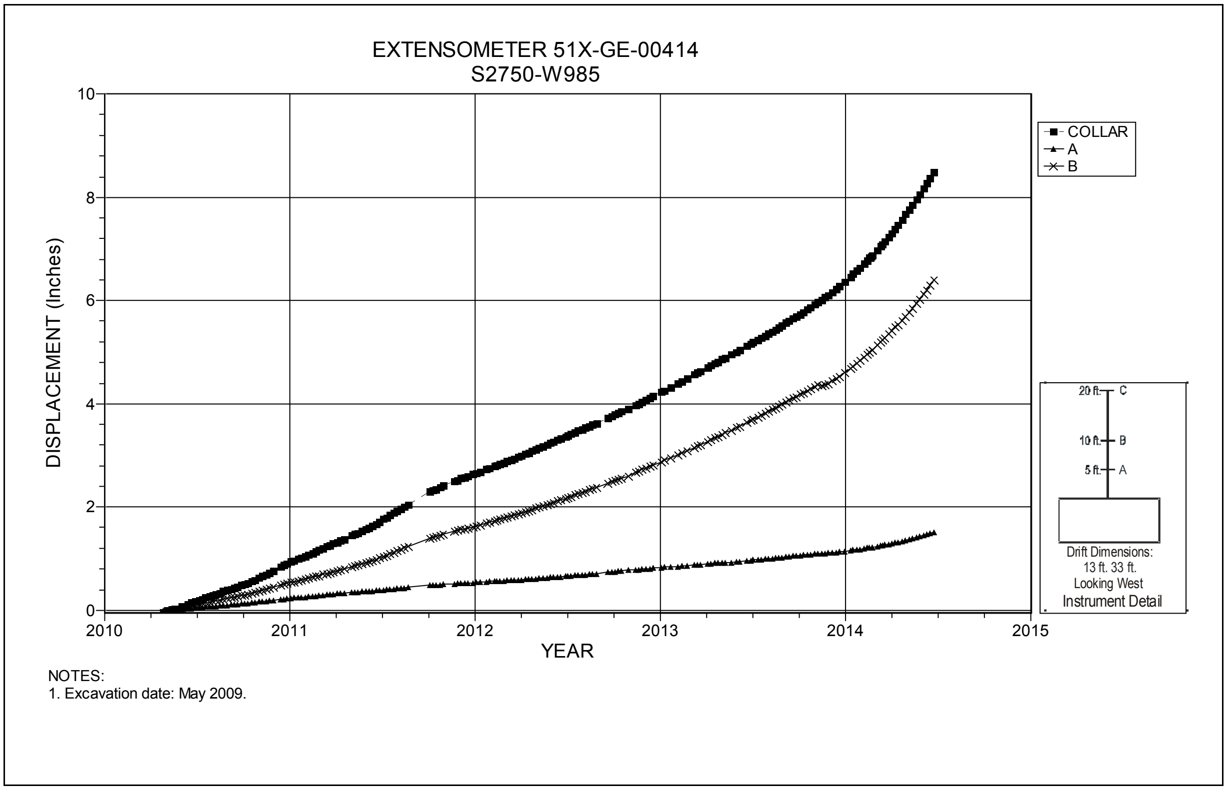

Figure 5-25 Extensometer 51X-GE-00414
S2750 W985 – Roof

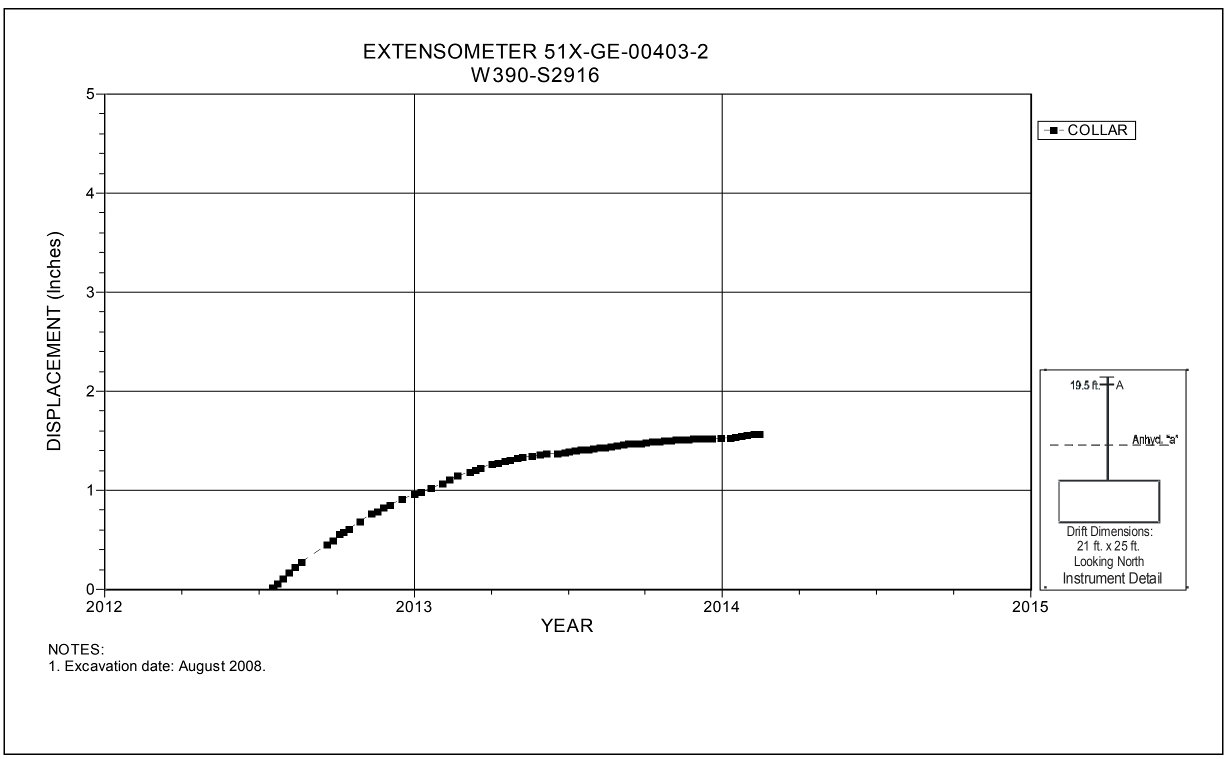

Figure 5-26 Extensometer 51X-GE-00403-2
Room 1, Panel 6 at W390 S2916 – Roof

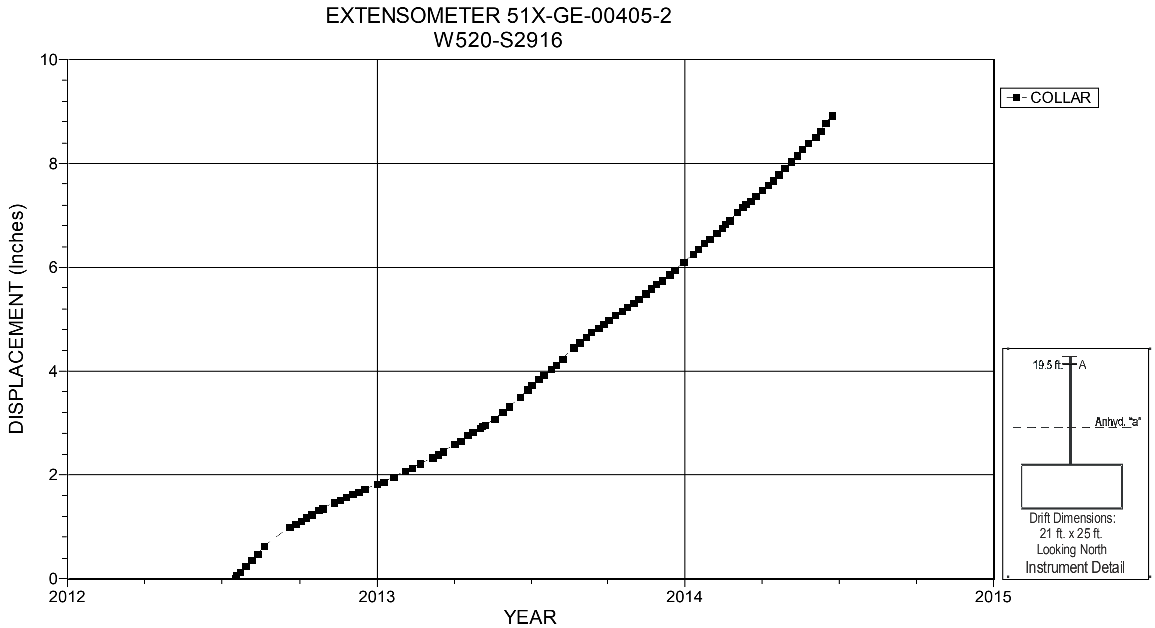

NOTES:
1. Excavation date: February 2009.

Figure 5-27 Extensometer 51X-GE-00405-2
Room 2, Panel 6 at W520 S2916 – Room Center – Roof

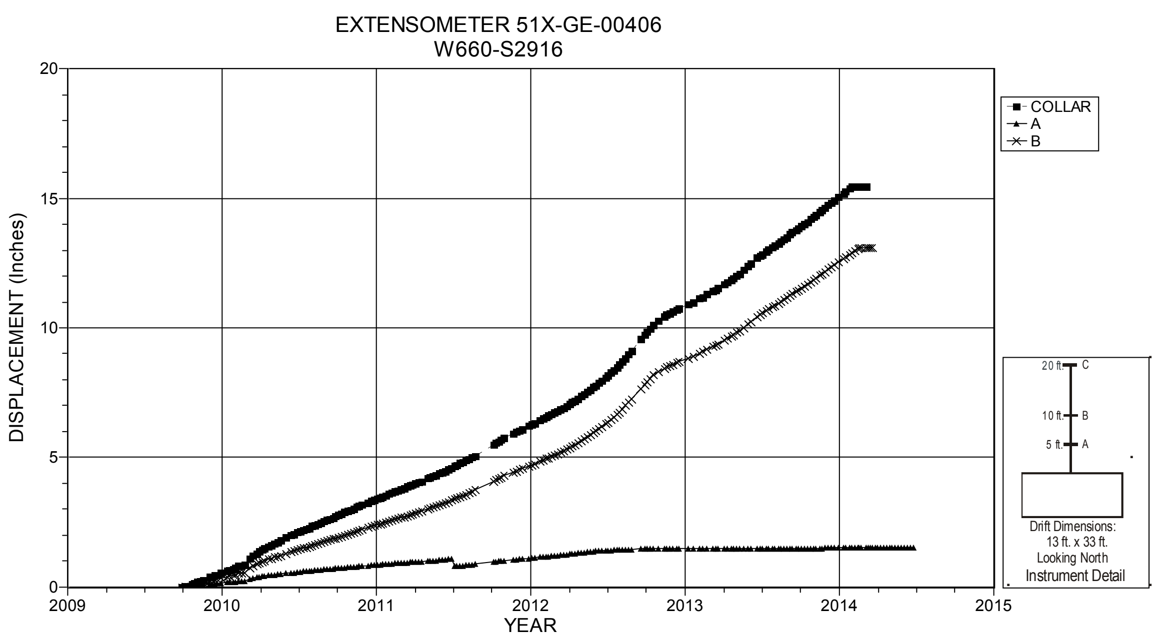

NOTES:
1. Excavation date: April 2009.
2. Anchors "B" and "C" have reached their maximum range and have failed.

Figure 5-28 Extensometer 51X-GE-00406
Room 3, Panel 6 at W660 S2916– Room Center – Roof

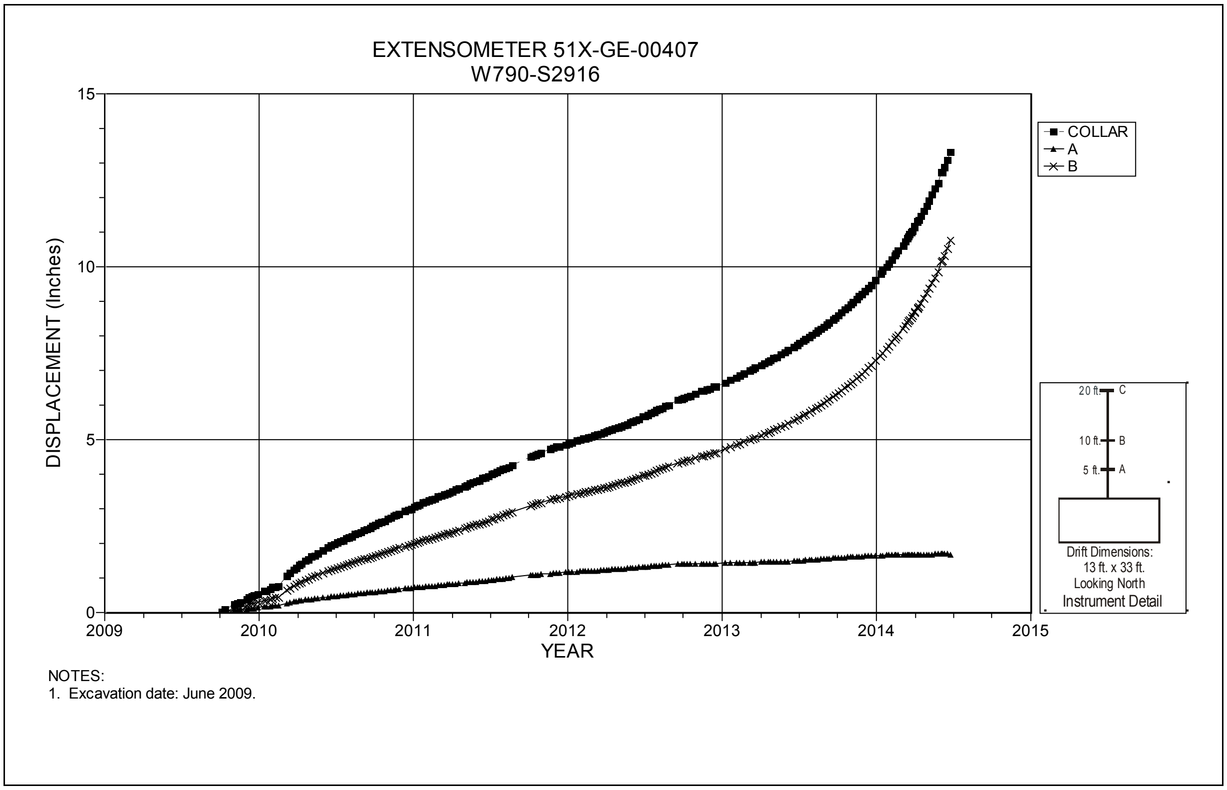

Figure 5-29 Extensometer 51X-GE-00407
Room 4, Panel 6 at W790 S2916 – Room Center – Roof

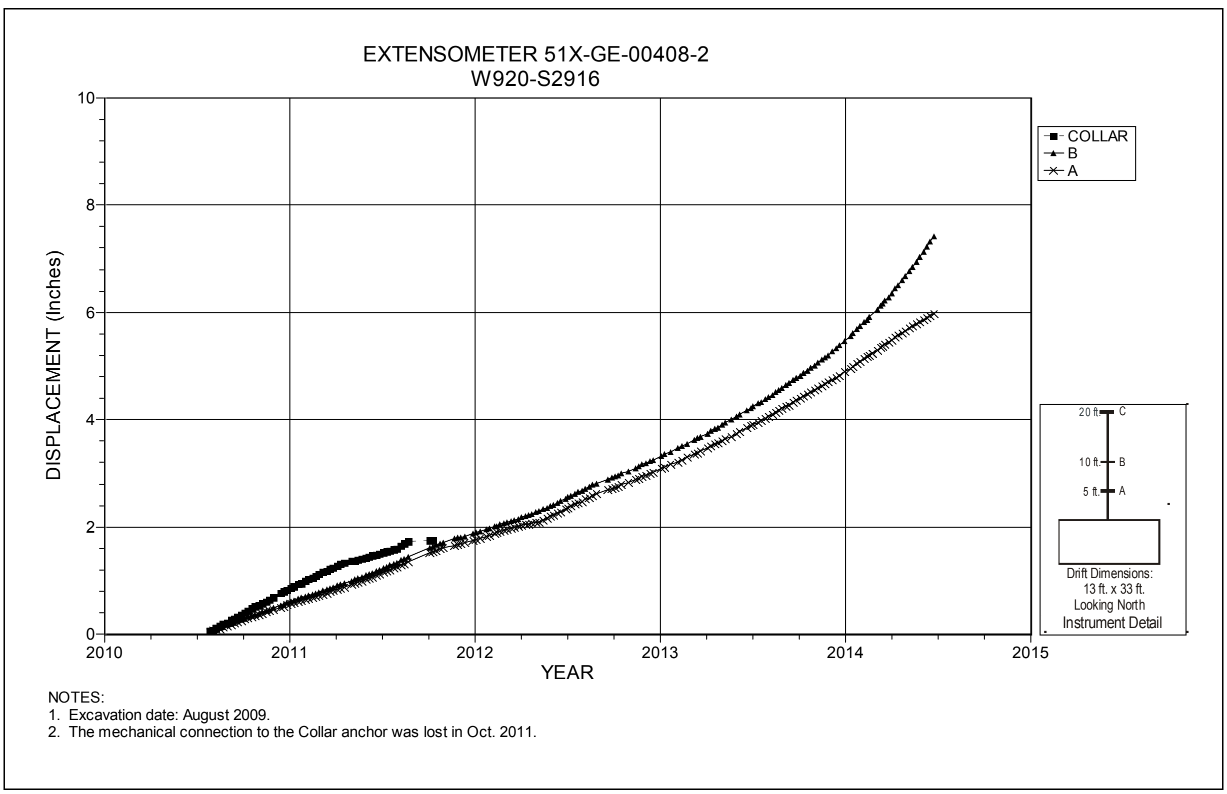

Figure 5-30 Extensometer 51X-GE-00408-2
Room 5, Panel 6 at W920 S2916 – Room Center – Roof

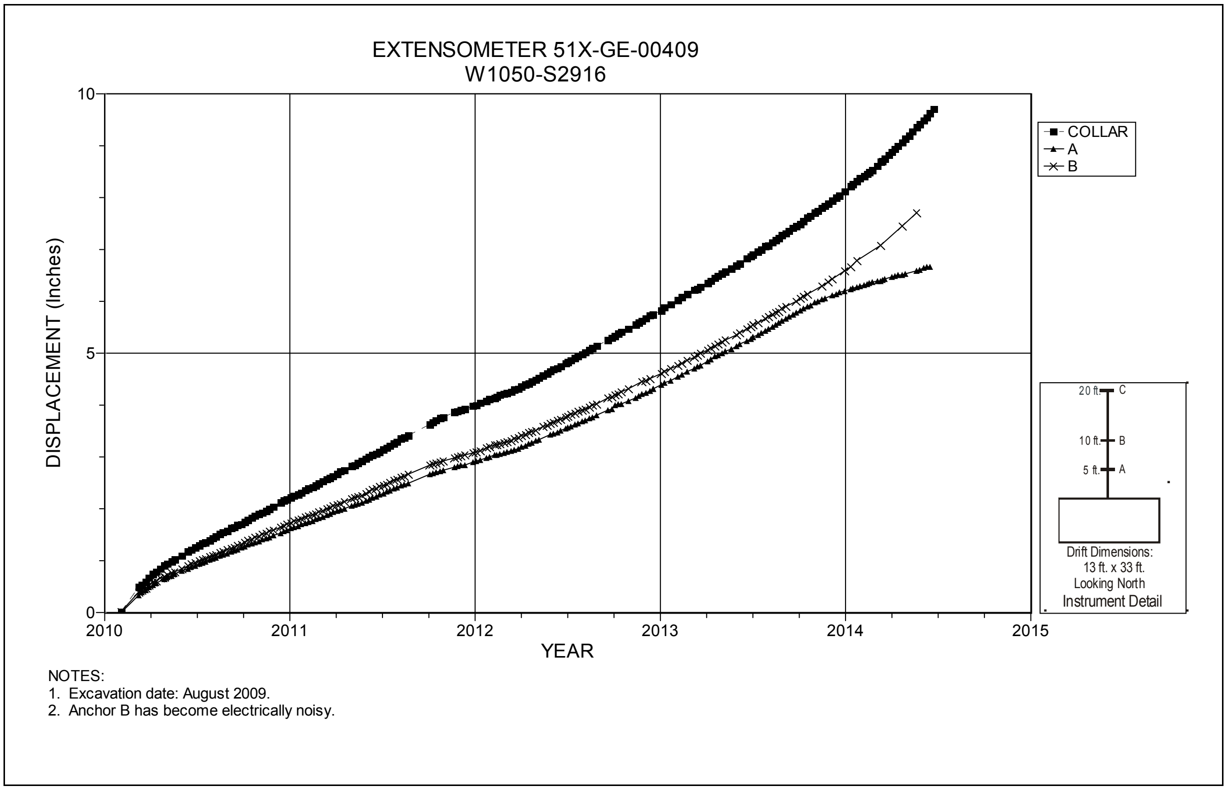

Figure 5-31 Extensometer 51X-GE-00409
Room 6, Panel 6 at W1050 S2916 – Room Center – Roof

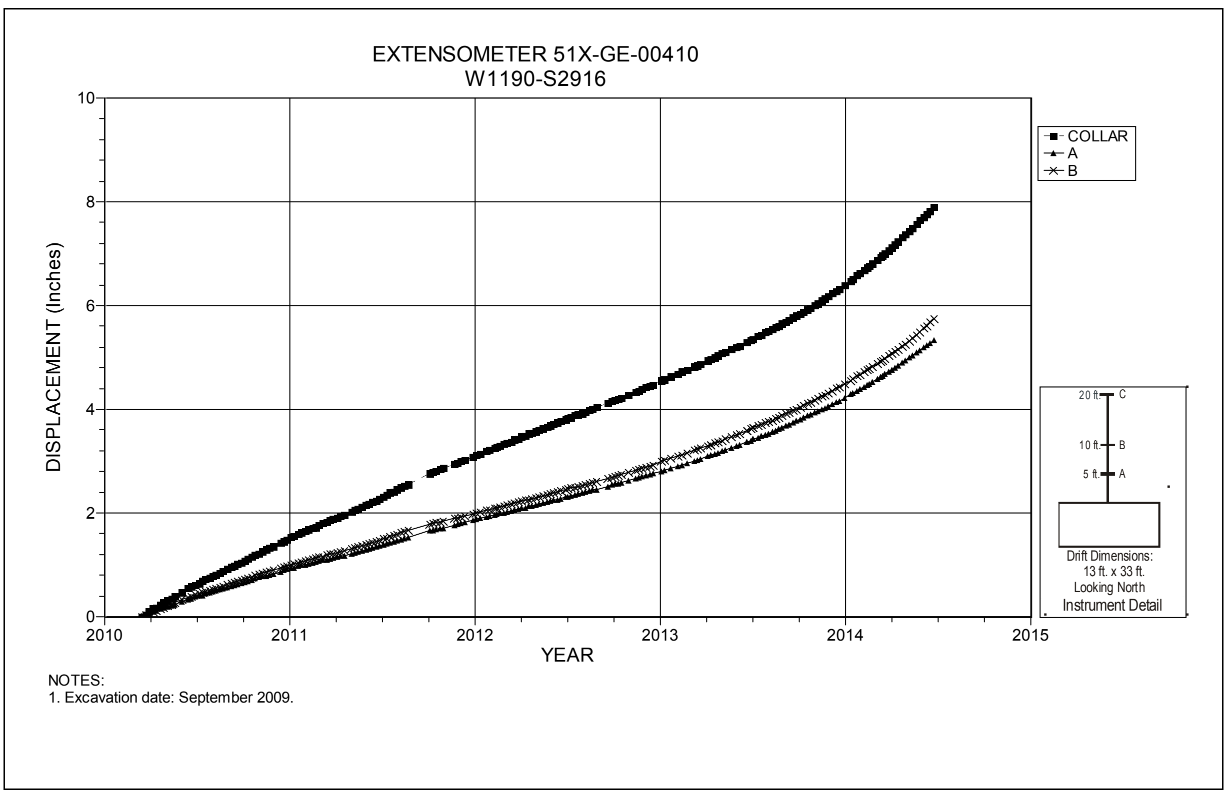

Figure 5-32 Extensometer 51X-GE-00410
Room 7, Panel 6 at W1190 S2916 – Room Center – Roof

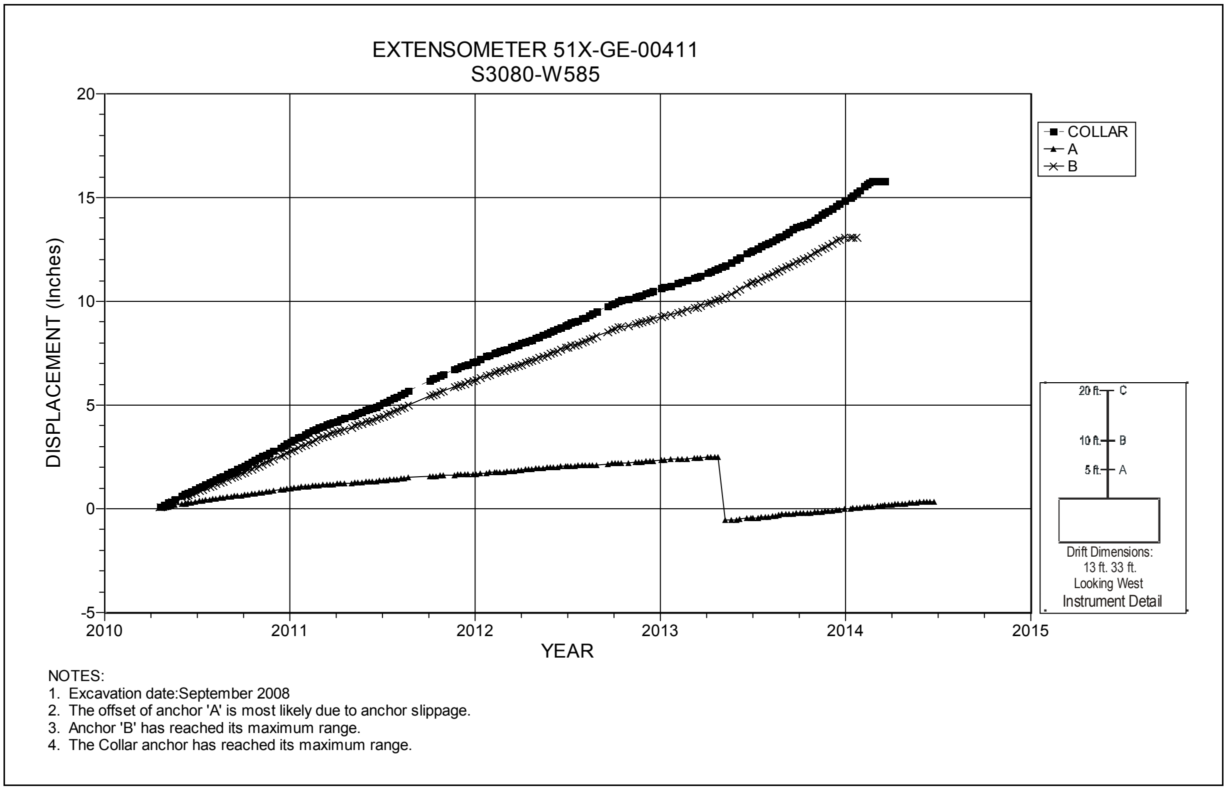

Figure 5-33 Extensometer 51X-GE-00411
S3080 W585 – Roof

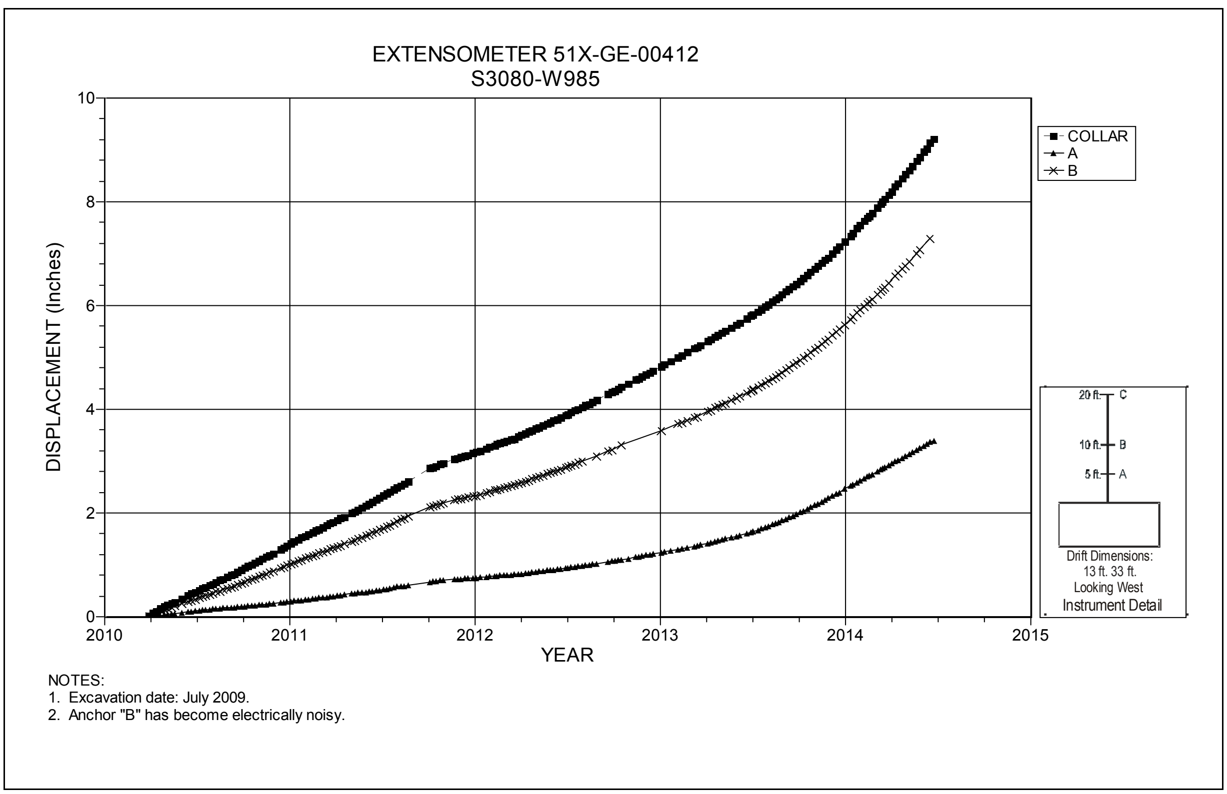

Figure 5-34 Extensometer 51X-GE-00412
S3080 W985 – Roof

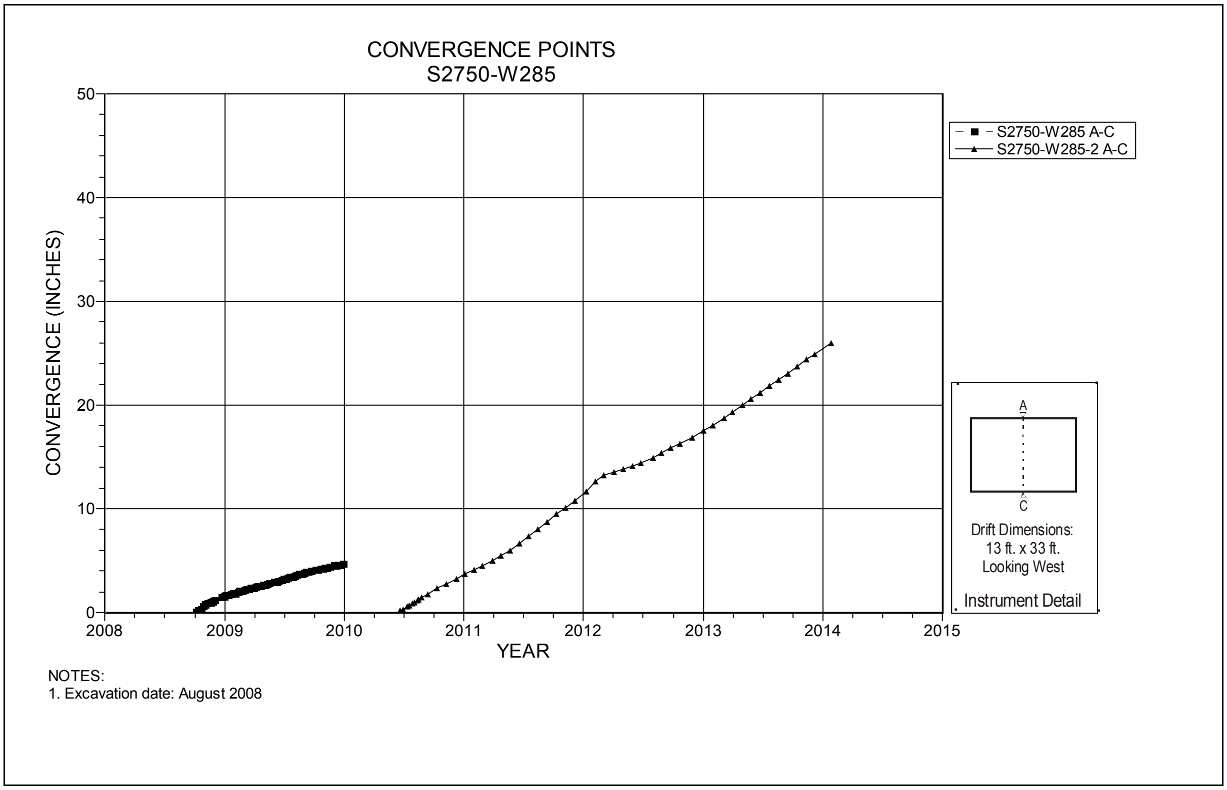

Figure 5-35 Convergence Point Array
S2750 W285 – Roof to Floor

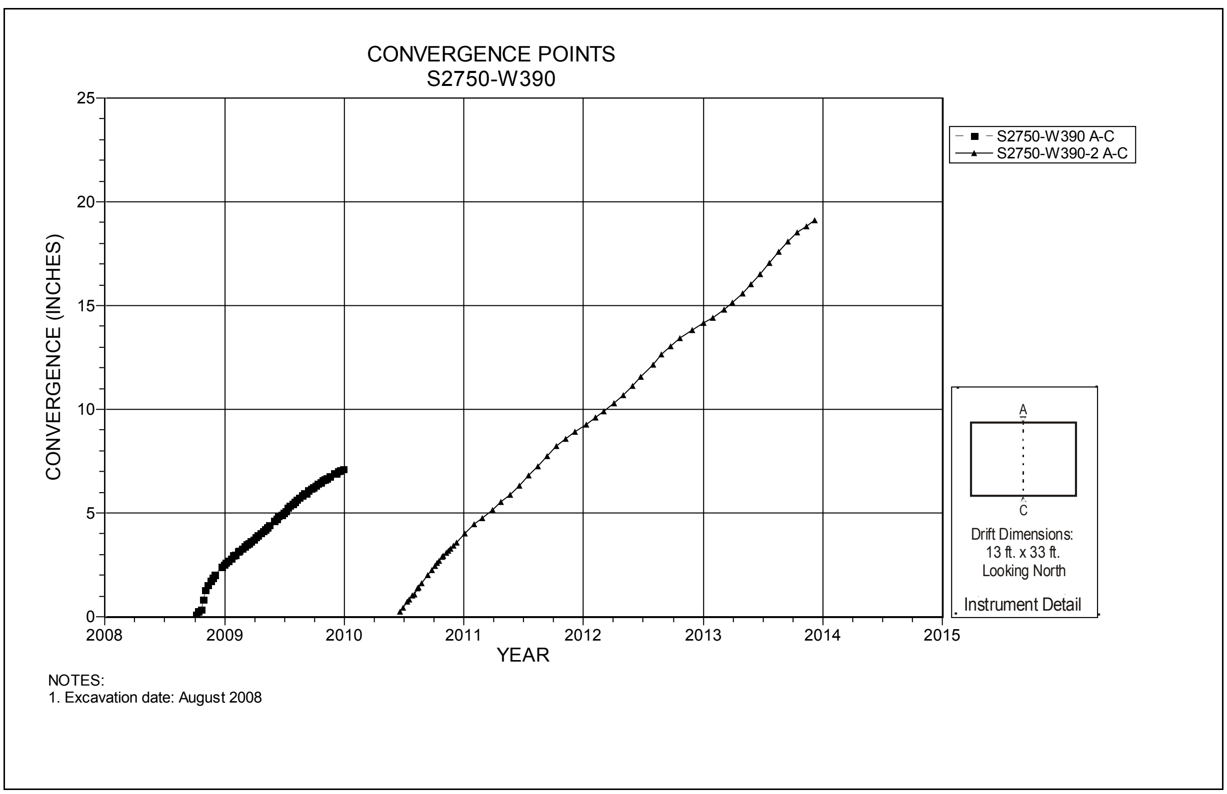

Figure 5-36 Convergence Point Array
S2750 W390 Intersection (Room 1, Panel 6) – Roof to Floor

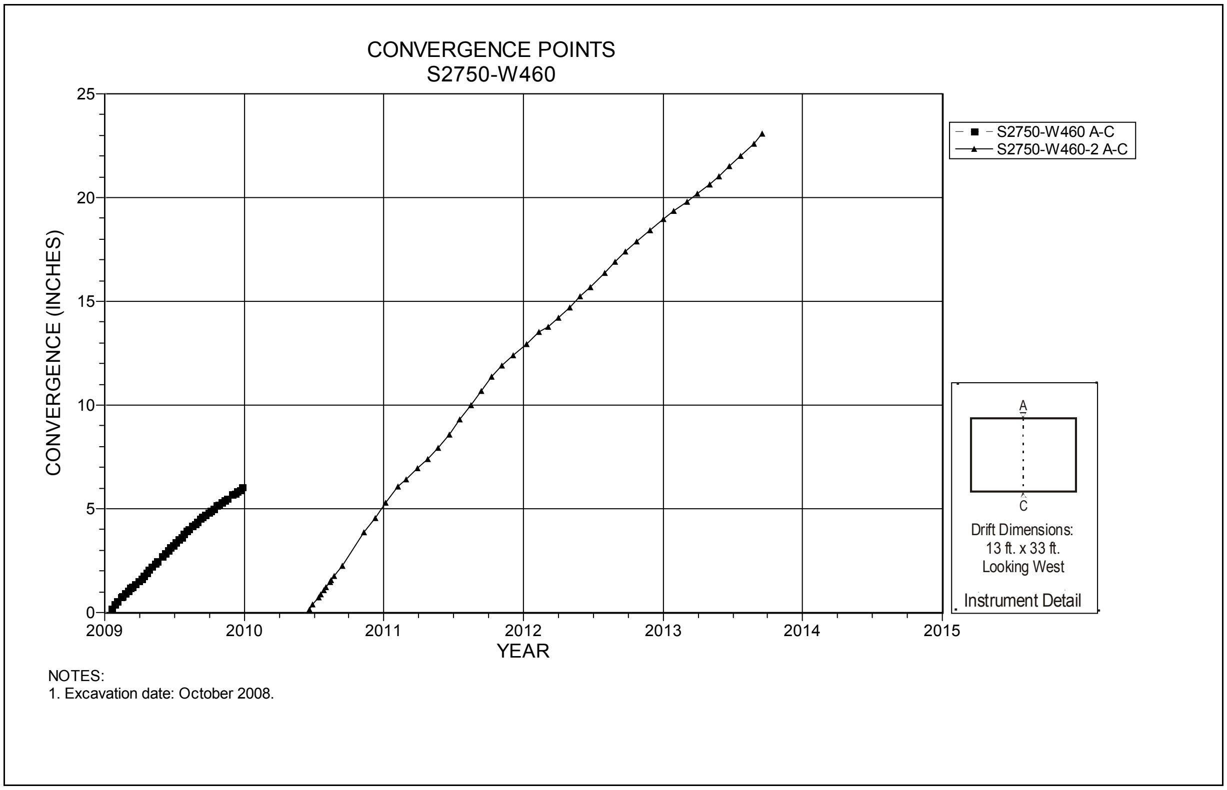

Figure 5-37 Convergence Point Array
S2750 W460 – Roof to Floor

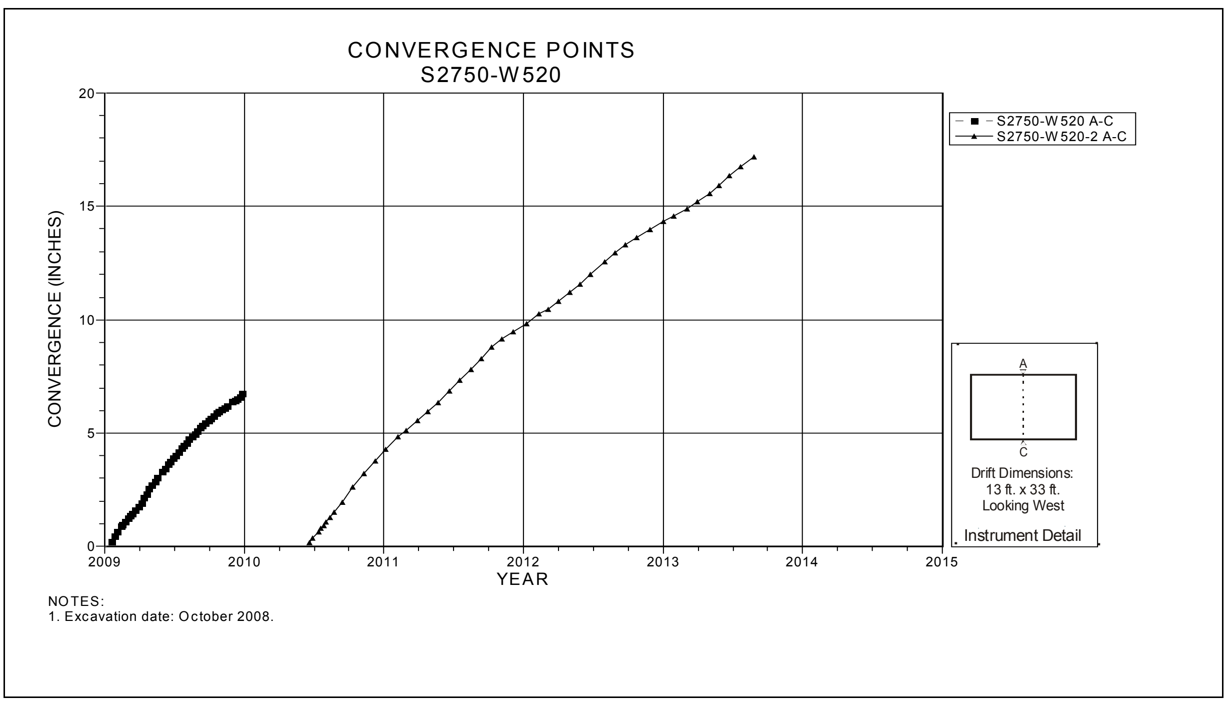

Figure 5-38 Convergence Point Array
S2750 W520 Intersection (Room 2, Panel 6) – Roof to Floor

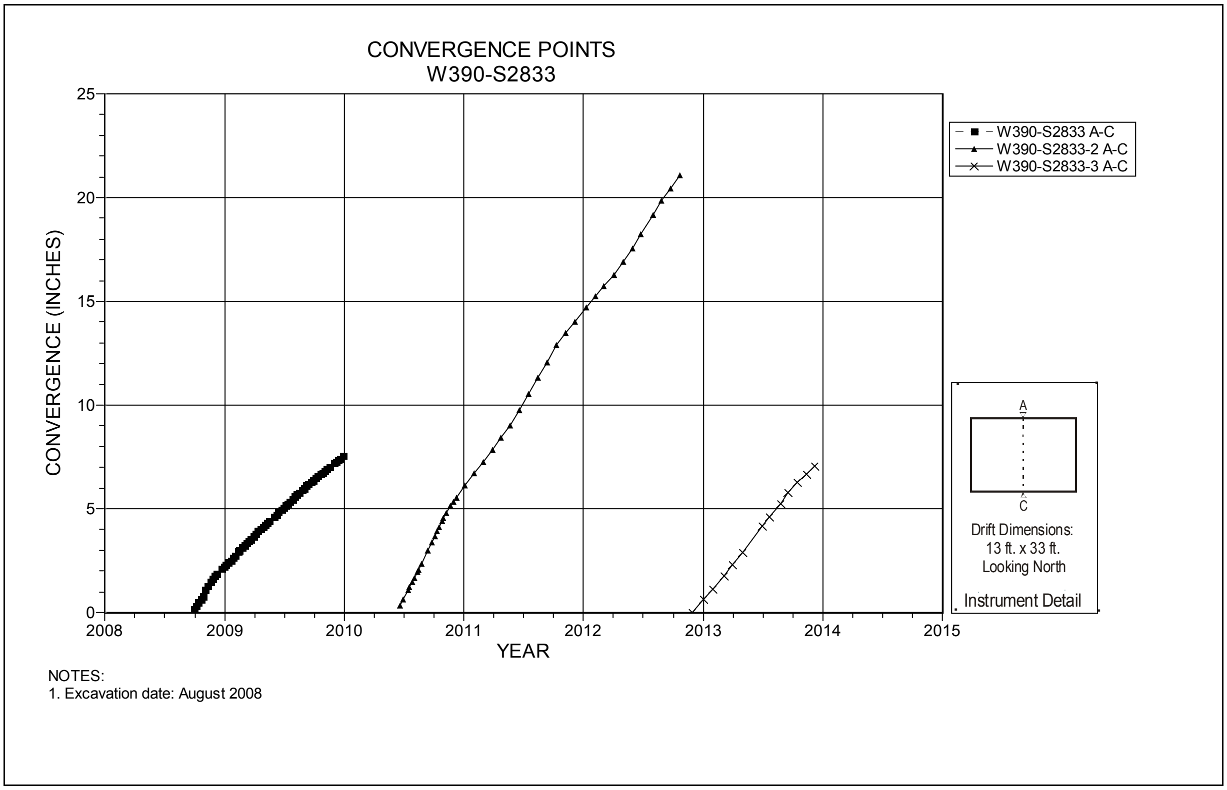

Figure 5-39 Convergence Point Array
Room 1, Panel 6 at W390 S2833 – Roof to Floor

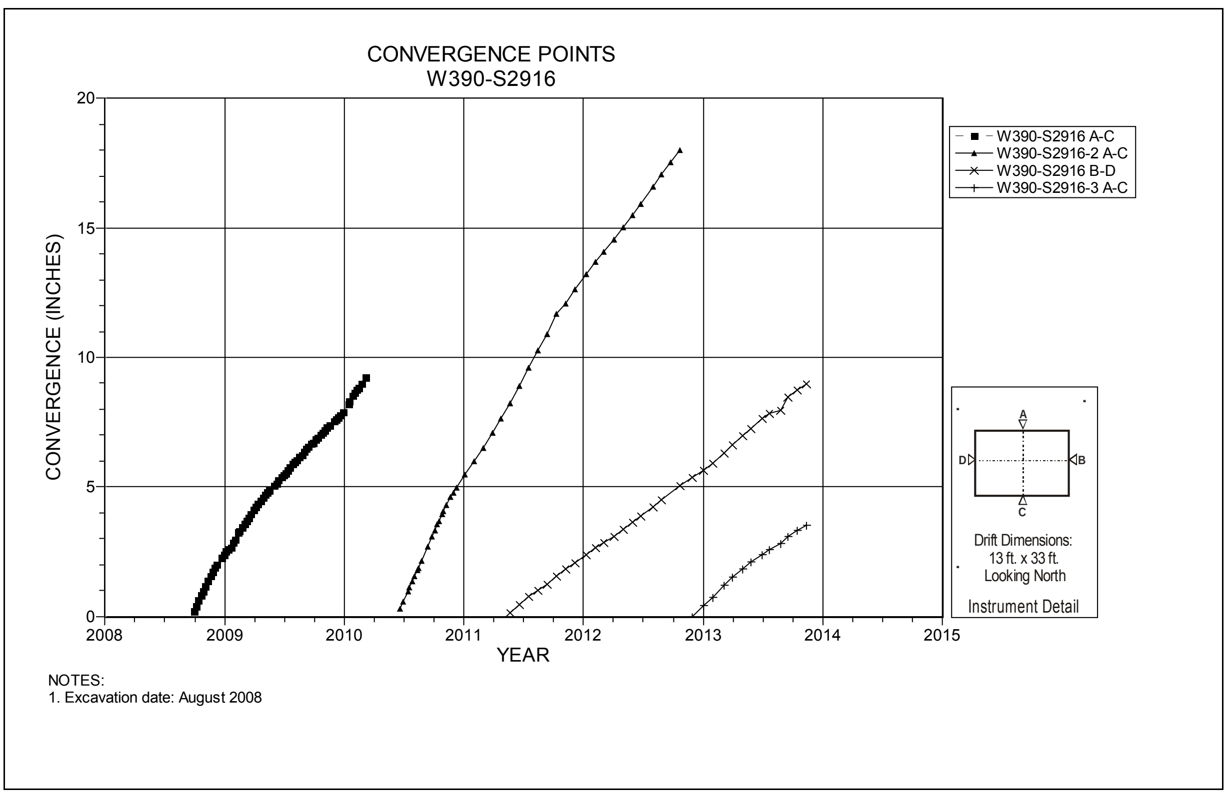

Figure 5-40 Convergence Point Array
Room 1, Panel 6 at W390 S2916 – Room Center – All Chords

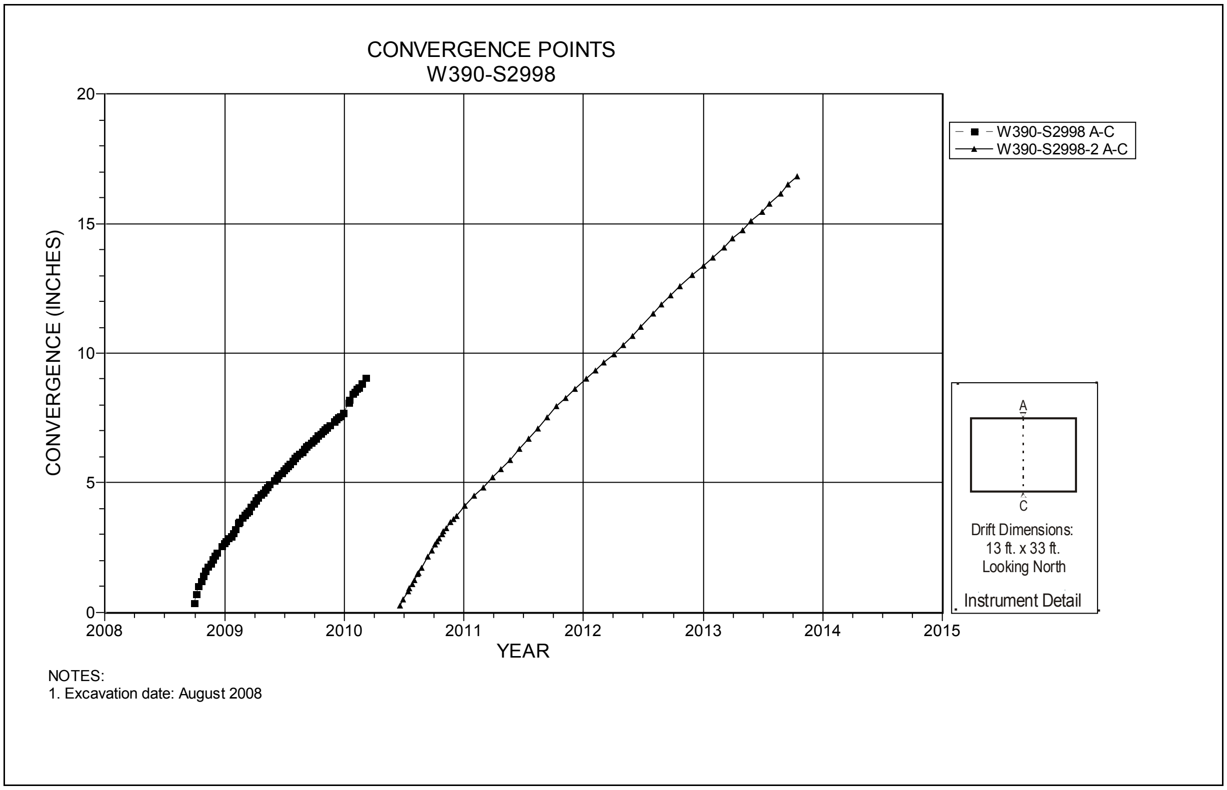

Figure 5-41 Convergence Point Array
Room 1, Panel 6 at W390 S2998 – Roof to Floor

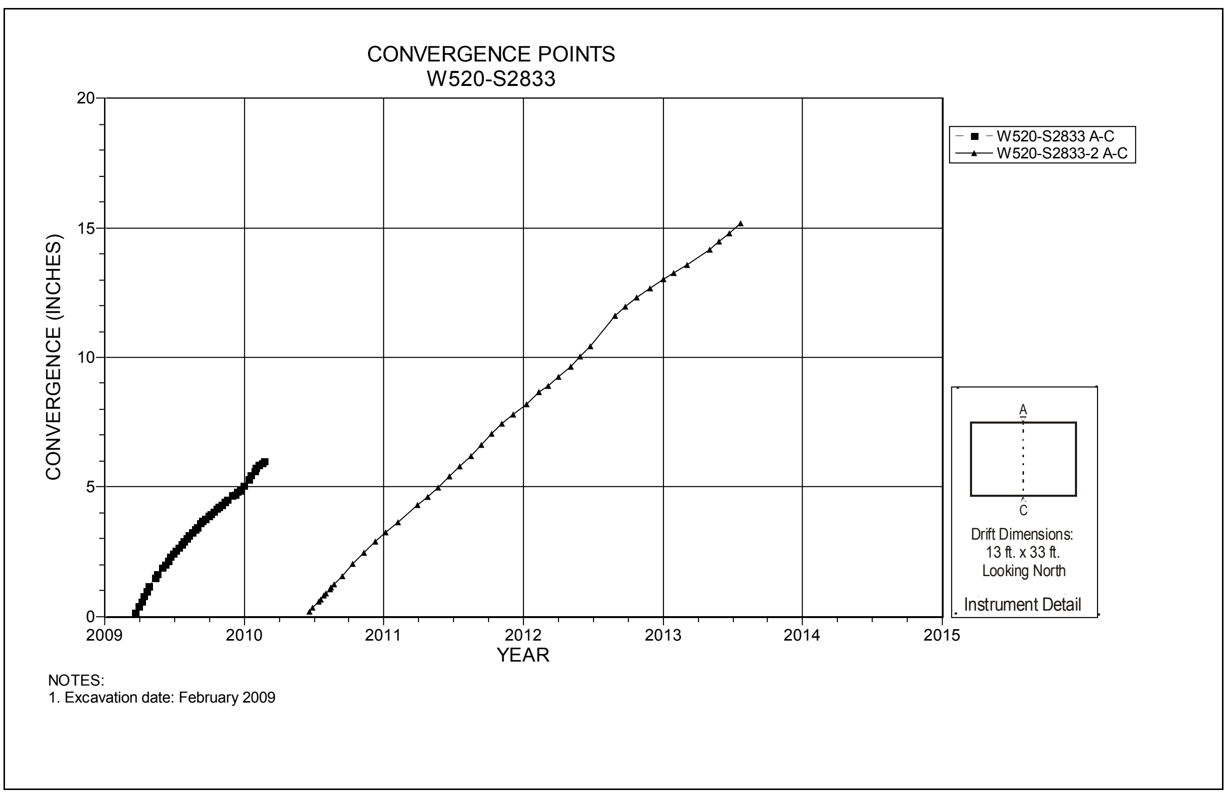

Figure 5-42 Convergence Point Array
Room 2, Panel 6 at W520 S2833 – Roof to Floor

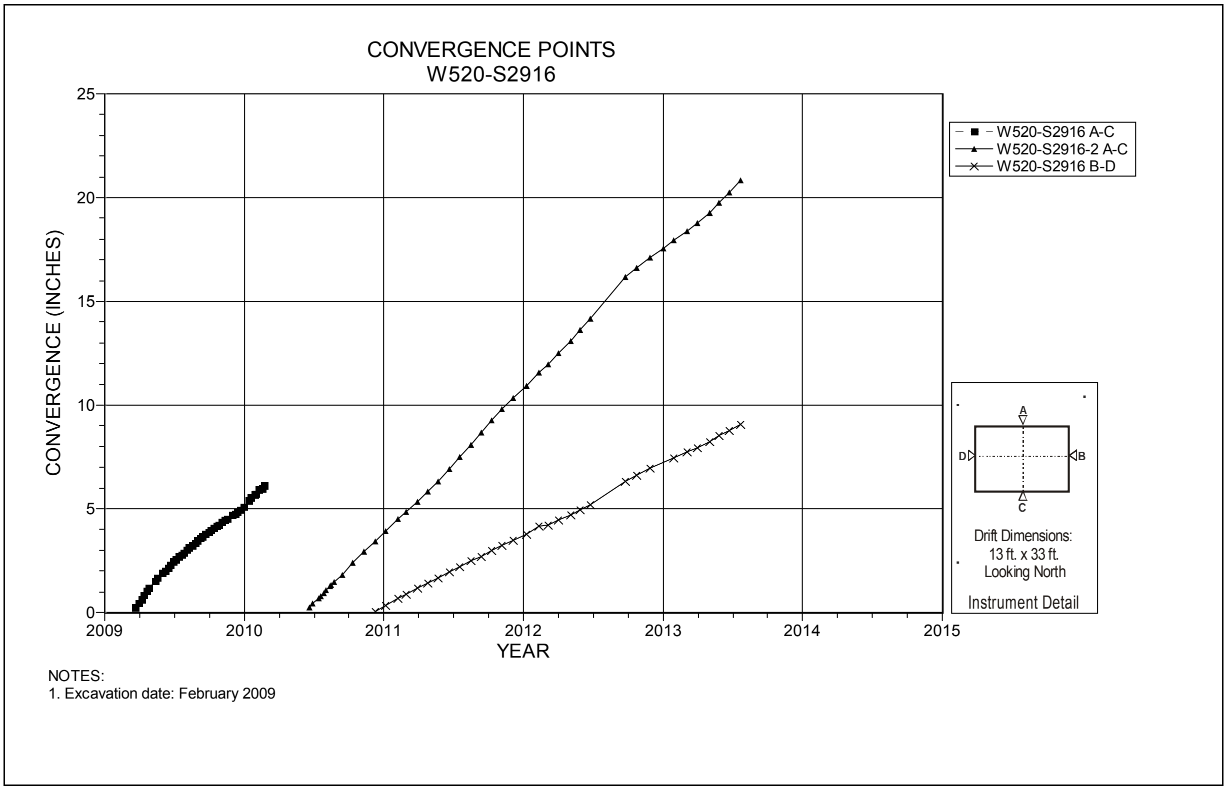

Figure 5-43 Convergence Point Array
Room 2, Panel 6 at W520 S2916 – Room Center – All Chords

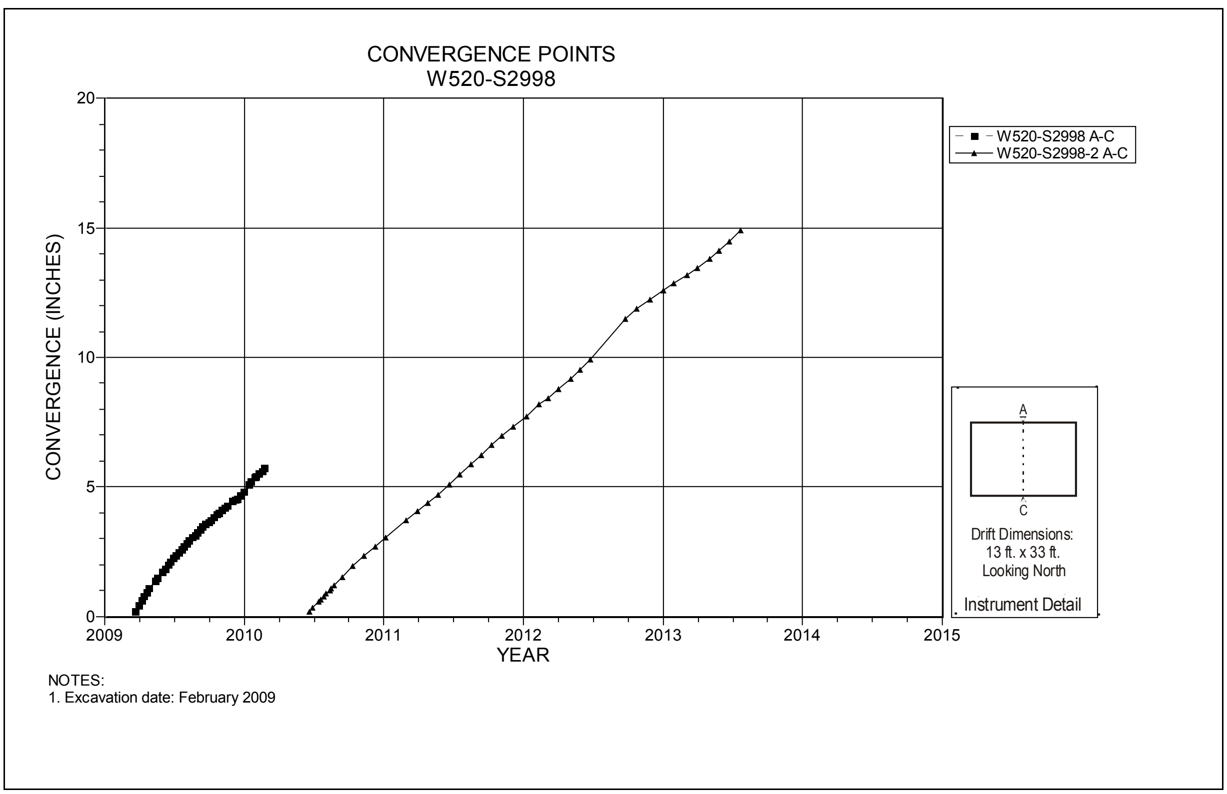

Figure 5-44 Convergence Point Array
Room 2, Panel 6 at W520 S2998 – Roof to Floor

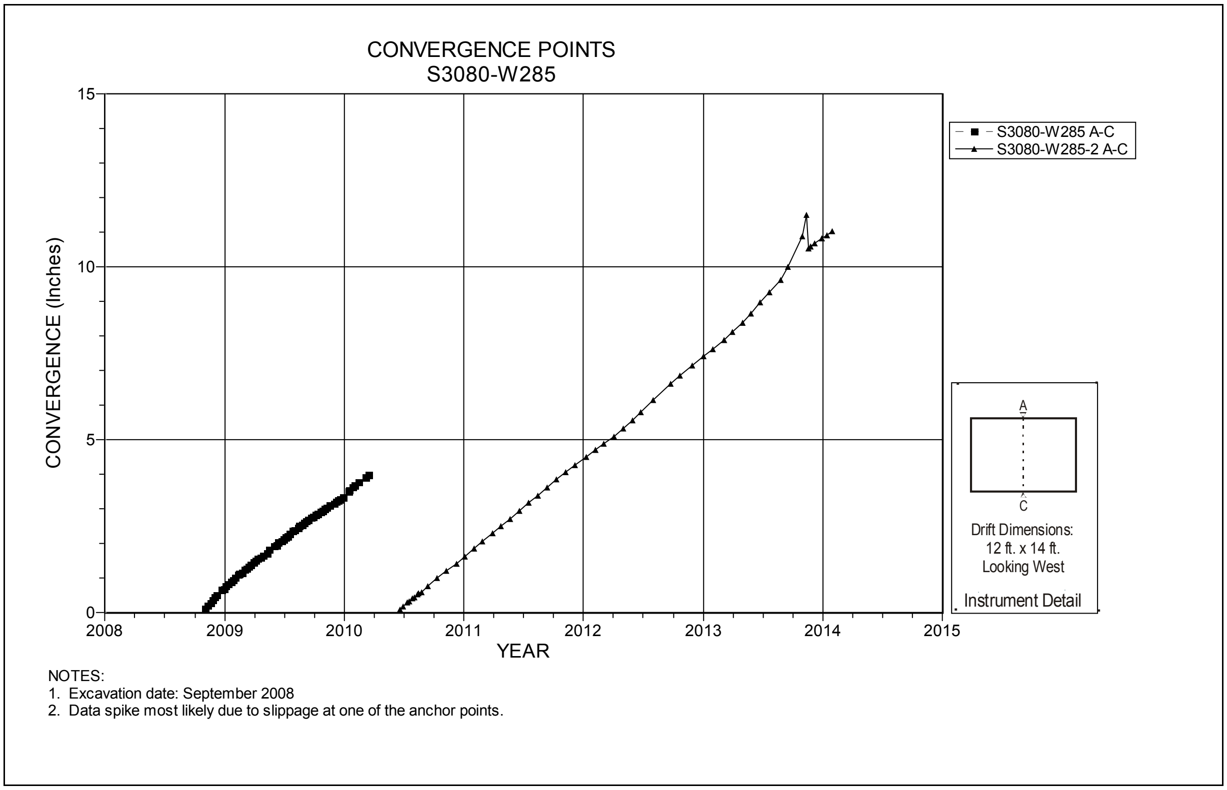

Figure 5-45 Convergence Point Array
S3080 W285 – Roof to Floor

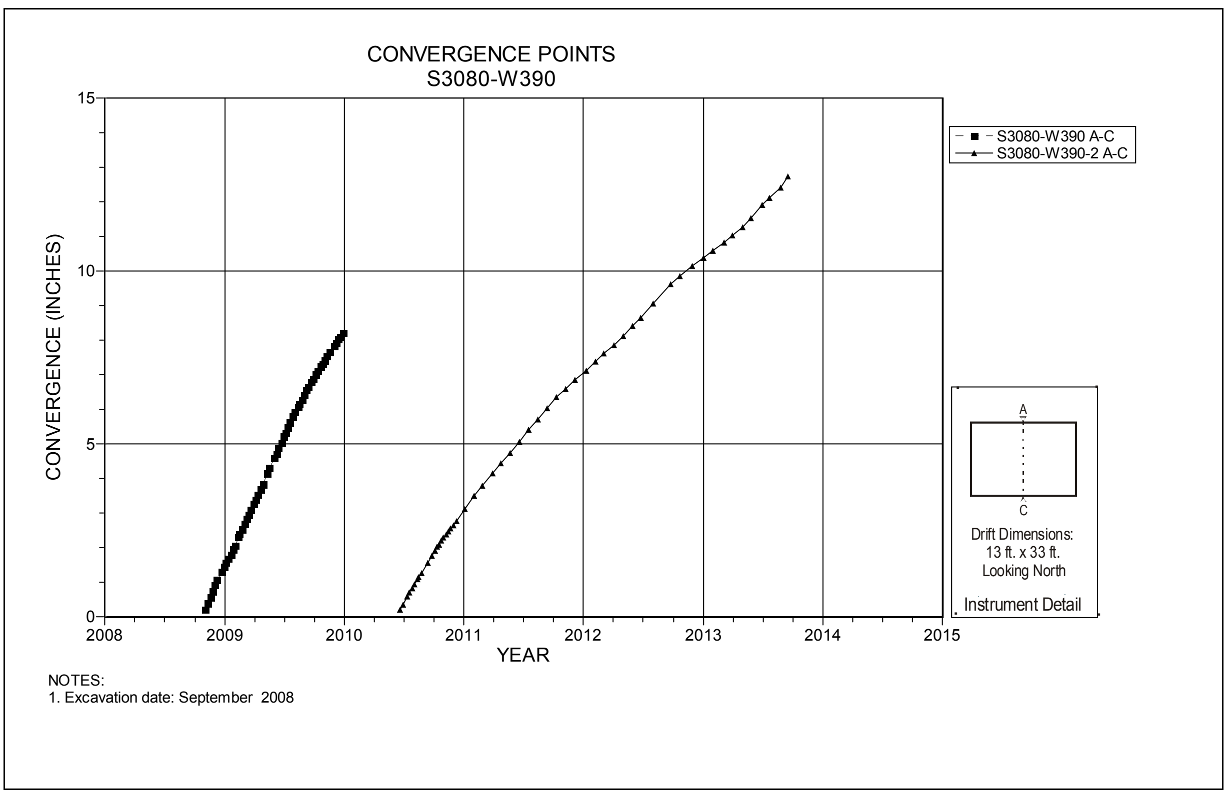

Figure 5-46 Convergence Point Array
S3080 W390 Intersection (Room 1, Panel 6) – Roof to Floor

Table 5-7
Panel 7 Data Analysis

Extensometers								
Field Tag	Location	Figure Number	Date of Last Reading	Collar Displacement Relative to Deepest Anchor (inches)	Displacement Rate 2012 to 2013 (in/year)	Displacement Rate[1] 2011 to 2012 (in/year)	Rate Change Percent[1]	Comments
51X-GE-00416	S2180-W585	5-47	06/24/14	3.699	1.4	1.1	27%	
51X-GE-00417	S2180-W985	5-48	06/24/14	4.664	2.1	1.3	62%	
51X-GE-00425	W390-S2350	5-49	06/24/14	2.789	1.0	0.9	11%	
51X-GE-00426	W520-S2350	5-50	06/24/14	3.253	1.1	1.1	0%	
51X-GE-00418	W660-S2350	5-51	06/24/14	3.964	1.5	1.3	15%	
51X-GE-00419	W790-S2350	5-52	06/24/14	3.365	1.4	1.2	17%	
51X-GE-00420	W920-S2350	5-53	06/24/14	2.205	1.8	1.2	50%	.
51X-GE-00421	W1050- S2350	5-54	06/24/14	3.451	1.2	1.1	9%	
51X-GE-00422	W1190-S2350	5-55	06/24/14	3.897	1.4	1.2	17%	
51X-GE-00423	S2520-W585	5-56	06/24/14	3.618	1.2	1.3	-8%	
51X-GE-00424	S2520-W985	5-57	06/24/14	3.866	1.5	1.3	15%	

Table 5-7
Panel 7 Data Analysis (Continued)

Convergence Points

Field Tag	Location	Figure Number	Last Reading 2013 to 2014		Cumulative Displacement (inches)	Closure Rate 2013 to 2014 (in/year)	Closure Rate 2012 to 2013 (in/year)	Rate Change Percent	Comments
			Date	Inches					
S2180-W285-2 A-C	S2180-W285	5-58	01/27/14	4.588	5.034	1.5	1.5	0%	
S2180-W390-3 A-C	S2180-W390	5-59	01/27/14	4.627	10.327	4.7	4.0	18%	
S2180-W460-3 A-C	S2180-W460	5-60	01/27/14	5.101	13.325	5.4	4.2	29%	
S2180-W520-3 A-C	S2180-W520	5-61	01/27/14	5.712	16.622	5.9	4.8	23%	
S2180-W585-4 A-C	S2180-W585	5-62	01/27/14	5.398	15.375	5.6	4.6	22%	
S2180-W660-4 A-C	S2180-W660	5-63	01/27/14	4.658	14.067	4.8	3.9	23%	
S2180-W725-4 A-C	S2180-W725	5-64	01/27/14	5.794	13.213	5.9	5.1	16%	
S2180-W790-3 A-C	S2180-W790	5-65	01/27/14	4.066	14.638	4.2	3.5	20%	
S2180-W855-3 A-C	S2180-W855	5-66	01/27/14	4.259	14.633	4.6	3.4	35%	
S2180-W920-3 A-C	S2180-W920	5-67	01/27/14	3.374	13.255	3.4	2.9	17%	
S2180-W985-4 A-C	S2180-W985	5-68	01/27/14	3.28	19.326	3.5	2.6	35%	
S2180-W1050-2 A-C	S2180-W1050	5-69	01/27/14	3.157	11.73	3.2	2.7	19%	
S2180-W1120-3 A-C	S2180-W1120	5-70	09/04/13	2.174	11.423	3.8	3.1	23%	Waste emplacement.
S2180-W1190-3 A-C	S2180-W1190	5-71	01/27/14	2.536	2.536	2.4	2.4	0%	
W390-S2275-3 A-C	W390-S2275	5-72	01/28/14	7.804	15.738	5.3	5.6	-5%	
W390-S2350-3 A-C	W390-S2350	5-73	01/28/14	5.538	12.102	2.7	5.4	-50%	
W390-S2350 B-D	W390-S2350	5-73	01/28/14	2.034	2.034	2.7	2.9	-7%	
W390-S2425-3 A-C	W390-S2425	5-74	01/28/14	5.092	15.159	3.4	3.7	-8%	
W520-S2275-3 A-C	W520-S2275	5-75	01/28/14	8.721	17.173	6.2	5.9	5%	
W520-S2350-3 A-C	W520-S2350	5-76	01/28/14	6.429	19.298	4.1	4.5	-9%	
W520-S2350 B-D	W520-S2350	5-76	01/28/14	2.133	2.133	2.9	3.2	-9%	
W520-S2425-3 A-C	W520-S2425	5-77	01/28/14	7.204	16.486	5.2	4.6	13%	
W660-S2275-3 A-C	W660-S2275	5-78	01/28/14	6.394	15.41	4.5	4.4	2%	
W660-S2350-3 A-C	W660-S2350	5-79	01/28/14	5.016	21.745	5.1	4.3	19%	
W660-S2350 B-D	W660-S2350	5-79	01/28/14	2.202	2.202	2.9	2.6	12%	
W660-S2425-3 A-C	W660-S2425	5-80	01/28/14	5.833	18.387	4.4	3.8	16%	
W790-S2275-3 A-C	W790-S2275	5-81	01/28/14	4.073	8.677	4.3	3.5	23%	
W790-S2350-3 A-C	W790-S2350	5-82	01/28/14	4.563	8.854	4.5	4.3	5%	
W790-S2350 B-D	W790-S2350	5-82	01/28/14	2.343	2.343	3.0	3.0	0%	

Table 5-7
Panel 7 Data Analysis (Continued)

Convergence Points (Continued)

Field Tag	Location	Figure Number	Last Reading 2013 to 2014		Cumulative Displacement (inches)	Closure Rate 2013 to 2014 (in/year)	Closure Rate 2012 to 2013 (in/year)	Rate Change Percent	Comments
			Date	Inches					
W790-S2425-2 A-C	W790-S2425	5-83	01/28/14	3.984	6.283	4.0	3.6	11%	
W920-S2275-3 A-C	W920-S2275	5-84	01/27/14	3.305	6.373	3.4	3.0	13%	
W920-S2350-3 A-C	W920-S2350	5-85	01/27/14	3.859	6.875	4.0	3.3	21%	
W920-S2350 B-D	W920-S2350	5-85	01/27/14	2.334	2.334	3.0	2.8	7%	
W920-S2425-3 A-C	W920-S2425	5-86	01/27/14	4.402	7.245	4.8	3.7	30%	
W1050-S2275-3 A-C	W1050-S2275	5-87	01/28/14	2.994	12.623	3.1	2.7	15%	
W1050-S2350-3 A-C	W1050-S2350	5-88	01/28/14	3.247	12.398	3.2	3.0	7%	
W1050-S2350 B-D	W1050-S2350	5-88	01/28/14	2.452	2.452	3.2	3.1	3%	
W1050-S2425-3 A-C	W1050-S2425	5-89	01/28/14	2.84	12.361	2.9	2.5	16%	
W1190-S2275-3 A-C	W1190-S2275	5-90	01/27/14	2.725	12.755	2.8	2.3	22%	
W1190-S2350-4 A-C	W1190-S2350	5-91	01/27/14	2.973	13.889	3.1	2.6	19%	
W1190-S2350 B-D	W1190-S2350	5-91	01/27/14	2.473	2.473	3.3	3.0	10%	
W1190-S2425-4 A-C	W1190-S2425	5-92	01/27/14	2.734	11.232	2.7	2.6	4%	
S2520-W285-4 A-C	S2520-W285	5-93	01/28/14	7.106	12.081	4.9	4.8	2%	
S2520-W390-3 A-C	S2520-W390	5-94	01/28/14	6.027	13.31	3.9	4.3	-9%	
S2520-W455-3 A-C	S2520-W455	5-95	01/28/14	6.08	13.77	3.9	4.3	-9%	
S2520-W520-3 A-C	S2520-W520	5-96	01/28/14	5.556	18.334	3.8	3.8	0%	
S2520-W585-4 A-C	S2520-W585	5-97	01/28/14	3.486	11.152	3.4	3.3	3%	
S2520-W660-3 A-C	S2520-W660	5-98	01/28/14	4.215	17.649	4.0	4.1	-2%	
S2520-W725-5 A-C	S2520-W725	5-99	01/28/14	4.671	13.622	4.5	4.5	0%	
S2520-W790-3 A-C	S2520-W790	5-100	01/28/14	3.966	12.067	3.9	3.7	5%	
S2520-W855-3 A-C	S2520-W855	5-101	01/28/14	5.101	19.034	4.9	4.9	0%	
S2520-W920-4 A-C	S2520-W920	5-102	01/28/14	3.589	12.958	3.5	3.4	3%	
S2520-W985-3 A-C	S2520-W985	5-103	01/28/14	3.707	13.921	3.7	3.4	9%	
S2520-W1050-4 A-C	S2520-W1050	5-104	01/28/14	3.147	11.66	3.1	2.9	7%	
S2520-W1120-4 A-C	S2520-W1120	5-105	01/28/14	2.854	17.926	2.9	2.5	16%	
S2520-W1190-3 A-C	S2520-W1190	5-106	01/27/14	2.281	9.481	2.3	2.1	10%	

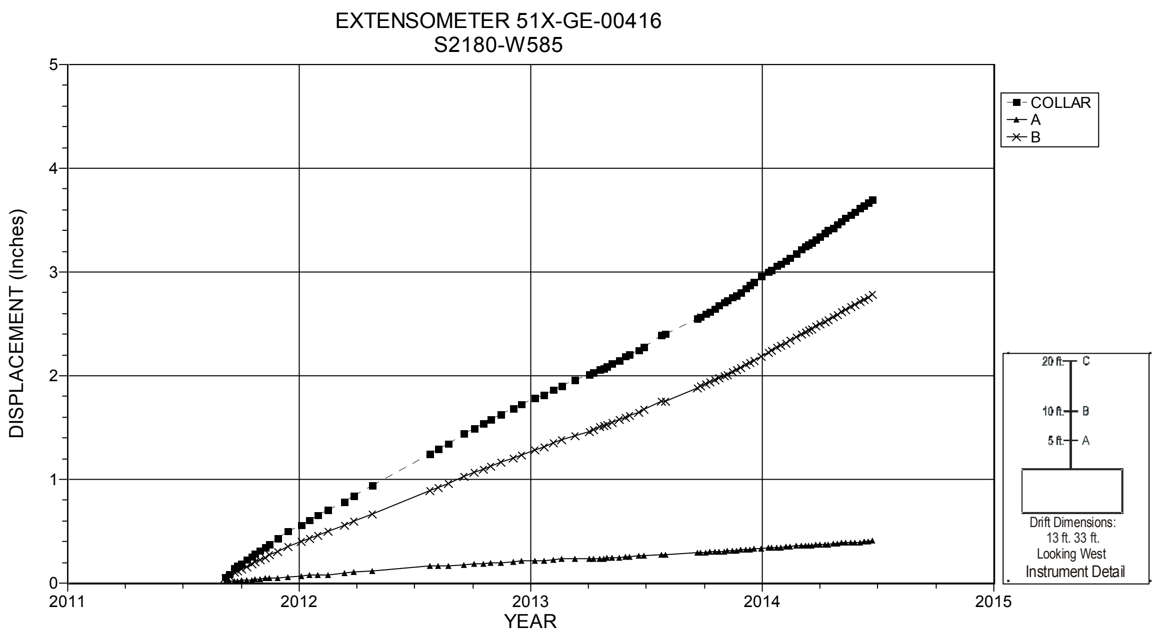

NOTES:
1. Excavation date: Augaust 2010.

Figure 5-47 Extensometer 51X-GE-00416
S2180 W585 – Roof

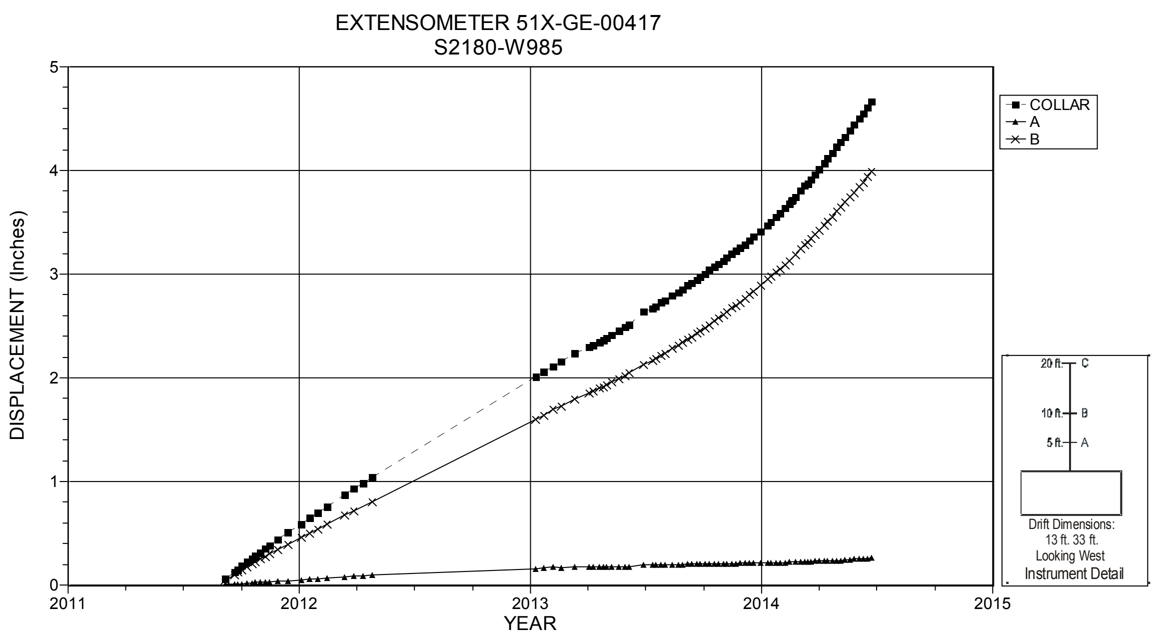

NOTES:
1. Excavation date: Augaust 2010.
2. The gap in readings is due to the area being inaccessible by aerial lift.

Figure 5-48 Extensometer 51X-GE-00417
S2180 W985 – Roof

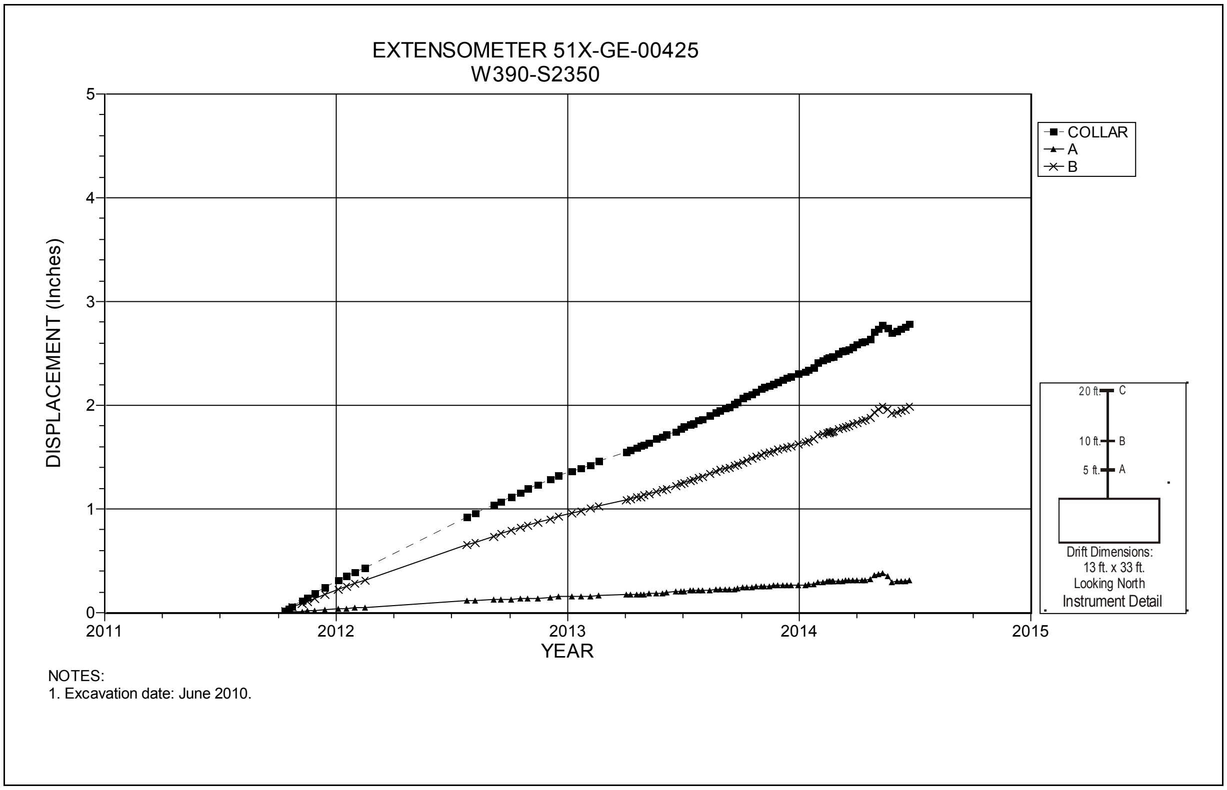

Figure 5-49 Extensometer 51X-GE-00425
Room 1, Panel 7 at W390 S2350 – Room Center – Roof

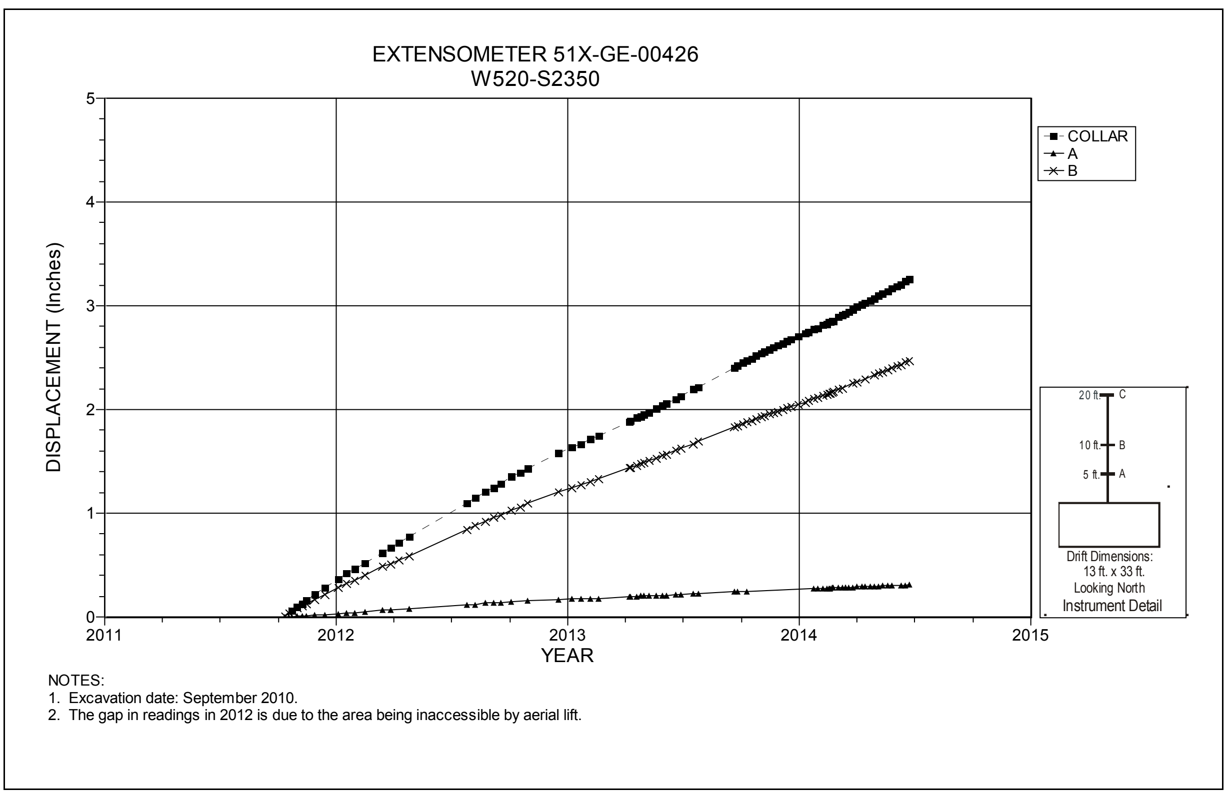

Figure 5-50 Extensometer 51X-GE-00426
Room 2, Panel 7 at W520 S2350 – Room Center – Roof

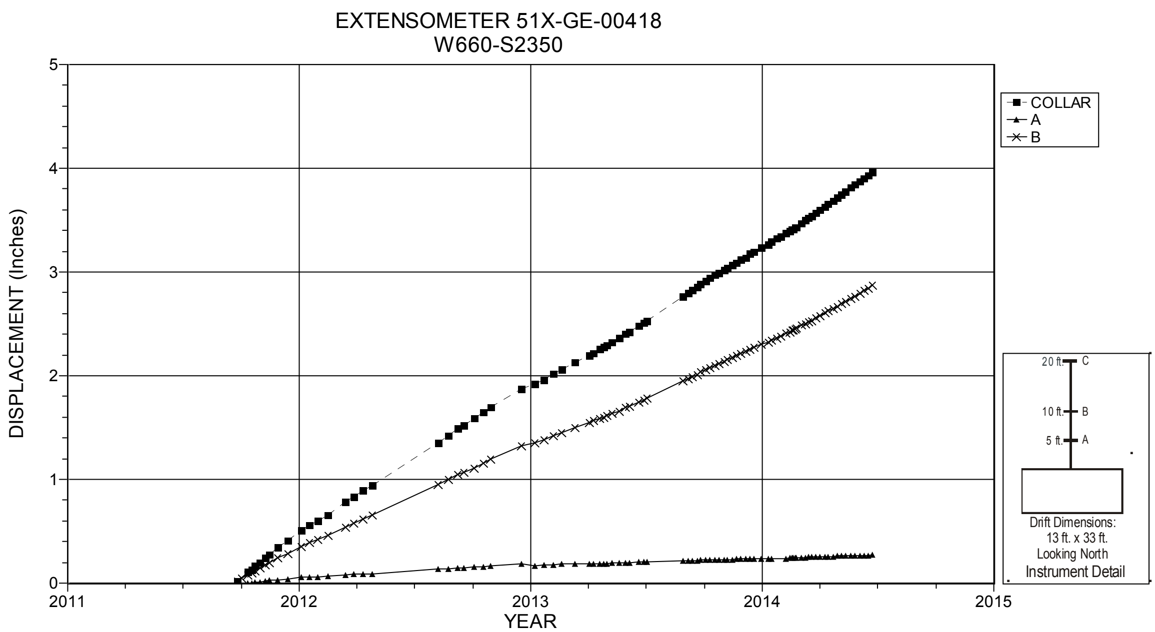

NOTES:
1. Excavation date: October 2010.
2. Anchor 'B' has become electrically noisy.

Figure 5-51 Extensometer 51X-GE-00418
Room 3, Panel 7 at W660 S2350 – Room Center – Roof

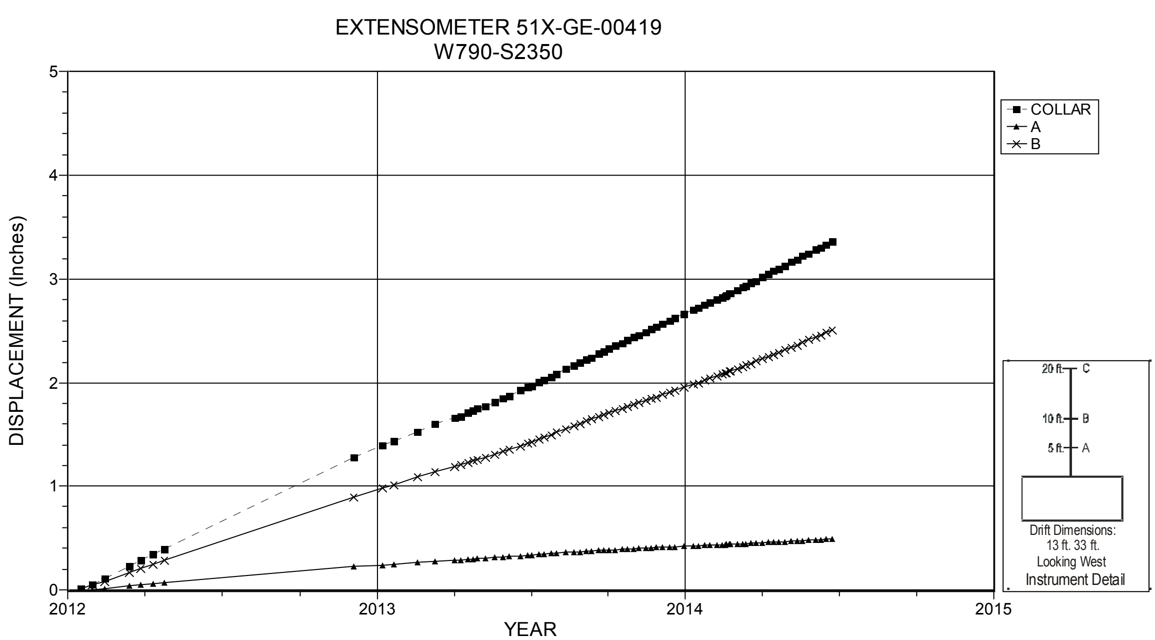

NOTES:
1. Excavation date: October 2010.
2. The gap in readings in 2012 is due to the area being inaccessible by aerial lift.

Figure 5-52 Extensometer 51X-GE-00419
Room 4, Panel 7 at W790 S2350 – Room Center – Roof

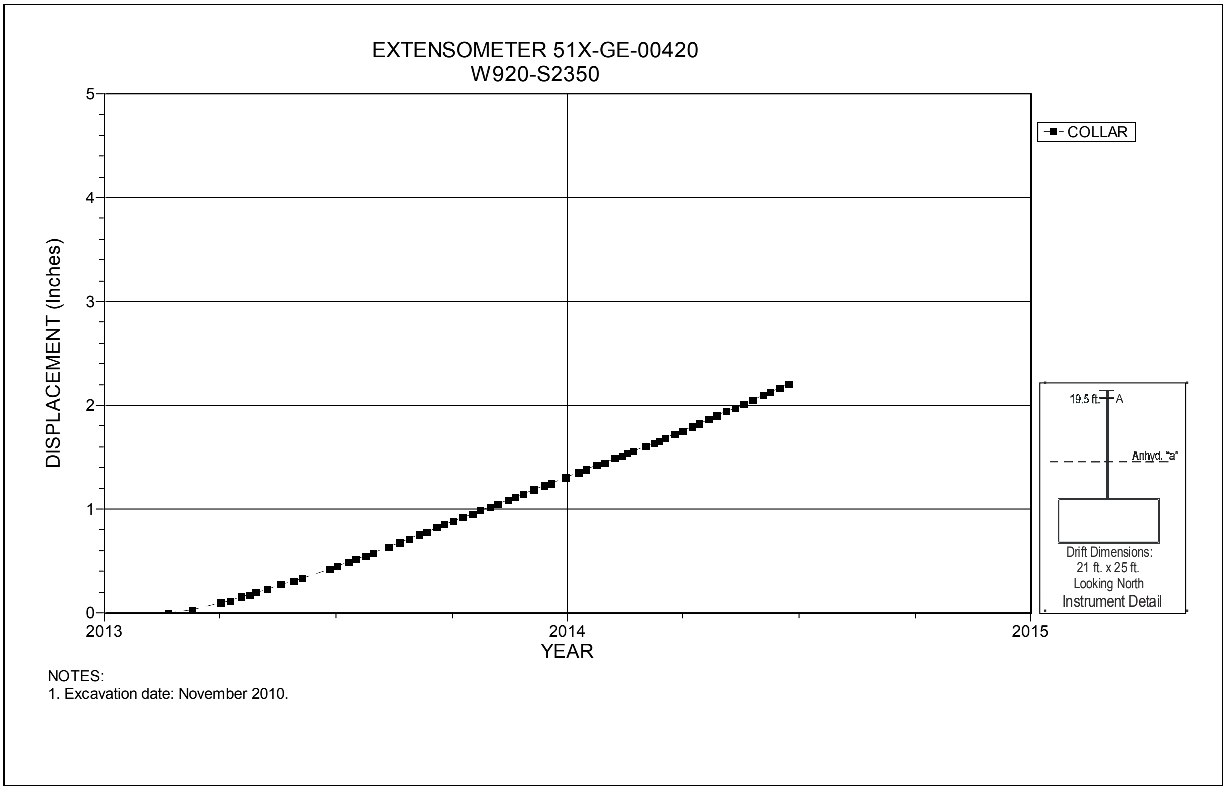

Figure 5-53 Extensometer 51X-GE-00420
Room 5, Panel 7 at W920 S2350 – Room Center – Roof

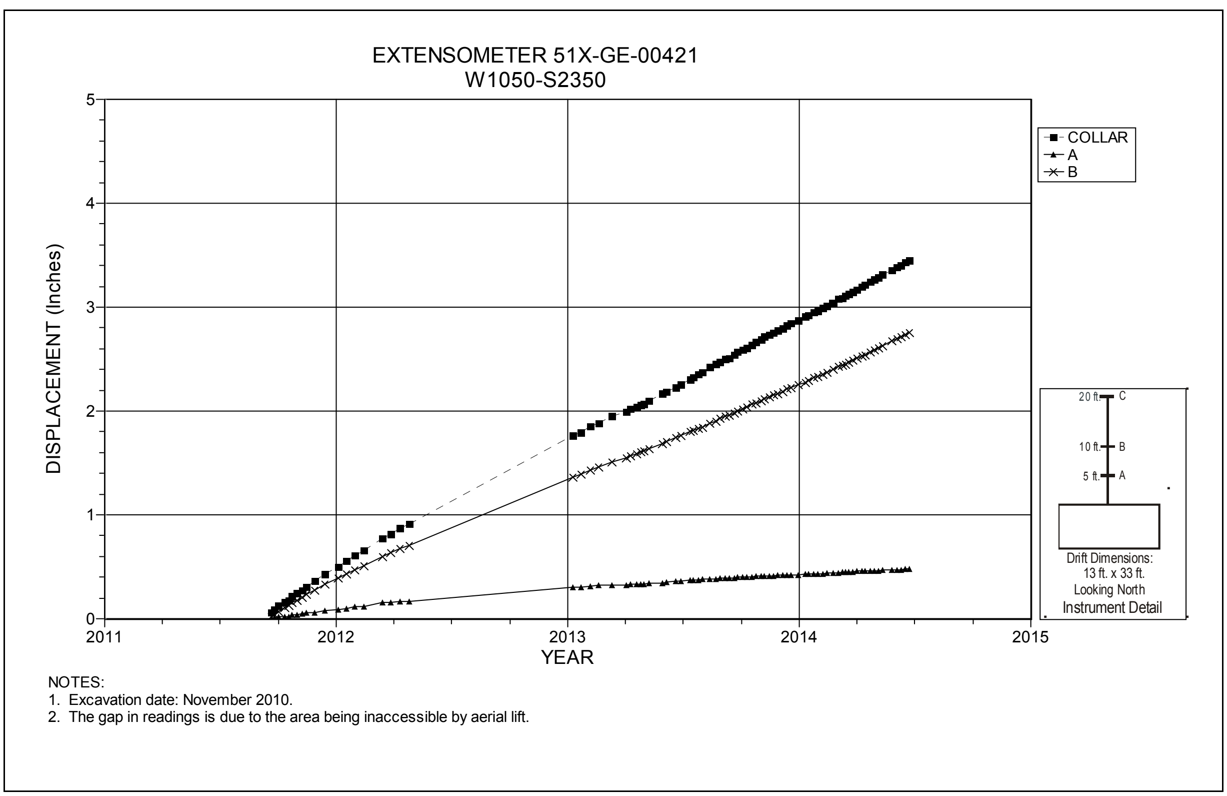

Figure 5-54 Extensometer 51X-GE-00421
Room 6, Panel 7 at W1050 S2350 – Room Center – Roof

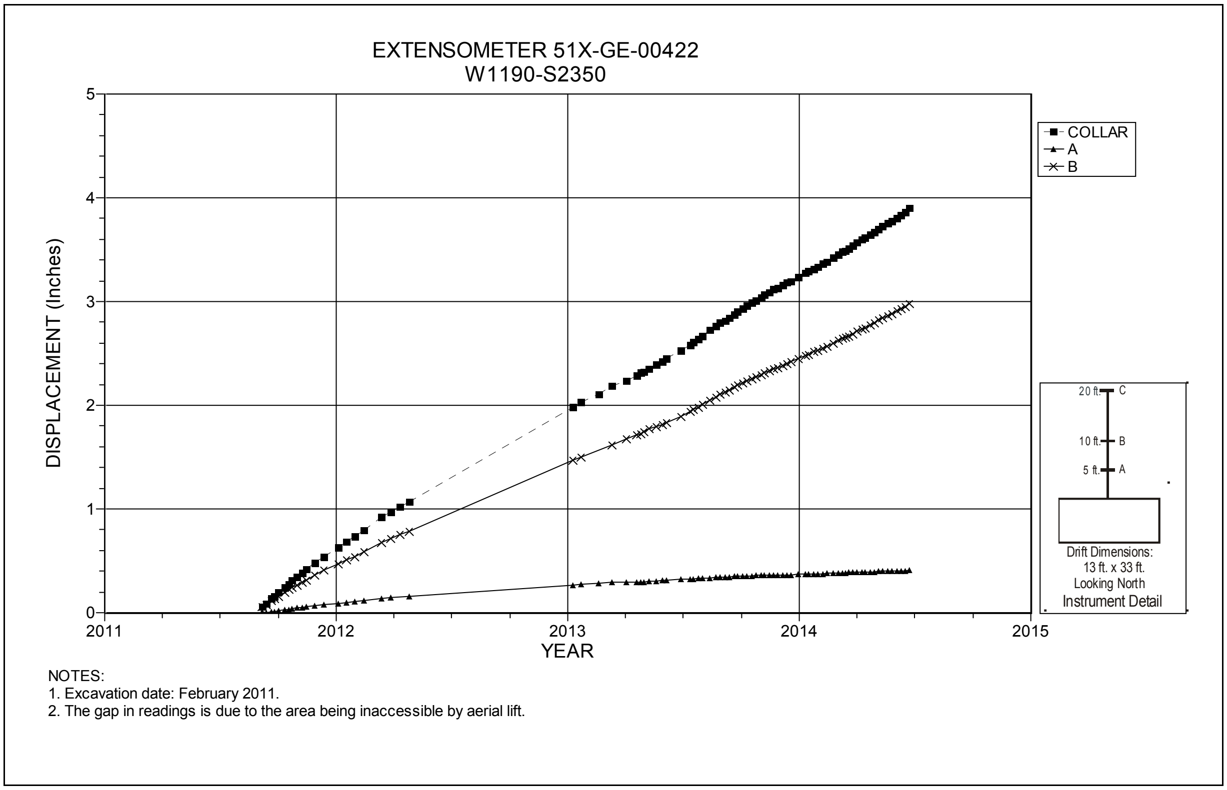

Figure 5-55 Extensometer 51X-GE-00422
Room 7, Panel 7 at W1190 S2350 – Room Center – Roof

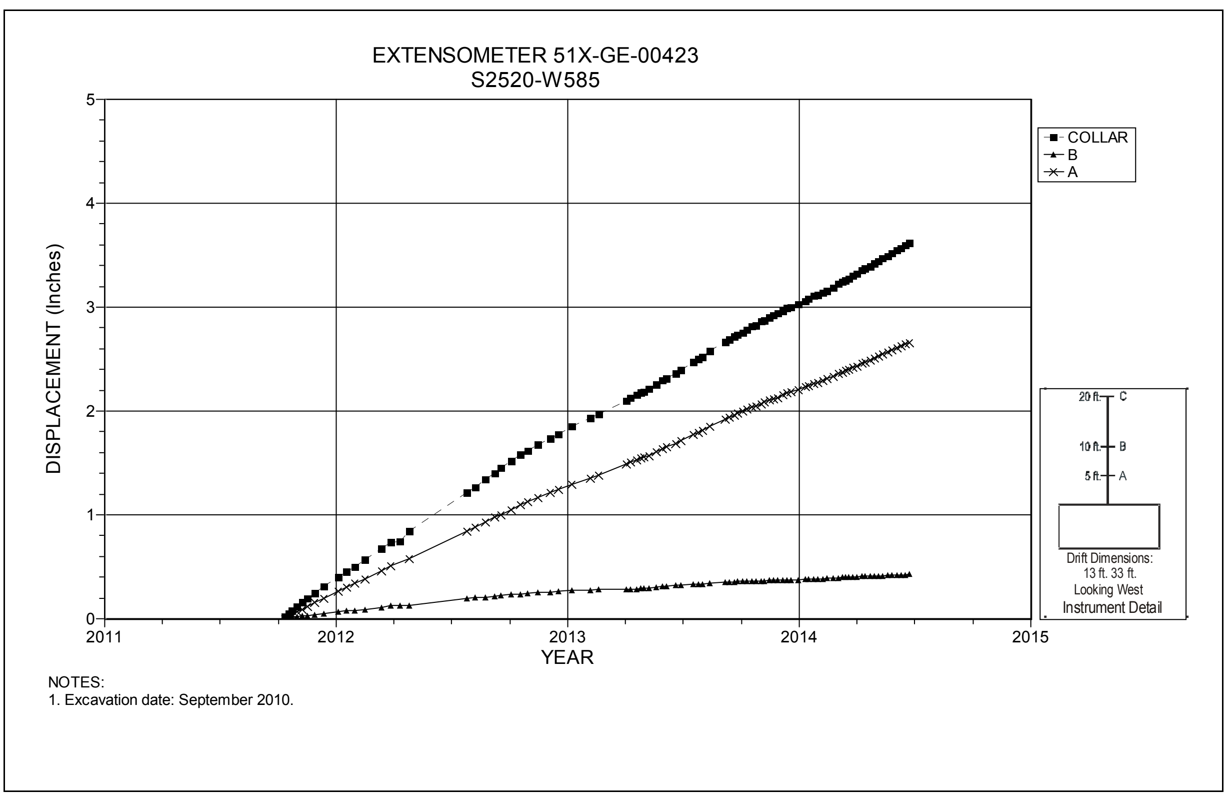

Figure 5-56 Extensometer 51X-GE-00423
S2520 W585 – Roof

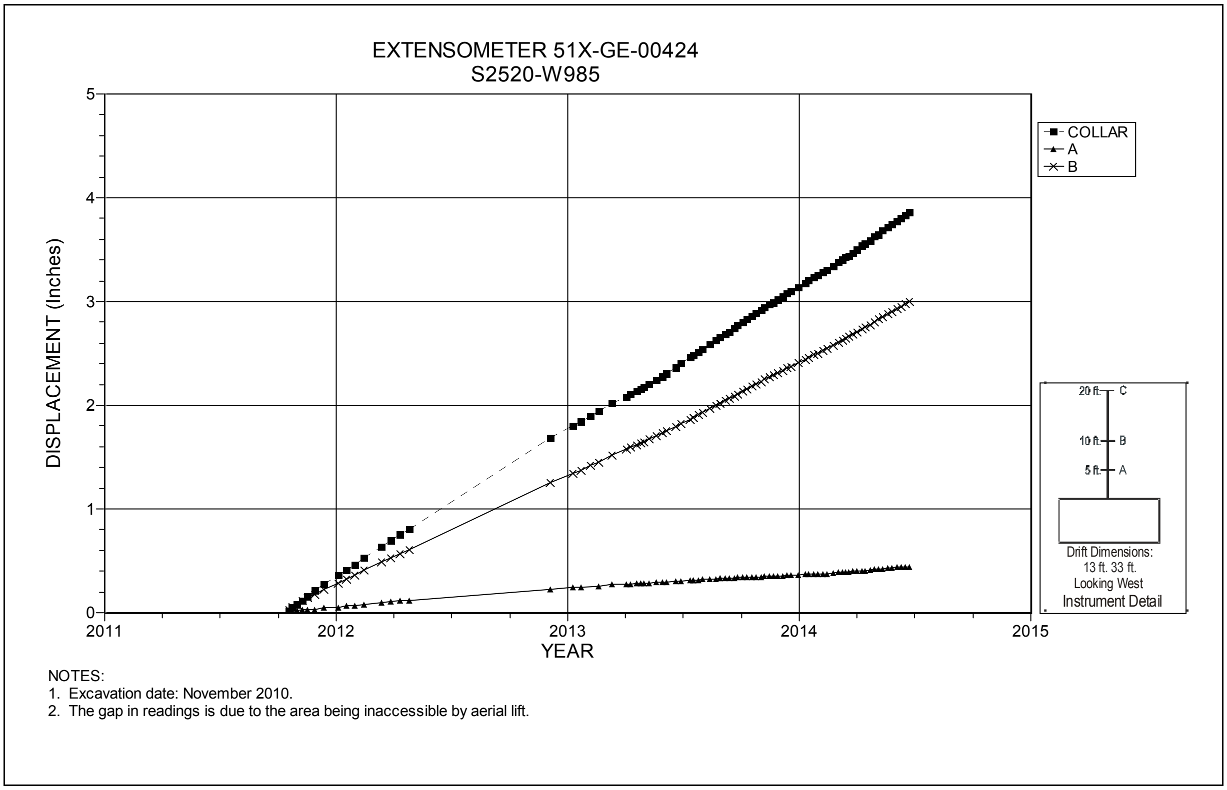

Figure 5-57 Extensometer 51X-GE-00424
S2520 W985 – Roof

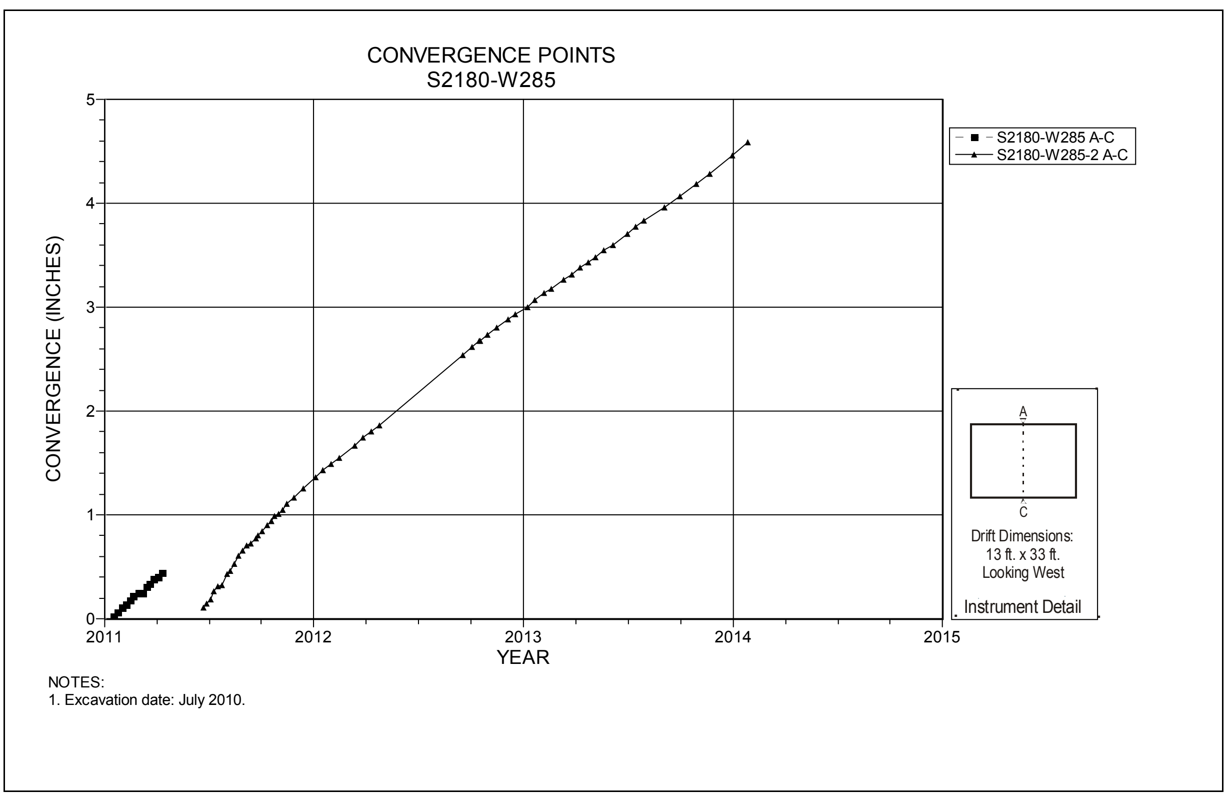

Figure 5-58 Convergence Point Array
S2180 W285 – Roof to Floor

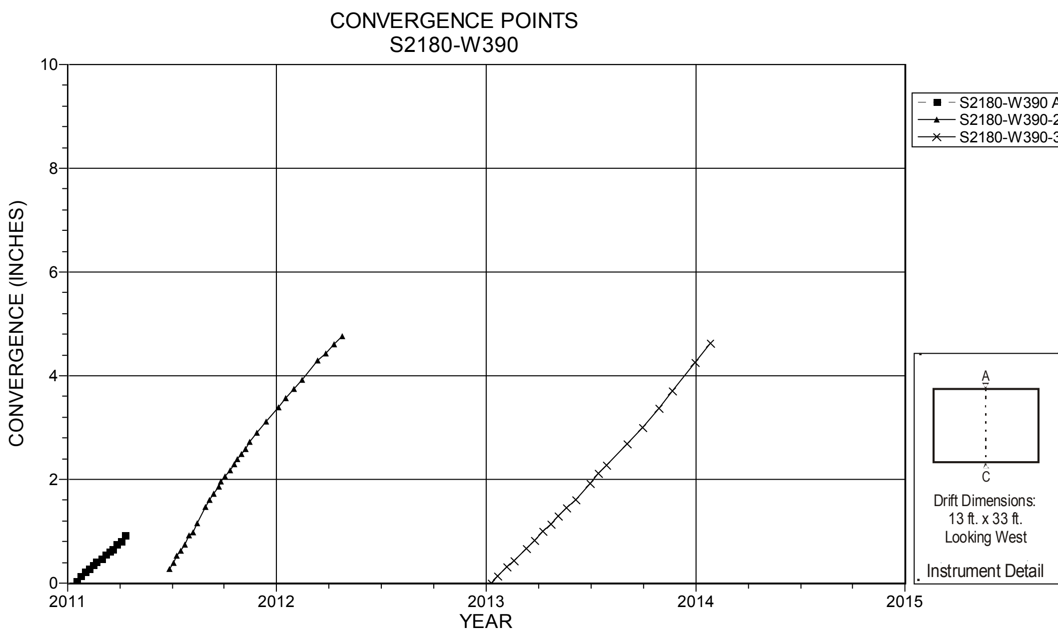

NOTES:
1. Excavation date: July 2010.
2. The gap in readings in 2011 and 2012 is due to the area being inaccessible by aerial lift.

Figure 5-59 Convergence Point Array
S2180 W390 Intersection (Room 1, Panel 7) – Roof to Floor

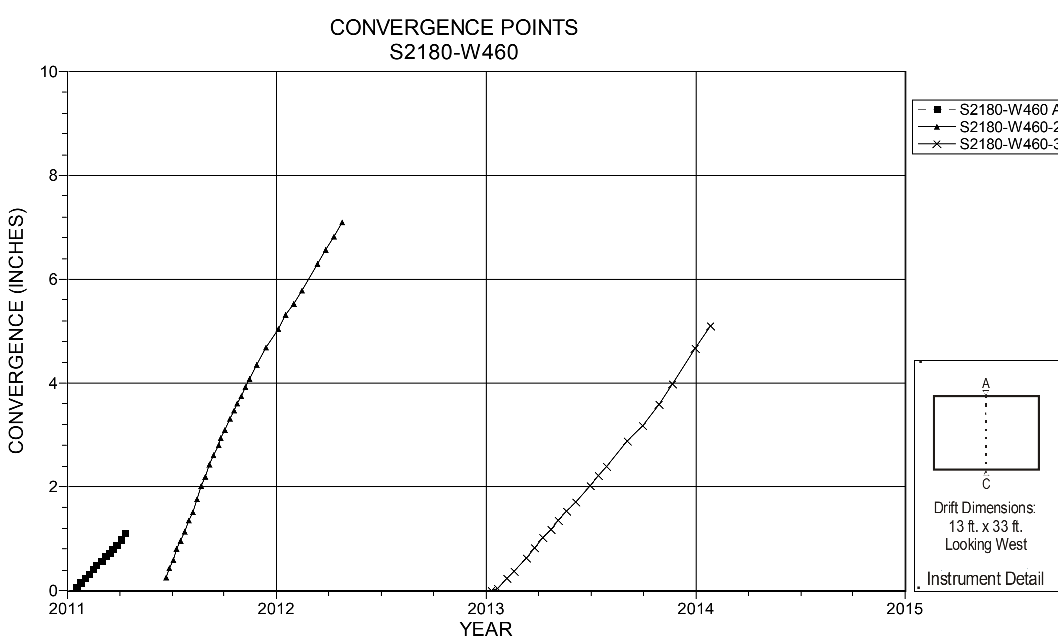

NOTES:
1. Excavation date: July 2010.
2. The gap in readings in 2011 and 2012 is due to the area being inaccessible by aerial lift.

Figure 5-60 Convergence Point Array
S2180 W460 – Roof to Floor

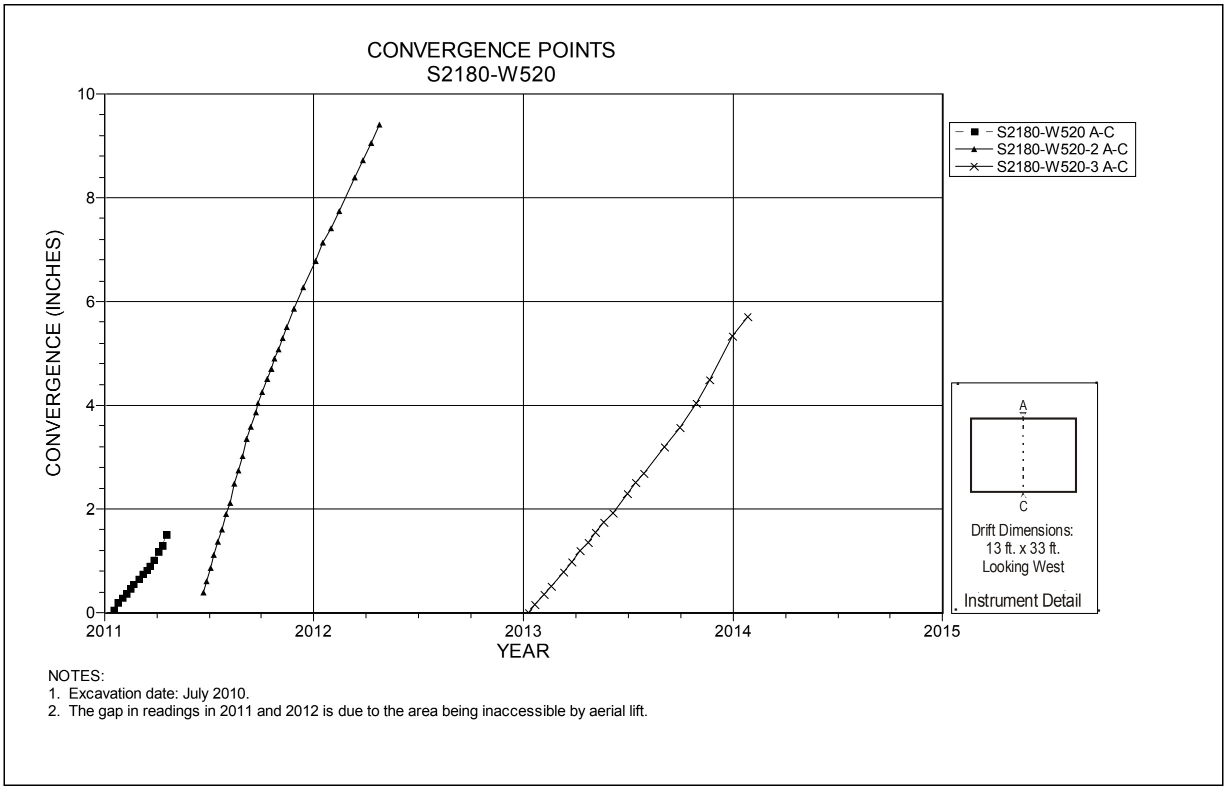

Figure 5-61 Convergence Point Array
S2180 W520 Intersection (Room 2, Panel 7) – Roof to Floor

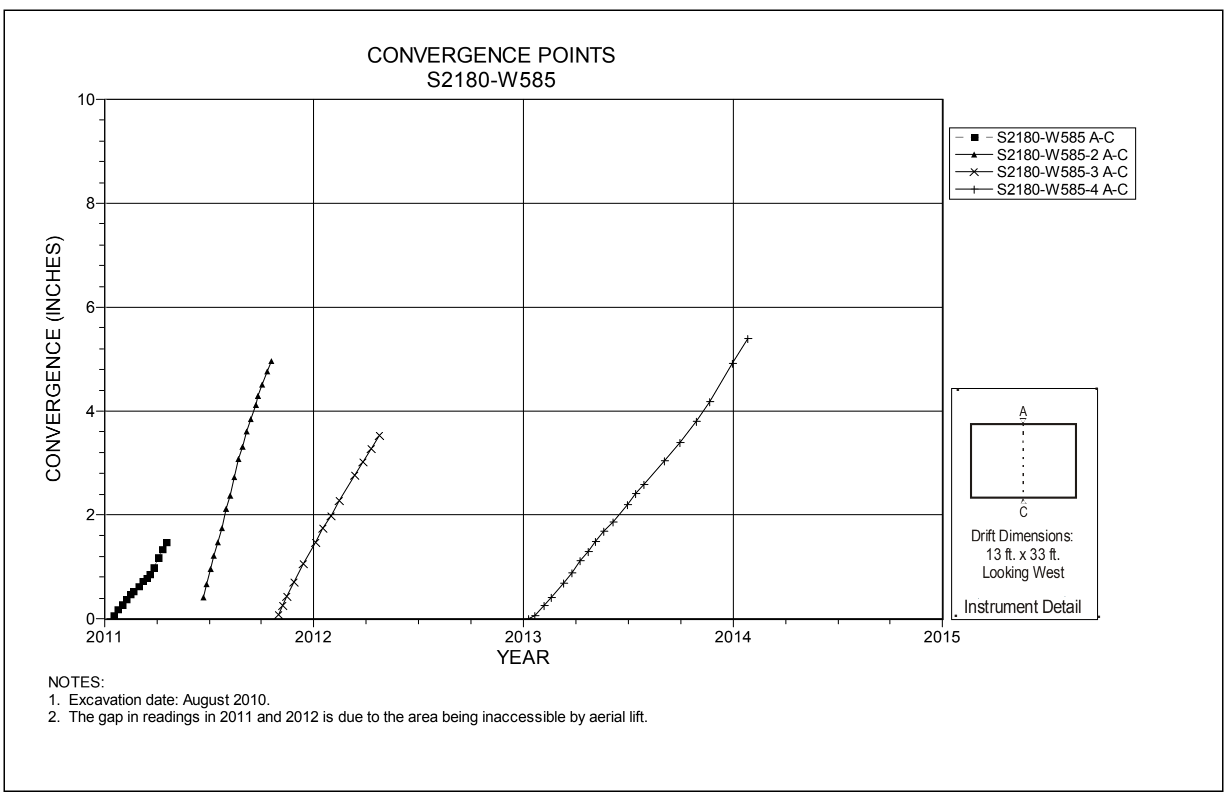

Figure 5-62 Convergence Point Array
S2180 W585 – Roof to Floor

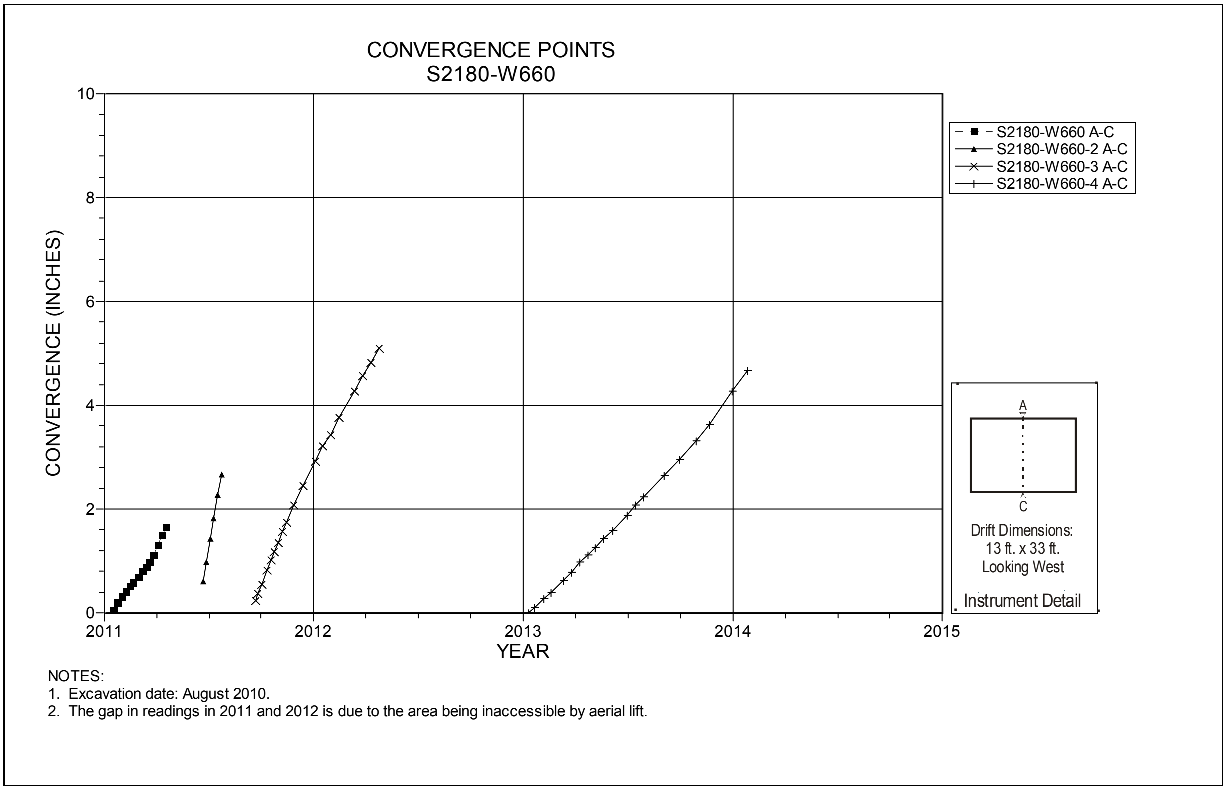

Figure 5-63 Convergence Point Array
S2180 W660 Intersection (Room 3 Panel 7) – Roof to Floor

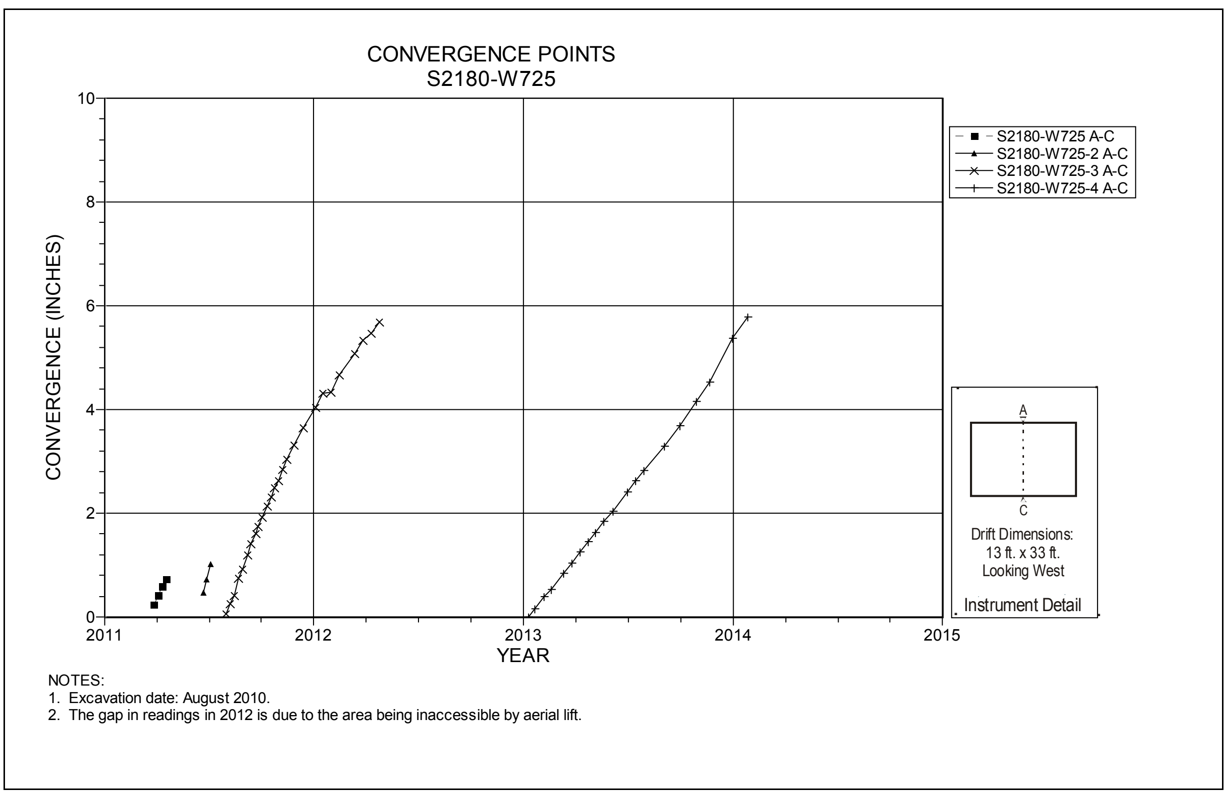

Figure 5-64 Convergence Point Array
S2180 W725 – Roof to Floor

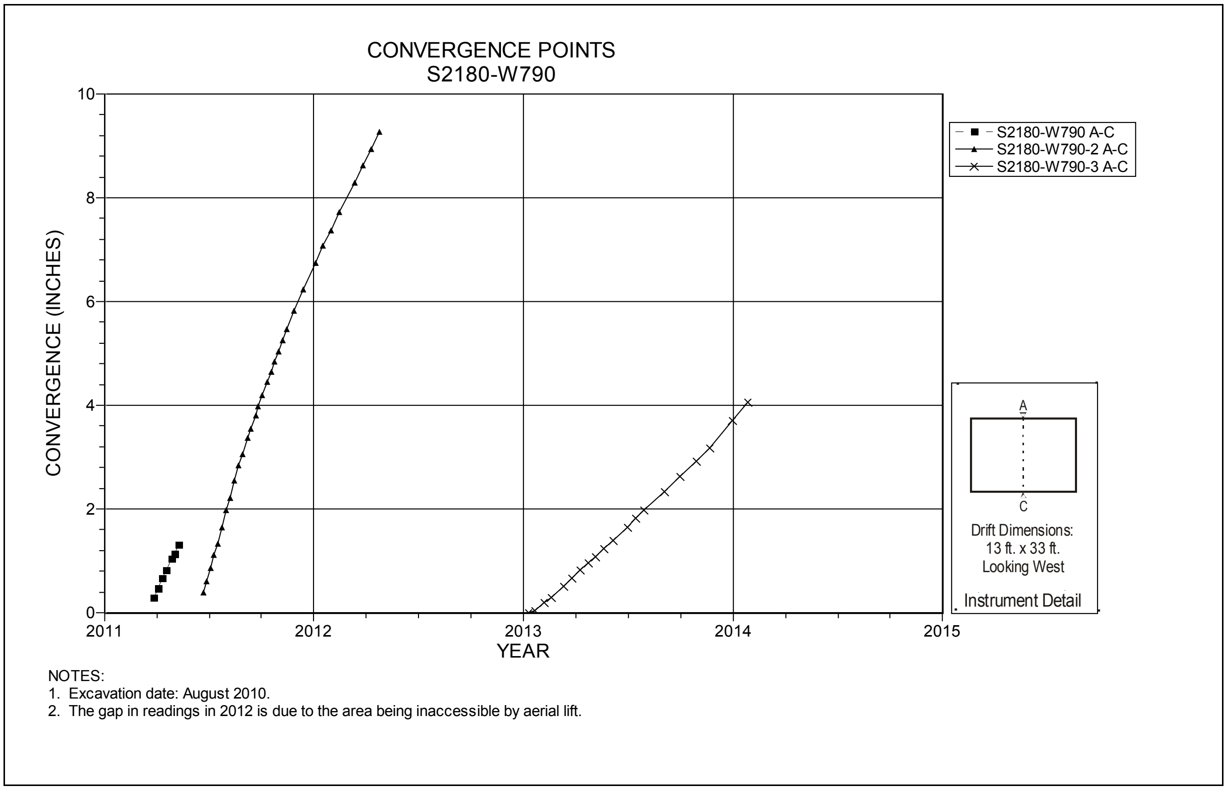

Figure 5-65 Convergence Point Array
S2180 W790 Intersection (Room 4, Panel 7) – Roof to Floor

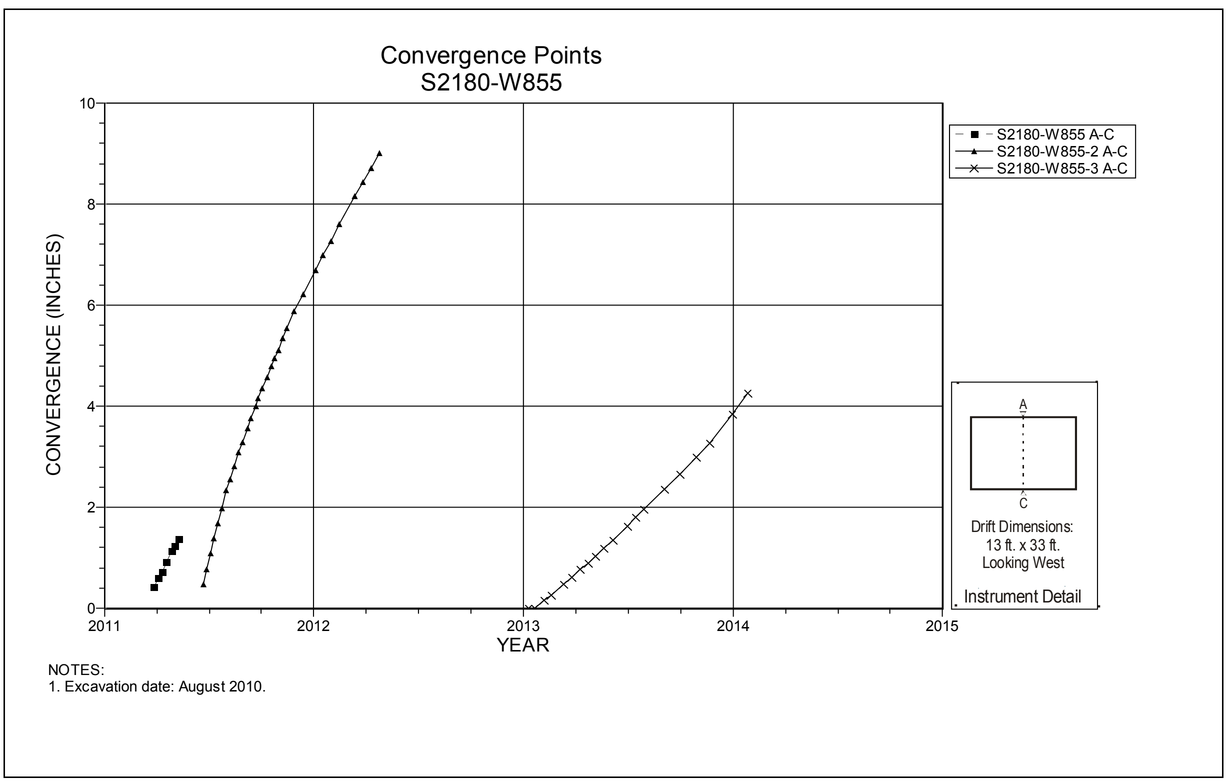

Figure 5-66 Convergence Point Array
S2180 W855 – Roof to Floor

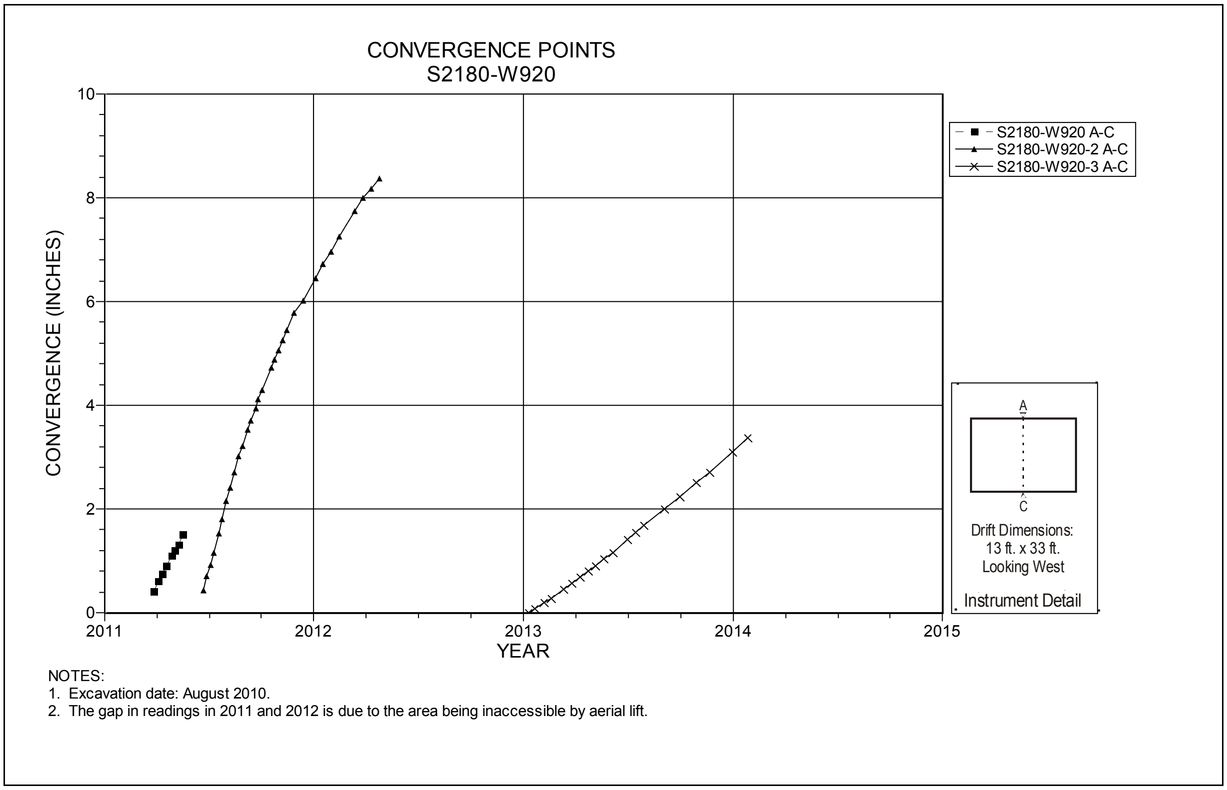

Figure 5-67 Convergence Point Array
S2180 W920 Intersection (Room 5, Panel 7) – Roof to Floor

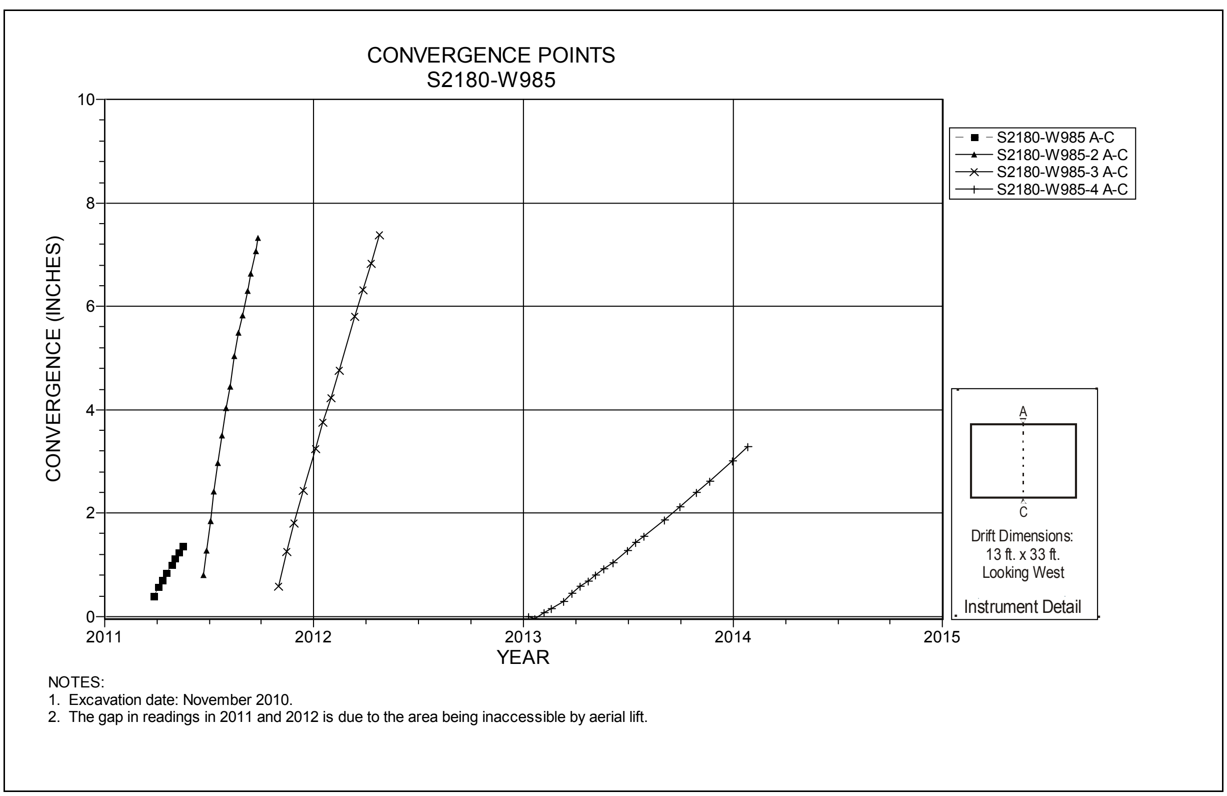

Figure 5-68 Convergence Point Array
S2180 W985 – Roof to Floor

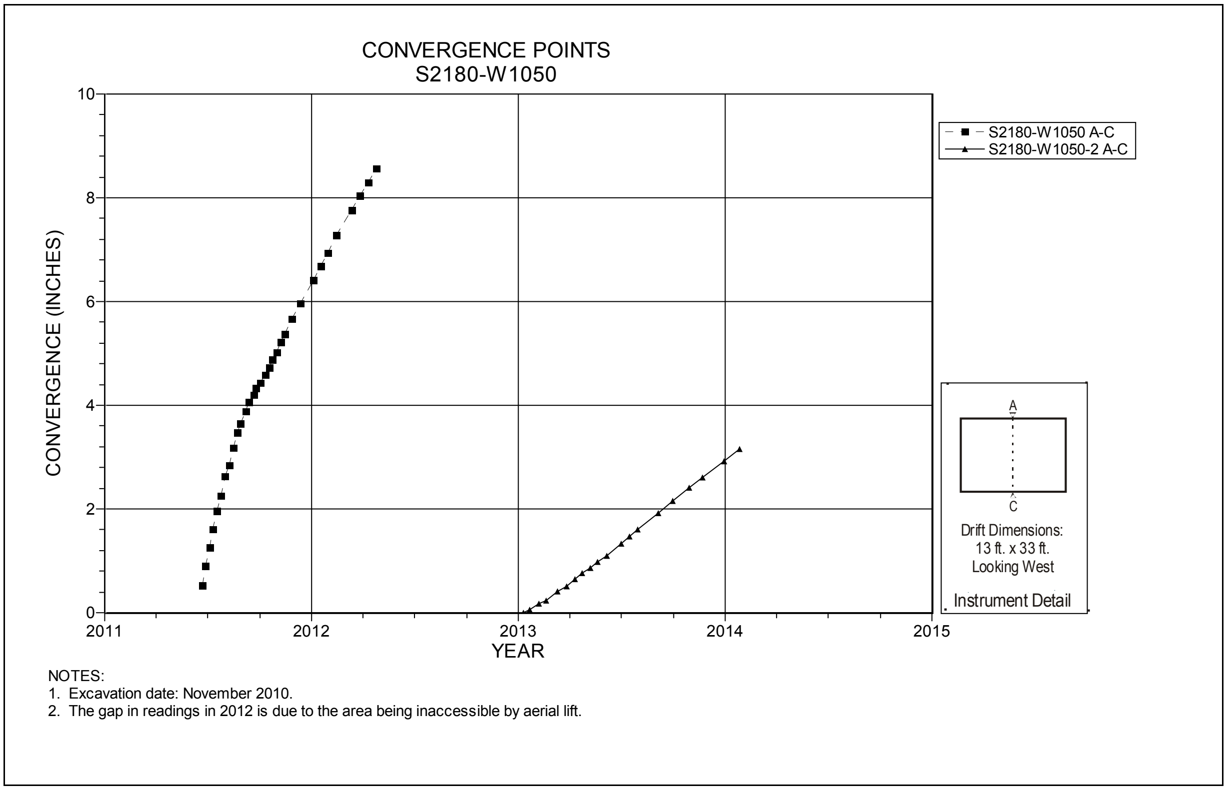

Figure 5-69 Convergence Point Array
S2180 W1050 Intersection (Room 6, Panel 7) – Roof to Floor

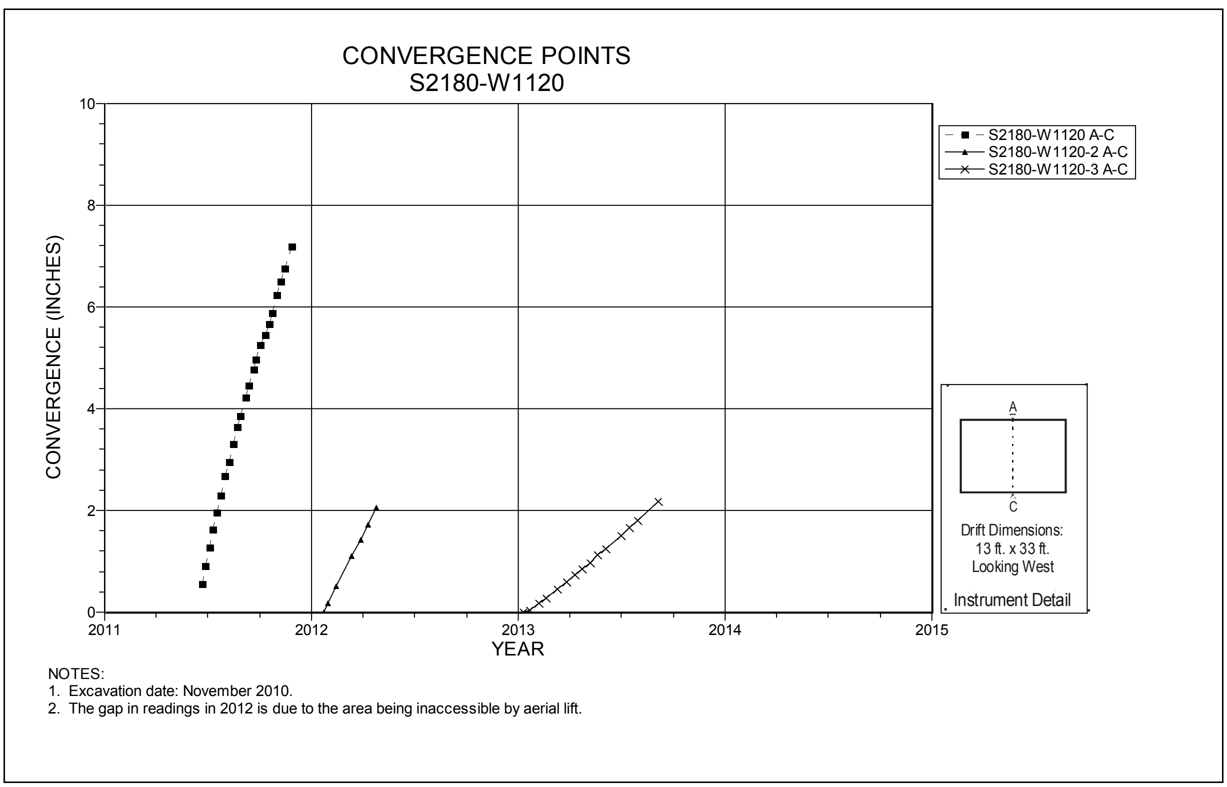

Figure 5-70 Convergence Point Array
S2180 W1120 – Roof to Floor

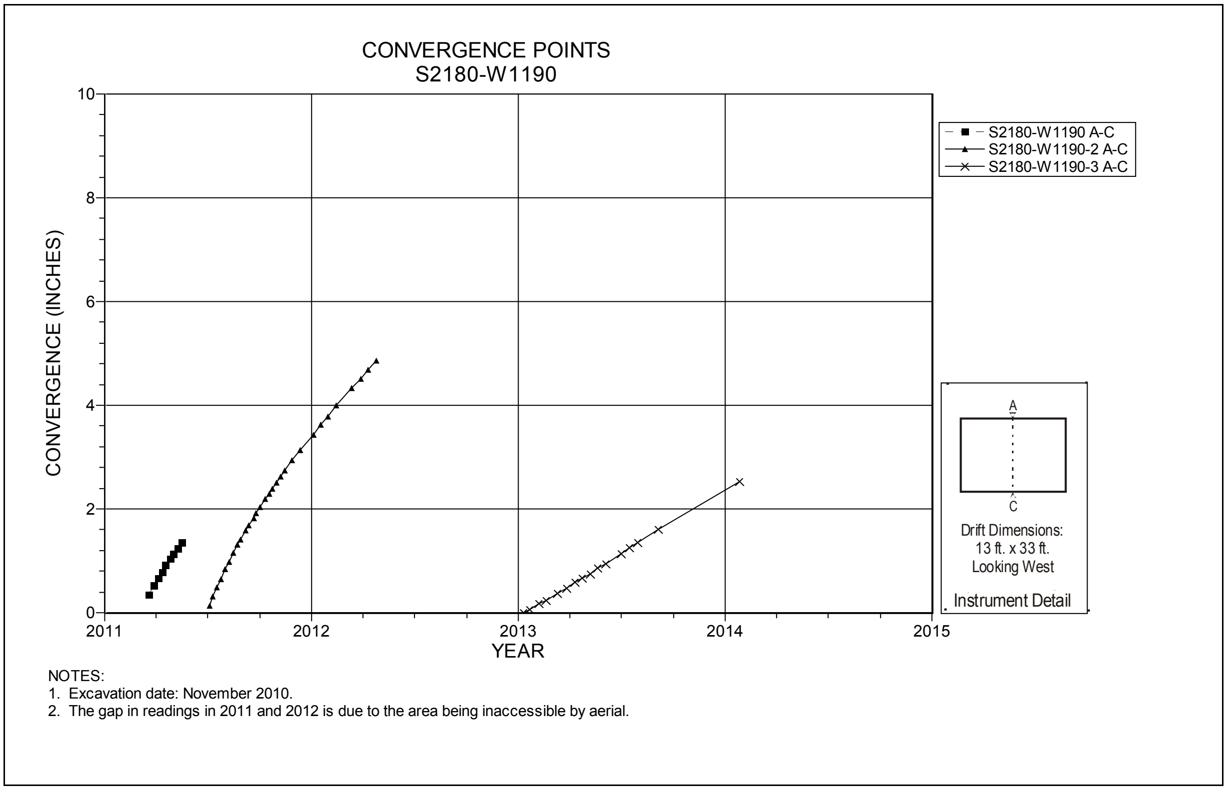

Figure 5-71 Convergence Point Array
S2180 W1190 Intersection (Room 7, Panel 7) – Roof to Floor

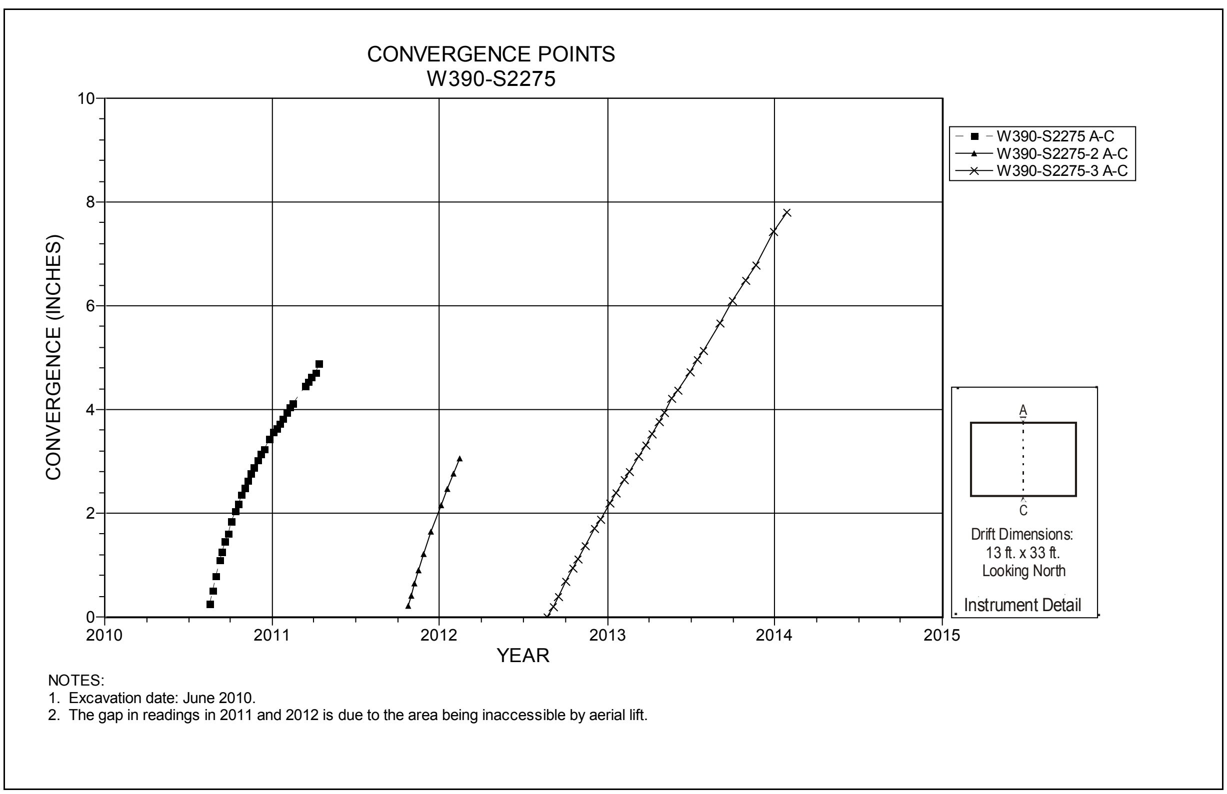

Figure 5-72 Convergence Point Array
Room 1, Panel 7 at W390 S2275 – Roof to Floor

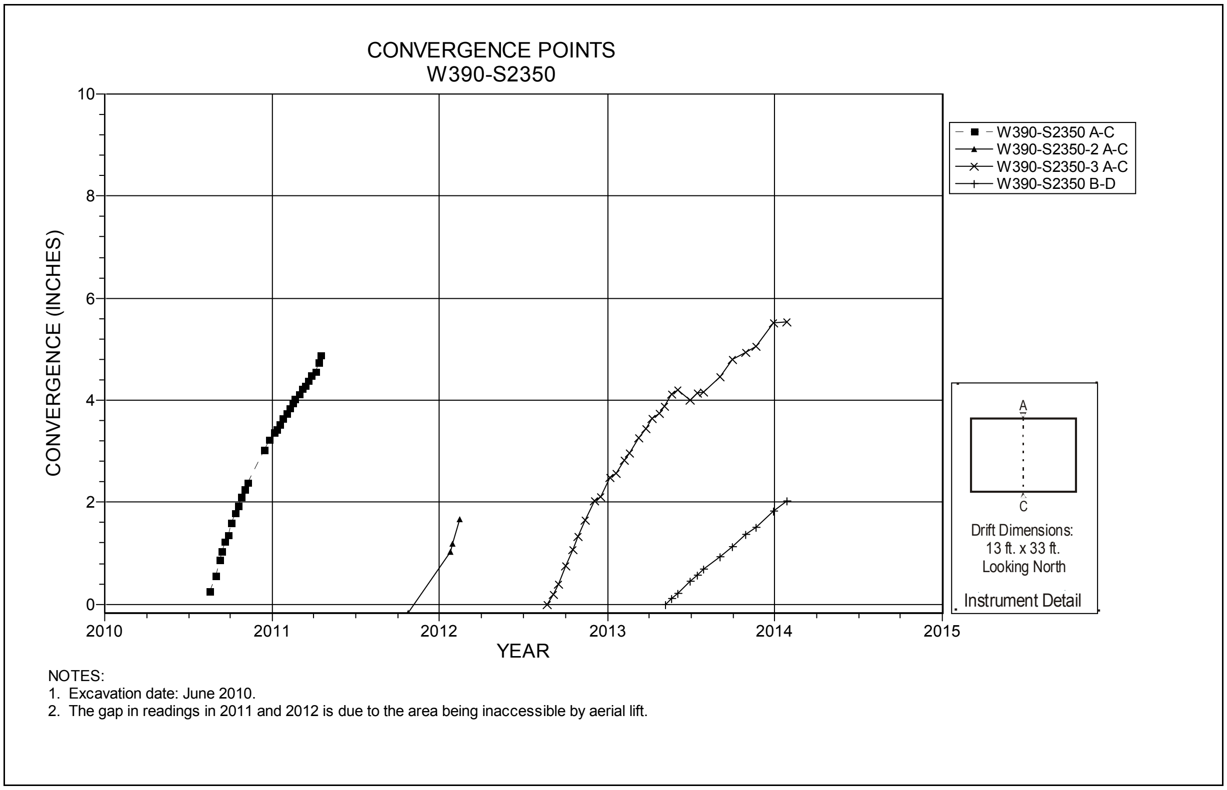

Figure 5-73 Convergence Point Array
Room 1, Panel 7 at W390 S2350– Room Center – All Chords

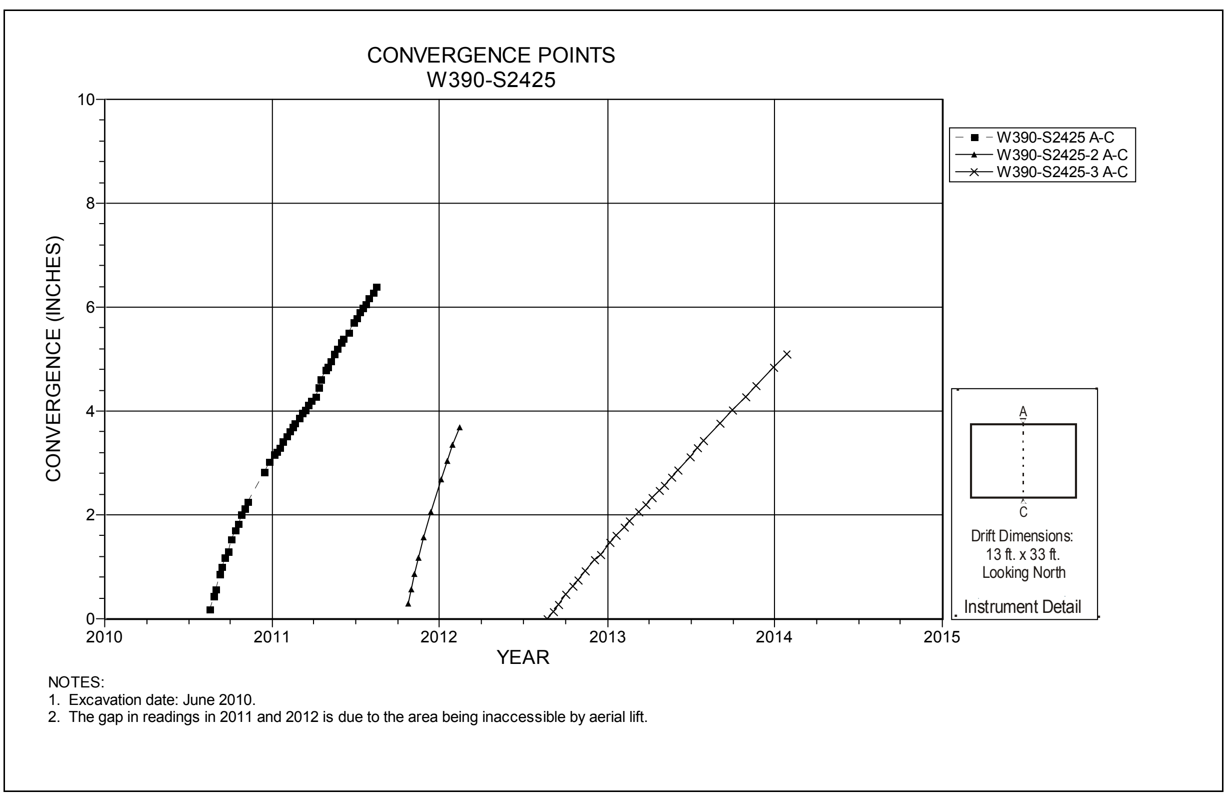

Figure 5-74 Convergence Point Array
Room 1, Panel 7 at W390 S2425 – Roof to Floor

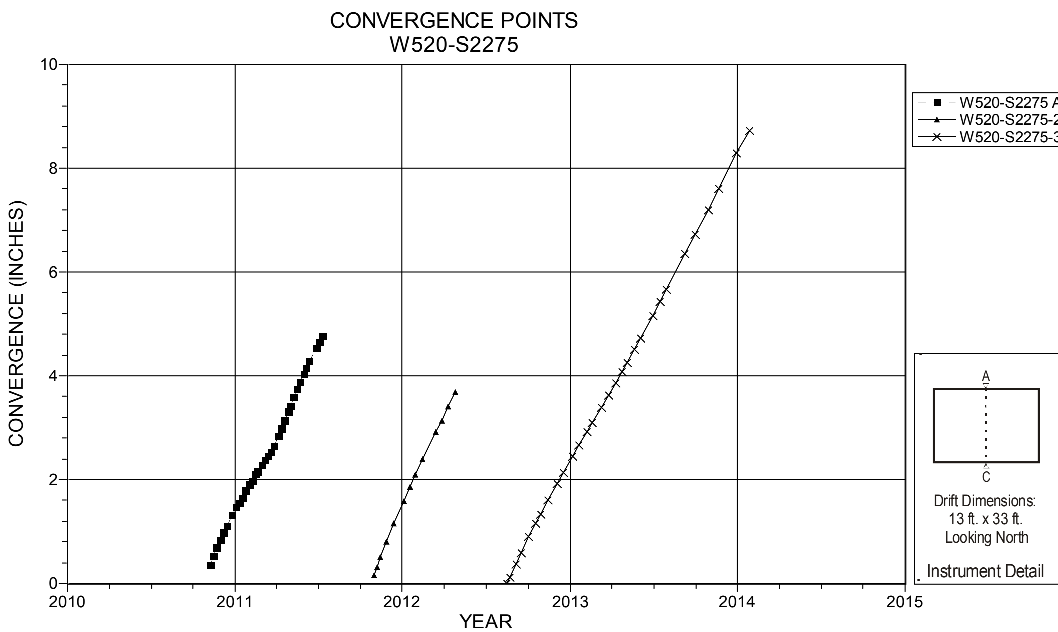

NOTES:
1. Excavation date: September 2010.
2. The gap in readings in 2011 and 2012 is due to the area being inaccessible by aerial lift.

Figure 5-75 Convergence Point Array
Room 2, Panel 7 at W520 S2275 – Roof to Floor

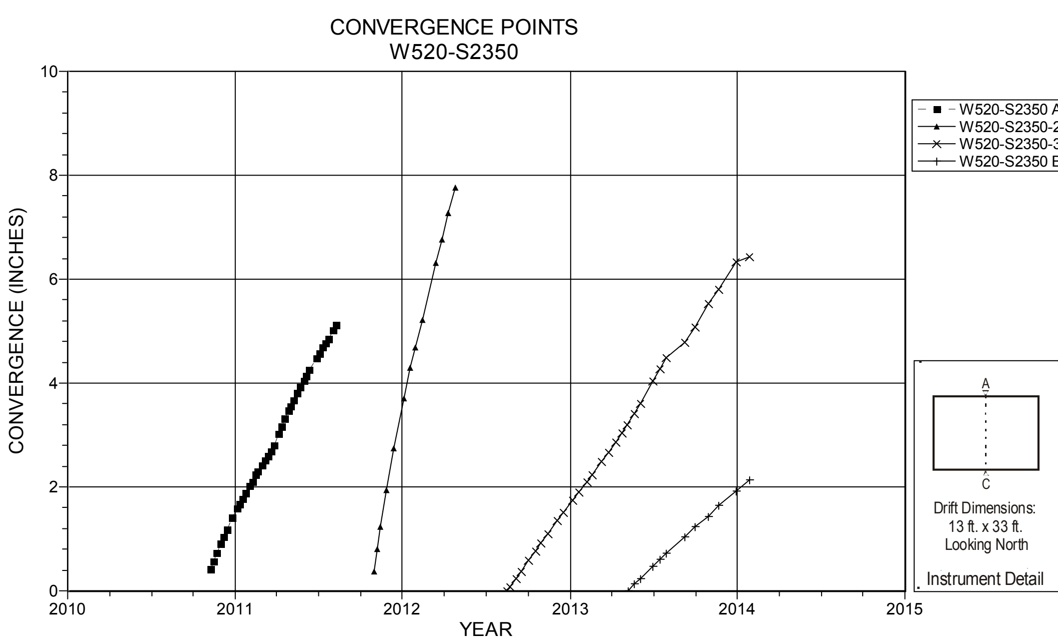

NOTES:
1. Excavation date: September 2010.
2. The gap in readings 2011 and 2012 is due to the area being inaccessible by aerial lift.

Figure 5-76 Convergence Point Array
Room 2, Panel 7 at W520 S2350 – Room Center – All Chords

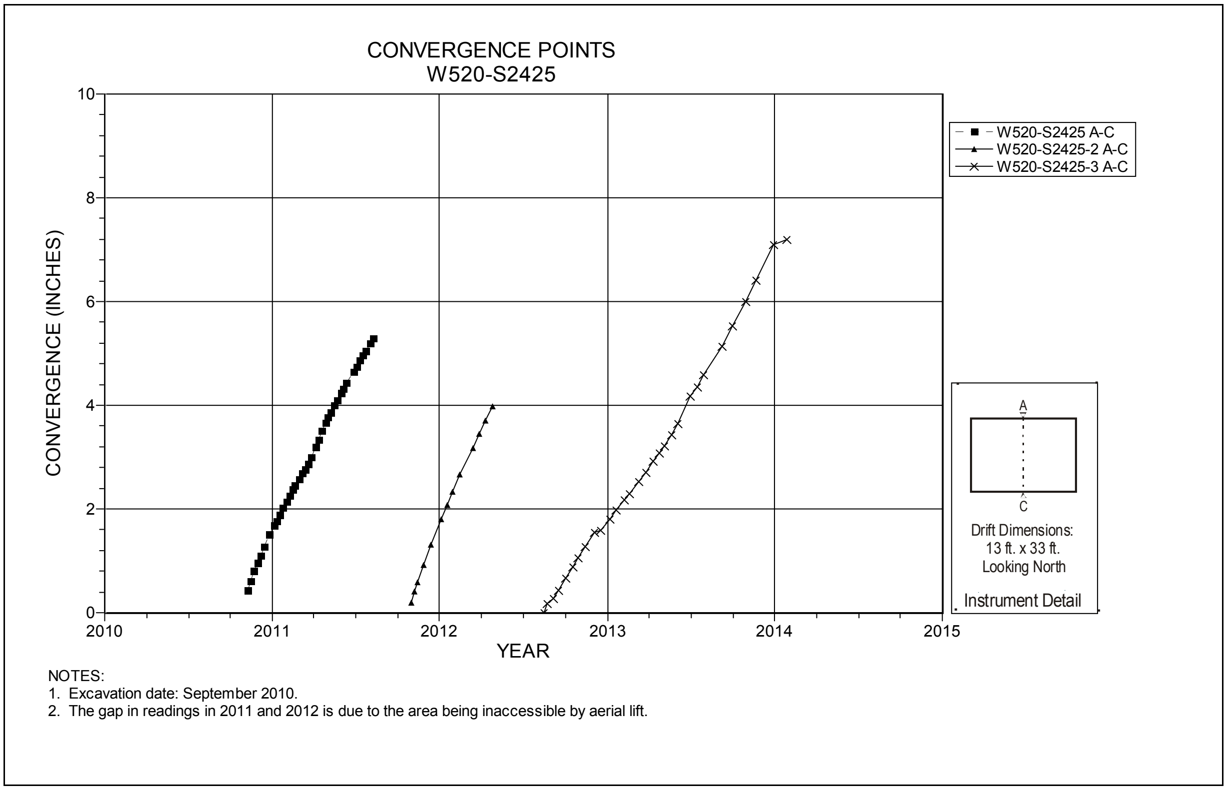

Figure 5-77 Convergence Point Array
Room 2, Panel 7 at W520 S2425 – Roof to Floor

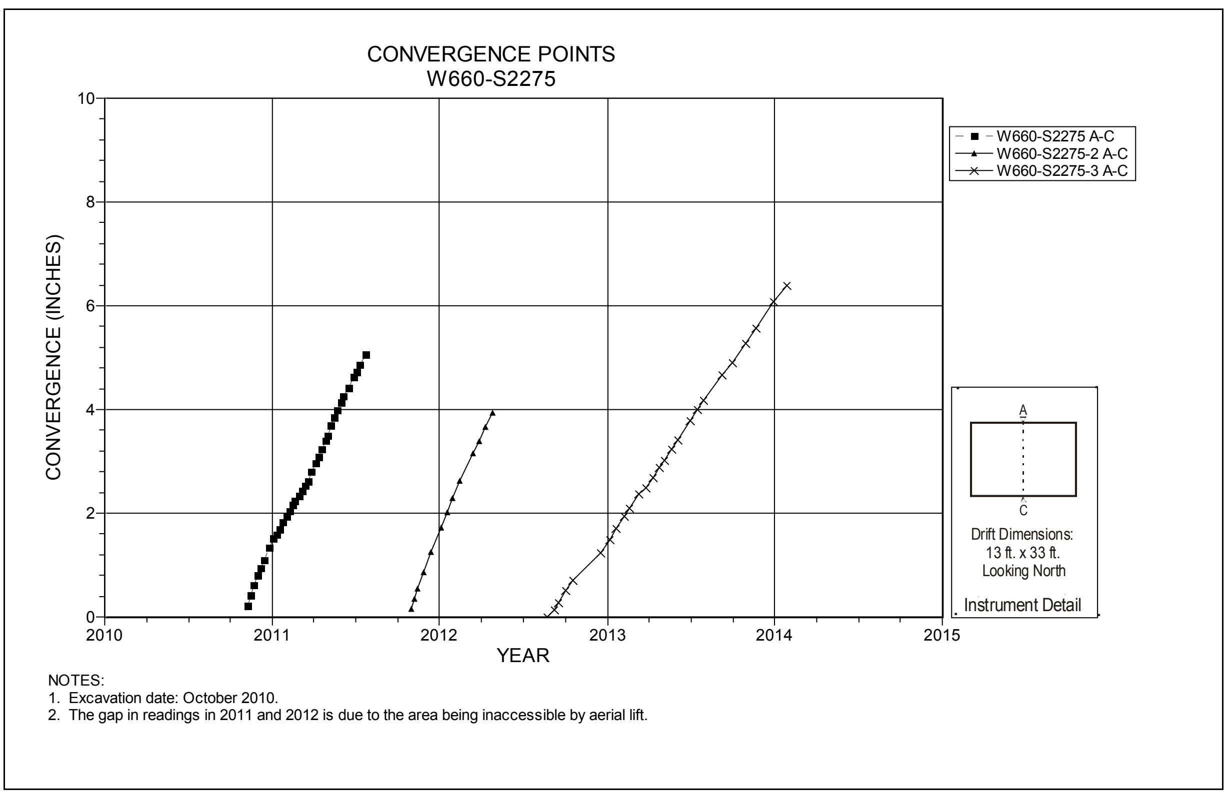

Figure 5-78 Convergence Point Array
Room 3, Panel 7 at W660 S2275 – Roof to Floor

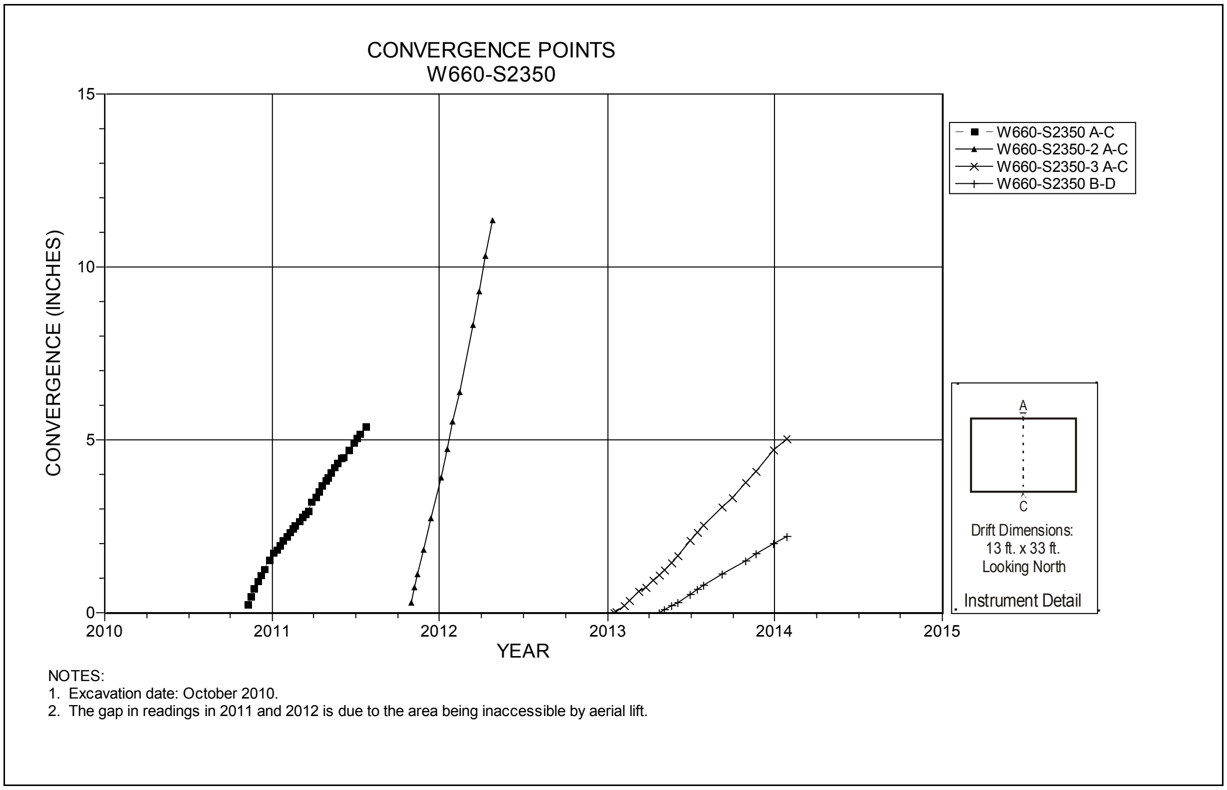

Figure 5-79 Convergence Point Array
Room 3, Panel 7 at W660 S2350 – Room Center – All Chords

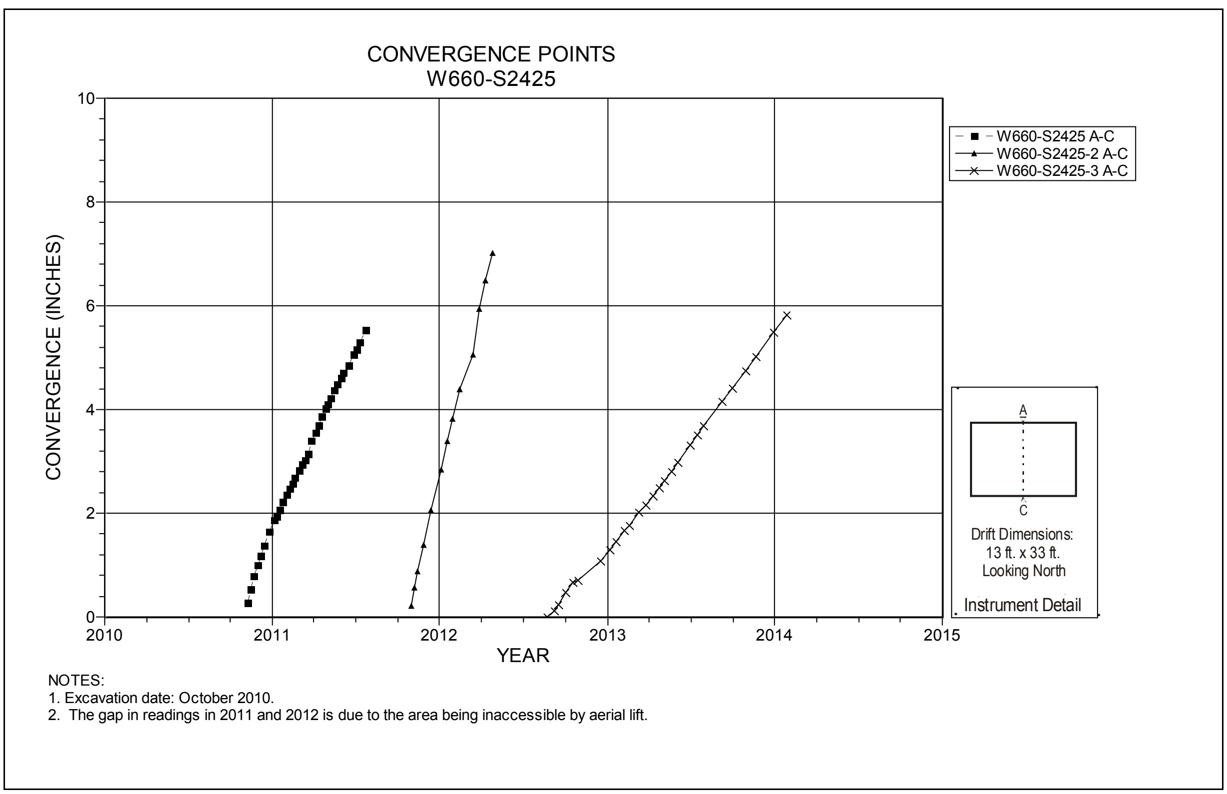

Figure 5-80 Convergence Point Array
Room 3, Panel 7 at W660 S2425 – Roof to Floor

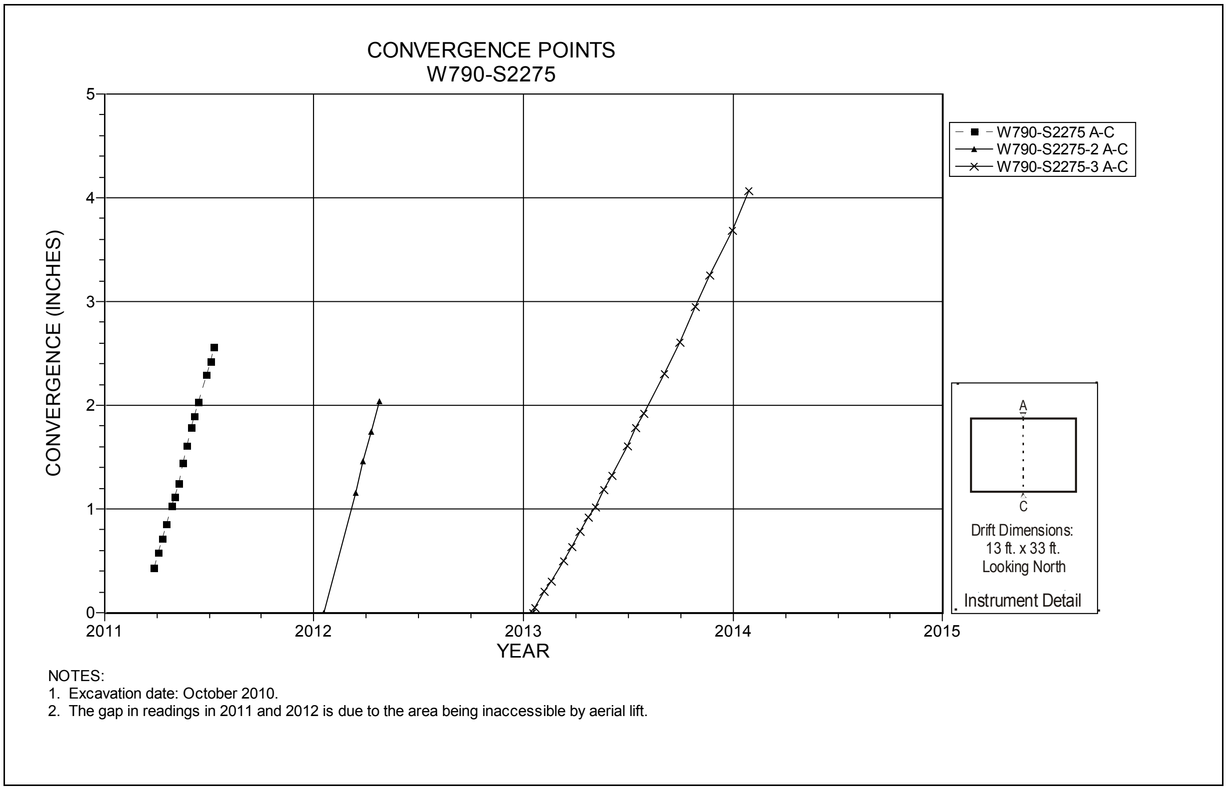

Figure 5-81 Convergence Point Array
Room 4, Panel 7 at W790 S2275 – Roof to Floor

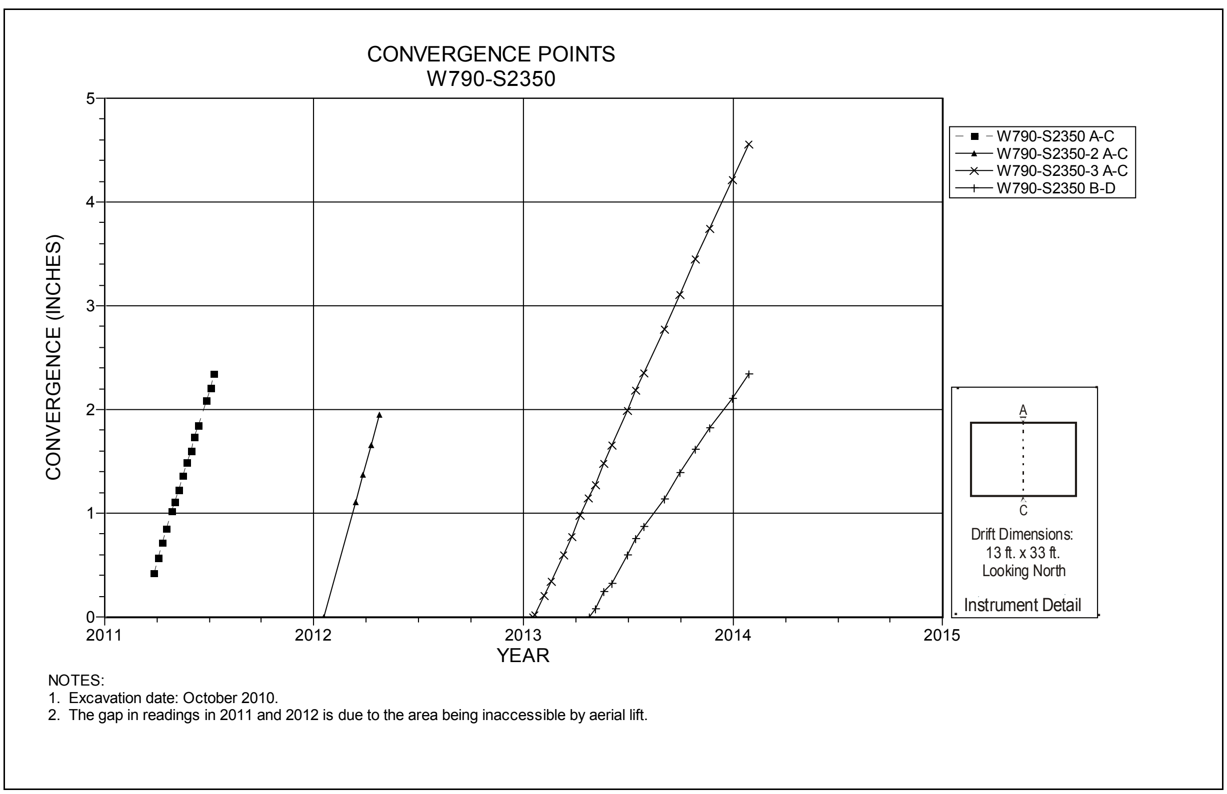

Figure 5-82 Convergence Point Array
Room 4, Panel 7 at W790 S2350 – Room Center – All Chords

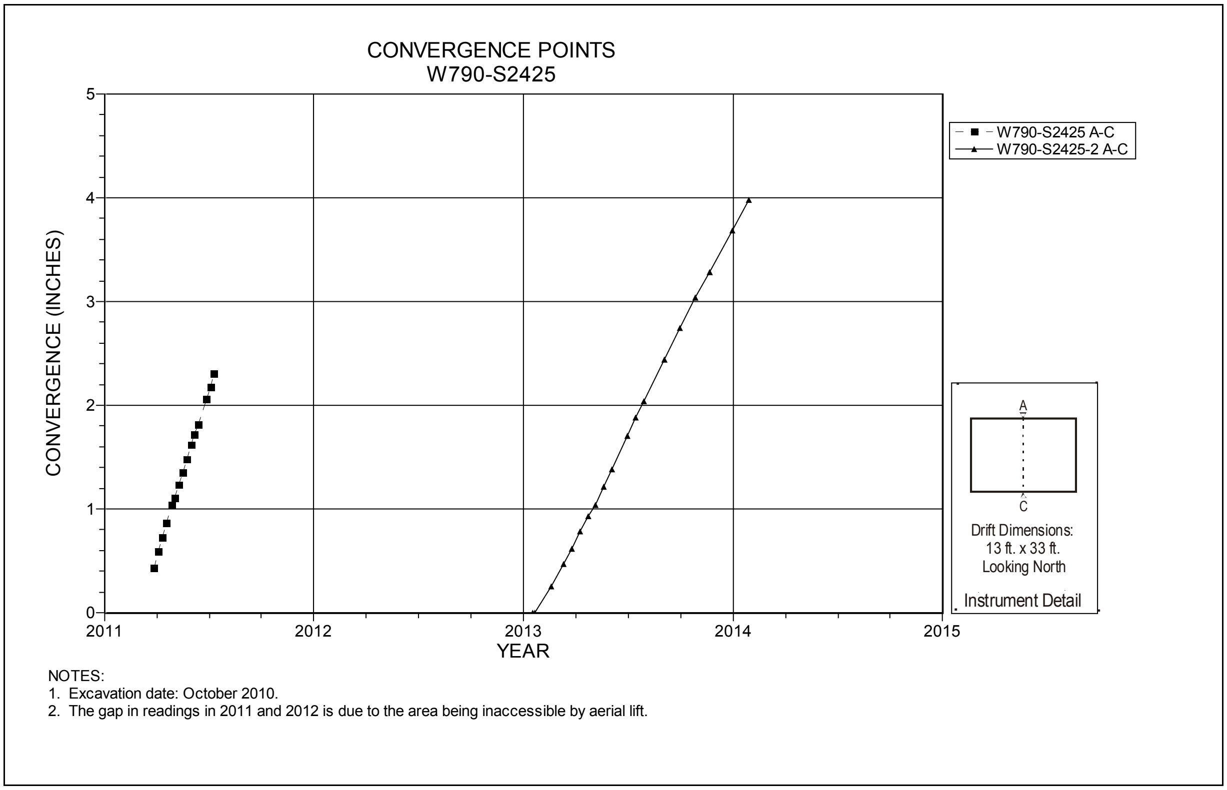

Figure 5-83 Convergence Point Array
Room 4, Panel 7 at W790 S2425 – Roof to Floor

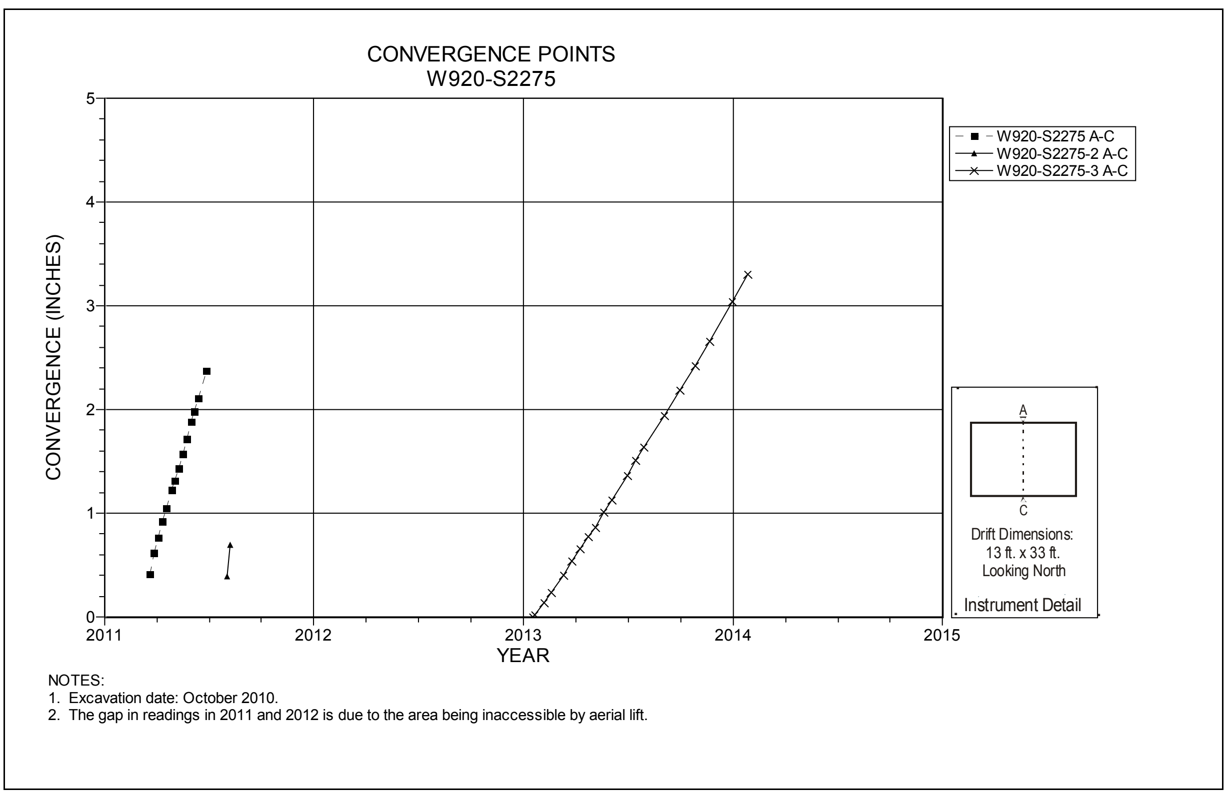

Figure 5-84 Convergence Point Array
Room 5, Panel 7 at W920 S2275 – Roof to Floor

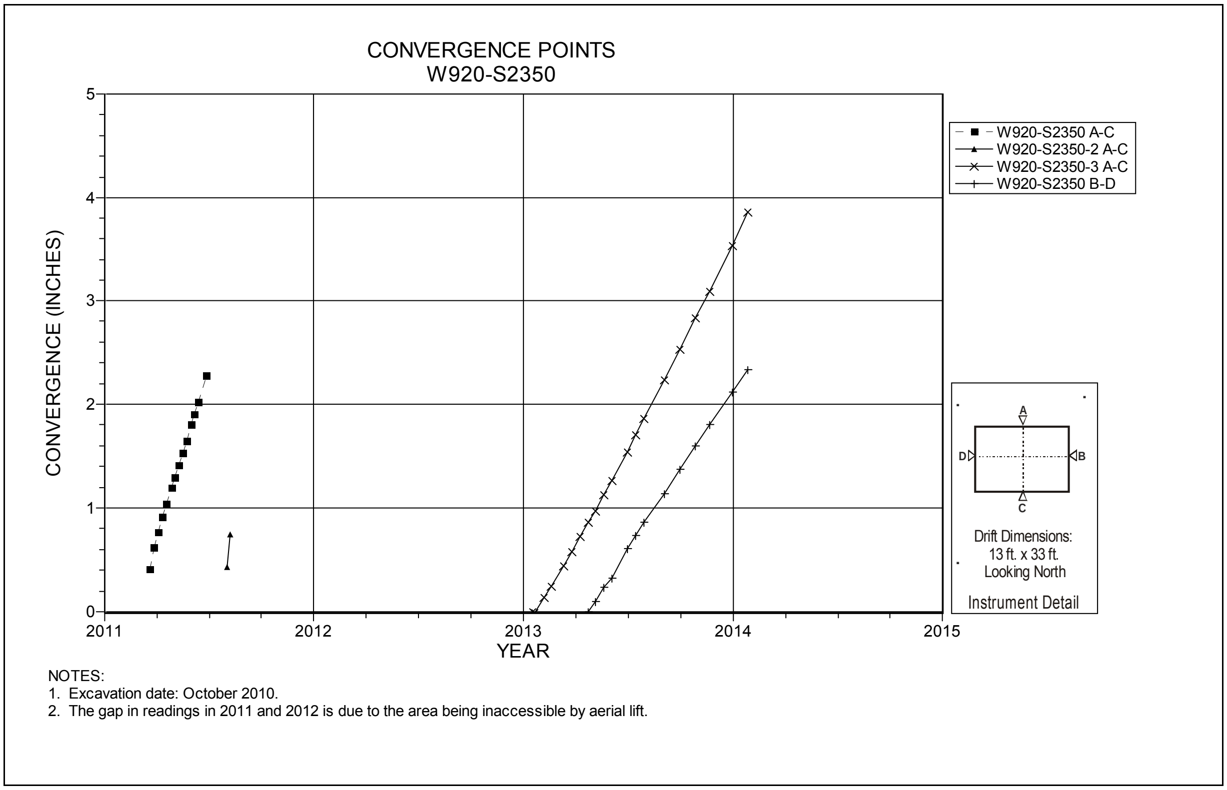

Figure 5-85 Convergence Point Array
Room 5, Panel 7 at W920 S2350 – Room Center – All Chords

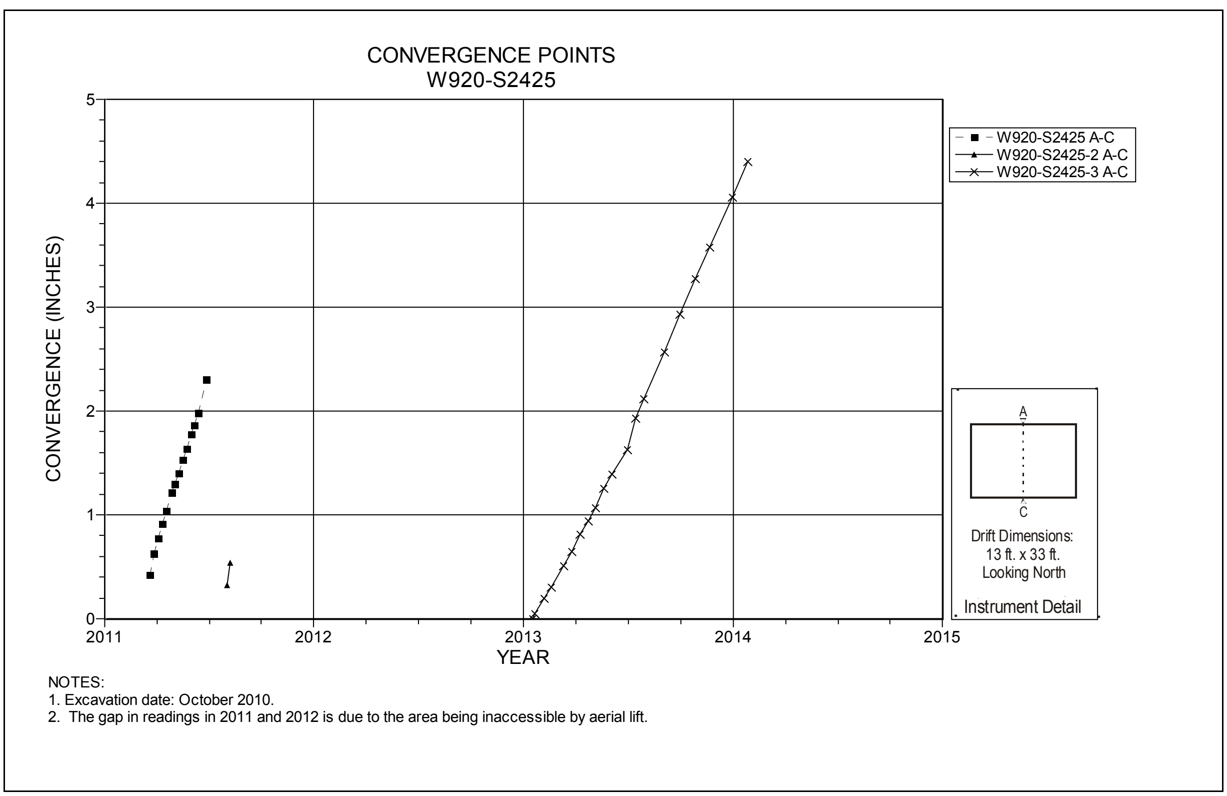

Figure 5-86 Convergence Point Array
Room 5, Panel 7 at W920 S2425 – Roof to Floor

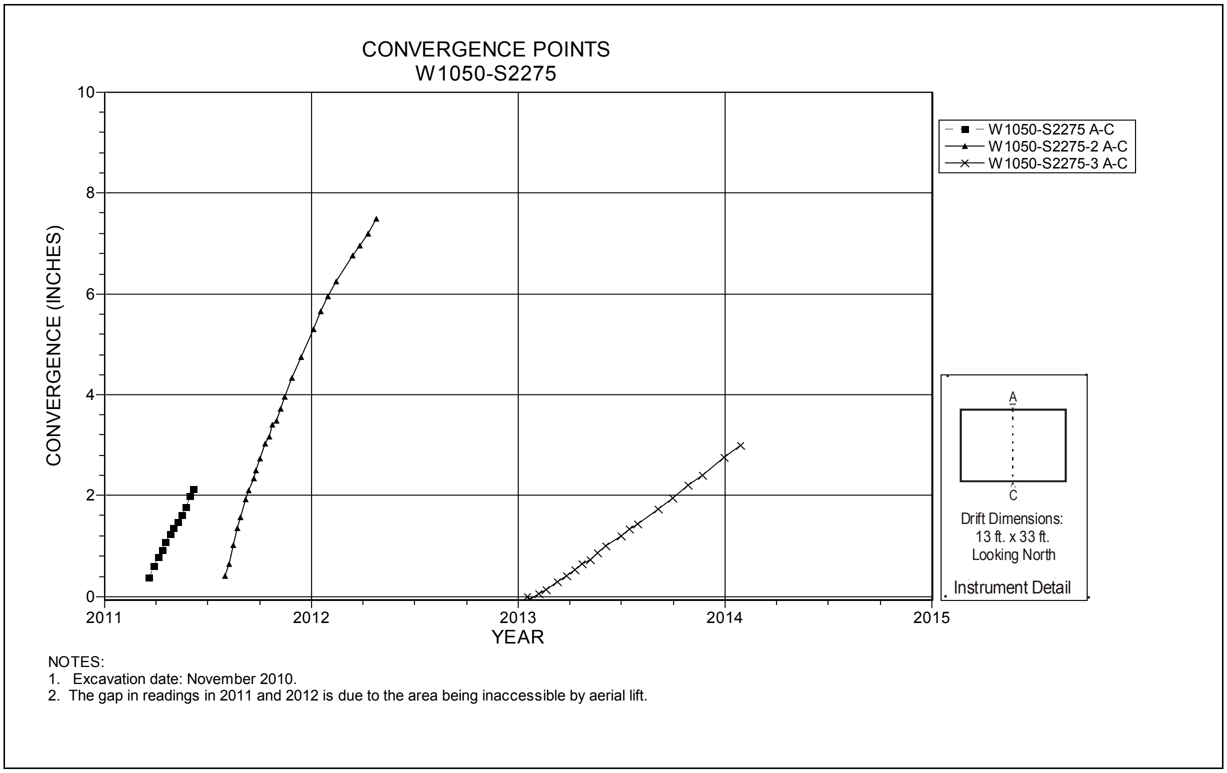

Figure 5-87 Convergence Point Array
Room 6, Panel 7 at W1050 S2275 – Roof to Floor

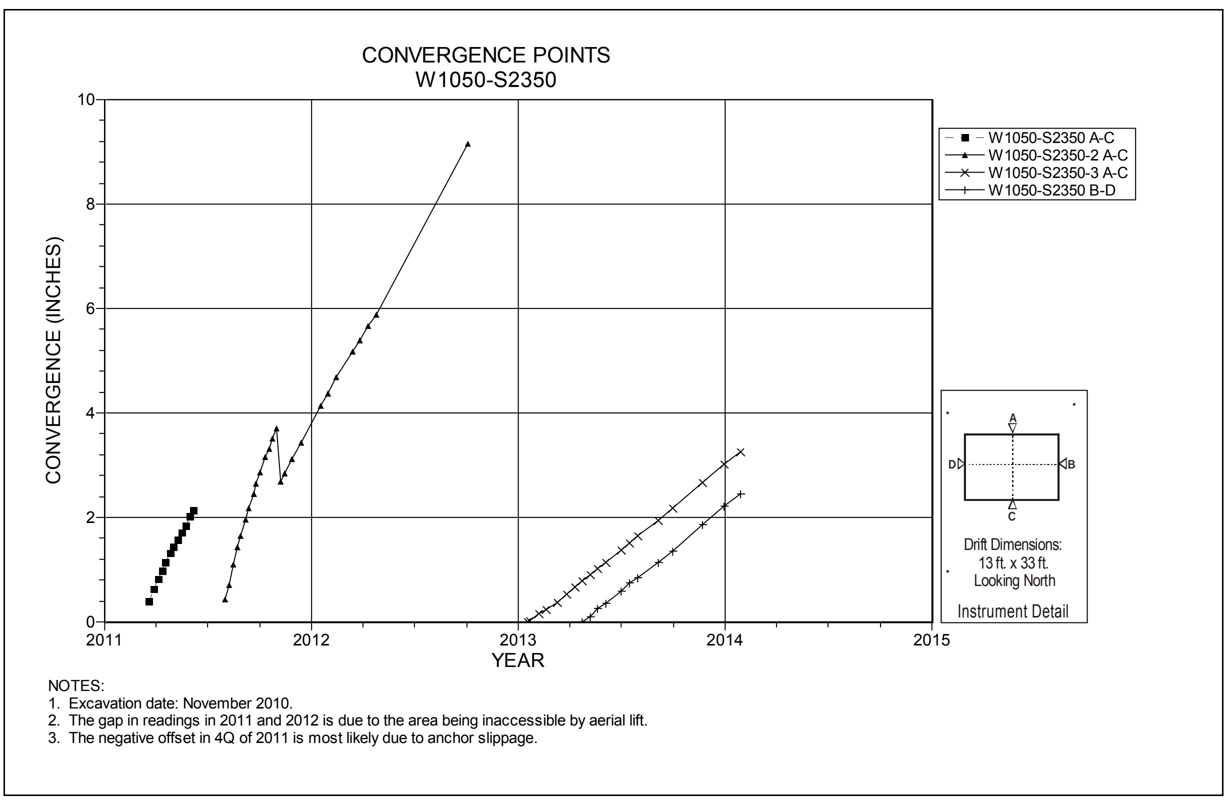

Figure 5-88 Convergence Point Array
Room 6, Panel 7 at W1050 S2350 – Room Center – All Chords

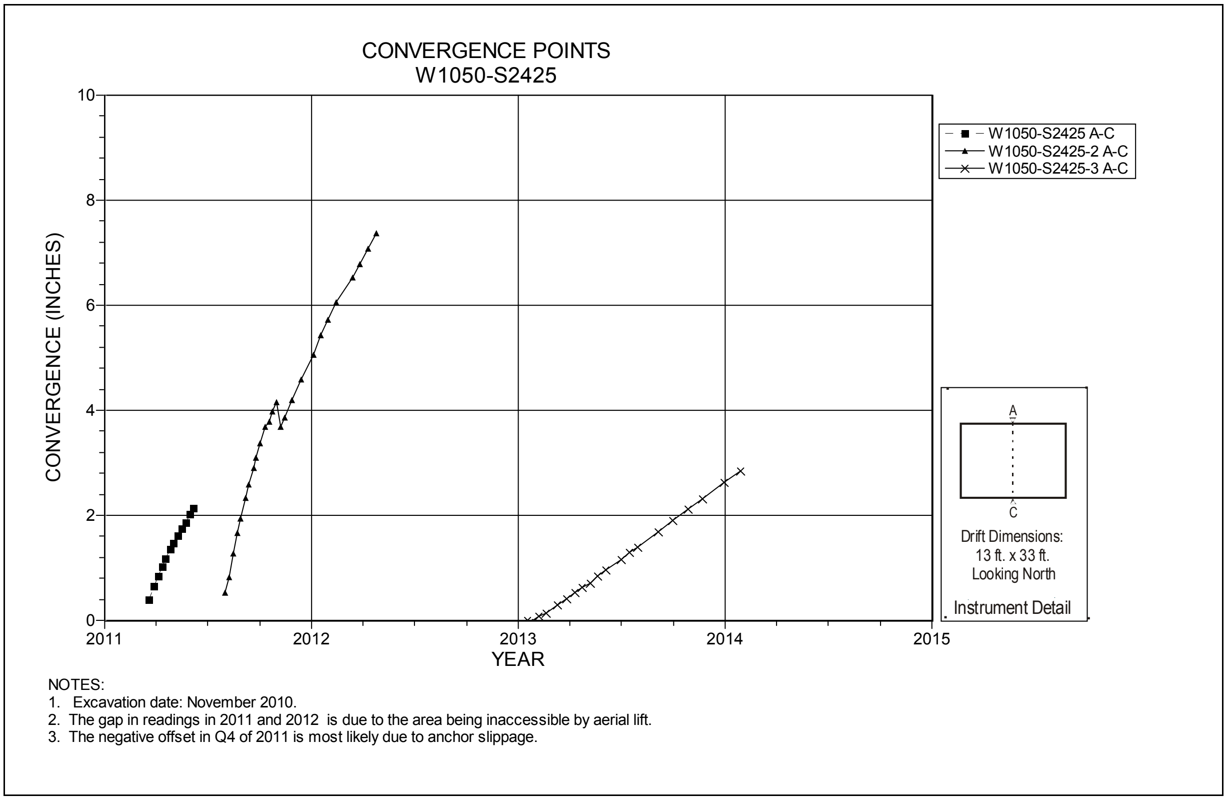

Figure 5-89 Convergence Point Array
Room 6, Panel 7 at W1050 S2425 – Roof to Floor

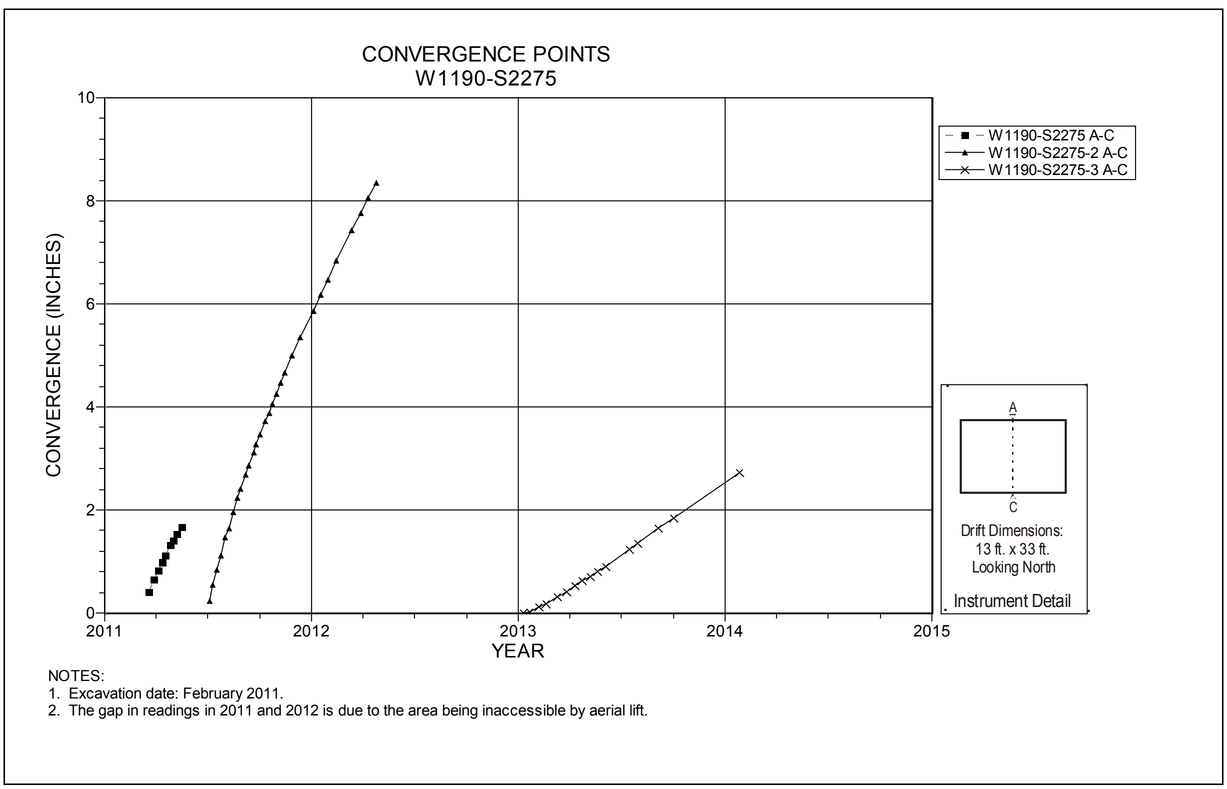

Figure 5-90 Convergence Point Array
Room 7, Panel 7 at W1190 S2275 – Roof to Floor

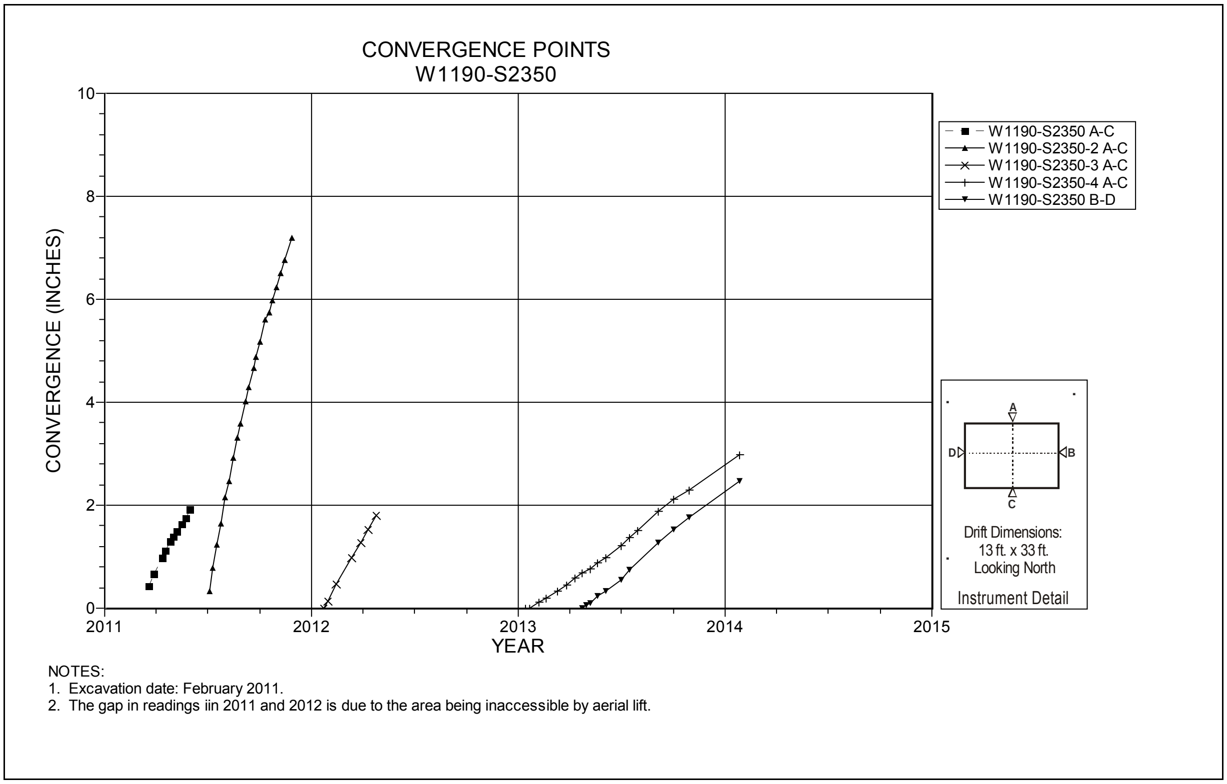

Figure 5-91 Convergence Point Array
Room 7, Panel 7 at W1190 S2350 – Room Center – All Chords

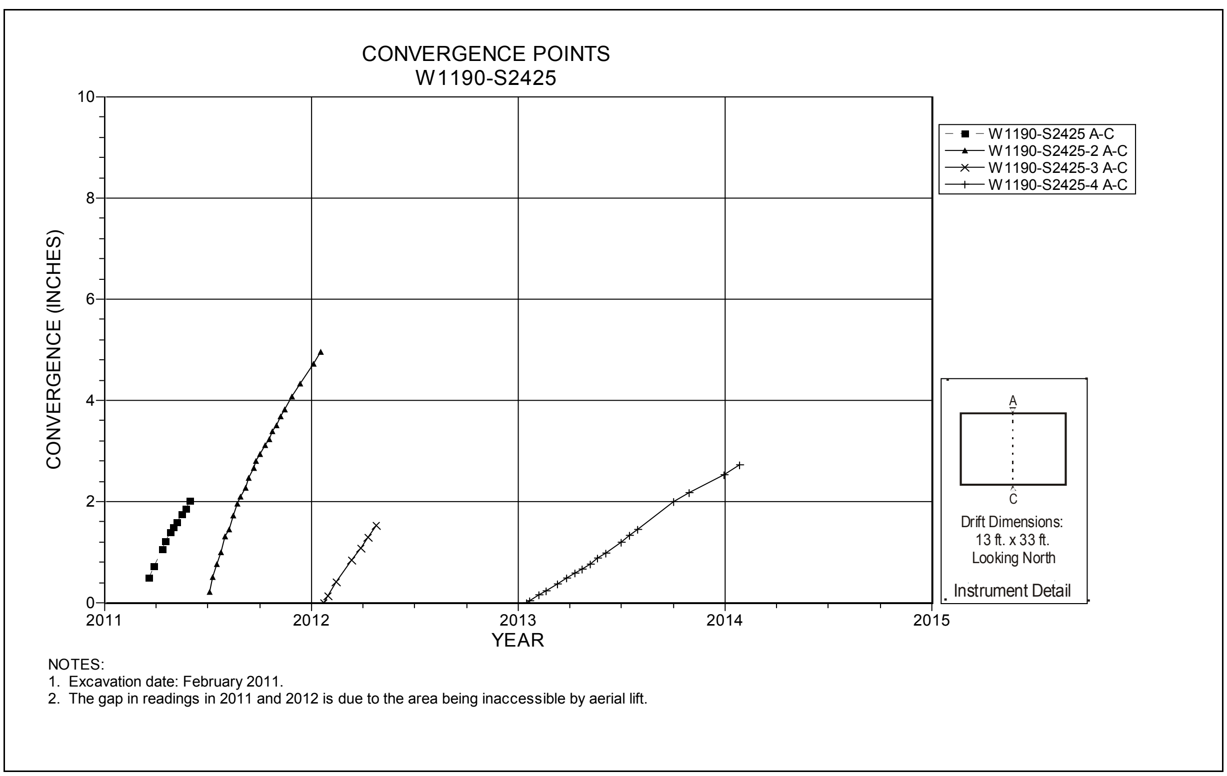

Figure 5-92 Convergence Point Array
Room 7, Panel 7 at W1190 S2425 – Roof to Floor

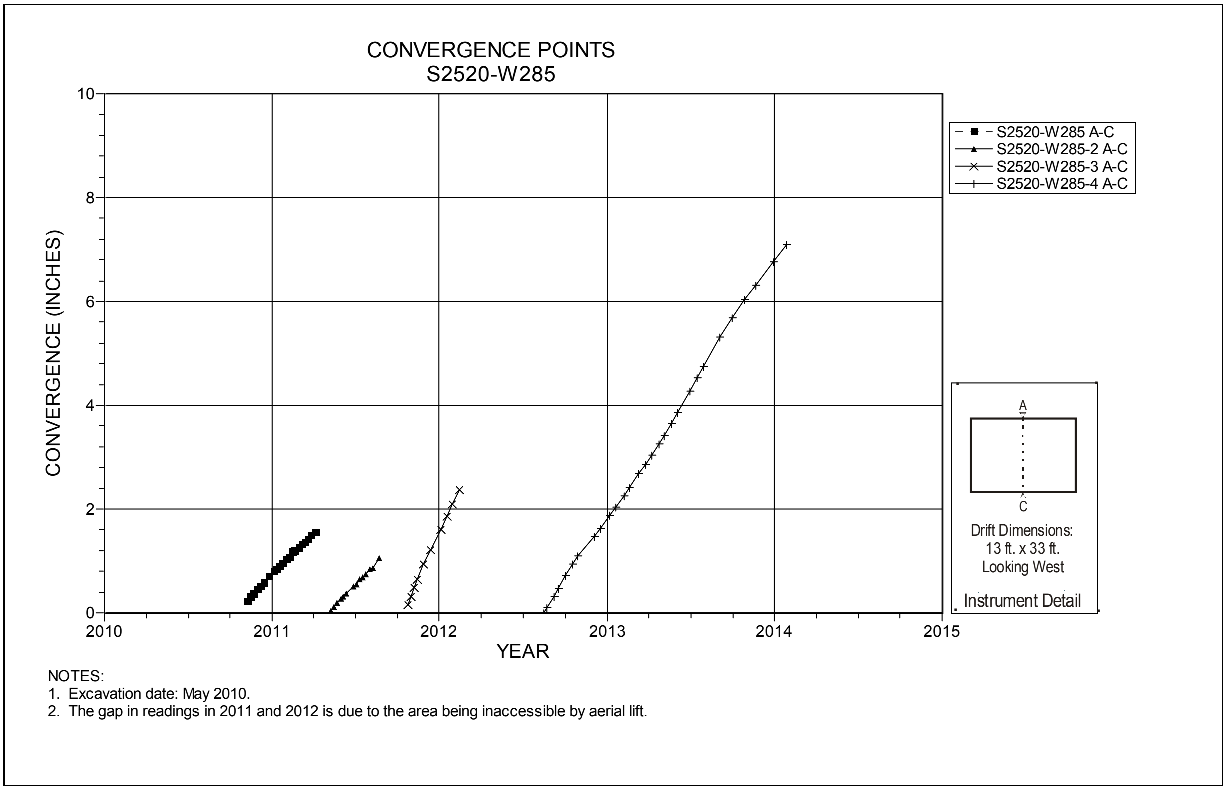

Figure 5-93 Convergence Point Array
S2520 W285 – Roof to Floor

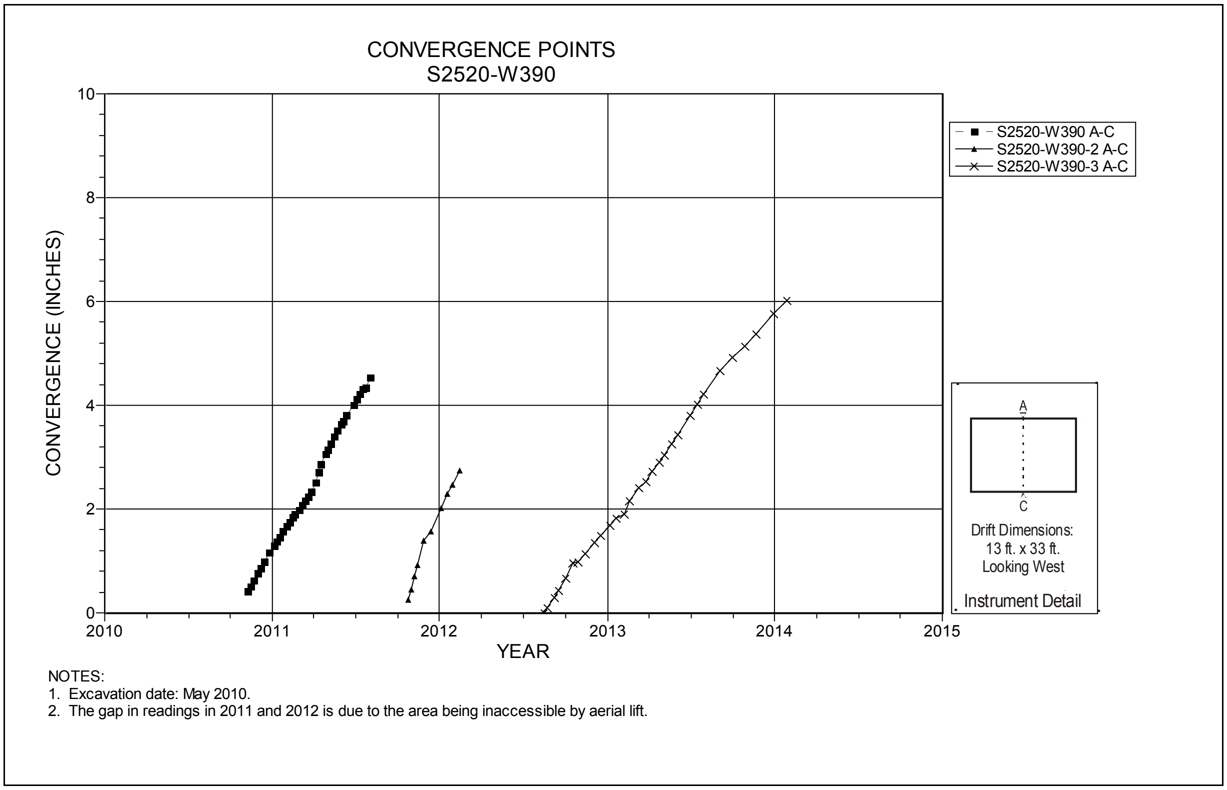

Figure 5-94 Convergence Point Array
S2520 W390 Intersection (Room 1, Panel 7) – Roof to Floor

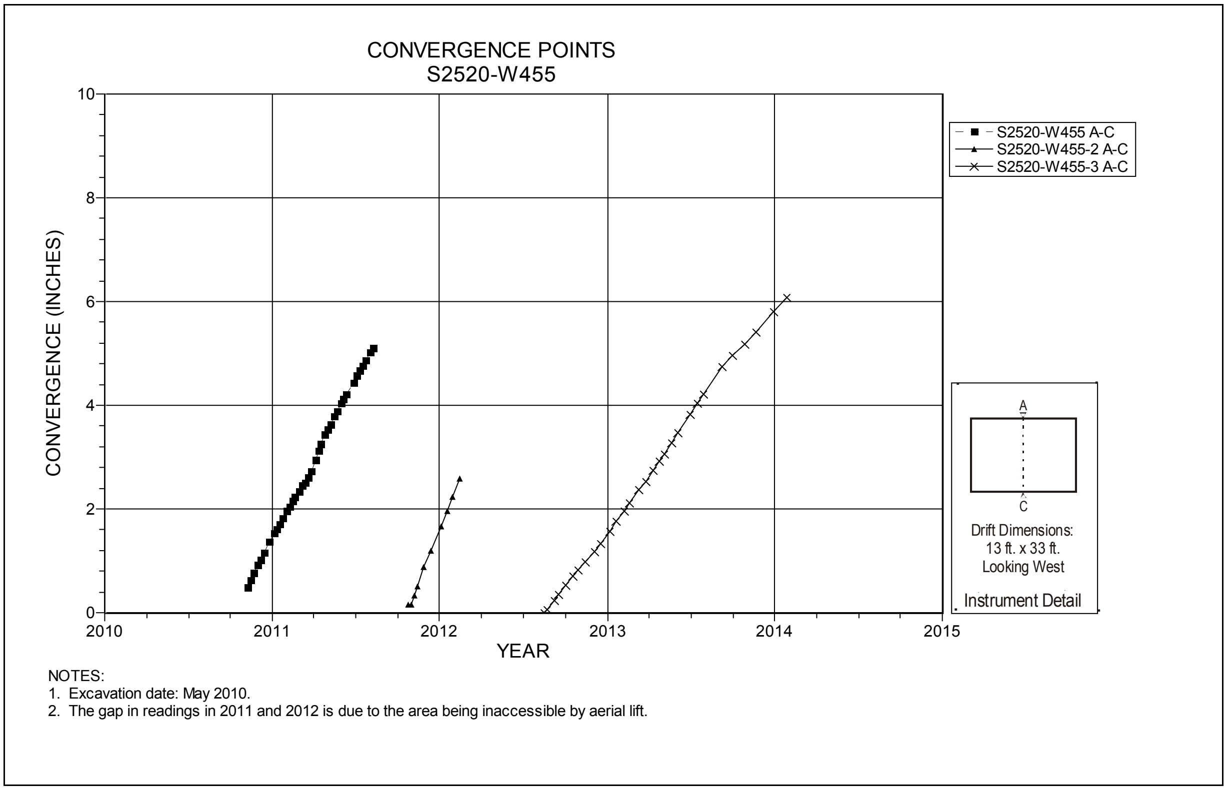

Figure 5-95 Convergence Point Array
S2520 W455 – Roof to Floor

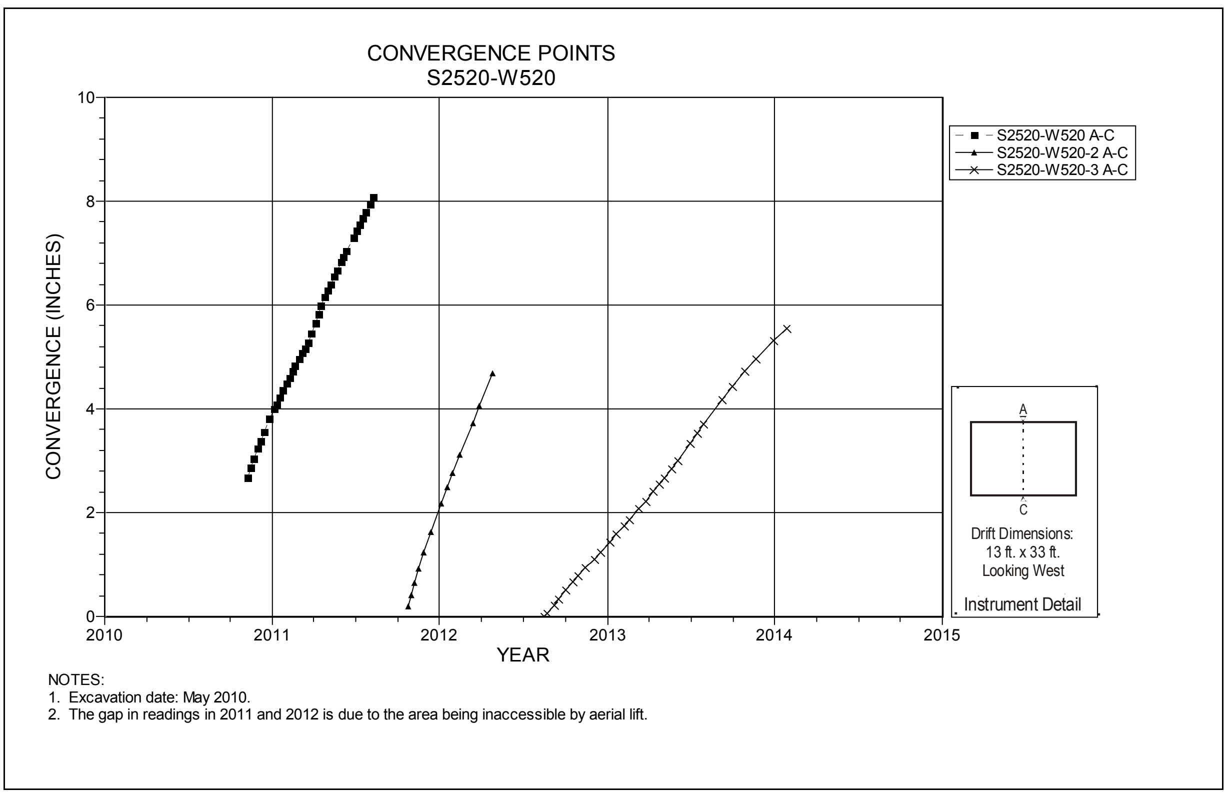

Figure 5-96 Convergence Point Array
S2520 W520 Intersection (Room 2, Panel 7) – Roof to Floor

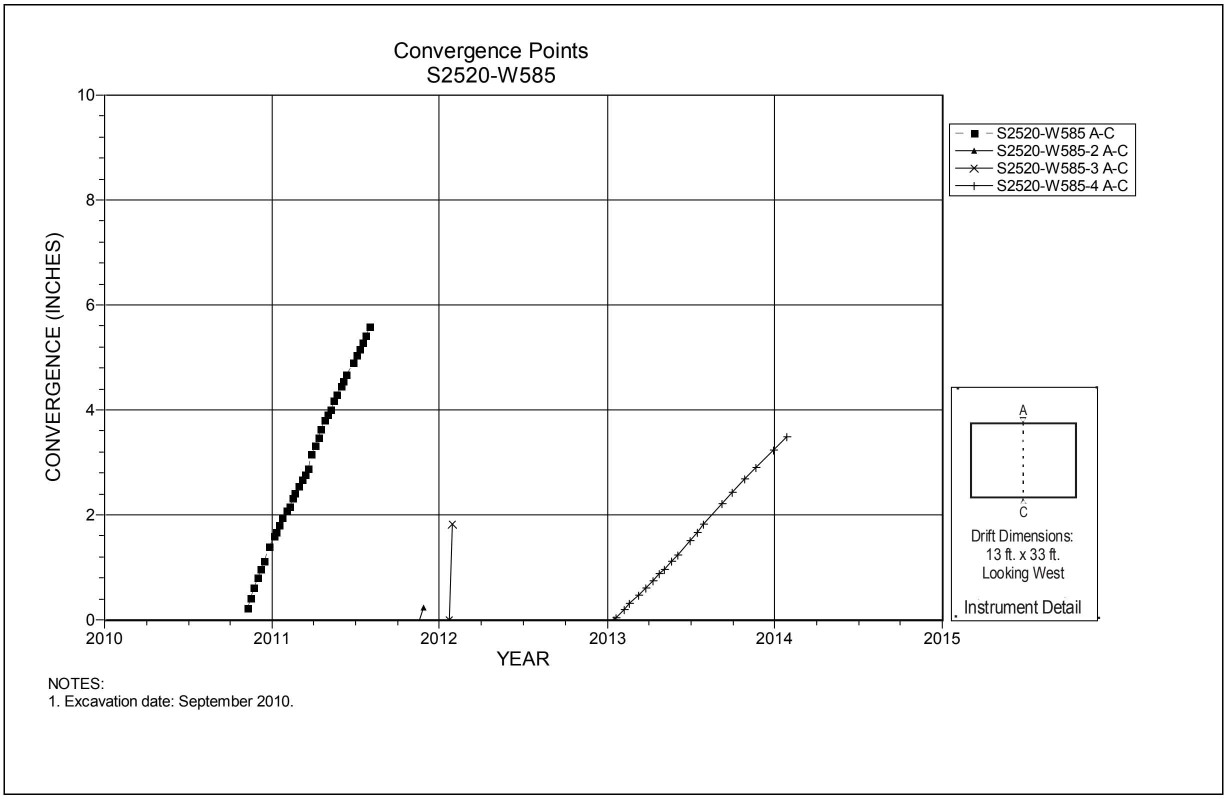

Figure 5-97 Convergence Point Array
S2520 W585 – Roof to Floor

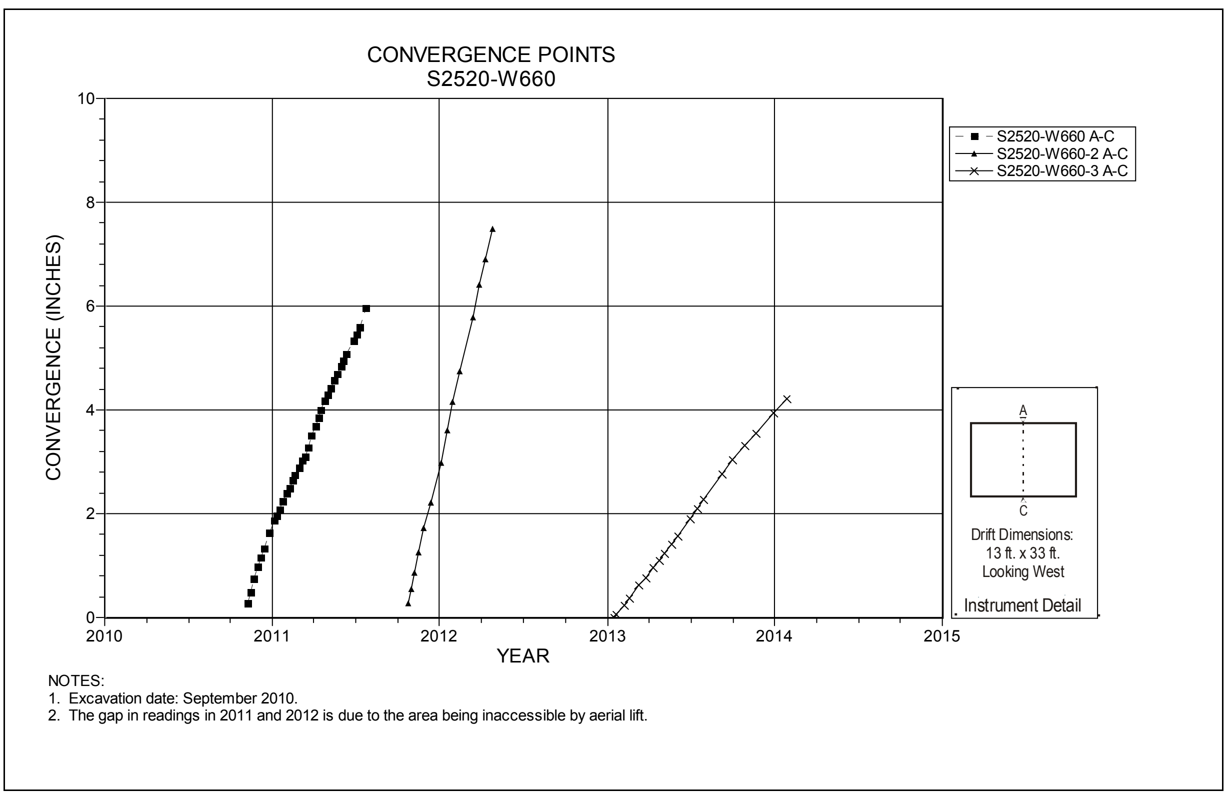

Figure 5-98 Convergence Point Array
S2520 W660 Intersection (Room 3, Panel 7) – Roof to Floor

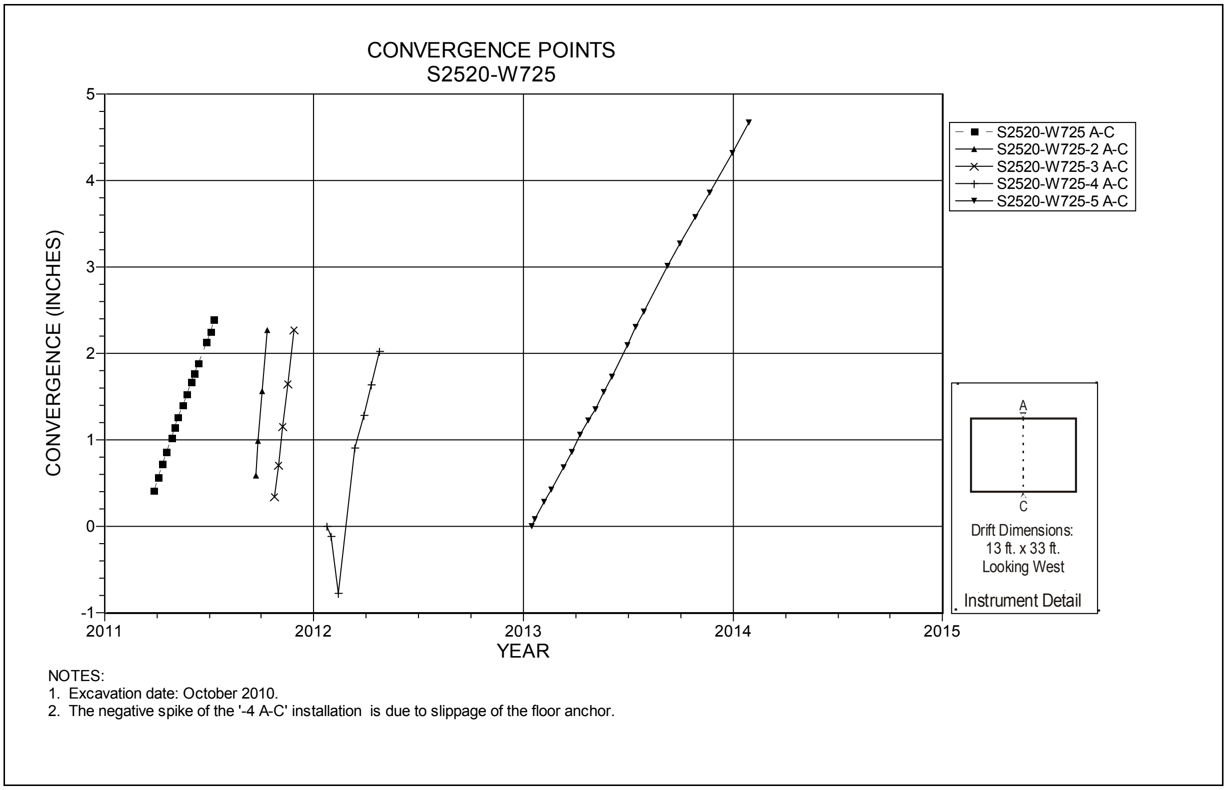

Figure 5-99 Convergence Point Array
S2520 W725 – Roof to Floor

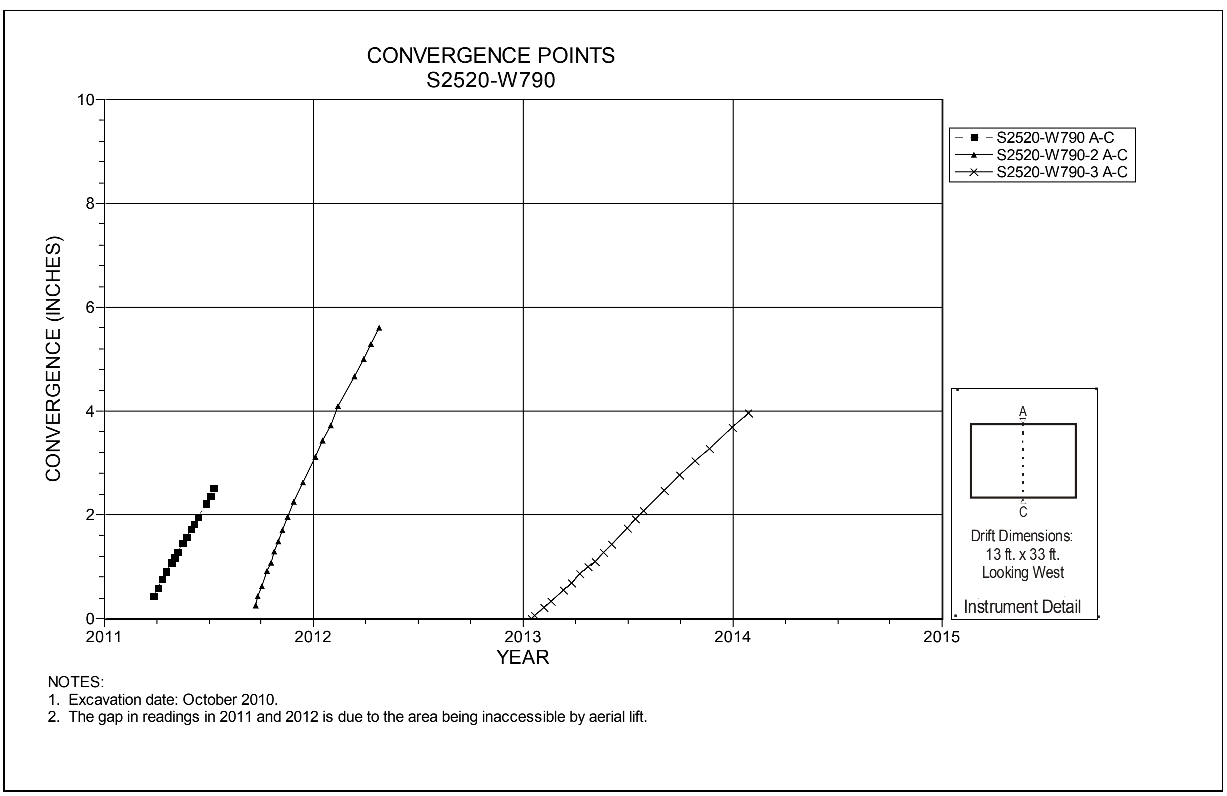

Figure 5-100 Convergence Point Array
S2520 W790 Intersection (Room 4, Panel 7) – Roof to Floor

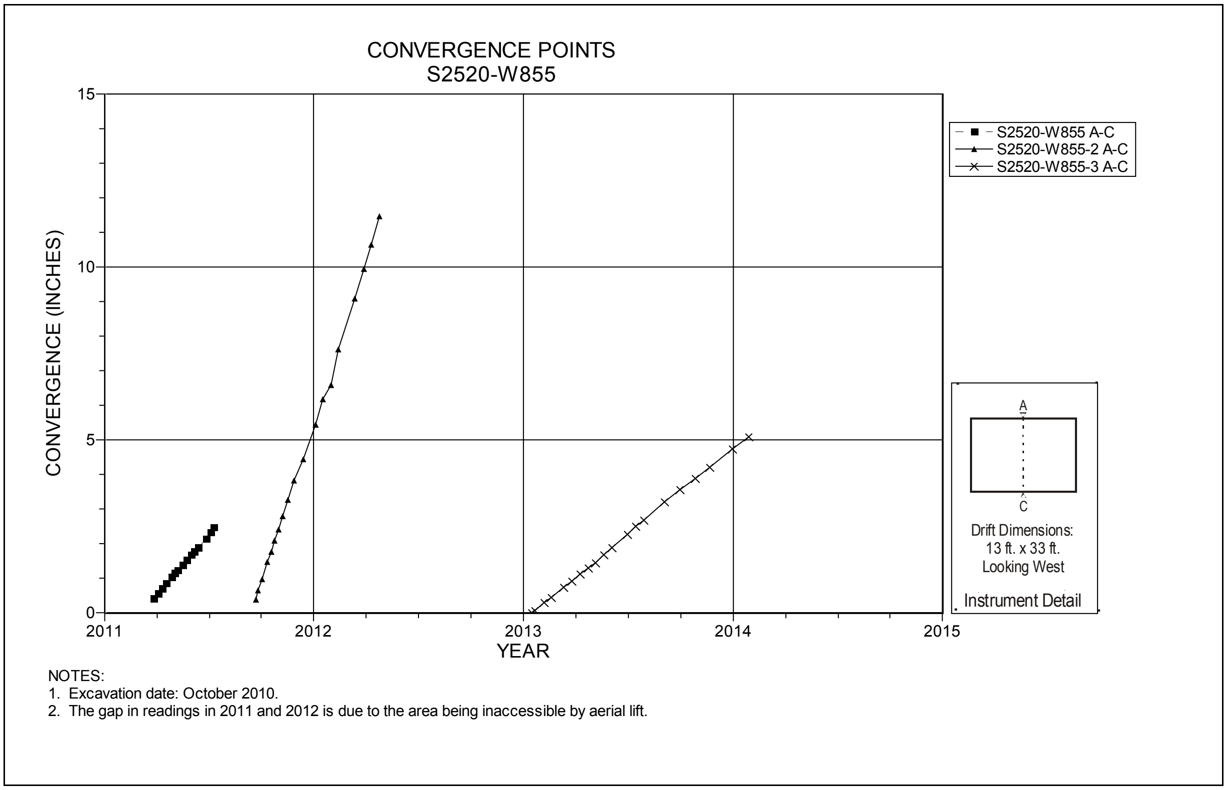

Figure 5-101 Convergence Point Array
S2520 W855 – Roof to Floor

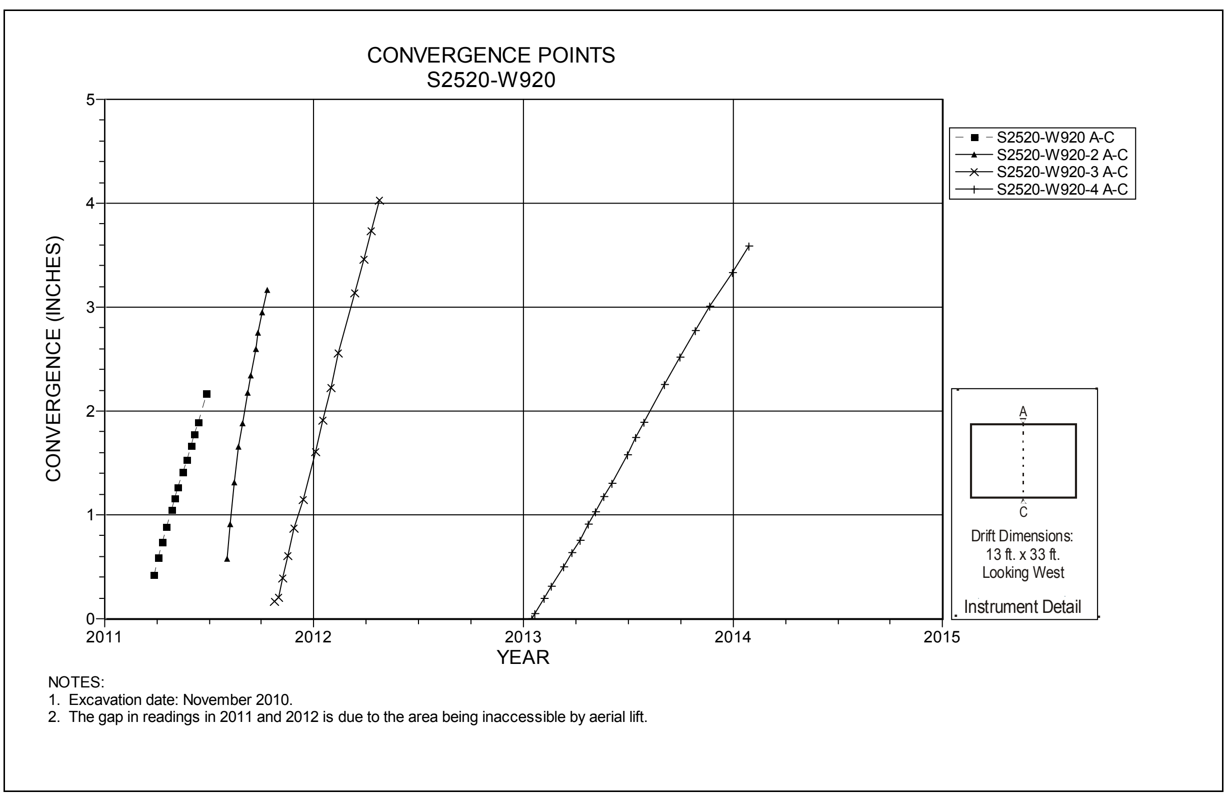

Figure 5-102 Convergence Point Array
S2520 W920 Intersection (Room 5, Panel 7) – Roof to Floor

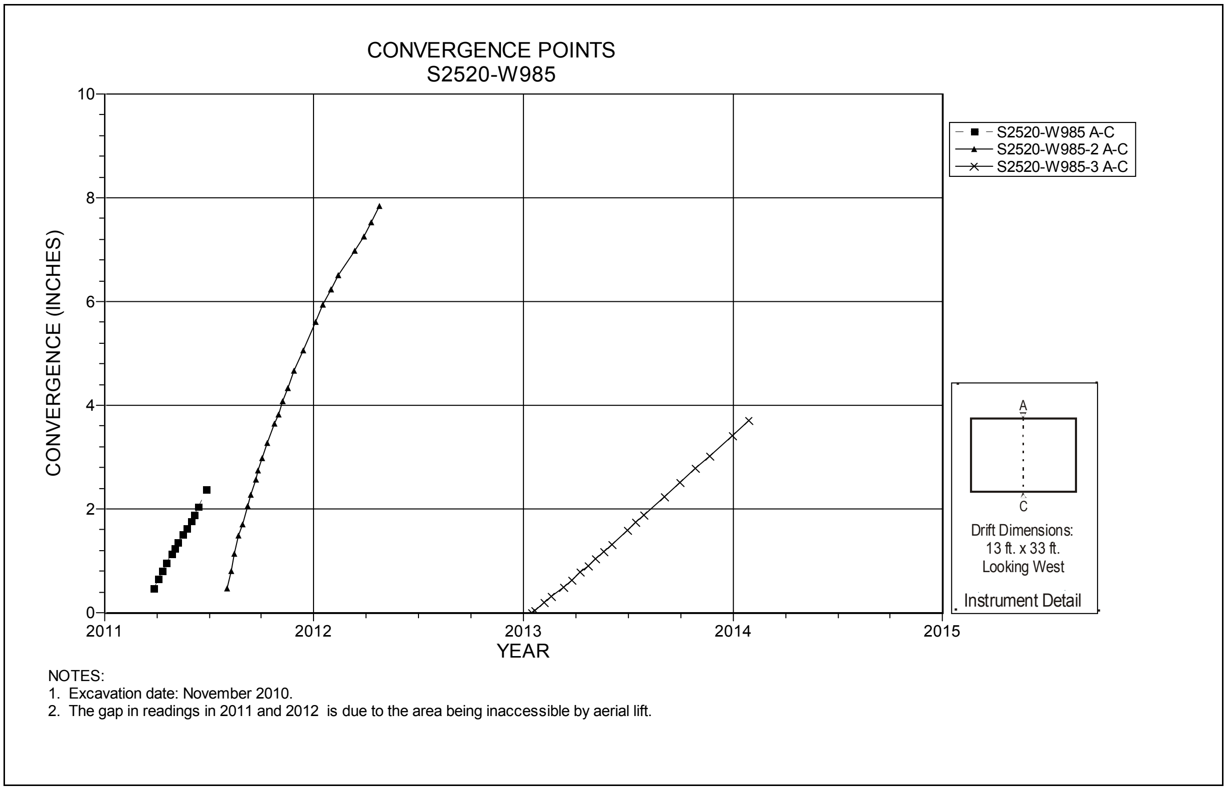

Figure 5-103 Convergence Point Array
S2520 W985 – Roof to Floor

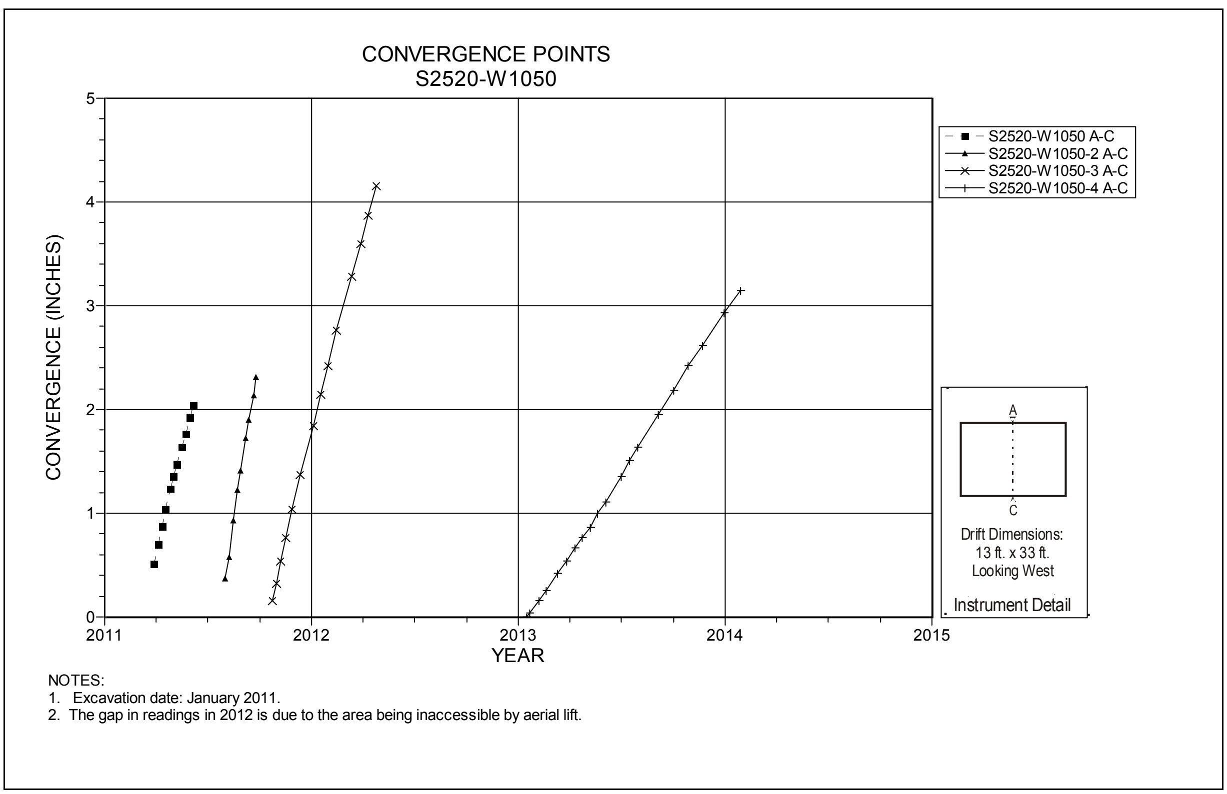

Figure 5-104 Convergence Point Array
S2520 W1050 Intersection (Room 6, Panel 7) – Roof to Floor

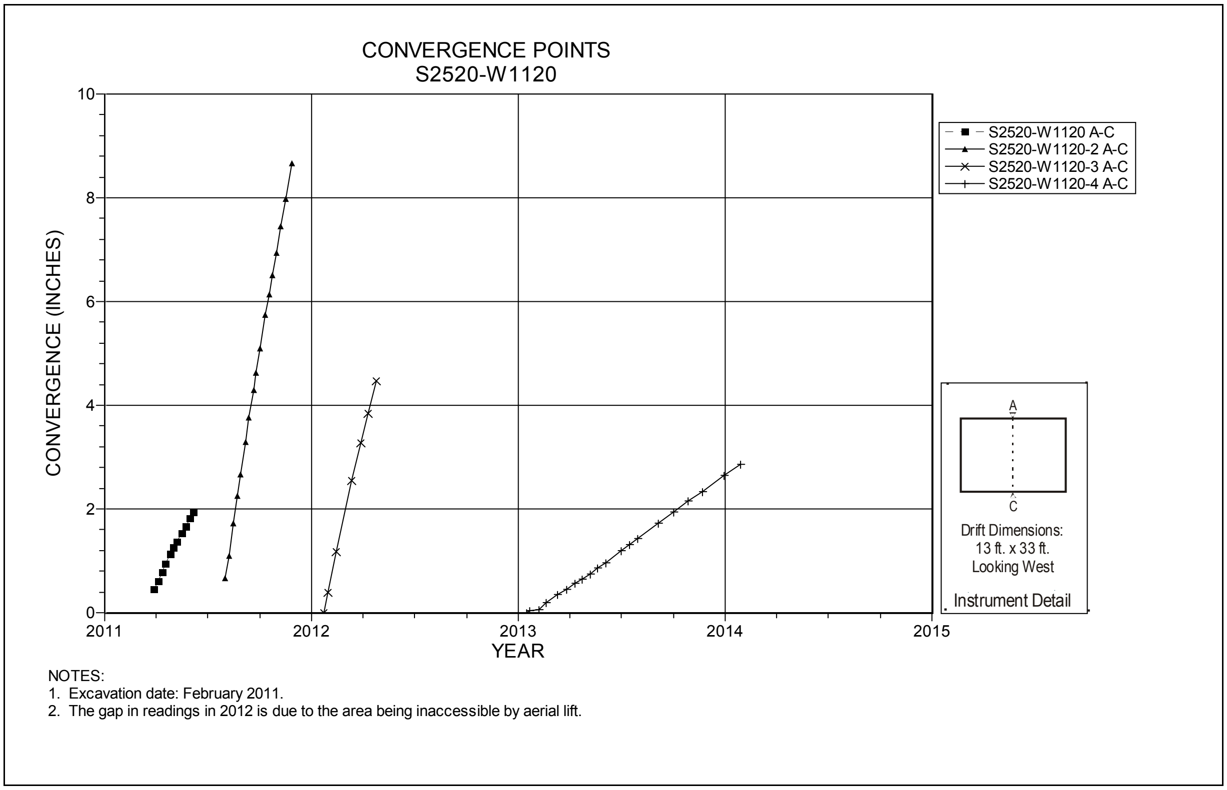

Figure 5-105 Convergence Point Array
S2520 W1120 – Roof to Floor

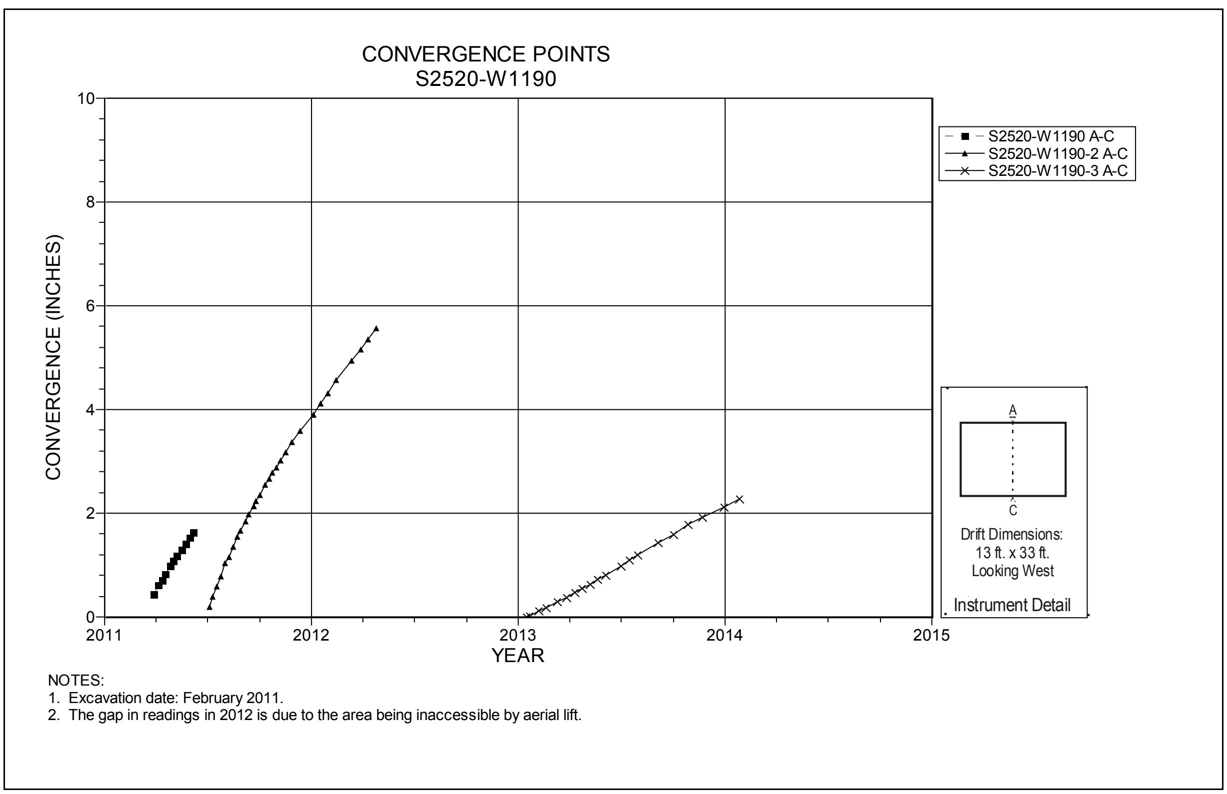

Figure 5-106 Convergence Point Array
S2520 W1190 – Roof to Floor

Table 5-8
Panel 8 Data Analysis

Convergence Points

Field Tag	Location	Figure Number	Last Reading 2013 to 2014 Date	Last Reading 2013 to 2014 Inches	Cumulative Displacement (inches)	Closure Rate 2013 to 2014 (in/year)[2]	Closure Rate 2012 to 2013 (in/year)[1]	Rate Change Percent[1]	Comments
S1600-W285 A-C	S1600-W285	5-107	01/22/14	0.155	0.155	3.8	N/A	N/A	
S1600-W390 A-C	S1600-W390	5-108	01/22/14	0.291	0.291	7.1	N/A	N/A	
S1600-W455 A-C	S1600-W455	5-109	01/22/14	0.447	0.447	10.9	N/A	N/A	
S1600-W520 A-C	S1600-W520	5-110	01/22/14	0.893	0.893	21.7	N/A	N/A	
W390-S1682 A-C	W390-S1682	5-111	01/22/14	0.384	0.384	9.4	N/A	N/A	
W390-S1765 A-C	W390-S1765	5-112	01/22/14	0.472	0.472	11.5	N/A	N/A	
W390-S1846 A-C	W390-S1846	5-113	01/22/14	0.435	0.435	10.6	N/A	N/A	
W520-S1682 A-C	W520-S1682	5-114	02/04/14	0.000	0.000	N/A	N/A	N/A	Only read one since installation
W520-S1765 A-C	W520-S1765	5-115	02/04/14	0.000	0.000	N/A	N/A	N/A	Only read one since installation
W520-S1846 A-C	W520-S1846	5-116	02/04/14	0.000	0.000	N/A	N/A	N/A	Only read one since installation
S1950-W285 A-C	S1950-W285	5-117	01/22/14	0.116	0.116	3.0	N/A	N/A	
S1950-W390 A-C	S1950-W390	5-118	01/22/14	0.339	0.339	8.8	N/A	N/A	
S1950-W455 A-C	S1950-W455	5-119	01/22/14	0.583	0.583	15.2	N/A	N/A	
S1950-W520 A-C	S1950-W520	5-120	01/22/14	1.750	1.750	45.7	N/A	N/A	
S1950-W585 A-C	S1950-W585	5-121	01/22/14	0.738	0.738	19.3	N/A	N/A	
S1950-W660 A-C	S1950-W660	5-122	01/22/14	0.487	0.487	12.7	N/A	N/A	
S1950-W725 A-C	S1950-W725	5-123	01/22/14	0.387	0.387	10.1	N/A	N/A	
S1950-W790 A-C	S1950-W790	5-124	01/22/14	0.350	0.350	9.1	N/A	N/A	

[1] N/A – Insufficient data available to perform the calculation. This is because the instruments were not installed until after the 2012 to 2013 reporting period.
[2] The convergence points in W520 (Panel 8, Room 2) were read at installation. Soon after the initial reading the release occurred and no further data were collected for the reporting period.

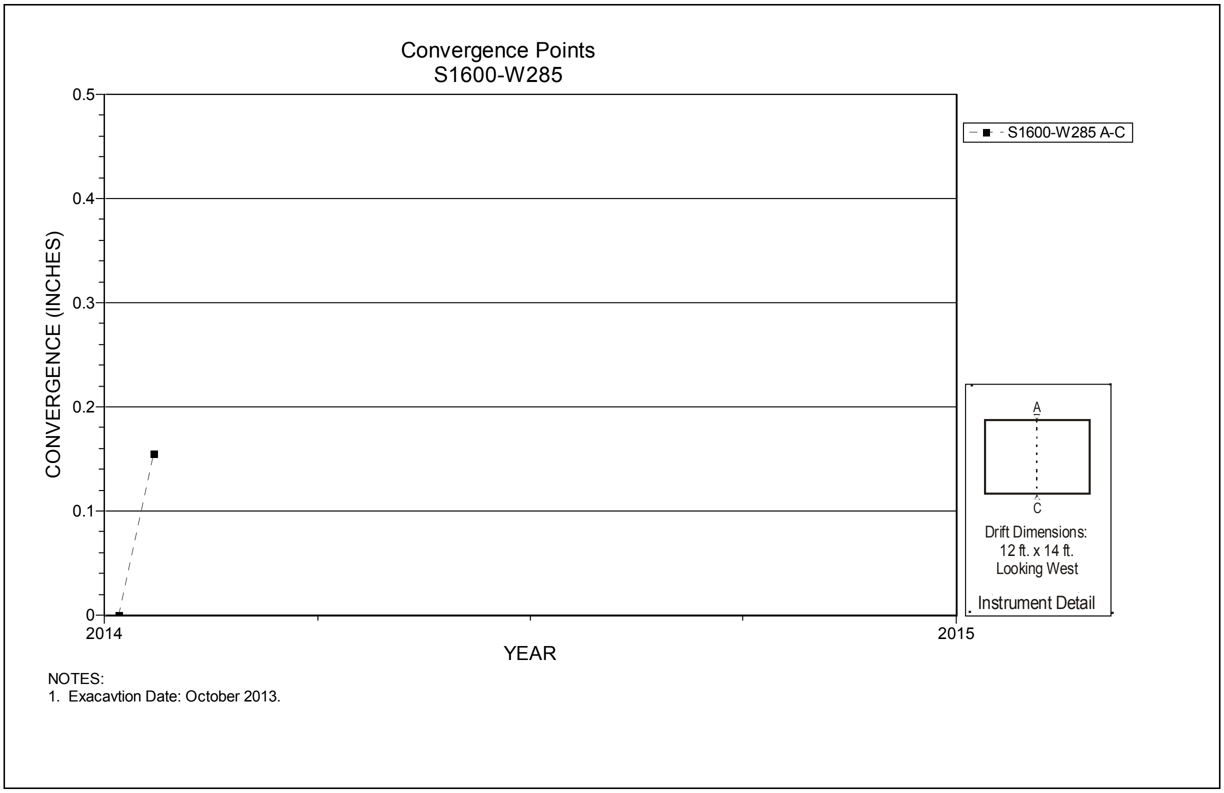

Figure 5-107 Convergence Point Array
S1600 W285 – Roof to Floor

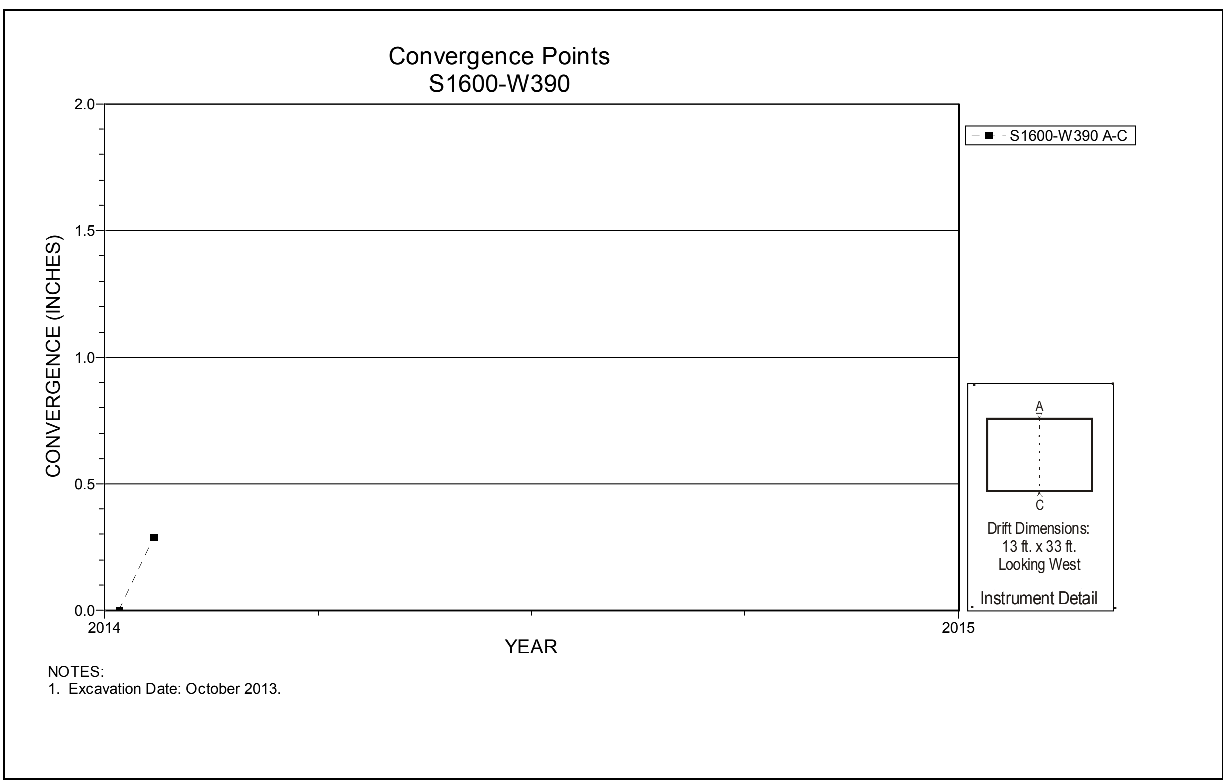

Figure 5-108 Convergence Point Array
S1600 W390 – Roof to Floor

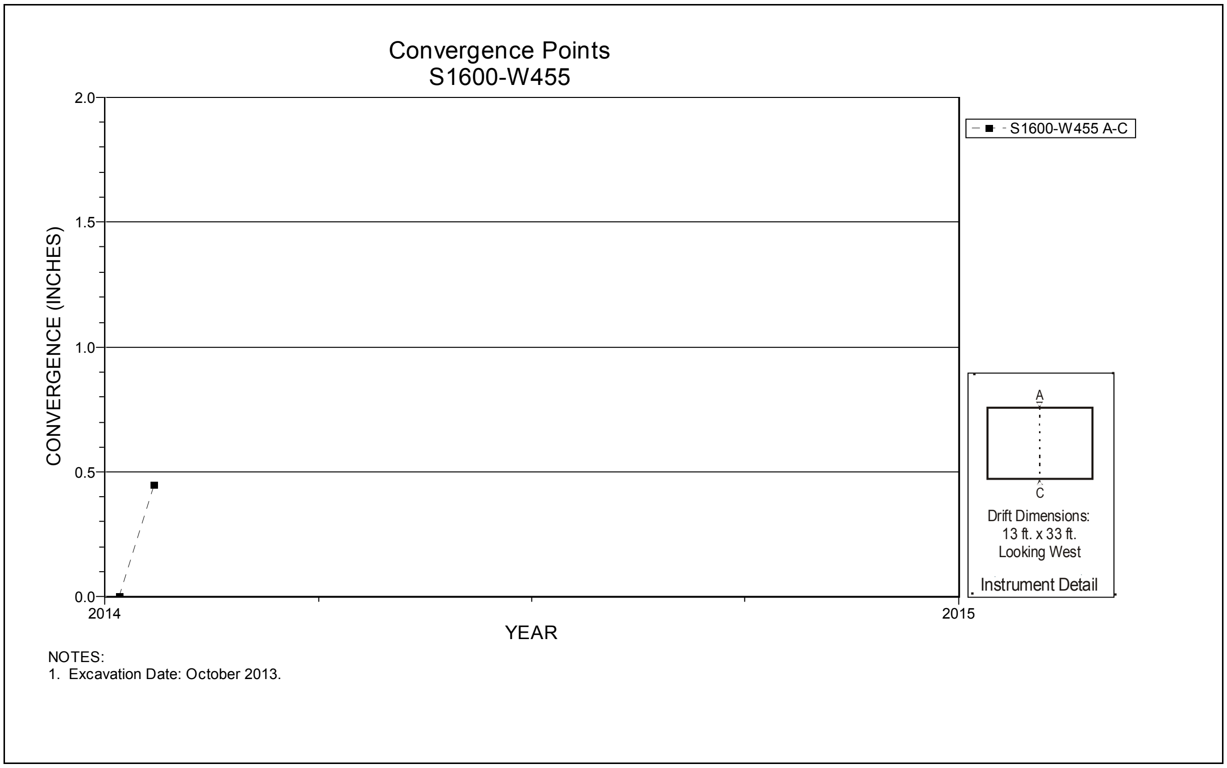

Figure 5-109 Convergence Point Array
S1600 W455 – Roof to Floor

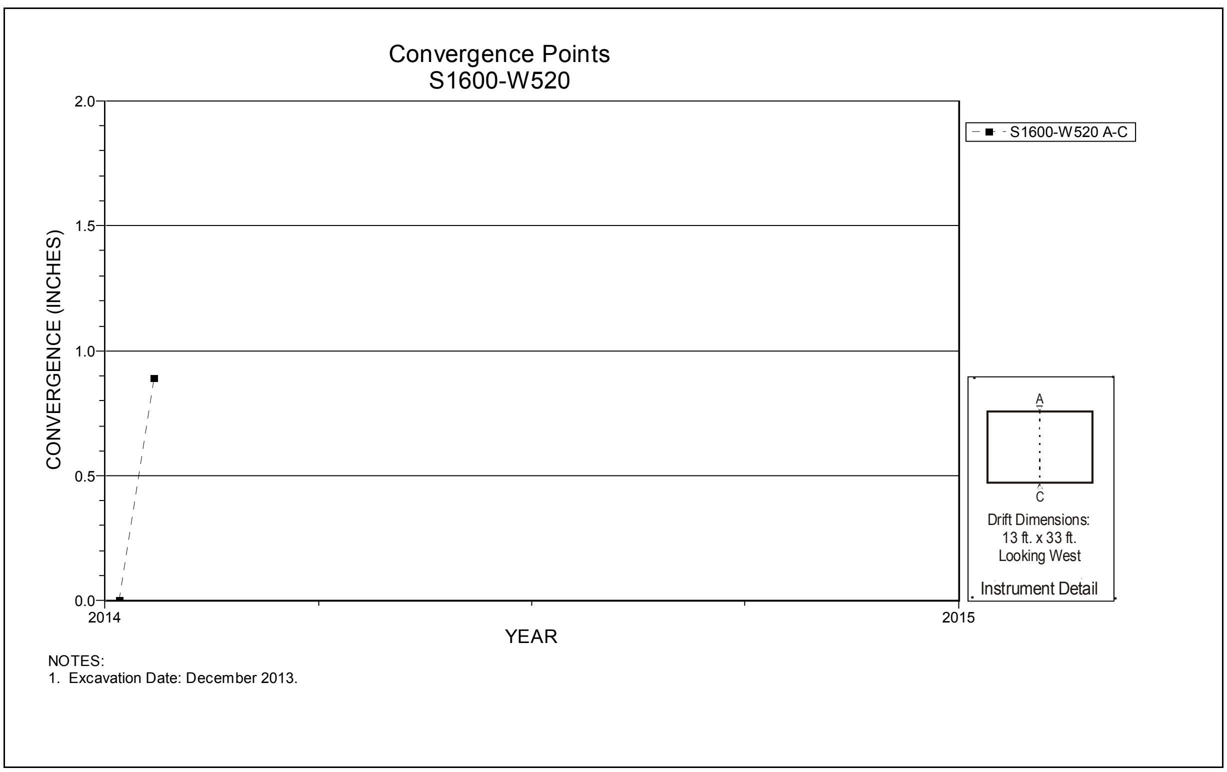

Figure 5-110 Convergence Point Array
S1600 W520 – Roof to Floor

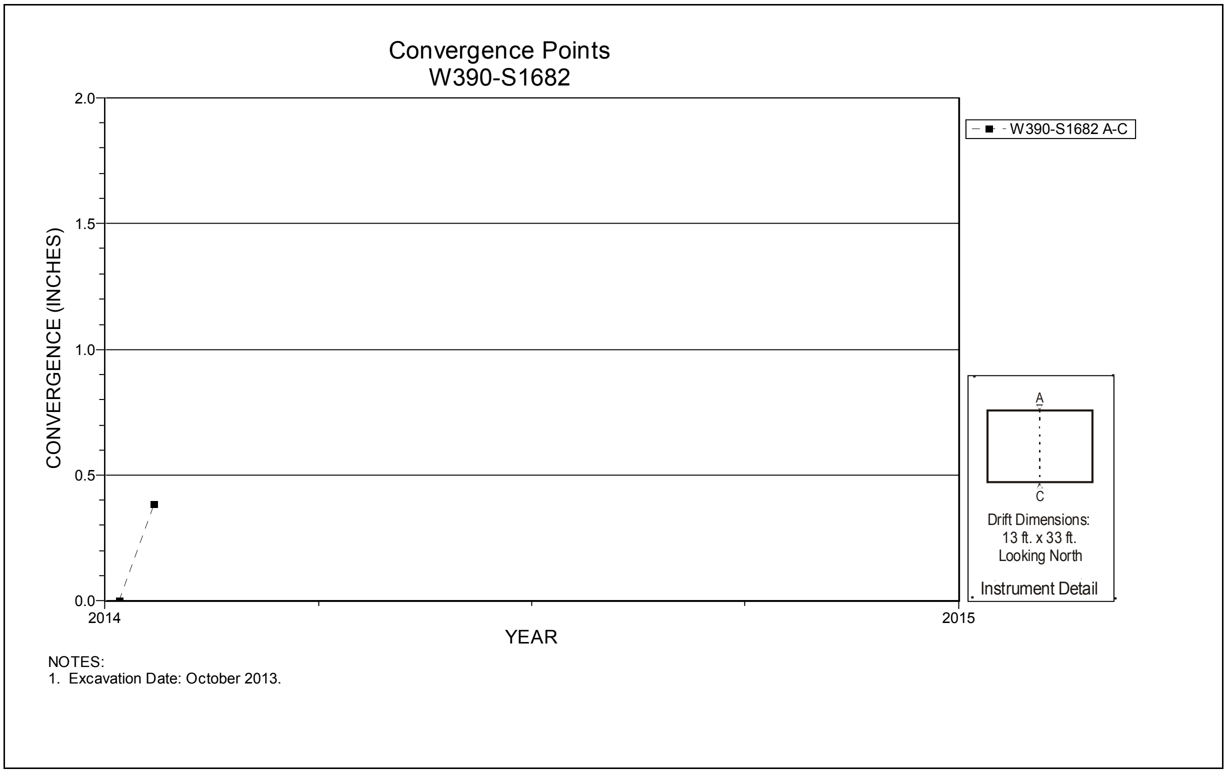

Figure 5-111 Convergence Point Array
W390 S1682 – Roof to Floor

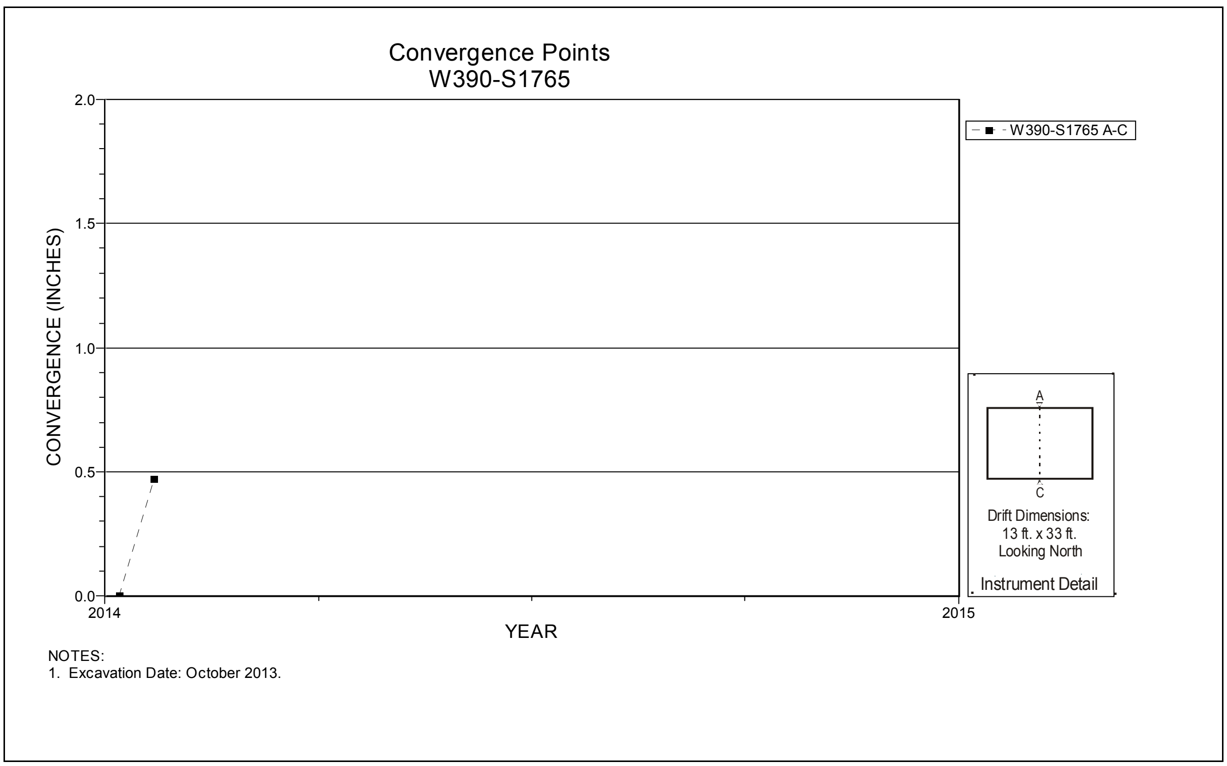

Figure 5-112 Convergence Point Array
W390 S1765 – Roof to Floor

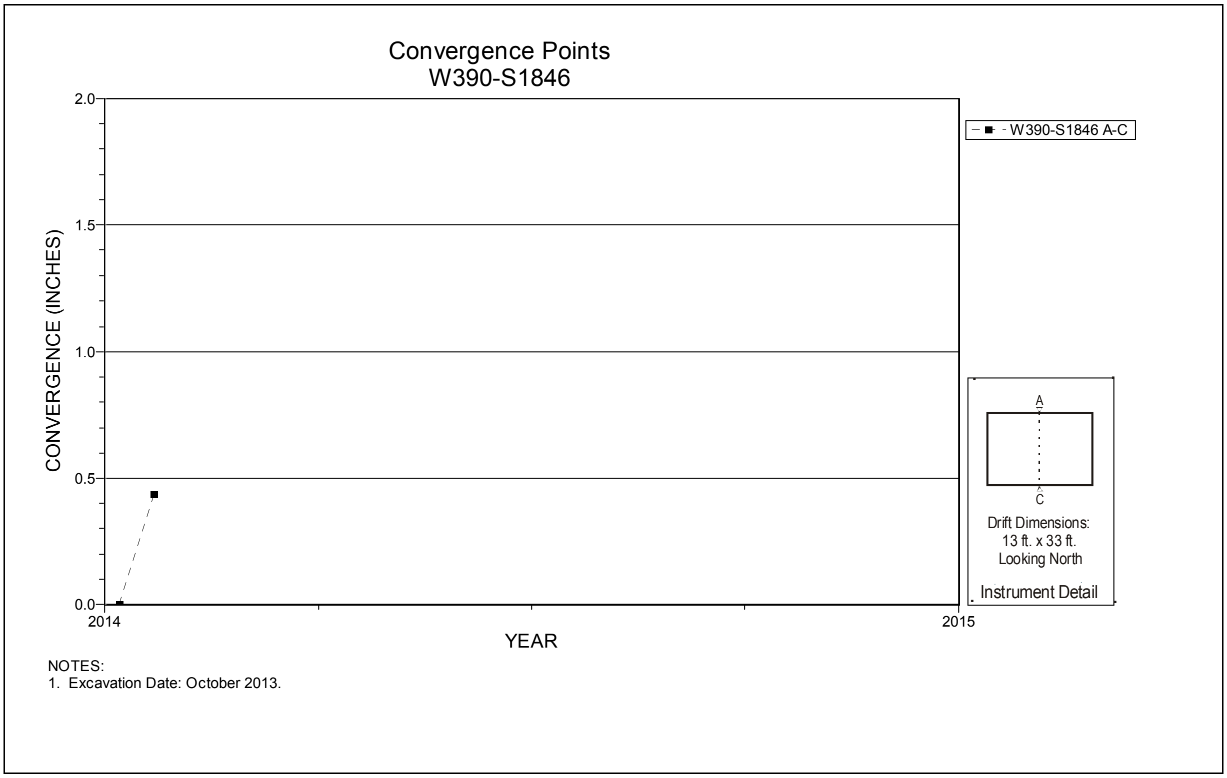

Figure 5-113 Convergence Point Array
W390 S1846 – Roof to Floor

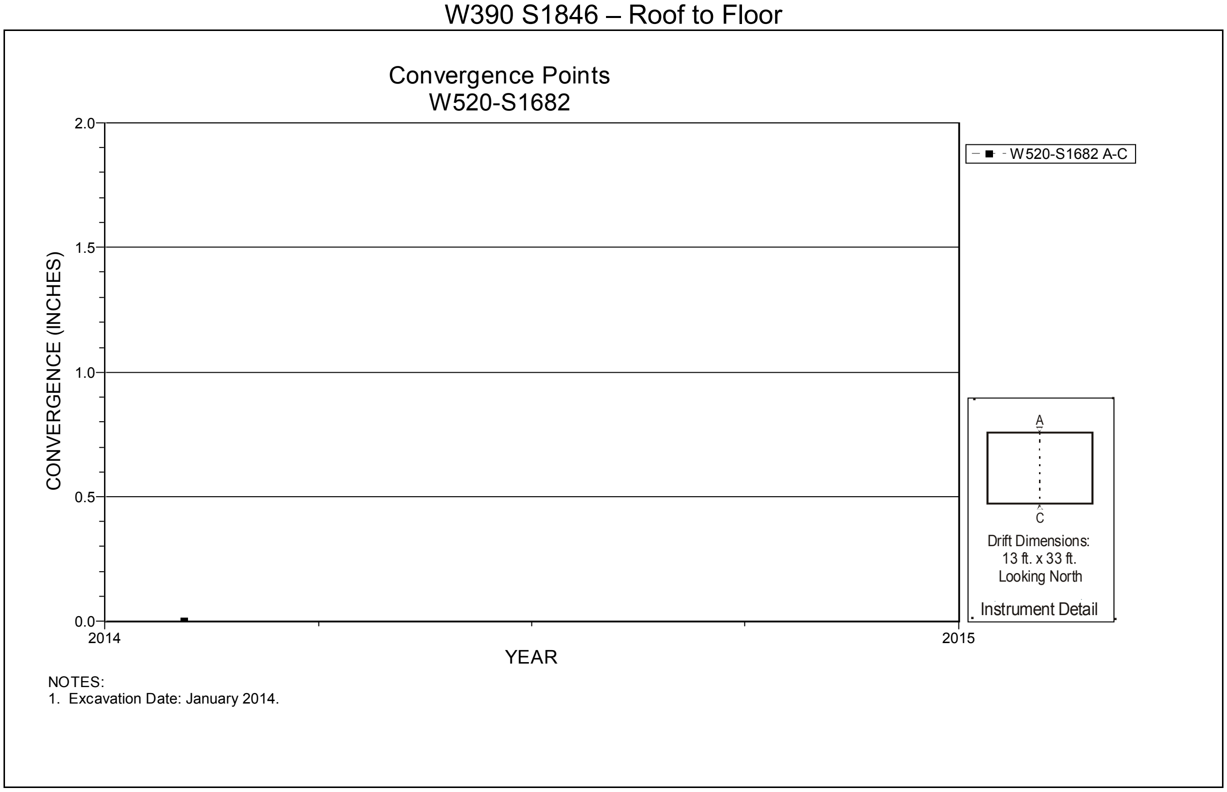

Figure 5-114 Convergence Point Array
W520 S1682 – Roof to Floor

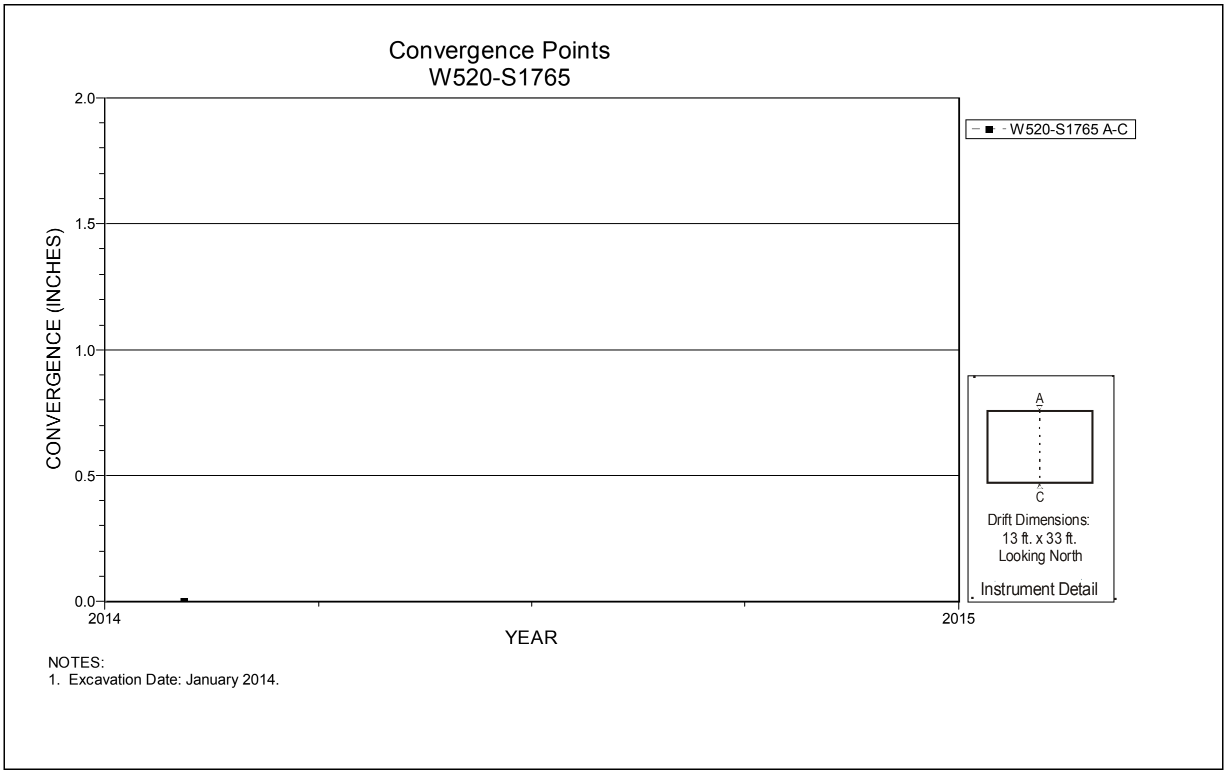

Figure 5-115 Convergence Point Array
W520 S1765 – Roof to Floor

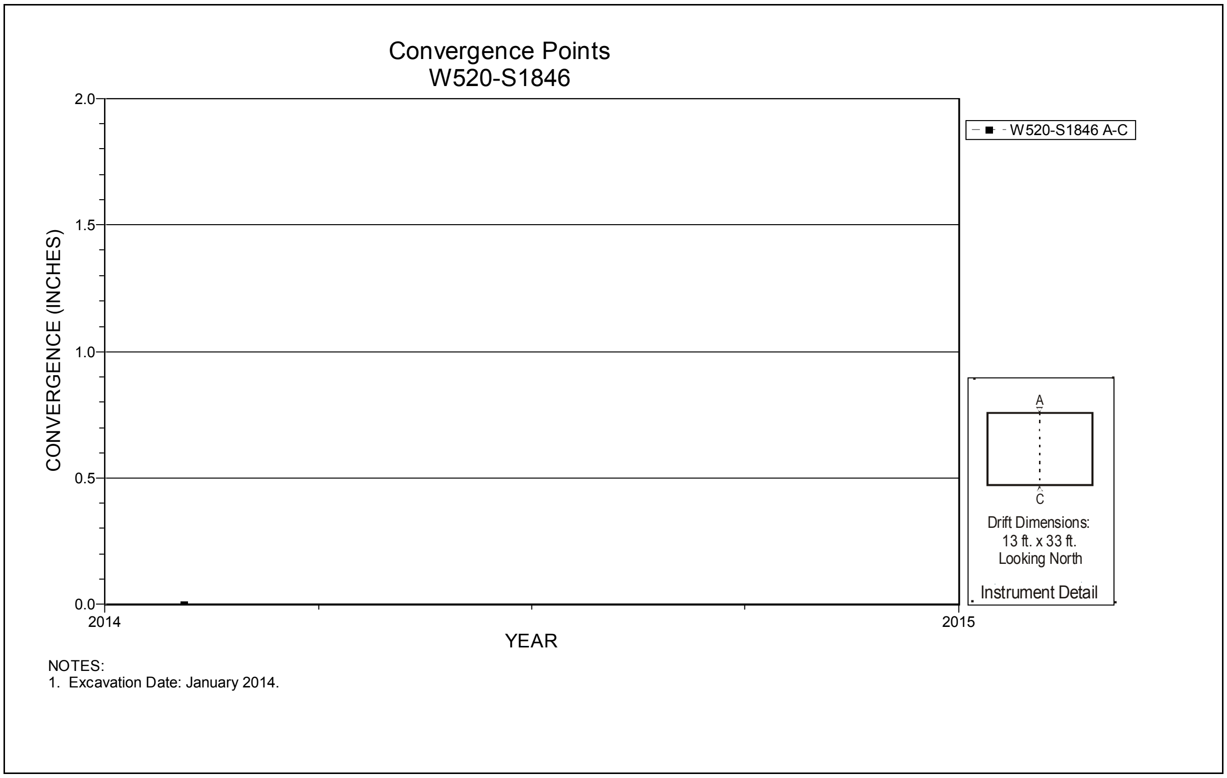

Figure 5-116 Convergence Point Array
W520 S1846 – Roof to Floor

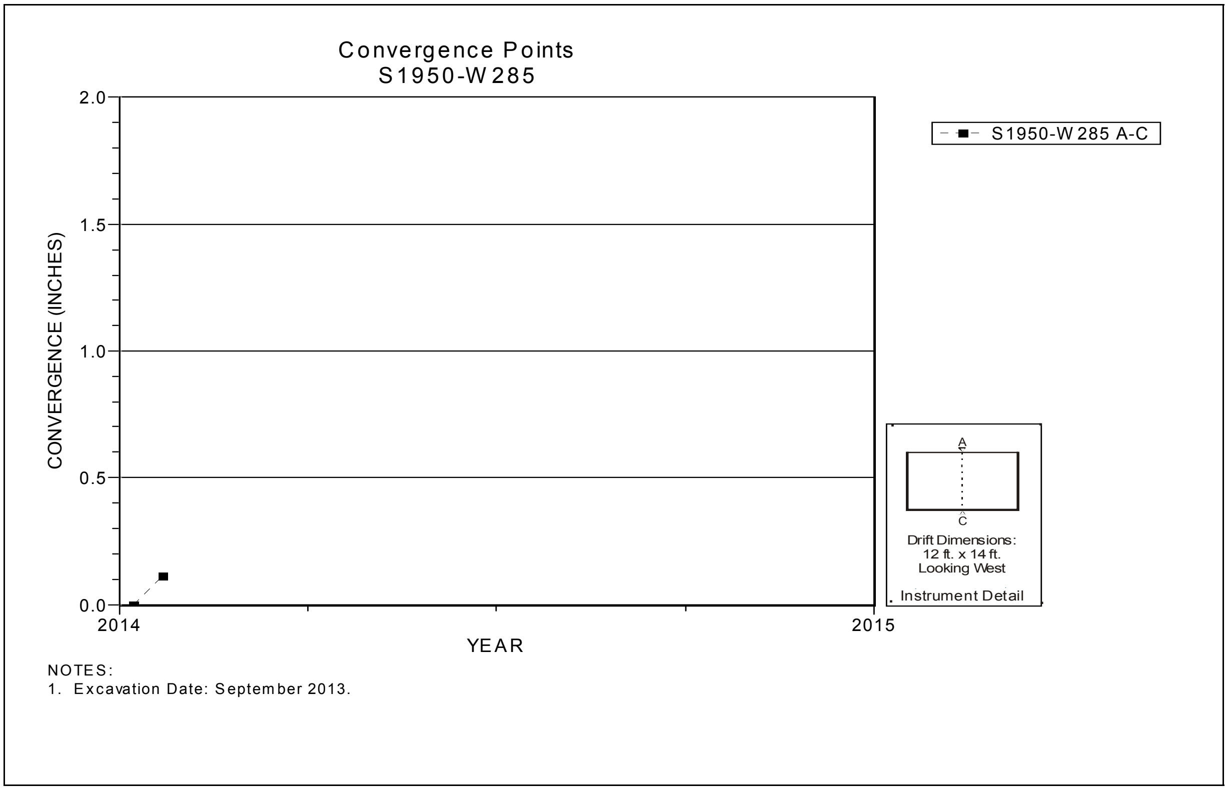

Figure 5-117 Convergence Point Array
S1950 W285 – Roof to Floor

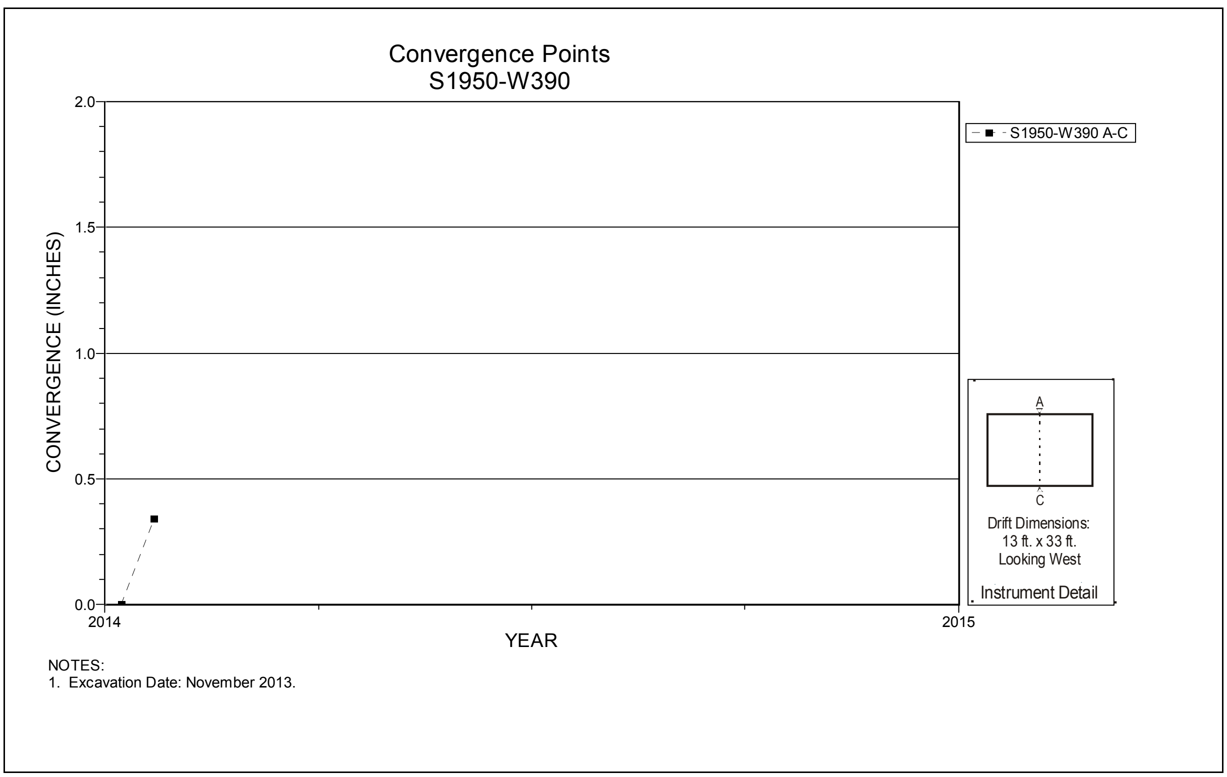

Figure 5-118 Convergence Point Array
S1950 W390 – Roof to Floor

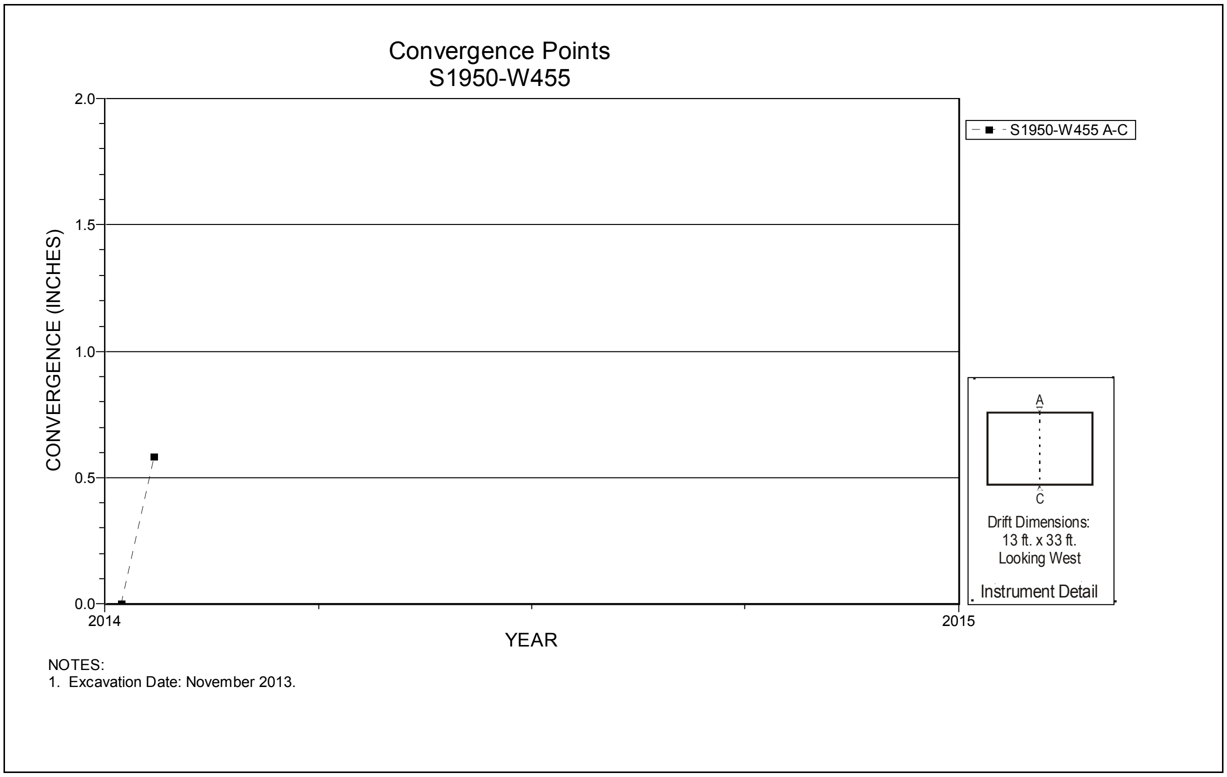

Figure 5-119 Convergence Point Array
S1950 W455 – Roof to Floor

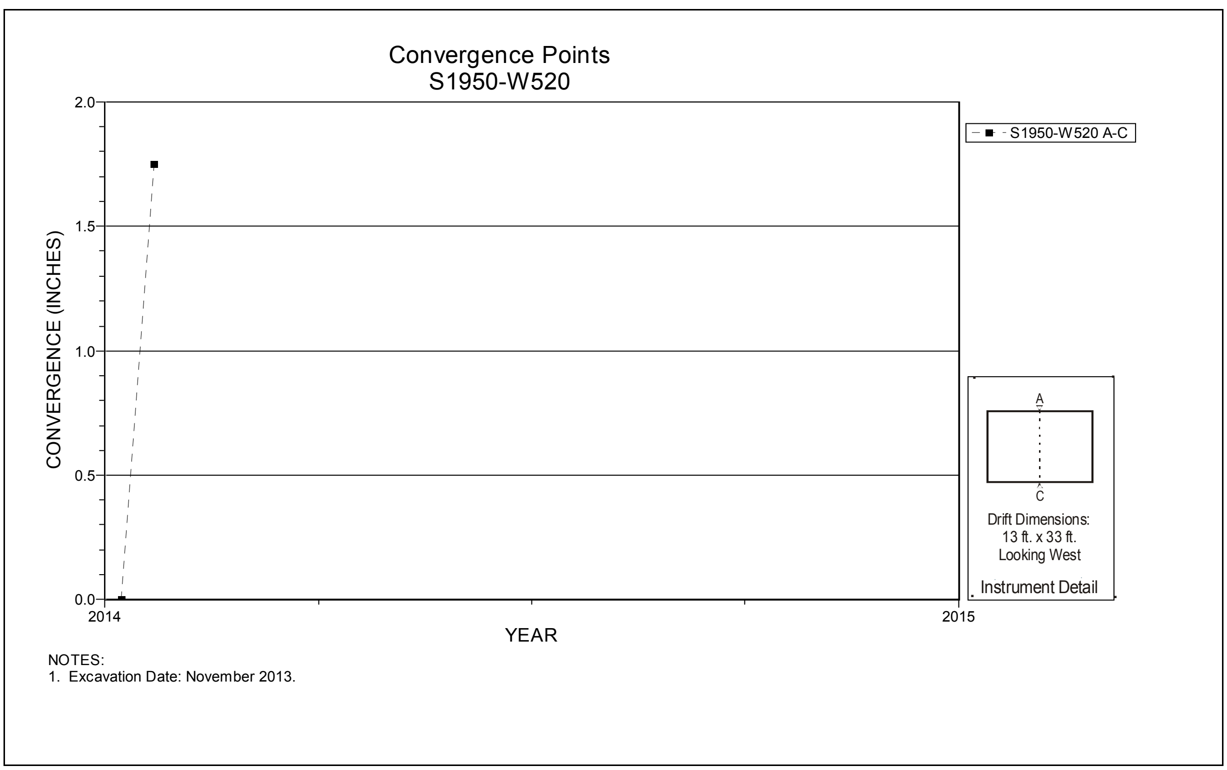

Figure 5-120 Convergence Point Array
S1950 W520 – Roof to Floor

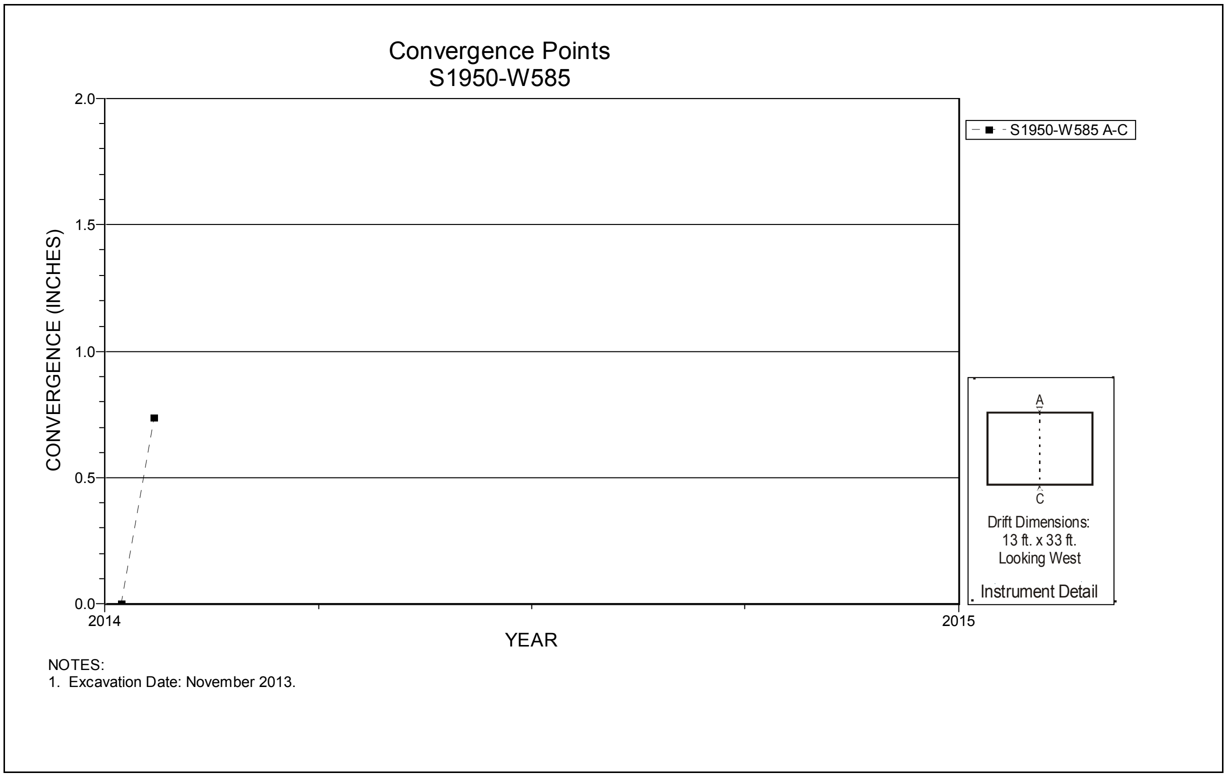

Figure 5-121 Convergence Point Array
S1950 W585 – Roof to Floor

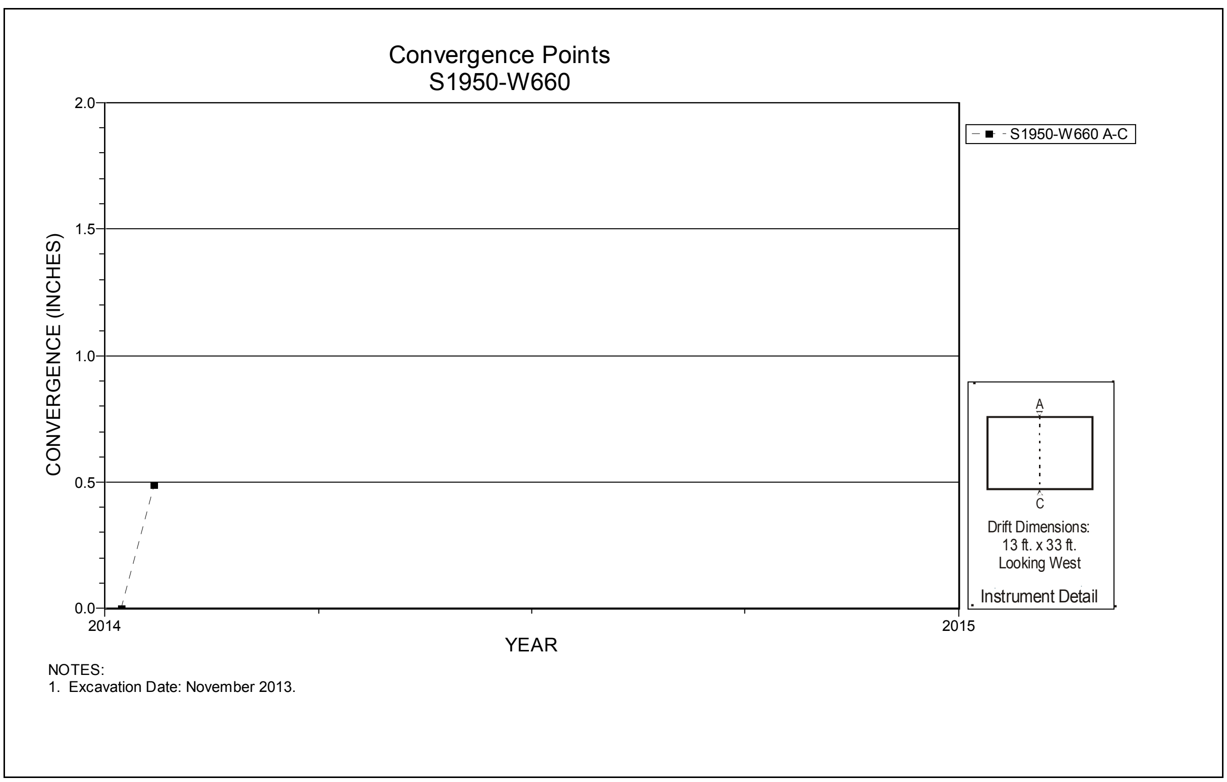

Figure 5-122 Convergence Point Array
S1950 W660 – Roof to Floor

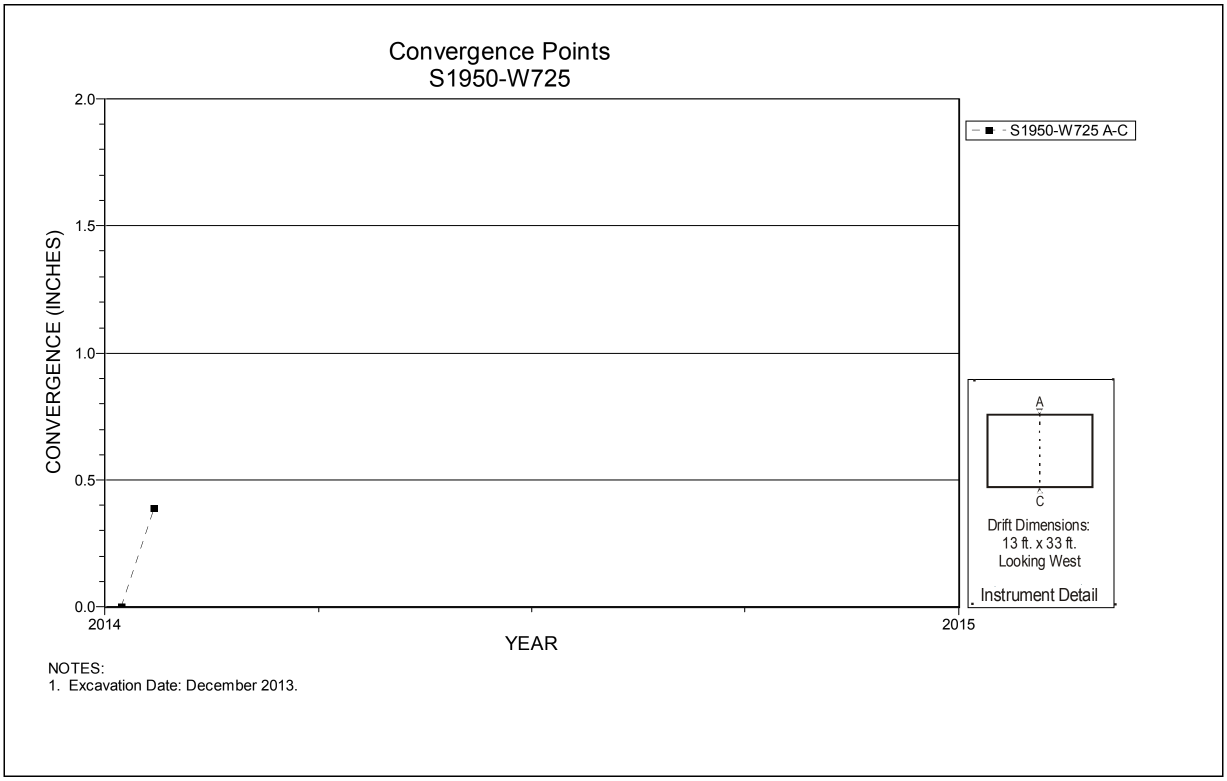

Figure 5-123 Convergence Point Array
S1950 W725 – Roof to Floor

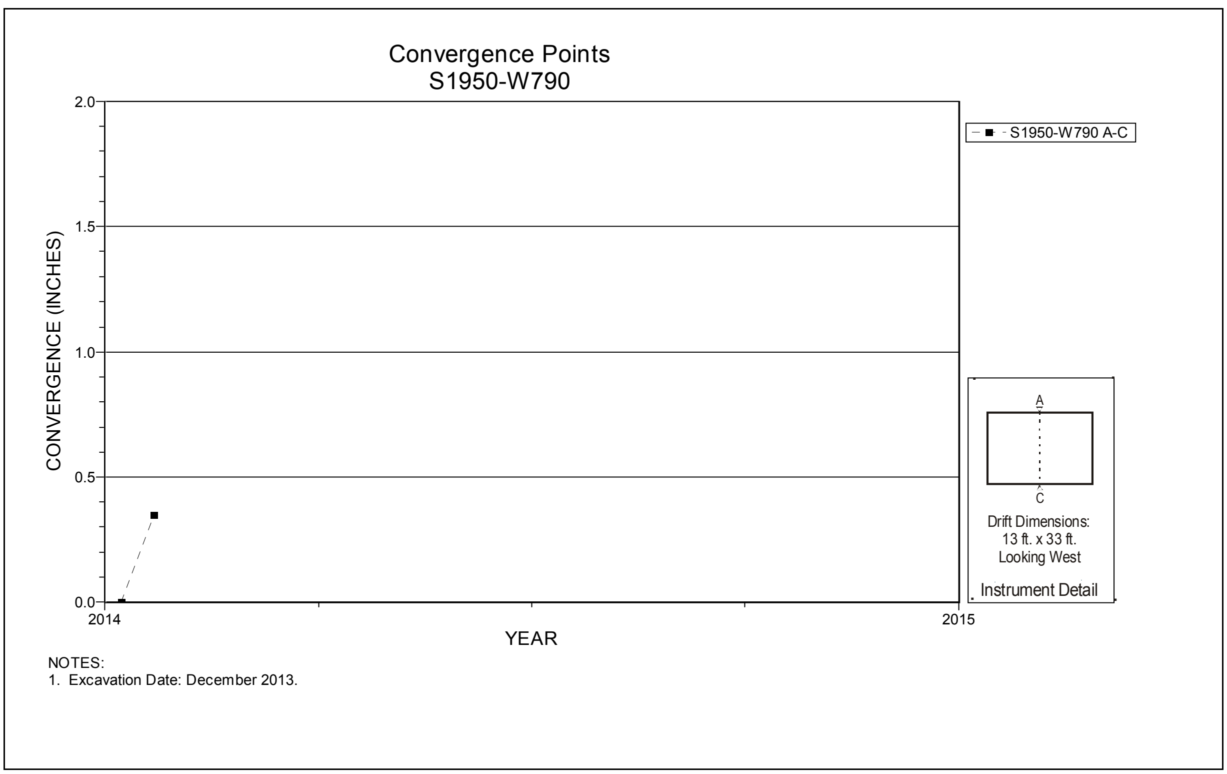

Figure 5-124 Convergence Point Array
S1950 W790 – Roof to Floor

This page was intentionally left blank.

6.0 Instrumentation Summary for the SDI Area

This chapter presents a summary of the data collected from radial convergence points located in the Storage Disposal Investigations (SDI) area at the WIPP. Table 6-1 presents data and analysis of the access drifts associated with the SDI area. Plots of the instrument data are presented as Figures 6-1 through 6-46.

Radial convergence points have been installed at the pillar midpoints, quarter points and drift intersections. The SDI area is still being mined. Hence, at times, access to many of the instruments may not be possible. Therefore, there will be intervals on some of the data plots void of any readings. Readings are resumed once access has been restored.

Table 6-1
SDI Data Analysis

Convergence Points

Field Tag	Location	Figure Number	Last Reading 2013 to 2014		Cumulative Displacement (inches)	Closure Rate 2013 to 2014 (in/year)	Closure Rate[1] 2012 to 2013 (in/year)	Rate Change Percent[1]	Comments
			Date	Inches					
E540-S17 A-C	E540-S17	6-1	01/13/14	1.504	1.504	1.8	2.2	-18%	
E540-S90 A-C	E540-S90	6-2	11/13/13	1.652	1.652	2.6	2.9	-11%	
E540-N55 A-C	E540-N55	6-3	01/13/14	1.776	1.776	2.1	2.6	-18%	
E540-N128 A-C	E540-N128	6-4	01/13/14	2.006	2.006	2.3	3.1	-24%	
E540-N200 A-C	E540-N200	6-5	01/13/14	2.109	2.109	2.5	3.1	-21%	
E540-N275 A-C	E540-N275	6-6	01/13/14	2.000	2.000	2.3	3.0	-21%	
E540-N350-2 A-C	E540-N350	6-7	01/13/14	2.022	2.022	2.4	3.0	-19%	
E540-N425 A-C	E540-N425	6-8	01/13/14	2.121	2.121	2.5	3.1	-21%	
E540-N500-2 A-C	E540-N500	6-9	01/13/14	2.222	2.222	2.6	3.2	-19%	
E540-N570 A-C	E540-N570	6-10	01/13/14	2.287	2.287	2.7	3.3	-18%	
E540-N640-2 A-C	E540-N640	6-11	01/13/14	2.393	2.393	2.8	3.5	-19%	
E540-N710 A-C	E540-N710	6-12	01/13/14	2.125	2.125	2.5	3.1	-20%	
E540-N860 A-C	E540-N860	6-13	01/14/14	2.330	2.330	2.3	3.0	-24%	
E690-S17-2 A-C	E690-S17	6-14	11/13/13	1.452	1.452	2.2	2.5	-13%	
E690-S90 A-C	E690-S90	6-15	11/13/13	1.560	1.560	2.4	2.7	-10%	
E690-N55-2 A-C	E690-N55	6-16	11/13/13	1.477	1.477	2.2	2.6	-16%	
E690-N128-2 A-C	E690-N128	6-17	11/13/13	1.626	1.626	2.4	2.9	-17%	
E690-N200-2 A-C	E690-N200	6-18	11/13/13	2.197	2.197	3.4	4.0	-14%	
E690-N275-2 A-C	E690-N275	6-19	11/13/13	1.856	1.856	2.8	3.5	-20%	
E690-N350-2 A-C	E690-N350	6-20	11/12/13	2.562	2.562	4.0	4.8	-18%	
E690-N425-2 A-C	E690-N425	6-21	11/12/13	1.962	1.962	3.0	3.7	-18%	
E690-N500-2 A-C	E690-N500	6-22	11/12/13	2.657	2.657	4.1	4.9	-16%	
E690-N640 A-C	E690-N640	6-23	11/12/13	1.051	1.051	3.1	N/A	N/A	
E690-N860 A-C	E690-N860	6-24	12/11/12	N/A	0.222	N/A	N/A	N/A	Not read this reporting period (blocked by equipment) [1].
N780-E220-4 A-C	N780-E220	6-25	01/13/14	2.483	2.483	3.4	2.3	-2%	
N780-E300-3 A-C	N780-E300	6-26	01/13/14	2.330	2.330	2.8	3	-15%	

Table 6-1, Continued
SDI Data Analysis

Convergence Points, Continued

Field Tag	Location	Figure Number	Last Reading 2013 to 2014		Cumulative Displacement (inches)	Closure Rate 2013 to 2014 (in/year)	Closure Rate 2012 to 2013 (in/year)	Rate Change Percent	Comments
			Date	Inches					
N780-E420-2 A-C	N780-E420	6-27	01/13/14	2.356	2.356	3.0	6.4	-23%	
N780-E540-2 A-C	N780-E540	6-28	01/13/14	3.269	3.269	4.1	15.4	-18%	
N780-E615-2 A-C	N780-E615	6-29	01/13/14	2.231	2.231	2.7	3.3	-16%	
N780-E690-2 A-C	N780-E690	6-30	11/12/13	2.748	2.748	4.1	5.2	-21%	
N780-E768 A-C	N780-E768	6-31	11/12/13	2.721	2.721	3.7	6.0	-38%	
N780-E845 A-C	N780-E845	6-32	11/12/13	3.074	3.074	4.0	7.0	-42%	
N780-E922 A-C	N780-E922	6-33	11/12/13	3.348	3.348	4.4	7.6	-43%	
N780-E1000 A-C	N780-E1000	6-34	10/15/13	3.588	3.588	5.6	11.5	-51%	
N780-E1050 A-C	N780-E1050	6-35	01/14/14	4.244	4.244	4.9	9.3	-48%	
N780-E1100 A-C	N780-E1100	6-36	01/14/14	4.589	4.589	5.0	10.6	-53%	
N780-E1150 A-C	N780-E1150	6-37	01/14/14	3.856	3.856	4.4	7.6	-43%	
N780-E1200 A-C	N780-E1200	6-38	01/14/14	3.995	3.995	4.4	7.0	-38%	
N780-E1250 A-C	N780-E1250	6-39	01/14/14	3.180	3.180	3.7	6.6	-44%	
N940-E220-2 A-C	N940-E220	6-40	01/14/14	1.288	1.288	1.4	1.5	-7%	
N940-E300-2 A-C	N940-E300	6-41	01/14/14	1.523	1.523	1.6	1.8	-12%	
N940-E420-2 A-C	N940-E420	6-42	01/14/14	2.226	2.226	2.4	2.6	-10%	
N940-E540-2 A-C	N940-E540	6-43	01/14/14	2.477	2.477	2.6	2.9	-8%	
N940-E615-2 A-C	N940-E615	6-44	01/14/14	2.656	2.656	2.7	3.3	-17%	
N940-E690-3 A-C	N940-E690	6-45	01/14/14	4.535	4.535	4.4	6.0	-28%	
S90-E615 A-C	S90-E615	6-46	11/13/13	1.407	1.407	2.1	2.5	-15%	

[1] N/A – Insufficient data available to perform the calculation. This is usually due to the inability to read the instruments because of activities such as: the temporary removal of an instrument due to floor, rib or back trimming; locations blocked by equipment or waste disposal, installation timing, etc.

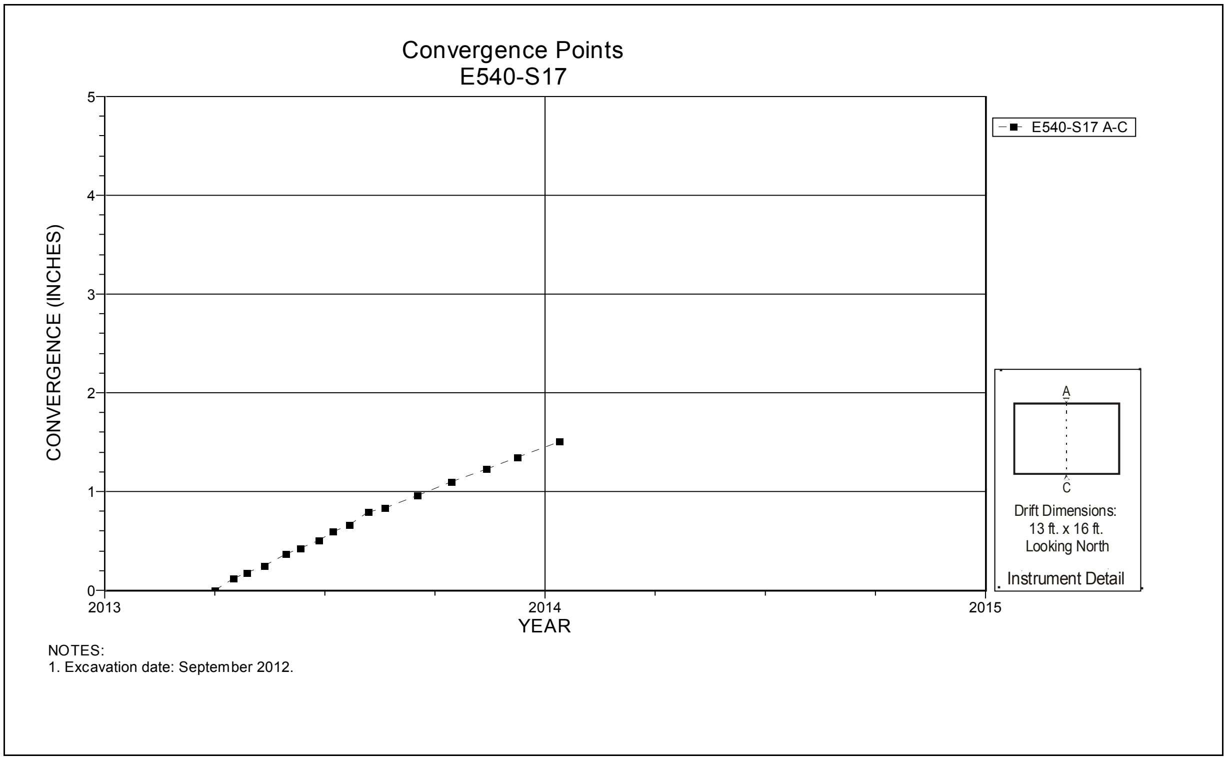

Figure 6-1 Convergence Point Array
E540 S17 – Roof to Floor

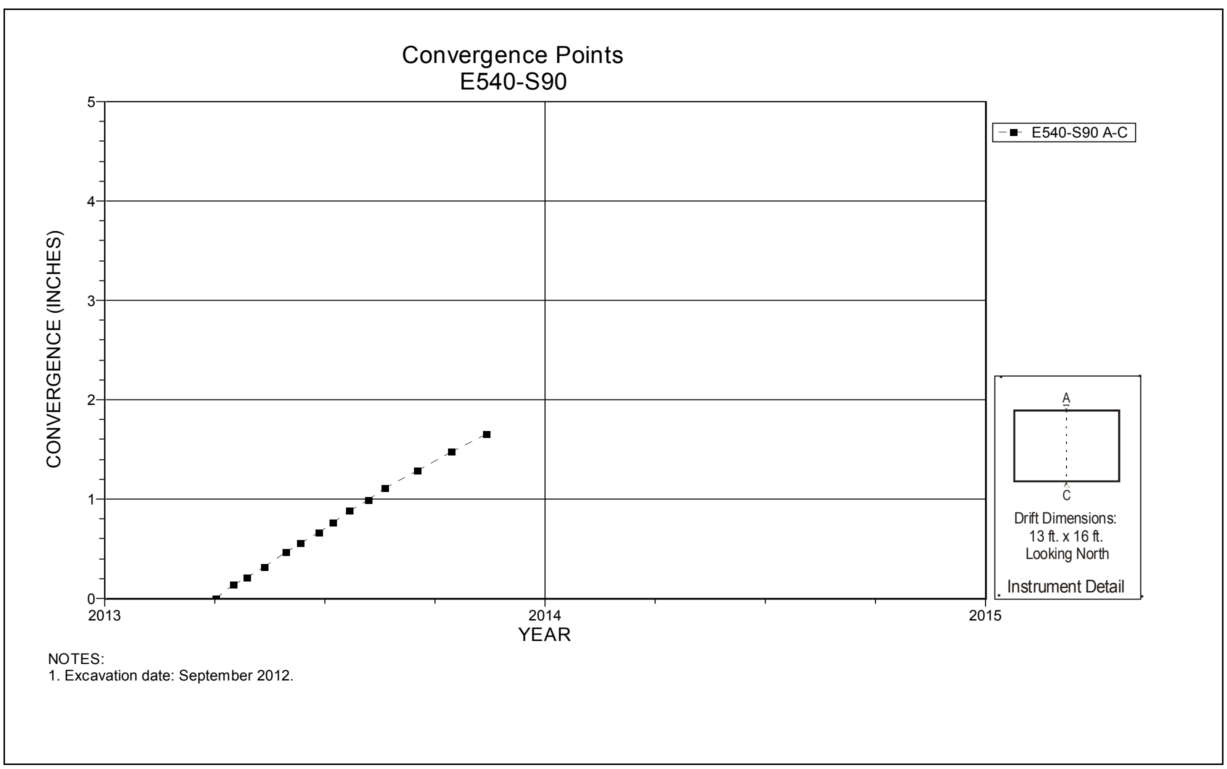

Figure 6-2 Convergence Point Array
E540 S90 – Roof to Floor

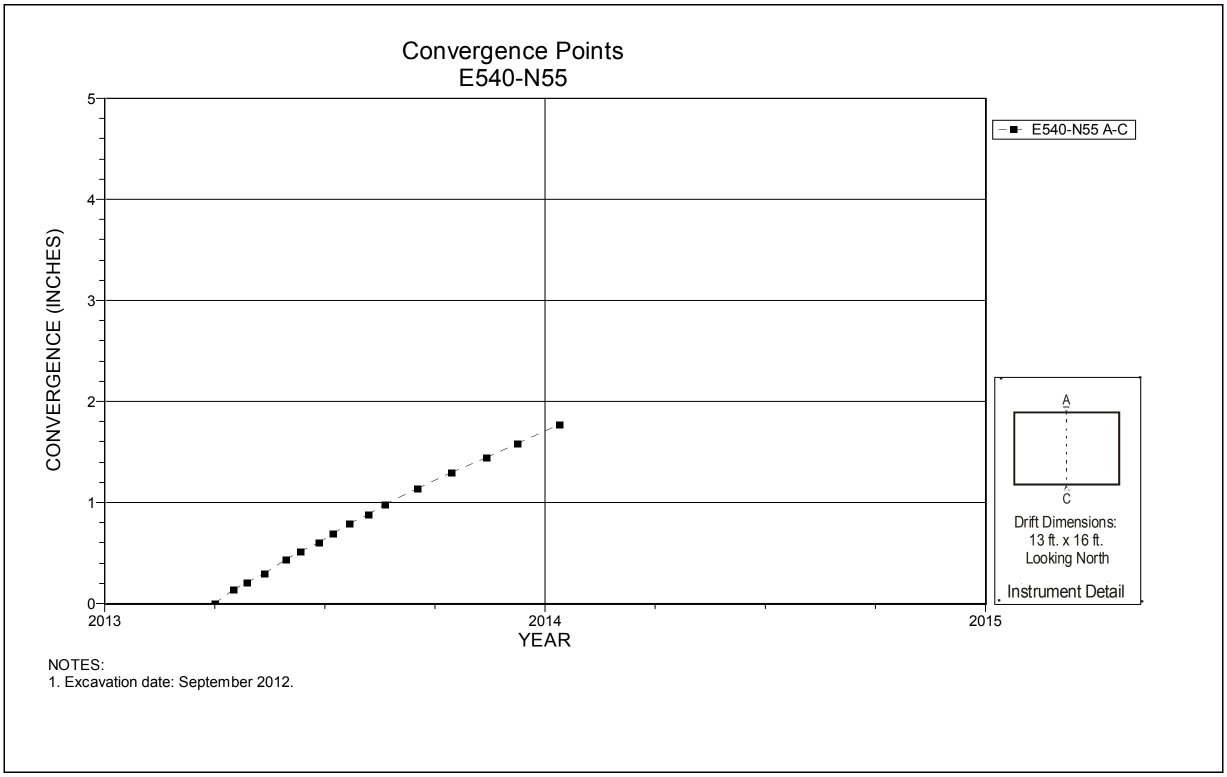

Figure 6-3 Convergence Point Array
E540 N55 – Roof to Floor

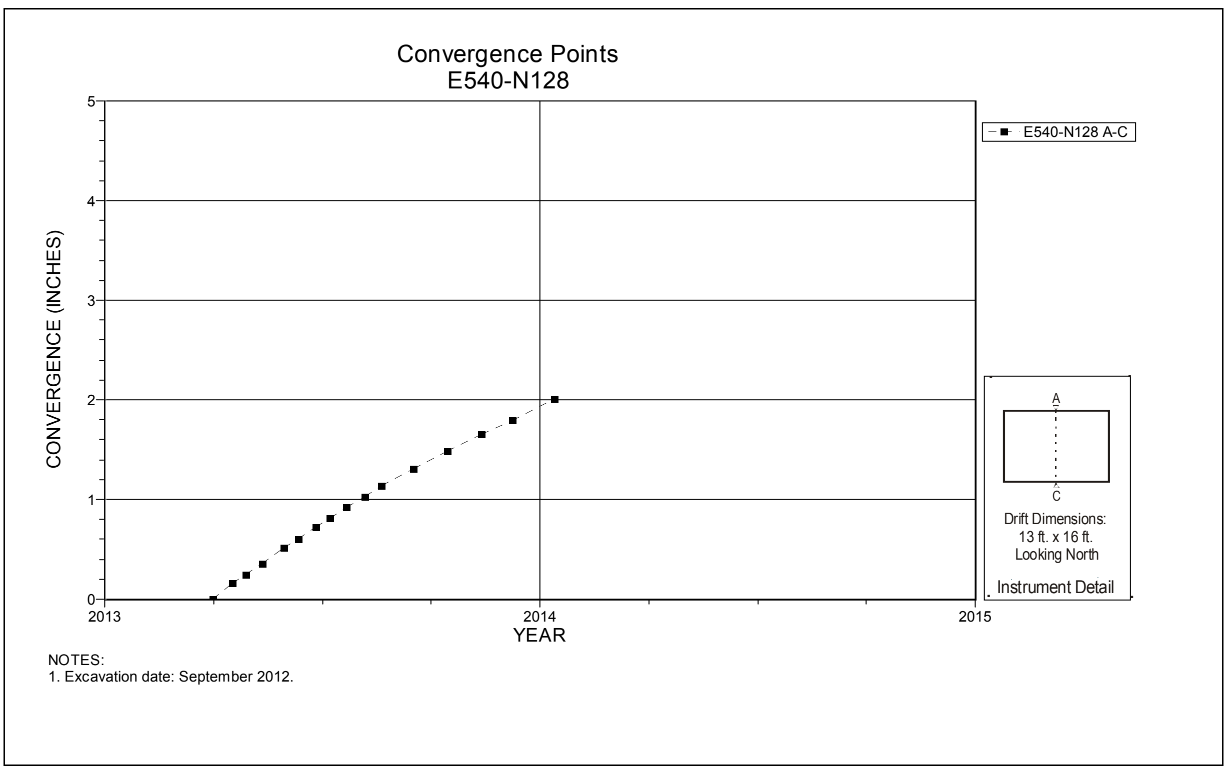

Figure 6-4 Convergence Point Array
E540 N128 – Roof to Floor

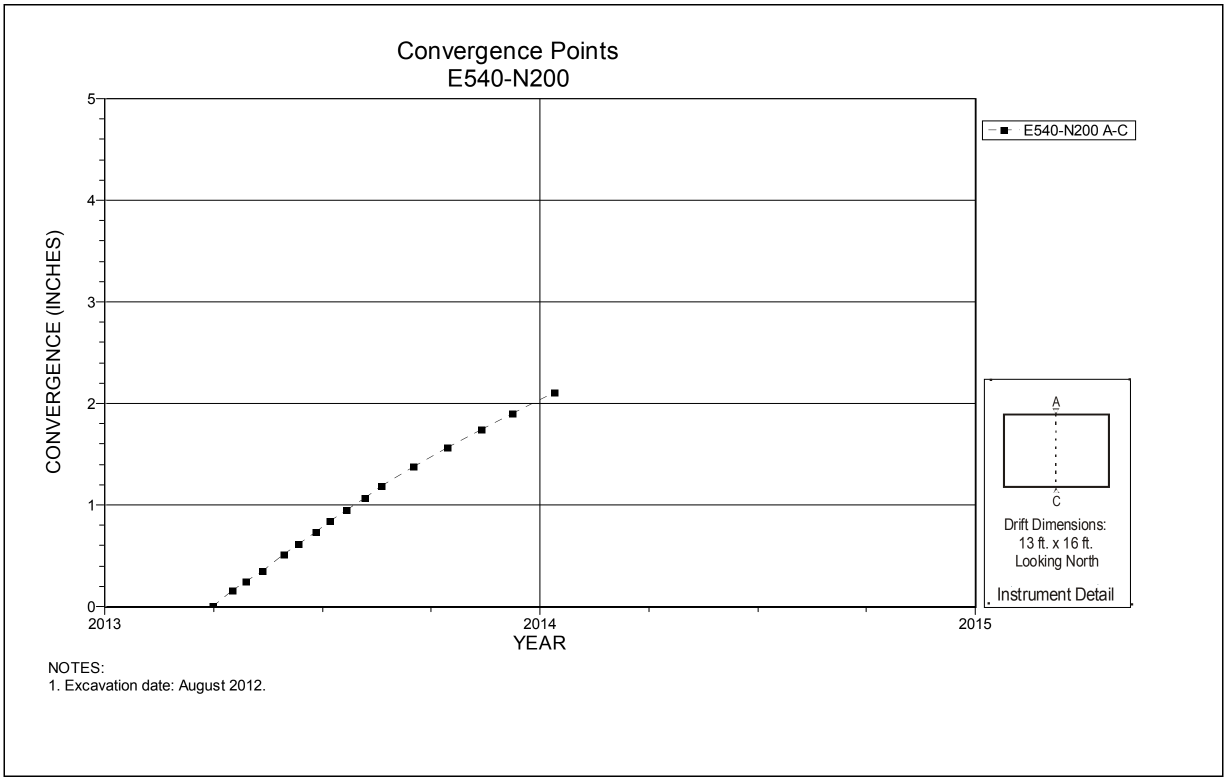

Figure 6-5 Convergence Point Array
E540 N200 – Roof to Floor

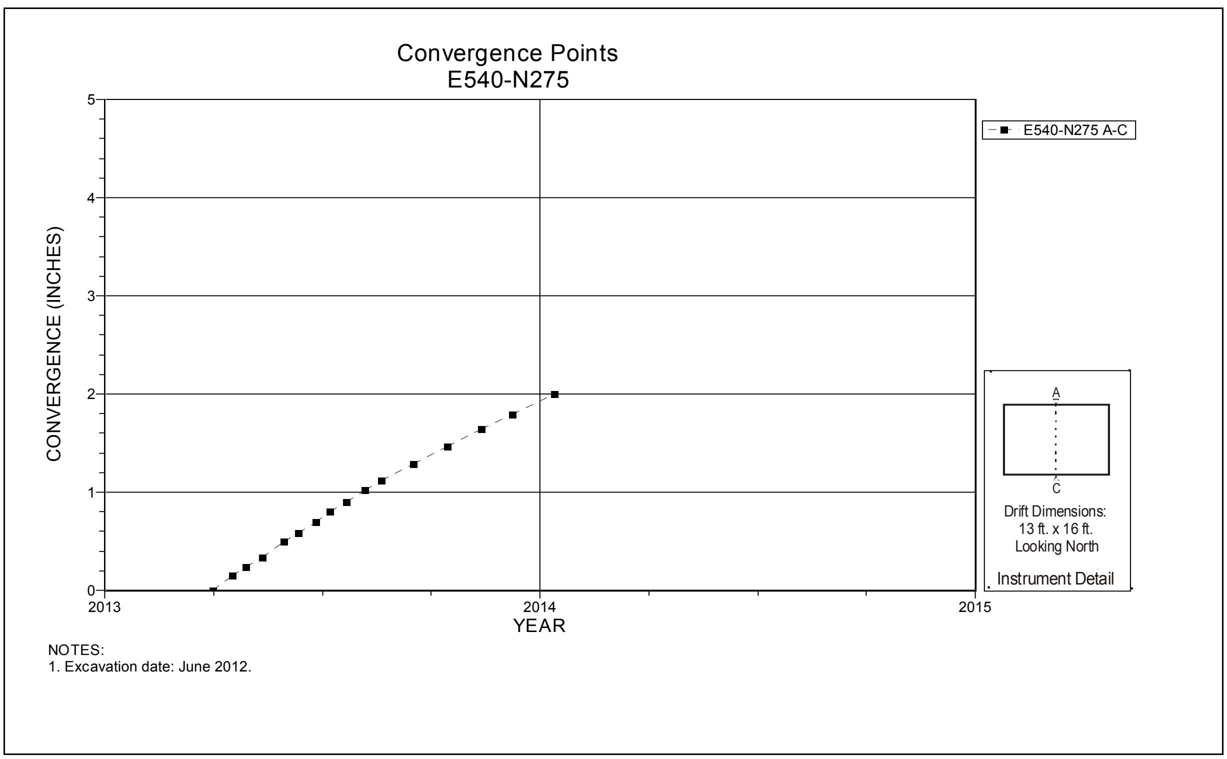

Figure 6-6 Convergence Point Array
E540 N275 – Roof to Floor

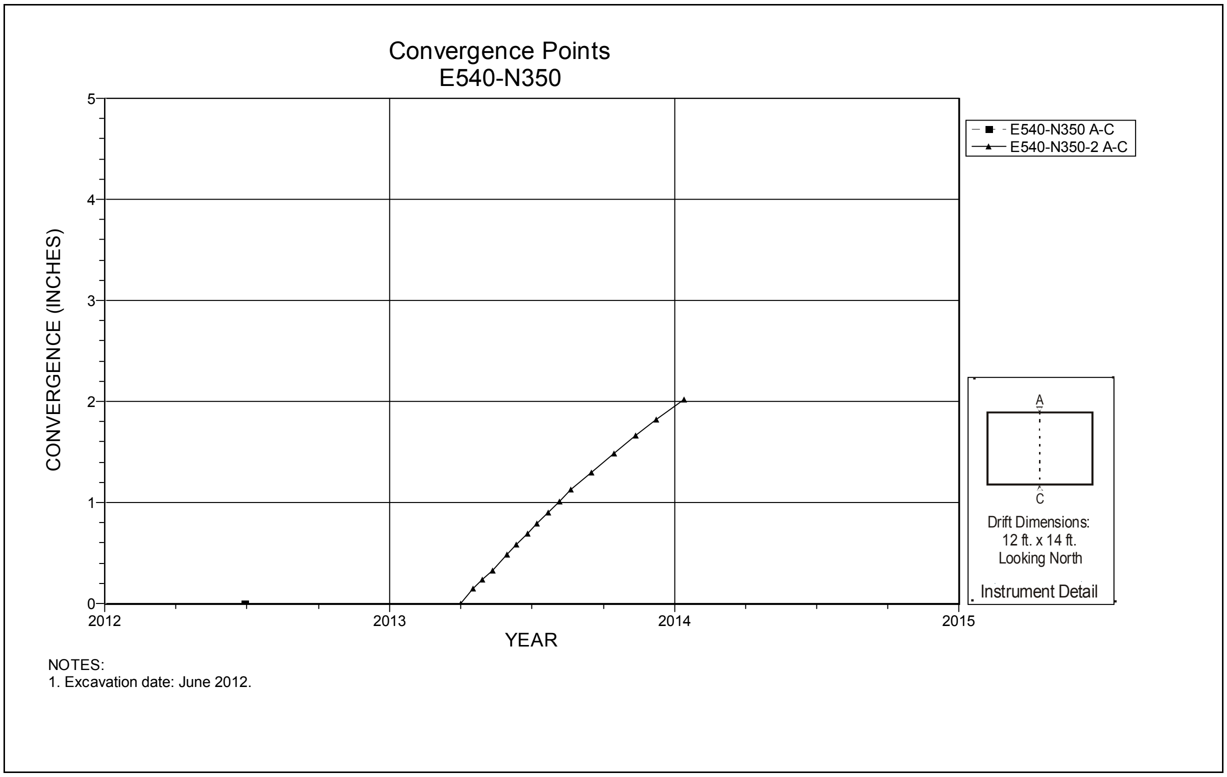

Figure 6-7 Convergence Point Array
E540 N350 – Roof to Floor

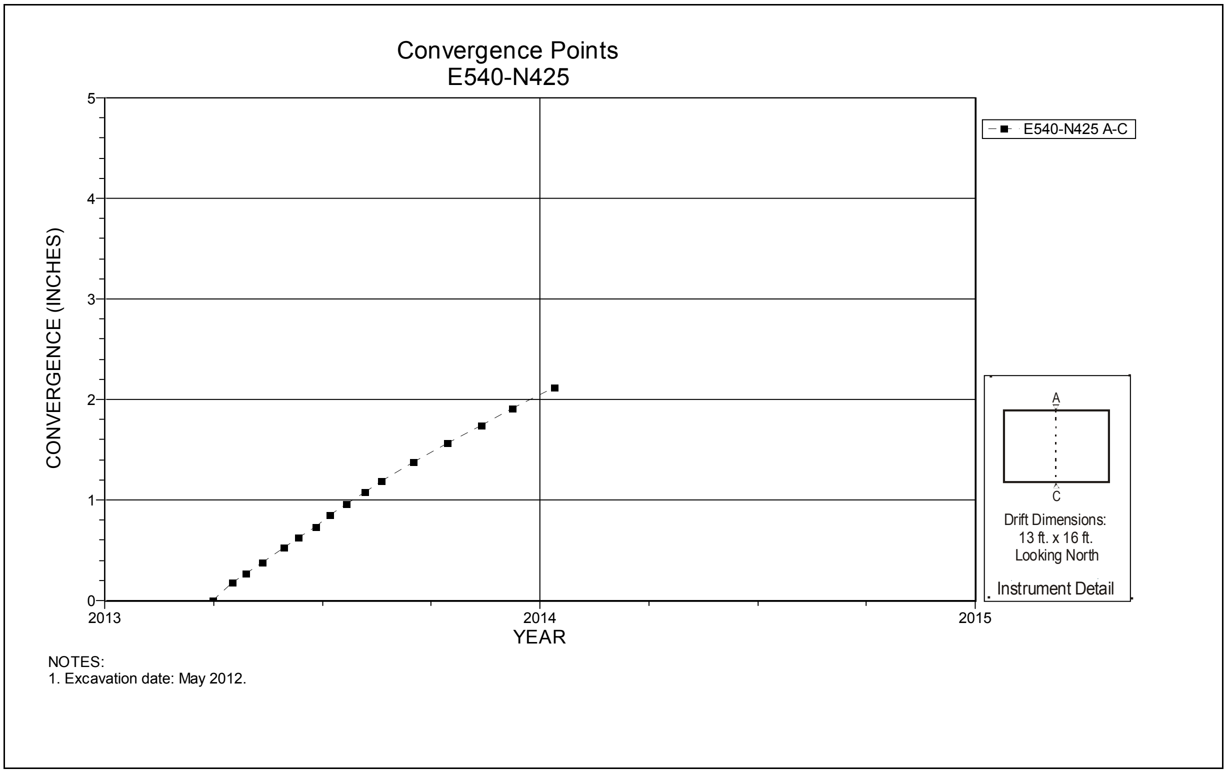

Figure 6-8 Convergence Point Array
E540 N425 – Roof to Floor

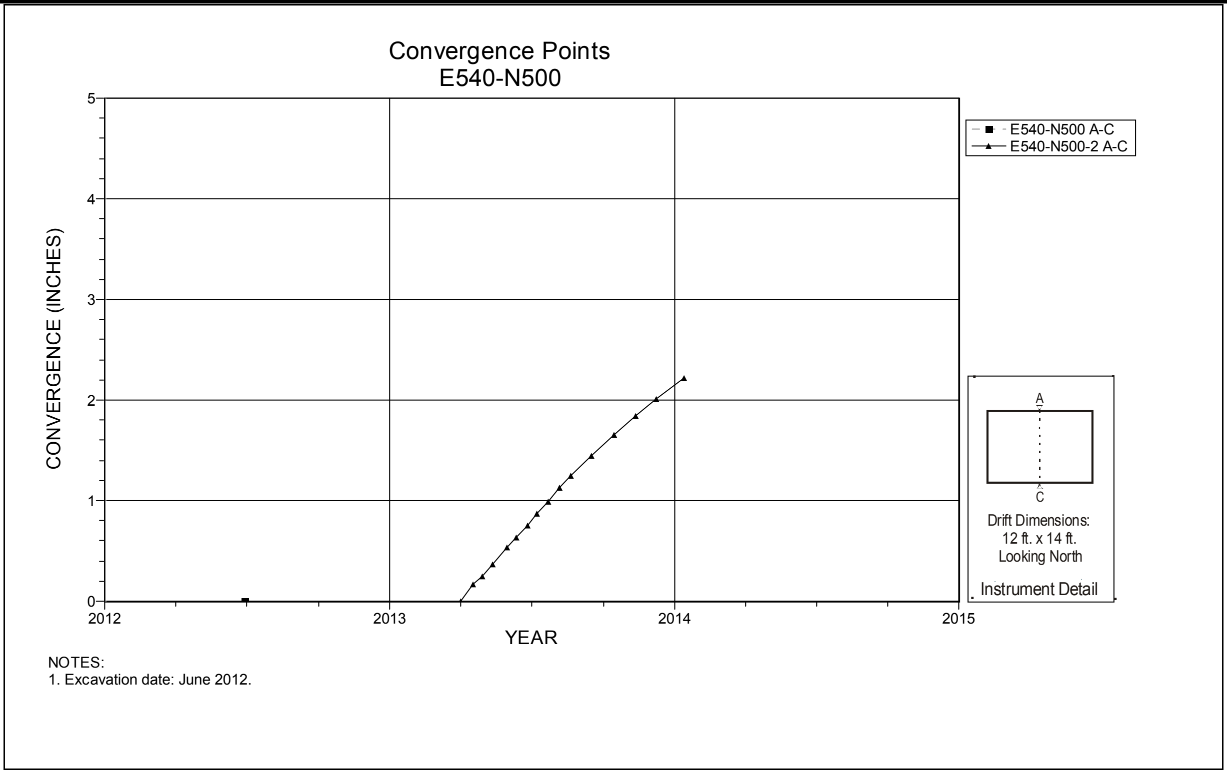

Figure 6-9 Convergence Point Array
E540 N500 – Roof to Floor

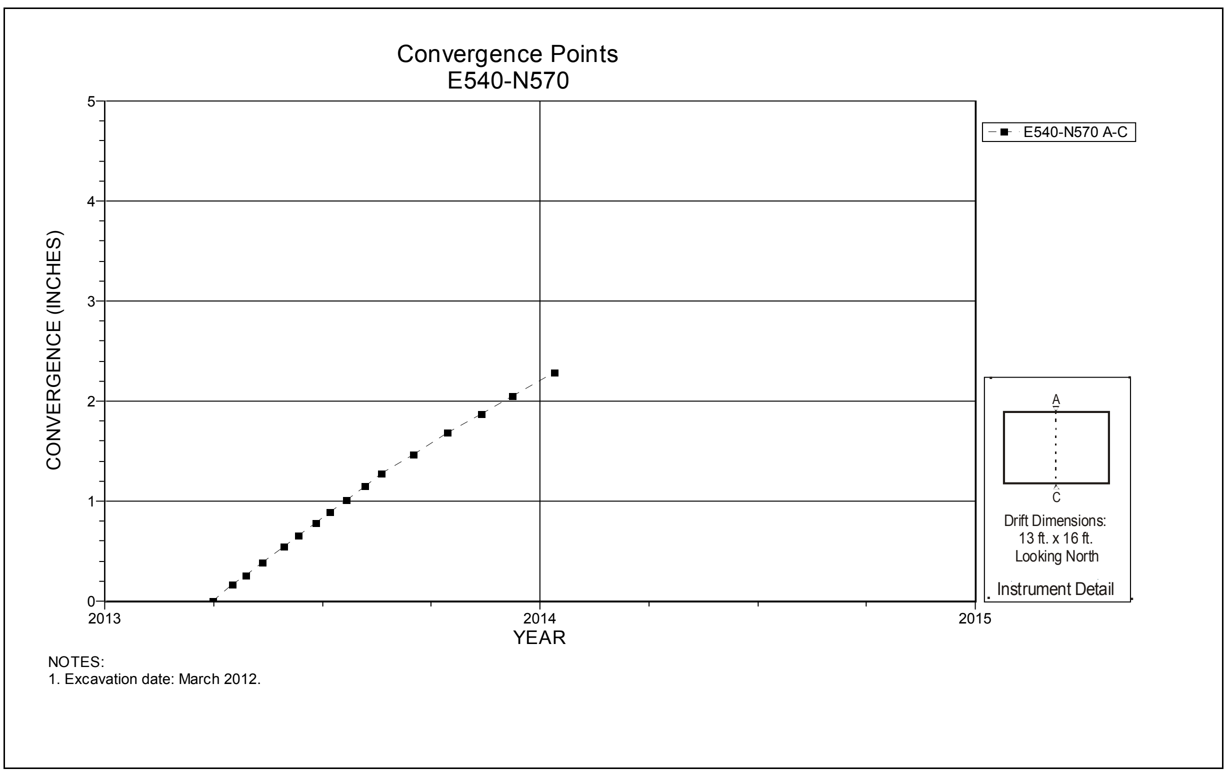

Figure 6-10 Convergence Point Array
E540 N570 – Roof to Floor

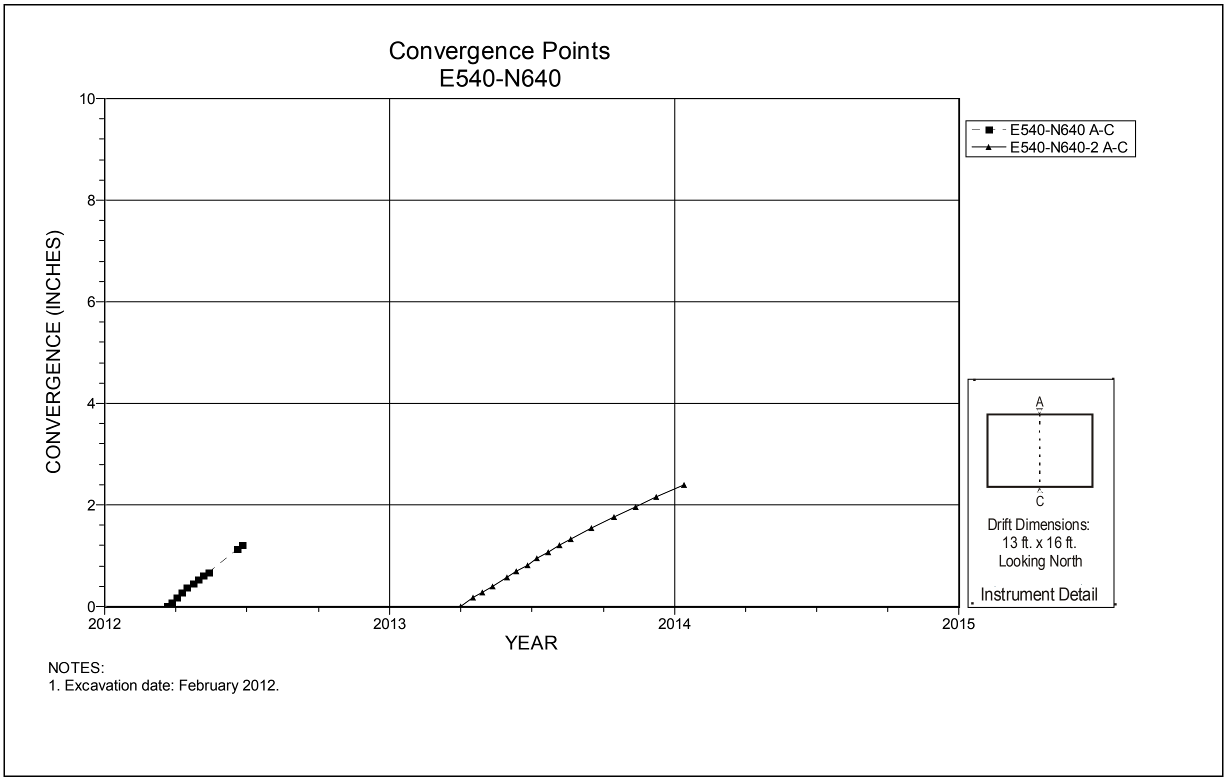

Figure 6-11 Convergence Point Array
E540 N640 – Roof to Floor

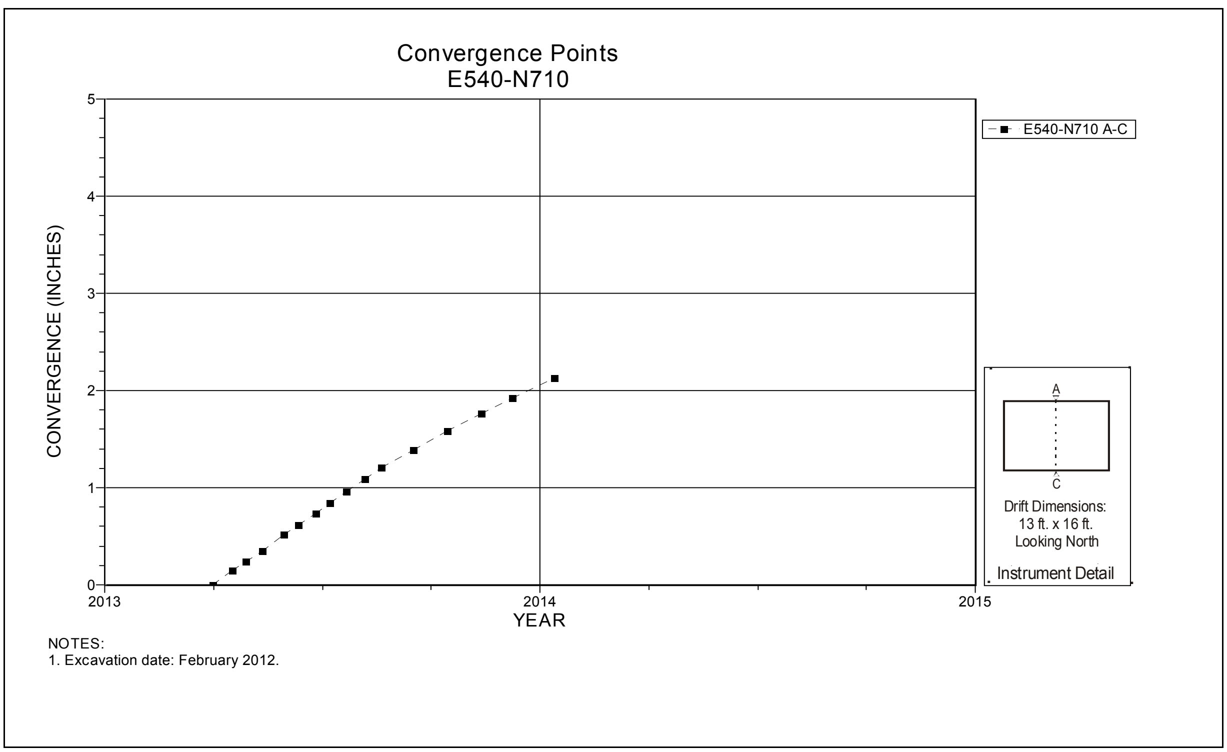

Figure 6-12 Convergence Point Array
E540 N710 – Roof to Floor

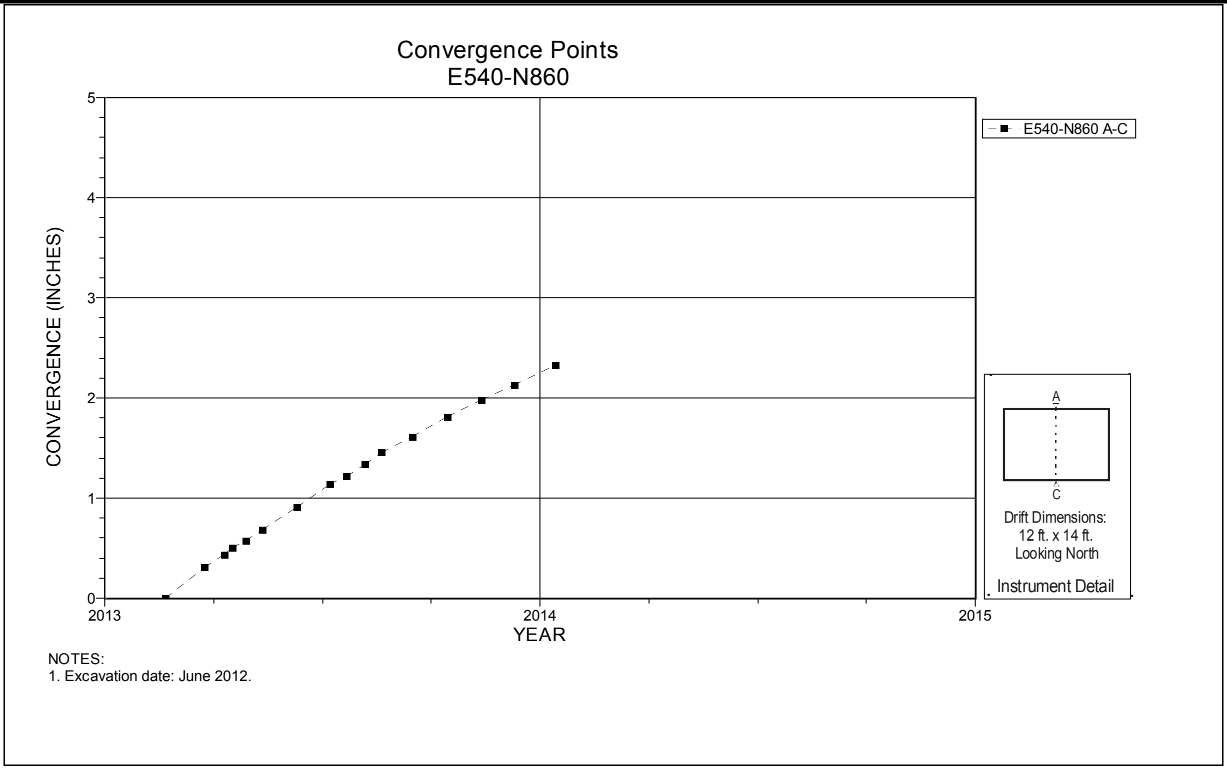

Figure 6-13 Convergence Point Array
E540 N860 – Roof to Floor

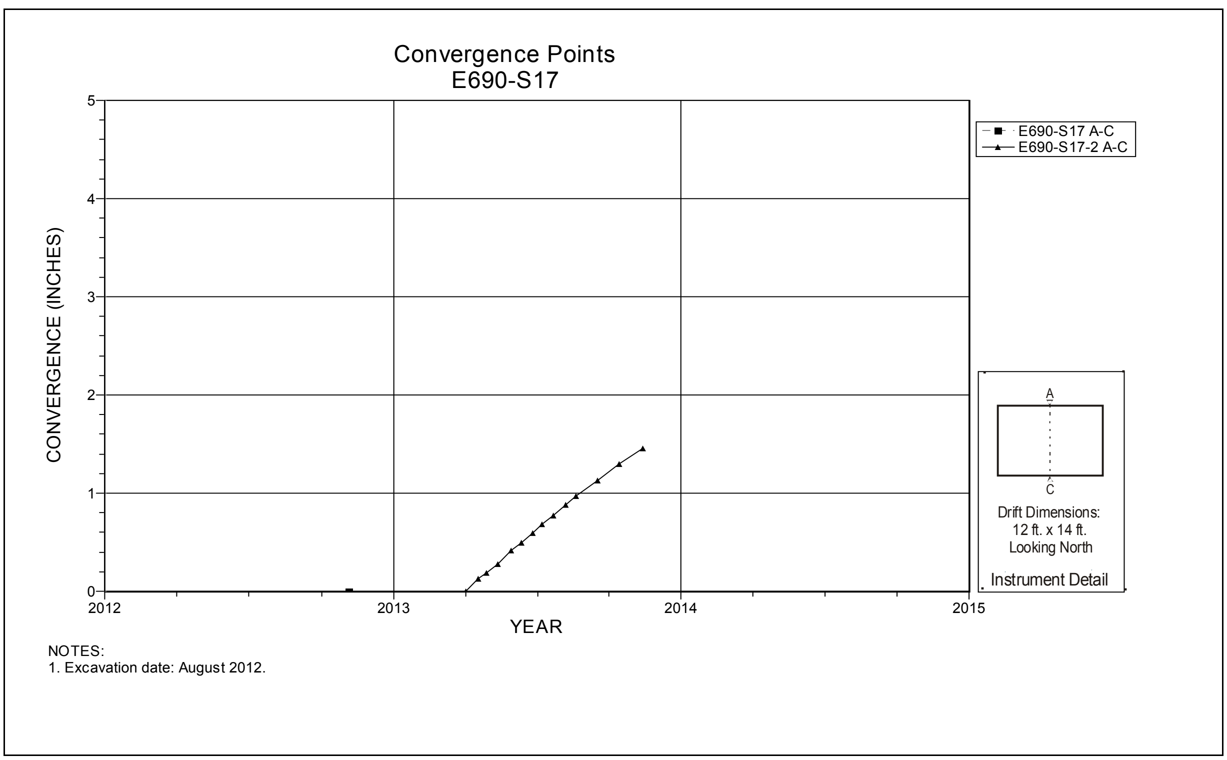

Figure 6-14 Convergence Point Array
E690 S17 – Roof to Floor

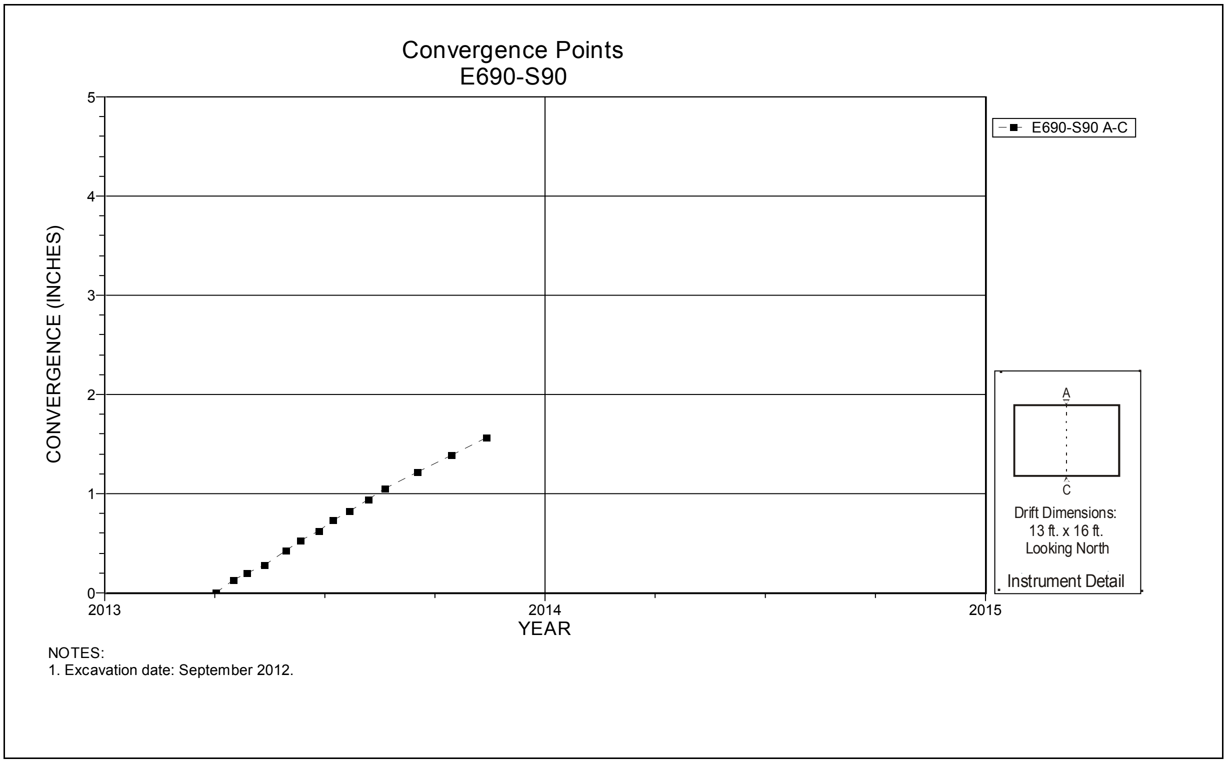

Figure 6-15 Convergence Point Array
E690 S90 – Roof to Floor

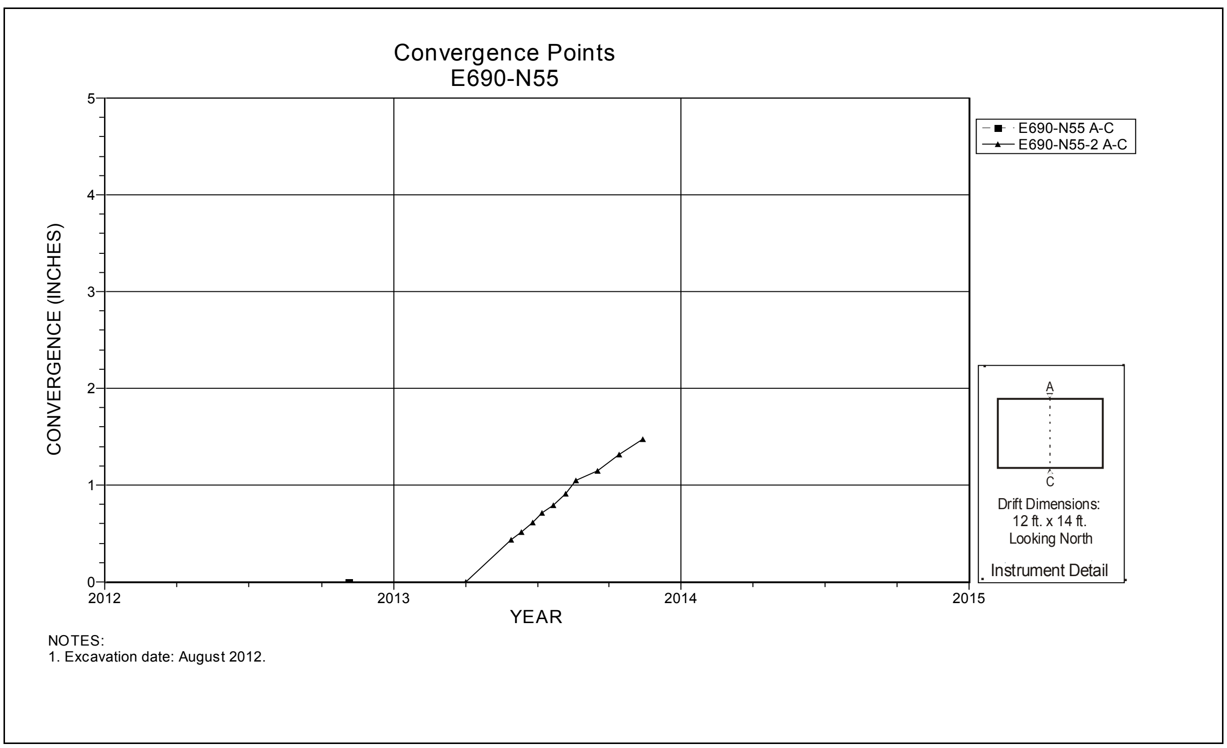

Figure 6-16 Convergence Point Array
E690 N55 – Roof to Floor

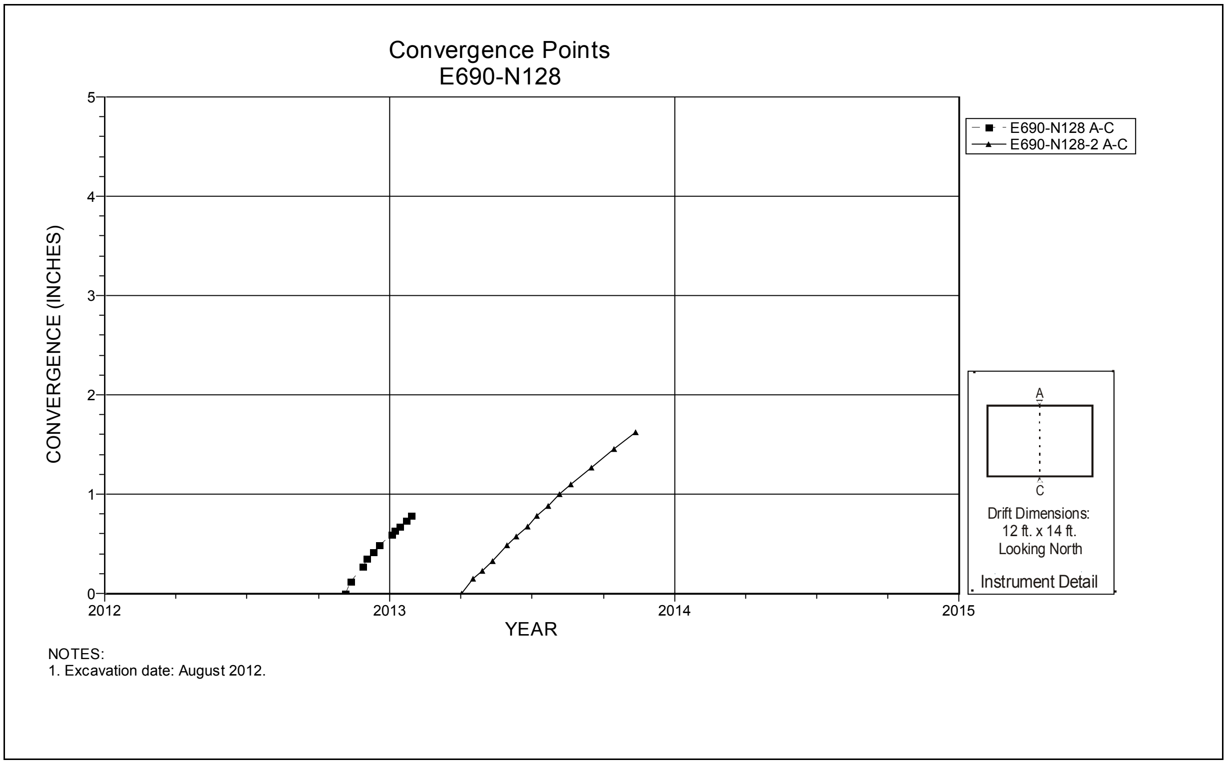

Figure 6-17 Convergence Point Array
E690 N128 – Roof to Floor

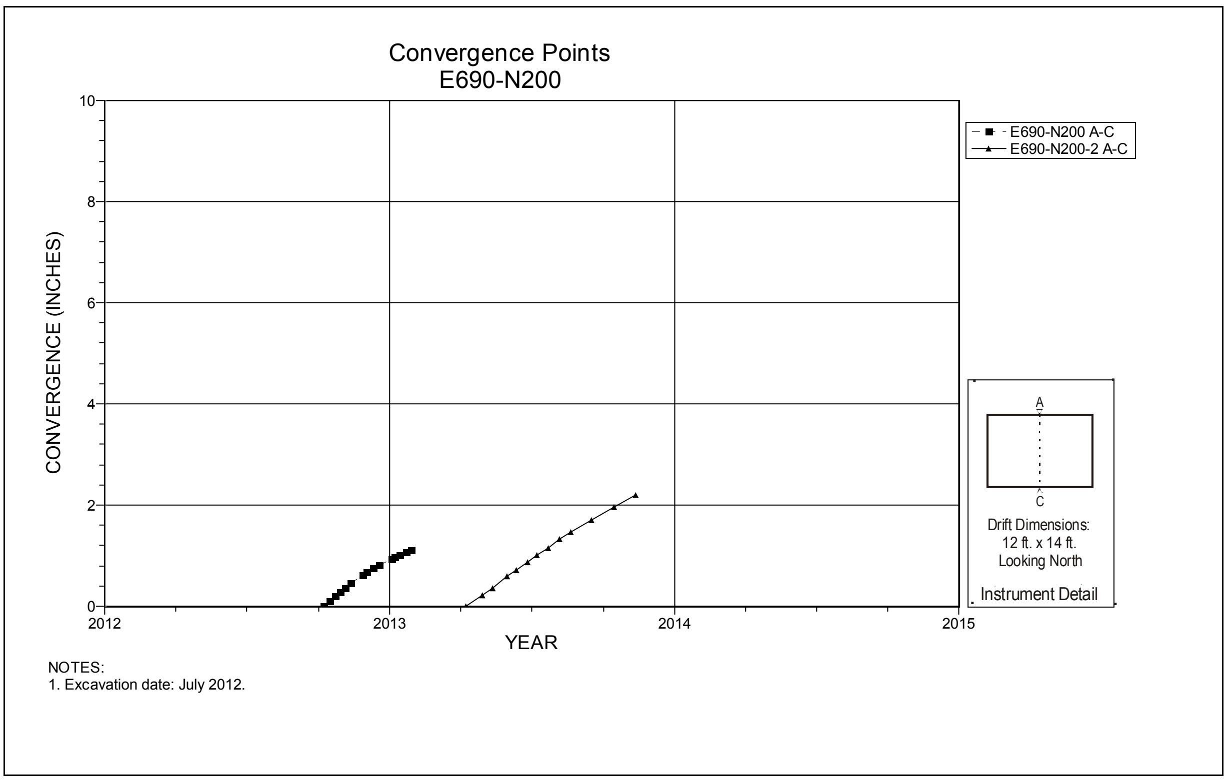

Figure 6-18 Convergence Point Array
E690 N200 – Roof to Floor

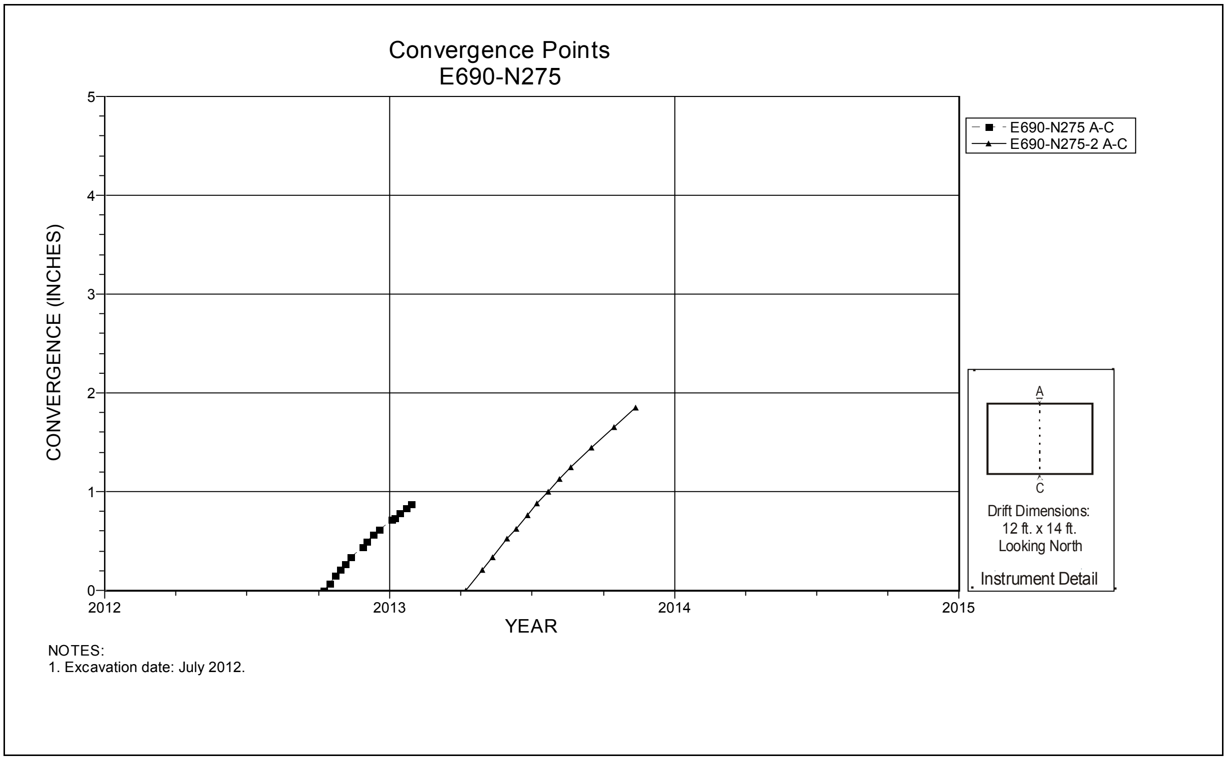

Figure 6-19 Convergence Point Array
E690 N275 – Roof to Floor

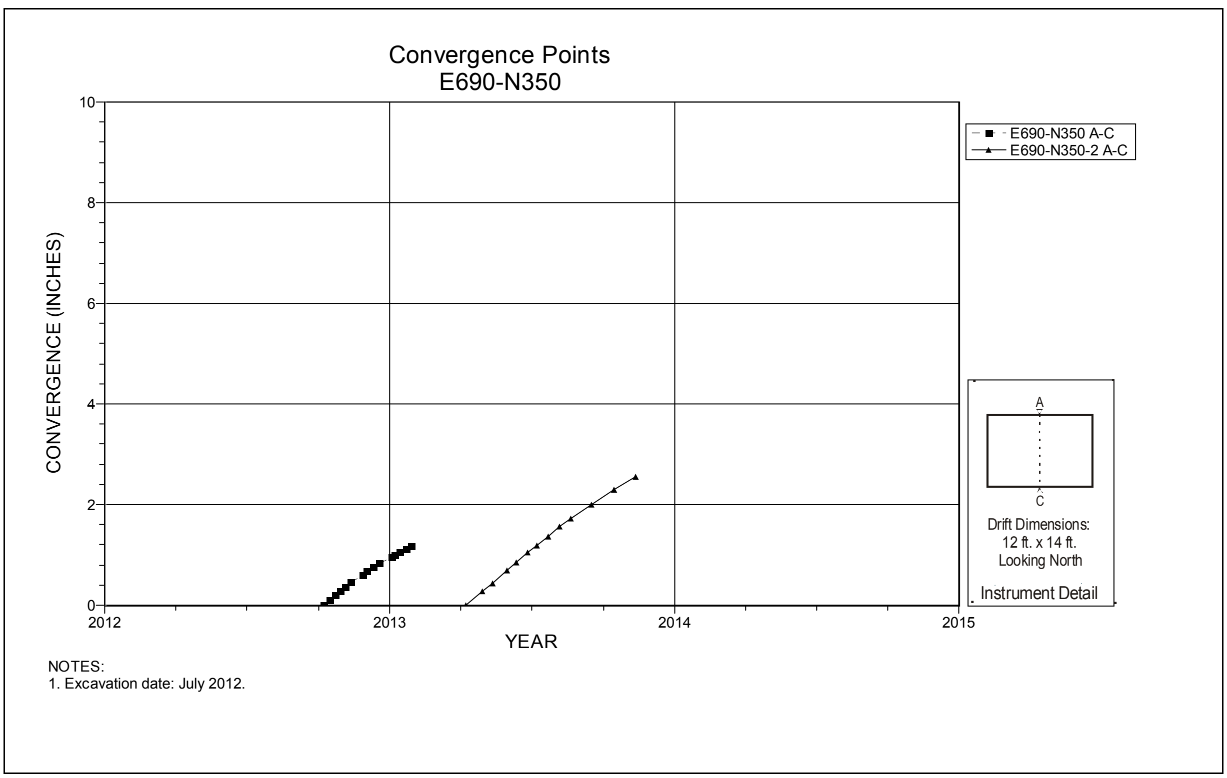

Figure 6-20 Convergence Point Array
E690 N350 – Roof to Floor

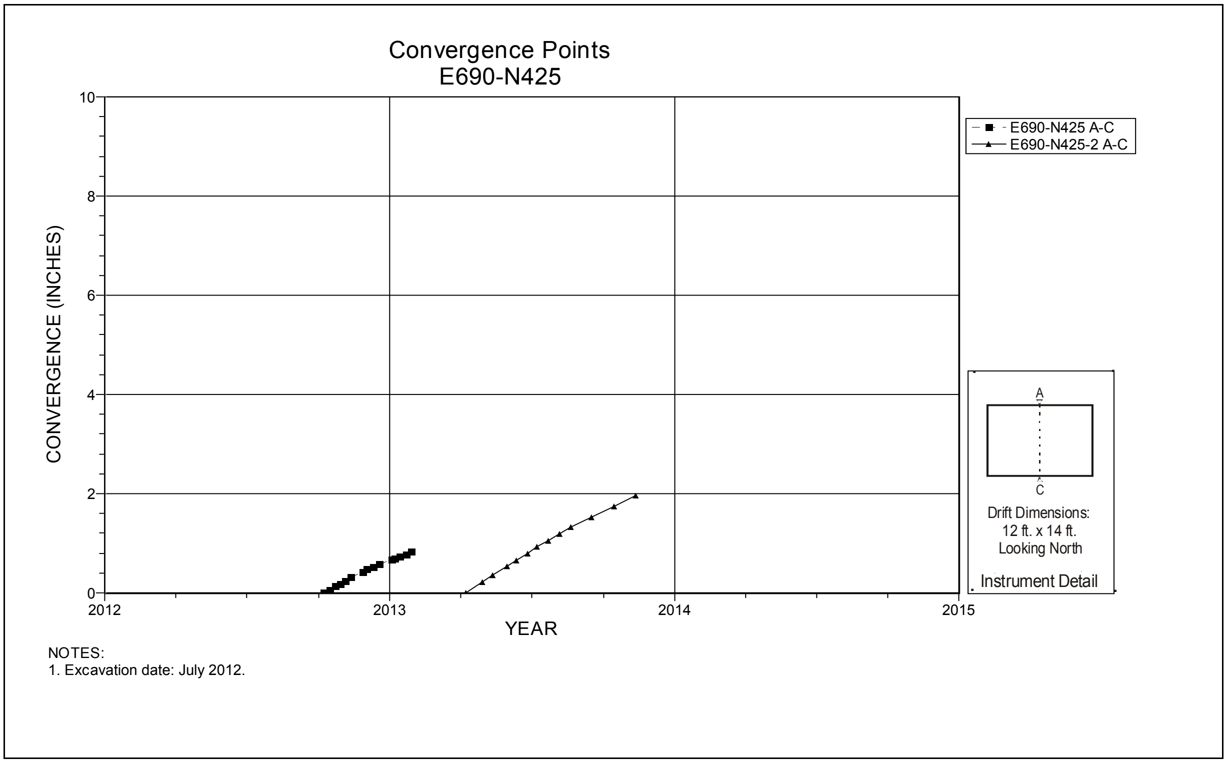

Figure 6-21 Convergence Point Array
E690 N425 – Roof to Floor

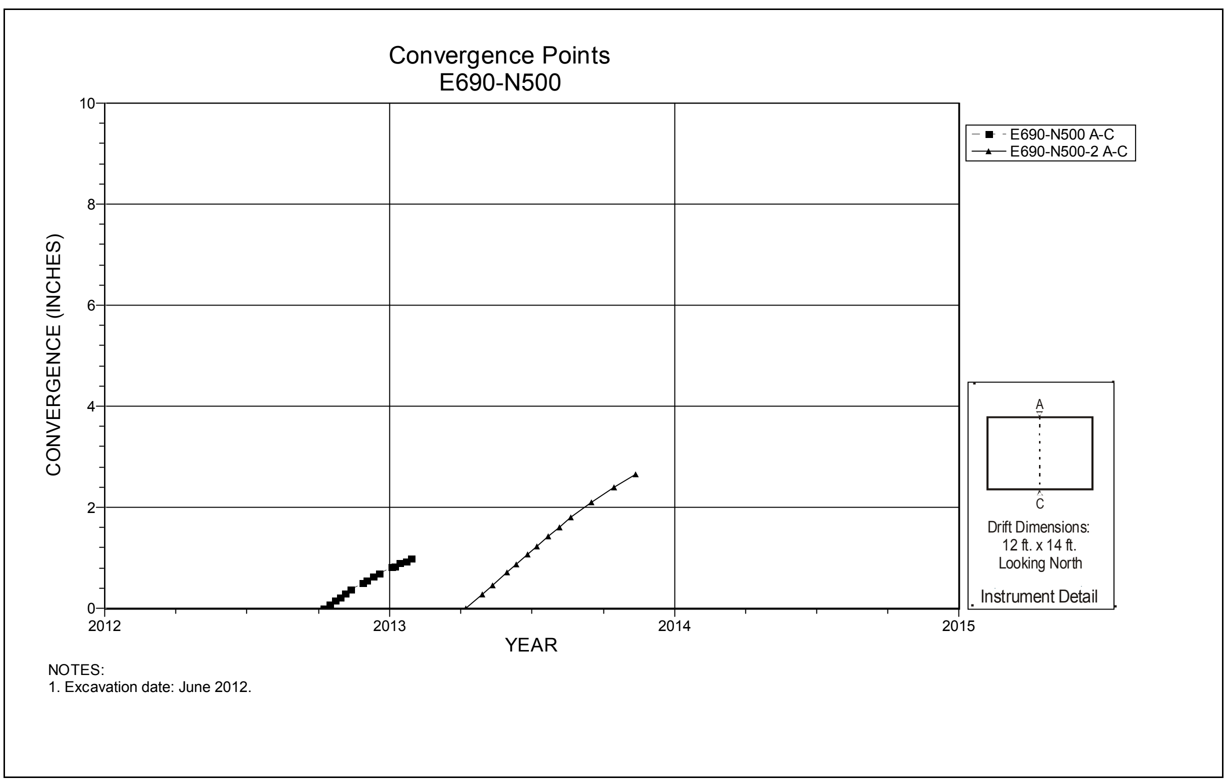

Figure 6-22 Convergence Point Array
E690 N500 – Roof to Floor

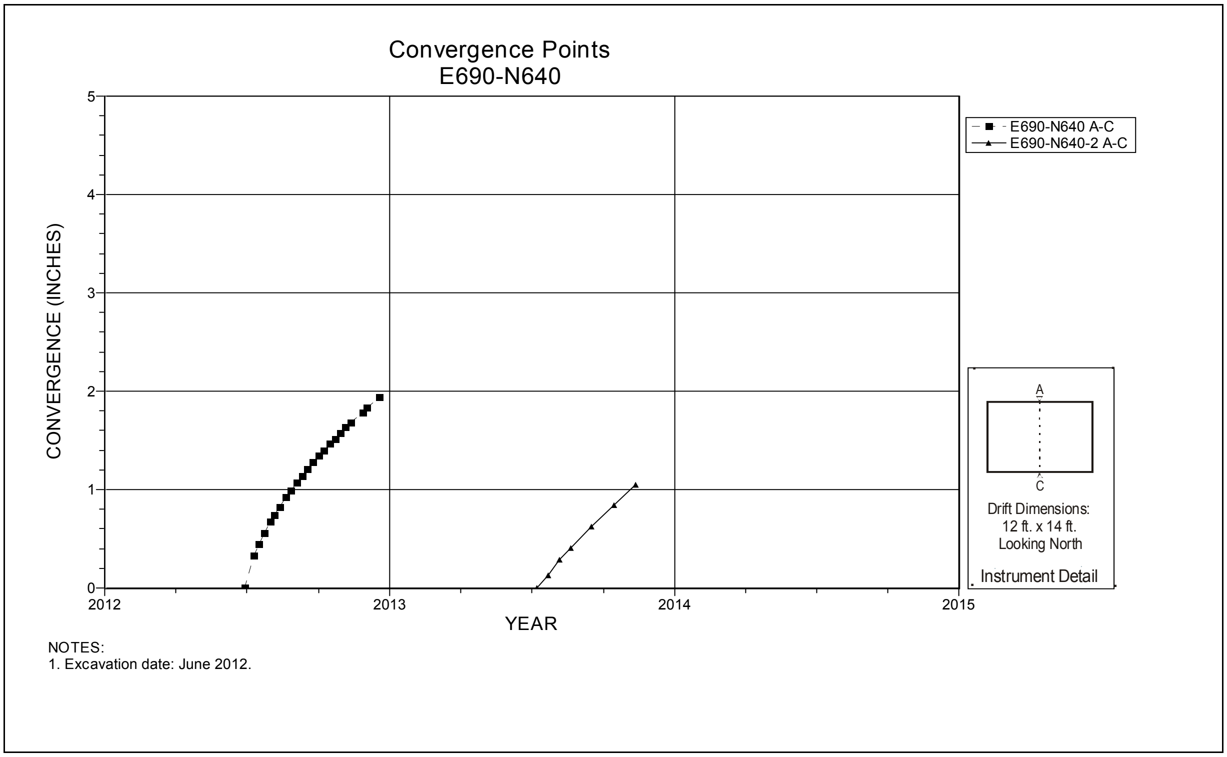

Figure 6-23 Convergence Point Array
E690 N640 – Roof to Floor

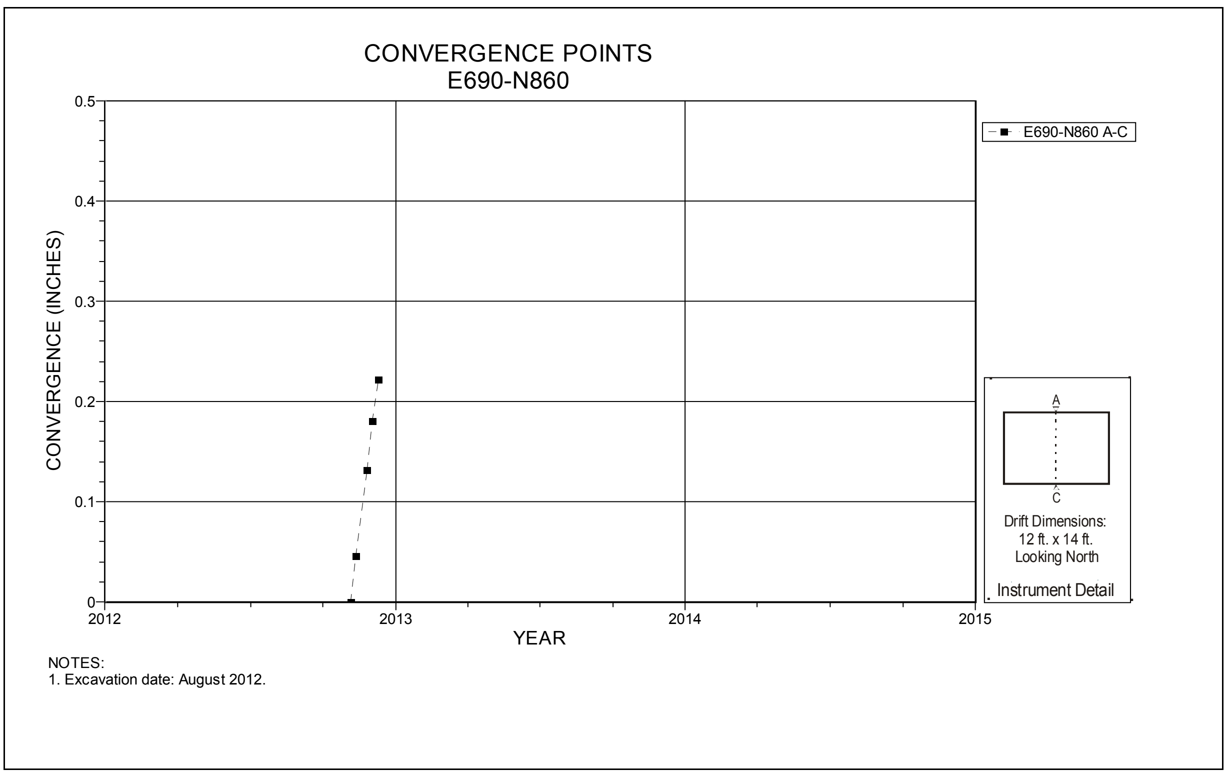

Figure 6-24 Convergence Point Array
E690 N860 – Roof to Floor

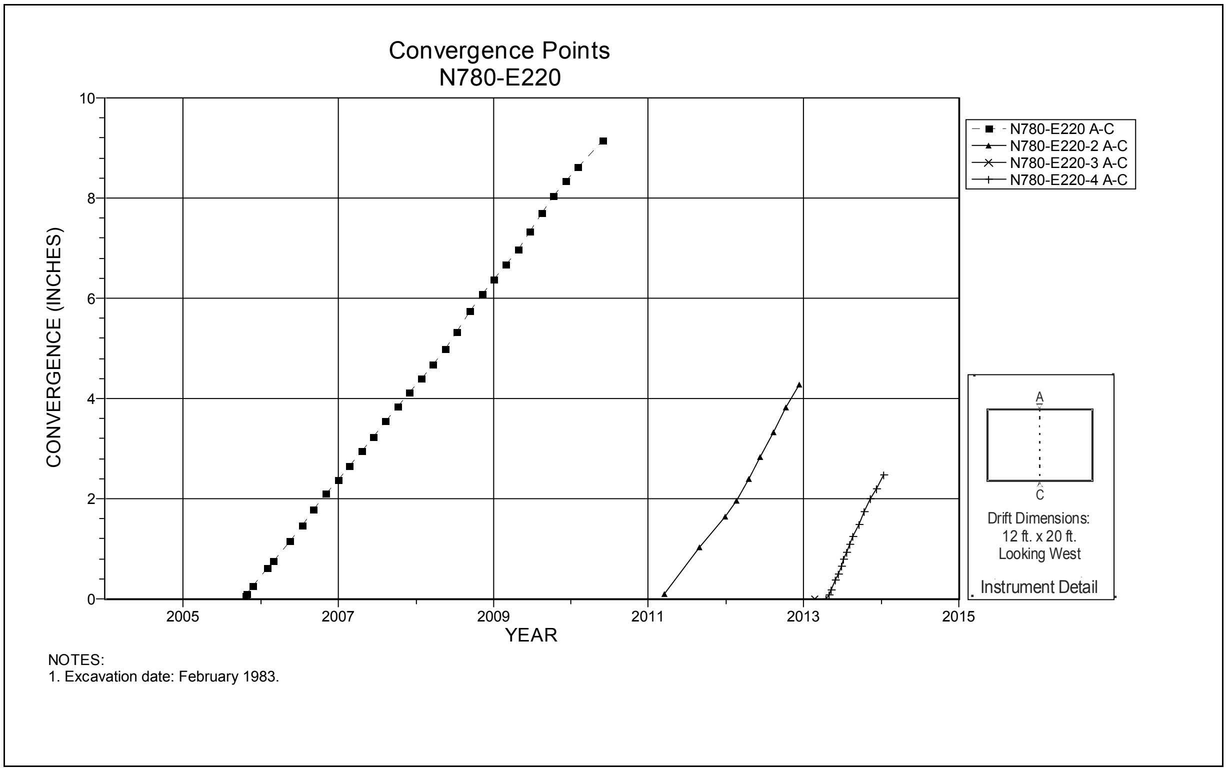

Figure 6-25 Convergence Point Array
N780 E220 – Roof to Floor

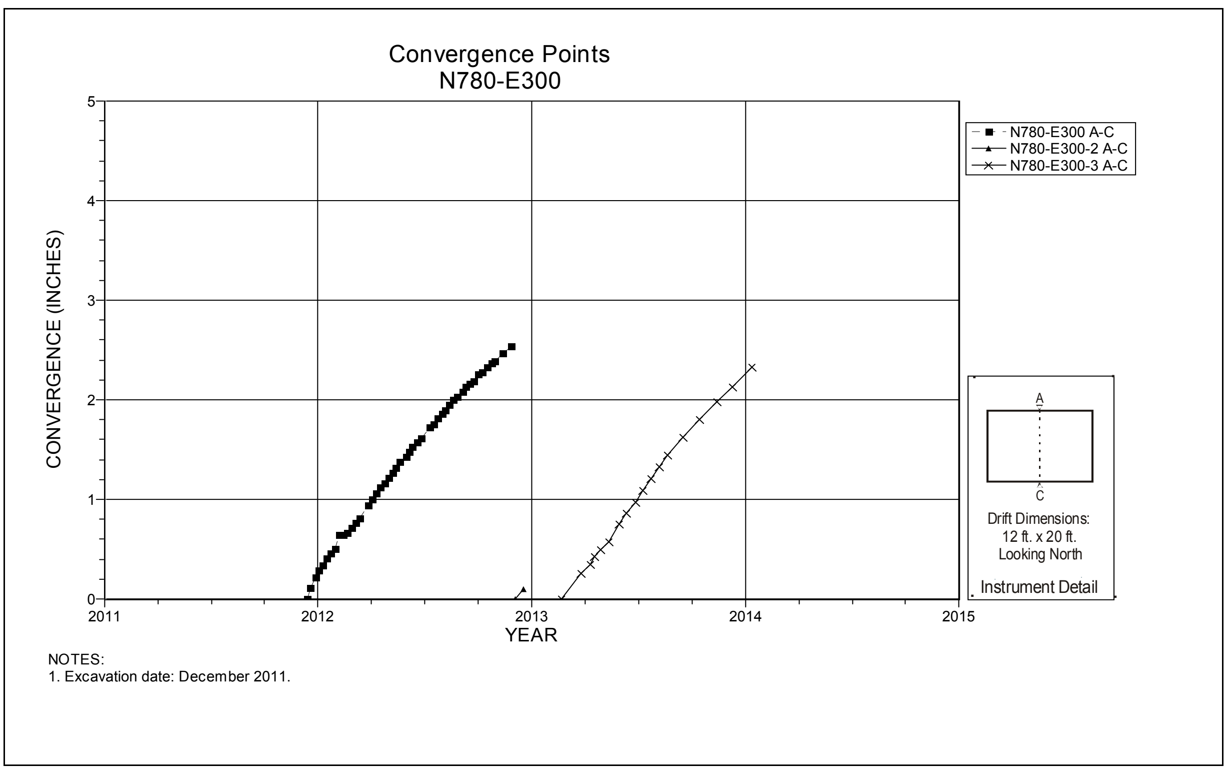

Figure 6-26 Convergence Point Array
N780 E300 – Roof to Floor

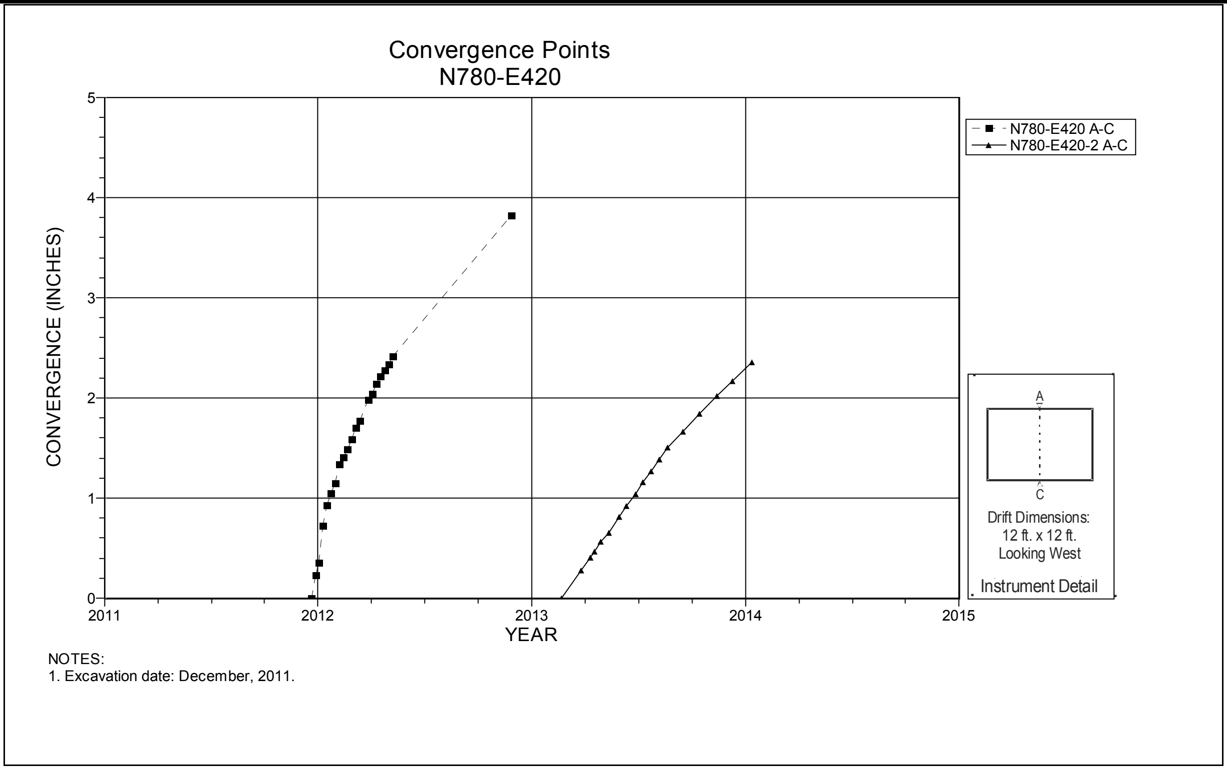

Figure 6-27 Convergence Point Array
N780 E420 – Roof to Floor

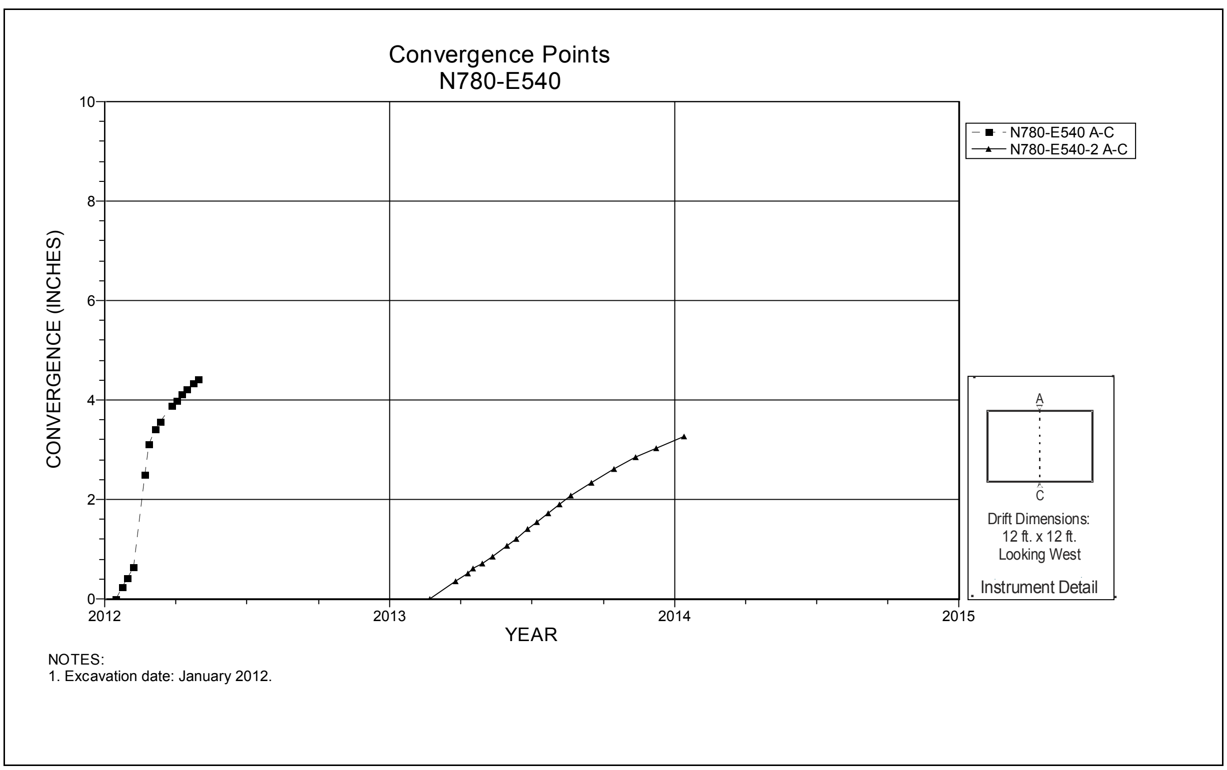

Figure 6-28 Convergence Point Array
N780 E540 – Roof to Floor

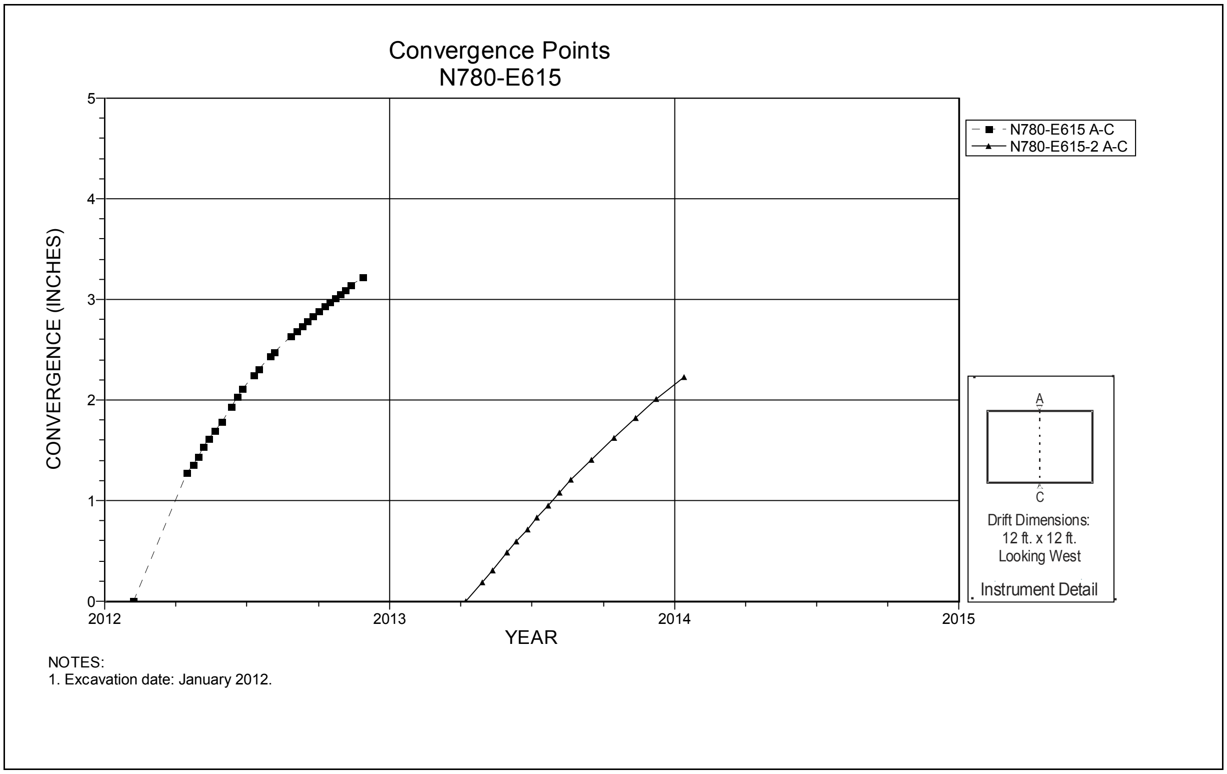

Figure 6-29 Convergence Point Array
N780 E615 – Roof to Floor

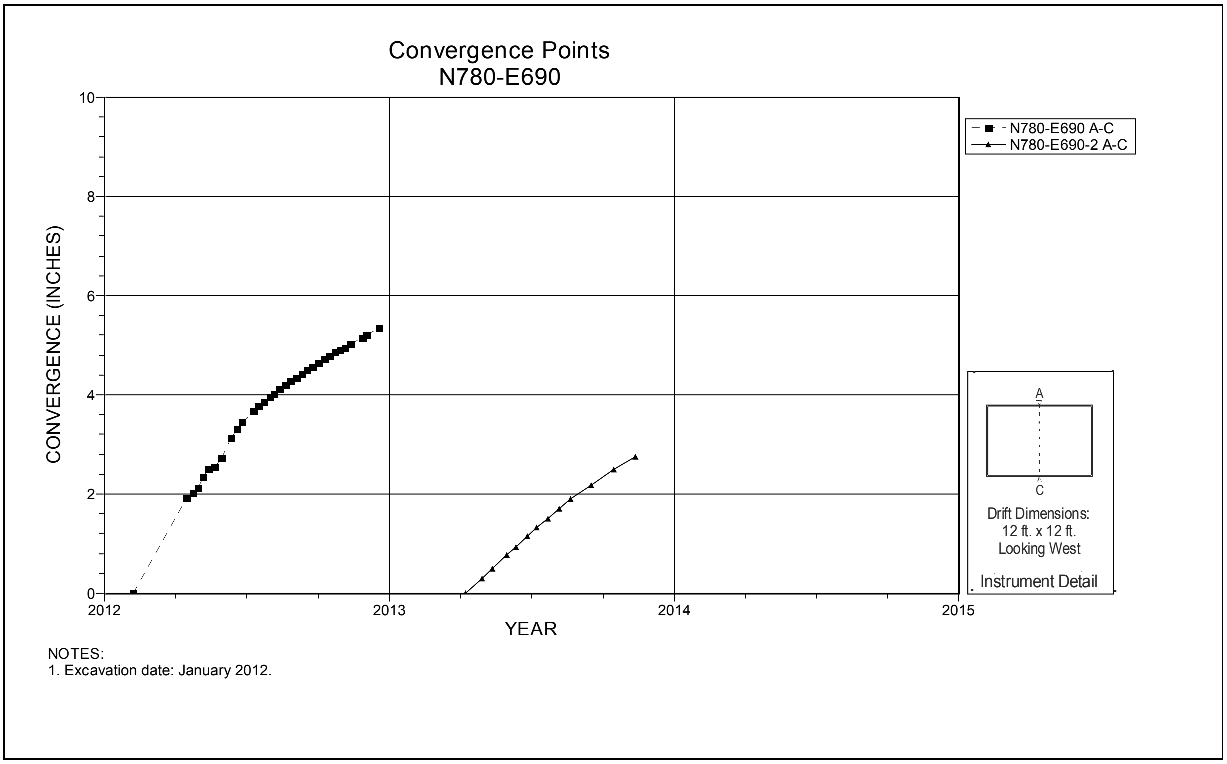

Figure 6-30 Convergence Point Array
N780 E690 – Roof to Floor

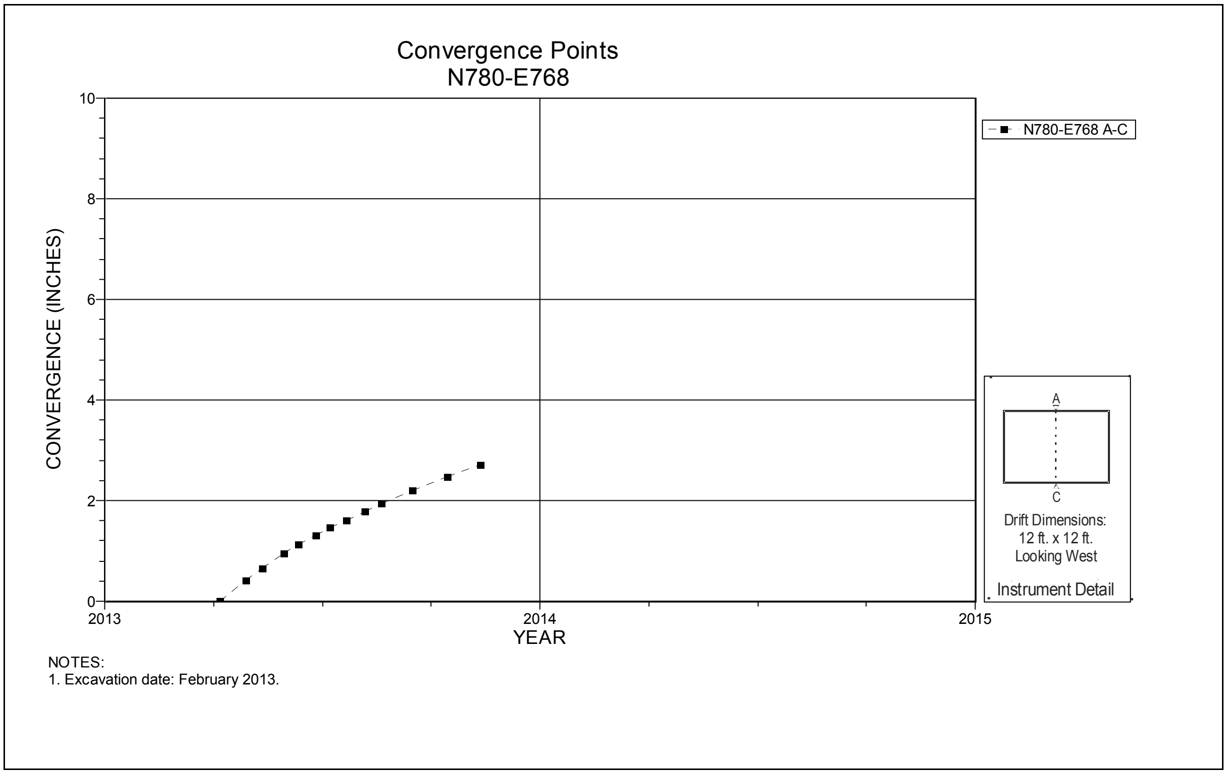

Figure 6-31 Convergence Point Array
N780 E768 – Roof to Floor

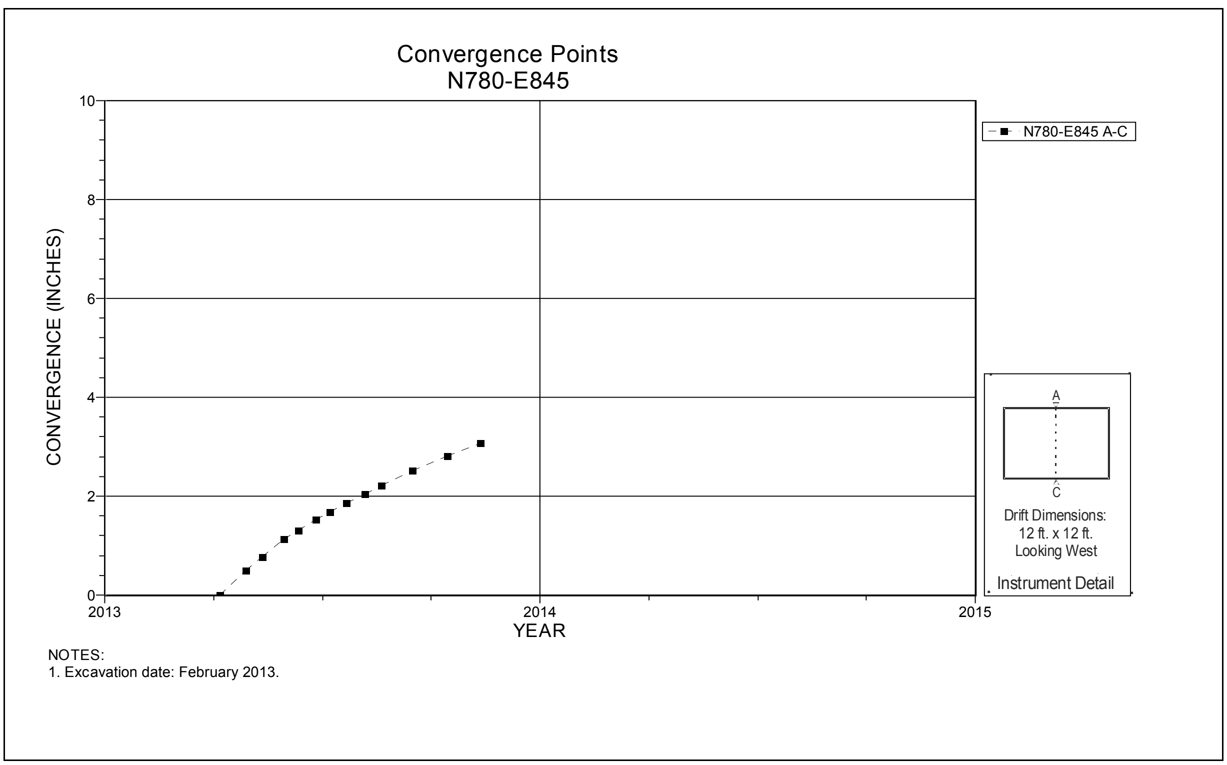

Figure 6-32 Convergence Point Array
N780 E845 – Roof to Floor

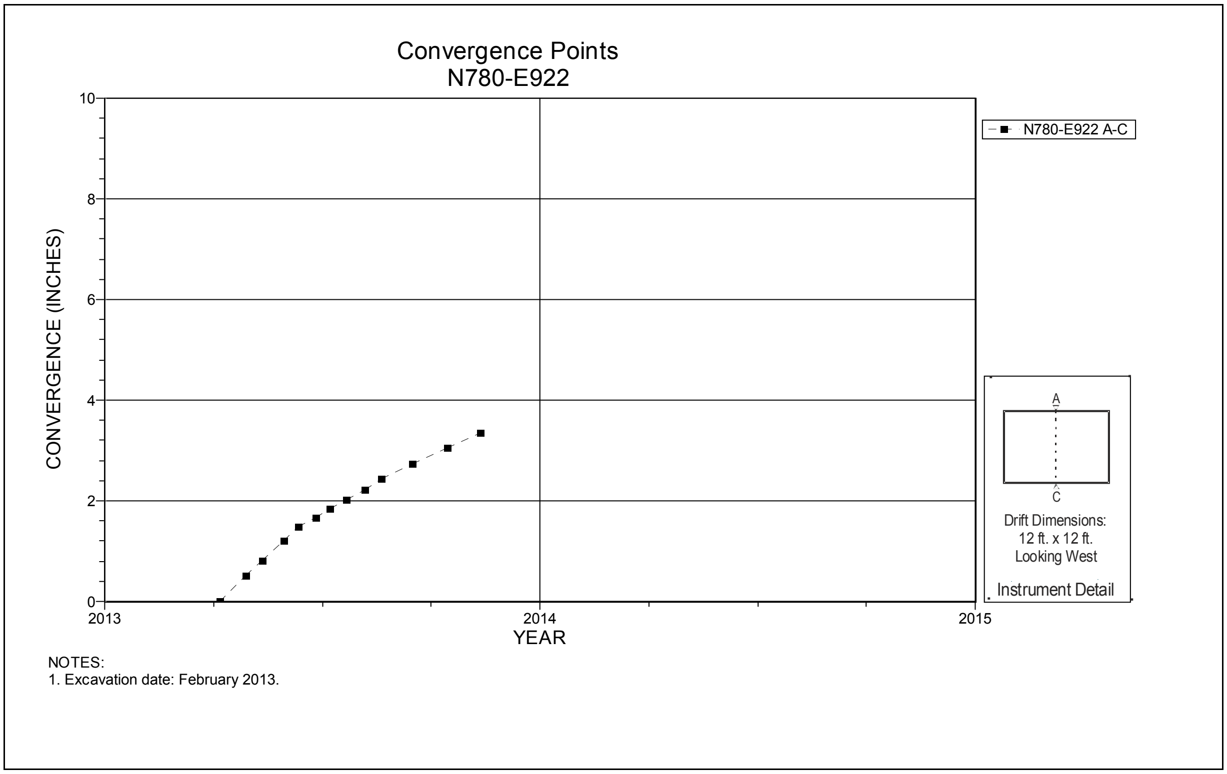

Figure 6-33 Convergence Point Array
N780 E922 – Roof to Floor

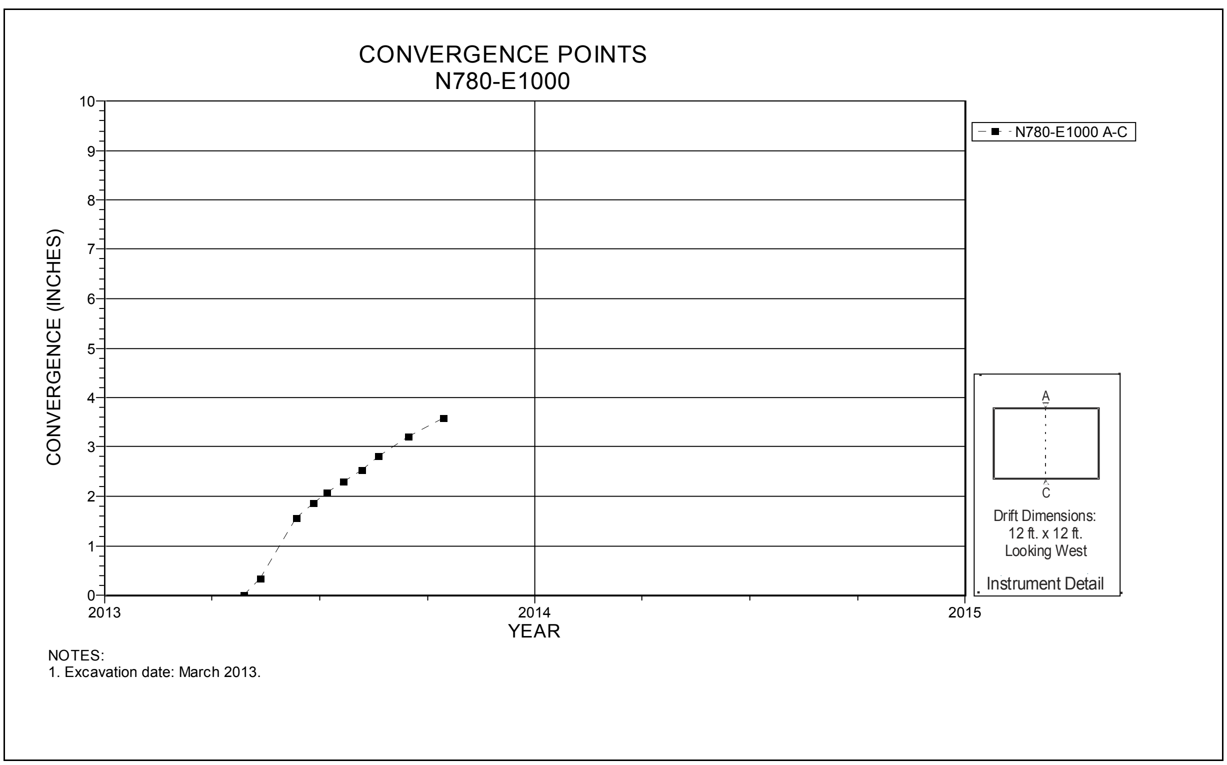

Figure 6-34 Convergence Point Array
N780 E1000 – Roof to Floor

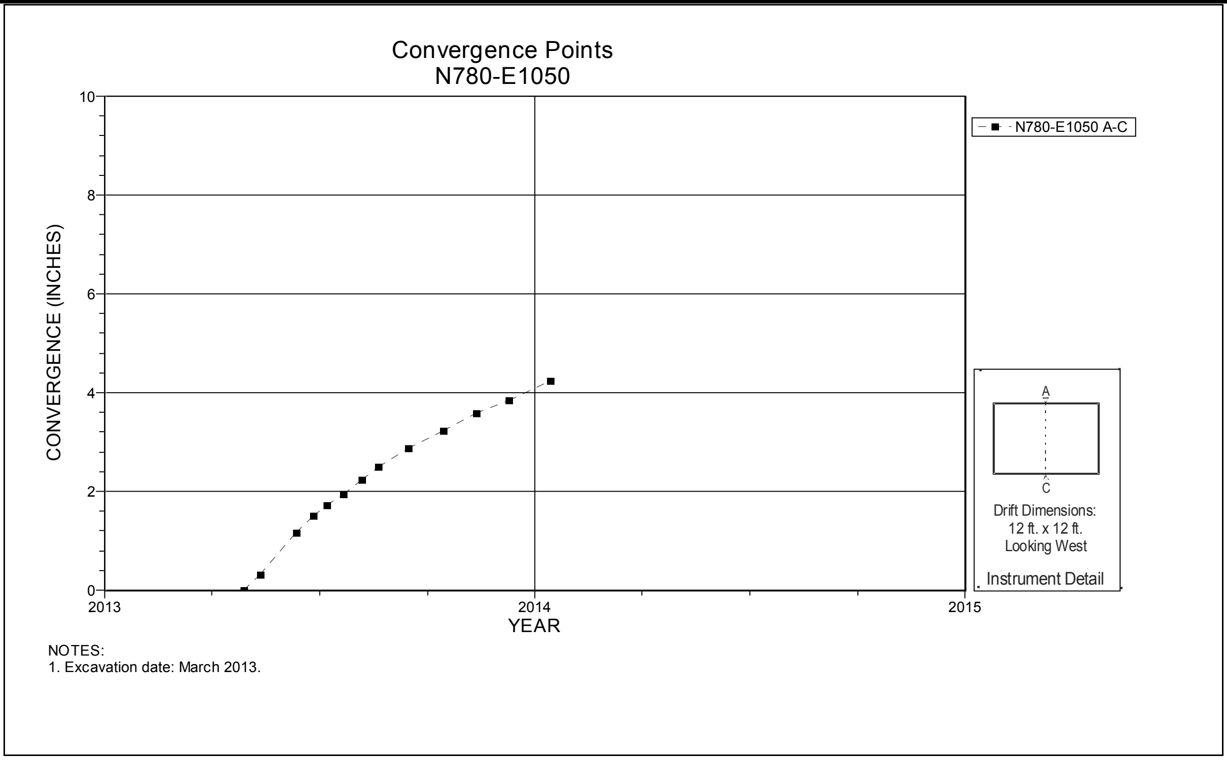

Figure 6-35 Convergence Point Array
N780 E1050 – Roof to Floor

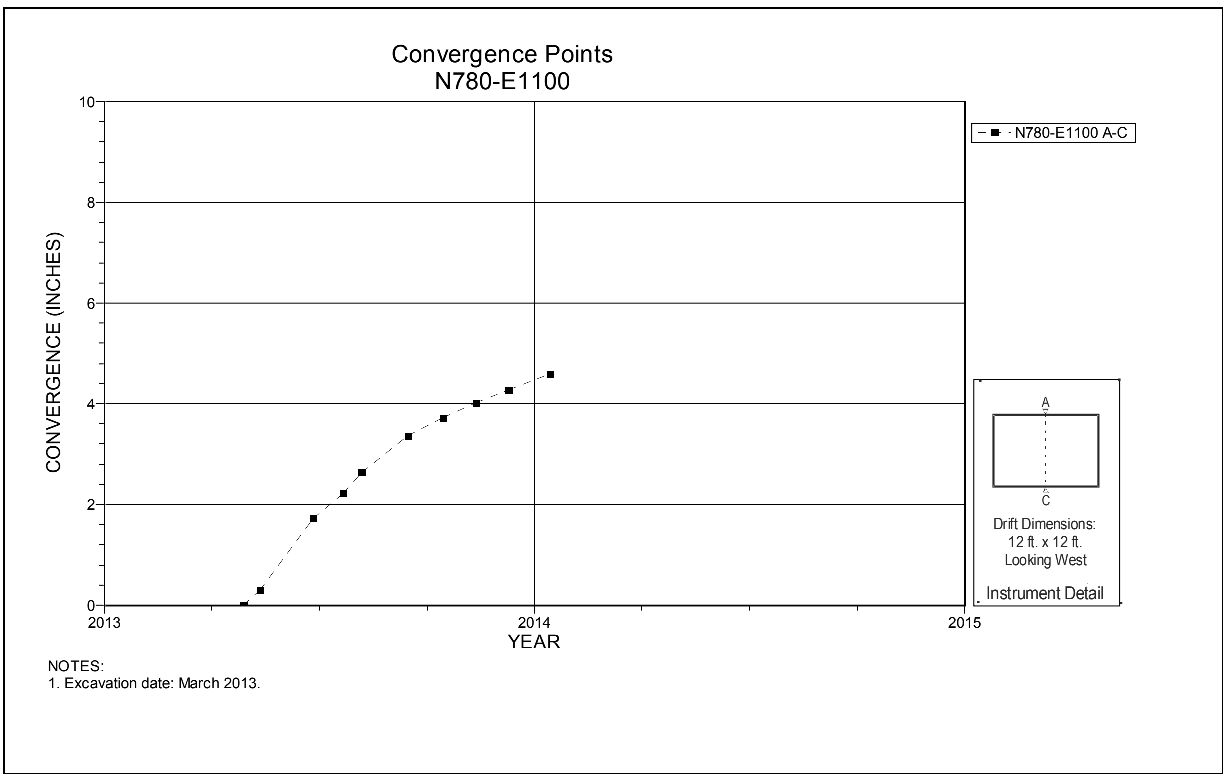

Figure 6-36 Convergence Point Array
N780 E1100 – Roof to Floor

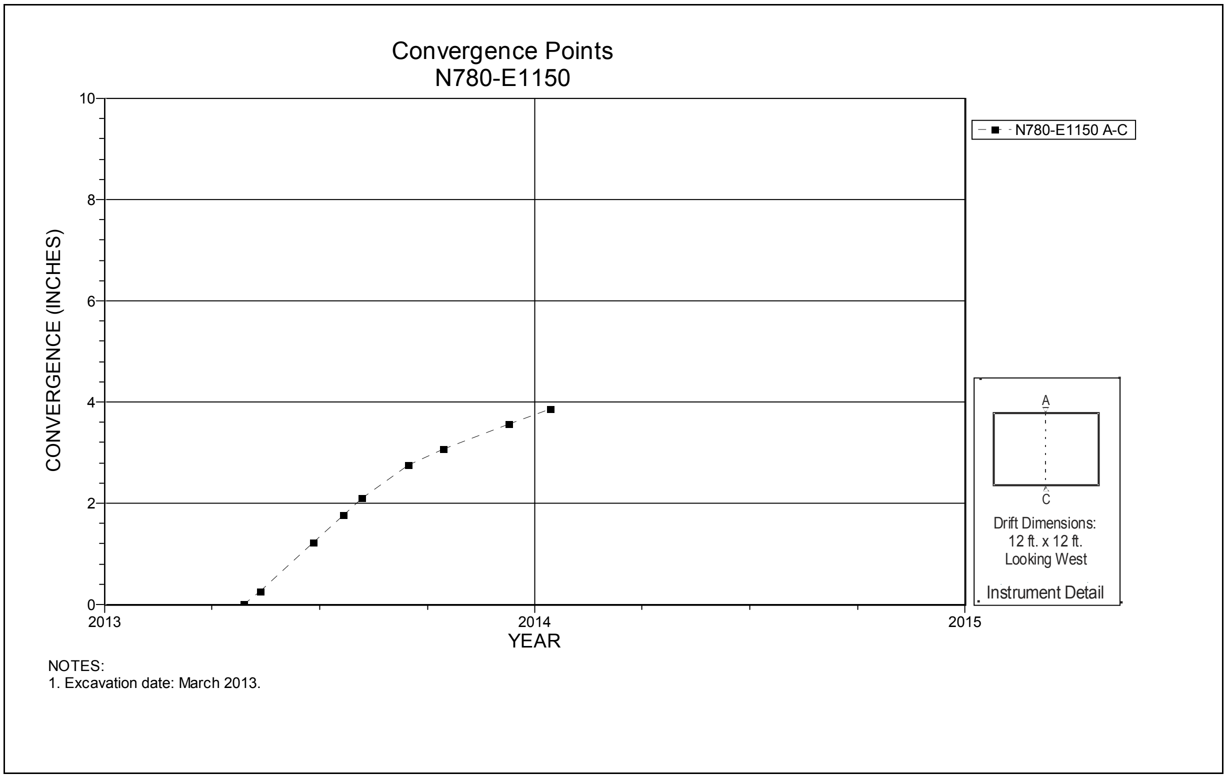

Figure 6-37 Convergence Point Array
N780 E1150 – Roof to Floor

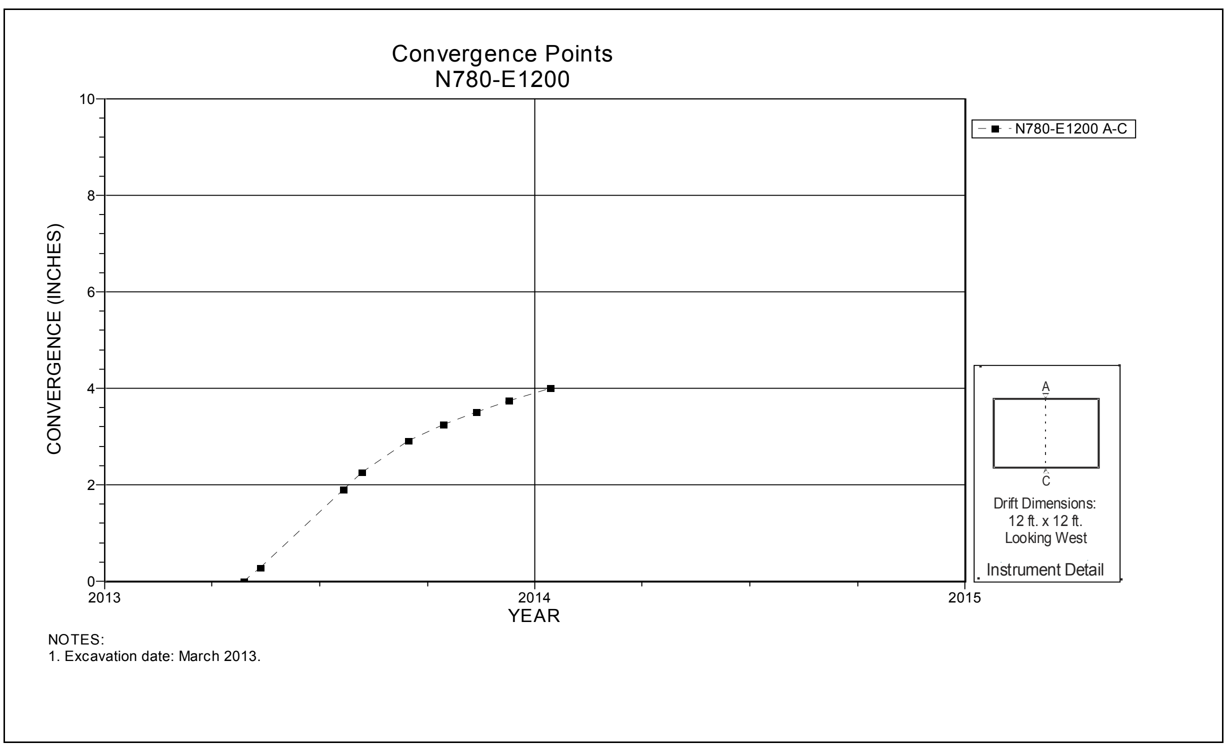

Figure 6-38 Convergence Point Array
N780 E1200 – Roof to Floor

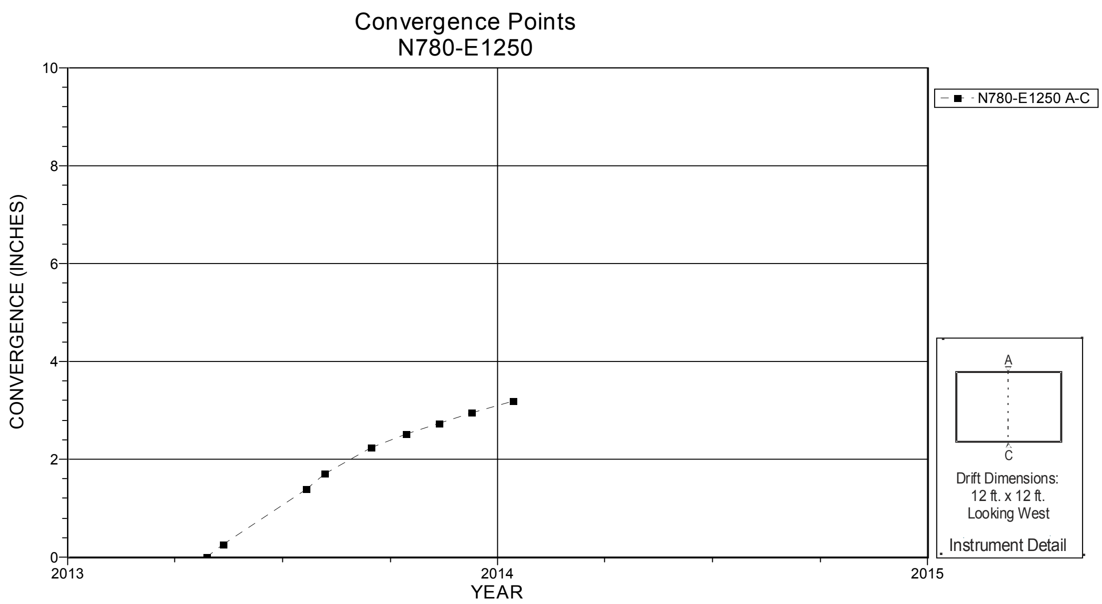

NOTES:
1. Excavation date: April 2013.

Figure 6-39 Convergence Point Array
N780 E1250 – Roof to Floor

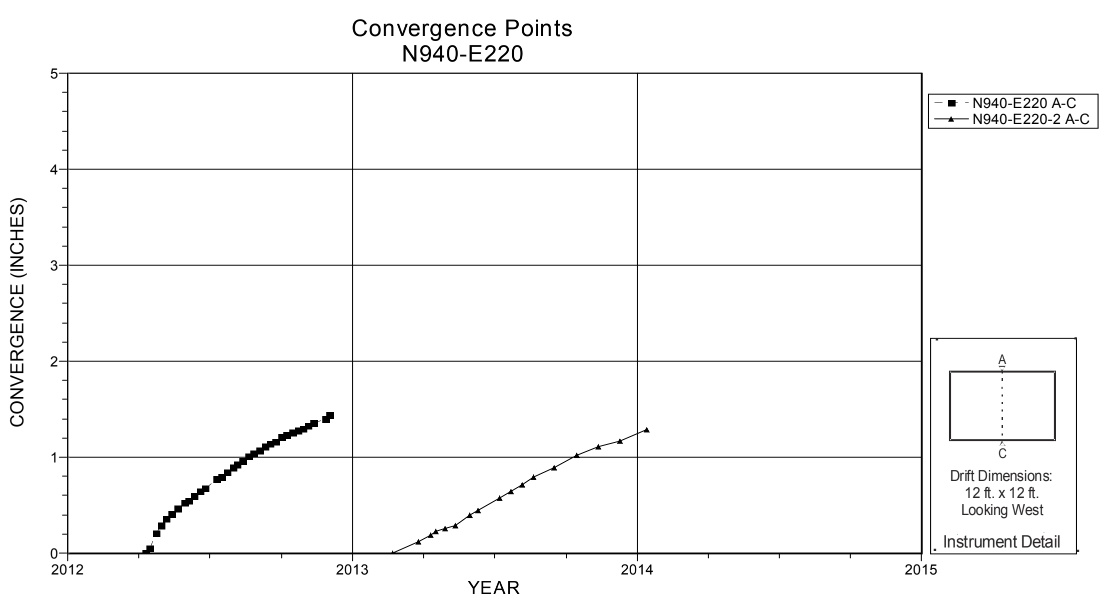

NOTES:
1. Excavation date: March 2012.

Figure 6-40 Convergence Point Array
N940 E220 – Roof to Floor

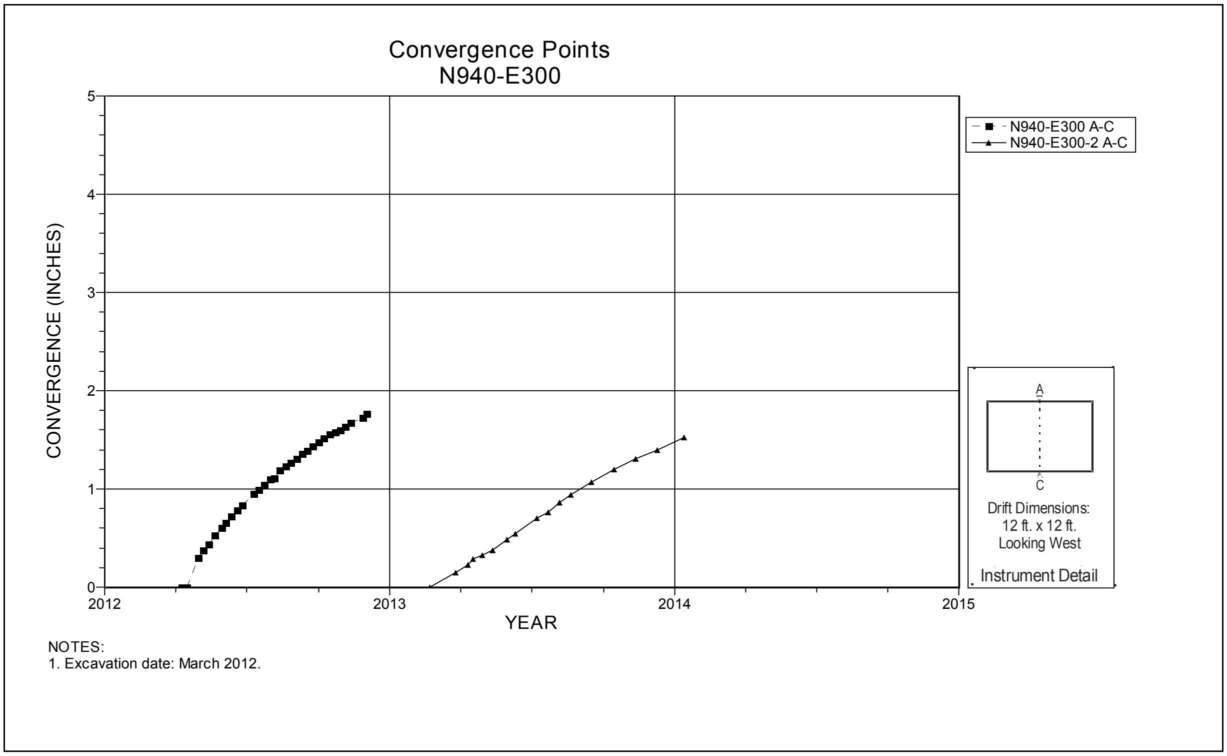

Figure 6-41 Convergence Point Array
N940 E300 – Roof to Floor

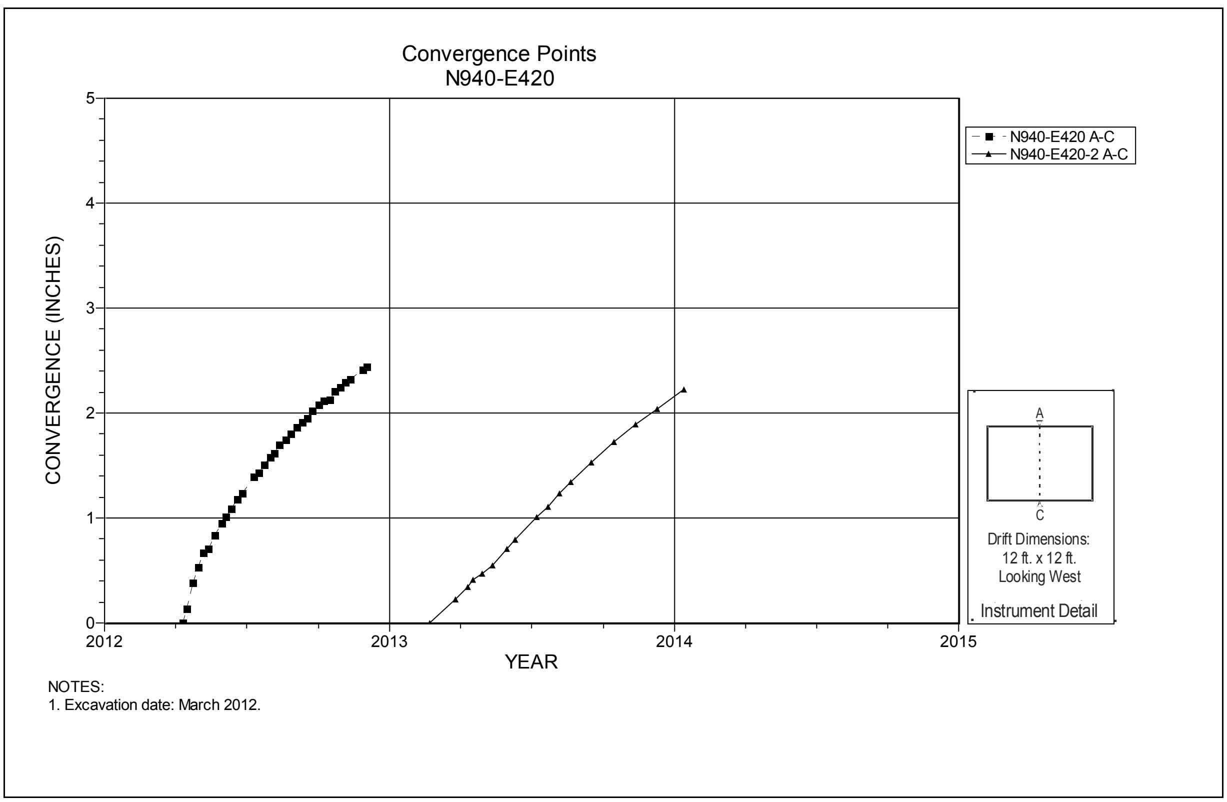

Figure 6-42 Convergence Point Array
N940 E420 – Roof to Floor

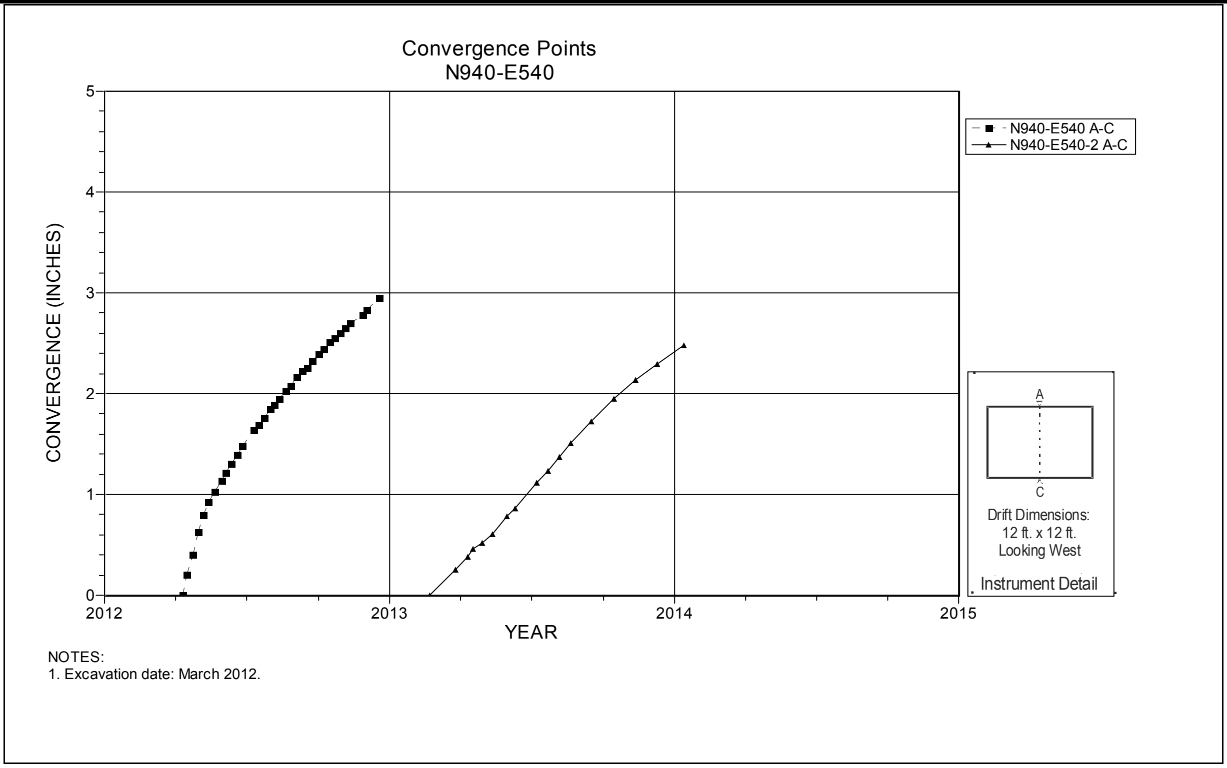

Figure 6-43 Convergence Point Array
N940 E540 – Roof to Floor

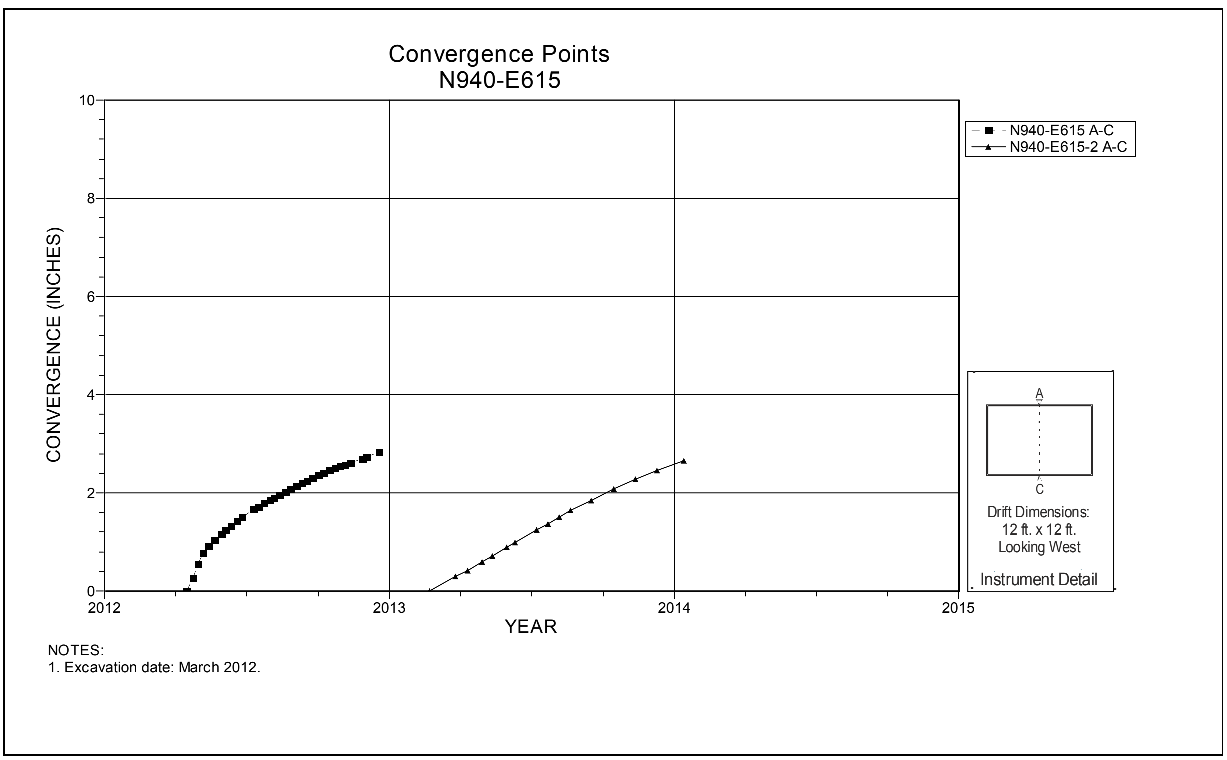

Figure 6-44 Convergence Point Array
N940 E615 – Roof to Floor

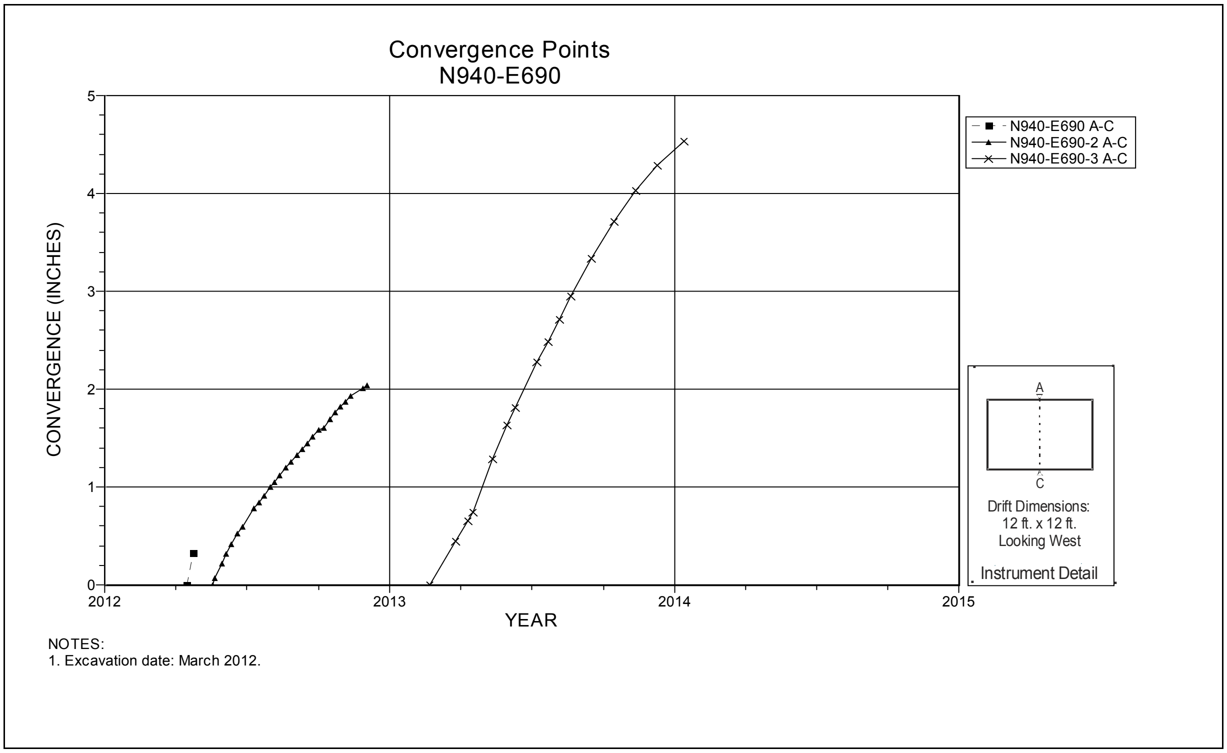

Figure 6-45 Convergence Point Array
N940 E690 – Roof to Floor

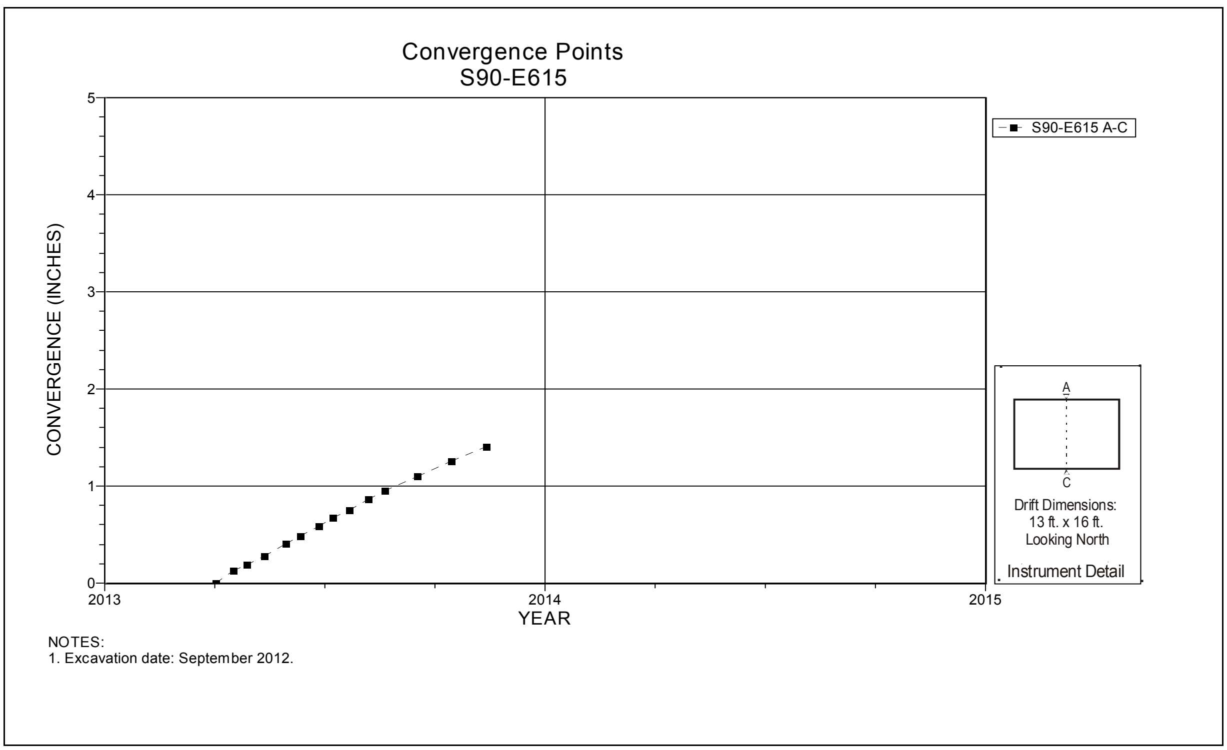

Figure 6-46 Convergence Point Array
S90 E615 – Roof to Floor

This page was intentionally left blank.

7.0 Geoscience Summary for the Waste Disposal Area

This chapter presents supporting data acquired as part of the Geoscience Program. It includes observations of clay seam displacements and other features in vertical observation holes, fracture maps of excavation surfaces, and stratigraphy mapping from the SDI.

7.1 Borehole Inspections

This section presents a summary of the clay seam displacements (offsets) and fracture densities measured in observation boreholes located through the WIPP underground facility. Relative lateral displacement of rock strata above and below a clay layer is measured as offset within a borehole. Fracture density is a calculated parameter based on the number of fractures (separations) and fracture zones observed in an observation borehole. Fracture density is calculated to be the number of fractures plus twice the number of fracture zones in a roof beam divided by the thickness of the beam (in feet). Table 7-1 presents the observed offset data for boreholes, the observed fractures and fracture zones, and the calculated fracture densities. Table 7-2 is a list of New Boreholes monitored during the July 2013- June 2014 reporting period.

7.2 Fracture Mapping

This section presents graphical results of the fracture mapping done in Panel 7 of the Waste Disposal Area. Figures 7-1 through 7-39 are plan view fracture maps for the roof and ribs for Panel 7 Rooms 1-7 and drifts S2180 and S2520.

7.3 Stratigraphic Mapping

This section presents graphical results of stratigraphic mapping conducted in the SDI Experimental Area located in the northeast portion of the WIPP underground in North 780 and 940 between E320 and E1310, East 690 between S70 and N780, and experimental rooms located between N780 and N940 in E1000, E1100, E1200, and E1310.

Table 7-1
Observation Borehole Fractures and Offset Data Summary

Hole	Location	Initial Inspection Date	Recent Inspection Date	FR[1]	FZ[2]	Beam Height (ft)	Feature	Fracture Density (frac/ft)	Feature Depth (ft)	Separation (in)	Offset (in.)	Compass	Hole Closure (%)	Offset Rate (in/yr)
OH1001	W390-S2268	9/23/2010	12/3/2013				BOH		20.6					
		9/23/2010	12/3/2013				Hangup		14.3	0.00	0.13	E	4	0.04
		9/23/2010	12/3/2013	1		8.7	Separation	0.11	8.7	0.25	0.75	E	25	0.23
		9/23/2010	12/3/2013				Separation		2.2	0.13	0.13	W	4	0.04
OH1002	W390-S2348	9/23/2010	12/3/2013				BOH		20.7					
		9/23/2010	12/3/2013	1		8.4	Separation	0.12	8.4	0.13	0.00			
		9/23/2010	12/3/2013				Separation		6.3	0.13	0.00			
OH1003	W390-S2432	9/23/2010	12/3/2013				BOH		20.4					
		9/23/2010	12/3/2013	0		8.0	Separation	0.00	8.0	0.13	0.00			
OH1004	W520-S2246	9/14/2010	11/13/2013				BOH		20.6					
		9/14/2010	11/13/2013	3		7.6	Hangup	0.39	7.6	0.00	0.00			
		9/14/2010	11/13/2013				Separation		6.6	0.13	0.00			
		9/14/2010	11/13/2013				Separation		3.0	0.13	0.19	W	6	0.06
		9/14/2010	11/13/2013				Separation		1.3	0.13	0.13	W	4	0.04
OH1005	W520-S2350	9/14/2010	11/13/2013				BOH		20.6					
		9/14/2010	11/13/2013	1		8.8	Separation	0.11	8.8	0.13	0.13	E	4	0.04
		9/14/2010	11/13/2013				Separation		6.9	0.13	0.13	E	4	0.04
OH1006	W520-S2429	9/14/2010	10/23/2013				BOH		20.2					
		9/14/2010	10/23/2013	1		7.6	Separation	0.13	7.6	0.13	0.00			
		9/14/2010	10/23/2013				Separation		0.4	0.38	0.00			

[1] Number of fractures (FR) in immediate roof beam

[2] Number of fracture zones (FZ) in immediate roof beam

[3] Fracture Density = (FR + 2 FZ)/beam height

Table 7-1
Observation Borehole Fractures and Offset Data Summary

Hole	Location	Initial Inspection Date	Recent Inspection Date	FR[1]	FZ[2]	Beam Height (ft)	Feature	Fracture Density (frac/ft)	Feature Depth (ft)	Separation (in)	Offset (in.)	Compass	Hole Closure (%)	Offset Rate (in/yr)
OH1001	W390-S2268	9/23/10	12/3/13				BOH		20.6					
		9/23/10	12/3/13				Hangup		14.3	0.00	0.13	E	0.04	0.01
		9/23/10	12/3/13	1		8.7	Separation	0.11	8.7	0.25	0.75	E	0.25	0.08
		9/23/10	12/3/13				Separation		2.2	0.13	0.13	W	0.04	0.01
OH1002	W390-S2348	9/23/10	12/3/13				BOH		20.7					
		9/23/10	12/3/13	1		8.4	Separation	0.12	8.4	0.13	0.00			
		9/23/10	12/3/13				Separation		6.3	0.13	0.00			
OH1003	W390-S2432	9/23/10	12/3/13				BOH		20.4					
		9/23/10	12/3/13	0		8.0	Separation	0.00	8.0	0.13	0.00			
OH1004	W520-S2246	9/14/10	11/13/13				BOH		20.6					
		9/14/10	11/13/13	3		7.6	Hangup	0.39	7.6	0.00	0.00			
		9/14/10	11/13/13				Separation		6.6	0.13	0.00			
		9/14/10	11/13/13				Separation		3.0	0.13	0.19	W	0.06	0.02
		9/14/10	11/13/13				Separation		1.3	0.13	0.13	W	0.04	0.01
OH1005	W520-S2350	9/14/10	11/13/13				BOH		20.6					
		9/14/10	11/13/13	1		8.8	Separation	0.11	8.8	0.13	0.13	E	0.04	0.01
		9/14/10	11/13/13				Separation		6.9	0.13	0.13	E	0.04	0.01
OH1006	W520-S2429	9/14/10	10/23/13				BOH		20.2					
		9/14/10	10/23/13	1		7.6	Separation	0.13	7.6	0.13	0.00			
		9/14/10	10/23/13				Separation		0.4	0.38	0.00			

[1] Number of fractures (FR) in immediate roof beam

[2] Number of fracture zones (FZ) in immediate roof beam

[3] Fracture Density = (FR + 2 FZ)/beam height

Table 7-1
Observation Borehole Fractures and Offset Data Summary

Hole	Location	Initial Inspection Date	Recent Inspection Date	FR[1]	FZ[2]	Beam Height (ft)	Feature	Fracture Density (frac/ft)	Feature Depth (ft)	Separation (in)	Offset (in.)	Compass	Hole Closure (%)	Offset Rate (in/yr)
OH1007	W660-S2267	11/15/2010	10/23/2013				BOH		20.6					
		11/15/2010	10/23/2013	1		8.2	Hangup	0.12	8.2	0.00	0.00			
		11/15/2010	10/23/2013				Separation		6.9	0.13	0.00			
OH1008	W660-S2351	11/15/2010	10/23/2013				BOH		20.6					
		11/15/2010	10/23/2013	1		7.8	Separation	0.13	7.8	0.13	0.00			
		11/15/2010	10/23/2013				Rough Spot		6.9	0.00	0.00			
		11/15/2010	10/23/2013				Separation		6.2	0.13	0.00			
OH1009	W660-S2433	11/15/2010	10/23/2013				BOH		20.5					
		11/15/2010	10/23/2013	0		7.5	Separation	0.00	6.7	0.13	0.00			
OH1010	W790-S2265	11/15/2010	10/23/2013				BOH		20.7					
		11/15/2010	10/23/2013	0		8.1	Separation	0.00	8.1	0.13	1.50	E	50	0.51
OH1011	W790-S2349	11/15/2010	10/23/2013				BOH		20.7					
		11/15/2010	10/23/2013				Hangup		13.6	0.00	0.00			
		11/15/2010	10/23/2013	1		7.6	Separation	0.13	7.6	0.13	0.25	E	8	0.09
		11/15/2010	10/23/2013				Separation		6.0	0.13	0.25	E	8	0.09
OH1012	W790-S2430	12/21/2010	10/23/2013				BOH		20.6					
		12/21/2010	10/23/2013				Rough Spot		6.9	0.00	0.00			
		12/21/2010	10/23/2013	0		6.7	Separation	0.00	6.7	0.13	1.50	E	50	0.53
OH1013	W920-S2231	3/1/2011	11/19/2013				BOH		20.1	0.00	0.00			
		3/1/2011	11/19/2013	0		7.3	Separation	0.00	7.3	0.25	0.00			

[1] Number of fractures (FR) in immediate roof beam

[2] Number of fracture zones (FZ) in immediate roof beam

[3] Fracture Density = (FR + 2 FZ)/beam height

Table 7-1
Observation Borehole Fractures and Offset Data Summary

Hole	Location	Initial Inspection Date	Recent Inspection Date	FR[1]	FZ[2]	Beam Height (ft)	Feature	Fracture Density (frac/ft)	Feature Depth (ft)	Separation (in)	Offset (in.)	Compass	Hole Closure (%)	Offset Rate (in/yr)
OH1014	W920-S2350	3/1/2011	12/4/2013				BOH		20.6					
		3/1/2011	12/4/2013	1		7.3	Separation	0.14	7.3	3.00	2.00	E	67	0.72
		3/1/2011	12/4/2013				Separation		6.7	0.13	0.00			
OH1015	W920-S2465	3/1/2011	12/4/2013				BOH		20.6					
		3/1/2011	12/4/2013	1		7.3	Separation	0.14	7.3	0.13	0.25	E	8	0.09
		3/1/2011	12/4/2013				Separation		6.7	0.13	0.25	E	8	0.09
OH1017	W1050-S2352	3/1/2011	11/13/2013				BOH		20.3					
		3/1/2011	11/13/2013				Separation		7.4	0.13	0.00			
		3/1/2011	11/13/2013	1		7.3	Separation	0.14	7.3	0.13	0.13	E	4	0.05
		3/1/2011	11/13/2013				Separation		7.1	0.13	0.13	W	4	0.05
OH1018	W1050-S2434	3/1/2011	10/23/2013				BOH		20.1					
		3/1/2011	10/23/2013				Hangup		7.7	0.00	0.00			
		3/1/2011	10/23/2013	0		6.9	Separation	0.00	6.9	0.13	0.13	E	4	0.05
		3/1/2011	10/23/2013				Hangup		6.5	0.00	0.00			
OH1022-1	W392-S2180	11/13/2013	11/13/2013				BOH		20.7					
		11/13/2013	11/13/2013				Offset		14.8	0.00	1.00	S	33	
		11/13/2013	11/13/2013	0		8.6	Separation	0.00	8.6	0.13	2.00	S	67	

[1] Number of fractures (FR) in immediate roof beam

[2] Number of fracture zones (FZ) in immediate roof beam

[3] Fracture Density = (FR + 2 FZ)/beam height

Table 7-1
Observation Borehole Fractures and Offset Data Summary

Hole	Location	Initial Inspection Date	Recent Inspection Date	FR[1]	FZ[2]	Beam Height (ft)	Feature	Fracture Density (frac/ft)	Feature Depth (ft)	Separation (in)	Offset (in.)	Compass	Hole Closure (%)	Offset Rate (in/yr)
OH1023	W460-S2180	9/14/2010	11/13/2013				BOH		20.6					
		9/14/2010	11/13/2013				Offset		14.9	0.00	0.38	N	13	0.12
		9/14/2010	11/13/2013	0		8.4	Separation	0.00	8.4	0.13	1.00	N	33	0.32
		9/14/2010	11/13/2013				Rough Spot		7.9	0.00	0.00			
OH1024	W522-S2180	9/14/2010	11/13/2013				BOH		20.5					
		9/14/2010	11/13/2013				Offset		14.9	0.00	1.50	S	50	0.47
		9/14/2010	11/13/2013	2		8.6	Separation	0.23	8.6	0.13	1.50	S	50	0.47
		9/14/2010	11/13/2013				Separation		7.9	0.13	0.00			
		9/14/2010	11/13/2013				Separation		0.7	0.13	0.13	S	4	0.04
OH1025	W593-S2180	9/14/2010	11/13/2013				BOH		20.5					
		9/14/2010	11/13/2013				Offset		14.5	0.00	0.25	N	8	0.08
		9/14/2010	11/13/2013	1		8.9	Separation	0.11	8.9	0.13	0.38	N	13	0.12
		9/14/2010	11/13/2013				Separation		8.0	0.06	0.00			
OH1026-1	W662-S2180	11/13/2013	11/13/2013				BOH		20.5					
		11/13/2013	11/13/2013				Offset		14.4	0.00	1.00	S	33	N/A
		11/13/2013	11/13/2013	1		8.2	Separation	0.12	8.2	0.13	1.75	S	58	N/A
		11/13/2013	11/13/2013				Separation		0.6	0.06	0.06	S	2	N/A
OH1027-1	W727-S2180	12/4/2013	12/4/2013				BOH		20.1					
		12/4/2013	12/4/2013	1		7.9	Separation	0.13	7.9	0.13	0.00			
		12/4/2013	12/4/2013				Separation		7.3	0.13	0.00			

[1] Number of fractures (FR) in immediate roof beam

[2] Number of fracture zones (FZ) in immediate roof beam

[3] Fracture Density = (FR + 2 FZ)/beam height

Table 7-1
Observation Borehole Fractures and Offset Data Summary

Hole	Location	Initial Inspection Date	Recent Inspection Date	FR[1]	FZ[2]	Beam Height (ft)	Feature	Fracture Density (frac/ft)	Feature Depth (ft)	Separation (in)	Offset (in.)	Compass	Hole Closure (%)	Offset Rate (in/yr)
OH1028	W793-S2180	9/14/2010	11/13/2013				BOH		20.4					
		9/14/2010	11/13/2013				Offset		14.6	0.00	0.75	S	25	0.24
		9/14/2010	11/13/2013				Separation		8.3	0.13	0.25	S	8	0.08
		9/14/2010	11/13/2013	2		8.1	Separation	0.25	8.1	0.50	0.25	S	8	0.08
		9/14/2010	11/13/2013				Separation		8.0	0.13	0.13	S	4	0.04
		9/14/2010	11/13/2013				Separation		2.3	0.13	0.00			
OH1029-1	W861-S2180	12/4/2013	12/4/2013				BOH		20.2					
		12/4/2013	12/4/2013	1		8.2	Separation	0.12	8.2	0.13	0.00			
		12/4/2013	12/4/2013				Separation		6.7	0.11	0.00			
OH1030-1	W928-S2180	11/13/2013	11/13/2013				BOH		20.3					
		11/13/2013	11/13/2013				Hangup		14.6	0.00	1.00	S	33	N/A
		11/13/2013	11/13/2013	2		8.4	Separation	0.24	8.4	0.13	0.25	S	8	N/A
		11/13/2013	11/13/2013				Separation		7.4	0.13	0.00			
		11/13/2013	11/13/2013				Separation		7.0	0.13	1.25	S	42	N/A
OH1031-1	W985-S2182	12/4/2013	12/4/2013				BOH		20.1					
		12/4/2013	12/4/2013	0		8.1	Separation	0.00	8.1	0.13	0.06	S	2	N/A
OH1032-1	W1058-S2180	12/4/2013	12/4/2013				BOH		20.1					
		12/4/2013	12/4/2013	1		7.5	Separation	0.13	7.5	0.13	0.00			
		12/4/2013	12/4/2013				Separation		7.0	0.13	0.00			

[1] Number of fractures (FR) in immediate roof beam

[2] Number of fracture zones (FZ) in immediate roof beam

[3] Fracture Density = (FR + 2 FZ)/beam height

Table 7-1
Observation Borehole Fractures and Offset Data Summary

Hole	Location	Initial Inspection Date	Recent Inspection Date	FR[1]	FZ[2]	Beam Height (ft)	Feature	Fracture Density (frac/ft)	Feature Depth (ft)	Separation (in)	Offset (in.)	Compass	Hole Closure (%)	Offset Rate (in/yr)
OH1035	W393-S2520	9/10/2010	10/23/2013				BOH		20.5					
		9/10/2010	10/23/2013				Hangup		13.9	0.00	1.25	N	42	0.40
		9/10/2010	10/23/2013	0		7.9	Separation	0.00	7.9	0.13	1.75	N	58	0.56
OH1036	W466-S2520	9/10/2010	10/23/2013				BOH		19.8					
		9/10/2010	10/23/2013	0		7.4	Separation	0.00	7.4	0.13	0.00			
		9/10/2010	10/23/2013				Rough Spot		5.6	0.00	0.00			
OH1037	W524-S2520	11/15/2010	10/23/2013				BOH		20.7					
		11/15/2010	10/23/2013				Hangup		14.1	0.00	0.00			
		11/15/2010	10/23/2013	0		7.9	Separation	0.00	7.9	0.13	0.00			
OH1038	W594-S2520	11/15/2010	10/23/2013				BOH		22.0					
		11/15/2010	10/23/2013	1		8.1	Separation	0.12	8.1	0.13	0.00			
		11/15/2010	10/23/2013				Separation		7.1	0.13	0.00			
OH1039	W659-S2520	11/15/2010	10/23/2013				BOH		20.5					
		11/15/2010	10/23/2013				Separation		13.8	0.13	1.00	N	33	0.34
		11/15/2010	10/23/2013	0		7.8	Separation	0.00	7.8	0.13	1.25	N	42	0.43
OH1040	W726-S2520	11/15/2010	10/23/2013				BOH		20.6					
		11/15/2010	10/23/2013				Hangup		13.9	0.00	0.00			
		11/15/2010	10/23/2013	1		7.5	Separation	0.13	7.5	0.13	0.00			
		11/15/2010	10/23/2013				Separation		6.8	0.13	0.00			

[1] Number of fractures (FR) in immediate roof beam

[2] Number of fracture zones (FZ) in immediate roof beam

[3] Fracture Density = (FR + 2 FZ)/beam height

Table 7-1
Observation Borehole Fractures and Offset Data Summary

Hole	Location	Initial Inspection Date	Recent Inspection Date	FR[1]	FZ[2]	Beam Height (ft)	Feature	Fracture Density (frac/ft)	Feature Depth (ft)	Separation (in)	Offset (in.)	Compass	Hole Closure (%)	Offset Rate (in/yr)
OH1041-1	W726-S2520	11/19/2013	11/19/2013				BOH		20.2					
		11/19/2013	11/19/2013	1		7.8	Rubble Zone	0.13	7.8	1.00	0.00			
		11/19/2013	11/19/2013				Separation		2.3	0.38	0.00			
OH1042-1	W860-S2520	11/19/2013	11/19/2013				BOH		20.1					
		11/19/2013	11/19/2013	2		7.2	Separation	0.28	7.2	1.00	0.00			
		11/19/2013	11/19/2013				Separation		6.8	0.13	0.00			
		11/19/2013	11/19/2013				Separation		3.1	0.13	0.00			
OH1043-1	W923-S2520	11/19/2013	11/19/2013				BOH		20.2					
		11/19/2013	11/19/2013	1		8.1	Separation	0.12	8.1	0.13	0.00			
		11/19/2013	11/19/2013				Separation		3.3	0.38	0.00			
OH1044	W993-S2520	12/4/2013	12/4/2013				BOH		20.6					
		12/4/2013	12/4/2013	0		7.5	Separation	0.00	7.5	0.13	0.38	N	13	N/A
OH1045-1	W1056-S2520	11/19/2013	11/19/2013				BOH		20.1					
		11/19/2013	11/19/2013	0		7.6	Separation	0.00	7.6	0.13				

[1] Number of fractures (FR) in immediate roof beam

[2] Number of fracture zones (FZ) in immediate roof beam

[3] Fracture Density = (FR + 2 FZ)/beam height

Table 7-1
Observation Borehole Fractures and Offset Data Summary

Hole	Location	Initial Inspection Date	Recent Inspection Date	FR[1]	FZ[2]	Beam Height (ft)	Feature	Fracture Density (frac/ft)	Feature Depth (ft)	Separation (in)	Offset (in.)	Compass	Hole Closure (%)	Offset Rate (in/yr)
OH620	E140-S700	11/17/2005	12/14/2013				BOH		16.8					
		11/17/2005	12/14/2013	2		5.9	Separation	0.34	5.9	0.25	0.50	E	17	0.06
		11/17/2005	12/14/2013				Separation		4.3	0.13	0.00			
		11/17/2005	12/14/2013				Separation		3.2	0.13	0.00			
OH750-1	E140-S773	2/4/2014	2/4/2014				BOH		20.2					
		2/4/2014	2/4/2014	1		5.0	Separation	0.20	5.0	0.25	0.00			
		2/4/2014	2/4/2014				Separation		4.8	1.00	0.06	E	2	N/A
OH751-1	E140-S920	2/4/2014	2/4/2014				BOH		20.1					
		2/4/2014	2/4/2014	4		5.7	Separation	0.70	5.7	0.13	0.00			
		2/4/2014	2/4/2014				Separation		5.5	0.13	0.00			
		2/4/2014	2/4/2014				Separation		5.1	0.13	0.00			
		2/4/2014	2/4/2014				Separation		4.8	0.13	0.00			
		2/4/2014	2/4/2014				Separation		4.4	0.13	0.00			
OH575-1	E140-S1000	9/29/2011	11/18/2013				BOH		20.8					
		9/29/2011	11/18/2013	2		5.4	Separation	0.37	5.4	0.13	0.00			
		9/29/2011	11/18/2013				Separation		4.2	1.00	1.75	E	58	0.82
		9/29/2011	11/18/2013				Separation		3.5	0.06	0.00			

[1] Number of fractures (FR) in immediate roof beam

[2] Number of fracture zones (FZ) in immediate roof beam

[3] Fracture Density = (FR + 2 FZ)/beam height

Table 7-1
Observation Borehole Fractures and Offset Data Summary

Hole	Location	Initial Inspection Date	Recent Inspection Date	FR[1]	FZ[2]	Beam Height (ft)	Feature	Fracture Density (frac/ft)	Feature Depth (ft)	Separation (in)	Offset (in.)	Compass	Hole Closure (%)	Offset Rate (in/yr)
OH752	E140-S1070	9/29/2011	11/18/2013				BOH		20.6					
		9/29/2011	11/18/2013	2		5.7	Separation	0.35	5.7	0.13	0.00			
		9/29/2011	11/18/2013				Hangup		2.3	0.00	0.00			
		9/29/2011	11/18/2013				Separation		1.4	0.13	0.00			
OH753-1	E140-S1226	2/5/2014	2/5/2014				BOH		20.1					
		2/5/2014	2/5/2014				Separation		1.1	0.13	0.00			
		2/5/2014	2/5/2014				Separation		1.2	0.13	0.00			
		2/5/2014	2/5/2014				Separation		2.8	0.75	0.00			
		2/5/2014	2/5/2014				Separation		4.3	0.25	0.00			
		2/5/2014	2/5/2014	3		5.7	Separation	0.53	5.7	2.00	0.00			
		2/5/2014	2/5/2014				Separation		6.0	0.25	0.00			
		2/5/2014	2/5/2014				Separation		6.6	0.13	0.00			
		2/5/2014	2/5/2014				RoughSpot		6.3	0.00	0.00			
		2/5/2014	2/5/2014				Separation		5.6	0.13	0.00			
OH578	E140-S1300	6/16/2005	11/18/2013				BOH		20.4					
		6/16/2005	11/18/2013	0		6.1	Rough Spot	0.00	6.1	0.00	0.00			

[1] Number of fractures (FR) in immediate roof beam

[2] Number of fracture zones (FZ) in immediate roof beam

[3] Fracture Density = (FR + 2 FZ)/beam height

Table 7-1
Observation Borehole Fractures and Offset Data Summary

Hole	Location	Initial Inspection Date	Recent Inspection Date	FR[1]	FZ[2]	Beam Height (ft)	Feature	Fracture Density (frac/ft)	Feature Depth (ft)	Separation (in)	Offset (in.)	Compass	Hole Closure (%)	Offset Rate (in/yr)
OH872-2	E140-S1390	2/4/2014	2/4/2014				BOH		20.0					
		2/4/2014	2/4/2014				Separation		6.1	0.13	0.00			
		2/4/2014	2/4/2014			5.9	Separation		5.9	1.00	0.00			
		2/4/2014	2/4/2014	4			Separation		5.5	0.13	0.13			
		2/4/2014	2/4/2014				Separation		4.2	0.13	0.50			
		2/4/2014	2/4/2014				Separation		3.0	0.13	0.13			
		2/4/2014	2/4/2014				Separation		1.5	0.13	0.13			
OH580-3	E140-S1463	2/4/2014	2/4/2014				BOH		20.0					
		2/4/2014	2/4/2014				Separation		6.7	0.13	0.00			
		2/4/2014	2/4/2014				Separation		5.5	6.00	0.00			
		2/4/2014	2/4/2014	3		5.0	Separation	0.60	5.0	5.00	0.00			
		2/4/2014	2/4/2014				Separation		2.5	5.00	0.00			
		2/4/2014	2/4/2014				Separation		1.0	1.00	0.00			
		2/4/2014	2/4/2014				Separation		0.7	0.13	0.00			
OH582	E140-S1600	6/16/2005	11/18/2013				BOH		20.5					
		6/16/2005	11/18/2013				Separation		6.8	0.13	0.00			
		6/16/2005	11/18/2013	0		6.1	Separation	0.00	6.1	0.13	0.25	S	8	0.03

[1] Number of fractures (FR) in immediate roof beam

[2] Number of fracture zones (FZ) in immediate roof beam

[3] Fracture Density = (FR + 2 FZ)/beam height

Table 7-1
Observation Borehole Fractures and Offset Data Summary

Hole	Location	Initial Inspection Date	Recent Inspection Date	FR[1]	FZ[2]	Beam Height (ft)	Feature	Fracture Density (frac/ft)	Feature Depth (ft)	Separation (in)	Offset (in.)	Compass	Hole Closure (%)	Offset Rate (in/yr)
OH143-5	E140-S1780	2/4/2014	2/4/2014				BOH		20.1					
		2/4/2014	2/4/2014				Separation		8.6	0.25	0.00			
		2/4/2014	2/4/2014	7		7.8	Separation	0.90	7.8	11.00	0.00			
		2/4/2014	2/4/2014				Separation		6.6	0.25	0.00			
		2/4/2014	2/4/2014				Separation		5.5	0.25	0.00			
		2/4/2014	2/4/2014				Separation		4.1	4.00	0.00			
		2/4/2014	2/4/2014				Separation		3.9	0.13	0.00			
		2/4/2014	2/4/2014				Separation		2.7	2.00	0.00			
		2/4/2014	2/4/2014				Separation		1.7	0.13	0.00			
		2/4/2014	2/4/2014				Separation		1.2	0.13	0.00			
OH583	E140-S1950	6/16/2005	11/26/2013				BOH		20.9					
		6/16/2005	11/26/2013				Separation		6.9	0.13	2.50	E	83	0.30
		6/16/2005	11/26/2013	3		6.0	Separation	0.50	6.0	0.13	0.25	W	8	0.03
		6/16/2005	11/26/2013				Separation		4.9	0.13	0.38	E	13	0.04
		6/16/2005	11/26/2013				Separation		2.9	0.25	0.00			
		6/16/2005	11/26/2013				Separation		1.9	0.25	0.38	E	13	0.04

[1] Number of fractures (FR) in immediate roof beam

[2] Number of fracture zones (FZ) in immediate roof beam

[3] Fracture Density = (FR + 2 FZ)/beam height

Table 7-1
Observation Borehole Fractures and Offset Data Summary

Hole	Location	Initial Inspection Date	Recent Inspection Date	FR[1]	FZ[2]	Beam Height (ft)	Feature	Fracture Density (frac/ft)	Feature Depth (ft)	Separation (in)	Offset (in.)	Compass	Hole Closure (%)	Offset Rate (in/yr)
OH583-1	E140-S1950	2/4/2014	2/4/2014				BOH		20.0					
		2/4/2014	2/4/2014				Separation		6.5	0.75	0.00			
		2/4/2014	2/4/2014	1		5.4	Separation	0.19	5.4	0.13	0.00			
		2/4/2014	2/4/2014				Separation		1.9	0.13	0.00			
OH474-2	E140-S2001	2/4/2014	2/4/2014				BOH		20.2					
		2/4/2014	2/4/2014				Separation		6.3	0.25	0.00			
		2/4/2014	2/4/2014				Separation		6.0	0.13	0.00			
		2/4/2014	2/4/2014	2		4.7	Separation	0.43	4.7	2.00	0.00			
		2/4/2014	2/4/2014				Separation		2.2	0.13	0.00			
		2/4/2014	2/4/2014				Separation		1.3	0.75	0.00			

[1] Number of fractures (FR) in immediate roof beam

[2] Number of fracture zones (FZ) in immediate roof beam

[3] Fracture Density = (FR + 2 FZ)/beam height

Table 7-1
Observation Borehole Fractures and Offset Data Summary

Hole	Location	Initial Inspection Date	Recent Inspection Date	FR[1]	FZ[2]	Beam Height (ft)	Feature	Fracture Density (frac/ft)	Feature Depth (ft)	Separation (in)	Offset (in.)	Compass	Hole Closure (%)	Offset Rate (in/yr)
OH473-4	E140-S2091	2/4/2014	2/4/2014				BOH		20.3					
		2/4/2014	2/4/2014				Separation		8.0	2.00	0.00			
		2/4/2014	2/4/2014				Separation		7.6	0.13	0.00			
		2/4/2014	2/4/2014				Separation		7.4	0.25	0.00			
		2/4/2014	2/4/2014				Separation		7.0	3.50	0.00			
		2/4/2014	2/4/2014				Separation		6.0	1.00	0.00			
		2/4/2014	2/4/2014	7		5.3	Separation	1.32	5.3	2.75	0.00			
		2/4/2014	2/4/2014				Separation		5.1	0.25	0.00			
		2/4/2014	2/4/2014				Separation		4.7	2.00	0.00			
		2/4/2014	2/4/2014				Separation		4.4	2.00	0.00			
		2/4/2014	2/4/2014				Separation		3.6	0.25	0.00			
		2/4/2014	2/4/2014				Separation		3.0	0.13	0.00			
		2/4/2014	2/4/2014				Separation		2.8	0.13	0.00			
		2/4/2014	2/4/2014				Separation		1.4	1.25	0.00			
OH472-2	E140-S2167	9/26/2011	2/4/2014				BOH		20.4					
		9/26/2011	2/4/2014				Separation		6.6	0.25	0.00			
		9/26/2011	2/4/2014	1		6.1	Separation	0.16	6.1	0.25	0.25	S	8	0.11
		9/26/2011	2/4/2014				Separation		5.0	0.13	0.00			

[1] Number of fractures (FR) in immediate roof beam

[2] Number of fracture zones (FZ) in immediate roof beam

[3] Fracture Density = (FR + 2 FZ)/beam height

Table 7-1
Observation Borehole Fractures and Offset Data Summary

Hole	Location	Initial Inspection Date	Recent Inspection Date	FR[1]	FZ[2]	Beam Height (ft)	Feature	Fracture Density (frac/ft)	Feature Depth (ft)	Separation (in)	Offset (in.)	Compass	Hole Closure (%)	Offset Rate (in/yr)
OH586-3	E140-S2359	2/4/2014	2/4/2014				BOH		20.1					
		2/4/2014	2/4/2014				Separation		7.7	0.75	0.00			
		2/4/2014	2/4/2014				Separation		6.6	0.13	0.00			
		2/4/2014	2/4/2014	4		5.2	Separation	0.77	5.2	5.00	0.00			
		2/4/2014	2/4/2014				Separation		4.2	4.50	0.00			
		2/4/2014	2/4/2014				Separation		2.5	0.38	0.00			
		2/4/2014	2/4/2014				Separation		1.5	0.25	0.00			
		2/4/2014	2/4/2014				Separation		1.0	0.13	0.00			
OH588-1	E140-S2520	9/26/2011	2/4/2014				BOH		20.7					
		9/26/2011	2/4/2014				Separation		6.5	0.25	0.00			
		9/26/2011	2/4/2014	1		5.3	Separation	0.19	5.3	2.50	1.75	E	58	0.74
		9/26/2011	2/4/2014				Separation		0.7	0.38	0.19	SE	6	0.08

[1] Number of fractures (FR) in immediate roof beam

[2] Number of fracture zones (FZ) in immediate roof beam

[3] Fracture Density = (FR + 2 FZ)/beam height

Table 7-1
Observation Borehole Fractures and Offset Data Summary

Hole	Location	Initial Inspection Date	Recent Inspection Date	FR[1]	FZ[2]	Beam Height (ft)	Feature	Fracture Density (frac/ft)	Feature Depth (ft)	Separation (in)	Offset (in.)	Compass	Hole Closure (%)	Offset Rate (in/yr)
OH468-3	E140-S2637	2/4/2014	2/4/2014				BOH		20.1					
		2/4/2014	2/4/2014				Separation		8.5	1.25	0.00			
		2/4/2014	2/4/2014				Separation		6.9	0.50	0.00			
		2/4/2014	2/4/2014				Separation		6.8	0.13	0.00			
		2/4/2014	2/4/2014				Separation		6.5	0.13	0.00			
		2/4/2014	2/4/2014				Separation		6.1	0.13	0.00			
		2/4/2014	2/4/2014				Separation		5.8	0.13	0.00			
		2/4/2014	2/4/2014	4		5.3	Rubble Zone	0.75	5.3	3.00	0.00			
		2/4/2014	2/4/2014				Separation		4.1	6.00	0.00			
		2/4/2014	2/4/2014				Separation		3.9	0.38	0.00			
		2/4/2014	2/4/2014				Separation		1.6	0.25	0.00			
		2/4/2014	2/4/2014				Separation		0.7	0.75	0.00			

[1] Number of fractures (FR) in immediate roof beam

[2] Number of fracture zones (FZ) in immediate roof beam

[3] Fracture Density = (FR + 2 FZ)/beam height

Table 7-1
Observation Borehole Fractures and Offset Data Summary

Hole	Location	Initial Inspection Date	Recent Inspection Date	FR[1]	FZ[2]	Beam Height (ft)	Feature	Fracture Density (frac/ft)	Feature Depth (ft)	Separation (in)	Offset (in.)	Compass	Hole Closure (%)	Offset Rate (in/yr)
OH589-2	E140-S2750	2/4/2014	2/4/2014				BOH		20.5					
		2/4/2014	2/4/2014				Rough Spot		8.6	0.00	0.00			
		2/4/2014	2/4/2014				Rough Spot		8.2	0.00	0.00			
		2/4/2014	2/4/2014				Rough Spot		8.1	0.00	0.00			
		2/4/2014	2/4/2014				Separation		8.0	0.25	0.00			
		2/4/2014	2/4/2014				Separation		6.9	0.13	0.00			
		2/4/2014	2/4/2014				Separation		6.4	0.13	0.00			
		2/4/2014	2/4/2014	0	1	5.1	Separation	0.39	5.1	0.13	0.00			
OH500-3	E140-S2920	2/4/2014	2/4/2014				BOH		20.1					
		2/4/2014	2/4/2014				Separation		8.3	1.75	0.00			
		2/4/2014	2/4/2014				Separation		6.7	2.50	0.00			
		2/4/2014	2/4/2014	4		5.6	Separation	0.71	5.6	7.50	0.00			
		2/4/2014	2/4/2014				Separation		5.3	1.00	0.00			
		2/4/2014	2/4/2014				Separation		4.9	0.13	0.00			
		2/4/2014	2/4/2014				Separation		2.0	2.00	0.00			
		2/4/2014	2/4/2014				Separation		1.0	1.00	0.00			

[1] Number of fractures (FR) in immediate roof beam

[2] Number of fracture zones (FZ) in immediate roof beam

[3] Fracture Density = (FR + 2 FZ)/beam height

Table 7-1
Observation Borehole Fractures and Offset Data Summary

Hole	Location	Initial Inspection Date	Recent Inspection Date	FR[1]	FZ[2]	Beam Height (ft)	Feature	Fracture Density (frac/ft)	Feature Depth (ft)	Separation (in)	Offset (in.)	Compass	Hole Closure (%)	Offset Rate (in/yr)
OH501-3	E140-S2984	2/4/2014	2/4/2014				BOH		20.1					
		2/4/2014	2/4/2014				Separation		7.1	5.00	0.00			
		2/4/2014	2/4/2014				Separation		6.8	0.13	0.00			
		2/4/2014	2/4/2014				Separation		6.2	0.13	0.00			
		2/4/2014	2/4/2014	2		5.2	Separation	0.38	5.2	7.00	0.00			
		2/4/2014	2/4/2014				Separation		1.8	1.00	0.00			
		2/4/2014	2/4/2014				Separation		0.8	1.00	0.00			
OH590-1	E140-S3080	11/18/2013	11/18/2013				BOH		20.7					
		11/18/2013	11/18/2013	5		5.9	Separation	0.85	5.9	1.00	1.25	E	42	N/A
		11/18/2013	11/18/2013				Separation		5.5	0.13	0.19	W	6	N/A
		11/18/2013	11/18/2013				Separation		5.2	0.13	0.00			
		11/18/2013	11/18/2013				Separation		2.4	0.13	0.00			
		11/18/2013	11/18/2013				Separation		1.5	1.50	0.38	SE	13	N/A
		11/18/2013	11/18/2013				Separation		0.4	0.13	0.00			

[1] Number of fractures (FR) in immediate roof beam

[2] Number of fracture zones (FZ) in immediate roof beam

[3] Fracture Density = (FR + 2 FZ)/beam height

Table 7-1
Observation Borehole Fractures and Offset Data Summary

Hole	Location	Initial Inspection Date	Recent Inspection Date	FR[1]	FZ[2]	Beam Height (ft)	Feature	Fracture Density (frac/ft)	Feature Depth (ft)	Separation (in)	Offset (in.)	Compass	Hole Closure (%)	Offset Rate (in/yr)
OH590-2	E140-S3080	2/4/2014	2/4/2014				BOH		20.0					
		2/4/2014	2/4/2014				Separation		7.6	0.13	0.00			
		2/4/2014	2/4/2014				Separation		6.1	0.50	0.00			
		2/4/2014	2/4/2014	3		5.8	Separation	0.52	5.8	2.00	0.00			
		2/4/2014	2/4/2014				Separation		5.4	0.13	0.00			
		2/4/2014	2/4/2014				Separation		4.8	0.13	0.00			
		2/4/2014	2/4/2014				Rough Spot		2.4	0.00	0.00			
		2/4/2014	2/4/2014				Separation		1.5	1.25	0.00			
OH493-3	E140-S3196	2/4/2014	2/4/2014				BOH		20.0					
		2/4/2014	2/4/2014				Separation		7.7	1.00	0.00			
		2/4/2014	2/4/2014				Separation		6.6	0.13	0.00			
		2/4/2014	2/4/2014				Separation		6.2	0.13	0.00			
		2/4/2014	2/4/2014	5		5.7	Separation	0.88	5.7	3.00	0.00			
		2/4/2014	2/4/2014				Separation		5.1	2.00	0.00			
		2/4/2014	2/4/2014				Separation		4.2	1.50	0.00			
		2/4/2014	2/4/2014				Separation		3.7	0.13	0.00			
		2/4/2014	2/4/2014				Separation		2.0	1.00	0.00			
		2/4/2014	2/4/2014				Separation		0.3	2.00	0.00			

[1] Number of fractures (FR) in immediate roof beam

[2] Number of fracture zones (FZ) in immediate roof beam

[3] Fracture Density = (FR + 2 FZ)/beam height

Table 7-1
Observation Borehole Fractures and Offset Data Summary

Hole	Location	Initial Inspection Date	Recent Inspection Date	FR[1]	FZ[2]	Beam Height (ft)	Feature	Fracture Density (frac/ft)	Feature Depth (ft)	Separation (in)	Offset (in.)	Compass	Hole Closure (%)	Offset Rate (in/yr)
OH571-1	E140-S3527	9/26/2011	12/9/2013				BOH		20.5					
		9/26/2011	12/9/2013				Separation		7.2	0.38	0.00			
		9/26/2011	12/9/2013	2	1	5.1	Rubble Zone	0.78	5.1	3.00	0.00			
		9/26/2011	12/9/2013				Separation		4.9	0.25	0.00			
		9/26/2011	12/9/2013				Separation		4.4	0.13	0.00			
OH607-1	E140-S3580	9/26/2011	12/9/2013				BOH		20.4					
		9/26/2011	12/9/2013				Separation		7.3	1.50	0.00			
		9/26/2011	12/9/2013	3		5.6	Separation	0.54	5.6	1.25	0.38	W	13	0.17
		9/26/2011	12/9/2013				Separation		5.1	0.25	0.00			
		9/26/2011	12/9/2013				Separation		4.8	0.13	0.13	W	4	0.06
		9/26/2011	12/9/2013				Separation		0.9	0.13	0.00			
OH567-1	E140-S3650	9/26/2011	12/9/2013				BOH		20.4					
		9/26/2011	12/9/2013				Separation		8.2	0.13	0.19	N	6	0.09
		9/26/2011	12/9/2013	3		6.7	Separation	0.45	6.7	1.00	0.50	N	17	0.23
		9/26/2011	12/9/2013				Separation		5.3	0.13	0.00			
		9/26/2011	12/9/2013				Separation		4.7	0.13	0.00			

[1] Number of fractures (FR) in immediate roof beam

[2] Number of fracture zones (FZ) in immediate roof beam

[3] Fracture Density = (FR + 2 FZ)/beam height

Table 7-1
Observation Borehole Fractures and Offset Data Summary

Hole	Location	Initial Inspection Date	Recent Inspection Date	FR[1]	FZ[2]	Beam Height (ft)	Feature	Fracture Density (frac/ft)	Feature Depth (ft)	Separation (in)	Offset (in.)	Compass	Hole Closure (%)	Offset Rate (in/yr)
OH565	W30-S3650	2/19/2005	12/9/2013				BOH		21.0					
		2/19/2005	12/9/2013				Hangup		16.6	0.00	0.00			
		2/19/2005	12/9/2013				Separation		7.2	1.00	0.00			
		2/19/2005	12/9/2013	3		5.7	Separation	0.53	5.7	1.00	2.25	N	75	0.26
		2/19/2005	12/9/2013				Separation		5.2	0.25	0.00			
		2/19/2005	12/9/2013				Separation		5.0	0.13	0.00			
		2/19/2005	12/9/2013				Separation		4.7	0.13	0.00			
		2/19/2005	12/9/2013				Separation		1.6	0.38	0.00			
OH566	E50-S3650	4/20/2005	12/9/2013				BOH		21.2					
		4/20/2005	12/9/2013	8		5.9	Separation	1.36	5.9	0.25	0.25	S	8	0.03
		4/20/2005	12/9/2013				Separation		5.7	0.13	0.00			
		4/20/2005	12/9/2013				Separation		5.4	0.13	0.00			
		4/20/2005	12/9/2013				Separation		5.3	0.25	0.00			
		4/20/2005	12/9/2013				Separation		5.0	0.13	0.00			
		4/20/2005	12/9/2013				Separation		4.9	0.13	0.00			
		4/20/2005	12/9/2013				Separation		4.6	0.13	0.00			
		4/20/2005	12/9/2013				Separation		2.3	1.50	0.00			
		4/20/2005	12/9/2013				Separation		1.4	0.13	0.00			

[1] Number of fractures (FR) in immediate roof beam

[2] Number of fracture zones (FZ) in immediate roof beam

[3] Fracture Density = (FR + 2 FZ)/beam height

Table 7-1
Observation Borehole Fractures and Offset Data Summary

Hole	Location	Initial Inspection Date	Recent Inspection Date	FR[1]	FZ[2]	Beam Height (ft)	Feature	Fracture Density (frac/ft)	Feature Depth (ft)	Separation (in)	Offset (in.)	Compass	Hole Closure (%)	Offset Rate (in/yr)
OH568	E235-S3650	4/20/2005	12/9/2013				BOH		21.0					
		4/20/2005	12/9/2013	4		5.9	Separation	0.68	5.9	0.13	0.13	S	4	0.02
		4/20/2005	12/9/2013				Separation		5.0	0.25	0.00			
		4/20/2005	12/9/2013				Separation		4.8	0.25	0.00			
		4/20/2005	12/9/2013				Separation		4.0	0.13	0.00			
		4/20/2005	12/9/2013				Separation		1.5	0.25	0.00			
OH569	E300-S3650	4/20/2005	12/9/2013				BOH		20.9					
		4/20/2005	12/9/2013				Rough Spot		15.5	0.00	0.00			
		4/20/2005	12/9/2013	2		5.9	Separation	0.34	5.9	0.25	1.75	N	58	0.20
		4/20/2005	12/9/2013				Separation		5.6	0.13	0.00			
		4/20/2005	12/9/2013				Separation		5.1	0.13	0.00			
		4/20/2005	12/9/2013				Rough Spot		4.8	0.00	0.00			
OH888	W30-S700	3/8/2009	12/3/2013				BOH		20.2					
		3/8/2009	12/3/2013	0		8.5	Separation	0.00	8.5	0.25	0.19	W	6	0.04
OH887	W30-S850	3/10/2009	12/3/2013				BOH		20.2					
		3/10/2009	12/3/2013	0		8.6	Separation	0.00	8.6	0.13	0.75	W	25	0.16
OH886	W30-S1000	3/3/2009	12/3/2013				BOH		20.2					
		3/3/2009	12/3/2013				Separation		16.1	0.13	0.13	S	4	0.03
		3/3/2009	12/3/2013				Separation		8.8	0.13	0.13	S	4	0.03
		3/3/2009	12/3/2013	0		8.1	Separation	0.00	8.1	0.25	0.50	S	17	0.11

[1] Number of fractures (FR) in immediate roof beam

[2] Number of fracture zones (FZ) in immediate roof beam

[3] Fracture Density = (FR + 2 FZ)/beam height

Table 7-1
Observation Borehole Fractures and Offset Data Summary

Hole	Location	Initial Inspection Date	Recent Inspection Date	FR[1]	FZ[2]	Beam Height (ft)	Feature	Fracture Density (frac/ft)	Feature Depth (ft)	Separation (in)	Offset (in.)	Compass	Hole Closure (%)	Offset Rate (in/yr)
OH885	W30-S1150	3/3/2009	12/3/2013				BOH		20.4					
		3/3/2009	12/3/2013				Separation		6.8	0.13	0.25	W	8	0.05
		3/3/2009	12/3/2013	5		6.6	Separation	0.76	6.6	0.13	1.50	W	50	0.32
		3/3/2009	12/3/2013				Separation		2.5	0.13	0.13	W	4	0.03
		3/3/2009	12/3/2013				Separation		2.2	0.38	0.25	W	8	0.05
		3/3/2009	12/3/2013				Separation		1.5	0.13	0.75	W	25	0.16
		3/3/2009	12/3/2013				Separation		0.7	0.13	0.50	W	17	0.11
		3/3/2009	12/3/2013				Separation		0.5	0.50	0.13	W	4	0.03
OH884	W30-S1300	3/3/2009	12/3/2013				BOH		20.2	0.00	0.00			
		3/3/2009	12/3/2013	0		8.5	Hangup	0.00	8.5	0.00	1.25	W	42	0.26
OH883	W30-S1485	3/3/2009	12/3/2013				BOH		20.3	0.00	0.00			
		3/3/2009	12/3/2013	0		8.8	Hangup	0.00	8.8	0.00	0.00			
OH882	W30-S1600	3/3/2009	12/9/2013				BOH		20.2					
		3/3/2009	12/9/2013				Hangup		9.0	0.00	0.00			
		3/3/2009	12/9/2013	1		8.3	Separation	0.12	8.3	0.13	0.00			
		3/3/2009	12/9/2013				Separation		0.5	0.13	0.00			
OH881	W30-S1780	3/3/2009	12/9/2013				BOH		20.2					
		3/3/2009	12/9/2013				Rough		2.0	0.00	0.00			
OH879	W30-S2060	3/3/2009	12/9/2013				BOH		20.2					
		3/3/2009	12/9/2013	0		7.7	Hangup	0.00	7.7	0.00	0.13	E	4	0.03

[1] Number of fractures (FR) in immediate roof beam

[2] Number of fracture zones (FZ) in immediate roof beam

[3] Fracture Density = (FR + 2 FZ)/beam height

Table 7-1
Observation Borehole Fractures and Offset Data Summary

Hole	Location	Initial Inspection Date	Recent Inspection Date	FR[1]	FZ[2]	Beam Height (ft)	Feature	Fracture Density (frac/ft)	Feature Depth (ft)	Separation (in)	Offset (in.)	Compass	Hole Closure (%)	Offset Rate (in/yr)
OH877	W30-S2350	3/11/2009	12/3/2013				BOH		20.3					
		3/11/2009	12/3/2013	1		8.0	Separation	0.13	8.0	0.13	0.19	E	6	0.04
		3/11/2009	12/3/2013				Separation		0.8	0.13	0.13	E	4	0.03
OH876	W30-S2520	3/2/2009	12/3/2013				BOH		18.0					
		3/2/2009	12/3/2013	3		7.6	Hangup	0.39	7.6	0.00	0.13	W	4	0.03
		3/2/2009	12/3/2013				Separation		7.2	0.13	0.00			
		3/2/2009	12/3/2013				Separation		7.1	0.13	0.13	S	4	0.03
		3/2/2009	12/3/2013				Separation		6.1	0.13	0.13	S	4	0.03
OH899	W170-S1000	3/24/2009	12/3/2013				BOH		20.1					
		3/24/2009	12/3/2013				Offset		16.0	0.00	0.19	E	6	0.04
		3/24/2009	12/3/2013	0		9.2	Separation	0.00	9.2	0.13	0.13	E	4	0.03
OH898	W170-1150	3/24/2009	12/3/2013				BOH		21.2	0.00	0.00			
		3/24/2009	12/3/2013	0		9.0	Hangup	0.00	9.0	0.00	0.00			
OH897	W170-S1300	3/24/2009	12/3/2013				BOH		20.2	0.00				
		3/24/2009	12/3/2013	0		8.6	Separation	0.00	8.6	0.13	1.00	NE	33	0.21
OH896	W170-S1482	3/24/2009	12/2/2013				BOH		17.3					
		3/24/2009	12/2/2013				Hangup		15.0	0.00	0.06	W	2	0.01
		3/24/2009	12/2/2013	0		8.2	Separation	0.00	8.2	0.25	0.13	W	4	0.03
OH895	W170-S1600	3/24/2009	12/3/2013				BOH		20.1					
		3/24/2009	12/3/2013	0		8.7	Separation	0.00	8.7	0.13	0.75	E	25	0.16

[1] Number of fractures (FR) in immediate roof beam

[2] Number of fracture zones (FZ) in immediate roof beam

[3] Fracture Density = (FR + 2 FZ)/beam height

Table 7-1
Observation Borehole Fractures and Offset Data Summary

Hole	Location	Initial Inspection Date	Recent Inspection Date	FR[1]	FZ[2]	Beam Height (ft)	Feature	Fracture Density (frac/ft)	Feature Depth (ft)	Separation (in)	Offset (in.)	Compass	Hole Closure (%)	Offset Rate (in/yr)
OH894	W170-S1780	3/24/2009	12/3/2013				BOH		20.1					
		3/24/2009	12/3/2013	0		9.4	Offset	0.00	9.4	0.00	0.25	E	8	0.05
OH893	W170-S1950	3/24/2009	12/9/2013				BOH		20.2					
		3/24/2009	12/9/2013	0		8.5	Separation	0.00	8.5	0.13	0.38	E	13	0.08
OH892	W170-S2055	3/24/2009	12/9/2013				BOH		19.6					
		3/24/2009	12/9/2013	2		7.9	Separation	0.25	7.9	0.13	0.00			
		3/24/2009	12/9/2013				Separation		1.9	0.13	0.00			
		3/24/2009	12/9/2013				Separation		1.1	0.13	0.00			
OH891	W170-S2180	3/24/2009	12/9/2013				BOH		20.2					
		3/24/2009	12/9/2013	0		7.8	Separation	0.00	7.8	0.13	0.38	E	13	0.08
OH890	W170-S2345	3/11/2009	12/9/2013				BOH		20.2					
		3/11/2009	12/9/2013				Offset		14.4	0.00	0.50	E	17	0.11
		3/11/2009	12/9/2013	0		8.0	Separation	0.00	8.0	0.13	1.50	E	50	0.32
OH889	W170-S2520	3/11/2009	12/3/2013				BOH		20.2					
		3/11/2009	12/3/2013	1		8.1	Hangup	0.12	8.1	0.00	0.25	E	8	0.05
		3/11/2009	12/3/2013				Hangup		7.7	0.00	0.00			
		3/11/2009	12/3/2013				Hangup		3.1	0.00	0.00			
		3/11/2009	12/3/2013				Separation		1.7	0.13	0.13	N	4	0.03

[1] Number of fractures (FR) in immediate roof beam

[2] Number of fracture zones (FZ) in immediate roof beam

[3] Fracture Density = (FR + 2 FZ)/beam height

Table 7-1
Observation Borehole Fractures and Offset Data Summary

Hole	Location	Initial Inspection Date	Recent Inspection Date	FR[1]	FZ[2]	Beam Height (ft)	Feature	Fracture Density (frac/ft)	Feature Depth (ft)	Separation (in)	Offset (in.)	Compass	Hole Closure (%)	Offset Rate (in/yr)
OH486	E0-N1400	1/7/2004	12/2/2013				BOH		20.5	0.00	0.00			
		1/7/2004	12/2/2013				Offset		16.3	0.00	0.00			
		1/7/2004	12/2/2013	1		6.6	Separation	0.15	6.6	4.00	2.00	S	67	0.20
		1/7/2004	12/2/2013				Separation		1.3	0.38	0.38	S	13	0.04
OH860	E0-N1266	3/8/2009	12/2/2013				BOH		20.3					
		3/8/2009	12/2/2013				Separation		7.3	0.25	0.00			
		3/8/2009	12/2/2013				Separation		6.9	0.25	0.13	W	4	0.03
		3/8/2009	12/2/2013	3		6.1	Separation	0.49	6.1	0.50	0.13	E	4	0.03
		3/8/2009	12/2/2013				Separation		5.8	0.13	0.13	W	4	0.03
		3/8/2009	12/2/2013				Separation		3.0	2.50	0.13	W	4	0.03
		3/8/2009	12/2/2013				Separation		1.6	2.00	0.13	W	4	0.03
OH488	E0-N1100	1/7/2004	12/2/2013				BOH		20.4					
		1/7/2004	12/2/2013	2		6.1	Separation	0.33	6.1	1.50	0.13	W	4	0.01
		1/7/2004	12/2/2013				Separation		5.1	0.13	0.13	W	4	0.01
		1/7/2004	12/2/2013				Separation		1.2	0.38	0.00			
OH859	E0-N920	3/8/2009	12/2/2013				BOH		20.4					
		3/8/2009	12/2/2013	2		6.6	Separation	0.30	6.6	1.25	0.06	W	2	0.01
		3/8/2009	12/2/2013				Separation		2.6	0.13	0.00			
		3/8/2009	12/2/2013				Separation		1.1	0.13	0.00			

[1] Number of fractures (FR) in immediate roof beam

[2] Number of fracture zones (FZ) in immediate roof beam

[3] Fracture Density = (FR + 2 FZ)/beam height

Table 7-1
Observation Borehole Fractures and Offset Data Summary

Hole	Location	Initial Inspection Date	Recent Inspection Date	FR[1]	FZ[2]	Beam Height (ft)	Feature	Fracture Density (frac/ft)	Feature Depth (ft)	Separation (in)	Offset (in.)	Compass	Hole Closure (%)	Offset Rate (in/yr)
OH755	E0-N460	3/9/2009	12/2/2013				BOH		20.2					
		3/9/2009	12/2/2013				Hangup		17.2	0.00	0.00			
		3/9/2009	12/2/2013				Separation		7.3	0.13	0.00			
		3/9/2009	12/2/2013	3		6.8	Separation	0.44	6.8	0.38	0.13	E	4	0.03
		3/9/2009	12/2/2013				Separation		5.7	0.13	0.13	E	4	0.03
		3/9/2009	12/2/2013				Separation		2.4	1.00	0.13	E	4	0.03
		3/9/2009	12/2/2013				Separation		1.3	0.25	0.13	E	4	0.03
OH485	E140-N1400	1/7/2004	12/2/2013				BOH		20.4					
		1/7/2004	12/2/2013				Hangup		10.2	0.00	0.38	S	13	0.04
		1/7/2004	12/2/2013	0		6.6	Hangup	0.00	6.6	0.00	1.75	S	58	0.18
OH492	E140-N790	1/9/2004	12/2/2013				BOH		20.5					
		1/9/2004	12/2/2013	0		6.7	Hangup		6.7	0.00	0.25	W	8	0.03
OH855	S90-W380	3/4/2009	12/2/2013				BOH		21.0					
OH856	S90-W620	3/4/2009	12/2/2013				BOH		20.2					
		3/4/2009	12/2/2013	1		9.1	Separation	0.11	9.1	0.13	0.19	W	6	0.04
		3/4/2009	12/2/2013				Separation		1.2	0.13	0.13	N	4	0.03
OH857	S90-W880	3/4/2009	12/2/2013				BOH		20.6					

[1] Number of fractures (FR) in immediate roof beam

[2] Number of fracture zones (FZ) in immediate roof beam

[3] Fracture Density = (FR + 2 FZ)/beam height

Table 7-1
Observation Borehole Fractures and Offset Data Summary

Hole	Location	Initial Inspection Date	Recent Inspection Date	FR[1]	FZ[2]	Beam Height (ft)	Feature	Fracture Density (frac/ft)	Feature Depth (ft)	Separation (in)	Offset (in.)	Compass	Hole Closure (%)	Offset Rate (in/yr)
OH755	E0-N460	3/9/2009	12/2/2013				BOH		20.2					
		3/9/2009	12/2/2013				Hangup		17.2	0.00	0.00			
		3/9/2009	12/2/2013				Separation		7.3	0.13	0.00			
		3/9/2009	12/2/2013	3		6.8	Separation	0.44	6.8	0.38	0.13	E	4	0.03
		3/9/2009	12/2/2013				Separation		5.7	0.13	0.13	E	4	0.03
		3/9/2009	12/2/2013				Separation		2.4	1.00	0.13	E	4	0.03
		3/9/2009	12/2/2013				Separation		1.3	0.25	0.13	E	4	0.03
OH485	E140-N1400	1/7/2004	12/2/2013				BOH		20.4					
		1/7/2004	12/2/2013				Hangup		10.2	0.00	0.38	S	13	0.04
		1/7/2004	12/2/2013	0		6.6	Hangup	0.00	6.6	0.00	1.75	S	58	0.18
OH492	E140-N790	1/9/2004	12/2/2013				BOH		20.5					
		1/9/2004	12/2/2013	0		6.7	Hangup		6.7	0.00	0.25	W	8	0.03
OH855	S90-W380	3/4/2009	12/2/2013				BOH		21.0					
OH856	S90-W620	3/4/2009	12/2/2013				BOH		20.2					
		3/4/2009	12/2/2013	1		9.1	Separation	0.11	9.1	0.13	0.19	W	6	0.04
		3/4/2009	12/2/2013				Separation		1.2	0.13	0.13	N	4	0.03
OH857	S90-W880	3/4/2009	12/2/2013				BOH		20.6					
OH850	N300-W80	3/8/2009	11/18/2013				BOH		6.1		3.00			
		3/8/2009	11/18/2013	0		6.1	Separation	0.00	5.8	2.50		0	0	0.00

[1] Number of fractures (FR) in immediate roof beam

[2] Number of fracture zones (FZ) in immediate roof beam

[3] Fracture Density = (FR + 2 FZ)/beam height

Table 7-1
Observation Borehole Fractures and Offset Data Summary

Hole	Location	Initial Inspection Date	Recent Inspection Date	FR[1]	FZ[2]	Beam Height (ft)	Feature	Fracture Density (frac/ft)	Feature Depth (ft)	Separation (in)	Offset (in.)	Compass	Hole Closure (%)	Offset Rate (in/yr)
OH850-1	N300-W80	12/2/2013	12/2/2013				BOH		20.0					
		12/2/2013	12/2/2013				Separation		7.4	0.00	0.00	0	0	N/A
		12/2/2013	12/2/2013	3		6.9		0.11	6.9	0.13	0.00			N/A
		12/2/2013	12/2/2013						5.3	0.00	0.00			N/A
		12/2/2013	12/2/2013						4.3	0.13	0.00			N/A
		12/2/2013	12/2/2013						3.0	0.06	0.00			N/A
OH858	W469-N216	3/8/2009	12/2/2013				BOH		20.2					
		3/8/2009	12/2/2013				Hangup		9.2	0.00	0.00			
		3/8/2009	12/2/2013				Separation		8.7	0.13	0.00			
		3/8/2009	12/2/2013	1		6.9	Separation	0.14	6.9	0.13	1.00	S	33	0.21
		3/8/2009	12/2/2013				Separation		5.6	0.13	0.00			

[1] Number of fractures (FR) in immediate roof beam

[2] Number of fracture zones (FZ) in immediate roof beam

[3] Fracture Density = (FR + 2 FZ)/beam height

Table 7-2
Summary of New Boreholes

Hole	Location	Northing	Easting	Drill Date	Depth	Diameter	Purpose
OH1022-1	S2180-W392	7507.23	6502.89	11/13/2013	20.7	3	Observation
OH1026-1	S2180-W662	7507.23	6232.89	11/13/2013	20.5	3	Observation
OH1027-1	S2180-W727	7507.23	6167.89	12/4/2013	20.1	3	Observation
OH1029-1	S2180-W861	7507.23	6033.89	12/4/2013	20.2	3	Observation
OH1030-1	S2180-W928	7507.23	5966.89	11/13/2013	20.3	3	Observation
OH1031-1	S2180-W985	7507.23	5909.89	12/4/2013	20.1	3	Observation
OH1032-1	S2180-W1058	7507.23	5836.89	12/4/2013	20.1	3	Observation
OH1041-1	S2520-W726	7167.23	6168.89	11/19/2013	20.2	3	Observation
OH1042-1	S2520-W860	7167.23	6034.89	11/19/2013	20.1	3	Observation
OH1043-1	S2520-W923	7167.23	5971.89	11/19/2013	20.2	3	Observation
OH1045-1	S2520-W1056	7167.23	5838.89	11/19/2013	20.1	3	Observation
OH750-1	E140-S773	8917.23	7034.89	2/4/2014	20.2	3	Observation
OH874-2	E140-S850	8837.23	7034.89	2/4/2014	20.1	3	Observation
OH751-1	E140-S920	8767.23	7034.89	2/4/2014	20.1	3	Observation
OH873-2	E140-S1145	8542.23	7034.89	2/4/2014	20.1	3	Observation
OH753-1	E140-S1226	8461.23	7034.89	2/5/2014	20.1	3	Observation
OH872-2	E140-S1391	8296.23	7034.89	2/4/2014	20	3	Observation
OH580-3	E140-S1463	8224.23	7034.89	2/4/2014	20	3	Observation
OH871-2	E140-S1675	8012.23	7034.89	2/4/2014	20.2	3	Observation
OH143-5	E140-S1780	7907.23	7034.89	2/4/2014	20.1	3	Observation
OH583-1	E140-S1950	7737.23	7034.89	2/4/2014	20	3	Observation
OH474-2	E140-S2001	7696.23	7034.89	2/4/2014	20.2	3	Observation
OH473-4	E140-S2091	7596.23	7034.89	2/4/2014	20.3	3	Observation
OH586-3	E140-S2359	7328.23	7034.89	2/4/2014	20.1	3	Observation
OH468-3	E140-S2637	7050.23	7034.89	2/4/2014	20.1	3	Observation
OH589-2	E140-S2750	6937.23	7034.89	2/4/2014	20.5	3	Observation
OH500-3	E140-S2920	6767.23	7034.89	2/4/2014	20.1	3	Observation
OH501-3	E140-S2984	6703.23	7034.89	2/4/2014	20.1	3	Observation
OH590-2	E140-S3080	6607.23	7034.89	2/4/2014	20	3	Observation
OH493-3	E140-S3196	6491.23	7034.89	2/4/2014	20	3	Observation
OH953	S2750-W285	6937.23	6609.89	2/3/2014	20.1	3	Observation
OH952	S2520-W285	7167.23	6609.89	2/3/2014	20	3	Observation
OH951	S2180-W285	7507.23	6609.89	2/3/1989	20.1	3	Observation
OH1102	S1763-W393	7924.23	6501.89	11/12/2013	20	3	Observation
OH1122	S1600-W400	8070.7	6494.9	11/12/2013	20.1	3	Observation
OH1135	S1950-W400	7737.23	6494.89	11/12/2013	20	3	Observation
OH850-1	W80-N300	9987.23	6814.89	12/2/2013	20	3	Observation

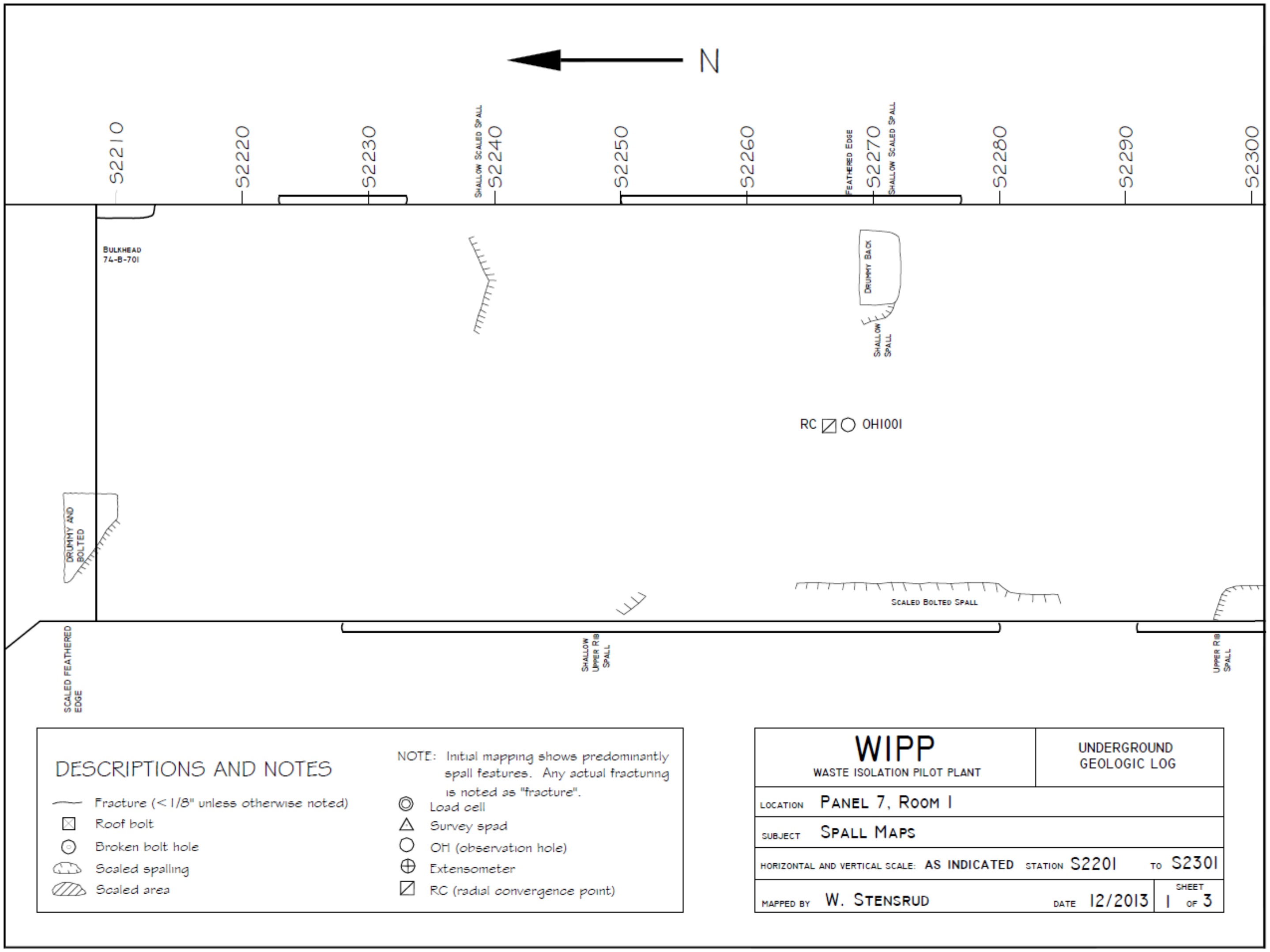

Figure - 1 Panel 7 Room 1, S2201-S2301 Roof Fractures

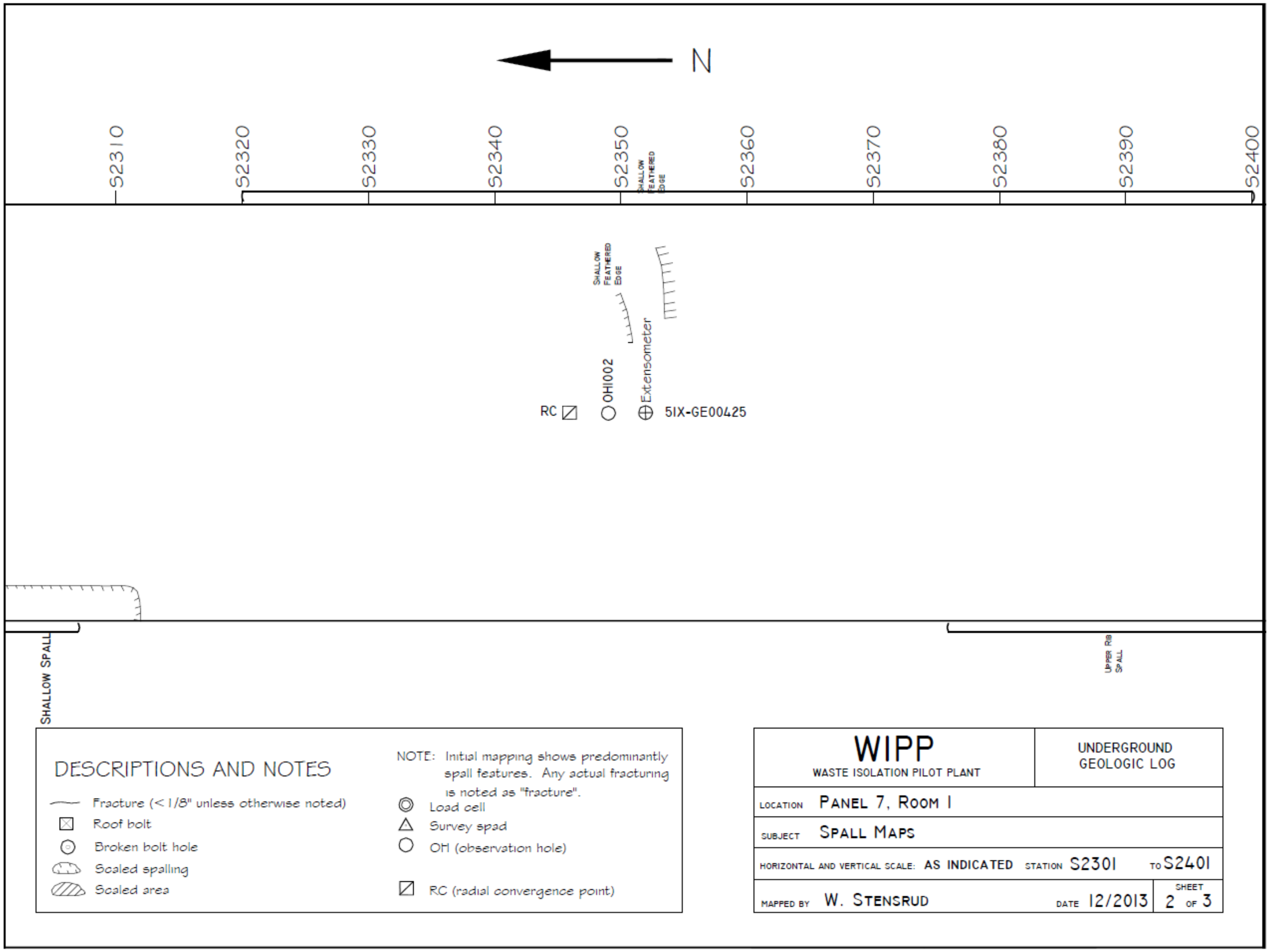

Figure - 2 Panel 7 Room 1, S2301-S2401 Roof Fractures

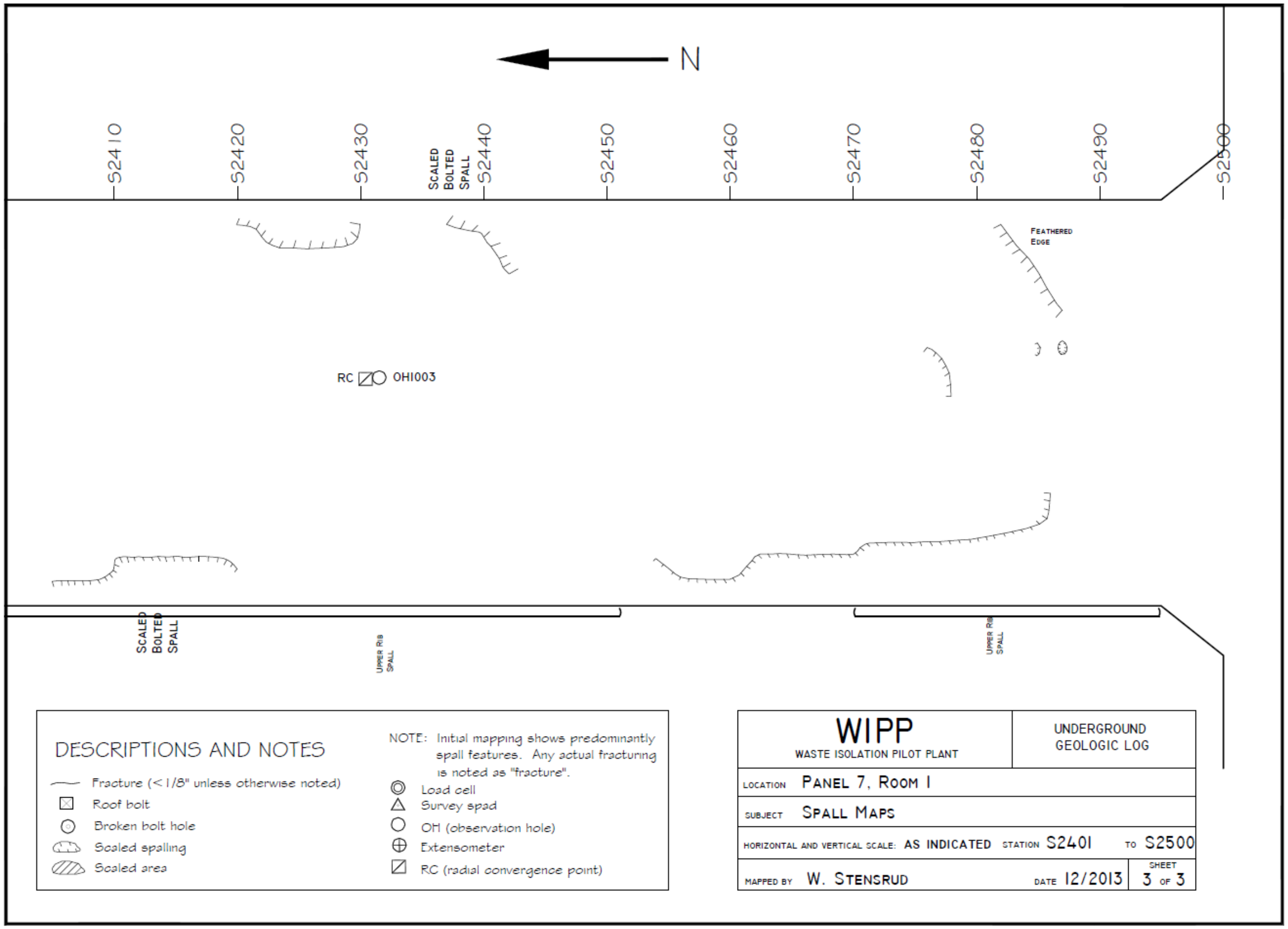

Figure - 3 Panel 7 Room 1, S2401-S2500 Roof Fractures

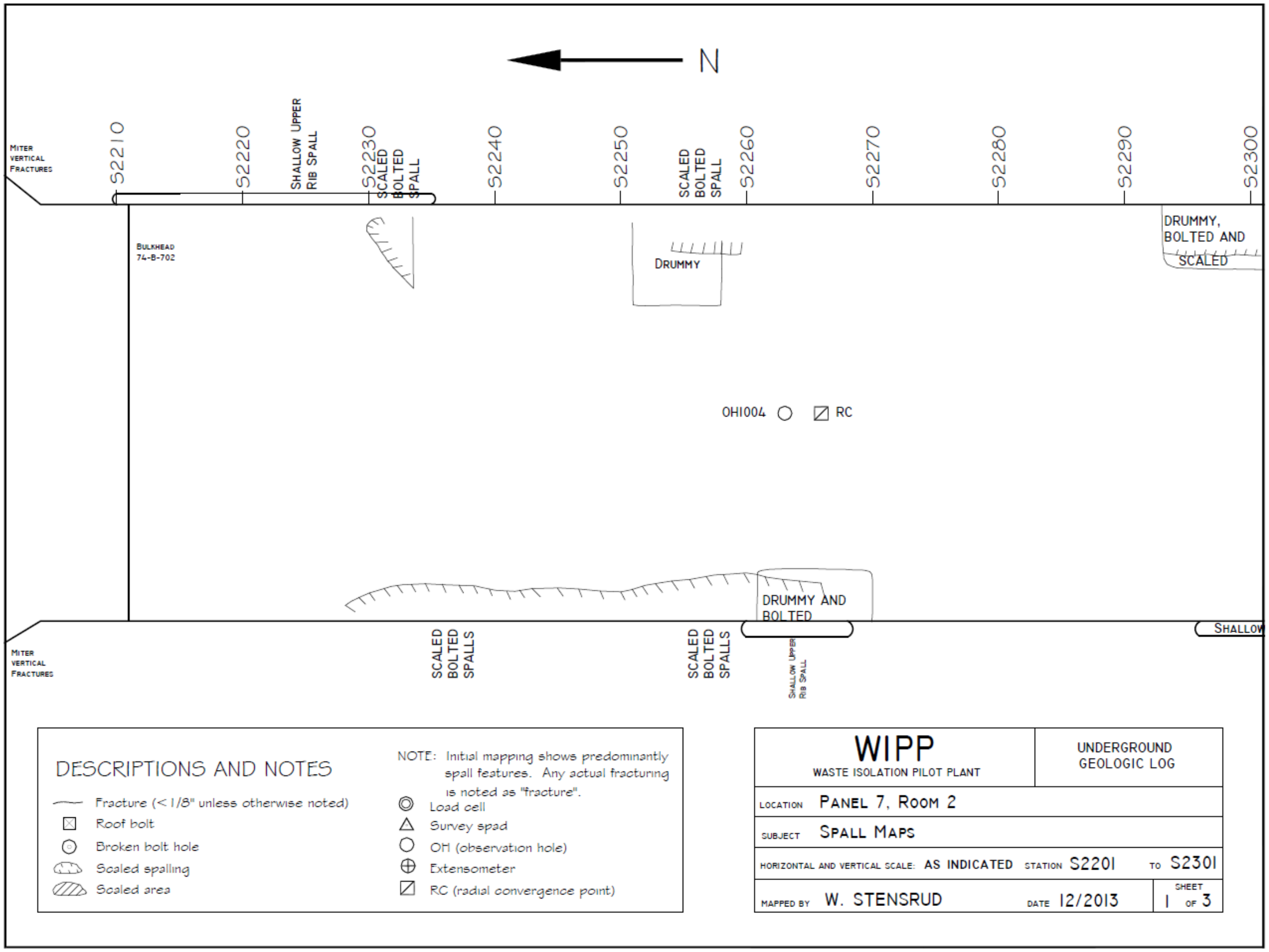

Figure - 4 Panel 7 Room 2, S2201-S2301 Roof Fractures

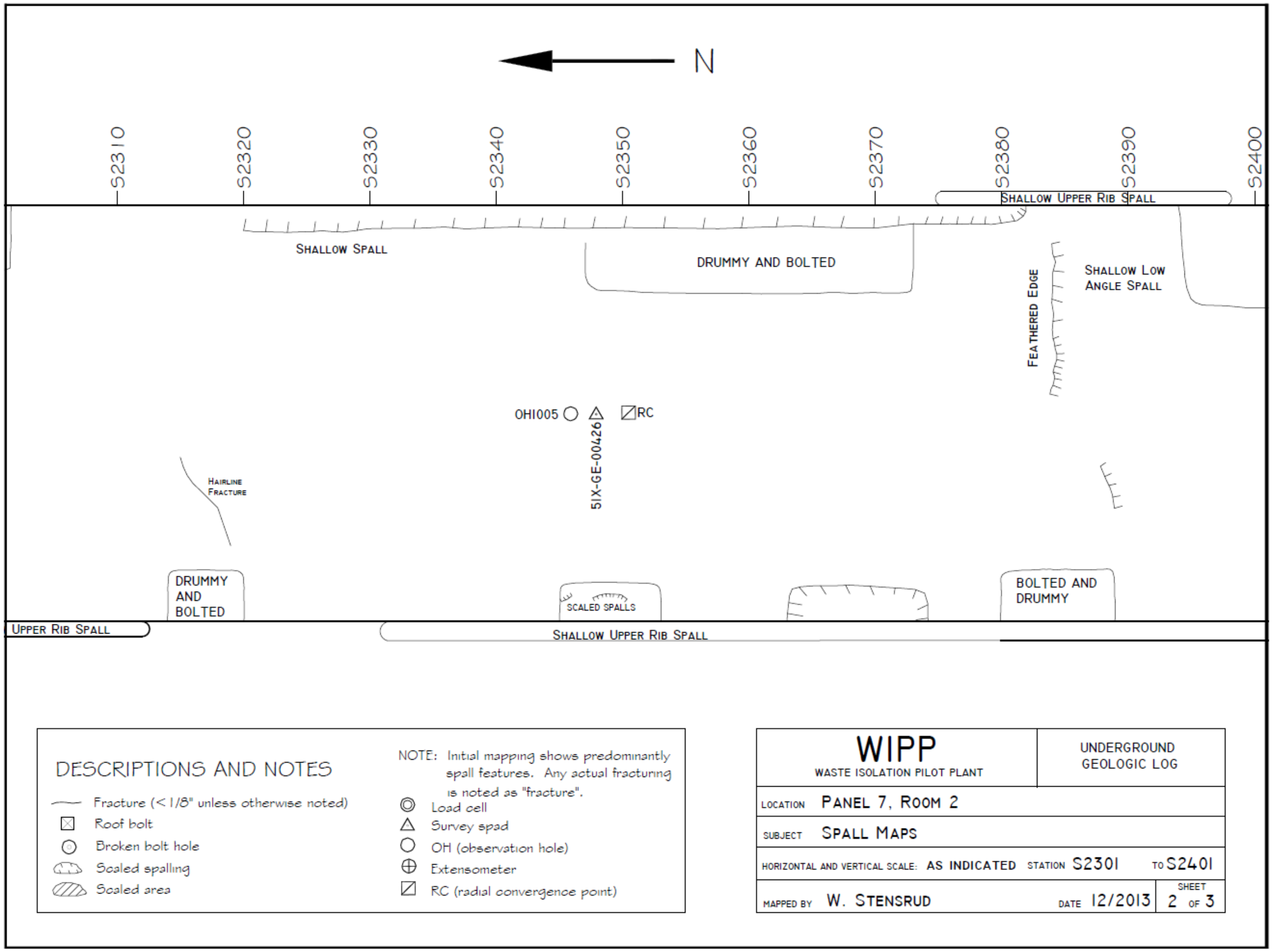

Figure - 5 Panel 7 Room 2, S2301-S2401Roof Fractures

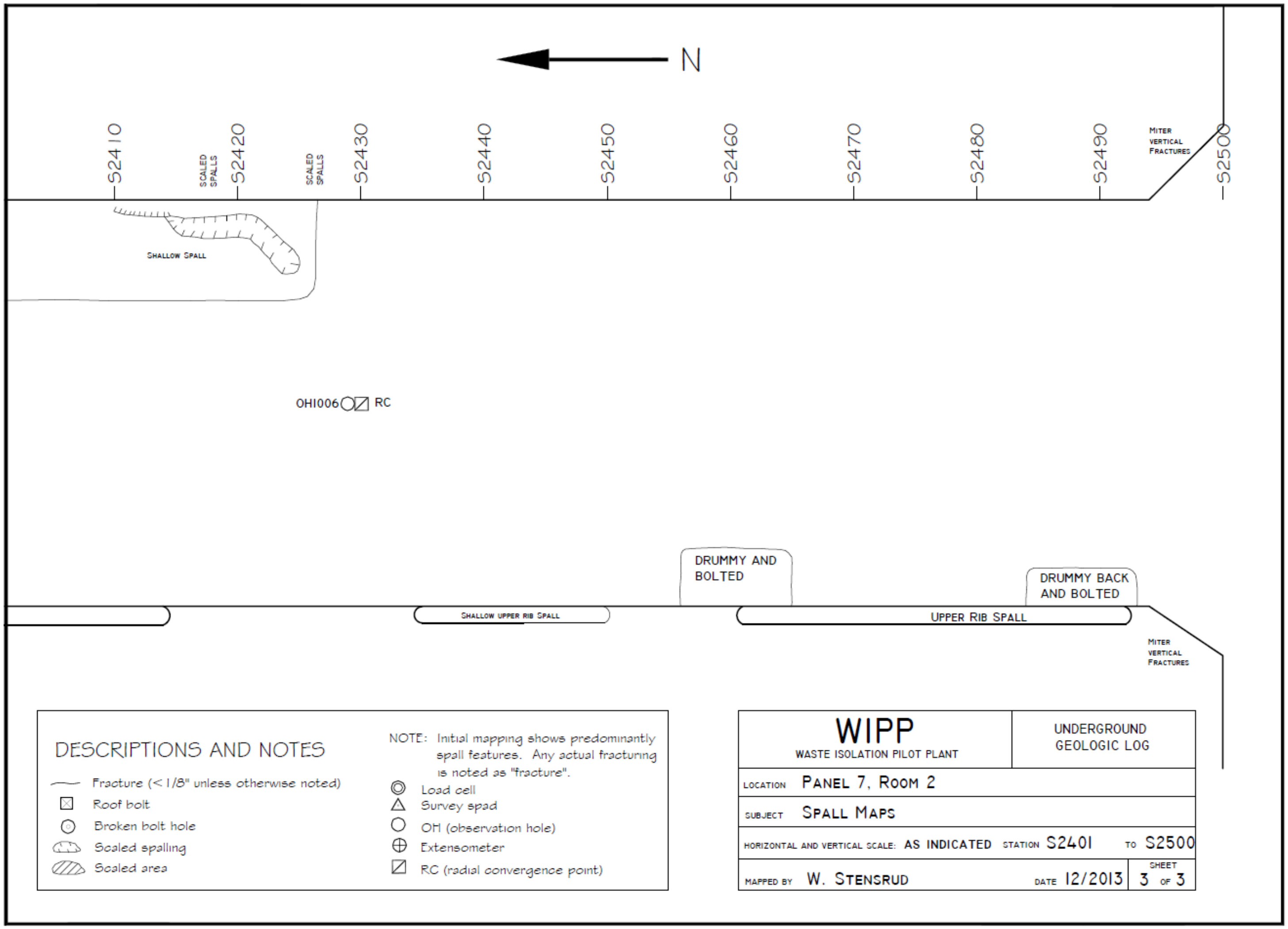

Figure - 6 Panel 7 Room 2, S2401-S2500 Roof Fractures

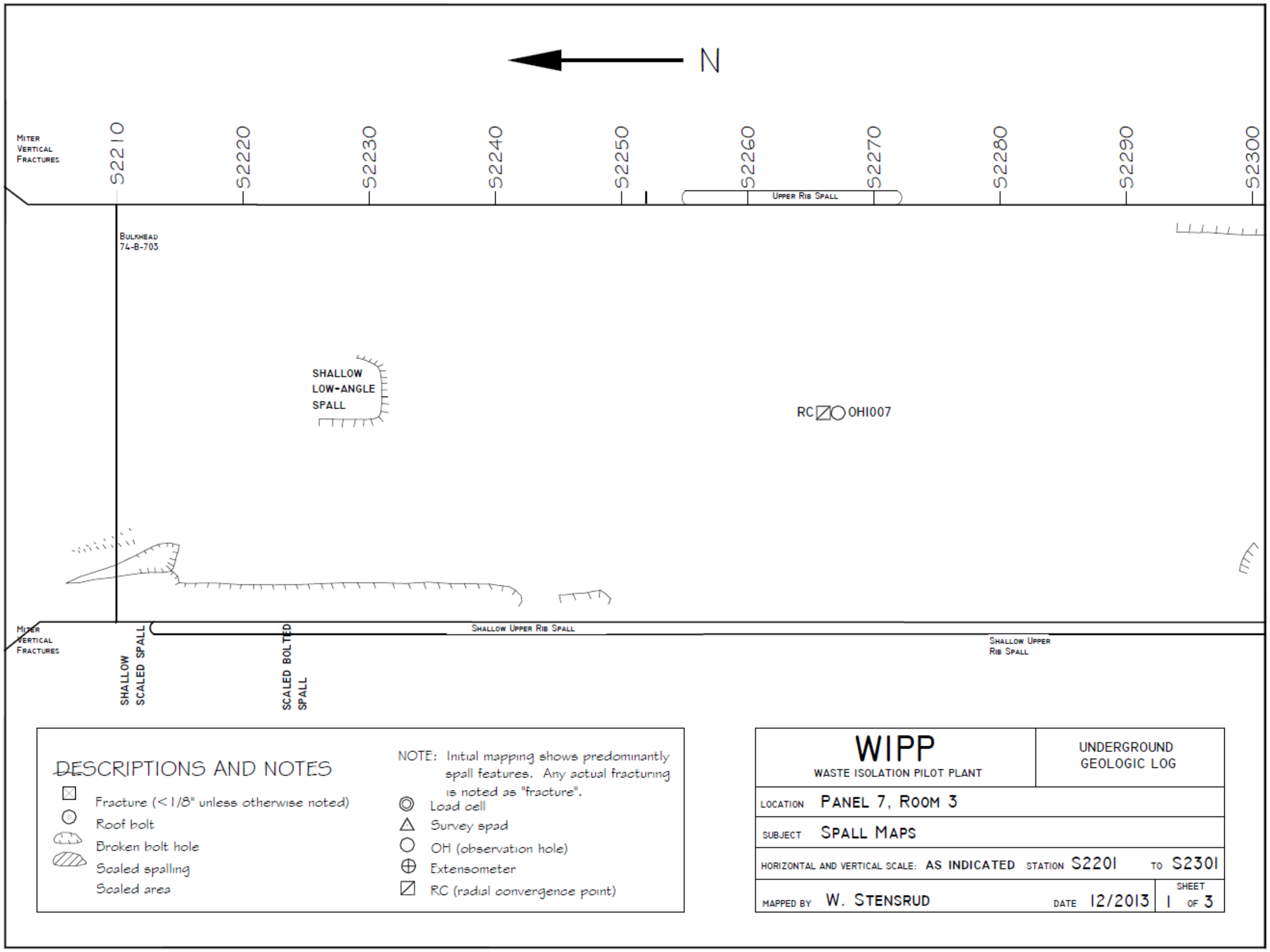

Figure - 7 Panel 7 Room 3, S2201-S2301 Roof Fractures

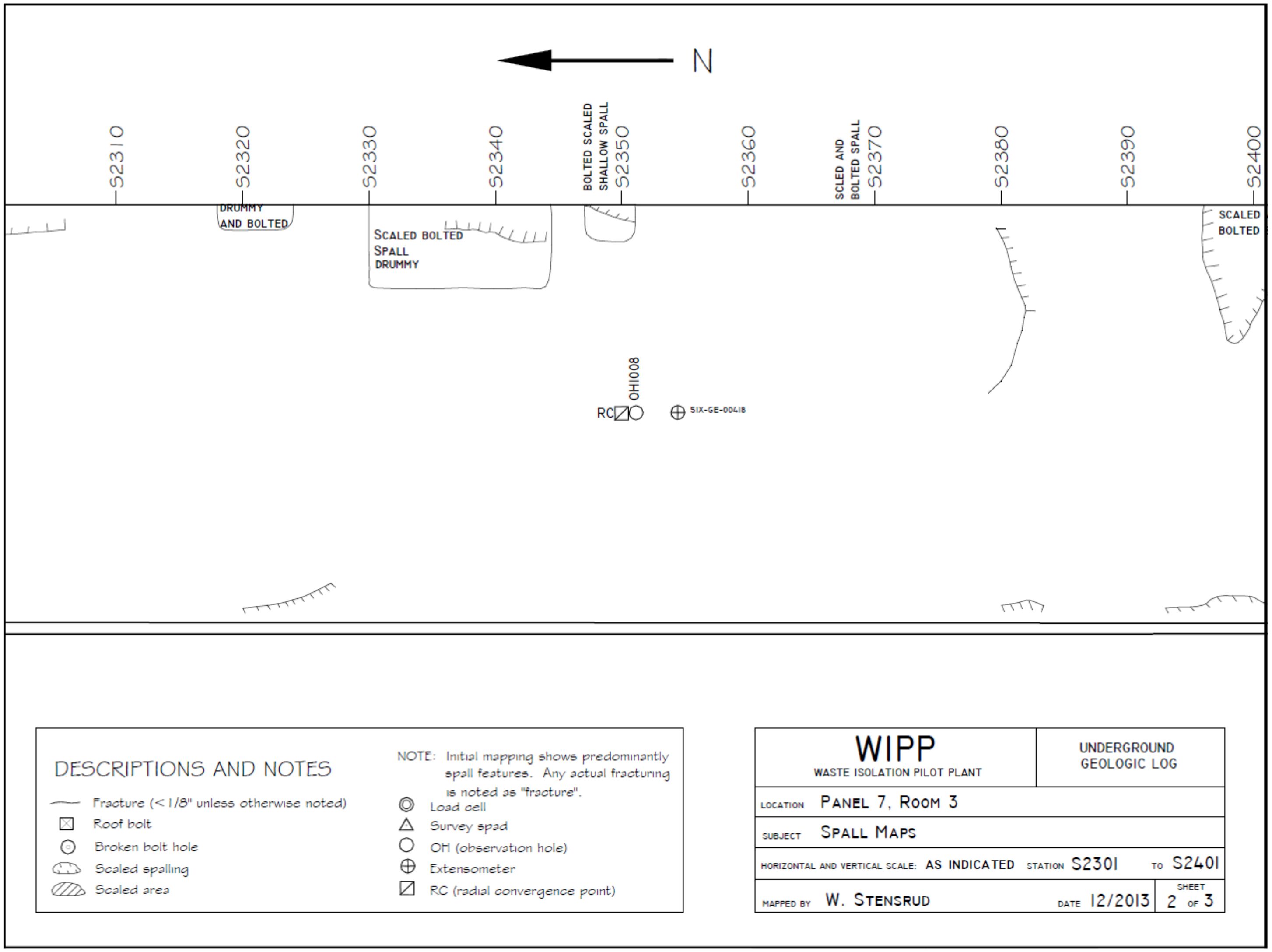

Figure - 8 Panel 7 Room 3, S2301-S2401 Roof Fractures

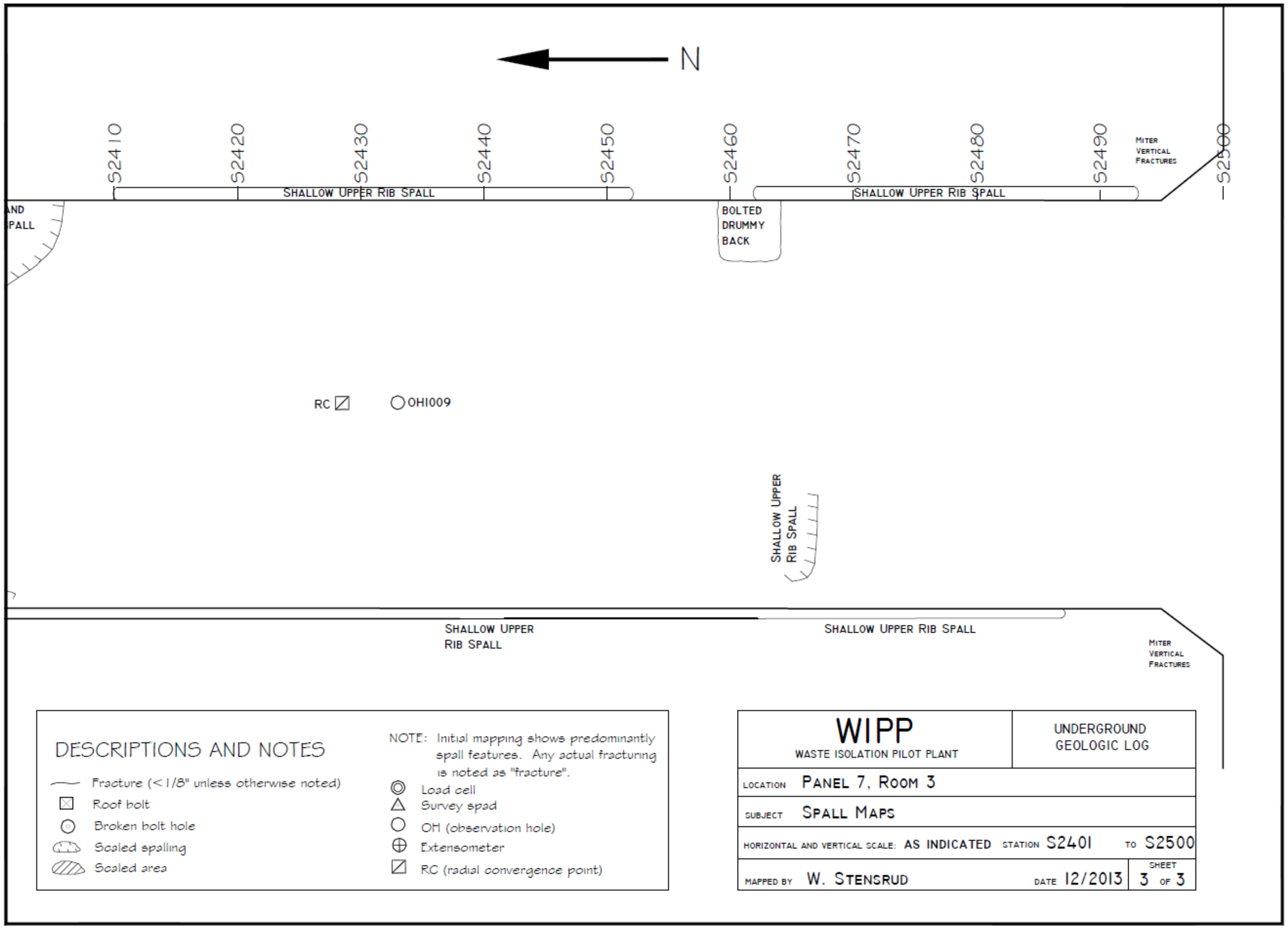

Figure - 9 Panel 7 Room 3, S2401-S2500 Roof Fractures

DRAFT

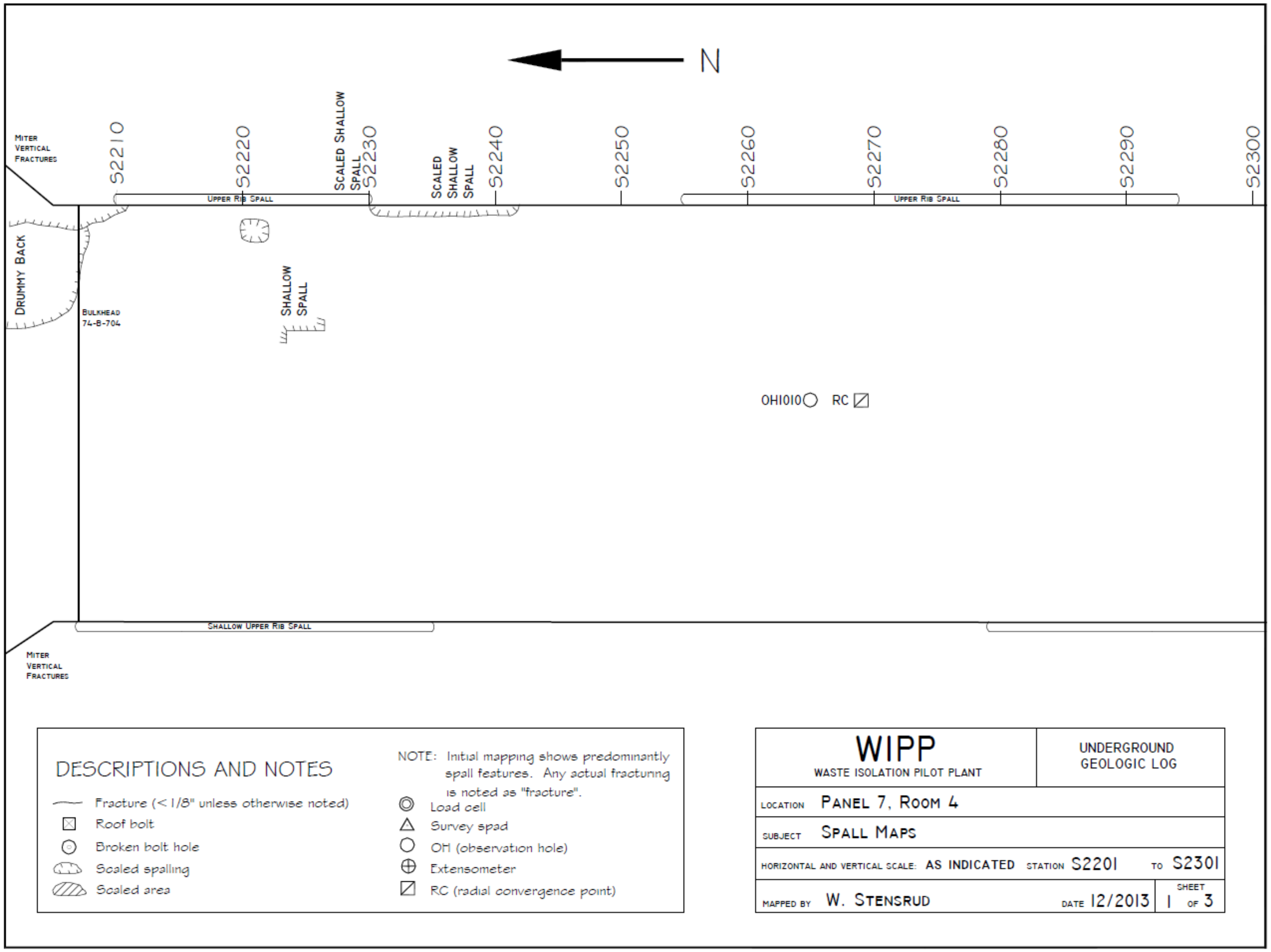

Figure - 10 Panel 7 Room 4, S2201-S2301 Roof Fractures

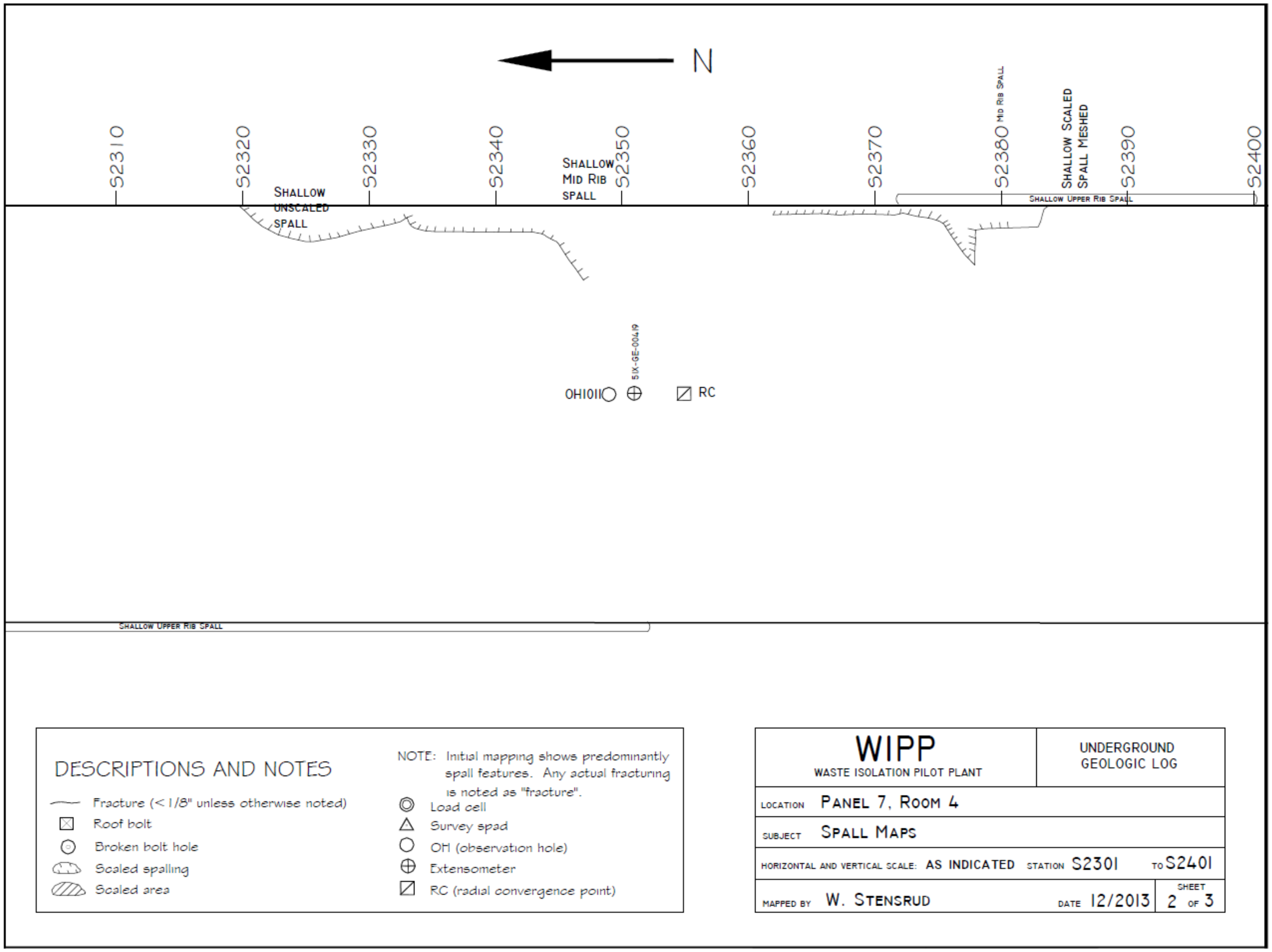

Figure - 11 Panel 7 Room 4, S2301-S2401 Roof Fractures

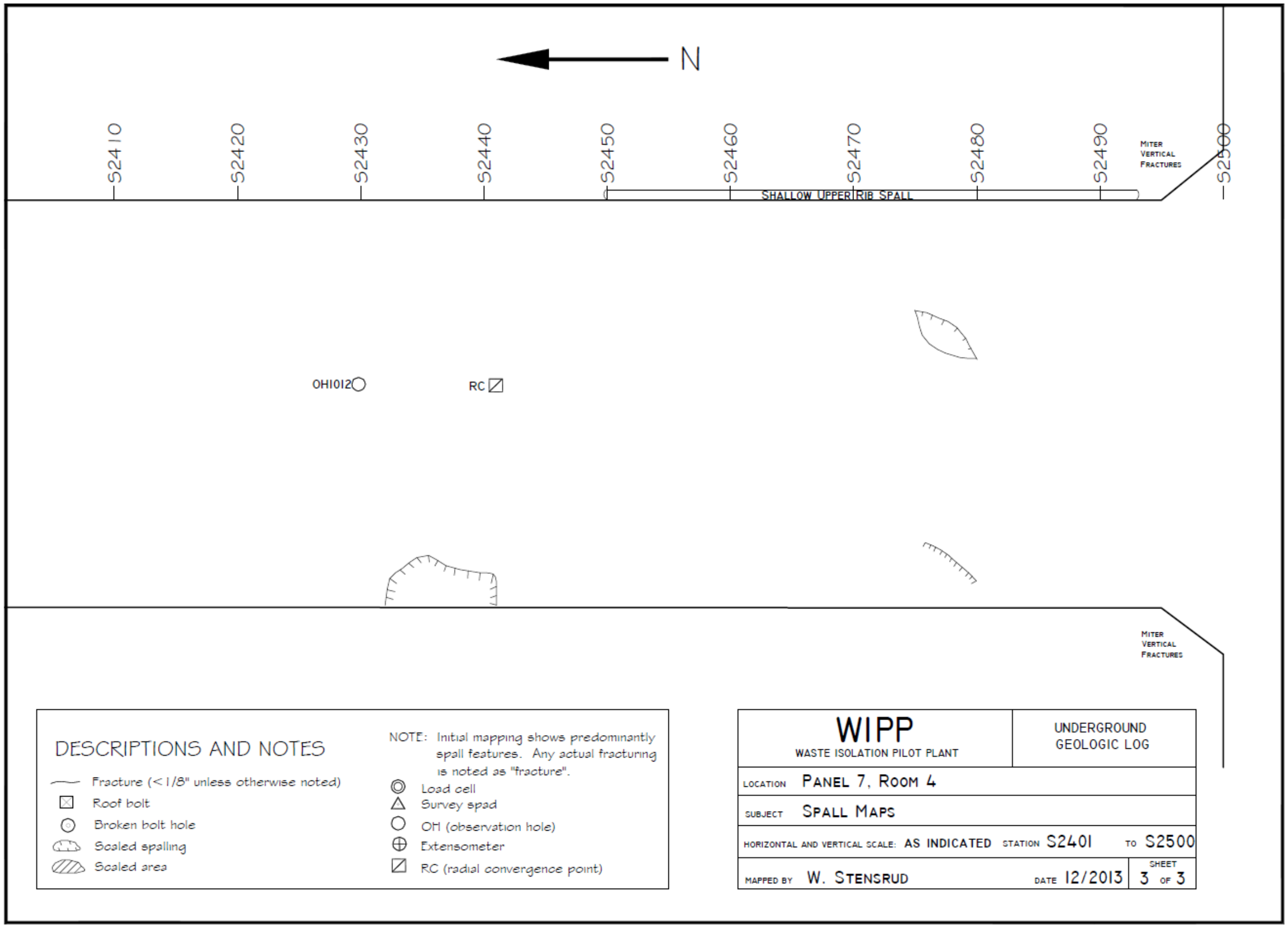

Figure - 12 Panel 7 Room 4, S2401-S2500 Roof Fractures

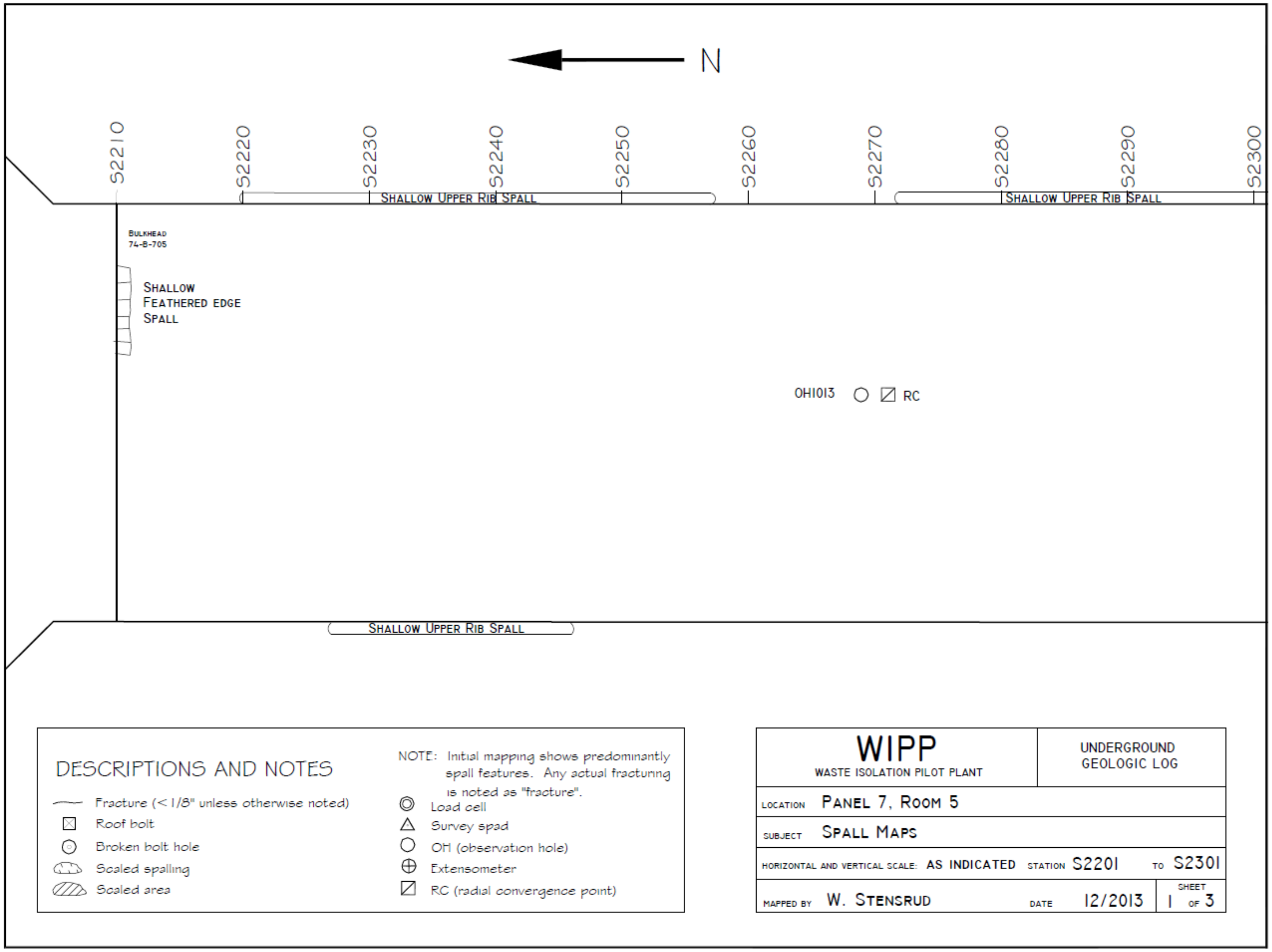

Figure - 13 Panel 7 Room 5, S2201-S2301 Roof Fractures

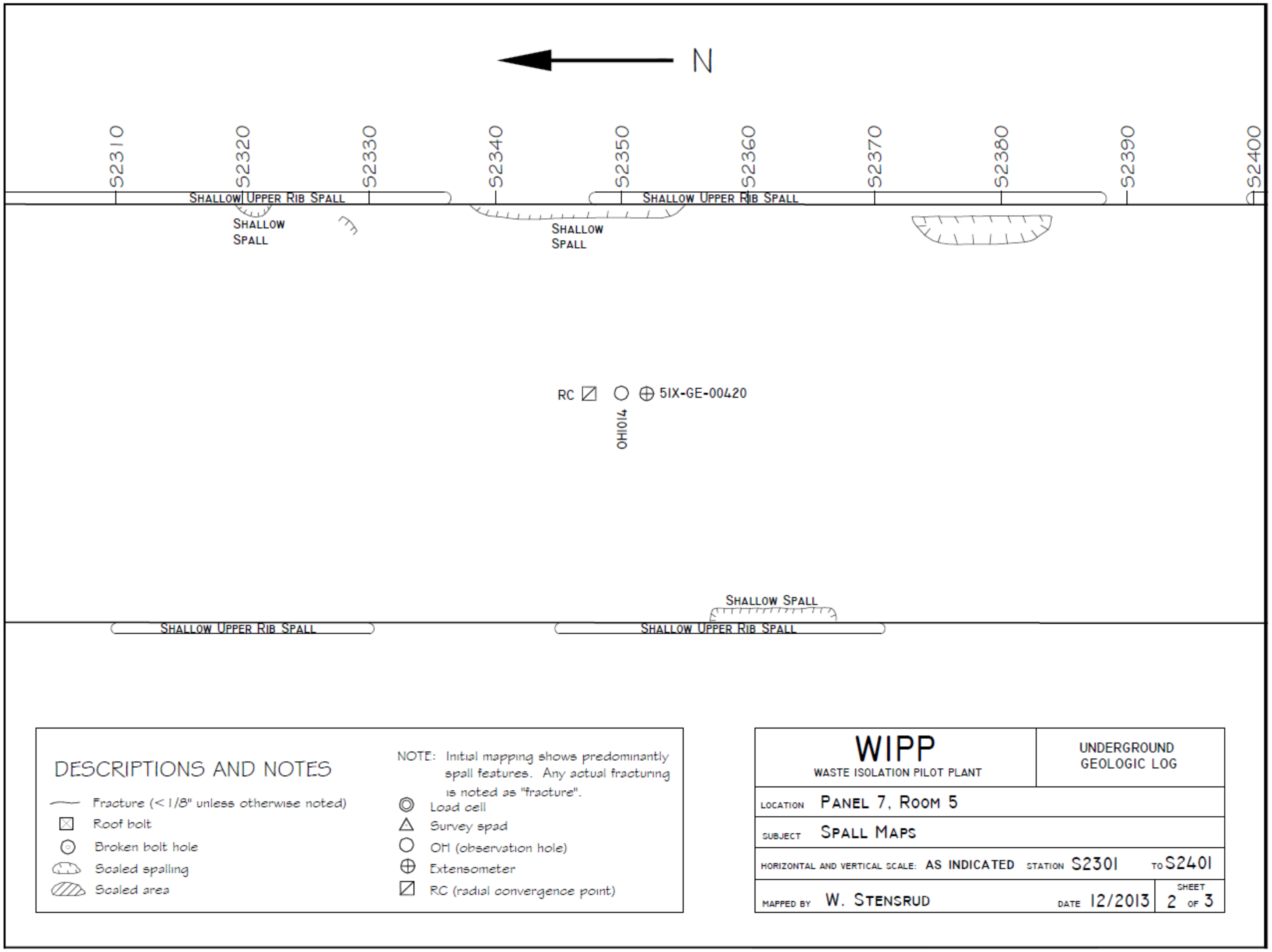

Figure - 14 Panel 7 Room 5 S2301-S2401 Roof Fractures

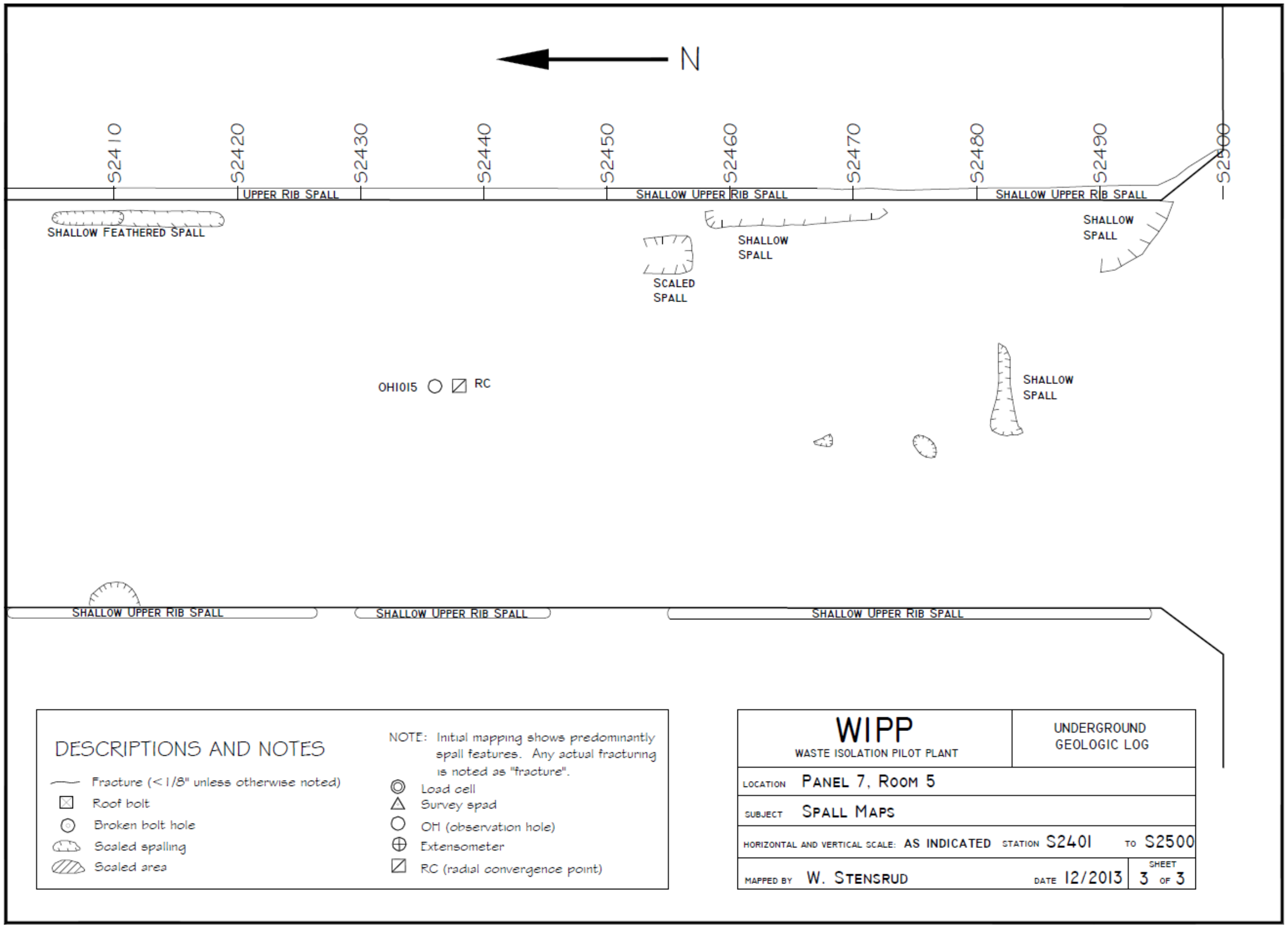

Figure - 15 Panel 7 Room 5, S2401-S2500 Roof Fractures

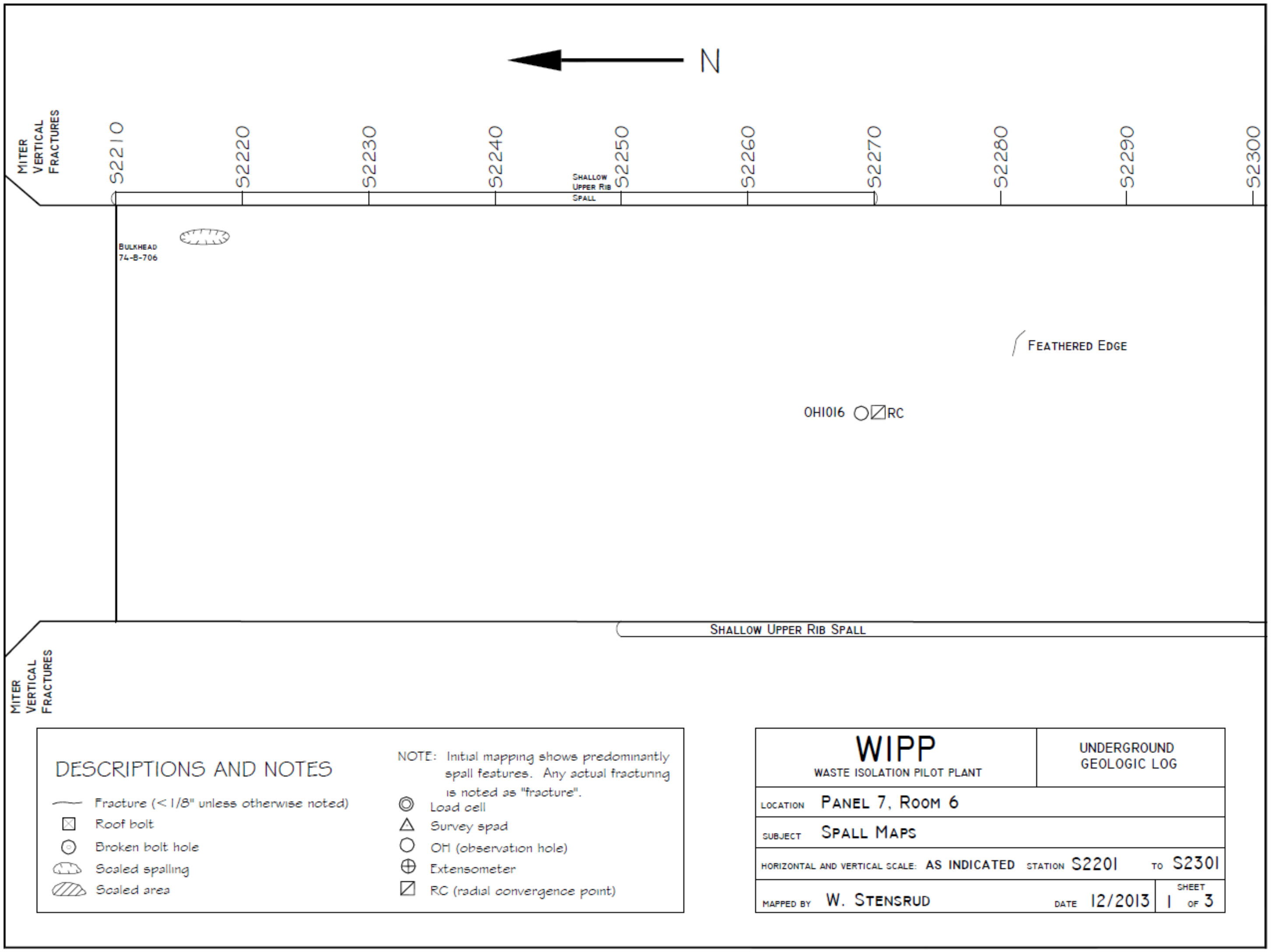

Figure - 16 Panel 7 Room 6, S2201-S2301 Roof Fractures

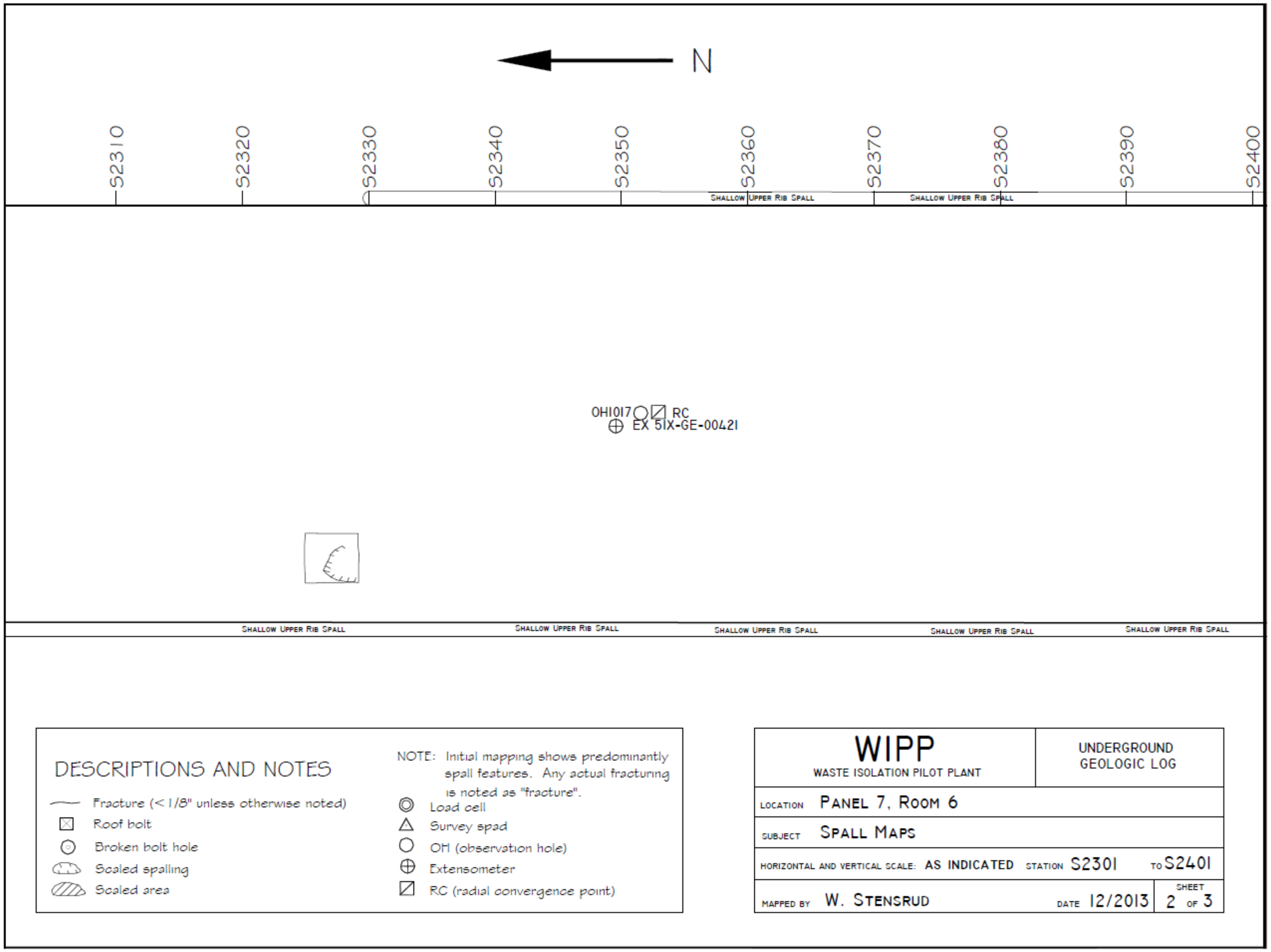

Figure - 17 Panel 7 Room 6, S2301-S2401 Roof Fractures

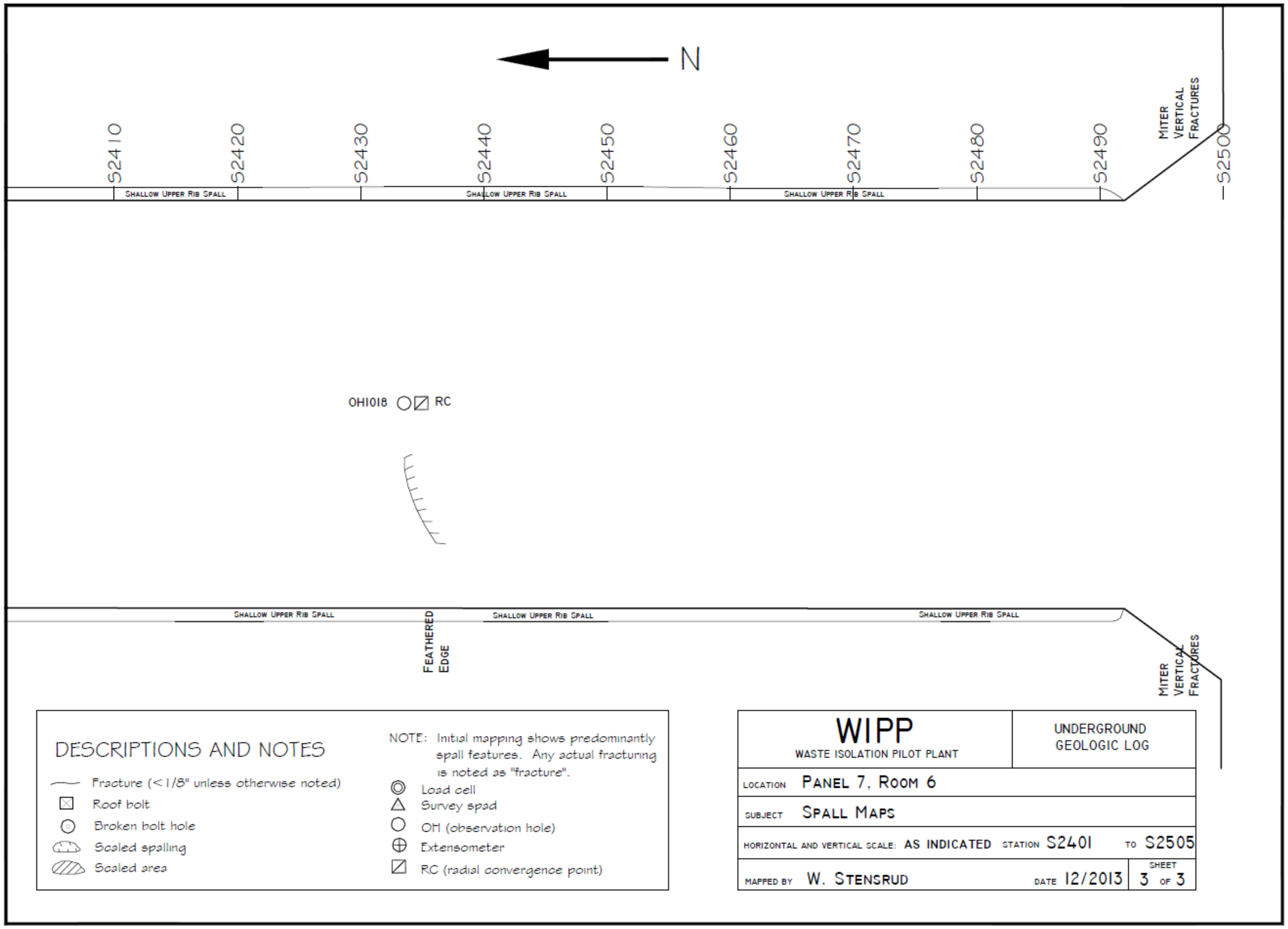

Figure - 18 Panel 7 Room 6, S2401-S2505 Roof Fractures

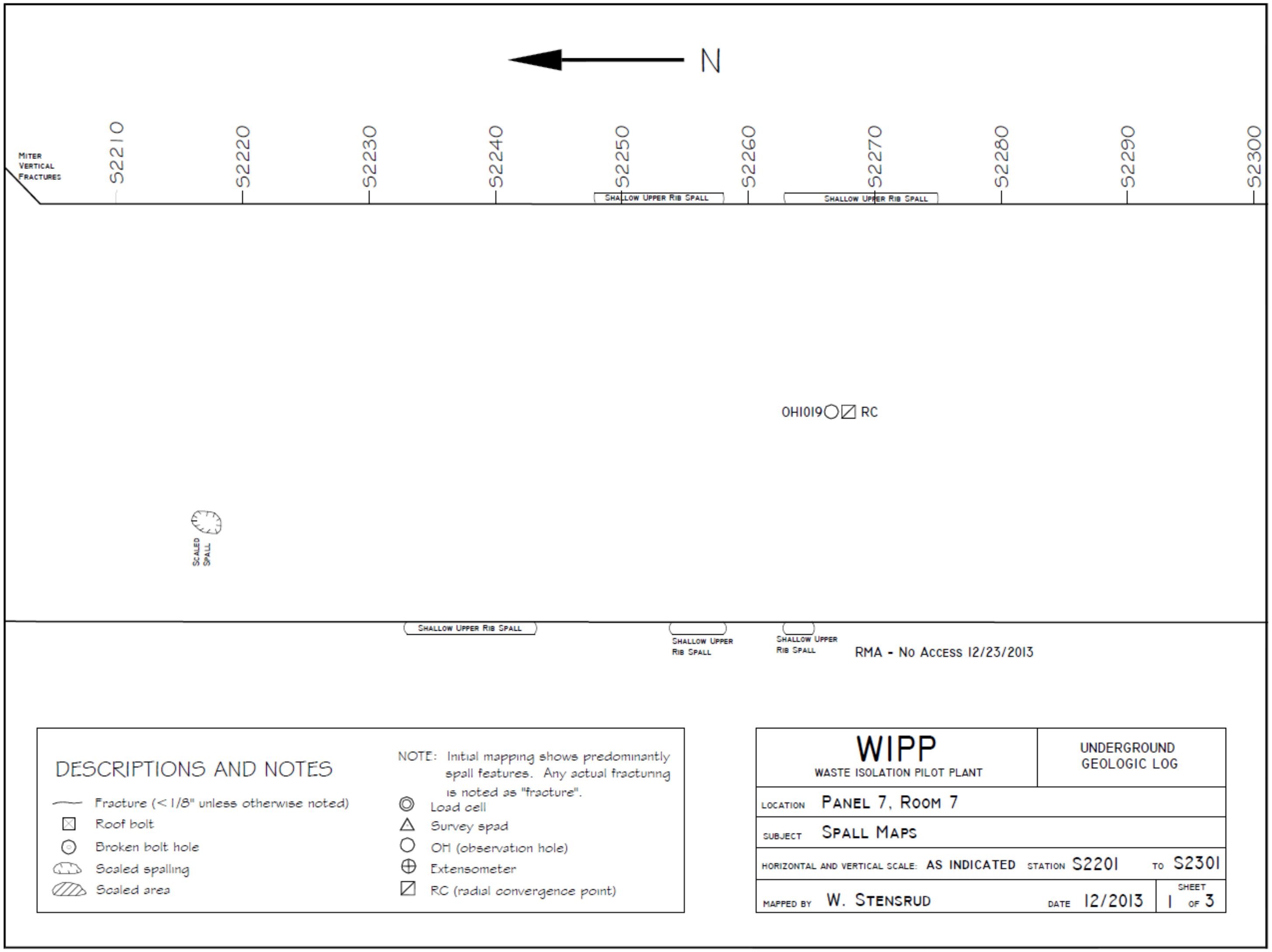

Figure - 19 Panel 7 Room 7, S2201-S2301 Roof Fractures

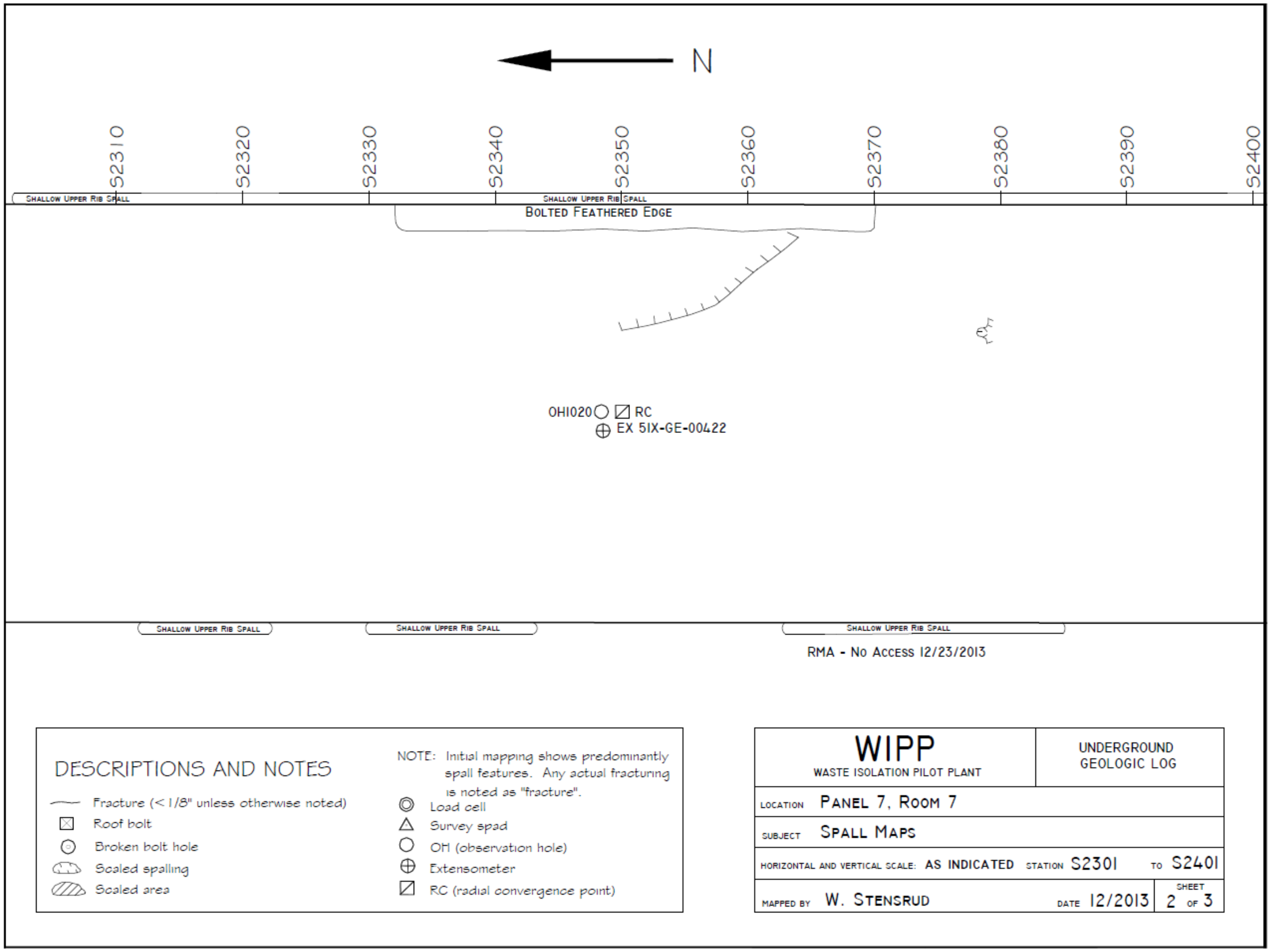

Figure - 20 Panel 7 Room 7, S2301-S2401 Roof Fractures

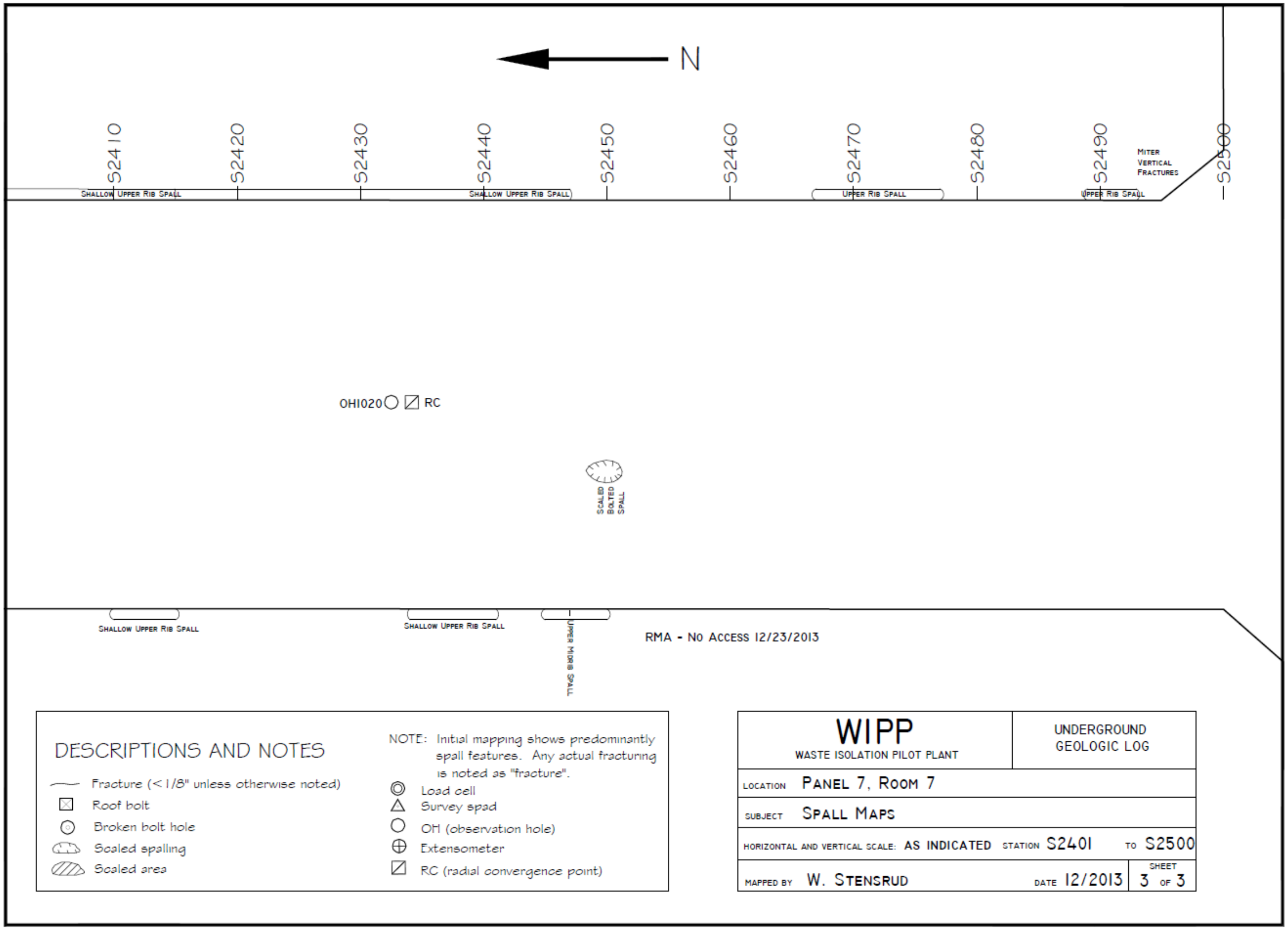

Figure - 21 Panel 7 Room 7, S2401-S2500 Roof Fractures

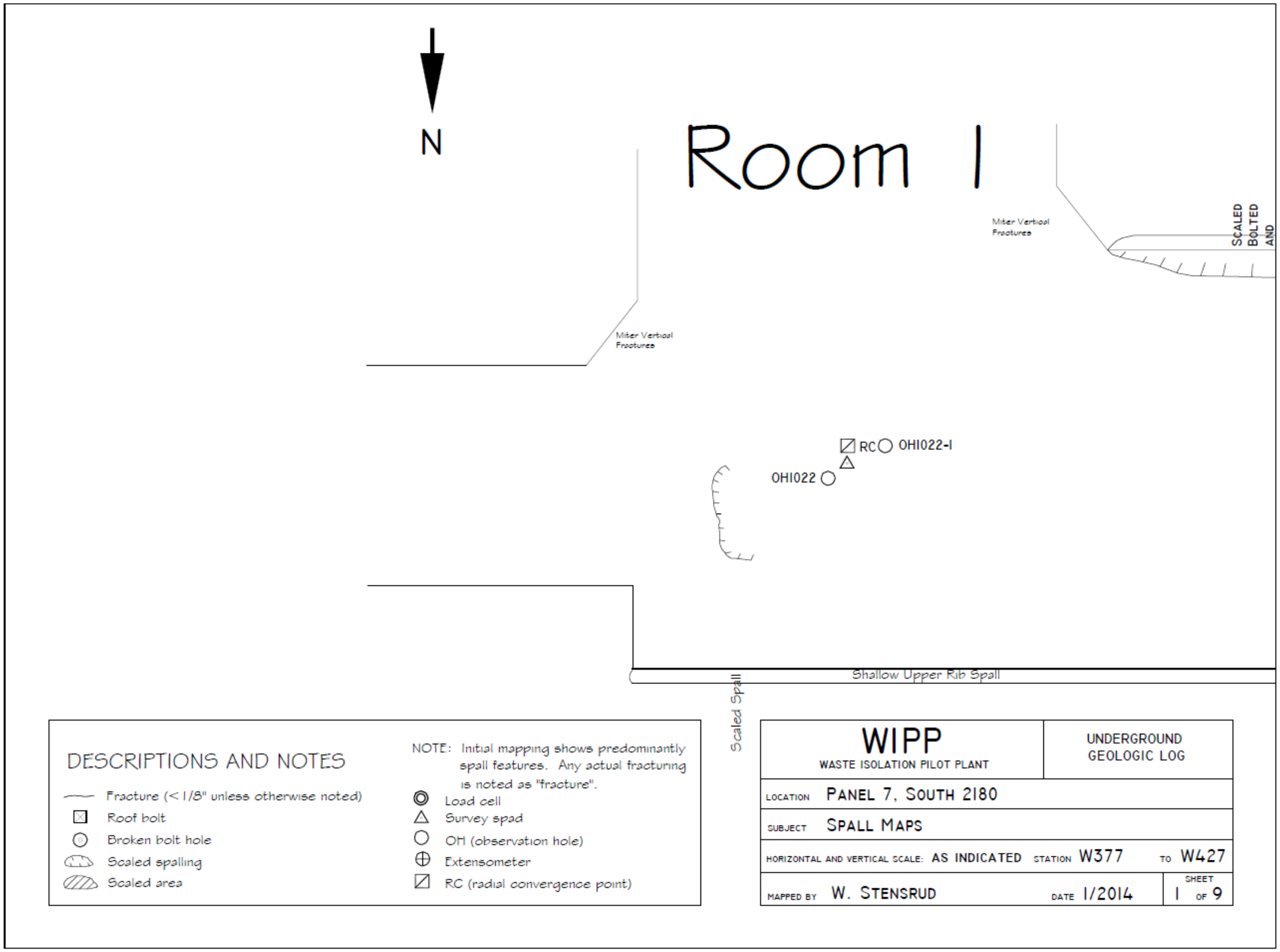

Figure - 22 Panel 7 S2180, W377-W427 Roof Fractures

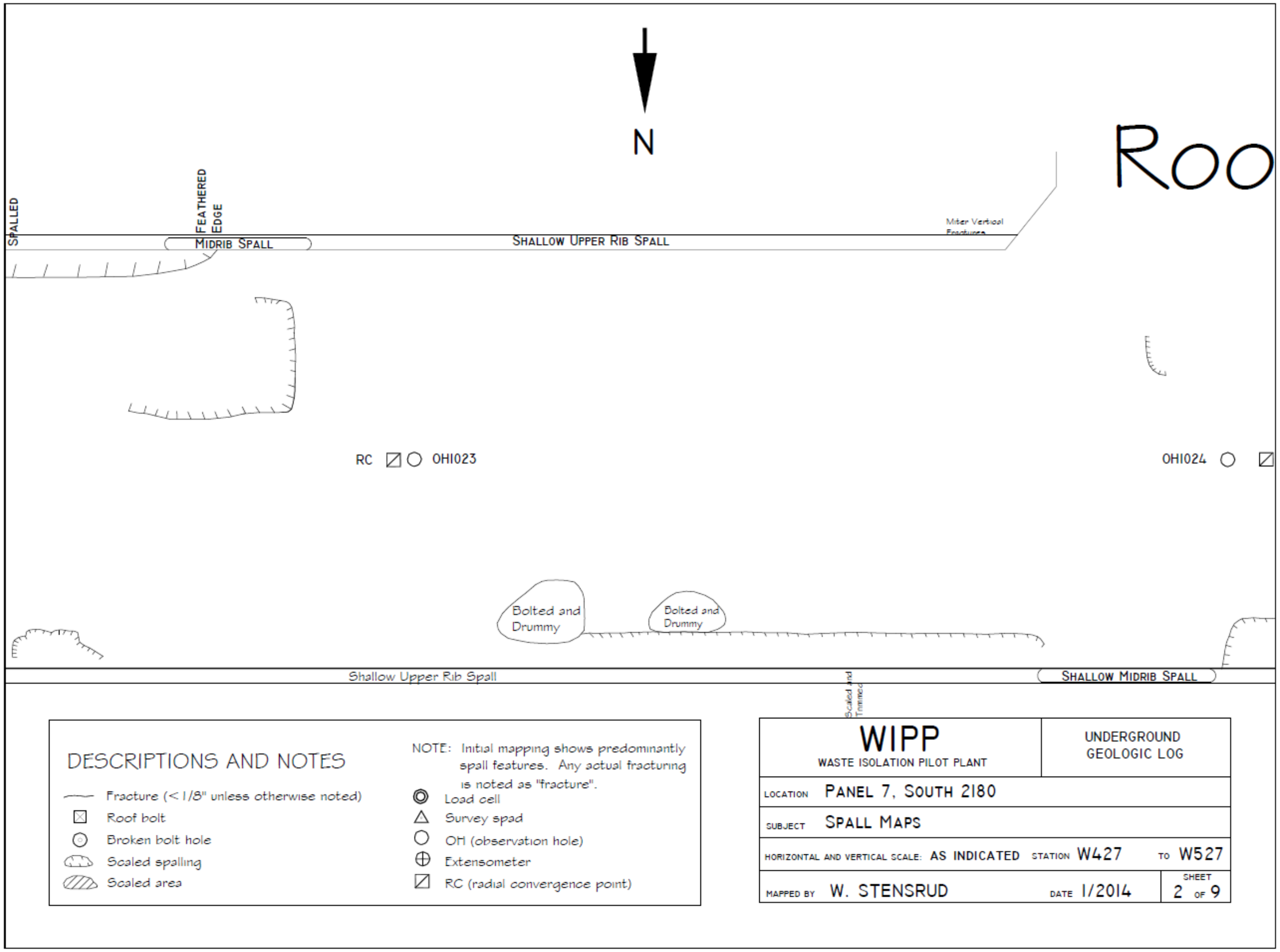

Figure - 23 Panel 7 S2780, W427-W527 Roof Fractures

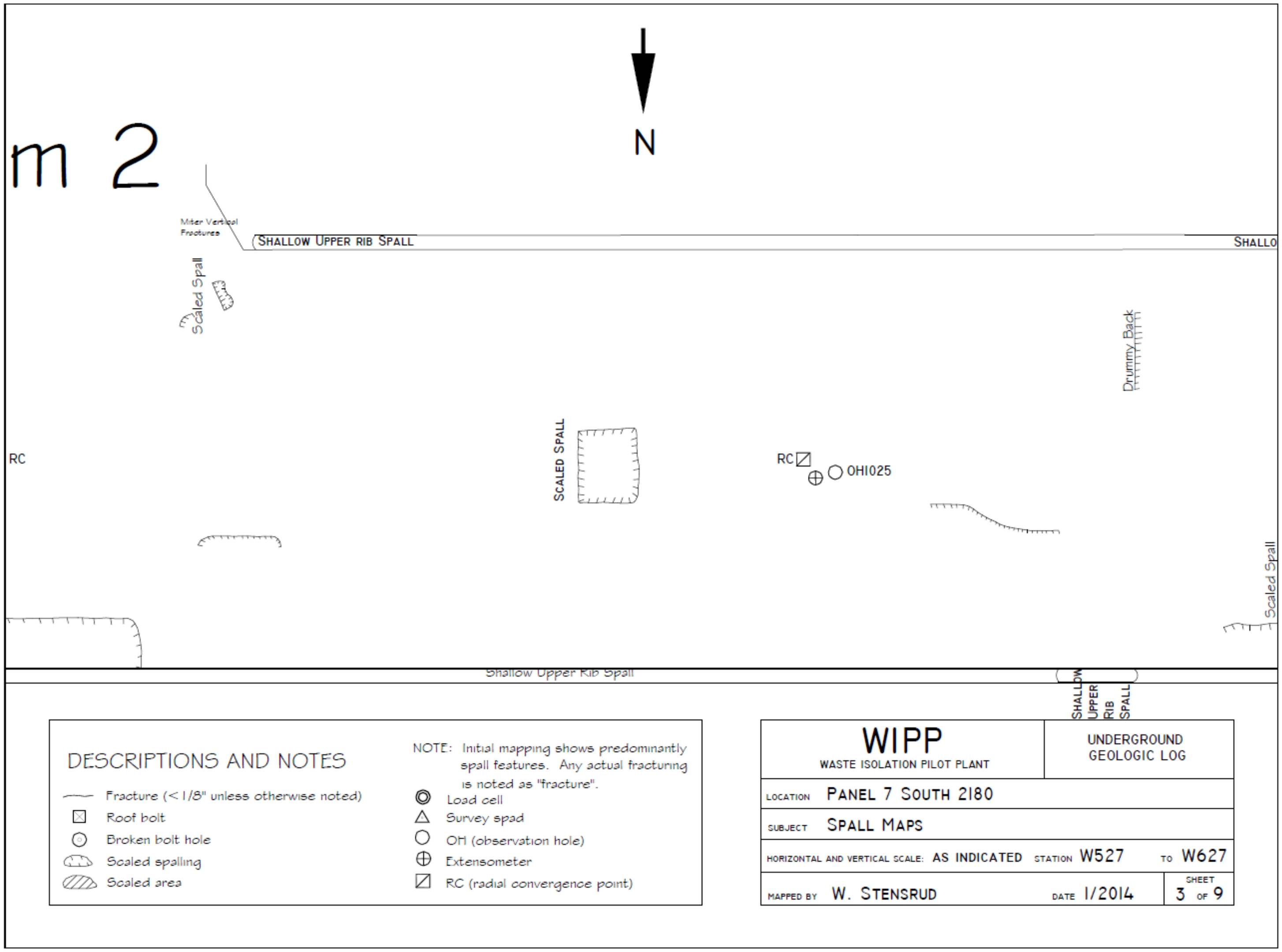

Figure - 24 Panel 7 S2180, W527-W627 Roof Fractures

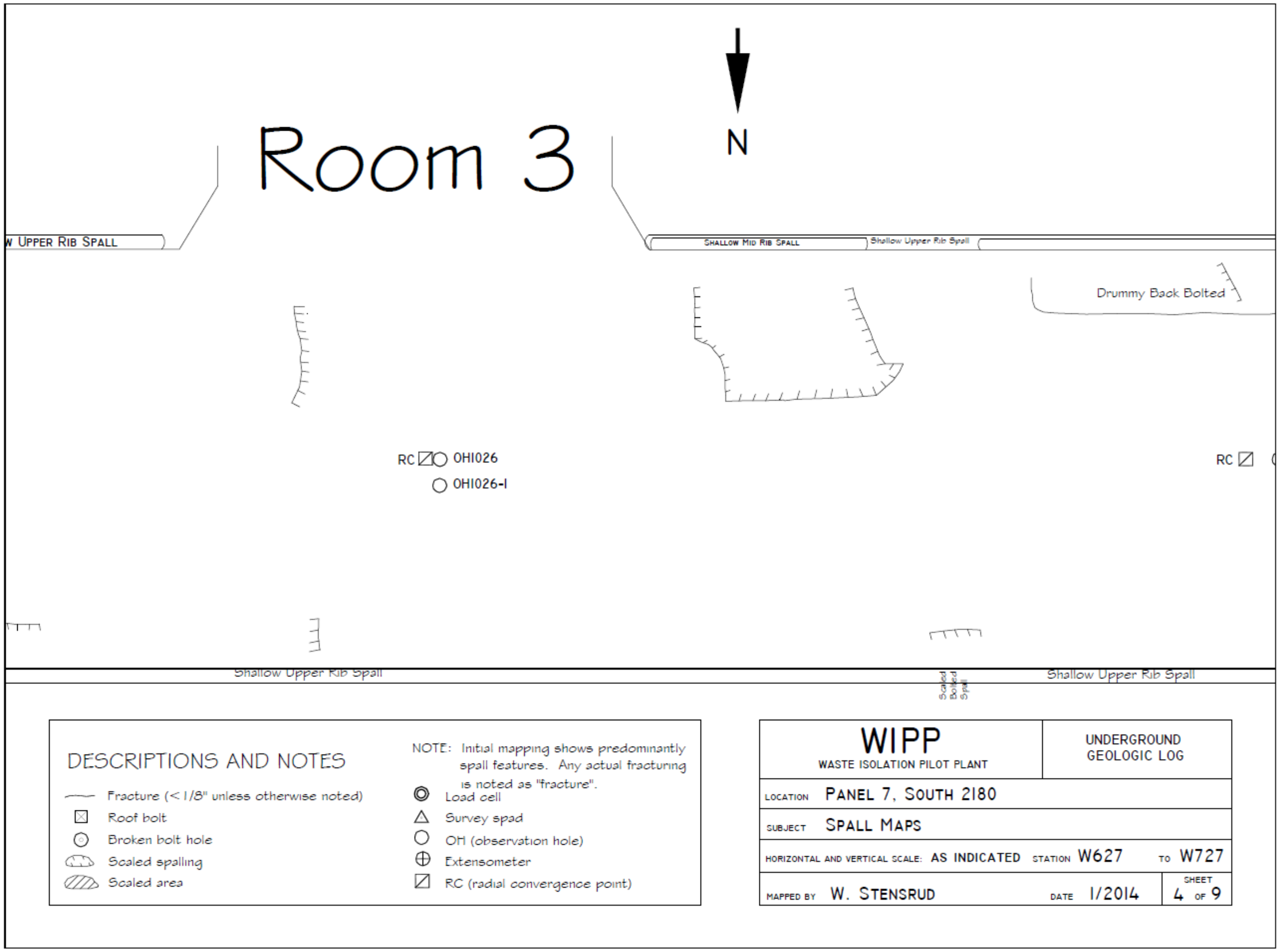

Figure - 25 Panel 7 S2180, W627-W727 Roof Fractures

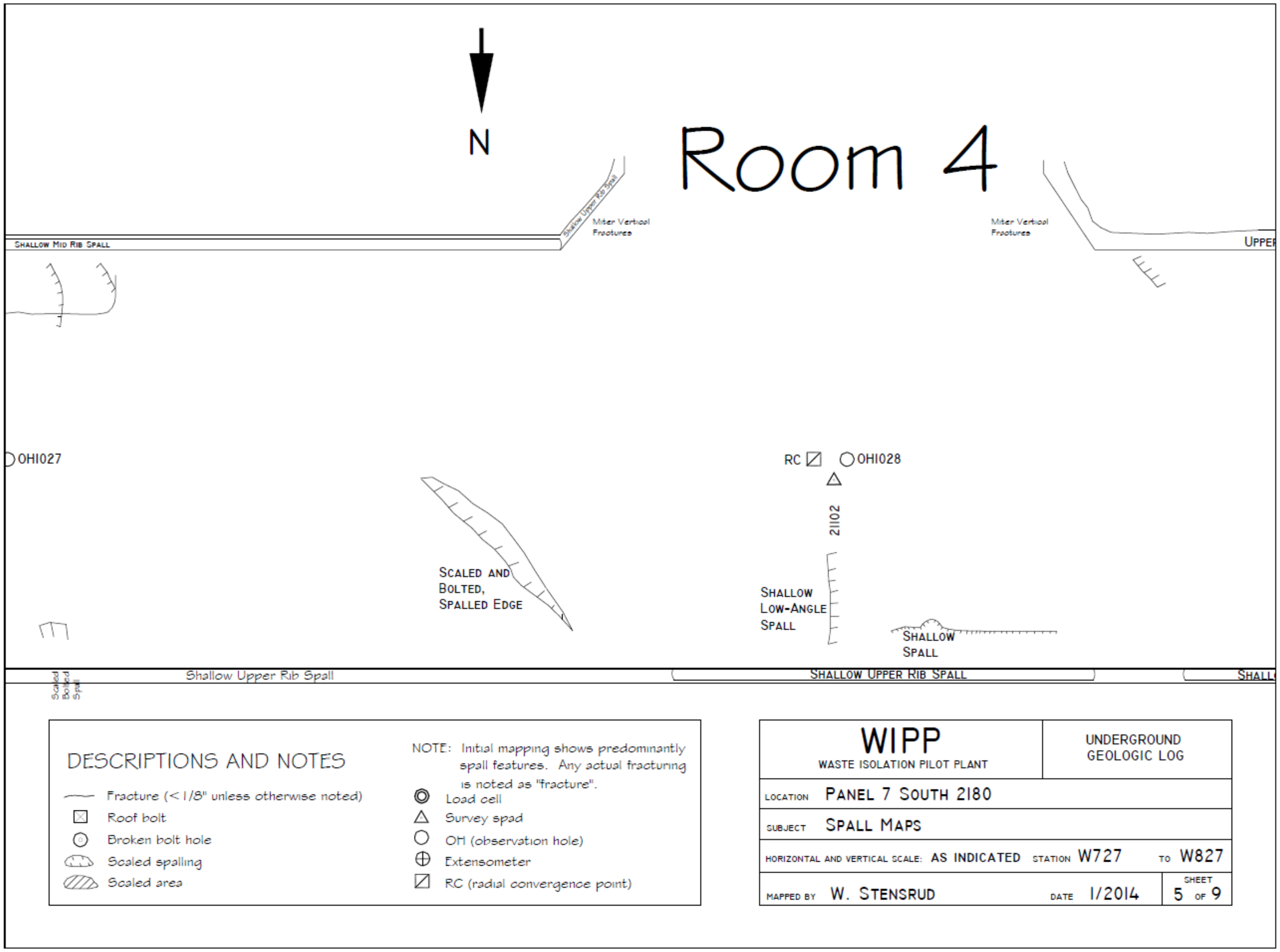

Figure - 26 Panel 7 S2180, W727-W827, Roof Fractures

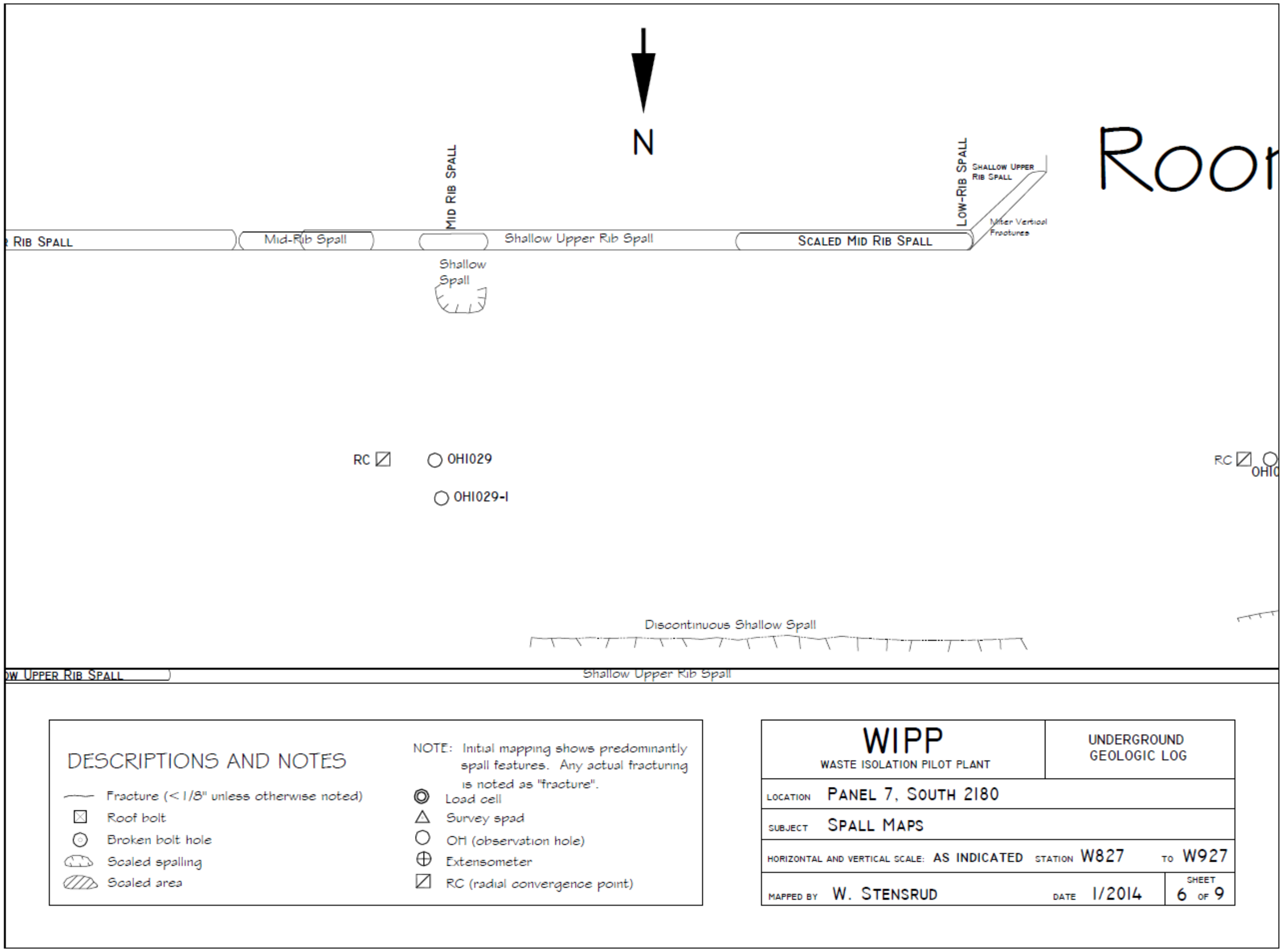

Figure - 27 Panel 7 S2180, W827-W927 Roof Fractures

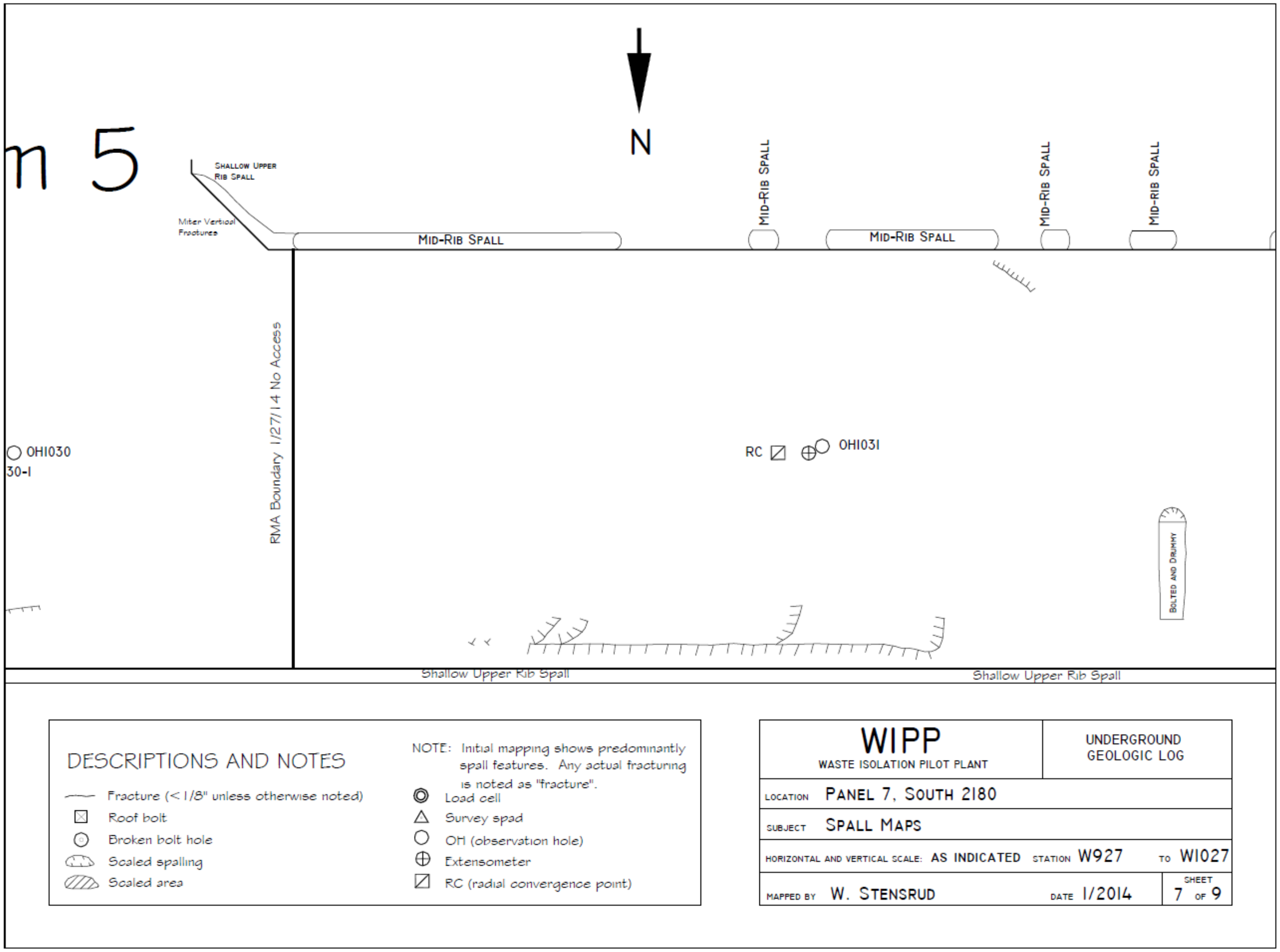

Figure -28 Panel 7 S2180, W927-W1027 Roof Fractures

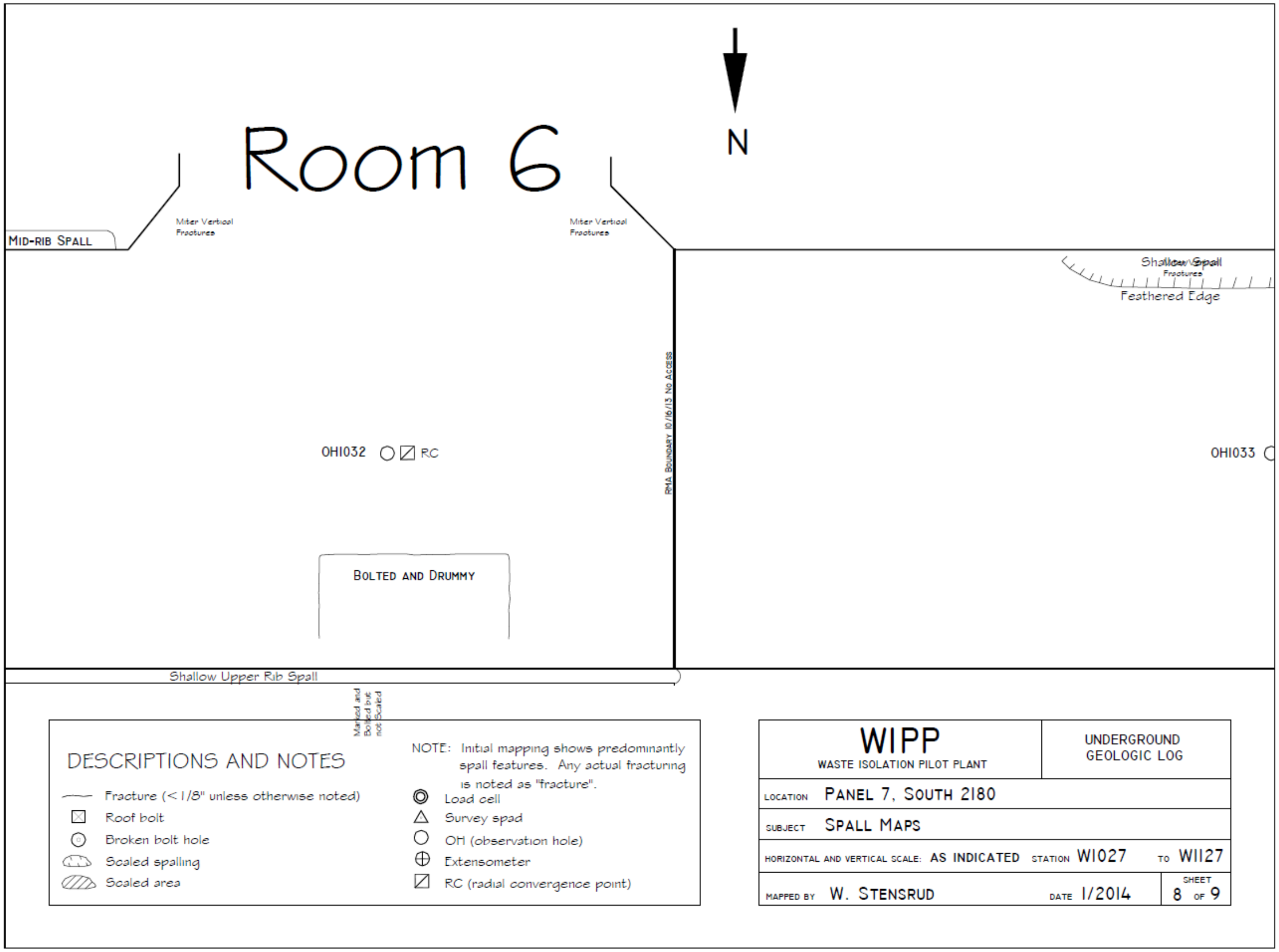

Figure-29 Panel 7 S2180, W1027-W1127 Roof Fractures

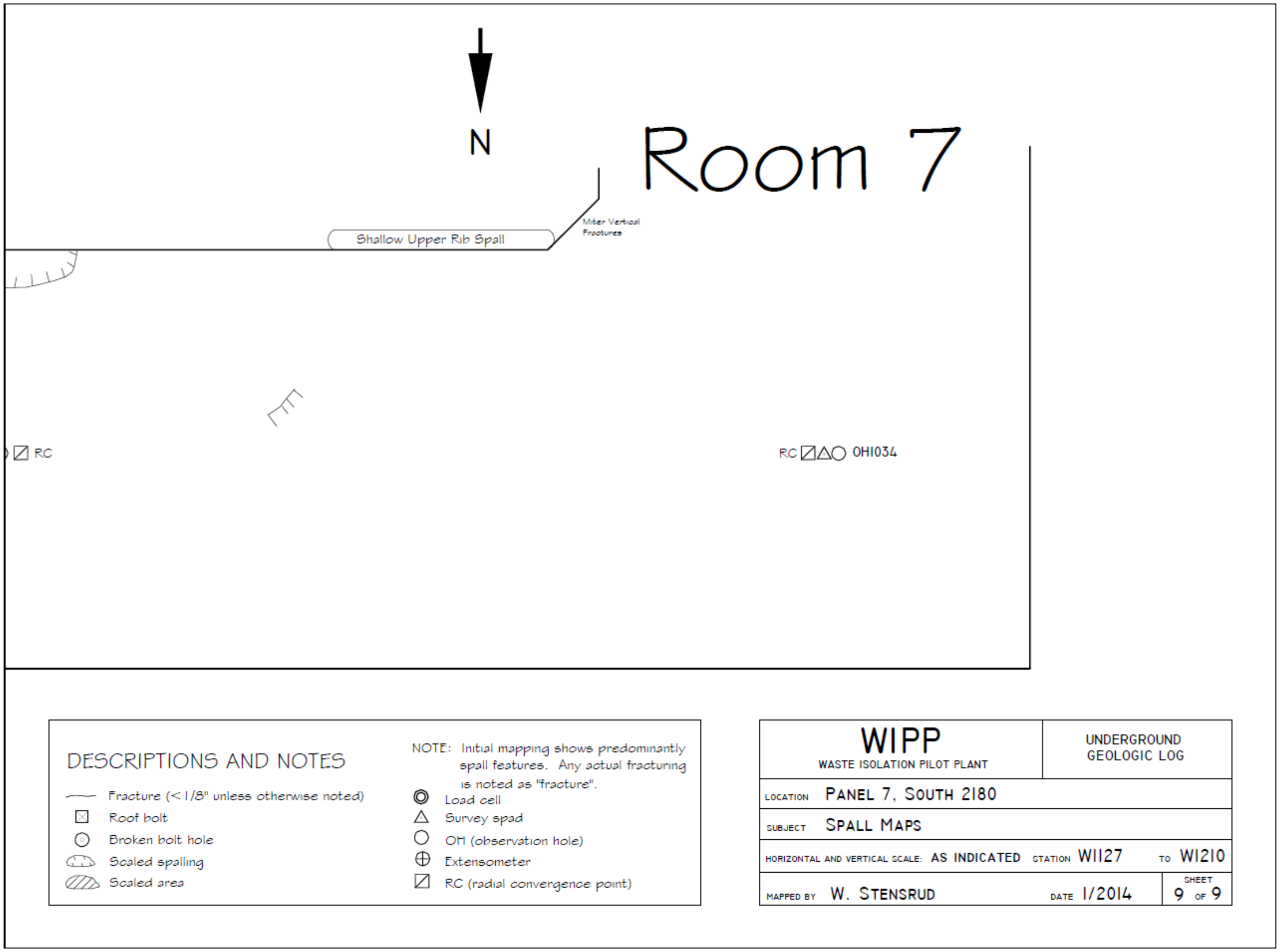

Figure-30 Panel 7 S2180, S1127-S1210 Roof Fractures

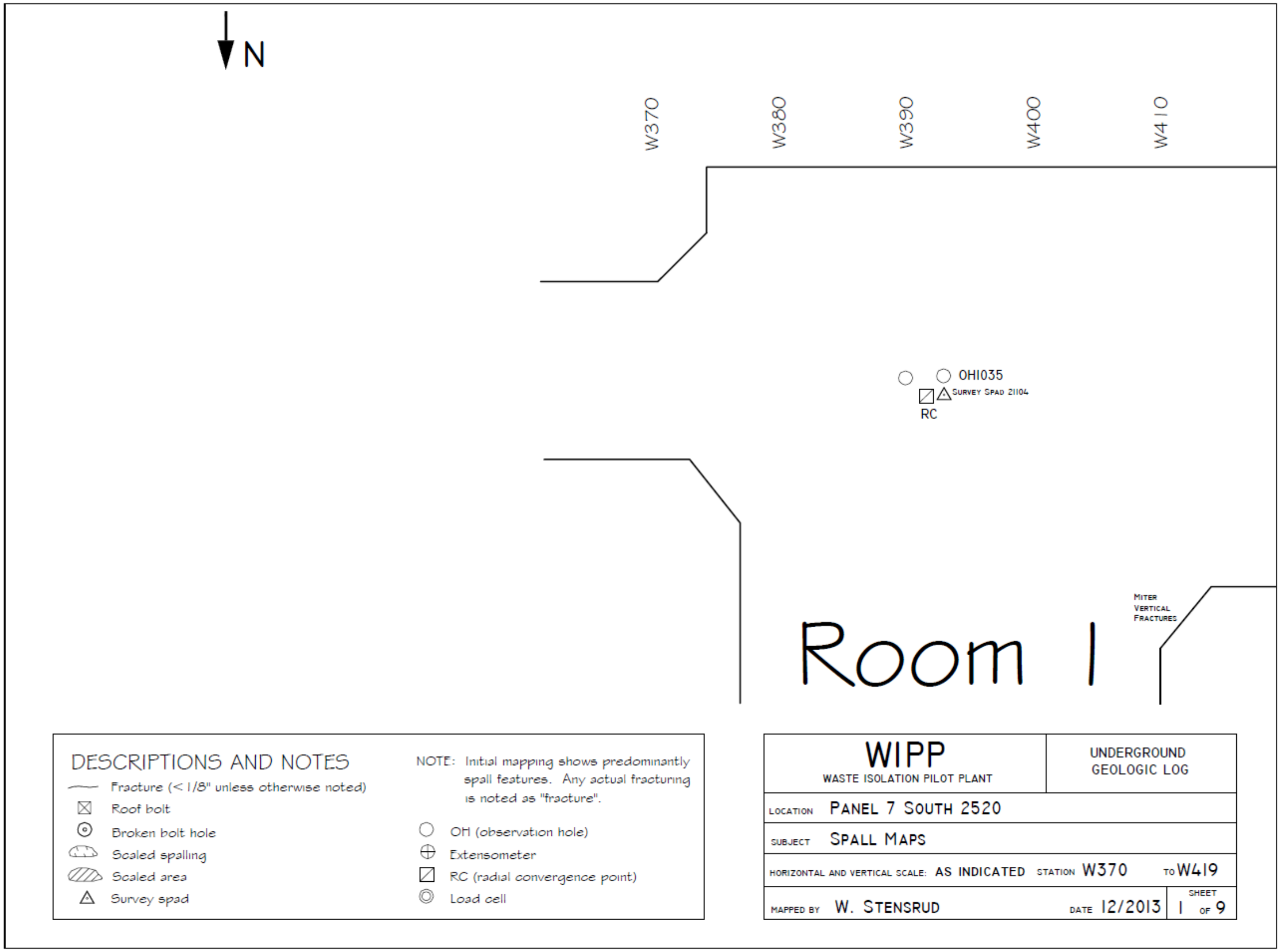

Figure-31Panel 7 S2520, W370-W419 Roof Fractures

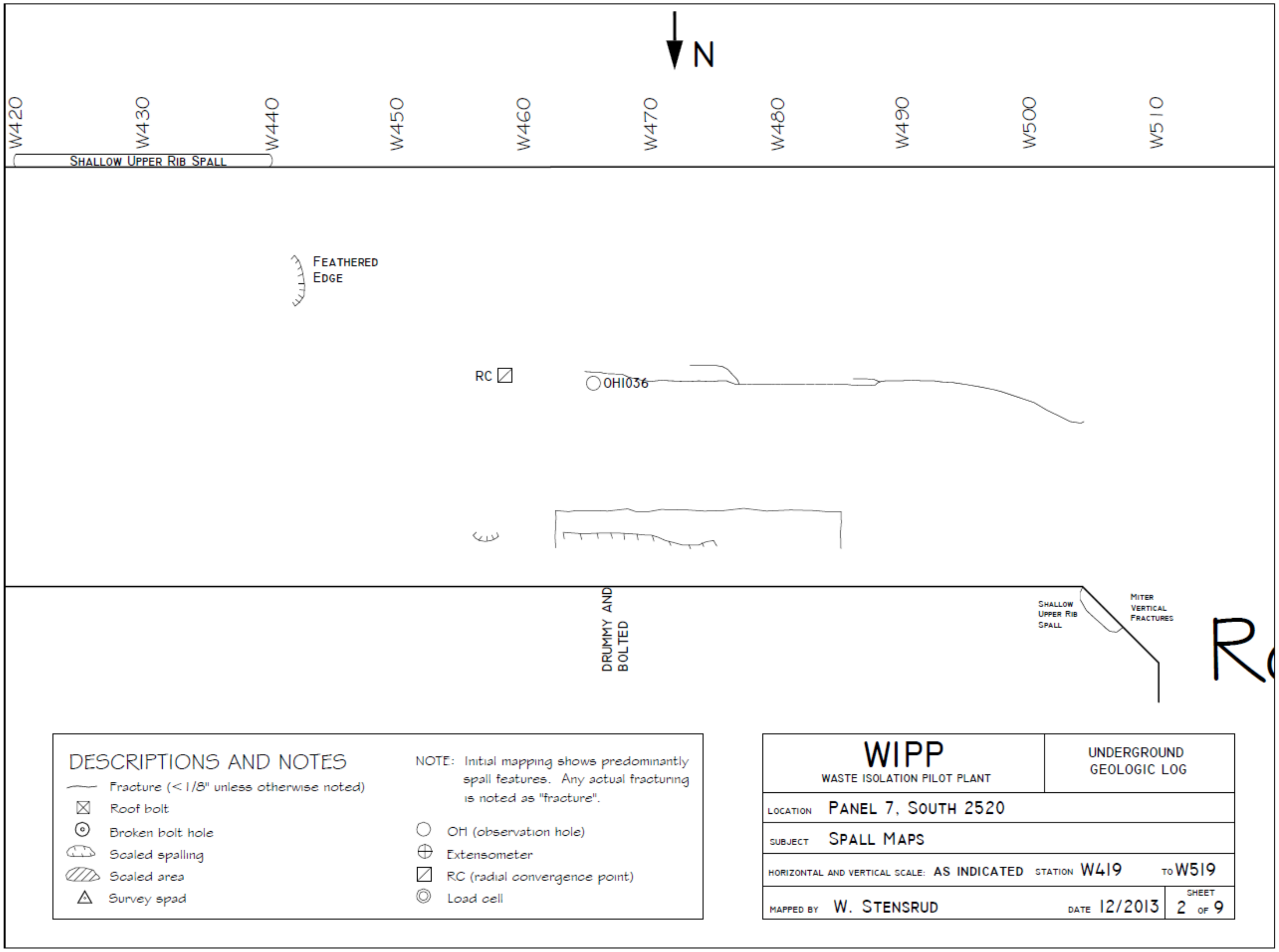

Figure-32 Panel 7 S2520, W419-W519 Roof Fractures

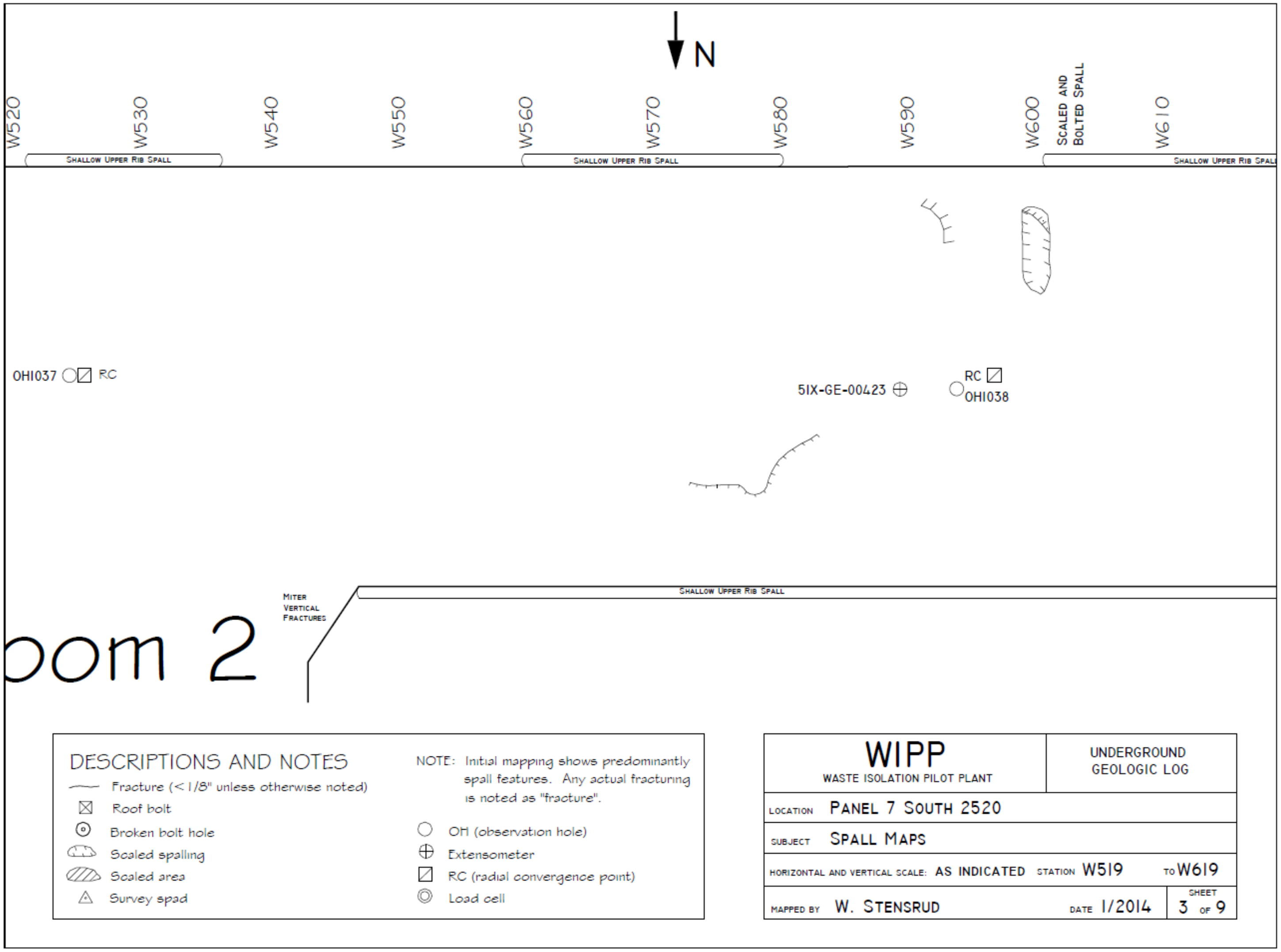

Figure-33 Panel 7 S2520, W519-W619 Roof Fractures

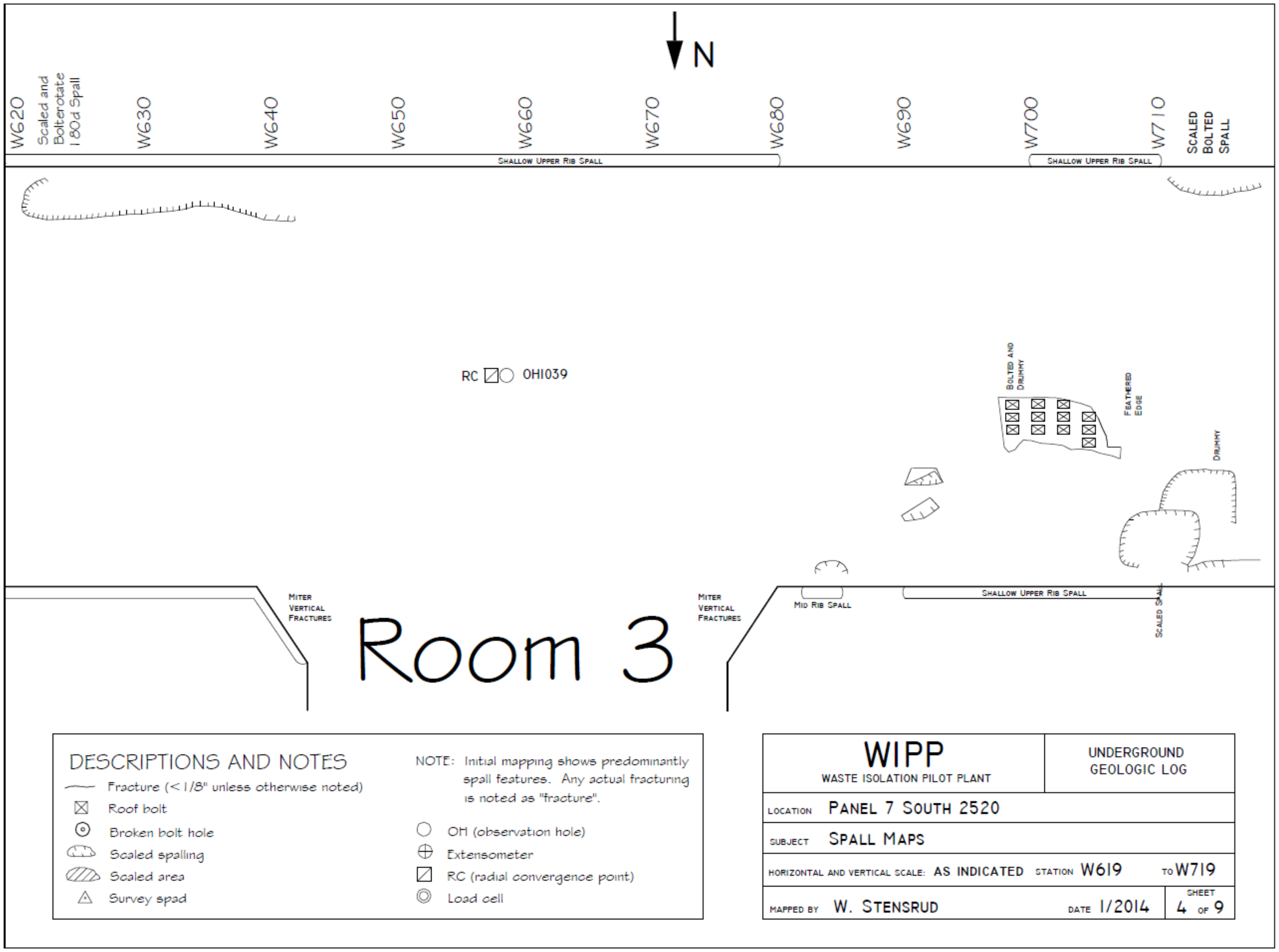

Figure-34 Panel 7 S2520, W619-W719 Roof Fractures

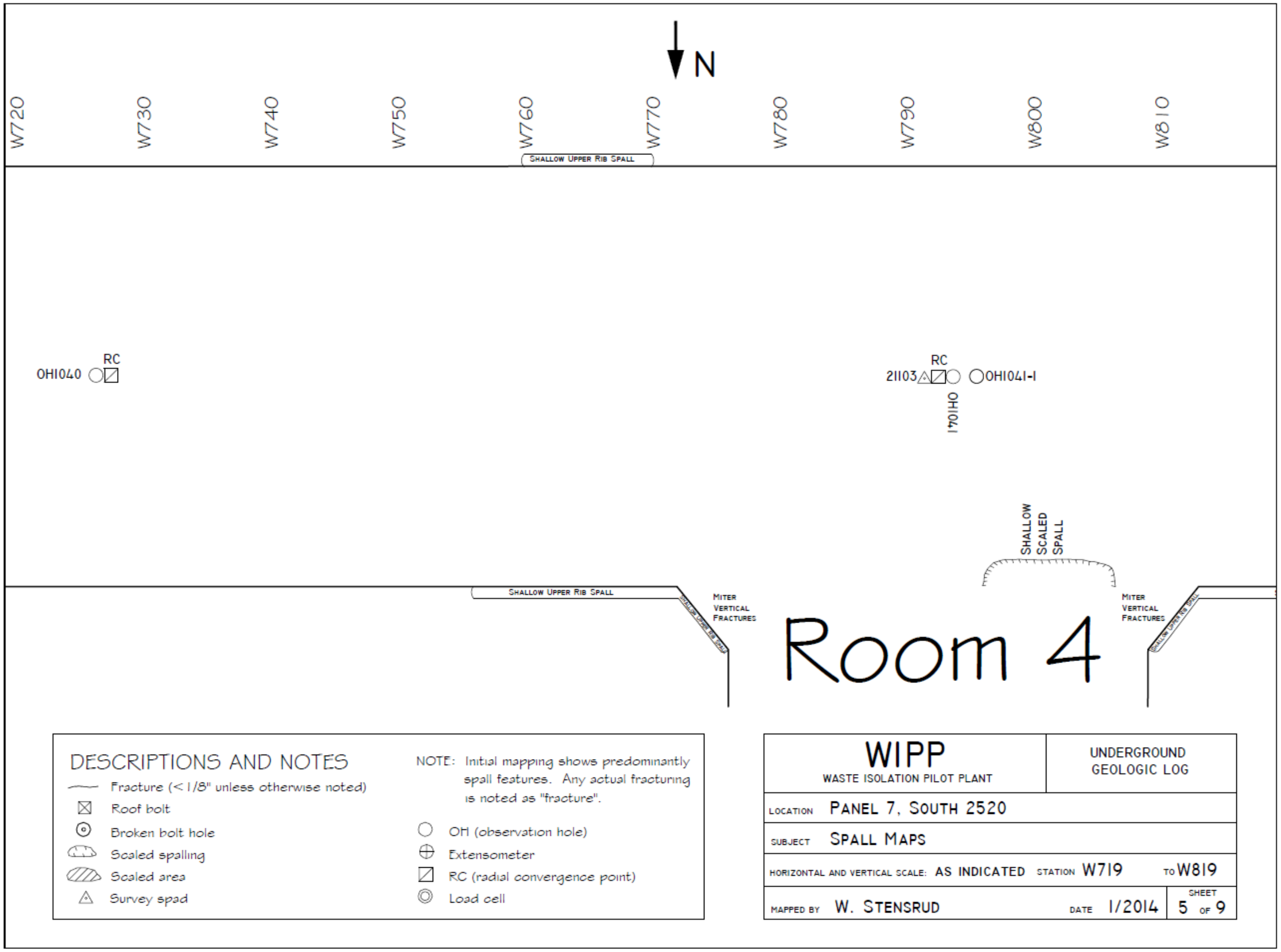

Figure-35 Panel 7 S2520, W719-W819 Roof Fractures

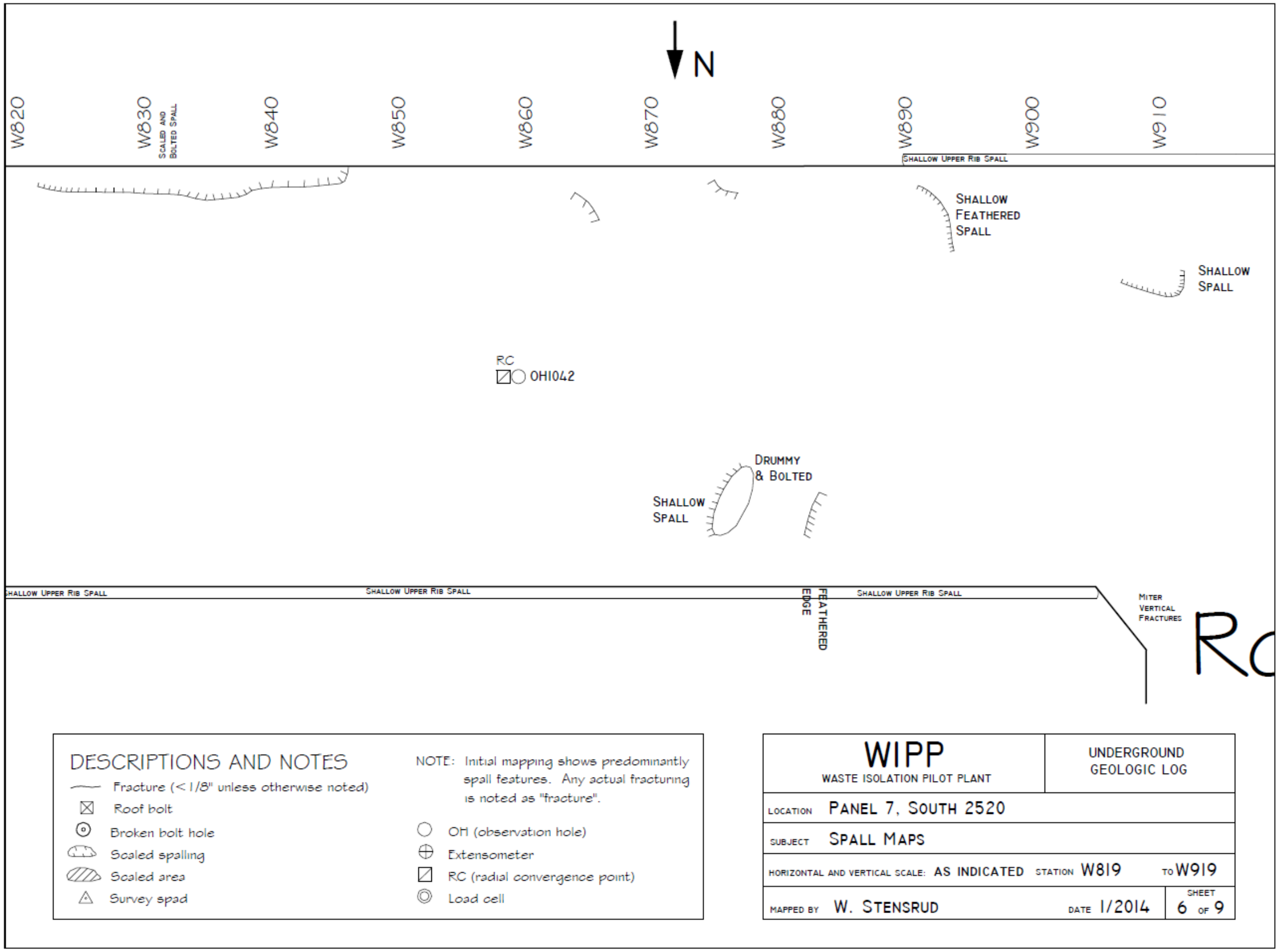

Figure-36 Panel 7 S2520, W819-W919 Roof Fractures

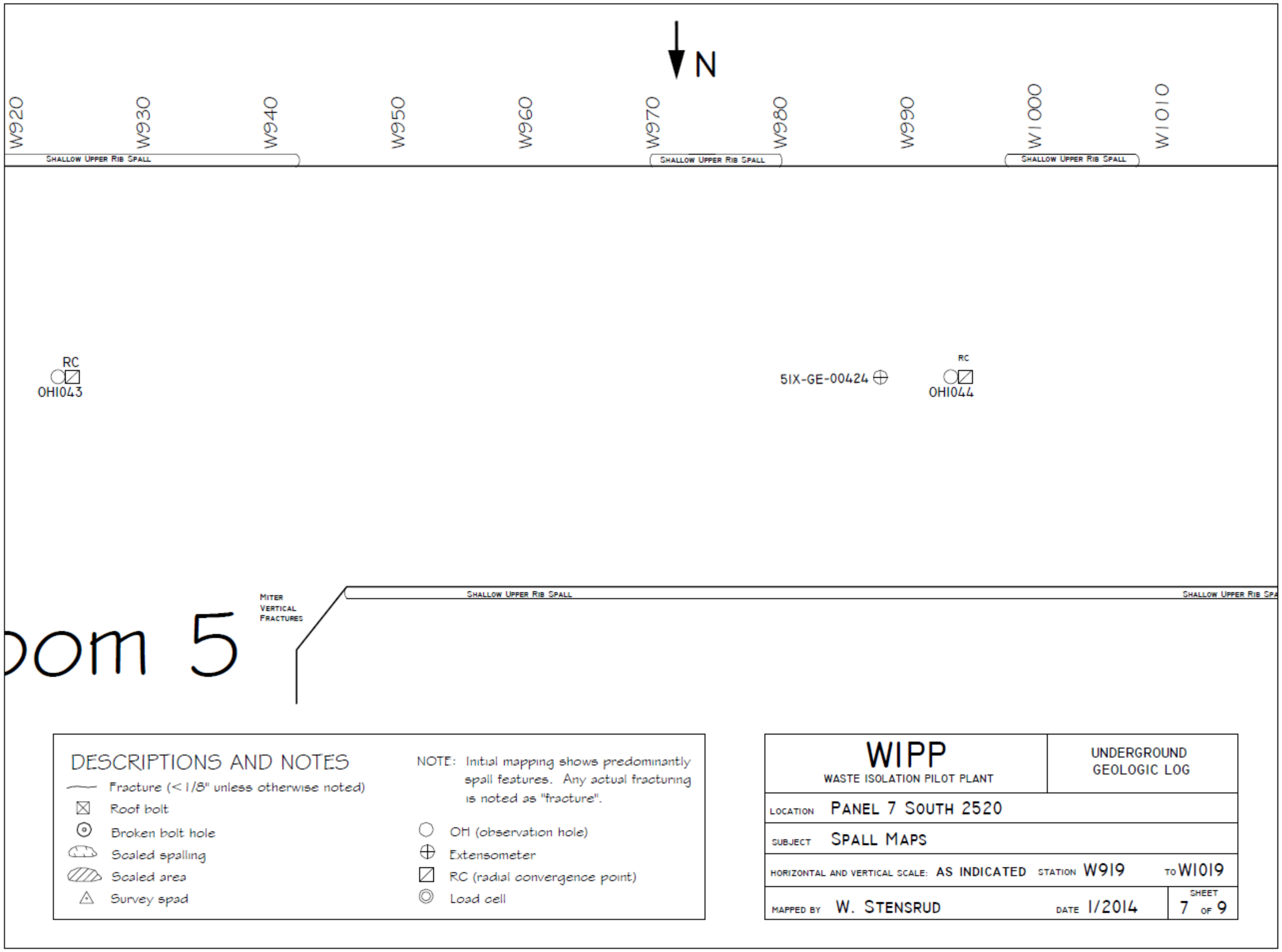

Figure-37 Panel 7 S2520, W919-W1019 Roof Fractures

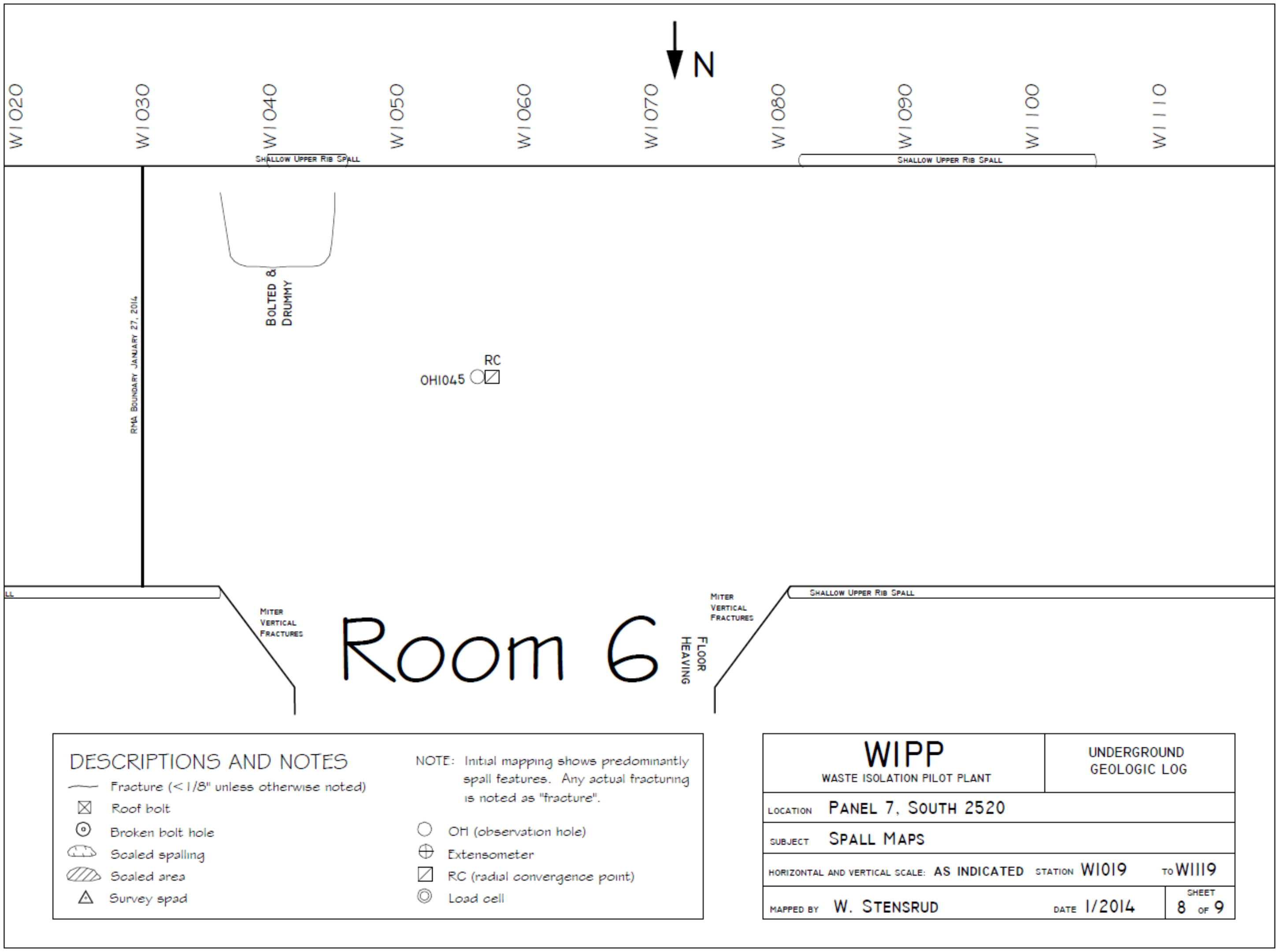

Figure-38 Panel 7 S2520, W1019-W1119 Roof Fractures

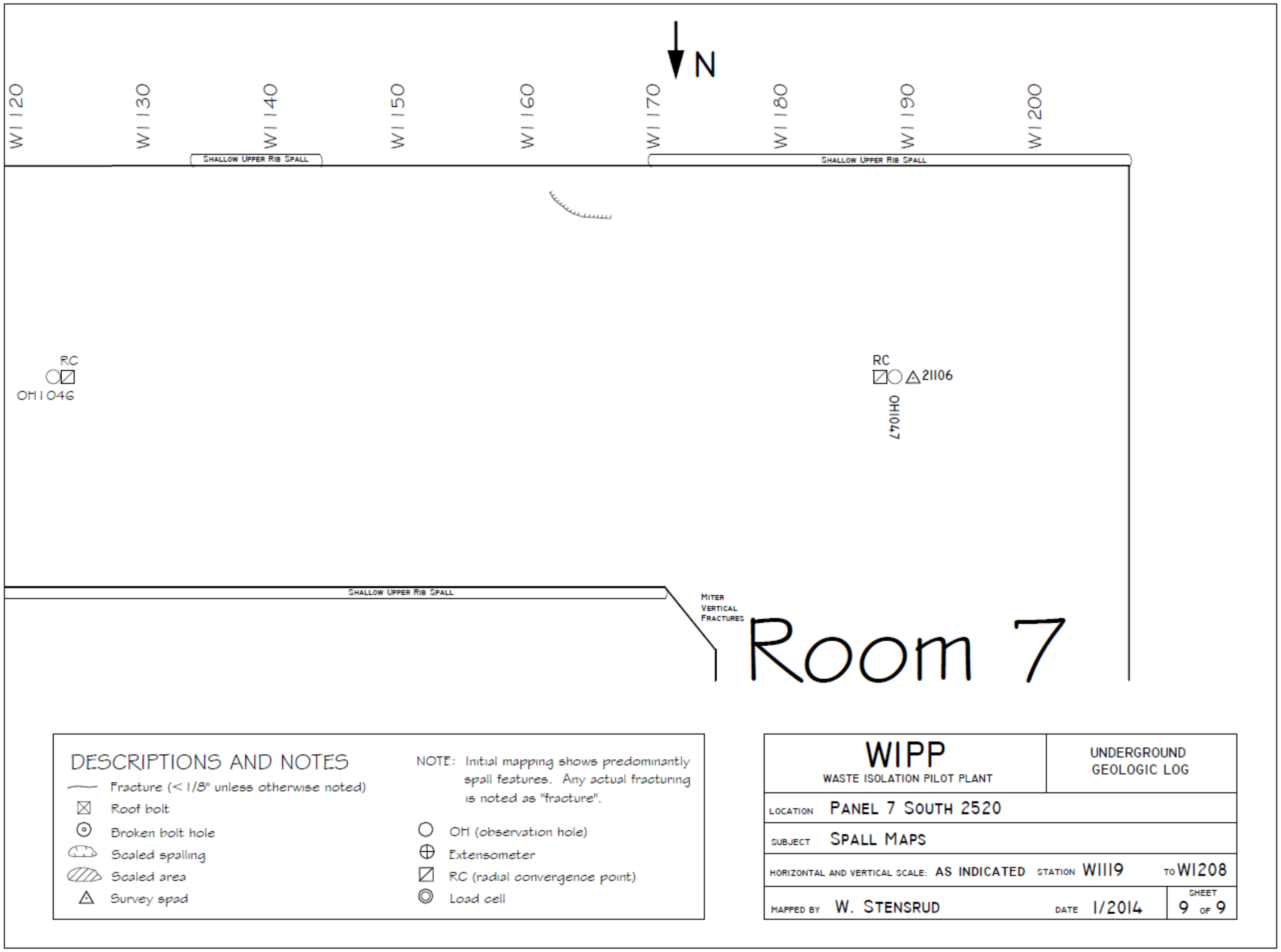

Figure-39 Panel 7 S2520, W1119-W1208 Roof Fractures

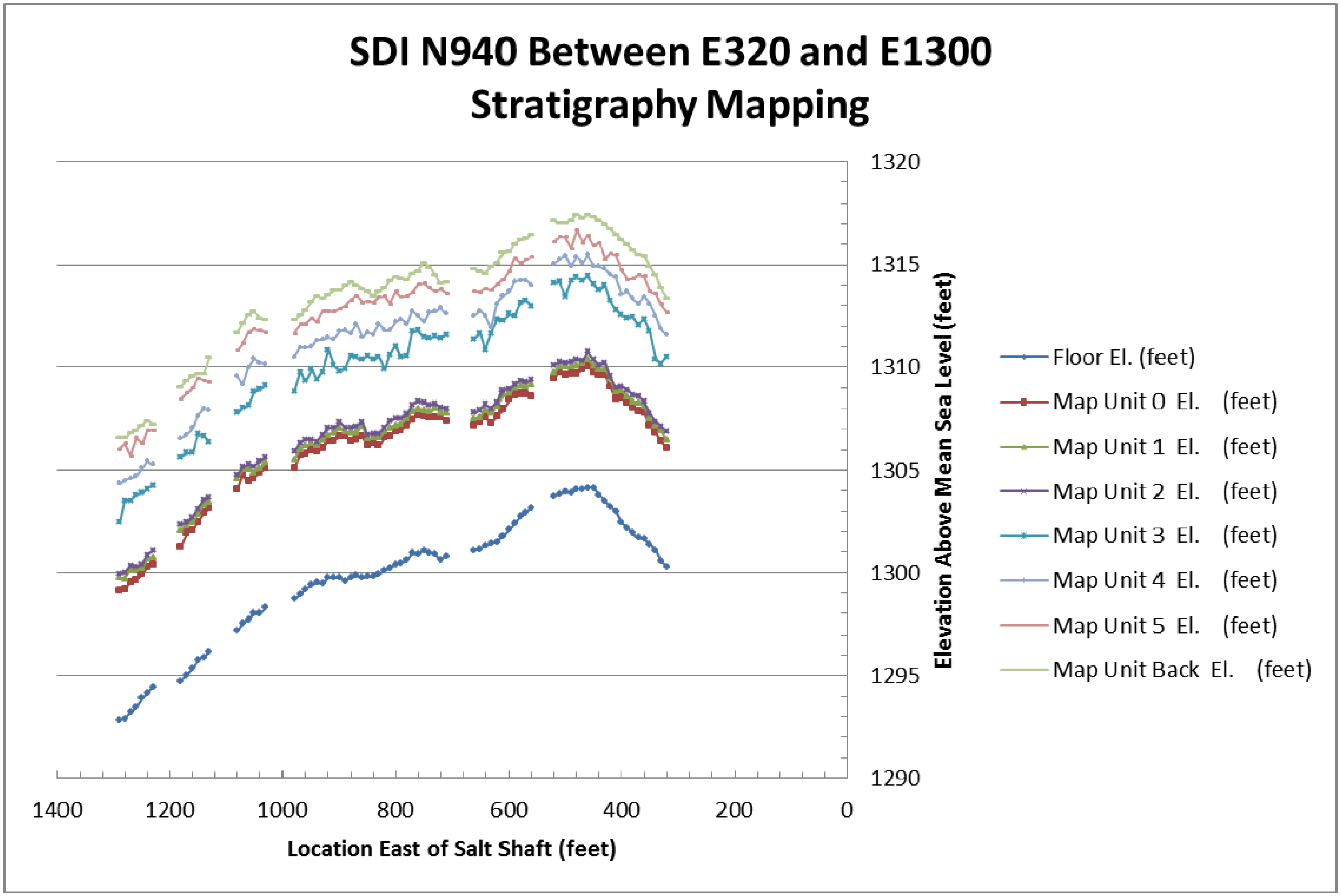

Figure-40 Stratigraphy Mapping, SDI N940 between E320 and E1300

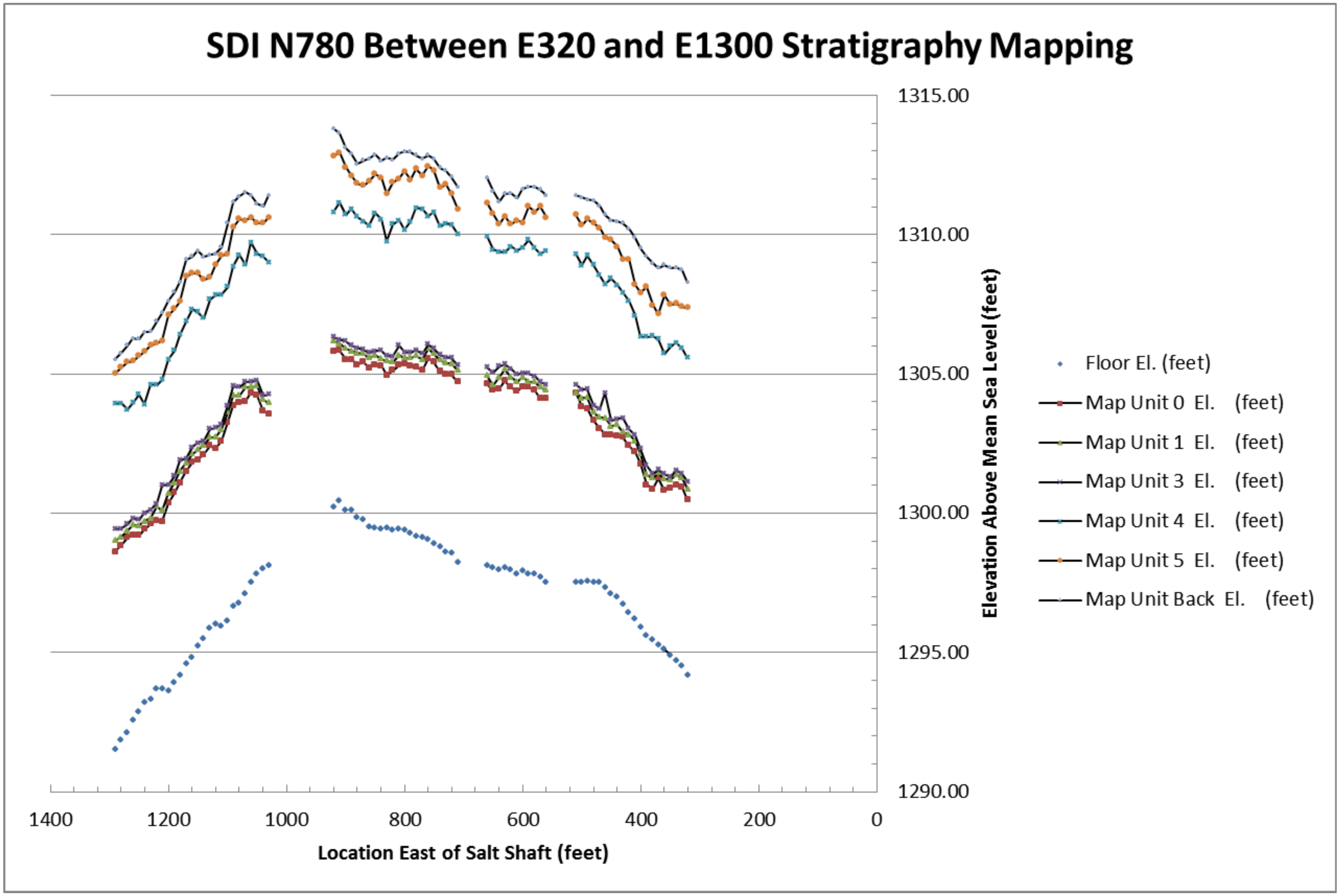

Figure-41 Stratigraphy Mapping, SDI N780 between E320 and E1300

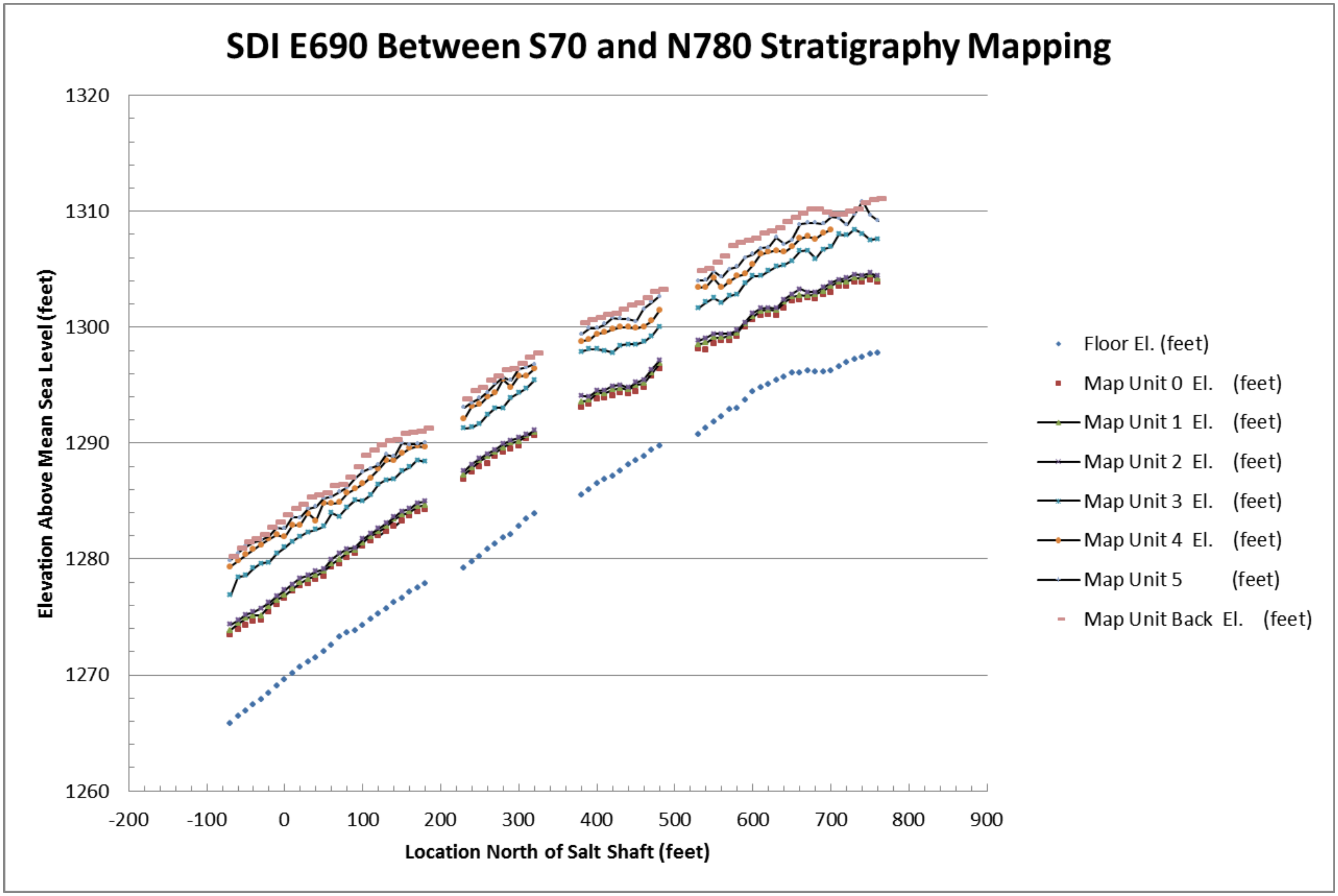

Figure-42 Stratigraphy Mapping, SDI E690 between S70 and N780

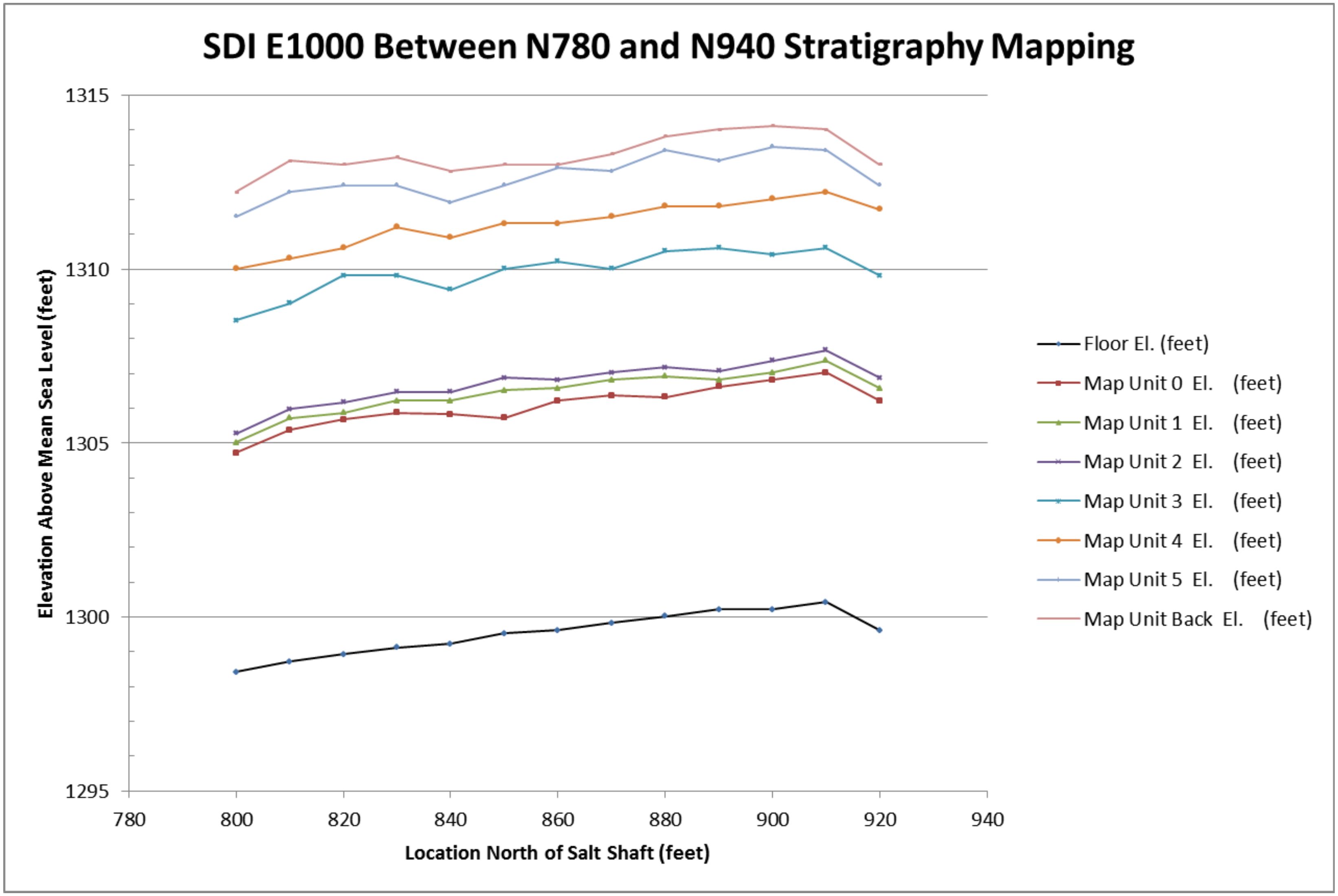

Figure-43 Stratigraphy Mapping, SDI E1000 between N780 and N940

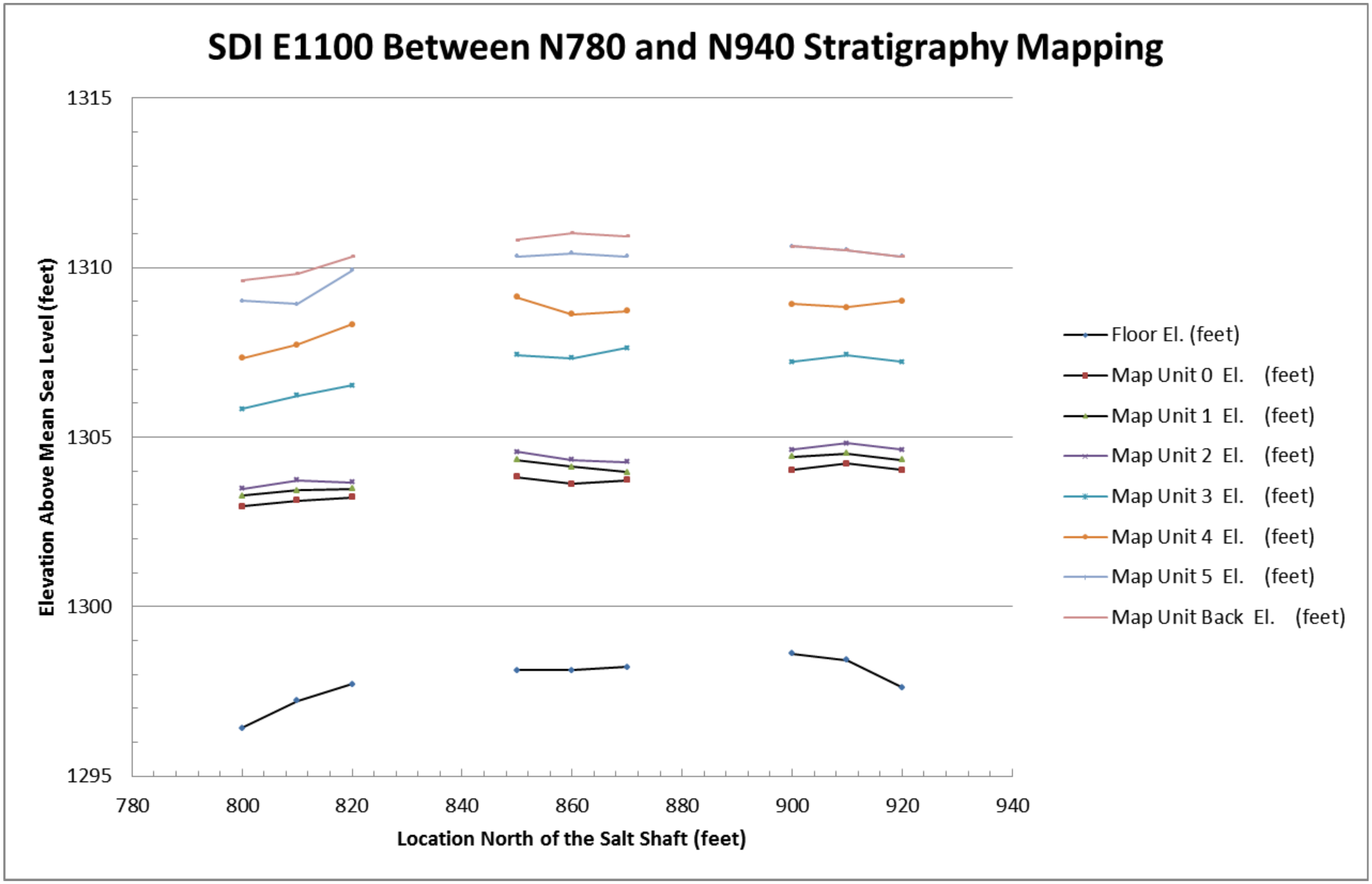

Figure-44 Stratigraphy Mapping, SDI E1100 between N780 and N940

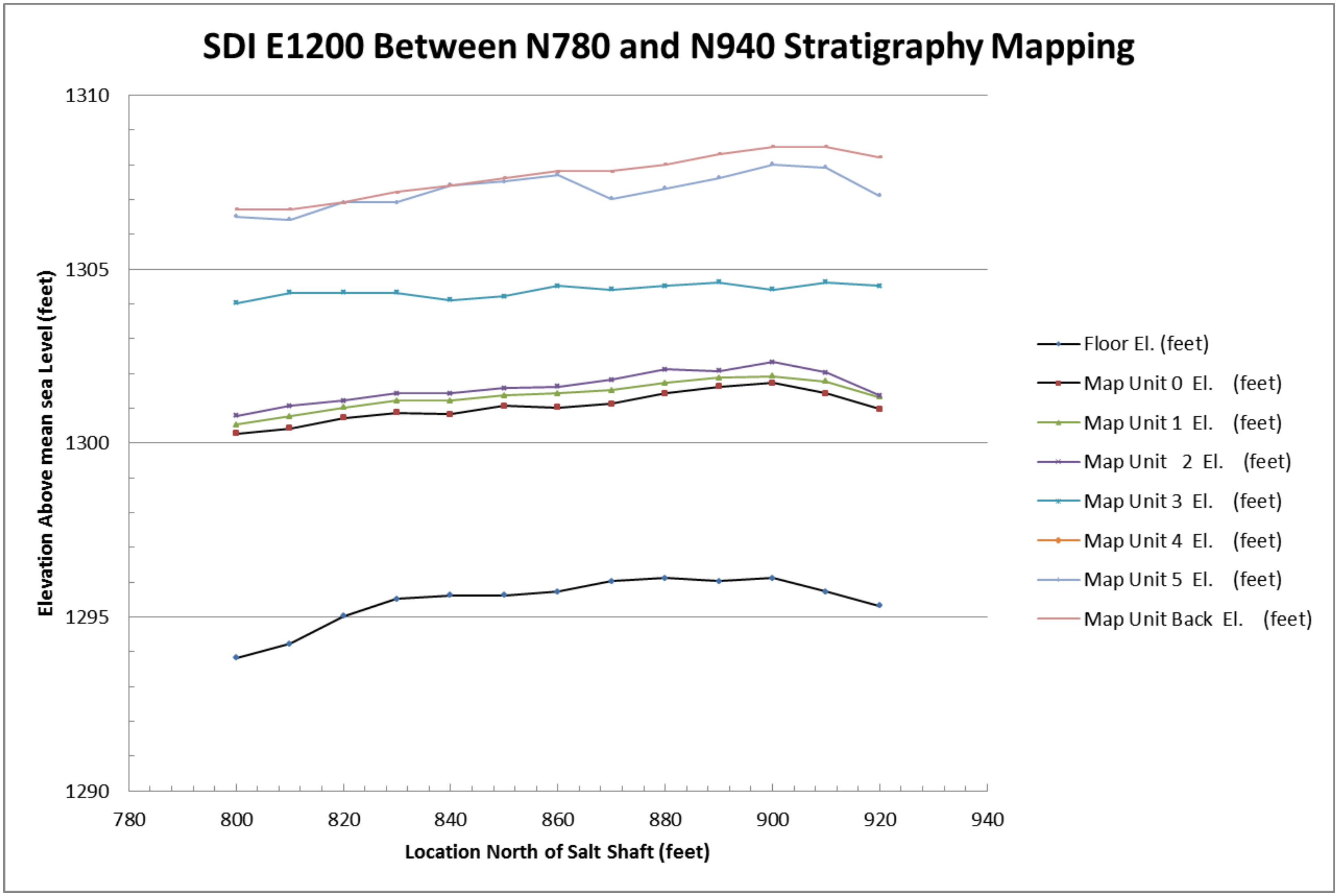

Figure-45 Stratigraphy Mapping, SDI E1200 between N780 and N940

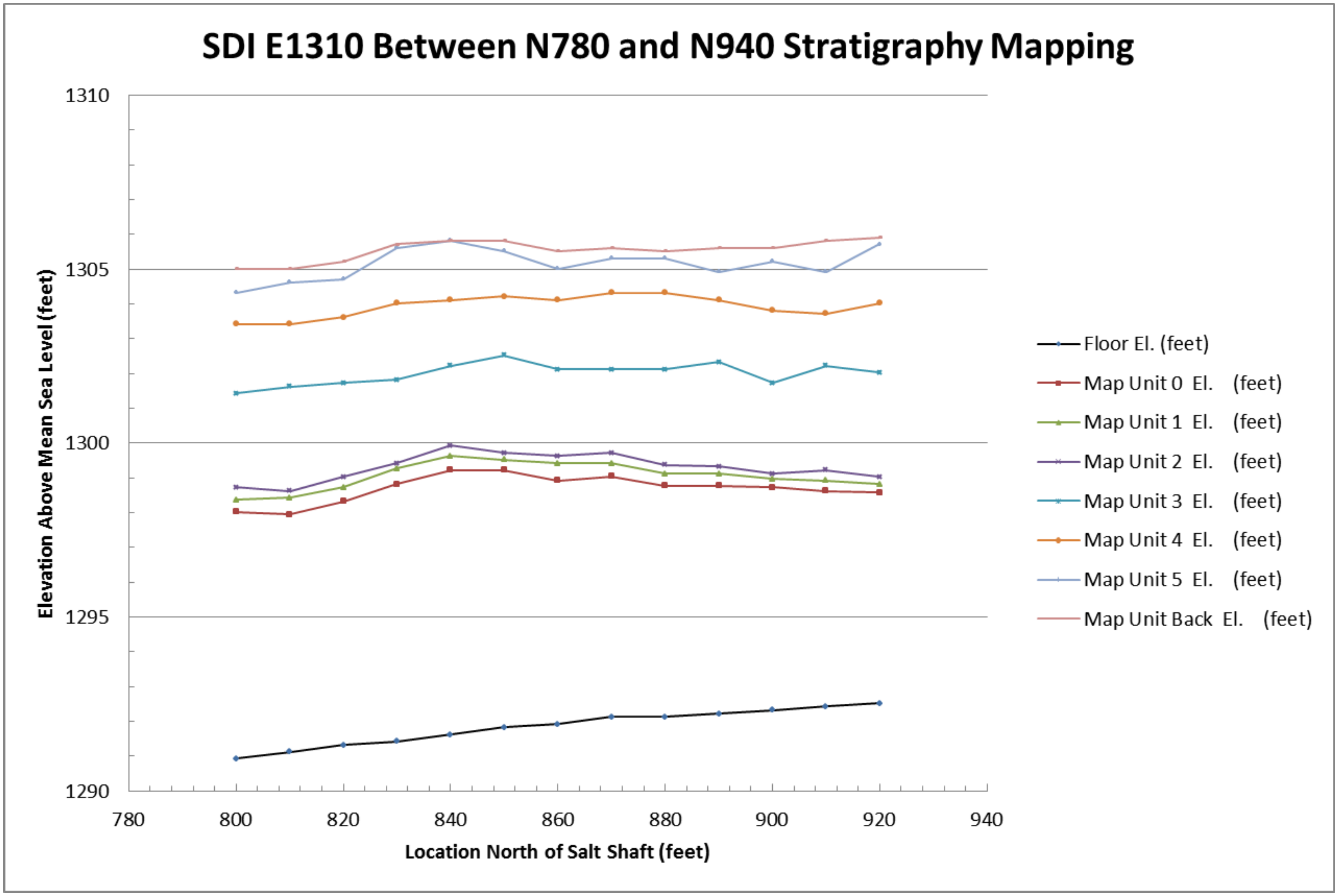

Figure-46 Stratigraphy Mapping, SDI E1310 between N780 and N940